STEPHEN M. KING

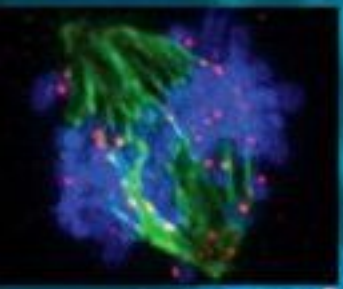

DYNEINS

STRUCTURE, BIOLOGY AND DISEASE

Dyneins

Structure, Biology and Disease

Stephen M. King

Department of Molecular, Microbial, and Structural Biology
University of Connecticut Health Center
Farmington
CT, USA

ELSEVIER

AMSTERDAM • BOSTON • HEIDELBERG • LONDON • NEW YORK • OXFORD • PARIS
SAN DIEGO • SAN FRANCISCO • SINGAPORE • SYDNEY • TOKYO

Academic Press is an imprint of Elsevier

Academic Press is an imprint of Elsevier
32 Jamestown Road, London NW1 7BY, UK
225 Wyman Street, Waltham, MA 02451, USA
525 B Street, Suite 1800, San Diego, CA 92101-4495, USA

First edition 2012
Copyright © 2012 Elsevier Inc. All rights reserved

Cover Image
The cover montage consists of two images that reflect the diverse activities of dynein motors.
At *top right* is a cryo-electron microscope tomographic reconstruction of the *Chlamydomonas* flagellum revealing the inner and outer arms associated with doublet microtubules of the axonemal superstructure, as well as the radial spokes and the central-pair microtubule complex that are involved in dynein regulation. In addition, an intraflagellar transport particle involved in organelle assembly is evident protruding between one doublet microtubule and the membrane. These particles are moved bidirectionally: a heterotrimeric kinesin is the motor necessary for movement from the cell body to the site of assembly at the distal tip, whereas an isoform of cytoplasmic dynein is required for recycling components in the retrograde direction back to the cell body. This image was prepared by Drs Khanh Huy Bui and Gaia Pigino in the laboratory of Dr Takashi Ishikawa at the Paul Scherrer Institute. The image at *left* is an immunofluorescent micrograph of a mitotic NRK2 cell stained for phosphorylated cytoplasmic dynein (red), tubulin (green), and chromatin (blue). The phosphorylated dynein is prominent at the kinetochores of chromosomes during prometaphase. This image was collected on a Deltavision API system by James Kasuboski, a PhD candidate in the laboratory of Dr Kevin T. Vaughan at the University of Notre Dame.

No part of this publication may be reproduced, stored in a retrieval system or transmitted in any form or by any means electronic, mechanical, photocopying, recording or otherwise without the prior written permission of the publisher

Permissions may be sought directly from Elsevier's Science & Technology Rights Department in Oxford, UK: phone (+ 44) (0) 1865 843830; fax (+44) (0) 1865 853333; email: permissions@elsevier.com. Alternatively, visit the Science and Technology Books website at www.elsevierdirect.com/rights for further information

Notice

No responsibility is assumed by the publisher for any injury and/or damage to persons or property as a matter of products liability, negligence or otherwise, or from any use or operation of any methods, products, instructions or ideas contained in the material herein. Because of rapid advances in the medical sciences, in particular, independent verification of diagnoses and drug dosages should be made

British Library Cataloguing-in-Publication Data
A catalogue record for this book is available from the British Library

Library of Congress Cataloging-in-Publication Data
A catalog record for this book is available from the Library of Congress

ISBN : 978-0-12-382004-4

For information on all Academic Press publications visit our website at www.elsevierdirect.com

Typeset by TNQ Books and Journals

Printed and bound in China

12 13 14 15 10 9 8 7 6 5 4 3 2 1

Working together to grow libraries in developing countries
www.elsevier.com | www.bookaid.org | www.sabre.org
ELSEVIER BOOK AID International Sabre Foundation

List of Contributors

Lea M. Alford

Emory University School of Medicine, Atlanta, GA, USA

Anita Becker-Heck

Klinik und Poliklinik für Kinder und Jugendmedizin, Allgemeine Pädiatrie, Universitätsklinik Münster, Münster, Germany

Frances K.Y. Cheong

Department of Biology, Johns Hopkins University, Baltimore, MD, USA

Amrita Dawn

Department of Molecular Medicine, Beckman Research Institute at the City of Hope, Duarte, CA, USA

Elizabeth M.C. Fisher

Department of Neurodegenerative Disease, Institute of Neurology, University College London, London, UK

I.R. Gibbons

Molecular and Cell Biology Department, University of California, Berkeley, CA, USA

Steven P. Gross

Department of Developmental and Cell Biology, University of California, Irvine, CA, USA

Keith Gull

Sir William Dunn School of Pathology, University of Oxford, Oxford, UK

Majid Hafezparast

School of Life Sciences, University of Sussex, Brighton, UK

Erika L.F. Holzbaur

Department of Physiology, University of Pennsylvania School of Medicine, Philadelphia, PA, USA

Takashi Ishikawa

Paul Scherrer Institute, Villigen, Switzerland

Ritsu Kamiya

Department of Biological Sciences, Graduate School of Science, University of Tokyo, Tokyo, Japan

Stephen M. King

Department of Molecular, Microbial, and Structural Biology, University of Connecticut Health Center, Farmington, CT, USA

Michael P. Koonce

Division of Translational Medicine, Wadsworth Center, Albany, NY, USA

Anna Kuta

Department of Neurodegenerative Disease, Institute of Neurology, University College London, London, UK

Christine M. Lightcap

Department of Molecular Medicine, Beckman Research Institute at the City of Hope, Duarte, CA, USA

Kevin W.-H. Lo

Department of Orthopaedic Surgery, University of Connecticut Health Center, Farmington, CT, USA

Niki T. Loges

Klinik und Poliklinik für Kinder und Jugendmedizin, Allgemeine Pädiatrie, Universitätsklinik Münster, Münster, Germany

Richard J. McKenney

Department of Pathology and Cell Biology, Columbia University, New York, NY, USA

Miroslav P. Milev

HIV-1 RNA Trafficking Laboratory, Lady Davis Institute for Medical Research – Sir Mortimer B. Davis Jewish General Hospital, Montréal, QC, Canada; Department of Medicine, Division of Experimental Medicine, McGill University, Montréal, QC, Canada

Armen J. Moughamian

Department of Physiology, University of Pennsylvania School of Medicine, Philadelphia, PA, USA

Andrew J. Mouland

HIV-1 RNA Trafficking Laboratory, Lady Davis Institute for Medical Research – Sir Mortimer B. Davis Jewish General Hospital, Montréal, QC, Canada; Department of Medicine, Division of Experimental Medicine, McGill University, Montréal, QC, Canada; Department of Microbiology and Immunology, McGill University, Montréal, QC, Canada

Heymut Omran

Klinik und Poliklinik für Kinder und Jugendmedizin, Allgemeine Pädiatrie, Universitätsklinik Münster, Münster, Germany

Kassandra M. Ori-McKenney

Department of Biological Sciences, Columbia University, New York, NY, USA
Department of Pathology and Cell Biology, Columbia University, New York, NY, USA

K. Kevin Pfister

Cell Biology Department, University of Virginia School of Medicine, Charlottesville, VA, USA

Stephen H. Pilder

Department of Anatomy and Cell Biology, Temple University School of Medicine, Philadelphia, PA, USA

Mary E. Porter

Department of Genetics, Cell Biology, and Development, University of Minnesota, Minneapolis, MN, USA

Winfield S. Sale

Emory University School of Medicine, Atlanta, GA, USA

Giampietro Schiavo

Molecular Neuropathology Laboratory, Cancer Research UK London Research Institute, London, UK

Trina A. Schroer

Department of Biology, Johns Hopkins University, Baltimore, MD, USA

Chikako Shingyoji

Department of Biological Sciences, Graduate School of Science, University of Tokyo, Tokyo, Japan

Amanda E. Siglin

Department of Molecular Medicine, Beckman Research Institute at the City of Hope, Duarte, CA, USA

Irina Tikhonenko

Division of Translational Medicine, Wadsworth Center, Albany, NY, USA

Paul A. Tucker

EMBL Hamburg Outstation, Hamburg, Germany

Richard B. Vallee

Department of Biological Sciences, Columbia University, New York, NY, USA
Department of Pathology and Cell Biology, Columbia University, New York, NY, USA

Kevin T. Vaughan

Department of Biological Sciences, University of Notre Dame, Notre Dame, IN, USA

Ken-ichi Wakabayashi

Department of Biological Sciences, Graduate School of Science, University of Tokyo, Tokyo, Japan

Bill Wickstead

Centre for Genetics and Genomics, University of Nottingham, Nottingham, UK

John C. Williams

Department of Molecular Medicine, Beckman Research Institute at the City of Hope, Duarte, CA, USA

Maureen Wirschell

Emory University School of Medicine, Atlanta, GA, USA

George B. Witman

Department of Cell Biology, University of Massachusetts Medical School, Worcester, MA, USA

Xin Xiang

Department of Biochemistry and Molecular Biology, Uniformed Services University of the Health Sciences – F. Edward Hébert School of Medicine, Bethesda, MD, USA

Jing Xu

Department of Developmental and Cell Biology, University of California, Irvine, CA, USA

Toshiki Yagi

Department of Cell Biology and Anatomy, Graduate School of Medicine, University of Tokyo, Tokyo, Japan

Ryosuke Yamamoto

Emory University School of Medicine, Atlanta, GA, USA

Preface

Molecular motor complexes are required for a vast array of cellular functions and consequently have attracted the attention of many biologists and clinicians. Over the last several decades, much has been learned about the mechanisms of action of molecular motors and the consequences of their dysfunction; for example, the manner in which members of the myosin and kinesin superfamilies convert ATP hydrolysis to mechanical work is now understood in exquisite detail. However, one class of motor — the dyneins, which translocate along microtubules — has stood out in terms of their complexity and the difficulties encountered in trying to understand their structural and functional attributes. Not only are the motor units themselves enormous (over 500 kDa each), which in and of itself imparts a whole host of technical challenges, but these motor subunits are associated with a complicated array of additional components that play key roles in stable formation of the holoenzymes, binding appropriate cargoes and regulating motor function in response to a wide variety of ever-changing regulatory inputs. Likewise, the array of activities that dyneins participate in and the consequences of their malfunction are myriad and complex. In this book, I have assembled a series of chapters written by some of the best-known dynein researchers who examine a broad array of topics ranging from the structural biology of dynein components and the details of the motor mechanism itself to how dyneins power ciliary motility and intracellular transport, the hijacking of dynein motors during viral pathogenesis, and the devastating consequences of dynein dysfunction for human disease.

This book is divided into five broad segments, which of necessity somewhat overlap. It begins with a section on **History and Evolution** that includes a fascinating article from Ian Gibbons (University of California, Berkeley), who first isolated axonemal dyneins from cilia of the alveolate *Tetrahymena pyriformis* in the early 1960s. Gibbons outlines the history of dynein research, incorporating his personal views of the field, and details some of the key insights that drove how our understanding of this complex motor progressed from the early days to the present. This is followed by a chapter from Wickstead (University of Nottingham) and Gull (University of Oxford), who consider the ancient evolutionary origins of dynein components and discuss how they might have arisen prior to the last common eukaryotic ancestor.

Section II focuses on the **Structure and Mechanics of Dynein Motors** and looks at the detailed structure of dynein components. Dyneins are members of the AAA^+ family of ATPases, and, although we have yet to obtain a high-resolution structure of the dynein heavy chain itself, multiple structures of other AAA^+ proteins have been solved. Tucker (EMBL Hamburg Outstation) describes how

this information can be used to inform our understanding of dynein heavy chain structure and this is followed by a chapter by Koonce and Tikhonenko (Wadsworth Center), who detail the current model of the general motor mechanism. Subsequently, Williams et al. (Beckman Research Institute at the City of Hope) describe the high-resolution crystallographic and NMR-based structural work on the intermediate and light chains associated with both cytoplasmic and some axonemal dyneins. The last chapter in this section, by Xu and Gross (University of California, Irvine), examines the biophysics of dynein action with an emphasis on *in vivo* measurements.

We then consider the role of **Dyneins in Ciliary Biology**, where multiple dyneins form the inner and outer arms associated with the axonemal doublet microtubules, which generate the force to power these motile organelles. In addition, a specific dynein isoform closely related to cytoplasmic dynein 1 is involved in assembly of the organelle at its distal tip. This section begins with a chapter by King (University of Connecticut Health Center) describing the basic composition and assembly of these complex axonemal motors. Ishikawa (Paul Scherrer Institute) then describes the latest information derived from cryo-electron microscopic tomography on the organization of these motors *in situ*. We then proceed to a detailed description of axonemal dynein genetics by Yagi and Kamiya (University of Tokyo) and to chapters by Wakabayashi (University of Tokyo) and Alford et al. (Emory University School of Medicine) that focus on the mechanisms by which outer- and inner-arm dyneins respond to a variety of regulatory cues. Subsequently, Porter (University of Minnesota) describes the dynein regulatory complex/nexin link that is a key component required for axonemal motility, and Shingyoji (University of Tokyo) provides a systems-level analysis of regulatory activity within the axoneme. In the final chapter in this section, Witman (University of Massachusetts Medical School) presents a detailed view of the dynein that powers retrograde intraflagellar transport and that is thus required for the assembly of both motile and sensory cilia.

The fourth section, **Cytoplasmic Dynein Biology**, focuses on dyneins that function within the cytoplasm. It begins with a description by Pfister (University of Virginia School of Medicine) and Lo (University of Connecticut Health Center) of the components present in these complexes and details the large isoform variation that can potentially occur and how this correlates with discrete cellular functions. Ori-McKenney et al. (Columbia University) then explain the current model for how force production by cytoplasmic dynein motor units is controlled through interaction with the Lis1 and NudE/NudEL regulatory proteins. This is followed by chapters from Xiang (Uniformed Services University of the Health Sciences) and Kuta et al. (Institute of Neurology, University College London, University of Sussex and Cancer Research UK) that discuss the insights into cytoplasmic dynein function that have been obtained from genetic studies in fungi and mammals. Schroer and Cheong (Johns Hopkins University) then provide an analysis of the dynactin complex, which associates with cytoplasmic

dynein to enhance processivity and is indispensible for many of its intracellular functions, and Vaughan (University of Notre Dame) discusses the specific roles played by dynein during mitosis.

The final section of this book, **Dynein Dysfunction and Disease**, examines what happens when dyneins fail to act appropriately. Pilder (Temple University School of Medicine) examines whether dynein dysfunction might be involved in the fascinating phenomenon of non-Mendelian chromosome segregation in mice. This is followed by a chapter from Mouland and Milev (McGill University), who discuss the role of dynein in viral pathogenesis and how a variety of viruses co-opts dynein motors to move the infectious particle along microtubules from the cell periphery to the nucleus. Moughamian and Holzbaur (University of Pennsylvania School of Medicine) then describe how disruption of cytoplasmic dynein activity is involved in a range of devastating neurodegenerative diseases (including amyotrophic lateral sclerosis, Huntington's disease, and Parkinson's disease). The final chapter, by Becker-Heck et al. (Universitätsklinik Münster), discusses the complex defects associated with primary ciliary dyskinesia and other ciliopathies (such as infertility, *situs inversus*, and other developmental problems) that occur in humans when axonemal dynein-powered ciliary motility is disrupted.

I would like to extend my thanks to all the authors, who put in so much effort to prepare the chapters for this volume, and also to the staff at Elsevier for their assistance in making this book a reality.

Stephen King

West Hartford, Connecticut

In this chapter

1

Discovery of Dynein and its Properties: A Personal Account

I.R. Gibbons
Molecular and Cell Biology Department, University of California, Berkeley, CA, USA

To Barbara

1.1 Introduction

This is an extremely exciting time for research on the dynein motor protein and its role in the life of a cell. Ever since dynein was first discovered in 1963, the study of

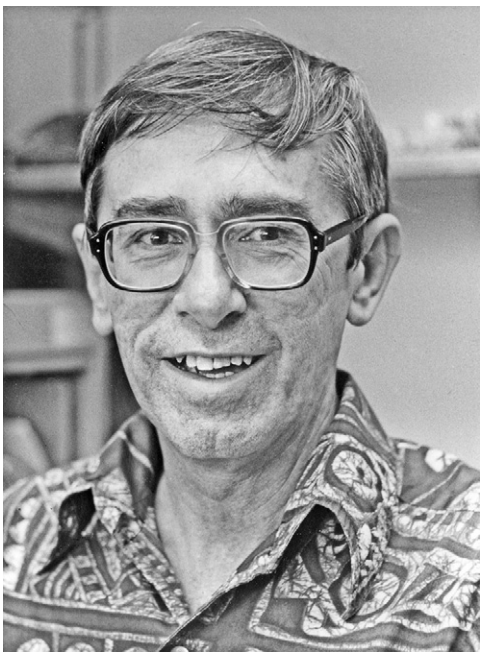

Figure 1.1
Ian Gibbons. The photograph was taken in 1983.

Dyneins DOI: 10.1016/B978-0-12-382004-4.10001-9
Copyright © 2012 by Elsevier Inc. All rights reserved.

its properties has been hindered by the unusually large size of the molecule and the relatively small quantities available from natural sources. The past few years have seen this constraint lifted by the development of procedures for *in vitro* expression of a functional cytoplasmic dynein motor [1,2]. The rapid advances in our understanding made possible by being able to apply the full range of contemporary molecular biology procedures have begun to appear [3–6]. At the time of writing, in December 2010, the first crystal structure for a complete dynein motor domain has just been presented at the 50th Annual Meeting of the American Society for Cell Biology. In this chapter, I have been invited to tell the story of how I, as the first person in my family to attend a university, have been privileged to participate in discovering the properties of this fascinating and extremely complex protein.

1.1.1 Early Years

I was born in 1931, at a time when my parents were living in Rye, a small town in the south-east of England. My father, Arthur Alwyn Gibbons, came from a family who had held smallholdings in Somerset, Essex and Guernsey during the nineteenth century. Perhaps because of the trauma he suffered as a British Army lieutenant in the trenches of Flanders during the First World War, he had fallen out with most of his family. He was frequently moody and I could never get him to talk to me of anything in his early life. Nevertheless, he was a committed freemason and had a stable job as a bank clerk; our family, although not well off, suffered no major financial upset during the depression of the 1930s and the subsequent Second World War. My mother, Hilda Read Cake, came from a family who had run small farms in Dorset for many generations. She had attended a cookery school and then worked as a pastry cook in a restaurant prior to her marriage. Her style of traditional English cooking still pervades our families today. Although she was a rather anxious person, who did not find it easy to make friends, she had a strong family tradition and enjoyed talking about her childhood. Even under the constraints imposed by the war, she frequently took my brother and me to visit our uncles and aunts, who were still farming in Dorset.

One of my earliest childhood memories is of my parents listening to Prime Minister Neville Chamberlain's radio broadcast on the day war broke out in September 1939 and then trying to explain to me what was happening. During the course of the war, I began eagerly listening to all the latest news on the radio that my parents allowed by my bedside. From this, I developed a more specific interest in the possibilities of radio. By starting with a kit purchased through a popular radio magazine, I managed to construct a shortwave radio that enabled me to listen to radio stations from around the globe. My subscription to the semi-professional magazine *Wireless World* gave me further theoretical and technical information, while encouraging my enthusiasm with its famously prescient 1945 article by Arthur C. Clarke on the potential for radio broadcasting from geostationary satellites. Pretty soon, I had taught myself enough about electric circuitry

and vacuum tubes to design and build a power amplifier that put out 25 watts of high-quality sound from an early LP recording of the Amadeus String Quartet playing a pair of Mozart quartets on an old record player with a rewired pick-up. These two quartets, K.465 in C major and K.575 in D major, have remained among my most favored works ever since.

In 1943, we were living in a small village in Kent when my parents enrolled me in the nearby Faversham Grammar School. Originally founded by Queen Elizabeth I in 1665 the school became fully state-funded as part of a general reorganization of education in England at the end of the war. At school in Faversham, I obtained an excellent education with a strong emphasis on mathematics, physics, and chemistry. Although I enjoyed maths and was reasonably good at it, my real enthusiasm was for physics, especially for its practical side, where my liking for details encouraged me to try out changes that would hopefully improve the accuracy of the final result. Towards the end of my schooling, when I sought advice as to where it would be best for me to go, my school headmaster, a classicist Kingsman himself, played a major role in my life by recommending that I decline an initial offer from one of the modern universities and instead stay an extra year at Faversham to apply for a scholarship at Cambridge. The entrance exams were both thorough and leisurely in those days and involved spending a full week in residence at the college of one's choice. The exam questions were frequently interesting and candidates were advised not to restrict themselves to answering the question directly but to give additional relevant information when they could. Through an odd coincidence, the vanadium compound that we were requested to study and attempt to identify in the practical chemistry exam would return later in my career as an important tool for my research on dynein. After hearing with almost disbelief that I had been awarded a scholarship at King's College, I took off on an 18-month detour performing my national service (conscription) as a pre-qualified radar mechanic in the Royal Air Force, before heading to Cambridge.

1.1.2 Life in Cambridge

When I entered King's College in October 1951 to read for a degree in physics, my advisor was already able to foresee the future expansion of biological research. He recommended that I prepare myself by taking physiology and biochemistry, in addition to my previous interests in physics, chemistry, and mathematics, for Part I of the Natural Sciences Tripos. In my third year, Part II of the Tripos involved more specialized lectures covering several different areas of physics. This was more difficult for me to get a grip on, but I managed to hang on and obtain a Class II (1) degree in physics. On the basis of this result, I was offered a research studentship on biological applications of electron microscopy in the unit headed by Vernon Cosslett in the Cavendish (physics) lab. My colleagues in the Electron Microscopy Unit were the first real social group that I had joined since leaving home and I found in them my first group of scientific kindred spirits.

The "sink or swim" style of graduate education in England at the time did not require me to take any formal courses in biology, but the lab encouraged me to obtain a general background knowledge of research in the field by providing me with funds to attend several major meetings, including the 1954 International Congress of Electron Microscopy in London; the following European Congress in Stockholm, where nearly half of the papers were devoted to biological applications; and the International Congress for Cell Biology at St. Andrews in 1957. My PhD supervisor, John Bradfield, was a zoologist who had a half-time appointment in the Cavendish. At this time he was studying cilia and flagella by electron microscopy and had proposed a contractile mechanism for their motility [7]. To get me started, he suggested that I use the then newly developed thin-sectioning procedure to study the structural changes in chromosome organization during mitosis and meiosis in locust testis. My results demonstrated that the chromatin aggregates into folded sheets during the reshaping of the rounded spermatid nuclei into the elongated shape of mature sperm heads, possibly as a result of the switch from histone to protamine as the major protein component of chromatin [8]. However, I was unable to make any progress in clarifying the mechanism of chromosome condensation during prophase, which had been my intended main topic. Fortunately, my examiners, Laurence Picken from the Zoology Department and Arthur Hughes from Oxford University, considered these mixed results sufficient for my PhD thesis.

1.1.3 Moving to the USA

In the spring of 1957, as I was starting to write my thesis, Tom Anderson, one of the eminent pioneers of biological electron microscopy, passed through the lab and offered me a postdoctoral position for the autumn in the Johnson Foundation at the University of Pennsylvania. By then, Bradfield had left the Cavendish to take a position managing the finances of Trinity College. Although Audrey Glauert from the Strangeways Laboratory dropped in to chat from time to time and the Cavendish MRC unit sponsored occasional seminars on topics in molecular biology, I had increasingly come to feel isolated from biologically oriented colleagues and decided that it was time for me to move on.

When I arrived in Philadelphia at the end of the summer in 1957, the director of the Johnson Foundation was Britton Chance, who had a large laboratory with about eight postdoctoral fellows working on different aspects of electron transport. Tom Anderson had recently returned from a sabbatical year at the Pasteur Institute in Paris. He was a warm and very friendly person, but experienced resistance in obtaining space in which to install the new electron microscope needed for his intended high-resolution work on negatively contrasted virus particles. Although I became good friends with some of Chance's postdoctoral researchers and learnt much from their breadth of scientific backgrounds, I sensed a lack of the momentum that I needed for my rather youthful research ambitions at the time. In my typical independent style, I perceived that my future at the lab

was limited and took it upon myself to respond to a job advertisement that happened to appear in *Nature*.

1.2 Research at Harvard

The following summer, I moved to Harvard University as an electron microscopist with the task of starting up a new service laboratory in the Biology department. Although this was a junior position with the formal status of a postdoctoral fellow, I had negotiated an agreement of devoting half my time to informal instruction of graduate students starting in electron microscopy and keeping the remainder available for my own research. This arrangement worked well, for the collaborations with other research groups did much to broaden my knowledge of biology while the departmental electron microscopy grant provided ample funds for my research. My supervisor, George Wald, was a kind and friendly man who did not object to my push for independence. He very helpfully provided me with a social center in the department by inviting me to join his active lunch group, where many eminent visitors to the department stopped by for lunch. One of my closest collaborations during this period was with John Dowling, who was then a graduate student in Wald's lab, studying the interactions of the retina with the pigment epithelium during embryonic development [9]. As time passed, I gradually took on additional responsibilities, including writing annual reports and the renewal application for the departmental NSF grant for electron microscopy.

By good fortune, the lunch meetings with Wald's group became a life-changing experience for me, personally, as through them I met my future wife, Barbara Hollingworth, with whom I was to have an enduringly happy marriage as well as a highly productive research collaboration over the 30 years of our life in Hawaii. Barbara had obtained her bachelor's degree in chemistry from Mount Holyoke College and had worked as a lab technician for Gerty Perlmann at the Rockefeller Institute in New York before moving to Harvard. At the time I met her, she was a graduate student studying for her PhD on the kinetics of carbonic anhydrase in the lab of John Edsall. In addition to science, we shared several interests including hiking and other outdoor recreations (Fig. 1.2), classical chamber music (with Barbara playing violin in a weekly string quartet group), and a strong belief in non-religious family bonds. We were married in the spring of 1961 and in the summer made an eight-week camping tour, passing through more than half of the 50 states.

1.2.1 Electron Microscopy of Cilia and Flagella

But this is skipping ahead in time. One day in the summer of 1959, my enthusiasm for studying cilia and flagella, which eventually led to the discovery of dynein, was sparked when I took some electron micrographs of a termite-inhabiting protozoan named *Pseudotrichonympha* that showed with unusual clarity that its flagellar system possessed an extraordinarily complex fibrous substructure

Figure 1.2
Barbara Hollingworth and Ian Gibbons sailing a canoe on the Charles River, Boston, before their marriage. The photograph was taken in September 1960 by Ken Simpson, a friend.

(Fig. 1.3; [10]). These micrographs formed the beginning of a collaboration with Bill Grimstone, a zoologist contemporary of mine at Cambridge, who had come to Harvard on a postdoctoral fellowship with L.R. Cleveland, the leading expert in such flagellates. We found that the large number of flagella emerging through deep grooves in the body surface of these protozoa constituted exceptionally favorable material for the analysis of flagellar structure. By electron microscopy of thin-sectioned specimens embedded in epoxy resin and then stained with heavy metal by a novel method, we were able to obtain excellent preservation of fine structure, combined with images of unusually high contrast.

This protocol enabled us to describe some features of the flagellar system — notably, of the basal body at the cytoplasmic end of each flagellum and of the transitional region between the basal body and the shaft of the flagellum — in greater detail than had hitherto been feasible [10]. Two structures of particular current interest were the fibrous cartwheel believed to underlie the nine-fold symmetry of basal bodies, cilia, and centrioles [11] and the transitional fibers involved in the intraflagellar transport (IFT)/cell signaling pathway [12]. We also confirmed the presence of outer and inner arms on the doublet tubules in the 9+2

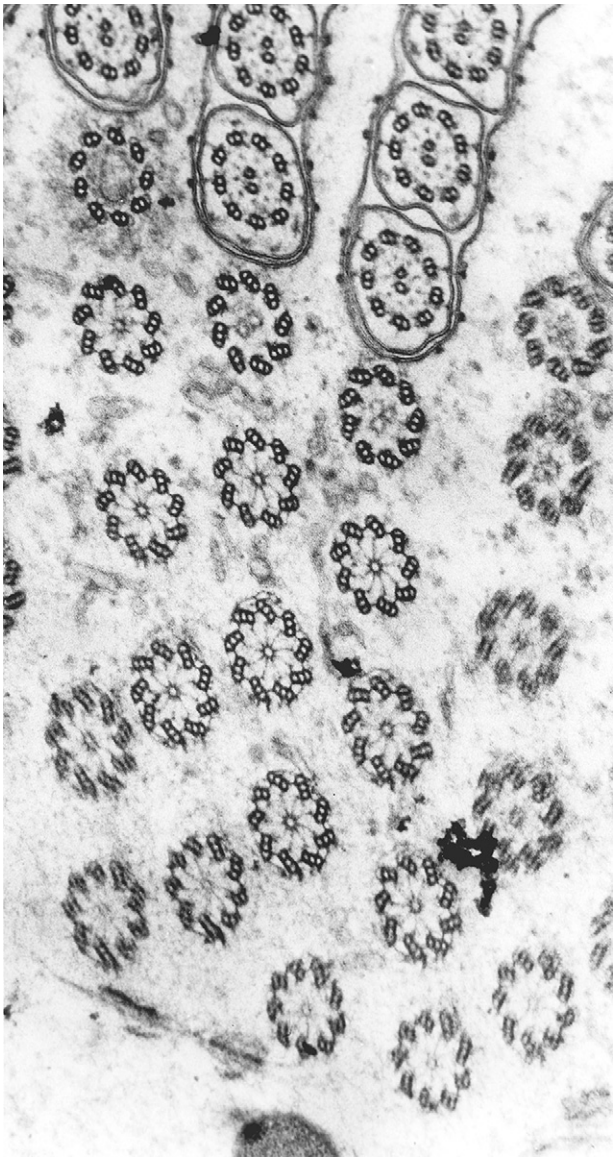

Figure 1.3
Electron micrograph showing transverse sections of flagella and basal bodies in *Pseudotrichonympha*, a protozoan that inhabits the gut of termites. At the top are the grooves through which the flagella exit the body and at the bottom are sections through the proximal ends of the basal bodies. *Reproduced from [10] with permission.*

structure of the flagellar axonemes; these arms were similar to those described in sperm flagella a few months earlier by Bjorn Afzelius [13], who suggested that they might function to produce sliding between tubules in a mechanism reminiscent of that proposed for the cross bridges between filaments in striated muscle [14]. In our own work at this time, we distinguished the two tubules of

each doublet as A and B, with the arms being permanently attached to the A-tubule of each doublet and extending toward the B-tubule of the adjacent doublet. We noted that the apparently unequal lengths of the doublet tubules in the flagellar tips would be consistent with a sliding tubule mechanism. However, we favored a contractile mechanism on the basis that in sperm flagella a sliding mechanism would necessitate limited regions at different positions along a given tubule moving simultaneously in opposite directions, which we (incorrectly, as we now know) deemed improbable.

Over the next couple of years, I extended the electron microscopic analysis to the ciliary and flagellar axonemes of a variety of other organisms. In all cases, the conspicuous enantiomorphic asymmetry indicated by the unilateral position of the arms on the axonemal doublets and by the inward tilt of the basal body triplets (Fig. 1.3) showed the same clockwise handedness, as viewed from base to tip [15]. This axonemal asymmetry seemed likely to underlie the clockwise conical component of the ciliary beat pattern reported in *Paramecium* by Parducz [16] and also by myself in reactivated cilia of *Tetrahymena* [17]. Much more recent work in the Hirokawa laboratory has demonstrated that a similar conical beat pattern occurs in vertebrate nodal cilia, where it initiates the left–right asymmetry in embryo development by distributing morphogens asymmetrically over the surface of embryos [18]. The enantiomorphism of ciliary structure thus constitutes one link in the chain that upscales the fundamental asymmetry of biological structures from the level of L-amino acids to proteins, to ciliary axonemes, to the asymmetric positioning of body organs in vertebrates.

The several specialized types of ciliated cell on a molluscan gill epithelium provided me with appropriate material to examine the relationship between ciliary beat patterns and axonemal structure in greater detail. Structurally, these cilia had 9+2 axonemes and basal bodies similar to those in the flagellated protozoa, but they contained additional features that gave them a more distinct polarity. The orientation of this ciliary polarity in the four different types of ciliated cell in these epithelia always coincided with the effective stroke direction for the cilia of that cell type. This correlation suggested that the polarized aspects of the structure were responsible for coordinating the beat pattern, although the mechanism was unclear.

Concurrently with this study of mine, Peter Satir, who was then a graduate student in Keith Porter's laboratory at the Rockefeller Institute, developed a procedure for using rapid fixation of actively beating cilia on lamellibranch gills in order to preserve changes in axonemal structure that occurred during a beat cycle for subsequent study by electron microscopy [19]. By quantitative analysis of the changes in ciliary tip structure in these samples, Satir was later able to demonstrate that the lengths of individual doublet tubules remained constant during a ciliary beat cycle and thus provided the first direct experimental support for a sliding tubule mechanism of ciliary motility [20,21]. However, some others in

the field, including myself, were not immediately ready to accept Satir's conclusion, largely because of the aforementioned complex patterns of sliding required to generate the planar and nearly symmetric bending waves of invertebrate sperm flagella. As late as 1968, a review of contractile versus sliding-tubule models concluded that neither appeared to provide a satisfactory working model for the varied bending patterns of cilia and flagella [22].

1.2.2 Discovery of Dynein

Several years earlier, during the summer of 1962, my familiarity with the variety of approaches that were being used productively to study striated muscle had led me to decide that biochemical characterization of the proteins responsible for axonemal bending waves would be prerequisite for general acceptance of any model of the underlying motility mechanism. Earlier work had shown that ATP can induce beating motility in glycerinated cilia and flagella [23,24] and that the isolated organelles possess ATPase activity [25,26], indicating that energy for motility comes from dephosphorylation of ATP. However, attempts to study ciliary proteins in any detail had been blocked by their apparent insolubility at neutral pH. I suspected that this reported insolubility was due to the cell membrane resealing over the broken ends of the detached cilia and that once the membranes were removed the axonemal proteins would be soluble under mild conditions.

In November 1962, with the benefit of considerable advice from Barbara, my wife, who had extensive previous experience with protein chemistry, I acquired a set of the famed Carlsberg micropipettes (hand-blown to $\pm 1\%$ accuracy by H. E. Pedersen) and began making preparations of isolated cilia from cultures of *Tetrahymena* using an ethanol-calcium procedure modified from that of Sir John Randall's group in London [26]. In the absence of polyacrylamide gel electrophoresis, which had not yet been developed, initial fractionation of axonemal protein involved a combination of protein and ATPase assays, supplemented with centrifugation of soluble fractions in the Beckman Model E analytical ultracentrifuge that I had access to in John Edsall's lab. The usual criterion for purity of an enzyme in those days was that the distribution of enzymatic activity should parallel the distribution of protein across a peak of the putatively purified material. As most cytoskeletal proteins did not chromatograph well, purification on a sucrose density gradient was preferred [27,28].

A trial of different ways to remove the ciliary membrane showed that extraction of the isolated cilia with a solution containing $MgSO_4$ and digitonin, a naturally occurring detergent, completely removed the ciliary membranes, leaving a preparation of free axonemes that appeared structurally intact by electron microscopy and that retained almost all the ATPase activity present in the original cilia (Fig. 1.4A,B; Table 1.1; [29]). These preparations of demembranated axonemes could be fully solubilized by 0.6 M salt solutions at neutral pH

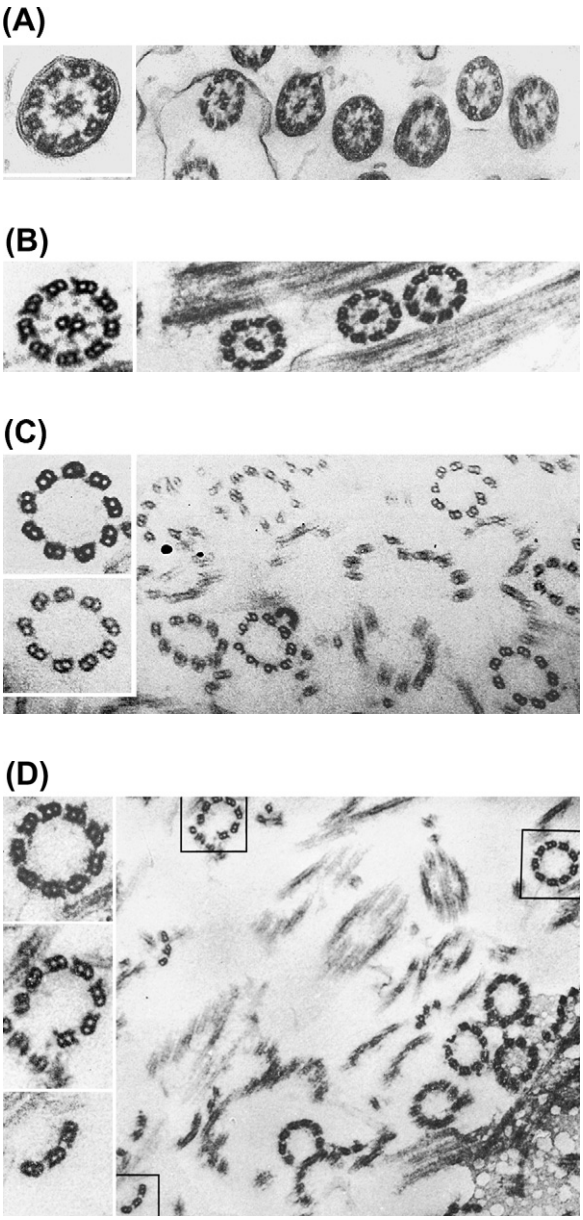

Figure 1.4 Reproductions of the original figures, legends, and tables in the 1963 paper that first described the principal physical and enzymatic properties of the protein forming the arms on the outer-doublet tubules in ciliary axonemes of *Tetrahymena* [29]. The protein was given the name of "dynein" in a follow-up 1965 paper after the 14 S and 30 S fractions – which we now know correspond to the inner and outer arms, respectively – had been separately purified and preliminary molecular weights established [32]. The arms had been earlier described in electron micrographs by Bjorn Afzelius [13], who speculated that they might correspond to the myosin cross-bridges in striated muscle. Figure legends have been reformatted for compatibility.

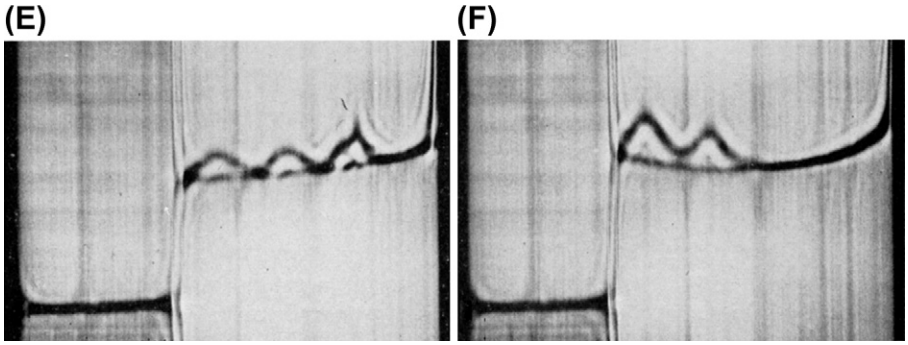

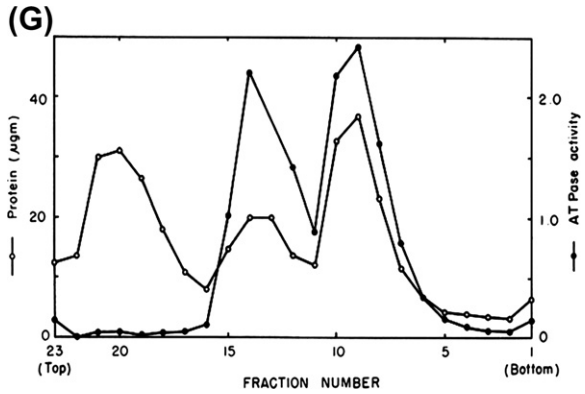

Figure 1.4 Continued

(A) Freshly isolated cilia. Inset shows detailed cross-section.

(B) Digitonin-extracted cilia. Inset shows detailed cross-section.

(C) Insoluble residue after dialyzing digitonin-extracted cilia against tris-EDTA solution. Inset shows detailed cross-sections.

(D) "Reconstituted" cilia obtained by restoring magnesium to a preparation of digitonin-extracted cilia that had been dialyzed against tris-EDTA solution; insets show portion of the same micrograph. (The same preparation of dialyzed cilia, but without the addition of magnesium, is shown in the upper inset of (C).)

(E and F) Analysis by ultracentrifugation of Fraction 1 of structural protein. Two cells were run, one containing sample and the other a solvent blank. (E) shows Fraction 1 in tris-EDTA solution. (F) shows the same preparation of Fraction 1 in tris-EDTA solution containing 0.1 M Na_2CO_3. Kel-F centerpiece; 59 000 rpm; 20°C; bar angle, 50°; time: 16 min. Fraction 1 is the soluble fraction after dialysis against 1 mM tris-HCl, 0.1 mM EDTA, and centrifugation.

(G) Separation of the components of Fraction 1 by centrifugation through a sucrose density gradient. 0.1 ml of Fraction 1 in tris-EDTA layered on top of a 5–30% sucrose gradient and centrifuged 7 h at 38 000 rpm in SW39 rotor of Spinco centrifuge. Contents of centrifuge tube collected in samples of three drops. ATPase activity in μmole P/hour. No activity measurement for sample 13.

Table 1.1 Extraction of Cilia with Digitonin

	Total Protein(mg)	Total ATPase Activity (μmoles P/hr)	Protein in Supernatant(mg)	ATPase Activity
in Supernatant(μmoles P/hr) Freshly isolated cilia in tris-Mg soln. Centrifuged.	4.8	15	0.6(12%)	—
Pellet resuspended in 0.5% digitonin in tris-Mg soln. Centrifuged.	—	—	1.4(30%)	2
Pellet resuspended in 0.5% digitonin in tris-Mg soln. Centrifuged.	—	—	0.3(6%)	—
Pellet resuspended in tris-Mg soln.	2.4(50%)	14	—	—

Figures in Parenthesis represent percentages of initial protein.

Table 1.2 Solubility of Digitonin-Extracted Cilia at pH 8.3

Extracting Solution	Time of Extraction	Per cent Protein in Solution	Per cent Activity in Solution	Specific Activity of Solution, μmoles P/(mg protein × hour)
0.6 *M* KCl, 30 mM tris-HCl, 2mM $MgSO_4$	18 hr	95	90	5.3
1 mM tris-HCl, 0.1 mM EDTA	Dialyzed 18 hr	31	90	20
1 mM tris-HCl, 1 mM $MgSO_4$	18 hr	7	4	—
10 mM KCl, 30 mM tris-HCl, 1 mM, EDTA	Dialyzed 18 hr	6	2	—
3 mM ATP, 30 mM tris-HCl, 2.5 mM $MgSO_4$	5 min	5	—	—

(Table 1.2). Analytical centrifugation of the resultant solution showed a large peak sedimenting at about 4 S, as well as smaller peaks at 14 S and 30 S[1]. This promising sedimentation pattern encouraged me to begin fractionating the axonemal proteins responsible for microtubule-based motility in cilia.

Within three months, I had succeeded in obtaining an initial fractionation of the axonemal protein by dialysis of the demembranated axonemes against a low-salt medium in the absence of magnesium. This dialysis solubilized almost all of the axonemal ATPase activity, but only about one-third of the total protein (Table 1.2). Electron microscopy showed that the fraction remaining insoluble consisted mostly of the axonemal doublet tubules, with all the other structural components, including the central tubules, the radial spokes, and the arms on the doublet

[1] *The sedimentation coefficients of these fractions were initially reported as 13 S and 25 S.*

tubules, almost completely removed (Fig. 1.4C). Despite so many structures having being removed, the cylindrical groups of nine doublets present in an intact cilium still largely persisted, apparently held together by a thin filament running around the inside of the cylinder. Analytical centrifugation of the soluble fraction from the dialysis showed the presence of the same three protein peaks as in solubilized whole axonemes (Fig. 1.4E), but with considerably less material in the 4 S peak. Subsequent density gradient analysis indicated that the axonemal ATPase activity was associated nearly equally with the 14 S and 30 S peaks, with the former having about twice the specific activity of the latter (Fig. 1.4G). At alkaline pH, the material in the 30 S peak appeared to break down to a mixture of 4 S and 14 S material (Fig. 1.4F). On the basis of these data, the 30 S particles were tentatively interpreted as a naturally occurring subunit of the cilium that became partly broken down to 14 S particles during normal preparation and more completely broken down at alkaline pH.

Importantly, the native axonemal structure could be partially reconstituted simply by restoring magnesium to the dialyzed preparation. Upon this addition of magnesium, about half of the solubilized protein and ATPase activity became re-bound to the suspension of doublet tubules. Electron microscopy of these preparations after re-binding showed that a high proportion of both the outer and inner arms had become restored to their original sites on the A-tubule of each doublet (Fig. 1.4D). This correlation between the presence or absence of arms on the doublet tubules and the presence or absence of pelletable ATPase activity strongly suggested that the arms projecting from each A-tubule of one doublet toward the B-tubule of the neighboring doublet are the site of most or all of the ATPase activity responsible for ciliary motility.

These results aroused significant interest when I first presented a preliminary account in a symposium organized by Tay Hayashi at the annual meeting of the Biophysical Society in March 1963. Ed Taylor, at the University of Chicago, very politely told me that Gary Borisy in his lab was working on related material, and, with slight understatement, suggested that there would be plenty of work for both our groups. At the urging of Keith Porter, who had moved to Harvard two years earlier, the Biology department agreed to release me from responsibility for the electron microscopy service lab that summer and to give me a faculty appointment as an Assistant Professor the following year. The increased funding provided by an NIH research grant in my own name enabled me to think of recruiting a postdoctoral researcher to participate in characterizing the axonemal proteins. With me enjoying my increased freedom and Barbara having just completed the requirements for her PhD degree, we decided to take off with our six-month-old daughter and spend the coming summer in Cambridge, England. In addition to visits with my family and some excellent hiking carrying our daughter on Mount Snowdon in Wales, I needed to finish writing and submit an initial paper on the localization and properties of the axonemal ATPase [29], and also planned to continue my collaboration with Grimstone on the unusually

structured centrioles and rostral apparatus of *Pseudotrichonympha* and the related genus *Trichonympha* [30]. While in Cambridge, I visited Paley Johnson, a protein chemist who worked on the physical chemistry of muscle proteins, in order to discuss my recent work on the axonemal proteins. It turned out that Johnson had a research student, Arthur Rowe, who was finishing up his PhD work and was interested in joining my lab at Harvard in the following spring.

By the time that Rowe came to join our lab in 1964, we had scaled up our preparations and were able to obtain sufficient of the density-gradient purified 14 S and 30 S ATPase fractions for more detailed characterization. Molecular mass determinations by analytical centrifugation gave values of 600 kD and 5400 kD for the 14 S and 30 S fractions, respectively. However, as noted at the time, the interpretation of these values was clouded by polydispersity and contaminating fragments of microtubules. More recent values for the molecular mass of the 30 S dynein have been about 2100 kD [31]. Nevertheless, the size of the monomeric ciliary ATPase and its relatively high nucleotide specificity for ATP clearly distinguished it from skeletal myosin (220 kD), the only other motility-associated ATPase known at the time. We proposed that the ciliary enzyme was one of a new class of ATP-dependent motor proteins that interact with microtubules to provide the energy for the beating of cilia and other forms of microtubule-based motility [32]. In a discussion one evening at home, Barbara came up with the name of "dynein," after the dyne, which had been the accepted unit of force when we were going through school. Re-binding experiments with the 30 S form of dynein restored the bound ATPase activity as well as the outer arms on the doublet tubules, confirming the localization we had reported earlier, but we were unable to localize the 14 S form of the dynein at that time. A more detailed characterization of the enzymatic properties of the 14 S and 30 S dyneins supported the close relationship of the two forms but was mostly useful for sensitizing me to the fact that some preparations of commercial ATP contained a potent inhibitor of dynein ATPase activity [33]. Although I did not go on to identify this inhibitor at the time, it was later to prove an important tool for studying dynein (Section 1.3.3.5).

An obvious next step in studying the properties of the isolated *Tetrahymena* axonemes was to add ATP to a suspension of the demembranated axonemes under conditions that might be expected to support motility. However, these experiments, begun in January 1963, yielded unexpected results showing that the addition of 10 μM ATP caused an irreversible decrease of ~20% in the turbidity of the suspension, although the axonemes appeared completely immotile by light microscopy. In the absence of any disintegration of the axonemal structure visible by electron microscopy and with no loss of protein or ATPase activity into solution, the turbidity decrease was interpreted as the result of a swelling of the axoneme structure, amounting to an increase of ~15% in its diameter [34,35], but the possible present-day significance of this turbidity change as indicative of an ATP-dependent state change in the strength of dynein arm attachment to the B-tubules of non-motile axonemes does not seem to have been followed up.

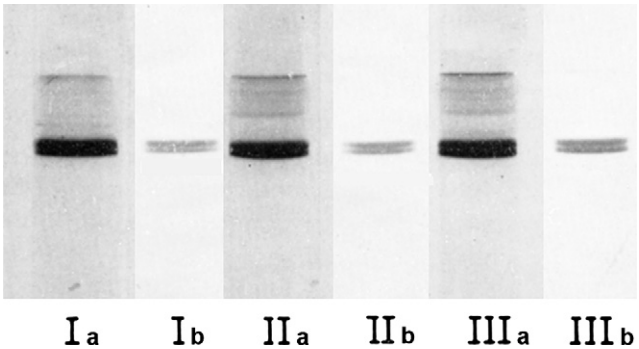

Figure 1.5 Reproductions of the original figure, legend, and table in the 1968 paper that first described the purification and principal physical properties of the protein forming the outer-doublet tubules in ciliary axonemes of *Tetrahymena* [36]. Disc electrophoresis in polyacrylamide gels made with 8 M urea. Samples of tubulin (outer fiber protein) purified by protocols 1, 2, and 3 were run simultaneously. All protein samples were reduced and alkylated prior to electrophoresis. a, printed darkly to show minor bands; b, printed lightly to show doubleness of principal band. Figure has been reformatted from original.

1.2.3 Co-Discovery of Tubulin

Two new postdoctoral researchers, Fernando Renaud from the University of Puerto Rico and Ray Stephens from Bob Kane's lab at Dartmouth, joined our group in 1966 and helped characterize the second major axonemal fraction, the protein forming the doublet microtubules. We were able to obtain monodisperse solutions of the native protein from *Tetrahymena* cilia by preparing an acetone powder of the demembranated axonemes and then extracting with a low ionic strength buffer — a protocol very similar to that then used to extract actin from skeletal muscle. When prepared in this way, the microtubule protein was a dimer of molecular mass 105 kD that migrated as a pair of closely spaced bands upon electrophoresis in 7 M urea and contained two moles of associated nucleotide (Fig. 1.5; Table 1.3; [36]). Thin-layer chromatography suggested the associated nucleotide was a mixture of GTP and GDP (Fig. 1.6A), rather than the ATP and ADP associated with actin. We confirmed this identity by hydrolysis of the nucleotides to the free base and chromatography against a known sample of guanine (Fig. 1.6B; [37]). Because this microtubule protein had some characteristics resembling skeletal actin, we refrained from taking the opportunity to name it, as did Dick Weisenberg and Gary Borisy in Ed Taylor's lab when they characterized it as the colchicine-binding protein from mammalian brain at about the same time [38]. But, a short while later, Hideo Mohri recognized correctly that it is a distinct protein and gave it the very appropriate name of "tubulin" [39]. Several years would elapse before it became possible to repolymerize tubulin dimers into microtubules and to show that microtubules are intrinsically

Table 1.3 Molecular Weight of Tubulin Dimer and its Subunits

Method	No. of Preparations	Molecular Weight*
Protein from procedure 1 in 1 mM Tris-HCl		
Sedimentation equilibrium	3	103,000 ± 14,000
Protein from procedures 1–3 in 5 M guanidine hydrochloride, 1% mercaptoethanol		
Archibald	6	55,200 ± 2,600
Sedimentation-equilibrium	3	49,300 ± 1,400
Sedimentation-diffusion	5	57,000 ± 5,400
Protein from procedure 1, reduced and alkylated in 5 M guanidine hydrochloride		
Archibald	1	58,800

**Partial specific volume was assumed to be 0.72.*

All protocols yielded purified tubulin (outer fiber protein). Protocol 1, involving extraction of an acetone powder of cilia with 1 mM tris-HCl, yielded monodisperse dimeric tubulin. Protocols 2 and 3 required use of guanidine bydrocbloride to disperse aggregates. See original paper for details.

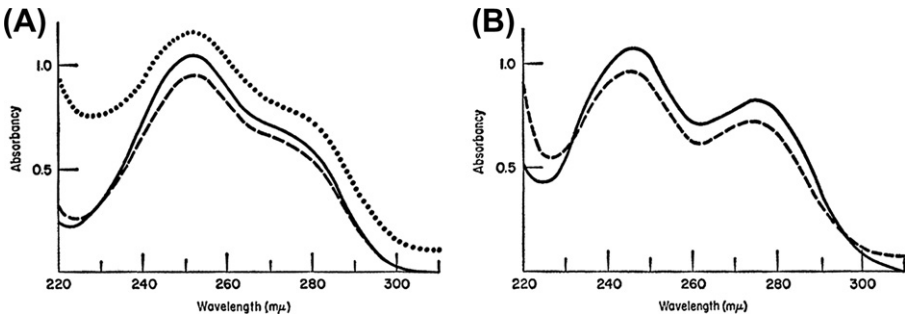

Figure 1.6 Reproductions of the original figures and legends in the 1967 paper that first characterized the nucleotide associated with the protein forming the outer-doublet tubules in ciliary and flagellar axonemes [37]. (A) Ultraviolet absorption spectrum of nucleotides from outer fibers (tubulin) of sea urchin flagella. The dotted line is the nucleotide soluble in 10% trichloracetic acid (TCA) after ether extraction. The dashed line is a chromatographed sample of the TCA-soluble nucleotide and corresponds in R_F value to GTP. The solid line is the spectrum of a known sample of GTP. The pH in all cases is 7 to 8. (B) Ultraviolet absorption spectrum of free base obtained by hydrolysis of the chromatographed sample described in (A). The dashed line is the hydrolyzed and neutralized sample. The solid line is the spectrum of a known sample of guanine. The hydrolyzed sample yielded approximately 3 mol of inorganic phosphate per mole of guanine. *Reproduced from [37] with permission.*

polarized structures, with their two ends distinguishable by polymerization occurring more rapidly at the distal ("plus") end than at the proximal ("minus") end [40, 41].

1.2.4 A Time for Decisions

With initial characterization of dynein and tubulin — the two major proteins responsible for axonemal motility — completed, I needed to make strategic decisions about the future directions of my research effort.

My first, and most important, decision was to continue working with the axoneme-based motility of cilia and sperm flagella, rather than to attempt to isolate dynein and tubulin from the cytoplasm. As with the early studies of myosin and actin from skeletal muscle, the advantages of starting with an easily isolated and highly structured microtubule system seemed likely to outweigh the disadvantage of it being specialized.

In order to correlate biochemical properties with motility, I needed an axonemal system that would permit me to quantify its motility parameters as well being appropriate for protein chemistry. Some preliminary experiments with reactivated cilia of *Tetrahymena* [17] had made me well aware of the difficulty of studying the motility of such short axonemes. The possibility of working with sea urchin sperm flagella was attractive, for they are about eight times as long as *Tetrahymena* cilia, and the classic paper of Sir James Gray [42] had shown that their planar beat pattern is easily recorded by cinematography. Moreover, these sperm flagella had yielded promising results when I tried to isolate their proteins during the summer of 1964, which we spent at Woods Hole [43].

So, when the opportunity came up to move to a marine lab in Hawaii, where sea urchins were abundant and sexually mature throughout the year, we were keen to move.

1.3 Research at the University of Hawaii

1.3.1 Moving to a New Lab in Honolulu

In the mid-1960s, the University of Hawaii had recruited Bob Kane to help design a new marine laboratory on an oceanfront site close to downtown Honolulu. When we moved to Hawaii in 1967, our research was accommodated in well-equipped laboratory space complete with a Beckman Spinco model E analytical ultracentrifuge and a new Philips electron microscope at the Waikiki Aquarium during construction of the new laboratory. The new Kewalo Marine Laboratory was completed in 1972 and had a spectacular oceanfront setting with the labs on one side looking out over a public park and the offices on the other looking over the surf line toward Diamond Head. Of course, our real reason for being on the waterfront was not the great views but the availability of freshly pumped sea water for maintaining the regular supply of sea urchins needed for our work.

1.3.2 Demembranated Axonemes Allow Direct Study of Motility

1.3.2.1 Uniform Preparations of Demembranated Flagellar Axonemes

1.3.2.1.1 Motility of Reactivated Sperm Flagella Closely Resembles that of Live Sperm

Shortly after the move to Hawaii, Barbara joined the project (Fig. 1.7) and set about developing methods for obtaining preparations of demembranated sea urchin sperm whose flagella would reactivate with uniform wave parameters close to those of live sperm. After attempts to use glycerol or digitonin gave poor results, Ray Stephens, who happened to be visiting the lab, made the brilliant suggestion that we try using the non-ionic detergent Triton X-100. This was far more satisfactory and yielded beautifully uniform preparations of completely demembranated sperm that were essentially 100% motile [44]. Under optimal conditions, the reactivated flagellar waveforms visually resembled those of the live sperm (Fig. 1.8), and measured values of average bend angle were essentially identical. As much as 72% of the axonemal ATP hydrolysis in the reactivated preparations was tightly coupled to the flagellar beating. These preparations of demembranated sperm axonemes formed the basis for most of our work on dynein and flagellar motility until the 1980s, when our enzyme kinetic studies of dynein ATPase showed that we could further improve the quality of reactivated

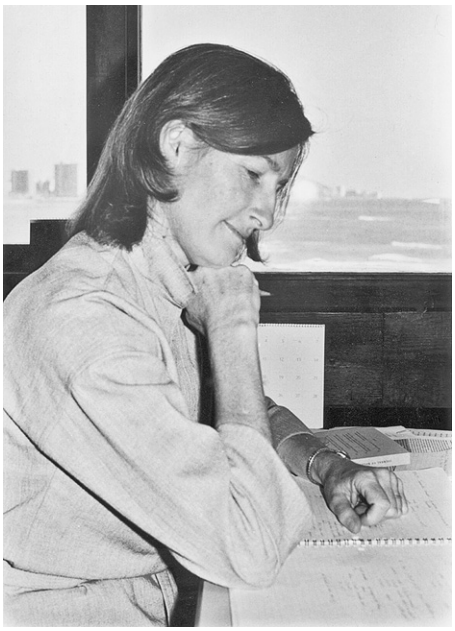

Figure 1.7
Barbara Gibbons. The photograph was taken at her desk in the Kewalo Marine Laboratory, University of Hawaii, in 1979.

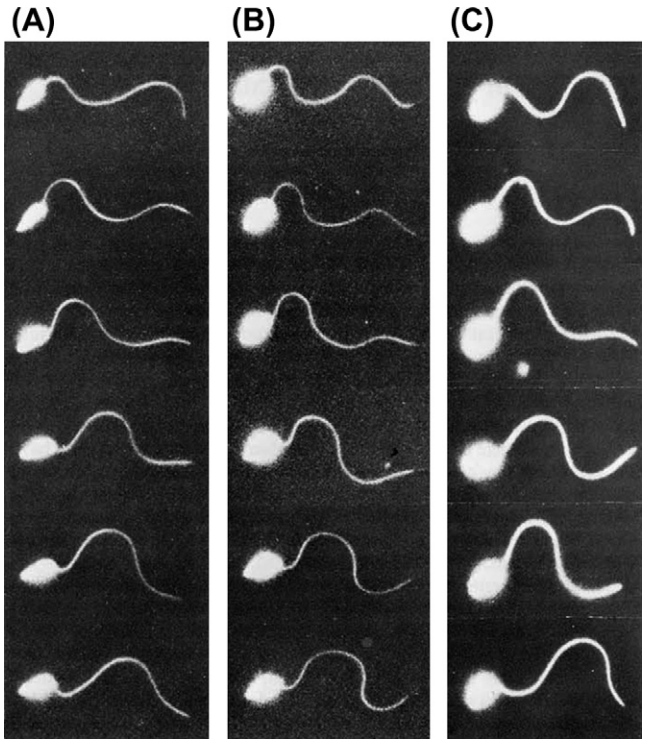

Figure 1.8 Flagellar waveforms of spermatozoa from sea urchin (*Colobocentrotus atratus*). (A) Dark-field light micrographs of a single live spermatozoon swimming in sea water. The individual images were selected to depict one beat cycle. (B) As in (A), except showing a Triton-demembranated spermatozoon in reactivation solution containing 1 mM ATP. (C) Spermatozoa with their flagella set into stationary rigor waves. Prepared by rapid dilution of reactivated sperm flagella to reduce the concentration of ATP below that needed for motility. Each micrograph shows a different sperm selected to depict one stage that occurs during a normal beat cycle. *Reproduced from [59,60].*

motility by substituting an organic anion for chloride in the reactivation medium (Section 1.3.2.1.3).

1.3.2.1.2 The Robustness of Flagellar Beating Indicates the Presence of a Well-Regulated Oscillatory System, with Independent Control Mechanisms Regulating the Flagellar Waveform and the Beat Frequency

A preliminary survey of the effects of different perturbing agents on the parameters of flagellar beating showed that the agents fall into three distinct categories. Those in the first group included ATP concentration, temperature, and changes in the number of dynein arms present. These agents all changed the rate of energy input to the flagellum, and they affect primarily the beat frequency with little effect on the waveform [45]. For example, the beat frequency of the

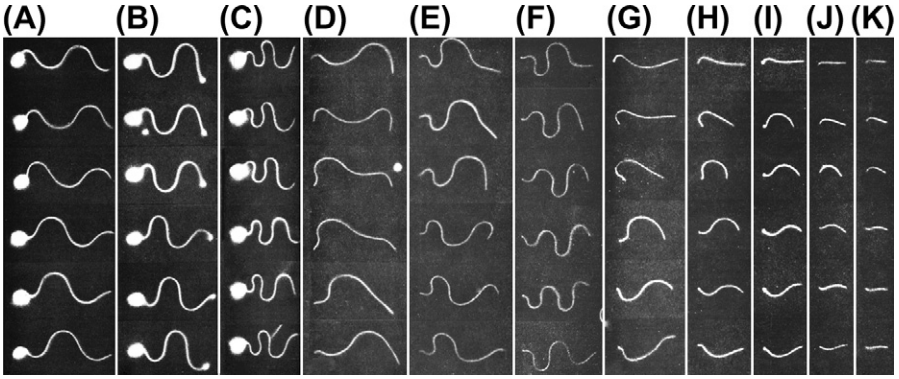

Figure 1.9 Effect of axonemal length and head attachment on flagellar waveforms of spermatozoa from sea urchin (*Tripneustes gratilla*). (A) Dark-field micrographs of a live sperm swimming in sea water at the undersurface of a cover glass. The micrographs, which were all of the same sperm, have been arranged to depict the form of the bending waves as they propagate. Flash exposures. (B) Same as (A), except that the sperm was attached to the coverglass by the tip of its head and pivoting slowly around its point of attachment. (C) Same as (B), except that the sperm head was attached more firmly to the cover glass and the sperm was not pivoting. (D) Dark-field micrographs of an intact axoneme isolated from sea urchin by gentle homogenizing. Other details as in (A). (E) Same as (D) except that the axoneme was attached to cover glass by its centriolar end and was pivoting slowly around its point of attachment. (F) Same as (E), except that the centriolar end was more firmly attached and the axoneme was not pivoting. (G) Movement of an axonemal fragment 28 μm long swimming freely at the underside of a cover glass. (H) Same as in (G), except fragment length was 21 μm. (I) Movement of axonemal fragment 16 μm long. Attached and pivoting slowly. (J) Movement of axonemal 12 μm long. Attached and not pivoting. (K) Movement of fragment 8.5 μm long. Attached and pivoting slowly. *Reproduced from [45] with permission.*

reactivated flagella could be reduced from 38 Hz to as low as 1.1 Hz by decreasing the concentration of ATP, with only a small accompanying change in flagellar waveform [44]. Similarly, selective extraction of the outer dynein arms caused a 50% decrease in beat frequency with little change in waveform [46]. On the other hand, agents in the second group, which included attachment of the sperm head (or the centriole of a headless flagellum) to the slide (Fig. 1.9A–F), flagellar length (Fig. 1.9G–K), and Ca^{2+} concentration[2], all had substantial effects on bend angles and on the asymmetry of the waveform, with only a small change in beat frequency. The third category was represented by the viscosity of the medium, which had only a relatively small effect upon both the beat frequency and the wavelength. In sea urchin sperm, for example, a two-fold increase in viscosity causes only about a 15% change in frequency and bend angle,

[2] *The action of Ca^{2+} in increasing the asymmetry of flagellar beating was discovered by Charles Brokaw [152] in work concurrent with our own, and is of particular importance because transient Ca^{2+}-dependent changes in waveform asymmetry result in changes in the direction of sperm swimming and so enable chemotaxis toward the egg [154].*

consistent with the level of available energy serving as a constraint under some conditions [47,48].

The existence of at least two sets of perturbing agents, one that primarily modifies the beat frequency and a second that primarily modifies the waveform, indicates that these parameters of the flagellar beating are regulated by distinct mechanisms within the axoneme, with little mutual interaction or dependence upon the external viscous resistance of the medium [45]. The implications of these data for the mechanisms regulating microtubule sliding will be considered in Section 1.3.7.2.

1.3.2.1.3 Organic Anions Stabilize the Reactivated Motility of Sperm Flagella and the Latency of Dynein ATPase

Although satisfactory for many purposes, the motility of the reactivated axonemes in these preparations was less than ideal in that their maximal beat frequency was only about ~35 Hz, as compared to 55 Hz in the flagella of live sperm at the same temperature. In the early 1980s, an important clue to further improving the quality of reactivation was discovered by my graduate student, John Evans, who found that chloride and other inorganic anions destabilized the product binding in the dynein.ADP.Pi complex and that this destabilization could be largely prevented by replacing chloride with an organic anion [49,50]. Sea urchin sperm axonemes reactivated in a medium with the chloride anions wholly replaced by acetate showed substantially improved motility parameters, including a 30% increase in maximal beat frequency, a five-fold decrease in the minimum concentration of MgATP required to support oscillatory beating, and a six- to fifteen-fold increase in sensitivity to inhibition by vanadate [51] (Section 1.3.3.5). We attributed these improved parameters to a tighter coupling of the free energy of ATP dephosphorylation to functional cross bridge cycling of the dynein arms, probably as a result of the organic anion helping to stabilize the high-energy dynein.ADP.Pi intermediate and thus to minimize the premature release of reaction products.

Although this change in the anionic component of the reactivation medium might seem minor, it made a qualitative difference in the work that we were doing at the time as we were unable to obtain any coordinated beating in the demembranated 9+0 flagella of eel sperm until we switched from using chloride to acetate as the major anion in the medium (Section 1.3.7.2.1).

1.3.2.2 ATP-Dependent Sliding of Doublet Tubules in Trypsin-Treated Flagella

In one of the earlier and most important sets of experiments, Keith Summers, my graduate student, and I were attempting to duplicate my observation of the ATP-dependent swelling response of *Tetrahymena* axonemes in an effort to study it further. When Keith was unable to reproduce this response in sea urchin

axonemes under the same conditions, he began looking at the effects of controlled pre-digestion by trypsin on the response to ATP. Unexpectedly, he found this induced a much larger decrease in turbidity upon the addition of ATP than I had earlier observed with the *Tetrahymena* axonemes. Preliminary electron microscopy of a digested preparation showed that the cylindrical structure of nine outer-doublet tubules remained largely intact in most axonemes (Fig. 1.10A) but that the structure had been modified in a way that made it highly sensitive to ATP. Addition of a low concentration of ATP to the digested preparation caused a rapid disintegration of the axonemes into individual doublet tubules and small groups (Fig. 1.10B). With my background in microscopy, it was natural to want to look at the axonemes to see what was actually happening to them during this transition. When viewed under our usual phase contrast light microscope, the trypsin-treated axonemes seemed to just fade and disappear upon exposure to ATP.

At this time, following the development of the "more powerful" electron microscope, use of light microscopy under dark-field conditions to observe objects smaller than the wavelength of light had fallen out of favor. However, as a beginning research student, I had once heard Andreanus Pijper describe the use of dark-field microscopy with the South African sun as a powerful light source to record individual bacterial flagella on film [52].

In our own lab at the time we did have dark-field condensers for our microscope, but our most powerful light source was the simple six-volt lamp built into the base. Not to be deterred, however, Barbara and I returned to the lab after dark one evening to test an idea. With Barbara watching over my shoulder, I was

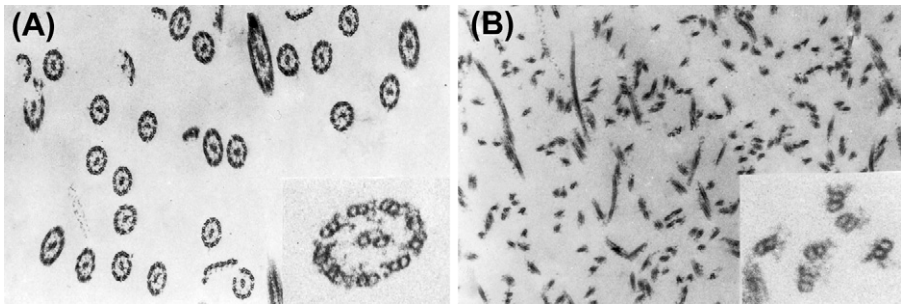

Figure 1.10 Electron micrographs of axonemes isolated from sea urchin sperm flagella and briefly digested with trypsin. (A) Part of a preparation was centrifuged into a pellet and fixed with osmium tetroxide without exposure to ATP. The cylindrical 9+2 organization of the axonemes remains largely intact. Dynein arms are still present, but the radial spokes are mostly disrupted. (B) A second part of the same preparation was exposed to 0.5 mM ATP for 3 min before centrifuging and fixing in the same manner as (A). Axonemes have almost completely disintegrated into single-doublet tubules and small groups. Inner and outer dynein arms are still present on most doublets, together with fragments of radial spokes in some cases. *Reproduced from [53] with permission.*

rewarded by being able to see for the first time the actual sliding apart of trypsin-treated axonemes into their component doublet microtubules in response to a front of ATP flowed in from the side. To a well-dark-adapted eye, the faint scattered light from individual microtubules was visible even with just that six-volt lamp. Our elation over the clarity and significance of this demonstration of ATP-dependent microtubule sliding certainly marked one of the major plus moments of life with dynein.

By using a very low concentration of ATP and 5–10 s time exposures, it was possible to take dark-field micrographs documenting the gradual disintegration of the axonemal fragments as the individual doublets telescoped out with each individual doublet sliding over its neighbor in the axoneme (Fig. 1.11). The lengths of the fully disintegrated structures ranged up to seven times that of the original fragment, demonstrating that most or all of the doublets were able to slide [53]. Subsequent upgrading of the microscope illumination made it possible to take 16 mm films showing that the speed of sliding between adjacent tubules was about 10 μm/sec, in agreement with the calculated maximal speed of sliding during normal flagellar beating [45,53]. Yet, although these quantitative details agreed with predictions for a sliding tubule model, it was really the visual impact of actually seeing the sliding happen in real time that was the most convincing. When shown an early version of this film at the Annual Meeting of the American Society for Cell Biology in 1971, the audience responded with a standing ovation, showing the same emotional enthusiasm as Barbara and I had experienced that first evening [54].

While I was working on the light microscopy, Keith had been using electron microscopy to study the rate at which trypsin disrupted the various structural components of the axoneme [55]. On the basis of his data, Keith and I proposed a mechanism for ATP-dependent motoring activity of the dynein arms in which the binding and hydrolysis of ATP causes a cyclic change in the angle of the arms, which coordinated with their repeated detachment and reattachment to successive sites along the B-tubule of the adjacent doublet, resulted in the arms permanently attached to the A-tubule of one doublet translocating this second doublet along the length of the first [53]. Simple geometry, based upon the tubules being inextensible, indicated that bends of the observed angle would require a sliding displacement of ~400 nm between the two sides of the axoneme, with at least 100 nm between adjacent doublets. This distance was considered greater than could be accommodated by the spokes and nexin links, unless they had an unusual ability to stretch or their links to the doublet tubules were broken and reformed.

More speculatively, we suggested [53] (1) that the dynein arms generate a force in only one direction between a given pair of tubules; (2) that the nexin links provide the major elastic resistance required to convert sliding into

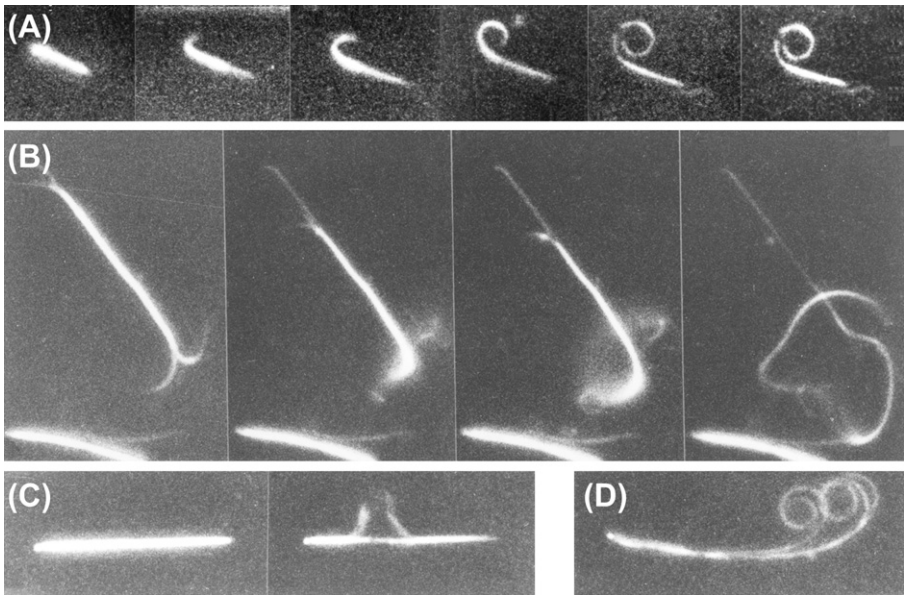

Figure 1.11 Dark-field light micrographs showing trypsin-treated axonemes from sea urchin sperm flagella undergoing sliding disintegration in the presence of MgATP. (A) Frames of a 16 mm cine film taken at two frames/sec. Frame 1 shows the initial position of a short axonemal fragment that has one side attached to the cover glass. Frames 2–4 show progressive extension of microtubule groups sliding over the stationary group toward the top left corner and then curving around. Frame 5 shows the final state after disintegration is complete. At this stage, an additional very thin twisted group (probably the central pair) is visible, having been extruded in the opposite direction toward the bottom right corner. Frame 6 shows superimposed images of two consecutive frames to enhance the visibility of structural detail. (B) Similar sliding disintegration of a longer axonemal fragment that slides toward the bottom right and then curls around out of the focal plane, returning into focus in the final frame. Successive micrographs in the series were taken at intervals of 10–30 s (C and D). In fragments originating from the proximal end of the flagellum, the centriole (visible as a white dot at the left-hand end in these images) blocks any sliding from occurring at that location; these fragments disintegrate either by looping out (C) or by splitting and curling from the distal end of the fragment (D). *Reproduced from [53] with permission.*

bending; (3) that the central tubules and sheath, together with the radial spokes that connect them to the outer doublets, are involved in the coordination process; and (4) that the 5–10 nm gap usually observed between arms and the adjacent B-tubule possibly also participates in regulation by preventing effective interaction of the arms with their corresponding sites on the B-tubule until the gap becomes closed by axonemal distortion resulting from curvature or shear elsewhere along the axoneme. As discussed in Section 1.3.7, some of these points have been confirmed by subsequent work and some remain controversial.

1.3.2.3 ATP-Dependent Sliding Between Adjacent Doublet Tubules Is Generated by the Enzymatic Dephosphorylation of ATP in the Dynein Arms

Afzelius' original suggestion that the arms are responsible for active sliding movements between the doublet tubules of flagellar axonemes was based solely upon their positioning between doublets [13]. Our work provided experimental support for his suggestion by showing that the nucleotide specificity and divalent cation requirement of the dynein ATPase located in the arms [33,56] closely match those required for reactivating movement in demembranated flagella [44] and for inducing sliding in trypsin-treated axonemes [53].

To obtain more direct evidence that the dynein arms are responsible for tubule sliding during the oscillatory beating of normal flagella, Barbara made use of a serendipitous observation that, when demembranated sperm are reactivated in a high-salt medium (0.5 M KCl), the flagellar beat frequency is initially normal but then decreases gradually over the next 2−3 min before stabilizing at a value of around half the initial value, all with no change in the flagellar waveform. Her results supported an active role of the dynein arms in beating flagella by showing that the outer dynein arms are selectively solubilized by the high-salt medium over a period of a few minutes and that the decrease in rate of sliding between tubules during this time is proportional to the fraction of outer dynein arms lost from the axoneme [46].

This interpretation was further strengthened a short while later, when Barbara showed that the diminished beat frequency of dynein-depleted sperm flagella could be largely restored by re-binding of purified outer-arm dynein, with the extent of beat frequency restoration being approximately proportional to the fraction of re-bound outer arms seen by electron microscopy [57,58].

1.3.2.4 Dynein Arms Make Fixed Cross Bridges in the Absence of MgATP

The properties of the postulated dynein cross bridges were studied by experiments in which a suspension of reactivated sperm axonemes beating in a medium containing a low concentration of MgATP was abruptly diluted to reduce the ATP concentration below the minimum required for motility [59]. This sudden depletion of MgATP causes the motile axonemes to set into stationary waves ("rigor waves") resembling those present at different phases of the normal beat cycle (Fig. 1.8C). Restoration of MgATP at a level too low for oscillatory beating causes the rigor waves to straighten gradually over 1−2 min; higher levels of MgATP result in immediate resumption of normal beating. Formation of the rigor waves is accompanied by increased axonemal stiffness, which supports the interpretation that the form of the rigor waves is maintained by the dynein arms that form fixed cross bridges between the double tubules in the absence of MgATP.

More detailed examination of localized flexural and torsional resistance by subjecting the rigor wave axonemes to fluid flow shows that all regions of the

axoneme, including both bends and interbends, are resistant to flexure, except under vigorous conditions sufficient to cause irreversible damage. On the other hand, torsional forces can twist the axoneme relatively easily without impairing subsequent reactivation with ATP [59].

1.3.2.5 High-Voltage Electron Microscopy of Axonemal Structure in Rigor Wave Flagella

In 1973–1974, I took a sabbatical leave to spend a year in France working at the Centre d'Etudes Nucléaires de Grenoble, where I was very kindly hosted in the laboratory of Pierre Vignais, who had an active group, including his wife, Paulette, working on mitochondria. While there, I used both normal and high-voltage electron microscopy to study the structure of axonemes that had been set into rigor waves by abrupt depletion of ATP. The results showed that the electron microscopic structure of the dynein arms in rigor wave axonemes depended upon the fixation conditions used to preserve the axonemes for microscopy. Fixation conditions that preserved the rigor waves showed the dynein arms tightly bridging the space between adjacent doublet tubules, whereas more usual fixation conditions that show a gap of ~5 nm between the end of the arm and the B-tubule of the adjacent doublet caused major distortion of the unfixed rigor waveform [60].

Barbara decided to take the year off from research and spent much time with a local chamber music group. Our two children, then aged 9 and 10, responded enthusiastically to the challenge of learning French by immersion at the local village primary school. They were especially delighted to discover that the whole school took off as a group to go skiing every Wednesday afternoon through the winter season.

1.3.2.6 ATP-Dependent Motility and Sliding of Filaments in Mammalian Sperm Flagella

After we returned to the Kewalo lab in 1974, we were joined by Charles Lindemann, who had previously studied theoretical models of bending wave propagation in bull sperm flagella and wanted to adapt our flagellar reactivation protocols for mammalian sperm. His work showed that, despite having an additional set of nine outer peripheral fibers that are much larger in size than the doublet tubules of a typical 9+2 axoneme, the motility mechanism of these sperm flagella appears to be very similar to that of sea urchin sperm flagella [61]. The patterns of ATP-induced disintegration after limited trypsin digestion were constrained by the mitochondrial and fibrous sheaths that surround the proximal region of the flagellum in mammalian sperm and by a tendency to extrude the pair of central tubules from the distal tip, but they otherwise resembled those of sea urchin sperm flagella. There was no indication of contractile or sliding activity associated with the peripheral fibers, suggesting that they principally serve as structural support for the 9+2 axoneme at their center.

1.3.2.7 Extension and Confirmation of the Sliding Microtubule Model

In 1977, Win Sale, then a graduate student in Satir's lab, made an important extension to the work of Summers and Gibbons by using critical-point drying to prepare clusters of partially disintegrated axonemes for examination by electron microscopy [62]. This procedure enabled him to convincingly demonstrate that the sliding produced by dynein arms is indeed unidirectional, and to show that the ATP-dependent cycling of dynein arms permanently attached on the A-tubule of one doublet (N) microtubule always results in translocation of the adjacent doublet (N+1) toward the minus end of the doublet to which the arms are attached. To explain how a unidirectional action of dynein arms distributed around the cylindrical axoneme could generate the oppositely directed effective and recovery strokes of the ciliary beat cycle, Sale and Satir reasoned that during the effective stroke the dynein on the doublets of one side of the axoneme must produce force while the dyneins on doublets of the other side are inactive and permit passive sliding; then during the recovery stroke of the beat cycle the active and passive sides would be reversed. This model was later extended to account for the oscillatory bending waves of sperm flagella [63] and further elaborated into a more detailed "switch-point" mechanism by Satir and Matsuoka [64], largely on the basis of the axonemal splitting observed when Mg.ATP is added to trypsin-weakened axonemes in which the proximal ends of doublet tubules continue to be held together by the trypsin-resistant basal body. Although it has proved difficult to identify the mechanism responsible for "switching" the activity from one side to the other, this model remains the most generally accepted one at the present time (Section 1.3.7).

An elegantly direct confirmation for the overall validity of the sliding microtubule model in sperm axonemes was provided in 1989 by Charles Brokaw, who attached small gold particles along the length of the doublet tubules and used them as position markers visible by light microscopy [65–67]. By automating the measurement of changes in relative position of multiple markers randomly attached to different doublets, he was able to quantify the relative sliding displacements between doublets over the course of a flagellar beat cycle and to show that observed displacements largely agreed with values predicted on the basis of the observed waveform and inextensible doublet tubules.

1.3.3 Protein Chemistry Reveals the Complexity of Dyneins

1.3.3.1 Revolution in Cell Biology: the Development of Denaturing Gel Electrophoresis

The development of electrophoresis in polyacrylamide gels containing Na dodecyl SO_4 [68–69] had a revolutionary impact on the whole field of cell biology. By enabling analysis of the number and size of distinct polypeptides in cell extracts at different stages of purification, it opened whole new areas of cell

biological research to the powerful techniques of protein chemistry. As the other side of the same coin, it also began to reveal the manifold levels of complexity in intracellular organization that have accrued over the course of biological evolution.

In our own studies of cilia and flagella, we could now use gel electrophoresis to assay the purity of our dynein preparations, rather than having to rely simply on the shape of an analytical centrifuge peak. This made it possible to begin characterizing the polypeptide subunits composing the outer and inner arms of flagellar axonemes.

1.3.3.2 Multiple Isoforms of Dynein

Richard Linck in Ray Stephens' lab at the Marine Biological Laboratory in Woods Hole was the first to apply Na.dodecyl.SO_4 gel electrophoresis to axonemal dynein (in 1970–1973) and he made the important discovery that the presence of dynein ATPase activity in axonemal extracts was correlated with a pair of electrophoretic bands that migrated considerably more slowly than the highest molecular marker proteins that were then available. By using crosslinked standard proteins as markers, he determined apparent molecular masses of 450–500 kD for the heavy chains (HCs) of axonemal dyneins in scallops [70,71]. Similar examination of cilia and flagella of other species soon indicated that possession of at least one HC polypeptide subunit of molecular mass 300–500 kD is a characteristic feature of all axonemal dyneins [72–74], with most of the uncertainty in mass being due to the difficulty of extrapolating from standard proteins of much lower mass. In 1974, the cytoplasmic isoform of dynein was first identified in brain extracts by Roy Burns and Tom Pollard, as a high molecular mass band that co-electrophoresed with the HCs of axonemal dynein [75].

Over the next few years, further improvements in electrophoretic technique resolved additional high-molecular-mass bands in the dynein HC region. In 1976, Kazuo Ogawa in my lab used gel electrophoresis and hydroxyapatite chromatography to purify a second dynein isoform from sea urchin sperm flagella [76]. Three years later, Chris Bell and Earl Fronk in my lab [77] resolved eight putative dynein HC bands in gels of sea urchin axonemes, while Gianni Piperno and David Luck partially purified as many as 10 HC subunits by chromatography of extracts of *Chlamydomonas* axonemes [78]. Use of two-dimensional electrophoresis to identify the full complement of lower-molecular-mass polypeptides in the whole axoneme of *Chlamydomonas* revealed at least 200 different polypeptides.

Awareness of these levels of complexity made protein work a whole new ball game. Clearly the usefulness of classical protein fractionation would be limited to favorable instances. An organism accessible to genetic manipulation would be essential for a complete study of the axonemal dyneins. The green alga *Chlamymonas reinhardtii* has served this purpose very well over the past 30 years. The many important studies of axonemal dyneins utilizing the genetics of

Chlamydomonas have been recently summarized in an excellent review by Steve King and Ritsu Kamiya [79].

1.3.3.3 The Subunit Composition of Outer-Arm Dynein Differs Between Sea Urchins and Chlamydomonas

Although such a genetic approach was not feasible with sea urchins, we were able to use selective extraction with 0.5 M NaCl, followed by density gradient centrifugation, to isolate the outer-arm dynein as a monodisperse preparation that sedimented at 21 S and had a native molecular mass of 1250 kD. Most importantly, these preparations had the functional capability to restore the flagellar beat frequency of dynein-depleted sperm axonemes [57,80]. Electrophoresis in denaturing gels showed that the particles of outer-arm dynein comprised two distinct HCs (β and γ[3]); three intermediate chains (ICs) of 128 kD, 68 kD, and 46 kD; and several light chains (LCs) of 10–15 kD.

Concurrent with our studies on this 21 S outer-arm dynein from sea urchin sperm flagella, other groups had obtained seemingly conflicting results on the outer-arm dyneins from *Tetrahymena* cilia and *Chlamydomonas* flagella. Fortunately, Baccio Baccetti took the opportunity of Barbara and me spending a sabbatical year in his laboratory at the University of Siena, Italy to organize an international meeting on development and function in cilia and sperm flagella at Siena in July 1982, with most major dynein groups well represented. At this meeting, the confusion over outer-arm dyneins was resolved by substantially improved electron microscopic images of soluble dynein by Johnson and Wall [31,81], who used dark-field scanning transmission electron microscopy of freeze-dried samples of soluble outer-arm dynein from *Tetrahymena* that were more purified than those that my lab had used 18 years earlier. These micrographs showed for the first time that the outer-arm dynein particle of *Tetrahymena* has a total mass of ~2000 kD and a substructure consisting of three globular heads of mass ~420 kD, each connected by a flexible tail to an extended base. This analysis of mass distribution confirmed and extended the earlier observation of Masami Takahashi and Yuji Tonomura [35] showing that the extended base of the outer-arm dynein forms a fixed structural attachment to the A-tubule of each doublet, while the ATP-dependent motility function is associated with the three globular heads that undergo cyclic detachment and reattachment to the B-tubule of the adjacent doublet concomitant with the binding and hydrolysis of ATP [81–83].

[3] *The non-β HC in outer-arm dynein of sea urchin sperm flagella was originally named the α HC. However, the recent availability of complete amino acid sequences for all the dynein HCs in sea urchins and other animals [198] shows that the non-β HC in this outer-arm dynein is actually orthologous to the γ HC of outer-arm dynein in* Tetrahymena *and* Chlamydomonas*, and that the sea urchin genome contains no ortholog of the α HC in the outer-arm dynein of* Tetrahymena *and* Chlamydomonas*. Accordingly, the former α-HC of outer-arm dynein in sea urchin and other animals is renamed to γ HC in this paper.*

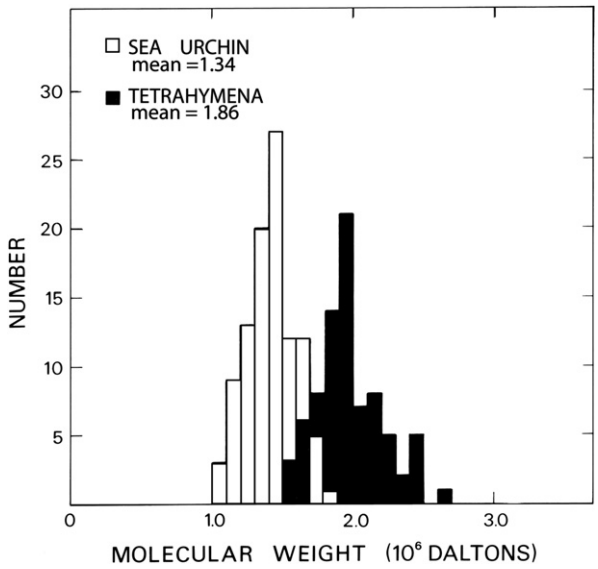

Figure 1.12
Molecular mass of outer-arm dynein. Histogram shows measured mass of individual molecules of outer-arm dynein from sea urchin (*Tripneustes gratilla*) sperm flagella and from cilia of *Tetrahymena* cilia, as determined by scanning transmission electron microscopy. Previously unpublished work by K. A. Johnson, I. R. Gibbons, and J. S. Wall (1981).

By the end of the Siena meeting, all dynein groups agreed that the outer-arm dynein of *Chlamydomonas* is three-headed, like that of *Tetrahymena*, except for splitting into two subparticles, (α, β) and γ, when solubilized [84]. At the same time, the outer-arm dynein of sea urchin sperm flagella was shown to differ fundamentally from those of *Tetrahymena* and *Chlamydomonas* in that it is a two-headed particle of mass ~1300 kD (Fig. 1.12) that contains only two HC subunits [80,85].

Much more recently, the evolutionary studies made possible by the availability of genomic sequence data revealed that the two HCs of sea urchin outer-arm dynein correspond to the β and γ HCs of outer-arm dynein in *Chlamydomonas*. This major structural difference between the outer-arm dynein of sea urchins and of *Chlamydomonas* possibly originated from the divergence of animals and plants that occurred at an early stage in the evolution of present eukaryotic organisms (see Section 1.4.2.3).

1.3.3.4 Discovery of Dynein's Microtubule-Binding Domain

Ursula Goodenough and John Heuser obtained generally similar results for the electron microscope structure of the solubilized outer-arm dynein from *Chlamydomonas* and *Tetrahymena*, but they also managed to identify an additional slender stalk ~15 nm long, with a tiny globular domain at its tip, that protruded from the globular head of each dynein HC [86]. When the outer and inner arms were bound on the intact axoneme, the large number of closely packed structures made their detailed arrangement hard to discern in these early studies [87].

Although the protruding 15 nm stalks were often seen making contact with the B-tubule of the adjacent doublet [88,89], their unconventional shape prevented them being generally accepted as the critically important ATP-dependent microtubule-binding domain (MTBD) of dynein until 15 years later, when Melissa Gee in Richard Vallee's lab made their function indisputably visible by expressing recombinant fragments of the HC containing the stalk domain and re-binding them to microtubules [90].

The substantial distance between the globular MTBD at the tip of its 15 nm stalk and the core of the motor raised the intriguing question of how transitions in the nucleotide-hydrolysis cycle occurring in the core of the motor are communicated to modulate the affinity of the binding domain for its sites on a microtubule; and conversely of how detachment and reattachment events at the MTBD are communicated back to the core of the motor so as to modulate the rate constants of the nucleotide-hydrolysis cycle. A possible mechanism for this bidirectional flow of information through the stalk forms the subject of our most recent work (Section 1.4.4).

1.3.3.5 Vanadate Inhibits the Cross Bridge Cycling of Dynein ATPase

Toward the end of 1977, when Lewis Cantley and Lee Josephson identified the vanadate anion VO_4^{2-} (V_i) as the Na/K-ATPase inhibitor that contaminated some commercial preparations of ATP [91], it was immediately apparent that the same anion could also well be the unidentified inhibitor of dynein ATPase that I had encountered earlier [33]. A couple of trial experiments confirmed this to be the case by showing that micromolar concentrations of V_i inhibited the ATPase activity of dynein by ~90% and completely blocked motility of reactivated sperm flagella. Although we knew that Marty Flavin's group at NIH was also interested in the previously unidentified inhibitor of dynein, a meeting of our lab group decided that it would be a fun experience to set up a short-term intensive project on V_i and dynein in a way that would give everybody in the group an active role at the wet bench biochemical work. This worked out very well as a morale booster for those whose work had been progressing slowly. Everybody was enthusiastic and, six weeks later, a paper with eight authors, Ian Gibbons, Marie Paule Cosson, John Evans, Barbara Gibbons, Becky Houck, Karl Martinson, Win Sale, and Wen-Jing Tang, was submitted [92]. Happily, Marty Flavin was apprised of what was afoot and a paper with similar results by his group was submitted and published at essentially the same time as ours [93].

After the submission of our group paper, Win Sale continued working along similar lines and showed that, although vanadate inhibits the MgATP-induced disruption of trypsin-treated axonemes, it does not inhibit the relaxation of rigor wave sperm flagella by MgATP. He deduced that V_i inhibits the ATP-driven cross bridge cycle of dynein at a step subsequent to the MgATP-induced release of the bridged dynein arm [94]. On the basis of this result, together with Barbara

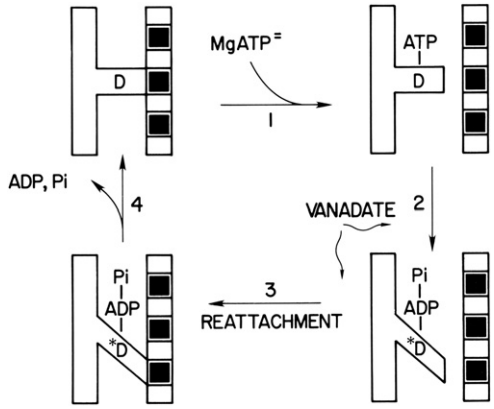

Figure 1.13 Model for dynein cross-bridge cycle, based upon that proposed for actomyosin by Richard Lymn and Edwin Taylor [95]. The kinetic steps in the dephosphorylation reaction of $MgATP^{2-}$ by dynein are associated with putative structural changes linked to the detachment/reattachment cycle of a dynein cross-bridge. In step I of the cycle, binding of $MgATP^{2-}$ to the dynein (D) initiates detachment of the cross-bridge. Step 2 is a conformational change in the dynein (*D) arm that is associated with hydrolysis of ATP. Step 3 is the reattachment of the dynein arm to the next site along the B-tubule of the adjacent doublet. Step 4 is the release of the reaction products, ADP and Pi, linked with the powerstroke of the dynein arm. Our data supporting this model were that (1) dynein forms fixed cross-bridges between doublet tubules in the absence of ATP [59]; (2) association of dynein with microtubules results in a six-fold activation of dynein ATPase [80]; and (3) vanadate inhibits dynein ATPase but does not inhibit the ATP-induced relaxation of the bend in rigor wave flagella. We concluded that dynein inhibits dynein ATPase at either step 2 or 3 of the model. *Reproduced from [94] with permission.*

Gibbons' earlier demonstration of fixed-rigor cross bridges in the absence of MgATP [59], and the six-fold activation of ATPase rate upon binding of soluble outer-arm dynein to extracted axonemes [80], we proposed a model for the ATP-dependent cycling of dynein cross bridges (Fig. 1.13), analogous to the model that had been proposed for myosin cross bridges in muscle by Richard Lymn and Ed Taylor several years earlier [95]. John Evans in our lab subsequently obtained additional evidence supporting the cross bridge model when he demonstrated an initial burst of P_i formation amounting to $\sim$1.8 mol P_i per mol of soluble outer-arm dynein [49,96].

Concurrently with Sale's work in our lab, Masami Takahashi in Yuji Tonomura's lab at Osaka University obtained qualitative evidence relating the kinetic steps of dynein ATPase to the cycling of its cross bridges. Also during this same period, Mary Porter and Takashi Shimizu in Ken Johnson's lab performed more detailed kinetic analyses of ATP hydrolysis by *Tetrahymena* outer-arm dynein, including the kinetics of vanadate inhibition [97,98]. Their results included rate constants for the individual reaction steps and fit well into the Lymn–Taylor cross bridge model. Vanadate inhibition was attributed to formation of a dead-end

dynein.ADP.V_i complex, with vanadate putatively replacing phosphate (P_i) at the γ-P_i position in the ATP-binding site.

1.3.3.6 Vanadate-Sensitized Photocleavage

In 1986, Alice Lee-Eiford, in my lab, was using the photo-affinity probe 8-azido-ATP to identify the ATP-binding sites in the HCs of outer-arm dynein. Finding it difficult to get sufficient probe incorporation for a reliable signal, she added vanadate to the UV-irradiated mixture of dynein and 8-azido ATP in an attempt to increase the efficiency of incorporation. This increased incorporation failed to occur, but instead she was surprised to observe that the UV irradiation in the presence of 8-azido ATP and vanadate appeared to cause a cleavage at a unique site (termed V1) in the mid-region of the β and γ HCs, forming two discrete polypeptide fragments of ~230 and 200 kD [99]. After we replaced 8-azido ATP with unmodified ATP and changed the UV irradiation from 254 nm to 365 nm to minimize side reactions, the photolytic reaction occurred with almost surgical specificity (Fig. 1.14). This high specificity made vanadate-sensitized photocleavage an obviously useful tool for studying dynein, and everyone in our lab at the time participated in further exploring its properties [100]. The results showed that the presence of micromolar vanadate and either ATP or ADP was required for photolysis to occur. The recovery of the two photocleaved peptides was ~95%

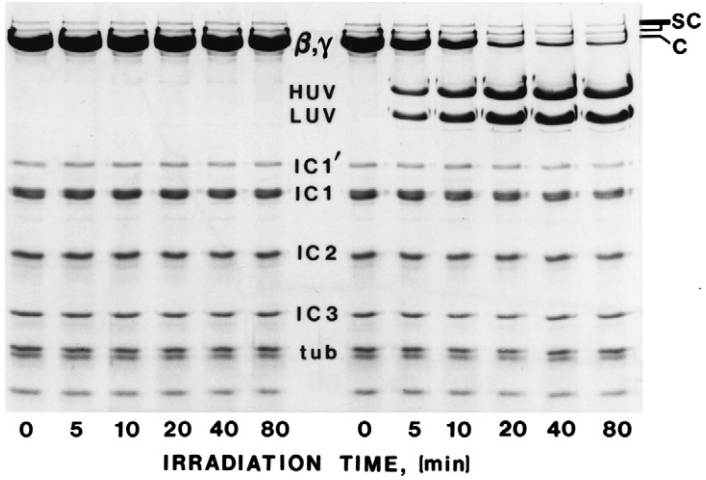

Figure 1.14 Specificity of vanadate-mediated photolysis of dynein HCs. Electrophoresis gels showing highly specific photolytic cleavage at the V1 site of the β and γ HCs of outer-arm dynein upon 365 nm irradiation for times indicated. The six right lanes show irradiation in the presence of 50 μM ATP and 10 μM vanadate. The six left lanes show irradiation in the presence of 50 μM adenosine and 10 μM vanadate as a control. β,γ: intact β and γ HCs (unresolved in this gel); HUV, LUV: products of cleavage at the V1 site; IC1′, IC1, IC2, IC3: dynein ICs as indicated; tub: tubulin; sc: sky chains. *Reproduced from [99] with permission.*

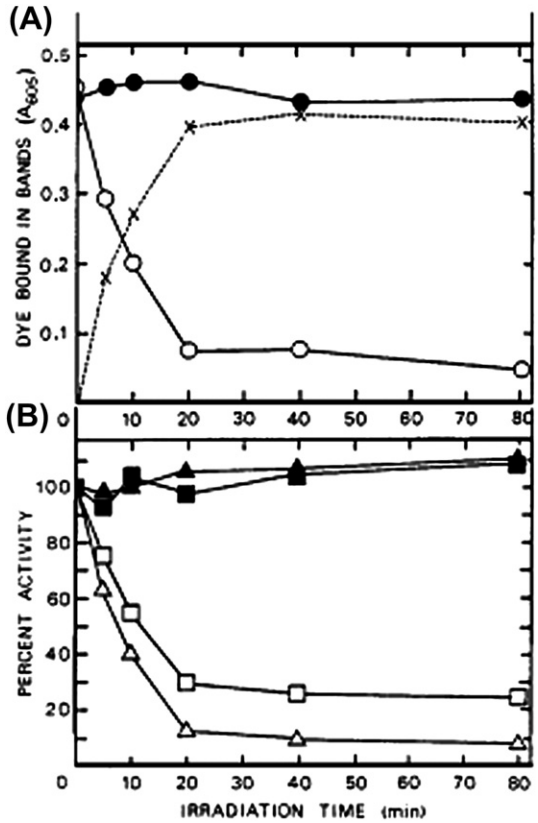

Figure 1.15 Vanadate-mediated cleavage of dynein HCs results in loss of ATPase activity. (A) Absorbance of dye extracted from excised bands of the gel shown in Figure 1.14. ○: β,γ bands of samples after irradiation in ATP and vanadate; ●: β,γ-bands of samples irradiated in adenosine and vanadate; ×: pooled HUV and LUV bands of samples irradiated in ATP and vanadate. (B) ATPase activity of the same irradiated samples as used for electrophoresis in Figure 1.14. △: samples irradiated in ATP and vanadate; ▲: samples irradiated in adenosine and vanadate. See original paper for details.
Reproduced from [100] with permission.

(Fig. 1.15A). Importantly, the cleavage of the dynein HC at this V1 site was accompanied by a parallel loss of its ATPase activity (Fig. 1.15B). On the basis of these and other supporting data, we suggested that photolysis at the V1 site is probably a local reaction resulting from photoexcitation of a vanadate anion bound to dynein at the hydrolytic ATP-binding site on each dynein HC, most likely in the dynein.MgADP.V_i complex that acts as a dead-end inhibitor of the dynein ATPase cycle.

At somewhat higher vanadate concentrations and in the absence of ATP, we were able to obtain photocleavage at a second site (V2), located ~100 kD from the V1

site on the dynein HCs [101,102], while yet a third site (located ~20 kD from the V1 site) undergoes photocleavage in the presence of Fe(III) and ATP [103]. At all these photocleavage sites, nucleotide appears to be involved in stabilizing the correct protein conformation for the reaction, with presence of ATP or ADP being required for cleavage at the V1 and Fe(III) sites but inhibiting cleavage at the V2 site [104].

A similar pattern of photocleavage sites is present in all the isoenzymic forms of dynein HC present in sea urchin flagella, as well as in dyneins from *Chlamydomonas* and *Tetrahymena* [105–110], indicating that most amino acid residues involved in the lytic pathways are well conserved and located in functionally important regions of the dynein.

At the time of their discovery, the photocleavage sites provided an important set of markers that facilitated mapping functional sites on the dynein HC polypeptides (Section 1.3.3.8). However, although these loci were considered putative phosphate-binding sites [102], nobody seems to have considered the possibility of multiple nucleotide-binding sites on an individual dynein HC before the coding sequence of the β-HC gene was determined in 1991 (Section 1.3.4.2).

1.3.3.7 Properties of the Isolated β Heavy Chain from Sea Urchin Sperm Flagella

With the sea urchin outer-arm dynein established as a two-headed heterodimeric particle, an obvious next step was to separate its component β and γ HC subunits for individual study. In our lab, a group including Grace Tang and Chris Bell separated the β and γ HC subunits by overnight dialysis against a low-salt buffer followed by zonal centrifugation [111]. Although both of the separated HCs possessed ATPase activity, our subsequent biochemical characterization of dynein HCs focused largely on the separated β HC because this formed a homogeneous preparation that sedimented (together with IC1) as a single peak of ~14 S, whereas the aggregating tendency of the γ HC made it more difficult to handle. This study showed that isolated β/IC1 subparticles retained capability for ATP-sensitive binding to dynein-depleted axonemes, but, rather than restoring the reactivated beat frequency in the manner of complete outer arm dynein, the β/IC1 became completely detached and passed into solution upon addition of ATP. We interpreted this result to indicate that the globular head of the separated β/IC1 subparticle retains its ATP-dependent motor function, whereas the tail domain of β/IC1 is unable to form a normal permanent attachment on the A-tubules, probably because this attachment also requires the additional presence of the tail of the γ-HC and of ICs 2 and 3. This interpretation was supported by Chris Bell, who used limited trypsin digestion to show that the fixed attachment of the complete outer arm dynein to the A-tubule is substantially weakened by an early tryptic nick in the tail region of the γ-HC [112]. The conclusion that isolated β/IC1 subparticles can function as ATP-dependent motors was confirmed by Sale, who, after establishing his own lab at Emory University, demonstrated that the

β/IC1 subparticles are capable of ATP-dependent translocation of microtubules in an *in vitro* assay [113].

1.3.3.8 Tryptic Digestion and a Linear Map of the β Heavy Chain

In the spring of 1985, we were joined by Gabor Mocz, who had earlier studied the tryptic digestion of myosin at Eötvös University in Budapest and was keen to map the functional domains of the dynein HCs by exploiting a broader range of digestion conditions than we had attempted previously. Working with an undergraduate honors student, Randy Ow, Gabor studied the proteolytic digestion pathways of the separated β and γ HCs in a low-salt medium [114–115]. Under these conditions, trypsin digestion attacks localized regions of the β HC relatively rapidly and selectively so that a simple pattern of cleavage at two major sites (T1 and T2) leads to formation of two subparticles (fragments A and B) that are separable by density-gradient centrifugation. The ATPase activity of the β-HC is associated with fragment A, which corresponds to the globular head of the complete chain, whereas fragment B corresponds to the flexible tail domain. A particle similar to our fragment A had been purified previously from digests of complete outer-arm dynein by Kazuo Ogawa [116].

With the help of a panel of monoclonal antibodies to the β HC of sea urchin dynein [117] kindly given us by Gianni Piperno of the Rockefeller University (New York), we were able to assemble the information provided by the various photolytic and proteolytic cleavage products and, thus, construct a linear map of the complete β HC identifying the approximate positions of all the cleavage sites (Fig. 1.16; [102]). The polarity of the map was determined by assay of the putative acetylated N-termini of intact and photocleaved HC.

Similar maps of the HCs in outer-arm dyneins of *Chlamydomonas* and of trout were obtained at about the same time by a group in George Witman's lab at the Worcester Foundation that included Steve King, Curtis Wilkerson, and Tony Moss [118,119].

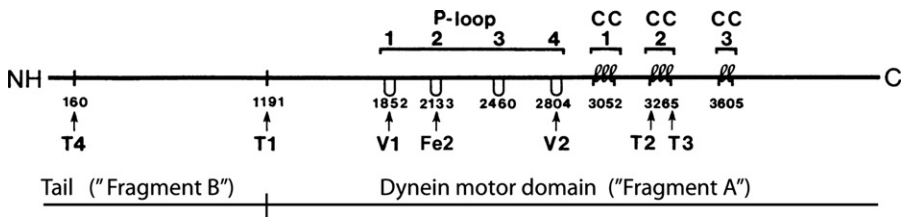

Figure 1.16 Map of photolytic and proteolytic cleavage sites on the β HC of outer-arm dynein from sea urchin. Cleavage sites shown were known prior to determination of the cDNA sequence of the gene in 1991 [125,126]. Short N-terminal amino acid sequences at the T1, T2, T3, and T4 tryptic sites were available at the time to validate the full-length sequence obtained. Also shown are the four ATP-binding sites indicated by Walker A (P-loop) sequence motifs and three regions of putative coiled-coil secondary structure, all revealed by the newly available amino acid sequence data. *Modified from [102,225].*

The development of these linear maps marked an important first step toward cloning and sequencing the genes encoding the HCs of axonemal dyneins in sea urchins (Section 1.3.4.2).

In the mid to late 1980s there were rapid advances in the knowledge of cytoplasmic dynein, due largely to the adaptation of Sheetz and Spudich's original *in vitro* assay for myosin [120] to microtubule-based motors. Rich Vallee's lab showed that a rat brain protein, earlier known as MAP1C, had the properties of a cytoplasmic dynein, including vanadate photocleavage [108]. Dick McIntosh's lab [109,121] characterized cytoplasmic dyneins from *Dictyostelium* and *Caenorhabditis.* These cytoplasmic dyneins, and the inner-arm dyneins studied in Win Sale's lab [113,122], all translocated microtubules in a minus direction when assayed *in vitro*. The availability of this *in vitro* motility assay also enabled discovery of the kinesin family of motor proteins, most members of which transport cargo along microtubules in a plus-direction, the opposite direction to that of dynein [123].

1.3.4 Transition from Protein Chemistry to Molecular Biology

1.3.4.1 Getting Set Up

By 1989, the genes for the other motor proteins, kinesin and myosin, had already been identified and cloned for several years, but there was still no sequence for any dynein gene in the database. With the map that we had derived for the β HC of sea urchin dynein, this axonemal dynein was the natural choice for us to use when we decided to get involved in molecular biology. With its predicted coding length of 13–15 kb, the dynein HC gene would probably be the longest gene sequenced at the time, but I felt confident that minimal retraining of our existing group of talented experimenters would enable them to handle the task efficiently. Greg Dolecki, an experienced molecular biologist in Tom Humphreys' group just down the hall from us, was looking for a new position at the time and agreed to join our group for a year to assist with the transition. Also, Dave Asai from Purdue University was keen to participate in the project and spent a sabbatical year with us as part of the team.

1.3.4.2 Sequencing the cDNA Encoding the β Heavy Chain of Outer Arm Dynein

After discussion with Humphreys, it seemed that the unusually large size of the HC gene and the lack of a decent protein expression system in sea urchins it would make it best for us to concentrate on determining the cDNA sequence and to leave the question of cloning for gene expression until later. In the absence of any previous dynein sequence, we had first to identify the gene by screening an expression library with a polyclonal antibody to the β-HC. To have the best chance of complete gene coverage, we decided to generate

a random-primed cDNA library from polyA(+) RNA of reciliating sea urchin embryos, followed by a polymerase chain reaction (PCR) procedure to take rapid successive walk steps through the library. The most fraught part of the process proved to be the antibody screening, where we found a number of antibody-positive clones that hybridized to a large mRNA on a Northern blot but proved to correspond to other known proteins upon sequencing. After about 12 months, we fortunately found a clone validated by Northern blotting that happened to overlap one of our N-terminal tryptic peptide sequences. From this point, we used a novel "leapfrog PCR" procedure to extend our sequence quickly along the gene and it took only three months to complete the 17 walk steps needed to obtain the full-length coding sequence of the β-HC gene [124].

As part of this team effort, Barbara Gibbons prepared the polyA(+) RNA for library generation, performed Northern blots, and organized everyone's scheduling; Gabor Mocz purified β-HC for antibody generation and tryptic peptides for N-terminal sequencing, as well as helping to interpret the final sequence; Nathan Ching, Wen-Jing Tang, and Hening Ren ran manual sequence gels and extension PCR reactions; Cheryl Phillipson synthesized oligonucleotide primers and read raw sequences into computer files; and I assembled raw sequences and designed oligonucleotides for extension PCR.

During the progress of this sequencing, Kazuo Ogawa, who had earlier been a postdoctoral student in my lab and had since returned to Japan, emailed me that he was engaged in sequencing the same dynein β-HC as us but from a different species of sea urchin. Fortunately, the two projects were on almost the same schedule and so we were able to agree on simultaneous publication [125,126]. When Kazuo and I exchanged derived amino-acid sequences for double-checking of discrepancies right before publication, we were delighted to find that we each needed to fix up only three or four out of the 4466 residues in the β chain.

Casual examination of the sequence indicated one striking feature to repay us for our efforts. This was the presence of four copies of the "P-loop" or Walker A motif for an ATP-binding site [127], located approximately 320 residues apart in the middle region of the HC. We identified these as P1, P2, P3, and P4, in order from the N-terminal end of the HC. The position of the P1 loop close to the V1 photocleavage site on the HC suggested that the P1 loop forms part of the principal hydrolytic ATP-binding site in the HC. The function of the other P-loops was less clear, but we suggested that they might function as sites of regulatory nucleotide binding, which would be consistent with their proximity to the V2 and Fe(III) sites of secondary photocleavage (Fig. 1.16).

Analysis of the amino-acid sequence of the β-HC for predicted secondary structure indicated the presence of an α/β-type structure over most of its length.

The only indication of a coiled-coil-type structure was in a region just downstream of the P4 nucleotide-binding motif that contained two long stretches of unbroken heptad hydrophobic repeat. We suggested that these stretches of heptad repeat might constitute a leucine-zipper-type structure and correspond to the short projection seen on the globular head of dynein HCs by electron microscopy [86].

The overall amino acid sequence of the β-HC confirmed that dynein represents a distinct class of motor protein with no homology to the other motor protein families, kinesin and myosin. We noted that the nearest neighbor to dynein in the protein database (PDB) at that time was ClpA, an ATP-dependent protease in *Escherichia coli*, but because of the very different function and size of the latter protein we did not take its relationship to dynein as seriously as we might have. It was not until eight years later that a more thorough sequence analysis by Andrew Neuwald and coworkers identified dynein's evolutionary origin, together with that of ClpA, within the large superfamily of AAA^+ ATPases [128,129] (see Section 1.4.1).

1.3.4.3 Experimental Assay of Nucleotide-Binding to β and γ Heavy Chain Subunits of Outer-Arm Dynein

Given that the amino acid sequence of the β-HC possesses four predicted nucleotide-binding sites, Gabor Mocz in our lab collaborated with Michael Helms and David Jameson in the Biochemistry department on campus to use two independent procedures to experimentally determine the number and affinities of nucleotide-binding sites in the outer dynein arm and its separated HC subunits.

Taken together, our results showed that moderate concentrations of 250 μM MgATP are sufficient to nearly saturate all four putative sites on each of the β and γ HCs of outer-arm dynein, whereas comparable concentrations of MgADP saturated only three sites per chain (Fig. 1.17; [130,131]). The stepwise dissociation constants for the binding ranged from ~10 μM up to ~100 μM, for both MgATP and MgADP. The different binding affinities at these sites were consistent with a model in which nucleotide binding occurs at a single high-affinity hydrolytic site, with additional nucleotide binding occurring at three regulatory sites whose functions remained to be determined.

More recent studies using molecular genetics to introduce site-specific mutations designed to block nucleotide binding and/or hydrolysis at each of the potential four nucleotide binding sites of cytoplasmic dynein in *Dictyostelium* [2] and in yeast [1,4] have confirmed that AAA1 is the principal site of ATP hydrolysis and energy transduction, but showed that ATP hydrolysis at the AAA3 site is also required for cytoplasmic dynein to function as an effective motor. Binding of nucleotide at the AAA2 and AAA4 sites can modulate the parameters of dynein function *in vitro*, but it is still unclear whether the regulatory effector *in vivo* is

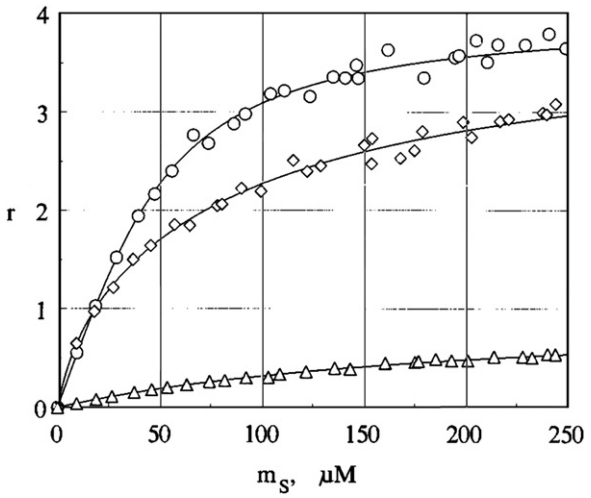

Figure 1.17 Binding of MgATP, MgADP, and MgAMP to the β HC subunit of outer-arm dynein by equilibrium partition. Data are shown as direct binding plot with *r* representing the moles of nucleotide bound per mole of dynein HC subunit (*Mol Wt.* 750 000) and m_S representing the concentration of unbound nucleotide in the dextran phase. ○: MgATP; ◇: MgADP; △: MgAMP. β HC concentration in the dextran phase was 4 μM. *Reproduced from [130] with permission.*

mechanical stress or allosteric interaction with a regulatory subunit, such as dynactin [132].

1.3.5 Exploring the Dynein Family of Multiple Isoforms

To facilitate classifying the family of dynein isoforms in two different organisms, we set up a collaborative sequence exchange with the lab of Tom Hays at the University of Minnesota. Our lab used PCR reactions with degenerate primers to obtain short clones of dynein isoforms in sea urchins, while the Hays lab did the same with *Drosophila*. By exchanging sequences of any new isoforms discovered, we hoped to identify a complete set of dynein isoforms more efficiently than either lab could alone.

Starting from poly(A+) RNA from reciliating sea urchin embryos, we identified 14 different genes that encoded for dynein HCs and hybridized with a ~14.5 kb transcript on a Northern blot [133]. Analysis of the changes in transcript levels during reciliation of embryonic external cilia showed that 11 or more of these genes became upregulated during reciliation, whereas the single gene that did not become upregulated closely resembled the reported sequences of cytoplasmic dynein in other organisms (Fig. 1.18). This work involved a significant number of poly(A+) RNA preparations from timed series of developing sea urchin embryos. These preparations were all prepared, blotted, and probed by Barbara Gibbons. Everybody who has worked with poly(A+) RNA knows how

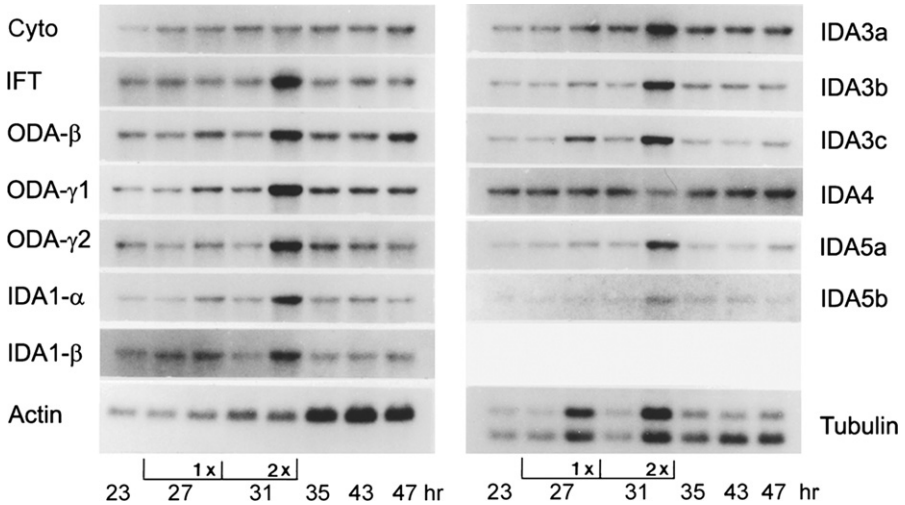

Figure 1.18 Change in abundance of poly(A)+ RNA transcripts of dynein HC genes after deciliation. Autoradiographs of Northern gels showing changes in abundance of poly(A)+ RNA transcripts from 15 dynein HC genes in response to deciliation of sea urchin embryos. The time shown is hours after fertilization. Portions of the 23 h embryos were deciliated once (1×) or twice (2×), as indicated. The Cyto transcript represents HC of cytoplasmic dynein and shows no change in abundance; all other dynein HC transcripts show increased abundance after deciliation. Abundance of tubulin and actin transcripts served as controls. Nomenclature of the dynein HC genes is updated as given in [198] (see Section 1.4.2.3). *Modified from [133] with permission.*

difficult it is not to have occasional degradation of a sample from contaminating ribonuclease. This becomes even more difficult when working with the unusually long 14 kb transcripts of dynein. It is a remarkable tribute to Barbara's meticulous experimental technique that she did not lose any step in her several timed RNA series.

Our sequence analysis of a ~400-amino-acid region encompassing the putative hydrolytic ATP-binding site showed that the sea urchin dynein genes fall into at least six classes [133]. Most of these classes in sea urchin had a high degree of sequence identity with one of the dynein HC genes identified in *Drosophila* by the Hays group [134], suggesting that the radiation of the dynein gene family into the present day classes occurred at an early stage in the evolution of eukaryotes [135]. The evolutionary history of the dynein gene family is discussed further in Section 1.4.2.3.

1.3.6 Function of Cytoplasmic Dynein in Yeast

At the time when most of our lab were turning to molecular biology, my postdoctoral student Dan Eshel was still in the midst of his productive collaboration with the Takahashi and Shingyoji group at the University of Tokyo (Section 1.3.7.3.2), but as soon as this work tapered down he was keen to shift to a project

using molecular genetics to study the function of cytoplasmic dynein in the budding yeast *Saccharomyces*.

With advice from others in our group, Dan was able to PCR-amplify a preliminary short clone of the putative single dynein HC gene that encoded a highly conserved region of the hydrolytic ATP-binding domain and map it to chromosome 11. As our lab had no experience with yeast genetics, I advised him to gain the necessary yeast skills by taking the Cold Spring Harbor yeast course that summer. While he was away on the course, I managed to arrange a collaborative project with Jean-Claude Jauniaux in Brussels and Rudy Planta in Amsterdam, the leaders of the two yeast sequencing groups responsible for that region of chromosome 11. With the benefit of complete nucleotide sequence provided by the sequencing groups, Eshel generated two knock-out mutations of the cytoplasmic dynein gene and found that the cells of both mutants continued to grow at nearly the normal rate. The sole phenotype noted was a misalignment of the mitotic spindle, seen in about a quarter of the cells. This misalignment initially blocks the normal passage of one end of the spindle into the daughter cell [136,137]. However, in almost all cases, the spindle misalignment in these cells becomes corrected after some delay and the cell then passes through the remaining stages of division with no further problem. This correction of misaligned spindles was taken to indicate that yeast cells possess a backup mechanism, independent of dynein, that comes into action to rescue cells that happen, for any reason, to have a misaligned mitotic spindle.

Further work by Bill Saunders in the lab of Andy Hoyt indicated that two kinesin-related gene products, Cin8p and Kip1p, participate with the dynein gene product Dyn1p in producing separation of chromosomes during mitosis in yeast, and that deletion of the dyn1, cin8 pair renders the yeast inviable [138].

1.3.7 Regulation of Microtubule Sliding in Cilia and Flagella

The molecular mechanisms responsible for coordinating the activity of axonemal dyneins to generate the typical oscillatory beating of cilia and flagella have proved difficult to investigate and are still not completely understood. The basic problem has been the lack of an experimental method to determine directly the distribution of dynein arm activity along each of the nine doublet tubules at different stages of a beat cycle so that these patterns can be correlated with the initiation, growth, and propagation of the principal and reverse bends in the axoneme. As a result, research on the regulation of microtubule sliding has been limited to indirect approaches, such as the quantitative analysis of flagellar waveforms [65,139,140]; the modification of flagellar beat patterns by use of mechanical, biochemical, or genetic perturbing agents [141–148]; and the construction of mathematical computer models that attempt to mimic the beating of real flagella

on the basis of postulated regulatory mechanisms [141,149,150]. As emphasized in a recent review by Charles Lindemann and Kathleen Lesich [151], the results obtained by these different approaches have yet to be assembled into a comprehensive model that includes all aspects of axonemal motility, with presumably only relatively minor variations among different organisms. As indicated in Section 1.3.2.7, the most broadly used model at the present time is the switch-point mechanism proposed by Satir and Matsuoka [64], but details of the mechanism responsible for contralateral switching of dynein activity during oscillatory beating have been difficult to establish.

Improved techniques of image reconstruction in cryo-electron microscopy (cryo-EM) have recently begun to visualize putative patterns of coordinated activity among dynein arms along the length of axonemal doublet tubules in unbent axonemes [5,6]. Future work along these lines will hopefully soon provide more direct evidence for the patterns of dynein activation that occur at the different stages of an axonemal beat cycle.

During the period 1975 to 1995, while the others in my group were deeply involved in the protein chemistry of dynein and later in molecular biology, I felt a need for a line of research that I could pursue with my own hands without the heavy time commitment involved in those approaches. With this in mind, I started thinking of possible experiments to clarify the factors involved in regulating microtubule sliding to generate the highly robust oscillatory beating of sperm flagella. My efforts were directed first toward the mechanisms involved in controlling the planar beating and the Ca^{2+}-mediated asymmetry of flagellar waveforms and later toward the influence of the hydromechanical boundary conditions at the flagellar base on the initiation and growth of new bends.

1.3.7.1 Modulation of Flagellar Beating by Ca^{2+}: Asymmetric Waveforms, Quiescence, and Chemotaxis

1.3.7.1.1 Background

Most organisms that utilize flagella or cilia for movement also possess a Ca^{2+}-mediated mechanism for modulating the beating movements of the organelles in ways that allow the organism to respond to changes in its surroundings by changing the speed and direction of this movement [152,153]. Working with hydroid sperm in the early 1970s, Richard Miller and Charles Brokaw were the first to show that the chemotactic response of these sperm involves short bursts of asymmetric flagellar beating that cause the sperm to turn its direction of swimming appropriately. They also noted that the asymmetric waveforms during these bursts resemble those produced in demembranated sperm flagella by an increased concentration of free Ca^{2+} in the medium [152,154]. More up-to-date work has shown that the Ca^{2+}-mediated asymmetry of flagellar beating in sea urchin sperm represents a critical step in an integrated pathway of chemotactic signaling that efficiently guides the helical trajectory of a swimming sperm toward the egg [155].

1.3.7.1.2 Increasing Concentrations of Intracellular Ca^{2+} Result in a Progressive Inhibition of Reverse Bend Growth, and Can Lead to Complete Blockage of Reverse Bend Initiation and Flagellar Quiescence

Our own interest in the Ca^{2+} response of sperm flagella was directed more toward regulation of microtubule sliding and began in the late 1970s with Barbara making the serendipitous observation that the live sperm of one particular species of Hawaiian sea urchin swim intermittently when observed in sea water by dark-field light microscopy [156]. In these sperm, the normal propagated bending waves of the flagellum are interrupted by brief episodes of quiescence in which the immotile flagellum assumes the shape of a cane, with a sharp bend of >3 rad at the proximal end and relatively little curvature over the rest of its length (Figs. 1.19 and 1.20). These episodes of quiescence require the normal presence of calcium in sea water and are thought to be the result of a spike in internal Ca^{2+} concentration resulting from a transient membrane depolarization that leads to opening of voltage-sensitive Ca^{2+} channels located at the flagellar base [156,157].

Analysis of flagellar waveforms in the stopping transient that precedes an episode of quiescence identified two stages. During the initial *transitional* stage, which lasts from two to six beat cycles, the asymmetry of the flagellar waveform increases gradually, with the angles of successive principal bends increasing and those of the intervening reverse bends decreasing correspondingly, so that the average angle of each pair of principal and reverse bends remains approximately constant, in a manner consistent with a gradually increasing intracellular concentration of free Ca^{2+} (Figs. 1.19 and 1.21; [139]). This stage continues until one principal bend at the base of the flagellum attains an angle of ~ 3 rad, whereupon initiation of the next following reverse bend fails to occur. The

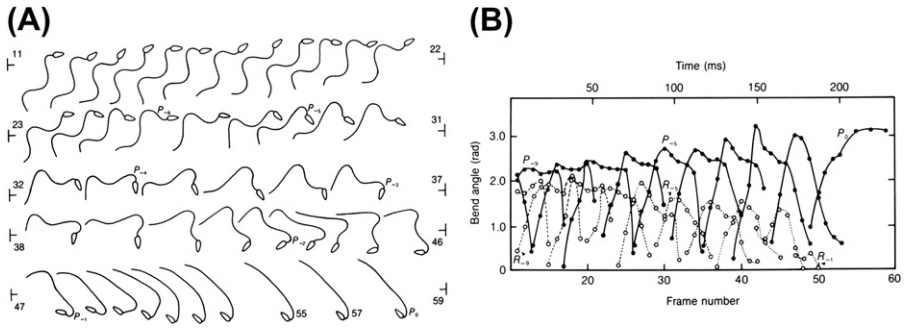

Figure 1.19 Asymmetric waveforms during transition between steady swimming and light-induced quiescence. (A) Tracings of successive frames of cine film during the stopping transient of a live sea urchin sperm swimming in sea water. Frames 11–22: steady-state beating; frames 22–48: transitional stage; frames 48–59: blocked stage. P_0: principal bend at base of quiescent flagellum; prior principal bends are labeled P_{-1}, P_{-2}, P_{-6} in reverse chronological order. (B) Progressive *increase* in angle of principal bends and the corresponding *decrease* in angle of reverse bends that occurs during the transitional stage of the above transient. *Reproduced from [158] with permission.*

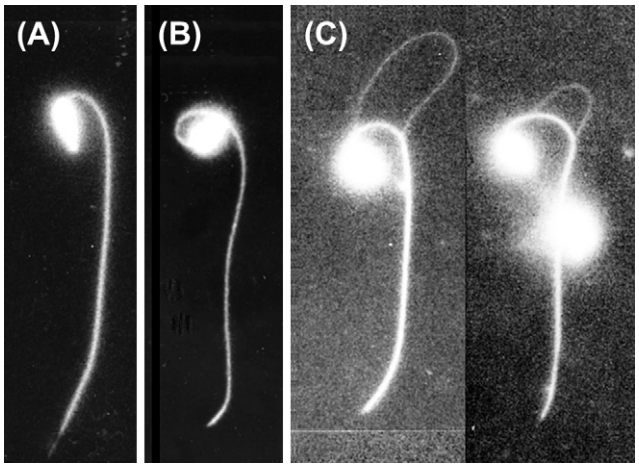

Figure 1.20 Quiescence waveforms and axonemal splitting. (A) Waveform of flagellum during a typical episode of Ca^{2+}-mediated quiescence provoked by irradiation of live sperm of *Tripneustes gratilla* swimming in sea water under intense blue light. See also Figure 1.19A. (B) Quiescent waveform resulting from over-activation of Ca^{2+}-mediated asymmetry in a reactivated sperm flagellum. (C) Typical examples of axonemal splitting and sliding observed in quiescent reactivated flagella. *Reproduced from [158,160] with permission.*

flagellum then enters a *blocked stage*, in which existing bends propagating through the mid-region decay before reaching the tip and the flagellum becomes quiescent [158,159]. After an interval of 0.2—2 s, flagellar motility resumes by initiation of a new reverse bend at the base and the original beat pattern recovers by reverse passage through the stages of the stopping transient.

To examine the nature of the quiescent state, we generated it in demembranated axonemes by adding a relatively high concentration of free Ca^{2+} to sperm flagella reactivated with MgATP under conditions favoring asymmetric beating [160]. Our results showed that quiescence represents an active, highly stressed state of the flagellum, with the sharp bend at the base being maintained by the continuing asymmetric activity of dynein arms in the more distal regions of the flagellum. The quiescent flagella were fragile, and disruption of the axoneme occurred spontaneously upon standing. This disruption usually involved a splitting of the axoneme in which one active group of microtubules looped out from the axoneme as it slid up over a second group of microtubules toward the sperm head (Fig. 1.20).

On the basis of these data, we concluded that the gradually increasing asymmetry of flagellar beating that occurs during a stopping transient is the result of a progressive increase in the Ca^{2+}-dependent inhibition of the microtubule sliding responsible for growth of reverse bends on the axoneme. When this inhibition attains a certain critical level, there is insufficient force at the base for new reverse bends to be initiated and the flagellum becomes quiescent [160].

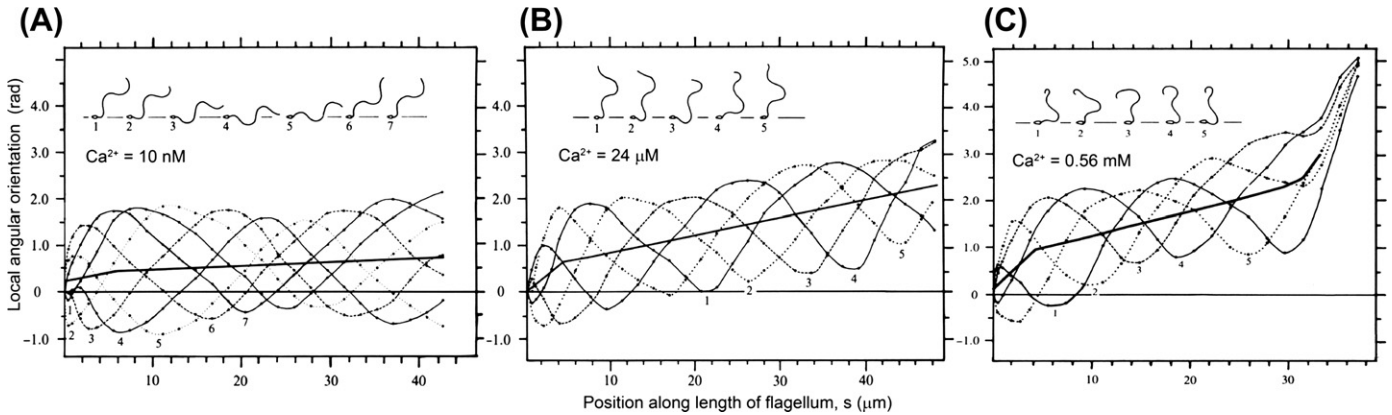

Figure 1.21 Effect of Ca^{2+} concentration on the asymmetry of flagellar beating. Plots of shear angle(s) (angle between longitudinal axis of sperm head and the local tangent angle of the flagellar waveform) as a function of distance(s) measured along the flagellum. The heavy black line indicates the time-averaged value of the local angular orientation over one beat cycle and is a measure of the waveform asymmetry. Inset shows the flagellar waveforms corresponding to each of the plots. (A) successive frames show approximately one cycle of steady-state beating of a demembranated sea urchin sperm flagellum beating in the presence of 1 mM ATP at a free Ca^{2+} concentration of ~10 nM. (B) same as (A) for a reactivated sperm flagellum in 1 mM ATP and 24 μM free Ca^{2+}. (C) same as (A) for a reactivated sperm in 1 mM ATP and 0.54 mM free Ca^{2+}. *Reproduced from [226] with permission.*

A subsequent electron microscopic analysis of the active splitting of quiescent axonemes in sperm flagella by Win Sale [63], together with other more recent and detailed studies in *Chlamydomonas* [145,146], have shown a consistent correlation between the position of one of the two central tubules and the identity of the doublet tubules participating most actively in disintegration of protease-treated axonemes. This provides evidence favoring a role of the central apparatus in regulating the switching of dynein activity in the switch-point model [64] although the interpretation has been disputed [161].

1.3.7.2 The Central Apparatus and Radial Spokes Govern the Plane of Beat and the Orientation of Ca^{2+}-Mediated Asymmetry in Sperm Flagella

1.3.7.2.1 Sperm Flagella Lacking the Two Central Tubules Propagate Only Three-Dimensional Helicoidal Bending Waves

Although targeted gene knock-out experiments are infeasible in the study of sperm flagella, much of the same information can be obtained by considering a different organism in which one of Nature's evolutionary experiments has resulted in the sperm flagella possessing a reduced axonemal structure. A good example is the Elopomorpha fish, which have 9+0 axonemes in their sperm flagella [162] but retain a standard 9+2 structure in their ependymal cilia [163]. The best-studied species of this taxon is the European eel, *Anguilla anguilla*, which can be made fertile in a laboratory aquarium by injections of chorionic gonadotropin. A structural study of these eel sperm flagella by Baccio Baccetti confirmed the presence of a 9+0 axoneme and showed that it contains the nine outer-doublet tubules and a complete set of inner dynein arms, but completely lacks the radial spokes and all elements of the central apparatus, as well as the outer dynein arms [164]. On the basis of these results, Baccetti invited Barbara and me to spend the 1981−1982 year in his laboratory at the University of Siena in Italy, studying the motility of these eel sperm flagella in detail. It was good timing, for we had just become due for a second sabbatical leave and were already considering where we might usefully go.

By the time we arrived in Siena, there was an aquarium containing fertile male *Anguilla* awaiting us. Our first observations showed us that the 9+0 flagella of *Anguilla* sperm beat unusually rapidly compared to those of the marine invertebrates with "normal" 9+2 flagella that we had worked with previously. After we had adapted our techniques to this unexpectedly rapid motion, we were able to show that the flagella of live *Anguilla* sperm propagate left-handed helicoidal waves distally along the flagellum (Fig. 1.22) at a true beat frequency of ~95 Hz and that this resulted in forward progression at a speed of about 140 μm/sec while rolling at a frequency of 19 Hz [165]. Demembranated *Anguilla* sperm could be reactivated with 0.8 mM MgATP and they swam in a manner that closely resembled that of the live sperm, exhibiting both the rolling motion and the propagation of helicoidal waves along the flagellum.

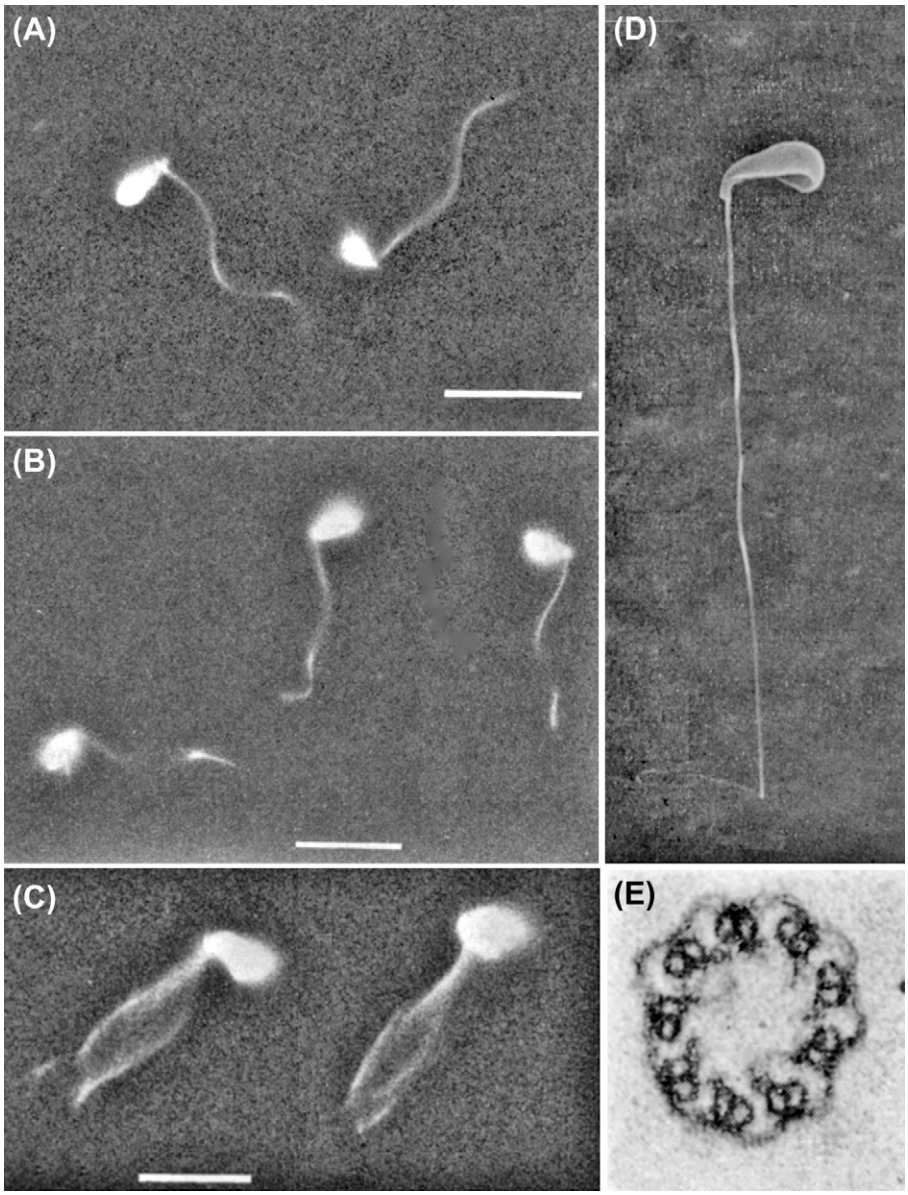

Figure 1.22 Structure and motility of the 9+0 flagellum of eel (*Anguilla anguilla*) spermatozoa. (A) Dark-field micrograph taken with flash illumination of live sperm swimming in saline solution, showing the three-dimensionality of the flagellar waves. Bar is 20 μm. (B) Dark-field micrograph taken with flash illumination of sperm swimming in demembranation/reactivation solution containing 0.8 mM $MgATP^{2-}$. Bar is 20 μm. (C) Dark-field micrograph of two individual live sperm stuck to the bottom surface of the observation dish by their heads. Taken with steady illumination (0.25 s) to show the wave envelope of the beating flagella. Bar is 20 μm. (D) Scanning electron micrograph of an intact sperm of *Anguilla*. The sperm head is eccentrically positioned relative to the longitudinal axis of the flagellum. (E) Transverse section through the flagellum, showing the 9+0 structure of the axoneme, with the flagellar membrane closely applied to the doublet tubules. Inner dynein arms are present on all doublet tubules. Outer dynein arms, radial spokes, and central apparatus are totally absent. *Reproduced from [165,229] with permission.*

However, the conditions for reactivated flagella motility in eel sperm were considerably more stringent than in sea urchin sperm and required the presence of acetate anions rather than chloride in the reactivation medium. No flagellar movement was seen at ATP concentrations below 40 μM, corresponding to a beat frequency of ~10 Hz. Importantly, concentrations of free Ca^{2+} ranging between 10^{-8} M and 10^{-4} M appeared to have no affect on either the beat frequency or the waveform of the beating flagella, suggesting that this 9+0 axoneme may lack the Ca^{2+}-mediated mechanism that regulates axonemal motility in the 9+2 axonemes of cilia and flagella in most other organisms that have been studied [153].

A second evolutionary instance of a 9+0 axonemal structure associated with helicoidal bending waves occurs in the Limulidae family of horseshoe crabs [166]. In this family, sperm of the Asian species, *Tachypleus tridentatus* and *T. giga*, have 9+0 axonemes and beat with helicoidal waveforms similar to those of *Anguilla*, although in this case the structural defect in the axoneme is more specific with the axonemes lacking only the paired central tubules and central sheath while retaining their radial spokes and outer dynein arms. Sperm of the closely related American species *Limulus polyphemis* have normal 9+2 flagellar axonemes and, as might be expected, they beat with planar waveforms very similar to those of sea urchin sperm.

When considered together with the properties of *Anguilla* sperm flagella, the more localized structural deficit in the 9+0 axonemes of *Tachypleus sp.* and their close evolutionary relationship to the 9+2 axonemes of *Limulus* support the hypothesis that the inability of the 9+0 axonemes in these two organisms to coordinate the patterns of tubule sliding required for planar beating in 9+2 sperm flagella is a direct effect of loss of the central pair, thereby revealing an underlying, less highly regulated, and possibly more primitive mechanism of sliding coordination that remains competent to generate helicoidal bending waves that are adequate, although less efficient, for sperm propulsion [167,168]. Support for the presence of two alternative modes of sliding regulation in sperm flagella is provided by the abrupt transitions between a normal planar beat pattern and an atypical helicoidal beat pattern that have been reported in the sperm flagella of marine invertebrates beating in highly viscous media [47,169].

1.3.7.2.2 Forced Rotation of the Central Complex Causes Rotation of the Flagellar Bend Plane and the Orientation of Ca^{2+}-Mediated Asymmetry

After completing work on spontaneous flagellar transients in 1985, I decided to test a new experimental approach to the regulation of microtubule sliding that would perturb the normal flagellar beat pattern by imposing vibratory movement on the head of a sea urchin sperm. When I suggested a US—Japan-funded international collaboration on this project to Keiichi Takahashi and Chikako Shingyoji

at the University of Tokyo, both of whom had had previous experience with micromanipulation of sea urchin sperm, they responded with enthusiasm. Dan Eshel, a graduate student working with Brokaw at CalTech, agreed to join the project and take charge of the Hawaiian side of the collaboration as soon as he had completed his PhD degree.

This approach involved holding the sperm head by suction in the tip of a micropipette mounted on a piezoelectric device that could be vibrated along any desired axis by sinusoidal voltages generated by a real-time computer program. Initial experiments showed that lateral vibration of the sperm head brought about a stable rhythmic beating of the flagellum synchronized to the movement of the pipette with the plane of flagellar beat coincident with that of the pipette vibration.

One of the earliest and most striking findings of this collaboration was that a gradual rotation of the plane of imposed vibration could induce the plane of flagellar beating to follow this rotation through as many as four complete revolutions (25 rad) relative to the clamped sperm head (Fig. 1.23). The direction of flagellar asymmetry, as indicated by the bends on one side of the flagellum being of greater angle than those on the other side, rotated along with the plane of beating. The large magnitude of possible beat-plane rotation surprised all of us in the room at the time of the first experiment, but cries of astonishment were heard when we stopped the forcing vibration and saw the beat plane spontaneously unwind four revolutions to its original orientation within the next few seconds. A video of an experiment showing imposed winding followed by spontaneous unwinding can be seen in the supplementary online data for [167].

The magnitude of this winding and unwinding immediately suggested that the forced rotation of the beat plane was causing a rotation of the pattern of sliding among nine outer doublet tubules, rather than just twisting the entire axonemal structure. The only axonemal structure seemingly available to rotate and store the elastic energy required for unwinding was the central tubule complex. Given that previous work from other labs had reported the occurrence of central-pair rotation during normal beating in protozoan cilia and algal flagella [167,169–171], we proposed that in sea urchin sperm the central complex does not normally rotate but that it can be forced to do so by an imposed rotation of the beat plane. A longitudinal displacement of the central complex resulting from such rotation over the path defined by the helical array of radial spokes could then provide the elastic restoring force for unwinding [172].

Subsequent experiments have supported this hypothesis, most importantly by excluding the alternative possibility of the entire axonemal structure becoming twisted (Fig. 1.24; [173]) as well as by demonstrating the elastic character of the force responsible for unwinding [174] and by verifying the rotation of Ca^{2+}-mediated asymmetry (Fig. 1.25; [173,175]).

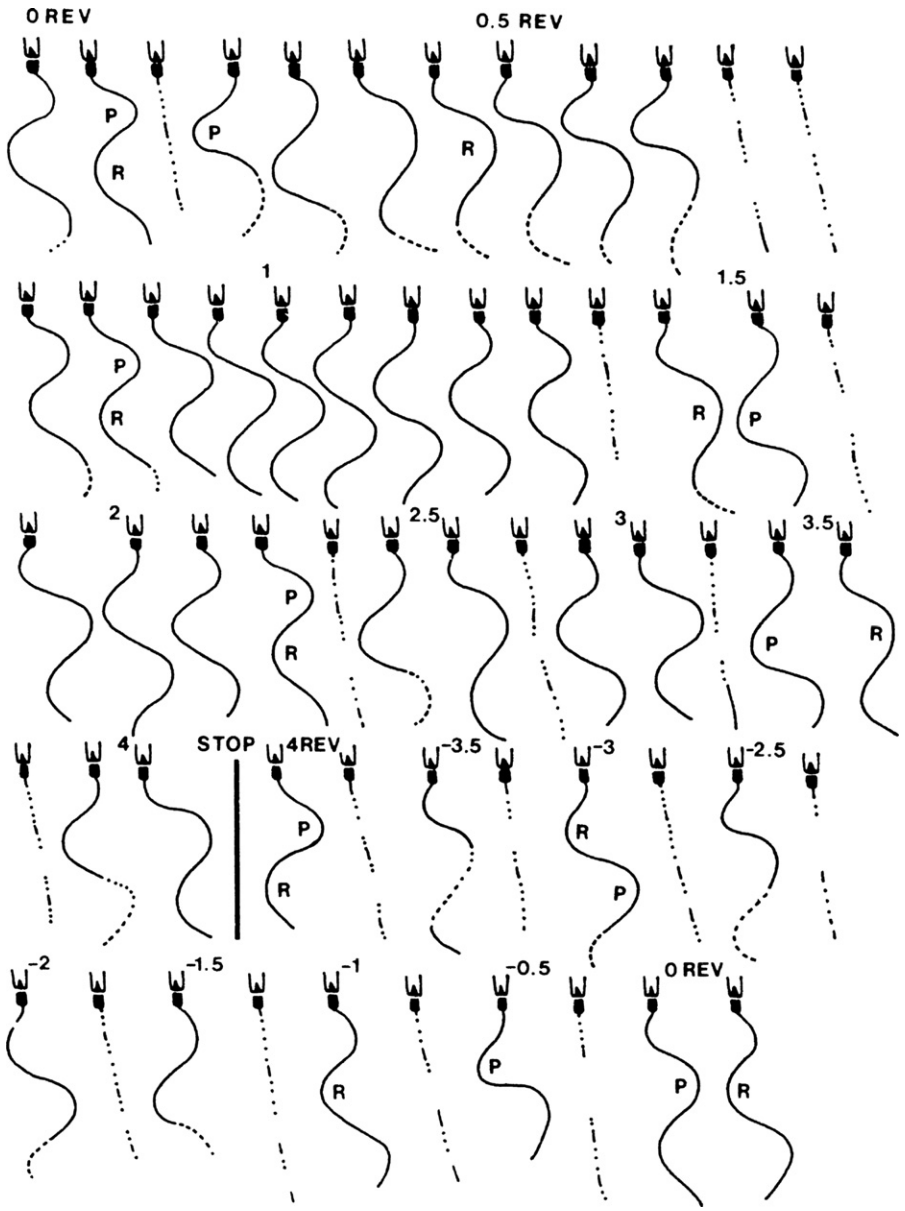

Figure 1.23 Spontaneous recovery after an imposed rotation of the plane of beating. (A) Tracing of selected frames from a cine film showing a live sea urchin spermatozoon undergoing four revolutions of its flagellar beat plane induced by gradual rotation of the plane of pipette vibration, followed by cessation of vibration (STOP) and the subsequent spontaneous unwinding of the beat plane. Orientations of the principal (P) and reverse (R) bends are indicated. The first 3.5 turns of unwinding were complete within 6 s and the final half turn occurred 10 s later. A video of this experiment can be viewed in the supplementary data for [167]. *Reproduced from [172] with permission.*

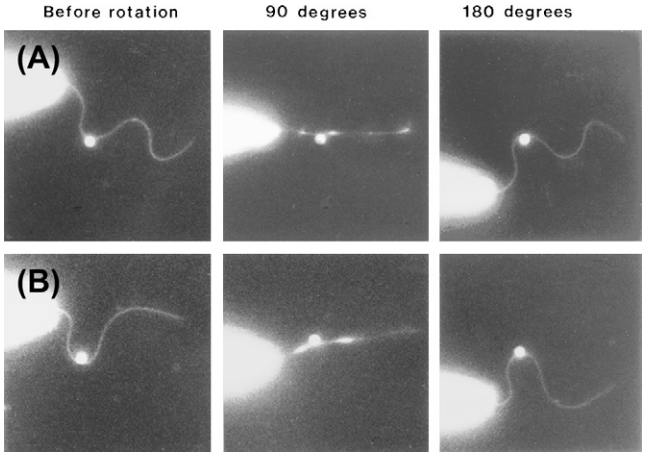

Figure 1.24 Doublet microtubules of axoneme remain untwisted after an imposed rotation of the flagellar bend plane. Dark-field light microscope images of demembranated sea urchin sperm with a marker bead stuck on one side of the flagellar axoneme. Two different sperm are shown before rotation and after imposing rotation of the bending plane through 90° and 180°, as indicated. The marker remains in the same position below (A) or above (B) the axoneme, unaffected by the rotation of the bending plane. Densities have been adjusted for visibility. *Reproduced from [173] with permission.*

1.3.7.3 Studies on Bend Initiation, Growth, and Propagation

1.3.7.3.1 Bend Initiation Requires a Block to Prevent Sliding Between Adjacent Doublet Tubules at the Flagellar Base

Early work by Stuart Goldstein in Charles Brokaw's lab had shown that, when an actively beating flagellum is amputated by a brief pulse of synchronized laser microbeam, the proximal section is usually able to continue oscillatory beating, whereas the distal section allows any pre-existing bends to propagate to the tip but then fails to initiate any new bends [176]. This important result indicated that something special about the base of the flagellum was required for initiation of new bends.

In 1972, Charles visited our lab in Honolulu for a couple of weeks and we collaborated on exploring the conditions required for bend initiation in more detail. By using a low concentration of ATP to obtain local reactivation of sperm flagella that had been demembranated over only a portion of their length, we were able to demonstrate that proximal, medial, and distal regions of the flagellum are all capable of autonomous oscillatory beating when supplied selectively with ATP. Thus, the presence of a proximally located section of inactive axoneme appeared to provide an adequate block to permit oscillatory beating in a more distal region of the axoneme that is selectively supplied with ATP [177]. From this, we concluded that the presence of some form of block to prevent sliding between tubules at the proximal end of a beating axoneme is required for bend initiation but that the presence of the centriole itself is not necessary. This

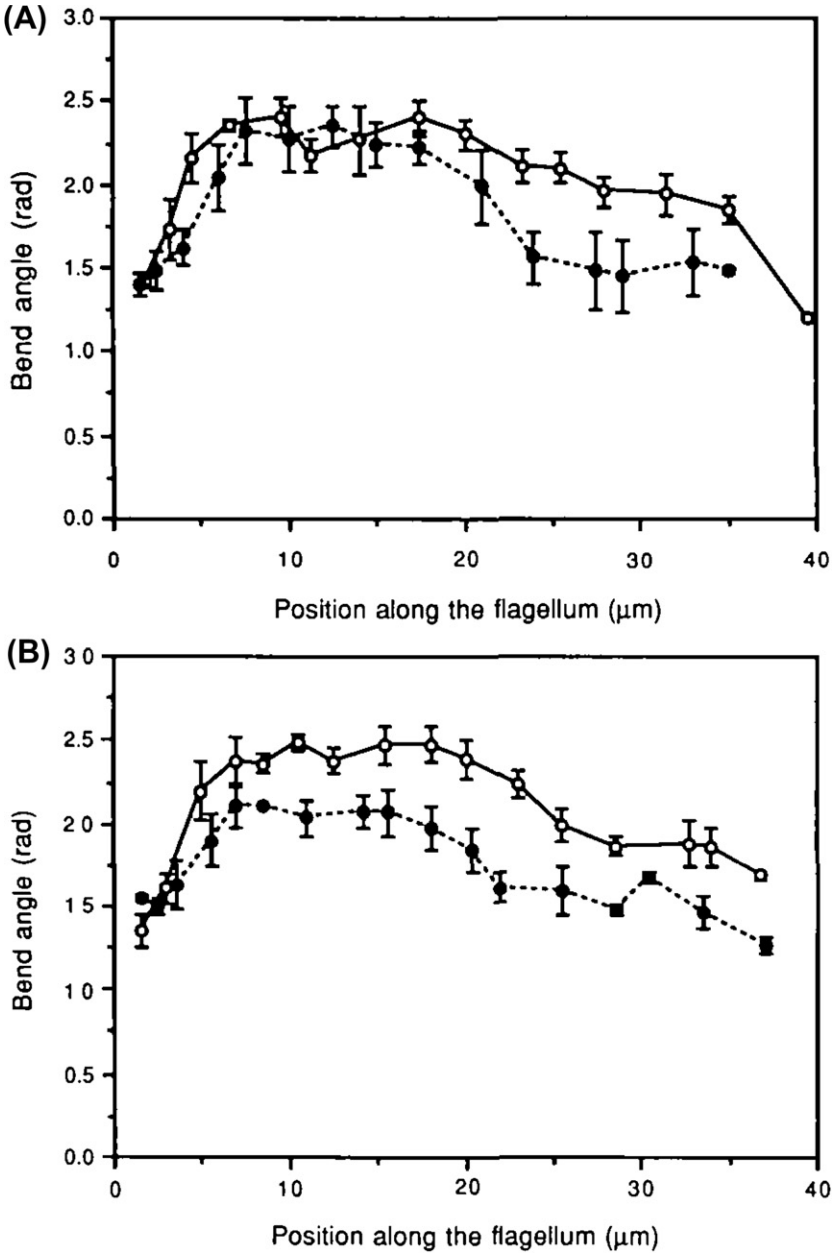

Figure 1.25 Imposed rotation of the flagellar beat plane results in an equal rotation of the orientation of Ca^{2+}-mediated asymmetry of waveform in the distal region of the flagellum. Changes of bend angles along the length of the flagellum in live sperm after (A) reversed orientation (2.5 counter-clockwise revolutions) and (B) normal orientation (three counter-clockwise revolutions). Angles of principal bends (O) are larger than those of reverse bends (●), except in the region close to the vibrating pipette where the movement of the pipette dominates the autonomous beating of the flagellum. *Reproduced from [173] with permission.*

result was later confirmed by Chikako Shingyoji, Akira Murakami, and Keiichi Takahashi at the University of Tokyo, who showed that iontophoretic application of a brief pulse of ATP at any position along the length of a demembranated flagellum generated a new pair of oppositely directed bends, in accord with the prediction by the sliding tubule model [178,179].

1.3.7.3.2 Mechanical Stress Applied to the Flagellar Base Can Advance or Retard the Timing of New Bend Initiation Without Disrupting Oscillatory Beating, but Only Within Limits Determined by the Unconstrained Beat Frequency

Starting in 1989 (Fig. 1.26), Dan Eshel extended our collaboration with Chikako Shingyoji, Akira Murakami, and Keiichi Takahashi at the University of Tokyo with a second series of vibrating micropipette experiments that probed the extent to which we could control the beat frequency of a flagellum by manipulating the vibration frequency of the micropipette holding the sperm head. The flagella of live sperm, with an average natural beat frequency of 48 Hz, showed stable beating synchronized to the pipette vibration over a frequency range of 35—90 Hz (Fig. 1.27A; [180]). The flagella of reactivated sperm with a natural beat frequency of 39 Hz at 2 mM ATP remained synchronized over the range 20—70 Hz

Figure 1.26 Gibbons lab group. From left: Ilana Eshel (visitor), Dan Eshel, Gabor Mocz, Barbara Gibbons, Keiichi Takahashi, Ian Gibbons, Greg Dolecki, Cheryl Phillipson, Pat Harwood, and Wen-Jing (Grace) Tang. Our collaborators Keiichi Takahashi and Chikako Shingyoji were visiting from the University of Tokyo. The photograph was kindly taken by Chikako Shingyoji in January 1989.

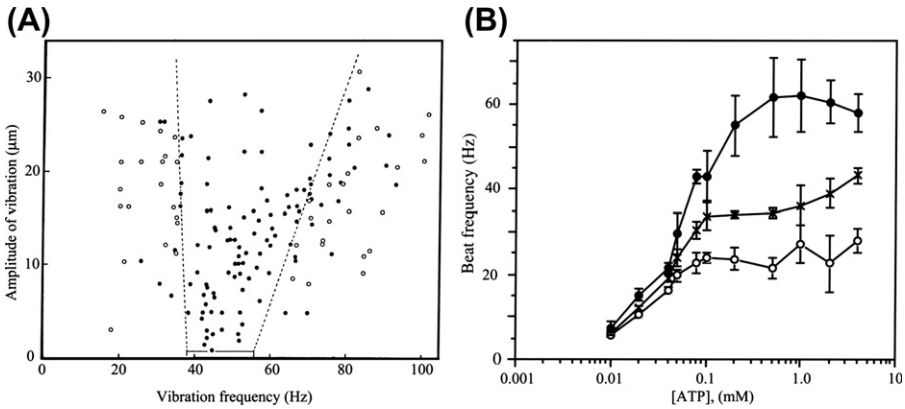

Figure 1.27 Range of vibration frequencies permitting stable synchronized flagellar beating. (A) live sperm in sea water at different amplitudes of imposed vibration. ●: stable beating synchronized to pipette vibration. O: unstable beating. Dashed lines show approximate boundaries of the region of stable beating. The rectangle on the abscissa indicates the range of beat frequencies in this population of spermatozoa when held in a stationary micropipette. (B) Reactivated flagella beating observed at different concentrations of ATP. ●: average maximum frequency capable of maintaining stable beating. O: average minimum frequency capable of maintaining stable beating synchronized to pipette vibration. x: average undriven beat frequency at each ATP concentration.
Reproduced from [180,181] with permission.

(Fig. 1.27B; [181]). In both live and reactivated sperm there was a characteristic difference between the behavior at the upper and lower limits. Vibration frequencies above the upper limit caused irregular, asymmetrical beating, whereas frequencies below the lower limit induced instability of the flagellar beat plane. Although the presence of an upper-limit frequency for synchronizing the flagellum to the vibrating micropipette may be due simply to energy factors, the presence of a lower limit frequency is more surprising and has the potential to reveal something of the basic oscillatory mechanism of the axoneme.

The ATP-dependence of both the upper- and lower-frequency limits for synchronizing (Fig. 1.27B) indicates that the timing of new bend initiation and the sliding velocity of axonemal microtubules are not determined solely by the [ATP]-dependent and mechanically-dependent cycling time of dynein cross bridges distributed along the length of the axoneme, although the energy provided by the latter can become a limiting factor and lead to a decrease in bend angles when the imposed beat frequency is significantly higher than the natural beat frequency [180]. At imposed beat frequencies below the natural value, the timing of new bend initiation appears to be constrained by a second, oscillatory clock mechanism that maintains its [ATP]-dependent cycling rate at the natural beat frequency of the flagellum even when the actual flagellar beat frequency is reduced by the influence of the vibrating micropipette. A plausible source for this second, [ATP]-dependent clock mechanism would be a circumferential propagation of dynein arm activity

around the nine doublet tubules at the proximal end of the axoneme. A clocking of this type in this location has been postulated previously to be responsible for the generation of helicoidal bending waves in sperm flagella having a 9+0 axonemal structure (Section 1.3.7.2.1; [167,168]).

1.3.7.3.3 Information About an Abrupt Change in Imposed Beat Frequency Is Communicated to the Distal Regions of the Flagellum at the Speed of Bend Propagation

We used a high-speed video system to analyze the flagellar wave parameters during the first few cycles following the abrupt change in beat frequency from 38 to 65 Hz and from 65 to 38 Hz [182]. Our results (Fig. 1.28) demonstrated that the initiation rate of new bends at the base is directly governed by the frequency of the vibration and changes immediately to the new frequency. However, the length and the propagation velocity of bends that are already fully developed remain constant as they propagate into the distal region of the flagellum. This indicates that information of the changed beat frequency propagates at the speed of the bend. Whether this occurs because the information is embedded in the autonomic structure of the bend itself or is propagated separately, perhaps through a side-to-side rocking motion of the central pair, is not yet clear. In either case, the result is consistent with previous observations that the propagation of a fully developed bend is unaffected by amputation of a more proximal region of the flagellum with a laser microbeam [176] or by an imposed mechanical blockage [183].

1.3.7.3.4 Hydrodynamic Boundary Conditions at the Basal End of the Flagellum Have an Important Role in Determining the Bend Angles and Asymmetry of Flagellar Bending Waves

A marked effect of head attachment on bend angles and asymmetry has been observed at the relatively high beat frequencies (~60 Hz) in live sperm of the Hawaiian sea urchin *Tripneustes gratilla* (see Fig. 1.9A–C) and in reactivated sperm of the same species (see Fig. 1.9D–F). This effect of head attachment on flagellar bend angles was previously attributed to compression of new bends during their period of growth in the basal region of the flagellum [48]. However, this interpretation appears less likely in reactivated sperm flagella beating in the presence of a low concentration of methanol, which show a substantial effect of head attachment on the waveform asymmetry even when beating in low concentrations

Figure 1.28 Transient flagellar waveforms following an imposed abrupt change in beat frequency. Live sperm in sea water. (A) Movement of the micropipet tip before, during, and after a vibration frequency change from 38 to 65 Hz. (B) Oscillations of shear angle with time at 3 μm (B) and 35 μm (C) from the base of the flagellum before and after a typical frequency increase. The solid lines show sine curves that were fitted separately to the data before and after the frequency change, using the Simplex method to vary the parameters for minimum root-mean-square deviation. Black arrows indicate where each of the fitted sine curves has been extended one-quarter period past the transition point. Shear angle(s) is defined as the angle between the longitudinal axis of the sperm head and the tangent to the flagellar waveform at distance s from the sperm head (measured along the length of the curved flagellum). *Reproduced from [182] with permission.*

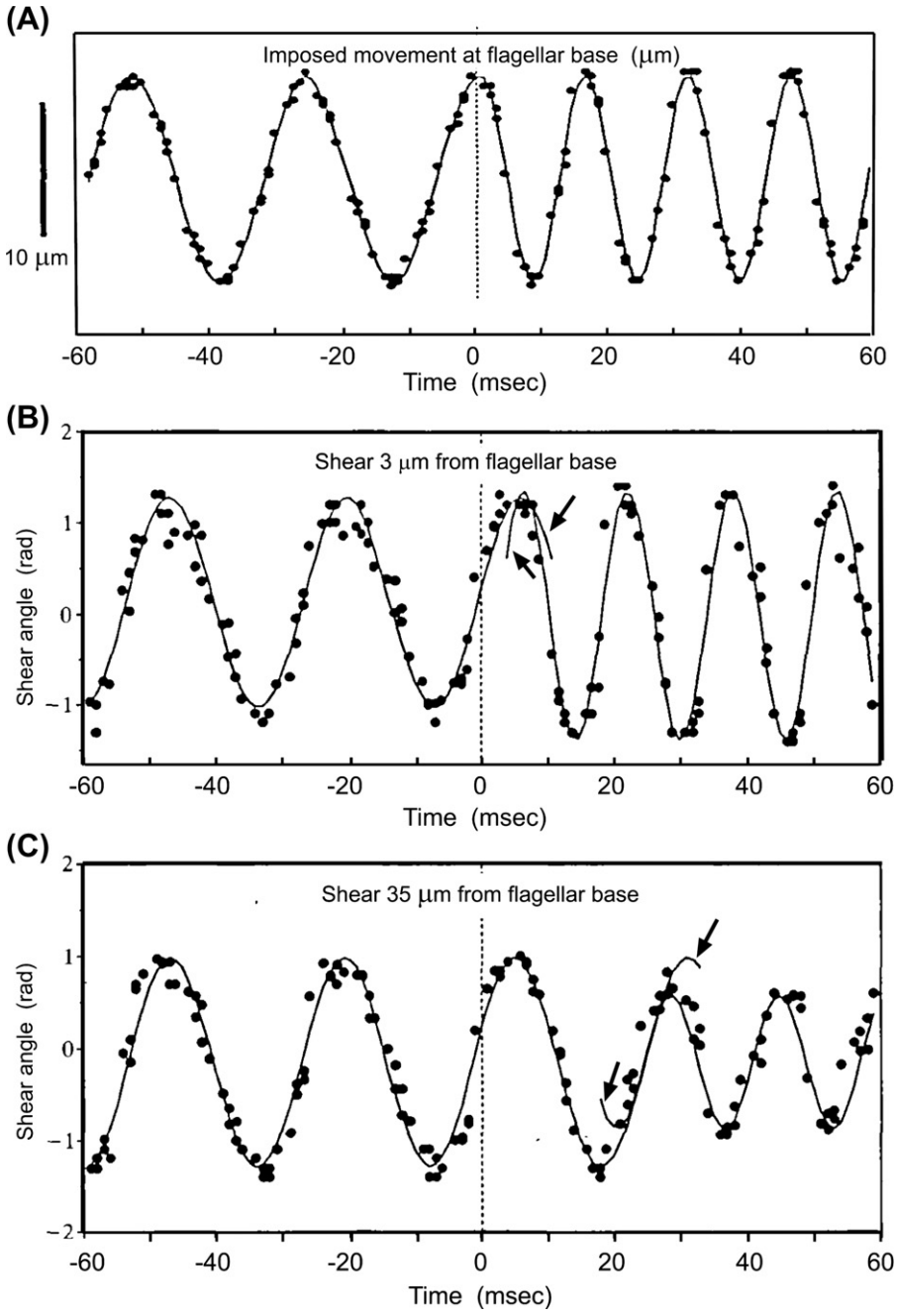
(A)
Imposed movement at flagellar base (μm)
10 μm
-60
-40
-20
0
20
40
60
Time (msec)
(B)
Shear 3 μm from flagellar base
Shear angle (rad)
2
1
0
−1
-60
-40
-20
0
20
40
60
Time (msec)
(C)
Shear 35 μm from flagellar base
Shear angle (rad)
2
1
0
−1
−2
-60
-40
-20
0
20
40
60
Time (msec)

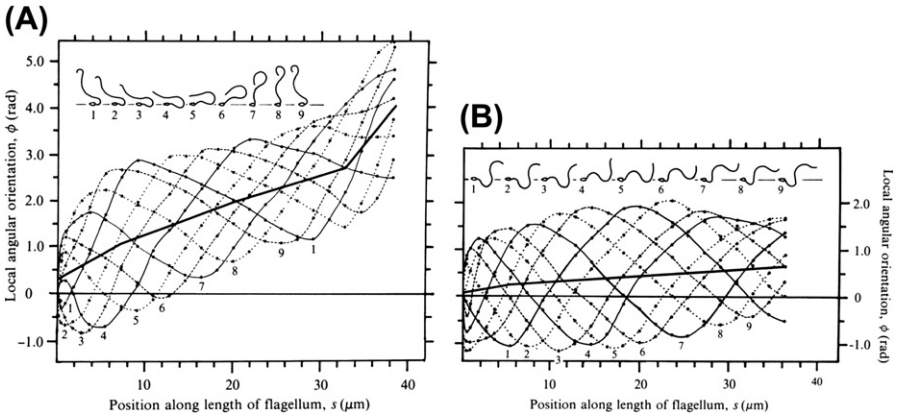

Figure 1.29 Effect of head attachment on Ca^{2+}-mediated asymmetry of flagellar beating. (A) Same as Figure 1.21A, but showing a freely swimming demembranated sperm with its flagellum reactivated in 20 μM ATP, 0.1 mM free Ca^{2+}, and 1.4 mole percent methanol. The flexible, but highly asymmetric, waveform was typical of all the freely swimming sperm in these preparations. Beat frequency: 2.5 Hz. Methanol was used to reduce the beat frequency sufficiently to obtain an adequate number of frames per beat cycle without need for stroboscopic filming [227]. In these flagella, the duration of basal growth for the principal bend occupies ~65% of the beat cycle and the waveform resembles that of typical cilia [228]. (B) Another sperm in the same preparation as that depicted in (A) but with its sperm head rigidly stuck to the dish. Beat frequency: 4.3 Hz. The flagella of all attached sperm in these preparations showed a similarly symmetrical waveform. A similar effect of attachment on Ca^{2+}-mediated asymmetry also occurs at higher beat frequencies in 1 mM ATP (Fig. 1.9D–F). *Reproduced from [226] with permission.*

of ATP at beat frequencies of 2–4 Hz (Fig. 1.29). The compressive forces at these low beat frequencies would be at least an order of magnitude smaller.

1.3.8 Loose Ends in Honolulu

Starting in around 1985, the contacts made through Barbara's weekly string quartet group gradually led to our increasing involvement with the Honolulu Chamber Music Series (HCMS), a non-profit organization, run almost completely by volunteers, that organized a series of five concerts by top international chamber music groups each year. As time passed, Barbara and I formed deep friendships with the other music enthusiasts on the Board of Directors. Barbara eventually became responsible for organizing the post-concert receptions, at which we shared the Aloha spirit with our donors and the visiting chamber groups. In 1994, I was surprised to be asked to take on a term as President. It was a novel and enjoyable experience for me to be negotiating fees with the musicians' agents and persuading them to request their clients to accept our offering of Aloha hospitality as a partial payment.

Toward the end of our time in Honolulu (Fig. 1.30), Barbara was looking forward to retiring and moving closer to our children, whereas I was reluctant to give up

Figure 1.30 Barbara and Ian Gibbons. The photograph was taken by Dave Au of the Pacific Biomedical Research Center in December 1994 to celebrate Barbara and Ian being awarded the E. B. Wilson Medal of the American Society for Cell Biology, a short while before Barbara's retirement. A video of their joint lecture at the ceremony can be downloaded from the companion website, www.king-dyneins.com. The video was kindly taken by Hening Ren, Ian's graduate student.

research as I still had ideas for new experiments and my NIH grant was funded for another five years, as well as saddened to lose our friendships with those on the Board of HCMS. We agreed to compromise on both retiring and moving from Hawaii to California in 1997, the year we would both turn 65. In the meantime, Barbara was able to cut back her work effort to 50% and started devoting more time to family visits and volunteer work trips with the Sierra Club.

For more than 25 years of our stay in Hawaii, we enjoyed Bob Kane's immensely skillful style of administration, which shielded our research from the daily nitty-gritty of building management. It was a shocking loss when Bob died suddenly about one year after retiring from his position as Director of the Kewalo Laboratory, just as he was getting back to his own research.

1.4 Semi-Retirement in Berkeley

A few months before our planned retirement and move to California, I spoke with some friends at the University of California, Berkeley to ask about the possibility of getting a small amount of research space there where I could continue my research on a part-time basis until my NIH grant ran out in 2002. Beth Burnside, whom I had known for many years, was extremely generous in

offering to host me and my assistant within her own allocation of research space. I am deeply grateful for her unstinting support for me and my research over what eventually turned into an extended stay of 12 years as a guest in her lab. Most of Beth's own research has involved the development and function of photoreceptor cells in the retina. My own early research on the retina, back when I was working with Dowling at Harvard, had acquainted me with the interesting aspects of this field. I felt comfortable and very much enjoyed participating in their discussions at the weekly meeting of Beth's lab group. Everybody in her group has been very friendly and helpful to me and I am most grateful for their friendship.

A few months after arrival in Berkeley, when the formalities of transferring my NIH grant from the University of Hawaii had been completed, I started to look around for a research assistant who would be able to continue a project independently of me when necessary. Within a short while, I was extremely fortunate in being able to recruit Joan Garbarino. After gaining her bachelor's degree in chemistry from the University of California, Berkeley, Joan had obtained her PhD in plant physiology from Cornell University. As the focus of my interest moved around, she enjoyed the challenge of learning new techniques, ranging from molecular genetics in yeast to growing protein crystals for X-ray diffraction. Her excellent technique and persistence in dealing with experimental difficulties have been remarkably successful with dynein.

1.4.1 Dynein as a Member of the AAA^+AAA^+ Class of Chaperone-Like ATPases

1.4.1.1 Background

In 1999, Andrew Neuwald and co-workers [128] used iterative sequence analysis to identify the four already-known nucleotide-binding domains of the dynein HC as modules of an expanded AAA^+ class of ATPases, as well as two additional poorly conserved and previously unrecognized AAA^+ modules closer to the C-terminus. They suggested that these six modules constitute a heterohexameric ring-shaped assembly in the motor domain of the dynein HC, similar to the homohexameric ring of AAA^+ modules already demonstrated in the biologically active form of the NSF membrane fusion factor (PDB: 1NSF) and considered likely also to occur in a variety of other AAA^+ proteins. In most AAA^+ proteins, the hexameric ring is formed by six identical AAA^+ modules located on separate polypeptide subunits. Dynein differs in that its six AAA^+ modules are arranged in tandem on a single polypeptide of unusually high molecular mass, the dynein HC. The only other protein known to resemble dynein in having six AAA^+ modules on a single polypeptide was a putative uncharacterized yeast protein (YLR106p) that had the distinction of being the largest open reading frame in the yeast genome. A review by Steve King discussed the functional implications of the AAA^+ structure of dynein in greater detail [184].

1.4.1.2 Homology-Based Model for the Motor Domain of β Heavy Chain of Sea Urchin Dynein

The concepts and techniques of protein crystallography were already somewhat familiar to me as I had taught this topic as part of the introductory biophysics course in the Department of Biochemistry and Biophysics at the University of Hawaii for several years. As the protein data bank already contained structures for the AAA^+ modules of other proteins, I thought that it might be worthwhile to use them as the basis for a homology-based model of a dynein HC and so I discussed this with Gabor Mocz, who had remained at the University of Hawaii after I retired. We agreed to collaborate on building a homology-based model for the structurally conserved regions in the AAA^+ domains of our favored β HC of axonemal dynein. Although we could not reasonably expect a fully correct model, we hoped to achieve sufficient accuracy for our model to serve as a guide for future high-resolution electron microscopy.

The secondary and tertiary levels of structure were modeled by Mocz during the summer of 2000, based upon their homology to a template of structurally conserved regions derived from the three AAA^+ proteins then available in the database. We were encouraged that most secondary structural elements in our model corresponded to regions of relatively-well-conserved sequence among different dynein isoforms. I assembled the structures of the six dynein AAA^+ modules into a ring by fitting them to the conserved structural regions in the hexameric crystal structure of PDB: 1NSF. The heterohexameric ring structure of our final model (PDB: 1HN5) had a diameter of 125−135 A and a central space of 15−20 A [185]. When compared to the electron microscopic structure of a dynein motor domain available at the time [186], our structure had six lobes, whereas the electron microscopic structure had seven. We attributed the extra lobe of the latter to an added contribution, probably from residues in the C-terminal domain beyond the AAA6 module.

Since publication of our paper, there have been major advances in identifying the structural basis of the ATP-dependent power stroke in the dynein motor. By using single-particle image averaging of electron micrographs, Stan Burgess, Anthony Roberts, and colleagues identified a previously unrecognized "linker domain" immediately N-terminal of the AAA1 domain [187]. This linker domain is about 10 nm long and lies across the top face of the AAA^+ ring. Most importantly, it appears to function as a lever, swinging its N-terminus a distance of ∼17 nm as the motor molecule transitions between the unprimed (nucleotide free) and the post-powerstroke (bound ADP and vanadate) steps of its ATPase cycle [3]. Our own earlier-predicted six-lobed structure generally resembles the AAA^+ core of the recent six-lobed structure, although without the additional linker domain and C-terminal domain formed by residues not included in our model.

1.4.1.3 Genomic Analysis of Midasin, Dynein's Nearest Neighbor in the AAA$^+$ Family

In the early summer of 2001, when Joan Garbarino and I were beginning to tire of failed attempts to express single or paired AAA$^+$ modules of cytoplasmic dynein in cultured insect cells, the challenge presented by the uncharacterized yeast open reading frame YLR106C, as potentially the closest evolutionary relative of dynein among the proteins of present-day eukaryotes, was too great for me to resist. I suggested to Joan that we perform a genomic survey of the YLR106C gene and determine the cellular location of its putative product in yeast in order to clarify whether this protein had some kind of motor function related to that of dynein.

A single-copy gene orthologous to YLR106C is present in all eukaryote genomes for which adequate sequence data are available. The six AAA$^+$ modules reported by Neuwald [128] form the N-terminal of its predicted product YLR106p. The carboxy-terminal region of YLR106p and its orthologs possesses a full set of the sequence motifs indicative of the MIDAS (metal-ion-dependent adhesion site) conformation that occurs in the I-domain of vertebrate integrin α-chains. In support of a uniform terminology over the broad range of eukaryotes in which the ortholog of YLR106p occurs, we proposed the name "midasin" (gene symbol: Mdn1, also known as Rea1 in yeast). To provide a reliable sequence of midasin in a second species for analysis of amino acid sequence conservation, we performed a full-length cDNA sequencing of the human gene for midasin.

Although Joan had not worked with yeast previously, she was happy to gain the experience. With help from the friendly yeast lab across the hall, she constructed a haploid hemagglutamin-tagged strain by homologous recombination into a diploid strain of *Saccharomyces*, followed by sporulation and tetrad dissection. After validating the mutated strain, she examined the immunostained cells by fluorescence microscopy and found that most or all of the hemagglutamin-tagged midasin was localized in the nucleus [188].

Amino acid sequence comparison between the AAA$^+$ domains of dynein and midasin confirmed that the two are substantially more closely related to each other than to any other protein in the AAA$^+$ superfamily. There is, however, an intriguing difference. Among the six AAA$^+$ modules of dynein, by far the most stringently conserved is the AAA1 module. On the other hand, in midasin the best-conserved modules are AAA2, AAA3, and AAA4 (Fig. 1.31). Despite this striking difference, the genes for dynein and midasin are clearly more closely related to each other than either of them is to any other known member of the AAA$^+$ family. This suggests that the genes for the HCs of dynein and of midasin diverged from their common ancestor at an early stage in the evolution of eukaryotes, before functional specialization of the concatenated six AAA$^+$ modules in the gene had occurred, possibly around the era of divergence between bacterial and eukaryotic ribosomes.

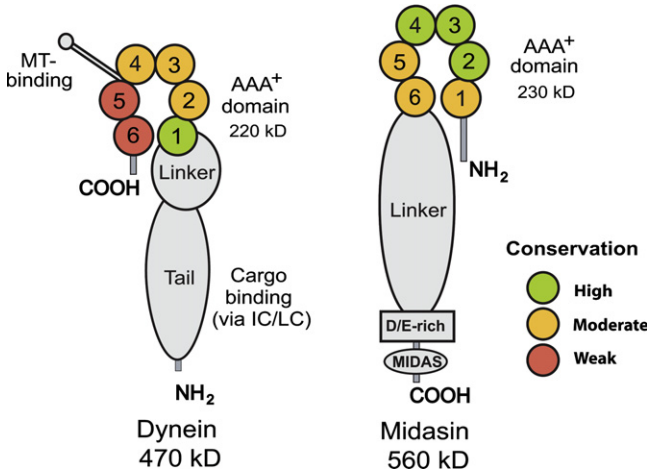

Figure 1.31 Comparison of domain organization inAAA$^+$ dynein and midasin. In dynein, the AAA$^+$ domain is at the C-terminal end of the HC, whereas in midasin it is at the N-terminal end of the HC. Within the AAA$^+$ domain of dynein, the amino acid sequence of the AAA1 module is substantially more highly conserved among organisms than those of the AAA2, AAA3, and AAA4 modules. The sequences of the AAA5 and AAA6 modules are sufficiently divergent that the modules have lost their ATP-binding sites and were not initially recognized as members of the AAA family. On the other hand, within the AAA$^+$ domain of midasin it is the AAA2, AAA3, and AAA4 modules that are most highly conserved, and the AAA1, AAA5, and AAA6 modules are substantially less well conserved [188].

Concurrently with our study, Ed Hurt's group in Heidelberg began a series of studies showing that Mdn1p/Rea1p plays a critical role as a chaperone during the maturation of the 60 S ribosome subunit in yeast [189,190].

Although Joan and I would have been content to explore midasin further, my NIH grant reviewers (sensibly) preferred otherwise and so we reverted to thinking of dynein (see Section 1.4.4).

1.4.2 Evolution Within the Dynein Gene Family

1.4.2.1 Early Studies

Preliminary indications of the extent of the dynein gene family and of the evolutionary relationships among its various members began to appear around 1995 as several research groups obtained partial sequences for different classes of dynein HC, together with full-length sequences for cytoplasmic dynein and a selected few isoforms of axonemal dynein [135,191–196]. Since around 2003, the increasing efficiency of genomic sequencing and assembly has resulted in the release of what amounts to almost a flood of sequence data, with genomes for well over 70 eukaryotic organisms being released so far.

1.4.2.2 Dynein Heavy Chains in the Sea Urchin Genome

When the annotation of the sea urchin (*Strongylocentrotus purpuratus*) genome was underway in the spring of 2006, I accepted an invitation from Bob Obar and Bob Morris to join the cytoskeleton team and be responsible for annotating the dynein HCs while Bob Obar annotated the dynein ICs and LCs. This provided me with an opportunity to complete full-length cDNA sequences for the 13 isoforms of dynein HC that I had deposited as partial sequences in Genbank 12 years earlier. The job of completing these dynein HC sequences turned out to be messier than I had anticipated because the 75–85 kb length of each HC gene spanned over two to five of the genomic scaffolds and the Sea Urchin Consortium had no plans for a more complete assembly. Fortunately, there was a complete annotated set of essentially full-length dynein HC sequences in the ensemble of mammalian genomes available on Jim Kent's excellent Blat server at the University of California, Santa Cruz [197] that could be used as indexing proteins [198]. Our complete set of cDNA sequences for the dynein light, intermediate, and HCs are available from the server of the Sea Urchin Genome Project [199] at http://annotation.hgsc.bcm.tmc.edu/Urchin/cgi-bin/pubLogin.cgi.

The earlier surveys of dynein genes in *Drosophila*, sea urchin, *Chlamydomonas*, *Tetrahymena*, and mammals had resulted in conflicting nomenclature for orthologous dynein genes in the different organisms. To encourage gradual adoption of a more uniform nomenclature, Bob Obar and I decided to use the internationally recognized names for dynein genes in the human genome [200,201] with as few changes as possible. The rate of evolutionary change in dynein HC genes has been sufficiently slow that full-length homologous genes of sea urchins and humans are 64–74% identical at the amino acid level and so are easily recognizable.

1.4.2.3 Natural History of the Dynein Heavy Chain Gene Family

Substantive evolutionary change in protein families occurs mostly through gene-duplication events, on a local or a whole-genome scale, followed either by selective fixation of the duplicated gene or by its loss from the genome [202]. In dynein, such duplications have become fixed more rarely than in most other gene families. This may be partly because the exceptionally large size of the dynein HC increases the cost of keeping it intact and possibly because the structural and functional integration of the several pre-existing dynein HC gene products in the highly conserved 9+2 axonemal structure of eukaryotes would make it difficult for a mutated newcomer to find even a temporary semi-stable niche. As a result of its relatively slow rate of change, the evolutionary history of the dynein HC family can be traced back to the last common ancestor of present eukaryotes with a fair degree of certainty [133,198].

For a study reported at the Second International Dynein Workshop in Kobe, 2009, I prepared a set of 496 approximately full-length dynein HC sequences (average

length: 4331 amino acids; range: 3157−7449) by manual homology-based curation of 50 diverse eukaryote genomes, representing five of the six currently accepted supergroups of deeply branched taxa. Analysis of multiple-sequence alignments of appropriate full-length subsets has confirmed that the dynein HC family consists of nine distinct subfamilies, each associated largely with a distinct cellular function or axonemal structure (Fig. 1.32). Of these subfamilies, cytoplasmic dynein and IFT dynein (also called cytoplasmic dynein 2) are homodimers; two subfamilies of outer-arm dyneins, ODA-β and ODA-γ, form the heterodimeric and heterotrimeric outer arms in the axonemal structure; two subfamilies of inner-arm dyneins, IDA1-α and IDA1-β, form the dimeric inner-arm 1 structure; while the remaining three subfamilies of inner-arm dyneins, IDA3, IDA4, and IDA5, are all monomeric and form the inner-arm-3, -4, and -5 structures, respectively [79,147,198].

More recent studies of the genomic distribution of the dynein HC genes corresponding to the α, β, and γ HCs of outer-arm dynein indicate that outer-arm dynein has a two-headed structure in animals, including sponges and chytrid fungi, whereas it is three-headed in algae, plants, alveolate protozoa, and most stramenopiles. In excavate protozoa, the distribution appears heterogeneous, with a two-headed outer arm in *Trichomonas*, *Giardia*, *Trypanosoma*, and *Leishmania* but probably a three-headed outer arm in *Naegleria* (Fig. 1.32; [198,203,204]). A classification of protozoa based upon the presence or absence of the α-HC gene that contributes the third head of a three-headed outer arm dynein would thus group most of the best-characterized excavate taxa together with animals and fungi. This grouping would not be in accord with recent work based principally upon a fusion of the pair of essential genes for dihydrofolate reductase and thymidylate synthase [205,206], and it is possible that the outer-arm dynein genes have traveled a more complex evolutionary pathway.

Loss of one or more dynein HC subfamilies has occurred during the evolution of some lines of present eukaryote taxa, so that many classes of present-day organisms contain only a subset of the full dynein HC family. Importantly, however, at least one representative of each dynein HC subfamily is found in all five of the eukaryotic taxonomic supergroups analyzed, indicating that all nine dynein HC subfamilies were already distinct in the last common ancestor of present eukaryotes [198,203,207,208].

Occasional dynein HC gene duplications have become fixed and propagated extensively through evolution into descendent taxa. Such fixation of duplicated genes has occurred most extensively in the monomeric inner arms, IDA3 and IDA5, but is also moderately common in the ODA-β and ODA-γ subfamilies of the outer arms (Fig. 1.32). On the other hand, fixation of duplicated copies of the dimeric inner arm 1 genes (IDA1-α and IDA1-β) has been extremely rare; these genes have clearly been the most stringently conserved of all the dynein HC genes, possibly indicating their origin in the early evolution of the 9+2 axoneme

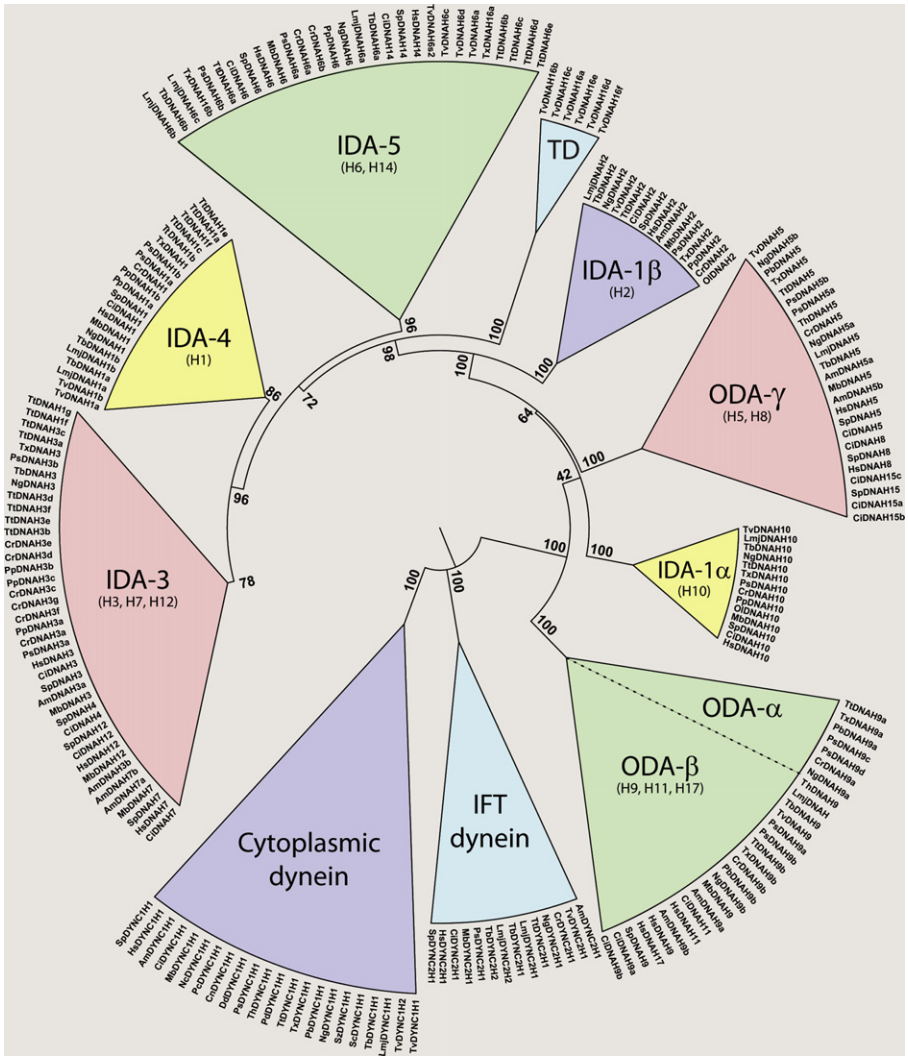

Figure 1.32 Phylogenetic tree of dynein HC genes in the genomes of 20 representative organisms. The genes for each of the nine subfamilies of dynein HC are collapsed into a circular segment. In each segment, the radius represents the sequence diversity of full-length genes among the members of that subfamily and the angle represents the total number of subfamily-member genes present in the 20 organisms. ODA-α, ODA-β, and ODA-γ: HC subfamilies forming outer arm dynein; IDA-1α and IDA-1β: HC subfamilies forming dimeric inner dynein arm1; IDA-3, IDA-4, and IDA-5: HC subfamilies forming monomeric inner dynein arm-3, -4, and -5, respectively; TD: orphan group of seven interrelated dynein HC genes of unknown function, as yet identified only in *Trichomonas vaginalis*. Organisms are: Am, *Apis mellifera*; Ce, *Caenorhabditis elegans*; Ci, *Ciona intestinalis*; Cr, *Chlamydomonas reinhardtii*; Dd, *Dictyostelium discoidium*; Hs, *Homo sapiens*; Lmj, *Leishmania major*; Mb, *Monosiga brevicollis*; Nc, *Neurospora crassa*; Ng, *Naegleria gruberi*; Pp, *Physcomitrella patens*; Ps, *Phytophthora sojae*; Sc, *Saccharomyces cerevisiae*; Sp, *Strongylocentrotus purpuratus*; Sz, *Schizosaccharomyces pombe*; Tb, *Trypanosoma brucei*; Th, *Thalassiosira pseudonana*; Tt, *Tetrahymena thermophila*; Tv, *Trichomonas vaginalis*; Tx, *Toxoplasma gondii*. Essentially full-length amino acid sequences were aligned with *Clustal* [230]. The number at each node of the tree indicates its percent statistical significance by bootstrap analysis in *Mega* (minimum evolution option and JTT matrix with $\gamma = 1.0$) [231]. The figure was prepared with *FigTree* (http://tree.bio.ed.ac.uk/software/figtree/).

[209]. Fixation of duplicated copies of the two homodimeric cytoplasmic dynein genes has also been extremely rare, but in this case the genes have been conserved somewhat less stringently, presumably because they have undergone occasional pressure to diverge as their products have taken on new tasks during cellular evolution (for example, the gene name *beethoven* that symbolizes the auditory role of the IFT dynein gene product in *Drosophila*).

The presence of a well-conserved, but hitherto underappreciated, sequence motif Exx(F/Y)W, located within the N-terminal 1 domain (Pfam: PF08385; [210]) approximately 240 residues from the N-terminus of all dimeric dynein HCs, both axonemal and cytoplasmic, together with its absence from all monomeric dynein HCs, suggests that the residues in this motif form a significant part of a highly conserved dimerizing interface that became established prior to the evolutionary split between cytoplasmic and axonemal dyneins.

In addition to the above-known dynein HC subfamilies, many eukaryote genomes possess one or more open reading frames of ~14 kb that encode what appears to be a highly aberrant form of "orphan" dynein HC. This putative protein retains critical conserved residues that characterize the four ATP-binding AAA domains, as well as the coiled-coil stalk and MTBD, of a typical dynein, whereas most other normally conserved residues are highly mutated. An example is the annotated human gene DNHD1, which is only 90 and 70% identical to its orthologs in chimpanzee and mouse, respectively, with an unusually low value of 3.4 for the ratio of synonymous to non-synonymous mutations between mouse and human, compared to ratios of 187 for cytoplasmic dynein and 70 for IDA3. I suggest that these open reading frames may represent "ghost genes" — remnants of earlier duplicated dynein HC genes, probably cytoplasmic dynein, that appear to have lost most or all of their functionality but are unable to decay at a normal rate, possibly because introduction of a premature stop codon usually results in an N-terminal dynein HC fragment that poisons the dimerization of cytoplasmic dynein and so is toxic to the organism [211].

1.4.3 Regulation of Binding Affinity in Dynein's Microtubule-Binding Domain

While browsing through the literature to look for a promising new dynein project of a size that would be manageable for Joan and myself, I happened upon Melissa Gee's excellent paper describing her expression of different regions of the dynein HC in tissue culture cells [90]. In describing the structure of the dynein coiled-coil stalk and its MTBD, she happened to mention seryl t-RNA synthetase (SRS) as an example of a second protein that possesses a similar projecting hairpin stalk. I was struck by the thought of constructing a chimeric protein in which a basal stub of the SRS coiled-coil stalk would be used to provide a stable platform onto which we could splice different lengths and heptad registries of the dynein coiled-coil stalk supporting the MTBD. By adding or removing a small number of residues from

the splice junction in one strand of the coiled coil, it would be possible to create a series of protein constructs with different heptad registries in the dynein portion of the fused stalk. My enthusiasm for this idea increased further upon checking the protein structure database and finding a 2.5 Å structure for the SRS from *Thermus thermophilus* (PDB: 1SRY) that was reported as stable at temperatures up to 70°C. If everything were to go really well, it might even be possible to use the SRS structure for phasing the X-ray diffraction pattern of the SRS-MTBD fusion protein. It is very, very rare in science for dreams of this kind to actually work out as planned, but in this case they essentially did.

We had only eight weeks to obtain enough preliminary results to convince the NIH reviewers that our project was feasible, so I undertook to do some of the molecular biology bench work myself, in spite of the fact that I had never performed these techniques with my own hands previously. Under Joan's expert tutelage, I designed, synthesized, and cloned an SRS construct with appropriate restriction sites and codons used efficiently by *E. coli*, while Joan was busy cloning cDNA inserts encoding the MTBD and its stalk from mouse cytoplasmic dynein. Working together, we managed to produce eight fusion constructs of the MTBD-SRS with different lengths of the coiled coil stalk and to show that they expressed well in *E. coli*, with most yielding ample amounts of soluble protein.

When it came to assaying the microtubule-binding affinity of the different MTBD-SRS constructs, we were happy to see that the protein products of these MTBD-SRS constructs showed significant binding to microtubules *in vitro*, although the native dimeric structure of the SRS introduced unwanted steric effects that complicated the assay of binding affinity. To avoid this complication, I synthesized three mutated monomeric versions of the SRS that contained 8, 15, or 21 amino acid substitutions in their dimerizing interface. The SRS construct with 15 mutations yielded protein that was monomeric at all concentrations, as well as being stable at temperatures up to 60°C. This monomerized SRS was used in subsequent assays of binding affinity.

For the main part of the project, Joan and her new assistant, Carol Tan, cloned and expressed the 100-odd different MTBD-SRS fusion constructs that we used, as well as performing the MTBD-SRS binding assays and their gels. Andrew Carter in the Vale lab at the University of California, San Francisco analyzed the hydrophobic heptad repeats in the two strands of the dynein coiled-coil stalk, built a homology-based space-filled model of the coiled coil to examine the possibility of a sliding motion between the two strands of the coil, and wrote the first draft of the paper. Sam Reck-Peterson, also in the Vale lab, performed the initial MTBD-SRS binding assays. I designed the MTBD-SRS constructs, quantified the electrophoresis gels of MTBD-binding assays, and calculated the microtubule-binding affinities of the constructs.

By surveying a variety of alignments between the heptad repeats in the two strands of the coiled coil, we identified three configurations that appeared the

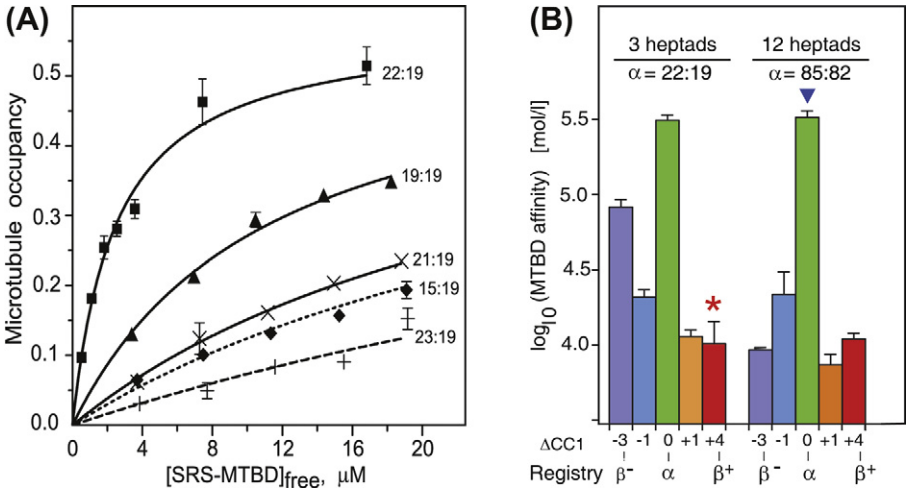

Figure 1.33 Microtubule-binding affinity of different MTBD-SRS constructs. (A) Microtubule-binding assays of dynein microtubule-binding domain-seryl tRNA-synthetase (MTBD-SRS) constructs containing the MTBD of mouse cytoplasmic dynein with a three-heptad length of its coiled-coil stalk in different registry alignments. Construct MTBD-SRS 22:19, with 22 amino acids in coiled coil 1 and 19 amino acids in coiled coil 2, represents the high-affinity α-registry; all other registries have a lower affinity. (B) Binding affinity of SRS-MTBD constructs with coiled-coil lengths of three heptads (one-quarter length) and 12 heptads (full length) in different registries. Red asterisk indicates the affinity of MTBD-SRS 26:19, the three-heptad β^+-registry construct used for crystallizing. *Reproduced from [212,214] with permission.*

most likely to be of biological importance (Fig. 1.33). One was an alignment (termed α) that yielded a protein displaying high affinity for microtubules (2.2 μM). The other two alignments (termed β^- and β^+) involved a half-heptad shift from the α-alignment, obtained by either shortening (by three residues) or lengthening (by four residues) of the upstream strand of the dynein coiled coil, and they yielded proteins of medium and low affinity, respectively. Essentially all other alignments showed at least 10-fold lower affinity for microtubules. Based upon these results and upon an unusual feature of the heptad periodicity in the coiled-coil stalk, we proposed that dynein utilizes small amounts of sliding displacement between the two strands of its coiled-coil stalk as a means of communication between the AAA^+ core of the motor and the MTBD during the ATP-dependent mechanochemical cycle of intact dynein [212].

1.4.4 Helix Sliding in the Dynein Stalk Couples ATPase and Microtubule Binding

In the winter of 2005, when our study of the MTBD-SRS binding affinity was nearly complete, we presented it as a poster at a meeting of the Biophysics Society that was also attended by Kazuo Sutoh, whose group at the University of Tokyo

was doing beautiful work on the enzymatic properties of the cytoplasmic dynein motor domain expressed in *Dictyostelium*. During the meeting, we discussed a possible future experiment in which his lab would use oxidation of introduced pairs of cysteine residues to lock the heptad repeats of the dynein coiled-coiled stalk into different registers, including α, β^-, and β^+ alignments that we had identified.

Using this procedure, Takahide Kon, a postdoctoral researcher in Sutoh's group was able to show that a change in stalk alignment between the α and β^+ registries modulated the microtubule-binding affinity of the *Dictyostelium* dynein motor domain in a manner very similar to that we had observed with our model MTBD-SRS constructs. Moreover, these new data substantially extended our results by demonstrating that the same registry change also modulates the rate of ATP hydrolysis by the dynein motor domain in a manner predicted for a two-way stalk-mediated communication between the AAA^+ core of the motor and its MTBD during the mechanochemical cycle of cytoplasmic dynein [213].

1.4.5 Crystal Structure of Dynein's ATP-Sensitive Microtubule-Binding Domain

In this case, our collaborator, Andrew Carter, an experienced crystallographer in the Vale lab at the University of California, San Francisco, headed the project. After some initial trials of crystal growing in the elaborate facility at the University of California, San Francisco, where Andrew taught her how to set up trays, Joan decided that it would be more efficient for her to set up the trays manually on her own lab bench in Berkeley, which stays at a nearly constant temperature year-round. My main role was to lead discussion on choosing which of our many constructs to work with.

As protein flexibility is generally inimical to crystallizing, we began trials with the monomeric short-stalked three-heptad MTBD-SRS construct in the high-affinity α-alignment which had been the center of our earlier work [212]. However, the results of these initial trials were unpromising, probably because of inadequate protein stability. Over the next 12 months, Joan achieved gradually improved trial results, first by switching to one of the low-affinity β^+ MTBD-SRS constructs that had consistently higher thermostability (Table 1.4) and later by reverting the construct to contain the native dimeric form of SRS so as to avoid the less-well-structured region of the SRS which had been introduced by our earlier mutations to generate a monomeric SRS for the binding studies.

Final success came when Joan was teaching her helper, Wesley Shipley, to set up crystal trays. His very first set contained wells at a lower pH, at which decent-looking crystals ranging up to 150 μm in size appeared overnight. The size of these crystals and the speed with which they appeared gave us serious doubts that they might simply be magnesium phosphate, but this proved an unnecessary

Table 1.4 Thermal stability of MTBD-SRS constructs

Registry	β^- (α-3)	α-1	α	α+1	β^+ (α+4)
Stalk length(heptads)	Protein Remaining in Supernatant (percent)				
3	42.3 ± 4.4	38.2 ± 2.8	51.0 ± 1.4	47.2 ± 2.6	*94.3 ± 0.5
7	3.8 ± 3.8	2.5 ± 0.1	4.9 ± 4.9	0	66.4 ± 1.2
10	18.7 ± 0.1	15.5 ± 4.7	42.7 ± 5.1	98.0 ± 0.1	94.B ± 2.1
11	30.7 ± 1.0	18.1 ± 0.4	13.8 ± 4.5	17.8 ± 0.6	98.3 ± 2.5
12	97.0 ± 4.2	86.9 ± 6.6	48.6 ± 0.7	30.9 ± 0.7	83.0 ± 0.9
14	34.1 ± 0.1	27.9 ± 8.7	39.3 ± 2.2	37.7 ± 2.7	48.1 ± 5.9

**Thermal stability was assayed by heating at 42° C for 30 min, followed by ammonium sulphate precipitation of denatured protein at 0° C and centrifugation. Constructs with the β+ registry, including the three-heptad construct (MTBD-SRS 26:19) that was crystallized showed consistently higher stability than all other constructs.*

worry. In the X-ray beam of the Advanced Light Source at the Lawrence Berkeley lab, the best of the crystals diffracted uniformly out to 2.3 Å. After phasing the reflections by molecular replacement with the dimeric SRS as a search model, Andrew skillfully used multiple rounds of building and refinement to obtain the structure of the MTBD and its partial stalk with an R_{free} quality of 0.25.

At this point, Andrew suggested that we might try a quick effort to confirm the helix linking in his structure by making fresh crystals of our protein containing selenomethionine. We had only two weeks in which to do this before the Advanced Light Source shut down for a period of extended maintenance. With superb teamwork, Joan and Wesley managed to grow up the bacteria, extract and purify the protein, and set up crystal trays by the day before our scheduled time on the Advanced Light Source. The protein cooperated by again producing crystals overnight and some of them diffracted to about 3.5 Å. From these data, Andrew was able to generate a phased anomalous difference map that confirmed the original build by showing all the selenium atoms close to their expected positions.

The MTBD is formed by a bundle of six short α-helices (H1 to H6) that has one side packed against the two strands of the coiled-coil stalk (Figs. 1.34 and 1.35; [214]). The probable microtubule-binding surface of the MTBD is located opposite the entry of the coiled coil into the domain and involves three helices — H1, H3, and H6 — that have a high density of conserved surface-accessible residues, including most of those known to block microtubule binding when mutated to alanine [212,215]. Confirmation for this identification of the microtubule contact surface was obtained through collaboration with Liz Wilson-Kubalek in Ron Milligan's lab, who made a cryo-EM helical reconstruction of one of our longer high-affinity MTBD-SRS constructs bound to microtubules [214]. Our crystal structure fit well

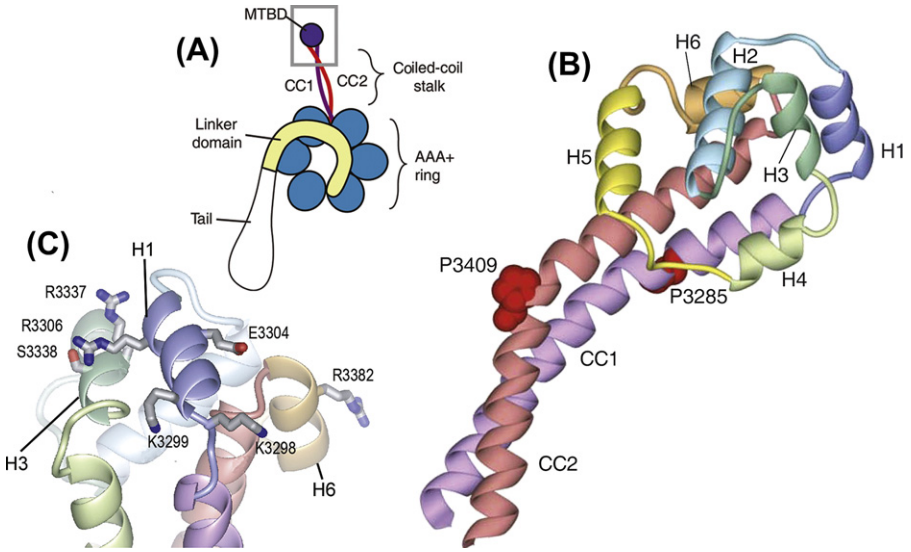

Figure 1.34 Crystal structure of the β^{+}-conformation of the microtubule-binding domain and partial coiled-coil stalk of cytoplasmic dynein from mouse. (A) Cartoon showing the sub-domain structure of the dynein motor domain that forms the C-terminal two-thirds of the HC. A gray box highlights the microtubule-binding domain and region of the stalk for which the atomic structure was obtained. (B) Crystal structure of the MTBD, showing the two α helices of the stalk (CC1, purple; CC2, red) that extend out of the SRS coiled coil and connect to the six-helix bundle (H1 to H6) forming the MTBD proper. (C) Microtubule-binding surface of the MTBD, formed by the three helices H1, H3 and H6. Side chains of seven amino acid residues known to block microtubule binding when mutated to alanine [212,215] are shown in stick format. *Reproduced from [214] with permission.*

Figure 1.35 Members of the dynein MTBD crystallizing team. From left: Andrew Carter, Joan Garbarino (front), Wesley Shipley (rear), and Ian Gibbons. The photograph was taken in May 2008 after collecting a 2.3 Å diffraction data set at the X-ray beam line of the ALS, Lawrence Berkeley National Laboratory.

into her cryo-EM density map and placed MTBD helices H1 and H3 into the same groove between the α and β tubulin subunits as the kinesin motor uses for binding to microtubules [216,217].

The structure of the MTBD reveals a pronounced asymmetry in the extent to which the two strands of the coiled-coil stalk, CC1 and CC2, are integrated into the body of the MTBD. This asymmetry suggests a plausible mechanism for modulating the affinity of the MTBD for microtubules that involves a sliding displacement of CC1, which connects directly to MTBD helix H1 in the microtubule-binding interface, relative to CC2, which is more deeply embedded into the structure of the MTBD. This mechanism supports our earlier hypothesis that bidirectional communication between the MTBD and the AAA^+ ATPase core of the dynein motor involves a sliding displacement between the two strands of the coiled-coil stalk [212,218]. However, a complete understanding of the communication mechanism will require structures of the stalk in different states of the dynein mechanochemical cycle, and no detailed structure for the strong microtubule-binding form of the stalk and MTBD is yet available.

1.5 The Pluses of Working on a Minus-End-Directed Motor

Looking back over my career, I realize how incredibly fortunate I was to have started my research in the late 1950s, just as the enormous expansion of biological research was getting started. Thanks to the strong public support of education in England at the time, I have been able to have a highly satisfying career and to enjoy the benefits of collaboration and friendship with an international group of committed scientists.

Even in the early days, I never doubted my liking for dynein as a topic for research. Its ATPase activity, its location on microtubules, and its relative quantity in the axoneme all led me to believe that it played a major role in the different transport systems that cells require for support of their growth, division, and differentiation. Although its high molecular mass and the relatively modest quantities available for study were sometimes constraining, the handle provided by its ATPase activity made it relatively easy to follow and assess its functioning. I've never regretted the decision to do so. Research with dynein has provided opportunities for utilizing a wide range of experimental techniques, from the simplicity of qualitative hydrodynamics on a microscope slide and the cookery of measuring protein thermostability, to the complexities of enzyme kinetics and protein crystallography. Dynein may be a minus-end directed motor, but working with it has had lots of pluses. I hope the fun that we have managed to have will encourage the highly talented young scientists who are bringing their powers to bear on the many fascinating secrets that remain in dynein, as well as in the other molecular motors, and, indeed, in most aspects of human biology.

Acknowledgments

In addition to the major research contributions of the students, associates, and collaborators mentioned in the text, my life as a scientist has benefited from the support of many friends, including A.V. (Bill) Grimstone, John T. Edsall, John W.S. Pringle, Keith R. Porter, Robert E. Kane, Lawrence H. Piette, Pierre and Paulette Vignais, Marie Paule and Jacky Cosson, Jerrold Chun, Terence A. Rogers, Baccio Baccetti, Hideo Mohri, Ron Vale, and Beth Burnside. Because of the focused approach of this account, it is not a complete history of dynein research and even less of cilia and flagella. Many important contributions from other research groups are omitted or mentioned only briefly for reasons of space. More comprehensive references are given in other reviews [79,150,219–224].

I thank our son and daughter, Pete and Wendy Gibbons, for their comments and suggestions regarding this chapter.

I gratefully acknowledge long-term funding, both to Barbara and myself, by the U.S. National Institutes of Health. Additional support has been provided by the National Science Foundation, and by a fellowship from the John Simon Guggenheim Foundation. Our research in Honolulu would have been impossible without the generous financial support of the State of Hawaii to the research activities of the kewalo Marine Laboratory and Pacific Biomedical Research Center of the University of Hawaii.

1.6 Epilogue

Portions of this text have been taken from a presentation made by my wife, Dr. Barbara Gibbons, at the annual meeting of the American Society for Cell Biology in 1994. Sadly, Barbara was diagnosed with Parkinson's disease in 2002 and is now too ill to participate in the preparation of this paper. I badly miss her organizing and communication skills. It is only recently that I have come to realize that my personality fits well into the Asperger's form of High Functioning Autism. For most of my life, I have managed to get along, just considering myself as a detail-oriented person who is shy and feels awkward in social intercourse. I hope that this paper succeeds in portraying how the collaboration between Barbara and myself allowed us to meet the challenges and thrive on a life in science and that our example will encourage others to follow up enthusiastically on all the opportunities that any special aspects of their personality may present them with.

References

[1] S.L. Reck-Peterson, R.D. Vale, Molecular dissection of the roles of nucleotide binding and hydrolysis in dynein's AAA domains in *Saccharomyces cerevisiae*, Proc. Natl. Acad. Sci. USA 101 (2004) 1491–1495.

[2] T. Kon, M. Nishiura, R. Ohkura, Y.Y. Toyoshima, K. Sutoh, Distinct functions of nucleotide-binding/hydrolysis sites in the four AAA modules of cytoplasmic dynein, Biochemistry 43 (2004) 11266–11274.

[3] A.J. Roberts, N. Numata, M.L. Walker, Y.S. Kato, B. Malkova, T. Kon, R. Ohkura, F. Arisaka, P.J. Knight, K. Sutoh, S.A. Burgess, AAA^{+} ring and linker swing mechanism in the dynein motor, Cell 136 (2009) 485–495.

[4] C. Cho, S.L. Reck-Peterson, R.D. Vale, Regulatory ATPase sites of cytoplasmic dynein affect processivity and force generation, J. Biol. Chem. 283 (2008) 25839–25845.

[5] T. Heuser, M. Raytchev, J. Krell, M.E. Porter, D. Nicastro, The dynein regulatory complex is the nexin link and a major regulatory node in cilia and flagella, J. Cell Biol. 187 (2009) 921–933.
[6] T. Movassagh, K.H. Bui, H. Sakakibara, K. Oiwa, T. Ishikawa, Nucleotide-induced global conformational changes of flagellar dynein arms revealed by *in situ* analysis, Nat. Struct. Mol. Biol. 17 (2010) 761–767.
[7] J.R.G. Bradfield, Fibre patterns in animal flagella and cilia, Symp. Soc. Exp. Biol. 9 (1955) 306–334.
[8] I.R. Gibbons, J.R.G. Bradfield, The fine structure of nuclei during sperm maturation in the locust, J. Biophys. Biochem. Cytol. 3 (1957) 133–140.
[9] J.E. Dowling, I.R. Gibbons, The fine structure of the pigment epithelium in the albino rat, J. Cell Biol. 14 (1962) 459–474.
[10] I.R. Gibbons, A.V. Grimstone, On flagellar structure in certain flagellates, J. Biophys. Biochem. Cytol. 7 (1960) 697–716.
[11] P. Strnad, P. Gonczy, Mechanisms of procentriole formation, Trends Cell Biol. 18 (2008) 389–396.
[12] J.A. Deane, D.G. Cole, E.S. Seeley, D.R. Diener, J.L. Rosenbaum, Localization of intraflagellar transport protein IFT52 identifies basal body transitional fibers as the docking site for IFT particles, Curr. Biol. 11 (2001) 1586–1590.
[13] B. Afzelius, Electron microscopy of the sperm tail: Results obtained with a new fixative, J. Biophys. Biochem. Cytol. 5 (1959) 269–278.
[14] H.E. Huxley, The double array of filaments in cross-striated muscle, J. Biophys. Biochem. Cytol. 3 (1957) 631–648.
[15] I.R. Gibbons, Structural asymmetry in cilia and flagella, Nature 190 (1961) 1128–1129.
[16] B. Parducz, [Physiological studies of excitation in Ciliata. I. The action system of Paramecium. J. Acta Microbiol. Acad. Sci. Hung. 1 (1954) 175–221.
[17] I.R. Gibbons, Reactivation of glycerinated cilia from *Tetrahymena pyriformis*, J. Cell Biol. 25 (1965) 400–402.
[18] N. Hirokawa, Y. Tanaka, Y. Okada, S. Takeda, Nodal flow and the generation of left–right asymmetry, Cell 125 (2006) 33–45.
[19] P. Satir, Studies on cilia: The fixation of the metachronal wave, J. Cell Biol. 18 (1963) 345–365.
[20] P. Satir, Studies on cilia: II. Examination of the distal region of the ciliary shaft and the role of the filaments in motility, J. Cell Biol. 26 (1965) 805–834.
[21] P. Satir, Studies on cilia. III. Further studies on the cilium tip and a "sliding filament" model of ciliary motility, J. Cell Biol. 39 (1968) 77–94.
[22] C.J. Brokaw, Mechanisms of sperm movement, Symp. Soc. Exp. Biol. 22 (1968) 101–116.
[23] H. Hoffmann-Berling, Geisselmodelle und adenosintriphosphat ATP, Biochim. Biophys. Acta. 16 (1955) 146–154.
[24] C.J. Brokaw, Decreased adenosine triphosphatase activity of flagella from a paralyzed mutant of *Chlamydomonas moewusii*, Exp. Cell Res. 19 (1960) 430–432.
[25] F.M. Child, Some aspects of the chemistry of cilia and flagella, Exp. Cell Res. Suppl. 8 (1961) 47–53.
[26] M.R. Watson, J.M. Hopkins, Isolated cilia from *Tetrahymena pyriformis*, Exp. Cell Res. 28 (1962) 280–895.
[27] R.J. Britten, R.B. Roberts, High-resolution density gradient sedimentation analysis, Science 131 (1960) 32–33.
[28] R.G. Martin, B.N. Ames, A method for determining the sedimentation behavior of enzymes: Application to protein mixtures, J. Biol. Chem. 236 (1961) 1372–1379.
[29] I.R. Gibbons, Studies on the protein components from cilia of *Tetrahymena pyriformis*, Proc. Natl. Acad. Sci. USA 50 (1963) 1002–1010.

[30] A.V. Grimstone, I.R. Gibbons, Fine structure of the centriolar apparatus and associated structures in the complex flagellates *Trichonympha* and *Pseudotrichonympha*, Phil. Trans. Royal Soc. London Series B 250 (1966) 215–242.
[31] K.A. Johnson, J.S. Wall, Structure and molecular weight of the dynein ATPase, J. Cell Biol. 96 (1983) 669–678.
[32] I.R. Gibbons, A.J. Rowe, Dynein: A protein with adenosine triphosphatase activity from cilia, Science. 149 (1965) 424–426.
[33] I.R. Gibbons, Studies on the adenosine triphosphatase activity of 14 S and 30 S dynein from cilia of *Tetrahymena*, J. Biol. Chem. 241 (1966) 5590–5596.
[34] I.R. Gibbons, An effect of adenosine triphosphate on the light scattered by suspensions of cilia, J. Cell Biol. 26 (1965) 707–712.
[35] M. Takahashi, Y. Tonomura, Binding of 30s dynein with the B-tubule of the outer doublet of axonemes from *Tetrahymena pyriformis* and adenosine triphosphate-induced dissociation of the complex, J. Biochem. 84 (1978) 1339–1355.
[36] F.L. Renaud, A.J. Rowe, I.R. Gibbons, Some properties of the protein forming the outer fibers of cilia, J. Cell Biol. 36 (1968) 79–90.
[37] R.E. Stephens, F.L. Renaud, I.R. Gibbons, Guanine nucleotide associated with the protein of the outer fibers of flagella and cilia, Science 156 (1967) 1606–1608.
[38] R.C. Weisenberg, G.G. Borisy, E.W. Taylor, The colchicine-binding protein of mammalian brain and its relation to microtubules, Biochemistry 7 (1968) 4466–4479.
[39] H. Mohri, Amino-acid composition of "Tubulin" constituting microtubules of sperm flagella, Nature 217 (1968) 1053–1054.
[40] R.C. Weisenberg, Microtubule formation *in vitro* in solutions containing low calcium concentrations, Science 177 (1972) 1104–1105.
[41] C. Allen, G.G. Borisy, Structural polarity and directional growth of microtubules of *Chlamydomonas* flagella, J. Mol. Biol. 90 (1974) 381–402.
[42] J. Gray, The movement of sea-urchin spermatozoa, J. Exp. Biol. 32 (1955) 775–801.
[43] I.R. Gibbons, Chemical dissection of cilia, Arch. Biol. Lige. 76 (1965) 317–352.
[44] B.H. Gibbons, I.R. Gibbons, Flagellar movement and adenosine triphosphatase activity in sea urchin sperm extracted with Triton X-100, J. Cell Biol. 54 (1972) 75–97.
[45] I.R. Gibbons, in: B.A. Afzelius (Ed.), the Functional Anatomy of the Spermatozoon, Pergamon Press, Oxford and New York, 1975, pp. 127–140.
[46] B.H. Gibbons, I.R. Gibbons, The effect of partial extraction of dynein arms on the movement of reactivated sea-urchin sperm, J. Cell Sci. 13 (1973) 337–357.
[47] C.J. Brokaw, Effects of increased viscosity on the movements of some invertebrate spermatozoa, J. Exp. Biol. 45 (1966) 113–139.
[48] C.J. Brokaw, I.R. Gibbons, Mechanisms of movement in flagella and cilia, in: T.T.Y. Wu, C.J. Brokaw, C. Brennen (Eds.), Swimming and Flying in Nature 1, Plenum Publishing Corp, New York, 1975, pp. 89–126.
[49] J.A. Evans, G. Mocz, I.R. Gibbons, Activation of dynein 1 adenosine triphosphatase by monovalent salts and inhibition by vanadate, J. Biol. Chem. 261 (1986) 14039–14043.
[50] J.A. Evans, I.R. Gibbons, Activation of dynein 1 adenosine triphosphatase by organic solvents and by Triton X-100, J. Biol. Chem. 261 (1986) 14044–14048.
[51] B.H. Gibbons, W.J. Tang, I.R. Gibbons, Organic anions stabilize the reactivated motility of sperm flagella and the latency of dynein 1 ATPase activity, J. Cell Biol. 101 (1985) 1281–1287.
[52] A. Pijper, Darkground studies of the flagellar and somatic aggregation of *B. typhosue*, J. Path. Bact. 47 (1938) 1–17.
[53] K.E. Summers, I.R. Gibbons, Adenosine triphosphate-induced sliding of tubules in trypsin-treated flagella of sea-urchin sperm, Proc. Natl. Acad. Sci. USA 68 (1971) 3092–3096.

[54] K. Whalley, Milestone 4(1965): Dynein, the first microtubule-dependent motor: Beating a path to success. Available from, Nature Reviews Neuroscience (2008), http://www.nature.com/milestones/milecyto/full/milecyto04.html.
[55] K.E. Summers, I.R. Gibbons, Effects of trypsin digestion on flagellar structures and their relationship to motility, J. Cell Biol. 58 (1973) 618–629.
[56] I.R. Gibbons, E. Fronk, Some properties of bound and soluble dynein from sea urchin sperm flagella, J. Cell Biol. 54 (1972) 365–381.
[57] B.H. Gibbons, I.R. Gibbons, Relationship between the latent adenosine triphosphatase state of dynein 1 and its ability to recombine functionally with KCl-extracted sea urchin sperm flagella, J. Biol. Chem. 254 (1979) 197–201.
[58] B.H. Gibbons, I.R. Gibbons, Functional recombination of dynein 1 with demembranated sea urchin sperm partially extracted with KC1, Biochem. Biophys. Res. Commun. 73 (1976) 1–6.
[59] B.H. Gibbons, I.R. Gibbons, Properties of flagellar "rigor waves" formed by abrupt removal of adenosine triphosphate from actively swimming sea urchin sperm, J. Cell Biol. 63 (1974) 970–985.
[60] I.R. Gibbons, The molecular basis of flagellar motility in sea urchin spermatozoa, in: S. Inoué, R.E. Stephens (Eds.), Molecules and Cell Movement, Raven Press, New York, 1975, pp. 207–232.
[61] C.B. Lindemann, I.R. Gibbons, Adenosine triphosphate-induced motility and sliding of filaments in mammalian sperm extracted with Triton X-100, J. Cell Biol. 65 (1975) 147–162.
[62] W.S. Sale, P. Satir, Direction of active sliding of microtubules in *Tetrahymena* cilia, Proc. Natl. Acad. Sci. USA 74 (1977) 2045–2049.
[63] W.S. Sale, The axonemal axis and Ca^{2+}-induced asymmetry of active microtubule sliding in sea urchin sperm tails, J. Cell Biol. 102 (1986) 2042–2052.
[64] P. Satir, T. Matsuoka, Splitting the ciliary axoneme: Implications for a "switch-point" model of dynein arm activity in ciliary motion, Cell Motil. Cytoskeleton 14 (1989) 345–358.
[65] C.J. Brokaw, Direct measurements of sliding between outer doublet microtubules in swimming sperm flagella, Science 243 (1989) 1593–1596.
[66] C.J. Brokaw, Microtubule sliding in swimming sperm flagella: Direct and indirect measurements on sea urchin and tunicate spermatozoa, J. Cell Biol. 114 (1991) 1201–1215.
[67] C.S. Dey, C.J. Brokaw, Activation of Ciona sperm motility: Phosphorylation of dynein polypeptides and effects of a tyrosine kinase inhibitor, J. Cell Sci. 100 (Pt 4) (1991) 815–824.
[68] K. Weber, M. Osborn, The reliability of molecular weight determinations by dodecyl sulfate-polyacrylamide gel electrophoresis, J. Biol. Chem. 244 (1969) 4406–4412.
[69] A.L. Shapiro, E. Vinuela, J.V. Maizel, Molecular weight estimation of polypeptide chains by electrophoresis in SDS-polyacrylamide gels, Biochem. Biophys. Res. Commun. 28 (1967) 815–820.
[70] R.W. Linck, Biochemical comparison of ciliary and flagellar axonemes from the bay scallop, *Aequipecten irradians*, Biol. Bull. Woods Hole. 139 (1970) 429a.
[71] R.W. Linck, Chemical and structural differences between cilia and flagella from the lamellibranch mollusc, *Aequipecten irradians*, J. Cell Sci. 12 (1973) 951–981.
[72] H.L. Kincaid, B.H. Gibbons, I.R. Gibbons, The salt-extractable fraction of dynein from sea urchin sperm flagella: An analysis by gel electrophoresis and by adenosine triphosphatase activity, J. Supramol. Struct. 1 (1973) 461–470.
[73] I. Mabuchi, T. Shimizu, Electrophoretic studies on dyneins from *Tetrahymena* cilia, J. Biochem. 76 (1974) 991–999.
[74] F.D. Warner, D.R. Mitchell, C.R. Perkins, Structural conformation of the ciliary ATPase dynein, J. Mol. Biol. 114 (1977) 367–384.

[75] R.G. Burns, T.D. Pollard, A dynein-like protein from brain, FEBS Lett. 40 (1974) 274–280.
[76] K. Ogawa, I.R. Gibbons, Dynein 2. A new adenosine triphosphatase from sea urchin sperm flagella, J. Biol. Chem. 251 (1976) 5793–5801.
[77] C.W. Bell, E. Fronk, I.R. Gibbons, Polypeptide subunits of dynein 1 from sea urchin sperm flagella, J. Supramol. Struct. 11 (1979) 311–317.
[78] G. Piperno, D.J. Luck, Axonemal adenosine triphosphatases from flagella of *Chlamydomonas reinhardtii*. Purification of two dyneins, J. Biol. Chem. 254 (1979) 3084–3090.
[79] S.M. King, R. Kamiya, in: G.B. Witman (Ed.), The *Chlamydomonas* Sourcebook, Elsevier, Amsterdam, 2009, pp. 131–208.
[80] I.R. Gibbons, E. Fronk, A latent adenosine triphosphatase form of dynein 1 from sea urchin sperm flagella, J. Biol. Chem. 254 (1979) 187–196.
[81] K.A. Johnson, Pathway of the microtubule-dynein ATPase and the structure of dynein: A comparison with actomyosin, Annu. Rev. Biophys. Biophys. Chem. 14 (1985) 161–188.
[82] M.E. Porter, K.A. Johnson, Transient state kinetic analysis of the ATP-induced dissociation of the dynein-microtubule complex, J. Biol. Chem. 258 (1983) 6582–6587.
[83] T. Shimizu, K.A. Johnson, Kinetic evidence for multiple dynein ATPase sites, J. Biol. Chem. 258 (1983) 13841–13846.
[84] G.B. Witman, K.A. Johnson, K.K. Pfister, J.S. Wall, Fine structure and molecular weight of the outer arm dyneins of *Chlamydomonas*, J. Submicros. Cytol. 15 (1983) 193–198.
[85] I.R. Gibbons, B.H. Gibbons, in: Y. Mukohata, M.F. Morales, S. Fleischei (Eds.), Perspectives of biological energy transduction, Academic Press Japan, Tokyo, 1987, pp. 107–116.
[86] U. Goodenough, J. Heuser, Structural comparison of purified dynein proteins with *in situ* dynein arms, J. Mol. Biol. 180 (1984) 1083–1118.
[87] U.W. Goodenough, J.E. Heuser, Substructure of the outer dynein arm, J. Cell Biol. 95 (1982) 798–815.
[88] W.S. Sale, U.W. Goodenough, J.E. Heuser, The substructure of isolated and *in situ* outer dynein arms of sea urchin sperm flagella, J. Cell Biol. 101 (1985) 1400–1412.
[89] L.A. Amos, Brain dynein crossbridges microtubules into bundles, J. Cell Sci. 93 (Pt. 1) (1989) 19–28.
[90] M.A. Gee, J.E. Heuser, R.B. Vallee, An extended microtubule-binding structure within the dynein motor domain, Nature 390 (1997) 636–639.
[91] L.C. Cantley Jr., L. Josephson, R. Warner, M. Yanagisawa, C. Lechene, G. Guidotti, Vanadate is a potent Na, K-ATPase inhibitor found in ATP derived from muscle, J. Biol. Chem. 252 (1977) 7421–7423.
[92] I.R. Gibbons, M.P. Cosson, J.A. Evans, B.H. Gibbons, B. Houck, K.H. Martinson, W.S. Sale, W.J. Tang, Potent inhibition of dynein adenosinetriphosphatase and of the motility of cilia and sperm flagella by vanadate, Proc. Natl. Acad. Sci. USA 75 (1978) 2220–2224.
[93] T. Kobayashi, T. Martensen, J. Nath, M. Flavin, Inhibition of dynein ATPase by vanadate, and its possible use as a probe for the role of dynein in cytoplasmic motility, Biochem. Biophys. Res. Commun. 81 (1978) 1313–1318.
[94] W.S. Sale, I.R. Gibbons, Study of the mechanism of vanadate inhibition of the dynein cross-bridge cycle in sea urchin sperm flagella, J. Cell. Biol. 82 (1979) 291–298.
[95] R.W. Lymn, E.W. Taylor, Mechanism of adenosine triphosphate hydrolysis by actomyosin, Biochemistry 10 (1971) 4617–4624.
[96] J.A. Evans, 1982 Kinetic study of latent and Triton-potentiated dynein-1 adenosine-triphosphatase, University of Hawaii, Honolulu, H. I, 1982.
[97] M.E. Porter, K.A. Johnson, Dynein structure and function, Annu. Rev. Cell Biol. 5 (1989) 119–151.

[98] T. Shimizu, K.A. Johnson, Presteady state kinetic analysis of vanadate-induced inhibition of the dynein ATPase, J. Biol. Chem. 258 (1983) 13833–13840.
[99] A. Lee-Eiford, R.A. Ow, I.R. Gibbons, Specific cleavage of dynein heavy chains by ultraviolet irradiation in the presence of ATP and vanadate, J. Biol. Chem. 261 (1986) 2337–2342.
[100] I.R. Gibbons, A. Lee-Eiford, G. Mocz, C.A. Phillipson, W.J. Tang, B.H. Gibbons, Photosensitized cleavage of dynein heavy chains. Cleavage at the "V1 site" by irradiation at 365 nm in the presence of ATP and vanadate, J. Biol. Chem. 262 (1987) 2780–2786.
[101] W.-J.Y. Tang, I.R. Gibbons, Photosensitized cleavage of dynein heavy chains. Cleavage at the V2 site by irradiation at 365 nm in the presence of oligovanadate, J. Biol. Chem. 262 (1987) 17728–17734.
[102] G. Mocz, W.J. Tang, I.R. Gibbons, A map of photolytic and tryptic cleavage sites on the beta heavy chain of dynein ATPase from sea urchin sperm flagella, J. Cell Biol. 106 (1988) 1607–1614.
[103] G. Mocz, I.R. Gibbons, III. Iron-mediated photolysis of outer arm dynein ATPase from sea urchin sperm flagella, J. Biol. Chem. 265 (1990) 2917–2922.
[104] I.R. Gibbons, G. Mocz, Photocatalytic cleavage of proteins with vanadate and other transition metal complexes, Methods Enzymol. 196 (1991) 428–442.
[105] B.H. Gibbons, I.R. Gibbons, Vanadate-sensitized cleavage of dynein heavy chains by 365-nm irradiation of demembranated sperm flagella and its effect on the flagellar motility, J. Biol. Chem. 262 (1987) 8354–8359.
[106] S.P. Marchese-Ragona, K.C. Facemyer, K.A. Johnson, Structure of the alpha-, beta-, and gamma-heavy chains of 22 S outer arm dynein obtained from *Tetrahymena* cilia, J. Biol. Chem. 264 (1989) 21361–21368.
[107] S.M. King, G.B. Witman, Structure of the gamma heavy chain of the outer arm dynein from *Chlamydomonas* flagella, J. Cell Biol. 107 (1988) 1799–1808.
[108] B.M. Paschal, H.S. Shpetner, R.B. Vallee, MAP 1C is a microtubule-activated ATPase which translocates microtubules *in vitro* and has dynein-like properties, J. Cell Biol. 105 (1987) 1273–1282.
[109] R.J. Lye, M.E. Porter, J.M. Scholey, J.R. McIntosh, Identification of a microtubule-based cytoplasmic motor in the nematode *C.* elegans, Cell 51 (1987) 309–318.
[110] H.S. Shpetner, B.M. Paschal, R.B. Vallee, Characterization of the microtubule-activated ATPase of brain cytoplasmic dynein MAP 1C, J. Cell Biol. 107 (1988) 1001–1009.
[111] W.-J.Y. Tang, C.W. Bell, W.S. Sale, I.R. Gibbons, Structure of the dynein-1 outer arm in sea urchin sperm flagella. I. Analysis by separation of subunits, J. Biol. Chem. 257 (1982) 508–515.
[112] C.W. Bell, I.R. Gibbons, Structure of the dynein-1 outer arm in sea urchin sperm flagella. II. Analysis by proteolytic cleavage, J. Biol. Chem. 257 (1982) 516–522.
[113] W.S. Sale, L.A. Fox, Isolated beta-heavy chain subunit of dynein translocates microtubules in vitro, J. Cell Biol. 107 (1988) 1793–1797.
[114] R.A. Ow, W.J. Tang, G. Mocz, I.R. Gibbons, Tryptic digestion of dynein 1 in low salt medium. Origin and properties of fragment A, J. Biol. Chem. 262 (1987) 3409–3414.
[115] G. Mocz, I.R. Gibbons, ATP-insensitive interaction of the amino-terminal region of the beta heavy chain of dynein with microtubules, Biochemistry 32 (1993) 3456–3460.
[116] K. Ogawa, Studies on flagellar ATPase from sea urchin spermatozoa. II. Effect of trypsin digestion on the enzyme, Biochim. Biophys. Acta. 293 (1973) 514–525.
[117] G. Piperno, Monoclonal antibodies to dynein subunits reveal the existence of cytoplasmic antigens in sea urchin egg, J. Cell Biol. 98 (1984) 1842–1850.
[118] S.M. King, G.B. Witman, Molecular structure of *Chlamydomonas* outer arm dynein, in: F.D. Warner, P. Satir, I.R. Gibbons (Eds.), Cell Movement I: Dynein ATPases., Alan R. Liss Inc, New York, 1975, pp. 61–75.
[119] S.M. King, J.L. Gatti, A.G. Moss, G.B. Witman, Outer-arm dynein from trout spermatozoa: Substructural organization, Cell Motil. Cytoskeleton 16 (1990) 266–278.

[120] J.A. Spudich, S.J. Kron, M.P. Sheetz, Movement of myosin-coated beads on oriented filaments reconstituted from purified actin, Nature 315 (1985) 584–586.
[121] M.P. Koonce, J.R. McIntosh, Identification and immunolocalization of cytoplasmic dynein in *Dictyostelium*, Cell Motil. Cytoskeleton 15 (1990) 51–62.
[122] L.A. Fox, W.S. Sale, Direction of force generated by the inner row of dynein arms on flagellar microtubules, J. Cell Biol. 105 (1987) 1781–1787.
[123] R.D. Vale, T.S. Reese, M.P. Sheetz, Identification of a novel force-generating protein, kinesin, involved in microtubule-based motility, Cell 42 (1985) 39–50.
[124] I.R. Gibbons, D.J. Asai, N.S. Ching, G.J. Dolecki, G. Mocz, C.A. Phillipson, H. Ren, W.-J.Y. Tang, B.H. Gibbons, A PCR procedure to determine the sequence of large polypeptides by rapid walking through a cDNA library, Proc. Natl. Acad. Sci. USA 88 (1991) 8563–8567.
[125] I.R. Gibbons, B.H. Gibbons, G. Mocz, D.J. Asai, Multiple nucleotide-binding sites in the sequence of dynein beta heavy chain, Nature 352 (1991) 640–643.
[126] K. Ogawa, Four ATP-binding sites in the midregion of the beta heavy chain of dynein, Nature 352 (1991) 643–645.
[127] J.E. Walker, M. Saraste, M.J. Runswick, N.J. Gay, Distantly related sequences in the alpha- and beta-subunits of ATP synthase, myosin, kinases and other ATP-requiring enzymes and a common nucleotide binding fold, EMBO J. 1 (1982) 945–951.
[128] A.F. Neuwald, L. Aravind, J.L. Spouge, E.V. Koonin, AAA^{+}: A class of chaperone-like ATPases associated with the assembly, operation, and disassembly of protein complexes, Genome Res. 9 (1999) 27–43.
[129] L.M. Iyer, D.D. Leipe, E.V. Koonin, L. Aravind, Evolutionary history and higher order classification of AAA^{+} ATPases, J. Struct. Biol. 146 (2004) 11–31.
[130] G. Mocz, I.R. Gibbons, Phase partition analysis of nucleotide binding to axonemal dynein, Biochemistry 35 (1996) 9204–9211.
[131] G. Mocz, M.K. Helms, D.M. Jameson, I.R. Gibbons, Probing the nucleotide binding sites of axonemal dynein with the fluorescent nucleotide analogue 2′3′-O–N-Methylanthraniloyl-adenosine 5′-triphosphate, Biochemistry 37 (1998) 9862–9869.
[132] M. Miura, A. Matsubara, T. Kobayashi, M. Edamatsu, Y.Y. Toyoshima, Nucleotide-dependent behavior of single molecules of cytoplasmic dynein on microtubules *in vitro*, FEBS Lett. 584 (2010) 2351–2355.
[133] B.H. Gibbons, D.J. Asai, W.J. Tang, T.S. Hays, I.R. Gibbons, Phylogeny and expression of axonemal and cytoplasmic dynein genes in sea urchins, Mol. Biol. Cell 5 (1994) 57–70.
[134] K. Rasmusson, M. Serr, J. Gepner, I. Gibbons, T.S. Hays, A family of dynein genes in *Drosophila melanogaster*, Mol. Biol. Cell 5 (1994) 45–55.
[135] I.R. Gibbons, Dynein family of motor proteins: Present status and future questions, Cell Motil. Cytoskeleton 32 (1995) 136–144.
[136] D. Eshel, L.A. Urrestarazu, S. Vissers, J.C. Jauniaux, J.C. van Vliet-Reedijk, R.J. Planta, I.R. Gibbons, Cytoplasmic dynein is required for normal nuclear segregation in yeast, Proc. Natl. Acad. Sci. USA 90 (1993) 11172–11176.
[137] Y.Y. Li, E. Yeh, T. Hays, K. Bloom, Disruption of mitotic spindle orientation in a yeast dynein mutant, Proc. Natl. Acad. Sci. USA 90 (1993) 10096–10100.
[138] W.S. Saunders, D. Koshland, D. Eshel, I.R. Gibbons, M.A. Hoyt, *Saccharomyces cerevisiae* kinesin- and dynein-related proteins required for anaphase chromosome segregation, J. Cell Biol. 128 (1995) 617–624.
[139] C.J. Brokaw, Calcium-induced asymmetrical beating of triton-demembranated sea urchin sperm flagella, J. Cell Biol. 82 (1979) 401–411.
[140] C.J. Brokaw, D.J. Luck, Bending patterns of chlamydomonas flagella: III. A radial spoke head deficient mutant and a central pair deficient mutant, Cell Motil. 5 (1985) 195–208.

[141] C.B. Lindemann, A model of flagellar and ciliary functioning which uses the forces transverse to the axoneme as the regulator of dynein activation, Cell Motil. Cytoskeleton 29 (1994) 141–154.
[142] S. Aoyama, R. Kamiya, Cyclical interactions between two outer doublet microtubules in split flagellar axonemes, Biophys. J. 89 (2005) 3261–3268.
[143] M.E. Porter, R. Bower, J.A. Knott, P. Byrd, W. Dentler, Cytoplasmic dynein heavy chain 1b is required for flagellar assembly in *Chlamydomonas*, Mol Biol. Cell 10 (1999) 693–712.
[144] M.E. Porter, W.S. Sale, The 9+2 axoneme anchors multiple inner arm dyneins and a network of kinases and phosphatases that control motility, J. Cell Biol. 151 (2000) F37–F42.
[145] E.E. Dymek, E.F. Smith, A conserved CaM- and radial spoke associated complex mediates regulation of flagellar dynein activity, J. Cell Biol. 179 (2007) 515–526.
[146] M.J. Wargo, M.A. McPeek, E.F. Smith, Analysis of microtubule sliding patterns in *Chlamydomonas* flagellar axonemes reveals dynein activity on specific doublet microtubules, J. Cell Sci. 117 (2004) 2533–2544.
[147] R. Kamiya, Functional diversity of axonemal dyneins as studied in *Chlamydomonas* mutants, Int. Rev. Cytol. 219 (2002) 115–155.
[148] A. Furuta, T. Yagi, H.A. Yanagisawa, H. Higuchi, R. Kamiya, Systematic comparison of *in vitro* motile properties between *Chlamydomonas* wild-type and mutant outer arm dyneins each lacking one of the three heavy chains, J. Biol. Chem. 284 (2009) 5927–5935.
[149] A. Hilfinger, A.K. Chattopadhyay, F. Julicher, Nonlinear dynamics of cilia and flagella, Phys. Rev. E Stat. Nonlin. Soft Matter Phys. 79 (2009) 051918.
[150] C.J. Brokaw, Thinking about flagellar oscillation, Cell Motil. Cytoskeleton 66 (2009) 425–436.
[151] C.B. Lindemann, K.A. Lesich, Flagellar and ciliary beating: The proven and the possible, J. Cell Sci. 123 (2010) 519–528.
[152] C.J. Brokaw, R. Josslin, L. Bobrow, Calcium ion regulation of flagellar beat symmetry in reactivated sea urchin spermatozoa, Biochem. Biophys. Res. Commun. 58 (1974) 795–800.
[153] I.R. Gibbons, Structure and function of flagellar microtubules, in: B.R. Brinkley, K.R. Porter (Eds.), International Cell Biology 1976–1977, Rockefeller University Press, New York, 1977, pp. 348–357.
[154] R.L. Miller, C.J. Brokaw, Chemotactic turning behaviour of *Tubularia* spermatzoa, J. Exp. Biol. 52 (1970) 799–806.
[155] A. Guerrero, T. Nishigaki, J. Carneiro, Y. Tatsu, C.D. Wood, A. Darszon, Tuning sperm chemotaxis by calcium burst timing, Dev Biol. 344 (2010) 52–65.
[156] B.H. Gibbons, Intermittent swimming in live sea urchin sperm, J. Cell Biol. 84 (1980) 1–12.
[157] J.J. Blum, M.H. Hines, Diffusion of Ca^{2+} and the quiescent response of sea urchin sperm flagella, J. Theor. Biol. 100 (1983) 511–523.
[158] I.R. Gibbons, B.H. Gibbons, Transient flagellar waveforms during intermittent swimming in sea urchin sperm. I. Wave parameters, J. Muscle Res. Cell Motil. 1 (1980) 31–59.
[159] I.R. Gibbons, Transient flagellar waveforms during intermittent swimming in sea urchin sperm. II. Analysis of tubule sliding, J. Muscle Res. Cell Motil. 2 (1981) 83–130.
[160] B.H. Gibbons, I.R. Gibbons, Calcium-induced quiescence in reactivated sea urchin sperm, J. Cell Biol. 84 (1980) 13–27.
[161] D.R. Mitchell, M. Nakatsugawa, Bend propagation drives central pair rotation in *Chlamydomonas reinhardtii* flagella, J. Cell Biol. 166 (2004) 709–715.
[162] C.M.X. Mattei, in: B.A. Afzelius (Ed.), The Functional Anatomy of the Spermatozoon, Pergamon Press, Oxford, 1975, pp. 211–221.

[163] B. Baccetti, A.G. Burrini, V. Pallini, Different axoneme patterns in cilia and flagella of the same animal, J. Submicrosc. Cytol. 13 (1981) 479–481.
[164] B. Baccetti, A.G. Burrini, R. Dallai, V. Pallini, The dynein electrophoretic bands in axonemes naturally lacking the inner or the outer arm, J. Cell Biol. 80 (1979) 334–340.
[165] B.H. Gibbons, B. Baccetti, I.R. Gibbons, Live and reactivated motility in the 9+0 flagellum of Anguilla sperm, Cell Motil. Cytoskel. 5 (1985) 333–350.
[166] S. Ishijima, K. Sekiguchi, Y. Hiramoto, Comparative study of the beat patterns of American and Asian horseshoe crab sperm: Evidence for a role of the central pair complex in forming planar waveforms in flagella, Cell Motil. Cytoskel. 9 (1988) 264–270.
[167] C.K. Omoto, I.R. Gibbons, R. Kamiya, C. Shingyoji, K. Takahashi, G.B. Witman, Rotation of the central pair microtubules in eukaryotic flagella, Mol. Biol. Cell 10 (1999) 1–4.
[168] C.J. Brokaw, Computer simulation of flagellar movement VIII: Coordination of dynein by local curvature control can generate helical bending waves, Cell Motil. Cytoskeleton 53 (2002) 103–124.
[169] D.M. Woolley, G.G. Vernon, A study of helical and planar waves on sea urchin sperm flagella, with a theory of how they are generated, J. Exp. Biol. 204 (2001) 1333–1345.
[170] C.K. Omoto, C. Kung, Rotation and twist of the central-pair microtubules in the cilia of *Paramecium*, J. Cell Biol. 87 (1980) 33–46.
[171] R. Kamiya, Extrusion and rotation of the central-pair microtubules in detergent-treated *Chlamydomonas* flagella, Prog. Clin. Biol. Res. 80 (1982) 169–173.
[172] I.R. Gibbons, C. Shingyoji, A. Murakami, K. Takahashi, Spontaneous recovery after experimental manipulation of the plane of beat in sperm flagella, Nature 325 (1987) 351–352.
[173] C. Shingyoji, J. Katada, K. Takahashi, I.R. Gibbons, Rotating the plane of imposed vibration can rotate the plane of flagellar beating in sea-urchin sperm without twisting the axoneme, J. Cell Sci. 98 (Pt. 2) (1991) 175–181.
[174] K. Takahashi, C. Shingyoji, J. Katada, D. Eshel, I.R. Gibbons, Polarity in spontaneous unwinding after prior rotation of the flagellar beat plane in sea-urchin spermatozoa, J. Cell Sci. 98 (Pt 2) (1991) 183–189.
[175] H. Bannai, M. Yoshimura, K. Takahashi, C. Shingyoji, Calcium regulation of microtubule sliding in reactivated sea urchin sperm flagella, J. Cell Sci. 113 (Pt. 5) (2000) 831–839.
[176] S.F. Goldstein, Irradiation of sperm tails by laser microbeam, J. Exp. Biol. 51 (1969) 431–441.
[177] C.J. Brokaw, I.R. Gibbons, Localized activation of bending in proximal, medial and distal regions of sea-urchins sperm flagella, J. Cell. Sci. 13 (1973) 1–10.
[178] C. Shingyoji, A. Murakami, K. Takahashi, Local reactivation of Triton-extracted flagella by iontophoretic application of ATP, Nature 265 (1977) 269–270.
[179] K. Takahashi, C. Shingyoji, S. Kamimura, Microtubule sliding in reactivated flagella, Symp. Soc. Exp. Biol. 35 (1982) 159–177.
[180] C. Shingyoji, I.R. Gibbons, A. Murakami, K. Takahashi, Effect of imposed head vibration on the stability and waveform of flagellar beating in sea urchin spermatozoa, J. Exp. Biol. 156 (1991) 63–80.
[181] C. Shingyoji, K. Yoshimura, D. Eshel, K. Takahashi, I.R. Gibbons, Effect of beat frequency on the velocity of microtubule sliding in reactivated sea urchin sperm flagella under imposed head vibration, J. Exp. Biol. 198 (1995) 645–653.
[182] D. Eshel, C. Shingyoji, K. Yoshimura, B.H. Gibbons, I.R. Gibbons, K. Takahashi, Transient behavior of sea urchin sperm flagella following an abrupt change in beat frequency, J. Exp. Biol. 152 (1990) 441–451.
[183] M. Okuno, Y. Hiramoto, Mechanical stimulation of starfish sperm flagella, J. Exp. Biol. 65 (1976) 401–413.
[184] S.M. King, AAA domains and organization of the dynein motor unit, J. Cell Sci. 113 (Pt. 14) (2000) 2521–2526.

[185] G. Mocz, I.R. Gibbons, Model for the motor component of dynein heavy chain based on homology to the AAA family of oligomeric ATPases, Structure 9 (2001) 93–103.
[186] M. Samso, M. Radermacher, J. Frank, M.P. Koonce, Structural characterization of a dynein motor domain, J. Mol. Biol. 276 (1998) 927–937.
[187] S.A. Burgess, M.L. Walker, H. Sakakibara, P.J. Knight, K. Oiwa, Dynein structure and power stroke, Nature 421 (2003) 715–718.
[188] J.E. Garbarino, I.R. Gibbons, Expression and genomic analysis of midasin, a novel and highly conserved AAA protein distantly related to dynein, BMC Genomics 3 (2002) 18.
[189] T.A. Nissan, J. Bassler, E. Petfalski, D. Tollervey, E. Hurt, 60 S pre-ribosome formation viewed from assembly in the nucleolus until export to the cytoplasm, EMBO J. 21 (2002) 5539–5547.
[190] C. Ulbrich, M. Diepholz, J. Bassler, D. Kressler, B. Pertschy, K. Galani, B. Bottcher, E. Hurt, Mechanochemical removal of ribosome biogenesis factors from nascent 60 S ribosomal subunits, Cell 138 (2009) 911–922.
[191] Y. Tanaka, Z. Zhang, N. Hirokawa, Identification and molecular evolution of new dynein-like protein sequences in rat brain, J. Cell Sci. 108 (Pt. 5) (1995) 1883–1893.
[192] D.R. Mitchell, K.S. Brown, Sequence analysis of the *Chlamydomonas* alpha and beta dynein heavy chain genes, J. Cell Sci. 107 (Pt. 3) (1994) 635–644.
[193] C.G. Wilkerson, S.M. King, G.B. Witman, Molecular analysis of the gamma heavy chain of *Chlamydomonas* flagellar outer-arm dynein, J. Cell Sci. 107 (Pt. 3) (1994) 497–506.
[194] M.E. Porter, J.A. Knott, S.H. Myster, S.J. Farlow, The dynein gene family in *Chlamydomonas reinhardtii*, Genetics 144 (1996) 569–585.
[195] K.L. Andrews, P. Nettesheim, D.J. Asai, L.E. Ostrowski, Identification of seven rat axonemal dynein heavy chain genes: Expression during ciliated cell differentiation, Mol. Biol. Cell 7 (1996) 71–79.
[196] C. Chapelin, B. Duriez, F. Magnino, M. Goossens, E. Escudier, S. Amselem, Isolation of several human axonemal dynein heavy chain genes: Genomic structure of the catalytic site, phylogenetic analysis and chromosomal assignment, FEBS Lett. 412 (1997) 325–330.
[197] W.J. Kent, C.W. Sugnet, T.S. Furey, K.M. Roskin, T.H. Pringle, A.M. Zahler, D. Haussler, The human genome browser at UCSC, Genome Res. 12 (2002) 996–1006.
[198] R.L. Morris, M.P. Hoffman, R.A. Obar, S.S. McCafferty, I.R. Gibbons, A.D. Leone, J. Cool, E.L. Allgood, A.M. Musante, K.M. Judkins, B.J. Rossetti, A.P. Rawson, D.R. Burgess, Analysis of cytoskeletal and motility proteins in the sea urchin genome assembly, Dev. Biol. 300 (2006) 219–237.
[199] E. Sodergren, G.M. Weinstock, E.H. Davidson, R.A. Cameron, R.A. Gibbs, R.C. Angerer, L.M. Angerer, M.I. Arnone, D.R. Burgess, R.D. Burke, J.A. Coffman, M. Dean, M.R. Elphick, C.A. Ettensohn, K.R. Foltz, A. Hamdoun, R.O. Hynes, W.H. Klein, W. Marzluff, D.R. McClay, R.L. Morris, A. Mushegian, J.P. Rast, L.C. Smith, M.C. Thorndyke, V.D. Vacquier, G.M. Wessel, G. Wray, L. Zhang, C.G. Elsik, O. Ermolaeva, W. Hlavina, G. Hofmann, P. Kitts, M.J. Landrum, A.J. Mackey, D. Maglott, G. Panopoulou, A.J. Poustka, K. Pruitt, V. Sapojnikov, X. Song, A. Souvorov, V. Solovyev, Z. Wei, C.A. Whittaker, K. Worley, K.J. Durbin, Y. Shen, O. Fedrigo, D. Garfield, R. Haygood, A. Primus, R. Satija, T. Severson, M.L. Gonzalez-Garay, A.R. Jackson, A. Milosavljevic, M. Tong, C.E. Killian, B.T. Livingston, F.H. Wilt, N. Adams, R. Belle, S. Carbonneau, R. Cheung, P. Cormier, B. Cosson, J. Croce, A. Fernandez-Guerra, A.M. Geneviere, M. Goel, H. Kelkar, J. Morales, O. Mulner-Lorillon, A.J. Robertson, J.V. Goldstone, B. Cole, D. Epel, B. Gold, M.E. Hahn, M. Howard-Ashby, M. Scally, J.J. Stegeman, E.L. Allgood, J. Cool, K.M. Judkins, S.S. McCafferty, A.M. Musante, R.A. Obar, A.P. Rawson, B.J. Rossetti, I.R. Gibbons, M.P. Hoffman, A. Leone, S. Istrail, S.C. Materna, M.P. Samanta, V. Stolc, W. Tongprasit, Q. Tu, K.F. Bergeron, B.P. Brandhorst, J. Whittle, K. Berney, D.J. Bottjer, C. Calestani, K. Peterson, E. Chow, Q.A. Yuan, E. Elhaik, D. Graur, J.T. Reese, I. Bosdet,

S. Heesun, M.A. Marra, J. Schein, M.K. Anderson, V. Brockton, K.M. Buckley, A.H. Cohen, S.D. Fugmann, T. Hibino, M. Loza-Coll, A.J. Majeske, C. Messier, S.V. Nair, Z. Pancer, D.P. Terwilliger, C. Agca, E. Arboleda, N. Chen, A.M. Churcher, F. Hallbook, G.W. Humphrey, M.M. Idris, T. Kiyama, S. Liang, D. Mellott, X. Mu, G. Murray, R.P. Olinski, F. Raible, M. Rowe, J.S. Taylor, K. Tessmar-Raible, D. Wang, K.H. Wilson, S. Yaguchi, T. Gaasterland, B.E. Galindo, H.J. Gunaratne, C. Juliano, M. Kinukawa, G.W. Moy, A.T. Neill, M. Nomura, M. Raisch, A. Reade, M.M. Roux, J.L. Song, Y.H. Su, I.K. Townley, E. Voronina, J.L. Wong, G. Amore, M. Branno, E.R. Brown, V. Cavalieri, V. Duboc, L. Duloquin, C. Flytzanis, C. Gache, F. Lapraz, T. Lepage, A. Locascio, P. Martinez, G. Matassi, V. Matranga, R. Range, F. Rizzo, E. Rottinger, W. Beane, C. Bradham, C. Byrum, T. Glenn, S. Hussain, G. Manning, E. Miranda, R. Thomason, K. Walton, A. Wikramanayke, S.Y. Wu, R. Xu, C.T. Brown, L. Chen, R.F. Gray, P.Y. Lee, J. Nam, P. Oliveri, J. Smith, D. Muzny, S. Bell, J. Chacko, A. Cree, S. Curry, C. Davis, H. Dinh, S. Dugan-Rocha, J. Fowler, R. Gill, C. Hamilton, J. Hernandez, S. Hines, J. Hume, L. Jackson, A. Jolivet, C. Kovar, S. Lee, L. Lewis, G. Miner, M. Morgan, L.V. Nazareth, G. Okwuonu, D. Parker, L.L. Pu, R. Thorn, R. Wright, The genome of the sea urchin *Strongylocentrotus purpuratus*, Science 314 (2006) 941–952.

[200] K.K. Pfister, E.M. Fisher, I.R. Gibbons, T.S. Hays, E.L. Holzbaur, J.R. McIntosh, M.E. Porter, T.A. Schroer, K.T. Vaughan, G.B. Witman, S.M. King, R.B. Vallee, Cytoplasmic dynein nomenclature, J. Cell Biol. 171 (2005) 411–413.

[201] R.L. Seal, S.M. Gordon, M.J. Lush, M.W. Wright, E.A. Bruford, genenames.org: The HGNC resources in 2011, Nucleic Acids Res 39 (Suppl. 1) (2011) D514–D519.

[202] I. Wapinski, A. Pfeffer, N. Friedman, A. Regev, Natural history and evolutionary principles of gene duplication in fungi, Nature 449 (2007) 54–61.

[203] B. Wickstead, K. Gull, Dyneins across eukaryotes: A comparative genomic analysis, Traffic 8 (2007) 1708–1721.

[204] D.E. Wilkes, V. Rajagopalan, C.W. Chan, E. Kniazeva, A.E. Wiedeman, D.J. Asai, Dynein light chain family in *Tetrahymena thermophila*, Cell Motil. Cytoskeleton 64 (2007) 82–96.

[205] T.A. Richards, T. Cavalier-Smith, Myosin domain evolution and the primary divergence of eukaryotes, Nature 436 (2005) 1113–1118.

[206] I.B. Rogozin, M.K. Basu, M. Csuros, E.V. Koonin, Analysis of rare genomic changes does not support the unikont-bikont phylogeny and suggests cyanobacterial symbiosis as the point of primary radiation of eukaryotes, Genome Biol. Evol. 1 (2009) 99–113.

[207] P. Hook, R.B. Vallee, The dynein family at a glance, J. Cell Sci. 119 (2006) 4369–4371.

[208] D.E. Wilkes, H.E. Watson, D.R. Mitchell, D.J. Asai, Twenty-five dyneins in *Tetrahymena*: A re-examination of the multidynein hypothesis, Cell Motil. Cytoskeleton 65 (2008) 342–351.

[209] H. Hartman, T.F. Smith, The evolution of the cilium and the eukaryotic cell, Cell Motil. Cytoskeleton 66 (2009) 215–219.

[210] R.D. Finn, J. Mistry, J. Tate, P. Coggill, A. Heger, J.E. Pollington, O.L. Gavin, P. Gunasekaran, G. Ceric, K. Forslund, L. Holm, E.L. Sonnhammer, S.R. Eddy, A. Bateman, The Pfam protein families database, Nucleic Acids Res. 38 (2010) D211–D222.

[211] M.P. Koonce, D.A. Knecht, Cytoplasmic dynein heavy chain is an essential gene product in *Dictyostelium*, Cell Motil. Cytoskeleton 39 (1998) 63–72.

[212] I.R. Gibbons, J.E. Garbarino, C.E. Tan, S.L. Reck-Peterson, R.D. Vale, A.P. Carter, The affinity of the dynein microtubule-binding domain is modulated by the conformation of its coiled-coil stalk, J. Biol. Chem. 280 (2005) 23960–23965.

[213] T. Kon, K. Imamula, A.J. Roberts, R. Ohkura, P.J. Knight, I.R. Gibbons, S.A. Burgess, K. Sutoh, Helix sliding in the stalk coiled coil of dynein couples ATPase and microtubule binding, Nat. Struct. Mol. Biol. 16 (2009) 325–333.

[214] A.P. Carter, J.E. Garbarino, E.M. Wilson-Kubalek, W.E. Shipley, C. Cho, R.A. Milligan, R.D. Vale, I.R. Gibbons, Structure and functional role of dynein's microtubule-binding domain, Science 322 (2008) 1691–1695.
[215] M.P. Koonce, I. Tikhonenko, Functional elements within the dynein microtubule-binding domain, Mol. Biol. Cell 11 (2000) 523–529.
[216] H. Hagiwara, H. Yorifuji, R. Sato-Yoshitake, N. Hirokawa, Competition between motor molecules kinesin and cytoplasmic dynein and fibrous microtubule-associated proteins in binding to microtubules, J. Biol. Chem. 269 (1994) 3581–3589.
[217] N. Mizuno, S. Toba, M. Edamatsu, J. Watai-Nishii, N. Hirokawa, Y.Y. Toyoshima, M. Kikkawa, Dynein and kinesin share an overlapping microtubule-binding site, EMBO J. 23 (2004) 2459–2467.
[218] N. Numata, T. Kon, T. Shima, K. Imamula, T. Mogami, R. Ohkura, K. Sutoh, K. Sutoh, Molecular mechanism of force generation by dynein, a molecular motor belonging to the AAA^+ family, Biochem. Soc. Trans. 36 (2008) 131–135.
[219] J. Gray, Ciliary Movement, Cambridge University Press, Cambridge, 1928.
[220] M.A. Sleigh, Cilia and Flagella, Academic Press, London, 1974.
[221] I.R. Gibbons, Cilia and flagella of eukaryotes, J. Cell Biol. 91 (1981) 107s–124s.
[222] P. Satir, S.T. Christensen, Overview of structure and function of mammalian cilia, Annu. Rev. Physiol. 69 (2007) 377–400.
[223] M. Fliegauf, T. Benzing, H. Omran, When cilia go bad: Cilia defects and ciliopathies, Nat. Rev. Mol. Cell Biol. 8 (2007) 880–893.
[224] D.M. Woolley, Flagellar oscillation: A commentary on proposed mechanisms, Biol. Rev. Camb. Philos. Soc. 85 (2010) 453–470.
[225] I.R. Gibbons, The role of dynein in microtubule-based motility, Cell Struct. Funct. 21 (1996) 331–342.
[226] I.R. Gibbons, Sliding and bending in sea urchin sperm flagella, Symp. Soc. Exp. Biol. 35 (1982) 225–287.
[227] B.H. Gibbons, I.R. Gibbons, Organic solvents modify the calcium control of flagellar movement in sea urchin sperm, Nature 292 (1981) 85–86.
[228] M.A. Sleigh, Patterns of ciliary beating, Symp. Soc. Exp. Biol. 22 (1968) 131–150.
[229] B.H. Gibbons, I.R. Gibbons, B. Baccetti, Structure and motility of the 9+0 flagellum of eel spermatozoa, J. Submicrosc. Cytol. 15 (1983) 15–20.
[230] M.A. Larkin, G. Blackshields, N.P. Brown, R. Chenna, P.A. McGettigan, H. McWilliam, F. Valentin, I.M. Wallace, A. Wilm, R. Lopez, J.D. Thompson, T.J. Gibson, D.G. Higgins, Clustal W and Clustal X version 2.0, Bioinformatics 23 (2007) 2947–2948.
[231] K. Tamura, J. Dudley, M. Nei, S. Kumar, MEGA4: Molecular Evolutionary Genetics Analysis MEGA. Software version 4.0, Mol. Biol. Evol. 24 (2007) 1596–1599.

In this chapter

2

Evolutionary Biology of Dyneins

Bill Wickstead [1], *Keith Gull* [2]
[1] Centre of Genetics and Genomics, University of Nottingham, Nottingham, UK
[2] Sir William Dunn School of Pathology, University of Oxford, Oxford, UK

2.1 Introduction

Dyneins are large molecular motors that hydrolyze ATP to generate a minus-end-directed force along microtubules. Each dynein consists of one to three dynein heavy chains (HCs), which encompass the ATPase activity, complexed to intermediate (IC), light-intermediate (LIC), and light (LC) chains, which provide regulatory roles and aid in tethering of the motor to cargo. Dynein HCs are very large polypeptides (~500 kDa) that have a very highly conserved sequence but exist in a number of specific types that are associated with specific cellular functions. Some specificity is also a feature of ICs and LICs, but LCs appear to be generally more promiscuous, with particular LCs being part of several different types of dynein (see [1,2]). Dyneins are not homologous to the other major families of cytoskeleton motors – the kinesins and myosins. Instead, they appear to have evolved from an ATPase involved in a different aspect of cellular biology.

To understand the evolution of dyneins it is necessary to classify their constituent parts, understand the relationships between them, and map this information onto the evolutionary tree of life. In this chapter, we review the present status of sequence-based classification and analysis of dynein components and show how genome-based knowledge of dynein repertoires informs our understanding of both the evolution of dyneins themselves and the biology of individual organisms. We trace the major dynein families back to their roots in the last common eukaryotic ancestor (LCEA). Moving further back in evolutionary time, we try to reconstruct the evolution of dyneins in the proto-eukaryote and explore the possible origins of dynein motors in the large biological gap between the prokaryotes and the last ancestor of all modern eukaryotic species. Finally, we ask about the functional conditions that might have led to the evolution of this important group of molecular motors.

Dyneins DOI: 10.1016/B978-0-12-382004-4.10002-0
Copyright © 2012 by Elsevier Inc. All rights reserved.

2.2 Dynein Classification

Dyneins are not a single monotonous group of proteins with only a single function. Instead, they are a collection of different complexes with specialized components in each. Of the four components of dynein complexes — dynein HCs, ICs, LICs, and LCs — it is the dynein HCs that define a particular type of dynein (although there is also some specificity in the ICs and LICs). All dynein complexes can be classified on the basis dynein HC that they contain. Such classification entails first aligning dynein HCs from different types of dynein and then inferring the relationships between them by molecular phylogenetics. Conveniently for such analyses, dynein HCs are highly conserved across most of their length and, being very large proteins, contain a large phylogenetic signal. Many phylogenies of dynein HCs have now been published [3–12]. Some of the most recent of these analyses take advantage of the emergence of genomic data to give a better sampling of the types of dynein HC found in extant organisms (a theme that will re-emerge in Section 2.3). In these analyses the strength of a particular grouping is usually given by a "bootstrap" value that shows the number of times the given grouping is recovered from independent inferences of the phylogeny, usually with resampling of the sequence dataset. At their best, bootstrap values are a conservative estimate of the confidence that a particular group is monophyletic (see [13]) — that is, the group is derived from a single common ancestor that is not also shared by other sequences in the analysis. However, systematic errors in either alignment or inference methodology can result in seemly strong support for erroneous groupings and only groups that are recovered by multiple methods, and preferably from different alignments, are robust. From several recent works, a consensus has emerged for the existence of nine major classes of dynein HC [7,9,10] — which can also be seen in the analysis presented in Figure 2.1. These nine classes encompass two "cytoplasmic" types and seven that are built into the axoneme of motile cilia and flagella. They are all conserved in diverse eukaryotic

Figure 2.1 Phylogeny of dynein HCs showing major families. The phylogeny is a consensus of 100 maximum-likelihood inferences using the program RAxML (LG matrix; GTR+Γ+I with Γ distribution approximated to eight discrete categories and shape parameters estimated from the data). The numbers at the nodes indicate the bootstrap support for that node from the 100 pseudo-replicates of the inference, and give a conservative estimate of the confidence that the sequences contained by the node are a true group. Phylogenies can change dramatically depending on the alignment, the sequences included, and the methodology used, with the "best" methods often being very computer intensive. The families identified here are generally supported in dynein HC phylogenies from varied organisms and methods [6,7,9–12], but there is currently less consensus regarding the branching order of the families. For display, the tree has been rooted between the "cytoplasmic" dynein families (Cyto1 and Cyto2) and those of the axoneme. Possible rooting of the tree is addressed in Figure 2.5. Organisms have been chosen to represent a broad diversity of eukaryotes. Batde, *Batrachochytrium dendrobatidis* (Fungi); Chlre, *Chlamydomonas reinhardtii* (Plantae); Dicdi, *Dictyostelium discoideum* (Amoebozoa); Homsa, *Homo sapiens* (Metazoa); Monbr, *Monosiga brevicollis* (Choanozoa); Naegr, *Naegleria gruberi* (Excavata); Sacce, *Saccharomyces cerevisiae* (Fungi); Tetth, *Tetrahymena thermophila* (Alveolata).

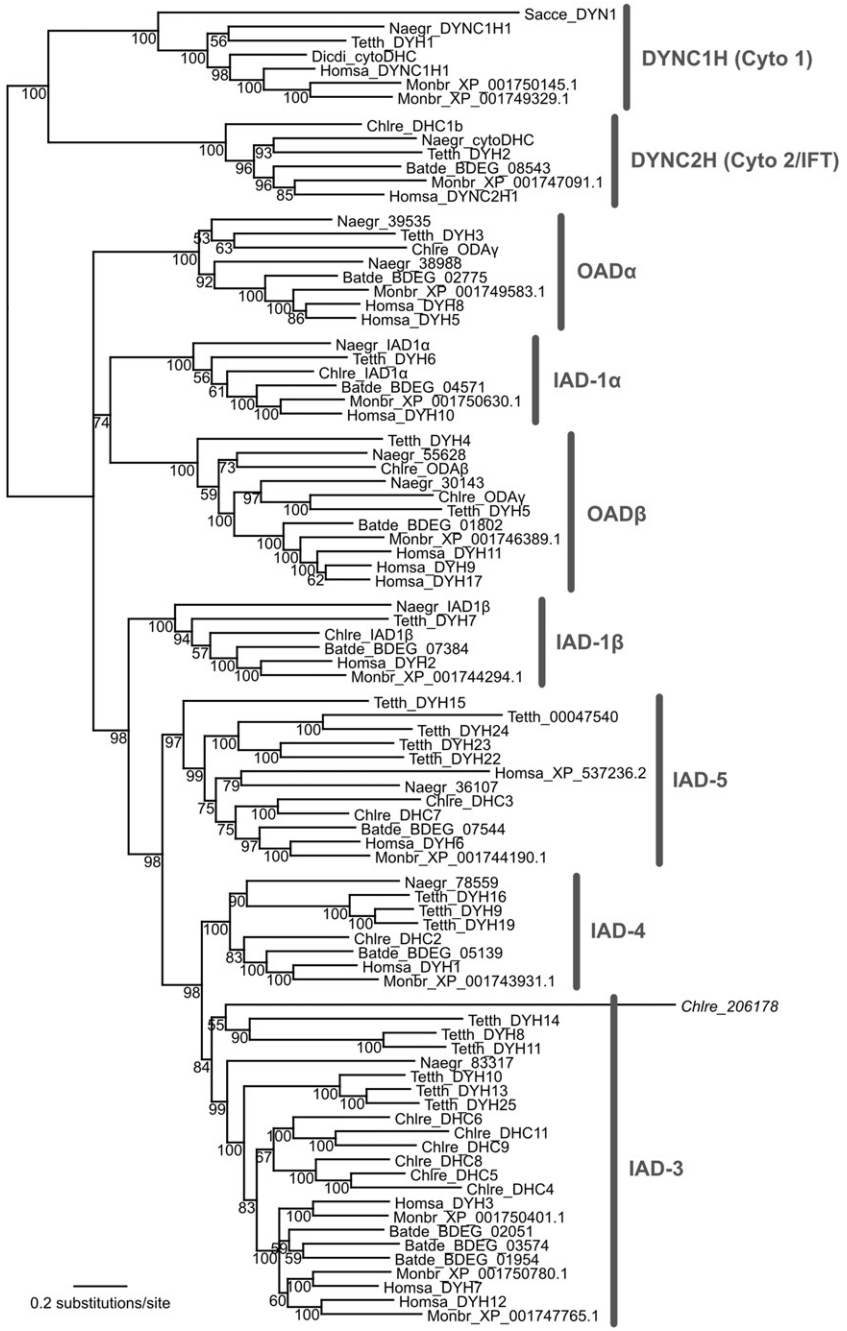
Sacce_DYN1
Naegr_DYNC1H1
Tetth_DYH1
Dicdi_cytoDHC
Homsa_DYNC1H1
Monbr_XP_001750145.1
Monbr_XP_001749329.1
DYNC1H (Cyto 1)
Chlre_DHC1b
Naegr_cytoDHC
Tetth_DYH2
Batde_BDEG_08543
Monbr_XP_001747091.1
Homsa_DYNC2H1
DYNC2H (Cyto 2/IFT)
Naegr_39535
Tetth_DYH3
Chlre_ODAγ
Naegr_38988
Batde_BDEG_02775
Monbr_XP_001749583.1
Homsa_DYH8
Homsa_DYH5
OADα
Naegr_IAD1α
Tetth_DYH6
Chlre_IAD1α
Batde_BDEG_04571
Monbr_XP_001750630.1
Homsa_DYH10
IAD-1α
Tetth_DYH4
Naegr_55628
Chlre_ODAβ
Naegr_30143
Chlre_ODAγ
Tetth_DYH5
Batde_BDEG_01802
Monbr_XP_001746389.1
Homsa_DYH11
Homsa_DYH9
Homsa_DYH17
OADβ
Naegr_IAD1β
Tetth_DYH7
Chlre_IAD1β
Batde_BDEG_07384
Homsa_DYH2
Monbr_XP_001744294.1
IAD-1β
Tetth_DYH15
Tetth_00047540
Tetth_DYH24
Tetth_DYH23
Tetth_DYH22
Homsa_XP_537236.2
Naegr_36107
Chlre_DHC3
Chlre_DHC7
Batde_BDEG_07544
Homsa_DYH6
Monbr_XP_001744190.1
IAD-5
Naegr_78559
Tetth_DYH16
Tetth_DYH9
Tetth_DYH19
Chlre_DHC2
Batde_BDEG_05139
Homsa_DYH1
Monbr_XP_001743931.1
IAD-4
Chlre_206178
Tetth_DYH14
Tetth_DYH8
Tetth_DYH11
Naegr_83317
Tetth_DYH10
Tetth_DYH13
Tetth_DYH25
Chlre_DHC6
Chlre_DHC11
Chlre_DHC9
Chlre_DHC8
Chlre_DHC5
Chlre_DHC4
Homsa_DYH3
Monbr_XP_001750401.1
Batde_BDEG_02051
Batde_BDEG_03574
Batde_BDEG_01954
Monbr_XP_001750780.1
Homsa_DYH7
Homsa_DYH12
Monbr_XP_001747765.1
IAD-3
0.2 substitutions/site

organisms, and functional analyses of particular model complexes have allowed them to be mapped into functional sets, as outlined below.

2.2.1 Dynein Heavy Chain Families

2.2.1.1 Cytoplasmic Dynein Families

The first family we consider here is the clade of dynein HCs specific for the cytoplasmic dynein 1 complex – which is herein referred to as the Cyto1 family of dynein HCs (variously also labeled Dynein-1 [6], DYNC1H1 [9,14], and Cytoplasmic [11]). Cytoplasmic dynein 1 is the principal minus-end-directed motor of cytoplasmic microtubules in animal cells, and it plays a role in many cellular processes including transport of vesicles, function of the Golgi apparatus, nuclear positioning, and spindle formation and function (see [15]). At the center of the cytoplasmic dynein 1 complex is a homodimer of Cyto1 dynein HCs – a situation that is apparently very stable in an evolutionary sense, since there appear to be very few examples of duplication of this gene family [7,9,10]. There are, however, some significant instances of loss of Cyto1 from particular lineages, which will be discussed later in this chapter.

The dynein HCs associated with cytoplasmic dynein 2 (as called dynein 1b or DYNC2) are closely related in primary sequence to Cyto1 (Fig. 2.1). However, in functional terms, rather than phylogenetically, the association of this complex is actually with flagella/cilia, since this dynein HC forms the basis of the retrograde motor for intraflagellar transport (IFT) – the conserved system for building and servicing cilia/flagella (see [16,17]). Herein, this dynein HC family is referred to as Cyto2, but it has also been labeled IFT dynein for its primary function [11] or DYNC2H1 to follow the standardized cytoplasmic nomenclature [9,14]. Like its "true" cytoplasmic counterpart, cytoplasmic dynein 2 is also thought to form around a dynein HC homodimer [18]. Furthermore, like Cyto1, there are interesting losses of Cyto2 in the history of eukaryotes that can be linked to the biology of particular organisms (see Section 2.3).

2.2.1.2 Outer-Arm Dyneins

Apart from Cyto1 and Cyto2, all the other dynein HC families are built into the axonemes of cilia/flagella where they are involved in axonemal motility through the doublet sliding. From a morphological (although not necessarily phylogenetic) point of view there are two general types of dyneins built into motile axonemes: the outer-arm dyneins found towards the outside of the axoneme, and inner-arm dyneins, which are positioned closest to the central-apparatus radial spokes.

The outer-arm dynein HCs encompass two well-supported families: OADα and OADβ (Fig. 2.1). These families are each well-supported individual groups, but in several phylogenies they are not monophyletic (i.e. they are not more closely related to one another than to other dynein HC families) [6,7,9,10]. There is an

important morphological difference between the outer-arm dynein complexes of some single-celled organisms and those of animal sperm. Animal sperm flagella contain two-headed outer-arm dynein complexes [19–25], whereas those of the *Chlamydomonas* and ciliate axonemes are three-headed [26–28]. The outer-arm dynein HC families are specialized for similar positions in the axoneme: the innermost head is composed of a member of the OADα family (i.e., the head closest to the center of the axoneme), while the adjacent dynein HC (the outermost of two-headed outer arms or the central head for three-headed forms) is an OADβ member [28,29]. Interestingly, the outermost head of the three-headed outer-arm dyneins is also an OADβ family member [30]. There does not appear to be a well-separated family of dynein HCs that is specific for this outermost position in the three-headed outer-arm dynein complexes (where they exist). Instead, both central and outermost heads are composed of similar OADβ family members that have become co-opted for the task. Animal OADβ sequences appear to be orthologous to *both* the outermost heads of ciliate or algal outer-arm dyneins – at least, detailed phylogenetic analysis is unable to split them into two monophyletic and well-supported sets [9,10].

An important point to note when discussing outer-arm dynein HCs is that they were originally named according to their order of migration in denaturing polyacrylamide gels before it was known which polypeptide correlated with which head of the dynein complex [31–33]. Only as sequence information later emerged did it become clear that the migration order of orthologous proteins was not necessarily the same across systems [3]. As a result, the same head is composed of a HC that has inherited a different name in different species. In *Chlamydomonas*, the α, β and, γ HCs correspond to the outermost, central, and innermost outer-arm dynein heads, respectively [29,30]. In contrast, for ciliates and animals, the nomenclature is reversed, with the heads corresponding to the α and β HCs (for animals) or α, β, and γ HCs (for ciliates) being positioned from innermost to outermost [10,28]. This reflects a difference in nomenclature only, not a different position for orthologous proteins in the axoneme – *Chlamydomonas* ODAγ is member of the OADα family (see Fig. 2.1) and occupies the innermost position in the outer-arm dyneins [29,30]. This can lead to some potentially confusing conflicts in nomenclature, dependent on the viewpoint from which an author is writing. For example, the OADα families herein and in [5,9–11] are the equivalent of the "ODA-gamma" and "γ outer-arm dynein" groups in [7] and [6], while OADβ encompasses both "ODA-alpha" and "ODA-beta" [7].

2.2.1.3 Inner-Arm Dyneins

Inner-arm dyneins are of two forms: the two-headed inner-arm complex (also called I1 or *f*-dynein), and "single-headed" dyneins. The two-headed inner-arm dynein complex is based around a dynein HC heterodimer composed of one protein from each of the IAD-1α and IAD-1β families [34,35]. As for the OADα and

OADβ families, there is strong support for the IAD-1α and IAD-1β groups. However, in spite of forming a dimer in the axoneme, the two groups appear to have different unique ancestors, since they are not found to be a monophyletic group in any published phylogeny of dynein HCs.

The single-headed dyneins form three classes, labeled IAD-3, -4, and -5 [9] to follow the respective group names in the nomenclature of Morris et al. [7]. Of all the dynein classes, these groups have the lowest coverage in terms of functional data. Yet, these are some of the largest dynein HC classes in organisms with motile axonemes. For example, the model *Chlamydomonas reinhardtii* encodes at least six members of the IAD-3 family alone [7,9,12] (see Fig. 2.1). Recent work combining ultrastructural work with analysis of genetic mutants has mapped some of the single-headed dyneins to specific densities in *Chlamydomonas* axonemes [36–38]. The three single-headed dynein HC classes, IAD-3, -4, and -5, are the families in the dynein HC phylogeny with the weakest support, and the membership of the groups can differ slightly according to the methods used for tree building [7,9,10]. The precise boundaries for these groups will likely become more refined as more sequences are incorporated into analyses (and as phylogenetic methods improve), but the general finding of three groups appears sound.

Although the nine dynein HC families outlined above are recovered in all modern analyses with good dynein HC sampling [7,9,10], there is as yet much less consensus for the relationships between these major classes. It is clear that there is a distinction between the "cytoplasmic" classes (Cyto1 and Cyto2) and the axonemal families (OADα/β, IAD-1α/β, and IAD-3/4/5). Monophyly of the single-headed inner-arm dynein HC families (IAD-3/4/5) is also generally well-supported. However, the branching order of the OADα/β and IAD-1α/β families changes considerably between differing alignments and phylogenetic approaches (see [3,5–7,9–11] and Fig. 2.1). Increasing bootstrap support for particular groups of interest by reducing the sequence set considered [11] does little to remove systematic errors, and at present it can only really be said that this issue has yet to be resolved in a phylogenetically satisfactory manner.

2.2.2 Intermediate Chains

Dynein ICs are proteins of 60–140 kDa in size that, like dynein HCs, are a single homologous superfamily that diverged from a common ancestor. This means that ICs can be meaningfully aligned and classified by phylogenetic analysis – although, because the identity of the dynein complexes is specified by the presence of particular classes of dynein HC (which also hold a richer phylogenetically signal), dynein ICs have not been subject to quite the same level of analysis as dynein HCs [9,39,40]. Phylogenetic classification of ICs shows there to be six well-supported classes of IC, as shown in Figure 2.2. As for dynein HCs, any taxonomy of ICs must contend with the difficult issue of nomenclature. Currently, there is no

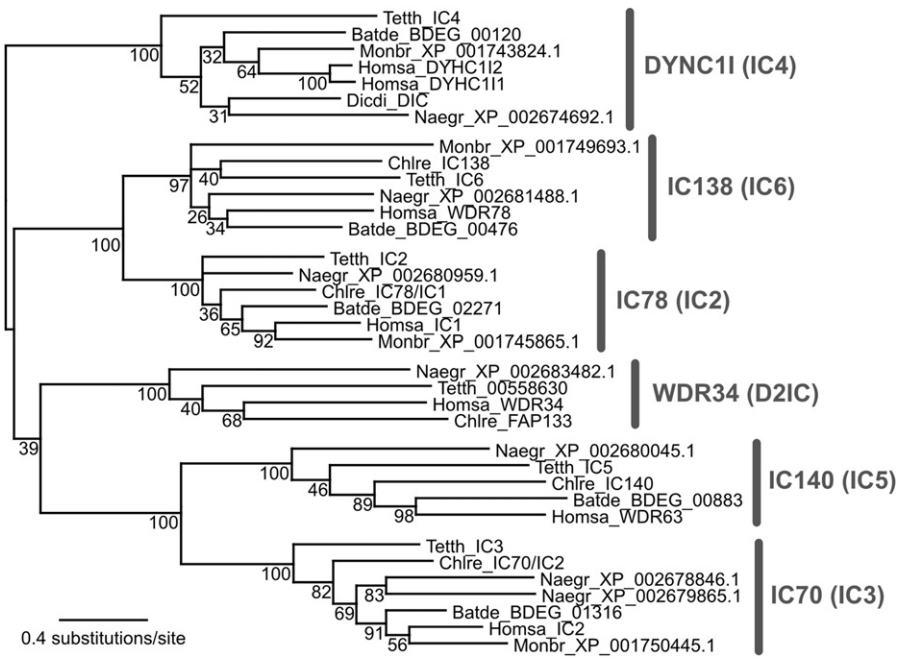

Figure 2.2 Phylogeny of dynein ICs showing major families. The phylogeny is a consensus of 100 maximum-likelihood inferences and was inferred as described in the legend to Figure 2.1. Published phylogenies support this inferred tree [9,40]. IC groups have been named as in [9] with the equivalent name from [40] in parentheses. Organisms and prefixes are the same as in Figure 2.1.

consensus nomenclature for the major IC families. In the following we use the nomenclature from [9], which is based largely on the "old" names for *Chlamydomonas* homologs contained in the classes. This system has the significant advantage of being relatively unambiguous, but is rather unsatisfactory in referring to groups according to the apparent molecular weight of subunits in SDS-PAGE gels. A more streamlined nomenclature based on *Tetrahymena* is proposed in [40] (in parentheses in Fig. 2.2). It is not employed here owing to the potential confusion with both animal and the new *Chlamydomonas* names (e.g. the "IC2" family (IC78) contains the IC1 chains of *Chlamydomonas* and human).

Classification of IC types reflects a specialization of the members for specific dynein classes: the DYNC1I family is specific for cytoplasmic dynein 1 [41]; WDR34 family members are associated with cytoplasmic dynein 2 [39]; a member of both the IC70 and the IC78 families is present in the outer-arm dynein complex [42–45]; whereas IC138 and IC140 are found in the two-headed inner-arm dynein complex [46–48]. Significantly, there is no known IC family that is specific for the single-headed dynein classes. Moreover, phylogenetic analysis would suggest that one is unlikely to be found, since all of the proteins that are readily identifiable as IC homologs can be grouped into the above six IC families. Hence, IC diversity does not include a class specific for single-headed dyneins and the presence of an IC may be one of the defining features of multi-head dynein complexes.

2.2.3 Light-Intermediate and Light Chains

Dynein LICs are 30–60 kDa in size. Unlike ICs and LCs, they are found only in the two "cytoplasmic" forms of dynein. In keeping with this, phylogenetic analysis of LICs shows only two families – one containing proteins specific for cytoplasmic dynein 1 (DYNC1LI) and one containing proteins specific for cytoplasmic dynein 2 (DYNC2LI) [9,40]. These LIC sequences have been phylogenetically compared to WDR34 IC sequences [40], although it is not clear that they are true homologs of these ICs, making the interpretation of these data problematic. Interestingly, there are two conserved proteins first identified in *Chlamydomonas*, called p38 and p44, that interact with DHC2 (an IAD-4 family member) [49,50]. On the basis of size only, these proteins would fit the description of "light-intermediate chain" molecules. However, they do not appear to be homologous to the LICs of cytoplasmic dyneins 1 and 2 or dynein IC proteins. It is not yet clear whether these proteins are part of a larger group of proteins that associate with other dynein HC classes.

The dynein LCs are more difficult to classify than dynein HCs and ICs because their small size and relatively high levels of sequence divergence lead to a lack of phylogenetic signal. Unlike dynein HCs, ICs, and LICs, LCs are probably not a homologous protein set with a single common ancestor, although it may be that sequence divergence makes a true homologous relationship difficult to detect (see [2,40] for analyses that assume homology between LC types). However, neither are they entirely separate orthologous sets, and some paralogous families are discernible (for example, LC2/LC9/Tctex1/Tctex2 homologs form an identifiable set [9]). This lack of overall homology allied with the presence of paralogous sets means that a combination of techniques for the separation of sets and also phylogenetics within sets is usually required for LC classification. LCs are also much more promiscuous than the other dynein components, with several LCs being found in more than one dynein complex (see [1,2]). Some LCs have roles that extend beyond dyneins altogether; for example, LC8 (DYNLL1/2) is a component of cytoplasmic dyneins 1 and 2 [51,52] but is also associated with a wide range of other cellular components, including myosin motors [53] and radial spokes [54], as well as being a dimerization hub [55]. Due to these difficulties in phylogenetic analysis and interpretation, dynein LCs will be largely excluded from the analysis that follows.

2.3 Dynein Evolution in Eukaryotes

With the advent of whole-genome sequencing for multiple eukaryotic organisms, there has been a step-change in the power of evolutionary analyses. Instead of merely classifying known sequences, it is now possible to delineate the whole repertoire of a particular family encoded by an organism. Moreover, by looking for the coexistence of other components of complexes or interacting proteins, it is possible to place a repertoire into a wider biological context in the cell. This is

hugely more powerful than phylogenies based on incomplete sets, since it directly speaks to what molecular machinery is — or is not — present in organisms and lineages.

Figure 2.3 shows the repertoires of dynein HCs, ICs, and LICs encoded in the genomes of a diverse set of eukaryotic organisms and also relates these to the IFT machinery. Such an approach enables us to look at how the evolution of eukaryotic lineages and the evolution of dynein types are linked. One of the most

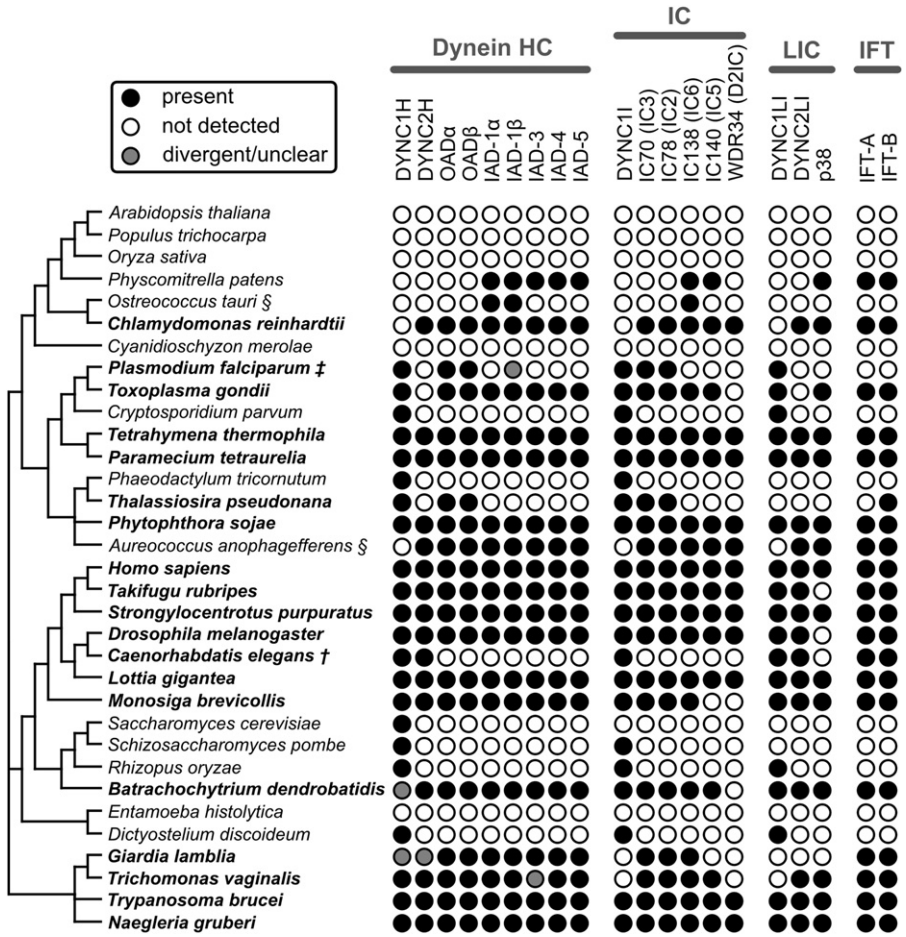

Figure 2.3 The distribution of dynein components across eukaryotes. A cladogram (left) shows the likely evolutionary relationships between the organisms in the analysis. Presence (dot) or absence (open circle) in the predicted proteomes of each organism is shown for identifiable orthologs of dynein HC, IC, or LIC families. Also shown is the presence/absence of some or all of the proteins of IFT-A or IFT-B particles. † *C. elegans* builds only immotile cilia; ‡ *P. falciparum* builds flagella by an IFT-independent mechanism [64]; § indicates organisms that have been described as non-ciliated but for which bioinformatic evidence suggests that cilia are built in a lifecycle stage that has yet to be observed (see Section 2.3.2).

striking things about the distribution of dynein families is that they are widely dispersed across the eukaryotic tree. In fact, from such analyses it can be seen that all of the major families of dynein date back at least as far as the last common ancestor of all eukaryotes (LCEA). Put another way: the dynein families pre-date the diversification of eukaryotes into the major lineages that survive to this day – rather than individual types of dyneins evolving in particular lineages (as appears to be the case for example for the myosins [56,57]), the dyneins existed prior to eukaryotic radiation and were then lost by individual lineages.

Tracing all the families of dyneins back to the root of eukaryotes implies that the LCEA already possessed differentiated cytoplasmic and IFT classes and all of the seven classes of dynein associated with axonemal motility. However, not all of these families are now found in extant species; from this relatively complex origin, the history of dyneins in eukaryotes is largely a history of loss. By incorporating information from dynein repertoires across the extant eukaryotic lineages, we can map the positions at which these losses most likely occurred on a tree of eukaryotic evolution, as in Figure 2.4. Many of these losses can be seen to be associated with the specific biology of organisms or lineages.

2.3.1 Dyneins: A History of Loss

2.3.1.1 Loss of Cytoplasmic Dynein 1

Given the importance of cytoplasmic dynein 1 in animal cells (and others), it is perhaps surprising to find that cytoplasmic dynein 1 has been independently lost a minimum of three times during the evolution of eukaryotes (Fig. 2.4 and [9]). We can be confident that this reflects true loss and is not simply a matter of the annotated genome for an individual organism lacking a good gene model for Cyto1 dynein HC, since these organisms are also missing the DYNC1I (IC) and DYNC1LI (LIC) components that are specific for this class of dynein (Fig. 2.3).

Arguably the most significant loss, and certainly the most ancient, is that in the ancestor of plants, red and green algae, and glaucophytes (collectively known as the Archaeplastida). Some confusion over the status of *Chlamydomonas* cytoplasmic dynein 1 was created by the early identification of a fragment of a dynein HC (denoted DHC1a) that appeared to group with the Cyto1 family [4,8]. Thanks to the sequencing of the *Chlamydomonas* genome [58], a full-length predicted sequence for the encoded protein is now available (JGI/ChlamyDB ID: 206178). However, inclusion of this full-length sequence in phylogenies with a wider range of dynein HCs has shown that this dynein HC is actually an axonemal dynein HC [9,59] and its original placement into the Cyto1 family was almost certainly an artefact of the fragmentary nature of the sequence and limited availability of dynein sequence data. In agreement with this conclusion, the IC and LIC proteins that are specific to cytoplasmic dynein 1 are also missing from the *Chlamydomonas* and *Ostreococcus* genomes (Fig. 2.3 and [9]). The same is true for dynein HCs encoded in the genome of *Volvox carteri*, which is closely related to

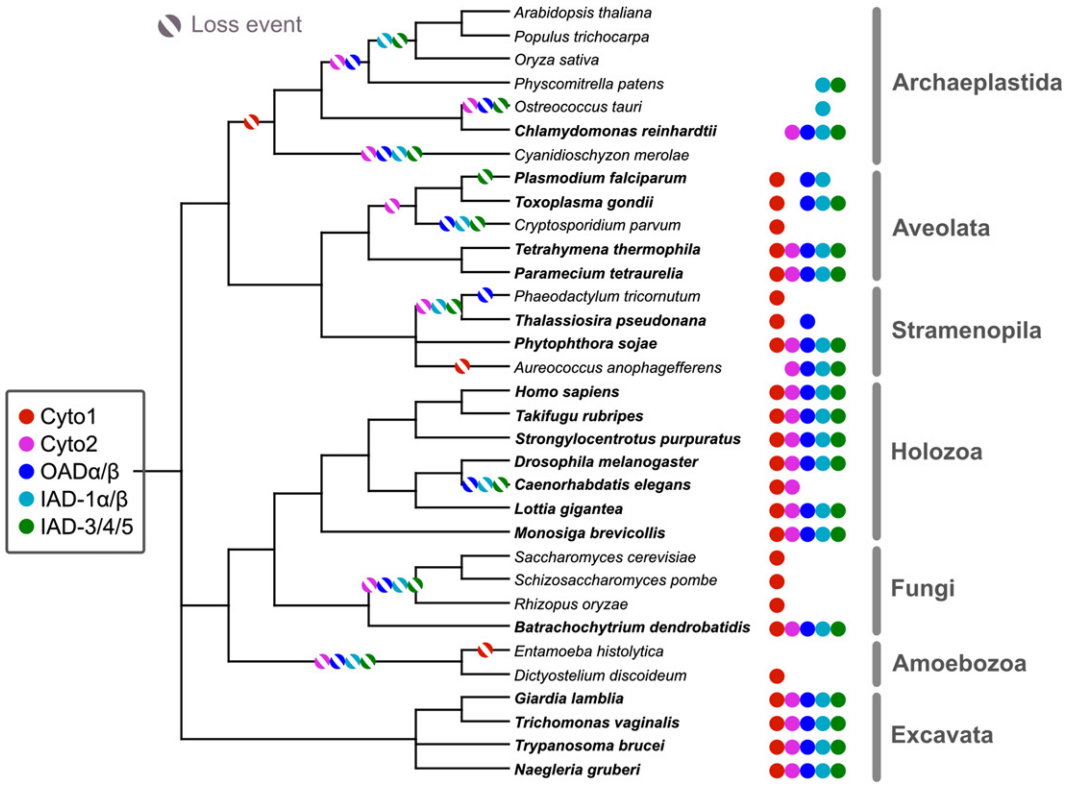

Figure 2.4 Evolution of the major classes of dynein in eukaryotes. All of the five major classes (Cyto1, Cyto2, OADα/β, IAD-1α/β, and IAD-3/4/5) were present in the LCEA of all extant eukaryotes, and their evolution from that point has involved multiple losses in several lineages. The positions of the loss events that provide the most parsimonious explanation for the modern-day distribution have been mapped onto a cladogram of the likely evolutionary relationships between the organisms.

Chlamydomonas and which also contain no identifiable Cyto1 sequence (data not shown).

These data show convincingly that the cytoplasmic dynein 1 complex has been lost in *Chlamydomonas* and its relatives. Moreover, since Cyto1 (and also DYNC1I and DYNC1LI) are missing from the land plants and also the red alga *Cyanidioschyzon merolae*, the most parsimonious explanation for the distribution now seen in extant organisms is that there was a single loss at or near the common ancestor that gave rise to all these organisms. This would make this specific loss of cytoplasmic dynein 1 very ancient (around 0.9–1.1 billion years ago [60]).

Cyto1, DYNC1I, and DYNC1LI are also missing from the genomes of the stramenopile *Aureococcus anophagefferens* and the amoeba *Entamoeba histolytica* (Fig. 2.3 and [9]). Neither of these organisms is closely related to the Archaeplastida, meaning that these losses must be independent of the loss in that

lineage. There is also a possible fourth loss of cytoplasmic dynein 1 in eukaryotes in the lineage giving rise to *Giardia*, although the situation is still unclear. Some analyses find no evidence for Cyto1 encoded in the genome of *Giardia lamblia* [61]. However, other work suggests that an ungrouped dynein HC in this organism is actually a difficult-to-detect member of the family [9]. The placing of the potential giardial Cyto1 dynein HC into this family certainly eludes simpler methods of tree inference, but this divergence of the sequence might also result in erroneous placement (due to so-called "long-branch attraction"). What is clear is that, even if *Giardia* does still contain a Cyto1 gene, the primary sequence of the protein is greatly altered from that of canonical dyneins in this family. Moreover, this divergence/loss also extends to the cytoplasmic dynein-1-specific IC and LIC families, which cannot be readily detected in the proteins predicted to be encoded by this organism (Fig. 2.3 and [9]).

Loss of cytoplasmic dynein 1 might be expected to deprive a cell of its principal minus-end-directed motor. Yet, evolution shows that other motors can fill this gap, at least in some evolutionary contexts. A biological analogy of this evolutionary scenario can be seen in experiments demonstrating that, despite roles in multiple cellular processes, *Saccharomyces cerevisiae* dynein HC mutants (*dyn1*) are viable unless combined with mutations in kinesin motors [62,63].

2.3.1.2 Loss of Cytoplasmic Dynein 2

As with cytoplasmic dynein 1, cytoplasmic dynein 2 has been lost multiple times during the evolution of eukaryotes (minimally seven times, as outlined in Fig. 2.4). Again, concomitant with the loss of the dynein HC are losses of the specific IC and LIC for this dynein. However, in contrast to cytoplasmic dynein 1, most of the losses of cytoplasmic dynein 2 can be linked to a specific piece of biology: IFT. Cytoplasmic dynein 2 and also a signature for IFT particles can be detected in nearly all organisms that build cilia/flagella at some point in their lifecycle (bold text in Fig. 2.3). A special deviation from this association is known to occur in *Plasmodium* species, which build their flagella in an IFT-independent manner [64]. To achieve this, flagella are assembled in the cytoplasm of the male gametocyte and then pushed out of the cell body in a process of exflagellation. Surprisingly, however, the loss of cytoplasmic dynein 2 appears to pre-date loss of IFT particles: *Toxoplasma* also has no detectable cytoplasmic dynein 2, but still has a signature for IFT [9].

In fact, in three organisms (*Toxoplasma gondii*, *Physcomitrella patens*, and *Thalassiosira pseudonana*), there are appears to be an IFT fingerprint with no retrograde motor. Interestingly, in all three cases, the IFT particle composition appears to be rather divergent (see [65]). For example, in *Thalassiosira pseudonana* there is a clear signal for proteins in IFT-B particles but no evidence for homologs of IFT44, IFT122, IFT139, IFT140, or IFT144, all of which are IFT-A proteins ([9] and this study). The lack of cytoplasmic dynein 2

in organisms that still possess a signature of the IFT machinery raises the important and currently unresolved question as to what is the retrograde motor for IFT in these organisms. Is it that no retrograde motor is required in these systems because another process such as diffusion is sufficient to return particles? Or is it that another motor, such as a minus-end-directed kinesin, has stepped in to perform this role? The situation in the moss *Physcomitrella patens* indicates that it is unlikely that cytoplasmic dynein 1 is fulfilling the role, since this organism also lacks this dynein.

2.3.1.3 Loss of Ciliary Dyneins

With so many of the dynein families having an axonemal function, it is unsurprising that there is a close association between the dynein repertoire and an organism's ability to build cilia/flagella. In several diverse lineages of eukaryotes, the axoneme as a motile organelle has been lost. As would be expected, the genomes of extant organisms from these lineages — which no longer build cilia/flagella at any lifecycle stage — are also devoid of genes encoding dyneins of the axonemal classes (i.e. those involved in bending of the axoneme), and also the retrograde motor of IFT, cytoplasmic dynein 2 (see Fig. 2.3). This complete loss of ciliary dyneins (i.e. the axonemal classes plus IFT) has occurred at least six times — and probably many more — in eukaryotes, most notably in angiosperms, Amoebozoa, and Fungi.

The nematode *Caenorhabditis elegans* represents a special case of ciliary dynein loss, since this organism and its relatives no longer build motile axonemes but still construct immotile cilia in some sensory neurons (see [66]). Again, the dynein family repertoire reflects this biology: *C. elegans* has retained cytoplasmic dynein 2 for IFT but lost all of the axonemal classes.

A different kind of loss event is also a feature of ciliary dynein evolution. This involves the loss of specific axonemal sets without the complete loss of motility. If we group the axonemal dyneins into functional sets — outer-arm dyneins (OADα/β), two-headed inner-arm dyneins (IAD-1α/β), and single-headed dyneins (IAD-3/4/5) — all three of these sets have been lost during the evolution of eukaryotes without full loss of axonemal motility. The moss *Physcomitrella patens* has lost all specific components of the outer-arm dyneins (OADα, OADβ, IC70, and IC78 families) but retained all two-headed and single-headed inner-arm dynein HC families (as well as IC138, IC140, and p38). The same genomic repertoire is very likely to be found in the fern *Marsilea vestita* (and most likely all lower land plants), in which spermatozoids show no ultrastructural evidence for outer-arm dyneins [67]. In contrast, the inverse dynein repertoire is found for the diatom *Thalassiosira pseudonana*: a full outer-arm dynein signature but no components (dynein HC, IC, or LIC) specific for inner-arm dyneins. The malaria parasite *Plasmodium falciparum* also encodes an unusual inner-arm dynein complement with no IAD-3/4/5 members and only a highly divergent possible member of the IAD-1β family.

None of these simplified repertoires represents the retention of a primitive ancestral form, since all of the respective lineages once possessed a full set of axonemal dyneins. Rather, these are repertoires that have been secondarily pared down from a more complex form. Hence, the loss of these dynein sets can be viewed as an evolutionary experiment in ciliary/flagellar function, investigating what can be removed without losing motility. They show that – even with the generally high conservation of axonemal dynein families in organisms with motile axonemes – neither inner- nor outer-arm dyneins are strictly required for axoneme-based motility. In analogy to the situation that has evolved in moss, mutants of *Chlamydomonas* that are unable to assemble outer-arm dyneins still build motile flagella [68,69]. However, mutants lacking both IAD-1α/β and also a LC that prevents several single-headed dyneins from assembling [70,71] are immotile in *Chlamydomonas* [72], unlike the diatom flagella, which lack all inner arms. Interesting, all of these stripped-down axonemes are built only during gametogenesis and all without the aid of cytoplasmic dynein 2. Such gamete-specific axonemes might in some ways be more "disposable" than more long-lived cilia/flagella and may not require the finer tuning of the beat that is likely to come with more axonemal dynein forms.

2.3.1.4 Organisms Possessing No Dynein

As can been seen from the above, no single family of dyneins appears to be essential for life as a eukaryote. In fact, the combination of the losses outlined above has produced three lineages that now exist without any dynein motors at all. The first good indication that there might be extant eukaryotic organisms with no dynein motors came from the sequencing of the *Arabidopsis thaliana* genome [73], when it was discovered that no components specific to dynein motors were encoded in the assembled sequence [74]. Subsequent examination of sequencing reads from the rice genome revealed good candidates for dynein HC genes [75], suggesting that the situation in plants might be more complicated than the initial findings in *Arabidopsis* had suggested. However, since that time, none of these dynein HC gene sequencing reads has assembled into the contigs covering the rice chromosomes ([76]; http://rice.plantbiology.msu.edu). Moreover, no dynein HC genes have been found in the completed *Populus trichocarpa* [77], *Vitis vinifera* [78], or *Zea mays* [79] genomes. These data, together with the fact that the original "rice" dynein HC reads appear to be of an axonemal dynein class [9], strongly indicate that the sequencing reads apparently from the rice genome were more likely sequence from a contaminating organism (probably a soil or phloem protozoan) and that flowering plants do indeed entirely lack dyneins. Furthermore, from the most probable position of the losses of the major dynein families on the tree of life (Fig. 2.3), we can predict that this lack of *all* dynein motors is common to all the flowering plants (angiosperms) and most likely any gymnosperms that lack flagella on their sperm (i.e. the conifers and gnetophytes). Such weight of genomic data makes the isolation by PCR of possible dynein HC gene fragments from *Nicotiana* [80] very unlikely to represent sequence of plant origin.

In addition to the large collection of dynein-less organisms above, the red alga *Cyanidioschyzon merolae* and the amoeba *Entamoeba histolytica* also lack dyneins of any kind (Fig. 2.3 and [9]). As more genome sequence emerges for organisms related to these, it will become clear how ancient (or recent) such total losses are. However, they do demonstrate that a dynein-less state has independently evolved at least three times in eukaryotes, without a great reduction in cytoplasmic microtubule function. An interesting parallel can be seen with the myosin motors of the actin cytoskeleton, which, despite their central cellular roles, have nonetheless been lost in their entirety in some lineages [56,57]. As yet, no organism that has lost all kinesin motors has been found [81].

2.3.2 Unexpected Presences

Particular cellular functions can be mapped onto specific dynein classes, meaning that some of the biology of an organism is reflected in its dynein repertoire. Some of the most unexpected findings that emerged after considering organisms' dynein repertoires in a "holistic" way were the discoveries of dynein families in places where there was no biology described to explain them. The green alga *Ostreococcus tauri* encodes what appears to be a canonical two-headed inner-arm dynein complex: the heterodimeric IAD-1α and IAD-1β dynein HC families, as well as at least one of the ICs (IC138) associated with it [9]. Yet this organism is not thought to build axonemes. In fact, *Ostreococcus* cells have been completely reconstructed ultrastructurally in three dimensions using electron tomography [82], and no centriole/basal body structure was present from which an axoneme might be extended. This does not, of course, preclude *de novo* formation of basal bodies, but this has never been described for this organism. An even clearer bioinformatic signal can be seen in the stramenopile *Aureococcus anophagefferens*, which also has no identified flagellate stage [83], yet encodes a clear signal for IFT [84] (including the retrograde motor) and all of the axonemal dynein classes (Fig. 2.3). Similar genomic signals have been seen in the encoded repertoires of kinesins [81] and centriolar proteins [65] and, for *Aureococcus*, in the flagellar apparatus [85].

These finding are significant because they predict unobserved biological features for organisms based only on genome sequence. It can be predicted from analysis of the dynein repertoire that both *Ostreococcus* and *Aureococcus* have flagellate lifecycle stages yet to be detected — either because they are very rare, because they are short-lived, or because the correct conditions have yet to be applied to cell cultures. We predict that both are motile male gamete stages.

2.3.3 Duplication and Diversification

Although the major theme in dynein evolution in eukaryotes is loss, on a smaller scale there have also been notable duplications of particular dynein classes. One of the most widespread has already been introduced: the duplication in the OADβ

dynein HC family to create three-headed outer-arm dynein. It is clear that, at one time, all proto-outer-arm dyneins were two-headed and consisted of a heterodimer of an OADα and an OADβ family member. At some stage, gene duplication occurred to produce what was probably a redundant OADβ copy. Diversification of the function of one copy created the third, outermost dynein head. The lack of phylogenetic resolution of the OADβ family into two well-supported "OADβ" and "OADγ" groups [9,10] means that it is currently not possible to accurately place the original duplication event on a tree of eukaryotic evolution. Indeed, it may not be only a single duplication event but several in different lineages. It is thus not clear whether the finding of only one OADβ family member in organisms such as trypanosomes [9] represents retention of an ancestral two-headed state or secondary loss of the outermost dynein head. However, the distribution does allow the prediction of specific axonemal ultrastructure from genome sequence alone: it is expected that all animal axonemes (not just sperm tails) will prove to be two-headed, as will the axonemes of chitrids and trypanosomes. In contrast, we expect that the axonemes of apicomplexans, diatoms, oomycetes, and *Naegleria* will prove to be three-headed, as are those of *Tetrahymena* and *Chlamydomonas*. It is noteworthy that, in organisms that possess three-headed outer-arm dyneins, the two OADβ family members (producing the β and γ heads in ciliates or α and β heads of *Chlamydomonas*) are still very similar in sequence, such that no separate OADγ class of dynein HC can be discerned. This almost certainly reflects a similar role for the dynein HCs involved, although it may also be due in part to the more recent nature of this duplication event compared to those that created the major dynein HC families.

As well as the duplication of the OADβ family, there are a number of more lineage-specific duplications in the dynein repertoires for some organisms, such as the expansion of the IAD-3 family in *Chlamydomonas*, the OADβ family in humans, or both the IAD-3 and IAD-5 families in *Tetrahymena* [9,10] (see Fig. 2.1). What function do these extra dyneins perform? The inner-arm dyneins of *Chlamydomonas* flagella repeat with a periodicity of 96 nm. Three-dimensional ultrastructural reconstructions show that, along with the two-headed IAD-1α/β complex, the 96 nm repeat contains an additional five [25,37] or six [36] single-headed inner-arm dynein densities. However, the genome of *C. reinhardtii* is predicted to encode at least nine dynein HCs in these families (see Fig. 2.1). This implies that either some of the dynein HCs are not used — unlikely, as they would quickly degenerate into pseudogenes in the absence of selective pressure — or that there is specialization of some of the dynein HCs for particular positions along the flagellum, stages in the organism lifecycle, or environmental conditions. Recent work suggests the former is the driving factor in *Chlamydomonas*, since low-abundance dynein isoforms DHC11 and possibly also DHC3 and DHC4 are specific to the proximal portion of the axoneme [59]. This creates a functionally differentiated portion of the flagellum, which it has been speculated might optimize the flagellar wave in this basal position.

This kind of diversification of function – encompassing either change in cellular role or specialization for specific cell types in multicellular organisms – is the most probable explanation for the persistence of many duplicated dynein HC types. For example, even a dynein with a clear cellular role, such as cytoplasmic dynein 2, also plays a role in other cellular processes [86,87], and duplications of the Cyto2 family within a single organism can create functional dynein HCs, only one of which is required for IFT [88].

The multi-dynein hypothesis states that multiple dynein HC genes exist in an organism's genome because they encode proteins with distinct functions. These functions are conserved across all organisms possessing that particular dynein HC type [89]. Redundancy or partial redundancy in dynein classes is thus in some senses a challenge to this central tenet of the multi-dynein hypotheses [10]. However, redundancy is also an essential intermediate in the evolution of multigene families with specialized functions. This is because the temporary redundancy created by gene duplication allows specialization of a protein that previously had pleiotropic functions. Alternatively, it can relax the evolutionary pressure that might otherwise prevent selection for additional functions. Such diversification of function following duplication is a common fate for gene duplications (see [90]).

2.4 Evolution in the Proto-Eukaryote

The majority of the dynein complexity seen in extant eukaryotes was already formed in the LCEA cell. Since that time, the evolutionary history of the dynein superfamily has been largely one of simplification – with losses of all of the major classes in some present-day lineages. Interestingly, this complexity in the LCEA is a surprising feature that is emerging from several different evolutionary analyses: the ancestral eukaryote had a complex kinesin repertoire [81], a heterogeneous replisome [91], and most of the machinery for endocytosis [92] and probably phagotrophy [93]. However, this complexity at the root of eukaryotes cannot have appeared fully formed. Somewhere during the evolution of the proto-eukaryote (i.e. in the ancestors to the LCEA), the different dynein families evolved through a series of steps involving duplication followed by functional diversification. These events must have been intimately linked with the evolution of the eukaryotic cytoskeleton more generally – particularly the evolution of the axoneme. As such, the evolutionary history of dynein is molecular archaeological evidence for the evolutionary events that gave rise to one of the signature features of the eukaryotes: the cilium.

The inference of the path of dynein evolution prior to the LCEA is considerably more demanding than inferences within the extant lines. This is because the events are more ancient (and hence have a weaker phylogenetic signal) and there are apparently no extant organisms that evolved from transitional forms to

support the existence of more primitive states. One of the key questions that must be addressed is: in what order did the dynein classes emerge? The problem is essentially one of rooting: if we either know or can infer the position on the dynein family tree of the single *ur*-dynein that evolved into all the others, then (given sufficient phylogenetic signal) we should be able to infer the branching order of the families. This then would represent the evolutionary history of dyneins *before* the LCEA.

2.4.1 A Cytoplasmic Dynein Root: Sensation Before Motility

Both Hartman and Smith [11] and Wilkes et al. [10] approached the problem of rooting the dynein tree in a similar way, by assuming that the root lies within the cytoplasmic dynein 1 family. When this is done, the first split in dynein evolution falls naturally between Cyto1 and an ancestor of all those involved in the cilium (i.e. Cyto2 and the axonemal dyneins). A second split in this latter lineage gives rise to the Cyto2 family and a proto-axonemal dynein – and at this point in evolution the motile cilium is born. This model is intuitively appealing, as it suggests that the primary division in dynein biology was between motors in the cytoplasm and those associated with the proto-cilium. Furthermore, it means that these cilium-associated motors were originally moving on an unbending structure and bending motility was only later produced by the specialization of these motors into IFT and axonemal dyneins.

Rooting the dynein tree on Cyto1 results in a dynein family branching order that supports either of two alternative hypotheses for the evolution of the cilium: (1) Sensation was the primary driver of proto-cilium evolution, with a specialized dynein (the ancestor of Cyto2 and axonemal dyneins) serving an IFT-like role on a sensory cilium before the emergence of motility via the incorporation of an IFT-like motor into the axoneme [16,94,95]; (2) The proto-cilium evolved as a motile rather than a sensory organelle, but this motility was originally based on gliding through the action of a specialized cytoplasmic dynein motor [96,97], with the later addition of bending motility from dyneins incorporated into the axoneme. In both scenarios the cilium exists before motility based on microtubule sliding is added, and in both cases the proto-cilium protrudes from the cell body and is serviced by specialized IFT machinery. However, support for these hypotheses from the dynein HC family phylogeny is entirely dependent on the validity of the assumption that the Cyto1 family was established before the other families. It is not at all clear that this assumption is valid. Gibbons [3] originally noted that the homodimeric nature of cytoplasmic dynein 1 was a more "primitive" arrangement than that of the heteromeric two-headed inner-arm dynein complex or two-/three-headed outer-arm dyneins, which might be indicative of ancestral simplicity. However, it has since become clear that the subunit composition of cytoplasmic dynein 1 is actually no simpler than that of many other dyneins. Cytoplasmic

dynein 2 is also homodimeric with respect to the dynein HC, and a large group of axonemal dyneins are single-headed, making cytoplasmic dynein 1 less primitive than it had first appeared.

The existence of organisms and cell types with immotile cilia built in an IFT-dependent fashion has been considered as support for this state as an evolutionary intermediate. However, all non-motile cilia in extant organisms evolved through the *loss* of motility from an ancestrally motile cilium. They do not therefore represent an ancestrally primitive state, but are a derived feature. As such, although the cilium *could* have evolved by the production first of a sensory, immotile axoneme onto which dynein-based sliding was subsequently added, the existence of present-day sensory cilia does not, in itself, provide evidence that this was a transitional state in ciliary evolution. It is axiomatic that a proto-eukaryote possessing a dynein-like motor, but yet to evolve the ability to build an axoneme, must contain only "cytoplasmic" dynein – but this is not equivalent to this proto-dynein being a member of the Cyto1 dynein HC family. Hence, rooting of the dynein HC phylogeny on Cyto1 is based on assumptions that are currently not well-supported.

2.4.2 Midasin-Based Rooting: Motility Drives Ciliary Evolution

An alternative approach to rooting the dynein HC tree is to use sequence data from a molecule that shares a common ancestor with dynein HCs but that diverged from them before the emergence of the dynein families. Midasins and related proteins are a family of large proteins that are widely conserved in eukaryotes and have a similar structure to dynein HCs (discussed further in Section 2.5). They have diverged a considerable distance from dynein HCs, but it is clear that they once had a common ancestor [98–100]. Dynein HC phylogenies rooted using midasins tell a rather different story from those rooted on Cyto1, as demonstrated in Figure 2.5. The inferred root of dyneins now lies between both classes of "cytoplasmic" dynein HC (Cyto1 and Cyto2) and the axonemal classes. This means that the primary division of the dynein HCs is between an ancestor of motors necessary for axonemal bending and those of the cytoplasm. Only later did the cytoplasmic motor specialize into a form dedicated to cytoplasmic traffic on single microtubules and a separate motor for IFT on doublets. This would not necessarily be incompatible with an evolution of the cilium involving an immotile sensory function or gliding motility prior to bending, but it does undermine some of the support for these hypotheses by removing the specialized IFT-like motor. In contrast to the analyses of Hartman and Smith [11] and Wilkes et al. [10], this rooting instead provides support for the idea that the cilium evolved as a bending organelle first, through the early evolution of axonemal motors. Such a proto-cilium could have evolved from a bundle of cytoplasmic microtubules that provided cellular motility without protruding from the cell body – a situation analogous to the axostyle-based motility of oxymonads [101–103]. Only later

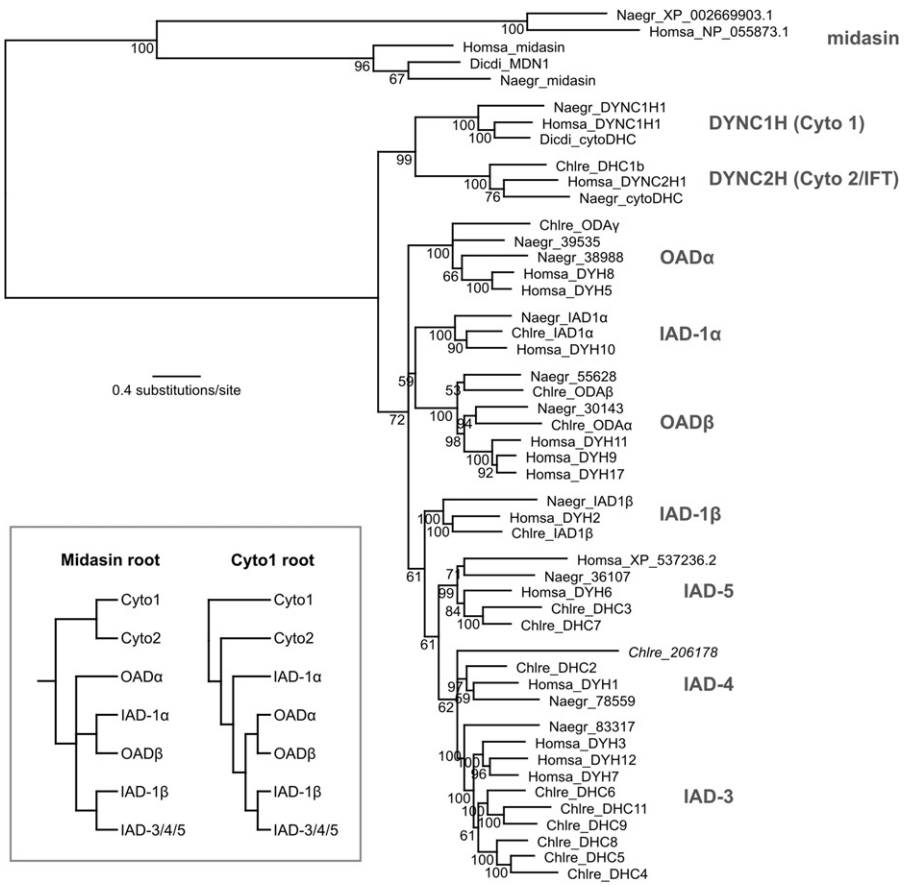

Figure 2.5 Rooting of the dynein HC tree using midasin sequences as an outgroup. The phylogeny is a consensus of 100 maximum-likelihood inferences and was inferred as described in Figure 2.1, but from a smaller set of model organisms. Inset summarizes the branching order of the dynein HC families seen in the tree and compares it with the order inferred by Hartman and Smith [11] by rooting a maximum parsimony tree on Cyto1. Chlre, *Chlamydomonas reinhardtii*; Dicdi, *Dictyostelium discoideum*; Homsa, *Homo sapiens*; Naegr, *Naegleria gruberi*.

would sensory functions and a specialized machinery necessary of IFT have been added to this motile structure. Without the aid of IFT, the proto-cilium may have remained confined within the cell body, but it could also have been assembled in the cytoplasm and then pushed out of the cell as are some IFT-independent axonemes today [64,104,105].

At first sight, rooting based on molecular sequence data might be assumed to be intrinsically preferable to analysis based on a prior assumption about the evolution of dyneins that lacks support. However, some caution is necessary when interpreting the dynein HC/midasin tree, just as it is when assuming other roots. Phylogenies inferred using very divergent paralogous sequences can potentially suffer from two sources of artefact: (1) High levels of divergence lead to homoplasy (sequence similarity due not to conservation but to

multiple substitutions at the same site), which can cause so-called "long-branch attraction." (2) Paralogous proteins with different functions have different evolutionary constraints. These different constraints can potentially mask phylogenetic signal and have a tendency to push paralogs to the base of a particular group. This second artefact in particular would encourage the placing of the midasin clade on the longest basal branch of the dynein tree. The methodology used in Figure 2.5 (maximum likelihood allowing for heterologous rates of evolution) copes much better with these potential artefacts than simpler methods (such as parsimony or minimum evolution), but the potential for such artefacts must not be overlooked. Nonetheless, the molecular evidence does strongly support monophyly for a single group containing both Cyto1 and Cyto2, which is inconsistent with "Cyto1-first" hypotheses.

2.5 The Origins of Dynein

Probing back further in evolutionary time from the single *ur*-dynein that was the ancestor of all present-day dyneins prompts the following seemingly simple question: from what sequence did this proto-dynein evolve? Moreover, how might the function of these huge molecular motors have evolved? There are no dyneins (or midasin) in either Bacteria or Archaea. In fact, although there is a prokaryotic tubulin homolog, FtsZ, which forms dynamic filaments that were probably the forerunners of microtubules (see [106–108]), there appear to be no motors that run these prokaryotic filaments. No orthologs for any of the components of dyneins have been identified in prokaryotic lineages.

Dynein HCs are members of the very large and diverse superfamily of AAA^+ proteins. AAA proteins (for ATPases associated with various cellular activities) are named for the broad variety of cellular roles with which they are associated. These include, amongst others, regulation of the eukaryotic 26 S proteasome, facilitation of vesicle fusion, biogenesis of the peroxisome, cell-cycle control, and transcription (see [109–112]). As if this were not diversity enough, subsequent bioinformatic analysis showed that the AAA proteins were themselves part of a larger superfamily of proteins, denoted "AAA^+" to differentiate this larger family from the established *sensu stricto* AAA set [113]. It is to this larger AAA^+ superfamily that the dynein HCs belong.

2.5.1 Evolution of Structure

The AAA^+ domain is based on an ATPase domain of ~220 aa. All dynein HCs contain six AAA^+ domains (see [1,114] and Fig. 2.6A) that come together in the folded structure to produce an intra-peptide hexameric ring of AAA^+ domains [115–117]. In contrast, most prokaryotic proteins contain only a single AAA^+ domain. However, many of these single AAA^+ domain proteins have been shown

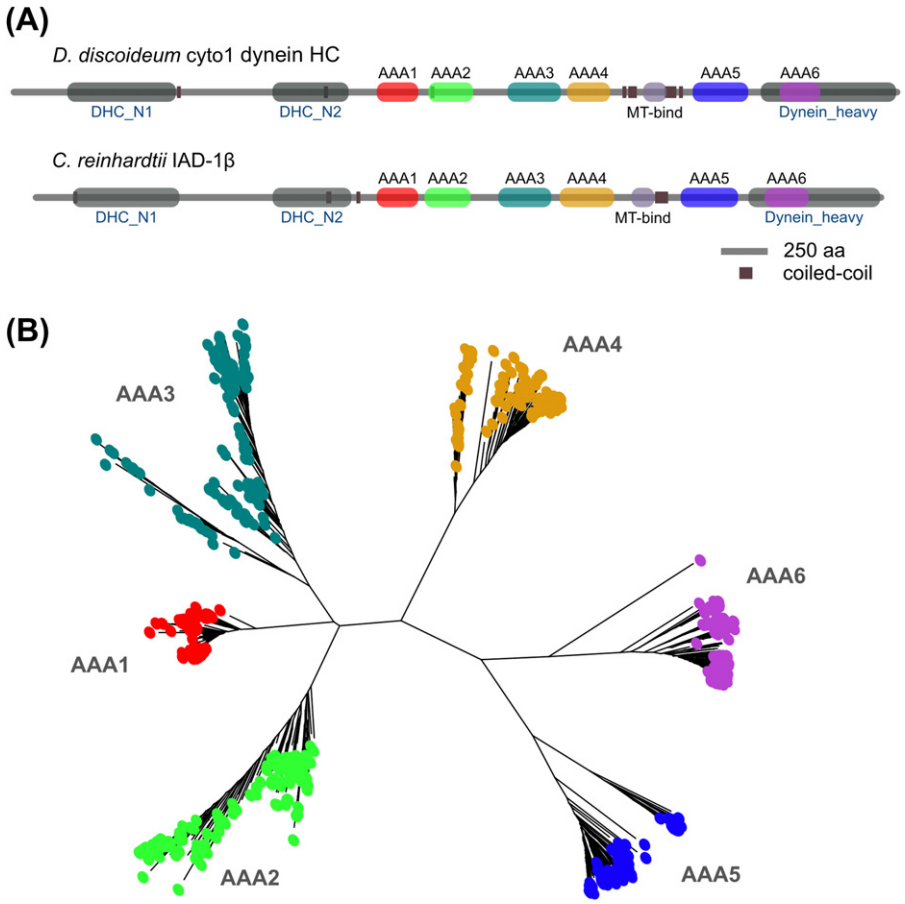

Figure 2.6 Evolution of dynein HC structure. (A) The domain structure of the dynein HC. Two dynein HCs from representative dynein HC families (Cyto1 *Dictyostelium discoideum* and IAD-1β from *Chlamydomonas reinhardtii*) are shown along with the positions of the AAA domains and microtubule-binding domain (MTBD). Also shown are the positions of all significant hits to domains in the Pfam-A database (blue text; [133]) and coiled-coil regions as predicted by the algorithm in [134]. (B) The relationship between the AAA domains of 158 dynein HCs from 24 diverse eukaryotes (sequences taken from [9]). Sequences were trimmed to the six AAA domains as defined by matching a hidden Markov model of each AAA domain to each predicted dynein HC. These trimmed AAA domains were then clustered on the basis of BLASTp score as described in [9].

to assemble into oligomeric ring complexes (often homomeric) composed of six or seven AAA^+ proteins (see [111]). Moreover, these rings are believed to change their shape during the ATPase cycle of their components. This arrangement implies that dynein HCs evolved by duplication of a single AAA^+ domain protein (a scenario involving fusion between already-diversified AAA^+ proteins cannot be ruled out, but it is rather unlikely as it would bring together proteins with different

functions). Following this original duplication event, the AAA^+ domains of dynein HCs diverged greatly, such that it is now difficult to align their primary sequences without employing sophisticated alignment methods [100]. Most of this divergence must have occurred *before* the LCEA and before the emergence of the major dynein classes, as can be seen from the fact that extant domains are much more similar to domains in the same position in other dynein HCs/organisms than to other AAA^+ domains in the same protein (Fig. 2.6B).

Of the six AAA^+ domains of the dynein HC, only the four nearest the N-terminus (AAA1−AAA4) contain Walker A (P-loop) and Walker B motifs and are able to bind ATP [118], but these are not present in AAA5 and AAA6. The first AAA^+ domain is the primary site of ATP hydrolysis [119], but hydrolysis at both AAA1 and AAA3 appears to be required for full function (see [120]). Asai and Koonce [121] have used the relationships between the AAA^+ domains in extant sequences to propose a "4+2" model of dynein HC evolution. In their model, the dynein HC structure is proposed to have developed from a single ATPase-competent domain (domain 1) by sequential duplications to produce domains 2, 3, and 4, onto which has been added the most divergent domains, 5 and 6.

This proposal is one of the few attempts to model proto-dynein HC evolution [121], but it does require some quirks relative to most models of sequence evolution. First, the more ancient duplications are proposed to have produced the more *similar* domains (rather than the more different, as would be expected if the rate of change of each was constant). Hence, the most divergent domains (AAA5 and AAA6) are proposed to have been added last, by fusion of a pre-existing divergent AAA^+ domain protein onto the $4\times AAA^+$ structure. Second, the model goes through a structure ($4\times AAA^+$) that cannot form a ring of six domains, requiring the supply of domains from a second protein of $2\times AAA^+$ structure that is latter fused to the former. This is not an insurmountable problem for the model, but it is greatly less parsimonious than models invoking only $2\times AAA^+$ and $3\times AAA^+$ intermediates. That said, there is biological precedent for a 4+2 arrangement: although the intramolecular $6\times AAA$ configuration is by far the most common, it is not strictly necessary, since the fungus *Ustilago maydis* encodes Cyto1 in two separate genes − one encoding AAA1−AAA4 and one encoding AAA5 and AAA6 [122]. However, as for the existence of sensory cilia in eukaryotes, this is not an ancestrally primitive state but a derived characteristic, and hence not necessarily good evidence that this was an intermediate in dynein evolution.

Models based on similar domains from more recent duplications are more conventional. However, these too create evolutionary scenarios in which it is difficult to have much faith. Since the AAA^+ domains are rather refractory to multiple sequence alignment encompassing all six modules, one of the easiest ways to investigate relationships between the domains is to cluster them based on local alignment scores. Figure 2.6B shows such an analysis by clustering all

domains from 158 dynein HCs by BLAST score. This suggests that the most basal division might be between domains AAA1–AAA3 and AAA4–AAA6. This can be readily explained by an ancestral duplication from a monomer to a dimer of AAA^+ domains, one half of which gave rise to domains AAA1–AAA3 and the other to domains AAA4–AAA6. However, both parts of this dimer would then have to independently duplicate within the protein, giving rise to both $4\times AAA^+$ and $5\times AAA^+$ intermediates that, as mentioned above, are rather improbable evolutionary intermediates.

There are potential systematic artefacts that may explain the unlikely scenarios suggested by phylogenies of dynein AAA^+ domains. First is the problem of different evolutionary pressure on paralogous sequences, as described above for the midasin/dynein HC tree. Such an issue is likely to be particularly acute in a protein in which AAA^+ domains have specialized to fulfill different functions. Second, since domains in the same protein interact, the assumption that the evolution of one domain is independent of changes in the other is almost certainly violated. These factors make it very tricky to infer ancestry between the AAA^+ domains with any great confidence. It is likely that it is also these factors that confound the inference of the evolution of the dynein HC structure.

Interestingly, the AAA^+ domains of midasin show different inter-domain relationships from that of the AAA^+ domains of dynein HCs [99], suggesting that midasin was the product of an independent series of duplication/fusion events but from a single protein that shares a common ancestor with dynein HC. The relationship between the AAA^+ domains in midasin – in which the most basal split is between domains 1, 3, and 5 and domains 2, 4, and 6 – is no more easily explained than the relationship between the domains of dynein HC. The same difficulties in inference of ancestry for dynein HCs are likely to apply to midasin.

2.5.2 Evolution of Function

Finally, we arrive at the question of the evolution of dynein function. In particular, what was the cellular role of the proto-dynein complex and how did that function evolve into those now seen for dynein molecular motors? The best clues to address these questions could be found by looking at the closest relatives to dynein HC in prokaryotes or eukaryotes. The closest eukaryotic relative to dynein HCs is midasin [99,100]. Midasin appears to be more closely related to dynein HC than any known prokaryotic protein. However, the function of midasin is strikingly different from that of dynein: midasin is a nuclear chaperone involved in the construction and maturation of the ribosome [100,123,124]. Is this sharp contrast in function also a feature of prokaryotic homologs? The combination of the small size of AAA^+ domains, the great diversity of their types, and the huge evolutionary distances involved make robust phylogenies of AAA^+ domains extremely challenging. Even producing alignments for inference is very difficult.

Attempting to address this, Iyer et al. [100] first aligned closely related AAA^+ domains and then created profile alignments (alignments of alignments) from these. Even employing this more sensitive technique, it was not possible to construct well-supported conventional phylogenetic trees from these alignments. Hence, the analysis of the relationships between AAA^+ types instead depended largely on comparisons of inferred structures and the presence of particular derived characters. By this approach, it is predicted that the closest prokaryotic family of AAA^+ proteins to eukaryotic dynein HC/midasin is the MoxR family [100].

The precise functional role of MoxR proteins in prokaryotes is unclear. The family contains proteins with a role in the biogenesis of methanol dehydrogenase [125], formation of nitric-oxide reductase [126,127], and gas vesicle biogenesis in certain organisms [128–131]. However, it has been suggested that the uniting feature behind these roles is that MoxR proteins are also primarily molecular chaperones [132]. This would mean that both the closest eukaryotic and also prokaryotic relatives of dynein HCs are chaperones that couple ATP hydrolysis to conformational change in other proteins. Might this also have been the ancestral role of proto-dynein in the pre-eukaryotic cell? The coincidence of function for the nearest relatives to dynein in both eukaryotes and prokaryotes is certainly provocative. A reasonable evolutionary pathway can also be drawn from an ancestral protein acting as a chaperone for a tubulin-like precursor, to a molecular motor walking on microtubules. From a very reductive perspective, the cycle of a NTPase chaperone is rather similar to that of a molecular motor: bind, change conformation, release. But from such a simplified point of view the same could be said for the activity of almost any NTPase. Dynein also differs significantly in that it must leave its binding partner unchanged after conformational change. Given the sparsity of data, such associations are tenuous at best, but the current data suggest that, somewhere in the large gulf between the prokaryotes and today's eukaryotes, the single ancestor of both midasin and dynein might have been a protein whose cellular role was to couple ATP hydrolysis to protein folding.

2.6 Summary

Dyneins are multi-subunit complexes that can be classified by phylogenetic analysis of the dynein HC and, to a lesser extent, IC and LIC, which they contain. Dynein HC phylogenies reveal nine major classes of dynein HC, one of which is specialized for cytoplasmic dynein function, one for IFT, and seven for roles in the axoneme. Combining phylogenetic analyses with whole-genome comparisons, it is possible to map the repertoires of dyneins in diverse eukaryotes and hence trace the evolution of dyneins for the past $\sim$1 billion years. Strikingly, the last common ancestor of all extant eukaryotes already

possessed a complex cytoskeleton containing all of the major dynein HC classes and, since that time, the evolutionary history of dyneins has been mainly one of loss. All of the major families of dynein have been lost independently multiple times during the evolution of eukaryotes, with some extant organisms now having no dyneins of any kind. Against these losses are relatively few well-conserved duplications and specializations within the families. These data both explain and also predict organism biology. They predict axonemal ultrastructure, show that neither inner- nor outer-arm dyneins are strictly required for axonemal motility, and imply a novel motor for IFT in a number of organisms with a divergent IFT machinery and no retrograde dynein motor. The presence of clear axonemal dyneins in organisms that were believed not to possess flagella/cilia also predicts the existence of a motile gamete stage that has not yet been described. If it is assumed that the cytoplasmic dynein 1 family existed before any others, then the branching order of the major dynein families supports the existence of sensory, immotile cilia/flagella as an intermediate in the evolution of the axoneme. However, molecular phylogenetics suggests a different origin for dynein HCs and places axonemal motility back near the very start of dynein evolution. Great challenges in alignment and tree building make it very difficult to infer an order for the evolution of the six-fold AAA^+ domain structure of the dynein HC, but the closest relatives in both eukaryotes and prokaryotes suggest that the role of dynein motors may have emerged from a chaperone-like function during the evolution of the cytoskeleton in the proto-eukaryote.

References

[1] S.M. King, Dynein motors: structure, mechanochemistry and regulation, in: M. Schliwa (Ed.), Molecular Motors, Wiley-VCH, Weinheim, 2002, pp. 45–78.

[2] D.E. Wilkes, V. Rajagopalan, C.W.C. Chan, E. Kniazeva, A.E. Wiedeman, D.J. Asai, Dynein light chain family in *Tetrahymena thermophila*, Cell Motil. Cytoskeleton 64 (2007) 82–96.

[3] I.R. Gibbons, Dynein family of motor proteins: Present status and future questions, Cell Motil. Cytoskeleton 32 (1995) 136–144.

[4] M.E. Porter, R. Bower, J.A. Knott, P. Byrd, W. Dentler, Cytoplasmic dynein heavy chain 1b is required for flagellar assembly in *Chlamydomonas*, Mol. Biol. Cell 10 (1999) 693–712.

[5] D.J. Asai, D.E. Wilkes, The dynein heavy chain family, J. Eukaryot. Microbiol. 51 (2004) 23–29.

[6] P. Höök, R.B. Vallee, The dynein family at a glance, J. Cell Sci. 119 (2006) 4369–4371.

[7] R.L. Morris, M.P. Hoffman, R.A. Obar, S.S. McCafferty, I.R. Gibbons, A.D. Leone, J. Cool, E.L. Allgood, A.M. Musante, K.M. Judkins, B.J. Rossetti, A.P. Rawson, D.R. Burgess, Analysis of cytoskeletal and motility proteins in the sea urchin genome assembly, Dev. Biol. 300 (2006) 219–237.

[8] G.J. Pazour, N. Agrin, B.L. Walker, G.B. Witman, Identification of predicted human outer dynein arm genes: Candidates for primary ciliary dyskinesia genes, J. Med. Genet. 43 (2006) 62–73.

[9] B. Wickstead, K. Gull, Dyneins across eukaryotes: A comparative genomic analysis, Traffic 8 (2007) 1708–1721.

[10] D.E. Wilkes, H.E. Watson, D.R. Mitchell, D.J. Asai, Twenty-five dyneins in *Tetrahymena*: A re-examination of the multidynein hypothesis, Cell Motil. Cytoskeleton 65 (2008) 342–351.
[11] H. Hartman, T.F. Smith, The evolution of the cilium and the eukaryotic cell, Cell Motil. Cytoskeleton 66 (2009) 215–219.
[12] T. Yagi, Bioinformatic approaches to dynein heavy chain classification, Methods Cell Biol. 92 (2009) 1–9.
[13] P.S. Soltis, D.E. Soltis, Applying the bootstrap in phylogeny reconstruction, Stat. Sci. 18 (2003) 256–267.
[14] K.K. Pfister, E.M.C. Fisher, I.R. Gibbons, T.S. Hays, E.L.F. Holzbaur, J.R. McIntosh, M.E. Porter, T.A. Schroer, K.T. Vaughan, G.B. Witman, S.M. King, R.B. Vallee, Cytoplasmic dynein nomenclature, J. Cell Biol. 171 (2005) 411–413.
[15] K.K. Pfister, P.R. Shah, H. Hummerich, A. Russ, J. Cotton, A.A. Annuar, S.M. King, E.M.C. Fisher, Genetic analysis of the cytoplasmic dynein subunit families, PLoS Genet. 2 (2006) e1.
[16] J.L. Rosenbaum, G.B. Witman, Intraflagellar transport, Nat. Rev. Mol. Cell Biol. 3 (2002) 813–825.
[17] J.M. Scholey, Intraflagellar transport motors in cilia: Moving along the cell's antenna, J. Cell Biol. 180 (2008) 23–29.
[18] C.A. Perrone, D. Tritschler, P. Taulman, R. Bower, B.K. Yoder, M.E. Porter, A novel dynein light intermediate chain colocalizes with the retrograde motor for intraflagellar transport at sites of axoneme assembly in *Chlamydomonas* and mammalian cells, Mol. Biol. Cell 14 (2003) 2041–2056.
[19] W.S. Sale, U.W. Goodenough, J.E. Heuser, The substructure of isolated and *in situ* outer dynein arms of sea urchin sperm flagella, J. Cell Biol. 101 (1985) 1400–1412.
[20] J.L. Gatti, S.M. King, A.G. Moss, G.B. Witman, Outer arm dynein from trout spermatozoa. Purification, polypeptide composition, and enzymatic properties, J. Biol. Chem. 264 (1989) 11450–11457.
[21] S.M. King, J.L. Gatti, A.G. Moss, G.B. Witman, Outer-arm dynein from trout spermatozoa: Substructural organization, Cell Motil. Cytoskeleton 16 (1990) 266–278.
[22] S. Wada, M. Okuno, K.I. Nakamura, H. Mohri, Dynein of sperm flagella of oyster belonging to Protostomia also has a 2-headed structure, Biol. Cell 76 (1992) 311–317.
[23] H. Mohri, M. Kubo-Irie, M. Irie, Outer arm dynein of sperm flagella and cilia in the animal kingdom, Memoires du Museum National d'Histoire Naturelle 166 (1995) 15–22.
[24] H. Mohri, K. Inaba, M. Kubo-Irie, H. Takai, Y. Yano-Toyoshima, Characterization of outer arm dynein in sea anemone, *Anthopleura midori*, Cell Motil. Cytoskeleton 44 (1999) 202–208.
[25] D. Nicastro, C. Schwartz, J. Pierson, R. Gaudette, M.E. Porter, J.R. McIntosh, The molecular architecture of axonemes revealed by cryoelectron tomography, Science 313 (2006) 944–948.
[26] K.A. Johnson, J.S. Wall, Structure and molecular weight of the dynein ATPase, J. Cell Biol. 96 (1983) 669–678.
[27] U. Goodenough, J. Heuser, Structural comparison of purified dynein proteins with *in situ* dynein arms, J. Mol. Biol. 180 (1984) 1083–1118.
[28] D. Nicastro, J.R. McIntosh, W. Baumeister, 3D structure of eukaryotic flagella in a quiescent state revealed by cryo-electron tomography, Proc. Natl. Acad. Sci. USA 102 (2005) 15889–15894.
[29] H. Sakakibara, S. Takada, S.M. King, G.B. Witman, R. Kamiya, A *Chlamydomonas* outer arm dynein mutant with a truncated β heavy chain, J. Cell Biol. 122 (1993) 653–661.
[30] H. Sakakibara, D.R. Mitchell, R. Kamiya, A *Chlamydomonas* outer arm dynein mutant missing the α heavy chain, J. Cell Biol. 113 (1991) 615–622.

[31] W.J. Tang, C.W. Bell, W.S. Sale, I.R. Gibbons, Structure of the dynein-1 outer arm in sea urchin sperm flagella. I. Analysis by separation of subunits, J. Biol. Chem. 257 (1982) 508–515.
[32] K.K. Pfister, G.B. Witman, Subfractionation of *Chlamydomonas* 18S dynein into two unique subunits containing ATPase activity, J. Biol. Chem. 259 (1984) 12072–12080.
[33] Y.Y. Toyoshima, Chymotryptic digestion of *Tetrahymena* 22S dynein. I. Decomposition of three-headed 22S dynein to one- and two-headed particles, J. Cell Biol. 105 (1987) 887–895.
[34] E.F. Smith, W.S. Sale, Structural and functional reconstitution of inner dynein arms in *Chlamydomonas* flagellar axonemes, J. Cell Biol. 117 (1992) 573–581.
[35] S.H. Myster, J.A. Knott, E. O'Toole, M.E. Porter, The *Chlamydomonas Dhc1* gene encodes a dynein heavy chain subunit required for assembly of the I1 inner arm complex, Mol. Biol. Cell 8 (1997) 607–620.
[36] K.H. Bui, H. Sakakibara, T. Movassagh, K. Oiwa, T. Ishikawa, Molecular architecture of inner dynein arms *in situ* in *Chlamydomonas reinhardtii* flagella, J. Cell Biol. 183 (2008) 923–932.
[37] T. Heuser, M. Raytchev, J. Krell, M.E. Porter, D. Nicastro, The dynein regulatory complex is the nexin link and a major regulatory node in cilia and flagella, J. Cell Biol. 187 (2009) 921–933.
[38] K.H. Bui, H. Sakakibara, T. Movassagh, K. Oiwa, T. Ishikawa, Asymmetry of inner dynein arms and inter-doublet links in *Chlamydomonas* flagella, J. Cell Biol. 186 (2009) 437–446.
[39] P. Rompolas, L.B. Pedersen, R.S. Patel-King, S.M. King, *Chlamydomonas* FAP133 is a dynein intermediate chain associated with the retrograde intraflagellar transport motor, J. Cell Sci. 120 (2007) 3653–3665.
[40] D.E. Wilkes, N. Bennardo, C.W.C. Chan, Y. Chang, E.O. Corpuz, J. DuMond, J.A. Eboreime, J. Erickson, J. Hetzel, E.E. Heyer, M.J. Hubenschmidt, E. Kniazeva, H. Kuhn, M. Lum, A. Sand, A. Schep, O. Sergeeva, N. Supab, C.R. Townsend, L.V. Ryswyk, H.E. Watson, A.E. Wiedeman, V. Rajagopalan, D.J. Asai, Identification and characterization of dynein genes in *Tetrahymena*, Methods Cell Biol. 92 (2009) 11–30.
[41] B.M. Paschal, A. Mikami, K.K. Pfister, R.B. Vallee, Homology of the 74-kD cytoplasmic dynein subunit with a flagellar dynein polypeptide suggests an intracellular targeting function, J. Cell Biol. 118 (1992) 1133–1143.
[42] D.R. Mitchell, Y. Kang, Identification of *oda6* as a *Chlamydomonas* dynein mutant by rescue with the wild-type gene, J. Cell Biol. 113 (1991) 835–842.
[43] S. Takada, R. Kamiya, Functional reconstitution of *Chlamydomonas* outer dynein arms from α-β and γ subunits: Requirement of a third factor, J. Cell Biol. 126 (1994) 737–745.
[44] K. Ogawa, R. Kamiya, C.G. Wilkerson, G.B. Witman, Interspecies conservation of outer arm dynein intermediate chain sequences defines two intermediate chain subclasses, Mol. Biol. Cell 6 (1995) 685–696.
[45] C.G. Wilkerson, S.M. King, A. Koutoulis, G.J. Pazour, G.B. Witman, The 78,000 M(r) intermediate chain of *Chlamydomonas* outer arm dynein is a WD-repeat protein required for arm assembly, J. Cell Biol. 129 (1995) 169–178.
[46] C.A. Perrone, P. Yang, E. O'Toole, W.S. Sale, M.E. Porter, The *Chlamydomonas IDA7* locus encodes a 140-kDa dynein intermediate chain required to assemble the I1 inner arm complex, Mol. Biol. Cell 9 (1998) 3351–3365.
[47] P. Yang, W.S. Sale, The Mr 140,000 intermediate chain of *Chlamydomonas* flagellar inner arm dynein is a WD-repeat protein implicated in dynein arm anchoring, Mol. Biol. Cell 9 (1998) 3335–3349.
[48] T.W. Hendrickson, C.A. Perrone, P. Griffin, K. Wuichet, J. Mueller, P. Yang, M.E. Porter, W.S. Sale, IC138 is a WD-repeat dynein intermediate chain required for light chain assembly and regulation of flagellar bending, Mol. Biol. Cell 15 (2004) 5431–5442.
[49] R. Yamamoto, H. Yanagisawa, T. Yagi, R. Kamiya, A novel subunit of axonemal dynein conserved among lower and higher eukaryotes, FEBS Lett. 580 (2006) 6357–6360.

[50] R. Yamamoto, H. Yanagisawa, T. Yagi, R. Kamiya, Novel 44-kiloDalton subunit of axonemal dynein conserved from *Chlamydomonas* to mammals, Eukaryot. Cell 7 (2008) 154–161.
[51] S.M. King, E. Barbarese, J.F. Dillman III, R.S. Patel-King, J.H. Carson, K.K. Pfister, Brain cytoplasmic and flagellar outer arm dyneins share a highly conserved Mr 8,000 light chain, J. Biol. Chem. 271 (1996) 19358–19366.
[52] G.J. Pazour, C.G. Wilkerson, G.B. Witman, A dynein light chain is essential for the retrograde particle movement of intraflagellar transport (IFT), J. Cell Biol. 141 (1998) 979–992.
[53] F.S. Espindola, D.M. Suter, L.B. Partata, T. Cao, J.S. Wolenski, R.E. Cheney, S.M. King, M.S. Mooseker, The light chain composition of chicken brain myosin-Va: calmodulin, myosin-II essential light chains, and 8-kDa dynein light chain/PIN, Cell Motil. Cytoskeleton 47 (2000) 269–281.
[54] P. Yang, D.R. Diener, J.L. Rosenbaum, W.S. Sale, Localization of calmodulin and dynein light chain LC8 in flagellar radial spokes, J. Cell Biol. 153 (2001) 1315–1326.
[55] E. Barbar, Dynein light chain LC8 is a dimerization hub essential in diverse protein networks, Biochemistry 47 (2008) 503–508.
[56] T.A. Richards, T. Cavalier-Smith, Myosin domain evolution and the primary divergence of eukaryotes, Nature 436 (2005) 1113–1118.
[57] B.J. Foth, M.C. Goedecke, D. Soldati, New insights into myosin evolution and classification, Proc. Natl. Acad. Sci. USA 103 (2006) 3681–3686.
[58] S.S. Merchant, S.E. Prochnik, O. Vallon, E.H. Harris, S.J. Karpowicz, G.B. Witman, A. Terry, A. Salamov, L.K. Fritz-Laylin, L. Maréchal-Drouard, W.F. Marshall, L. Qu, D.R. Nelson, A.A. Sanderfoot, M.H. Spalding, V.V. Kapitonov, Q. Ren, P. Ferris, E. Lindquist, H. Shapiro, S.M. Lucas, J. Grimwood, J. Schmutz, P. Cardol, H. Cerutti, G. Chanfreau, C. Chen, V. Cognat, M.T. Croft, R. Dent, S. Dutcher, E. Fernández, H. Fukuzawa, D. González-Ballester, D. González-Halphen, A. Hallmann, M. Hanikenne, M. Hippler, W. Inwood, K. Jabbari, M. Kalanon, R. Kuras, P.A. Lefebvre, S.D. Lemaire, A.V. Lobanov, M. Lohr, A. Manuell, I. Meier, L. Mets, M. Mittag, T. Mittelmeier, J.V. Moroney, J. Moseley, C. Napoli, A.M. Nedelcu, K. Niyogi, S.V. Novoselov, I.T. Paulsen, G. Pazour, S. Purton, J. Ral, D.M. Riaño-Pachón, W. Riekhof, L. Rymarquis, M. Schroda, D. Stern, J. Umen, R. Willows, N. Wilson, S.L. Zimmer, J. Allmer, J. Balk, K. Bisova, C. Chen, M. Elias, K. Gendler, C. Hauser, M.R. Lamb, H. Ledford, J.C. Long, J. Minagawa, M.D. Page, J. Pan, W. Pootakham, S. Roje, A. Rose, E. Stahlberg, A.M. Terauchi, P. Yang, S. Ball, C. Bowler, C.L. Dieckmann, V.N. Gladyshev, P. Green, R. Jorgensen, S. Mayfield, B. Mueller-Roeber, S. Rajamani, R.T. Sayre, P. Brokstein, et al., The *Chlamydomonas* genome reveals the evolution of key animal and plant functions, Science 318 (2007) 245–250.
[59] T. Yagi, K. Uematsu, Z. Liu, R. Kamiya, Identification of dyneins that localize exclusively to the proximal portion of *Chlamydomonas* flagella, J. Cell Sci. 122 (2009) 1306–1314.
[60] E.J.P. Douzery, E.A. Snell, E. Bapteste, F. Delsuc, H. Philippe, The timing of eukaryotic evolution: Does a relaxed molecular clock reconcile proteins and fossils? Proc. Natl. Acad. Sci. USA 101 (2004) 15386–15391.
[61] H.G. Morrison, A.G. McArthur, F.D. Gillin, S.B. Aley, R.D. Adam, G.J. Olsen, A.A. Best, W.Z. Cande, F. Chen, M.J. Cipriano, B.J. Davids, S.C. Dawson, H.G. Elmendorf, A.B. Hehl, M.E. Holder, S.M. Huse, U.U. Kim, E. Lasek-Nesselquist, G. Manning, A. Nigam, J.E.J. Nixon, D. Palm, N.E. Passamaneck, A. Prabhu, C.I. Reich, D.S. Reiner, J. Samuelson, S.G. Svard, M.L. Sogin, Genomic minimalism in the early diverging intestinal parasite *Giardia lamblia*, Science 317 (2007) 1921–1926.
[62] W.S. Saunders, D. Koshland, D. Eshel, I.R. Gibbons, M.A. Hoyt, *Saccharomyces cerevisiae* kinesin- and dynein-related proteins required for anaphase chromosome segregation, J. Cell Biol. 128 (1995) 617–624.
[63] E.R. Hildebrandt, M.A. Hoyt, Mitotic motors in *Saccharomyces cerevisiae*, Biochim. Biophys. Acta 1496 (2000) 99–116.

[64] L.J. Briggs, J.A. Davidge, B. Wickstead, M.L. Ginger, K. Gull, More than one way to build a flagellum: Comparative genomics of parasitic protozoa, Curr. Biol. 14 (2004) R611–R612.
[65] M.E. Hodges, N. Scheumann, B. Wickstead, J.A. Langdale, K. Gull, Reconstructing the evolutionary history of the centriole from protein components, J. Cell Sci. 123 (2010) 1407–1413.
[66] D.H. Hall, Z.F. Altun, *C. elegans* Atlas, Cold Spring Harbor Laboratory Press, Cold Spring Harbor, N.Y, 2008, pp. 57–95.
[67] J.S. Hyams, Binding of *Tetrahymena* dynein to axonemes of *Marsilea vestita* lacking the outer dynein arm, J. Cell Sci. 73 (1985) 299–310.
[68] R. Kamiya, M. Okamoto, A mutant of *Chlamydomonas reinhardtii* that lacks the flagellar outer dynein arm but can swim, J. Cell Sci. 74 (1985) 181–191.
[69] C.J. Brokaw, R. Kamiya, Bending patterns of *Chlamydomonas* flagella: IV. Mutants with defects in inner and outer dynein arms indicate differences in dynein arm function, Cell Motil. Cytoskeleton 8 (1987) 68–75.
[70] O. Kagami, R. Kamiya, Translocation and rotation of microtubules caused by multiple species of *Chlamydomonas* inner-arm dynein, J. Cell Sci. 103 (1992) 653–664.
[71] M. LeDizet, G. Piperno, The light chain p28 associates with a subset of inner dynein arm heavy chains in *Chlamydomonas* axonemes, Mol. Biol. Cell 6 (1995) 697–711.
[72] R. Kamiya, E. Kurimoto, E. Muto, Two types of *Chlamydomonas* flagellar mutants missing different components of inner-arm dynein, J. Cell Biol. 112 (1991) 441–447.
[73] The Arabidopsis Genome Initiative, Analysis of the genome sequence of the flowering plant *Arabidopsis thaliana*, Nature 408 (2000) 796–815.
[74] C.J. Lawrence, N.R. Morris, R.B. Meagher, R.K. Dawe, Dyneins have run their course in plant lineage, Traffic 2 (2001) 362–363.
[75] S.M. King, Dyneins motor on in plants, Traffic 3 (2002) 930–931.
[76] J. Yu, S. Hu, J. Wang, G.K. Wong, S. Li, B. Liu, Y. Deng, L. Dai, Y. Zhou, X. Zhang, M. Cao, J. Liu, J. Sun, J. Tang, Y. Chen, X. Huang, W. Lin, C. Ye, W. Tong, L. Cong, J. Geng, Y. Han, L. Li, W. Li, G. Hu, X. Huang, W. Li, J. Li, Z. Liu, L. Li, J. Liu, Q. Qi, J. Liu, L. Li, T. Li, X. Wang, H. Lu, T. Wu, M. Zhu, P. Ni, H. Han, W. Dong, X. Ren, X. Feng, P. Cui, X. Li, H. Wang, X. Xu, W. Zhai, Z. Xu, J. Zhang, S. He, J. Zhang, J. Xu, K. Zhang, X. Zheng, J. Dong, W. Zeng, L. Tao, J. Ye, J. Tan, X. Ren, X. Chen, J. He, D. Liu, W. Tian, C. Tian, H. Xia, Q. Bao, G. Li, H. Gao, T. Cao, J. Wang, W. Zhao, P. Li, W. Chen, X. Wang, Y. Zhang, J. Hu, J. Wang, S. Liu, J. Yang, G. Zhang, Y. Xiong, Z. Li, L. Mao, C. Zhou, Z. Zhu, R. Chen, B. Hao, W. Zheng, S. Chen, W. Guo, G. Li, S. Liu, M. Tao, J. Wang, L. Zhu, L. Yuan, H. Yang, A draft sequence of the rice genome (*Oryza sativa* L. ssp. *indica*), Science 296 (2002) 79–92.
[77] G.A. Tuskan, S. Difazio, S. Jansson, J. Bohlmann, I. Grigoriev, U. Hellsten, N. Putnam, S. Ralph, S. Rombauts, A. Salamov, J. Schein, L. Sterck, A. Aerts, R.R. Bhalerao, R.P. Bhalerao, D. Blaudez, W. Boerjan, A. Brun, A. Brunner, V. Busov, M. Campbell, J. Carlson, M. Chalot, J. Chapman, G. Chen, D. Cooper, P.M. Coutinho, J. Couturier, S. Covert, Q. Cronk, R. Cunningham, J. Davis, S. Degroeve, A. Déjardin, C. Depamphilis, J. Detter, B. Dirks, I. Dubchak, S. Duplessis, J. Ehlting, B. Ellis, K. Gendler, D. Goodstein, M. Gribskov, J. Grimwood, A. Groover, L. Gunter, B. Hamberger, B. Heinze, Y. Helariutta, B. Henrissat, D. Holligan, R. Holt, W. Huang, N. Islam-Faridi, S. Jones, M. Jones-Rhoades, R. Jorgensen, C. Joshi, J. Kangasjärvi, J. Karlsson, C. Kelleher, R. Kirkpatrick, M. Kirst, A. Kohler, U. Kalluri, F. Larimer, J. Leebens-Mack, J. Leplé, P. Locascio, Y. Lou, S. Lucas, F. Martin, B. Montanini, C. Napoli, D.R. Nelson, C. Nelson, K. Nieminen, O. Nilsson, V. Pereda, G. Peter, R. Philippe, G. Pilate, A. Poliakov, J. Razumovskaya, P. Richardson, C. Rinaldi, K. Ritland, P. Rouzé, D. Ryaboy, J. Schmutz, J. Schrader, B. Segerman, H. Shin, A. Siddiqui, F. Sterky, A. Terry, C. Tsai, E. Uberbacher, P. Unneberg, et al., The genome of black cottonwood, *Populus trichocarpa* (Torr. & Gray), Science 313 (2006) 1596–1604.

[78] O. Jaillon, J. Aury, B. Noel, A. Policriti, C. Clepet, A. Casagrande, N. Choisne, S. Aubourg, N. Vitulo, C. Jubin, A. Vezzi, F. Legeai, P. Hugueney, C. Dasilva, D. Horner, E. Mica, D. Jublot, J. Poulain, C. Bruyère, A. Billault, B. Segurens, M. Gouyvenoux, E. Ugarte, F. Cattonaro, V. Anthouard, V. Vico, C. Del Fabbro, M. Alaux, G. Di Gaspero, V. Dumas, N. Felice, S. Paillard, I. Juman, M. Moroldo, S. Scalabrin, A. Canaguier, I. Le Clainche, G. Malacrida, E. Durand, G. Pesole, V. Laucou, P. Chatelet, D. Merdinoglu, M. Delledonne, M. Pezzotti, A. Lecharny, C. Scarpelli, F. Artiguenave, M.E. Pè, G. Valle, M. Morgante, M. Caboche, A. Adam-Blondon, J. Weissenbach, F. Quétier, P. Wincker, The grapevine genome sequence suggests ancestral hexaploidization in major angiosperm phyla, Nature 449 (2007) 463–467.

[79] P.S. Schnable, D. Ware, R.S. Fulton, J.C. Stein, F. Wei, S. Pasternak, C. Liang, J. Zhang, L. Fulton, T.A. Graves, P. Minx, A.D. Reily, L. Courtney, S.S. Kruchowski, C. Tomlinson, C. Strong, K. Delehaunty, C. Fronick, B. Courtney, S.M. Rock, E. Belter, F. Du, K. Kim, R.M. Abbott, M. Cotton, A. Levy, P. Marchetto, K. Ochoa, S.M. Jackson, B. Gillam, W. Chen, L. Yan, J. Higginbotham, M. Cardenas, J. Waligorski, E. Applebaum, L. Phelps, J. Falcone, K. Kanchi, T. Thane, A. Scimone, N. Thane, J. Henke, T. Wang, J. Ruppert, N. Shah, K. Rotter, J. Hodges, E. Ingenthron, M. Cordes, S. Kohlberg, J. Sgro, B. Delgado, K. Mead, A. Chinwalla, S. Leonard, K. Crouse, K. Collura, D. Kudrna, J. Currie, R. He, A. Angelova, S. Rajasekar, T. Mueller, R. Lomeli, G. Scara, A. Ko, K. Delaney, M. Wissotski, G. Lopez, D. Campos, M. Braidotti, E. Ashley, W. Golser, H. Kim, S. Lee, J. Lin, Z. Dujmic, W. Kim, J. Talag, A. Zuccolo, C. Fan, A. Sebastian, M. Kramer, L. Spiegel, L. Nascimento, T. Zutavern, B. Miller, C. Ambroise, S. Muller, W. Spooner, A. Narechania, L. Ren, S. Wei, S. Kumari, B. Faga, M.J. Levy, L. McMahan, P. Van Buren, M.W. Vaughn, et al., The B73 maize genome: Complexity, diversity, and dynamics, Science 326 (2009) 1112–1115.

[80] M. Scali, R. Vignani, A. Moscatelli, S. Jellbauer, M. Cresti, Molecular evidence for a cytoplasmic dynein heavy chain from Nicotiana tabacum L, Cell Biol. Int. 27 (2003) 261–262.

[81] B. Wickstead, K. Gull, T.A. Richards, Patterns of kinesin evolution reveal a complex ancestral eukaryote with a multifunctional cytoskeleton, BMC Evol. Biol. 10 (2010) 110.

[82] G.P. Henderson, L. Gan, G.J. Jensen, 3-D ultrastructure of *O. tauri*: Electron cryotomography of an entire eukaryotic cell, PLoS ONE 2 (2007) e749.

[83] J.M. Sieburth, P.W. Johnson, P.E. Hargraves, Ultrastructure and ecology of *Aureococcus anophagefferens* Gen-Et-Sp-Nov (Chrysophyceae) – the dominant picoplankter during a bloom in Narragansett Bay, Rhode-Island, Summer 1985, J. Phycol. 24 (1988) 416–425.

[84] H.R. Woodland, A.M. Fry, Pix proteins and the evolution of centrioles, PLoS ONE 3 (2008) e3778.

[85] M. Elias, J.M. Archibald, The RJL family of small GTPases is an ancient eukaryotic invention probably functionally associated with the flagellar apparatus, Gene 442 (2009) 63–72.

[86] E.A. Vaisberg, P.M. Grissom, J.R. McIntosh, Mammalian cells express three distinct dynein heavy chains that are localized to different cytoplasmic organelles, J. Cell Biol. 133 (1996) 831–842.

[87] S. Lee, J.C. Wisniewski, W.L. Dentler, D.J. Asai, Gene knockouts reveal separate functions for two cytoplasmic dyneins in *Tetrahymena thermophila*, Mol. Biol. Cell 10 (1999) 771–784.

[88] C. Adhiambo, J.D. Forney, D.J. Asai, J.H. LeBowitz, The two cytoplasmic dynein-2 isoforms in *Leishmania mexicana* perform separate functions, Mol. Biochem. Parasitol. 143 (2005) 216–225.

[89] D.J. Asai, The multi-dynein hypothesis, Cell Motil. Cytoskeleton 32 (1995) 129–132.

[90] E.J. Louis, Evolutionary genetics: Making the most of redundancy, Nature 449 (2007) 673–674.

[91] Y. Liu, T.A. Richards, S.J. Aves, Ancient diversification of eukaryotic MCM DNA replication proteins, BMC Evol. Biol. 9 (2009) 60.

[92] J.B. Dacks, M.C. Field, Evolution of the eukaryotic membrane-trafficking system: Origin, tempo and mode, J. Cell Sci. 120 (2007) 2977–2985.
[93] T. Cavalier-Smith, The phagotrophic origin of eukaryotes and phylogenetic classification of Protozoa, Int. J. Syst. Evol. Microbiol. 52 (2002) 297–354.
[94] G. Jékely, D. Arendt, Evolution of intraflagellar transport from coated vesicles and autogenous origin of the eukaryotic cilium, Bioessays 28 (2006) 191–198.
[95] P. Satir, C. Guerra, A.J. Bell, Evolution and persistence of the cilium, Cell Motil. Cytoskeleton 64 (2007) 906–913.
[96] D.R. Mitchell, Speculations on the evolution of 9+2 organelles and the role of central pair microtubules, Biol. Cell 96 (2004) 691–696.
[97] D.R. Mitchell, The evolution of eukaryotic cilia and flagella as motile and sensory organelles, Adv. Exp. Med. Biol. 607 (2007) 130–140.
[98] G. Mocz, I.R. Gibbons, Model for the motor component of dynein heavy chain based on homology to the AAA family of oligomeric ATPases, Structure 9 (2001) 93–103.
[99] J.E. Garbarino, I.R. Gibbons, Expression and genomic analysis of midasin, a novel and highly conserved AAA protein distantly related to dynein, BMC Genomics 3 (2002) 18.
[100] L.M. Iyer, D.D. Leipe, E.V. Koonin, L. Aravind, Evolutionary history and higher order classification of AAA^+ ATPases, J. Struct. Biol. 146 (2004) 11–31.
[101] J.R. McIntosh, E.S. Ogata, S.C. Landis, The axostyle of *Saccinobaculus*. I. Structure of the organism and its microtubule bundle, J. Cell Biol. 56 (1973) 304–323.
[102] J.R. McIntosh, The axostyle of *Saccinobaculus*. II. Motion of the microtubule bundle and a structural comparison of straight and bent axostyles, J. Cell Biol. 56 (1973) 324–339.
[103] M.S. Mooseker, L.G. Tilney, Isolation and reactivation of the axostyle. Evidence for a dynein-like ATPase in the axostyle, J. Cell Biol. 56 (1973) 13–26.
[104] R.E. Sinden, Cell biology, in: R. Killick-Kendric, W. Jones (Eds.), Rodent malaria, Academic Press, New York, 1978, pp. 85–168.
[105] G.B. Witman, Cell motility: Deaf *Drosophila* keep the beat, Curr. Biol. 13 (2003) R796–R798.
[106] D. Scheffers, A.J. Driessen, The polymerization mechanism of the bacterial cell division protein FtsZ, FEBS Lett. 506 (2001) 6–10.
[107] S. Vaughan, B. Wickstead, K. Gull, S.G. Addinall, Molecular evolution of FtsZ protein sequences encoded within the genomes of archaea, bacteria, and eukaryota, J. Mol. Evol. 58 (2004) 19–29.
[108] W. Margolin, FtsZ and the division of prokaryotic cells and organelles, Nat. Rev. Mol. Cell Biol. 6 (2005) 862–871.
[109] F. Confalonieri, M. Duguet, A 200-amino acid ATPase module in search of a basic function, Bioessays 17 (1995) 639–650.
[110] S. Patel, M. Latterich, The AAA team: Related ATPases with diverse functions, Trends Cell Biol. 8 (1998) 65–71.
[111] R.D. Vale, AAA proteins. Lords of the ring, J. Cell Biol. 150 (2000) F13–F19.
[112] A.N. Lupas, J. Martin, AAA proteins, Curr. Opin. Struct. Biol. 12 (2002) 746–753.
[113] A.F. Neuwald, L. Aravind, J.L. Spouge, E.V. Koonin, AAA^+: A class of chaperone-like ATPases associated with the assembly, operation, and disassembly of protein complexes, Genome Res. 9 (1999) 27–43.
[114] S.M. King, AAA domains and organization of the dynein motor unit, J. Cell Sci. 113 (2000) 2521–2526.
[115] M. Samsó, M. Radermacher, J. Frank, M.P. Koonce, Structural characterization of a dynein motor domain, J. Mol. Biol. 276 (1998) 927–937.
[116] S.A. Burgess, M.L. Walker, H. Sakakibara, P.J. Knight, K. Oiwa, Dynein structure and power stroke, Nature 421 (2003) 715–718.

[117] A.J. Roberts, N. Numata, M.L. Walker, Y.S. Kato, B. Malkova, T. Kon, R. Ohkura, F. Arisaka, P.J. Knight, K. Sutoh, S.A. Burgess, AAA^+ ring and linker swing mechanism in the dynein motor, Cell 136 (2009) 485–495.
[118] G. Mocz, I.R. Gibbons, Phase partition analysis of nucleotide binding to axonemal dynein, Biochemistry 35 (1996) 9204–9211.
[119] I.R. Gibbons, A. Lee-Eiford, G. Mocz, C.A. Phillipson, W.J. Tang, B.H. Gibbons, Photosensitized cleavage of dynein heavy chains. Cleavage at the "V1 site" by irradiation at 365 nm in the presence of ATP and vanadate, J. Biol. Chem. 262 (1987) 2780–2786.
[120] N. Numata, T. Kon, T. Shima, K. Imamula, T. Mogami, R. Ohkura, K. Sutoh, K. Sutoh, Molecular mechanism of force generation by dynein, a molecular motor belonging to the AAA^+ family, Biochem. Soc. Trans. 36 (2008) 131–135.
[121] D.J. Asai, M.P. Koonce, The dynein heavy chain: Structure, mechanics and evolution, Trends Cell Biol. 11 (2001) 196–202.
[122] A. Straube, W. Enard, A. Berner, R. Wedlich-Söldner, R. Kahmann, G. Steinberg, A split motor domain in a cytoplasmic dynein, EMBO J. 20 (2001) 5091–5100.
[123] J. Talkish, J.L.J. Woolford, The Rea1 tadpole loses its tail, Cell 138 (2009) 832–834.
[124] J. Bassler, M. Kallas, B. Pertschy, C. Ulbrich, M. Thoms, E. Hurt, The AAA-ATPase Rea1 drives removal of biogenesis factors during multiple stages of 60S ribosome assembly, Mol. Cell 38 (2010) 712–721.
[125] R.J. van Spanning, C.W. Wansell, T. De Boer, M.J. Hazelaar, H. Anazawa, N. Harms, L.F. Oltmann, A.H. Stouthamer, Isolation and characterization of the *moxJ, moxG, moxI*, and *moxR* genes of *Paracoccus denitrificans*: Inactivation of *moxJ, moxG*, and *moxR* and the resultant effect on methylotrophic growth, J. Bacteriol. 173 (1991) 6948–6961.
[126] A.P. de Boer, J. van der Oost, W.N. Reijnders, H.V. Westerhoff, A.H. Stouthamer, R.J. van Spanning, Mutational analysis of the *nor* gene cluster which encodes nitric-oxide reductase from *Paracoccus denitrificans*, Eur. J. Biochem. 242 (1996) 592–600.
[127] T.B. Bartnikas, I.E. Tosques, W.P. Laratta, J. Shi, J.P. Shapleigh, Characterization of the nitric oxide reductase-encoding region in *Rhodobacter sphaeroides* 2.4.3, J. Bacteriol. 179 (1997) 3534–3540.
[128] C. Englert, G. Wanner, F. Pfeifer, Functional analysis of the gas vesicle gene cluster of the halophilic archaeon *Haloferax mediterranei* defines the vac-region boundary and suggests a regulatory role for the *gvpD* gene or its product, Mol. Microbiol. 6 (1992) 3543–3550.
[129] S. DasSarma, P. Arora, F. Lin, E. Molinari, L.R. Yin, Wild-type gas vesicle formation requires at least ten genes in the *gvp* gene cluster of *Halobacterium halobium* plasmid pNRC100, J. Bacteriol. 176 (1994) 7646–7652.
[130] S. Offner, G. Wanner, F. Pfeifer, Functional studies of the *gvpACNO* operon of *Halobacterium salinarium* reveal that the GvpC protein shapes gas vesicles, J. Bacteriol. 178 (1996) 2071–2078.
[131] A. Mlouka, K. Comte, A. Castets, C. Bouchier, N. Tandeau de Marsac, The gas vesicle gene cluster from *Microcystis aeruginosa* and DNA rearrangements that lead to loss of cell buoyancy, J. Bacteriol. 186 (2004) 2355–2365.
[132] J. Snider, W.A. Houry, MoxR AAA^+ ATPases: A novel family of molecular chaperones? J. Struct. Biol. 156 (2006) 200–209.
[133] A. Bateman, L. Coin, R. Durbin, R.D. Finn, V. Hollich, S. Griffiths-Jones, A. Khanna, M. Marshall, S. Moxon, E.L.L. Sonnhammer, D.J. Studholme, C. Yeats, S.R. Eddy, The Pfam protein families database, Nucleic Acids Res. 32 (2004) D138–D141.
[134] A. Lupas, M. Van Dyke, J. Stock, Predicting coiled coils from protein sequences, Science 252 (1991) 1162–1164.

In this chapter

3

The AAA$^+$ Powerhouse — Trying to Understand How it Works

Paul A. Tucker
EMBL Hamburg Outstation, Hamburg, Germany

3.1 Introduction

AAA$^+$ (ATPases associated with various cellular activities) domains are classified as P-loop NTPases. They occur throughout all kingdoms of life as components of molecules or complexes where ATP hydrolysis is used to generate a molecular movement [1]. They serve in proteases such as the proteosome, in chaperones that are required to unfold polypeptides prior to refolding, in helicases required to unwind double-stranded DNA, in transcriptional activators that require ATP to facilitate processive transcription by formation of an "open" RNA polymerase complex at the promoter, and, the subject of this book, in some motor proteins. The evolutionary history and classification of the AAA$^+$ ATPases has been discussed extensively [2,3]. Seven clades have been described involving 24 major protein families [3]. AAA$^+$ domains, irrespective of other domains present in the protein, often form hexameric rings. The exceptions are primarily in the clamp loader and initiator clades, which function by causing a remodeling, typically of DNA, upon ATP binding rather than acting as processive machines that hydrolyze ATP. In some cases, for example for PspF, nucleotide binding appears to be a factor stabilizing the oligomer. As a further example, ATP binding, rather than ADP binding, is necessary to assemble the helical oligomer formed by DnaA (initiator clade) at bacterial replication origins [4]. The common sequence signatures and basic structure of the AAA$^+$ domain have been known for some time. The important features (see Fig. 3.1 — a structure belonging to the clade to which dynein presumably belongs has been chosen for illustration) are:

- A basic two-subdomain structure involving an $(\alpha/\beta)_5$ subdomain with a β2-β3-β4-β1-β5 topology of the central β-sheet and a smaller $(\alpha)_4$ subdomain. The ATP-binding site is located between the two subdomains.

Dyneins DOI: 10.1016/B978-0-12-382004-4.10003-2
Copyright © 2012 by Elsevier Inc. All rights reserved.

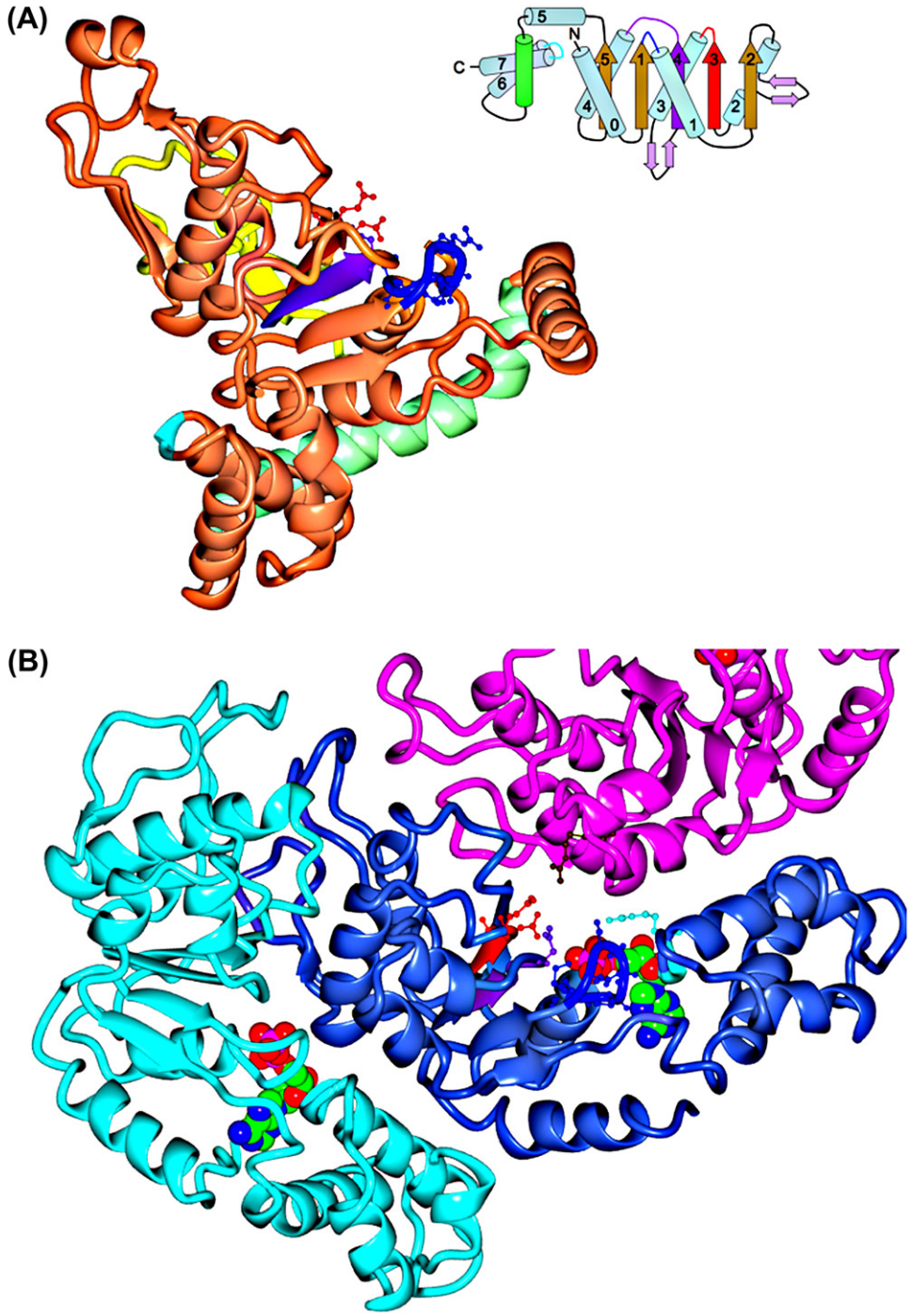
(A)
5
N
C
7
6
5
1
4
3
2
4
0
3
1
2
(B)

- A Walker A (P-loop) sequence signature at the end of strand β1 (see the inset in Fig. 3.1 for the numbering and [3]) that has the form GxxGx[G/A]K[T/S]. The loop is required for ATP binding, but not hydrolysis, and for magnesium ion coordination.
- A Walker B motif, associated with β3, that has the form hhhhDE where h is a hydrophobic residue. The glutamate is required to activate nucleophilic attack on the γ phosphate of ATP and is therefore essential for ATP hydrolysis.
- A sensor-I region involving β4. It contains a polar residue, often asparagine, which is thought to be more important for ATP hydrolysis than for ATP binding.
- A sensor-II region at the N-terminus of α7 in the helical subdomain, which often contains arginine, a mutation of which impairs ATP hydrolysis. The region is also important because there is frequently a conformational change dependent upon whether ATP or ADP is bound.
- One or more arginine fingers stabilizing triphosphate binding, usually with one at the end of α4, mutation of which impairs ATP hydrolysis, and often one coming from an adjacent protomer in oligomeric AAA$^+$ structures. They will be mentioned briefly below but are discussed in some detail by Ogura, Whiteheart, and Wilkinson [5].

It is worthwhile summarizing what is known about the structural changes that occur upon ATP turnover. Ignoring for the moment transition states, there are notionally three possible "states" of the AAA$^+$ domain: the apo form, the ADP bound form, and the ATP bound form. Investigation of the latter structurally requires either a non-hydrolyzing mutant or a non-hydrolyzable ATP analog such as AMPPNP or AMPPCP, although often the absence of Mg^{2+} will allow ATP binding but not hydrolysis. The changes in conformation of the AAA$^+$ domain during the hydrolysis cycle are modest and until the middle of the last decade high-resolution structures in the different states were not available. Work on the transcriptional activator PspF [6] and the SV40 large tumor antigen (Ltag) [7] show broadly similar structural differences between varying states despite their being members of different AAA$^+$ clades. The major conformational change occurs (Fig. 3.2A) on going from the apo to ATP (with Mg^{2+} but

Figure 3.1 The structural features of AAA$^+$ domains. (A) The structure of BchI (PDB: 1g8p [18]) showing the Walker A motif (P-loop) in blue, the Walker B motif in red, and the sensor-I region in purple. The important residues of the Walker A, Walker B, and sensor-I regions are shown in ball-and-stick representation. The helical insertion after α5, a feature of this clade, is colored light green, while the insertion between α1 and β2, unique to this particular protein family, is colored yellow. The inset is the numbering scheme after reference [3]. (B) The arrangement of three monomers (cyan, blue, and magenta) of the heptamer of the AAA$^+$ domain of the activated form of NtrC1 (PDB: 1ny6 [48]) in ribbon representation with the same orientation of the central monomer as in A). Also shown are bound ADP in sphere representation, the sensor-II region colored cyan, and a putative arginine finger from an adjacent monomer colored tan. The images were produced with ccp4mg [50].

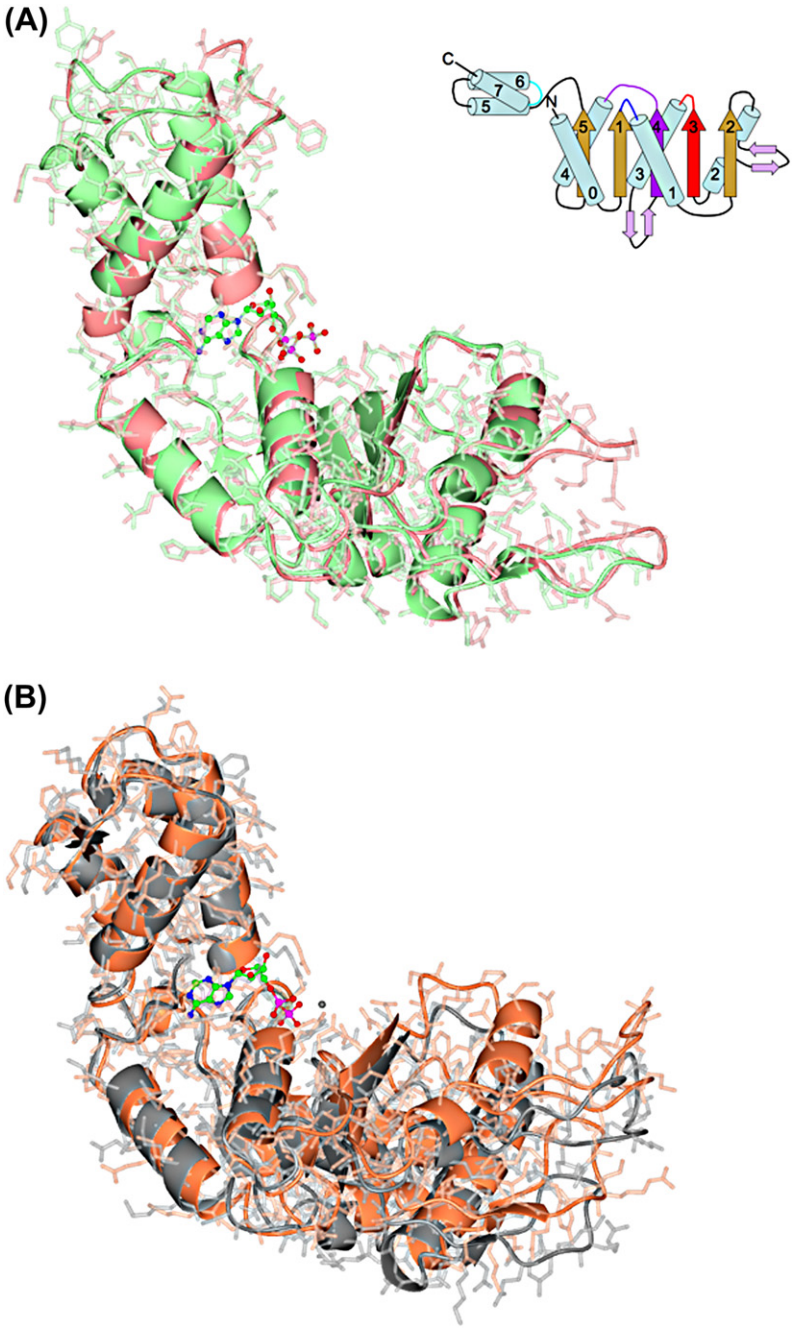

Figure 3.2 Changes in the structure of the AAA$^+$ domain during the ATP hydrolysis cycle. (A) The structure of the AAA$^+$ domain of the σ^{54} activator PspF with bound ATP (green: PDB 2c96 [6]) and in the apo form (pink: PDB 2bjw [49]). The major changes are in the two loops to the right (the α2 insertion and the loop between α3 and β4) and are probably caused by a change in conformation of the linker region between β2 and α2. The inset is the numbering scheme after reference [3]. (B) The structures of the AAA$^+$ domain of the σ^{54} activator NtrC1 in the inactive conformation (coral: PDB 1ny5 [48]) and in the active conformation with Mg^{2+} (grey sphere) and ADP (ball-and-stick representation) bound (grey: PDB 1ny6).

using the inactive R277A mutant) bound form, especially in the linker between β2 and α2 (again using the labeling from [3]). Differences between the ADP bound and apo states are smaller. Figure 3.2B also illustrates that changes in the relative positioning of the two subdomains can occur, indicating that ATP hydrolysis in one monomer can also affect adjacent monomers in oligomeric structures and/or can alter the relative positions of adjacent domains. These small changes can, and do, generate much larger changes either in other parts of the structure (PspF) or in the central aperture of the hexameric ring (Ltag). The transition state, which is thought to be mimicked by binding of ADP-AlF_x, appears to be similar to the ATP bound form – at least for the transcriptional activator NtrC1 [8].

The high-resolution structures referred to above have all protomers in one particular state. For functional hexameric AAA+ assemblies, one of the arginine fingers is often in close proximity to the nucleotide-binding site of an adjacent protomer in the ring (Fig. 3.1B). This naturally leads to the thought that this is another means by which the state of the nucleotide in one protomer can be sensed by an adjacent protomer. It is, therefore, possible that in the functioning assembly the different protomers bind and hydrolyze ATP randomly, or in a concerted fashion, or even strictly sequentially. This has been tested for the AAA+ domain (ClpX) of the chambered protease ClpXP, where the protomers were connected with polypeptide linkers between AAA+ domains, forming proteins with two, three, or six AAA+ domains, all of which formed hexameric structures similar to that formed by a single domain. In this work [9], different arrangements of active or inactive protomers were functionally characterized. The conclusion was that, for ClpX at least, the mechanism of action is random. In contrast, for the transcriptional activator PspF, coordinated hydrolysis has been proposed [10], based on the observation that the presence of ADP increases the rate of ATP hydrolysis with communication between adjacent protomers structurally dependent on two arginine fingers located at the protomer interface.

A number of proteins contain multiple AAA+ domains such that some of the domains exhibit nucleotide binding but little or no ATPase activity. For example, p97 [11,12] contains an N-terminal domain that binds adaptor proteins and two AAA+ domains (D1 and D2). The C-terminal domain (D2) is an active ATPase, while the central domain (D1) does not hydrolyze ATP but binds ADP tightly. D1 is involved in transmitting the structural changes that occur in D2, primarily on nucleotide binding and release, to the N-terminal domain. The purpose of AAA+ hexamers with little or no ATPase activity may be either to be involved in amplifying or transmitting the signal, as for p97, or possibly as an anchor for the active domain to work against.

This brief introduction, biased as it is towards aspects of the AAA+ cassette that may be relevant to our understanding of dynein, nevertheless illustrates just how

varied the detailed mechanisms of the transduction of ATP hydrolysis into mechanical energy can be.

3.2 Sequence analysis of the Dynein AAA^+ Domains

Dyneins are complex multi-protein motors very different in size and operating characteristics from the myosins and kinesins. Cytosolic dyneins contain two identical heavy chains (HCs), each with a C-terminal globular head that is believed [13] to contain a motor unit built around six AAA^+ domains. Axonemal dyneins contain one, two, or three non-identical HCs. The interaction region between HCs and intermediate chains (ICs) is in the N-terminal part of the protein while the microtubule-binding domain (MTBD), flanked by coiled-coil sequences is situated between the fourth and fifth AAA^+ modules. Sequence alignments of axonemal (β chain) and cytoplasmic dynein AAA^+ domains (Fig. 3.3A; a schematic of the HC sequence is shown in Fig. 3.3B) based on the alignments reported in [2,14] show some interesting features. Only the first four modules have clearly recognizable Walker A (P-loop) sequences and only the first and third have a convincing Walker B motif. In good agreement with the experiments discussed in Section 3.3, the conclusion would then be that, whereas all of the first four domains could bind nucleotide, only the first and third could hydrolyze ATP.

Erzberger and Berger [3] place the dynein AAA^+ domains in a clade together with midasins, the minichromosome maintenance (MCM) proteins, the BchI subunit of Mg^{2+} chelatase, and the MoxR chaperones. The N-terminus of Rea1 [15], involved in ribosomal biogenesis, also has similarities to dynein [16]. The feature of this clade that distinguishes it from other clades is a helical insertion

Figure 3.3 (A) A sequence alignment, based on that reported in [2], of the first four AAA^+ domains from an axonemal (P23098: *Tripneustes gratilla*, ciliary dynein β chain) and cytoplasmic (Q9JHU4: Murine cytoplasmic dynein 1 HC 1) dynein, with BchI (PDB: 1g8p [18]), an AAA^+ domain from *Giardia intestinalis* midasin (Q8T5T1), an archaeal MCM homolog (PDB: 3f8t [17]), and an MCM protein from *Sulfolobus solfataricus* P2. The secondary structure elements are shown for the two known structures as magenta (α-helices) and light-blue (β-strands) boxes. Strong secondary structure prediction, using the JPRED server [51] for the aligned dynein AAA^+ domains, is shown as mauve (α-helices) and blue (β-strands) letters. AAA5 and AAA6 show the same (approximate) secondary structure prediction trends as the other AAA^+ domains in agreement with having the same AAA^+ fold. The residues of the α1-β2 insertion unique to BchI are not shown. The insertion helix in the helical subdomain in the archaeal MCM analog is assumed to be in the major disordered region of this structure. (B) A schematic representation of a dynein HC. The following are indicated: regions that interact with other HCs and LCs, the six AAA^+ modules, the stalk structure comprising the coiled-coil region and the MTBD, and the C-terminal domain.

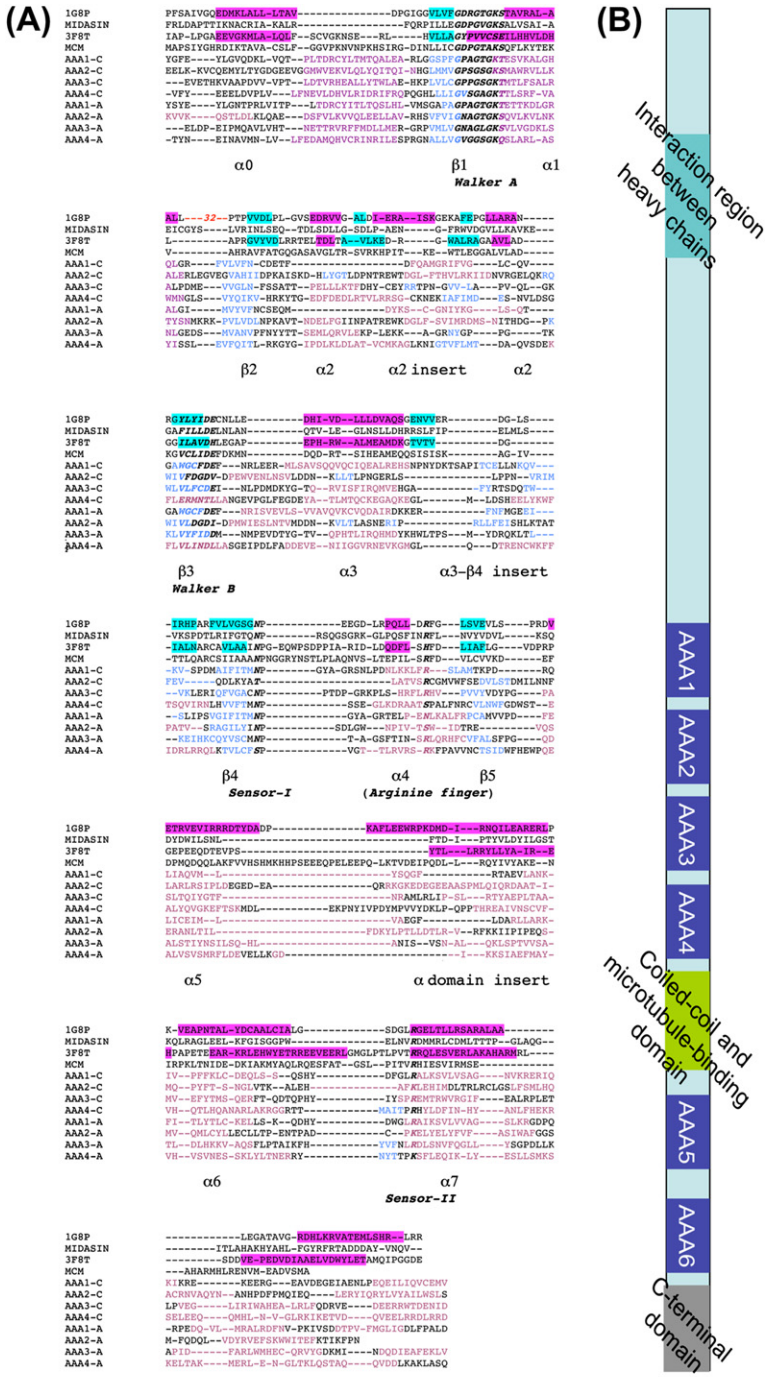
(A)
(B)
Interaction region between heavy chains
AAA1
AAA2
AAA3
AAA4
Coiled-coil and microtubule-binding domain
AAA5
AAA6
C-terminal domain

between helices α5 and α6 in the α-helical subdomain, which results in a repositioning of the sensor-II motif (see the schematic in Fig. 3.4A). Crudely, the result is that the α-helical subdomain, including the sensor-II motif, comes from the adjacent protomer in oligomers rather than from the same protomer. This

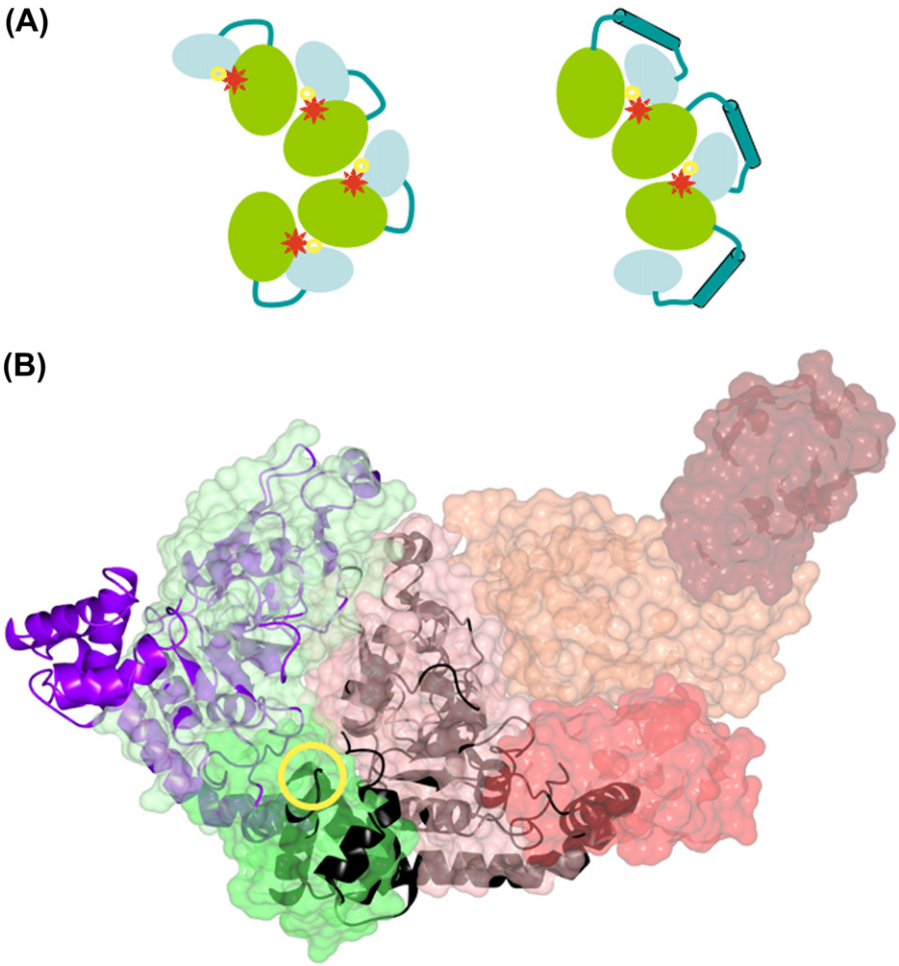

Figure 3.4 (A) A schematic representation of the effect of the helical insertion (on the right) on an oligomer of AAA^+ domains. The α/β subdomain is colored green and the α subdomain is colored light blue. The ATP-binding site is indicated by a red star and the sensor-II region by a yellow doughnut. (B) Three monomers of the AAA^+ domain of NtrC1 (PDB: 1ny6 [48]) are shown in semi-transparent surface representation. The α subdomains are colored green, red, and brown and the α/β subdomains light green, pink, and tan. Superimposed are two molecules of BchI (PDB: 1g8p [18]) in black and purple ribbon representation. The "composite" α subdomain consists of one helix from the mauve monomer and three from the black monomer. The sensor 2 region is indicated by a yellow circle showing its position in *trans*.

trans interaction, and the difference between it and the classical *cis* interaction, is illustrated in Figure 3.4B. It is described in more detail for an archaeal MCM homolog [17] and for BchI [18]. If it is indeed the case that the dynein AAA$^+$ domains belong to this clade — and there is no high-resolution structural confirmation yet — then structures of dynein based on homology models with AAA$^+$ domains of other clades, such as those suggested by Mocz and Gibbons [14], Samso and Koonce [19], and Serohijos et al. [20], must be regarded with caution.

3.3 Nucleotide Binding in the Motor Domain

Most biochemical studies of dynein motor domains are performed on constructs with the first ~1400 amino acids of the HC missing. These constructs exclude the HC/HC-interaction region and are consequently monomeric.

As mentioned above, only the first and third (AAA1) AAA$^+$ domains have the Walker A and B motifs expected for an active ATPase. Experimentally, Mocz et al. [21] used a fluorescent nucleotide analog (2′(3′)-O-(-N-Methylanthraniloyl)-adenosine 5′-triphosphate) to show that there is one high and one low affinity binding site in the motor domain. Double labeling *Dictyostelium discoideum* dynein HC at different places with blue (either before or after AAA2 or in the C-terminus) and green (either at the start of N-terminally truncated constructs or in the C-terminus) fluorescent protein and performing fluorescence resonance energy transfer experiments demonstrates [22] that there must be at least two different conformations during the motor duty cycle. In one, the N-terminal tail is close to the C-terminal domain but in the other it is close to AAA2. The interpretation is to some extent dependent on the assumption that the central "ring" of the dynein motor is comprised of the six AAA$^+$ domains and the C-terminal domain (see below). However, despite this uncertainty it is clear that the N-terminal tail undergoes motion relative to the central "ring" of the AAA$^+$ motor during the ATP hydrolysis cycle.

It has long been known [23,24] that, at least for axonemal dyneins, force production is coupled with ATP product release and that, although there is nucleotide binding at multiple sites (which is important for function), hydrolysis principally occurs at only one site. Although it was known that AAA1 had ATPase activity, Silvanovich et al. [25] showed that the Walker A motif of AAA3 is essential for cytoplasmic dynein function and is required for ATP-induced release of dynein from microtubules. Proteins with mutations in the Walker A (K and T replaced with I and A) of AAA1 and AAA3 for the *Drosophila melanogaster* cytoplasmic dynein HC have been functionally characterized. The mutations give rise to ATP-insensitive microtubule binding. The AAA3 mutations do not stop hydrolysis of ATP by AAA1. Although ATP bound in AAA3 might alter the rate of hydrolysis by

AAA1, it is more likely that nucleotide binding in AAA3 causes a conformational change required for proper function in a later step; in other words, the binding of ATP to AAA3 is regulatory. Walker A mutations (K to T or GK to AS) have been investigated [26] in a *D. discoideum* cytoplasmic dynein HC N-terminal deletion construct (missing the majority of the tail) in order to investigate the effect of blocking nucleotide binding in AAA1 through AAA4. The AAA1 mutant was trapped in a strong microtubule binding state but exhibited no motility on microtubules. The AAA3 mutant had high microtubule binding affinity but exhibited little ATPase activity. AAA2 and AAA4 mutations reduced, but did not eliminate, ATPase and microtubule-sliding activities.

There is evidence that communication between the ATPase region and the MTBD must pass through the AAA1 to AAA4 section of the molecule. This is because a construct with just AAA1 through AAA4 hydrolyzes ATP faster (probably due to an increase in the rate of release of ADP) and exhibits no inhibition by vanadate relative to the full-length construct. Since the stalk is missing from this half motor and the C-terminus can be cleaved (except when ATP-bound), it is possible that the C-terminal domain interacts with AAA1, being close to the hydrolysis site, and is thus a regulator of ATPase activity [27]. Zhuang et al. [28] demonstrated that the *Aspergillus nidulans* homolog of the human *Lis1* gene (a cytosolic dynein accessory protein) enhances microtubule-stimulated ATPase activity. It is known that Lis1 interacts with the N-terminal third of dynein (i.e. the stem region). These authors also showed that mutations at the end of AAA4 negatively regulate ATPase activity of dynein.

3.4 How are the AAA$^+$ Modules Spatially Arranged?

The size, complexity, likely flexibilities, heterogeneity, and possible difficulty of heterologous expression mean that until now high-resolution crystallographic data have not been available for the central part of the motor domain of any dynein — or even any of the individual AAA$^+$ modules. Fortunately, structural information is available from electron microscopy studies. Even taking into consideration the technical difficulties of single-particle averaging, there are some general problems that lead to results which are, in terms of broad brush strokes, consistent, but leave leave uncertainty in the details. There is always the potential with negative-stain electron microscopy that samples will be preferentially oriented on the supporting grid, or even trapped in non-physiologically-meaningful conformations. Single-particle reconstructions using cryo-electron microscopy (cryo-EM) would be a welcome addition to the experimentally available data.

The flagellar inner-arm dynein (subspecies c) from *Chlamydomonas reinhardtii* has been examined in the apo and ADP/vanadate complex (formed by incubation of protein with ATP and orthovanadate, thus preventing product release)

forms by negative-stain electron microscopy [29,30]. The apo protein corresponds to a post-powerstroke (unprimed) form and the ADP/vanadate complex to a pre-powerstroke (or primed) form. As previously mentioned, the release of ADP and phosphate from (principally) AAA1 is associated with a conformational change and therefore presumably the powerstroke. In this study a range of conformations was observed and the density for the relatively small stalk was, most likely, averaged out. Class averages of species with a longer stem indicated that it consists of three regions: base, neck, and linker. The stalk was observed to stiffen in molecules in the apo state. Movement occurs by a change in the orientation between head and stem and the angle between the stem and the stalk decreases on changing from the ADP/vanadate complex to the apo state. The data support the idea of a toroidal structure with a linker lying across one face of the head such that the two faces look different (Fig. 3.5). A follow-up paper [31] provided confirmation that the stem has neck, shaft, and base subdomains, with flexibility in the stem occurring in the neck. The stalk was also reported to be flexible. The authors sound two notes of caution, however: First, their preparations may have contained other dynein-associated molecules, such as p28. Second, they recognize that cryo-EM is likely to be a preferable technology in terms of avoiding artifacts caused by sample preparation. Two models (indistinguishable from this work) were proposed (Fig. 3.5), but from pre- to post-powerstroke, or vice versa, the linker changes its interaction point from AAA6 to the region AAA2 to AAA5. As a consequence, the motor duty cycle would not just produce movement along microtubules but would also be predicted to generate a rotation.

Possible communication between motor domains in oligomeric dynein complexes has received little attention. One study, however, indicates that, for the more complex structural arrangement of the axonemal outer dynein arm [32] containing three HCs, which shows a likely stacking of AAA$^+$-containing "rings," there is no evidence of communication between motor "rings."

A 25 Å resolution electron microscopic study in negative stain of a cytoplasmic dynein (*Dictyostelium discoideum*) that used a tilt series to obtain a three-dimensional reconstruction [19] is largely in agreement with the results described in the previous paragraphs. In this instance, the heterologously expressed construct used was missing the first 1383 N-terminal residues of the dynein HC and so was without the bulk of the stem. An antibody against the MTBD was used as a reference point. The reconstruction showed a flattish elliptical ring with seven regions of density into which positions for AAA1 through AAA6 were modeled. The seventh density was not assigned, although the authors considered that it could be the C-terminal domain. In the model, derived from the experimental observations, AAA1, connected to the stem, would be on the opposite side of the ring to the stalk that emerges between AAA4 and AAA5. Density was observed within the ring and this was suggested to be the linker referred to by others [30,31]. The authors suggested that apparent differences in the results from

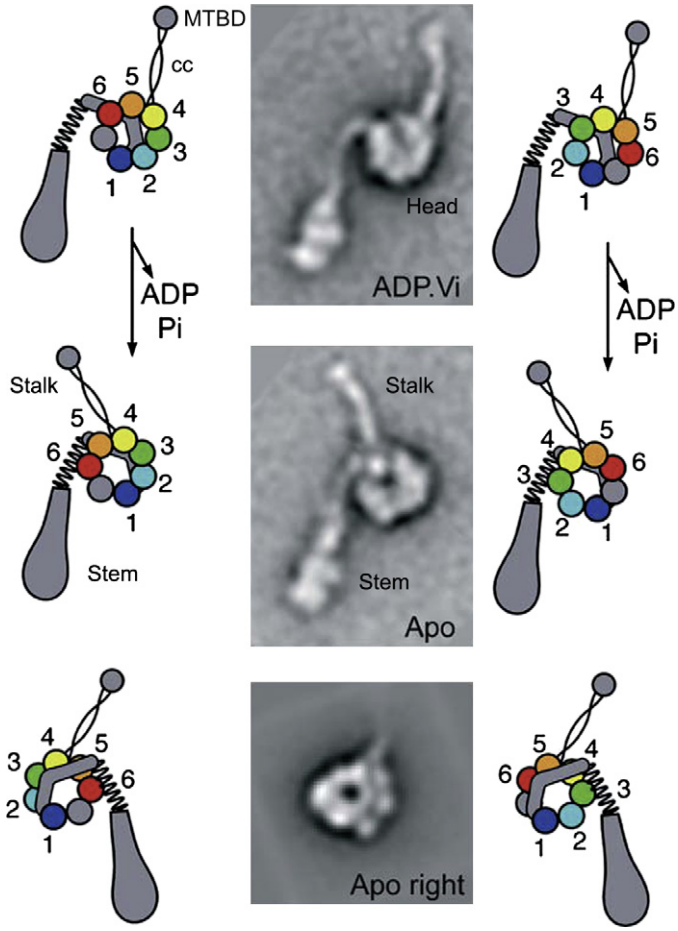

Figure 3.5 Two models (left and right) illustrating how the powerstroke, occurring upon ATP hydrolysis and product release, could be generated with class average images in the center. The AAA^{+} domains are labeled 1 though 6 for AAA1 through AAA6 (blue, cyan, green, yellow, orange, and red). The MTBD and coiled coil together form the stalk. The stem consists of a neck, shaft, and base. In the center are electron microscopy class averages of *C. reinhardtii* dynein c with ADP/vanadate (top) and in the apo form (middle). The asymmetry of the structure results in two views (top and center, called the "top" view, and bottom, called the "right" view) amongst the electron microscopy images. cc: coiled coil; MTBD: microtubule-binding domain. Reproduced from figure 6 of [30].

different groups might be the result of differences in technique and not of any fundamental difference between axonemal and cytosolic dyneins.

In further negative-stain electron microscopy work [33] on *Dictyostelium* dynein, a c-myc antibody epitope was attached to the linker region end of the construct

and the antibody was used as a reference point for analyzing the micrographs. Class averages gave seven blobs of density, in agreement with other electron microscopy results [22], although early literature sometimes refers to a six-membered AAA$^+$ ring. Perhaps more important is the deduction that the connection to the stem originates from near the center of the "ring" and is highly flexible. The interaction of dynein with microtubules has been visualized by cryo-EM to 26 Å resolution using a recombinant truncated cytoplasmic dynein [34], although the authors did not analyze different binding states. The motor ring was observed to be ~280 Å away from the microtubule center. The dynein stalk was reported to be rigid and connected to the microtubule in a defined geometry with the plane of the motor ring parallel to the microtubule axis. The motor ring was modeled in a similar fashion to that of Serohijos et al. [20], with seven blobs of density in the ring and a bridge across the front. The AAA1 through AAA6 domains are arranged in a clockwise fashion looking from the side of the ring containing the bridge (left side in Fig. 3.5). The ~120 Å stalk was not observed in this image reconstruction and was visualized separately. This is similar to the model [30] for flagellar dynein described above (Fig. 3.5). This model, which would argue for a lever-arm mechanism for dynein force production, is not entirely consistent with the flexibility suggested by Meng et al. [33]. The discrepancy could be the effect of the negative-stain preparation or the fact that no microtubules were bound in that study. The most recent report on cytoplasmic dynein by negative-stain electron microscopy [35] used constructs with green fluorescent protein (GFP) fusions at different places in order to locate the various parts of the motor ring. It is reassuring to note that cytoplasmic and axonemal dyneins look very similar at low resolution in at least one view of the molecule. The sample preparation resulted in two different views (called "top" and "right" and probably related to each other by a 180° rotation about the long axis of the molecule), which were used in the class classifications. In the unprimed motor (apo form), the stalk emerges at a range of angles from the head. The C-terminal domain is not required for basal ATPase activity but is required for motility and if it is deleted the motor still looks much the same, suggesting that the seventh blob of density seen in other work (see above) is probably not the C-terminal domain. Indeed, fungal isoforms miss most of the C-sequence yet are still processive motors. In contrast, if the N-terminal sequence is removed, the ring looks more symmetric. It was suggested in [35] that AAA1 through AAA6 form a ring and that the N-terminus lies near the base of the stalk. In this latest model, AAA1 is opposite the stalk and the N-terminal sequence (which includes the linker domain) spans the head. AAA1 through AAA6 are arranged counterclockwise around the ring, as seen from the side spanned by the N-terminal sequence. The C-terminal domain then spans from AAA6 towards AAA5 (and the base of stalk) and returns to AAA6. In the ADP/vanadate complex (primed), the N-terminal region is shifted towards AAA2. The angle the stalk makes with the ring changes relative to the head on going from the primed to unprimed states and there is a three-dimensional movement of the N-terminus of the linker during the priming stroke. This model

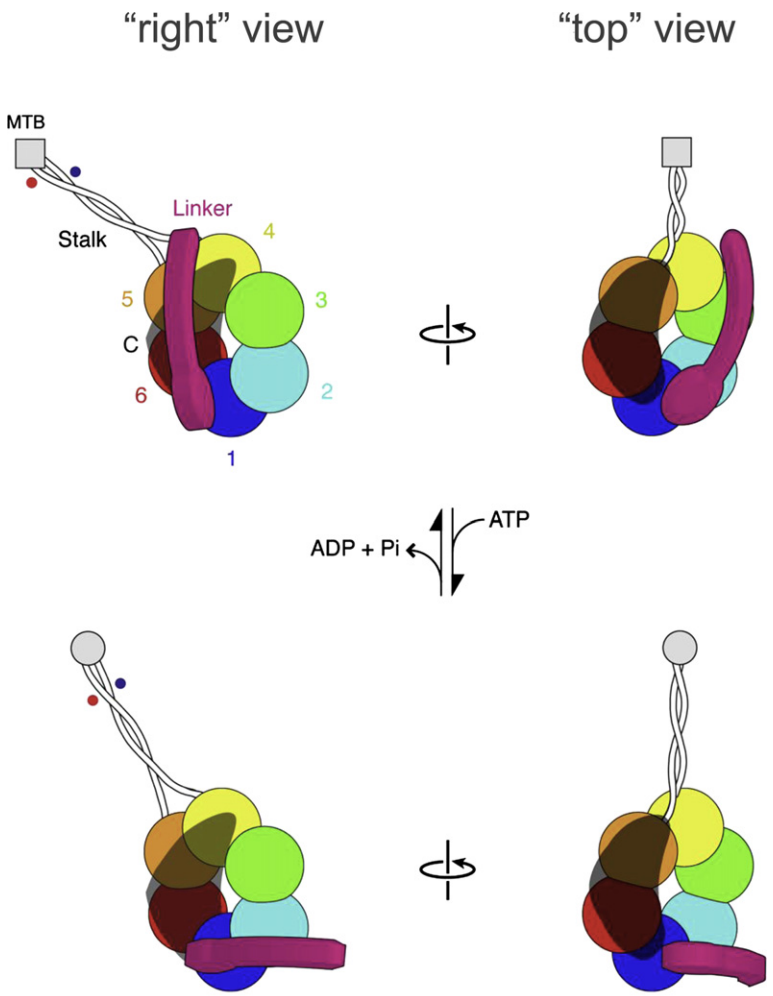

Figure 3.6 A model of the structure and priming stroke of dynein. (A) Six AAA$^+$ modules (numbered) form a hexameric ring. The C sequence (translucent black) is represented speculatively as an elongated structure interacting with (one or another face of) AAA6, AAA5, and AAA4. The N sequence (magenta) contains the linker, which runs from AAA1 across the head to AAA4 (yellow) in the unprimed (top pair) conformation and switches to a position close to AAA2 in the primed conformation, thereby moving the N-terminus of the motor by ~17 nm (in the right view in a plane parallel to the page). The N sequence may also contain non-linker structures, for example near the junction with AAA1 (magenta ellipse). Tilting of the stalk, shown here to occur entirely in the plane of the page in right view, displaces the MTBD by ~5 nm and could shift the registration of the two α helices of the coiled coil (indicated by red and blue spots). Stalk tilting perpendicular to the page is not seen in the top view, probably because the stalk flattens down onto the electron microscopy grid in this orientation. Reproduced from figure 7 of [35].

can be regarded simply as a revision of previous "heptameric" models [20]. The C-terminal region overlaps with AAA6, AAA5, and perhaps AAA4, and the N-terminal region includes a lever-like linker. In the unprimed state this goes across the head from AAA1 to near the base of the stalk at AAA4 and AAA5, whereas during the priming stroke it swings close to AAA2 (Fig. 3.6).

In an attempt to add atomic detail to the low-resolution electron microscopy-based models, a detailed homology model of the motor unit of cytoplasmic dynein from *D. discoideum*, improving upon previous work [19], was produced [20]. Using the programs 2DJury and Insight II, improved folds of the AAA+ subunits were obtained. However (see Section 3.2) the proteins (having protein data bank (PDB) IDs 1hqc, 1jr3, and 1sxj) used as AAA+ templates are from other clades that do not contain the expected helical domain insert. Although R2145 is, indeed, a well-conserved residue in the sensor-II region, it is not clear how this might act in *trans*. Complement protein C3d (an α-α toroid, PDB: 1ghq) plus a PH domain (PDB: 1txd) were used to model the C-terminus. High-resolution experimental verification is still missing; however, the model does fit exceptionally well into the 25 Å negatively stained electron microscopy density of *D. discoideum* cytoplasmic dynein. In the HC sequence the region between AAA5 and AAA6 is especially long (231 residues) and it is suggested that a coiled-coil structure (modeled using PDB 1qu7) spans the ring (in contrast to the model [35] described above). Normal mode analysis was used to try to identify pivot points within the structure. In this analysis, AAA5, AAA6, and the C-terminal domain move most. AAA5 is at the base of the stalk, which tilts upon the powerstroke. The authors suggest that micrographs forced to be flat on a substrate would not capture conformations that occur during force generation. As mentioned previously, the small structural changes that occur upon ATP hydrolysis have to be amplified by the rest of the molecule. In this regard, the AAA1 β-hairpin shows a large movement in the normal mode analysis, which could result in a coupling of ATP hydrolysis to movement of the C-domain.

3.5 Communication of the Motor Domain with the Microtubule-Binding Domain

There appears to be two-way communication between the motor domain and the MTBD that must be transmitted via the coiled coil of the stalk. Not only is the hydrolysis of ATP associated with a transition between weak (ADP/vanadate complex) and strong (apo form) microtubule binding, but ATP hydrolysis is also stimulated by microtubule binding [30]. Possible coiled-coil alignments have been examined [36] by creating fusions with a template (seryl t-RNA synthetase) containing the base of an established coiled-coil structure. The helix following the MTBD, which has a regular heptad repeat, was kept in

a fixed orientation while the leading helix was varied in length. Two registers of the helices were identified (α and $+\beta$), with only the α registry exhibiting strong binding. This work demonstrated that the transition, involving a half-heptad slide, generated at the base of the coiled coil a translation of 4.5 Å and a rotation of 58°, causing a transition from a high-affinity to a low-affinity microtubule binding state. This region is the only one, to date, for which there is high-resolution structural information [37], although only the weak binding fusion could be crystallized. Docking the structure into the available density from a helical cryo-EM reconstruction places the binding interface between α- and β-tubulin subunits. One consequence of this structural analysis is that an additional heptad might be expected to change directionality of movement. Unfortunately, this appears to be contradictory to experimental results. It is therefore necessary to postulate that the stalk is tilted towards the microtubule-binding end at the time when the powerstroke occurs. More direct evidence for the signal being passed via a change in coiled-coil registry [38] was obtained by using disulphide crosslinks to lock into either the $+\beta$ and α registries of the coiled coil, again showing the α registry to be the high-affinity microtubule binding state. Binding to microtubules favors the α registry whereas binding of ATP plus orthovanadate in the motor domain favors the $+\beta$ registry. It is clear then that microtubule binding can drive conformational changes in the stalk, which could have an effect on the ability of AAA3 to bind or hydrolyze ATP.

3.6 Transduction of Local Conformational Changes into Motion

Inner-arm axonemal dynein-c is a processive motor that moves in 8 nm steps but that can slide back under tension [29]. Of the inner-arm axonemal dyneins, one is heterodimeric and six are monomeric. They appear to be more essential for flagellar movement than the outer-arm dynein. It has been suggested that monomeric inner-arm dyneins function as dimers, and a study by Bui et al. [39] as well as work on cytoplasmic dyneins indicate that this is likely. In micrographs of the flagellum one can see rings of motor domains, which appear parallel to the microtubules.

Since only full-length cytosolic dyneins will be dimeric, versions with substantial N-terminal truncations (used in most of the structural work mentioned in Section 3.4) are expected to be monomeric. A comparative investigation [40] suggests that two heads of a single cytoplasmic dynein must communicate with each other for processive movement along microtubules to occur, although this does not apparently require communication between the motor domains. Interestingly, processivity can be restored by using a chimeric dimerization domain.

3.7 Conclusion

Figure 3.6 captures in a simplified manner much of the biochemical and structural information on the motor domain of cytoplasmic and axonemal dyneins, and high-resolution crystal structures give some idea of how AAA+ domains change in structure during the ATP hydrolysis cycle. Despite this, the way in which rather small structural changes in the AAA+ domains give rise to the much larger movements observed during the dynein powerstroke remains to be determined. For the reader who would like further information and an idea of how our knowledge has developed over the last decade, a number of authoritative reviews [41–47] are available.

References

[1] P.A. Tucker, L. Sallai, The AAA+ superfamily – a myriad of motions, Curr. Opin. Struc. Biol. 17 (2007) 641–652.

[2] L.M. Iyer, D.D. Leipe, E.V. Koonin, L. Aravind, Evolutionary history and higher order classification of AAA+ ATPases, J. Struct. Biol. 146 (2004) 11–31.

[3] J.P. Erzberger, J.M. Berger, Evolutionary relationships and structural mechanisms of AAA+ proteins, Annu. Rev. Bioph. Biom. 35 (2006) 93–114.

[4] J.P. Erzberger, M.L. Mott, J.M. Berger, Structural basis for ATP-dependent DnaA assembly and replication-origin remodeling, Nat. Struct. Mol. Biol. 13 (2006) 676–683.

[5] T. Ogura, S.W. Whiteheart, A.J. Wilkinson, Conserved arginine residues implicated in ATP hydrolysis, nucleotide-sensing, and inter-subunit interactions in AAA and AAA+ ATPases, J. Struct. Biol. 146 (2004) 106–112.

[6] M. Rappas, J. Schumacher, H. Niwa, M. Buck, X. Zhang, Structural basis of the nucleotide driven conformational changes in the AAA+ domain of transcription activator PspF, J. Mol. Biol. 357 (2006) 481–492.

[7] D. Gai, R. Zhao, D. Li, C.V. Finkielstein, X.S. Chen, Mechanisms of conformational change for a replicative hexameric helicase of SV40 large tumor antigen, Cell 119 (2004) 47–60.

[8] B. Chen, M. Doucleff, D.E. Wemmer, S. De Carlo, H.H. Huang, E. Nogales, T.R. Hoover, E. Kondrashkina, L. Guo, B.T. Nixon, ATP ground and transition states of bacterial enhancer binding AAA+ ATPases support complex formation with their target protein, sigma54, Structure 15 (2007) 429–440.

[9] A. Martin, T.A. Baker, R.T. Sauer, Rebuilt AAA + motors reveal operating principles for ATP-fuelled machines, Nature 437 (2005) 1115–1120.

[10] N. Joly, J. Schumacher, M. Buck, Heterogeneous nucleotide occupancy stimulates functionality of phage shock protein F, an AAA+ transcriptional activator, J. Biol. Chem. 281 (2006) 34997–35007.

[11] B. DeLaBarre, A.T. Brunger, Nucleotide dependent motion and mechanism of action of p97/VCP, J. Mol. Biol. 347 (2005) 437–452.

[12] J.M. Davies, H. Tsuruta, A.P. May, W.I. Weis, Conformational changes of p97 during nucleotide hydrolysis determined by small-angle X-ray scattering, Structure 13 (2005) 183–195.

[13] A.F. Neuwald, L. Aravind, J.L. Spouge, E.V. Koonin, AAA+: A class of chaperone-like ATPases associated with the assembly, operation, and disassembly of protein complexes, Genome research 9 (1999) 27–43.

[14] G. Mocz, I.R. Gibbons, Model for the motor component of dynein heavy chain based on homology to the AAA family of oligomeric ATPases, Structure 9 (2001) 93–103.

[15] K. Galani, T.A. Nissan, E. Petfalski, D. Tollervey, E. Hurt, Rea1, a dynein-related nuclear AAA-ATPase, is involved in late rRNA processing and nuclear export of 60 S subunits, J. Biol. Chem. 279 (2004) 55411–55418.
[16] J.E. Garbarino, I.R. Gibbons, Expression and genomic analysis of midasin, a novel and highly conserved AAA protein distantly related to dynein, BMC Genomics 3 (2002) 18.
[17] B. Bae, Y.H. Chen, A. Costa, S. Onesti, J.S. Brunzelle, Y. Lin, I.K. Cann, S.K. Nair, Insights into the architecture of the replicative helicase from the structure of an archaeal MCM homolog, Structure 17 (2009) 211–222.
[18] M.N. Fodje, A. Hansson, M. Hansson, J.G. Olsen, S. Gough, R.D. Willows, S. Al-Karadaghi, Interplay between an AAA module and an integrin I domain may regulate the function of magnesium chelatase, J. Mol. Biol. 311 (2001) 111–122.
[19] M. Samso, M.P. Koonce, 25 Angstrom resolution structure of a cytoplasmic dynein motor reveals a seven-member planar ring, J. Mol. Biol. 340 (2004) 1059–1072.
[20] A.W. Serohijos, Y. Chen, F. Ding, T.C. Elston, N.V. Dokholyan, A structural model reveals energy transduction in dynein, Proc. Natl. Acad. Sci. USA 103 (2006) 18540–18545.
[21] G. Mocz, M.K. Helms, D.M. Jameson, I.R. Gibbons, Probing the nucleotide binding sites of axonemal dynein with the fluorescent nucleotide analogue 2′(3′)-O-(-N-Methylanthraniloyl)-adenosine 5′-triphosphate, Biochemistry 37 (1998) 9862–9869.
[22] T. Kon, T. Mogami, R. Ohkura, M. Nishiura, K. Sutoh, ATP hydrolysis cycle-dependent tail motions in cytoplasmic dynein, Nat. Struct. Mol. Biol. 12 (2005) 513–519.
[23] E.L. Holzbaur, K.A. Johnson, Microtubules accelerate ADP release by dynein, Biochemistry 28 (1989) 7010–7016.
[24] E.L. Holzbaur, K.A. Johnson, ADP release is rate limiting in steady-state turnover by the dynein adenosinetriphosphatase, Biochemistry 28 (1989) 5577–5585.
[25] A. Silvanovich, M.G. Li, M. Serr, S. Mische, T.S. Hays, The third P-loop domain in cytoplasmic dynein heavy chain is essential for dynein motor function and ATP-sensitive microtubule binding, Mol. Biol. Cell 14 (2003) 1355–1365.
[26] T. Kon, M. Nishiura, R. Ohkura, Y.Y. Toyoshima, K. Sutoh, Distinct functions of nucleotide-binding/hydrolysis sites in the four AAA modules of cytoplasmic dynein, Biochemistry 43 (2004) 11266–11274.
[27] P. Hook, A. Mikami, B. Shafer, B.T. Chait, S.S. Rosenfeld, R.B. Vallee, Long range allosteric control of cytoplasmic dynein ATPase activity by the stalk and C-terminal domains, J. Biol. Chem. 280 (2005) 33 045–33 054.
[28] L. Zhuang, J. Zhang, X. Xiang, Point mutations in the stem region and the fourth AAA domain of cytoplasmic dynein heavy chain partially suppress the phenotype of NUDF/LIS1 loss in *Aspergillus nidulans*, Genetics 175 (2007) 1185–1196.
[29] H. Sakakibara, H. Kojima, Y. Sakai, E. Katayama, K. Oiwa, Inner-arm dynein c of *Chlamydomonas* flagella is a single-headed processive motor, Nature 400 (1999) 586–590.
[30] S.A. Burgess, M.L. Walker, H. Sakakibara, P.J. Knight, K. Oiwa, Dynein structure and power stroke, Nature 421 (2003) 715–718.
[31] S.A. Burgess, M.L. Walker, H. Sakakibara, K. Oiwa, P.J. Knight, The structure of dynein-c by negative stain electron microscopy, J. Struct. Biol. 146 (2004) 205–216.
[32] T. Ishikawa, H. Sakakibara, K. Oiwa, The architecture of outer dynein arms *in situ*, J. Mol. Biol. 368 (2007) 1249–1258.
[33] X. Meng, M. Samso, M.P. Koonce, A flexible linkage between the dynein motor and its cargo, J. Mol. Biol. 357 (2006) 701–706.
[34] N. Mizuno, A. Narita, T. Kon, K. Sutoh, M. Kikkawa, Three-dimensional structure of cytoplasmic dynein bound to microtubules, Proc. Natl. Acad. Sci. USA 104 (2007) 20832–20837.
[35] A.J. Roberts, N. Numata, M.L. Walker, Y.S. Kato, B. Malkova, T. Kon, R. Ohkura, F. Arisaka, P.J. Knight, K. Sutoh, S.A. Burgess, AAA^+ ring and linker swing mechanism in the dynein motor, Cell 136 (2009) 485–495.

[36] I.R. Gibbons, J.E. Garbarino, C.E. Tan, S.L. Reck-Peterson, R.D. Vale, A.P. Carter, The affinity of the dynein microtubule-binding domain is modulated by the conformation of its coiled-coil stalk, J. Biol. Chem. 280 (2005) 23960–23965.
[37] A.P. Carter, J.E. Garbarino, E.M. Wilson-Kubalek, W.E. Shipley, C. Cho, R.A. Milligan, R.D. Vale, I.R. Gibbons, Structure and functional role of dynein's microtubule-binding domain, Science 322 (2008) 1691–1695.
[38] T. Kon, K. Imamula, A.J. Roberts, R. Ohkura, P.J. Knight, I.R. Gibbons, S.A. Burgess, K. Sutoh, Helix sliding in the stalk coiled coil of dynein couples ATPase and microtubule binding, Nat. Struct. Mol. Biol. 16 (2009) 325–333.
[39] K.H. Bui, H. Sakakibara, T. Movassagh, K. Oiwa, T. Ishikawa, Molecular architecture of inner dynein arms *in situ* in *Chlamydomonas reinhardtii* flagella, J. Cell Biol. 183 (2008) 923–932.
[40] T. Shima, K. Imamula, T. Kon, R. Ohkura, K. Sutoh, Head–head coordination is required for the processive motion of cytoplasmic dynein, an AAA$^+$ molecular motor, J. Struct. Biol. 156 (2006) 182–189.
[41] S.M. King, AAA domains and organization of the dynein motor unit, Journal of Cell Science 113 (Pt 14) (2000) 2521–2526.
[42] R.D. Vale, The molecular motor toolbox for intracellular transport, Cell. 112 (2003) 467–480.
[43] M. Sakato, S.M. King, Design and regulation of the AAA$^+$ microtubule motor dynein, J. Struct. Biol. 146 (2004) 58–71.
[44] S.A. Burgess, P.J. Knight, Is the dynein motor a winch? Curr. Opin. Struc. Biol. 14 (2004) 138–146.
[45] R.B. Vallee, P. Hook, Autoinhibitory and other autoregulatory elements within the dynein motor domain, J. Struct. Biol. 156 (2006) 175–181.
[46] N. Numata, T. Kon, T. Shima, K. Imamula, T. Mogami, R. Ohkura, K. Sutoh, K. Sutoh, Molecular mechanism of force generation by dynein, a molecular motor belonging to the AAA$^+$ family, Biochem. Soc. T. 36 (2008) 131–135.
[47] A.P. Carter, R.D. Vale, Communication between the AAA$^+$ ring and microtubule-binding domain of dynein, Biochem. Cell. Biol. 88 (2010) 15–21.
[48] S.Y. Lee, A. De La Torre, D. Yan, S. Kustu, B.T. Nixon, D.E. Wemmer, Regulation of the transcriptional activator NtrC1: Structural studies of the regulatory and AAA$^+$ ATPase domains, Gene Dev. 17 (2003) 2552–2563.
[49] M. Rappas, J. Schumacher, F. Beuron, H. Niwa, P. Bordes, S. Wigneshweraraj, C.A. Keetch, C.V. Robinson, M. Buck, X. Zhang, Structural insights into the activity of enhancer-binding proteins, Science 307 (2005) 1972–1975.
[50] L. Potterton, S. McNicholas, E. Krissinel, J. Gruber, K. Cowtan, P. Emsley, G.N. Murshudov, S. Cohen, A. Perrakis, M. Noble, Developments in the CCP4 molecular-graphics project, Acta Cryst. D60 (2004) 2288–2294.
[51] C. Cole, J.D. Barber, G.J. Barton, The Jpred 3 secondary structure prediction server, Nucleic Acids Res. 36 (2008) W197–W201.

In this chapter

4

Dynein Motor Mechanisms

Michael P. Koonce, Irina Tikhonenko
Division of Translational Medicine, Wadsworth Center, Albany, NY, USA

4.1 The Dynein Engine Room

The dynein motor domain comprises a concatenated assembly of six non-identical AAA modules that are arranged to form a ring-shaped core (Figs. 4.1 and 4.2) [2,3]. The first four AAA domains (AAA1 to AAA4) bind and hydrolyze nucleotide [4], but only hydrolysis at AAA1 is cyclically linked to force production [5–7]. Connecting upstream to AAA1 and extending outside of the motor core is a linker domain that arcs across one side of the ring surface [8] and connects the motor to a stem/tail region that mediates motor interactions and cargo-binding activities [9,10]. Most dyneins contain additional polypeptide sequence downstream of AAA6, forming a mass approximately the same size as an AAA module. Although absent in yeast and fungal dyneins, this seventh domain may contribute to the ring structure or form part of the surface densities that are visible on the sides of the ring (Fig. 4.1) [11,12]. The motor ring is interrupted between AAA4 and AAA5 by the microtubule-binding domain (MTBD) (Fig. 4.1).

UV-vanadate cleavage experiments and targeted mutational analyses demonstrate that nucleotide hydrolysis at AAA1 is absolutely required for dynein force production [13–17]. Early kinetic studies indicated that ATP binding weakens dynein's affinity for microtubules, that nucleotide hydrolysis is required for tight microtubule binding, and that ADP release represents the rate-limiting step of force production [18–21]. More recent efforts – using combinations of green fluorescent protein (GFP)-based fluorescence resonance energy transfer tags, motor domain mutations, and nucleotide analogs that trap the motor at intermediate states in the catalytic cycle – have added significant detail to these processes [22–24]. ATP binding to AAA1 initiates a relatively rapid ($180\,s^{-1}$) isomerization phase of the motor's catalytic cycle, whereby microtubule affinity converts from a tight to weak bound state and the linker arm repositions from a post- to a pre-powerstroke state (Fig. 4.2). These steps then lead to nucleotide hydrolysis and release of the cleaved phosphate. Phosphate release leaves ADP bound to AAA1, resulting in a second isomerization phase. During this relatively

Dyneins DOI: 10.1016/B978-0-12-382004-4.10004-4
Copyright © 2012 by Elsevier Inc. All rights reserved.

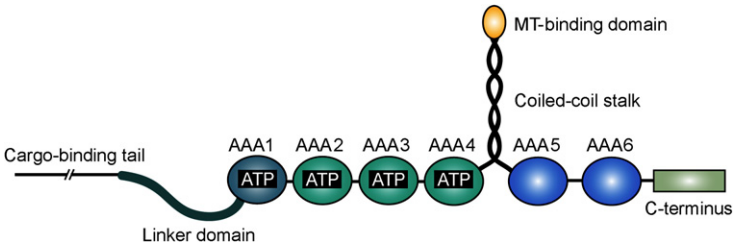

Figure 4.1 Schematic of the dynein motor domain. Linear representation of the six AAA^+ modules, the MTBD, the linker, and the C-terminus sequence. The region including AAA1 to the C-terminus folds into a ring-shaped motor core, as depicted in Figure 4.2. The amino terminal tail domain of the dynein HC sequence binds accessory proteins (e.g. intermediate chains (ICs), light-intermediate chains (LICs), light chains (LCs), and dynactin) that target the motor to the cargo and mediate motor–motor interactions [9,10].

slow (0.2 s^{-1}) step, microtubule affinity is increased and is presumably followed by the linker arm powerstroke. The motor maintains a tight affinity for microtubules, even after ADP is released.

AAA domains 2, 3, and 4 also bind and hydrolyze nucleotide, but their activities are not directly linked to force production. Instead, these AAA domains appear more involved with the conformational coupling process that links nucleotide hydrolysis with microtubule affinity, and thus are considered regulatory modules that govern engine operation. Mutations in AAA2 that prevent nucleotide binding produce a mild reduction in the microtubule-stimulated ATPase activity of AAA1 and show reduced microtubule binding and gliding in *in vitro* assays [15,25]. Of the first four AAA domains, AAA2 appears to play the least active role in engine modulation. Disruption of ATP binding in AAA3 produces motors that bind and

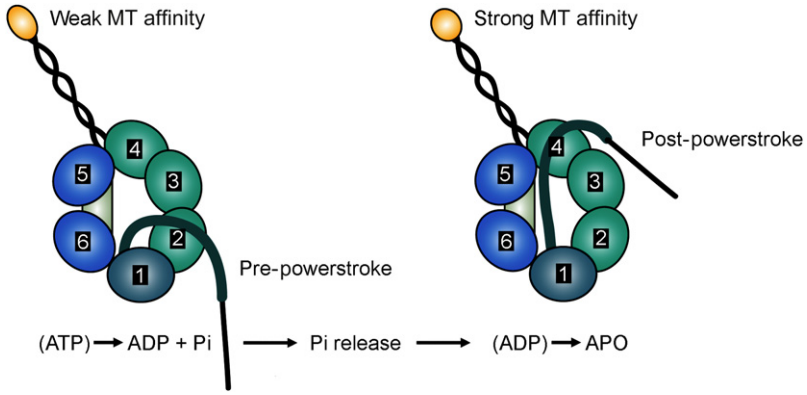

Figure 4.2 Two-dimensional representation of the motor domain in two catalytic states. ATP binding (left) converts the motor into a weak-microtubule-affinity state that is primed to undergo a powerstroke. Nucleotide hydrolysis and phosphate release produces an ADP bound motor (right) that binds tightly to a microtubule and generates force. The motor remains in a tight binding configuration even after ADP is released.

remain bound to microtubules, even in the presence of ATP [15,16,26]. A mutation in AAA3 that allows nucleotide binding but not hydrolysis produces a motor capable of processive movement along the microtubule, but this movement occurs at a reduced velocity [26]. Thus, it appears that nucleotide occupancy at AAA3 is critical for coupling microtubule release to the catalytic cycle. Mutations in AAA4 that prevent nucleotide binding also reduce the rate of dynein-driven microtubule gliding and microtubule-stimulated ATPase activity, yet blocking nucleotide hydrolysis at this site enhances motor processivity and microtubule affinity [15,25,26].

The AAA5 and AAA6 domains continue the ring structure downstream of the microtubule-binding region. These two domains lack the complete assemblage of motifs required for ATP binding [3] and thus are not likely to actively generate or enhance conformational changes. Rather, they may provide key structural elements that direct conformational changes between AAA1 and AAA4, and/or act as a static component to enhance force production at AAA1. A division of labor among subunits in AAA^+ proteins is not uncommon. For example, the AAA^+ *E. coli* clamp loader protein is assembled from five major subunits: three identical γ subunits (AAA motor domains), a δ domain, and a δ' domain [27]. Nucleotide binding in the γ subunits results in a wrench-like movement of the δ domain to open a β-clamp that encircles DNA and provides a sliding platform to guide DNA polymerase activity. The δ' domain serves as a structurally stable stator that facilitates the wrench movement. For the clamp loader, nucleotide catalysis in three AAA domains works against two non-catalytic subunits to generate force production and modulate substrate affinity. Even identical subunits within AAA^+ proteins can generate heterogeneous functions. ClpX is a hexameric AAA^+ protein that functions in protein unfolding. Although composed of identical subunits, recent crystal structures have revealed a striking asymmetry in the ring assembly [28,29]. Rotational differences between the large and small AAA domains of individual subunits result in conformations that prevent nucleotide binding in two of the six subunits. This structural heterogeneity suggests a mechanism to direct conformation changes to adjacent, functional subunits and/or alter ring geometry to accommodate variably sized substrates. The parallel of these two examples to dynein is that all three AAA proteins appear to have a static component that the ring can work against. The additional sequence downstream of AAA6 in most dyneins has been localized to a region that roughly covers the AAA5 and AAA6 domains [12]. Thus, it is conceivable that AAA5, AAA6, and the C-terminal domains form a static structural component to the dynein ring that guides conformational changes.

Molecular modeling and simulation efforts will no doubt be required to understand the structural dynamics of the motor ring movements. Significant analyses need to address the pathway from catalysis in AAA1 to conformation changes that affect microtubule affinity; how nucleotide occupancy in AAA2, AAA3, and AAA4 affects this communication; and whether or how motor activity is regulated by

globally altering ring structure. Interestingly, fragments of the dynein motor containing only the AAA1 domain show very limited catalytic activity [17]. Expression and analysis of motor fragments demonstrates that combinations of AAA modules are required for robust ATPase activity, and that the entire ring-shaped geometry is necessary for complete motor function [17,30]. Thus, the interactions between adjacent AAA domains are important in generating the proper nucleotide binding geometry and therefore indicate that the AAA domains are conformationally linked to one another. Although preliminary attempts at modeling have been made [11,31,32], greater structural detail of the motor domain will be required to fully understand how the AAA modules interact with each other and direct motor activity.

4.2 The Linker Arm and Powerstroke

Early electron microscopy micrographs of the dynein molecule depicted motors with the MTBD on one side of the motor density and the cargo-binding tail projecting out at the opposite side (e.g. [13]). However, detailed analyses of an inner-arm axonemal dynein from *Chlamydomonas* revealed a more complex tail structure, with a distinctive near-180° bend as the tail extends away from the motor mass [8]. As GFP tags were incorporated into the heavy chain (HC) sequence of the *Dictyostelium* dynein and motors were analyzed by both fluorescence resonance energy transfer and electron microscopy image averaging methods, it became even more apparent that the dynein tail does not simply extend off one edge of the ring [12,23]. Instead, there appears to be a linker region connecting the motor and tail that arcs in some fashion across the ring surface (Fig. 4.2; see also Chapter 3 and [33]). The ultrastructure of the linker domain is currently unknown. The linker sequence clearly has some affinity for the ring surface since it can be found in both docked and detached configurations [12]. In motors that are "primed" (e.g. ATP-bound, weak microtubule affinity state prior to producing a powerstroke), the tail extends off the ring at a position near AAA2. In "unprimed" motors (apo-ATP, tight microtubule affinity, post-powerstroke state) the tail emerges near the base of the microtubule-binding stalk, close to AAA4 [12,23]. These efforts provide the best available evidence for a dynein powerstroke, a movement of the linker region from a position near AAA2 to a position near AAA4 (Fig. 4.2).

The dynein powerstroke differs from force-generating strokes found in the other cytoskeleton-based motors. In kinesins and myosins, the head actively rotates a lever arm to drive a forward motion of the motor complex (Fig. 4.3) [1]. Dynein, however, is thought to undergo a winch-like movement, where cargo is pulled forward [33–36]. This powerstroke reduces the distance between the motor and cargo while roughly maintaining the angle by which the motor is bound to a microtubule [35,36], (Fig. 4.3). Movement direction is conferred through the angle by which the stalk contacts the microtubule surface [34]. A missing

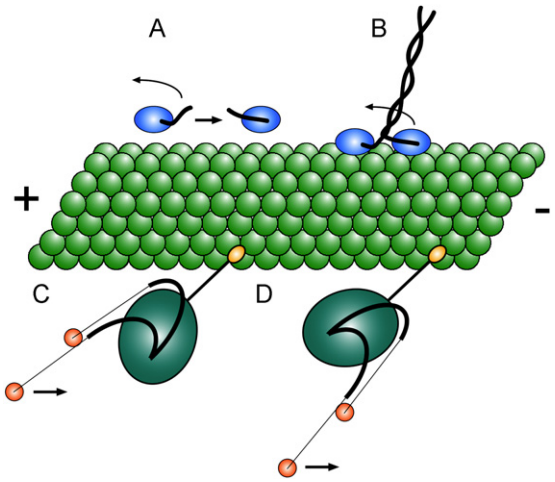

Figure 4.3 Powerstrokes and directionality. (A) A powerstroke in a single kinesin motor domain. The neck linker domain (in black) rotates toward the microtubule-plus end upon ATP binding and hydrolysis. (B) An intact dimeric kinesin molecule on a microtubule (green); the powerstroke on the leading motor head drives the trailing motor toward the microtubule-plus end. For details and a movie of this type of movement, see [1]. (C) The dynein powerstroke. Both pre- and post-powerstroke positions of the linker domain (black) are superimposed on the same single head. The orange spheres serve as reference marks to indicate cargo movement toward the microtubule-minus end. (D) A motor domain rotated 180° relative to the MTBD orientation, as described in [34]. Note that, despite reversing the motor orientation relative to the microtubule, the powerstroke still produces movement toward the microtubule-minus end.

component of dynein movement lies in understanding how the motor head repositions itself further along the microtubule surface. The mechanics of head stepping are not likely to be trivial since dyneins appear to show load-dependent variations in step sizes [5,37].

4.3 Microtubule Affinity: Binding at A Distance

The ATP-sensitive interaction of dyneins with microtubules occurs in a small globular region at the distal end of a ~10 nm length coiled-coil stalk [11,13]. The proximal end of the stalk emerges from the main motor mass at AAA4 and reconnects to the ring at AAA5, as shown in Figure 4.1. This unusual structural arrangement positions the MTBD well away from the motor surface, extending from a point on the ring nearly opposite the AAA1 domain. An atomic-level structure for the binding domain from mouse cytoplasmic dynein has been developed [34], demonstrating six short α-helices that cluster around the end of the coiled-coil stalk (Fig. 4.4). Four of these helices make lateral contacts with the coiled-coil ends, indicating that their positions would be sensitive to structural changes within the stalk. Alanine substitution experiments have identified several

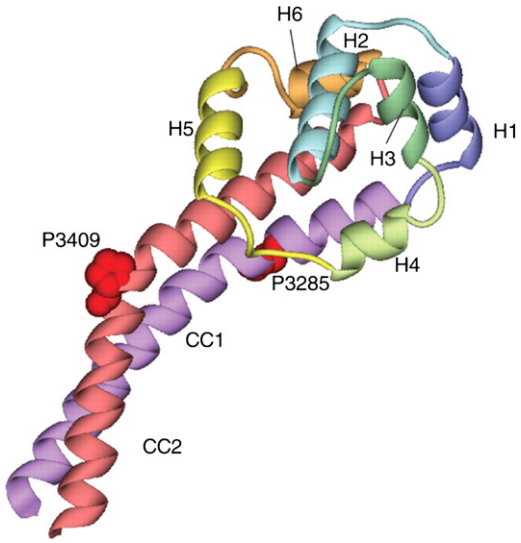

Figure 4.4 Atomic structure of the murine cytoplasmic dynein MTBD. Six helical domains (H1–6) are clustered around the distal tip of the ~10 nm-length antiparallel coiled-coil stalk (CC1, CC2; not shown in its entirety). This structure depicts the weak-microtubule-affinity state. Shifting the registries in the coiled coil is thought to produce subtle changes in helix positions and thus alter microtubule affinity. Depending on the docking orientation, microtubule interaction could occur through H1 and H3 or through H2 and H5. Reproduced from [34] with permission from AAAS.

conserved charged residues in the globular tip that are significant for microtubule binding [38] and highlight helices one and three as regions particularly important for microtubule contact [34]. Electron microscopy analyses indicate that dynein binds to both α- and β-tubulin, at the junction between these two subunits along the microtubule protofilament [34,39]. Interestingly, dynein binds to microtubules in nearly the same location as kinesin [39].

There are two general ideas concerning how dynein could engage microtubules at its binding domain. The first idea posits that affinity with the substrate remains constant and individual motors attach and detach through the movement of a second (or third) head in a motor complex. The second idea postulates that, despite a considerable spatial distance between the two functional sites, affinity at the microtubule-binding interface is actively controlled by the ATP catalytic cycle in AAA1 to achieve tight and weak binding states. Although single-headed motors have long been known to readily detach from microtubules in the presence of ATP without assistance from an additional motor, key support for the second idea came from molecular fusion experiments. Gibbons et al. [40] demonstrated that alterations in the coiled-coil registry of the stalk produced dynein MTBDs with different microtubule affinities. One coiled-coil registry (by default designated as α) produced a polypeptide that bound tightly to microtubules (1–3 μM binding affinity). Shifting

the coiled-coil registry by half-heptad distances in either direction (so-called β^- and β^+ registries) produced constructs with intermediate and weak microtubule affinity (10–15 μM and >20 μM, respectively). These results indicate that microtubule affinity is actively modulated and that shifting the stalk's coiled-coil registry transduces nucleotide-dependent changes in affinity. The ultrastructural details that confer tight or weak affinity to microtubules remain to be discovered.

A direct test of this active-affinity mechanism came from Kon et al. [41]. These authors engineered pairs of cysteine residues into the coiled-coil stalk of an otherwise fully functional *Dictyostelium* dynein motor domain, which could then be used as crosslinks to fix the registry under different oxidizing or reducing conditions. Consistent with the Gibbons et al. [40] study, disulfide crosslinks predicted to stabilize the α registry produced a motor with high microtubule affinity. A four-residue shift in the crosslink position to the predicted β^+ helical registry yielded an ATP-independent, low microtubule affinity motor.

A combination of nuclear magnetic resonance (NMR) analyses and molecular modeling was further used to develop a solution model for the distal tip of the dynein MTBD from *Dictyostelium* [42]. As in the crystal structure of murine dynein [34], six α-helical regions were identified and modeling efforts showed a similar positioning of these helices around the distal three turns of the stalk's coiled coil. Whereas the murine dynein was physically constrained into the low-microtubule-affinity β^+ registry by fusion onto the seryl tRNA-synthetase, the NMR work analyzed an unconstrained fragment, in solution. Nuclear Overhauser Effect (NOE) analysis of connectivities in the *Dictyostelium* stalk segment demonstrates that the default coiled-coil registry of this fragment is the low-affinity, β^+ conformation. Microtubule-binding measurements of this fragment further show that it has a relatively weak affinity for microtubules. These results not only validate the registry assignment imposed by the fusion experiments but also indicate that the energy minimum conformation for the MTBD lies in a weak affinity state. Interestingly, appending the full-length coiled-coil stalk onto the microtubule-binding tip converted the tip structure into a high-affinity binding state. These results suggest that the energetics of interaction within the full-length coiled-coil favor the α-registry and are sufficient to drive the globular tip structure into a conformationally unstable high-affinity binding state. Thus, it is possible that there exists an energetic tension between the stalk and the MTBD components that acts as a switch between high and low binding affinities. This tension may form an important, bidirectional response element to modulate microtubule affinity.

Carter et al. [34] also addressed the interesting question of whether orientation of the MTBD can confer directionality of motor movement. By lengthening or shortening the coiled-coil stalk by seven heptads, the authors calculated that the orientation of the microtubule-binding interface would rotate 180° relative to the AAA^+ ring. These modifications would enable the MTBD to engage microtubules in the same manner as unaltered motors, but position the ring-shaped motor core

in the opposite orientation. However, instead of motors reversing their direction, these modified dyneins moved in the same direction as native dynein, albeit at reduced velocities [34]. The winch-like movement of the dynein powerstroke helps to explain this result. Despite a 180° rotation of the motor core, the angle of microtubule contact relative to force production would not have changed, and thus movement direction is preserved (Fig. 4.4). Taking this idea one step further, sequence variations or ring conformations that alter the stalk–microtubule-binding angle ought to influence dynein direction, step size, or step mechanics [5,37,43,44]. Thus, relatively simple modifications to the dynein polypeptide sequence that alter the binding angle may underlie the subtle differences in movement between different dynein isoforms (e.g. [44]).

4.4 A Three-Part Harmony in A Big Block V-8

To function as a robust processive motor, dynein must coordinate force production of the linker arm with alternating tight and weak binding affinities of the MTBD. These three components – the linker, stalk, and ring – must work together, and their synchrony is sensitive to multiple constraints. Clearly the catalytic cycle at AAA1 drives the engine, but nucleotide occupancy at AAA domains 2, 3, and 4 appears to influence the coupling between the catalytic cycle, force production, and microtubule affinity. Altering this coupling will enhance, retard, or prevent force-producing motor engagements with a microtubule and potentially provides at least one mechanism to regulate motor activity. Tension applied to the motor ring could act to inhibit or gate nucleotide interactions at AAA2, AAA3, or AAA4 and thus provide real-time adjustments to the motor as it moves along a microtubule. Various gating mechanisms have been described for the kinesin motors, and these, in general, are likely to be useful for dynein [45,46].

In the bigger picture, most dyneins function as combinations of multiple motor domains. In cytoplasmic isoforms, two motors are linked together through dimerization motifs in the tail domain, forming a V-shaped molecule (with eight nucleotide binding domains). Cytoplasmic dynein moves along a microtubule through a coordinated hand-over-hand-type fashion [7], but how the two heads advance along a microtubule is currently unknown. One recent idea is that the two motor heads coordinate their steps through physical interactions with one another [6,37,47]. The stepping movements apply cyclical strain and tension on dynein motors that likely influence their mechanical coupling (e.g. [5,37,48]). Moreover, as discussed in Chapters 10–12 and 16, dynein-based movement is also regulated through interactions with a number of accessory proteins. While some of these proteins act to alter dynein–cargo interactions, it would not be surprising to find that others directly influence motor activity. Dynein activity potentially could be modified through ring tension, which regulates nucleotide occupancy in the catalytic AAA domains by altering the angle of the MTBD, and

through load-based dynamics, that involves how the two heads in a complex coordinate their actions. For example, unlike kinesin or myosin, dynein molecules lack a neck-like region that tightly coordinates activity between the two heads. Electron microscopy micrographs of isolated dynein motors typically show a range of morphologies, from the two heads being tightly grouped together to their being widely splayed apart [2,49]. These images suggest that the head–head interactions are variable, and thus could help explain how motors under different nucleotide conditions and loads show variation in step sizes and movements [5,37]. Altogether, there are a number of different factors that potentially tune how the motor moves.

Over the past decade and a half, the inner workings of the dynein engine have been explored via a number of bench-top mechanics. However, a complete understanding of dynein mechanics is far from complete, and we suspect that the dynein engine still has many secrets to reveal.

During the proofing stage for this chapter, an atomic structure for the yeast cytoplasmic dynein appeared in print [50]. This structure initiates the molecular mapping of atomic detail into the motor domain and identifies a new component, the buttress, which interacts with the coiled-coil stalk and may facilitate transitions between weak and tight microtubule-binding affinity.

Acknowledgments

Work in our laboratory is supported in part by the National Science Foundation (MCB-0542731 to M.P.K.).

References

[1] R.D. Vale, R.A. Milligan, The way things move: Looking under the hood of molecular motor proteins, Science 288 (2000) 88–95.
[2] M.P. Koonce, M. Samsó, Of rings and levers: The dynein motor comes of age, Trends Cell Biol. 14 (2004) 612–619.
[3] A.F. Neuwald, L. Aravind, J.L. Spouge, E.V. Koonin, AAA^{+}: A class of chaperone-like ATPases associated with the assembly, operation, and disassembly of protein complexes, Genome Res. 9 (1999) 27–43.
[4] G. Mocz, I.R. Gibbons, Phase partition analysis of nucleotide binding to axonemal dynein, Biochemistry 35 (1996) 9204–9211.
[5] R. Mallik, B.C. Carter, S.A. Lex, S.J. King, S.P. Gross, Cytoplasmic dynein functions as a gear in response to load, Nature 427 (2004) 649–652.
[6] S.L. Reck-Peterson, A. Yildiz, A.P. Carter, A. Gennerich, N. Zhang, R.D. Vale, Single-molecule analysis of dynein processivity and stepping behavior, Cell 126 (2006) 335–348.
[7] S. Toba, T.M. Watanabe, L. Yamaguchi-Okimoto, Y.Y. Toyoshima, H. Higuchi, Overlapping hand-over-hand mechanism of single molecular motility of cytoplasmic dynein, Proc. Natl. Acad. Sci. USA 103 (2006) 5741–5745.
[8] S.A. Burgess, M.L. Walker, H. Sakakibara, P.J. Knight, K. Oiwa, Dynein structure and power stroke, Nature 421 (2003) 715–718.

[9] A. Habura, I. Tikhonenko, R.L. Chisholm, M.P. Koonce, Interaction mapping of a dynein heavy chain. Identification of dimerization and intermediate-chain binding domains, J. Biol. Chem. 274 (1999) 15447–15453.
[10] S.H. Tynan, M.A. Gee, R.B. Vallee, Distinct but overlapping sites within the cytoplasmic dynein heavy chain for dimerization and for intermediate chain and light intermediate chain binding, J. Biol. Chem. 275 (2000) 32 769–32 774.
[11] M. Samsó, M.P. Koonce, 25-Angstrom resolution structure of a cytoplasmic dynein motor reveals a seven-member planar ring, J. Mol. Biol. 340 (2004) 1059–1072.
[12] A.J. Roberts, N. Numata, M.L. Walker, Y.S. Kato, B. Malkova, T. Kon, R. Ohkura, F. Arisaka, P.J. Knight, K. Sutoh, S.A. Burgess, AAA$^+$ ring and linker swing mechanism in the dynein motor, Cell 136 (2009) 485–495.
[13] M.A. Gee, J.E. Heuser, R.B. Vallee, An extended microtubule-binding structure within the dynein motor domain, Nature 390 (1997) 636–639.
[14] I.R. Gibbons, A. Lee-Eiford, G. Mocz, C.A. Phillipson, W.J. Tang, B.H. Gibbons, Photosensitized cleavage of dynein heavy chains. Cleavage at the "V1 site" by irradiation at 365 nm in the presence of ATP and vanadate, J. Biol. Chem. 262 (1978) 2780–2786.
[15] T. Kon, M. Nishiura, R. Ohkura, Y.Y. Toyoshima, K. Sutoh, Distinct functions of nucleotide-binding/hydrolysis sites in the four AAA modules of cytoplasmic dynein, Biochem. 43 (2004) 11266–11274.
[16] A. Silvanovich, M.-G. Li, M. Serr, S. Mische, T.S. Hays, The third P-loop domain in cytoplasmic dynein heavy chain is essential for dynein motor function and ATP-sensitive microtubule binding, Mol. Biol. Cell 14 (2003) 1355–1365.
[17] Y. Takahashi, M. Edamatsu, Y.Y. Toyoshima, Multiple ATP-hydrolyzing sites that potentially function in cytoplasmic dynein, Proc. Natl. Acad. Sci. USA 101 (2004) 12865–12869.
[18] E.L. Holzbaur, K.A. Johnson, Microtubules accelerate ADP release by dynein, Biochemistry 28 (1989) 7010–7016.
[19] E.L. Holzbaur, K.A. Johnson, ADP release is rate limiting in steady-state turnover by the dynein adenosinetriphosphatase, Biochem. 28 (1989) 5577–5585.
[20] K.A. Johnson, The pathway of ATP hydrolysis by dynein. Kinetics of a presteady state phosphate burst, J. Biol. Chem. 258 (1983) 13825–13832.
[21] M.E. Porter, K.A. Johnson, Transient state kinetic analysis of the ATP-induced dissociation of the dynein-microtubule complex, J. Biol. Chem. 258 (1983) 6582–6587.
[22] K. Inamula, T. Kon, R. Ohkura, K. Sutoh, The coordination of cyclic microtubule association/dissociation and tail swing of cytoplasmic dynein, Proc. Natl. Acad. Sci. USA 104 (2007) 16134–16139.
[23] T. Kon, T. Mogami, R. Ohkura, M. Nishiura, K. Sutoh, ATP hydrolysis cycle-dependent tail motions in cytoplasmic dynein, Nat. Struct. Mol. Biol. 12 (2005) 513–519.
[24] T. Mogami, T. Kon, K. Ito, K. Sutoh, Kinetic characterization of tail swing steps in the ATPase cycle of Dictyostelium cytoplasmic dynein, J. Biol. Chem. 282 (2007) 21 639–21 644.
[25] S.L. Reck-Peterson, R.D. Vale, Molecular dissection of the roles of nucleotide binding and hydrolysis in dynein's AAA domains in *Saccharomyces cerevisiae*, Proc. Natl. Acad. Sci. USA 101 (2004) 1491–1495.
[26] C. Cho, S.L. Reck-Peterson, R.D. Vale, Regulatory ATPase sites of cytoplasmic dynein affect processivity and force generation, J. Biol. Chem. 283 (2008) 25 839–25 845.
[27] M.J. Davey, D. Jeruzalmi, J. Kuriyan, M. O'Donnell, Motors and switches: AAA$^+$ machines within the replisome, Nat. Rev. Mol. Cell Biol. 3 (2002) 826–835.
[28] S.E. Glynn, A. Martin, A.R. Nager, T.A. Baker, R.T. Sauer, Structures of asymmetric ClpX hexamers reveal nucleotide-dependent motions in a AAA$^+$ protein-unfolding machine, Cell 139 (2009) 744–756.
[29] P. Pietroni, P.H. von Hippel, Multiple ATP binding is required to stabilize the "activated" (clamp open) clamp loader of the T4 DNA replication complex, J. Biol. Chem. 283 (2008) 28338–28353.

[30] P. Höök, A. Mikami, B. Shafer, B.T. Chait, S. Rosenfeld, R.B. Vallee, Long range allosteric control of cytoplasmic dynein ATPase activity by the stalk and C-terminal domains, J. Biol. Chem. 280 (2005) 33045–33054.
[31] A.W. Serohijos, Y. Chen, F. Ding, T.C. Elston, N.V. Dokholyan, A structural model reveals energy transduction in dynein, Proc. Natl. Acad. Sci. U.S.A. 103 (2006) 18540–18545.
[32] G. Mocz, I.R. Gibbons, Model for the motor component of dynein heavy chain based on homology to the AAA family of oligomeric ATPases, Structure 9 (2001) 93–103.
[33] S.A. Burgess, P.J. Knight, AAA^+ is the dynein motor a winch? Curr. Opin. Struct. Biol. 14 (2004) 138–146.
[34] A.P. Carter, J.E. Garbarino, E.M. Wilson-Kubalek, W.E. Shipley, C. Cho, R.A. Milligan, R.D. Vale, I.R. Gibbons, Structure and functional role of dynein's microtubule-binding domain, Science 322 (2008) 1691–1695.
[35] H. Ueno, T. Yasunaga, C. Shingyoji, K. Hirose, Dynein pulls microtubules without rotating its stalk, Proc. Natl. Acad. Sci. USA 105 (2008) 19 702–19 707.
[36] T. Movassagh, K.H. Bui, H. Sakakibara, K. Oiwa, T. Ishikawa, Nucleotide-induced global conformational changes of flagellar dynein arms revealed by *in situ* analysis, Nat. Struct. Mol. Biol. 17 (2010) 761–767.
[37] A. Gennerich, A.P. Carter, S.L. Reck-Peterson, R.D. Vale, Force-induced bidirectional stepping of cytoplasmic dynein, Cell 131 (2007) 952–965.
[38] M.P. Koonce, I. Tikhonenko, Functional elements within the dynein microtubule-binding domain, Mol. Biol. Cell 11 (2000) 523–529.
[39] N. Mizuno, S. Toba, M. Edamatsu, J. Watai-Nishli, N. Hirokawa, Y. Toyoshima, M. Kikkawa, Dynein and kinesin share an overlapping microtubule-binding site, EMBO J. 23 (2004) 2459–2467.
[40] I.R. Gibbons, J.E. Garbarino, C.E. Tan, S.L. Reck-Peterson, R.D. Vale, A.P. Carter, The affinity of the dynein microtubule-binding domain is modulated by the conformation of its coiled-coil stalk, J. Biol. Chem. 280 (2005) 23960–23965.
[41] T. Kon, K. Imamula, A.J. Roberts, R. Ohkura, P.J. Knight, I.R. Gibbons, S.A. Burgess, K. Sutoh, Helix sliding in the stalk coiled coil of dynein couples ATPase and microtubule binding, Nat. Struct. Mol. Biol. 16 (2009) 325–333.
[42] L. McNaughton, I. Tikhonenko, N.K. Banavali, D.M. LeMaster, M.P. Koonce, A low affinity ground state conformation for the dynein microtubule binding domain, J. Biol. Chem. 285 (2010) 15994–16002.
[43] J.L. Ross, K. Wallace, H. Shuman, Y.E. Goldman, E.L.F. Holzbaur, Processive bidirectional motion of dynein-dynactin complexes in vitro, Nat. Cell Biol. 8 (2006) 562–570.
[44] R.D. Vale, Y. Yano Toyoshima, Rotation and translocation of microtubules in vitro induced by dyneins from Tetrahymena cilia, Cell 52 (1988) 459–469.
[45] A. Gennerich, R.D. Vale, Walking the walk: How kinesin and dynein coordinate their steps, Curr. Opin. Cell Biol. 21 (2009) 59–67.
[46] D.D. Hackney, Evidence for alternating head catalysis by kinesin during microtubule-stimulated ATP hydrolysis, Proc. Natl. Acad. Sci. USA 91 (1994) 6865–6869.
[47] T. Shima, K. Imamula, T. Kon, R. Ohkura, K. Sutoh, Head–head coordination is required for the processive motion of cytoplasmic dynein, an AAA^+ molecular motor, J. Struct. Biol. 156 (2006) 182–189.
[48] W.J. Walter, B. Brenner, W. Steffen, Cytoplasmic dynein is not a conventional processive motor, J. Struct. Biol. 170 (2010) 266–269.
[49] L.A. Amos, Brain dynein crossbridges microtubules into bundles, J. Cell Sci. 93 (1989) 19–28.
[50] A.P. Carter, C. Cho, L. Jin, R.D. Vale, Crystal structure of the dynein motor domain, Science 331 (2011) 1159–1165.

In this chapter

5

Structural Analysis of Dynein Intermediate and Light Chains

John C. Williams, Amanda E. Siglin, Christine M. Lightcap, Amrita Dawn
Department of Molecular Medicine, Beckman Research Institute at the City of Hope, Duarte, CA, USA

5.1 Introduction

Cytoplasmic and axonemal dyneins are multiple-component complexes that share some common features but participate in fundamentally different processes. In both complexes, the heavy chain (HC) subunits hydrolyze ATP and interact with microtubules to generate force. The N-termini of the dynein HCs act as scaffolds for the accessory proteins, which include the dynein intermediate chain (IC), the dynein light-intermediate chains (LICs), and the dynein light chains (LCs) [1]. These accessory subunits interact with other target proteins or macromolecules and have also been suggested to directly and indirectly regulate dynein ATPase activity [2,3]. In the case of cytoplasmic dynein, cellular targets that interact with the dynein IC, LICs, and LCs are frequently considered as cargo for retrograde microtubule transport [1,4]. While the IC and LIC make specific, but limited, interactions with cargo (e.g. dynactin [5,6] and pericentrin [7]), the dynein LCs bind to a large number of proteins [1,8], including signaling molecules (TrkA [9]), transcription factors [10], and viruses (see Tables 5.1 and 5.2). With the limited number of cytoplasmic dyneins (i.e. nearly all tissues appear to express only one isoform [11,12]) and noting that cytoplasmic dynein is the dominant retrograde motor protein in the cell (see Chapter 14), the diversity of LC binding partners originally lead to the notion that they bridge cargo to dynein [13]. Structural and thermodynamic studies of the LCs and their different targets shortly followed these initial *in vitro* experiments. These studies of the LCs bound to fragments of the IC do not support this bridging model [14]. Rather, they argue for a role in the assembly of the dynein complex and/or a regulatory role of the IC subunits.

Dyneins DOI: 10.1016/B978-0-12-382004-4.10005-6
Copyright © 2012 by Elsevier Inc. All rights reserved.

Table 5.1 LC8 Targets and their Associated Sequences

Target	LC8 Sequence	Sequence Location	Dimer[1]	NLS/ Nuclear[2]	NLS Location	References
53BP1	VSAATQTI	167–174	Yes	Yes/Yes	1395–1401 1626–1629 1668–1685	[58,119]
A. Moorei entomopoxvirus AMV179 ORF	NIKSTQTC	152–159	N/A	Yes/No	194–210	[120,121]
African swine fever virus p54	QNTASQTM	256–263	Yes	Yes/Yes	55–58	[66,122]
Bassoon	TANYGSQTQ TAEFSTQTP MVAQGTQTP	1425–1433 1501–1509 1529–1537	Yes*	Yes/No	791–893 1012–1028 1072–1088 2600–2604 2625–2636	[123]
BimEL	CDKSTQTP	110–117	N/A	No/No	–	[76,113]
BimL	CDKSTQTP	50–57	N/A	No/No	–	[76,113]
Bmf	EDKATQTL	143–150	N/A	No/Yes	–	[76,124]
Cdk2	Unknown	–	N/A	No/Yes	–	[125,126]
Ciz1	Unknown	–	Yes*	Yes/Yes	689–714	[126,127]
DazI	VDRSIQTV	268–275	Yes	No/Yes	–	[8,128]
Dynein HC	QDKLVQTP	1876–1883	Yes*	No/No	–	[129,130]
Dynein IC	YTKETQTP	166–173	Yes*	Yes/Yes	13–29 42–58	[14,64]
Egl	VDAESQTL	950–957	Yes	No/Yes	–	[10,131]
Estrogen Receptor α	Unknown	AB Domain	Yes	Yes/Yes	243–272	[132,133]
Gephyrin	EDKGVQCE	206–213	Yes	Yes/Yes	347–350	[129,134]
GKAP	LSIGIQVD	650–657	N/A	Yes/No	338–344 904–910	[57,135]
GRINL1A	REIGVGCDL	424–432	Yes*	Yes/Ukn	365–381	[136]
Grp3	TSQATQTE	610–617	N/A	No/No	–	[137]
Human adenovirus protease	LIKSTQTV	107–114	Yes	No/Yes	–	[120,138]
Human herpes simplex virus helicase	LAKSTQTF	760–767	Yes	No/Yes	–	[120,139]
Human herpesvirus U19 gene	FSRHTQTD	260–267	N/A	No/Yes	–	[120,140]
IκBα	Disulfide?	–	N/A	Yes/Yes	83–128	[79,141]
Kibra	Unknown	–	Yes*	Yes/Yes	361–376	[142]
Kid-1	TTKSTQTQ	93–100	Yes	Yes/Yes	180–186	[8,143,144]
MAP-4	GSKSTQTV	627–634		No/No	–	[8,144]
Mokola virus	EDKSTQTP	140–147	Yes	No/Yes	–	[120,145]
Myosin Va	EDKNTMTD	1284–1291	Yes	Yes/Yes	858–874 1467–1473 1643–1649	[8,146]
nNOS	KDTGIQVD	234–241	Yes	Yes/Yes	728–734 993–996 1323–1326	[147,148]
NRF-1	EHGVTQTE	3–10	Yes	Yes/Yes	89–108	[10,149]
Nup159	ADRDVQTS AESGIQTD	1105–1112 1118–1125	Yes*	No/Yes	–	[150]

Table 5.1 LC8 Targets and their Associated Sequences—cont'd

Target	LC8 Sequence	Sequence Location	Dimer[1]	NLS/ Nuclear[2]	NLS Location	References
	KENEVQTD	1131–1138				
	KHNSTQTV	1143–1150				
	VDNGLQTR	1155–1162				
	CNFSVQTP	1167–1174				
Pak1	RDVATSPI	212–224	Yes	Yes/Yes	243–245	[30,151]
Rabies virus	EDKSTQTT	142–149	Yes	Yes/Yes	211–214	[119,152]
Respiratory syncitial virus attachment glycoprotein	TTTSTQTN	137–144	Yes	Yes/No	155–162 190–200	[120,153]
Swallow	SAKATQTD	280–287	Yes*	Yes/Yes	349–352 485–488	[154,155]
TRP14	Unknown	–	No	No/No	–	[156]
TRPS1	VDRSTQDE	1219–1226	Yes	Yes/Yes	900–903	[157,158]
Viral protein VP35 of ebolavirus	*Zaire* SQTQT *Sudan* KQVQT *Reston* SSSQT	71–75 All species	Yes	No/Yes	–	[65,159]

[1]* *denotes either reported in the literature or noted in public databases to contain a highly predicted coiled coil (http://www.isrec.isb-sib.ch/webmarcoil/webmarcoilC1.html).*

[2]*Reported nuclear localization sequences (NLSs) and their sequence locations. The PSORT II NLS prediction program (http://psort.hgc.jp/form2.html) was used to determine potential NLS sequences for LC8 binding proteins that have not been experimentally verified.*

Table 5.2 Reported Tctex1 Binding Proteins[1]

Target	Dimerization Domain[2]	References
BMPR-II	Yes	[59]
CD5	Yes	[160]
CD155	Yes	[161]
DOC2a	N/A	[74]
Dynein IC	Yes	[14]
FIP-1	Unknown	[162]
p59 Fyn kinase	N/A	[108]
G protein βγ subunit	N/A	[163]
Herpes simplex virus 1	Yes	[164]
Lfc	Yes	[165,166]
PTH receptor	Yes	[72]
Rhodopsin	Yes	[61]
SATB1	Yes	[64]
TrkA	Yes	[167]
VDAC	Yes	[60]
VP26	Yes	[168]

[1]*The reported Tctex1 binding site in these binding partners is not clear based on the structural data and thus not determined.*

[2]* *denotes either reported in the literature or noted in public databases to contain a highly predicted coiled coil (http://www.isrec.isb-sib.ch/webmarcoil/webmarcoilC1.html).*

This chapter focuses on these structural and biochemical investigations of the LCs and ICs. It also addresses the promiscuity of the dynein LCs LC8 and Tctex1, as well as their potential role in dynein function. Since much of the structural and biochemical efforts focus on cytoplasmic dynein, and in particular on dynein of animal origin (rat and drosophila), the primary emphasis will be on cytoplasmic dynein. Information from other dynein complexes will be used to illustrate potential structural differences among the different dynein family members.

5.2 Abbreviated Background of Light Chains

The dynein LCs were identified as accessory subunits of axonemal and cytoplasmic dynein isolated and purified from sea urchins [15], *Chlamydomonas* flagella [16], and bovine brain tissue [17]. Treatment of isolated dynein with potassium iodide produced two distinct fractions, one containing the dynein HCs and LICs and the other containing the dynein IC and LCs [18]. LCs isolated from cytoplasmic dynein include three polypeptides: Tctex1 (DYNLT1/3) [19], LC8 (DYNLL1/2) [20], and LC7/Robl (DYNLRB1/2) [21]. In addition to these LCs, other low-molecular-weight polypeptides, also denoted as LCs, have been isolated from axonemal dynein complexes [22].

Among the cytoplasmic LCs, LC8 is the best-characterized dynein subunit. It is an essential gene that is expressed in all tissues but found at higher levels in brain and testes [23]. LC8 is highly conserved across all eukaryotes but also found in plants, which are devoid of both dynein HC and IC [24]. Initial studies characterizing LC8 function did so by impairing or completely blocking its expression. These studies found that complete loss of LC8 function in drosophila results in embryonic lethality, and partial loss of function produces apoptotic signatures (e.g. nuclear envelope breakdown) [25]. Additional genetic screens in drosophila showed that mutations of LC8 disrupt axon trajectories [26]. In *A. nidulans*, deletion of LC8 prevented asexual reproduction and affected the localization and function of the dynein HC [27]. RNA-mediated interference of LC8 in *C. elegans* inhibited pronuclear migration in males as well as reduction or absence of the mitotic spindle in early embryonic cells [28]. Recent studies have shown that overexpression of LC8 plays a critical role in breast cancer [29,30] and plays an important role in the early transcription and localization of the rabies virus [29,31]. LC8 has also been shown to play a critical role in cell stress [32] and autophagy [33].

Tctex1 was originally identified as part of the t-complex and its mutation causes male sterility [34]. Unlike LC8, it is not as well conserved across eukaryotes and is absent in yeast and plants. Viable drosophila were obtained upon the deletion of Tctex1, suggesting it is not essential for development; however, males missing

the Tctex1 gene were completely sterile [35]. Additionally, cytoplasmic dynein failed to localize to the nuclear membrane in early spermatids [35]. Tctex1 is also frequently observed to play critical roles in viral pathogenesis. For instance, depletion of Tctex1 by siRNA affected the pericentriolar targeting of Mason-Pfizer monkey virus [36]. Finally, depletion of Tctex1 (and LC8) was recently shown to play an important role in endoplasmic-reticulum-to-Golgi transport [37].

LC7, also known as roadblock and km23, is the least studied of the dynein LCs. Like LC8 and Tctex1, it was found to bind to both axonemal and cytoplasmic dynein [21]. There are two isoforms, which are expressed in a tissue-dependent manner [21]. Studies aimed at identifying proteins that regulate axonal transport in drosophila identified a 193 bp deletion in LC7 in EMS-treated flies. Axons isolated from these flies showed axon swelling, the accumulation of synaptotagmin and choline acetyltransferase, and nerve degeneration [21]. LC7 has also been implicated in cancer. In patients with hepatocellular carcinoma the LC7 isoform, DYNLRB1, is upregulated while DYNLRB2 is suppressed [38]. Mutations in LC7 have also been reported at a high frequency in tissue samples isolated from patients with ovarian cancer [39]; however, an independent study did not confirm these initial findings [40].

5.3 Structure of The Apo Light Chains

Since dynein participates in multiple processes and disruption of its function either through mutation or suppression of its subunits produces pleiotropic effects, structural investigations were initiated to more fully understand the function of the LCs in terms of target recognition as well as the regulation of LC function. The solution structure of LC8 was first published in 1998 [41] and was subsequently shown by NMR to interact with a 17-residue fragment of neuronal nitric-oxide synthase (nNOS) [42]. The crystal structure showed that LC8 forms a symmetric homodimer with a core consisting of two β-sheets, each flanked by two antiparallel α-helices (Fig. 5.1). Each β-sheet is formed by five anti-parallel β-strands: β1, β4, β5, β2, and β3′. Strand β3′ originates from the other monomer and thus there are two swapped β-strands in the dimer [43]. In addition to the interactions arising from the swapped β-strands, there are a number of hydrogen bonds and hydrophobic interactions at the dimer interface. Of interest are His55 and Ser88. At low pH, His55 becomes protonated, placing two charges adjacent to each other and creating a stable monomer [44]. Similarly, Ser88 was recently proposed to be phosphorylated by Pak1 [30] placing charges adjacent to each other and affording a stable monomer [45–47]. While the stability of the LC8 monomer provides insight to the molecular mechanism of its folding and assembly, it is not clear whether a monomeric form is physiologically relevant (see below).

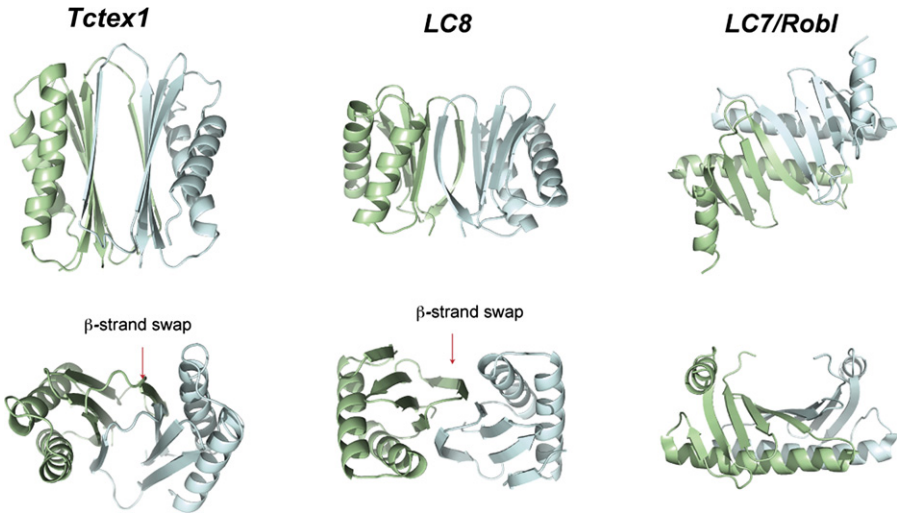

Figure 5.1 Ribbon diagrams of each member of the dynein LCs. All three LCs are homodimeric. One protomer is colored pale green and the other is colored pale cyan. Tctex1 and LC8 are structural homologs, though they share very little in terms of sequence similarity. In both cases, Tctex1 and LC8 form homodimers through a swapped strand β3. The fold of LC7 is clearly different from Tctex1 and LC8. The second α-helix and third β-strand of each protomer interact extensively with the same elements of the other protomer.

Like LC8, Tctex1 was also reported to bind to multiple proteins (Table 5.2), but these binding proteins are distinct from those identified for LC8. In addition, there is no sequence similarity between LC8 and Tctex1. On the other hand, both LC8 and Tctex1 showed the same order of predicted secondary elements (e.g. β1-β2-α2-α3-β3-β4-β5). NMR studies confirmed the secondary structure arrangement and suggested that Tctex1 and LC8 shared a common fold [48]. Crystallographic [49] and NMR [50] investigations showed that Tctex1 is structurally homologous to LC8, including the dimer swapped strand β3 (Fig. 5.1). Superposition of the LC8 and Tctex1 structures indicates that Tctex1 is extended along the two-fold axis (e.g. the α-helices and β-strands are longer). Consistent with this observation, each Tctex1 protomer buries ~1500 $Å^2$ of surface area, compared to ~750 $Å^2$ in LC8 [49]. In contrast to LC8, the symmetric Tctex1 homodimer does not contain histidines at the dimer interface and its dimerization is not pH sensitive [49,51].

The third class of dynein LCs, LC7/Robl, shows no sequence similarity to either LC8 or Tctex1 and has a limited number of known binding partners (dynein ICs, TGFβ, or Rab6). In addition, secondary structure predictions indicated that its arrangement of secondary-structure elements was significantly different from that of LC8 and Tctex1 (e.g. α1-β2-α2-β3-β4-β5). NMR [52] and diffraction studies

[53] proved in fact that the LC7 fold is distinctly different from that of Tctex1 and LC8 (Fig. 5.1). It too is a symmetric homodimer with extensive contacts across the dimer interface. Specifically, the 10-strand β-sheet of the dimer is formed by anti-parallel strands β2, β1, β5, β4, and β3 of one monomer connect to strand β3′ of the other monomer via a two-fold axis. This extended β-sheet wraps around a long, anti-parallel helical bundle formed by helix α2 of each monomer. Helices α1 and α1′ are located on the other side of the β-sheet and run perpendicular to the coiled coil, producing a "saddle-like" shape. LC7 also shows structural similarity to MglB from *Thermus thermophilus,* a protein proposed to modulate the Ras/Rab/Rho GTPase [52,54].

5.4 Structure of Liganded Light Chains

Both LC8 and Tctex1 bind to numerous targets whereas the number of binding partners of LC7 is far more limited (see Tables 5.1 and 5.2). Reported LC8 binding partners include cytoplasmic partners such as dynein IC [55], myosin Va [56], Pak1 [30], GKAP [57], and 53BP1 [58]. Likewise, Tctex1 binds to a large number of cytoplasmic proteins including membrane-associated proteins. These include dynein IC [19], Fyn and Trk kinases [9], bone morphogenetic receptor type II [59], voltage-dependent anion-selective channel (VDAC) [60], and rhodopsin [61]. Both LC8 and Tctex1 have been shown to bind to transcription factors as well, including TRPS1 [62], Swallow [63], and SATB1 [64]. In addition, a large number of viruses have been reported to bind to LC8 and Tctex1. The expanding list includes ebolavirus VP38 [65], lyssavirus [31], African swine fever [66], herpes VP26 caspid protein [67], and human papillomavirus type 16 L2 capsid protein [68]. While LC8 and Tctex1 have been shown to bind to a large number of proteins, LC7 is much more restricted. Beyond the dynein IC [21], the only other proteins reported to bind to LC7 are TGFβ [69] and Rab6 [70].

There are four distinct X-ray structures of LC8 bound to unique ligands: dynein IC peptide [14], NOS peptide [43], Swallow peptide [71], and Pak1 peptide [30]. In addition, the binding site of several peptides derived from LC8 binding proteins has been identified through NMR perturbation methods. Superposition of the X-ray structures shows that the LC8 binding peptide forms an edge-on β-strand to the swapped β3-strand of LC8 (Fig. 5.2). In addition, a large number of the LC8 binding peptides encode a glutamine flanked by hydrophobic residues (Fig. 5.2D). The structures of the dynein IC, nNOS, and Swallow show that the side chain amine group of this glutamine caps helix α2 of LC8 through a backbone hydrogen bond to Lys36. The flanking hydrophobic groups are buried in pockets formed by strands β2, β4, and β5 of LC8. These structures indicate that these two pockets can accommodate small hydrophobic side chains (e.g. Thr, Val, Ile); sequences from reported LC8-binding proteins

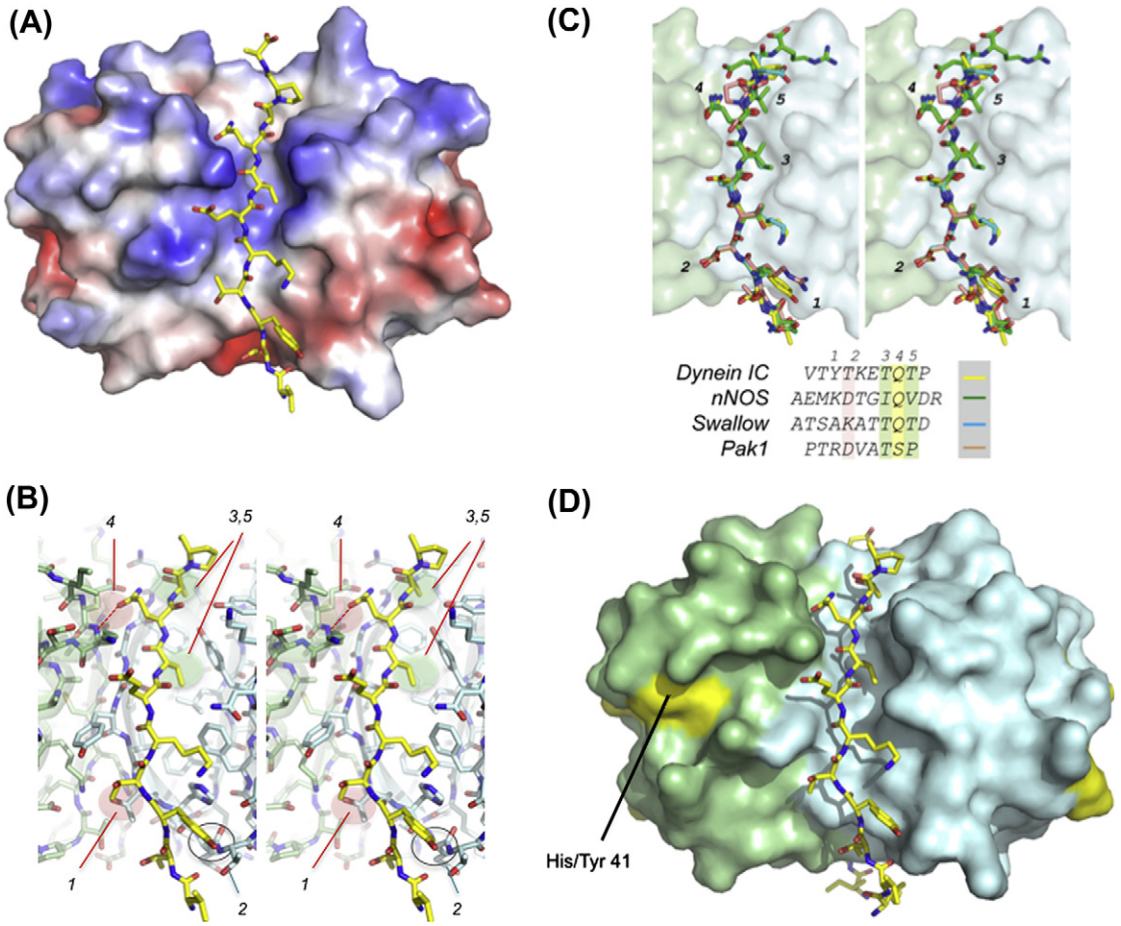

Figure 5.2 Liganded LC8. (A) The IC peptide is shown on the electrostatic surface of LC8 (contoured at +/−5 kT [169]). (B) A stereo view of the interaction between the IC ligand and LC8. Important interactions are highlighted and denoted by numbers from the N-terminus to the C-terminus of the peptide. Thr67 of LC8 is highly conserved and makes a critical salt bridge to a number of LC8-binding proteins (position 1). All cytoplasmic dynein ICs from yeast to humans encode a tyrosine (position 2). The hydrophobic pockets that intercalate the hydrophobic groups surrounding the highly conserved glutamine are highlighted in green (positions 3 and 5). Finally, the highly conserved glutamine makes a hydrogen bond to Lys36 and caps the N-terminus of helix α2. (C) Superposition of liganded LC8, determined by diffraction methods, is shown in stereo. nNOS (green carbons), swallow (cyan carbons), and Pak1 (wheat carbons) are superimposed on the dynein IC (yellow carbons). Note that the backbone of each target is nearly indistinguishable. (D) The sequence difference between each isoform is shown on the surface of each LC. Surfaces colored pale cyan or pale green are identical. Surfaces colored yellow indicate similar residues.

suggest that these hydrophobic pockets can also accommodate Ser, Cys, and Leu. We observe that the reported LC8-binding sequence in TRPS1 would place an Asp at the second (C-terminal) pocket. The effect of this substitution remains to be characterized.

We also observe that a small number of reported LC8 binding sequences encode a different residue at the predominantly conserved glutamine found in dynein IC, nNOS, Swallow, etc. This includes myosin Va, Pak1, and GrinL1A. To test whether these "non-canonical" ligands could bind to distinct regions on LC8 (i.e. the flanking α-helices) and constitute a unique class of dynein cargo, the point mutation, Lys36$\rightarrow$Pro, was created in LC8 to block the capping interaction between the target peptide and helix α2 backbone. Binding studies confirmed that the dynein IC failed to interact with the mutant LC8 whereas the Pak1 peptide bound to the mutant at a similar level [46]. The X-ray structure of this "non-canonical" peptide bound to LC8 indicated that the Pak1 peptide binds to LC8 in the same manner as the other LC8-binding peptide. In this structure, the highly conserved glutamine is replaced by a serine that could potentially cap helix α2 at Lys36.

The Pak1-LC8 structure did draw attention to a second important interaction. Namely, an aspartate that is located i$-$4 residues from the predominantly conserved glutamine that is present in Pak1 as well as many other LC8-binding peptides including Myosin Va. The aspartate side chain interacts with hydroxyl group of Thr67 located in the swapped strand β3 of LC8. Mutation of Thr67 to Ala in LC8 significantly reduced the binding affinity of the Pak1 peptide but not of the dynein IC [46]. Lastly, there appears to be some preference for a lysine/arginine at the i$-$3 position (underlined in Table 5.1). Taken together, these data suggest a potential hierarchy of LC8-binding peptides based on affinity.

Finally, we note that titration experiments of ^{15}N-labeled LC8 followed by NMR using unlabeled myosin Va or GrinL1A peptides found that both of these peptides bind to the same groove as the other peptide ligands. Myosin Va encodes a Met at the conserved glutamine position but also encodes an aspartate at the i$-$4 position. GrinL1A encodes a glycine at this position but does not encode an aspartate. The GrinL1A peptide was modeled onto the structure of the nNOS peptide and places an Ile at the i$-$4 position, a Gly at the i$-$3 position, and a Cys at the i$+$1 position. However, shifting the GrinL1A peptide by two residues to the C-terminus also seems to produce a plausible model. This would also place a glycine at the predominantly conserved glutamine, but would place a Thr at the i$-$4 position, an Arg at the i$-$3 position, and an Ile and Val at the hydrophobic positions. This shift would mimic the dynein IC, Swallow, and other structures. Additional studies including structural and biochemical investigations are required to determine the register and affinities of these targets.

In the case of Tctex1, there is only one liganded structure, namely the dynein IC peptide bound to Tctex1 and LC8 [14]. Not surprisingly, the IC fragment

binds to Tctex1 in a similar manner to the way in which the IC binds to LC8. Specifically, the IC also forms an edge-on interaction with the swapped strand β3. As Tctex1 is slightly extended compared to LC8, there are additional backbone hydrogen bonds between the IC peptide and Tctex1. The IC peptide also buries hydrophobic residues, V110 and F112, in Tctex1 at similar positions to those found in LC8. However, the helix α2 in Tctex1 is extended compared to LC8 and self-capped. Thus, there is no obvious selection pressure for a glutamine or a different "capping" residue at this position, as observed for LC8. This observation may partially account for the lack of overlap between Tctex1 and LC8 reported targets. While an arginine-rich sequence was originally proposed to be the "Tctex1" binding motif [48], the IC peptide used in the structural studies included these N-terminal arginines. However, none of these arginines were observed in the electron density maps, suggesting that they are not required for Tctex1 binding. Consequently, it remains difficult to identify a Tctex1 "canonical" sequence from the reported Tctex1 binding partners.

Without a clear signature, we have mutated a number of residues in the IC peptide and used size exclusion chromatography to characterize the effect of these point mutations (data not published, A. Dawn and J. C. Williams). We observe Leu112, Met114, and Phe122 mutated individually to alanine effectively abrogated the interaction (numbering from rat IC2, isoform C). Mutation of the other residues to alanine, on the other hand, did not strongly affect the IC–Tctex1 interaction. These preliminary binding studies suggest that the specificity of Tctex1 for its peptide targets requires hydrophobic residues at the N- and C-termini spanned by eight residues, and further explains the observation that Tctex1 and LC8 bind distinct and non-overlapping targets. Applying these observations to reported Tctex1 targets (e.g. rhodopsin [61], PTHRa [72], CD155 [73], etc.) to determine the Tctex1 binding site remains challenging. In one case, there is reasonable agreement between the reported Tctex1 binding peptide in Doc2A [74] and the structure and mutagenesis data of the IC–Tctex1 interaction (Fig. 5.3). Clearly, more structural and binding assays are required to define a Tctex1 binding motif.

Lastly, the structure of a dynein IC fragment bound to LC7 was recently solved [53]. The peptide fragment spans residues 182 to 219 of the IC (rat IC2, isoform C) and forms a short α-helix, followed by a two-residue break and a long α-helix, which wraps along the β-sheet and helix α1. The first α-helix from IC places the Ile190 side chain into a shallow pocket formed by strands β1, β2, and β5. The second α-helix from the IC–LC7 interface predominantly consists of hydrophobic residues from the IC peptide fitting into a deep groove formed by the helix α1 and strands β3, β4, and β5 of LC7. In addition, the end of the IC peptide encodes a glutamate that interacts with the completely conserved Arg located in strand β3. Unlike LC8 or Tctex1, where the target peptides bind in a parallel fashion, the IC ligand binds to LC7 in an anti-parallel manner.

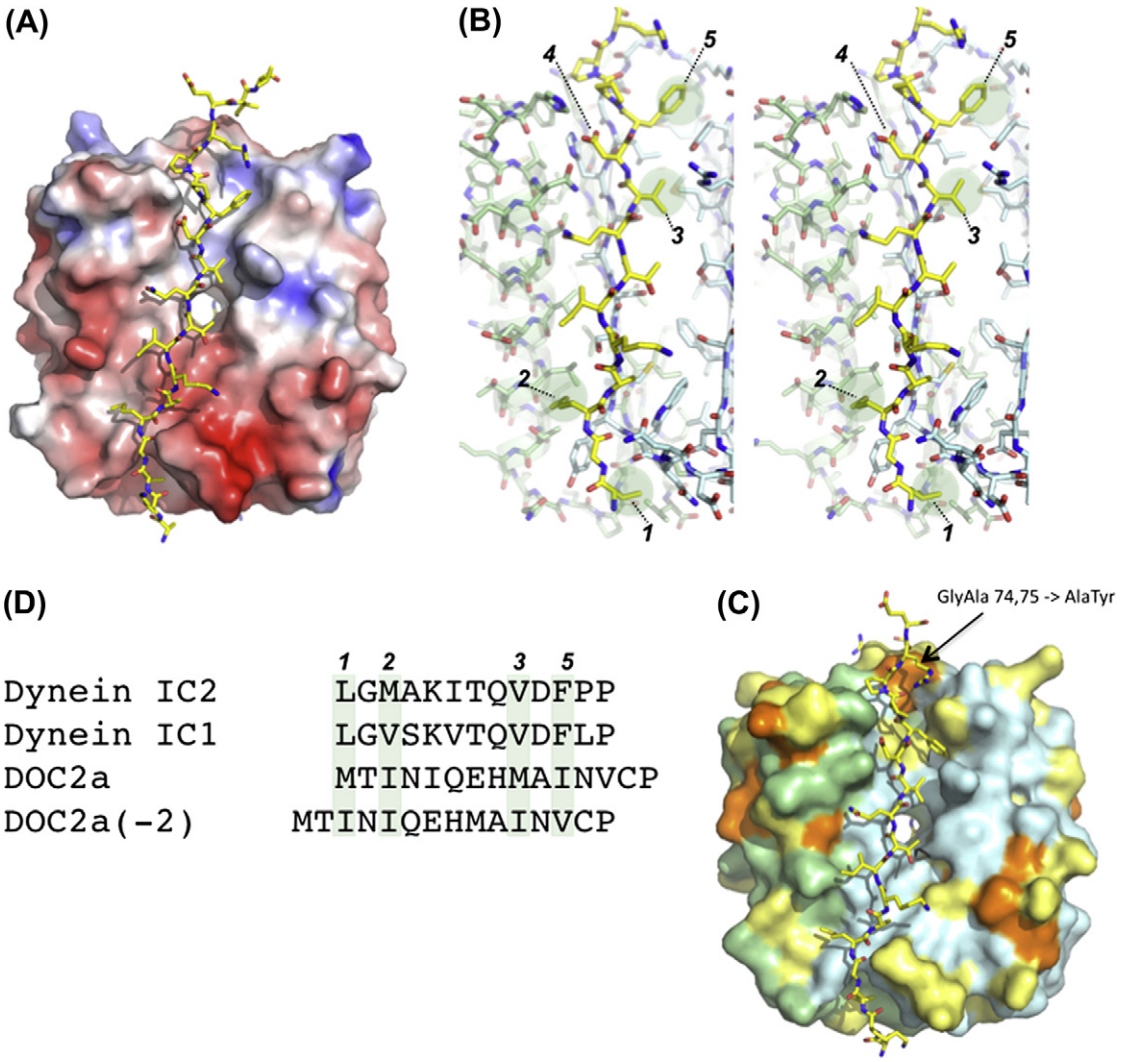

Figure 5.3 Liganded Tctex1. (A) The IC peptide is shown on the electrostatic surface of Tctex1. Note that the charge distribution differs from LC8, which may also affect ligand selection (contoured at +/−5 kT [169]). (B) Stereo view of the IC bound to Tctex1. Residues found to be required for binding are shadowed in green. Mutation of Leu112 (position 1), Met114 (position 2), and Phe122 (position 5) to alanine significantly reduces the IC—Tctex1 interaction. Positions 3 and 5, respectively, occupy positions analogous to the hydrophobic positions on LC8. Position 4, Asp121, occupies a position similar to the conserved glutamine found in the LC ligands but does not cap the helix α2 of Tctex1. Its mutation to alanine does not strongly affect the IC binding. The requirement of hydrophobic residues leucine and methionine at positions 1 and 2 likely accounts for the difference in ligand selection between Tctex1 and LC8. (C) Potential Tctex1 ligand. Based on the alanine mutagenesis, the reported binding region of Doc2 aligns well to both cytoplasmic IC isoforms. An alternative alignment requires a shift of two residues towards the N-terminus. (D) Isoform differences between Tctex1 and RP3. Unlike the LC8 isoforms, there are a number of sequence differences between Tctex1 and its family member RP3. Surfaces colored orange indicate no similarity. Sequence differences in the ligand binding site are marked with an arrow.

5.5 LC8 and Tctex1 Promiscuity

These liganded atomic structures of the LCs provide a plausible explanation for the promiscuity of LC8 and Tctex1 and the limited number of LC7 binding proteins. The interface between LC8 and Tctex1 and their respective peptide ligands consists primarily of backbone hydrogen bonds through the edge-on strand interaction and the placement of several hydrophobic interactions (Fig. 5.4A,B). Neither backbone nor hydrophobic interactions are strongly sequence specific. In this sense, the interactions between LC8 and its targets and Tctex1 and its targets resemble the mechanism by which MHC recognizes a large number of antigenic peptides [75]. This is in stark contrast to the LC7–IC interaction. In this case, the interface is dominated by side chain interactions between the IC peptide and LC7. While a number of the side chain interactions are hydrophobic (Fig. 5.4C), there are several conserved hydrogen bonds and salt bridges. Specifically, a mixed hydrogen bond/salt bridge network, formed by residues Glu252 and Asn253 in the IC and Arg71 and Gln93 in LC7, is present at the C-terminal end of the IC peptide (Fig. 5.4D – Drosophila numbering). In addition, Glu247 of the IC (denoted by *) also forms a salt bridge to the backbone carbonyl of Arg10 in LC7. Taken together, these observations indicate that the LC7 binding site is far more selective than Tctex1 or LC8. In addition, BLAST searches using the LC7 peptide failed to identify additional LC7 targets. On the other hand, BLAST searches using the LC8 sequence produce a number of targets, many of them shown experimentally to bind to LC8.

5.6 Light Chain Isoforms

In mammals, there are two isoforms of each LC, each located on a different chromosome [12]. For Tctex1, LC8, and LC7, the isoforms are 54% identical and 76% similar, 93% identical and 98% similar, and 77% identical and 87% similar, respectively. Mapping these differences to the surface of each structure suggests that the sequence differences in LC8 and LC7 should not affect IC binding. While phenotypic and biochemical differences between the LC7 isoforms have yet to be identified, residue 41 located on helix $\alpha 2$ has been demonstrated to differentially direct the LC8 isoforms to bind to dynein or myosin Va [76]. Moreover, BimL and Bmf, which encode nearly identical LC8 binding sequences, preferentially bind to one isoform over the other [76–78]. While detailed biochemical studies demonstrated that both LC8 isoforms bound to peptides derived from Bmf with equal affinity, *in vivo* assays demonstrated that the exogenous expression of the His41→Tyr LC8 mutant in HEK-293 cells redirected the first LC8 isoform (DYNLL1) to myosin. The exogenous expression of the complementary mutation in the second isoform encoding the Tyr41→His mutation redirects this mutant isoform to dynein [76]. The origin of this differential localization remains unclear and should be reconfirmed in other cell lines;

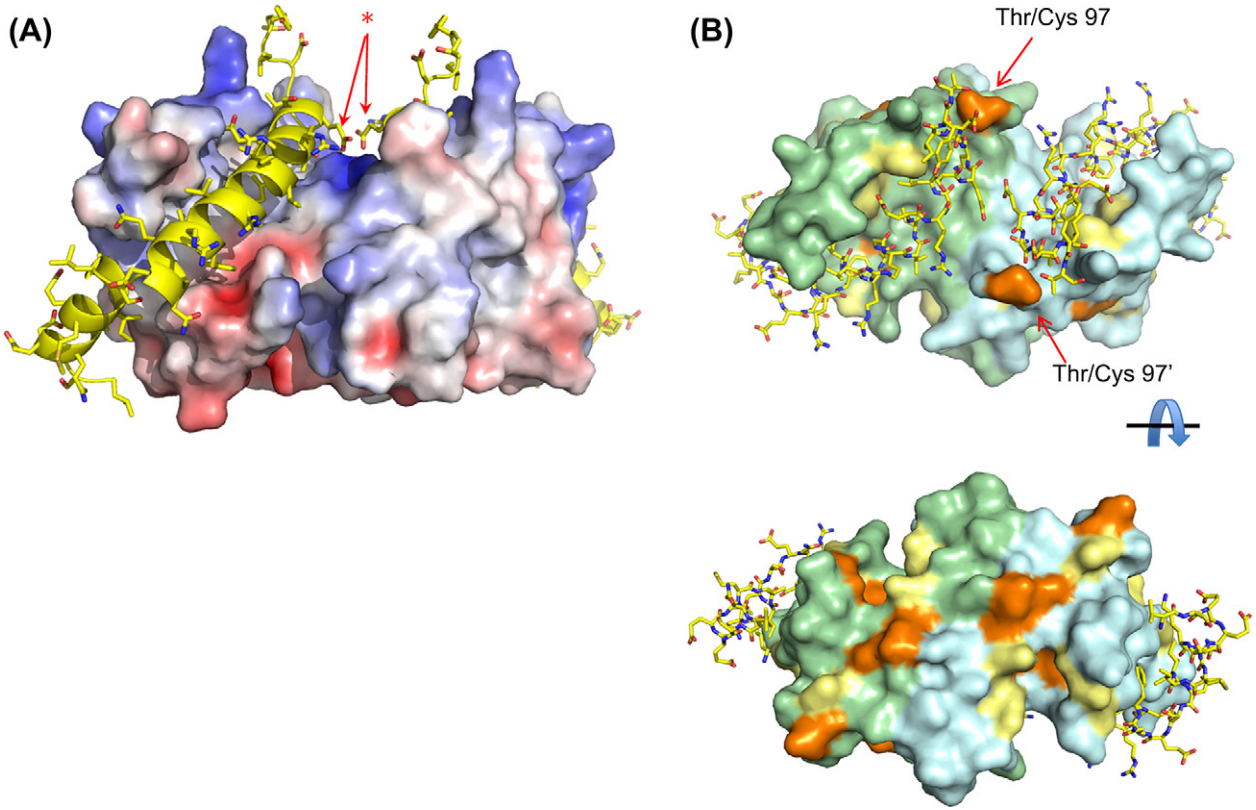

Figure 5.4 Promiscuous ligand binding. Cross-sections of Tctex1 and LC8 show the IC (yellow) binds to the swapped strand β3 (cyan) of Tctex1 (A) and LC8 (B), primarily through backbone hydrogen bonds (black dashes). Important side-chain interactions are also highlighted. (C) The IC fragment that binds to LC7 encodes a large number of hydrophobic groups along one face of the α-helix. At the C-terminal end, the IC makes several side-chain interactions (boxed region). An extended hydrogen bond/salt bridge network (red dashes) is shown in stereo (D). Sequence alignment of the human cytoplasmic and axonemal dynein ICs indicates that axonemal IC1 encodes similar residues that form the extended side-chain network and encodes hydrophobic residues at many of the same sites as cytoplasmic IC. Thus, axonemal IC1 likely binds LC7. However, axonemal IC2 differs significantly at these sites.

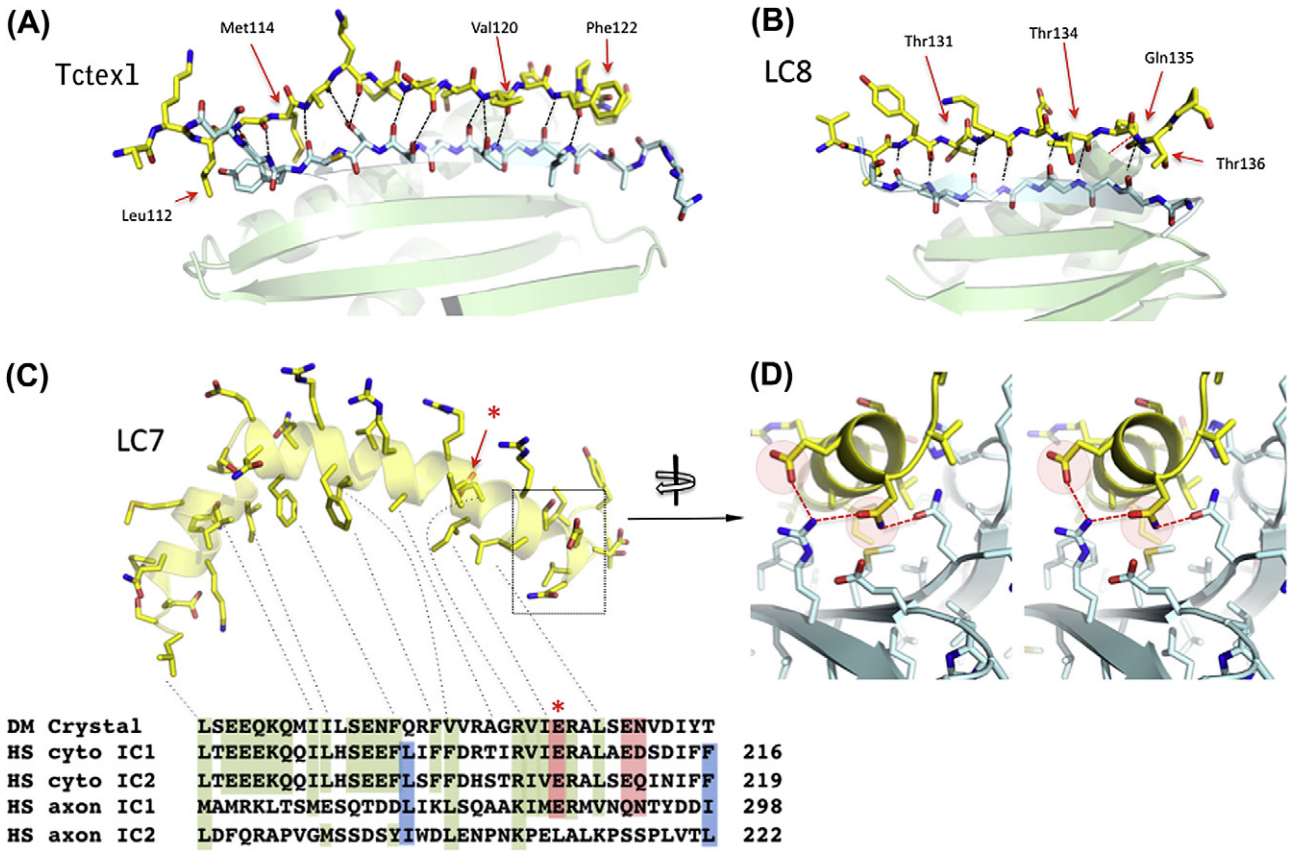

Figure 5.5 Liganded LC7. (A) The IC peptide (yellow) is shown on the electrostatic surface of LC7. Note that the IC—LC7 occurs predominantly through side-chain interactions and is distinctly different from the IC and Tctex1 or LC8 interfaces. (B) Differences between LC7 isoforms. There are several minor sequence differences lining the IC binding site on LC7. Highlighted is residue 97, which is either a threonine or a cysteine. The side chain does not contact the IC peptide; however, oxidation of the sulfhydral group could affect ligand binding. Otherwise, the remaining differences are located on the opposite surface of the IC binding site.

however, these findings suggest that additional cellular factors are required for this differential localization [76].

In addition, the first five residues of LC8 are disordered and not visible in the electron density maps; however, the second residue in this disordered region also differs between the two isoforms. Specifically, the first isoform (DYNLL1) encodes a cysteine and the second isoform (DYNLL2) encodes a serine. The cysteine isoform of LC8 was shown to bind to IκBα [79] and inhibit its phosphorylation by IKK through a redox mechanism [80,81]. Trp14, a novel disulfide reductase, was shown to reduce DYNLL1 through disulfide trapping experiments [80,81]. Furthermore, the depletion of Trp14 or LC8 by siRNA was shown to interfere with TNFα-induced NFκB activation. Collectively, these results suggest that binding activity of the DYNLL1 isoform is regulated in part by the redox state of the cell [82].

The differences in Tctex1 and RP3 appear to be more significant and may affect ligand selection. While both isoforms bind to the dynein IC, Tctex1, but not RP3, binds to the PTH receptor [72]. In addition, RP3, but not Tctex1, was demonstrated to bind to and modulate the activity of the nuclear matrix-associated protein SATB1 [83]. This differential binding may be explained by substitutions at residues 74 and 75, where glycine and alanine in Tctex1 are substituted by alanine and tyrosine in RP3. In addition, the flanking helices also show a number of differences. These could affect Tctex1/RP3 distributions in a similar manner to that observed in the LC8 isoforms [76]. Finally, Tctex1 and RP3 have been demonstrated to form heterodimers, although these heterodimers were not capable of binding to the dynein IC [84]. Currently no structural data is available for RP3; such data may help to elucidate the isoform-specific binding properties.

Lastly, while the differential expression of LC7 has been associated with hepatocellular carcinoma, there are no significant substitutions between the LC7 isoforms that should strongly affect IC binding. The second isoform of LC7, DYNLRB2, encodes a cysteine located at the C-terminus, residue 97. Oxidation of this cysteine could affect its interaction with the IC (Fig. 5.5). Many of the remaining sequence differences in LC7 map to the opposite surface, formed in part by the antiparallel α-helix bundle (Fig. 5.5), suggesting that this surface interacts with TGFβ or Rab6. Reversion of these surface residues to the other isoform followed by *in vivo* assays could provide insight into both cellular and isoform-specific functions of LC7.

5.7 Mammalian Dynein Intermediate Chains

There are six dynein IC homologs identified in the human genome IC [24]. Four, including DNAI1 and DNAI2, are associated with axenomal dynein. The other two, DYNC1I1 (IC1) and DYNC1I2 (IC2), are associated with cytoplasmic dynein. Of the

two cytoplasmic dynein ICs, there are two splice variants for each, both occurring at essentially equivalent positions. Of these, the IC2 isoform C (the shortest isoform) is ubiquitously expressed. The remaining isoforms are primarily expressed in brain tissues [85]. All IC homologs encode a C-terminal WD domain (amino acids ~220–580; around two-thirds of molecules located at the C-terminus) that has been demonstrated to bind to the dynein HC [86]. In addition, secondary structure prediction algorithms predict short α-helices immediately before and after the WD domain of each IC [87] (Fig. 5.6).

The N-termini of the ICs, however, differ significantly between the cytoplasmic and axonemal IC isoforms. Specifically, the first 42 residues of both cytoplasmic ICs are highly charged (17 lysines and arginines and 12 aspartates and glutamates in the first 44 residues of rat IC). This region is also strongly predicted to form a coiled coil and has been demonstrated by multiple groups to interact with dynactin, a critical multi-subunit complex that is essential for many of the functions of cytoplasmic dynein (see Chapter 19) [6,88–90]. Immediately following this stretch is a disordered region that is rich in proline and serine residues. Several of these serines have been shown to be phosphorylated in a cell-cycle-dependent manner [91,92]. In addition, the splice sites for both cytoplasmic ICs in mammals are located in this region. Immediately following this serine- and proline-rich stretch is the binding site of the LCs Tctex1 and LC8 (residues 112 to 138 – numbering based on Rat IC2 isoform C). The LC7 binding site (residues 182 to 218) follows a short acidic stretch. Immediately following the LC7 site is the WD domain.

The N-termini of the axonemal IC isoforms not only differ significantly from cytoplasmic dynein ICs but also differ significantly between themselves. Using Jpred3 to predict secondary structure [87] and RONN to predict disorder [93], the first 90 residues of axonemal IC2 (e.g. DNAI2) encode a significant number of β-strands and show little disorder, suggesting that the domain is folded. Similar predictions of the N-terminus of axonemal IC1 (e.g. DNAI1) show that the N-terminus is largely disordered, with the exception of a small region – residues 55 to 130 – that contains a mix of predicted α-helices and β-strands. As noted above, the extreme N-terminus of cytoplasmic dynein IC specifically binds to dynactin and is critical to many of the cytoplasmic dynein functions. By analogy, differences in secondary structure of the N-termini of each axonemal IC isoform suggest that each interacts with a different macromolecule and likely acts in different processes.

The precise position of the LC binding sites within mammalian axonemal ICs remains undetermined. There are several sites within the axonemal ICs that could potentially bind to LC8. For instance, searching the human DNAI1 coding sequence for all glutamines immediately surrounded by threonine, valine, or isoleucine and within a disordered region produces several hits including 207-RDRECQT-213. Using similar criteria for human DNAI2, several

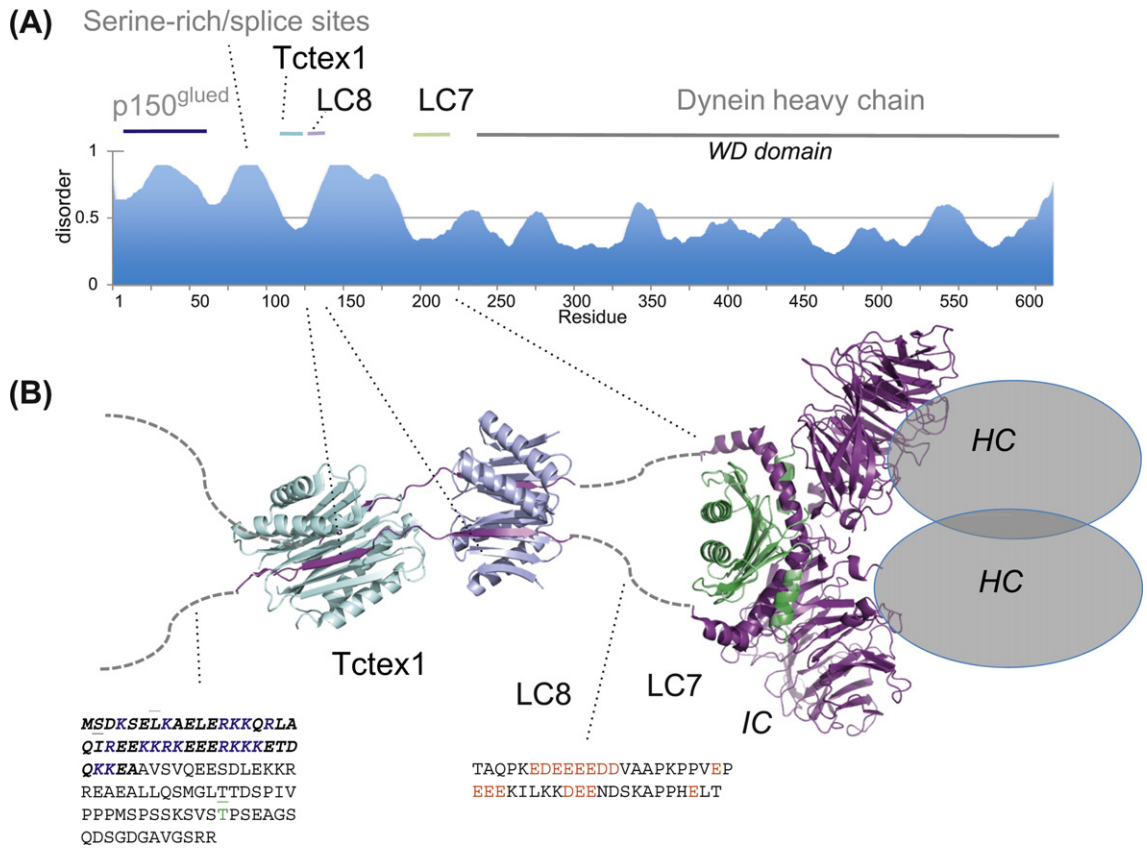

Figure 5.6 Model of the cytoplasmic IC–LC complex. (A) The binding sites of the LCs, p150^{Glued}, and the HC domain are shown above the predicted disorder of cytoplasmic dynein IC2. The first 180 residues of the IC are predicted to be disordered (e.g. values above 0.5). Of interest, this region encodes the binding sites of the LCs LC8 and Tctex1, as well as p150^{Glued}. This region also contains the serine-rich region, which has been shown to be phosphorylated in a cell-dependent manner. (B) The structures of the IC (purple) bound to Tctex1 (cyan) and LC8 (light blue) (2PG1.pdb) and the IC bound to LC7 (green) (3L9K.pdb) were combined with the WD domain of Rbbp4 (purple) (3GFC.pdb) to produce a spatial model of the LC–IC complex. The IC α-helix was manually superimposed on the N-terminal helix preceding the WD domain of Rbb4. The position of the Tcex1 and LC8 with respect to LC7 and the WD domains is not known, but likely constrained through the dimer of dimers. The position of the HC with respect to the WD domains is based on peptide–WD domain complexes but is also tentative. Also shown are the amino acid sequences of IC N-terminus and the region between the LC8 and LC7 binding sites. The predicted coiled-coil region and the p150^{Glued} binding site at the N-terminus are highlighted in bold italics. The phosphorylation site T89< is highlighted in green. AUC, CD, and NMR studies indicate that the first 112 residues are disordered and do not dimerize. Consequently, these are depicted as random coils.

potential sites have been identified, including 47-VDTGIQCS-54. On the other hand, without a clear canonical sequence it is difficult to identify a Tctex1 binding site. Finally, using the secondary structure prediction and the cytoplasmic IC-LC7 structure (Fig. 5.4), it appears that DNAI1, but not DNAI2, encodes an LC7 binding site. Specifically, many of the hydrophobic residues in DNAI1 closely match the hydrophobic residues in the cytoplasmic IC sequences. The same region in DNAI2, however, encodes a number of proline residues that should destablize the formation of an α-helix (Fig. 5.4). While there have been inroads made in understanding cytoplasmic dynein, there is a significant lack of structural data for axonemal dynein, especially concerning mammalian axonemal dynein.

5.8 Molecular Model of the Light Chain–Intermediate Chain Structure

With the structures of Tctex1, LC8, and LC7 bound to their respective fragments of the dynein IC, it is possible to generate a plausible model of the cytoplasmic IC–LC complex. At the C-terminus, a number of the WD domains deposited in the protein database (PDB) encode an N-terminal and C-terminal helix, which is similar to what is predicted from the primary sequences of the dynein IC. A BLAST search [94] using the rat cytoplasmic IC2C sequence and the PDB indentified the WD domain of histone-binding protein, Rbbp4 (3GFC.pdb), as a close structural homolog. It is 43% similar to the IC WD domain over residues 307 to 534. Moreover, the "sequence register" of the N-terminal helix of Rbbp4 with respect to the WD domain closely matches the sequence register of the IC α-helix that binds to LC7. Superposition of the N-terminal α-helix of Rbbp4 domain to each α-helix of the ICs that is bound to LC7 affords a model with minimal steric clashes and no overlap between the WD domains. The relative orientation of the two β-propeller domains also appears to be well-positioned to bind to the dimeric dynein HC (Fig. 5.6).

At the N-terminus of the cytoplasmic ICs, the crystal structure of the co-complex of Tctex1, LC8, and the IC shows that ICs bind as extended strands along each LC binding site in a parallel manner [14]. The remaining N-terminal region of the ICs, residues 1 to 111 and 138 to 214, are predicted to be disordered and are highly, but oppositely, charged. The isoelectric point of the IC fragment that binds to dynactin, residues 1–44, is 10.5, whereas the isoelectric point of the region between the LC8 binding site and the LC7 binding site, residues 138 to 182, is 3.9. This observation suggests that their potential interaction with other cellular components will be dominated by electrostatic interactions. While the IC–LC8–Tctex1 complex also indicates that there is no contact between LC8 and Tctex1 LCs, their position in the middle of a highly disordered region suggests that they restrict the conformation and/or radius of gyration of the IC, potentially

enhancing the apparent affinity of potential targets binding to these disordered regions (e.g. $p150^{Glued}$ – see Section 5.10).

5.9 Light Chains and Cargo

The observation that LC8 and Tctex1 bind to a large number of proteins led to the hypothesis that they act as adaptors to bind cargo to the dynein motor complex [13,95]. This hypothesis was partially bolstered by the observation that, in mammals, there is essentially one cytoplasmic dynein [96]. Thus, it was hypothesized that different combinations of the promiscuous LCs could potentially expand the repertoire of cargo that required retrograde transport. As structural data became available, the validity of this model became suspect. Specifically, each characterized cargo peptide binds in precisely the same groove as the IC peptide (demonstrated for LC8). However, since the homodimeric LCs encode two binding surfaces, it is possible to envision a model where one interface binds to the IC and the other binds to the cargo peptide.

There are, however, compelling thermodynamic arguments against this model. First, the cytoplasmic dynein motor complex is composed of homodimeric subunits. The dynein HC is homodimeric through its N-terminal domain [86], and this region acts as a scaffold for the dynein IC and LICs [97]. In turn, these chains are either dimeric in and of themselves or dimeric through their association with the dynein HC. As a consequence, the dimeric ICs can act as a bivalent ligand for the bivalent LCs. Bivalent–bivalent interactions afford energy additivity and higher apparent affinities. Specifically, the free energy at each site can be added modulated by a "linkage" term [98,99]. Mathematically, $\Delta G_{Total} = \Delta G_1 + \Delta G_2 + \Delta G_{linker}$. While the contribution of the linker invariably counteracts energy additivity, in the case where it is negligible ($\Delta G_{linker} = 0$) the binding constants of each interaction are multiplicative (e.g., $-RT \ln (k_{total}) = -RT \ln (k_{total}) - RT \ln (k_{total})$, which simplifies to $k_{total} = k_1 k_2$). A powerful example of this principle, demonstrated by the Whitesides group, shows that coupling vancomycin and D-Ala-D-Ala to trimeric scaffolds dramatically reduces the dissociation constant of the monomeric interaction from $\sim 10^{-6}$ M to $\sim 10^{-17}$ M [100], which far exceeds the dissociation constant of biotin and avidin. While geometric and entropic effects of the linker interfere with simple multiplication of the individual affinities, modest but significant gains in the apparent affinity are observed in most cases [98].

Enhanced affinity due to multivalency has been observed for LC8 and Tctex1 [14,101]. First, SUPREX studies, a mass spectrometry method that follows hydrogen-deuterium exchange and extracts thermodynamic information, showed substantial gains in the stability of LC8 in the presence of an IC peptide encoding both LC8 and Tctex1, pre-bound to Tctex1. These original experiments have been independently verified [102]. The affinity for the LC8 binding peptide

derived from the IC is ~10 mM for a single site on LC8. The affinity of an "optimal" dimer of this peptide for LC8 would be 100 pM (e.g. 10^{-5} M × 10^{-5} M). A peptide that encodes tandem LC8 binding sites afforded a 1000-fold increase in the apparent affinity for LC8 compared to a peptide with a single LC8 binding site [102].

Second, molecular traps developed to determine the effect of LC8 and Tctex1 on dynein *in vivo* were developed based on this additivity principle [101]. Specifically, peptide fragments based on the LC8 binding site or Tctex1 binding site of the dynein IC were fused to FKBP. Dimerization of FKBP using the small molecule AP20187 [103] dramatically enhanced the weak affinity of the monomeric LC binding peptides, producing high-affinity, bivalent "receptors" or traps for the LCs [101]. The expression of these traps *in vivo* did not produce significant defects associated with acute dynein inhibition (which would be expected for the bridging model). The addition of AP20187 to cells expressing these traps, however, led to rapid endosome and lysosome dispersion, presumably by sequestering the LCs from endogenous dynein. These observations reinforce the proposal that bivalent—bivalent interactions out-compete trivalent interactions.

Lastly, nearly all characterized proteins that bind to the LCs LC8 or Tctex1 are dimeric (see Tables 5.1 and 5.2) [14]. Thus, the interaction of these LC binding proteins with their respective LCs (LC8 or Tctex1) is also likely to be exclusive, or dynein independent. In fact, replacing the LC8 binding region in Pak1 with FKBP and using AP20187 to dimerize Pak1 permitted rapid nuclear localization of Pak1 [104]. In other words, dimerization of Pak1, mediated by LC8, is required for its nuclear import. In this sense, LC8 has recently been described as a dimerization hub [105]. However, this term must be used carefully. The LC8 binding partner must be dimeric or encode a region that will dimerize after sufficiently high concentrations are achieved to saturate both LC8 binding sites [106], otherwise energy additivity is lost. Thus, it is more accurate to consider the LCs as allosteric effectors. Regardless, these data strongly argue against the original cargo or bridging models.

5.10 Post-Translational Modifications

Post-translational modification of the LCs and/or ICs by phosphorylation, ubiquination, and so on is a potential means to regulate their interaction with targeted proteins. While sumoylation, acetylation, and other modifications have not been reported for the LCs or ICs, phosphorylation has been reported for each LC and the ICs.

Interest in the phosphorylation of LC8 stems from a recent report indicating that Pak1 binds to and phosphorylates Ser88 and plays an important role in breast

cancer [30]. As noted earlier, LC8 bearing the phosphomimic Ser88→Glu or Ser88→Asp is monomeric and fails to bind IC peptides encoding the LC8 binding site. However, careful examination of the LC8 structure indicates that Ser88, part of strand β5, is buried at the dimer interface. As such, it is sterically occluded from the kinase. Moreover, analytical ultracentrifugation [46] and NMR [107] studies indicate that LC8 is a relatively tight dimer ($K_D < 50$ nM).While wildtype LC8 could not be phosphorylated by Pak1 in *in vitro* assays using purified reagents, phosphorylation was observed using a his-tagged LC8 encoding a thrombin cleavage site [46]. The thrombin cleavage site, coincidentally, closely matches the canonical Pak1 phosphorylation consensus sequence. Thus, the inclusion of tags for immunochemistry and purification can lead to false positives and may account for the original observation that LC8 can be phosphorylated.

Tctex1 and LC7 have also been proposed to be phosphorylated *in vivo* [69,83,108]. In each case these sites are remote from the peptide-binding interface. Moreover, a number of these reported sites are located in ordered secondary structure elements, analogous to Ser88 in LC8. Recently, it has been shown that the majority of well-characterized phosphorylation sites are located within intrinsically disordered regions [109]. In fact, no phosphorylation sites were identified when applying a disorder-enhanced phosphorylation site prediction algorithm to each LC sequence [109]. While these sites may very well be bona fide kinase targets, they remain tenuous without further investigation.

Phosphorylation of cytoplasmic dynein ICs in a cell-cycle-dependent manner has also been reported. In these studies, phosphorylation of Ser84 was found to block $p150^{Glued}$ binding using blot overlay assays [92]. However, a separate study demonstrated that phosphorylation of Ser84 does not affect the dynein–dynactin interaction [110]. This latter study is also consistent with our biophysical studies, which indicate that a fragment containing residues 1 to 44 of the IC is sufficient to bind to $p150^{Glued}$ (A. E. Siglin and J. C. Williams, unpublished data). Rather than physically blocking dynactin binding, it is possible that phosphorylation of this site creates a binding site for a separate protein and this interaction effectively decouples the IC from $p150^{Glued}$. Recent studies support this notion [91].

Of note, a number of sites at the N-terminus of both cytoplasmic ICs were identified using the same disorder-enhanced phosphorylation site prediction algorithm, including Ser84 and Thr89 [109].

5.11 The Roles of LC8 and Tctex1 on Dynein

In the absence of a "bridging model," the role of the LCs on dynein function remains unresolved; however, there are several alternative hypotheses [84]. First, it is possible that the LCs are required for the assembly of the dynein complex. As shown in Figure 5.6, the use of different LCs would ensure the

register of the IC, enforce a parallel architecture, and lead to the efficient binding of the dimeric HC through the WD domains. This is supported in part by the observation that treatment of purified cytoplasmic dynein with potassium iodide produces two distinct fractions, one containing the dynein HC and LICs and the other containing the ICs and LCs [18]. Moreover, in Chlamydomonas, the LCs have been observed to bind to axonemal ICs [111,112]. Collectively, these data support the notion that the LCs are necessary for the assembly of the dynein complex.

A second potential role for the LCs is to modulate the phosphorylation of the sequences encoded by LC binding proteins. For instance, Thr56 located within the LC8 binding site on BimL/EL, *DKSTQTSP*, has been shown to be phosphorylated by JNK kinase [113]. Phosphorylation of this site was demonstrated to abrogate LC8 binding and to increase apoptotic activity [113]. Likewise, Cdk5, Erk2, and Cdc2 have been shown to phosphorylate Pak1 at Thr212, the residue that immediately precedes the LC8 binding site on Pak1 (212-TP*TRDVTSPI*). While the phosphomimic of the Pak1 LC8 binding site, T212E, still bound LC8 *in vitro* [46], it is possible that LC8 occupancy of these targets could sterically occlude the site to kinase activity. In this sense, LC8 could regulate the activity of these molecules; however, experimental evidence for this mechanism is still required. By analogy, Tctex1 could operate through a similar mechanism on its target proteins.

Lastly, LC occupancy could regulate the function of the dynein ICs. This hypothesis stems from several observations. First, the N-terminal region of the dynein IC is intrinsically disordered [114]. While the first ~42 residues are predicted to form a coiled coil, CD and NMR studies clearly indicate that it is unfolded [114] (A. E. Siglin and J. C. Williams, unpublished data). Disordered regions in other sytems have been shown recently to "fold" on their target [115]. Such interactions can be highly specific as the disordered region makes multiple contacts over an extended region of the target. A disordered-to-coiled-coil folding transition has been observed for the IC in the presence of dimeric $p150^{Glued}$, the principle dynactin subunit (A. E. Siglin and J. C. Williams, unpublished data). In addition, these disordered/order interactions are frequently of low affinity due to an entropic penalty of structuring an unfolded polypeptide [109]. However, both the dynein IC and dynactin $p150^{Glued}$ are dimeric under physiological conditions and the loss in binding affinity due to entropy should be compensated in part by bivalency. More importantly, the binding site for the LCs Tctex1 and LC8 is located in the middle of the disordered IC N-terminus, residues 112 to 138. By binding the IC at this point, the LCs can restrict the "radius of gyration" of the N-terminal 44 residues, which in turn can enhance the apparent affinity of the interaction. The dynein LC traps were initially designed to test this hypothesis [101]. Specifically, if LC8 and Tctex1 act as allosteric regulators of dynein function, sequestering the LCs from *preassembled* dynein (e.g. not possible with RNA interference (RNAi)) should produce defects commonly

associated with dynein interference (e.g. microinjection techniques). Such effects were observed. As noted, chemically induced dimerization of the LC8 or the Tctex1 traps expressed in Cos1 or Cos7 cells produced rapid endosome and lysosome dispersion [101], consistent with the reduction of the IC-p150^{Glued} interaction.

Finally, it was observed that the affinity for LC7 was not significantly enhanced using an IC preassembled with Tctex1 and LC8 compared to the same IC construct without the LCs [53]. The three-fold difference suggests that the slight increase in affinity is due to local concentration effects as opposed to energy additivity. In other words, Tctex1 and LC8 appear to act independently of LC7. This observation also points to a regulatory role for LC8 and Tctex1 and an assembly role for LC7.

Collectively, these examples are consistent with the hypothesis that LC occupancy of the cytoplasmic IC affects p150^{Glued} binding. These investigations also suggest a different model for retrograde transport of critical macromolecules that addresses the lack of multiple members in the cytoplasmic dynein family. Specifically, it is possible to locally sort macromolecules into vesicles, load these vesicles onto dynactin, and use dynein to carry these vesicles along microtubules. This mitigates conceptual issues of using one cytoplasmic dynein to transport one molecule (e.g. TrkA bridge to the IC through Tctex1). In this sense, this model is very similar to conventional cargo transport where dynein is the tractor and dynactin is the trailer. Evidence supporting such a model is beginning to appear [116–118].

5.12 Summary

Structural investigations of the LCs, initially performed to understand their role in the context of the cytoplasmic dynein, have met their mark. These investigations provide compelling evidence that the LCs do not bridge cargo to cytoplasmic dynein, but rather play important roles in the assembly of the dynein complex (e.g. LC7) and potentially in the regulation of the N-terminus of cytoplasmic dynein IC (e.g. LC8 and Tctex1). Currently, less than ~10% of the cytoplasmic dynein complex and even less of axonemal dynein complexes has been structurally characterized. Clearly, there is much left to be done.

References

[1] R.B. Vallee, J.C. Williams, D. Varma, L.E. Barnhart, Dynein: An ancient motor protein involved in multiple modes of transport, J. Neurobiol. 58 (2004) 189–200.
[2] A.R. Kini, C.A. Collins, Modulation of cytoplasmic dynein ATPase activity by the accessory subunits, Cell Motil. Cytoskeleton 48 (2001) 52–60.
[3] R.J. McKenney, M. Vershinin, A. Kunwar, R.B. Vallee, S.P. Gross, LIS1 and NudE induce a persistent dynein force-producing state, Cell 141 (2010) 304–314.

[4] S.M. King, The dynein microtubule motor, Biochim. Biophys. Acta. 1496 (2000) 60–75.
[5] K.T. Vaughan, E.L. Holzbaur, R.B. Vallee, Subcellular targeting of the retrograde motor cytoplasmic dynein, Biochem. Soc. Trans. 23 (1995) 50–54.
[6] S. Karki, E.L. Holzbaur, Affinity chromatography demonstrates a direct binding between cytoplasmic dynein and the dynactin complex, J. Biol. Chem. 270 (1995) 28 806–28 811.
[7] A. Purohit, S.H. Tynan, R. Vallee, S.J. Doxsey, Direct interaction of pericentrin with cytoplasmic dynein light intermediate chain contributes to mitotic spindle organization, J. Cell. Biol. 147 (1999) 481–492.
[8] I. Rodriguez-Crespo, B. Yelamos, F. Roncal, J.P. Albar, P.R. Ortiz de Montellano, F. Gavilanes, Identification of novel cellular proteins that bind to the LC8 dynein light chain using a pepscan technique, FEBS Lett. 503 (2001) 135–141.
[9] H. Yano, F.S. Lee, H. Kong, J. Chuang, J. Arevalo, P. Perez, C. Sung, M.V. Chao, Association of Trk neurotrophin receptors with components of the cytoplasmic dynein motor, J. Neurosci. 21 (2001) RC125.
[10] R.P. Herzig, U. Andersson, R.C. Scarpulla, Dynein light chain interacts with NRF-1 and EWG, structurally and functionally related transcription factors from humans and drosophila, J. Cell Sci. 113 (Pt 23) (2000) 4263–4273.
[11] R.D. Vale, The molecular motor toolbox for intracellular transport, Cell. 112 (2003) 467–480.
[12] K.K. Pfister, P.R. Shah, H. Hummerich, A. Russ, J. Cotton, A.A. Annuar, S.M. King, E.M. Fisher, Genetic analysis of the cytoplasmic dynein subunit families, PLoS Genet. 2 (2006) e1.
[13] S.J. King, M. Bonilla, M.E. Rodgers, T.A. Schroer, Subunit organization in cytoplasmic dynein subcomplexes, Protein Sci. 11 (2002) 1239–1250.
[14] J.C. Williams, P.L. Roulhac, A.G. Roy, R.B. Vallee, M.C. Fitzgerald, W.A. Hendrickson, Structural and thermodynamic characterization of a cytoplasmic dynein light chain-intermediate chain complex, Proc. Natl. Acad. Sci. USA 104 (2007) 10 028–10 033.
[15] C.W. Bell, E. Fronk, I.R. Gibbons, Polypeptide subunits of dynein 1 from sea urchin sperm flagella, J. Supramol. Struct. 11 (1979) 311–317.
[16] K.K. Pfister, R.B. Fay, G.B. Witman, Purification and polypeptide composition of dynein ATPases from *Chlamydomonas* flagella, Cell Motil. 2 (1982) 525–547.
[17] R.B. Vallee, S.E. Davis, Low molecular weight microtubule associated proteins are light chains of MAP 1, Proc. Natl. Acad. Sci. USA 80 (1983) 1342–1346.
[18] S.R. Gill, D.W. Cleveland, T.A. Schroer, Characterization of DLC-A and DLC-B, two families of cytoplasmic dynein light chain subunits, Mol. Biol. Cell 5 (1994) 645–654.
[19] S.M. King, J.F. Dillman 3rd, S.E. Benashski, R.J. Lye, R.S. Patel-King, K.K. Pfister, The mouse t-complex-encoded protein Tctex-1 is a light chain of brain cytoplasmic dynein, J. Biol. Chem. 271 (1996) 32 281–32 287.
[20] S.M. King, R.S. Patel-King, The $M_r = 8{,}000$ and 11,000 outer arm dynein light chains from *Chlamydomonas* flagella have cytoplasmic homologues, J. Biol. Chem. 270 (1995) 11445–11452.
[21] A.B. Bowman, R.S. Patel-King, S.E. Benashski, J.M. McCaffery, L.S. Goldstein, S.M. King, Drosophila roadblock and Chlamydomonas LC7: A conserved family of dynein-associated proteins involved in axonal transport, flagellar motility, and mitosis, J. Cell Biol. 146 (1999) 165–180.
[22] K.K. Pfister, G.B. Witman, Subfractionation of *Chlamydomonas* 18 S dynein into two unique subunits containing ATPase activity, J. Biol. Chem. 259 (1984) 12072–12080.
[23] S.M. King, E. Barbarese, J.F. Dillman 3rd, R.S. Patel-King, J.H. Carson, K.K. Pfister, Brain cytoplasmic and flagellar outer arm dyneins share a highly conserved Mr 8,000 light chain, J. Biol. Chem. 271 (1996) 19 358–19 366.
[24] B. Wickstead, K. Gull, Dyneins across eukaryotes: A comparative genomic analysis, Traffic 8 (2007) 1708–1721.

[25] T. Dick, K. Ray, H.K. Salz, W. Chia, Cytoplasmic dynein (ddlc1) mutations cause morphogenetic defects and apoptotic cell death in *Drosophila melanogaster*, Mol. Cell Biol. 16 (1996) 1966–1977.
[26] R. Phillis, D. Statton, P. Caruccio, R.K. Murphey, Mutations in the 8 kDa dynein light chain gene disrupt sensory axon projections in the Drosophila imaginal CNS, Development 122 (1996) 2955–2963.
[27] B. Liu, X. Xiang, Y.R. Lee, The requirement of the LC8 dynein light chain for nuclear migration and septum positioning is temperature dependent in *Aspergillus nidulans*, Mol. Microbiol. 47 (2003) 291–301.
[28] P. Gonczy, C. Echeverri, K. Oegema, A. Coulson, S.J. Jones, R.R. Copley, J. Duperon, J. Oegema, M. Brehm, E. Cassin, E. Hannak, M. Kirkham, S. Pichler, K. Flohrs, A. Goessen, S. Leidel, A.M. Alleaume, C. Martin, N. Ozlu, P. Bork, A.A. Hyman, Functional genomic analysis of cell division in *C. elegans* using RNAi of genes on chromosome III, Nature 408 (2000) 331–336.
[29] G.S. Tan, M.A. Preuss, J.C. Williams, M.J. Schnell, The dynein light chain 8 binding motif of rabies virus phosphoprotein promotes efficient viral transcription, Proc. Natl. Acad. Sci. USA 104 (2007) 7229–7234.
[30] R.K. Vadlamudi, R. Bagheri-Yarmand, Z. Yang, S. Balasenthil, D. Nguyen, A.A. Sahin, P. den Hollander, R. Kumar, Dynein light chain 1, a p21-activated kinase 1-interacting substrate, promotes cancerous phenotypes, Cancer Cell 5 (2004) 575–585.
[31] Y. Jacob, H. Badrane, P.E. Ceccaldi, N. Tordo, Cytoplasmic dynein LC8 interacts with lyssavirus phosphoprotein, J. Virol. 74 (2000) 10 217–10 222.
[32] Y.W. Chang, R. Jakobi, A. McGinty, M. Foschi, M.J. Dunn, A. Sorokin, Cyclo-oxygenase 2 promotes cell survival by stimulation of dynein light chain expression and inhibition of neuronal nitric oxide synthase activity, Mol. Cell Biol. 20 (2000) 8571–8579.
[33] Y. Batlevi, D.N. Martin, U.B. Pandey, C.R. Simon, C.M. Powers, J.P. Taylor, E.H. Baehrecke, Dynein light chain 1 is required for autophagy, protein clearance, and cell death in Drosophila, Proc. Natl. Acad. Sci. USA 107 (2010) 742–747.
[34] E. Lader, H.S. Ha, M. O'Neill, K. Artzt, D. Bennett, Tctex-1: A candidate gene family for a mouse t complex sterility locus, Cell 58 (1989) 969–979.
[35] M.G. Li, M. Serr, E.A. Newman, T.S. Hays, The Drosophila tctex-1 light chain is dispensable for essential cytoplasmic dynein functions but is required during spermatid differentiation, Mol. Biol. Cell 15 (2004) 3005–3014.
[36] J. Vlach, J. Lipov, M. Rumlova, V. Veverka, J. Lang, P. Srb, Z. Knejzlik, I. Pichova, E. Hunter, R. Hrabal, T. Ruml, D-retrovirus morphogenetic switch driven by the targeting signal accessibility to Tctex-1 of dynein, Proc. Natl. Acad. Sci. USA 105 (2008) 10 565–10 570.
[37] K.J. Palmer, H. Hughes, D.J. Stephens, Specificity of cytoplasmic dynein subunits in discrete membrane trafficking steps, Mol. Biol. Cell. 20 (2009) 2809.
[38] J. Jiang, L. Yu, X. Huang, X. Chen, D. Li, Y. Zhang, L. Tang, S. Zhao, Identification of two novel human dynein light chain genes, DNLC2A and DNLC2B, and their expression changes in hepatocellular carcinoma tissues from 68 Chinese patients, Gene 281 (2001) 103–113.
[39] W. Ding, Q. Tang, V. Espina, L.A. Liotta, D.T. Mauger, K.M. Mulder, A transforming growth factor-beta receptor-interacting protein frequently mutated in human ovarian cancer, Cancer Res. 65 (2005) 6526–6533.
[40] I.G. Campbell, W.A. Phillips, D.Y. Choong, Genetic and epigenetic analysis of the putative tumor suppressor km23 in primary ovarian, breast, and colorectal cancers, Clin. Cancer Res. 12 (2006) 3713–3715.
[41] H. Tochio, S. Ohki, Q. Zhang, M. Li, M. Zhang, Solution structure of a protein inhibitor of neuronal nitric oxide synthase, Nat. Struct. Biol. 5 (1998) 965–969.

[42] J.S. Fan, Q. Zhang, M. Li, H. Tochio, T. Yamazaki, M. Shimizu, M. Zhang, Protein inhibitor of neuronal nitric-oxide synthase, PIN, binds to a 17-amino acid residue fragment of the enzyme, J. Biol. Chem. 273 (1998) 33 472–33 481.
[43] J. Liang, S.R. Jaffrey, W. Guo, S.H. Snyder, J. Clardy, Structure of the PIN/LC8 dimer with a bound peptide, Nat. Struct. Biol. 6 (1999) 735–740.
[44] A. Nyarko, L. Cochrun, S. Norwood, N. Pursifull, A. Voth, E. Barbar, Ionization of His 55 at the dimer interface of dynein light-chain LC8 is coupled to dimer dissociation, Biochemistry 44 (2005) 14 248–14 255.
[45] Y. Song, G. Benison, A. Nyarko, T.S. Hays, E. Barbar, Potential role for phosphorylation in differential regulation of the assembly of dynein light chains, J. Biol. Chem. 282 (2007) 17 272–17 279.
[46] C.M. Lightcap, S. Sun, J.D. Lear, U. Rodeck, T. Polenova, J.C. Williams, Biochemical and structural characterization of the Pak1-LC8 interaction, J. Biol. Chem. 283 (2008) 27314–27324.
[47] C. Song, W. Wen, S.K. Rayala, M. Chen, J. Ma, M. Zhang, R. Kumar, Serine 88 phosphorylation of the 8-kDa dynein light chain 1 is a molecular switch for its dimerization status and functions, J. Biol. Chem. 283 (2008) 4004–4013.
[48] Y.K. Mok, K.W. Lo, M. Zhang, Structure of Tctex-1 and its interaction with cytoplasmic dynein intermediate chain, J. Biol. Chem. 276 (2001) 14067–14074.
[49] J.C. Williams, H. Xie, W.A. Hendrickson, Crystal structure of dynein light chain TcTex-1, J. Biol. Chem. 280 (2005) 21 981–21 986.
[50] H. Wu, M.W. Maciejewski, S. Takebe, S.M. King, Solution structure of the Tctex1 dimer reveals a mechanism for dynein-cargo interactions, Structure (Camb) 13 (2005) 213–223.
[51] M. Talbott, M. Hare, A. Nyarko, T.S. Hays, E. Barbar, Folding is coupled to dimerization of Tctex-1 dynein light chain, Biochemistry 45 (2006) 6793–6800.
[52] J. Song, R.C. Tyler, M.S. Lee, E.M. Tyler, J.L. Markley, Solution structure of isoform 1 of Roadblock/LC7, a light chain in the dynein complex, J. Mol. Biol. 354 (2005) 1043–1051.
[53] J. Hall, Y. Song, P.A. Karplus, E. Barbar, The crystal structure of dynein intermediate chain-light chain roadblock complex gives new insights into dynein assembly, J. Biol. Chem. 285 (2010) 22 566–22 575.
[54] E.V. Koonin, L. Aravind, Dynein light chains of the Roadblock/LC7 group belong to an ancient protein superfamily implicated in NTPase regulation, Curr. Biol. 10 (2000) R774–R776.
[55] J. Fan, Q. Zhang, H. Tochio, M. Li, M. Zhang, Structural basis of diverse sequence-dependent target recognition by the 8 kDa dynein light chain, J. Mol. Biol. 306 (2001) 97–108.
[56] F.S. Espindola, D.M. Suter, L.B. Partata, T. Cao, J.S. Wolenski, R.E. Cheney, S.M. King, M.S. Mooseker, The light chain composition of chicken brain myosin-Va: calmodulin, myosin-II essential light chains, and 8-kDa dynein light chain/PIN, Cell Motil. Cytoskeleton 47 (2000) 269–281.
[57] S. Naisbitt, J. Valtschanoff, D.W. Allison, C. Sala, E. Kim, A.M. Craig, R.J. Weinberg, M. Sheng, Interaction of the postsynaptic density-95/guanylate kinase domain-associated protein complex with a light chain of myosin-V and dynein, J. Neurosci. 20 (2000) 4524–4534.
[58] K.W. Lo, H.M. Kan, L.N. Chan, W.G. Xu, K.P. Wang, Z. Wu, M. Sheng, M. Zhang, The 8-kDa dynein light chain binds to p53-binding protein 1 and mediates DNA damage-induced p53 nuclear accumulation, J. Biol. Chem. 280 (2005) 8172–8179.
[59] R.D. Machado, N. Rudarakanchana, C. Atkinson, J.A. Flanagan, R. Harrison, N.W. Morrell, R.C. Trembath, Functional interaction between BMPR-II and Tctex-1, a light chain of dynein, is isoform-specific and disrupted by mutations underlying primary pulmonary hypertension, Hum. Mol. Genet. 12 (2003) 3277–3286.

[60] C. Schwarzer, S. Barnikol-Watanabe, F.P. Thinnes, N. Hilschmann, Voltage-dependent anion-selective channel (VDAC) interacts with the dynein light chain Tctex1 and the heat-shock protein PBP74, Int. J. Biochem. Cell Biol. 34 (2002) 1059–1070.
[61] A.W. Tai, J.Z. Chuang, C. Bode, U. Wolfrum, C.H. Sung, Rhodopsin's carboxy-terminal cytoplasmic tail acts as a membrane receptor for cytoplasmic dynein by binding to the dynein light chain Tctex-1, Cell 97 (1999) 877–887.
[62] F.J. Kaiser, K. Tavassoli, G.J. van den Bemd, G.T.G. Chang, B. Horsthemke, T. Moroy, H.J. Ludecke, Nuclear interaction of the dynein light chain LC8a with the TRPS1 transcription factor suppresses the transcriptional repression activity of TRPS1, Hum. Mol. Genet. 12 (2003) 1349–1358.
[63] F. Schnorrer, K. Bohmann, C. Nusslein-Volhard, The molecular motor dynein is involved in targeting Swallow and bicoid RNA to the anterior pole of Drosophila oocytes, Nat. Cell Biol. 2 (2000) 185–190.
[64] T.Y. Yeh, J.Z. Chuang, C.H. Sung, Dynein light chain rp3 acts as a nuclear matrix-associated transcriptional modulator in a dynein-independent pathway, J. Cell Sci. 118 (2005) 3431–3443.
[65] T. Kubota, M. Matsuoka, T.H. Chang, M. Bray, S. Jones, M. Tashiro, A. Kato, K. Ozato, Ebolavirus VP35 interacts with the cytoplasmic dynein light chain 8, J. Virol. 83 (2009) 6952–6956.
[66] C. Alonso, J. Miskin, B. Hernaez, P. Fernandez-Zapatero, L. Soto, C. Canto, I. Rodriguez-Crespo, L. Dixon, J.M. Escribano, African swine fever virus protein p54 interacts with the microtubular motor complex through direct binding to light-chain dynein, J. Virol. 75 (2001) 9819–9827.
[67] M.W. Douglas, R.J. Diefenbach, F.L. Homa, M. Miranda-Saksena, F.J. Rixon, V. Vittone, K. Byth, A.L. Cunningham, Herpes simplex virus type 1 capsid protein VP26 interacts with dynein light chains RP3 and Tctex1 and plays a role in retrograde cellular transport, J. Biol. Chem. 279 (2004) 28 522–28 530.
[68] M.A. Schneider, G.A. Spoden, L. Florin, C. Lambert, Identification of the dynein light chains required for human papillomavirus infection, Cell Microbiol. 13 (1) (2010) 32–46.
[69] Q. Tang, C.M. Staub, G. Gao, Q. Jin, Z. Wang, W. Ding, R.E. Aurigemma, K.M. Mulder, A novel transforming growth factor-beta receptor-interacting protein that is also a light chain of the motor protein dynein, Mol. Biol. Cell 13 (2002) 4484–4496.
[70] B. Wanschers, R. van de Vorstenbosch, M. Wijers, B. Wieringa, S.M. King, J. Fransen, Rab6 family proteins interact with the dynein light chain protein DYNLRB1, Cell Motil. Cytoskeleton 65 (2008) 183–196.
[71] G. Benison, P.A. Karplus, E. Barbar, Structure and dynamics of LC8 complexes with KXTQT-motif peptides: Swallow and dynein intermediate chain compete for a common site, J. Mol. Biol. 371 (2007) 457–468.
[72] M. Sugai, M. Saito, I. Sukegawa, Y. Katsushima, Y. Kinouchi, N. Nakahata, T. Shimosegawa, T. Yanagisawa, J. Sukegawa, PTH/PTH-related protein receptor interacts directly with Tctex-1 through its COOH terminus, Biochem. Biophys. Res. Commun. 311 (2003) 24–31.
[73] S. Mueller, X. Cao, R. Welker, E. Wimmer, Interaction of the poliovirus receptor CD155 with the dynein light chain Tctex-1 and its implication for poliovirus pathogenesis, J. Biol. Chem. 277 (2002) 7897–7904.
[74] F. Nagano, S. Orita, T. Sasaki, A. Naito, G. Sakaguchi, M. Maeda, T. Watanabe, E. Kominami, Y. Uchiyama, Y. Takai, Interaction of Doc2 with tctex-1, a light chain of cytoplasmic dynein. Implication in dynein-dependent vesicle transport, J. Biol. Chem. 273 (1998) 30 065–30 068.
[75] D.H. Fremont, M. Matsumura, E.A. Stura, P.A. Peterson, I.A. Wilson, Crystal structures of two viral peptides in complex with murine MHC class I H-2Kb, Science 257 (1992) 919–927.

[76] C.L. Day, H. Puthalakath, G. Skea, A. Strasser, I. Barsukov, L.Y. Lian, D.C. Huang, M.G. Hinds, Localization of dynein light chains 1 and 2 and their pro-apoptotic ligands, Biochem. J. 377 (2004) 597–605.
[77] H. Puthalakath, A. Villunger, L.A. O'Reilly, J.G. Beaumont, L. Coultas, R.E. Cheney, D.C. Huang, A. Strasser, Bmf: A proapoptotic BH3-only protein regulated by interaction with the myosin V actin motor complex, activated by anoikis, Science 293 (2001) 1829–1832.
[78] H. Puthalakath, D.C. Huang, L.A. O'Reilly, S.M. King, A. Strasser, The proapoptotic activity of the Bcl-2 family member Bim is regulated by interaction with the dynein motor complex, Mol. Cell 3 (1999) 287–296.
[79] P. Crepieux, H. Kwon, N. Leclerc, W. Spencer, S. Richard, R. Lin, J. Hiscott, I kappaB alpha physically interacts with a cytoskeleton-associated protein through its signal response domain, Mol. Cell Biol. 17 (1997) 7375–7385.
[80] W. Jeong, T.S. Chang, E.S. Boja, H.M. Fales, S.G. Rhee, Roles of TRP14, a thioredoxin-related protein in tumor necrosis factor-alpha signaling pathways, J. Biol. Chem. 279 (2004) 3151–3159.
[81] Y. Jung, H. Kim, S.H. Min, S.G. Rhee, W. Jeong, Dynein light chain LC8 negatively regulates NF-kappaB through the redox-dependent interaction with IkappaBalpha, J. Biol. Chem. 283 (2008) 23 863–23 871.
[82] S.M. King, Dynein-independent functions of DYNLL1/LC8: Redox state sensing and transcriptional control, Sci. Signal (2008). 1, pe51.
[83] T.Y. Yeh, D. Peretti, J.Z. Chuang, E. Rodriguez-Boulan, C.H. Sung, Regulatory dissociation of Tctex-1 light chain from dynein complex is essential for the apical delivery of rhodopsin, Traffic 7 (2006) 1495–1502.
[84] K.W. Lo, J.M. Kogoy, B.A. Rasoul, S.M. King, K.K. Pfister, Interaction of the DYNLT (TCTEX-1/RP3) light chains and the intermediate chains reveals novel intersubunit regulation during assembly of the dynein complex, J. Biol. Chem. 282 (2007) 36 871–36 878.
[85] S.J. Susalka, K.K. Pfister, Cytoplasmic dynein subunit heterogeneity: Implications for axonal transport, J. Neurocytol. 29 (2000) 819–829.
[86] S.H. Tynan, M.A. Gee, R.B. Vallee, Distinct but overlapping sites within the cytoplasmic dynein heavy chain for dimerization and for intermediate chain and light intermediate chain binding, J. Biol. Chem. 275 (2000) 32 769–32 774.
[87] C. Cole, J.D. Barber, G.J. Barton, The Jpred 3 secondary structure prediction server, Nucleic. Acids. Res. 36 (2008) W197–W201.
[88] K.T. Vaughan, R.B. Vallee, Cytoplasmic dynein binds dynactin through a direct interaction between the intermediate chains and $p150^{Glued}$, J. Cell. Biol. 131 (1995) 1507–1516.
[89] K.T. Vaughan, S.H. Tynan, N.E. Faulkner, C.J. Echeverri, R.B. Vallee, Analysis of $p150^{Glued}$ as the cytoplasmic dynein-binding component of dynactin: Evidence for colocalization with CLIP-170 at microtubule distal-ends, Mol. Biol. Cell 7 (1996) 403a.
[90] C.M. Waterman-Storer, S. Karki, E.L.F. Holzbaur, The $p150^{Glued}$ component of the dynactin complex binds to both microtubules and the actin-related protein centractin (Arp-1), Proc. Natl. Acad. Sci. USA 92 (1995) 1634–1638.
[91] J. Whyte, J.R. Bader, S.B. Tauhata, M. Raycroft, J. Hornick, K.K. Pfister, W.S. Lane, G.K. Chan, E.H. Hinchcliffe, P.S. Vaughan, K.T. Vaughan, Phosphorylation regulates targeting of cytoplasmic dynein to kinetochores during mitosis, J. Cell Biol. 183 (2008) 819–834.
[92] P.S. Vaughan, J.D. Leszyk, K.T. Vaughan, Cytoplasmic dynein intermediate chain phosphorylation regulates binding to dynactin, J. Biol. Chem. 276 (2001) 26 171–26 179.
[93] Z.R. Yang, R. Thomson, P. McNeil, R.M. Esnouf, RONN: The bio-basis function neural network technique applied to the detection of natively disordered regions in proteins, Bioinformatics 21 (2005) 3369–3376.

[94] S.F. Altschul, T.L. Madden, A.A. Schaffer, J. Zhang, Z. Zhang, W. Miller, D.J. Lipman, Gapped BLAST and PSI-BLAST: A new generation of protein database search programs, Nucleic Acids Res. 25 (1997) 3389–3402.
[95] K.K. Pfister, Dynein cargo gets its groove back, Structure 13 (2005) 172–173.
[96] R.D. Vale, R.A. Milligan, The way things move: Looking under the hood of molecular motor proteins, Science 288 (2000) 88–95.
[97] S.H. Tynan, A. Purohit, S.J. Doxsey, R.B. Vallee, Light intermediate chain 1 defines a functional subfraction of cytoplasmic dynein which binds to pericentrin, J. Biol. Chem. 275 (2000) 32 763–32 768.
[98] M. Mammen, S.K. Choi, G.M. Whitesides, Polyvalent interactions in biological systems: Implications for design and use of multivalent ligands and inhibitors, Angew. Chem., Int. Ed. Eng. 37 (1998) 2755–2794.
[99] W.P. Jencks, On the attribution and additivity of binding energies, Proc. Natl. Acad. Sci. USA 78 (1981) 4046–4050.
[100] J. Rao, J. Lahiri, L. Isaacs, R.M. Weis, G.M. Whitesides, A trivalent system from vancomycin.D-ala-D-Ala with higher affinity than avidin.biotin, Science 280 (1998) 708–711.
[101] D. Varma, A. Dawn, A. Ghosh-Roy, S.J. Weil, K.M. Ori-McKenney, Y. Zhao, J. Keen, R.B. Vallee, J.C. Williams, Development and application of *in vivo* molecular traps reveals that dynein light chain occupancy differentially affects dynein-mediated processes, Proc. Natl. Acad. Sci. USA 107 (2010) 3493–3498.
[102] J. Hall, P.A. Karplus, E. Barbar, Multivalency in the assembly of intrinsically disordered dynein intermediate chain, J. Biol. Chem. 284 (2009) 33 115–33 121.
[103] T. Clackson, W. Yang, L.W. Rozamus, M. Hatada, J.F. Amara, C.T. Rollins, L.F. Stevenson, S.R. Magari, S.A. Wood, N.L. Courage, X. Lu, F. Cerasoli Jr., M. Gilman, D.A. Holt, Redesigning an FKBP-ligand interface to generate chemical dimerizers with novel specificity, Proc. Natl. Acad. Sci. USA 95 (1998) 10 437–10 442.
[104] C.M. Lightcap, G. Kari, L.E. Arias-Romero, J. Chernoff, U. Rodeck, J.C. Williams, Interaction with LC8 is required for Pak1 nuclear import and is indispensable for zebrafish development, PLoS One 4 (2009) e6025.
[105] E. Barbar, Dynein light chain LC8 is a dimerization hub essential in diverse protein networks, Biochemistry 47 (2008) 503–508.
[106] E.T. Mack, R. Perez-Castillejos, Z. Suo, G.M. Whitesides, Exact analysis of ligand-induced dimerization of monomeric receptors, Anal. Chem. 80 (2008) 5550–5555.
[107] G. Benison, M. Chiodo, P.A. Karplus, E. Barbar, Structural, thermodynamic, and kinetic effects of a phosphomimetic mutation in dynein light chain LC8, Biochemistry 48 (2009) 11 381–11 389.
[108] K.S. Campbell, S. Cooper, M. Dessing, S. Yates, A. Buder, Interaction of p59fyn kinase with the dynein light chain, Tctex-1, and colocalization during cytokinesis, J. Immunol. 161 (1998) 1728–1737.
[109] L.M. Iakoucheva, P. Radivojac, C.J. Brown, T.R. O'Connor, J.G. Sikes, Z. Obradovic, A.K. Dunker, The importance of intrinsic disorder for protein phosphorylation, Nucleic Acids Res. 32 (2004) 1037–1049.
[110] S.J. King, C.L. Brown, K.C. Maier, N.J. Quintyne, T.A. Schroer, Analysis of the dynein–dynactin interaction *in vitro* and *in vivo*, Mol. Biol. Cell 14 (2003) 5089–5097.
[111] L.M. DiBella, M. Sakato, R.S. Patel-King, G.J. Pazour, S.M. King, The LC7 light chains of *Chlamydomonas* flagellar dyneins interact with components required for both motor assembly and regulation, Mol. Biol. Cell 15 (2004) 4633–4646.
[112] C.A. Tanner, P. Rompolas, R.S. Patel-King, O. Gorbatyuk, K. Wakabayashi, G.J. Pazour, S.M. King, Three members of the LC8/DYNLL family are required for outer arm dynein motor function, Mol. Biol. Cell 19 (2008) 3724–3734.

[113] K. Lei, R.J. Davis, JNK phosphorylation of Bim-related members of the Bcl2 family induces Bax-dependent apoptosis, Proc. Natl. Acad. Sci. USA 100 (2003) 2432–2437.
[114] E.J. Barbar, S. Norwood, M. Hare, Increase in flexibility upon dissociation of dynein light chain LC8 dimer as probed by NMR and mass spectrometry, Biophys. J. 82 (2002) 1701.
[115] H.J. Dyson, P.E. Wright, Coupling of folding and binding for unstructured proteins, Curr. Opin. Struct. Biol. 12 (2002) 54–60.
[116] N. Sharma, C.D. Deppmann, A.W. Harrington, C. St Hillaire, Z.Y. Chen, F.S. Lee, D.D. Ginty, Long-distance control of synapse assembly by target-derived NGF, Neuron 67 (2010) 422–434.
[117] M.P. McShane, M. Zerial, Survival of the weakest: Signaling aided by endosomes, J. Cell. Biol. 182 (2008) 823–825.
[118] S. Kermorgant, P.J. Parker, Receptor trafficking controls weak signal delivery: A strategy used by c-Met for STAT3 nuclear accumulation, J. Cell Biol. 182 (2008) 855–863.
[119] G.W. Moseley, D.M. Roth, M.A. Dejesus, D.L. Leyton, R.P. Filmer, C.W. Pouton, D.A. Jans, Dynein light chain association sequences can facilitate nuclear protein import, Mol. Biol. Cell. 18 (8) (2007) 3204–3213.
[120] M. Martinez-Moreno, I. Navarro-Leida, F. Roncal, J.P. Albar, C. Alonso, F. Gavilanes, I. Rodriguez-Crespo, Recognition of novel viral sequences that associate with the dynein light chain LC8 identified through a pepscan technique, FEBS Lett. 544 (2003) 262–267.
[121] T.G. Senkevich, L.S. Wyatt, A.S. Weisberg, E.V. Koonin, B. Moss, A conserved poxvirus NlpC/P60 superfamily protein contributes to vaccinia virus virulence in mice but not to replication in cell culture, Virology 374 (2008) 506–514.
[122] B. Hernaez, G. Diaz-Gil, M. Garcia-Gallo, J. Ignacio Quetglas, I. Rodriguez-Crespo, L. Dixon, J.M. Escribano, C. Alonso, The African swine fever virus dynein-binding protein p54 induces infected cell apoptosis, FEBS Lett. 569 (2004) 224–228.
[123] A. Fejtova, D. Davydova, F. Bischof, V. Lazarevic, W.D. Altrock, S. Romorini, C. Schone, W. Zuschratter, M.R. Kreutz, C.C. Garner, N.E. Ziv, E.D. Gundelfinger, Dynein light chain regulates axonal trafficking and synaptic levels of Bassoon, J. Cell Biol. 185 (2009) 341–355.
[124] M.D. Show, J.S. Folmer, M.D. Anway, B.R. Zirkin, Testicular expression and distribution of the rat bcl2 modifying factor in response to reduced intratesticular testosterone, Biol. Reprod. 70 (2004) 1153–1161.
[125] D.A. Blanchard, S. Mouhamad, M.T. Auffredou, A. Pesty, J. Bertoglio, G. Leca, A. Vazquez, Cdk2 associates with MAP kinase in vivo and its nuclear translocation is dependent on MAP kinase activation in IL-2-dependent Kit 225 T lymphocytes, Oncogene 19 (2000) 4184–4189.
[126] P. den Hollander, R. Kumar, Dynein light chain 1 contributes to cell cycle progression by increasing cyclin-dependent kinase 2 activity in estrogen-stimulated cells, Cancer Res. 66 (2006) 5941–5949.
[127] A. Lukasik, K.A. Uniewicz, M. Kulis, P. Kozlowski, Ciz1, a p21 cip1/Waf1-interacting zinc finger protein and DNA replication factor, is a novel molecular partner for human enhancer of rudimentary homolog, FEBS J. 275 (2008) 332–340.
[128] R.A. Anderson, N. Fulton, G. Cowan, S. Coutts, P.T. Saunders, Conserved and divergent patterns of expression of DAZL, VASA and OCT4 in the germ cells of the human fetal ovary and testis, BMC Dev. Biol. 7 (2007) 136.
[129] A.D. Lajoix, R. Gross, C. Aknin, S. Dietz, C. Granier, D. Laune, Cellulose membrane supported peptide arrays for deciphering protein–protein interaction sites: The case of PIN, a protein with multiple natural partners, Mol. Divers. 8 (2004) 281–290.
[130] X. Xiang, C. Roghi, N.R. Morris, Characterization and localization of the cytoplasmic dynein heavy chain in *Aspergillus nidulans*, Proc. Natl. Acad. Sci. USA 92 (1995) 9890–9894.
[131] W.M. Saxton, Microtubules, motors, and mRNA localization mechanisms: Watching fluorescent messages move, Cell 107 (2001) 707–710.

[132] S.K. Rayala, P. den Hollander, S. Balasenthil, Z. Yang, R.R. Broaddus, R. Kumar, Functional regulation of oestrogen receptor pathway by the dynein light chain 1, EMBO Rep. 6 (6) (2005) 538–544.
[133] Y. Xu, R.J. Traystman, P.D. Hurn, M.M. Wang, Membrane restraint of estrogen receptor alpha enhances estrogen-dependent nuclear localization and genomic function, Mol. Endocrinol. 18 (2004) 86–96.
[134] R. Studer, L. von Boehmer, T. Haenggi, C. Schweizer, D. Benke, U. Rudolph, J.M. Fritschy, Alteration of GABAergic synapses and gephyrin clusters in the thalamic reticular nucleus of GABAA receptor alpha3 subunit-null mice, Eur. J. Neurosci. 24 (2006) 1307–1315.
[135] E. Kim, S. Naisbitt, Y.P. Hsueh, A. Rao, A. Rothschild, A.M. Craig, M. Sheng, GKAP, a novel synaptic protein that interacts with the guanylate kinase-like domain of the PSD-95/SAP90 family of channel clustering molecules, J. Cell Biol. 136 (1997) 669–678.
[136] M.F. Garcia-Mayoral, M. Martinez-Moreno, J.P. Albar, I. Rodriguez-Crespo, M. Bruix, Structural basis for the interaction between dynein light chain 1 and the glutamate channel homolog GRINL1A, FEBS J. 277 (2010) 2340–2350.
[137] S.M. Okamura, C.E. Oki-Idouchi, P.S. Lorenzo, The exchange factor and diacylglycerol receptor RasGRP3 interacts with dynein light chain 1 through its C-terminal domain, J. Biol. Chem. 281 (2006) 36 132–36 139.
[138] A. Webster, I.R. Leith, R.T. Hay, Activation of adenovirus-coded protease and processing of preterminal protein, J. Virol. 68 (1994) 7292–7300.
[139] A.D. Kwong, B.G. Rao, K.T. Jeang, Viral and cellular RNA helicases as antiviral targets, Nat. Rev. Drug Discov. 4 (2005) 845–853.
[140] E. Kofod-Olsen, K. Ross-Hansen, J.G. Mikkelsen, P. Hollsberg, Human herpesvirus 6B U19 protein is a PML-regulated transcriptional activator that localizes to nuclear foci in a PML-independent manner, J. Gen. Virol. 89 (2008) 106–116.
[141] S. Sachdev, A. Hoffmann, M. Hannink, Nuclear localization of IkappaB alpha is mediated by the second ankyrin repeat: The IkappaB alpha ankyrin repeats define a novel class of cis-acting nuclear import sequences, Mol. Cell Biol. 18 (1998) 2524–2534.
[142] S.K. Rayala, P. den Hollander, B. Manavathi, A.H. Talukder, C. Song, S. Peng, A. Barnekow, J. Kremerskothen, R. Kumar, Essential role of KIBRA in co-activator function of dynein light chain 1 in mammalian cells, J. Biol. Chem. 281 (2006) 19 092–19 099.
[143] J.D. Huang, S.T. Brady, B.W. Richards, D. Stenolen, J.H. Resau, N.G. Copeland, N.A. Jenkins, Direct interaction of microtubule- and actin-based transport motors, Nature 397 (1999) 267–270.
[144] N. Tekki-Kessaris, J.V. Bonventre, C.A. Boulter, Characterization of the mouse Kid1 gene and identification of a highly related gene, Kid2, Gene 240 (1999) 13–22.
[145] D. Pasdeloup, N. Poisson, H. Raux, Y. Gaudin, R.W. Ruigrok, D. Blondel, Nucleocytoplasmic shuttling of the rabies virus P protein requires a nuclear localization signal and a CRM1-dependent nuclear export signal, Virology 334 (2005) 284–293.
[146] M.C. Pranchevicius, M.M. Baqui, H.C. Ishikawa-Ankerhold, E.V. Lourenco, R.M. Leao, S.R. Banzi, C.T. dos Santos, M.C. Roque-Barreira, E.M. Espreafico, R.E. Larson, Myosin Va phosphorylated on Ser1650 is found in nuclear speckles and redistributes to nucleoli upon inhibition of transcription, Cell Motil. Cytoskeleton 65 (2008) 441–456.
[147] S.R. Jaffrey, S.H. Snyder, PIN: An associated protein inhibitor of neuronal nitric oxide synthase, Science 274 (1996) 774–777.
[148] Z. Yuan, B. Liu, L. Yuan, Y. Zhang, X. Dong, J. Lu, Evidence of nuclear localization of neuronal nitric oxide synthase in cultured astrocytes of rats, Life Sci. 74 (2004) 3199–3209.
[149] M. Hertel, S. Braun, S. Durka, C. Alzheimer, S. Werner, Upregulation and activation of the Nrf-1 transcription factor in the lesioned hippocampus, Eur. J. Neurosci. 15 (2002) 1707–1711.

[150] P. Stelter, R. Kunze, D. Flemming, D. Hopfner, M. Diepholz, P. Philippsen, B. Bottcher, E. Hurt, Molecular basis for the functional interaction of dynein light chain with the nuclear-pore complex, Nat. Cell. Biol. 9 (2007) 788–796.
[151] R.R. Singh, C. Song, Z. Yang, R. Kumar, Nuclear localization and chromatin targets of p21-activated kinase 1, J. Biol. Chem. 280 (2005) 18 130–18 137.
[152] H. Raux, A. Flamand, D. Blondel, Interaction of the rabies virus P protein with the LC8 dynein light chain, J. Virol. 74 (2000) 10 212–10 216.
[153] F.P. Polack, P.M. Irusta, S.J. Hoffman, M.P. Schiatti, G.A. Melendi, M.F. Delgado, F.R. Laham, B. Thumar, R.M. Hendry, J.A. Melero, R.A. Karron, P.L. Collins, S.R. Kleeberger, The cysteine-rich region of respiratory syncytial virus attachment protein inhibits innate immunity elicited by the virus and endotoxin, Proc. Natl. Acad. Sci. USA 102 (2005) 8996–9001.
[154] J. Hegde, E.C. Stephenson, Distribution of swallow protein in egg chambers and embryos of *Drosophila melanogaster*, Development 119 (1993) 457–470.
[155] L. Wang, M. Hare, T.S. Hays, E. Barbar, Dynein light chain LC8 promotes assembly of the coiled-coil domain of swallow protein, Biochemistry 43 (2004) 4611–4620.
[156] W. Jeong, Y. Jung, H. Kim, S.J. Park, S.G. Rhee, Thioredoxin-related protein 14, a new member of the thioredoxin family with disulfide reductase activity: Implication in the redox regulation of TNF-alpha signaling, Free Radic. Biol. Med. 47 (2009) 1294–1303.
[157] F.J. Kaiser, K. Tavassoli, G.J. van den Bemd, G.T. Chang, B. Horsthemke, T. Moroy, H.J. Ludecke, Nuclear interaction of the dynein light chain LC8a with the TRPS1 transcription factor suppresses the transcriptional repression activity of TRPS1, Hum. Mol. Genet. 12 (2003) 1349–1358.
[158] F.J. Kaiser, P. Brega, M.L. Raff, P.H. Byers, S. Gallati, T.T. Kay, S. de Almeida, B. Horsthemke, H.J. Ludecke, Novel missense mutations in the TRPS1 transcription factor define the nuclear localization signal, Eur. J. Hum. Genet. 12 (2004) 121–126.
[159] W.B. Cardenas, Y.M. Loo, M. Gale Jr., A.L. Hartman, C.R. Kimberlin, L. Martinez-Sobrido, E.O. Saphire, C.F. Basler, Ebola virus VP35 protein binds double-stranded RNA and inhibits alpha/beta interferon production induced by RIG-I signaling, J. Virol. 80 (2006) 5168–5178.
[160] A. Bauch, K.S. Campbell, M. Reth, Interaction of the CD5 cytoplasmic domain with the Ca^{2+}/calmodulin-dependent kinase IIdelta, Eur. J. Immunol. 28 (1998) 2167–2177.
[161] S. Ohka, N. Matsuda, K. Tohyama, T. Oda, M. Morikawa, S. Kuge, A. Nomoto, Receptor (CD155)-dependent endocytosis of poliovirus and retrograde axonal transport of the endosome, J. Virol. 78 (2004) 7186–7198.
[162] S.A. Lukashok, L. Tarassishin, Y. Li, M.S. Horwitz, An adenovirus inhibitor of tumor necrosis factor alpha-induced apoptosis complexes with dynein and a small GTPase, J. Virol. 74 (2000) 4705–4709.
[163] P. Sachdev, S. Menon, D.B. Kastner, J.Z. Chuang, T.Y. Yeh, C. Conde, A. Caceres, C.H. Sung, T.P. Sakmar, G protein beta gamma subunit interaction with the dynein light-chain component Tctex-1 regulates neurite outgrowth, EMBO J. 26 (2007) 2621–2632.
[164] K. Dohner, K. Radtke, S. Schmidt, B. Sodeik, Eclipse phase of herpes simplex virus type 1 infection: Efficient dynein-mediated capsid transport without the small capsid protein VP26, J. Virol. 80 (2006) 8211–8224.
[165] A. Gauthier-Fisher, D.C. Lin, M. Greeve, D.R. Kaplan, R. Rottapel, F.D. Miller, Lfc and Tctex-1 regulate the genesis of neurons from cortical precursor cells, Nat. Neurosci. 12 (2009) 735–744.
[166] D. Meiri, M.A. Greeve, A. Brunet, D. Finan, C.D. Wells, J. LaRose, R. Rottapel, Modulation of Rho guanine exchange factor Lfc activity by protein kinase A-mediated phosphorylation, Mol. Cell Biol. 29 (2009) 5963–5973.

[167] H. Yano, M.V. Chao, Biochemical characterization of intracellular membranes bearing Trk neurotrophin receptors, Neurochem. Res. 30 (2005) 767–777.
[168] J.H. Carter, L.E. Douglass, J.A. Deddens, B.M. Colligan, T.R. Bhatt, J.O. Pemberton, S. Konicek, J. Hom, M. Marshall, J.R. Graff, Pak-1 expression increases with progression of colorectal carcinomas to metastasis, Clin. Cancer Res. 10 (2004) 3448–3456.
[169] N.A. Baker, D. Sept, S. Joseph, M.J. Holst, J.A. McCammon, Electrostatics of nanosystems: Application to microtubules and the ribosome, Proc. Natl. Acad. Sci. USA 98 (2001) 10037–10041.

In this chapter

6

Biophysics of Dynein *In Vivo*

Jing Xu, Steven P. Gross
Department of Developmental and Cell Biology, University of California, Irvine, CA, USA

One of the challenges in understanding molecular motors is that they are mechano-enzymes, whose function is to physically exert force and move cargos of a variety of types from one place to another inside cells. Because of this physical component, we must understand them both from an enzymatic point of view and from a biophysical one. A key question concerns determination of how their function is regulated in order to achieve the wide range of things they do. Because the requirements for successful function will be different depending on what is being moved, there will be a variety of routes for appropriate regulation of function. Almost all regulatory pathways will need to control how groups of motors function together, but at the single-molecule level this could in principle be achieved in a variety of ways. This chapter will summarize what we know about how single-molecule properties relate to ensemble function and how such properties can be regulated.

Our ultimate goal is to understand the regulated transport of cargos *in vivo*, starting from single-molecule properties of motors such as dynein *in vitro*. *A priori*, molecular motors may behave the same *in vivo* as *in vitro*, or they may function somewhat differently due to the differences between their *in vitro* and *in vivo* environments. In particular, *in vivo* the motors may interact with a variety of co-factors not present *in vitro*, and, furthermore, they likely function in groups rather than as individual motors. Thus, we will start by describing the functions determined for single dynein motors *in vitro*, in a purified and controlled environment, and then turn to how the motors function in groups *in vitro*. From these studies, we will not only discover what properties emerge from groups of motors but also which aspects of the single motors are important for their function as a group. Which single-molecule properties turn out to be important depends on what kinds of "challenges" the cargo's motion is likely to face.

6.1 Single-Molecule Properties of Dynein *In Vitro*

Dynein is an enzyme that converts ATP to ADP and free Pi, and in the process is able to generate useful work by "walking" along a microtubule. The dynein

Dyneins DOI: 10.1016/B978-0-12-382004-4.10006-8
Copyright © 2012 by Elsevier Inc. All rights reserved.

"motor" is in fact already a large protein complex, with two heavy chains (HCs) (AAA-domain proteins that are the force-producing part of dynein) together with intermediate chains (ICs) and light chains (LCs) (the details of these proteins are discussed in Chapters 7 and 15). Dynein also typically (though not always) functions with dynactin, another large protein complex (see Chapter 19).

Cytoplasmic dynein has been purified from bovine, murine, chicken, and other sources so that it can be studied at the single-molecule level. In this case, the dynein motor proteins are attached to glass or polystyrene beads or quantum dots (artificial cargos), and the motor then moves the cargo along microtubules. At saturating (~1 mM) ATP, dynein typically moves in the range of 600 nm/s to 1 μm/s at room temperature. It is able to take a variety of step sizes (including 8, 16, 24, 32, and 40 nm) [9], though most frequently appears to take 8 nm steps [1]. The extent to which steps other than 8 nm occur is still under investigation, though larger steps have been detected *in vivo* (see Section 6.5 and [2]). Dynein is a processive enzyme; that is, it is able to undergo multiple enzymatic cycles before releasing from the microtubule. Without dynactin, bovine dynein has been measured to have an average single-molecule travel of approximately 700 nm [3,4], reflecting somewhere between 100 (8 nm) and 25 (32 nm) steps. However, murine dynein is less processive, with a mean travel of ~300 nm [5]. The presence of dynactin approximately doubles the mean travel distance of single dynein molecules *in vitro*, to about 1.5 μm for bovine dynein [3] and 800 nm for murine dynein [6]. The reason for murine dynein's lower processivity relative to bovine dynein is unknown. Dynactin binds to the microtubule independently of dynein, which could provide an independent tether between cargo and microtubule, thus potentially explaining its functional increase in dynein processivity [7]. However, other studies suggest that dynactin's ability to bind to microtubules is in fact not required in order to increase its mean travel distance [8]. Overall, dynactin's mechanism and function are very much under investigation.

Dynein's force production has also been measured. *In vitro*, our lab measures purified bovine dynein to stall at approximately 1.1–1.2 pN of force [9–11], the same as for murine [5] and rat dyneins (J. Xu and S. P. Gross, unpublished work). The ~1.1 pN stall force has also been measured for murine dynein by the Holzbaur group (personal communication) and for Dictystelium dynein by the Mallik Group [12]. However, yeast dynein is reported to stall at 5–7 pN [13]. Interestingly, the Higuchi group reports a stall force of 5–7 pN for bovine dynein [14], which they attribute to the details of how the dynein is attached to the cargo. This seems unlikely to us, since our group received their protocol but was unable to reproduce their findings. The overall cause of this discrepancy is unknown, but we have suggested it may reflect kinesin contamination [11]. The bona fide differences between bovine dynein and yeast dynein may reflect cellular specialization, because yeast does not use dynein/microtubule-based transport for vesicular transport but rather for slowly moving/repositioning large cargos

such as the nucleus. Consistent with such specialization, yeast dynein is very slow, moving at ~50–80 nm/s.

In summary, by itself at the single-molecule level *in vitro*, dynein moves at approximately 800 nm/s, with approximately one μm of mean travel (with the exception of murine dynein [5]). It can move against loads of up to 1.2 pN. Note that these stated velocity and travel distances reflect "unloaded" dynein – when moving a cargo against a load, dynein moves slower and is more prone to detachment from the microtubule. The larger the opposing load, the slower the motion and the shorter the mean travel.

6.2 Multiple-Motor Properties of Dynein *In Vitro*

Distances in cells are frequently more than 1 μm and, in principle, the forces opposing motion could be larger than 1.2 pN. This suggests that perhaps multiple motors move cargos *in vivo*. Can this longer-distance transport be achieved simply by putting more motors on the cargo or are additional proteins required to coordinate the motors and help them work well together? As a first step to understanding such *in vivo* transport, there have been characterizations of how multiple motors function together *in vitro*.

Such studies have shown that, indeed, multiple dynein motors work relatively well together. That is, when moving an unloaded cargo, two or three motors can move much further than one [4,5], at the same velocity as a single motor. Our theoretical studies [15] show that the average number of engaged motors moving a cargo plays a critical role in determining how far the cargo moves. In principle, this average number can be tuned in a number of ways. First, consider the case of a cargo with three motors present, all clustered together at a single point (and thus all able to reach the microtubule simultaneously). Starting from a case of a single motor engaged, that motor could detach, in which case the "run" would end. Obviously, the further the single motor tends to go before detaching, the further the cargo will go. So, increased single-motor processivity will obviously increase mean cargo transport. However, increasing single-motor transport has a slightly less obvious advantage as well: by taking longer to detach, the first motor gives more time to the other motors to attach. On average, at any given time, this will lead to a higher percentage of the total available motors being active, and this in turn leads to further transport because when more than one motor is attached to the microtubule both must detach before the runs end (Fig. 6.1). Alternatively, one could leave processivity alone and simply tune the "on" rate of the motors – that is, how long it takes a "free" motor (i.e. one attached to the cargo but unbound from the microtubule) to (re-)bind to the microtubule. Increasing the effective on-rate will also increase the mean number of engaged motors, consequently leading to longer mean runs. Finally, one can

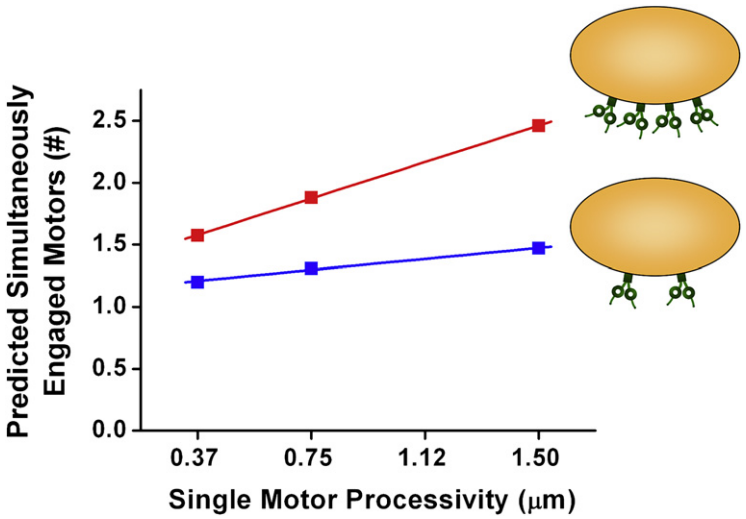

Figure 6.1 **Single-motor processivity contributes to the number of simultaneously engaged motors.** For a given number of available motors (N = 2, blue, and N = 4, red), the number of simultaneously engaged dyneins increases with increased processivity (theoretically tested for 0.4, 0.75, and 1.5 μm). The scatter represents simulation data and the lines represent linear fit. The simulation algorithm is detailed in [5,11]; the motors' assumed "on" rate was 1 per second.

leave all the single-molecule properties alone but simply recruit more motors. The more motors present, on average, the more that will be engaged. Thus, regulation of multiple-motor function *in vivo* can in principle use any of these three routes (or all of them combined) to tune how far cargos move on average. The extent to which one strategy is favored *in vivo* is currently unclear but is obviously of great interest.

6.3 Regulation of Dynein *In Vitro*

In Section 6.2, we highlighted three factors contributing to the number of engaged motors and thus to the mean transport of the cargo moving under no load. In principle, a fourth aspect can also be regulated: how likely the motors are to detach when under load (e.g. detachment kinetics at high forces). The slower the motors are to detach under load (even if they still stall at the same maximum load), the more they are able to remain attached and share load between motors present. Thus, in principle, one can tune ensemble function by altering detachment kinetics under load as well as the motors' on-rate and off-rate, and the total number of motors present.

So far, there are two established classes of dynein regulatory complexes (DRC): the dynactin complex and the NudE/Lis1 complex [11]. Each affects dynein function *in vitro*, at both the single-molecule and multiple-motor level. As stated above,

dynactin increases the mean travel for single dynein motors, causing a roughly two-times increase in mean travel distance [3,8]. *In vivo* studies (see Section 6.8) suggest that dynactin (possibly in conjunction with other proteins) may affect dynein function in other ways as well, but this has not been investigated *in vitro*. One expected result of dynactin's increase in mean travel for single dynein motors is that cargos moved by multiple motors will go significantly further; however, exactly how this plays out depends on the magnitude of the single-motor processivity. For example, if a single dynein has a very low processivity of $\sim$300 nm (that of mouse), the contribution from dynactin may be critical. In contrast, for higher processivity (e.g. bovine) dynein, multiple dynein motors can move very long distances even without dynactin [4], so the dynactin's processivity role may be less important and its established importance may reflect other functions. Overall, then, dynactin helps dynein move cargos further but the importance of this might depend on the specific organism, cargo, or situation. So far there is no clear indication that dynactin plays a role in altering or regulating dynein force production.

In contrast, NudE and Lis1 do alter dynein force production. By itself, NudE turns dynein "off," and Lis1 reverses this inhibition. Although this "off" and "on" mechanism may by itself be quite useful for the cell, there is an additional effect: Lis1-activated dynein is more persistent in its force-producing ability. That is, while Lis1-activated dynein still stalls at 1.2 pN, under load it is more able to "hold on" and avoid detaching from the microtubule. This persistence under load enhances the ability of multiple dynein motors to work together — they share load better, and for the same number of motors the addition of NudE and Lis1 results in improved ability to move cargos against significant opposing forces [11]. This enhanced ability of multiple motors to exert load together is likely to be of great importance *in vivo* when moving large cargos against high load, for example during nuclear migration (see Section 6.7). In summary, so far at least, it appears that dynactin may be important to allow vesicular cargos to be moved over longer distances, whereas NudE/Lis1 may be important to allow dyneins to work well together in high-force applications. With this background for *in vitro* dynein function, we now turn to how dynein functions and is regulated in a cellular context. *In vivo*, there are likely other players (e.g. kinases) that contribute to dynein function either by helping to recruit (or release) dynein from the cargo or by altering dynein's on-rate or its processivity. However, such players have not been characterized cleanly *in vitro*, so at this point we can only speculate about their existence and properties.

6.4 Regulation of Dynein *In Vivo*

Many classes of cargos are moved by dynein *in vivo*, including endosomes and lysosomes, mitochondria, mRNA particles, virus particles, lipid droplets, nuclei, and complete microtubule spindles engaged in chromosome segregation. Thus, when we start discussing "*in vivo* dynein function," we must first be careful about

what class of cargo we are discussing, because many aspects of the dynein's function may depend on the specific cargo in question – there is not a single "dynein" *in vivo* but rather a set of dynein motors functioning with a variety of co-factors that could alter their function, with different combinations of co-factors for different cargos. This makes for a very rich, but complicated, landscape. Nonetheless, we can try to artificially group classes of cargos together to try to make some general observations. After discussing what is known about the single-molecule function of dynein *in vivo*, we separately consider unidirectionally and bidirectionally moving cargos. By "unidirectional" we mean moving in a single direction along microtubules (in this case towards the microtubule minus end). By "bidirectional" we refer to the class of cargos that frequently (every few seconds) reverses course, switching between plus-end motion and minus-end motion. The minus-end motion is always driven by dynein and typically the plus-end motion is driven by kinesin-1, though sometimes by kinesin-2.

6.5 Single-Molecule Properties of Dynein *In Vivo*

Actual stall forces for individual dynein motors inside a cell have now been measured for three different systems. Mitochondria moving in Reticulomyxa, likely moved by dyneins, were estimated to have a single-motor stalling force of approximately 2.4 pN [16]. Similarly, dynein moving lipid droplets in *Drosophila* embryos appear to have a single-molecule stalling force of approximately 2.5 pN [17]. Finally, in cultured human cancer cells, lipid droplets likely moved by dynein stall at approximately 3.5 pN (+/−1 pN) [2]. Thus, these measurements would suggest that single dynein motors stall in the 2.5−3.5 pN range. This is different from the 1.2 pN stall we measured *in vitro*, and the mechanism leading to this discrepancy is unknown. However, all three of these cargos are bidirectional, frequently reversing between plus-end and minus-end motion, and the function of the motors could be modified by accessory factors. Intriguingly, while the dynein motors appear to stall at a higher stall force *in vivo* than they do *in vitro*, the kinesin moving the lipid droplets appears to stall at a lower force, resulting in balanced plus-end and minus-end single motor stall forces *in vivo*.

There have been a number of other semi-*in-vivo* force measurements that have led to different conclusions about dynein's single-molecule function. In one [18], a bead was used to study flagellar surface motility by attaching the bead outside the flagella to motors moving inside, via the FMG-1 flagellar membrane protein. The force required to stop the bead from moving was measured to be quite high – up to 60 pN. While individual motor forces could not be measured, the high magnitude overall was interpreted to reflect approximately ten 6 pN motors (though in principle there could equally be twenty 3 pN motors). A different study [12] measured overall escape percentages of endosomes in cells and also forces of purified endosomes *in vitro*. They found that the overall forces required

to stall endosomes were approximately the same in both directions (in the 5–10 pN range), but, based on single-molecule properties *in vitro* (1.1 pN for dynein and 5 pN for kinesin), proposed that this reflects very different numbers of kinesin versus dynein motors. However, the "unit" stall force for single dynein motors *in vivo* was never actually measured; to really establish that dynein was stalling at 1.1 pN as opposed to 2.5 pN, one would need to measure stalling force "peaks" *in vivo* and detect the location of the smallest peak, as was done in both the Shubeita study [17] and the Simms study [2].

Dynein's *in vivo* velocity can vary significantly, but is typically in the same range as its *in vitro* velocity – that is, from 500 nm/s up to about 1.5 μm/s – although in mammalian neurons dynein-driven cargos can move faster, up to 2–3 μm/s. This excludes yeast cytoplasmic dynein, which moves extremely slowly (~50–80 nm/s) both *in vitro* and *in vivo* [8,13].

Dynein's stepping behavior *in vivo* is also relatively similar to its behavior *in vitro*. Initial single-molecule measurements on dynein reported a variable step size, including 8, 16, 24, and 32 nm steps [9]. This variable distribution of step sizes of cargos moved by single dyneins has been observed *in vivo*, for lipid droplets moved by single dynein motors [2], though there are typically more 8 nm steps than steps of other sizes. Another *in vivo* study [19] suggested that a different set of vesicles moved by dynein took only 8 nm steps, but in this case there was no differentiation between cargos moved by single versus multiple dyneins. This is important because studies [15,20,21] show that, at least for multiple kinesin motors on a cargo, the motors do not coordinate their stepping, so, when multiple motors are present, the cargo's center of mass moves only a fraction of the distance each motor steps. For example, if two motors are bound and moving the cargo, the observation of an 8 nm step might reflect one motor moving 16 nm while the other remains instantaneously stationary (for kinesins, which take 8 nm steps, the cargo's center of mass moves 4 nm).

6.6 Regulation of Unidirectional Dynein-Based Transport: Vesicular Cargos

What does it mean to regulate unidirectional transport? During unidirectional transport, cargo motion is interrupted by periods of dissociations from microtubules ("pauses") before reattachment and continued motion in the same direction. Here, the segmental travel of each cargo in a specific direction determines how far it can travel per unit time (with some additional time spent paused). The motion of the individual cargos compounds, so that together they determine the net flux of a type of transported cargo (e.g. how many cargos pass a certain point per unit time). This flux is crucial in deciding the long-term global cargo

distribution. Therefore, we can effectively tune the unidirectional transport by influencing the average velocity of individual cargos.

Three factors contribute to a cargo's average velocity: the cargo's velocity during continuous travel (i.e. its "instantaneous velocity"), the cargo's run length between attachment and detachment, and the duration of the pauses. Put another way, imagine a cargo moving down an axon, occasionally pausing and then continuing on. This cargo's average velocity can be tuned by the relative amount of time it spends moving and pausing. Clearly, in the absence of any pauses, the cargo's "average velocity" would be approximately the same as its typical instantaneous velocity. In this scenario, regulation of net cargo flux would rely entirely on how fast each cargo moved. It is of course unlikely that a cargo would advance infinitely without detachment, and this is where the relative interplay of run length and pause duration comes into play. Cargo run length determines pausing frequency. The shorter the cargo run length, the more likely it is that it will fall off the microtubule track and, hence, the higher the pause frequency. Furthermore, the longer it takes the cargo to reattach to the microtubule, the longer the pause. Combined, both pause frequency and pause duration contribute to the cargo's non-moving state. The more time the cargo spends in the non-moving, paused state, the lower its average velocity will be.

The number of simultaneously engaged motors has the potential to influence all three factors important for unidirectional dynein transport *in vivo*. First, let us consider the cargo's instantaneous velocity. A number of studies have demonstrated that, in the absence of a significant opposing force, cargo velocity during continuous travel is minimally sensitive to motor numbers both *in vitro* and *in vivo* [4,5,17,22]. However, some *in vivo* conditions can introduce significant load, such as the crowded environment of neuronal blockages. Here it is entirely possible that cargos carried by fewer motors will move slower, because the force on average per motor is higher. In this case, whatever dynein's force velocity curve may be *in vivo*, and regardless of load-sharing details [15,23], more load per motor will result in slower motion.

The number of engaged motors is also crucial for cargo run length. We have recently identified dynein's single-motor processivity as an important contributor to retrograde axonal transport. We found that wild-type murine dynein has a single molecule processivity of ~300 nm [5]. This value, though surprisingly short compared to that of bovine dynein (~600–800 nm), is in good agreement with measurements of the murine dynein–dynactin complex [6]. We find a striking enhancement of multiple-motor dynein run lengths *in vivo* with increasing single-dynein processivity (measured *in vitro)*. A seemingly small −25% (or 50%) − reduction in murine dynein processivity alone compounds to a 55% (and 83%) reduction in retrograde lysosomal run length in mutant neurons. Theoretical modeling suggests that an additional consequence of reduced

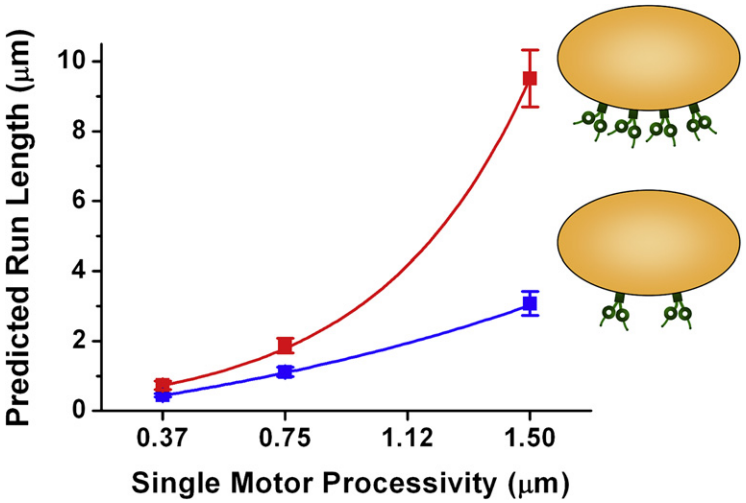

Figure 6.2 Cargo run length depends on single-motor processivity, as well as the number of available motors. The three single-motor processivities tested theoretically (J. Xu and S. P. Gross, unpublished simulation results) represent those of mouse dynein (0.4 μm), bovine dynein or mouse dynein–dynactin complex (0.75 μm), and bovine dynein with the addition of potential processivity factor dynactin (1.5 μm). The scatter represents simulation data and the lines represent first-order exponential fits. The simulation algorithm is detailed in [5,11].

processivity for each dynein is a reduction in the number of simultaneously engaged motors [5]. This study highlights a previously unappreciated role of single-motor processivity, and hence potential processivity factors *in vivo*, in regulating multiple dynein transport: the longer the travel for each individual dynein, the less dynein a cargo needs to recruit to reach a destination when on-rate and detachment kinetics of individual motors are held constant (Fig. 6.2).

Finally, the pausing duration can also correlate with the average number of simultaneously engaged motors. Obviously, during pausing, the number of engaged motors is zero. An increase in the on-rate of individual dyneins will act to both reduce pause duration and to upregulate the number of engaged motors, as discussed earlier. One mechanism for tuning individual dynein on-rate may be via decoration of microtubules with microtubule-associated proteins (MAPs), and MAP2 is one such candidate. MAP2 has been identified to compete with dynein in their microtubule binding [24,25]. The molecular detail of such competition has yet to be identified to differentiate between potential decrease in dynein on-rate and processivity (off-rate under no load), and in fact the MAP Tau has little effect on dynein function *in vitro* [10,26].

In Section 6.3 we highlighted the possibility of regulating unidirectional dynein transport *in vivo* by tuning the single-motor properties (detachment kinetics, processivity, and on-rate) to change the number of engaged motors. Now let

us consider the effect of cargo recruitment. Intuitively, assuming homogeneous behavior for each individual dynein, the greater the dynein presence on a cargo, the more dynein can contribute to transport. Dynein's cargo association *in vivo* is not yet well established. Both the dynein HC (tail) and accessory subunits (light-intermediate chains (LICs), LCs, and ICs) can mediate cargo association. As the main minus-end motor in most eukaryotic cells, the complexity of the dynein–cargo association may be the key for specificity in retrograde transport. For example, different isoforms of the IC have been shown to differentiate between different classes of cargos for transport [27,28]. Additionally, dynactin [29] and huntingtin [30] can also act as cargo adaptors via binding to the dynein IC. Such complexity imposes certain difficulties in regulating the amount of dynein present on a cargo. So far, hyperphosphorylation in the dynein LIC has been shown to cause detachment from cargo [31,32], and phosphorylation of the IC has been found to disrupt dynein–dynactin binding [33]. The regulatory mechanism for dynein–cargo association remains a rich area for exploration.

6.7 Regulation of Unidirectional Dynein-Based Transport: Large Cargos

There is another class of cargos that may have different requirements: large cargos (nuclei, microtubule spindles, etc.) that face significant opposition to motion. Such opposition could reflect either a need to either push filaments and other subcellular components out of the way as the cargo moves, or the fact that these cargos "drag" other things with them as they are moved. In such cases, force production is critical – one needs many motors to work well together. Our studies *in vitro* and *in vivo* suggest that force production is proportional to the number of engaged motors. Thus, to increase force production one needs to increase this number.

There are several obvious ways in which to increase the number of engaged motors. First, one can simply increase the number of motors present on the cargo. While these mechanisms are not yet that well understood, dynactin clearly plays a role in recruiting dynein to cargos, and recent work suggests that BicD [45] may as well. Furthermore, is seems highly likely that kinases, perhaps acting via phosphorylating either the dynein ICs, dynactin, or BicD, could play a role in regulating recruitment or release of dynein, though much work remains to be done to fully understand this.

A second way to increase the number of engaged motors is to increase the number of "active" motors on the cargo. Examples of co-factors that can do this are NudE and Lis1. Dynein on a cargo and bound to NudE is significantly downregulated or inactive, and this is reversed by the addition of Lis1. Thus,

increasing Lis1 dosage can increase the number of active dynein motors per cargo, up to the limit where all NudE-bound dyneins are active. In principle, there could be other regulatory factors able to activate and/or inactivate dynein, though they are not yet determined.

A third way to alter the number of engaged motors is to alter how they function in response to load. That is, if motors are prone to detach from the microtubule when under load, then when high loads are present (pulling on the cargo) it will be difficult to achieve a situation where many motors are engaged simultaneously. In contrast, if the motors are tenacious and "hang on" under load, they can all remain bound and help each other by sharing the burden. The NudE/Lis1 co-factors help in this regard: Lis1 significantly decreases dynein's "off" rate under load, allowing the same number of motors to work better together under load; so, for the same number of motors present, in the presence of Lis1, at high loads on average more motors are engaged, resulting in improved ensemble performance [11].

In principle, many of the factors discussed above in the context of vesicular transport could also contribute in the high-force regime. For instance, as above, any increase in single-motor processivity will increase the mean number of engaged motors when multiple motors are present, as will any increase in single-motor on-rate. The extent to which the factors are interchangeable between the two general classes of cargos remains to be determined, and is a focus of ongoing research.

6.8 Regulation of Bidirectional Dynein-Based Transport

Many cargos move bidirectionally, frequently reversing the direction of travel along microtubules. Such cargos are typically moved by dynein in the minus-end direction, and kinesin (and/or) kinesin-2 in the plus-end direction. Past studies by our group and others suggest that, in many cases, net (average) transport of a bidirectionally moving cargo can be controlled by regulating the travel distance in one direction while leaving the other direction unchanged. For instance, in the case of lipid droplets [17,34] and mitochondria [35], the length of plus-end "runs" (periods of uninterrupted motion in a give direction) is regulated, whereas minus-end runs remain constant. (Note: for lipid droplets there is a transient phase, IIB [36], where travel is upregulated in both directions, though there is no net transport, indicating that, although predominantly plus-end motion is altered to control average transport, both directions are under regulatory control.) Thus, in these systems, net plus-end transport results from long plus-end runs and moderate-length minus-end runs, whereas net minus-end transport results from short plus-end runs and moderate minus-end runs. In these cases, understanding net regulation then comes down to understanding how run lengths are

controlled. In contrast to the unidirectional transport discussed above, it is important to stress that one cannot consider plus-end or minus-end transport in isolation — studies repeatedly show strong "coupling" between the two travel directions, and factors that alter one direction of transport usually affect the other as well, though often in unexpected ways.

How are run lengths controlled? *In vitro*, more motors move further, so the simplest way to regulate run lengths would appear to be control of the number of active/engaged motors. This turns out not to be true: for bidirectionally moving cargos, there is no simple relationship between run lengths and the number of engaged motors [17]. In fact, in many cases something appears to cut the runs short. That is, given the number of engaged motors, one would expect the cargo to move much further than it actually does. This unexpectedly short travel is found for lipid droplets in drosophila embryos [17] and endosomes [12], and possibly other systems where the number of active/engaged motors is still unknown. Thus, one key question centers on what the "switching" mechanism is that cuts runs short.

There are currently two competing hypotheses for the nature of the "switch." The first is that it reflects an unregulated "tug of war" between opposite motors; that is, the plus-end runs are shorter than expected because the minus-end motors present become randomly engaged, and a tug of war ensues, with each set of motors attempting to move the cargo in opposite directions. In this model, sometimes the plus-end motors "lose" the tug of war, resulting in shorter plus-end travels. Similarly, sometimes the minus-end motors lose the tug of war, resulting in shorter minus-end travels. The tug of war model was first seriously proposed theoretically as a possible explanation for bidirectional lipid droplet motion [37], and has since been embraced by two independent groups to explain bidirectional motion of endosomes [12] and lysosomes [38]. The second model postulates a "switch" that is able to activate (or inactivate) the group of motors, terminating the run when it inactivates the group of inactive motors. We currently favor the latter model as an explanation for lipid droplet motion, but cannot completely eliminate the possibility that some variant of the tug of war model may be correct (see following paragraph). However, at least in one case — the flagellar surface motility system mentioned above [18] — there clearly is a switch rather than a tug of war, because there is a very short pause between the successful disengagement/inactivation of one set of motors and the subsequent activation of the second set. The mechanism of the switch is unknown.

The tug of war hypothesis may turn out to be true in some circumstances, but there are a number of reasons to doubt it — or, at the very least, to modify it significantly. First, there is clearly a second layer of regulation, not simply reflecting an unregulated tug of war because the opposite forces are almost always balanced. For instance, when the number of engaged plus-end motors is decreased, the

number of engaged minus-end motors is also decreased to compensate [17]. *In vitro*, individual kinesin and dynein motors are active even if they are not experiencing an opposing force, so this downregulation of the second set of motors appears to reflect an active process. Second, our data suggest that a number of dynein co-factors, such as klar [34] and dynactin [39], may contribute to coordination between opposing motors; that is, in contrast to the wild type, in mutants that alter their function the data is consistent with the induction of a tug of war. Research that aims to clarify which scenario is really correct in each case is ongoing.

Regardless of the actual mechanism, however, the functional question remains: how are the switching properties of the cargo altered to control net transport? Here, a variety of studies in a number of systems have provided key molecular players, though we do not know exactly how they work together. First, it is important to note that, although frequently only one set of run lengths is altered during normal regulation of travel, in fact there is evidence that both travel directions are being altered. For instance, studies of pigment-granule motion show that kinase activity can tune both sets of run lengths quite substantially [40]. Similarly, a variety of mutant studies show effects on both directions: in *Drosophila* lipid droplets, halo protein levels tune plus-end run lengths but complete loss of halo also alters minus-end motion, increasing minus-end run lengths (the mechanism is unclear) [41]. Similarly, in this system the klar and LSD2 proteins are required in order to regulate net transport [34,42]. In this and other systems, the BicD protein also plays a role in regulating dynein function [36,43]. The Huntington protein has been reported to play a role in controlling the motion of some bidirectional cargos, and there an exciting study [44] shows that a single phosphorylation can result in a change in the net direction of transport. However, mechanistic details of how the Huntington protein is actually able to achieve these effects are still somewhat lacking. A recent review [28] discusses a number of these dynein-interacting factors in more detail, though we do not know their mechanisms. What remains, then, is the observation that a great many proteins contribute to appropriate regulation of bidirectionally moving cargos, and that these proteins are likely do this not simply by recruiting or releasing one class of motors but rather by changing how the motors function. We know that kinases are involved in this regulation, but we are still attempting to understand how the kinases ultimately change the motors' function, both at the single-molecule level and also at the ensemble-function level.

Looking forward, this is a very exciting time for the field. In the last few years quite a number of factors regulating dynein function have been determined, and combining single-molecule-type approaches to quantifying function *in vitro* and *in vivo* with a variety of advanced fluorescence techniques *in vivo* should allow rapidly accelerating progress in understanding the mechanisms of dynein regulation at a fundamental level.

References

[1] S.L. Reck-Peterson, A. Yildiz, A.P. Carter, A. Gennerich, N. Zhang, R.D. Vale, Single-molecule analysis of dynein processivity and stepping behavior, Cell 126 (2006) 335–348.

[2] P.A. Sims, X.S. Xie, Probing dynein and kinesin stepping with mechanical manipulation in a living cell, Chemphyschem 10 (2009) 1511–1516.

[3] S.J. King, T.A. Schroer, Dynactin increases the processivity of the cytoplasmic dynein motor, Nat. Cell. Biol. 2 (2000) 20–24.

[4] R. Mallik, D. Petrov, S.A. Lex, S.J. King, S.P. Gross, Building complexity: An *in vitro* study of cytoplasmic dynein with *in vivo* implications, Curr. Biol. 15 (2005) 2075–2085.

[5] K.M. Ori-McKenney, J. Xu, S.P. Gross, R.B. Vallee, A Cytoplasmic Dynein Tail Mutation Impairs Motor Processivity, Nat. Cell Biol. 12 (2010) 1228–1234.

[6] J.L. Ross, K. Wallace, H. Shuman, Y.E. Goldman, E.L. Holzbaur, Processive bidirectional motion of dynein–dynactin complexes in vitro, Nat. Cell. Biol. 8 (2006) 562–570.

[7] T.L. Culver-Hanlon, S.A. Lex, A.D. Stephens, N.J. Quintyne, S.J. King, A microtubule-binding domain in dynactin increases dynein processivity by skating along microtubules, Nat. Cell. Biol. 8 (2006) 264–270.

[8] J.R. Kardon, S.L. Reck-Peterson, R.D. Vale, Regulation of the processivity and intracellular localization of *Saccharomyces cerevisiae* dynein by dynactin, Proc. Natl. Acad. Sci. USA 106 (2009) 5669–5674.

[9] R. Mallik, B.C. Carter, S.A. Lex, S.J. King, S.P. Gross, Cytoplasmic dynein functions as a gear in response to load, Nature 427 (2004) 649–652.

[10] M. Vershinin, J. Xu, D.S. Razafsky, S.J. King, S.P. Gross, Tuning microtubule-based transport through filamentous MAPs: The problem of dynein, Traffic 9 (2008) 882–892.

[11] R.J. McKenney, M. Vershinin, A. Kunwar, R.B. Vallee, S.P. Gross, LIS1 and NudE induce a persistent dynein force-producing state, Cell 141 (2010) 304–314.

[12] V. Soppina, A.K. Rai, A.J. Ramaiya, P. Barak, R. Mallik, Tug-of-war between dissimilar teams of microtubule motors regulates transport and fission of endosomes, Proc. Natl. Acad. Sci. USA 106 (2009) 19381–19386.

[13] A. Gennerich, A.P. Carter, S.L. Reck-Peterson, R.D. Vale, Force-induced bidirectional stepping of cytoplasmic dynein, Cell 131 (2007) 952–965.

[14] S. Toba, T.M. Watanabe, L. Yamaguchi-Okimoto, Y.Y. Toyoshima, H. Higuchi, Overlapping hand-over-hand mechanism of single molecular motility of cytoplasmic dynein, Proc. Natl. Acad. Sci. USA 103 (2006) 5741–5745.

[15] A. Kunwar, M. Vershinin, J. Xu, S.P. Gross, Stepping, strain gating, and an unexpected force-velocity curve for multiple-motor-based transport, Curr. Biol. 18 (2008) 1173–1183.

[16] A. Ashkin, K. Schutze, J.M. Dziedzic, U. Euteneuer, M. Schliwa, Force generation of organelle transport measured in vivo by an infrared laser trap, Nature 348 (1990) 346–348.

[17] G.T. Shubeita, S.L. Tran, J. Xu, M. Vershinin, S. Cermelli, S.L. Cotton, M.A. Welte, S.P. Gross, Consequences of motor copy number on the intracellular transport of kinesin-1-driven lipid droplets, Cell 135 (2008) 1098–1107.

[18] J.A. Laib, J.A. Marin, R.A. Bloodgood, W.H. Guilford, The reciprocal coordination and mechanics of molecular motors in living cells, Proc. Natl. Acad. Sci. USA 106 (2009) 3190–3195.

[19] T.M. Watanabe, H. Higuchi, Stepwise movements in vesicle transport of HER2 by motor proteins in living cells, Biophys. J. 92 (2007) 4109–4120.

[20] C. Leduc, F. Ruhnow, J. Howard, S. Diez, Detection of fractional steps in cargo movement by the collective operation of kinesin-1 motors, Proc. Natl. Acad. Sci. USA 104 (2007) 10847–10852.

[21] B.C. Carter, M. Vershinin, S.P. Gross, A comparison of step-detection methods: How well can you do? Biophys. J. 94 (2008) 306–319.

[22] J.E. Martinez, M.D. Vershinin, G.T. Shubeita, S.P. Gross, On the use of *in vivo* cargo velocity as a biophysical marker, Biochem. Biophys. Res. Commun. 353 (2007) 835–840.
[23] S. Klumpp, R. Lipowsky, Cooperative cargo transport by several molecular motors, Proc. Natl. Acad. Sci. USA 102 (2005) 17284–17289.
[24] B.M. Paschal, R.A. Obar, R.B. Vallee, Interaction of brain cytoplasmic dynein and MAP2 with a common sequence at the C terminus of tubulin, Nature 342 (1989) 569–572.
[25] L.A. Lopez, M.P. Sheetz, Steric inhibition of cytoplasmic dynein and kinesin motility by MAP2, Cell Motil. Cytoskeleton 24 (1993) 1–16.
[26] R. Dixit, J.L. Ross, Y.E. Goldman, E.L. Holzbaur, Differential regulation of dynein and kinesin motor proteins by tau, Science 319 (2008) 1086–1089.
[27] J. Ha, K.W. Lo, K.R. Myers, T.M. Carr, M.K. Humsi, B.A. Rasoul, R.A. Segal, K.K. Pfister, A neuron-specific cytoplasmic dynein isoform preferentially transports TrkB signaling endosomes, J. Cell Biol. 181 (2008) 1027–1039.
[28] J.R. Kardon, R.D. Vale, Regulators of the cytoplasmic dynein motor, Nat. Rev. Mol. Cell Biol. 10 (2009) 854–865.
[29] K.T. Vaughan, R.B. Vallee, Cytoplasmic dynein binds dynactin through a direct interaction between the intermediate chains and p150Glued, J. Cell Biol. 131 (1995) 1507–1516.
[30] J.P. Caviston, J.L. Ross, S.M. Antony, M. Tokito, E.L. Holzbaur, Huntingtin facilitates dynein/dynactin-mediated vesicle transport, Proc. Natl. Acad. Sci. USA 104 (2007) 10045–10050.
[31] J. Niclas, V.J. Allan, R.D. Vale, Cell cycle regulation of dynein association with membranes modulates microtubule-based organelle transport, J. Cell Biol. 133 (1996) 585–593.
[32] S.G. Addinall, P.S. Mayr, S. Doyle, J.K. Sheehan, P.G. Woodman, V.J. Allan, Phosphorylation by cdc2-CyclinB1 kinase releases cytoplasmic dynein from membranes, J. Biol. Chem. 276 (2001) 15939–15944.
[33] P.S. Vaughan, J.D. Leszyk, K.T. Vaughan, Cytoplasmic dynein intermediate chain phosphorylation regulates binding to dynactin, J. Biol. Chem. 276 (2001) 26171–26179.
[34] M.A. Welte, S.P. Gross, M. Postner, S.M. Block, E.F. Wieschaus, Developmental regulation of vesicle transport in *Drosophila* embryos: Forces and kinetics, Cell 92 (1998) 547–557.
[35] P.J. Hollenbeck, The pattern and mechanism of mitochondrial transport in axons, Front. Biosci. 1 (1996) d91–d102.
[36] K.S. Larsen, J. Xu, S. Cermelli, Z. Shu, S.P. Gross, BicaudalD actively regulates microtubule motor activity in lipid droplet transport, PLoS One 3 (2008) e3763.
[37] M.J. Muller, S. Klumpp, R. Lipowsky, Tug-of-war as a cooperative mechanism for bidirectional cargo transport by molecular motors, Proc. Natl. Acad. Sci. USA 105 (2008) 4609–4614.
[38] A.G. Hendricks, E. Perlson, J.L. Ross, H.W. Schroeder 3rd, M. Tokito, E.L. Holzbaur, Motor coordination via a tug-of-war mechanism drives bidirectional vesicle transport, Curr. Biol. 20 (2010) 697–702.
[39] S.P. Gross, M.A. Welte, S.M. Block, E.F. Wieschaus, Coordination of opposite-polarity microtubule motors, J. Cell Biol. 156 (2002) 715–724.
[40] V. Rodionov, J. Yi, A. Kashina, A. Oladipo, S.P. Gross, Switching between microtubule- and actin-based transport systems in melanophores is controlled by cAMP levels, Curr. Biol. 13 (2003) 1837–1847.
[41] S.P. Gross, Y. Guo, J.E. Martinez, M.A. Welte, A determinant for directionality of organelle transport in *Drosophila* embryos, Curr. Biol. 13 (2003) 1660–1668.
[42] M.A. Welte, S. Cermelli, J. Griner, A. Viera, Y. Guo, D.H. Kim, J.G. Gindhart, S.P. Gross, Regulation of lipid-droplet transport by the perilipin homolog LSD2, Curr. Biol. 15 (2005) 1266–1275.
[43] S.L. Bullock, D. Ish-Horowicz, Conserved signals and machinery for RNA transport in *Drosophila* oogenesis and embryogenesis, Nature 414 (2001) 611–616.

[44] E. Colin, D. Zala, G. Liot, H. Rangone, M. Borrell-Pages, X.J. Li, F. Saudou, S. Humbert, Huntingtin phosphorylation acts as a molecular switch for anterograde/retrograde transport in neurons, EMBO J. 27 (2008) 2124–2134.
[45] D. Splinter, M.E. Tanenbaum, A. Lindqvist, D. Jaarsma, A. Flotho, K.L. Yu, I. Grigoriev, D. Engelsma, E.D. Haasdijk, N. Keijzer, J. Demmers, M. Fornerod, F. Melchior, C.C. Hoogenraad, R.H. Medema, A. Akhmanova, Bicaudal D2, dynein, and kinesin-1 associate with nuclear pore complexes and regulate centrosome and nuclear positioning during mitotic entry, PLoS Biol. 8 (4) (2010) e1000350.

In this chapter

7

Composition and Assembly of Axonemal Dyneins

Stephen M. King
Department of Molecular, Microbial, and Structural Biology, University of Connecticut Health Center, Farmington, CT, USA

7.1 Introduction

Axonemal dyneins form the inner and outer arms that are associated with doublet microtubules within cilia and flagella. Specifically, these enzymes are permanently attached to the A-tubule of the outer doublets and transiently interact in an ATP-dependent manner with the B-tubule of the adjacent doublet. The axoneme contains multiple different motors that have distinct functions in ciliary/flagellar beating; this variation derives from different motor components (heavy chains (HCs))[1] as well as from distinct arrays of associated proteins that are involved in targeting and regulation. In general, axonemal dyneins can be classified based on whether they contain either a single or multiple motor units [1]. The inner-arm system consists of a differentially organized array of monomeric motors as well as a dimeric motor complex, which are arranged in a complicated 96 nm repeating pattern. The number of motor units associated with outer-arm dyneins appears to vary depending on a deep phylogenetic division [2,3]. In unikonts (organisms with a single flagellum), which includes mammals and sea urchins, the outer arm contains two distinct HCs, whereas in bikonts (such as green algae, excavates, and

[1]**A cautionary note about nomenclature**. *It is extremely important to recognize that the currently employed nomenclatures for axonemal dynein components are historically based on biochemical studies that date to the early 1980s before sequence data was available. These naming schemes derived from how proteins migrated during SDS-PAGE and consequently are specific to each particular organism. Thus, although* Chlamydomonas *and sea urchin outer-arm dyneins contain several very similar LCs these were originally assigned completely different designations due to electrophoretic variations and/or the total number of LCs evident. For example, the ubiquitous LC now termed DYNLL1/2 in mammals is known as LC8 in* Chlamydomonas *and LC6 in sea urchin. Furthermore, when cloned from* Drosophila *and* Saccharomyces cerevisiae *the orthologous proteins were assigned as DDLC1 and SLC1, respectively. To add further complexity, in* Chlamydomonas *outer-arm dynein, LC1 is a leucine-rich repeat (LRR) protein whereas in the sea urchin* Anthocidaris, *a Tctex1 was assigned as LC1. Similar confusion surrounds the naming of many other axonemal dynein components including the HCs.*

Dyneins DOI: 10.1016/B978-0-12-382004-4.10007-X
Copyright © 2012 by Elsevier Inc. All rights reserved.

chromalveolates) outer-arm dyneins incorporate a third HC motor. This chapter discusses the composition of axonemal dyneins and the roles of individual components, their phylogenetic variation, and the mechanisms by which they are assembled in the cytoplasm.

7.2 Classes of Dynein Components

Detailed study of axonemal and cytoplasmic dyneins has revealed several distinct classes of component, some of which are specifically found only in particular dynein subtypes (Fig. 7.1 and 7.2A,B). Dyneins that contain a single HC motor unit have a relatively simple array of additional components that includes a single molecule of actin and either an essential light chain (LC) (termed p28, p29, or p33 depending on the species) or the Ca^{2+}-binding protein centrin [4,5]. At least in *Chlamydomonas*, one monomeric inner arm also contains two larger components (p38 and p44) that are thought to be involved in attachment to the A-tubule [6]. For dyneins containing multiple HCs (Fig. 7.1 and 7.2A,B) there is a core group of conserved components that includes at least two intermediate chains (ICs) that contain C-terminal WD-repeat β-propeller structures [7–11] and LCs belonging to the DYNLL/LC8, DYNLT/Tctex1, and DYNLRB/LC7/Roadblock families [12–15]. Furthermore, additional ICs and LCs are present in various forms that appear to transduce regulatory

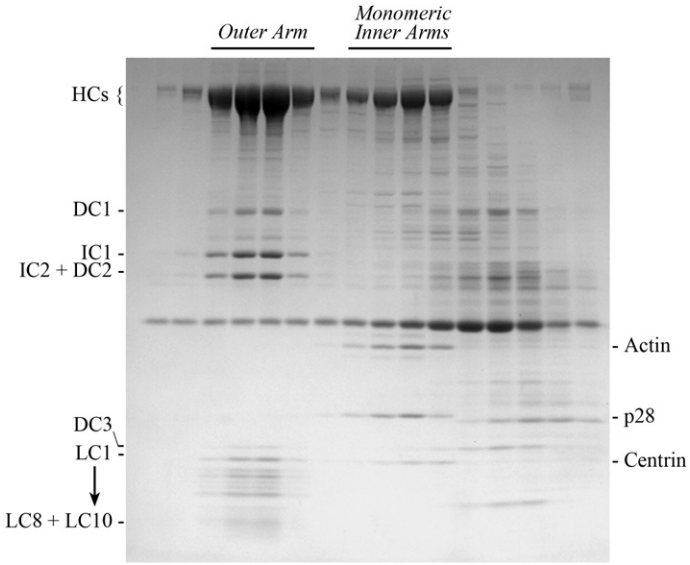

Figure 7.1 Electrophoretic analysis of axonemal dyneins. Sucrose density gradient purification of outer-arm dynein and monomeric inner-arm dyneins from flagella of a *Chlamydomonas* mutant (*ida1*) lacking inner arm I1/f: this strain was used as the I1/f and outer-arm dynein peaks partially overlap. The bottom of the sucrose gradient is at the left. The locations at which the various components migrate in this 5–15% acrylamide gradient SDS gel are indicated. *Modified from [123] © 2005 by the American Society for Cell Biology.*

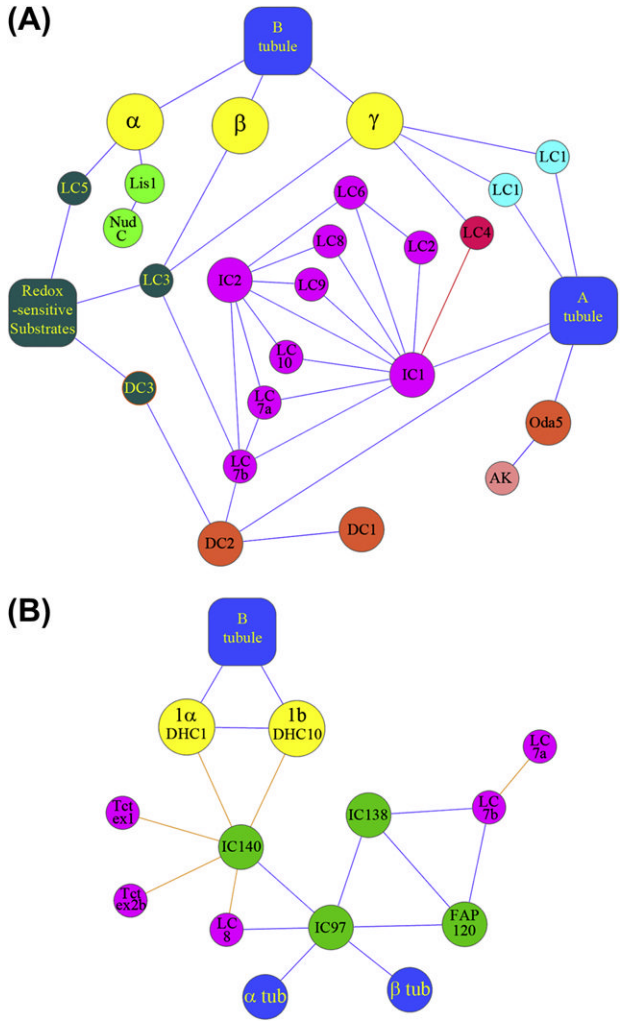

Figure 7.2 Interaction maps for outer-arm dynein and inner dynein arm I1/f. (A) Interaction map for the *Chlamydomonas* outer dynein arm. Associations for which there is direct experimental evidence are indicated by solid blue lines; the red line indicates an interaction between LC4 and IC1 that occurs only in the presence of Ca^{2+}. The various outer-arm components are color-coded: HCs, yellow; redox-sensitive components, dark green; IC–LC complex, purple; docking complex, orange; motor-domain-associated LCs, light blue; Ca^{2+}-sensitive LC, red; adenylate kinase, pink; A and B tubules of the outer doublets, blue. Note that LC6, LC8, LC9, and LC10 are homodimeric. Close examination reveals some surprising features. For example, there is little evidence to indicate whether the HCs interact with each other or how they are actually attached to the remainder of the complex. In addition, the LC3 thioredoxin appears to occupy a key position in the network and has been demonstrated to interact with three different integral dynein components as well as various currently unidentified redox-sensitive substrates. Redrawn and modified from [34] © 2010 Wiley-Liss, Inc. (B) Interaction map for inner-arm dynein I1/f. The components are color-coded as follows: HCs, yellow; ICs and FAP120, green; LCs, purple; B tubule and α- and β-tubulin, blue. Interactions for which there is direct experimental evidence are indicated by blue lines whereas interactions that are less certain are shown in orange.

signals that impinge on specific dyneins (e.g. [16–23]). Interestingly, the light-intermediate chains (LICs) present in both canonical cytoplasmic dynein [24] and the dynein that powers retrograde intraflagellar transport (IFT) [25] have not been identified associated with integral axonemal dynein motors. Finally, it has become clear that axonemal outer-arm dyneins require various "docking complex" components, many of which contain large segments of coiled-coil structure, in order to be targeted and assembled at the correct location within the axoneme [26–30]. In some organisms such as *Chlamydomonas*, these additional components readily dissociate from the motors during purification [26], whereas for others (e.g. *Ciona* and *Salmo*) they remain tightly bound [30,31]. Thus, many of the apparent differences in composition seen during dynein purifications from various organisms may actually be ascribed to variations in the stability of dyneins and their associated components during high salt extraction from the axoneme and/or subsequent purification steps.

Interestingly, electron microscopy of axonemes from a broad array of species combined with recent genomic studies reveals that some motile axonemes have dispensed with either the outer or inner rows of dynein arms. For example, the genome of the bryophyte *Physcomitrella* does not encode outer-arm dynein proteins but has a full complement of inner-arm components and other axonemal substructures [32]. In contrast, there are cases such as the centric diatom *Thalassiosira* where inner arms have been lost in addition to radial spokes and the central-pair microtubule complex [33]. Thus, these axonemes contain only outer dynein arms but retain the ability to beat. This finding has been used to bolster the hypothesis that the outer- and inner-arm systems are regulated by different intrinsic mechanosensory mechanisms ([34] and Section 7.11.2).

7.3 Monomeric Inner Dynein Arms

Biochemical studies have revealed that certain dyneins within the flagellum act as monomeric motors and have a distinct complement of associated proteins including actin and either an essential LC (termed p28 in *Chlamydomonas*) or the calcium-binding calmodulin homolog centrin [4,5,35]; certain HCs are associated with additional components as well (Table 7.1) [6,36]. Genomic studies have now complemented these initial efforts and revealed that *Chlamydomonas* axonemes contain 10 different members of this monomeric motor class whereas *Tetrahymena* expresses 18 (Table 7.2) [37]. This large expansion in the inner-arm dynein repertoire of *Tetrahymena* may reflect the presence of two ciliary types with distinctive motile properties in this organism. These dyneins are not only differentially arranged along the ciliary/flagellar length [38,39] but distinct complements of monomeric motors are also present on the various doublet microtubules [40] (see Chapter 8). Although the functional consequences of these complex assembly patterns are unclear at present, they presumably reflect specific requirements for generating particular waveforms. Furthermore, the AAA rings of

Table 7.1 Integral Components of *Chlamydomonas* Inner-Arm Dyneins*

Inner-Arm Dynein	Protein	Description	Number of Residues	Mass (kDa)	Stoichiometry per Dynein Complex	Protein Accession Number
a	DHC6	ATPase/motor	3553[1]	397[1]	1	XP_001700741
	Actin	Monomeric; required for assembly	377	42	1	P53498
	p28	Dimer; required for assembly	253	29	2	Q39604
b	DHC5	ATPase/motor	3299[1]	368[1]	1	XP_001699742
	Actin	Monomeric; not essential: can be replaced by NAP (see below)	377	42	1	P53498
	Centrin	Binds Ca^{2+}	169	19	1	P05434
c	DHC9	ATPase/motor required for motility under high viscous load	4149	465	1	BAE19786
	Actin	Monomeric; required for assembly	377	42	1	P53498
	p28	Dimer; required for assembly	253	29	2	Q39604
d	DHC2	ATPase/motor	4069	457	1	XP_001694660
	p44	Contains TPR repeats; associates only with dynein d	408	44	1	BAF98914
	Actin	Monomeric; required for assembly	377	42	1	P53498
	p38	Associates only with dynein d	380	41	1	BAG07147
	p28	Dimer; required for assembly	253	29	2	Q39604
e	DHC8	ATPase/motor	3241[1]	362[1]	1	XP_001692092
	Actin	Monomeric; required for assembly	377	42	1	P53498
	Centrin	Binds Ca^{2+}	169	19	1	P05434
f (I1)	DHC1 (1α)	ATPase/motor	4625	523	1	Q9SMH3
	DHC10 (1β)	ATPase/motor	4513	510	1	Q9MBF8
	IC140	WD-repeat protein	1024	110	1	AAD45352
	IC138	WD-repeat phosphoprotein	1057	111	1	AAU93505
	IC97	FAP94; Las1 homolog	550	90	1	EDP03678
	FAP120	Ankyrin repeat protein	294	32	1	EDP07339
	Tctex1	DYNLT1 and outer-arm LC9 homolog	114	12	1	AAC18035
	Tctex2b	Tctex2 and outer-arm LC2 homolog	120	14	1	DAA05278
	LC7a	DYNLRB/Roadblock homolog; also present in outer arm	105	12	1	AAD45881
	LC7b	DYNLRB/Roadblock homolog; also present in outer arm	100	11	1	EDP03034
	LC8	Highly conserved; also present in outer-arm retrograde IFT dynein and radial spokes; essential for assembly	91	10	2	Q39580

(Continued)

Table 7.1 Integral Components of *Chlamydomonas* Inner-Arm Dyneins[*]—cont'd

Inner-Arm Dynein	Protein	Description	Number of Residues	Mass (kDa)	Stoichiometry per Dynein Complex	Protein Accession Number
g	DHC7	ATPase/motor	3540[1]	399[1]	1	XP_001692695
	Actin	Monomeric; not essential: can be replaced by NAP (see below)	377	42	1	P53498
	Centrin	Binds Ca^{2+}	169	19	1	P05434
Alternative component						
b/g	NAP	Novel actin-related protein; can replace actin in dyneins b and g	380	41	1	AAC49834
Minor dynein HCs whose associations have not been defined[2]						
Not assigned	DHC3	ATPase/motor[3]			5353(estimate)	n.d.[4]
1						
Not assigned	DHC4	ATPase/motor	Unknown	n.d.	1	
Not assigned	DHC11	ATPase/motor	Unknown	n.d.	1	
Not assigned	DHC12	ATPase/motor	Unknown	n.d.	Unknown	

[*] *This table was adapted and modified from [1].*

[1] *These dynein HC sequences are incomplete as they have highly truncated N-terminal domains.*

[2] *Based on HC abundance in mutant axonemes, all three HCs are thought to interact with actin, whereas DHC3 and DHC4 likely associate with centrin and DHC11 with p28 [39].*

[3] *This dynein is estimated to be ~100 kDa larger than DHC1 due to a series of insertions within AAA domains 2, 5, and 6, and within the C-terminal segment [39].*

[4] *Not determined as complete sequence is uncertain.*

Table 7.2 Inner-Arm Dynein Orthologs[1]

Dynein	Chlamydomonas reinhardtii	*Anthocidaris crassispina*	*Tetrahymena thermophila*	*Homo sapiens*
Inner arm I1/f	DHC1 (1a)	DNAH10	DYH6	DNAH10
	DHC10 (1b)	DNAH2	DYH7	DNAH2
	IC140	XP_780818[2]	IC5	IC140, WD63 (NYD-SP29)
	IC138	–	IC6	IC138, WD78 (predicted)
	IC97	XP_001176114; similar to p83.9 isoform 1[2]	TTHERM_00437360 (predicted)	CASC1 (LAS1)
	Tctex1	LC3?	Tctex1A or Tctex1B	DYNLT1 or DYNLT3
	Tctex2b	Tctex2	LC2B	TCX2(Tctex2)
	LC7a / LC7b	XP_001186907[1]; similar to light polypeptide 2A[2]	LC7A/LC7B	DYNLRB1 or DYNLRB2
	LC8	LC6	LC8	DYNLL1 or DYNLL2
Monomeric HCs, group 3[3]	DHC4, DHC5, DHC6, DHC8, DHC9, DHC11	DNAH3, DNAH4, DNAH7, DNAH12	DYH10, DYH12, DYH13, DYH25[1](DYH8, DYH11, DYH14, DYH17 also related)	DNAH3, DNAH7, DNAH12
Monomeric HCs, group 4[3]	DHC2	DNAH1	DYH9, DYH16, DYH19, DYH20, DYH21	DNAH1
Monomeric HCs, group 5[3]	DHC3, DHC7	DNAH6, DNAH14	DYH15, DYH18, DYH22, DYH23, DYH24	DNAH6, DNAH14
Unassigned HCs[3]	DHC12 (aka 206178)	–	–	–
	Actin	Actin	Actin	Actin
	Centrin	Centrin	Centrin	Centrin
	p28	p33	p28A, p28B, p28C	p28

[1] *This tabulation derives from phylogenies described in [1,3,15,37,164] and from BLAST searches of the NCBI databases.*
[2] *Predicted from the genome sequence of the sea urchin* Strongylocentrotus purpuratus.
[3] *The equivalence of the various monomeric inner-arm HCs is uncertain and so they are listed here by group as defined in [3,37,164].*

these dynein motors are arrayed at a variety of angles with respect to the microtubule long axis [41]. This suggests that their powerstroke may not occur directly along the axonemal long axis but may also contain an off-axis vector. Indeed, this concept is supported by the observation that, when examined using an *in vitro* microtubule-gliding assay, many of these dyneins generate torque that causes the unloaded microtubules to rotate as they translocate [42].

7.4 Dimeric Inner Dynein Arm I1/f

Dimeric inner dynein arm I1/f contains two distinct HC motors and plays a key role in the regulation of axonemal motility. The complete composition of this dynein is presented in Table 7.1 and the equivalent proteins present in sea urchins, *Tetrahymena*, and humans are indicated in Table 7.2 [43]. A map of the various interactions is shown in Figure 7.2B. Mutants that lack this dynein exhibit

slow swimming due to alterations in flagellar waveform that result in a less efficient beat [44]. There is one copy of the I1/f dynein located within each 96 nm axonemal repeat and both HCs are necessary for its assembly [45,46]. *In vitro*, these individual HCs and the intact motor translocate microtubules only very slowly (1.5–3.0 μm/s) [45–47], which is somewhat surprising given that microtubule sliding in axonemes can proceed at rates up to ~20 μm/s. One model that presents a possible solution to this conundrum is that the I1/f dynein may act as a brake to locally limit the rate of sliding in an ATP-dependent manner rather than actually driving the motility *per se* [48]; a similar activity has also been proposed for the function of one HC within the outer arm [22].

7.5 Outer Dynein Arms

Functional analysis has revealed that the outer arms provide much (perhaps as much as 80%) of the power generated during flagellar beating. Consequently, cilia/flagella that lack these structures beat significantly more slowly than wild type [49,50], and thus defects in the outer arms are a major cause of primary ciliary dyskinesia (PCD) in humans (see Chapter 24). In all organisms examined to date, outer arms contain multiple – either two (e.g. mammals and sea urchins) or three (e.g. *Chlamydomonas* and *Tetrahymena*) – HCs associated with two WD-repeat ICs, a core set of LCs, and coiled-coil proteins involved in assembly within the axoneme [51–56]. Furthermore, outer arms contain additional components (depending on the species examined) that act in various signaling pathways to control motor function [22,23,57–61]. The interaction map of *Chlamydomonas* outer-arm dynein is shown in Figure 7.2B, its composition is detailed in Table 7.3, and the names of orthologous components from other species are shown in Table 7.4. Experiments that have used mechanical activation to induce flagellar beating in a variety of paralyzed mutant strains suggest that axonemes contain a dedicated mechanosensory system that allows outer-arm dyneins to respond to alterations in curvature [62]. Intriguingly, analysis of *Chlamydomonas* flagella beating under varying viscous loads has revealed that outer-arm-less strains are incapable of increasing flagellar power output in response to an increase in solution viscosity (Fig. 7.3) [63]. This suggests that outer-arm dyneins contain a system that senses mechanical strain and allows the motors to compensate for increased load.

7.6 Inter-Dynein Linkers

Cryo-electron microscope (cryo-EM) tomography has revealed that axonemal dyneins are connected *in situ* via a series of linker structures that interconnect the outer arms to each other and also every fourth outer arm to inner arm I1/f [64]. Although the role of these linkages remains uncertain, they potentially provide a direct signaling conduit to allow for coordination of motor activity. The leucine-rich repeat (LRR) protein ODA7 has been proposed as a component of the inner-arm–outer-arm dynein linker based on biochemical studies [65]. Lack of this

Table 7.3 Integral Components of *Chlamydomonas* Outer-Arm Dynein*

Protein	Description	Number of Residues	Mass (kDa)	Stoichiometry per Outer-Arm Complex	Protein Accession Number
α HC	ATPase/motor; kelch repeat domain at N-terminus	4499	504	1	Q39610
β HC	ATPase/motor; essential for assembly	4568	520	1	Q39565
γ HC	ATPase/motor; essential for assembly	4485	513	1	Q39575
IC1	WD repeats; essential for assembly	683	76	1	Q39578
IC2	WD repeats; essential for assembly	567	63	1	P27766
LC1	LRR protein; mechano-sensor	198	22	2	AAD41040
LC2	Tctex2 homolog	136	16	1	AAB58383
LC3	Thioredoxin	156	17	1	Q39592
LC4	Calmodulin homolog; specifically binds Ca^{2+} with high affinity	159	18	1	Q39584
LC5	Thioredoxin	129	14	1	Q39591
LC6	LC8 homolog	120	14	2	Q39579
LC7a	DYNLRB/Roadblock homolog; also present in inner arm I1/f	105	12	1	AAD45881
LC7b	DYNLRB/Roadblock homolog; also present in inner arm I1/f	100	11	1	EDP03034
LC8	Highly conserved; also present in inner arm I1/f, retrograde IFT dynein, and radial spokes; essential for assembly	91	10	4	Q39580
LC9	DYNLT1 homolog	117	13	2	AAZ95589
LC10	LC8 homolog	103	12	2	EDP00562
DC1	Coiled-coil protein	749	83	1	AAC49732
DC2	Coiled-coil protein	552	62	1	AAK72125
DC3	Calmodulin homolog; binds Ca^{2+} with high affinity and Mg^{2+} with low affinity	184	21	1	AAP49435
ODA5	Coiled-coil protein	652	66	Unknown	AAS10183
Lis1	WD-repeat protein; homolog of cytoplasmic dynein regulator lacking dimerization domain	347	37	<1 in wild-type flagella but enhanced in flagella with radial spoke/central pair defects[1]	ABG33844

** This table was adapted and modified from [1].*

[1] P. Rompolos and S.M. King, unpublished results.

Table 7.4 Outer-Arm Dynein Orthologs[1]

Chlamydomons reinhardtii	*Anthocidaris crassispina*	*Tetrahymena thermophila*	*Homo sapiens*
α HC	Not present	DYH5 (γ HC)	Not present
β HC	β HC	DYH4 (β HC)	DNAH9, DNAH11, DNAH17
γ HC	α HC	DYH3 (α HC)	DNAH5, DNAH8
Not present[2]	IC1	Not present	TXNDC3 (Sptrx2)
IC1	IC2	IC2	DNAI1
IC2	IC3	IC3	DNAI2
LC1	LC2	LC1	DNAL1
LC2	LC1	LC2A	TCTE3 (Tctex2)
LC3	Not present[3]	LC3-likeA/LC3-likeB	Not present[4]
LC4	Not present	LC4A/LC4B	Not present
LC5	Not present[3]	Not present	Not present[4]
LC6	Not present	Uncertain	Not present
LC7a/LC7b	XP_001186907; similar to light polypeptide 2A[e]	LC7A / LC7B	DYNLRB1 or DYNLRB2
LC8	LC6	LC8	DYNLL1 or DYNLL2
LC9	LC3	Tctex1A or Tctex1B	DYNLT1 or DYNLT3
LC10	LC4	LC10	DNAL4

[1] *This tabulation derives from phylogenies described in [1,3,15,37,164]. The coiled-coil docking complex proteins are not included as their equivalence across species is uncertain at present [30].*
[2] *Thioredoxin-related modules in LC3/LC5. No NDK modules are present in this dynein.*
[3] *Related thioredoxin module present in IC1.*
[4] *Related thioredoxin module present in TXNDC3.*
[5] Predicted from the genome sequence of the sea urchin *Strongylocentrotus purpuratus.*

protein results in the complete failure of outer-arm assembly; however, the linker occurs on only one outer arm in every four. When dyneins are re-bound to microtubules *in vitro*, they assemble in long continuous arrays, indicating a significant level of cooperativity [66]. Thus, although it remains uncertain why ODA7 is needed for assembly of all outer arms, a single missing arm within every repeat may be sufficient to disrupt the overall pattern of sequential incorporation.

7.7 Properties and Organization of Axonemal Dynein Motor Units

Each HC consists of an N-terminal domain that is highly specific for individual enzymes and a motor unit that has the general composition of four AAA domains

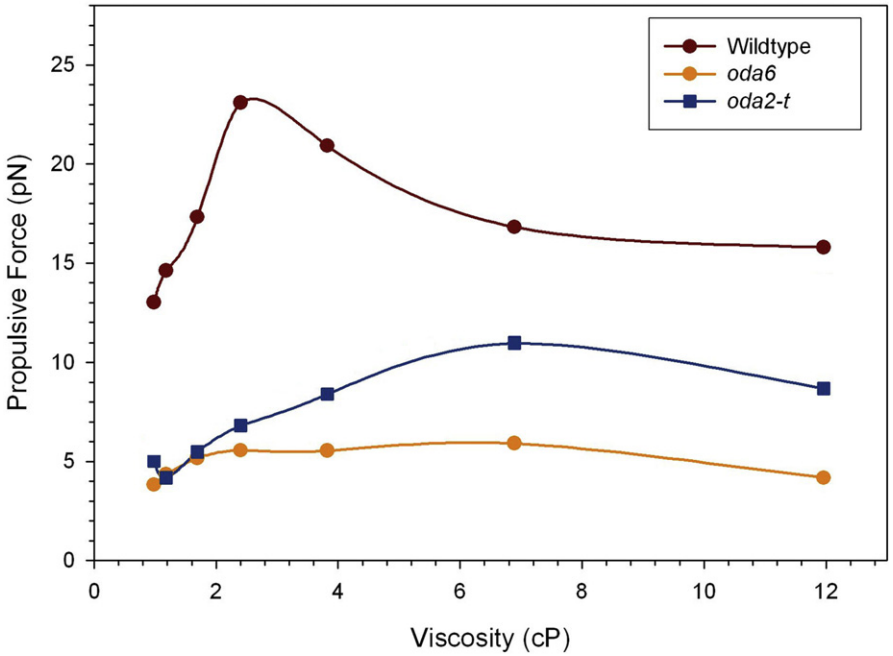

Figure 7.3 Outer-arm dyneins increase propulsive force under high viscous load. This plot illustrates how the propulsive force generated by the two flagella of *Chlamydomonas* varies under increasing viscous load conditions imposed by the addition of Ficoll to the medium. As viscosity increases, wild-type cells are able to almost double the flagellar force output over the range of ~1.5–3.0 cP. In contrast, this response is completely missing in a mutant (*oda6*) that lacks outer dynein arms. This illustrates that the outer- and inner-arm systems have distinct capacities for force generation. Interestingly, another mutant (*oda2-t*) that lacks only the motor domain of the γ HC and the associated LC1 proteins behaves like an outer-arm-less strain under low viscous load but tends towards wild-type behavior as the viscosity increases. These data are from [22].

followed by two regions of coiled coil bracketing the microtubule-binding domain (MTBD), two additional degenerate AAA domains, and a final C-terminal unit [67–72]; the organization of the N-terminal regions of the three *Chlamydomonas* outer-arm HCs and the generic structure of the C-terminal motor unit are indicated in Figure 7.4. What has previously been considered as the N-terminal region includes not only segments involved in binding ICs, LCs, and other components, but also the region near AAA1 is now recognized to be of key importance for the motor mechanism as it contains the linker/neck regions that traverse the plane of the AAA ring and actually mediate the powerstroke [73–77]. One key defining feature of the oligomeric axonemal dynein motors is that, unlike canonical cytoplasmic dyneins, they consist of heterodimers or heterotrimers of HCs with very distinct sequences and functional attributes rather than being homodimers of apparently identical motor proteins. This diversity reflects the growing body of evidence that suggests that these individual HCs play very distinctive roles in motility.

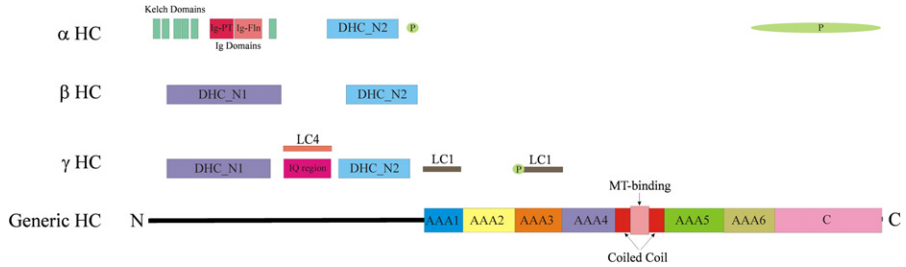

Figure 7.4 Domain organization of *Chlamydomonas* outer-arm HCs. The generic organization of dynein HC domains within the motor unit is illustrated in the lower portion of the figure. This region consists of six AAA domains forming a hexameric ring structure, a MTBD at the tip of an anti-parallel coiled-coil stalk, and a C-terminal unit that traverses the plane of the AAA ring. The N-terminal domains exhibit considerable variation in organization. Two generic domains have been identified within the N-terminal regions. One (DHC_N1) appears to coincide with a segment proposed to mediate HC–HC interactions and the second (DHC_N2) with the hinge/linker region that is key to the powerstroke mechanism. Also illustrated are sites of phosphorylation (green labeled P), the IQ motif region, and kelch and Ig domains. The segments involved in binding both LC1 and LC4 are also indicated; although the LC3 and LC5 thioredoxins bind the N-terminal regions of the β and α HCs, respectively, the precise interaction sites are unclear.

The β HC of sea urchin outer-arm dynein acts as an ATP-dependent motor that provides much of the power for flagellar beating, although it cannot form a stable rigor bond with microtubules *in vitro* [78]. In contrast, the α HC of this dynein mediates the ATP-dependent formation of microtubule bundles and can form both structural (ATP-independent) and rigor bond attachments [79]. Similarly, in *Chlamydomonas*, the β HC is essential for outer-arm function and a mutant (*oda4-s7*) lacking only the motor domain of this component has a motility phenotype comparable to that of strains that lack the entire complex [80]. A related mutant strain (*oda2-t*) that is missing the γ HC motor unit (this HC is equivalent to the sea urchin α HC) also exhibits significant motility defects, indicating that both functions are required for efficient axonemal beating [81]. The motor domain of this HC is tethered to the outer doublet A-tubule via the LC1 protein and it is thus conceivable that this HC acts as an ATP-dependent brake rather than a motor *in situ* [22]. This latter hypothesis is supported by the observation that dynein lacking this HC motor unit and LC1 translocates microtubules *in vitro* at a rate faster than wild type [82]. The equivalent HC in mammals (Dnahc5) is also important for normal motility, and mutations in this gene can result in structural defects in heart development and other phenotypes associated with PCD [83].

The *Chlamydomonas* α HC, which is located towards the axonemal perimeter, appears less essential for both assembly and motility, as a mutant lacking this component incorporates a full complement of outer arms and swims only slightly more slowly than wild type [84]. However, analysis of ATP-dependent microtubule binding of mutant dyneins lacking various HC combinations led to the suggestion that the α HC may act in a regulatory pathway that controls the function of the other HCs [58]. Biochemical analysis of these mutant dyneins *in*

vitro determined that dyneins lacking this particular HC have an increased basal ATPase but a dramatically decreased microtubule gliding velocity, suggesting that mechanochemical coupling has been disrupted [82]. Intriguingly, this HC has a very distinctive N-terminal region that is not found in any other HC from that organism and is separated from the rest of the protein by multiple degenerate copies of the motif EPAA; a related region is present in one HC of *Plasmodium* [1,70]. Specifically, the first ~1000 residues of this HC are predicted to form a β-propeller structure from a series of kelch repeats and contain two subdomains formed from Ig-like motifs; both these subdomains must protrude to the same side of the propeller [1]. What distinctive functions this region of the α HC performs remain uncertain.

Distinct regions of the N-terminal region of the mammalian cytoplasmic dynein HC have been identified as being involved in HC—HC and HC—IC interactions [85]. Surprisingly, although such interactions (as well as HC-regulatory LC associations) must still occur in the axonemal enzymes, with the exception of the binding site for a *Chlamydomonas* calmodulin homolog on the γ HC [86] there is no good evidence indicating the regions involved.

7.8 Core WD-Repeat Intermediate Chains Associated with Oligomeric Motors

All oligomeric dynein motors include two ICs (Fig. 7.5) that contain WD-repeat β-propellers — a toroidal structure consisting of interlocking repeats each forming a series of four β strands. In cytoplasmic dyneins these ICs are apparently identical in some organisms (e.g. yeast and fungi), although mammals contain several distinct but closely related IC genes and generate multiple isoforms through alternative splicing that are expressed in a tissue-specific manner [87,88]. In contrast, oligomeric axonemal dynein ICs contain distinctive WD repeats and highly divergent N- and C-terminal extensions [7,8,10,11]. As the first and last WD repeats within a β-propeller interact, the N- and C-terminal regions must actually be located close together, which has implications for the association of various LCs and other components. For example, studies on several different dyneins suggest that the LC7/roadblock LCs may interact with IC regions either N-terminal or C-terminal [10,89] of the WD segment; however, as these sections must be spatially close, it is likely that the LCs actually bind both.

The WD-repeat ICs play a key role in dynein assembly and function. In *Chlamydomonas*, null mutants for outer-arm IC1 or IC2 result in the complete failure of dynein assembly [7,8]. Similarly, mutations in the human DNAI2 gene lead to PCD through the disruption of outer-arm assembly [90]. Although complete lack of IC140 in inner arm I1/f is also highly disruptive, surprisingly, genetic and biochemical studies have revealed that a large N-terminal segment of IC140 is

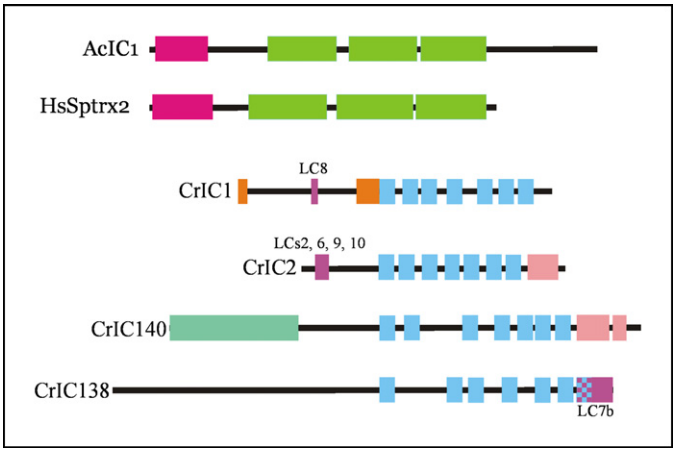

Figure 7.5 Organization of ICs. Maps of outer-arm dynein ICs are shown two modular at top. The upper IC (837 residues) derives from the sea urchin *Anthocidaris crassispina* and consists of an N-terminal thioredoxin module (red) followed by three catalytic NDK domains (green). Similar proteins (e.g. *Homo sapiens* Sptrx2) are present in the dyneins of mammals. The lower four maps detail WD-repeat ICs from *Chlamydomonas reinhardtii* axonemal dyneins (CrIC1, CrIC2, CrIC140, CrIC138). The seven repeats within each protein that fold to form toroidal β-propellers are indicated in blue. Other features include coiled-coil domains (pink), microtubule-binding regions (dark orange), and a segment of IC140 that is apparently non-essential (green). Also shown are LC binding sites (magenta) for which there is experimental evidence or that are predicted based on analysis of other dyneins. The outer-arm proteins (IC1 and IC2) and inner arm I1/f IC140 are all required for assembly whereas IC138 is not.

dispensable for assembly [91]. At least within the outer arm, there is direct biochemical evidence that the two ICs interact directly [92,93].

In the outer-arm dynein ICs, the N-terminal IC regions interact with a complex array of LC dimers that appear to be necessary to mediate IC–IC interactions. Although the current models would suggest that all these LCs are arranged in a linear fashion [1], some are clearly more important for assembly, stability, and/or regulation than others. For example, lack of the LC8 dimer leads to the failure of arm assembly [94] whereas strains lacking the close homologs LC6 or LC10 both assemble considerable numbers of outer arms but have other, more subtle, defects [95]. Why this is so and how these LCs differentially modulate dynein IC assembly and activity remains uncertain.

The WD-repeat ICs are also directly involved in motor regulation. In inner-arm I1/f, IC138 is the key phosphoprotein that is modified in response to signals derived from the radial spokes/central pair complex and plays an essential role in controlling motor function [17]. Phosphorylation of IC138 by casein kinase 1 and/or protein kinase A leads to an inactive I1-dynein motor [96]. In contrast, dephosphorylation by protein phosphatases 1 and 2A reverses the effect (see Chapter 11 for a detailed analysis of this regulatory pathway). What remains unclear though is precisely how phosphorylation of this component is

transduced to the HCs so as to lead to altered motor function. In contrast to IC140, lack of IC138 does not result in the failure of I1/f assembly although the IC97 component (see Section 7.9) is not incorporated.

Both outer-arm dynein IC2 and IC140 from inner arm I1/f have C-terminal coiled-coil domains that presumably bind other axonemal components. The targets of these domains have not been ascertained.

7.9 Additional Intermediate Chains

In addition to WD-repeat-containing ICs, some dyneins have been found to include an intriguing and diverse array of other IC components. Some of these are coiled-coil proteins homologous to the docking complex proteins DC1 and DC2 and the ODA5 protein required for outer-arm dynein assembly in *Chlamydomonas*. The key difference between these dyneins appears to be simply that in *Chlamydomonas* association of the assembly factors with the core motor is sensitive to disruption by high ionic strength and/or high hydrostatic pressure, whereas in dyneins from other organisms these coiled-coil proteins remain tightly associated. Consequently, these components are described in Section 7.12.

Outer-arm dynein from sea urchin sperm flagella contains a modular protein (termed here suIC1) that consists of an N-terminal thioredoxin unit followed by three nucleoside diphosphate kinase (NDK) catalytic domains (Fig. 7.5) [16,97]. This protein is tightly associated with the sea urchin β HC and copurifies with that motor. Similar proteins (Sptrx-1 and Txl-1) have been identified in mammals, indicating that the requirement for a dynein-associated NDK spans a broad phylogenetic range [98]. Intriguingly, although *Chlamydomonas* outer-arm dynein contains thioredoxins, NDKs are not directly associated with this motor; rather a calcium-dependent NDK (RSP23) is located within the radial spokes [99]. Phylogenetic analysis suggests that the RSP23 NDK domain is most closely related to human nm23-H7. Axonemes from both *Chlamydomonas* and mammals also contain an additional NDK (nm23-H5 in humans) that is tightly associated with the doublet microtubules [99]. Thus, although there is strong evidence for multiple catalytically functional NDKs in axonemes (e.g. [100]), the reason why in some organisms one of these enzymes is outer-arm-associated, whereas in others there is a module present in the radial spokes remains unclear. Genetic evidence that these modular proteins play an important role in dynein function came from the observation that mutations that affect alternative splicing and reduce the levels of a thioredoxin-NDK protein (TXNDC3) in humans result in PCD [101].

A third non-WD-repeat class of dynein ICs has been identified in the dimeric inner arm I1/f in *Chlamydomonas*. This protein, termed IC97, does not contain obvious structural motifs that would provide a clue as to its precise function. Intriguingly, however, IC97 is homologous to the mammalian protein LAS1, which is present in axonemes and has been implicated in murine lung tumor formation. IC97 can

be directly crosslinked to both α and β-tubulin, suggesting that it may act as a dynein attachment factor [102]. However, this protein is missing from the IC138 truncation mutant *bop5*, which still assembles this dynein, and so IC97 cannot be essential for inner arm I1/f assembly [102]. IC97 appears to play a central role in the I1/f dynein as it interacts directly with at least five other components (see Fig. 7.2B) and acts in the control of interdoublet microtubule sliding.

7.10 Core Light Chains Associated with Oligomeric Motors

Three sets of LCs (originally termed the LC8, Tctex1, and LC7/Roadblock families) fall into this category and form groups that in mammals are now termed DYNLL, DYNLT, and DYNLRB, respectively [103,104]. Although not obviously similar at the sequence level, the first two groups are actually closely related at the structural level, whereas the DYNLRB class is quite distinct (see Chapter 5 for detailed discussion of the structural biology of these proteins). These LC groups are present in both cytoplasmic and oligomeric axonemal dynein isoforms and in some cases have also been found associated with a broad array of unrelated cellular enzymes and systems. They are all important in dynein assembly and associate with ICs, and most occur as dimers; there is also evidence to suggest that control of dimerization of some of these proteins through differential phosphorylation may be employed to regulate assembly of these complex motors [105].

7.10.1 The DYNLL/LC8 Group

In axonemal dyneins, three distinct groupings within the DYNLL class have been identified (LC6, LC8, and LC10 in *Chlamydomonas*) [12,95]. Two of these (LC8 and LC10) have been highly conserved over a very broad phylogenetic range whereas the third species (LC6) has to date been identified only in *Chlamydomonas*. Intriguingly, the *Tetrahymena* genome encodes multiple additional LC8-related proteins, one of which is distantly grouped with LC6 [15]. As DYNLL1 and DYNLL2 (the mammalian equivalents of *Chlamydomonas* LC8) occur in multiple essential enzyme systems including cytoplasmic dynein [106], myosin V [107], neuronal nitric oxide synthase [108], and many others, lack of these proteins in multicellular organisms results in highly pleitropic phenotypes and leads to lethality [109]. In contrast, LC8 null mutants in the unicellular alga *Chlamydomonas*, which lacks canonical cytoplasmic dynein 1, exhibit only a flagellar phenotype but grow and divide at normal rates [94].

Null mutants have been identified for all three of these dynein proteins and each yields a distinct ciliary/flagellar phenotype in *Chlamydomonas*. LC8 is found in at least four flagellar complexes (outer arms, inner arm I1/f, radial spokes, and the dynein that powers IFT) [12,13,94,110]. Thus, the LC8 mutant *fla14* has a complex phenotype that includes the failure of axonemal dynein and radial spoke assembly and the formation of only small flagellar stubs due to the

inhibition of retrograde IFT. As a consequence, *fla14* cells are immotile. This analysis clearly demonstrates that LC8 is absolutely required for dynein assembly.

Mutant strains lacking LC6 and LC10 have more subtle defects. LC6 is 41% identical to LC8 and contains an extended N-terminal region and a seven-residue insertion in a loop prior to the β strand segment. The *oda13* strain completely lacks LC6 [111], assembles a normal complement of outer arms, and exhibits a beat frequency only slightly reduced from the wild-type rate [112]. LC6 is known to interact directly with LC2 [113].

The gene for the third member of this group (LC10) is located close to the *ODA12* locus, which encodes the LC2 outer-arm LC [95]. The *oda12-1* mutant lacks both these genes and exhibits a beat frequency that is less than that observed in strains (such as oda1) that completely lack outer arms. When this strain was rescued with a plasmid containing only the LC2 gene, beat frequency returned to near-wild-type levels. Thus, lack of LC10 alone is only slightly disruptive, whereas in combination with the loss of LC2 it results in a phenotype more disruptive than the complete failure of outer-arm assembly. This might result either from residual outer arms missing these components acting in a dominant negative manner (essentially as a brake) or possibly through alterations in feedback to the inner-arm system. In mammals, LC10 is known as DNAL4 and is present in cilia from a variety of tissues and in sperm [95]. Surprisingly, DNAL4 is very highly expressed compared to other axonemal dynein genes in many tissues during embryogenesis; it is also prominently expressed in the hippocampus of the brain. This has raised the possibility that in some organisms LC10/DNAL4 plays additional roles unrelated to its function in the axoneme.

7.10.2 The DYNLT/LC9/Tctex1/Tctex2 Group

Members of this LC group were originally identified in mammalian cytoplasmic dynein [114] and subsequently found in oligomeric axonemal dyneins [13,112,115–118]. Prior to this, these proteins had been suggested as potential "distorters" involved in the non-Mendelian segregation of *t* haplotypes in mice [119,120] (see Chapter 21 for detailed discussion of this fascinating phenomenon). Four members of this LC group are present in axonemal dyneins; two are monomeric Tctex2-like proteins and two are dimeric Tctex1 relatives. Both outer arms and inner arm I1/f contain a single Tctex2 (LC2 and Tctex2b in *Chlamydomonas*) and a Tctex1 dimer (termed LC9 and Tctex1 in *Chlamydomonas*). In mammals, canonical Tctex1 is shared by both cytoplasmic and axonemal dyneins, whereas Tctex2 appears to be mainly axoneme-specific although there is some immunological evidence to suggest that a subgroup of cytoplasmic dyneins may also contain this protein [113].

No mutants are currently available that are solely missing either of the Tctex1-related proteins and thus their precise functional role within oligomeric axonemal dyneins remains uncertain. However, these proteins are known to associate with

the N-terminal regions of the WD-repeat ICs present in these dyneins. Furthermore, analysis of the LCs assembled in a *Chlamydomonas* pseudorevertant strain (*oda6-r88*) that expresses an IC2 outer-arm protein with an internal sequence alteration of 23 residues [121] revealed that LC9 (along with LC2 and LC6) fail to assemble but that all other components do [112]. Thus, these three LCs are likely to all bind IC2 via sites located within this small N-terminal region.

In *Drosophila*, homozygous defects in Tctex1 (this appears to be the closest homolog to the Tctex1 in *Chlamydomonas* inner arm I1/f) lead to male sterility but not to any obvious decrease in viability [117]. Thus, these observations suggest that Tctex1 proteins indeed play an essential role in dynein function *per se* and/or in the assembly and development of sperm flagella.

In contrast, *Chlamydomonas* strains lacking either outer-arm LC2 or inner arm I1/f Tctex2b are available [115,122]. The *TCTEX2b* gene is located close to *PF16* (which encodes a component of the central-pair microtubule complex) and both genes were found to be completely missing in a strain (*pf16-D2*) generated by insertional mutagenesis that exhibits paralyzed flagella. When this strain was rescued with a cloned genomic fragment containing both wild-type genes, flagellar swimming velocity and beat frequency were restored to wild-type levels. In contrast, when the *PF16* gene was restored but *TCTEX2b* was not, a residual swimming phenotype was observed, suggesting that Tctex2b is indeed required for wild-type inner arm I1/f function. This prediction was confirmed using *in vitro* axoneme sliding disintegration assays, which revealed that lack of Tctex2b reduced microtubule-sliding velocity [115].

The outer-arm Tctex2 protein (LC2 in *Chlamydomonas*) is encoded at *ODA12* [122]. Two alleles are available: one (*oda12-1*) is a complete null for both LC2 and the adjacent gene, which encodes the LC10 outer-arm component (see Section 7.10.1). The second allele (*oda12-2*) lacks only the 3′ end of the LC2 gene and expresses wild-type levels of LC10. Although *oda12-2* axonemes still retain outer arms, this strain exhibits a beat frequency that is approximately the same as that of those that completely lack these motors. This strongly suggests that LC2 is a key player in controlling the function of the outer arm. More surprisingly, the *oda12-1* strain lacking both LC2 and LC10 also assembles at least some outer arms but has a beat frequency that is worse than strains with no outer arms at all. The most likely explanation is that these LC2/LC10-defective motors act in a dominant negative fashion to inhibit motility driven by the inner-arm system.

Further evidence that Tctex2 proteins are important in the control of outer-arm motor function came from analysis of the orthologous protein in salmonid fish and sea urchin sperm [23]. In sperm from these organisms, Tctex2 is phosphorylated in a cAMP-dependent manner during activation of sperm motility. This of course is consistent with the proposed involvement of Tctex2 in control of murine sperm motility (see Chapter 21).

7.10.3 The DYNLRB/LC7/Roadblock Group

The role of this protein class in axonemal dyneins has to date been explored only in *Chlamydomonas* [14,123]. This organism expresses two members of this group (LC7a and LC7b) and both are present in outer-arm dynein and in inner arm I1/f at a stoichiometry of one per complex. Although significantly depleted in outer-arm-less mutants, both proteins are only completely absent from double mutants that lack both dyneins [123]. Structural studies indicate that mammalian DYNLRB proteins [124] are dimeric and so presumably LC7a/LC7b form heterodimers, although this has not been demonstrated directly. Lack of LC7a in the *oda15* mutant results in a reduced number of outer arms assembled but a swimming phenotype similar to that seen for a complete loss of these structures. Furthermore, dyneins isolated from the *oda15* strain are much more labile and dissociate readily; this includes LC7b, which can be obtained as the free LC. In addition to interactions between LC7a and LC7b, and association of both LCs with the ICs, LC7b appears to be a central component of the outer-arm complex, as crosslinking revealed that it binds directly to the LC3 thioredoxin and also to the coiled-coil protein DC2, which is part of the outer-arm docking complex.

7.11 Regulatory Components

In order to achieve a coordinated beat, axonemal dynein function must be precisely coordinated so that individual motors with specific motor properties act at appropriate times to generate forward and reverse bends and to propagate those bends along the axonemal length. Furthermore, in some systems, additional controls must determine whether flagella beat with a simple oscillatory motion or switch to a more complex asymmetric beat pattern. Multiple regulatory mechanisms that lead to motor regulation have been uncovered in a variety of organisms. Some of these involve the direct binding of ligands, whereas others are mediated through post-translational modifications or via alterations in direct protein–protein interactions. A systems diagram of the various inputs, effectors, motors, and functional outputs for the *Chlamydomonas* outer arm is shown in Figure 7.6. Further discussion of these regulatory systems and the evidence supporting inter-HC control of motor and ATPase activity is presented in Chapter 10.

7.11.1 Phosphorylation

Multiple dynein components are subject to reversible phosphorylation; however, the particular target depends on the species of origin and the dynein subtype. For example, in the *Chlamydomonas* outer arm the α HC is modified at a minimum of six sites, which are all located near the AAA1 domain or in the C-terminal unit (note these regions are potentially close together in the final folded structure) [125]. There is also mass spectrometry evidence for modification of the outer-arm γ HC at one site [126]. Within the inner-arm system, many

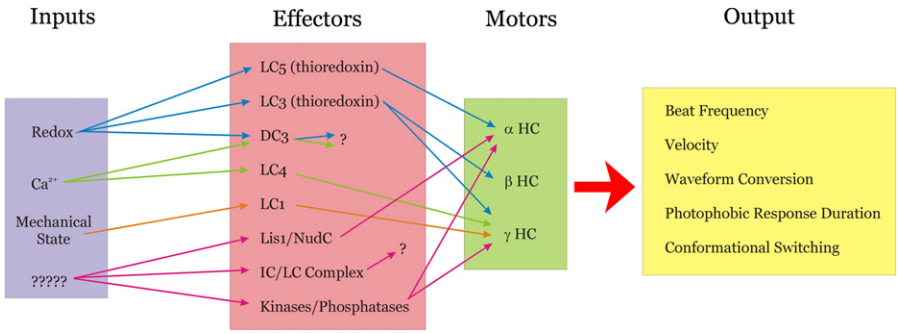

Figure 7.6 Systems analysis of outer-arm dynein regulation. The regulatory pathways impinging on the *Chlamydomonas* outer dynein arm are subdivided into inputs, effectors, motors, and outputs. Although it is not yet completely clear how variations in motor function lead to altered physiological outputs, recent studies have started to uncover details of how these complex systems are integrated at the molecular level and suggest that the γ HC represents a key regulatory node (e.g. [34]). For example, the mechanical state of the axoneme appears to be sensed by a tripartite system consisting of the microtubule, LC1, and the γ HC and to allow for conformational switching. However, whether these effects are mediated solely through the γ HC or are propagated to the other motor units remains uncertain. Similarly, Ca^{2+} binding to LC4 (and possibly also DC3) leads to an alteration in conformation of the γ HC N-terminal domain and results in waveform conversion from an asymmetric to a symmetric beat pattern.

(perhaps most) of the monomeric motors are heavily phosphorylated *in vivo* [127] and the IC138 component of inner arm I1/f is also hyperphosphorylated and intimately involved in the control of flagellar beating [17] (see Chapter 11). However, in this organism no LCs have been found to be modified even after continuous growth in medium containing radioactive phosphate for several days [125]. In contrast, LC phosphorylation has been described in *Paramecium* [21], sea urchin, and *Ciona* sperm [23]. The *Paramecium* LC (termed p29) is phosphorylated in a cAMP-dependent manner. This modification results in an increase in microtubule gliding velocity *in vitro*, suggesting that LC phosphorylation regulates motor output [57].

7.11.2 Motor Domain Tethering

A LRR protein that interacts with the motor domain of one outer-arm HC is a highly conserved feature of dynein design. There is an N-terminal helical segment followed by six LRRs, which form a barrel structure, and a terminal helical domain, which protrudes from the major axis [128]. In *Chlamydomonas*, two copies of this protein (termed LC1) associate with the AAA1 and AAA3 or AAA4 units [129]. Furthermore, crosslinking and immunoelectron microscopy revealed that LC1 also interacts directly with tubulin within the A-tubule of the axonemal outer doublets and thus tethers the AAA ring of the γ HC to that microtubule [22]. Expression of various mutant forms of LC1 in wild-type *Chlamydomonas* led to only minor changes in beat frequency but dramatic reduction in swimming velocity. More detailed analysis revealed that the two flagella beat almost

completely out of phase, leading to a rocking forward motion. This was caused by the flagella randomly stalling for a few milliseconds at or near the switch point governing the power/recovery stroke transition. RNA interference (RNAi) of LC1 in trypanosomes resulted in a variety of phenotypes including an alteration in swimming direction due to a change in the direction of flagella beating, failure of some dynein arms to assemble, and misorientation of the central apparatus [61]. More recently, knockdown of LC1 in planaria has been found to reduce beat frequency, cause cilia to randomly stall during the beat cycle, and inhibit the formation of metachronal waves [130]. These observations have led to the suggestion that the LC1-γ HC-microtubule ternary complex acts as a conformational switch that alters outer-arm dynein function in response to variations in curvature. Such an outer-arm-specific mechanosensor was initially proposed based on the observation that various paralyzed mutant flagella could be induced to beat following mechanical activation [62].

7.11.3 Ca^{2+} Binding

Axonemal dyneins must respond to alterations in Ca^{2+} concentration that ultimately result in changes in waveform [131,132]. A subset of inner-arm dyneins is associated with centrin [5], which binds Ca^{2+} with high affinity within four EF hand motifs [133,134]. No centrin null mutants have been obtained (as they likely result in lethality) and thus the precise role of centrin in dynein assembly and Ca^{2+} regulation remains uncertain. A centrin mutant strain (VFL2) has defects in basal body positioning and cytokinesis although no specific effects on inner-arm function have been noted [135]. RNAi strains that still make some protein exhibit basal body deficiencies, which is consistent with the presence of centrin in basal body-associated fibers [136]. However, vfl2 has been reported to exhibit aberrant phototaxis [133,137] but normal flagellar reversal during the photoshock response [138]. In *Tetrahymena*, addition of Ca^{2+} to centrin-containing dynein preparations increased the rate of microtubule translocation *in vitro* [139].

In *Chlamydomonas*, a second Ca^{2+} binding calmodulin homolog (termed LC4) is associated with the N-terminal region of the γ HC [20,52]. LC4 binds 1–2 Ca^{2+} ions with an affinity of ~$3\times10-5$ M [20]. This affinity would be appropriate for detecting the change in intraflagellar Ca^{2+} from 10^{-6} to 10^{-4} M that signals the photophobic response which involves a change in waveform and consequent reversal of swimming direction [140]. LC4 interacts with the HC via two distinct sites, only one of which is Ca^{2+} sensitive, and indeed appears to control the conformation of this HC domain in a ligand-dependent manner [86]. In the absence of Ca^{2+}, isolated γ HC particles have a relatively rigid N-terminal domain that includes a kink with an angle of ~120^{o} located about two thirds of the way along its length. However, in the presence of Ca^{2+} this region becomes much more flexible and the angle measured following negative-stain electron microscopy much more variable. Given that recent structural studies suggest that this HC domain is key to the proposed winch mechanism [74–77], this

ligand-induced structural alteration may have profound implications for force generation by the γ HC motor unit.

Within the *Chlamydomonas* outer-arm γ HC, there are two IQ motifs that are predicted to bind calmodulin or related proteins [86]. This region is clearly involved in the association of LC4 (which is 42% identical to calmodulin) [86]. However, as there is a 1:1 stoichiometry between this HC and LC4, the possibility remains that the γ HC also binds soluble calmodulin present in the flagellar matrix under certain conditions; this hypothesis has not yet been explored experimentally.

A different calcium-binding component has been identified in outer-arm dynein from *Ciona*; orthologs are also present in the genomes of various metazoans but not *Chlamydomonas*. This 25 kDa protein (termed calaxin) contains three EF hands potentially capable of binding Ca^{2+} ions, and also can be directly cross-linked to β-tubulin [141].

7.11.4 Redox Sensors

Outer-arm dyneins from diverse organisms have been found to contain one or more components that are redox-sensitive [16,19,142,143]. The outer arms, but not inner arms, can even be purified based on their affinity for trivalent arsenic, as proteins containing vicinal dithiols form a covalent dithioarsine ring that can be disrupted by dithiol-reducing agents such as dithiothreitol [19]. Thioredoxin modules have been found either as individual LCs associated with HC N-terminal domains (e.g. *Chlamydomonas*) [19] or as part of multi-domain proteins consisting of an N-terminal thioredoxin followed by several NDK catalytic domains (sea urchins and chordates) [16,101,142]. Redox state has also been shown to be important for activation of mammalian sperm [144]. Furthermore, reversible sulfhydryl oxidation activates outer-arm ATPase activity [59]. Together these observations led to the hypothesis that dynein function might be controlled based on the redox balance of the ciliary/flagellar cytoplasm. This was tested directly by manipulating redox poise in live cells by the addition of oxidizing agents or membrane-permeable reactive oxygen species scavengers [60]. The observed alterations in flagellar beat frequency could also be mimicked using reactivated cell models where the redox state was defined by the ratio of oxidized:reduced glutathione buffers. For wild-type *Chlamydomonas* cell models, beat frequency was greatest under reducing conditions and decreased significantly as conditions became more oxidizing. Importantly, this response was essentially absent from a strain that completely lacked outer dynein arms. In addition, the response was substantially modified in a strain that lacked one HC and its associated thioredoxin LC. Specifically, this strain had a beat frequency less than wild type under reducing conditions, but greater than wild type when placed in an oxidizing environment. Biochemical analysis suggested that these redox-sensitive dynein proteins form mixed disulfides with multiple different partners within the flagellum and that these

partners change depending on the redox state. However, the identity of these transient dynein-associated components remains to be determined. Furthermore, reduction in the expression of the thioredoxin/NDK TXNDC3 in humans results in PCD [101], again emphasizing the important role played by these dynein components.

In *Chlamydomonas*, the DC3 component of the docking complex (see Section 7.12) is also redox-sensitive [143]. In this calmodulin-related protein, Ca^{2+} binding by one EF-hand motif is modulated depending on whether two Cys residues located within the ligand binding site are in the reduced state or have been oxidized to form a disulfide. Although the role of Ca^{2+} binding to DC3 remains uncertain, these observation do suggest that these two signaling systems are integrated at the level of individual dynein motors.

7.12 Docking Motors onto the Axoneme

In order for dyneins to assemble at the correct location within the axoneme, there must be components that direct the assembly process to specific sites. Within outer-arm dyneins a series of coiled-coil proteins have been identified in several organisms that fulfill this role although the precise manner in which they achieve this is still the subject of considerable debate. In *Chlamydomonas*, this docking structure consists of the DC1 and DC2 proteins and their associated calmodulin homolog DC3 [26–28,145,146]. Re-binding of dynein onto various mutant axonemes revealed that the docking complex also plays a key role in the beat frequency imbalance that is observed between the two flagella in wild-type cells and demembranated cell models [147]. The ODA5 protein is also essential for assembly, contains multiple coiled-coil segments, and interacts with an adenylate kinase [29]; genetic studies support an association of ODA5 with both ODA8 and ODA10 proteins [148], although this has yet to be confirmed. During some extraction/purification schemes, these *Chlamydomonas* proteins dissociate from the core motor (e.g. [52]). However, if care is taken to keep the imposed hydrostatic pressure to a minimum and to also include Mg^{2+}, then the docking complex remains associated with all three outer-arm HCs and their ancillary components [26,149]. In contrast, in outer-arm dyneins from other organisms (e.g. *Ciona* and *Salmo*) these proteins remain tightly associated [31,142]. In *Ciona*, three proteins related to *Chlamydomonas* DC2 have been identified, one of which (Ci-Axp66.0) is present in substoichiometric levels following outer-arm purification [142]. The variations in association of these coiled-coil docking components seen in dyneins from different organisms appear to reflect altered sensitivities of the *in situ* complex for various chemical and physical treatments. For example, it has become clear that both hydrostatic pressure (from ultracentrifugation) and lack of Mg^{2+} in the buffers can lead to disruption of dynein complexes [149].

7.13 Other Dynein-Associated Components

The ODA7 protein is a member of the SDS22 subgroup of the LRR family (as is LC1) containing six repeats [65] and was initially identified in *Chlamydomonas* from mutant studies that determined that the gene product is essential for outer-arm assembly [148]. Strains defective for the *oda7* gene contain approximately normal levels of most outer-arm dynein components within the cytoplasm [150]. However, intriguingly, the α HC is completely absent from the cytoplasm of these cells, suggesting that ODA7 protein is involved in stabilizing and/or incorporating this HC into the complex during cytoplasmic pre-assembly. Most ODA7 protein resides in the cytoplasm; however, fractionation experiments revealed that it does associate with both the outer arm and inner arm I1 [65] and it has been proposed to form the linker identified by cryo-EM tomography that spans these structures [64]. Four families with loss-of-function defects in the human ortholog of ODA7 (termed LRRC50) resulting in outer-arm assembly defects and PCD have been identified [151,152]. Intriguingly, LRRC50-deficient patients also lack inner arms, whereas these structures remain unaffected in *Chlamydomonas*.

A protein (Ap58) containing tetratricopeptide repeats has been identified as potentially interacting with outer-arm dyneins from the sea urchin *Anthocidaris crassispina* [153]. This protein is extracted from axonemes under high salt conditions and is also arrayed along the doublet microtubules with a spacing of ~25 nm reminiscent of assembled outer arms. However, Ap58 does not co-purify with outer-arm dynein in sucrose density gradients or following gel filtration. The potential role of this protein in dynein assembly and function remains to be ascertained. Another TPR protein is associated with inner dynein arm d but again its role is unclear [36].

The lissencephaly protein Lis1 was initially identified as associated with cytoplasmic dynein function in fungi and was subsequently found to be a key regulator of the mammalian enzyme [154,155] (see Chapters 16 and 17). Further studies in mice revealed that Lis1 is present in motile cilia in the trachea and oviduct, but is apparently completely absent from immotile primary or sensory cilia [156]. The orthologous protein in *Chlamydomonas* was also found to be present in flagella and to be completely absent from strains lacking either the entire outer dynein arm or the outer-arm α HC [156]. There are two pools of Lis1 in flagella: one is detergent-soluble and the second is axoneme-associated. In wild-type flagella, Lis1 is present in substiochiometric amounts compared to the outer arms. However, intriguingly, the levels of Lis1 are significantly enhanced in flagella of several strains that exhibit poor or no motility as they are lacking other axonemal substructures (i.e. radial spokes and the central-pair microtubule complex). This suggests that Lis1 levels within the flagellum are actively monitored and adjusted in response to a currently unknown signal [157].

7.14 Pathways of Axonemal Dynein Assembly and Transport

Although axonemal dyneins function in cilia/flagella, these complex multicomponent enzymes are assembled in the cytoplasm and then transported into the cilium. Initial evidence for this came from the analysis of the assembly state of outer-arm dynein components in the cytoplasm of *Chlamydomonas* mutants defective for various dynein proteins and assembly factors [150]. No assembly of the outer-arm HCs and ICs with the β HC was observed in the cytoplasm of strains lacking IC1, IC2, or the γ HC. In contrast, the core motor was completely assembled in the absence of the docking complex or ODA5 proteins. Two strains revealed partial cytoplasmic assembly with the β HC: *oda11* lacking the α HC and *oda7*, which occurs mainly in cytoplasm but is also devoid of the α HC. Oda7 is a LRR protein that is present in axonemes [65]. Fractionation experiments revealed that it is associated with both outer arms and inner arm I1/f, but is substiochiometric compared to the bulk dynein; most of this protein resides in the cell body. One possibility is that this protein forms part of the linker that joins these two dyneins together. An alternative view is that Oda7 is a cytoplasmic assembly factor that is mostly dissociated from the dynein complexes prior to their transport into the cilium [65].

Additional cytoplasmic assembly factors for axonemal dyneins have recently been described; both are members of the PIH group, which interact with heat-shock family proteins. One protein encoded by the *kintoun*(*ktu*) gene was identified in medaka following a mutant screen and also in humans with PCD [158]. In addition, the *Chlamydomonas* ortholog was found to be encoded at *PF13* defects in which result in the failure of both outer and inner dynein arm assembly [158,159]. The Ktu/*PF*13 protein was found to bind both dyneins and Hsp70, leading to the hypothesis that it acts as a co-chaperone to aid dynein assembly in cytoplasm. A second PIH protein (MOT48) that is encoded at the *IDA10* locus was identified as being required for the assembly of a subset of monomeric inner dynein arms, including dyneins b, c, d, and e, but not for outer arm or inner arm I1/f assembly [160]. Bioinformatics analysis has identified several additional PIH domain proteins in *Chlamydomonas* and indicates that these PIH proteins are present only in organisms that bear motile cilia [160]. Furthermore, one of the uncharacterized *Chlamydomonas* PIH proteins appears to be homologous to the TWISTER protein in zebrafish defects in which leads to polycystic kidneys and morphogenetic abnormalities [161].

Further mutant analysis in *Chlamydomonas* revealed that an additional protein encoded at ODA16 is required for transport of outer-arm dyneins into the flagellum [162]. This protein interacts directly with IFT46, which is part of the IFT complex B and is thought to act essentially as a cargo adaptor for outer-arm transport [163].

7.15 Conclusions

Genetic and biochemical studies in a variety of model organisms have revealed the enormously complex nature of axonemal dyneins. This complexity presumably underlies subtle requirements for particular motor activities and also allows for the integration of various signaling pathways to impinge on motor function in response to particular cellular cues. Although most of the core dynein components have now been identified, there still remain challenges, especially as regards defining inner arms that are present in very low amounts and in identifying proteins that only transiently interact with the *in situ* arms.

Acknowledgments

I thank Dr Toshiki Yagi (University of Tokyo) for his assistance with the phylogeny of inner-arm dynein HC sequences. My laboratory is supported by grant GM51293 from the National Institutes of Health.

References

[1] S.M. King, R. Kamiya, Axonemal dyneins: Assembly, structure and force generation, in: G.B. Witman (Ed.), second ed, The *Chlamydomonas* Sourcebook, vol. 3, Elsevier, San Diego, 2009, pp. 131–208.

[2] T. Cavalier-Smith, The phagotrophic origin of eukaryotes and phylogenetic classification of protozoa, Int. J. Syst. Evol. Micr. 52 (2002) 297–354.

[3] B. Wickstead, K. Gull, Dyneins across eukaryotes: A comparative genomic analysis, Traffic 8 (2007) 1708–1721.

[4] O. Kagami, R. Kamiya, Translocation and rotation of microtubules caused by multiple species of *Chlamydomonas* inner-arm dynein, J. Cell Sci. 103 (1992) 653–664.

[5] G. Piperno, Z. Ramanis, E.F. Smith, W.S. Sale, Three distinct inner dynein arms in *Chlamydomonas* flagella: Molecular composition and location in the axoneme, J. Cell Biol. 110 (1990) 379–389.

[6] R. Yamamoto, H. Yanagisawa, T. Yagi, R. Kamiya, A novel subunit of axonemal dynein conserved among lower and higher eukaryotes, FEBS Lett. 580 (2006) 6357–6360.

[7] D.R. Mitchell, Y. Kang, Identification of *oda6* as a *Chlamydomonas* dynein mutant by rescue with the wild-type gene, J. Cell Biol. 113 (1991) 835–842.

[8] C.G. Wilkerson, S.M. King, A. Koutoulis, G.J. Pazour, G.B. Witman, The 78,000 $M_{(r)}$ intermediate chain of *Chlamydomonas* outer arm dynein is a WD-repeat protein required for arm assembly, J. Cell Biol. 129 (1995) 169–178.

[9] K. Ogawa, R. Kamiya, C.G. Wilkerson, G.B. Witman, Interspecies conservation of outer arm dynein intermediate chain sequences defines two intermediate chain subclasses, Mol. Biol. Cell 6 (1995) 685–696.

[10] T.W. Hendrickson, C.A. Perrone, P. Griffin, K. Wuichet, J. Mueller, P. Yang, M.E. Porter, W.S. Sale, IC138 is a WD-repeat dynein intermediate chain required for light chain assembly and regulation of flagellar bending, Mol. Biol. Cell 15 (2004) 5431–5442.

[11] P. Yang, W.S. Sale, The M_r 140,000 intermediate chain of *Chlamydomonas* flagellar inner arm dynein is a WD-repeat protein implicated in dynein arm anchoring, Mol. Biol. Cell 9 (1998) 3335–3349.

[12] S.M. King, R.S. Patel-King, The $M_{(r)} = 8{,}000$ and 11,000 outer arm dynein light chains from *Chlamydomonas* flagella have cytoplasmic homologues, J. Biol. Chem. 270 (1995) 11445–11452.

[13] A. Harrison, P. Olds-Clarke, S.M. King, Identification of the *t* complex-encoded cytoplasmic dynein light chain Tctex1 in inner arm I1 supports the involvement of flagellar dyneins in meiotic drive, J. Cell Biol. 140 (1998) 1137–1147.
[14] A.B. Bowman, R.S. Patel-King, S.E. Benashski, J.M. McCaffery, L.S. Goldstein, S.M. King, *Drosophila* roadblock and *Chlamydomonas* LC7: a conserved family of dynein-associated proteins involved in axonal transport, flagellar motility, and mitosis, J. Cell Biol. 146 (1999) 165–180.
[15] D. Wilkes, V. Rajagopalan, C. Chan, E. Kniazeva, A. Wiedeman, D. Asai, Dynein light chain family in *Tetrahymena thermophila*, Cell Motil. Cytoskeleton 64 (2007) 82–96.
[16] K. Ogawa, H. Takai, A. Ogiwara, E. Yokota, T. Shimizu, K. Inaba, H. Mohri, Is outer arm dynein intermediate chain 1 multifunctional? Mol. Biol. Cell 7 (1996) 1895–1907.
[17] G. Habermacher, W.S. Sale, Regulation of flagellar dynein by phosphorylation of a 138-kD inner arm dynein intermediate chain, J. Cell Biol. 136 (1997) 167–176.
[18] S.J. King, S.K. Dutcher, Phosphoregulation of an inner dynein arm complex in *Chlamydomonas reinhardtii* is altered in phototactic mutant strains, J. Cell Biol. 136 (1997) 177–191.
[19] R.S. Patel-King, S.E. Benashki, A. Harrison, S.M. King, Two functional thioredoxins containing redox-sensitive vicinal dithiols from the *Chlamydomonas* outer dynein arm, J. Biol. Chem. 271 (1996) 6283–6291.
[20] S.M. King, R.S. Patel-King, Identification of a $Ca^{(2+)}$-binding light chain within *Chlamydomonas* outer arm dynein, J. Cell Sci. 108 (1995) 3757–3764.
[21] T. Hamasaki, K. Barkalow, J. Richmond, P. Satir, cAMP-stimulated phosphorylation of an axonemal polypeptide that copurifies with the 22S dynein arm regulates microtubule translocation velocity and swimming speed in Paramecium, Proc. Natl. Acad. Sci. USA 88 (1991) 7918–7922.
[22] R.S. Patel-King, S.M. King, An outer arm dynein light chain acts in a conformational switch for flagellar motility, J. Cell Biol. 186 (2009) 283–295.
[23] K. Inaba, O. Kagami, K. Ogawa, Tctex2-related outer arm dynein light chain is phosphorylated at activation of sperm motility, Biochem. Biophys. Res. Commun. 256 (1999) 177–183.
[24] S.M. Hughes, K.T. Vaughan, J.S. Herskovits, R.B. Vallee, Molecular analysis of a cytoplasmic dynein light intermediate chain reveals homology to a family of ATPases, J. Cell Sci. 108 (1995) 17–24.
[25] Y. Hou, G.J. Pazour, G.B. Witman, A dynein light intermediate chain, D1bLIC, is required for retrograde intraflagellar transport, Mol. Biol. Cell 15 (2004) 4382–4394.
[26] S. Takada, R. Kamiya, Functional reconstitution of *Chlamydomonas* outer dynein arms from alpha- beta and gamma subunits: Requirement of a third factor, J. Cell Biol. 126 (1994) 737–745.
[27] S. Takada, C.G. Wilkerson, K. Wakabayashi, R. Kamiya, G.B. Witman, The outer dynein arm-docking complex: Composition and characterization of a subunit (Oda1) necessary for outer arm assembly, Mol. Biol. Cell 13 (2002) 1015–1029.
[28] A. Koutoulis, G.J. Pazour, C.G. Wilkerson, K. Inaba, H. Sheng, S. Takada, G.B. Witman, The *Chlamydomonas reinhardtii ODA3* gene encodes a protein of the outer dynein arm docking complex, J. Cell Biol. 137 (1997) 1069–1080.
[29] M. Wirschell, G. Pazour, A. Yoda, M. Hirono, R. Kamiya, G. Witman, Oda5p, a novel axonemal protein required for assembly of the outer dynein arm and an associated adenylate kinase, Mol. Biol. Cell 15 (2004) 2729–2741.
[30] A. Hozumi, Y. Satouh, Y. Makino, T. Toda, H. Ide, K. Ogawa, S.M. King, K. Inaba, Molecular characterization of *Ciona* sperm outer arm dynein reveals multiple components related to outer arm docking complex protein 2, Cell Motil. Cytoskeleton 63 (2006) 591–603.
[31] J.L. Gatti, S.M. King, A.G. Moss, G.B. Witman, Outer arm dynein from trout spermatozoa. Purification, polypeptide composition, and enzymatic properties, J. Biol. Chem. 264 (1989) 11450–11457.

[32] S.A. Rensing, D. Lang, A.D. Zimmer, A. Terry, A. Salamov, H. Shapiro, T. Nishiyama, P.-F. Perroud, E.A. Lindquist, Y. Kamisugi, T. Tanahashi, K. Sakakibara, T. Fujita, K. Oishi, T. Shin-I, Y. Kuroki, A. Toyoda, Y. Suzuki, S.-i. Hashimoto, K. Yamaguchi, S. Sugano, Y. Kohara, A. Fujiyama, A. Anterola, S. Aoki, N. Ashton, W.B. Barbazuk, E. Barker, J.L. Bennetzen, R. Blankenship, S.H. Cho, S.K. Dutcher, M. Estelle, J.A. Fawcett, H. Gundlach, K. Hanada, A. Heyl, K.A. Hicks, J. Hughes, M. Lohr, K. Mayer, A. Melkozernov, T. Murata, D.R. Nelson, B. Pils, M. Prigge, B. Reiss, T. Renner, S. Rombauts, P.J. Rushton, A. Sanderfoot, G. Schween, S.-H. Shiu, K. Stueber, F.L. Theodoulou, H. Tu, Y. Van de Peer, P.J. Verrier, E. Waters, A. Wood, L. Yang, D. Cove, A.C. Cuming, M. Hasebe, S. Lucas, B.D. Mishler, R. Reski, I.V. Grigoriev, R.S. Quatrano, J.L. Boore, The *Physcomitrella* genome reveals evolutionary insights into the conquest of land by plants, Science 319 (2008) 64–69.

[33] E.V. Armbrust, J.A. Berges, C. Bowler, B.R. Green, D. Martinez, N.H. Putnam, S. Zhou, A.E. Allen, K.E. Apt, M. Bechner, M.A. Brzezinski, B.K. Chaal, A. Chiovitti, A.K. Davis, M.S. Demarest, J.C. Detter, T. Glavina, D. Goodstein, M.Z. Hadi, U. Hellsten, M. Hildebrand, B.D. Jenkins, J. Jurka, V.V. Kapitonov, N. Kroger, W.W.Y. Lau, T.W. Lane, F.W. Larimer, J.C. Lippmeier, S. Lucas, M. Medina, A. Montsant, M. Obornik, M.S. Parker, B. Palenik, G.J. Pazour, P.M. Richardson, T.A. Rynearson, M.A. Saito, D.C. Schwartz, K. Thamatrakoln, K. Valentin, A. Vardi, F.P. Wilkerson, D.S. Rokhsar, The genome of the diatom *Thalassiosira pseudonana*: Ecology, evolution, and metabolism, Science 306 (2004) 79–86.

[34] S.M. King, Sensing the mechanical state of the axoneme and integration of Ca^{2+} signaling by outer arm dynein, Cytoskeleton 67 (2010) 207–213.

[35] G. Piperno, Isolation of a sixth dynein subunit adenosine triphosphatase of *Chlamydomonas* axonemes, J. Cell Biol. 106 (1988) 133–140.

[36] R. Yamamoto, H.-a. Yanagisawa, T. Yagi, R. Kamiya, Novel 44-kilodalton subunit of axonemal dynein conserved from *Chlamydomonas* to mammals, Eukaryot. Cell 7 (2008) 154–161.

[37] D.E. Wilkes, H.E. Watson, D.R. Mitchell, D.J. Asai, Twenty-five dyneins in *Tetrahymena*: A re-examination of the multidynein hypothesis, Cell Motil. Cytoskeleton 65 (2008) 342–351.

[38] G. Piperno, Z. Ramanis, The proximal portion of *Chlamydomonas* flagella contains a distinct set of inner dynein arms, J. Cell Biol. 112 (1991) 701–709.

[39] T. Yagi, K. Uematsu, Z. Liu, R. Kamiya, Identification of dyneins that localize exclusively to the proximal portion of *Chlamydomonas* flagella, J. Cell Sci. 122 (2009) 1306–1314.

[40] K.H. Bui, H. Sakakibara, T. Movassagh, K. Oiwa, T. Ishikawa, Asymmetry of inner dynein arms and inter-doublet links in *Chlamydomonas* flagella, J. Cell Biol. 186 (2009) 437–446.

[41] K.H. Bui, H. Sakakibara, T. Movassagh, K. Oiwa, T. Ishikawa, Molecular architecture of inner dynein arms *in situ* in *Chlamydomonas reinhardtii* flagella, J. Cell Biol. 183 (2008) 923–932.

[42] O. Kagami, S. Takada, R. Kamiya, Microtubule translocation caused by three subspecies of inner-arm dynein from *Chlamydomonas* flagella, FEBS Lett. 264 (1990) 179–182.

[43] M.E. Porter, W.S. Sale, The 9+2 axoneme anchors multiple inner arm dyneins and a network of kinases and phosphatases that control motility, J. Cell Biol. 151 (2000) F37–F42.

[44] R. Kamiya, E. Kurimoto, E. Muto, Two types of *Chlamydomonas* flagellar mutants missing different components of inner-arm dynein, J. Cell Biol. 112 (1991) 441–447.

[45] S.H. Myster, J.A. Knott, E. O'Toole, M.E. Porter, The *Chlamydomonas* Dhc1 gene encodes a dynein heavy chain subunit required for assembly of the I1 inner arm complex, Mol. Biol. Cell 8 (1997) 607–620.

[46] C.A. Perrone, S.H. Myster, R. Bower, E.T. O'Toole, M.E. Porter, Insights into the structural organization of the I1 inner arm dynein from a domain analysis of the 1β dynein heavy chain, Mol. Biol. Cell 11 (2000) 2297–2313.

[47] E.F. Smith, W.S. Sale, Microtubule binding and translocation by inner dynein arm subtype I1, Cell Motil. Cytoskeleton 18 (1991) 258–268.
[48] M. Wirschell, T. Hendrickson, W. Sale, Keeping an eye on I1: I1 dynein as a model for flagellar dynein assembly and regulation, Cell Motil. Cytoskeleton 64 (2007) 569–579.
[49] R. Kamiya, M. Okamoto, A mutant of *Chlamydomonas reinhardtii* that lacks the flagellar outer dynein arm but can swim, J. Cell Sci. 74 (1985) 181–191.
[50] D.R. Mitchell, J.L. Rosenbaum, A motile *Chlamydomonas* flagellar mutant that lacks outer dynein arms, J. Cell Biol. 100 (1985) 1228–1234.
[51] G. Piperno, D.J. Luck, Axonemal adenosine triphosphatases from flagella of *Chlamydomonas reinhardtii*. Purification of two dyneins, J. Biol. Chem. 254 (1979) 3084–3090.
[52] K.K. Pfister, R.B. Fay, G.B. Witman, Purification and polypeptide composition of dynein ATPases from *Chlamydomonas* flagella, Cell Motil. 2 (1982) 525–547.
[53] A.T. Hastie, S.P. Marchese-Ragona, K.A. Johnson, J.S. Wall, Structure and mass of mammalian respiratory ciliary outer arm 19S dynein, Cell Motil. Cytoskeleton 11 (1988) 157–166.
[54] S.P. Marchese-Ragona, K.C. Facemyer, K.A. Johnson, Structure of the alpha-, beta-, and gamma-heavy chains of 22 S outer arm dynein obtained from *Tetrahymena* cilia, J. Biol. Chem. 264 (1989) 21361–21368.
[55] C.W. Bell, I.R. Gibbons, Structure of the dynein-1 outer arm in sea urchin sperm flagella. II. Analysis by proteolytic cleavage, J. Biol. Chem. 257 (1982) 516–522.
[56] M. Belles-Isles, C. Chapeau, D. White, C. Gagnon, Isolation and characterization of dynein ATPase from bull spermatozoa, Biochem. J. 240 (1986) 863–869.
[57] K. Barkalow, T. Hamasaki, P. Satir, Regulation of 22S dynein by a 29-kD light chain, J. Cell Biol. 126 (1994) 727–735.
[58] M. Sakato, S. King, Calcium regulates ATP-sensitive microtubule binding by *Chlamydomonas* outer arm dynein, J. Biol. Chem. 278 (2003) 43571–43579.
[59] A. Harrison, M. Sakato, H.W. Tedford, S.E. Benashski, R.S. Patel-King, S.M. King, Redox-based control of the γ heavy chain ATPase from *Chlamydomonas* outer arm dynein, Cell Motil. Cytoskeleton 52 (2002) 131–143.
[60] K. Wakabayashi, S.M. King, Modulation of *Chlamydomonas reinhardtii* flagellar motility by redox poise, J. Cell Biol. 173 (2006) 743–754.
[61] D.M. Baron, Z.P. Kabututu, K.L. Hill, Stuck in reverse: loss of LC1 in *Trypanosoma brucei* disrupts outer dynein arms and leads to reverse flagellar beat and backward movement, J. Cell Sci. 120 (2007) 1513–1520.
[62] K. Hayashibe, C. Shingyoji, R. Kamiya, Induction of temporary beating in paralyzed flagella of *Chlamydomonas* mutants by application of external force, Cell Motil. Cytoskeleton 37 (1997) 232–239.
[63] I. Minoura, R. Kamiya, Strikingly different propulsive forces generated by different dynein-deficient mutants in viscous media, Cell Motil. Cytoskeleton 31 (1995) 130–139.
[64] D. Nicastro, C. Schwartz, J. Pierson, R. Gaudette, M.E. Porter, J.R. McIntosh, The molecular architecture of axonemes revealed by cryoelectron tomography, Science 313 (2006) 944–948.
[65] J. Freshour, R. Yokoyama, D.R. Mitchell, *Chlamydomonas* flagellar outer row dynein assembly protein Oda7 interacts with both outer row and I1 inner row dyneins, J. Biol. Chem. 282 (2007) 5404–5412.
[66] L.T. Haimo, B.R. Telzer, J.L. Rosenbaum, Dynein binds to and crossbridges cytoplasmic microtubules, Proc. Natl. Acad. Sci. USA 76 (1979) 5759–5763.
[67] K. Ogawa, Four ATP-binding sites in the midregion of the beta heavy chain of dynein, Nature 352 (1991) 643–645.
[68] I.R. Gibbons, B.H. Gibbons, G. Mocz, D.J. Asai, Multiple nucleotide-binding sites in the sequence of dynein beta heavy chain, Nature 352 (1991) 640–643.

[69] C.G. Wilkerson, S.M. King, G.B. Witman, Molecular analysis of the γ heavy chain of *Chlamydomonas* flagellar outer-arm dynein, J. Cell Sci. 107 (1994) 497–506.
[70] D.R. Mitchell, K.S. Brown, Sequence analysis of the *Chlamydomonas* alpha and beta dynein heavy chain genes, J. Cell Sci. 107 (1994) 635–644.
[71] G. Mocz, I.R. Gibbons, Model for the motor component of dynein heavy chain based on homology to the AAA family of oligomeric ATPases, Structure (Camb) 9 (2001) 93–103.
[72] S.M. King, AAA domains and organization of the dynein motor unit, J. Cell Sci. 113 (2000) 2521–2526.
[73] S.A. Burgess, M.L. Walker, H. Sakakibara, P.J. Knight, K. Oiwa, Dynein structure and power stroke, Nature 421 (2003) 715–718.
[74] A.J. Roberts, N. Numata, M.L. Walker, Y.S. Kato, B. Malkova, T. Kon, R. Ohkura, F. Arisaka, P.J. Knight, K. Sutoh, S.A. Burgess, AAA^{+} ring and linker swing mechanism in the dynein motor, Cell 136 (2009) 485–495.
[75] A.P. Carter, J.E. Garbarino, E.M. Wilson-Kubalek, W.E. Shipley, C. Cho, R.A. Milligan, R.D. Vale, I.R. Gibbons, Structure and functional role of dynein's microtubule-binding domain, Science 322 (2008) 1691–1695.
[76] H. Ueno, T. Yasunaga, C. Shingyoji, K. Hirose, Dynein pulls microtubules without rotating its stalk, Proc. Natl. Acad. Sci. USA 105 (2008) 19702–19707.
[77] T. Movassagh, K. Bui, H. Sakakibara, K. Oiwa, T. Ishikawa, Nucleotide-induced global conformational changes of flagellar dynein arms revealed by *in situ* analysis, Nat. Struct. Mol. Biol. 17 (2010) 761–767.
[78] A.G. Moss, J.L. Gatti, G.B. Witman, The motile beta/IC1 subunit of sea urchin sperm outer arm dynein does not form a rigor bond, J. Cell Biol. 118 (1992) 1177–1188.
[79] A.G. Moss, W.S. Sale, L.A. Fox, G.B. Witman, The alpha subunit of sea urchin sperm outer arm dynein mediates structural and rigor binding to microtubules, J. Cell Biol. 118 (1992) 1189–1200.
[80] H. Sakakibara, S. Takada, S.M. King, G.B. Witman, R. Kamiya, A *Chlamydomonas* outer arm dynein mutant with a truncated β heavy chain, J. Cell Biol. 122 (1993) 653–661.
[81] Z. Liu, H. Takazaki, Y. Nakazawa, M. Sakato, T. Yagi, T. Yasunaga, S.M. King, R. Kamiya, Partially functional outer arm dynein in a novel *Chlamydomonas* mutant expressing a truncated γ heavy chain, Eukaryot. Cell 7 (2008) 1136–1145.
[82] A. Furuta, T. Yagi, H. Yanagisawa, H. Higuchi, R. Kamiya, Systematic comparison of *in vitro* motile properties between *Chlamydomonas* wild-type and mutant outer arm dyneins each lacking one of the three heavy chains, J. Biol. Chem. 284 (2009) 5927–5935.
[83] S.Y. Tan, J. Rosenthal, X.-Q. Zhao, R.J. Francis, B. Chatterjee, S.L. Sabol, K.L. Linask, L. Bracero, P.S. Connelly, M.P. Daniels, Q. Yu, H. Omran, L. Leatherbury, C.W. Lo, Heterotaxy and complex structural heart defects in a mutant mouse model of primary ciliary dyskinesia, J. Clin. Invest. 117 (2007) 3742–3752.
[84] H. Sakakibara, D.R. Mitchell, R. Kamiya, A *Chlamydomonas* outer arm dynein mutant missing the α heavy chain, J. Cell Biol. 113 (1991) 615–622.
[85] A. Habura, I. Tikhonenko, R.L. Chisholm, M.P. Koonce, Interaction mapping of a dynein heavy chain. Identification of dimerization and intermediate-chain binding domains, J. Biol. Chem. 274 (1999) 447–453.
[86] M. Sakato, H. Sakakibara, S.M. King, *Chlamydomonas* outer arm dynein alters conformation in response to Ca^{2+}, Mol. Biol. Cell 18 (2007) 3620–3634.
[87] K.K. Pfister, M.W. Salata, J.F. Dillman 3rd, E. Torre, R.J. Lye, Identification and developmental regulation of a neuron-specific subunit of cytoplasmic dynein, Mol. Biol. Cell 7 (1996) 331–343.
[88] A. Kuta, W. Deng, A. Mosrsi El-Kadi, G. Banks, M. Hafezparast, K.K. Pfister, E.M.C. Fisher, Mouse cytoplasmic dynein intermediate chains: Identification of new isoforms, alternative splicing and tissue distribution of transcripts, PLoS One 5 (2010) e11682.

[89] S.J. Susalka, K. Nikulina, M.W. Salata, P.S. Vaughan, S.M. King, K.T. Vaughan, K.K. Pfister, The roadblock light chain binds a novel region of the cytoplasmic dynein intermediate chain, J. Biol. Chem. 277 (2002) 939–946.
[90] N.T. Loges, H. Olbrich, L. Fenske, H. Mussaffi, J. Horvath, M. Fliegauf, H. Kuhl, G. Baktai, E. Peterffy, R. Chodhari, E.M.K. Chung, A. Rutman, C. O'Callaghan, H. Blau, L. Tiszlavicz, K. Voelkel, M. Witt, E. Zitkiewicz, J. Neesen, R. Reinhardt, H.M. Mitchison, H. Omran, DNAI2 mutations cause primary ciliary dyskinesia with defects in the outer dynein arm, Am. J. Hum. Genet. 83 (2008) 547–558.
[91] C.A. Perrone, P. Yang, E. O'Toole, W.S. Sale, M.E. Porter, The *Chlamydomonas IDA7* locus encodes a 140-kDa dynein intermediate chain required to assemble the I1 inner arm complex, Mol. Biol. Cell 9 (1998) 3351–3365.
[92] D.R. Mitchell, J.L. Rosenbaum, Protein–protein interactions in the 18S ATPase of *Chlamydomonas* outer dynein arms, Cell Motil. Cytoskeleton 6 (1986) 510–520.
[93] S.M. King, C.G. Wilkerson, G.B. Witman, The M_r 78,000 intermediate chain of *Chlamydomonas* outer arm dynein interacts with α-tubulin *in situ*, J. Biol. Chem. 266 (1991) 8401–8407.
[94] G.J. Pazour, C.G. Wilkerson, G.B. Witman, A dynein light chain is essential for the retrograde particle movement of intraflagellar transport (IFT), J. Cell Biol. 141 (1998) 979–992.
[95] C. Tanner, P. Rompolas, R.S. Patel-King, O. Gorbatyuk, K. Wakabayashi, G.J. Pazour, S.M. King, Three members of the LC8/DYNLL family are required for outer arm dynein motor function, Mol. Biol. Cell 19 (2008) 3724–3734.
[96] P. Yang, W.S. Sale, Casein kinase I is anchored on axonemal doublet microtubules and regulates flagellar dynein phosphorylation and activity, J. Biol. Chem. 275 (2000) 18 905–18 912.
[97] C.W. Bell, E. Fronk, I.R. Gibbons, Polypeptide subunits of dynein 1 from sea urchin sperm flagella, J. Supramol. Struct. 11 (1979) 311–317.
[98] C.M. Sadek, A.E. Damdimopoulos, M. Pelto-Huikko, J.A. Gustafsson, G. Spyrou, A. Miranda-Vizuete, Sptrx-2, a fusion protein composed of one thioredoxin and three tandemly repeated NDP-kinase domains is expressed in human testis germ cells, Genes Cells 6 (2001) 1077–1090.
[99] R. Patel-King, O. Gorbatyuk, S. Takebe, S. King, Flagellar radial spokes contain a Ca^{2+}-sensitive nucleoside diphosphate kinase, Mol. Biol. Cell 15 (2004) 3891–3902.
[100] T. Watanabe, M. Flavin, Nucleotide-metabolizing enzymes in *Chlamydomonas* flagella, J. Biol. Chem. 251 (1976) 182–192.
[101] B. Duriez, P. Duquesnoy, E. Escudier, A.-M. Bridoux, D. Escalier, I. Rayet, E. Marcos, A.-M. Vojtek, J.-F. Bercher, S. Amselem, A common variant in combination with a nonsense mutation in a member of the thioredoxin family causes primary ciliary dyskinesia, Proc. Natl. Acad. Sci. USA 104 (2007) 3336–3341.
[102] M. Wirschell, C. Yang, P. Yang, L. Fox, H.-a. Yanagisawa, R. Kamiya, G.B. Witman, M.E. Porter, W.S. Sale, IC97 is a novel intermediate chain of I1 dynein that interacts with tubulin and regulates interdoublet sliding, Mol. Biol. Cell 20 (2009) 3044–3054.
[103] K.K. Pfister, E.M.C. Fisher, I.R. Gibbons, T.S. Hays, E.L.F. Holzbaur, J.R. McIntosh, M.E. Porter, T.A. Schroer, K.T. Vaughan, G.B. Witman, S.M. King, R.B. Vallee, Cytoplasmic dynein nomenclature, J. Cell Biol. 171 (2005) 411–413.
[104] K.K. Pfister, P.R. Shah, H. Hummerich, A. Russ, J. Cotton, A.A. Annuar, S.M. King, E.M.C. Fisher, Genetic analysis of the cytoplasmic dynein subunit families, PLoS Genetics 2 (2006) e1.
[105] Y. Song, G. Benison, A. Nyarko, T.S. Hays, E. Barbar, Potential role for phosphorylation in differential regulation of the assembly of dynein light chains, J. Biol. Chem. 282 (2007) 17272–17279.
[106] S.M. King, E. Barbarese, J.F. Dillman III, R.S. Patel-King, J.H. Carson, K.K. Pfister, Brain cytoplasmic and flagellar outer arm dyneins share a highly conserved M_r 8,000 light chain, J. Biol. Chem. 271 (1996) 358–366.

[107] F.S. Espindola, D.M. Suter, L.B. Partata, T. Cao, J.S. Wolenski, R.E. Cheney, S.M. King, M.S. Mooseker, The light chain composition of chicken brain myosin-Va: calmodulin, myosin-II essential light chains, and 8-kDa dynein light chain/PIN, Cell Motil. Cytoskeleton 47 (2000) 269–281.
[108] S.R. Jaffrey, S.H. Snyder, PIN: An associated protein inhibitor of neuronal nitric oxide synthase, Science 274 (1996) 774–777.
[109] T. Dick, K. Ray, H.K. Salz, W. Chia, Cytoplasmic dynein (*ddlc1*) mutations cause morphogenetic defects and apoptotic cell death in *Drosophila melanogaster*, Mol. Cell Biol. 16 (1996) 1966–1977.
[110] P. Yang, D.R. Diener, J.L. Rosenbaum, W.S. Sale, Localization of calmodulin and dynein light chain LC8 in flagellar radial spokes, J. Cell Biol. 153 (2001) 1315–1326.
[111] G.J. Pazour, G.B. Witman, Forward and reverse genetic analysis of microtubule motors in *Chlamydomonas*, Methods 22 (2000) 285–298.
[112] L.M. DiBella, O. Gorbatyuk, M. Sakato, K. Wakabayashi, R.S. Patel-King, G.J. Pazour, G.B. Witman, S.M. King, Differential light chain assembly influences outer arm dynein motor function, Mol. Biol. Cell 16 (2005) 5661–5674.
[113] L.M. DiBella, S.E. Benashski, H.W. Tedford, A. Harrison, R.S. Patel-King, S.M. King, The Tctex1/Tctex2 class of dynein light chains. Dimerization, differential expression, and interaction with the LC8 protein family, J. Biol. Chem. 276 (2001) 14366–14373.
[114] S.M. King, J.F. Dillman 3rd, S.E. Benashski, R.J. Lye, R.S. Patel-King, K.K. Pfister, The mouse *t*-complex-encoded protein Tctex1 is a light chain of brain cytoplasmic dynein, J. Biol. Chem. 271 (1996) 281–287.
[115] R.S. Patel-King, S.E. Benashski, A. Harrison, S.M. King, A *Chlamydomonas* homologue of the putative murine *t* complex distorter Tctex2 is an outer arm dynein light chain, J. Cell Biol. 137 (1997) 1081–1090.
[116] L.M. DiBella, E.F. Smith, R.S. Patel-King, K. Wakabayashi, S.M. King, A novel Tctex2-related light chain is required for stability of inner dynein arm I1 and motor function in the *Chlamydomonas* flagellum, J. Biol. Chem. 279 (2004) 666–676.
[117] O. Kagami, M. Gotoh, Y. Makino, H. Mohri, R. Kamiya, K. Ogawa, A dynein light chain of sea urchin sperm flagella is a homolog of mouse Tctex 1, which is encoded by a gene of the *t* complex sterility locus, Gene. 211 (1998) 383–386.
[118] C. Caggese, R. Moschetti, G. Ragone, P. Barsanti, R. Caizzi, *dtctex1*, the *Drosophila melanogaster* homolog of a putative murine *t*-complex distorter encoding a dynein light chain, is required for production of functional sperm, Mol. Genet. Genomics 265 (2001) 436–444.
[119] E. Lader, H.S. Ha, M. O'Neill, K. Artzt, D. Bennett, *tctex1*: A candidate gene family for a mouse *t* complex sterility locus, Cell 58 (1989) 969–979.
[120] L.Y. Huw, A.S. Goldsborough, K. Willison, K. Artzt, Tctex2: A sperm tail surface protein mapping to the *t*-complex, Dev. Biol. 170 (1995) 183–194.
[121] D.R. Mitchell, Y. Kang, Reversion analysis of dynein intermediate chain function, J. Cell Sci. 105 (1993) 1069–1078.
[122] G.J. Pazour, A. Koutoulis, S.E. Benashski, B.L. Dickert, H. Sheng, R.S. Patel-King, S.M. King, G.B. Witman, LC2, the *Chlamydomonas* homologue of the *t* complex-encoded protein Tctex2, is essential for outer dynein arm assembly, Mol. Biol. Cell 10 (1999) 3507–3520.
[123] L.M. DiBella, M. Sakato, R.S. Patel-King, G.J. Pazour, S.M. King, The LC7 light chains of *Chlamydomonas* flagellar dyneins interact with components required for both motor assembly and regulation, Mol. Biol. Cell 15 (2004) 4633–4646.
[124] J. Song, R.C. Tyler, M.S. Lee, E.M. Tyler, J.L. Markley, Solution structure of isoform 1 of Roadblock/LC7, a light chain in the dynein complex, J. Mol. Biol. 354 (2005) 1043–1051.
[125] S.M. King, G.B. Witman, Multiple sites of phosphorylation within the α heavy chain of *Chlamydomonas* outer arm dynein, J. Biol. Chem. 269 (1994) 5452–5457.

[126] V. Wagner, G. Gessner, I. Heiland, M. Kaminski, S. Hawat, K. Scheffler, M. Mittag, Analysis of the phosphoproteome of *Chlamydomonas reinhardtii* provides new insights into various cellular pathways, Eukaryot. Cell 5 (2006) 457–468.
[127] G. Piperno, D.J. Luck, Inner arm dyneins from flagella of *Chlamydomonas reinhardtii*, Cell 27 (1981) 331–340.
[128] H. Wu, M.W. Maciejewski, A. Marintchev, S.E. Benashski, G.P. Mullen, S.M. King, Solution structure of a dynein motor domain associated light chain, Nature Struct. Biol. 7 (2000) 575–579.
[129] S.E. Benashski, R.S. Patel-King, S.M. King, Light chain 1 from the *Chlamydomonas* outer dynein arm is a leucine-rich repeat protein associated with the motor domain of the γ heavy chain, Biochemistry 38 (1999) 7253–7264.
[130] P. Rompolas, R.S. Patel-King, S.M. King, An outer arm dynein conformational switch is required for metachronal synchrony of motile cilia in planaria, Mol. Biol. Cell 21 (2010) 3669–3679.
[131] J. Hyams, G. Borisy, Isolated flagellar apparatus of *Chlamydomonas*: Characterization of forward swimming and alteration of waveform and reversal of motion by calcium ions in vitro, J. Cell Sci. 33 (1978) 235–253.
[132] R. Kamiya, G.B. Witman, Submicromolar levels of calcium control the balance of beating between the two flagella in demembranated models of *Chlamydomonas*, J. Cell Biol. 98 (1984) 97–107.
[133] B.E. Taillon, S.A. Adler, J.P. Suhan, J.W. Jarvik, Mutational analysis of centrin: An EF-hand protein associated with three distinct contractile fibers in the basal body apparatus of *Chlamydomonas*, J. Cell Biol. 119 (1992) 1613–1624.
[134] C. Weber, V.D. Lee, W.J. Chazin, B. Huang, High level expression in *Escherichia coli* and characterization of the EF-hand calcium-binding protein caltractin, J. Biol. Chem. 269 (1994) 15795–15802.
[135] B. Koblenz, J. Schoppmeier, A. Grunow, K.-F. Lechtreck, Centrin deficiency in *Chlamydomonas* causes defects in basal body replication, segregation and maturation, J. Cell Sci. 116 (2003) 2635–2646.
[136] B. Koblenz, K.-F. Lechtreck, The *NIT1* promoter allows inducible and reversible silencing of centrin in *Chlamydomonas reinhardtii*, Eukaryot. Cell 4 (2005) 1959–1962.
[137] M. Hayashi, T. Yagi, K. Yoshimura, R. Kamiya, Real-time observation of Ca^{2+}-induced basal body reorientation in *Chlamydomonas*, Cell Motil. Cytoskeleton 41 (1998) 49–56.
[138] D.R. Mitchell, *Chlamydomonas* flagella, J. Phycol. 36 (2000) 261–273.
[139] C. Guerra, Y. Wada, V. Leick, A. Bell, P. Satir, Cloning, localization, and axonemal function of *Tetrahymena* centrin, Mol. Biol. Cell 14 (2003) 251–261.
[140] M. Bessen, R.B. Fay, G.B. Witman, Calcium control of waveform in isolated flagellar axonemes of *Chlamydomonas*, J. Cell Biol. 86 (1980) 446–455.
[141] K. Mizuno, P. Padma, A. Konno, Y. Satouh, K. Ogawa, K. Inaba, A novel neuronal calcium sensor family protein, calaxin, is a potential Ca^{2+}-dependent regulator for the outer arm dynein of metazoan cilia and flagella, Biol. Cell 101 (2009) 91–103.
[142] P. Padma, A. Hozumi, K. Ogawa, K. Inaba, Molecular cloning and characterization of a thioredoxin/nucleoside diphosphate kinase related dynein intermediate chain from the ascidian, *Ciona intestinalis*, Gene. 275 (2001) 177–183.
[143] D. Casey, T. Yagi, R. Kamiya, G. Witman, DC3, the smallest subunit of the *Chlamydomonas* flagellar outer dynein arm-docking complex, is a redox-sensitive calcium-binding protein, J. Biol. Chem. 278 (2003) 42652–42659.
[144] R.J. Aitken, D. Harkiss, W. Knox, M. Paterson, D.S. Irvine, A novel signal transduction cascade in capacitating human spermatozoa characterised by a redox-regulated, cAMP-mediated induction of tyrosine phosphorylation, J. Cell Sci. 111 (1997) 645–656.

[145] S. Takada, C.G. Wilkerson, R. Kamiya, G.B. Witman, The *ODA1* gene encodes a 62 kDa component of a complex necessary for outer arm dynein docking on the doublet microtubules of *Chlamydomonas* flagella, Mol. Biol. Cell 7 (1996) 568a.
[146] D. Casey, K. Inaba, G. Pazour, S. Takada, K. Wakabayashi, C. Wilkerson, R. Kamiya, G. Witman, DC3, the 21-kD subunit of the outer dynein arm-docking complex (ODA-DC), is a novel EF-hand proten important for assembly of both the outer arm and the ODA-DC, Mol. Biol. Cell 14 (2003) 3650–3663.
[147] S. Takada, R. Kamiya, Beat frequency difference between the two flagella of *Chlamydomonas* depends on the attachment site of outer dynein arms on the outer-doublet microtubules, Cell Motil. Cytoskeleton 36 (1997) 68–75.
[148] R. Kamiya, Mutations at twelve independent loci result in absence of outer dynein arms in *Chlamydomonas reinhardtii*, J. Cell Biol. 107 (1988) 2253–2258.
[149] S. Takada, H. Sakakibara, R. Kamiya, Three-headed outer arm dynein from *Chlamydomonas* that can functionally combine with outer-arm-missing axonemes, J. Biochem. (Tokyo) 111 (1992) 758–762.
[150] M.E. Fowkes, D.R. Mitchell, The role of preassembled cytoplasmic complexes in assembly of flagellar dynein subunits, Mol. Biol. Cell 9 (1998) 2337–2347.
[151] N.T. Loges, H. Olbrich, A. Becker-Heck, K. Häffner, A. Heer, C. Reinhard, M. Schmidts, A. Kispert, M.A. Zariwala, M.W. Leigh, M.R. Knowles, H. Zentgraf, H. Seithe, G. Nürnberg, P. Nürnberg, R. Reinhardt, H. Omran, Deletions and point mutations of LRRC50 cause primary ciliary dyskinesia due to dynein arm defects, Am. J. Hum. Genet. 85 (2009) 883–889.
[152] P. Duquesnoy, E. Escudier, L. Vincensini, J. Freshour, A.-M. Bridoux, A. Coste, A. Deschildre, J. de Blic, M. Legendre, G. Montantin, H. Tenreiro, A.-M. Vojtek, C. Loussert, A. Clément, D. Escalier, P. Bastin, D.R. Mitchell, S. Amselem, Loss-of-function mutations in the human ortholog of *Chlamydomonas reinhardtii* ODA7 disrupt dynein arm assembly and cause primary ciliary dyskinesia, Am. J. Hum. Genet. 85 (2009) 890–896.
[153] K. Ogawa, K. Inaba, Ap58: A novel *in situ* outer dynein arm-binding protein, Biochem. Biophys. Res. Comm. 343 (2006) 385–390.
[154] X. Xiang, A.H. Osmani, S.A. Osmani, M. Xin, N.R. Morris, NUDF, a nuclear migration gene in *Aspergillus nidulans*, is similar to the human LIS-1 gene required for neuronal migration, Mol. Biol. Cell 6 (1995) 297–310.
[155] N.E. Faulkner, D.L. Dujardin, C.Y. Tai, K.T. Vaughan, C.B. O'Connell, Y. Wang, R.B. Vallee, A role for the lissencephaly gene LIS1 in mitosis and cytoplasmic dynein function, Nat. Cell Biol. 2 (2000) 784–791.
[156] L. Pedersen, P. Rompolas, S. Christensen, J.L. Rosenbaum, S.M. King, The lissencephaly protein Lis1 is present in motile mammalian cilia and requires outer dynein arm for targeting to *Chlamydomonas* flagella, J. Cell Sci. 120 (2007) 858–867.
[157] P. Rompolas, S.M. King, Regulated association of CrLis1 with the outer dynein arm, Mol. Biol. Cell 19 (2008). CD supplement.
[158] H. Omran, D. Kobayashi, H. Olbrich, T. Tsukahara, N.T. Loges, H. Hagiwara, Q. Zhang, G. Leblond, E. O'Toole, C. Hara, H. Mizuno, H. Kawano, M. Fliegauf, T. Yagi, S. Koshida, A. Miyawaki, H. Zentgraf, H. Seithe, R. Reinhardt, Y. Watanabe, R. Kamiya, D.R. Mitchell, H. Takeda, Ktu/PF13 is required for cytoplasmic pre-assembly of axonemal dyneins, Nature 456 (2008) 611–616.
[159] B. Huang, G. Piperno, D.J.L. Luck, Paralyzed flagellar mutants of *Chlamydomonas reinhardtii* defective for axonemal doublet microtubule arms, J. Biol. Chem. 254 (1979) 3091–3099.
[160] R. Yamamoto, M. Hirono, R. Kamiya, Discrete PIH proteins function in the cytoplasmic preassembly of different subsets of axonemal dyneins, J. Cell Biol. 190 (2010) 65–71.

[161] Z. Sun, A. Amsterdam, G.J. Pazour, D.G. Cole, M.S. Miller, N. Hopkins, A genetic screen in zebrafish identifies cilia genes as a principal cause of cystic kidney, Development 131 (2004) 4085–4093.
[162] N.T. Ahmed, D.R. Mitchell, ODA16p, a *Chlamydomonas* flagellar protein needed for dynein assembly, Mol. Biol. Cell 16 (2005) 5004–5012.
[163] N. Ahmed, C. Gao, B. Lucker, D. Cole, D. Mitchell, ODA16 aids axonemal outer row dynein assembly through an interaction with the intraflagellar transport machinery, J. Cell Biol. 183 (2008) 313–322.
[164] T. Yagi, Bioinformatic approaches to dynein heavy chain classification, Methods Cell Biol. 92 (2009) 1–9.

In this chapter

8

Organization of Dyneins in the Axoneme

Takashi Ishikawa
Paul Scherrer Institute, Villigen, Switzerland

This chapter reviews the recent progress in our understanding of axonemal dynein in the context of flagellar/ciliary bending motion, focusing mainly on structural studies using electron microscopy/tomography but also correlating these studies with functional motility assays and theoretical studies. Significant questions to be addressed in the near future will also be presented.

8.1 Introduction

Flagella/cilia are bending organelles that drive cells or produce extracellular flow. Axonemal dyneins are motor proteins responsible for the generation of force, and are one of more than 600 proteins in the flagella/cilia [1]. While the mechanism of the dynein powerstroke itself has been under investigation for a long time (see Chapter 4), the mechanism that integrates the sliding of individual dyneins into a flagellar/ciliary bending motion is another challenging question that is now attracting scientists. A number of dyneins (which form outer and inner dynein arms, located between the A-microtubule and the adjacent B-microtubule), along with regulatory and cytoskeletal proteins, are likely indispensable for bending motion. This makes axonemal bending activity much more complicated than, for example, actomyosin sliding in skeletal muscle. Thus, to elucidate the mechanism by which dynein generates flagellar/ciliary motion, we must examine structure and function at various scales: (1) within each dynein heavy chain (HC) (AAA domains, the coiled-coil stalk, the N-terminal tail), (2) between dynein HCs (within an inner or outer dynein arm), (3) between dynein arms on one microtubule doublet, (4) among the nine microtubule doublets, and (5) between flagella/cilia. To tackle questions at different scales, multidisciplinary approaches are inevitable (Fig. 8.1).

The characterization of single axonemal dynein HCs is the area that has been worked on most intensively in recent decades. Single-particle analysis electron microscopy gave us an idea of dynein conformation at ~20 Å resolution [2,3]. Functional studies were carried out using the *in vitro* motility assay to measure the velocity and force generation of single dyneins or groups of dyneins (Review [4]).

Dyneins DOI: 10.1016/B978-0-12-382004-4.10008-1
Copyright © 2012 by Elsevier Inc. All rights reserved.

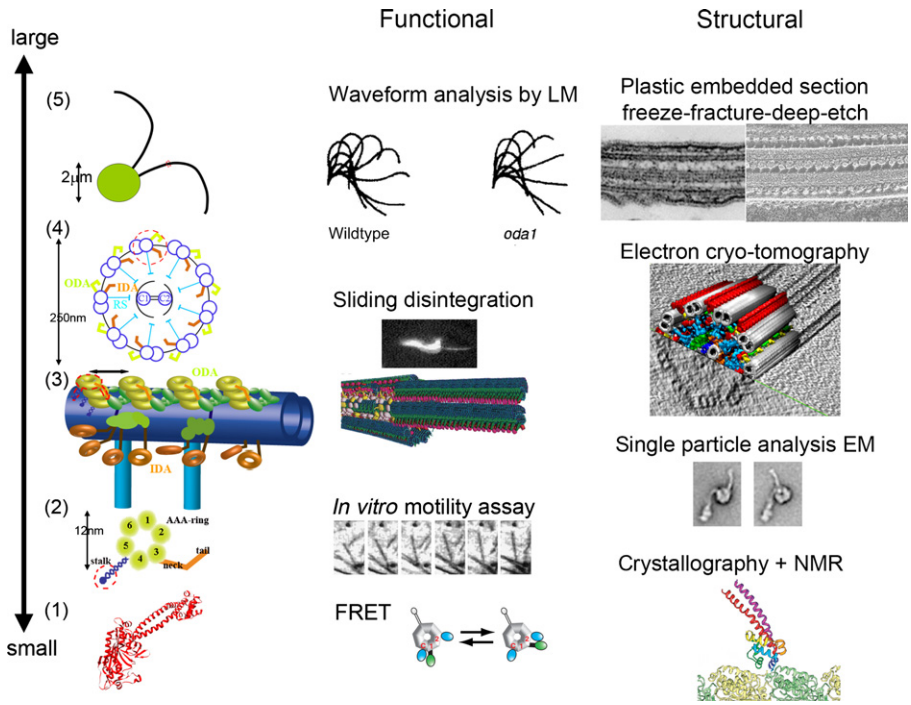

Figure 8.1 Diagram of scales of various flagellar/ciliary studies. Reproduced from the following: fluorescence resonance energy transfer [52], *in vitro* motility assay [6] (Macmillan Publication Ltd) and, sliding disintegration [13] (Copyright, 2005, Wiley). Modified from the following: freeze-fracture-deep-etch [55], plastic embedded section [93], sliding disintegration [13], waveform analysis [94], and crystallography [26].

There must be a reason why flagella/cilia need such gigantic motors (~4500 amino acids) with multiple AAA domains [5] instead of compact motors like myosin and kinesin. Higher velocity cannot be the reason: the *in vitro* motility assay demonstrated that the velocity of axonemal dynein is not higher than that of kinesin and cytoplasmic dynein (Table 8.1). Furthermore, the force generated by dynein c (1.6 pN) [6] is lower than that of kinesin (7 pN) [7].

At the scale of dynein arms, we should know how these complexes are formed and what is the meaning of the complex formation. Although *in vitro* motility assays show similar activity in inner-arm dyneins and outer-arm dyneins when they are purified [6,8] (Table 8.1), their *in situ* roles are distinct: the inner dynein arm is responsible for waveform determination and the outer dynein arm for force generation and acceleration [9], which means that extra functions are created when dyneins are assembled into arms.

The *in vitro* motility assay showed that dyneins that form arrays on microtubules, either *in situ* (sliding disintegration) [10] or by *in vitro* reconstitution [11], can drive another microtubule much faster than isolated dyneins on glass slides [8,12]

Table 8.1 Velocity of Axonemal Dyneins Under Various Experimental Conditions: *In Vitro* Motility Assay

Dynein components	Velocity	References
Dynein f (single motor)	0.62 ± 0.32 μm/s	[49]
Dynein f	0.99 ± 0.37 μm/s	[49]
Dynein c (single motor)	0.7 μm/s	[6]
Dynein c	5.1 μm/s	[6]
Dynein b	1.8–2.7 μm/s	[8]
Dynein c	6.7–6.8 μm/s	[8]
Dynein g	2.5–3.9 μm/s	[8]
Dynein β	~0.7 μm/s	[12]
Dynein γ	3.8 ± 1.2 μm/s	[12]
Dynein β, γ	0.87 ± 0.34 μm/s	[64]
Dynein α, γ	2.3 ± 0.65 μm/s	[64]
Dynein α, β	6.8 ± 1.3 μm/s	[64]
Dynein α, β, γ	4.8 ± 1.1 μm/s	[64]
Dynein α, β, γ; processive motion with low ATP	~0.2 μm/s	[83]

Under the condition of multiple motors, unless otherwise indicated. Velocity of kinesin: ~2 μm/s (multiple motors) and ~0.3 μm/s (single motor) for KIF1D[95]

Table 8.2 Sliding Disintegration and Sliding by Outer Dynein Arm Bundle

Dynein components	Velocity	References
WT, ODA bundle	30.2 ± 6.0 μm/s	[11]
WT, sliding disintegration	19.2 ± 6.4 μm/s	[11]
Oda1, sliding disintegration	4.1 ± 1.9 μm/s	[11]
Oda11, sliding disintegration	~10.0 ± 4.5 μm/s	[11]
Oda2-t, sliding disintegration	~16 ± 4 μm/s	[11]
Tetrahymena WT, sliding disintegration	3.1 ± 2.1 μm/s	[96]
Tetrahymena WT, sliding disintegration	9.8 ± 2.6 μm/s	[13]

(Tables 8.1 and 8.2). Seetharam and Satir discovered high-speed sliding by outer dynein arms during sliding disintegration by high-frame rate video; this is not detectable using normal *in vitro* motility assays [13]. These results suggest a form of synergy between dyneins when arrayed on the microtubule. Dynein arms lined

up on microtubule doublets cause a unique oscillatory motion [14]. It is not known whether this oscillatory movement is a driving force of bending when the microtubule doublet is embedded in the axoneme.

The bending mechanism is one of the scientific community's main interests. Sliding or oscillatory motions of the dynein/microtubule in an axoneme must be integrated into bending by generating torque. According to a calculation based on the stiffness of flagella [15], ~0.5 nN/μm is necessary to bend a flagellum [16]. This is a reasonable value, judging from the number of dynein heads (~1000 heads/μm). However, the sliding force must be converted to a bending force. This conversion seems to require the whole axoneme: there has been no report of two microtubules linked by dynein arms bending (they only slide past each other). It seems that nine microtubule doublets (or at least several) must form a bundle to produce bending. Although functional analysis at this level has been carried out actively for a long time using waveform analysis, structural studies were limited to two-dimensional work. However, ground-breaking recent progress in electron cryo-tomography has enabled three-dimensional structural analysis of the whole axoneme. This will be described in detail in Sections 8.3 to 8.6.

Almost all the efforts to build theoretical models to explain the function of flagella/cilia and axonemal dynein address this scale. They formalize the bending motion as a self-organized motion [17]. Brokaw made computational simulations to reproduce flagellar waveforms assuming switching between two distinct modes (on/off) of dynein activity, regulated either by displacement or curvature of microtubules (see review [18]). Lindeman proposed a geometric clutch mechanism based on the transverse force (t-force), which depends on the distance between two adjacent microtubules (see review [19,20]). Jülicher and colleagues [21] analytically solved non-linear equations depending on microtubule rigidity, length, friction, and external viscosity, under the condition that dynein takes two states. This model can also explain linear oscillation [22]. In Sections 8.7.3 we will compare these theoretical studies with recent experimental work.

Inter-flagella (or inter-cilia) interactions generate, for example, metachronal waves of ependymal cilia or synchronized unidirectional rotation of nodal cilia. There have been proposed a few hypotheses on the mechanism that generates cooperativity among flagella/cilia – involving, for example, osmotic pressure or mechanical force [23,24,25] – but the details will not be described in the present review.

8.2 The History of Methodological Development in Structural Research into Axonemal Dynein

This section will survey a variety of methods to investigate dynein structure *in vitro* and *in situ*.

Although the structure and function of single axonemal dynein HCs have been under investigation for a long time, the information produced is still limited compared to what is known about other motor proteins (myosin, kinesin, FoF1 ATPase). Due to the huge molecular weight of the dynein HC (~500 000 Da), characterization of single dynein HCs is already challenging. So far only the microtubule-binding domain (MTBD) of cytoplasmic dynein and the whole dynein head have been analyzed at atomic resolution and at relatively low (~6 Å) resolution, respectively, by X-ray crystallography in Vale's group. The interface of the MTBD and the microtubules was modeled based on helical reconstruction from cryo-electron microscopy (cryo-EM) [26]. Structural analysis of the whole dynein HC has been carried out by single-particle analysis from cryo-EM . Despite the fact that this method can obtain 7–8 Å resolution [27,28,29], which is enough to visualize secondary structures, single-particle analysis of dynein is still carried out at ~25 Å resolution [2,3]. This is probably due to the flexibility of dynein. Burgess and colleagues demonstrated how flexible the tail is by two-dimensional image classification from electron micrographs of negatively stained dynein c [3]. Because nobody has yet succeeded in the directed mutagenesis of axonemal dynein HCs, the structural study of genetically engineered axonemal dynein mutant with less flexibility remains an exciting future topic.

As regards questions to do with the interactions between dyneins, microtubules, and other molecules, electron microscopy has been the most popular method since the 1970s. For *in situ* studies, freeze-fracture-deep-etch [30], plastic embedded sections [31], and negative stain [32] were the dominant specimen preparation techniques until the 1990s. Importantly, with these techniques the 96 nm periodicity of inner dynein arm and 24 nm periodicity of outer dynein arm were established. Furthermore, these electron microscopy studies mapped dynein isoforms and regulatory proteins two-dimensionally [33]. The way in which the heads and the tails of dynein HCs as well as the intermediate chains (ICs), light chains (LCs), and radial spokes are aligned on the microtubule was modeled based on these results and they are in principle consistent with the most recent three-dimensional work. However, the output from these methodologies was limited to two dimensions. Although cryo-EM appeared in early 1980s and became one of the mainstays of three-dimensional structural analysis due to hydrated and intact (without staining) specimen preparation, it was hard to apply it to the axoneme. One major reason was thickness: one microtubule doublet with dynein arms has a thickness of ~50 nm while the whole axoneme has a thickness of about ~250 nm, which causes an abundance of inelastic scattering of electrons and lowers the contrast. Another reason delaying the application of three-dimensional cryo-TEM to the axoneme was the highly complex nature of the organelle. Since contrast obtained by cryo-TEM is quite poor, micrographs must be averaged to improve the signal-to-noise ratio. While this approach has been quite successful for relatively rigid complexes such as ribosomes or periodic objects such as viruses, flagella/cilia are highly flexible with a heterogeneous arrangement of components inside and are therefore not suitable for averaging. Only in the last decade has electron cryo-tomography with energy-filtered TEM,

which removes inelastically scattered electrons, been developed to address such complicated and heterogeneous targets as a whole cell [34]. This technique has allowed us to reconstruct the three-dimensional structure of the whole axoneme to reveal the *in situ* structure of dyneins and other axonemal proteins by three-dimensional averaging, as described in Sections 8.3, 8.4, and 8.5.

8.3 Dynein Arm Arrangement *In Situ*

Recent progress in electron cryo-tomography has enabled us to see detailed three-dimensional structure [35,36,37,38,39,40,41], and this section will

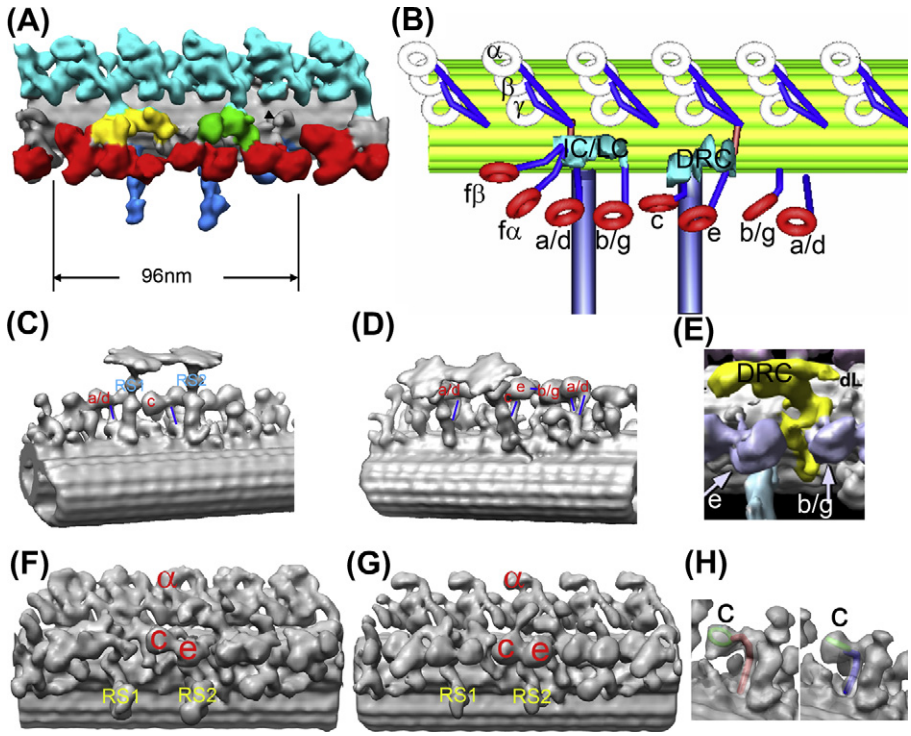

Figure 8.2 Arrangements of dyneins and other molecules within the 96 nm periodic unit revealed by electron cryo-tomography. (A) Averaged tomogram: IDA (red), ODA (light blue), IC/LC of dynein f (yellow), DRC (green), radial spokes (blue). (B) Assignment of molecules based on tomographic analysis of mutants [37, 38]. The rings of outer-arm dyneins (α, β, γ) (white) and the inner-arm dyneins (red) are indicated. Tails are shown in blue. (C,D) Different views of the structure to emphasize the connection between inner dynein arm tails (Lines) and radial spokes (RS1, RS2) and the various conformations of the tails, respectively. (E) Connections between DRC and inner-arm dyneins. (F,G) Structure with (left) and without (right) ADP.Vi (vanadate), which stand for pre- and post-powerstroke states, respectively. Inner-arm dyneins c and e and outer-arm dynein α are indicated. (H) The shift of the head and the conformational change of the tail in dynein c during the powerstroke: left, pre-powerstroke (ADP.Vi); right, post-powerstroke (apo). (A,B) modified from [38]; (C,D,E) from Bui et al. (unpublished data); (E) modified from [40]; (F,G,H) modified from [41].

review the architecture of axonemal dyneins in inner dynein arms and outer dynein arms.

Within the 96 nm periodic unit (Fig. 8.2A), eight inner-arm dynein HCs form a colinear array along the A-microtubule, while three outer-arm dynein HCs stack vertically (Fig. 8.2B). By mutant analysis, three outer-arm dynein HC isoforms and eight inner-arm dynein HC isoforms have been identified (assignments of two pairs are still ambiguous) [37,38]. Outer dynein arms and inner dynein arms are connected at two interfaces (Fig. 8.2B). One is through the IC/LC of dynein f, while the other is the dynein regulatory complex (DRC) (nexin). The tails of two inner dyneins are connected to the radial spokes (Fig. 8.2C,D), suggesting that these tails are the pathways of regulation from radial spokes and the central apparatus [42]. The DRC connects to dyneins c, e, b, or g [40] (Fig. 8.2E). A more detailed description of DRC is given in Chapter 12.

The γ-ring of the outer dynein arm binds on the A-microtubule at two interfaces (Fig. 8.3E). One interface may be the docking complex [43]. Outer-arm dyneins can bind without the docking complex [44], but this might occur in a slightly different way. IC78, a WD-repeat IC, binds both the outer dynein arm and the A-microtubule [45] and is thus a candidate for the other interface.

Sections 8.4 and 8.5 will outline the structures of dynein arms in more detail and discuss their functional significance.

8.4 Inner Dynein Arm Structure *In Situ*

8.4.1 Overall Structure

In a three-dimensional density map of the 96 nm periodic unit extracted and averaged from tomograms of ice-embedded *Chlamydomonas* flagella, all eight inner-arm dyneins that have been biochemically identified [8] were observed. Both the ring-shaped heads and the tails were visualized [38] (Fig. 8.2B). The eight heads are located as a colinear array, while all the tails extend from the ring toward the distal end (i.e. the tip of the flagellum). Comparing the structures of mutants lacking isoforms of inner-arm dyneins, four isoforms (c, e, fα, and fβ) were indexed in the map, while there are two pairs with ambiguity (a/d and b/g) [38] (Fig. 8.2B).

Six single-headed dyneins are located at the same distance (184 Å) from the A-microtubule and seem to form three dyads around the two radial spokes and one protrusion, which is shorter than the radial spokes but is located at the same place as the third radial spoke of *Tetrahymena* (Fig. 8.2D). This might suggest a pair-wise function of inner dyneins: with this combination each dyad can contain p28, actin, and centrin [46,47,48].

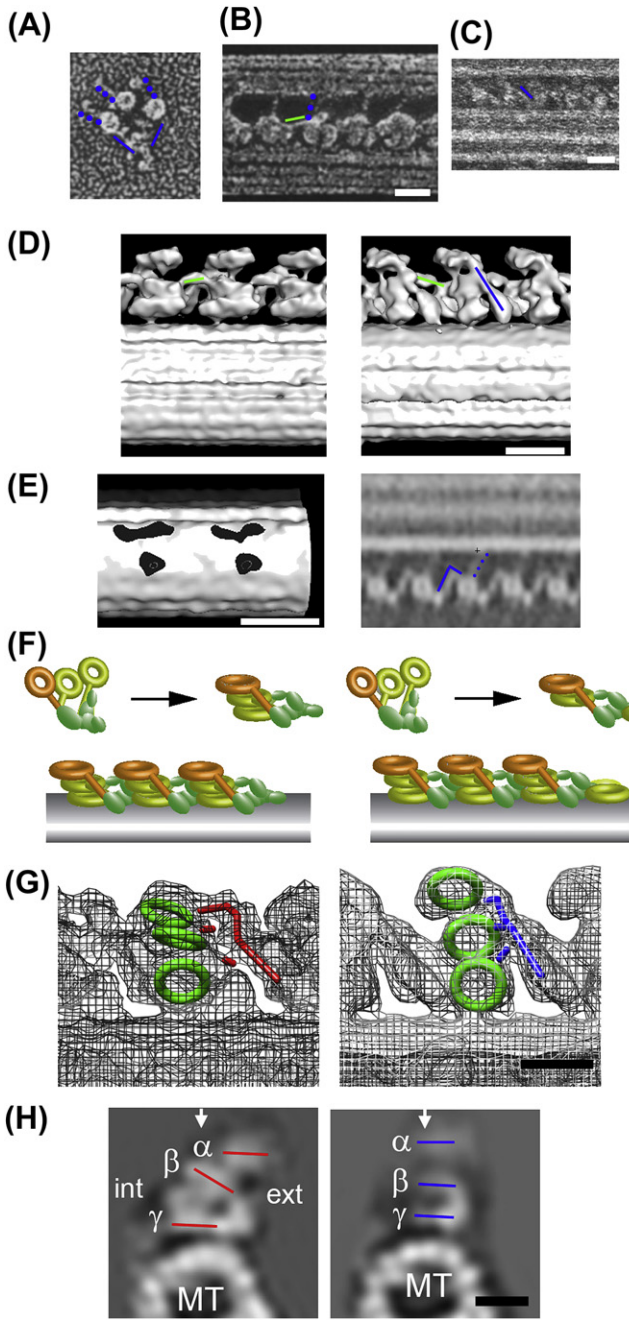
(A)
(B)
(C)
(D)
(E)
(F)
(G)
(H)
α
β
γ
int
ext
MT
α
β
γ
MT

8.4.2 Distinct Conformation and Function of Dynein f

The dimeric isoform dynein f is located closer to the A-microtubule than the other single-headed dyneins (Fig. 8.2B). Dyneins fα and fβ are located 130 Å and 60 Å away from the surface of the A-microtubule, respectively. This means that dynein f has a different binding angle to the B-microtubule from those of the other six single-headed dyneins. The conformation of the dynein f tail is also exceptional. While other dyneins have tails that are sharply kinked at the neck domain to join the A-microtubule, dynein f tails protrude from the ring and extend straight forward [38].

Dynein f is also functionally distinct from other inner dyneins. Dynein f has a higher duty ratio (0.62 [49]) compared to that of dynein c (0.14 [6]) and a lower velocity (~1 μm/s [49]) compared to that of dynein c (~6.7 μm/s [8]) (Table 8.1). When dynein c and dynein f were mixed for the *in vitro* motility assay, the velocity decreased compared to when pure dynein c was used [49]. These structural and functional results suggest a unique role of dynein f: it could be either a modulator or a brake.

8.4.3 Structural Change of Inner-Arm Dyneins *In Situ*: Powerstroke Mechanism

According to kinetics studies [50], dynein with ATP or with ADP.Pi is considered to be in the pre-powerstroke state, while dynein with ADP or without nucleotides (apo) is considered to be in the post-powerstroke state. When ATP and vanadate are added to dynein, vanadate occupies the space of the γ-phosphate and thus mimics the ADP.Pi state [51,52]. The averaged tomogram of *Chlamydomonas* flagella in the presence of ADP and vanadate (ADP.Vi) has shown remarkable differences from the one without nucleotides (apo) [41]. By using radial spokes — which are not affected by nucleotides — as landmarks, an 8 nm shift of the rings of inner- and outer-arm dyneins toward the distal end was detected in the structure with ADP.Vi (ADP.Vi form) compared to the structure without nucleotides (the apo form) (Fig. 8.2F,G). The tail undergoes conformational change: with ADP.Vi it protrudes horizontally (i.e. parallel to the A-microtubule) and gradually curves to

Figure 8.3 Structure of outer dynein arms. (A) Electron micrograph of purified and rotary shadowed outer dynein arm. (B) Array of outer dynein arms *in situ* by the freeze-fracture-deep-etch method. (C) Outer dynein arms observed in a negatively stained flagellum. (D) Outer dynein arms reconstructed from electron cryo-tomograms: left, seen from the external side of the axoneme; right, seen from the internal side. (E) Left, section of a flagellum at the base of the outer dynein arm; right, longitudinal section of a tomogram. The stalk connects the B-microtubule and a β-ring. (F) Two possible models of outer dynein arm assembly. (G,H) Structural change of outer dynein arm induced by nucleotides, shown by wire-frame model (top; side views) and vertical sections (bottom; end view), respectively: left, ADP.Vi form (pre-powerstroke); right, apo-form (post-powerstroke). In (G), AAA-rings (green) and tails (red, blue) are indicated. In H, AAA-rings are shown in red and blue. In (A,E), stalks and tails are indicated by blue dotted and solid lines, respectively. Green lines in (B) and (D) indicate the other linker. (A,B) modified from [62]. (C) modified from [32]. (D—F) modified from [37,39]. (G,H) modified from [41]. (B—E) Bar = 20 nm. (G,H) Bar = 10 nm.

the A-microtubule, while in the apo form it kinks sharply as soon as it extends from the ring (Fig. 8.2H).

8.4.4 Variation of Single-Headed Dyneins

There must be functional reasons why six isoforms of single-headed inner-arm dyneins, rather than six identical dyneins, form the array on the A-microtubule. These isoforms have diverse biophysical and biochemical characteristics. While dynein c has a velocity of ~6.7 μm/s in the *in vitro* motility assay, other dyneins are slower (Table 8.1). Dynein c is important in the maintenance of velocity in highly viscous solutions [53]. There are a number of publications reporting different performances of the inner-arm dynein isoforms [54]. The orientations of the heads of the six single-headed dyneins have slight variations (up to ~35° [38]) (Fig. 8.2B). The manner in which their conformations change during the powerstroke varies as well. While the shift induced by ADP.Vi binding is parallel to the microtubule in the case of outer-arm dynein α and inner-arm dynein e, the head of inner-arm dynein c shows a lateral shift as well (Fig. 8.2F,G). This suggests that the role of dynein c is not only to drive the B-microtubule but also to generate torque. This activity might be related to the ability of dynein c to rotate microtubules during the *in vitro* motility assay [54].

The question of what mechanism locates each isoform in the correct position is also still open. Since the microtubule itself has an 8 nm periodicity, there should be binding proteins on either the outer or inner surface of the microtubule to function as landmarks or rulers. To bind to the proper positions, inner-arm dynein isoforms must be able to recognize specific features on the uneven surface. Conformations of the tails of dynein isoforms differ (blue lines in Fig. 8.2D), reflecting the diverse sequences of the N-terminal domains.

8.5 Outer Dynein Arm Structure *In Situ*

8.5.1 Overall Structure

Outer dynein arms form an array on microtubule doublets with a 24 nm periodicity [32,55]. Each unit of outer dynein arm in flagella of *Chlamydomonas* and *Tetrahymena* consists of three vertically stacked disks [36,37] (Figs. 8.2A and 8.3). Cross-sections of each of the three discs show a ring, indicating a AAA ring of the three outer-arm dyneins to be genetically [56] and biochemically [53] characterized. The docking complex is located at the external side of the γ-head [38], which is consistent with observations from plastic embedded sections [43] (details of the docking complex are described in Chapter 7). In sea urchin sperm flagella, which have only two outer-arm dyneins, two discs are stacked vertically [35].

Adjacent periodic units are connected by two slender linkers [37] (Fig. 8.3D), which are likely the N-terminal tails of the three dynein HCs. One is located at the

inner side of the axoneme and tilted at ~45° (blue line in Fig. 8.3D), whereas the other linker (green lines) at the external side is horizontal at the height of the middle disc (top disc when there are only two discs, as in the sea urchin sperm). These results from electron cryo-tomography are consistent with previous reports based on electron microscopy with traditional specimen-preparation techniques (Fig. 8.3A,B,C). The tilted linker ("slender rod"[37]) probably corresponds to the "lobe" described in the study of negatively stained axonemes [32,57] (blue line in Fig. 8.3C), whereas the external linker was observed via the freeze-fracture-deep-etch technique [55] (green line in Fig. 8.3B). A more detailed comparison is made elsewhere [58].

Three-dimensional visualization of the coiled-coil stalk came later than that of the ring and the tail because of the stalk's thin nature. Freeze-fracture-deep-etch was the most powerful approach to visualizing this coiled coil [30,59]. However, averaging 24 nm periodic units (instead of 96 nm for inner dynein arms) improves the signal-to-noise ratio and thus enables us to see the coiled-coil stalk three-dimensionally via cryo-tomography (Fig. 8.3E) [39]. The stalk extends from the ring toward the B-microtubule and is slightly tilted toward the proximal end, which is consistent with tomography of the replica [59]. The stalk from cytoplasmic dynein alone binds on the reconstituted microtubule at the same angle [26,60,61], suggesting that this binding angle results from an intrinsic property of MTBD and the stalk.

8.5.2 The Difference Between Native Outer Dynein Arms *In Situ* and Purified Outer Dynein Arms *In Vitro*

The isolated outer dynein arm, when observed by the rotary shadowing technique [62] and negative stain [37], shows a completely different structure, termed a "bouquet" (Fig. 8.3A). *In situ*, the bundled tails of this bouquet are likely bound on the A-microtubule and three heads stack vertically when outer dynein arms are arrayed on the microtubules (Fig. 8.3F). Indeed, when the isolated outer dynein arms are mixed with reconstituted microtubules, AAA rings form stacks [44,63]. However, the way in which the three heads stack in the *in situ* constitution is slightly different from the *in vitro* reconstitution [44], which likely lacks the docking complex [36,37,38]. Functional differences are reported as well: reconstituted outer dynein arm/microtubule complexes, in which outer dynein arms form arrays on the the microtubules, drive additional microtubules one and a half times faster than the native outer dynein arms on microtubule doublets [11].

8.5.3 Tail Conformation

It is less straightforward to identify the tail for each outer-arm dynein than it is to identify the tail for inner-arm dyneins. Data from the *Chlamydomonas oda11* mutant (lacking α-dynein) indicates that the tilted slender rod is the α-tail. This

means that the N-terminal tail extends toward the distal end of the flagellum in a similar manner to the inner-arm dyneins. The pathway of the β-tail is still not clear: it could merge with the α-tail in the "slender rod" at the internal side or could be the external linker (Fig. 8.3D). In either case, the β-tail, similarly to the α-tail, extends toward the distal end. Less certain is the direction of the γ-tail, which is not visible as a direct connection between the γ-head and the slender rod. Currently two models have been proposed [37] (Fig. 8.3F): (1) The γ-tail is the external linker and extends from the head toward the distal end in parallel with the α and β dyneins (Fig. 8.3F, left). (2) The γ-tail extends from the γ-head belonging to the adjacent (distal) complex and toward the proximal end, and merges with the α- and β-tails. In this scenario three heads do not stack as one complex, but the adjacent complexes form a tandem array (Fig. 8.3F, right). If the conformation of the γ-HC is different from that of HCs α and β, the γ-dynein will have a different function (perhaps regulatory), which is in agreement with the *in vitro* motility assay data, which show an increased velocity in the absence of the γ-dynein [64]. Genomic analysis also indicates the similarity of the α and β HCs of *Chlamydomonas* compared to the γ chain [65]. However, the direction of the stalk is the same (slightly tilted toward the proximal end) for all three HCs in *Chlamydomonas* (Fig. 8.3E, right) [39]. Furthermore, the stalk orientation does not change upon nucleotide binding both for the β- and γ-dyneins [41] (see Section 8.5.4), suggesting that the roles of β- and γ-dynein are rather similar. Structural analysis at higher resolution and functional analysis in more intact states are awaited.

8.5.4 Conformational Change Induced by Nucleotides: Winch Model

As with the inner-arm dyneins, structural changes take place in the outer dynein arm during the powerstroke. However, interestingly, in the presence of nucleotides only some of the outer dynein arms undergo conformational changes while the others stay in a non-nucleotide-bound form (apo form) (Fig. 8.4). The detail of this heterogeneity will be described in Section 8.6.1. Here we will focus on the conformation specifically appearing in the presence of ADP.Vi (termed the ADP.Vi form).

The rings shift ~8 nm toward the proximal end in the outer dynein arm in the ADP.Vi form (left in Fig. 8.3G) compared to the apo form (right). A conformational change of the tail domain occurs in a similar manner to that of the inner dynein arms (Fig. 8.2H): the tail extends from the ring and gradually curves toward the A-microtubule in the presence of ADP.Vi (pre-powerstroke) but kinks sharply in the apo form (post-powerstroke) (Fig. 8.3G). In contrast, there is no obvious change in the coiled-coil stalk, which extends from the ring toward the B-microtubule and is slightly tilted toward the proximal end (Fig. 8.5D, E). Since the stalk is located between the AAA4 and AAA5 domains, the constant angle of the stalk indicates that there is no rotation of the ring during the powerstroke. The shift of the ring could pull (winch)

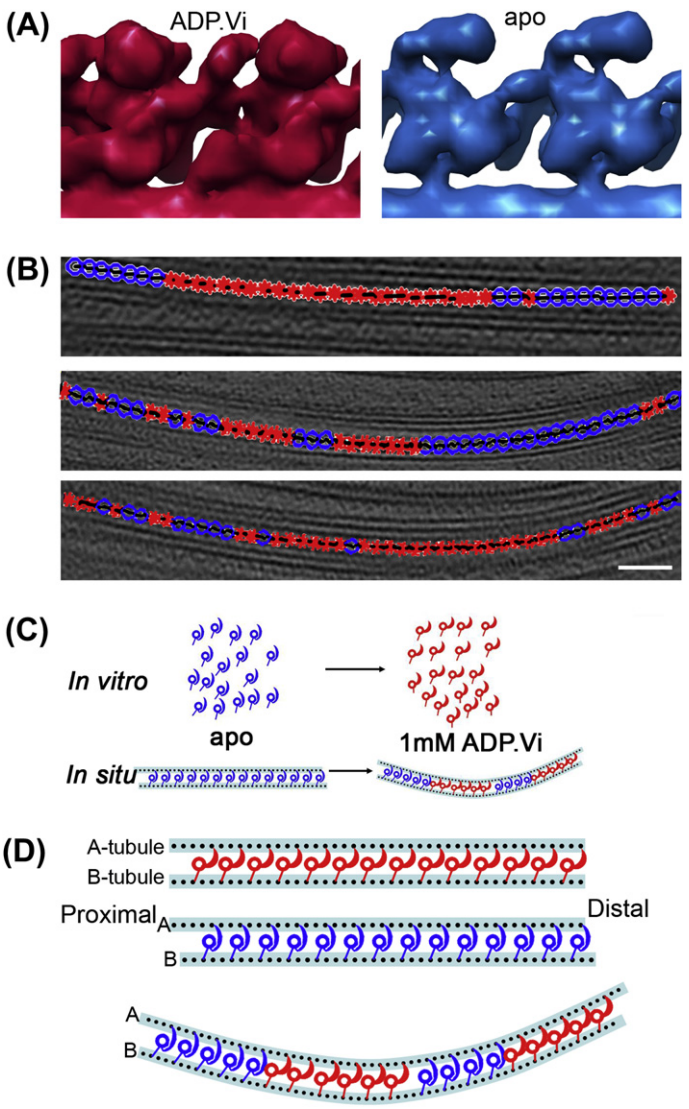

Figure 8.4 **Nucleotide-induced heterogeneous structural change of outer dynein arms *in situ*.** (A) Two conformations coexisting in the flagella with ADP.Vi: the apo form (blue) and the ADP.Vi form (red). (B) Outer dynein arms arrayed on three microtubule doublets are classified based on the two forms given in (A) as templates. Blue and red figures indicate outer dynein arms that show similarity to the apo and ADP.Vi forms, respectively. Bar = 100 nm. (C) Diagram of nucleotide-induced structural change of dyneins. Above: When 1 mM ADP.Vi is added, all the purified dyneins (without microtubules) turn into the ADP.Vi form. Bottom: Only some fractions of dyneins in flagella, however, change their conformations (red); the rest remain as the apo form (blue). (D) Bending mechanism based on the heterogeneity. Upper: if the conformations of all the dyneins change in a synchronized manner, the adjacent microtubules only slide past each other. Lower: when regions of two (or more) structures coexist, torsion is generated at the interface between the regions. *Modified from [41].*

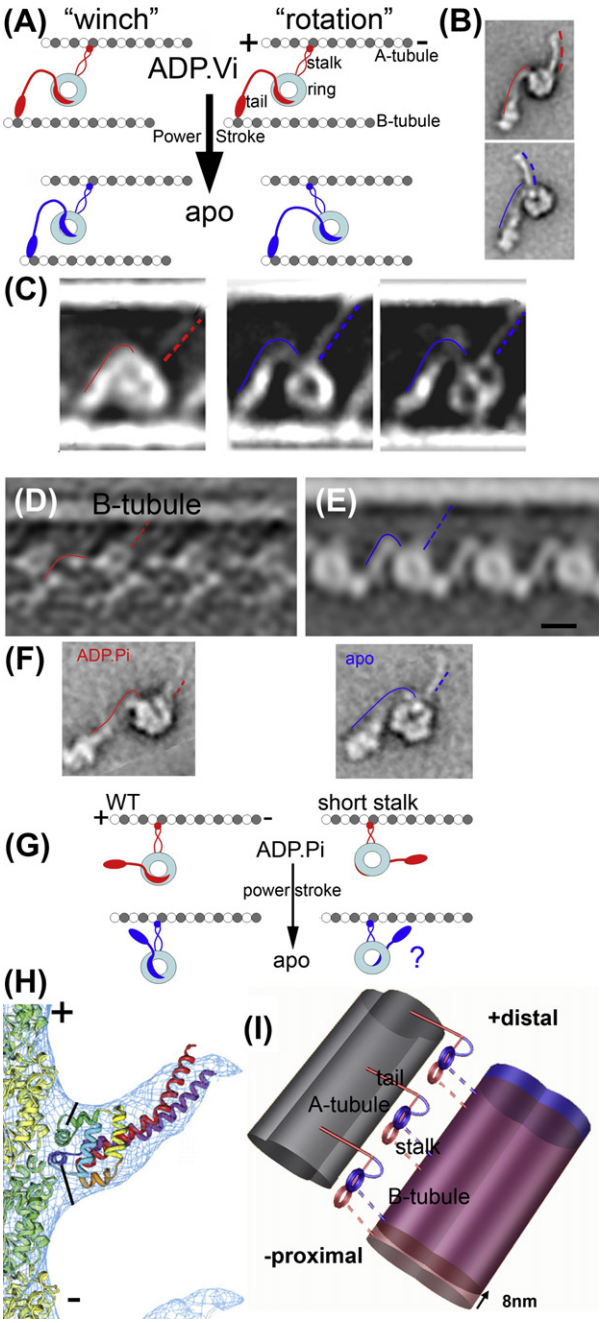
(A)
"winch"
"rotation"
(B)
+
-
ADP.Vi
stalk
ring
tail
A-tubule
B-tubule
Power Stroke
apo
(C)
(D)
B-tubule
(E)
(F)
ADP.Pi
apo
(G)
WT
short stalk
+
-
ADP.Pi
power stroke
apo
?
(H)
+
-
(I)
+distal
tail
A-tubule
stalk
B-tubule
-proximal
8nm

the adjacent B-microtubule by 8 nm. Section 8.7.1 will examine the winch mechanism.

The vertical section of the tomogram gives us an insight into the strong/weak binding process [41] (Fig. 8.3H). In the ADP.Vi form the β-ring is tilted at ~30° and the distance between the α-ring and the adjacent B-microtubule is ~400 Å. After the powerstroke, in the apo form the β-ring becomes horizontal (i.e. parallel to the γ-ring) and, probably as a result, the α-ring moves closer to the B-microtubule (distance: ~200 Å). This lateral rotation and shift could explain the transitional mechanism between the weak binding and strong binding states. A similar experiment carried out with the two-headed outer dynein arm (e.g. sea urchin sperm flagella) would aid our comprehension.

The structure of the outer dynein arm in the presence of ADP is similar to the apo form. This finding is consistent with kinetics studies [50].

8.6 Heterogeneity and Asymmetry of Structure and Arrangement of Dynein in the Axoneme

For a long time it was believed that inner dynein arm and outer dynein arm have 96 nm and 24 nm periodicities, respectively, and that most axonemes have a symmetric arrangement of nine microtubule doublets with only a few exceptional asymmetries: one doublet of *Chlamydomonas* lacks outer dynein arm and only three doublets have a beak-like structure inside the B-microtubules [66] (Fig. 8.6A). However, progress in electron cryo-tomography, genomic studies, and light microscopy has revealed additional exceptional molecular arrangements and structural heterogeneity of dyneins and other proteins in the axoneme. Cryo-tomography revealed asymmetric structural change of dyneins induced by nucleotides.

Figure 8.5 Rotation mechanism. (A) "Rotation" and "winch" models. (B) Two-dimensional averages of negatively stained dynein c showed structural change induced by ADP.Vi. (C) Two-dimensional averages of sea urchin sperm outer-arm dyneins arrayed on microtubules. (D,E) Sections from electron cryo-tomograms, with and without ADP.Vi, respectively. Bar = 10 nm. (F) Images in (B) are rotated to fit to the orientation of (D,E). (G) Genetic engineering and the *in vitro* motility assay approach prove that the "rotation" hypothesis is wrong. Cytoplasmic dynein with a half-pitch-shorter stalk (right) will run to the opposite direction if the rotation is a driving force. However, such an engineered dynein also moves to the minus end. (H) Pseudo-atomic model of a microtubule and a cytoplasmic dynein stalk. The direction of the stalk is the same as that of axonemal dynein. (I) Model of microtubule sliding *in situ*. (A) modified from [63]. (B) modified from [3]. (C) modified from [63]. (D,E) modified from [41]. (G,H) modified from [26]. (I) modified from [41].

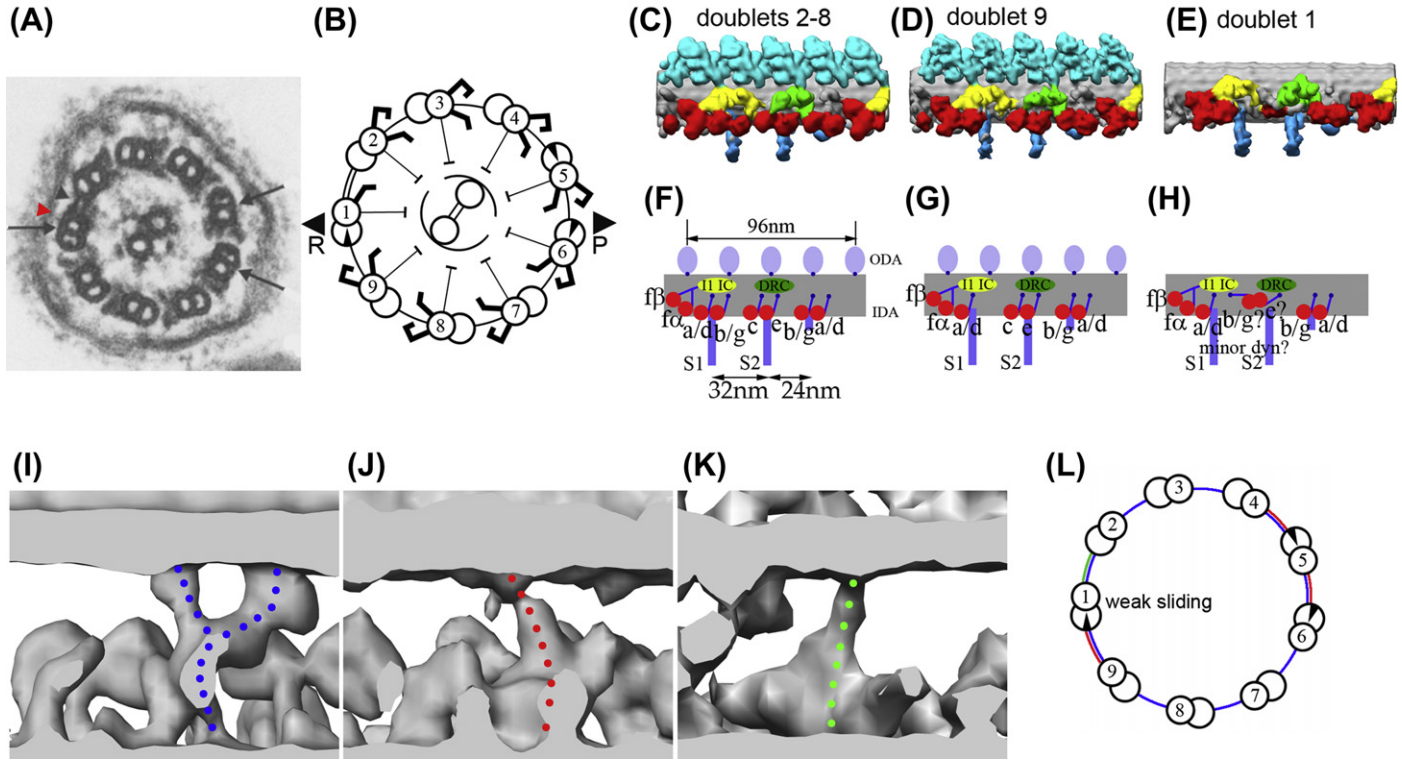

Figure 8.6 Asymmetric arrangements of dyneins and other molecules in the axoneme. (A) Cross-section of *Chlamydomonas* axoneme reveals the absence of outer dynein arm on one doublet (red arrowhead); the 1–2 bridge (black arrowhead); and the beak-like structure inside B-microtubules 1, 5 and 6 (arrows). (B) Numbering of microtubule doublets based on (A). The two arrowheads show the direction of principle (P) and reverse (R) bending. (C–H) Asymmetry of dynein arrangements demonstrated by electron cryo-tomography. (C–E) are tomograms; (F–H) are schematic diagrams. Doublets 1 and 9 have exceptional arrangement of inner-arm dyneins. (I–L) Asymmetry of interdoublet linkers. (I) Nexin (blue dotted lines), which links all the adjacent pairs. (J) IDL2 (red) between doublets 9/1, 4/5, and 5/6. (K) IDL3 (green) between doublets 1 and 2. (L) Locations of the linkers plotted on the section. (A) Modified from [66]. (B–L) Modified from [39].

8.6.1 Cluster Formation Observed in Tomograms with Nucleotides

If all the dyneins were to change their form simultaneously, they would cause the microtubules to slide past each other rather than bend. Electron cryo-tomography revealed the coexistence of at least two forms *in situ* in the presence of ADP.Vi. In *Chlamydomonas* flagella with 1 mM ADP.Vi, ~52% of outer dynein arms take the ADP.Vi form and the rest of the outer dynein arms stay in the apo form. Furthermore, the two forms do not appear randomly but exist as clusters [41] (Fig. 8.4A,B). This suggests that, by integrating dyneins on microtubules, a force different from simple sliding can be generated in the axoneme; for example, torsion or strain between two clustering areas, which could cause bending. The length of each cluster varies from several outer dynein arms to 30 outer dynein arms. From outer dynein arms on eight microtubules in one segment of one flagellum, we have so far found no obvious relationships between the cluster distribution and macroscopic flagellar bending. Apparently it is not as simple as one side being active and the other inactive; both sides of the curvature have clusters of both the ADP.Vi form and the apo form. In fact, it is not even clear whether this cluster formation is the cause or the result of the bending. We do at least know, however, that it is not simple, passive morphological change caused by the binding of the microtubule [41].

What is the mechanism that creates this clustering? Here two possibilities will be considered. One is cooperativity among outer dynein arms. Adjacent outer dynein arms are connected by various pathways: two linkers (Fig. 8.3D), the A-microtubule, and the adjacent B-microtubule. It is yet to be determined whether cluster formation occurs in outer dynein arms on a doublet isolated from the axoneme. Another possibility is that dynein is a mechanical sensor. Oscillation of the outer dynein arms themselves during *in vitro* motility assays [14,64] could be interpreted as repetitive forward and backward motions caused by the load from optical tweezers [67]. Single dyneins can move backwards under high loads [6]. In the case of cytoplasmic dynein, asymmetric load-dependent (and nucleotide-independent) step-wise motion was observed: 3 pN is enough to drive dynein forward, while 7−10 pN is necessary for backward motion [68]. In any case, these observations suggest that dyneins have unique properties. These special characteristics could induce flagellar/ciliary bending.

8.6.2 Asymmetry of Dynein and Interdoublet Linker Proteins

Progress in *in situ* electron cryo-tomography has revealed an asymmetric arrangement of both dyneins and other linkers among the nine microtubule doublets. It is known that outer dynein arms are missing on one doublet[1] of

[1] *This doublet was named doublet 1: other doublets are numbered clockwise as seen from the base (Fig. 8.6B). In the two flagella of one* Chlamydomonas *cell, the doublet 1s appose each other.*

Chlamydomonas [66] (Fig. 8.6A). However, it is hard to explain the mechanism of the asymmetric flagellar waveform based on this specific distribution of outer dynein arms because the *oda1* mutant, which lacks all outer dynein arms, can swim with the regular waveform [69]. The new asymmetry found by cryo-tomography involves the inner dynein arm [39]: doublet 9 lacks one dynein besides radial spoke 1, while three dyneins are either missing or folded differently on doublet 1 (Fig. 8.6C–H). Since doublets 1 and 9 are located at the inner side of the two flagella, this finding suggests an asymmetry of sliding force between the inside and the outside of the flagellum, which could cause the asymmetric waveforms of the principle bend and the reverse bend.

Asymmetry also exists for the interdoublet linkers [39] (Fig. 8.6I–L). Besides the well-known nexin linker (see Chapter 12), which exists between all the adjacent doublets, another linker has been found to connect doublets 4/5, 5/6, and 9/1 (we call this linker IDL2), while the third linker (IDL3) links doublets 1 and 2. Since all these extra linkers are located on the plane of bending, they could be considered as extra linkages that restrict the bending plane.

The mechanism of the asymmetric flagellar/ciliary formation is not clear. It might result from the asymmetry of the basal body or the asymmetric design of the intraflagellar transport (IFT).

8.6.3 Longitudinal Asymmetry

The longitudinal periodicity (96 nm) was found to break down at the proximal end of the *Chlamydomonas* flagellum. Between doublets 1 and 2 there is a dense connection near the basal body (1–2 bridge) [39,66]. Cryo-tomography clarified that there are highly dense linkers with 8 nm periodicity that also could suppress the sliding between doublets 1 and 2. The proximal domain has an unusual dynein distribution. Yagi et al. [70] demonstrated that minor dyneins, which are found in the *Chlamydomonas* genome but have never been detected biochemically, exist only in the proximal region. These specific features of the proximal end might be relevant to the sharp bend $\sim 2\mu m$ away from the base of *Chlamydomonas* flagella.

8.6.4 Cylindrical or Helical?

It will be very interesting to see how the 96 nm units are aligned in the cylindrical axoneme: do they have cylindrical symmetry or helical symmetry? Based on the freeze-fracture-deep-etch electron microscopy of *Tehtrahymena* cilia, Goodenough and Heuser [30] proposed that the 96 nm units form a three-start right-handed helix. X-ray fiber diffraction of sea urchin sperm flagella also supports the idea that the units form a helix [71]. This problem must be re-examined by cryo-tomography, and it will be intriguing to find out whether it is affected by nucleotides or regulatory mechanisms.

8.7 Thoughts on Dynein Functions Based on *In Situ* Structure

8.7.1 Powerstroke Mechanism of the Single Dynein Monomer

Controversy exists over the mechanism of the dynein powerstroke: dynein generates force either by rotating or shifting its head (the "rotation" and "winch" hypotheses) (Fig. 8.5A). Three-dimensional structural analysis supports the model in which the shift of dynein heads winches (without rotation) the adjacent B-microtubule through the stalk [41]. This structural change of the dynein HC *in situ* is consistent with that observed by cryo-positive stain electron microscopy of purified and reconstituted dynein and microtubules [63] (Fig. 8.5C). Burgess et al. [3], using negative stain and two-dimensional averaging from electron microscopy, demonstrated that, in purified dynein c, the relative angle between the tail and the stalk changes by the binding of ADP.Vi (Fig. 8.5B) (see Chapter 4). This result, since it does not involve microtubules in the system, could be fitted to both models (winch and rotation) and does not contradict the result obtained by tomography (Fig. 8.5D–F).

Functional studies also support the winch model. Carter et al. [26] showed that the orientation of microtubule sliding by dynein is not affected by the length of the stalk. If the stalk is rigid enough to push the microtubule by rotation, when the stalk is shorter or longer by half the pitch of the coiled coil it will flip the orientation of the dynein head and thus induce the powerstroke in the opposite direction (Fig. 8.5G). The fact that the orientation of the sliding of the microtubule is independent of the stalk length supports the winch hypothesis.

The mechanism of winching must be investigated and will require a higher-resolution structure. The tail conformation in the averaged tomogram might give us a hint. The length of the tail between the neck region and the joint to the A-microtubule is shorter in the apo form than in the ADP.Vi form (Fig. 8.2H). This indicates a conformational change within the tail. One possibility is that the linker region, which extends across the ring, folds into the inside of the ring more deeply in the apo form, making the rest of the tail shorter. The activity of dynein as a AAA protein makes such a rearrangement possible. Most of the AAA proteins have substrates threaded into their rings [72]. If dynein has its own linker region as a substrate, it will be drawn inside the ring more deeply and leave the rest of the tail shorter.

During the force-generating cycle, the binding constant between dynein and the B-microtubules must be changed and this transition must be induced by the nucleotide states. Since the distance between the MTBD and the ATP-binding domain of dynein is greater than that of myosin, the mechanism to modulate the microtubule-binding affinity of dynein should also be different from that of myosin [73]. Gibbons et al. [74] hypothesized that this modulation occurs by

sliding of the two α helices composing the coiled-coil stalk. Carter et al. [26] and Kon et al. [75] proved this hypothesis by mutating residues within the stalk to lock the sliding at different stages.

8.7.2 Powerstroke of Dimeric Dyneins: Hand-Over-Hand or Synchronized?

From the *in vitro* motility assay it is known that cytoplasmic dynein processively walks on microtubules in a "hand-over-hand" manner [76], in which the two heads of the dynein dimer alternate during the advances. However, we still do not know whether axonemal dyneins, especially outer-arm dyneins, move in a synchronized or hand-over-hand manner. This question could be relevant to another question: why are there two-headed outer dynein arms and three-headed outer dynein arms?

Electron microscopy/tomography has not yet made the answer clear. Three-dimensional image classification did not detect any three-headed outer dynein arms with the three heads in different forms, suggesting a synchronized power-stroke. However, this could be the result of the limitations of the classification. Two-dimensional classification and averaging of single particles of reconstituted outer dynein arms show shifted pairs of outer-arm dyneins as well as overlapped pairs, suggesting that they walk [63]. However, since this is a two-dimensional study, it is hard to distinguish real shifted pairs from overlapped pairs seen at a tilted angle. Considering the low duty ratio (0.08) of outer dynein arms [64], outer-arm dyneins are not processive motors (at least as an isolated form) and thus do not necessarily have to walk along microtubules at all.

According to comparative genomic studies [65], *Chlamydomonas* α and β outer-arm dyneins (which correspond to the γ and β outer-arm dyneins, respectively, of *Tetrahymena*) belong to one class, whereas γ belongs to another class. This apparently makes the possibility of the outer dynein arm walking using only the upper two dyneins (α and β of *Chlamydomonas* and β and γ of *Tetrahymena*) unlikely as a universal model (it cannot explain the motion of two-headed outer dynein arms). There is still a possibility that the two lower dyneins (β and γ of *Chlamydomonas* and α and β in *Tetrahymena*) generate a walking motion.

8.7.3 Bending Mechanism

If force generation is uniform along the axoneme, microtubules will slide past each other and cannot produce bending motion. Some part of the axoneme must generate more force than other parts or generate forces in the opposite direction and this local distribution must move as a package during propagation of the wave form. This has been pointed out by theoretical model building [77]. Classification from tomograms of ice-embedded *Chlamydomonas* flagella with ADP.Vi demonstrated that two structures (the ADP.Vi form and the apo form) coexist and form clusters, thus supporting this idea [41]. However, judging from the pattern

of the heterogeneity, a simple model such as "sliding at one side of the axoneme while relaxed (or halting) at the other side," as conceptualized frequently [18,78], is not correct. Theoretical modeling and more data under various bending conditions are required to explain these complex patterns.

The system to propagate dynein activity along (or among) doublets must be either programmed inside the axoneme or self-organized by a feedback mechanism. For the latter, dynein must sense local sliding/bending conditions. Until now, however, there has been no direct report of sensory proteins participating in the bending function. Displacement or force could be sensed by dynein itself. In other words, dynein might change gears under sliding/bending conditions. There have been quite a few theoretical studies aiming to explain physiological flagellar/ciliary bending motion by introducing models in which such characteristics as force–velocity curves and attachment/detachment rates are influenced by the sliding displacement of microtubules [21,79], curvature [78], sliding velocity [80], load [79], and distance between adjacent doublets [16,19,20,81]. Electron cryotomography has not demonstrated a correlation between outer dynein arm structures and curvature or interdoublet distances, at least with current resolution [41]. The roles of dynein isoforms are also yet to be characterized. Brokaw proposed a non-linear force–velocity relationship in outer dynein arms to explain the effects of the removal of outer dynein arms [82], but this has not so far been proved by *in vitro* motility assays of purified outer-arm dyneins [83], although outer dynein arms may behave differently in flagella *in situ*. Additionally, the characteristics of single dynein motors and the effects of basal sliding [21] and head motility (clamped, fixed and free heads) [84] – which have been proposed to be influential in bending motion – must be experimentally examined.

The structural heterogeneity of inner-arm dyneins in the presence of nucleotides is even more complicated. Three-dimensional classification from tomograms has demonstrated that different isoforms have different distributions of pre- and post-powerstroke conformations; when both dynein c and dynein e are in the nucleotide-free form in one 96 nm unit, another unit can have dynein c in the apo form and dynein e in the ADP.Vi form (Bui et al. manuscript in preparation). A variety of duty ratios (dynein f: 0.63 [49]; dynein c: 0.14 [6]; ODA: 0.08 [64]) and ATPase activities could explain the unsynchronized distributions of dynein conformations. However, the meaning of this heterogeneity in the context of the bending motion must be examined with more datasets in the future.

8.7.4 How are the Dyneins Located Appropriately in the Axoneme?

Our knowledge of the mechanism by which dyneins and other molecules are arranged in the axoneme is quite limited. Although it is known that flagella/cilia are built at the tip by IFT, there should be landmarks or rulers to indicate where the transported protein should bind. The docking complex is essential for outer

dynein arm binding on the A-microtubule and is responsible for the ordered binding of outer dynein arms with 24 nm periodicity (see Chapter 10) [85]. However, this fact only raises a further question: how is the location of the docking complex determined?

For inner dynein arms, no proteins have yet been identified as rulers. Proteins binding to the inside of the microtubules of a doublet might be candidates to influence dynein binding on the microtubules. Not much is known about such candidates as tektin, Sp77, and Sp83. The structure on the inside [86] might affect the structure on the outside of the microtubules, which controls the binding of dyneins and other microtubule binding proteins to organize the architecture in a 96 nm unit and the targeted binding of stalks.

Further open questions concern the manner and the mechanism by which the stalk targets the B-microtubule. According to cryo-EM studies on cytoplasmic dyneins, the dynein MTBD and kinesin bind to the same region of reconstituted microtubules [60]; that is, on the protofilament rather than between protofilaments. It is not known whether the stalks bind only on microtubules that have a B-lattice, such as most reconstituted microtubules [87] and the B-microtubule [88] (it will be worthwhile to determine this assignment via modern techniques such as electron tomography of kinesin-decorated doublets). In the apo form of the outer dynein arm, the MTBD (the tip of the coiled coil) of the three outer dynein arms binds on protofilaments 4, 5, and 6 of the B-microtubule, respectively [38]. It is not clear whether the stalk targets the same protofilament under different nucleotide conditions.

8.8 Outlook

The current knowledge on axonemal dyneins has been presented and questions still to be answered have been raised. Which technology will help us to learn more about axonemal dyneins? In specimen preparation, targeted mutagenesis of axonemal dynein HCs is an urgent issue. Currently, genetic engineering of flagellar/ciliary dynein HC is limited to knockout [89,90,91] and RNA interference (RNAi) techniques. If mutant axonemal dynein HCs can be designed and expressed, it will enable various functional techniques (such as fluorescence resonance energy transfer, which has been carried out for cytoplasmic dynein [52]) to be used and also will help structural analysis (crystallography and single-particle analysis electron microscopy) by reducing the flexibility of dynein molecules. Furthermore, homologous recombination of dynein HC and expression in the axoneme will make various physiological studies and *in situ* labeling possible (at the levels of both light and electron microscopy).

Analytical methods also have room for improvement. For electron cryo-tomography larger detectors will enable us to cover wider areas of flagella (hopefully a full-length flagellum in the future) without loss of resolution. Currently, data for

cryo-tomography of flagella/cilia are collected on 2048×2048 pixel detectors, which corresponds to ~1 μm at a resolution of ~35 Å [38]. If tomographic data acquisition using a larger camera becomes possible, longer fragments of flagella/cilia can be visualized and will give us more insight into the dynamic structural pattern of dyneins along microtubules. To localize the ~600 proteins identified in *Chlamydomonas* flagella by proteomics [1], we need systematic labeling methods. Motility assays under more intact conditions will be informative. TIRF to detect single ATPase events and force measurement (by optical tweezers or AFM) [92] – not only with purified dyneins but also for dyneins in more complex structures, such as in dynein arms or on the microtubule doublets – will give us a better idea as to how dyneins function as a group in flagella/cilia. To examine the characteristics of dyneins under strain, velocity, and load as modeled (see Section 8.7.2), we need to fuse electron cryo-tomography and *in vitro* motility assays. It is to be hoped that dynein research will inspire the development of new technology.

Acknowledgments

I acknowledge Dr. David Sargent (ETH Zurich) for critical reading of the manuscript. Figure 8.2C,D are courtesy of Dr. Khanh Huy Bui (ETH Zurich/PSI).

References

[1] G.J. Pazour, N. Agrin, J. Leszyk, G.B. Witman, Proteomic analysis of a eukaryotic cilium, J. Cell Biol. 170 (2005) 103–113.
[2] M. Samso, M.P. Koonce, 25 angstrom resolution structure of a cytoplasmic dynein motor reveals a seven-member planar ring, J. Mol. Biol. 340 (2004) 1059–1072.
[3] S.A. Burgess, M.L. Walker, H. Sakakibara, P.J. Knight, K. Oiwa, Dynein structure and power stroke, Nature 421 (2003) 715–718.
[4] H. Kojima, S. Toba, H. Sakakibara, K. Oiwa, Biophysical measurements on axonemal dyneins, Methods Cell Biol. 92 (2009) 83–105.
[5] A.F. Neuwald, L. Aravind, J.L. Spouge, E.V. Koonin, AAA^{+}: A class of chaperone-like ATPases associated with the assembly, operation, and disassembly of protein complexes, Genome Res. 9 (1999) 27–43.
[6] H. Sakakibara, H. Kojima, Y. Sakai, E. Katayama, K. Oiwa, Inner-arm dynein c of *Chlamydomonas* flagella is a single-headed processive motor, Nature 400 (1999) 586–590.
[7] H. Kojima, E. Muto, H. Higuchi, T. Yanagida, Mechanics of single kinesin molecules measured by optical trapping nanometry, Biophys. J. 73 (1997) 2012–2022.
[8] O. Kagami, R. Kamiya, Translocation and rotation of microtubules caused by multiple species of *Chlamydomonas* inner-arm dynein, J. Cell Sci. 103 (1992) 653–664.
[9] R. Kamiya, Exploring the function of inner and outer dynein arms with *Chlamydomonas mutants*, Cell Motil. Cytoskel. 32 (1995) 98–102.
[10] K.E. Summers, I.R. Gibbons, Adenosine triphosphate-induced sliding of tubules in trypsin-treated flagella of sea-urchin sperm, Proc. Natl. Acad. Sci. U.S.A. 68 (1971) 3092–3096.
[11] S. Aoyama, R. Kamiya, Strikingly fast microtubule sliding in bundles formed by Chlamydomonas axonemal dynein, Cytoskeleton (Hoboken) 67 (2010) 365–372.
[12] H. Sakakibara, H. Nakayama, Translocation of microtubules caused by the alphabeta, beta and gamma outer arm dynein subparticles of *Chlamydomonas*, J. Cell Sci. 111 (Pt 9) (1998) 1155–1164.

[13] R.N. Seetharam, P. Satir, High speed sliding of axonemal microtubules produced by outer arm dynein, Cell Motil. Cytoskeleton 60 (2005) 96–103.
[14] C. Shingyoji, H. Higuchi, M. Yoshimura, E. Katayama, T. Yanagida, Dynein arms are oscillating force generators, Nature 393 (1998) 711–714.
[15] D.L. Holcomb-Wygle, K.A. Schmitz, C.B. Lindemann, Flagellar arrest behavior predicted by the Geometric Clutch model is confirmed experimentally by micromanipulation experiments on reactivated bull sperm, Cell Motil. Cytoskeleton 44 (1999) 177–189.
[16] C.B. Lindemann, Structural-functional relationships of the dynein, spokes, and central-pair projections predicted from an analysis of the forces acting within a flagellum, Biophys. J. 84 (2003) 4115–4126.
[17] T.J. Mitchison, H.M. Mitchison, Cell biology: How cilia beat, Nature 463 (2010) 308–309.
[18] C.J. Brokaw, Thinking about flagellar oscillation, Cell Motil. Cytoskeleton 66 (2009) 425–436.
[19] C.B. Lindemann, Testing the geometric clutch hypothesis, Biol. Cell 96 (2004) 681–690.
[20] C.B. Lindemann, The geometric clutch as a working hypothesis for future research on cilia and flagella, Ann. N.Y. Acad. Sci. 1101 (2007) 477–493.
[21] I.H. Riedel-Kruse, A. Hilfinger, J. Howard, F. Julicher, How molecular motors shape the flagellar beat, HFSP J. 1 (2007) 192–208.
[22] F. Julicher, J. Prost, Spontaneous oscillations of collective molecular motors, Phys. Rev. Lett. 78 (1997) 4510–4513.
[23] A. Vilfan, F. Julicher, Hydrodynamic flow patterns and synchronization of beating cilia, Phys. Rev. Lett. 96 (2006) 058102.
[24] B. Guirao, J.F. Joanny, Spontaneous creation of macroscopic flow and metachronal waves in an array of cilia, Biophys. J. 92 (2007) 1900–1917.
[25] W.F. Marshall, Cilia self-organize in response to planar cell polarity and flow, Nat. Cell. Biol. 12 (2010) 314–315.
[26] A.P. Carter, J.E. Garbarino, E.M. Wilson-Kubalek, W.E. Shipley, C. Cho, R.A. Milligan, R.D. Vale, I.R. Gibbons, Structure and functional role of dynein's microtubule-binding domain, Science 322 (2008) 1691–1695.
[27] M. van Heel, B. Gowen, R. Matadeen, E.V. Orlova, R. Finn, T. Pape, D. Cohen, H. Stark, R. Schmidt, M. Schatz, A. Patwardhan, Single-particle electron cryo-microscopy: Towards atomic resolution, Q. Rev. Biophys. 33 (2000) 307–369.
[28] E.V. Orlova, H.R. Saibil, Structure determination of macromolecular assemblies by single-particle analysis of cryo-electron micrographs, Curr. Opin. Struct. Biol. 14 (2004) 584–590.
[29] J. Frank, Single-particle imaging of macromolecules by cryo-electron microscopy, Annu. Rev. Biophys. Biomol. Struct. 31 (2002) 303–319.
[30] U. Goodenough, J. Heuser, Substructure of inner dynein arms, radial spokes, and the central pair/projection complex of cilia and flagella, J. Cell Biol. 100 (1985) 2008–2018.
[31] D.N. Mastronarde, E.T. O'Toole, K.L. McDonald, J.R. McIntosh, M.E. Porter, Arrangement of inner dynein arms in wild-type and mutant flagella of *Chlamydomonas*, J. Cell Biol. 118 (1992) 1145–1162.
[32] J. Avolio, S. Lebduska, P. Satir, Dynein arm substructure and the orientation of arm-microtubule attachments, J. Mol. Biol. 173 (1984) 389–401.
[33] M.E. Porter, Axonemal dyneins: Assembly, organization, and regulation, Curr. Opin. Cell Biol. 8 (1996) 10–17.
[34] O. Medalia, I. Weber, A.S. Frangakis, D. Nicastro, G. Gerisch, W. Baumeister, Macromolecular architecture in eukaryotic cells visualized by cryoelectron tomography, Science 298 (2002) 1209–1213.
[35] D. Nicastro, J.R. McIntosh, W. Baumeister, 3D structure of eukaryotic flagella in a quiescent state revealed by cryo-electron tomography, Proc. Natl. Acad. Sci. U.S.A. 102 (2005) 15889–15894.

[36] D. Nicastro, C. Schwartz, J. Pierson, R. Gaudette, M.E. Porter, J.R. McIntosh, The molecular architecture of axonemes revealed by cryoelectron tomography, Science 313 (2006) 944–948.
[37] T. Ishikawa, H. Sakakibara, K. Oiwa, The architecture of outer dynein arms *in situ*, J. Mol. Biol. 368 (2007) 1249–1258.
[38] K.H. Bui, H. Sakakibara, T. Movassagh, K. Oiwa, T. Ishikawa, Molecular architecture of inner dynein arms *in situ* in *Chlamydomonas reinhardtii* flagella, J. Cell Biol. 183 (2008) 923–932.
[39] K.H. Bui, H. Sakakibara, T. Movassagh, K. Oiwa, T. Ishikawa, Asymmetry of inner dynein arms and inter-doublet links in *Chlamydomonas* flagella, J. Cell Biol. 186 (2009) 437–446.
[40] T. Heuser, M. Raytchev, J. Krell, M.E. Porter, D. Nicastro, The dynein regulatory complex is the nexin link and a major regulatory node in cilia and flagella, J. Cell Biol. 187 (2009) 921–933.
[41] T. Movassagh, K.H. Bui, H. Sakakibara, K. Oiwa, T. Ishikawa, Nucleotide-induced global conformational changes of flagellar dynein arms revealed by *in situ* analysis, Nat. Struct. Mol. Biol. 17 (2010) 761–767.
[42] E.F. Smith, P. Yang, The radial spokes and central apparatus: Mechano-chemical transducers that regulate flagellar motility, Cell Motil. Cytoskeleton 57 (2004) 8–17.
[43] S. Takada, H. Sakakibara, R. Kamiya, Three-headed outer arm dynein from *Chlamydomonas* that can functionally combine with outer-arm-missing axonemes, J. Biochem. 111 (1992) 758–762.
[44] T. Oda, N. Hirokawa, M. Kikkawa, Three-dimensional structures of the flagellar dynein-microtubule complex by cryoelectron microscopy, J. Cell Biol. 177 (2007) 243–252.
[45] S.M. King, R.S. Patel-King, C.G. Wilkerson, G.B. Witman, The 78,000-M(r) intermediate chain of *Chlamydomonas* outer arm dynein is a microtubule-binding protein, J. Cell Biol. 131 (1995) 399–409.
[46] G. Piperno, K. Mead, W. Shestak, The inner dynein arms I2 interact with a "dynein regulatory complex" in *Chlamydomonas* flagella, J. Cell Biol. 118 (1992) 1455–1463.
[47] M. LeDizet, G. Piperno, The light chain p28 associates with a subset of inner dynein arm heavy chains in *Chlamydomonas* axonemes, Mol. Biol. Cell 6 (1995) 697–711.
[48] H.A. Yanagisawa, R. Kamiya, Association between actin and light chains in *Chlamydomonas* flagellar inner-arm dyneins, Biochem. Biophys. Res. Commun. 288 (2001) 443–447.
[49] N. Kotani, H. Sakakibara, S.A. Burgess, H. Kojima, K. Oiwa, Mechanical properties of inner-arm dynein-f (dynein I1) studied with *in vitro* motility assays, Biophys. J. 93 (2007) 886–894.
[50] K.A. Johnson, Pathway of the microtubule-dynein ATPase and the structure of dynein: A comparison with actomyosin, Annu. Rev. Biophys. Biophys. Chem. 14 (1985) 161–188.
[51] T. Shimizu, K. Furusawa, S. Ohashi, Y.Y. Toyoshima, M. Okuno, F. Malik, R.D. Vale, Nucleotide specificity of the enzymatic and motile activities of dynein, kinesin, and heavy meromyosin, J. Cell Biol. 112 (1991) 1189–1197.
[52] T. Kon, T. Mogami, R. Ohkura, M. Nishiura, K. Sutoh, ATP hydrolysis cycle-dependent tail motions in cytoplasmic dynein, Nat. Struct. Mol. Biol. 12 (2005) 513–519.
[53] T. Yagi, I. Minoura, A. Fujiwara, R. Saito, T. Yasunaga, M. Hirono, R. Kamiya, An axonemal dynein particularly important for flagellar movement at high viscosity. Implications from a new *Chlamydomonas* mutant deficient in the dynein heavy chain gene DHC9, J. Biol. Chem. 280 (2005) 41412–41420.
[54] K. Kikushima, R. Kamiya, Clockwise translocation of microtubules by flagellar inner-arm dyneins *in vitro*, Biophys. J. 94 (2008) 4014–4019.
[55] U.W. Goodenough, J.E. Heuser, Substructure of the outer dynein arm, J. Cell Biol. 95 (1982) 798–815.
[56] M.E. Porter, J.A. Knott, S.H. Myster, S.J. Farlow, The dynein gene family in *Chlamydomonas reinhardtii*, Genetics 144 (1996) 569–585.

[57] G.B. Witman, N. Minervini, Dynein arm conformation and mechanochemical transduction in the eukaryotic flagellum, Symp. Soc. Exp. Biol. 35 (1982) 203–223.
[58] T. Ishikawa, 3D structures of axoneme, in: K. Hirose, L. Amos (Eds.), Dynein Handbook, Pan Stanford, Singapore, 2011.
[59] P. Lupetti, S. Lanzavecchia, D. Mercati, F. Cantele, R. Dallai, C. Mencarelli, Three-dimensional reconstruction of axonemal outer dynein arms *in situ* by electron tomography, Cell Motil. Cytoskeleton 62 (2005) 69–83.
[60] N. Mizuno, S. Toba, M. Edamatsu, J. Watai-Nishii, N. Hirokawa, Y.Y. Toyoshima, M. Kikkawa, Dynein and kinesin share an overlapping microtubule-binding site, EMBO J. 23 (2004) 2459–2467.
[61] N. Mizuno, A. Narita, T. Kon, K. Sutoh, M. Kikkawa, Three-dimensional structure of cytoplasmic dynein bound to microtubules, Proc. Natl. Acad. Sci. U.S.A. 104 (2007) 20832–20837.
[62] U. Goodenough, J. Heuser, Structural comparison of purified dynein proteins with *in situ* dynein arms, J. Mol. Biol. 180 (1984) 1083–1118.
[63] H. Ueno, T. Yasunaga, C. Shingyoji, K. Hirose, Dynein pulls microtubules without rotating its stalk, Proc. Natl. Acad. Sci. U.S.A. 105 (2008) 19702–19707.
[64] A. Furuta, T. Yagi, H.A. Yanagisawa, H. Higuchi, R. Kamiya, Systematic comparison of *in vitro* motile properties between *Chlamydomonas* wild-type and mutant outer arm dyneins each lacking one of the three heavy chains, J. Biol. Chem. 284 (2009) 5927–5935.
[65] B. Wickstead, K. Gull, Dyneins across eukaryotes: A comparative genomic analysis, Traffic 8 (2007) 1708–1721.
[66] H. Hoop, G.B. Witman, Outer doublet heterogeneity reveals structural polarity related to beat direction in *Chlamydomonas* flagella, J. Cell Biol. 97 (1983) 902–909.
[67] C.J. Brokaw, Stochastic simulation of processive and oscillatory sliding using a two-headed model for axonemal dynein, Cell Motil. Cytoskeleton 47 (2000) 108–119.
[68] A. Gennerich, A.P. Carter, S.L. Reck-Peterson, R.D. Vale, Force-induced bidirectional stepping of cytoplasmic dynein, Cell 131 (2007) 952–965.
[69] R. Kamiya, Mutations at twelve independent loci result in absence of outer dynein arms in *Chlamydomonas reinhardtii*, J. Cell Biol. 107 (1988) 2253–2258.
[70] T. Yagi, K. Uematsu, Z. Liu, R. Kamiya, Identification of novel dyneins that localized exclusively to the proximal portion of *Chlamydomonas* flagella, J. Cell Sci. 122 (2009) 1306–1314.
[71] K. Oiwa, S. Kamimura, H. Iwamoto, X-ray fiber diffraction studies on flagellar axonemes, Methods Cell Biol. 91 (2009) 89–109.
[72] T. Ogura, A.J. Wilkinson, AAA^{+} superfamily ATPases: Common structure–diverse function, Genes Cells 6 (2001) 575–597.
[73] K.C. Holmes, I. Angert, F.J. Kull, W. Jahn, R.R. Schroder, Electron cryo-microscopy shows how strong binding of myosin to actin releases nucleotide, Nature 425 (2003) 423–427.
[74] I.R. Gibbons, J.E. Garbarino, C.E. Tan, S.L. Reck-Peterson, R.D. Vale, A.P. Carter, The affinity of the dynein microtubule-binding domain is modulated by the conformation of its coiled-coil stalk, J. Biol. Chem. 280 (2005) 23960–23965.
[75] T. Kon, K. Imamula, A.J. Roberts, R. Ohkura, P.J. Knight, I.R. Gibbons, S.A. Burgess, K. Sutoh, Helix sliding in the stalk coiled coil of dynein couples ATPase and microtubule binding, Nat. Struct. Mol. Biol. 16 (2009) 325–333.
[76] S. Toba, T.M. Watanabe, L. Yamaguchi-Okimoto, Y.Y. Toyoshima, H. Higuchi, Overlapping hand-over-hand mechanism of single molecular motility of cytoplasmic dynein, Proc. Natl. Acad. Sci. U.S.A. 103 (2006) 5741–5745.
[77] C.J. Brokaw, Flagellar movement: A sliding filament model, Science 178 (1972) 455–462.
[78] C.J. Brokaw, Computer simulation of flagellar movement VIII: Coordination of dynein by local curvature control can generate helical bending waves, Cell Motil. Cytoskeleton 53 (2002) 103–124.

[79] A. Hilfinger, A.K. Chattopadhyay, F. Julicher, Nonlinear dynamics of cilia and flagella, Phys. Rev. E Stat. Nonlin. Soft Matter Phys. 79 (2009) 051918.
[80] C.J. Brokaw, Computer simulation of flagellar movement IX. Oscillation and symmetry breaking in a model for short flagella and nodal cilia, Cell Motil. Cytoskeleton 60 (2005) 35–47.
[81] C.B. Lindemann, A model of flagellar and ciliary functioning which uses the forces transverse to the axoneme as the regulator of dynein activation, Cell Motil. Cytoskeleton 29 (1994) 141–154.
[82] C.J. Brokaw, Computer simulation of flagellar movement: VII. Conventional but functionally different cross-bridge models for inner and outer arm dyneins can explain the effects of outer arm dynein removal, Cell Motil. Cytoskeleton 42 (1999) 134–148.
[83] E. Hirakawa, H. Higuchi, Y.Y. Toyoshima, Processive movement of single 22S dynein molecules occurs only at low ATP concentrations, Proc. Natl. Acad. Sci. U.S.A. 97 (2000) 2533–2537.
[84] S. Camalet, F. Julicher, J. Prost, Self-organized beating and swimming of internally driven filaments, Phys. Rev. Lett. 82 (1999) 1590–1593.
[85] K. Wakabayashi, S. Takada, G.B. Witman, R. Kamiya, Transport and arrangement of the outer-dynein-arm docking complex in the flagella of *Chlamydomonas* mutants that lack outer dynein arms, Cell Motil. Cytoskeleton 48 (2001) 277–286.
[86] H. Sui, K.H. Downing, Molecular architecture of axonemal microtubule doublets revealed by cryo-electron tomography, Nature 442 (2006) 475–478.
[87] M. Kikkawa, T. Ishikawa, T. Nakata, T. Wakabayashi, N. Hirokawa, Direct visualization of the microtubule lattice seam both *in vitro* and *in vivo*, J. Cell Biol. 127 (1994) 1965–1971.
[88] L. Amos, A. Klug, Arrangement of subunits in flagellar microtubules, J. Cell Sci. 14 (1974) 523–549.
[89] S.P. Angus, R.E. Edelmann, D.G. Pennock, Targeted gene knockout of inner arm 1 in *Tetrahymena thermophila*, Eur. J. Cell Biol. 80 (2001) 486–497.
[90] S. Liu, R. Hard, S. Rankin, T. Hennessey, D.G. Pennock, Disruption of genes encoding predicted inner arm dynein heavy chains causes motility phenotypes in *Tetrahymena*. Cell Motil, Cytoskeleton 59 (2004) 201–214.
[91] C.R. Wood, R. Hard, T.M. Hennessey, Targeted gene disruption of dynein heavy chain 7 of *Tetrahymena thermophila* results in altered ciliary waveform and reduced swim speed, J. Cell Sci. 120 (2007) 3075–3085.
[92] Y. Harada, T. Funatsu, M. Tokunaga, K. Saito, H. Higuchi, Y. Ishii, T. Yanagida, Single molecule imaging and nanomanipulation of biomolecules, Methods Cell Biol. 55 (1998) 117–128.
[93] G. Pigino, S. Geimer, S. Lanzavecchia, E. Paccagnini, F. Cantele, D.R. Diener, J.L. Rosenbaum, P. Lupetti, Electron-tomographic analysis of intraflagellar transport particle trains *in situ*, J. Cell Biol. 187 (2009) 135–148.
[94] R. Kamiya, Functional diversity of axonemal dyneins as studied in *Chlamydomonas* mutants, Int. Rev. Cytol. 219 (2002) 115–155.
[95] K.R. Rogers, S. Weiss, I. Crevel, P.J. Brophy, M. Geeves, R. Cross, KIF1D is a fast non-processive kinesin that demonstrates novel K-loop-dependent mechanochemistry, EMBO J. 20 (2001) 5101–5113.
[96] A. Yamada, T. Yamada, H. Sakakibara, H. Nakayama, K. Oiwa, Unidirectional movement of fluorescent microtubules on rows of dynein arms of disintegrated axonemes, J. Cell Sci. 111 (1998) 93–98.

In this chapter

Genetic Approaches to Axonemal Dynein Function in *Chlamydomonas* and Other Organisms

Toshiki Yagi [1], Ritsu Kamiya [2]
[1] Department of Cell Biology and Anatomy, Graduate School of Medicine, University of Tokyo, Tokyo, Japan
[2] Department of Biological Sciences, Graduate School of Science, University of Tokyo, Tokyo, Japan

9.1 Introduction

Cilia and flagella are equipped with various species of dyneins each consisting of multiple subunits (see Chapter 7). For studying the organization and function of the complex axonemal dyneins, use of mutants lacking specific dyneins or their subunits is essential. Genetic disorders in axonemal dyneins were first identified as an absence of dynein arms in the sperm of an infertile man [1] and in the cilia of patients suffering from primary ciliary dyskinesia (PCD), a congenital disorder also called immotile cilia syndrome (see Chapter 24) [2]. However, genetic studies of axonemal dynein have been most extensively carried out using *Chlamydomonas,* a unicellular organism that yields a variety of flagella-deficient mutants [3,118]. An outstanding merit of *Chlamydomonas* is that a mutation in a flagella-related gene immediately results in defective motility in daughter cells, because its vegetative cells are haploid. The cells can be easily cultivated in defined medium and their flagella can be isolated and analyzed using biochemical methods and electron microscopy. In addition, a mutant can be genetically crossed with other mutants, which enables detailed genetic analysis as well as production of double mutants suitable for biochemical and physiological analyses. *Chlamydomonas* dynein-deficient mutants were first isolated by Luck and others by screening non-motile cells produced by chemical mutagenesis [4]. Later studies identified a number of mutants defective in either outer-arm dynein or inner-arm dynein by screening mutants that swam slowly [5–10].

Dyneins DOI: 10.1016/B978-0-12-382004-4.10009-3
Copyright © 2012 by Elsevier Inc. All rights reserved.

Genome analyses of various organisms have revealed that major dynein subunits are well conserved. Most dynein components identified in *Chlamydomonas* have homologs in vertebrates and other ciliated organisms (see Chapters 2 and 7) [11,12]. The forward genetic approach using *Chlamydomonas* has thus greatly contributed to the studies of axonemal dyneins in general. On the other hand, reverse genetic techniques – for example, targeted gene disruption or expression suppression by RNA interference (RNAi) – are used in several other organisms and have proven powerful in elucidating the function of dynein subunits [13–16]; this approach is complementary to the forward genetic approach because some dynein-related proteins are present only in multi-cellular organisms and because mutants deficient in some axonemal proteins are not available in *Chlamydomonas*.

9.2 Genetic Studies of *Chlamydomonas* Axonemal Dyneins

Chlamydomonas dynein-deficient mutants are isolated from cells displaying slow-swimming or non-motile phenotypes, as noted above. The isolation method used is described elsewhere [17]. For mutagenesis, application of UV light or chemicals and plasmid insertion at random positions in the genome (insertional mutagenesis) are most commonly used. Because mutants with motility defects tend to grow at the bottom of culture flasks, we can concentrate slow swimmers or non-motile cells from a population of mutagenized cells by collecting cells from the bottom of test-tube cultures. For isolation of individual mutants, the collected cells are streaked on agar plates to produce single colonies, and each colony is examined for motility under a microscope. After isolation of candidate cells, flagella are isolated and deficiencies in the dynein composition are examined via an SDS-PAGE system capable of resolving dynein heavy chain (HC) bands. For more detailed analysis, dynein is extracted from the axoneme with high-salt concentration solution and analyzed by ion-exchange chromatography [18–20]. Most species of *Chlamydomonas* dyneins can be resolved by this procedure.

Any new isolates must also be genetically analyzed. For this, the isolates are mated with various known mutants and the progeny with distinct phenotypes are scored. A genetic method uniquely applicable to *Chlamydomonas* is a "temporary dikaryon rescue" assay, which is useful for determining the relationship between the new mutant and known mutants. When two mutants are mated, they transiently form zygotes (temporary dikaryons) that swim with four flagella until the flagella are resorbed ~3 h after mating. During this time, the two flagella of mutants may be repaired and recover wild-type motility if the defects in the mated pair are genetically distinct [3,21]. If a pair of mutants displays clear rescue, we can unambiguously conclude that they have mutations in different genes. However, if a pair does not undergo rescue, we cannot

conclude that their mutations are in the same gene. This is because there are various reasons why failure of rescue may result. For example, some structural defects in dynein or other axonemal components may be irreversible and cannot be repaired by supplying correct subunits after the axoneme has been assembled. Another case of rescue failure is observed when dikaryons are formed between pairs with closely related mutations. Suppose two dynein-related proteins, A and B, are those that form a stable complex in the cytoplasm. In such a case, the absence of A or B in the cytoplasm of a mutant may cause destabilization and degradation of the other protein. If so, temporary dikaryons formed between a mutant lacking A and another mutant lacking B do not undergo rescue, because both proteins are missing in either mutant and hence in the zygote. This kind of rescue failure has actually been observed between several pairs of dynein-deficient mutants [7].

The final stage of genetic analysis of a given mutant is the determination of the mutated gene. Insertional mutagenesis has the potential to allow rapid identification of the mutated gene, by recovering the inserted plasmid sequence [22]. As another method, RFLP mapping can be used to narrow down the position of the mutation in the genome: in one such method, a mutant is mated with a variant strain, S1D2, that has a variety of sequence polymorphism in the nuclear genome; the mutation is mapped using polymorphic markers; and candidate genes contained in the mapped region are sequenced [23].

9.2.1 General Characteristics of *Chlamydomonas* Mutants

Tables 9.1 and 9.2 show the list of currently known *Chlamydomonas* mutants deficient in outer-arm dynein or inner-arm dyneins. Mutants lacking either the entire outer-arm dynein or any one kind of inner-arm dynein display slow swimming rather than a complete loss of motility (Fig. 9.1). Mutants lacking outer-arm dynein swim slower than wild type because their flagellar beat frequency is reduced while the waveform is not changed so much. Because of the low-frequency beating of the flagella, the swimming of outer-arm-deficient mutants is often described as “jerky.” In contrast, mutants lacking inner-arm dynein swim slower because the flagellar bend angle is reduced, while the flagellar beat frequency is not so greatly altered. Their swimming is smooth. Therefore, the loss of outer-arm dynein and the loss of inner-arm dynein have different effects on flagellar beating, which suggests a functional difference between inner-arm dynein and outer-arm dynein [24].

Chlamydomonas axonemal dyneins are comprised of three distinct types of dyneins: an outer-arm dynein containing three HCs, a two-headed inner-arm dynein (containing two HCs), and multiple species of single-headed dyneins (containing single HCs) (see Chapter 7). As is evident from the above observations, flagella can beat even if they lack any one of the three types. However,

Table 9.1 *Chlamydomonas* Outer-Arm Mutants

Strain	Missing Structure/Components	Protein Affected	References
oda1	Outer arm, ODA-DC	DC2	[5,7,25,26]
oda2/pf28	Outer arm	γHC	[6,7,27]
oda3	Outer arm, ODA-DC	DC1	[7,25,28]
oda4	Outer arm	β HC	[7,29,64]
oda5	Outer arm	ODA5	[7,30]
oda6	Outer arm	IC2	[7,31]
oda7	Outer arm	ODA7	[7,32]
oda8	Outer arm	–	[7]
oda9	Outer arm	IC1	[7,33]
oda10	Outer arm	–	[7]
oda11	α-HC + LC5 + Lis1	α-HC	[34–36]
oda12	Outer arm	LC2	[37]
oda13	–	LC6	[37,38]
oda14	Outer arm (partial)	DC3	[28,37,39]
oda15	Outer arm (partial)	LC7a	[40]
oda16	Outer arm (partial)	ODA16	[41]
pf13	Outer arm, Inner-arm dynein (c)	KTU/PF13	[4,42]
pf22	Outer arm, Inner-arm dyneins	–	[4]
fla14	Various structures	LC8	[38,43]
Mutants lacking part of the HCs			
oda2-t	γ HC motor domain	γ HC	[44]
oda4-s7	β HC motor domain	β HC	[45]
sup-pf-1	No visible change	β HC	[46,47]
sup-pf-2	Partial loss of outer arm	γ HC	[46,48]

– : currently unknown. Modified from [118].

double mutants lacking two types of dyneins are generally non-motile [8,119] (Fig. 9.1). Thus, the presence of two types of dyneins appears necessary for the axoneme to beat. This finding explains why the three dynein-deficient mutants studied by Luck and others [4] were non-motile; these mutants are likely to lack two of the three types of axonemal dyneins.

Table 9.2 *Chlamydomonas* Inner-Arm Mutants

Strain	Missing Components	Mutated Gene	References
ida1/pf9[1]	f[2]	1α (DHC1)	[8,20,49–51]
ida2	f	1β (DHC10)	[8,52]
ida3	f	–	[8]
ida4	a c d	p28	[8,20,53]
ida5	a c d e	actin	[9,54]
ida6	e	–	[9]
ida7	f	IC140	[55]
ida8/bop2	152 kD	–	[56]
ida9	c	DHC9	[10]
ida10	b, c, d, e (reduced)	MOT48	[57]
pf23	a, c, d, f	–	[4]
pf2	b, e (reduced), DRC	Gas11/Gas8	[58,59]
pf3	e, DRC	PF3	[58]
bop5	IC138, IC97, FAP120	IC138	[60–63]

[1] *Also called* pf30 *([24], [29]).*
[2] *Also called dynein I1.*
DRC: dynein regulatory complex (see Chapter 12); – : currently unknown. Modified from [118].

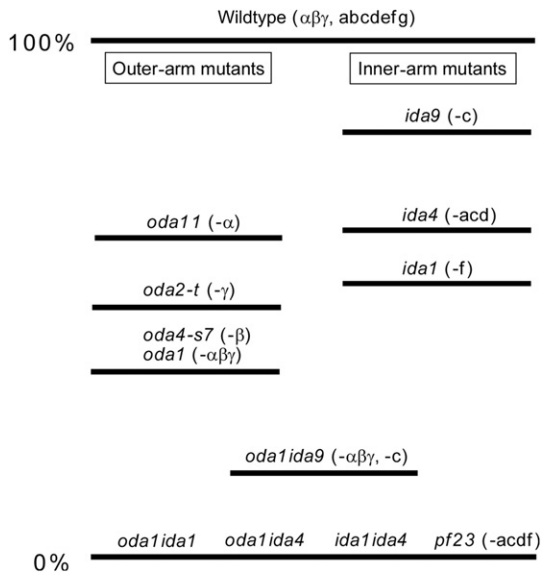

Figure 9.1
Motility of *Chlamydomonas* dynein-deficient mutants. Approximate swimming velocities of mutants are shown as the percentage of wild-type velocity (130–160 μm/s). The letters in parentheses denote the dynein species missing in each mutant. For example, *oda11* lacks the outer-arm1 dynein α HC and *ida9* lacks inner-arm dynein species c.

9.2.2 Mutants Deficient in Outer-Arm Dynein

Currently about 20 mutants are known that lack all or part of outer-arm dynein (Table 9.1). The causal mutations so far determined can be classified into three distinct categories: (1) deficient in various dynein subunits (*oda2*, *oda4*, *oda6*, *oda9*, *oda11*, *oda12*, *oda13*, and *oda15*); (2) deficient in the dynein attachment site (outer-arm docking complex (ODA-DC)) (*oda1*, *oda3*, and *oda14*); and (3) deficient in the assembly of outer-arm precursor within the cytoplasm (*oda7*, *oda16*, and *pf13*). Outer-arm dynein is almost completely lost in mutants that lack the β HC (*oda4*) [64], γ HC (*oda2*) [27], IC1 intermediate chain (IC) (*oda9*) [33], or IC2 IC (*oda6*) [31], while it is only partially lost in most mutants that lack light chains (LCs). An exception is the mutant *fla14*, a mutant of LC8, which has only very short flagella without outer-arm dynein [43]. This severe phenotype most likely represents the unique importance of LC8; it has been shown to be present in various protein complexes including outer-arm dynein, inner-arm dynein, and cytoplasmic dynein, possibly participating in the process of protein dimerization [65].

Mutants lacking β or γ HCs lack the entire outer arm whereas those lacking the α HC assemble outer arms that lack only the α HC and LC5 [34]. It is likely that the N-terminal tail portions of the β and γ HCs are necessary for the attachment of the outer arm to the outer doublet, whereas that of the α HC is not necessary. In support of this idea, mutants that have a truncated β HC (*oda4-s7*) [45] or a truncated γ HC (*oda2-t*) [44] assemble outer-arm dyneins that lack only the head domain of the β or γ HCs, respectively.

Interestingly, a mutant lacking a short segment in the stalk of the β HC has an activity ("suppressor") that restores motility in paralyzed-flagella mutants defective in the central pair or radial spokes. The stalk is a coiled-coil projection that, together with the stalk head at the tip, functions in the ATP-dependent binding of dynein to the adjacent outer doublet (see Chapter 4). This mutation is called *sup-pf-1* [46,47]. Some mutations in the γ HC also have a similar activity. This mutation is called *sup-pf-2* [46,48]. Although the exact mechanism underlying this phenomenon is not understood, these mutations may cause a change in the affinity of outer-arm dynein for the adjacent outer doublets, thereby bypassing the loss of control by the central pair/radial spokes. Suppressor activities have also been found in certain alleles of *ida1*/*pf9* deficient in two-headed inner-arm dynein f/I1 [66].

The mutants *oda5*, *oda8*, and *oda10* may be deficient in the attachment of outer-arm dynein to the outer doublet microtubules [30]. The products of their causal genes are likely to form a stable complex, because temporary dikaryon rescue does not readily take place between them [7]. This is similar to the case with *oda1* and *oda3*, which also do not undergo rescue. The products of the genes *oda1* and *oda3* are thought to form a stable complex in the cytoplasm and are transported into flagella as the ODA-DC.

Analyses of the assembly state of dynein subunits within the cytoplasm [41,67,68] have shown that outer-arm dynein is first assembled within the cytoplasm and transported into the flagella by means of the intraflagellar transport (IFT) system (see Chapter 14). The mutant *oda7* is apparently deficient in dynein preassembly. The product of the *oda7* gene contains leucine-rich repeats (LRRs) and coiled-coil domains, and its homologs are present in almost all ciliated organisms. In mammals, it is called LRRC50. Genetic and biochemical studies suggest that it also functions as a structural link between inner- and outer-row dyneins [32]. ODA16 contains WD repeats and is present in the flagellar matrix. It binds to an IFT protein, suggesting that it functions as an adaptor between IFT particles and outer-arm dyneins [68]. Its homologs are widely conserved in ciliated organisms [69]. Another mutant deficient in outer-arm dynein transport has been isolated and shown to be deficient in an IFT protein, IFT46 [70]. It is conceivable that other proteins will be found that are responsible for the transport of outer-arm dynein, ODA-DC, or various inner-arm dyneins. Outer-arm dynein and ODA-DC are apparently transported separately since mutants deficient in outer-arm subunits retain ODA-DC.

Several mutants are thought to be defective in the cytoplasmic assembly of outer-arm dynein. The mutant *pf13*, first shown by Huang et al. [4] to lack outer-arm dynein, was later found to encode a protein homologous to Kintoun (Ktu), a dynein preassembly factor present in medaka fish [42]. This protein is widely conserved in ciliated organisms including humans, in which genetic loss of this protein was found to cause Kartagener's syndrome, a severe PCD accompanied by defects in the determination of left–right asymmetry of the body (see Chapter 24). This protein is present in the cellular cytoplasm rather than in cilia. *Chlamydomonas pf13* axonemes were found to lack inner-arm dynein species c in addition to the entire outer arm. From these and other observations, the protein Ktu/PF13 is thought to function in the preassembly of outer-arm dynein and some inner-arm dyneins. It may function to help the folding of HCs as a co-chaperon, as experiments with mouse cells indicate that it interacts with a molecular chaperon, HSP70. Interestingly, *Chlamydomonas* and other ciliated organisms have two or three other proteins (called the PIH proteins) that share a protein motif with Ktu/PF13. A *Chlamydomonas* mutant (*ida10*) lacking one of the PIH proteins, MOT48, has been found to lack some single-headed inner-arm dyneins and have a slightly reduced amount of outer-arm dynein [57].

9.2.3 Mutants Lacking Inner-Arm Dyneins

Mutants lacking one or a few species of inner-arm dyneins usually display better motility than mutants lacking outer-arm dynein, so that it is sometimes difficult to distinguish them from wild-type cells. One way to circumvent this problem is to take advantage of the fact that double mutants that lack both outer-arm dynein and inner-arm dynein are non-motile in most cases; the procedure is to mutagenize *oda* mutants, isolate completely non-motile cells,

and backcross them with wild-type cells to obtain cells without the *oda* mutation [8].

About 10 mutants have thus far been isolated that lack some of the inner-arm dyneins. As shown in Chapter 7, *Chlamydomonas* inner-arm dynein is comprised of one species of two-headed dynein (called dynein f or dynein I1) and multiple species of single-headed dyneins. The single-headed dyneins comprise six major types (dyneins a, b, c, d, e, and g) and four minor types that contain DHC3, DHC4, DHC11, and DHC12 [71]; [T. Yagi, unpublished result]. Most minor types appear to localize only to the proximal portion of the axoneme. Sequence analyses in various organisms have shown that the HCs of single-headed inner-arm dyneins can be further classified into three groups: IAD-3, IAD-4, and IAD-5 [12,72]. In *Chlamydomonas*, DHC2 (dynein d HC) belongs to IAD-4, DHC3 and DHC7 (dynein g) belong to IAD-5, and all others except DHC12 belong to IAD-3. DHC12 has a very diverged sequence that does not conform to this classification.

Subunit compositions of the two-headed type and the single-headed types are totally different. The two-headed dynein is composed of two HCs (DHC1 and DHC10) [49,52,73]; three ICs of 140 kD, 138 kD, and 97 kD; and several LCs (see Chapter 7). In contrast, single-headed dyneins are composed of single distinct HCs, actin, and either centrin or a protein of 28 kD (p28). Dynein d has additional LCs of 44 kD (p44) and 38 kD (p38).

The majority of currently available inner-arm-deficient mutants have defects in genes that code for dynein subunits. For the two-headed isotype (dynein f/I1), mutants lacking the DHC1 (the f/I1α HC) (*ida1*/*pf9*/*pf30*), DHC10 (the f/I1β HC) (*ida2*), or the IC140 IC (*ida7*) lack the entire dynein [55]. In contrast, null mutants of the IC138-encoding gene (*bop5*) assemble an incomplete dynein f/I1 complex that lacks IC138, IC97, and a protein termed FAP120 [60–63]. Transformation of a null mutant of DHC1 (*pf9-2*) with a gene coding for its N-terminal sequence produces an incomplete dynein f/I1 that lacks the motor domain of DHC1 (f/I1α HC) [50]. Similarly, transformation of a null mutant of DHC10 (*ida2-6*) with a gene coding for its N-terminal sequence produces another type of incomplete dynein f/I1 without the motor domain of DHC10 (f/I1β HC) [52]. Hence, as in outer-arm dynein, the N-terminal tail regions of HCs (DHC1 and DHC10) are the sites where all subunits associate to assemble on the doublet microtubules.

For single-headed dyneins, only one mutant has been isolated that lacks a particular HC: *ida9*, which lacks the dynein c HC, DHC9 [10]. Two mutants are known to lack other subunits. The mutant *ida4* has a mutation in the gene coding for the LC p28 [53]. It lacks the dynein species containing this subunit – that is, dyneins a, c, d, and two minor dynein species that contain DHC11 or DHC12 [20,71; T. Yagi, unpublished results]. The other mutant, *ida5*, lacks conventional actin and, as a result, lacks dyneins a, c, d, e, and some minor dyneins. An

interesting feature of *ida5* is that, while all single-headed dyneins contain monomeric actin as a subunit [74,75], this mutant lacks only a subset of these dyneins. It was found that *Chlamydomonas* has a second actin gene, whose product (NAP) has a low (~64%) homology to conventional actin. NAP can replace actin in dyneins b and g but not in dyneins a, c, d, or e [54]. Interestingly, while NAP is expressed in only a negligibly small amount in wild-type cells, a significant amount is expressed in *ida5* cells [76].

Some inner-arm-deficient mutants appear to have defects in the proteins responsible for the cytoplasmic preassembly of certain kinds of dyneins. As stated above, PF13 and MOT48 are thought to function in the assembly of some inner-arm dynein and outer-arm dynein. A mutant, *ida10*, has a mutation in the MOT48 gene and expresses reduced amounts of single-headed dyneins, most notably dyneins b, c, d, and e [57].

Mutants deficient in the dynein regulatory complex (DRC) (see Chapter 12) show reduced amounts of some single-headed dyneins [58,120]. The mutant *pf3* lacks dynein e and the mutant *pf2* has reduced amounts of dyneins e and b [58]. The loss or reduction of dynein e in these mutants reflects a close association of dynein e with the DRC, a structure that has been suggested to function as the link between adjacent outer-doublet microtubules [77]. Another mutant *ida6* also lacks dynein e [9] and part of the DRC (see Chapter 12). The DRC may function as a docking site for dynein e.

9.3 Genetic Studies in Various Organisms

Other than *Chlamydomonas*, mutants deficient in axonemal dyneins have been obtained in several unicellular and multicellular organisms (Table 9.3). In most cases, mutants were generated by reverse genetics techniques, using information from genome databases. Following are brief summaries of what has been reported for each organism.

9.3.1 *Tetrahymena*

In *Tetrahymena*, several dynein-deficient mutants have been generated using gene knockdown techniques based on homologous recombination. The *Tetrahymena* genome has as many as 25 HC-encoding genes (DYH1—DYH25) [104]. DYH1 and DYH2 encode cytoplasmic dyneins that function in the cytoplasm and IFT, respectively; DYH3, DYH4, and DYH5 encode the three HCs of the three-headed outer-arm dynein; DYH6 and DYH7 encode the two HC genes of the two-headed type inner-arm dynein, dynein f/I1; the remaining 18 HC genes are likely to encode single-headed inner-arm dyneins [104]). Thus far, gene knockdowns have been performed for five HC genes (DYH6, DYH7, DYH8, DYH9, and DYH12) and several genes encoding other subunits (Table 9.3).

Table 9.3 Dynein-Related Genes Studied in Various Organisms

Species	Category	Gene Studied	Phenotype	Corresponding *Chlamydomonas* Mutant	References
Tetrahymena	HC (IA[1])	*DYH6*	Slow swimming	*ida1*	[14,78]
	HC (IA)	*DYH7*	Slow swimming	*ida2*	[15]
	HC (IA)	*DYH8*	Slow swimming	—	[79,80]
	HC (IA)	*DYH9*	Slow swimming	—	[79,80]
	HC (IA)	*DYH12*	Slow swimming	—	[79,80]
	LC (OA[2])	*LC4*	Delayed recovery from ciliary reversal response	—	[81]
Trypanosome	IC (OA)	*TbDNAI1*	No effective movement[3]	*oda9*	[82]
	IC (IA)	*TbIC140*	N/A	*ida7*	[83]
	LC (OA)	*TbLC1*	Backward swimming	—	[16]
	LC (OA)	*TbLC2*	Slow swimming	*oda12*	[82]
	Dynein preassembly factor	*TbLRRC50*	N/A	*oda7*	[84]
Zebrafish	HC (OA)	*DNAH9*	LR defect[4], hydrocephalus, PN-cysts[5], curly tail[6]	*oda4*	[85]
	HC (OA)	*DNAH11*	LR defect	*oda4*	[86]
	Dynein preassembly factor	*LRRC50*	LR defect, PN-cysts, curly tail	*oda7*	[87,88]
	Transport adaptor (OA)	*wdr69*	LR defect, PN-cysts, curly tail	*oda16*	[69]

Medaka	Dynein preassembly factor	*Ktu/PF13*	LR defect, PN-cysts, reduced fertility	*pf13*	[42]
	IC (OA)	*DNAI2*	LR defect, curly tail	*oda6*	[89,90]
Frog	HC (OA)	*DNAH5*	LR defect	*oda2*	[91]
	HC (OA)	*DNAH9*	LR defect, reduced hovering movement[7]	*oda4*	[91]
Mouse	HC (OA)	*DNAH5*	LR defect, hydrocephalus, respiratory defect[8], perinatal death	*oda2*	[92,93]
	HC (OA)	*DNAH11*	LR defect	*oda4*	[94,95]
	HC (IA)	*DNAH1*[9]	Infertility	—	[13,96]
Human	HC (OA)	*DNAH5*	PCD	*oda2*	[97]
	HC (OA)	*DNAH11*	PCD	*oda4*	[98]
	IC (OA)	*DNAI1*	PCD	*oda9*	[99,100]
	IC (OA)	*DNAI2*	PCD	*oda6*	[101]
	IC (OA)	*TXNDC3*	PCD	—	[102]
	Dynein preassembly factor	*LRRC50*	PCD	*oda7*	[84,103]
	Dynein preassembly factor	*KTU/PF13*	PCD	*pf13*	[42]

[1] *Inner-arm dynein.*
[2] *Outer-arm dynein.*
[3] *No effective movement is produced although flagella beat.*
[4] *Randomization of left–right body axis.*
[5] *Polycysts formation in pronephros.*
[6] *The tail is curled downward.*
[7] *Reduced cilia-driven hovering movements of tadpoles.*
[8] *Recurrent respiratory infection.*
[9] *Previous name: MDHC7.*
PCD: primary ciliary dyskenesia (see Chapter 24); *TXNDC3*: thioredoxin-domain-containing protein.

Strains in which one of the two HCs of the two-headed inner-arm type (DYH6 and DYH7) is disrupted display swimming at about half the wild-type velocity while their ciliary beat frequency is almost normal [14,15,78]. This suggests that the defects in two-headed inner-arm dynein cause abnormal ciliary waveform, a phenotype similar to that observed in *Chlamydomonas* mutants lacking this type of dynein (see Section 9.2). The DYH7-knockdown strain has actually been observed to display abnormal ciliary beating patterns; its cilia frequently entangle and impede neighboring cilia, resulting in disruption of metachronal waves [15]. Since DYH6 and DYH7 most likely constitute the same two-headed dynein together, we may expect that knockdown of either gene results in the same phenotype, as in *Chlamydomonas* flagella. However, unexpectedly, knockdown of the two genes has been reported to produce somewhat different phenotypes regarding regulation of ciliary beating. *Tetrahymena*, like *Paramecium* [105], displays a Ca^{2+}-dependent ciliary reversal reaction upon receiving mechanical stimuli [14,79]. A DYH6-knockdown strain, KO-6, does not display this response [14]. However, curiously, a DYH7-knockdown strain, DYH7neo3, readily displays the ciliary reversal response [15]. The reason for this discrepancy is not clear. However, it is possible that DYH6 knockdown results in more severe defects in two-headed inner-arm dynein and that this dynein plays a crucial role in the conversion of ciliary waveform.

For single-headed inner-arm dynein, three strains have been produced that lack particular HCs [80]: DYH8 (which belongs to an IAD-3 type [12,72]), DYH9 (IAD-4 type), and DYH12 (IAD-3 type). The three HC mutants all swim at ~70% the wild-type velocity, but only the DYH8-knockout strain shows a reduction in ciliary beat frequency. The other two strains are likely to swim slower because of a change in the ciliary waveform [80]. Unexpectedly, all of them tend to exhibit a more sensitive ciliary reversal reaction than wild type [79]. Thus, apparently single-headed dyneins and two-headed dynein antagonize with each other in ciliary waveform regulation.

In addition to HCs, several LCs have been chosen as the targets for gene knockout [81]. A strain whose light chain 4 (LC4) is disrupted shows a clear phenotype. LC4 is a Ca^{2+}-binding protein first identified in *Chlamydomonas* (see Chapter 7 and [106]), but no mutants deficient in LC4 have been obtained in *Chlamydomonas*. The *Tetrahymena* genome contains two LC4-related genes, LC4A and LC4B, of which only LC4B is induced after deciliation [107]. Possibly LC4B is the ortholog of the *Chlamydomonas* LC4. Interestingly, however, the LC4A-disrupted strain, but not the LC4B-disrupted strain, displays a delay in the recovery from depolalization-induced ciliary reversal. The interpretation of this phenomenon awaits further studies.

9.3.2 *Trypanosoma*

In *Trypanosoma brucei*, inducible RNAi is used to knock down the expression of specific genes. Most dynein genes thus far disrupted are those that code for homologs of *Chlamydomonas* dynein subunits, which include outer-arm dynein

intermediate chain 1 (IC1), light chain 1 (LC1), light chain 2 (LC2), light chain 7a (LC7a), inner-arm intermediate chain (IC140), and cytoplasmic preassembly factor of dynein (ODA7/LRRC50) (Table 9.3). (These homologs will be indicated with the prefix Tb).

Suppression of TbIC1 results in the total absence of outer-arm dynein and a striking motility phenotype [82]. Wild-type cells usually swim forward with flagella that propagate bending waves from tip to base but occasionally alter the swimming direction by changing the bend propagation direction from base to tip. Interestingly, the TbIC1-knockout cells show only base-to-tip flagellar bend propagation and the cells cannot move in any direction. Thus, outer-arm dynein appears to be important for the tip-to-base bend propagation and the production of propulsive force. In addition, the mutant displays growth defects; cells tend to have multiple nuclei and multiply only slowly [82]. Lowered growth rate has also been observed in other motility mutants [82,83]. Flagellar motility is likely to play an important role in cell cycle progression. It may help daughter cells to divide after completion of cytokinesis [82].

While the TbIC1 mutant cannot swim in any direction, the TbLC1-suppressed strain can swim backwards with a base-to-tip flagellar bend propagation [16]. It cannot swim forward. The different motility phenotypes probably result from different structural defects in the outer dynein arm; in contrast to the TbIC1 mutant, the TbLC1 mutant retains residual outer arms on the doublet microtubules [16]. *Chlamydomonas* LC1 is associated with the motor domains of the γ HC [108] while other LCs and ICs are likely to localize to the base of outer-arm dynein. The results in *Trypanosoma* are consistent with the idea that LC1 functions in the bend propagation mechanism [109], while IC1 functions in the attachment of outer-arm dynein to the outer doublet.

A TbLC2-disrupted strain displays jerky swimming [82] reminiscent of *Chlamydomonas* outer-arm-deficient mutants, including an LC2 null mutant, which lacks the outer arm almost completely [110,111]. However, as stated above, the TbIC1 mutant, lacking the entire outer arm, does not swim. The different phenotypes may have resulted from a less efficient silencing of the LC2 mRNA.

Other than TbLC2, two additional genes for dynein subunits, TbLC7a and TbIC140, have been silenced in a comparative genomic study in which 41 genes out of 50 cilia-related genes identified in the genome database were silenced by RNAi [83]. These mutants display reduced growth rates. However, their motility phenotypes have not been analyzed in detail.

9.3.3 Zebrafish

In zebrafish (*Danio rerio*), morpholino antisense oligonucleotides can be used to suppress the expression of the target gene. Injection of antisense oligonucleotides into an embryo cell suppresses the transcription of the target gene, thereby

enabling inference of the function of the gene in the developmental process. Dynein-related proteins thus far used for morpholino oligonucleotide-based gene suppression include those coding for homologs of DNAH9 and DNAH11 (both are outer-arm HCs), a cytoplasmic factor for dynein assembly (Oda7/LRRC50), and an outer-arm dynein transport adaptor protein, Oda16/Wdr69. Reduction of DNAH9 transcription interferes with the left–right asymmetry determination of the body and causes hydrocephalus [86], as often observed in human PCD patients (see Chapter 24). In the gene-suppressed fish, fluid flow in the Kupffer's vesicle and in the spinal cord is reduced because ciliary beat frequency is reduced to half the normal frequency. The Kupffer's organ corresponds to the node in mammalian embryos. Ciliary defects in Kupffer's vesicle most likely cause the abnormal left–right determination, while those in the spinal cord cause hydrocephalus. In addition, the treated fish also display cyst formation in the pronephros (fish kidney), similar to human polycystic kidney disease patients. However, unlike the mammalian renal tubule epithelial cells having non-motile primary cilia, fish kidney epithelial cells have motile multi-cilia. Therefore, in zebrafish, fluid flow produced by cilia is important for the proper development of the nephron as well as the determination of left–right asymmetry and neuron development [86]. Like DNAH9 disruption, DNAH11 disruption reduces fluid flow in the Kupffer's vesicle and perturbs left–right development [85].

Mutants in a gene encoding a homolog of *Chlamydomonas* ODA7 have been found in zebrafish by a forward genetic screen [87,88]. The gene product is homologous to human LRRC50. Following this finding, the function of LRRC50 was studied in *Trypanosoma* and humans, as well as in zebrafish [84,87,88,103]. The zebrafish LRRC50-deficient mutant has defects in left–right asymmetry determination, as do other cilia-deficient mutants [87,88]. Electron microscopy shows that, unlike *Chlamydomonas oda7* flagella, which lack only outer-arm dynein and are motile, the cilia in LRRC50-deficient mutants of zebrafish, as well as humans [84,103], lack both inner and outer dynein arms and are non-motile. Thus, there may be a slight organism-dependent difference in the function of ODA7/LRRC50.

Likewise, a homolog of *Chlamydomonas* ODA16 has been identified in zebrafish as a protein encoded by the *wdr69* gene [69]. It is expressed in organs with motile cilia. Antisense morpholino knockdown of *wdr69* disrupts ciliary motility and causes multiple phenotypes associated with vertebrate ciliopathies. Outer dynein arms are lost in morphant embryos. These results indicate that, in zebrafish as well as in *Chlamydomonas*, the ODA16/Wdr69 protein functions as an adaptor between outer-arm dynein and IFT particles, which are needed for dynein transport into the flagellar compartment [41].

9.3.4 Medaka

Forward genetic screens, followed by positional cloning of the mutated gene, are feasible in medaka fish (*Oryzias latipes*). Screening for PCD has yielded several

mutants that include those deficient in Ktu, a protein involved in the cytoplasmic preassembly of outer- and inner-arm dyneins [42], and DNAI2, intermediate chain 2 of outer-arm dynein [89,90]. As stated in Section 9.2, Ktu has been found to be homologous to the *Chlamydomonas* PF13 protein.

9.3.5 Frog

Expression levels of three outer-arm dynein HCs, DNAH5, DNAH9, and DNAH11, have been examined in *Xenopus laevis* during development [91]. DNAH9 is expressed more abundantly than the other two genes in the epidermis and in the gastrocoel roof plate, an organ homologous to the mouse node. Injection of morpholino antisense oligonucleotides against *DNAH9* reduces ciliary motility in these sites, resulting in perturbation of left–right axis formation and reduction of the hovering movement of tadpoles driven by epidermal cilia.

9.3.6 Mouse

In mouse (*Mus musculus*), mutants can be generated by targeted gene disruption through homologous recombination as well as by insertional mutagenesis. Knockout mutants of two outer-arm HCs (DNAH5 and DNAH11) and one inner-arm HC (DNAH1) have been generated and analyzed. In addition, a mutation *inversus viscerum* (*iv*) showing defects in left–right determination has been isolated from a litter produced in non-inbred mice [112]. The *iv* mutant has a point mutation in the *DNAH11* gene. From the mutant's phenotype, DNAH11 is also called left–right dynein [94]. A DNAH11-knockout mouse displays an identical phenotype [95]. *DNAH11* is abundantly transcribed in the node region of a mouse embryo [94], which suggests its importance for the determination of left–right axis. The functional meaning of this observation was made clear when cilia-driven nodal flow was found to be crucial for the left–right asymmetry determination [113,114].

The DNAH5-knockout mouse displays recurrent respiratory infection, hydrocephalus, and *situs inversus*, and most of them die during the first two or three weeks of life [92,97]. These phenotypes are caused by ciliary malfunction in the respiratory epithelial cells, in the brain ventricle ependymal cells, and in the node of embryos. In fact, cilia in the respiratory epithelial cells and the brain ependymal cells completely lack outer-arm dynein and are immotile [92,93]. *DNAH5* mutation is thus apparently more severe than *DNAH11* mutation. This difference may well reflect the difference in their localization in the body. At any rate, a complete absence of motility in outer-arm-missing cilia has not been observed in other organisms. Whether or not outer-arm dynein is essential for the beating of certain kinds of mammalian cilia warrants further experiments.

Loss of an inner-arm HC apparently causes less severe damage to mice. The only inner-arm dynein mutant was produced by gene knockout of DNAH1, a homolog

of *Chlamydomonas* inner-arm dynein d HC (IDA-4-type dynein) [13]. The homozygous and heterozygous strains are viable and have no abnormality except that the homozygous strain shows reduced beat frequency of tracheal cilia and male infertility. In solutions of low viscosity, the mutant sperm swim at about 50% of the wild-type velocity with no reduction in beat frequency, indicating that the absence of inner-arm dynein affects flagellar waveform. Interestingly, the mutant sperms are incapable of swimming in media of raised viscosity, in which wild-type sperm can swim [96]. A high susceptibility to increased viscosity has also been observed in a *Chlamydomonas* mutant that lacks a single-headed inner-arm dynein [10]. In electron micrographs of longitudinal sections, electron density corresponding to an inner-arm dynein is diminished [115].

9.3.7 Human

As described in Chapter 24, a number of mutations in axonemal dyneins and related genes have been identified in patients with PCD. Genes thus far examined include *DNAH5*, *DNAH11*, *DNAI1*, *DNAI2*, *KTU/PF13*, *ODA7/LRRC50*, and *TXNDC3* (Table 9.3). TXNDC3 is one of the three ICs found only in metazoan cilia and flagella (see Chapter 7 and [116]).

9.4 Conclusion and Perspective

Forward and reverse genetic studies of axonemal dynein, as outlined in this chapter, indicate that the functional characteristics of various types of dyneins are well-conserved among organisms. For example, outer-arm dynein is important for cilia and flagella to beat at high frequency whereas two-headed inner-arm dynein, dynein f/I1, is important for producing proper waveforms. Therefore, in most cases the information obtained from *Chlamydomonas* mutants should be relevant to the studies of cilia and flagella in other organisms. However, it is also clear that studies with *Chlamydomonas* alone cannot elucidate the function of every dynein species or subunit in cilia/flagella motility. One serious drawback with *Chlamydomonas* is that it is not easy to knock down a particular gene, despite the recent significant improvement in RNAi techniques. Thus, we can infer the function of a particular species of dynein only if a mutant that lacks it has been isolated by chance. Currently it is not possible to infer the specific function of most single-headed inner-arm dyneins in detail because only one mutant has been isolated that lacks a particular HC. For an understanding of the function of every kind of dynein, we must await the development of techniques that enable targeted gene knockdown in *Chlamydomonas*. Alternatively, we can study the function of various dynein species in organisms in which such gene disruption is feasible. For this purpose, *Tetrahymena* and *Trypanosoma* have already provided some important information. In the future, it should be possible to examine the functional significance of a given protein domain by transforming these organisms with mutated genes.

Although cilia/flagella and axonemal dyneins are widely conserved in their fundamental function, the manner of movement and its regulation must vary greatly among organisms and, in many cases, organism-specific functions are important. For example, the nodal cilia in mammalian embryos produce leftward flow by producing three-dimensional helical waves [117]. The function of dynein and cilia in such a system cannot be studied in *Chlamydomonas*. For studies of axonemal dynein function in vertebrates, zebrafish and medaka fish will be very useful since they allow use of both forward and reverse genetics while requiring much less labor than mouse. It is suggestive that a medaka mutant has provided the first clue to the function of a homolog of the *Chlamydomonas* protein PF13. Investigations using a variety of organisms will be crucial for elucidation of the function and significance of various species of axonemal dyneins in diverse biological phenomena, as well as in ciliary motility itself.

References

[1] H. Pedersen, H. Rebbe, Absence of arms in the axoneme of immobile human spermatozoa, Biol. Reprod. 12 (1975) 541–544.

[2] B.A. Afzelius, A human syndrome caused by immotile cilia, Science 193 (1976) 317–319.

[3] R.A. Lewin, Mutants of *Chlamydomonas moewusii* with impaired motility, J. Gen. Microbiol. 11 (1954) 358–363.

[4] B. Huang, G. Piperno, D.J.L. Luck, Paralyzed flagellar mutants of *Chlamydomonas reinhardtii* defective for axonemal doublet microtubule arms, J. Biol. Chem. 254 (1979) 3091–3099.

[5] R. Kamiya, M. Okamoto, A mutant of *Chlamydomonas reinhardtii* that lacks the flagellar outer dynein arm but can swim, J. Cell Sci. 74 (1985) 181–191.

[6] D.R. Mitchell, J.L. Rosenbaum, A motile *Chlamydomonas* flagellar mutant that lacks outer dynein arms, J. Cell Biol. 100 (1985) 1228–1234.

[7] R. Kamiya, Mutations at twelve independent loci result in absence of outer dynein arms in *Chlamydomonas reinhardtii*, J. Cell Biol. 107 (1988) 2253–2258.

[8] R. Kamiya, E. Kurimoto, E. Muto, Two types of *Chlamydomonas* flagellar mutants missing different components of inner-arm dynein, J. Cell Biol. 112 (1991) 441–447.

[9] T. Kato, O. Kagami, T. Yagi, R. Kamiya, Isolation of two species of *Chlamydomonas reinhardtii* flagellar mutants, *ida5* and *ida6*, that lack a newly identified heavy chain of the inner dynein arm, Cell Struct. Funct. 18 (1993) 371–377.

[10] T. Yagi, I. Minoura, A. Fujiwara, R. Saito, T. Yasunaga, M. Hirono, R. Kamiya, An axonemal dynein particularly important for flagellar movement at high viscosity: Implications from a new *Chlamydomonas* mutant deficient in the dynein heavy chain gene DHC9, J. Biol. Chem. 280 (2005) 41412–41420.

[11] G.J. Pazour, N. Agri, J. Leszyk, G.B. Witman, Proteomic analysis of a eukaryotic cilium, J. Cell Biol. 170 (2005) 103–113.

[12] B. Wickstead, K. Gull, Dyneins across eukaryotes: A comparative genomic analysis, Traffic 8 (2007) 1708–1721.

[13] J. Neesen, R. Kirschner, M. Ochs, A. Schmiedl, B. Habermann, C. Mueller, A.F. Holstein, T. Nuesslein, I. Adham, W. Engel, Disruption of an inner arm dynein heavy chain gene results in asthenozoospermia and reduced ciliary beat frequency, Hum. Mol. Genet. 10 (2001) 1117–1128.

[14] T.M. Hennessey, D.Y. Kim, D.J. Oberski, R. Hard, S.A. Rankin, D.G. Pennock, Inner arm dynein 1 is essential for Ca^{+}-dependent ciliary reversals in *Tetrahymena thermophila*, Cell Motil. Cytoskel. 53 (2002) 281–288.

[15] C.R. Wood, R. Hard, T.M. Hennessey, Targeted gene disruption of dynein heavy chain 7 of *Tetrahymena thermophila* results in altered ciliary waveform and reduced swim speed, J. Cell Sci. 120 (2007) 3075–3085.
[16] D.M. Baron, Z.P. Kabututu, K.L. Hill, Stuck in reverse: Loss of LC1 in *Trypanosoma brucei* disrupts outer dynein arms and leads to reverse flagellar beat and backward movement, J. Cell Sci. 120 (2007) 1513–1520.
[17] R. Kamiya, Selection of *Chlamydomonas* dynein mutants, Methods in Enzymology 196 (1991) 348–355.
[18] G. Piperno, D.J. Luck, Axonemal adenosine triphosphatases from flagella of *Chlamydomonas reinhardtii*. Purification of two dyneins, J. Biol. Chem. 254 (1979) 3084–3090.
[19] K.K. Pfister, R.B. Fay, G.B. Witman, Purification and polypeptide composition of dynein ATPases from *Chlamydomonas* flagella, Cell Motility 2 (1982) 525–547.
[20] O. Kagami, R. Kamiya, Translocation and rotation of microtubules caused by multiple species of *Chlamydomonas* inner-arm dynein, J. Cell Sci. 103 (1992) 653–664.
[21] B. Huang, G. Piperno, Z. Ramanis, D.J. Luck, Radial spokes of *Chlamydomonas* flagella: Genetic analysis of assembly and function, J. Cell Biol. 88 (1981) 80–88.
[22] L.W. Tam, P.A. Lefebvre, Cloning of flagellar genes in *Chlamydomonas reinhardtii* by DNA insertional mutagenesis, Genetics 135 (1993) 375–384.
[23] P. Kathir, M. LaVoie, W.J. Brazelton, N.A. Haas, P.A. Lefebvre, C.D. Silflow, Molecular map of the *Chlamydomonas reinhardtii* nuclear genome, Eukaryot. Cell 2 (2003) 362–379.
[24] C.J. Brokaw, R. Kamiya, Bending patterns of *Chlamydomonas* flagella: IV. Mutants with defects in inner and outer dynein arms indicate differences in dynein arm function, Cell Motil. Cytoskel. 8 (1987) 68–75.
[25] S. Takada, R. Kamiya, Functional reconstitution of *Chlamydomonas* outer dynein arms from α, β and γ subunits: requirement of a third factor, J. Cell Biol. 126 (1994) 737–745.
[26] S. Takada, C.G. Wilkerson, K. Wakabayashi, R. Kamiya, G.B. Witman, The outer dynein arm-docking complex: composition and characterization of a subunit (Oda1) necessary for outer-arm assembly, Mol. Biol. Cell 13 (2002) 1015–1029.
[27] C.G. Wilkerson, S.M. King, G.B. Witman, Molecular analysis of the γ heavy chain of *Chlamydomonas* flagellar outer arm dynein, J. Cell Sci. 107 (1994) 497–506.
[28] A. Koutoulis, G.J. Pazour, C.G. Wilkerson, K. Inaba, H. Sheng, S. Takada, G.B. Witman, The *Chlamydomonas reinhardtii ODA3* gene encodes a protein of the outer dynein arm docking complex, J. Cell Biol. 137 (1997) 1069–1080.
[29] D.J.L. Luck, G. Piperno, Dynein arm mutants of *Chlamydomonas*, in: F.D. Warner, P. Satir, I.R. Gibbons (Eds.), Cell Movement, the Dynein ATPases, vol. 1, Alan R. Liss, Inc., New York, 1989, pp. 49–60.
[30] M. Wirschell, G. Pazour, A. Yoda, M. Hirono, R. Kamiya, G.B. Witman, *Oda5*p, a novel axonemal protein required for assembly of the outer dynein arm and an associated adenylate kinase, Mol. Biol. Cell 6 (2004) 2729–2741.
[31] D.R. Mitchell, Y. Kang, Identification of *oda6* as a *Chlamydomonas* dynein mutant by rescue with the wild-type gene, J. Cell Biol. 113 (1991) 835–842.
[32] J. Freshour, R. Yokoyama, D.R. Mitchell, *Chlamydomonas* flagellar outer row dynein assembly protein *ODA7* interacts with both outer row and I1 inner row dyneins, J. Biol. Chem. 282 (2007) 5404–5412.
[33] C.G. Wilkerson, S.M. King, A. Koutoulis, G.J. Pazour, G.B. Witman, The 78,000 Mr intermediate chain of *Chlamydomonas* outer arm dynein is a WD-repeat protein required for arm assembly, J. Cell Biol. 129 (1995) 169–178.
[34] H. Sakakibara, D.R. Mitchell, R. Kamiya, A *Chlamydomonas* outer arm dynein mutant missing the α heavy chain, J. Cell Biol. 113 (1991) 615–622.
[35] D.R. Mitchell, K.S. Brown, Sequence analysis of the *Chlamydomonas reinhardtii* flagellar α dynein gene, Cell Motil. Cytoskel. 37 (1997) 120–126.

[36] L.B. Pedersen, P. Rompolas, S.T. Christensen, J.L. Rosenbaum, S.M. King, The lissencephaly protein Lis1 is present in motile mammalian cilia and requires outer arm dynein for targeting to *Chlamydomonas* flagella, J. Cell Sci. 120 (2007) 858–867.

[37] G.J. Pazour, A. Koutoulis, S.E. Benashski, B.L. Dickert, H. Sheng, R.S. Patel-King, S.M. King, G.B. Witman, LC2, the *Chlamydomonas* homolog of the *t* complex-encoded protein Tctex2, is essential for outer dynein arm assembly, Mol. Biol. Cell 10 (1999) 3507–3520.

[38] S.M. King, R.S. Patel-King, The $M_{(r)} = 8{,}000$ and 11,000 outer-arm dynein light chains from *Chlamydomonas* flagella have cytoplasmic homologs, J. Biol. Chem. 270 (1995) 11445–11452.

[39] D. Casey, K. Inaba, G. Pazour, S. Takada, K. Wakabayashi, C. Wilkerson, R. Kamiya, G. Witman, DC3, the 21-kD subunit of the outer dynein arm-docking complex (ODA-DC), is a novel EF-hand protein important for assembly of both the outer arm and the ODA-DC, Mol. Biol. Cell 14 (2003) 3650–3663.

[40] L.M. DiBella, M. Sakato, R.S. Patel-King, G.J. Pazour, S.M. King, The LC7 light chains of *Chlamydomonas* flagellar dyneins interact with components required for both motor assembly and regulation, Mol. Biol. Cell 15 (2004) 4633–4646.

[41] N.T. Ahmed, D.R. Mitchell, ODA16p, a *Chlamydomonas* flagellar protein needed for dynein assembly, Mol. Biol. Cell 16 (2005) 5004–5012.

[42] H. Omran, D. Kobayashi, H. Olbrich, T. Tsukahara, N.T. Loges, H. Hagiwara, Q. Zhang, G. Leblond, E. O'Toole, C. Hara, H. Mizuno, H. Kawano, M. Fliegauf, T. Yagi, S. Koshida, A. Miyawaki, H. Zentgraf, H. Seithe, R. Reinhardt, Y. Watanabe, R. Kamiya, D.R. Mitchell, H. Takeda, Ktu/PF13 is required for cytoplasmic pre-assembly of axonemal dyneins, Nature 456 (2008) 611–616.

[43] G.J. Pazour, C.G. Wilkerson, G.B. Witman, A dynein light chain is essential for the retrograde particle movement of intraflagellar transport (IFT), J. Cell Biol. 141 (1998) 979–992.

[44] Z. Liu, H. Takazaki, Y. Nakazawa, M. Sakato, T. Yagi, T. Yasunaga, S.M. King, R. Kamiya, Partially functional outer-arm dynein in a novel *Chlamydomonas* mutant expressing a truncated γ heavy chain, Eukaryot. Cell 7 (2008) 1136–1145.

[45] H. Sakakibara, S. Takada, S.M. King, G.B. Witman, R. Kamiya, A *Chlamydomonas* outer arm dynein mutant with a truncated β heavy chain, J. Cell Biol. 122 (1993) 653–661.

[46] B. Huang, Z. Ramanis, D.J. Luck, Suppressor mutations in *Chlamydomonas* reveal a regulatory mechanism for flagellar function, Cell 28 (1982) 115–124.

[47] M.E. Porter, J.A. Knott, L.C. Gardner, D.R. Mitchell, S.K. Dutcher, Mutations in the SUP-PF-1 locus of *Chlamydomonas reinhardtii* identify a regulatory domain in the beta-dynein heavy chain, J. Cell Biol. 126 (1994) 1495–1507.

[48] G. Rupp, E. O'Toole, L.C. Gardner, B.F. Mitchell, M.E. Porter, The *sup-pf-2* mutations of *Chlamydomonas* alter the activity of the outer dynein arms by modification of the γ-dynein heavy chain, J. Cell Biol. 135 (1996) 1853–1865.

[49] S.H. Myster, J.A. Knott, E. O'Toole, M.E. Porter, The *Chlamydomonas Dhc1* gene encodes a dynein heavy chain subunit required for assembly of the I1 inner arm complex, Mol. Biol. Cell 8 (1997) 607–620.

[50] S.H. Myster, J.A. Knott, K.M. Wysocki, E. O'Toole, M.E. Porter, Domains in the 1α dynein heavy chain required for inner arm assembly and flagellar motility in *Chlamydomonas*, J. Cell Biol. 146 (1999) 801–818.

[51] G. Piperno, Z. Ramanis, E.F. Smith, W.S. Sale, Three distinct inner dynein arms in *Chlamydomonas* flagella: molecular composition and location in the axoneme, J. Cell Biol. 110 (1990) 379–389.

[52] C.A. Perrone, S.H. Myster, R. Bower, E.T. O'Toole, M.E. Porter, Insights into the structural organization of the I1 inner arm dynein from a domain analysis of the 1β dynein heavy chain, Mol. Biol. Cell 11 (2000) 2297–2313.

[53] M. LeDizet, G. Piperno, *ida4-1*, *ida4-2*, and *ida4-3* are intron splicing mutations affecting the locus encoding p28, a light chain of *Chlamydomonas* axonemal inner dynein arms, Mol. Biol. Cell 6 (1995) 713–723.
[54] T. Kato-Minoura, M. Hirono, R. Kamiya, *Chlamydomonas* inner-arm dynein mutant, *ida5*, has a mutation in an actin encoding gene, J. Cell Biol. 137 (1997) 649–656.
[55] C.A. Perrone, P. Yang, E. O'Toole, W.S. Sale, M.E. Porter, The *Chlamydomonas* IDA7 locus encodes a 140-kDa dynein intermediate chain required to assemble the I1 inner arm complex, Mol. Biol. Cell 9 (1998) 3351–3365.
[56] S.J. King, W.B. Inwood, E.T. O'Toole, J. Power, S.K. Dutcher, The *bop2–1* mutation reveals radial asymmetry in the inner dynein arm region of *Chlamydomonas reinhardtii*, J. Cell Biol. 126 (1994) 1255–1266.
[57] R. Yamamoto, M. Hirono, R. Kamiya, Discrete PIH proteins function in the cytoplasmic preassembly of different subsets of axonemal dyneins, J. Cell Biol. 190 (2010) 65–71.
[58] L.C. Gardner, E. O'Toole, C.A. Perrone, T. Giddings, M.E. Porter, Components of a "dynein regulatory complex" are located at the junction between the radial spokes and the dynein arms in *Chlamydomonas* flagella, J. Cell Biol. 127 (1994) 1311–1325.
[59] G. Rupp, M.E. Porter, A subunit of the dynein regulatory complex in *Chlamydomonas* is a homolog of a growth arrest-specific gene product, J. Cell Biol. 162 (2003) 47–57.
[60] T.W. Hendrickson, C.A. Perrone, P. Griffin, K. Wuichet, J. Mueller, P. Yang, M.E. Porter, W.S. Sale, IC138 is a WD-repeat dynein intermediate chain required for light chain assembly and regulation of flagellar bending, Mol. Biol. Cell 15 (2004) 5431–5442.
[61] M. Wirschell, C. Yang, P. Yang, L. Fox, H. Yanagisawa, R. Kamiya, G.B. Witman, M. Porter, W.S. Sale, IC97 is a novel intermediate chain of I1 dynein that interacts with tubulin and regulates interdoublet sliding, Mol. Biol. Cell 20 (2009) 3044–3054.
[62] R. Bower, K. VanderWaal, E. O'Toole, L. Fox, C. Perrone, J. Mueller, M. Wirschell, R. Kamiya, W.S. Sale, M.E. Porter, IC138 defines a subdomain at the base of the I1 dynein that regulates microtubule sliding and flagellar motility, Mol. Biol. Cell 20 (2009) 3055–3063.
[63] K. Ikeda, R. Yamamoto, M. Wirschell, T. Yagi, R. Bower, M.E. Porter, W.S. Sale, R. Kamiya, A novel ankyrin-repeat protein interacts with the regulatory proteins of inner arm dynein f (I1) of *Chlamydomonas reinhardtii*, Cell Motil. Cytoskel. 66 (2009) 448–456.
[64] D.R. Mitchell, K.S. Brown, Sequence analysis of the *Chlamydomonas* α and β dynein heavy chain genes, J. Cell Sci. 107 (1994) 635–644.
[65] E. Barbar, Dynein light chain LC8 is a dimerization hub essential in diverse protein networks, Biochemistry 47 (2008) 503–508.
[66] M.E. Porter, J. Power, S.K. Dutcher, Extragenic suppressors of paralyzed flagellar mutations in *Chlamydomonas reinhardtii* identify loci that alter the inner dynein arms, J. Cell Biol. 118 (1992) 1163–1176.
[67] M.E. Fowkes, D.R. Mitchell, The role of preassembled cytoplasmic complexes in assembly of flagellar dynein subunits, Mol. Biol. Cell 9 (1998) 2337–2347.
[68] N.T. Ahmed, C. Gao, B.F. Lucker, D.G. Cole, D.R. Mitchell, ODA16 aids axonemal outer row dynein assembly through an interaction with the intraflagellar transport machinery, J. Cell Biol. 183 (2008) 313–322.
[69] C. Gao, G. Wang, J.D. Amack, D.R. Mitchell, Oda16/Wdr69 is essential for axonemal dynein assembly and ciliary motility during zebrafish embryogenesis, Dev. Dynam. 239 (2010) 2190–2197.
[70] Y. Hou., H. Qin, J.A. Follit, G.J. Pazour, J.L. Rosenbaum, G.B. Witman, Functional analysis of an individual IFT protein: IFT46 is required for transport of outer dynein arms into flagella, J. Cell Biol. 176 (2007) 653–665.
[71] T. Yagi, K. Uematsu, Z. Liu, R. Kamiya, Identification of novel dyneins that localize exclusively to the proximal portion of *Chlamydomonas* flagella, J. Cell Sci. 122 (2009) 1306–1314.

[72] R.L. Morris, M.P. Hoffman, R.A. Obar, S.S. McCafferty, I.R. Gibbons, A.D. Leone, J. Cool, E.L. Allgood, A.M. Musante, K.M. Judkins, B.J. Rossetti, A.P. Rawson, D.R. Burgess, Analysis of cytoskeletal and motility proteins in the sea urchin genome assembly, Dev. Biol. 300 (2006) 219–237.
[73] M.E. Porter, J.A. Knott, S.H. Myster, S.J. Farlow, The dynein gene family in *Chlamydomonas reinhardtii*, Genetics 144 (1996) 569–585.
[74] G. Piperno, D.J. Luck, An actin-like protein is a component of axonemes from *Chlamydomonas* flagella, J. Biol. Chem. 254 (1979) 2187–2190.
[75] H. Yanagisawa, R. Kamiya, Association between actin and light chains in *Chlamydomonas* flagellar inner-arm dyneins, Biochem. Bioph. Res. Co. 288 (2001) 443–447.
[76] M. Hirono, S. Uryu, A. Ohara, T. Kato-Minoura, R. Kamiya, Expression of conventional and unconventional actins in *Chlamydomonas reinhardtii* upon deflagellation and sexual adhesion, Eukaryot. Cell 2 (2003) 486–493.
[77] T. Heuser, M. Raytchev, J. Krell, M.E. Porter, D. Nicastro, The dynein regulatory complex is the nexin link and a major regulatory node in cilia and flagella, J. Cell Biol. 187 (2009) 921–933.
[78] S.P. Angus, R.E. Edelmann, D.G. Pennock, Targeted gene knockout of inner arm 1 in Tetrahymena thermophila, Eur. J. Cell Biol. 80 (2001) 486–497.
[79] S. Liu, T. Hennessey, S. Rankin, D.G. Pennock, Mutations in genes encoding inner arm dynein heavy chains in *Tetrahymena thermophila* lead to axonemal hypersensitivity to Ca^{2+}, Cell Motil. Cytoskel. 62 (2005) 133–140.
[80] S. Liu, R. Hard, S. Rankin, T. Hennessey, D.G. Pennock, Disruption of genes encoding predicted inner arm dynein heavy chains causes motility phenotypes in *Tetrahymena*, Cell Motil. Cytoskel. 59 (2004) 201–214.
[81] D.E. Wilkes, N. Bennardo, C.W. Chan, Y.L. Chang, E.O. Corpuz, J. DuMond, J.A. Eboreime, J. Erickson, J. Hetzel, E.E. Heyer, M.J. Hubenschmidt, E. Kniazeva, H. Kuhn, M. Lum, A. Sand, A. Schep, O. Sergeeva, N. Supab, C.R. Townsend, L.V. Ryswyk, H.E. Watson, A.E. Wiedeman, V. Rajagopalan, D.J. Asai, Identification and characterization of dynein genes in *Tetrahymena*, Method. Cell Biol. 92 (2009) 11–30.
[82] C. Branche, L. Kohl, G. Toutirais, J. Buisson, J. Cosson, P. Bastin, Conserved and specific functions of axoneme components in trypanosome motility, J. Cell Sci. 119 (2006) 3443–3455.
[83] D.M. Baron, K.S. Ralston, Z.P. Kabututu, K.L. Hill, Functional genomics in *Trypanosoma brucei* identifies evolutionarily conserved components of motile flagella, J. Cell Sci. 120 (2007) 478–491.
[84] P. Duquesnoy, E. Escudier, L. Vincensini, J. Freshour, A.M. Bridoux, A. Coste, A. Deschildre, J. de Blic, M. Legendre, G. Montantin, H. Tenreiro, A.M. Vojtek, C. Loussert, A. Clément, D. Escalier, P. Bastin, D.R. Mitchell, S. Amselem, Loss-of-function mutations in the human ortholog of *Chlamydomonas reinhardtii ODA7* disrupt dynein arm assembly and cause primary ciliary dyskinesia, Am. J. Hum. Genet. 85 (2009) 890–896.
[85] J.J. Essner, J.D. Amack, M.K. Nyholm, E.B. Harris, H.J. Yost, Kupffer's vesicle is a ciliated organ of asymmetry in the zebrafish embryo that initiates left–right development of the brain, heart and gut, Development 132 (2005) 1247–1260.
[86] A.G. Kramer-Zucker, F. Olale, C.J. Haycraft, B.K. Yoder, A.F. Schier, I.A. Drummond, Cilia-driven fluid flow in the zebrafish pronephros, brain and Kupffer's vesicle is required for normal organogenesis, Development 132 (2005) 1907–1921.
[87] J. Sullivan-Brown, J. Schottenfeld, N. Okabe, C.L. Hostetter, F.C. Serluca, S.Y. Thiberge, R.D. Burdine, Zebrafish mutations affecting cilia motility share similar cystic phenotypes and suggest a mechanism of cyst formation that differs from *pkd2* morphants, Dev. Biol. 314 (2008) 261–275.
[88] E. van Rooijen, R.H. Giles, E.E. Voest, C. van Rooijen, S. Schulte-Merker, F.J. van Eeden, LRRC50, a conserved ciliary protein implicated in polycystic kidney disease, J. Am. Soc. Nephrol. 19 (2008) 1128–1138.

[89] D. Kobayashi, N. Iijima, H. Hagiwara, K. Kamura, H. Takeda, T. Yokoyama, Characterization of the medaka (*Oryzias latipes)* primary ciliary dyskinesia mutant, *jaodori*: Redundant and distinct roles of *dynein axonemal intermediate gene 2 (dnai2)* in motile cilia. Dev. Biol. 347 (2010) 62–70.

[90] Y. Nagao, J. Cheng, K. Kamura, R. Seki, A. Maeda, D. Nihei, S. Koshida, Y. Wakamatsu, T. Fujimoto, M. Hibi, H. Hashimoto, Dynein axonemal intermediate chain 2 is required for formation of the left–right body axis and kidney in medaka. Dev. Biol. 347 (2010) 53–61.

[91] P. Vick, A. Schweickert, T. Weber, M. Eberhardt, S. Mencl, D. Shcherbakov, T. Beyer, M. Blum, Flow on the right side of the gastrocoel roof plate is dispensable for symmetry breakage in the frog *Xenopus laevis*, Dev. Biol. 331 (2009) 281–291.

[92] I. Ibañez-Tallon, S. Gorokhova, N. Heintz, Loss of function of axonemal dynein *Mdnah5* causes primary ciliary dyskinesia and hydrocephalus, Hum. Mol. Genet. 11 (2002) 715–721.

[93] I. Ibañez-Tallon, A. Pagenstecher, M. Fliegauf, H. Olbrich, A. Kispert, U.P. Ketelsen, A. North, N. Heintz, H. Omran, Dysfunction of axonemal dynein heavy chain Mdnah5 inhibits ependymal flow and reveals a novel mechanism for *hydrocephalus* formation, Hum. Mol. Genet. 13 (2004) 2133–2141.

[94] D.M. Supp, D.P. Witte, S.S. Potter, M. Brueckner, Mutation of an axonemal dynein affects left–right asymmetry in *inversus viscerum* mice, Nature 389 (1997) 963–966.

[95] D.M. Supp, M. Brueckner, M.R. Kuehn, D.P. Witte, L.A. Lowe, J. McGrath, J. Corrales, S.S. Potter, Targeted deletion of the ATP binding domain of left–right dynein confirms its role in specifying development of left–right asymmetries, Development 126 (1999) 5495–5504.

[96] D.M. Woolley, J. Neesen, G.G. Vernon, Further studies on knockout mice lacking a functional dynein heavy chain (*MDHC7*). 2. A developmental explanation for the asthenozoospermia, Cell Motil. Cytoskel. 61 (2005) 74–82.

[97] H. Olbrich, K. Häffner, A. Kispert, A. Völkel, A. Volz, G. Sasmaz, R. Reinhardt, S. Hennig, H. Lehrach, N. Konietzko, M. Zariwala, P.G. Noone, M. Knowles, H.M. Mitchison, M. Meeks, E.M. Chung, F. Hildebrandt, R. Sudbrak, H. Omran, Mutations in *DNAH5* cause primary ciliary dyskinesia and randomization of left–right asymmetry, Nat. Genet. 30 (2002) 143–144.

[98] L. Bartoloni, J.L. Blouin, Y. Pan, C. Gehrig, A.K. Maiti, N. Scamuffa, C. Rossier, M. Jorissen, M. Armengot, M. Meeks, H.M. Mitchison, E.M. Chung, C.D. Delozier-Blanchet, W.J. Craigen, S.E. Antonarakis, Mutations in the *DNAH11* (axonemal heavy chain dynein type 11) gene cause one form of situs inversus totalis and most likely primary ciliary dyskinesia, Proceedings of the National Academy of Science USA 99 (2002) 10282–10286.

[99] G. Pennarun, E. Escudier, C. Chapelin, A.M. Bridoux, V. Cacheux, G. Roger, A. Clément, M. Goossens, S. Amselem, B. Duriez, Loss-of-function mutations in a human gene related to *Chlamydomonas reinhardtii* dynein IC78 result in primary ciliary dyskinesia, Am. J. Hum. Genet. 65 (1999) 1508–1519.

[100] C. Guichard, M.C. Harricane, J.J. Lafitte, P. Godard, M. Zaegel, V. Tack, G. Lalau, P. Bouvagnet, Axonemal dynein intermediate-chain gene (*DNAI1*) mutations result in situs inversus and primary ciliary dyskinesia (Kartagener syndrome), Am. J. Hum. Genet. 68 (2001) 1030–1035.

[101] N.T. Loges, H. Olbrich, L. Fenske, H. Mussaffi, J. Horvath, M. Fliegauf, H. Kuhl, G. Baktai, E. Peterffy, R. Chodhari, E.M. Chung, A. Rutman, C. O'Callaghan, H. Blau, L. Tiszlavicz, K. Voelkel, M. Witt, E. Zietkiewicz, J. Neesen, R. Reinhardt, H.M. Mitchison, H. Omran, *DNAI2* mutations cause primary ciliary dyskinesia with defects in the outer dynein arm, Am. J. Hum. Genet. 83 (2008) 547–558.

[102] B. Duriez, P. Duquesnoy, E. Escudier, A.M. Bridoux, D. Escalier, I. Rayet, E. Marcos, A.M. Vojtek, J.F. Bercher, S. Amselem, A common variant in combination with a nonsense mutation in a member of the thioredoxin family causes primary ciliary dyskinesia, Proceedings of the National Academy of Science USA 104 (2007) 3336–3341.

[103] N.T. Loges, H. Olbrich, A. Becker-Heck, K. Häffner, A. Heer, C. Reinhard, M. Schmidts, A. Kispert, M.A. Zariwala, M.W. Leigh, M.R. Knowles, H. Zentgraf, H. Seithe, G. Nürnberg, P. Nürnberg, R. Reinhardt, H. Omran, Deletions and point mutations of *LRRC50* cause primary ciliary dyskinesia due to dynein arm defects, Am. J. Hum. Genet. 85 (2009) 883–889.
[104] D.E. Wilkes, H.E. Watson, D.R. Mitchell, D.J. Asai, Twenty-five dyneins in *Tetrahymena*: A re-examination of the multidynein hypothesis, Cell Motil. Cytoskel. 65 (2008) 342–351.
[105] Y. Naito, H. Kaneko, Reactivated triton-extracted models of *Paramecium*: Modification of ciliary movement by calcium ions, Science 176 (1972) 523–524.
[106] S.M. King, R.S. Patel-King, Identification of a Ca^{2+}-binding light chain within *Chlamydomonas* outer arm dynein, J. Cell Sci. 108 (1995) 3757–3764.
[107] D.E. Wilkes, V. Rajagopalan, C.W. Chan, E. Kniazeva, A.E. Wiedeman, D.J. Asai, Dynein light chain family in *Tetrahymena thermophila*, Cell Motil. Cytoskel. 64 (2007) 82–96.
[108] S.E. Benashski, R.S. Patel-King, S.M. King, Light chain 1 from the *Chlamydomonas* outer dynein arm is a leucine-rich repeat protein associated with the motor domain of the γ heavy chain, Biochemistry 38 (1999) 7253–7264.
[109] R.S. Patel-King, S.M. King, An outer arm dynein light chain acts in a conformational switch for flagellar motility, J. Cell Biol. 186 (2009) 283–295.
[110] G.J. Pazour, N. Agrin, B.L. Walker, G.B. Witman, Identification of predicted human outer dynein arm genes: Candidates for primary ciliary dyskinesia genes, J. Med. Genet. 43 (2006) 62–73.
[111] L.M. DiBella, O. Gorbatyuk, M. Sakato, K. Wakabayashi, R.S. Patel-King, G.J. Pazour, G.B. Witman, S.M. King, Differential light chain assembly influences outer arm dynein motor function, Mol. Biol. Cell 16 (2005) 5661–5674.
[112] M. Brueckner, P. D'Eustachio, A.L. Horwich, Linkage mapping of a mouse gene, *iv*, that controls left–right asymmetry of the heart and viscera, Proc. Nat. Acad. Sci. USA 86 (1989) 5035–5038.
[113] S. Nonaka, Y. Tanaka, Y. Okada, S. Takeda, A. Harada, Y. Kanai, M. Kido, N. Hirokawa, Randomization of left–right asymmetry due to loss of nodal cilia generating leftward flow of extraembryonic fluid in mice lacking KIF3B motor protein, Cell 95 (1998) 829–837.
[114] S. Nonaka, H. Shiratori, Y. Saijoh, H. Hamada, Determination of left–right patterning of the mouse embryo by artificial nodal flow, Nature 418 (2002) 96–99.
[115] G.G. Vernon, J. Neesen, D.M. Woolley, Further studies on knockout mice lacking a functional dynein heavy chain (*MDHC7*). 1. Evidence for a structural deficit in the axoneme, Cell Motil. Cytoskel. 61 (2005) 65–73.
[116] K. Ogawa, H. Takai, A. Ogiwara, E. Yokota, T. Shimizu, K. Inaba, H. Mohri, Is outer-arm dynein intermediate chain 1 multifunctional? Mol. Biol. Cell 7 (1996) 1895–1907.
[117] Y. Okada, S. Takeda, Y. Tanaka, J.C. Belmonte, N. Hirokawa, Mechanism of nodal flow: A conserved symmetry breaking event in left–right axis determination, Cell 121 (2005) 633–644.
[118] S.M. King, R. Kamiya, in: G.B. Witman (Ed.), The Chlamydomonas Sourcebook, Axonemal dyneins: Assembly, structure and force generation, vol. 3, Elsevier, Amsterdam, 2009, pp. 129–206.
[119] R. Kamiya, Functional diversity of axonemal dyneins as studied in *Chlamydomonas* mutants, Int. Rev. Cytol. 219 (2002) 115–155.
[120] G. Piperno, K. Mead, W. Shestak, The inner dynein arms I2 interact with a "dynein regulatory complex" in *Chlamydomonas* flagella, J. Cell Biol. 118 (1992) 1455–1463.

In this chapter

10

Regulation of Axonemal Outer-Arm Dyneins in Cilia

Ken-ichi Wakabayashi
Department of Biological Sciences, Graduate School of Science, University of Tokyo, Tokyo, Japan

10.1 Introduction: Structure, Subunit Composition, and Arrangement of Outer-Arm Dynein

To describe the regulation of outer-arm dynein (OAD), it is necessary to briefly discuss its structure and composition and the various functional motifs present in OAD subunits. Although these features are described in detail in Chapter 7, they are summarized here as an introduction.

OAD in eukaryotic cilia/flagella is a multimeric complex that is composed of heavy chains (HCs) that contain ATPase/motor domains, intermediate chains (ICs), and several light chains (LCs). The structure, subunit composition, and regulation of OAD are best studied using the green alga *Chlamydomonas reinhardtii* because numerous mutants with defects in the OAD subunit genes have been isolated. In *Chlamydomonas*, three HCs are bound like a bouquet, and two ICs and several LCs form a complex at the base of the bouquet (IC—LC complex). The exceptions are LC1, LC3, LC4, and LC5, which are bound to either the motor domains or N-terminal regions of the HCs (Fig. 10.1) [1]. OADs in other organisms have slightly different subunit compositions: a comparison of the OAD subunit composition of *Chlamydomonas* and the ascidian *Ciona intestinalis* is detailed in Table 10.1 [2].

OADs are arranged linearly on specific sites of the A-tubule of doublet microtubules with a regular spacing of 24 nm, through interaction with the outer-dynein-arm docking complex (ODA-DC) [3]. In this chapter, the term "OAD" is defined to include the ODA-DC. The ODA-DC was first identified as a projection on the OAD-lacking mutants in *Chlamydomonas*. Biochemical and genetic analyses revealed that ODA-DC is composed of three subunits (termed DC1, DC2, and DC3) [4,5,6]. The subunit composition of ODA-DC in other organisms is different from that in *Chlamydomonas*. For example, in *Ciona*, salmonid fish, and mollusca,

Dyneins DOI: 10.1016/B978-0-12-382004-4.10010-X
Copyright © 2012 by Elsevier Inc. All rights reserved.

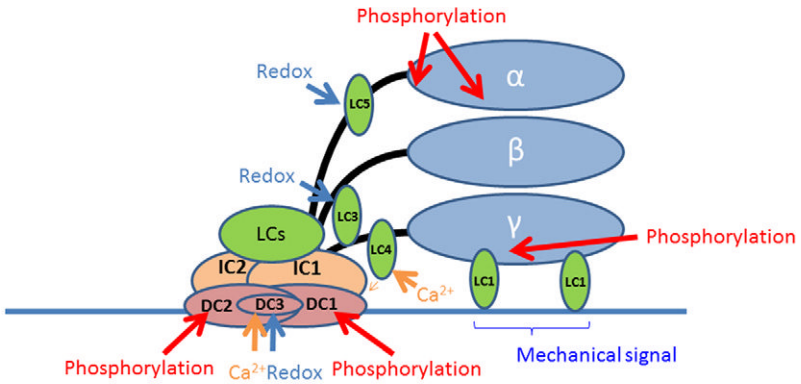

Figure 10.1 Model for the arrangement of *Chlamydomonas* OAD subunits potentially related to OAD regulation. Various kinds of signals are suggested to regulate OAD activities, such as phosphorylation (of the α HC, γ HC, DC1, and DC2), Ca^{2+} binding (to LC4 and DC3), and redox poise (sensed by LC3, LC5, and DC3). Since binding of Ca^{2+} to LC4 changes the conformation of the γ HC tail and LC1 anchors the γ HC motor domain to tubulin in the A-tubule, the γ HC may act as a mechanosensor. Arrangements of OAD subunits are from [1].

OAD contains two or three ICs containing coiled-coil domains, which have sequence similarities to DC2 [7,8]. In humans, DC1 does not appear to be conserved but two genes seem to be DC2 orthologs [9].

Many electron microscopic studies using *Chlamydomonas* OAD have revealed structural features of OAD both *in situ* and *in vitro* [10–14]. In the axoneme, three AAA^+ rings of HCs form stacked plates and the planes of all three rings appear parallel to the longitudinal axis of outer doublet microtubules [10,12]. In contrast, single-molecule observation of purified OADs suggests that the ring planes of α and β HCs are parallel but that of γ HC is in a different plane [13]. Two models of how three-headed OADs are aligned in the axoneme have been proposed: in the first model, all three HCs are stacked and OADs are aligned in an end-to-end manner; in the second model, the α and β HCs are stacked while γ HC belongs to the adjacent complex [12]. Taken together with single-molecule observations, the second model is so far more likely to be the case; however, it is still contradictory that the γ HC is in a different plane from those of the α and β HCs *in vitro* but that the three HCs are in the same plane *in situ*.

10.2 Fundamental Sliding Activity of Outer-Arm Dynein

10.2.1 Outer-Arm Dynein Functioning *In Situ*

Phenotypic analyses of *Chlamydomonas* mutants lacking OAD have revealed several features of OAD that are different from inner-arm dyneins (IADs). First,

Table 10.1 Subunit Composition of OADs from *Chlamydomonas* and *Ciona*

Chlamydomonas			*Ciona*		
Subunit	**Motif/Family**	**Possible Regulation**	**Subunit**	**Motif/Family**	**Possible Regulation**
α HC	AAA	Phosphorylation	α HC	AAA	
β HC	AAA		β HC	AAA	Phosphorylation
γ HC	AAA, IQ	Phosphorylation			
IC1	WD		IC1	WD	
IC2	WD, CC		IC2	WD	
			IC3	NDK, TRX	Redox
			TPR58	TPR	
LC1	LRR		LC1	LRR	
LC2	Tctex2		LC2	Tctex2	Phosphorylation
LC3	TRX	Redox	LC3	Tctex1	
LC4	EF	Ca^{2+}	LC4	LC8	
LC5	TRX	Redox	LC5	Robl	
LC6	LC8		LC6	LC8	
LC7a	Robl		Calaxin	EF	Ca^{2+}
LC7b	Robl				
LC8	LC8				
LC9	Tctex1				
LC10	LC8				
DC1	CC	Phosphorylation	IC4	CC	
DC2	CC	Phosphorylation	IC5	CC	
DC3	EF	Ca^{2+}, redox	p66	CC	

AAA, ATPases associated with diverse cellular activity; CC, coiled coil; IQ, IQ-motif; LRR, leucine-rich repeat; NDK, nucleoside diphosphate kinase; Robl, roadblock; TPR, tetratricopeptide repeat; TRX, thioredoxin; WD, WD-repeat. *Modified from [1,2].*

wild-type flagellar beat frequency is ~60 Hz whereas that of strains lacking OAD (*oda*) is ~20 Hz, and thus those mutants show jerky, slow swimming [15,16]. Mutants lacking IADs (*ida*) exhibit almost wild-type beat frequency levels (40~50 Hz) and lower amplitude waveforms, and thus those mutants exhibit smooth, slow swimming. These data show that OAD is important for maintaining high beat frequency whereas IADs are important for generating high-amplitude waveforms [15]. Second, wild-type flagella generate propulsive force of ~10 pN whereas *oda* mutants only produce ~3 pN [17]. Moreover, when in viscous media, wild-type flagella generate greater force (~20 pN) whereas OAD-lacking flagella do not show such amplification of propulsive force [17]. These data suggest that OAD is mechanosensitive such that it generates greater force than usual when under high load.

10.2.2 Translocation of Microtubules by Outer-Arm Dynein

Purified OADs coated on a glass surface can generate force against brain cytoplasmic microtubules (the so-called "gliding assay" or "*in vitro* motility assay").

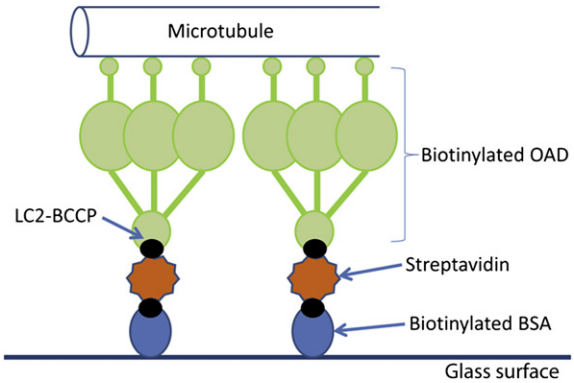

Figure 10.2 Schematic diagram of the improved system for the microtubule-gliding assay. Biotinylated OAD is fixed onto a glass surface via streptavidin, which is specifically bound to biotinamidocaproyl-BSA attached to the glass surface. Thus, OAD molecules are oriented so that they interact with microtubules only via the motor domains. Modified from [22].

This kind of experiment has been performed with *Tetrahymena* IADs and OADs (14 S and 22 S dyneins, respectively), sea urchin sperm OADs, and *Chlamydomonas* OADs [18]. However, it has been difficult to accurately estimate the gliding activity of OAD *in vitro*, since the basal domain of the OADs (IC—LC complex and the ODA-DC) can also bind to microtubules. Thus, if some OADs attach to the glass surface via their head domains (upside-down), those basal domains act as a load to the "upside-up" molecules [19,20]. To place OADs on the glass surface in a controlled manner, OADs were produced from an LC2-deficient *Chlamydomonas* mutant (*oda12*) that expressed biotinylated LC2 [21,22,23]. Using these biotinylated OADs and an avidin-coated glass surface, OADs were bound to the glass surface in a controlled and "upside-up" manner (Fig. 10.2). Those OADs translocated brain cytoplasmic microtubules at ~5 μm/s [22]. As described below, two-headed (αβ) OADs show higher gliding speed than three-headed (αβγ) OADs. The translocation velocity for biotinylated αβ OADs (~7 μm/s) is faster than that previously reported for wild-type αβ OADs (~4.6 μm/s), suggesting that this controlled binding of OADs to the glass surface is effective in obtaining an accurate measurement of OAD activity [24].

10.3 Intra-Outer-Arm Dynein (Inter-Heavy Chain) Regulations

Several lines of experiments have revealed that each HC in OADs has different properties and that those HCs are functionally coordinated when assembled into the OAD complex. *Chlamydomonas* mutants lacking single HCs (*oda11* lacking the α HC, *oda4s7* lacking the β HC motor domain, and *oda2-t* lacking the γ HC motor domain) provide an advantageous system with which to assay intra-OAD (or inter-HC) regulatory mechanisms [14,25,26].

When assayed separately, the ATPase activity of the α, β, and γ HCs are 0.6, 7.3, and 1.1 μmol phosphate released/min/mg, respectively [27,28]. However, when the α HC and β HC are mixed (or the αβ dimer is purified), the ATPase activity of these two-headed OADs is ~2.0 μmol phosphate released/min/mg, which is much lower than simple addition of the ATPase values of the α and β HCs would suggest [27,28]. Addition of the γ HC to the αβ dimer further suppresses the total ATPase [29]. These data strongly suggest that inter-HC regulation exists. Consistent with this idea, the ATPase activities of purified OADs from *Chlamydomonas* mutant axonemes lacking single HC are in the order αβ>βγ>αβγ>αγ [22]. However, interestingly, the order changed to αβ>αβγ>αγ>βγ when the gliding velocity of cytoplasmic microtubules by the biotinylated OAD described above was measured [22]. This difference in the order of activities may not be a result of the presence of microtubules, since OADs from *Chlamydomonas*, *Tetrahymena*, and sea urchin sperm do not show significant ATPase activation following addition of microtubules [22,30,31]. One possible interpretation is that the α HC functions as an energy converter and the βγ HCs cannot effectively convert the chemical energy from ATP hydrolysis to mechanical motion to slide microtubules without the α HC.

Intra-OAD regulation is also suggested from microtubule co-sedimentation assays of OAD from *Chlamydomonas* mutants. When mixed with cytoplasmic microtubules, most wild-type OADs are co-precipitated with microtubules in an ATP-sensitive manner. However, without the α HC, considerable amounts of βγ HC particles remain unbound to microtubules [32]. Intriguingly, when OADs are pretreated with tubulin and ATP so that ATP-insensitive microtubule binding sites (IC—LC complex and ODA-DC) are filled, those OADs do not bind to microtubules [32]. Moreover, without the α HC, βγ HC particles pretreated with tubulin bind microtubules in an ATP-sensitive manner only in the presence of Ca^{2+} [32]. These data suggest that the α HC functions as a transducer for a negative signal that controls the response of other HCs to Ca^{2+} and that the α HC plays opposite roles depending on the presence of tubulin and Ca^{2+}. Further experiments *in situ* will be necessary to clarify how these roles are regulated and contribute to ciliary/flagellar beating.

10.4 Inter-Outer-Arm Dynein Regulation

There are two major methods to estimate the motor activity of OADs against microtubules: one is the gliding assay described above and the other is the sliding disintegration assay, in which ATP is applied to protease-treated ciliary axonemes and doublet microtubules are extruded. Interestingly, the velocity of microtubule translocation of purified OADs in the gliding assay is only 15—30% of that observed in the sliding disintegration assay in *Chlamydomonas* [22,24]. To understand why OADs show faster sliding velocity in the axoneme, sliding

between cross-bridged microtubules by purified OADs was observed to estimate the sliding velocity of aligned OAD [33]. Purified OADs from *Chlamydomonas* or *Tetrahymena* are known to cross-bridge microtubules via an ATP-sensitive motor domain (HCs) and an ATP-insensitive tail domain (IC–LC complex and ODA-DC) [19,34]. Application of ~0.5 mM ATP induced sliding between these cross-bridged microtubules with a velocity of ~30 μm/s, which is 1.5 times faster than the microtubule sliding observed in the sliding disintegration assay and five times faster than that in the gliding assay. These data suggest that OADs generate greater force when aligned. There are two possible interpretations of this observation: one is that there occur protein–protein interactions between individual OADs when aligned and the force generation is amplified when multiple molecules interact together; the other is that OADs generate greater force when the polarity of multiple molecules is aligned (even if the OADs are not interacting). So far it is difficult to rule out either interpretation, since purified OADs tend to bind to microtubules in a cooperative manner to form patches and they rarely bind to microtubules separately from each other [19].

10.5 Regulation of Outer-Arm Dynein Activity by External Signals

10.5.1 Phosphorylation

Phosphorylation is a well-studied regulation mechanism for IADs [35–39] (see Chapter 11) but several studies suggest that it also regulates OAD activity.

For sperm initiation, motility activation, and hyperactivation, cAMP-dependent protein phosphorylation is the most important trigger in many organisms including sea urchin, salmonid fish, and mammals [40–43]. The Tctex2 LCs of OAD (LC1 in sea urchin sperm and LC2 in salmonid fish, rainbow trout, and *Ciona* sperm) are phosphorylated in a cAMP-dependent manner upon motility activation [44–47]. The phosphorylation site in these sperm Tctex2 LCs is not conserved in the *Chlamydomonas* homolog LC2 [45]. Since cAMP has an inhibitory effect on *Chlamydomonas* flagella motility [48], phosphorylation may play opposite roles in ciliary/flagellar motility regulation, depending on whether OADs contain phosphorylation-regulated Tctex2 or not.

Biochemical analyses revealed that several OAD subunits other than Tctex2 LCs are phosphorylated. The *Chlamydomonas* α HC is phosphorylated at several sites including one close to AAA1, which is a nucleotide binding and hydrolysis site [49]. Furthermore, phosphoproteome analysis using mass spectrometry revealed that the γ HC (at AAA3), DC1, and DC2 are also phosphorylated [50,51]. In *Ciona*, sperm motility is activated upon the addition of SAAF (sperm-activating and -attracting factor), which activates calmodulin-dependent kinase II through the influx of Ca^{2+} that is followed by an increase in cAMP levels [52,53].

Autoradiography and/or 2D-PAGE of sperm flagella before and after treatment with SAAF in combination with mass spectrometry revealed that the β HC and LC2 are phosphorylated and that IC2 is dephosphorylated after treatment with SAAF [47,53,54]. These data strongly suggest that OAD motor and/or ATPase activity are regulated by phosphorylation but so far there is no evidence from *in vitro* experiments to directly demonstrate this.

10.5.2 Calcium Ions

Ca^{2+} plays important roles in the control of ciliary/flagellar activity, such as phototaxis and photophobic response in *Chlamydomonas* [55,56] and animal sperm chemotaxis to the egg [52,57–59]. Among these, the photophobic response in *Chlamydomonas* has been suggested to involve OADs since it is missing or aberrant in OAD-lacking mutants [60,61].

Chlamydomonas flagella exhibit waveform conversion: they beat with a ciliary (or asymmetric) waveform when the intraflagellar Ca^{2+} concentration is ~10^{-8} M, but with a flagellar (or symmetric) waveform when the Ca^{2+} concentration is raised to ~10^{-4} M [56]. This waveform conversion of *Chlamydomonas* flagella occurs in response to a sudden change in the surrounding light intensity (termed the "photoshock response" or "photophobic response") or a mechanical shock, which induce Ca^{2+} influx into the flagella via a voltage-dependent Ca^{2+} channel at the flagellar tip [56,62].

Chlamydomonas OAD contains at least two subunits (LC4 and DC3) that have four helix-loop-helix motifs, several of which conform to the EF-hand consensus. LC4 is a calmodulin-like protein that binds to the N-terminal stem region of γ HC [27,63,64]. LC4 binds one or two Ca^{2+} with a K_{Ca} of ~3×10^{-5} M, and its binding is highly specific and not affected by Mg^{2+} [63]. LC4 associates with γ HC at two sites, one of which is Ca^{2+} dependent and one that is Ca^{2+} independent (Fig. 10.3A) [64]. When Ca^{2+} is bound to LC4, one site releases the γ HC and instead interacts with IC1. This Ca^{2+}-dependent alteration in binding causes a conformational change in the γ HC [64]. DC3 is a redox-sensitive protein belonging to the CTER (calmodulin, troponin C, essential, and regulatory myosin LCs) group, and is a subunit of the ODA-DC [6,65]. DC3 binds one Ca^{2+} with a K_{Ca} of ~1×10^{-5} M only when it is reduced; it also binds Mg^{2+} but with much lower affinity [65]. Since a *Chlamydomonas* transformant expressing DC3 with a mutation in the functional EF hand showed normal photoshock response (and other Ca^{2+}-related responses such as phototaxis), DC3 may not be involved in waveform conversion regulation [65]. However, there is also no direct evidence that LC4 is involved in the waveform conversion. What directs OAD function to yield waveform conversion is still to be clarified.

In *Ciona*, a neuronal calcium sensor family protein named calaxin has been found to be a subunit of OAD in epithelial cilia and sperm flagella [66]. It has three EF hands and binds to the β HC in the presence of Ca^{2+}. Since calaxin is suggested to

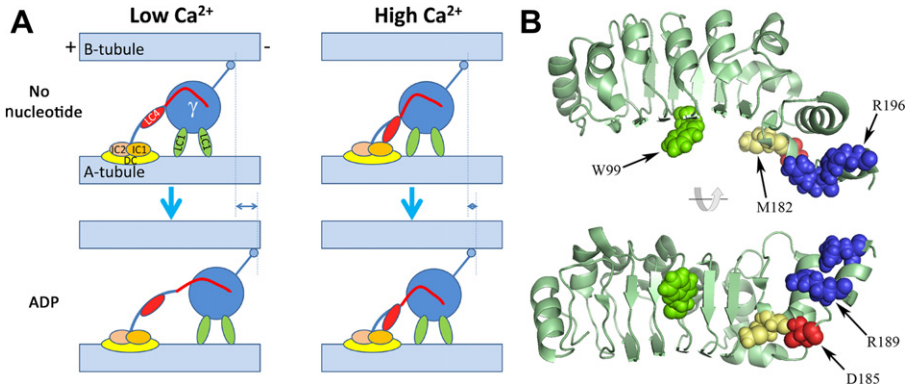

Figure 10.3 (A) Models for mechanoreception and Ca^{2+} signaling by OAD. At least one of two LC1s anchors the γ HC motor domain to the A-tubule (in this diagram, both copies are bound). LC4 has two γ HC binding domains. When Ca^{2+} is bound, one of these domains is released and instead interacts with IC1 at the base of the OAD. Taken together with the "winch" model of OAD function, the γ HC may change the manner of interaction with the B-tubule in a Ca^{2+}-dependent manner. Modified from [87]. **(B) The structure of LC1 and its important residues for OAD regulation.** NMR studies revealed that LC1 contains an N-terminal helix, six ββα motifs of leucine-rich repeats, and a C-terminal helical domain. Important residues for OAD regulation in the text are mentioned. This figure was generated by PyMOL from accession number 1M9L.

bind IC2 in a Ca^{2+}-independent manner and the β HC in *Ciona* is orthologous to the γ HC in *Chlamydomonas*, it is likely that Ca^{2+}-sensitive conformational alterations in OAD HCs are evolutionarily conserved [66].

In *Chlamydomonas*, in addition to phototaxis and the photophobic response, a third Ca^{2+}-regulated motility change related to OAD has been found: a transient increase in beat the flagellar frequency following the mechanical agitation of the flagella [67]. This response is caused by Ca^{2+} influx into flagella to a concentration of ~10^{-7} M via voltage-dependent Ca^{2+} channels, and is missing in OAD-lacking mutants [67,68]. However, so far no OAD-related Ca^{2+}-binding protein with such high affinity for Ca^{2+} has been found, suggesting the existence of an external Ca^{2+} binding factor that regulates OAD activity.

10.5.3 Redox Poise

Redox (reduction and oxidation) has been known for many years to play key roles in respiration and photosynthesis, and it has essential roles in many kinds of cellular regulation such as transcription factor activation, proliferation, and apoptosis [69]. In *Chlamydomonas*, photokinesis (alterations in swimming speed in response to changes in the surrounding light intensity) and duration of the photophobic response are shown to be redox-regulated through the variations in the *in vivo* redox state as a consequence of changes in photosynthetic output [70,71,72,73]. *In vitro* reactivation of demembranated cell models in redox buffers revealed that the flagellar beat frequency was significantly decreased

when oxidized but that the effect of oxidation on OAD-lacking mutant cell models was only modest, suggesting that OAD activity is redox-regulated [72].

In *Chlamydomonas* OADs, several subunits have been shown to be redox-sensitive by biochemical experiments. Upon thiol modification (oxidation), ATPase activity of 18 S dynein (which contains the αβ HC dimer) decreases, whereas 12 S dynein (which contains the γ HC) increases [74]. Two LCs (LC3 and LC5) are thioredoxin-related proteins [75]. Both proteins have perfect copies of the WCGPCK thioredoxin active site motif, which contains a redox-sensitive vicinal dithiol; LC3 contains a second potentially redox-sensitive vicinal dithiol (VCAEKCN) [74,75]. LC3 interacts with the N-terminal stem region of both the β and γ HCs, whereas LC5 associates with a similar region of the α HC [26,64,74]. In addition, the ODA-DC subunit DC3 is a redox-sensitive Ca^{2+} binding protein and contains a redox-sensitive vicinal dithiol within an EF hand motif (DCDGCI) [65]. These three OAD subunits interact with several flagellar proteins (other than OAD subunits) in a redox-sensitive manner, and those substrate proteins change depending on the *in vivo* redox state [72]. However, the identity of these redox-binding partners remains to be ascertained.

The presence of thioredoxin-related subunits and redox regulation of OAD is not specific to *Chlamydomonas*. A catalytic thioredoxin module has been found in IC1 of sperm flagellar OAD from the sea urchin *Anthocidaris crassispina* and *Ciona* [7,8]. Human TXNDC3 (otherwise known as NM23-H8) and TXNDC6 (otherwise known as thioredoxin-like 2 (TXL-2)) are suggested to be orthologous to LC3, LC5, and sea urchin IC1 [9]. In addition, modulation of ATPase activity after thiol modification, which was observed for the *Chlamydomonas* γ HC, has also been demonstrated for both sea urchin sperm and *Tetrahymena thermophila* dyneins [76,77,78]. Thus, redox-based regulation of OAD activity seems to be evolutionarily conserved. Further investigation to identify the substrate proteins interacting with these redox-sensitive OAD subunits may clarify how OAD is involved in redox signaling pathways *in vivo*.

10.5.4 Mechanical Signals

To propagate a wave along the length of the axoneme, axonemal dyneins should become active or inactive at certain times in a periodic manner. For this switching regulation to occur, dyneins are likely regulated by mechanical signals derived from alterations in flagellar curvature. Indeed, mechanical activation experiments suggest the presence of two distinct mechanosensory systems that control IAD and OAD function independently [79].

In *Chlamydomonas* OAD, a candidate system for such mechanoreception has been found in the LC1 and γ HC complex. Two copies of LC1, a leucine-rich repeat (LRR) protein, associate with the AAA^{+} domains of the γ HC, and at least one of them has been shown to bind tubulin from the A-tubule in a nucleotide- and Ca^{2+}-independent manner [80,81]. From the NMR-based structural analysis

of LC1, a hydrophobic patch centered on Trp99 was suggested to be important for the binding of LC1 to the AAA^+ domains. Met182 and Asp185 appear to control the orientation of a C-terminal helix, and Arg189 and Arg196, located within that helix, potentially make ionic contacts with the HC or nucleotide bound within the AAA^+ domains (Fig. 10.3B) [82,83]. Expression of LC1 with mutations at some of these residues caused dominant-negative effects such as a decrease in the flagellar beat frequency and/or defects in the power/recovery stroke transition. These data suggest the possibility that tethering of the γ HC to the A-tubule by two sites (the N-terminal region via the IC—LC complex and the C-terminal motor unit by LC1) acts as a conformational switch that alters dynein motor function in response to changes in flagellar curvature. This system appears to be conserved in other organisms, since RNA interference (RNAi)-based knockdown of LC1 orthologs in *Typanosoma bruciai* and the planarian *Schmidtea* caused severe defects in ciliary/flagellar beating [84,85].

Though the interaction between LC1 and tubulin is Ca^{2+}-independent, LC4 at the N-terminal stem of the γ HC changes its mode of binding in a Ca^{2+}-dependent manner. Together with the "winch" model for dynein motion, which proposes that the microtubule-binding stalk in dyneins pulls the B-microtubule, it is possible that the γ HC changes its manner of interaction with the B-tubule in a Ca^{2+}-sensitive manner (Fig. 10.3A) [86,87].

10.6 Conclusion

As we might expect from its complex structure and the many subunits with various functional motifs, OAD receives and integrates many kinds of external signals, such as phosphorylation, Ca^{2+}, redox, and mechanical strain. Most experiments illustrating the function of these signals have utilized biochemical approaches; however, further physiological and/or biophysical studies will be necessary to understand how these signals modify OAD activities and how they contribute to ciliary/flagellar beating.

Furthermore, though each signal is described separately above, these regulatory pathways must function in combination. For example, the *Chlamydomonas* α HC is a target of phosphorylation and it also interacts with LC5, which receives a redox signal. Furthermore, the *Chlamydomonas* γ HC receives phosphorylation signals and interacts with LC1, LC3, and LC4, which appear to receive/mediate mechanical, redox, and Ca^{2+} signals, respectively. Moreover, because of intra- and inter-OAD regulation, the responses of OAD to these signals may change when combinations of HCs change or multiple OAD molecules are aligned. However, most of the *in vitro* experiments described in this chapter restrict the experimental conditions so that only one signaling pathway functions. For further understanding of how OAD is regulated during ciliary/flagellar beating, combinatorial analyses of different signaling pathways with different HC combinations will be necessary.

Acknowledgments

I would like to thank Prof. Stephen M. King (University of Connecticut Health Center) for providing the LC1 structure figure and for his critical reading of this manuscript. This work was supported by a Grant-in-Aid for Young Scientists (B) from the Japan Society for Promotion of Sciences to K. W.

References

[1] S.M. King, R. Kamiya, Axonemal dyneins: Assembly, structre and force generation, in: G.B. Witman (Ed.), second ed, The Chlamydomonas Sourcebook, volume 3, Academic Press, Amsterdam, 2009, pp. 131–208.

[2] K. Inaba, Molecular basis of sperm flagellar axonemes: Structural and evolutionary aspects, Ann. N.Y. Acad. Sci. 1101 (2007) 506–526.

[3] S. Takada, R. Kamiya, Functional reconstitution of *Chlamydomonas* outer dynein arms from alpha, beta and gamma subunits: Requirement of a third factor, J. Cell Biol. 126 (1994) 737–745.

[4] A. Koutoulis, G.J. Pazour, C.G. Wilkerson, K. Inaba, H. Sheng, S. Takada, G.B. Witman, The *Chlamydomonas reinhardtii* ODA3 gene encodes a protein of the outer dynein arm docking complex, J. Cell Biol. 137 (1997) 1069–1080. Erratum appears in J. Cell Biol. 138(3), (1997) 729.

[5] S. Takada, C.G. Wilkerson, K. Wakabayashi, R. Kamiya, G.B. Witman, The outer dynein arm-docking complex: Composition and characterization of a subunit (oda1) necessary for outer arm assembly, Mol. Biol. Cell 13 (2002) 1015–1029.

[6] D.M. Casey, K. Inaba, G.J. Pazour, S. Takada, K. Wakabayashi, C.G. Wilkerson, R. Kamiya, G.B. Witman, DC3, the 21-kDa subunit of the outer dynein arm-docking complex (ODA-DC), is a novel EF-hand protein important for assembly of both the outer arm and the ODA-DC, Mol. Biol. Cell 14 (2003) 3650–3663.

[7] K. Ogawa, H. Takai, A. Ogiwara, E. Yokota, T. Shimizu, K. Inaba, H. Mohri, Is outer arm dynein intermediate chain 1 multifunctional? Mol. Biol. Cell 7 (1996) 1895–1907.

[8] P. Padma, A. Hozumi, K. Ogawa, K. Inaba, Molecular cloning and characterization of a thioredoxin/nucleoside diphosphate kinase related dynein intermediate chain from the ascidian, *Ciona intestinalis.* Gene 275 (2001) 177–183.

[9] G.J. Pazour, N. Agrin, B.L. Walker, G.B. Witman, Identification of predicted human outer dynein arm genes: Candidates for primary ciliary dyskinesia genes, J. Med. Genet. 43 (2006) 62–73.

[10] D. Nicastro, C. Schwartz, J. Pierson, R. Gaudette, M.E. Porter, J.R. McIntosh, The molecular architecture of axonemes revealed by cryoelectron tomography, Science 313 (2006) 944–948.

[11] T. Oda, N. Hirokawa, M. Kikkawa, Three-dimensional structures of the flagellar dynein-microtubule complex by cryoelectron microscopy, J. Cell Biol. 177 (2007) 243–252.

[12] T. Ishikawa, H. Sakakibara, K. Oiwa, The architecture of outer dynein arms *in situ*, J. Mol. Biol. 368 (2007) 1249–1258.

[13] H. Takazaki, Z. Liu, M. Jin, R. Kamiya, T. Yasunaga, Three outer arm dynein heavy chains of *Chlamydomonas reinhardtii* operate in a coordinated fashion both *in vitro* and *in vivo*, Cytoskeleton (Hoboken) 67 (2010) 466–476.

[14] Z. Liu, H. Takazaki, Y. Nakazawa, M. Sakato, T. Yagi, T. Yasunaga, S.M. King, R. Kamiya, Partially functional outer-arm dynein in a novel *Chlamydomonas* mutant expressing a truncated gamma heavy chain, Eukaryot. Cell 7 (2008) 1136–1145.

[15] C.J. Brokaw, R. Kamiya, Bending patterns of *Chlamydomonas* flagella: IV. Mutants with defects in inner and outer dynein arms indicate differences in dynein arm function, Cell Motil. Cytoskeleton 8 (1987) 68–75.

[16] R. Kamiya, Mutations at twelve independent loci result in absence of outer dynein arms in *Chlamydomonas reinhardtii*, J. Cell Biol. 107 (1988) 2253–2258.
[17] I. Minoura, R. Kamiya, Strikingly different propulsive forces generated by different dynein-deficient mutants in viscous media, Cell Motil. Cytoskeleton 31 (1995) 130–139.
[18] R.D. Vale, Y.Y. Toyoshima, Rotation and translocation of microtubules *in vitro* induced by dyneins from *Tetrahymena cilia*, Cell 52 (1988) 459–469.
[19] L.T. Haimo, B.R. Telzer, J.L. Rosenbaum, Dynein binds to and crossbridges cytoplasmic microtubules, Proc. Natl. Acad. Sci. USA 76 (1979) 5759–5763.
[20] S.M. King, R.S. Patel-King, C.G. Wilkerson, G.B. Witman, The 78,000-M(r) intermediate chain of *Chlamydomonas* outer arm dynein is a microtubule-binding protein, J. Cell Biol. 131 (1995) 399–409.
[21] G.J. Pazour, A. Koutoulis, S.E. Benashski, B.L. Dickert, H. Sheng, R.S. Patel-King, S.M. King, G.B. Witman, LC2, the *Chlamydomonas* homologue of the t complex-encoded protein Tctex2, is essential for outer dynein arm assembly, Mol. Biol. Cell 10 (1999) 3507–3520.
[22] A. Furuta, T. Yagi, H.A. Yanagisawa, H. Higuchi, R. Kamiya, Systematic comparison of *in vitro* motile properties between *Chlamydomonas* wild-type and mutant outer arm dyneins each lacking one of the three heavy chains, J. Biol. Chem. 284 (2009) 5927–5935.
[23] L.M. DiBella, O. Gorbatyuk, M. Sakato, K. Wakabayashi, R.S. Patel-King, G.J. Pazour, G.B. Witman, S.M. King, Differential light chain assembly influences outer arm dynein motor function, Mol. Biol. Cell 16 (2005) 5661–5674.
[24] H. Sakakibara, H. Nakayama, Translocation of microtubules caused by the alphabeta, beta and gamma outer arm dynein subparticles of *Chlamydomonas*, J. Cell Sci. 111 (1998) 1155–1164.
[25] H. Sakakibara, D.R. Mitchell, R. Kamiya, A *Chlamydomonas* outer arm dynein mutant missing the alpha heavy chain, J. Cell Biol. 113 (1991) 615–622.
[26] H. Sakakibara, S. Takada, S.M. King, G.B. Witman, R. Kamiya, A *Chlamydomonas* outer arm dynein mutant with a truncated beta heavy chain, J. Cell Biol. 122 (1993) 653–661.
[27] K.K. Pfister, R.B. Fay, G.B. Witman, Purification and polypeptide composition of dynein ATPases from *Chlamydomonas* flagella, Cell Motil. 2 (1982) 525–547.
[28] K.K. Pfister, G.B. Witman, Subfractionation of *Chlamydomonas* 18 S dynein into two unique subunits containing ATPase activity, J. Biol. Chem. 259 (1984). 12072–12080.
[29] K. Nakamura, C.G. Wilkerson, G.B. Witman, Functional interaction between *Chlamydomonas* outer arm dynein subunits: The gamma subunit suppresses the ATPase activity of the alpha beta dimer, Cell Motil. Cytoskeleton 37 (1997) 338–345.
[30] C.K. Omoto, K.A. Johnson, Activation of the dynein adenosinetriphosphatase by microtubules, Biochemistry 25 (1986) 419–427.
[31] E. Yokota, I. Mabuchi, C/A dynein isolated from sea urchin sperm flagellar axonemes. Enzymatic properties and interaction with microtubules, J. Cell Sci. 107 (Pt 2) (1994) 353–361.
[32] M. Sakato, S. King, Calcium regulates ATP-sensitive microtubule binding by *Chlamydomonas* outer arm dynein, J. Biol. Chem. 278 (2003). 43571–43579.
[33] S. Aoyama, R. Kamiya, Strikingly fast microtubule sliding in bundles formed by *Chlamydomonas* axonemal dynein, Cytoskeleton (Hoboken) 67 (2010) 365–372.
[34] M.E. Porter, K.A. Johnson, Characterization of the ATP-sensitive binding of Tetrahymena 30 S dynein to bovine brain microtubules, J. Biol. Chem. 258 (1983) 6575–6581.
[35] G. Habermacher, W.S. Sale, Regulation of flagellar dynein by phosphorylation of a 138-kD inner arm dynein intermediate chain, J. Cell Biol. 136 (1997) 167–176.
[36] G. Piperno, D.J. Luck, Inner arm dyneins from flagella of *Chlamydomonas reinhardtii*, Cell 27 (1981) 331–340.
[37] S.J. King, S.K. Dutcher, Phosphoregulation of an inner dynein arm complex in *Chlamydomonas reinhardtii* is altered in phototactic mutant strains, J. Cell Biol. 136 (1997) 177–191.

[38] T.W. Hendrickson, C.A. Perrone, P. Griffin, K. Wuichet, J. Mueller, P. Yang, M.E. Porter, W.S. Sale, IC138 is a WD-repeat dynein intermediate chain required for light chain assembly and regulation of flagellar bending, Mol. Biol. Cell 15 (2004) 5431–5442.
[39] R. Bower, K. VanderWaal, E. O'Toole, L. Fox, C. Perrone, J. Mueller, M. Wirschell, R. Kamiya, W.S. Sale, M.E. Porter, IC138 defines a subdomain at the base of the I1 dynein that regulates microtubule sliding and flagellar motility, Mol. Biol. Cell 20 (2009) 3055–3063.
[40] K. Ishiguro, H. Murofushi, H. Sakai, Evidence that cAMP-dependent protein kinase and a protein factor are involved in reactivation of triton X-100 models of sea urchin and starfish spermatozoa, J. Cell Biol. 92 (1982) 777–782.
[41] R.E. Stephens, G. Prior, Dynein from serotonin-activated cilia and flagella: Extraction characteristics and distinct sites for cAMP-dependent protein phosphorylation, J. Cell Sci. 103 (1992) 999–1012.
[42] M. Morisawa, M. Okuno, Cyclic AMP induces maturation of trout sperm axoneme to initiate motility, Nature 295 (1982) 703–704.
[43] J.S. Tash, A.R. Means, Regulation of protein phosphorylation and motility of sperm by cyclic adenosine monophosphate and calcium, Biol. Reprod. 26 (1982) 745–763.
[44] K. Inaba, O. Kagami, K. Ogawa, Tctex2-related outer arm dynein light chain is phosphorylated at activation of sperm motility, Biochem. Biophys. Res. Commun. 256 (1999) 177–183. Erratum appears in Biochem. Biophys. Res. Comm. 268(3), 952 (2000).
[45] K. Inaba, Dephosphorylation of Tctex2-related dynein light chain by type 2A protein phosphatase, Biochem. Biophys. Res. Comm. 297 (2002) 800–805.
[46] K. Inaba, S. Morisawa, M. Morisawa, Proteasomes regulate the motility of salmonid fish sperm through modulation of cAMP-dependent phosphorylation of an outer arm dynein light chain, J. Cell Sci. 111 (1998) 1105–1115.
[47] M. Nomura, K. Inaba, M. Morisawa, Cyclic AMP- and calmodulin-dependent phosphorylation of 21 and 26 kda proteins in axoneme is a prerequisite for SAAF-induced motile activation in ascidian spermatozoa, Dev. Growth Differ. 42 (2000) 129–138.
[48] E. Hasegawa, H. Hayashi, S. Asakura, R. Kamiya, Stimulation of *in vitro* motility of *Chlamydomonas* axonemes by inhibition of cAMP-dependent phosphorylation, Cell Motil. 8 (1987) 302–311.
[49] S.M. King, G.B. Witman, Multiple sites of phosphorylation within the alpha heavy chain of *Chlamydomonas* outer arm dynein, J. Biol. Chem. 269 (1994) 5452–5457.
[50] V. Wagner, G. Gessner, I. Heiland, M. Kaminski, S. Hawat, K. Scheffler, M. Mittag, Analysis of the phosphoproteome of *Chlamydomonas reinhardtii* provides new insights into various cellular pathways, Eukaryot. Cell 5 (2006) 457–468.
[51] J. Boesger, V. Wagner, W. Weisheit, M. Mittag, Analysis of flagellar phosphoproteins from *Chlamydomonas reinhardtii*, Eukaryot. Cell 8 (2009) 922–932.
[52] M. Yoshida, K. Inaba, K. Ishida, M. Morisawa, Calcium and cyclic AMP mediate sperm activation, but Ca21 alone contributes sperm chemotaxis in the ascidian. Ciona savignyi, Dev. Growth Differ. 36 (1994) 589–595.
[53] M. Nomura, M. Yoshida, M. Morisawa, Calmodulin/calmodulin-dependent protein kinase II mediates SAAF-induced motility activation of ascidian sperm, Cell Motil. Cytoskeleton 59 (2004) 28–37.
[54] A. Hozumi, P. Padma, T. Toda, H. Ide, K. Inaba, Molecular characterization of axonemal proteins and signaling molecules responsible for chemoattractant-induced sperm activation in Ciona intestinalis, Cell Motil. Cytoskeleton 65 (2008) 249–267.
[55] R. Kamiya, G.B. Witman, Submicromolar levels of calcium control the balance of beating between the two flagella in demembranated models of *Chlamydomonas*, J. Cell Biol. 98 (1984) 97–107.
[56] M. Bessen, R.B. Fay, G.B. Witman, Calcium control of waveform in isolated flagellar axonemes of *Chlamydomonas*, J. Cell Biol. 86 (1980) 446–455.

[57] M.P. Cosson, D. Carre, J. Cosson, Sperm chemotaxis in siphonophores. II. Calcium-dependent asymmetrical movement of spermatozoa induced by the attractant, J. Cell Sci. 68 (1984) 163–181.
[58] M. Bohmer, Q. Van, I. Weyand, V. Hagen, M. Beyermann, M. Matsumoto, M. Hoshi, E. Hildebrand, U.B. Kaupp, Ca^{2+} spikes in the flagellum control chemotactic behavior of sperm, EMBO J. 24 (2005) 2741–2752.
[59] C.D. Wood, T. Nishigaki, T. Furuta, S.A. Baba, A. Darszon, Real-time analysis of the role of Ca(2+) in flagellar movement and motility in single sea urchin sperm, J. Cell Biol. 169 (2005) 725–731.
[60] R. Kamiya, M. Okamoto, A mutant of *Chlamydomonas reinhardtii* that lacks the flagellar outer dynein arm but can swim, J. Cell Sci. 74 (1985) 181–191.
[61] D.R. Mitchell, J.L. Rosenbaum, A motile *Chlamydomonas* flagellar mutant that lacks outer dynein arms, J. Cell Biol. 100 (1985) 1228–1234.
[62] K. Fujiu, Y. Nakayama, A. Yanagisawa, M. Sokabe, K. Yoshimura, *Chlamydomonas* CAV2 encodes a voltage-dependent calcium channel required for the flagellar waveform conversion, Curr. Biol. 19 (2009) 133–139.
[63] S.M. King, R.S. Patel-King, Identification of a Ca(2+)-binding light chain within *Chlamydomonas* outer arm dynein, J. Cell Sci. 108 (1995) 3757–3764.
[64] M. Sakato, H. Sakakibara, S.M. King, *Chlamydomonas* outer arm dynein alters conformation in response to Ca2+, Mol. Biol. Cell 18 (2007) 3620–3634.
[65] D. Casey, T. Yagi, R. Kamiya, G. Witman, DC3, the smallest subunit of the *Chlamydomonas* flagellar outer dynein arm-docking complex, is a redox-sensitive calcium-binding protein, J. Biol. Chem. 278 (2003). 42652–42659.
[66] K. Mizuno, P. Padma, A. Konno, Y. Satouh, K. Ogawa, K. Inaba, A novel neuronal calcium sensor family protein, calaxin, is a potential Ca(2+)-dependent regulator for the outer arm dynein of metazoan cilia and flagella, Biol. Cell 101 (2009) 91–103.
[67] K. Wakabayashi, T. Ide, R. Kamiya, Calcium-dependent flagellar motility activation in *Chlamydomonas reinhardtii* in response to mechanical agitation, Cell Motil. Cytoskeleton 66 (2009) 736–742.
[68] C.K. Omoto, C.J. Brokaw, Bending patterns of *Chlamydomonas* flagella: II. Calcium effects on reactivated *Chlamydomonas* flagella, Cell Motil. 5 (1985) 53–60.
[69] T. Finkel, N.J. Holbrook, Oxidants, oxidative stress and the biology of ageing, Nature 408 (2000) 239–247.
[70] G. Pazour, O. Sineschekov, G. Witman, Mutational analysis of the phototransduction pathway of *Chlamydomonas reinhardtii*, J. Cell Biol. 131 (1995) 427–440.
[71] A.G. Moss, D.D. Morgan, Rapid analysis of *Chlamydomonas reinhardtii* flagellar beat activity with a LSCM, Microsc. Anal. 34 (1999) 7–9.
[72] K. Wakabayashi, S.M. King, Modulation of *Chlamydomonas reinhardtii* flagellar motility by redox poise, J. Cell Biol. 173 (2006) 743–754.
[73] G. Forti, A. Furia, P. Bombelli, G. Finazzi, *In vivo* changes of the oxidation-reduction state of NADP and of the ATP/ADP cellular ratio linked to the photosynthetic activity in *Chlamydomonas reinhardtii*, Plant Physiol. 132 (2003) 1464–1474.
[74] A. Harrison, M. Sakato, H.W. Tedford, S.E. Benashski, R.S. Patel-King, S.M. King, Redox-based control of the gamma heavy chain ATPase from *Chlamydomonas* outer arm dynein, Cell Motil. Cytoskeleton 52 (2002) 131–143.
[75] R.S. Patel-King, S.E. Benashki, A. Harrison, S.M. King, Two functional thioredoxins containing redox-sensitive vicinal dithiols from the *Chlamydomonas* outer dynein arm, J. Biol. Chem. 271 (1996) 6283–6291.
[76] K. Ogawa, H. Mohri, Studies on the flagellar ATPase from sea urchin spermatozoa. I. Purification and some properties of the enzyme, Biochim. Biophys. Acta 256 (1972) 142–155.
[77] T. Shimizu, I. Kimura, Effects of N-ethylmaleimide on dynein adenosinetriphosphatase activity and its recombining ability with outer fibers, J. Biochem. (Tokyo) 76 (1974) 1001–1008.

[78] I.R. Gibbons, E. Fronk, A latent adenosine triphosphatase form of dynein 1 from sea urchin sperm flagella, J. Biol. Chem. 254 (1979) 187–196.
[79] K. Hayashibe, C. Shingyoji, R. Kamiya, Induction of temporary beating in paralyzed flagella of *Chlamydomonas* mutants by application of external force, Cell Motil. Cytoskeleton 37 (1997) 232–239.
[80] S.E. Benashski, R.S. Patel-King, S.M. King, Light chain 1 from the *Chlamydomonas* outer dynein arm is a leucine-rich repeat protein associated with the motor domain of the gamma heavy chain, Biochemistry 38 (1999) 7253–7264.
[81] R.S. Patel-King, S.M. King, An outer arm dynein light chain acts in a conformational switch for flagellar motility, J. Cell Biol. 186 (2009) 283–295.
[82] H. Wu, M. Blackledge, M.W. Maciejewski, G.P. Mullen, S.M. King, Relaxation-based structure refinement and backbone molecular dynamics of the dynein motor domain-associated light chain, Biochemistry 42 (2003) 57–71.
[83] H. Wu, M.W. Maciejewski, A. Marintchev, S.E. Benashski, G.P. Mullen, S.M. King, Solution structure of a dynein motor domain associated light chain, Nat. Struct. Biol. 7 (2000) 575–579.
[84] P. Rompolas, R.S. Patel-King, S.M. King, An outer arm Dynein conformational switch is required for metachronal synchrony of motile cilia in planaria, Mol. Biol. Cell 21 (2010) 3669–3679.
[85] D.M. Baron, Z.P. Kabututu, K.L. Hill, Stuck in reverse: Loss of LC1 in *Trypanosoma brucei* disrupts outer dynein arms and leads to reverse flagellar beat and backward movement, J. Cell Sci. 120 (2007) 1513–1520.
[86] H. Ueno, T. Yasunaga, C. Shingyoji, K. Hirose, Dynein pulls microtubules without rotating its stalk, Proc. Natl. Acad. Sci. USA 105 (2008). 19702–19707.
[87] S.M. King, Sensing the mechanical state of the axoneme and integration of Ca^{2+} signaling by outer-arm dynein, Cytoskeleton (Hoboken) 67 (2010) 207–213.

In this chapter

11

Control of Axonemal Inner Dynein Arms

Lea M. Alford, Maureen Wirschell, Ryosuke Yamamoto, Winfield S. Sale
Emory University School of Medicine, Atlanta, GA, USA

11.1 Overview

The focus of this chapter is on the regulation of axonemal inner dynein arms and control of ciliary/flagellar bending. Motile cilia and flagella are highly conserved from protozoa to human, where they play vital roles in movement, sensory transduction, and cell regulation [1–3]. The fundamental, motile machinery is the 9+2 axoneme, composed of nine outer doublet microtubules and two central singlet microtubules with associated structural projections (Fig. 11.1A). The axoneme is enclosed by the ciliary membrane, a highly specialized extension of the plasma membrane required for both the regulation of ciliary motility and for sensory functions of the cilium [4–9]. Studies using diverse, experimental systems have also revealed that second messengers and target signaling proteins, physically built into the 9+2 axoneme, regulate ciliary and flagellar motility. Data indicates that the downstream regulation of the axonemal signaling pathway occurs through localized control of the dynein motors [10,11]. In particular, a subset of dyneins called the inner dynein arms are regulated by phosphorylation [10–12]. Thus, the inner dynein arms, in addition to their role in driving inter-microtubule sliding, also play a role in regulation and are required for effective and precise forward and reverse axonemal bends [13,14]. Important questions include: what is the exact role of each dynein structure for generation and control of bending? And, what are the mechanisms that regulate the dynein motors?

Projecting from each outer doublet microtubule are the outer dynein arms, inner dynein arms, radial spokes, and dynein regulatory complex/nexin structures (DRC-nexin) (Fig. 11.1 and see Section 11.2). Analysis of *Chlamydomonas* mutants and experimental study of sea urchin sperm tail flagella reveal that the outer dynein arm is required for normal beat frequency and power, features required for efficient movement [15]. Moreover, diverse studies have revealed that beat frequency and force can be regulated though calcium regulation of outer dynein arms (reviewed in [16,17]); however, this topic will not be reviewed

Dyneins DOI: 10.1016/B978-0-12-382004-4.10011-1
Copyright © 2012 by Elsevier Inc. All rights reserved.

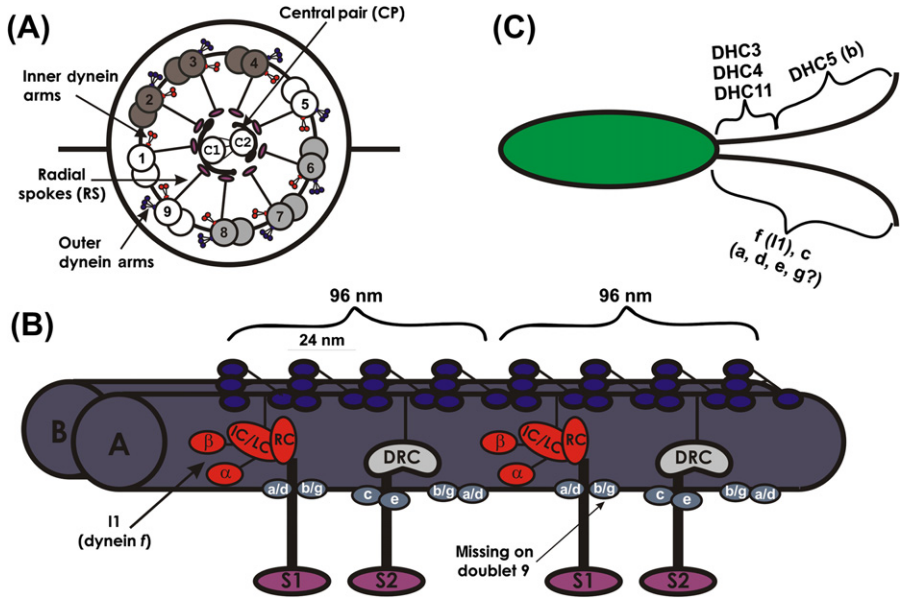

Figure 11.1 Organization of inner dynein arms in the axoneme. (A) A cross-section of the *Chlamydomonas* axoneme shows the 9+2 arrangement of the outer doublet microtubules and central pair apparatus, and the radial spoke structures. The dynein arms attach to the A-tubule of the outer doublets and I1 dynein is depicted in red. (B) The predicted positions of each inner dynein arm species in the 96 nm repeat are indicated. I1 dynein at the base of radial spoke S1 is colored in red. The precise arrangement of dyneins a/d and b/g is still unclear within the 96 nm repeat. (C) The localization of inner dynein arms along the length of the axoneme is shown. The minor inner arms (DHC3, DHC4, and DHC11) are located at the proximal end of both flagella, whereas dynein b (DHC5) is localized to the distal region. Dyneins f and c are along the entire length of the flagella, but the precise distribution of dyneins a, d, e, and g along the length of the axoneme remains unclear.

here. The inner dynein arms, an array of several distinct dyneins, can also generate oscillatory bending, independent of the outer dynein arms, but at greatly reduced beat frequency [18–20]. Furthermore, based on analysis of *Chlamydomonas* mutants lacking subsets of dyneins, the inner dynein arms are important for control of the size and shape of the axonemal bend, parameters referred to as "waveform" [14,21]. Important questions include: what is the precise role of each inner dynein arm in the control of waveform? And, do the inner dynein arms contribute to the modulation of axonemal bending in response to changes in second messengers such as calcium or cyclic nucleotides?

Effective ciliary movement and bend propagation require the coordinated activity of the inner and outer dynein arms in a temporal and spatial manner. How this is accomplished is the focus of intense study. The prevailing concept for ciliary movement is the sliding microtubule model [22]. In this model, axonemal dynein motor activity results in a relative sliding motion between adjacent outer doublet

microtubules: the "sliding microtubule" mechanism for ciliary/flagellar bending [22–25]. The dynein arms induce relative sliding motions that are precisely controlled around the circumference and along the length of the axoneme. However, we have little understanding of either the patterns of active dynein-driven microtubule sliding (versus the patterns of passive outer doublet microtubule sliding) or the structural/mechanical mechanisms that regulate the location or timing of dynein activity (discussed in [26–29]).

The heavy chain (HC) subunits of each dynein arm complex are exceptionally large polypeptides and each contain conserved ATP-binding and motor domains responsible for coupling ATPase activity to translocation of microtubules [15,30,31]. In addition, since the outer and inner dynein arms generate force in one direction (the dyneins are "minus"-end motors [32,33]), active dyneins must switch ("switching model" [34–38]) from one side of an axonemal axis to the other in order to generate alternating bends (axis defined in Fig. 11.1A). Thus, the major challenge for understanding axonemal motility is to determine the mechanism and spatial/temporal regulation of the dynein motors. Evidence indicates that the basic oscillatory mechanism leading to alternating bends is an inherent property of the dynein [14,39–41] and a structural/mechanical feedback mechanism that controls the position of active dyneins. For example, theoretical and experimental evidence indicates that curvature and direction of the bend play a role in the control of dynein activity [27,42–46].

The inherent regulation of dynein by structural/mechanical feedback is not addressed in this chapter. Rather, we focus on a secondary level of regulation, superimposed on the basic dynein-driven oscillatory mechanism, designed to modulate and precisely control the waveform of forward and reverse axonemal bends. The mechanism we focus upon involves second messenger signaling, a phosphorylation pathway, and the inner dynein arms [11,12]. The pathway also includes the central pair apparatus, radial spokes, and conserved protein kinases and phosphatases localized to the axoneme. We review the composition, organization, and general functions of the inner dynein arms. We then focus on a specific inner dynein arm, I1 dynein, also known as dynein-f, which is an unusual, conserved dynein, required for normal motility and composed of two highly conserved HCs [47–49]. I1 dynein is important for control of the size and shape of the axonemal bend (reviewed in [50]). It is required for control of microtubule sliding by an axonemal phosphorylation pathway that includes signals from the central pair, radial spoke, and a network of axonemal kinases and phosphatases [10,11,50]. The mechanism involves a phosphoregulatory complex called the IC138 regulatory subcomplex [51–53]. We discuss models in which I1 dynein can play a "negative" role, locally inhibiting microtubule sliding driven by other dyneins [54], or a "positive" role, locally activating the outer dynein arm and/or other inner dynein arms.

11.2 Organization of the Inner Dynein Arms in the Axoneme

In contrast to the outer dynein arm, which is homogeneous in composition and organization, genetic, biochemical, and structural analysis in *Chlamydomonas* have revealed seven major species of inner-arm dyneins: a, b, c, d, e, f (I1 dynein), and g, and at least three minor species of inner-arm dyneins: DHC3, DHC4, and DHC11 (Tables 11.1 and 11.2) [49]. The identification of inner dynein arm structural heterogeneity began when Goodenough and Heuser [55] noted two different morphologies of inner-arm dyneins in rapid-freeze, deep-etch electron microscopy of axonemes from *Chlamydomonas*, *Tetrahymena*, *Strongelocentrotus*, and *Mnemiopsis*: a tri-lobed structure, termed the triad, at the base of radial spoke S1 and bi-lobed densities, called dyads, which have the same periodicity as the radial spokes. Based on genomic [47–49] and structural [55–60] analyses, the organization and complexity of the inner dynein arms and 96 nm axonemal repeat was shown to be a highly conserved feature of all motile axonemes.

Two years later, Goodenough and colleagues published the first fractionation of inner-arm dyneins by HPLC with a MonoQ anion exchange column [61]. Their analysis of high-salt extracts of *Chlamydomonas* axonemes revealed five distinct fractions, three of which represented inner-arm dyneins as they were not present in extracts from a mutant cell lacking inner dynein arms. Electron microscopy of the fractions corresponding to the inner arms confirmed that there are two structural species that correspond to the dyads and triads: single-headed dyneins and two-headed dyneins, respectively [61]. Piperno [62] further characterized the inner arms and termed three species I1, I2, and I3. Importantly, the electron microscopic analysis of mutants lacking a single species of inner dynein arm revealed regular, 96 nm gaps in structure, confirming the 96 nm repeat model for the axoneme. This result also indicated that each of the different inner dynein arm species was targeted to a precise position and independent of assembly of the other dynein species. Biochemical and electron microscopic analysis of dynein mutants led to the discovery of six distinct HCs comprising these species and the uniqueness of the I1 species [62]. In particular, two HCs and a 140 kDa subunit comprise I1 dynein, which sediments near 21 S on a sucrose gradient, after extraction from the axoneme. In contrast, the other inner-arm dyneins consist of one HC, one LC, and actin, sedimenting at 11 S on a sucrose gradient.

Several subsequent studies have confirmed the composition and organization of I1 (f) dynein [50,63,64]. Electron microscopy [63,65,66], biochemical fractionation [67–71], and localization studies [49,72] revealed that the organization of the single-headed inner dynein arms is far more complex than explained by the I2 and I3 nomenclature. Thus, the "I2" and "I3" nomenclature has been abandoned. Kagami and Kamiya [68] defined what we currently know as the seven major inner-arm dynein subtypes (dyneins a, b, c, d, e, f/I1 dynein, and g) based on fast protein liquid chromatography (FPLC)-MonoQ elution

Table 11.1 Axonemal Inner-Arm Dyneins of *Chlamydomonas reinhardtii*

	Major							Minor		
Species[1]	a	b	c	d	e	f	g	–		
Other name[2]	I2′	I3′	I2A	I2′	I2B	I1	I3	–		
Gene[3]	DHC6	DHC5	DHC9	DHC2	DHC8	DHC1 DHC10	DHC7	DHC3	DHC4	DHC11
Group[4]	IAD3	IAD3	IAD3	IAD4	IAD3	IAD1α IAD1β	IAD5	IAD5	IAD3	IAD3
Subunits[5]	DHC6 actin p28	DHC5 actin centrin	DHC9 actin p28	DHC2 p44 actin p38 p28	DHC8 actin centrin	DHC1 DHC10 IC140 IC138 IC97 FAP120 Tctex1 Tctex2b LC7a LC7b LC8	DHC7 actin centrin	DHC3 actin centrin	DHC4 actin centrin	DHC11 actin p28
DHC gene mutation[6]	–	–	*ida9*	–	–	*ida1* *ida2*	–	–	–	–
Mutants with defects in this species[7]	*ida4* *ida5* *pf23*	*ida10* *pf3*	*ida4* *ida5* *ida9* *ida10* *pf23*	*ida4* *ida5* *ida10* *pf23*	*ida5* *ida6* *ida10* *pf3*	*ida1* *ida2* *ida3* *ida7* *pf23*	–	*ida5*	*ida5*	*ida4* *ida5*
Microtubule rotation[8]	+	–	+	+	+	+	+	?	?	?
Microtubule bending[9]	–	–	–	+	–	–	+	?	?	?

[1] *See [140].*
[2] *See [141].*
[3] *See [49,72,90,142].*
[4] *See [47].*
[5] *See [15,53].*
[6] *See [72,90,142].*
[7] *See [15,49,71].*
[8] *See [54,140].*
[9] *See [143].*

Table 11.2 Inner-Arm-Dynein-Deficient Mutants of *Chlamydomonas reinhardtii*

Mutant	Defective Protein	Defects	References
ida1	DHC1	Loss of dynein f/I1	[66,92]
ida2	DHC10	Loss of dynein f/I1	[66,90]
ida3	?	Loss of dynein f/I1	[66]
ida4	p28	Loss of dynein a, c, d Reduction of DHC11	[66,144]
ida5	Actin	Loss of dynein a, c, d, e Reduction of DHC3, 4, 11	[145]
ida6	?	Loss of dynein e Reduction of tektin DRC defects	[146,147]
ida7	IC140	Loss of dynein f/I1	[91]
ida8/bop2	?	Loss of 152-kDa phospho-protein	[75]
ida9	DHC9	Loss of dynein c	[72]
ida10	MOT48	Reduction of dynein b, c, d, e; slight reduction of outer-arm dynein	[71]
pf3	DRC1	Reduction of dynein b, e DRC defects Reduction of tektin	[147,148]
pf23	?	Loss of dynein a, c, d, f	[149]
bop5	IC138	Loss of dynein regulatory sub-complex of dynein f/I1	[51,85]

profile. Six of the seven major inner-arm dynein species are monomeric — that is, they contain only one HC motor domain (dyneins a, b, c, d, e, and g) — while one inner dynein arm, I1 or dynein f, is dimeric — that is, it contains two HCs, a two-headed dynein. The monomeric species (a, b, c, d, e, and g) are comprised of an actin and either a 28 kDa protein (p28) or a centrin exclusively, while the subunit composition of I1 dynein is more complex (described in Section 11.2.2). With the discovery of this extraordinary complexity and conservation of inner dynein arms, researchers began to question the precise arrangement of each inner dynein arm component: which structure corresponds to which proteins? And, what is the functional role of each dynein in flagellar motility?

Brokaw and Kamiya [21] analyzed motility in *Chlamydomonas* mutants deficient in inner arms to begin to elucidate their role in flagellar motility. The experimental advantages of *Chlamydomonas* allow for determining the position, role, and significance of a specific axonemal component by examining mutant

strains deficient in that component. In a detailed and quantitative analysis of a range of dynein mutants, Brokaw and Kamiya determined that the inner and outer dynein arms have distinct roles for generation and control of axonemal motility. In contrast to outer-arm mutants, *pf30* (a mutant that fails to assemble I1) exhibits a reduction in the amplitude of the bending pattern while maintaining a relatively normal beat frequency. Therefore, outer-arm dyneins are responsible for the beat frequency and power required for generation of normal axonemal motility, whereas the inner-arm dyneins regulate the size and shape of the axonemal bend, parameters we refer to here as "waveform" (reviewed in [15]). These conclusions are consistent with those of Gibbons and Gibbons [18] in study of motility in sea urchin sperm tail axonemes lacking outer dynein arms.

11.2.1 Each Inner Dynein Arm Species is Targeted to a Precise Position in the 96 nm Repeat

By comparing wild-type and mutant axonemes, the inner-arm dyneins exhibit a specific arrangement in the 96 nm repeat (Table 11.1; Fig. 11.1). For example, image averaging of electron micrographs from longitudinal sections of the mutant *pf9* [65] confirmed the location of I1 dynein [62]. These results also confirmed that I1 dynein is the "triad" structure defined in the freeze-etch rotary shadow analysis of axonemal structure [55]. Analysis of the *Chlamydomonas* mutants *pf3* (lacking the DRC and inner-arm species b and e) and *ida4* (lacking species a, c, and d) confirmed that the DRC and these single-headed dynein isoforms also correspond to precisely ordered densities within the 96 nm repeat (Fig. 11.1) [65,73]. Most recently, the positions and structures of the inner dynein arms were further defined using cryo-electron tomography (cryo-ET) of axonemes from wild type and inner and outer dynein arm mutants [56–59,74]. Cryo-electron microscopy (cryo-EM) tomography also confirmed the position of I1 dynein at the proximal position of the 96 nm repeat and revealed that I1 dynein is located on every doublet and along the length of the axoneme [59].

Localization of individual single-headed inner dynein arms has been more challenging due to the limited number of mutants lacking specific subsets of single-headed inner dyneins. However, taking advantage of complementary inner-arm mutants, we now have an idea of the organization of the single-headed inner arms (Fig. 11.1). For example, the mutant *ida9* lacks inner-arm dynein c and, thus, averaging of longitudinal sections of *ida9* axonemes defined the position of dynein c near the base of the S2 radial spoke [72]. Moreover, using cryo-EM tomography and axonemes from *ida1* (lacking I1), *ida9* (lacking dynein c), *ida5* (lacking dyneins a, c, d, and e), and *ida4* (lacking dyneins a, c, and d) mutants, and by process of elimination, we now have a working model for the positions of inner-arm dynein species a/d, b/g, c, e, and f (Fig. 11.1) [58]. However, we cannot yet directly clarify the positions of dynein a and d, or dynein b and g. One approach to directly defining the positions of these dyneins is to combine electron

microscopy analysis with either RNA interference (RNAi) knockdown of specific dynein species or labeling specific species with anti-dynein HC antibodies.

Further analyses, of informative mutants by biochemical and structural approaches, have revealed additional complexity in inner dynein arm organization. This includes the presence of relatively minor subsets of dyneins that localize to the proximal or distal end of the axoneme or to specific doublet microtubules. For example, as determined by electron microscopic analysis, the *bop2* mutant (bypass of paralysis) results in failure of inner dynein arm assembly in a doublet-specific manner, providing evidence of radial asymmetry in inner dynein arms [75]. Cryo-EM tomography also demonstrated heterogeneity to the inner-arm dynein positioning among doublet microtubules [59]. That is, using doublet number nomenclature as defined by Hoops and Witman [76], doublet 9 specifically lacks the dynein b/g structure at the base of radial spoke S1. Furthermore, doublet 1 has a unique structural density located where dyneins b/g, c, and e are typically found on the other doublet microtubules. These are important observations since they may define the position of specialized dyneins or other structures important for control of the bending plane and bend direction.

Heterogeneity in inner dynein arms along the length of the flagella has also been described [49,67]. In detailed biochemical studies of dynein subunits in *Chlamydomonas* mutants defective in flagellar length, or regenerating flagella following de-flagellation, Piperno and Ramanis [67] provided the first evidence that the inner-arm dynein composition differs proximally versus distally. These creative and careful studies relied on high-resolution separation of dynein HCs by SDS-PAGE analysis. More recently, Yagi et al. [49] used direct localization approaches to determine that a subset of inner dyneins localize exclusively to the proximal region of the axoneme. They found three minor inner-arm dynein species (DHC3, DHC4, and DHC11) that localize to the proximal end of the axoneme (Fig. 11.1C; Table 11.1). In contrast, dynein b (DHC5), one of the major inner dynein arm species, appears to be located in a complementary position toward the distal region of the axoneme (Fig. 11.1C). Dynein c (DHC9), another major species, localizes uniformly along the length of the axoneme. These are important observations indicating that the positioning of certain dynein species may play a critical role in ciliary movement. For example, the minor dyneins may replace some of the major dynein species at the proximal region of flagella and play a special role at the base of the axoneme to generate the force required for the initiation of flagellar bending.

Despite the extensive information we have gathered about the conservation and positioning of inner dynein arms, we have yet to elucidate the mechanism for targeting and docking to the axoneme. For example, as described above, we have a good idea about the precise position of most inner dynein arm species [49,58,59,72], and we know from mutant analysis and *in vitro* reconstitution studies that each inner dynein is targeted to a precise position, independent of the others [77,78]. However, to date, neither specific docking proteins nor the "ruler"

proteins determining the 96 nm periodicity of inner-arm dyneins have been identified. In contrast, two independently assembled docking complexes have been identified for the outer dynein arms (ODA-DC and the Oda5 complex), which together specifically anchor four equally spaced outer-arm dyneins per 96 nm repeat [79–82]. Predictably, each inner dynein arm is targeted and anchored in the 96 nm repeat by analogous docking proteins.

11.2.2 Functional Roles of I1 Dynein and Dynein c

I1 dynein is one of the best-characterized of the inner dynein arms. It is the only two-headed inner-arm dynein and its HCs (1α and 1β) are very highly conserved [47–49]. Electron microscopy analysis revealed that, like other dyneins, the HC subunits are organized into two large domains: a tail domain connects to an IC–LC complex at the base of the dynein motor, where the dynein is docked to the A-microtubule, and a globular head-motor domain [54,83]. In addition to the two HC subunits, I1 dynein also contains three ICs (IC140, IC138, and IC97), FAP120, and five LCs (LC8, LC7a, LC7b, Tctex1, and Tctex2b) (Table 11.1; Fig. 11.2) [51–53,84–89]. Based on analysis of I1-dynein mutants, the ICs and LCs play important roles in motor assembly and regulation of motor activity [51,52,90,91].

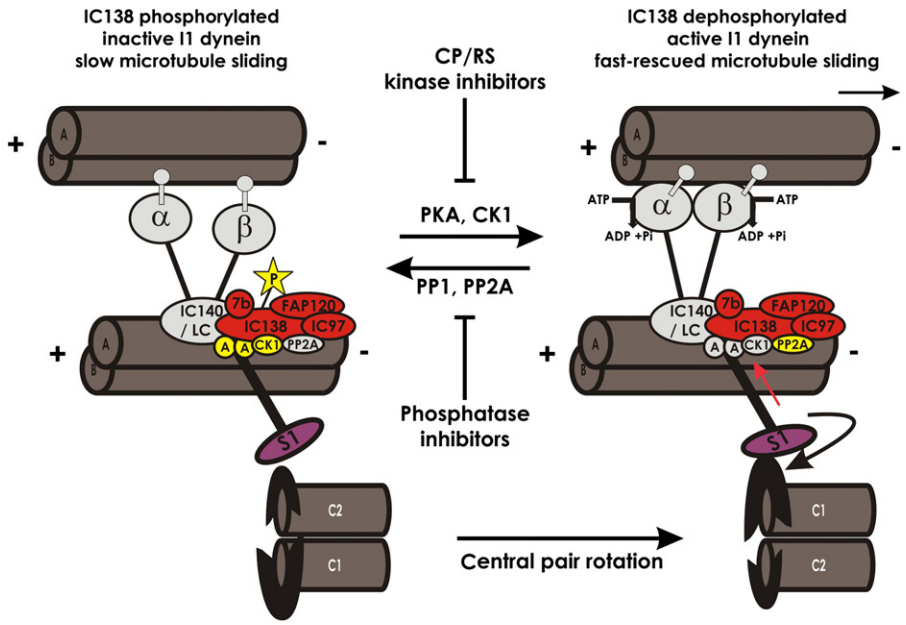

Figure 11.2 Model for the conserved central pair–radial spoke–I1 dynein phosphoregulatory pathway. I1 dynein activity is regulated by axonemal kinases and phosphatases. Central pair rotation provides a mechanical signal to the radial spokes, which activates PKA and CK1, resulting in phosphorylation of IC138. When IC138 is phosphorylated, I1 is inactive and microtubule sliding is inhibited; when IC138 is dephosphorylated, I1 dynein is active and microtubules slide, producing a flagellar bend.

Moreover, analysis of mutants expressing truncated HCs that lack the motor domain of the 1α or 1β HC indicate that each individual I1 dynein HC plays a distinct role in motility [90,92].

The three ICs play distinct roles in the assembly and regulation of I1 dynein; IC140 is critical for assembly and anchoring of I1 in the axoneme [84,91], while IC97 and IC138 play predominantly regulatory roles (see Section 11.3) [51,52]. Notably, LC8, LC7a, LC7b, and Tctex1 are also found in other dyneins, enzymes, and structures (see Chapters 5 and 7) [87,93–95]. These LCs may function in the stable assembly of multi-subunit complexes such as the dynein motors (LC8) [93,96,97] or cargo binding (e.g. the Tctex1–rhodopsin interaction) [98], or perform regulatory functions (LC7b) [15,85,88]. Four of these subunits – IC138, IC97, FAP120, and LC7b – form a distinct sub-complex called the regulatory sub-complex [51–53], which is critical for regulation of I1-dynein activity by phosphorylation.

In addition to I1 dynein, the only other well-characterized inner-arm dynein is dynein c [54,72,99–101]. As discussed above, Yagi and colleagues [72] localized this dynein to the base of radial spoke S2 by electron microscopy of wild-type and *ida9*-mutant axonemes. The dynein c HC is encoded by the *DHC9* gene, is a processive motor, and is one of the "fastest" inner-arm dyneins [54,99]. *In vitro* functional and structural analysis of purified dynein c has played an important role in defining structural changes associated with ATP hydrolysis and force generation [99–101]. Analysis of the *ida9* mutant revealed the role of dynein c in force generation: *ida9* cells undergo a significant reduction of swimming speed in viscous media, indicating that dynein c is required for force generation [72].

The inner dynein arms are highly conserved, very complex structures organized within the 96 nm repeat, along the length of the axoneme, and among the individual outer doublet microtubules (Fig. 11.1) [57–59,72,74]. Although analysis of inner-arm-deficient motility phenotypes clearly implicates their role in the control of waveform, the challenge is to determine how each different inner dynein arm contributes to the bending movement and whether there is a functional/regulatory interaction among different dyneins [14,15,21]. For the remainder of the chapter, we focus on I1 dynein, its regulation, and its role in axonemal bending.

11.3 Regulation of I1 Dynein by Second Messengers and Phosphorylation

Diverse data have revealed that second messengers, including calcium and cyclic nucleotides, can directly or indirectly control ciliary motility by modulation of dynein activity [10,16,50,102]. Here we focus on data generated in the model

genetic organism, *Chlamydomonas*, which has revealed a conserved phosphoregulatory pathway for control of dynein motor activity that involves the central pair, radial spokes, and I1 dynein (reviewed in [11]). This pathway utilizes highly conserved kinases (PKA, CK1) [103–105], anchoring proteins (e.g. AKAP) [106,107], and phosphatases (PP1, PP2A) [108–110] that are physically located in the axoneme, where they play a direct role in the control of motility.

Critical to understanding the regulation of dynein-driven motility in cilia was the development of two types of *in vitro* motility assays. The first is the ATP-induced reactivation of movement of axonemes [111–113]. Not only did this approach reveal that the machinery required for motility is an inherent part of the 9+2 axoneme, but also that change in the reactivation buffer could alter ATP-driven motility in isolated axonemes. For example, in *Chlamydomonas*, this approach led to discovery that both calcium and cAMP addition could alter motility in isolated axonemes [112,114,115]. These, and studies in other experimental systems, revealed that the calcium-binding proteins and cyclic nucleotide-binding proteins are physical components of the axoneme. For example, calmodulin is found in a number of protein complexes in the axoneme [116–120]. Experimental studies also reveal that PKA is an important component for regulation of ciliary motility (reviewed in [16]). For the future, high-speed film analysis (see [121]) of motility in ATP-induced reactivation of axonemes lacking selected subsets of dyneins, or lacking calmodulin or signaling enzymes, will be a particularly important approach for defining the role and regulation of each inner dynein arm.

The second *in vitro* motility assay is the microtubule sliding, or sliding disintegration assay, which has provided an extremely reliable means to assess the mechanochemical properties of the ciliary dynein motors by measuring microtubule sliding [122]. The assay was first developed by Summers and Gibbons [23], who used dark-field microscopy for observation and directly demonstrated *in vitro* dynein-driven sliding of outer doublet microtubules in sea urchin sperm tail axonemes. The microtubule-sliding assay has been adapted for axonemes from a wide variety of organisms, revealing important features of the control of axonemal movement [32,123–130]. Subsequent experiments refined the microtubule-sliding assay for *Chlamydomonas* axonemes, allowing for highly reproducible results in wild-type and mutant axonemes [127]. Using the improved assay, microtubule-sliding velocities for mutants lacking specific dynein arms, or other axonemal components, were determined, revealing distinct functional capabilities of different axonemal dyneins [131].

11.3.1 Regulation of the Inner Dynein Arms: The Central Pair/Radial Spoke Phosphoregulatory Pathway and I1 Dynein

As indicated above, the central pair and radial spoke structures are required for normal ciliary motility [130] and regulated microtubule sliding by a control

mechanism involving axonemal protein phosphorylation [10,50,132]. This control system was first identified through a series of bypass suppressor mutations in *Chlamydomonas* that restore motility to paralyzed central-pair or radial-spoke mutants without restoring assembly of the missing axonemal structures [63,133–136]. Consistent with this discovery, dynein activity can be induced in mutant central pair or radial spoke axonemes, using the *in vitro* microtubule-sliding assay, indicating that the dynein arms are functional in these paralyzed axonemes. However, the velocity of microtubule sliding is greatly reduced in axonemes from the paralyzed flagellar mutants relative to wild-type axonemes [137].

These results indicated that dynein activity is inhibited in axonemes from central-pair or radial-spoke mutants. To test this idea, Smith and Sale [137] measured microtubule-sliding velocities in reconstituted axonemes (rebinding of dynein arms to dynein-depleted axonemes from either wild-type or radial-spoke-defective axonemes). They determined that the reduced dynein activity in radial-spoke mutant axonemes was due to a reversible phosphorylation and that the alteration occurred in an inner dynein arm component. Moreover, the key kinases (PKA, CK1) [103–105] are localized to the axoneme, presumably by specialized anchoring proteins such as AKAPs (A-kinase anchoring proteins) [10,11,106,107]. The question was which inner dynein arm is the target for regulation by the axonemal phosphoregulatory pathway?

Subsequent analysis of axonemes from double mutants, lacking the radial spoke structures and selected dynein arms, demonstrated that I1 dynein is a critical target for regulation by the central-pair and radial-spoke pathway [104,109,138]. Furthermore, these studies revealed that phosphorylation of the I1-dynein IC, IC138, correlated with inactive I1 dynein (i.e. inhibited axonemal microtubule sliding – Fig. 11.2) and de-phosphorylation correlated with active I1 dynein ("rescued" axonemal microtubule sliding – Fig. 11.2; reviewed in [10,50]). When the regulatory pathway is defective, such as in central-pair and radial-spoke mutant axonemes, it appears that axonemal kinases are unregulated, resulting in abnormal IC138 phosphorylation and reduced microtubule-sliding velocities [85,109]. Importantly, the addition of kinase inhibitors rescues microtubule sliding [103,104,105] consistently with the model shown in Figure 11.2. This model is also supported by the identification of mutants defective in IC138 phosphorylation or assembly or I1-dynein assembly [51,85,138]. Additional studies of IC138 null alleles characterized a novel sub-complex, called the IC138 regulatory sub-complex (Fig. 11.2), which is required for I1-dynein activity; rescue of microtubule sliding by protein kinase inhibitors requires assembly of the IC138 sub-complex [51].

While there is strong evidence that microtubule sliding correlates with changes in IC138 phosphorylation, the assembly of IC97 is also important for regulation of I1-dynein activity (Fig. 11.2) [52]. IC97 may function together with the IC138

phosphorylation cycle and may function to mediate changes in I1-dynein conformation that are associated with phosphorylation; however, we know little about how phosphorylation and the IC138 complex operate to control I1 dynein and microtubule sliding [52]. Multiple lines of evidence have shown that IC97 interacts directly with tubulin in the axoneme; this interaction may function in the docking of I1 dynein to the outer doublet microtubules or as a "curvature sensor" to detect changes in the bend of the flagellum (see [52]). The requirement for the assembly of the IC138 regulatory sub-complex for regulation indicates that I1 dynein plays an active role in the regulation of microtubule sliding.

Although I1 dynein and phosphorylation of IC138 appear to play a critical role for normal motility, we do not know the mechanisms. Questions include: how does I1 dynein regulate microtubule sliding and axonemal bending? And, how does change in phosphorylation alter I1-dynein activity? One model is that I1 dynein plays a role as a "negative" regulator and, through localized signals, inhibits microtubule sliding on subsets of microtubules driven by other dynein motors. Consistent with this model, compared to other axonemal dyneins, I1 dynein can only generate slow microtubule movement [54,83]. Moreover, in *in vitro* competition assays using purified dynein complexes, Kotani et al. [54] determined that I1 dynein could inhibit dynein c microtubule translocation. Change in phosphorylation of IC138 could modulate the capability of I1 dynein to resist microtubule sliding.

I1 dynein could also act in a "positive" manner by permitting full motor activity of other axonemal dyneins such as the outer dynein arm. For example, in the absence of I1 dynein [90,92] or in the absence of the IC138 complex [51], cells swim at a reduced velocity. Furthermore, microtubule sliding in axonemes lacking I1 dynein or IC138 is reduced to near half [51]. One interpretation of these observations is that, in the absence of I1 or IC138, the outer dynein arm can only operate at a reduced level of activity. Interestingly, recent structural studies have revealed a linker structure that extends between I1 dynein and the adjacent outer dynein arm [57,58,59]. Further tests of this idea will require identification of new motility mutants and the molecular identification of the linker and structural–functional interactions between I1 and the outer dynein arms.

11.3.2 The Regulatory Components of the Axonemal Phosphoregulatory Mechanism: The Kinases and Phosphatases

Combining pharmacological agents and microtubule-sliding assays in paralyzed axonemes provided the initial evidence that conserved kinases (PKA, CK1) and phosphatases (PP2A, PP1) are physically located in the axoneme for control of I1 dynein [10,11,50,103–105,110,139]. For example, as indicated in Section 11.3.1, addition of specific kinase inhibitors to central-pair or radial-spoke mutant axonemes increased microtubule-sliding velocities to wild-type levels (Fig. 11.2)

[103,104,108]. This result demonstrated that these kinases are inherent components of the axoneme and that they play a role in the control of dynein-driven microtubule sliding. To determine whether these kinases are directly involved in phosphorylation of IC138, incorporation of radioactive phosphate into IC138 was measured in the presence of the kinase inhibitors. Interestingly, while PKA inhibitors rescue microtubule-sliding velocities in radial-spoke mutant axonemes, they do not prevent phosphorylation of IC138 [103,104]. Thus, cAMP, while an important second messenger that regulates motility through PKA, does not appear to act alone in control of IC138 phosphorylation. These signaling components may reside upstream in the regulatory pathway or may form part of a parallel pathway that involves phosphorylation of other, unidentified axonemal proteins. In contrast, CK1 inhibitors not only rescue microtubule-sliding velocities but also block IC138 phosphorylation, suggesting that CK1 may directly control phosphorylation of IC138. Consistent with this model, the axonemal CK1 was recently characterized and found to directly regulate I1-dynein-dependent microtubule sliding [105]. These results indicate that, in wild-type axonemes, the central-pair and radial-spoke structures operate, in part, to regulate the axonemal protein kinases for precise control of flagellar motility. One prevailing model indicates that signals, generated by the central pair, are transmitted via the radial-spoke structures and result in tight regulation of kinase activity. This, in turn, alters the phosphorylation state of IC138 and results in changes in I1-dynein activity and microtubule sliding. Predictably, local changes in I1-dynein activity and microtubule sliding on one side of an axonemal axis (Fig. 11.1A) will influence the pattern of microtubule sliding and the size and shape of the flagellar bend.

The "rescue" of microtubule-sliding velocities by kinase inhibitors is prevented by treatment with phosphatase inhibitors, demonstrating that the key phosphatases involved in the regulation of I1 dynein are also axonemal components [108–110]. Initially, the protein phosphatase, PP1, was thought to be critical for the rescue of microtubule sliding [108]. PP1 is a prominent component of the central-pair apparatus and may function upstream in the regulatory pathway [110]. The same studies revealed that the protein phosphatase, PP2A, localizes to the outer-doublet microtubules [110]. As such, PP2A is a prime candidate for regulation of I1 dynein (Fig. 11.2). Current questions relate to how PP2A is localized in the axoneme and whether PP2A is associated with I1 dynein.

11.4 Current Questions

This chapter provides an overview of the structure, organization, and regulation of the inner dynein arms, with particular focus on I1 dynein/dynein f. Although there is much evidence from *Chlamydomonas* for the presence of seven distinct major inner-arm dyneins, their precise arrangement in the axoneme and regulation by second messengers are not completely understood.

Immediate questions regarding the positioning of inner dynein arms include: (1) Is there a docking complex associated with I1 dynein that targets it to the base of S1? (2) Do the other inner arms have similar docking complexes? Analysis of mutants lacking subsets of inner dynein arms indicates they are each assembled independently of one another [62]. Thus, predictably there must be conserved proteins that target and anchor each dynein in a unique position. Such targeting and docking proteins can be revealed by additional dynein assembly mutants and by analysis of protein–protein interactions. (3) How are the minor species of inner dynein arms localized in the proximal region of the axoneme [49] or on subsets of doublet microtubules [59]? Presumably, the mechanisms for docking and localization of each dynein species require at least the same number of docking complexes, or docking domains on a multi-purpose docking protein.

There may be functional interactions between different axonemal dyneins: (1) Does I1 dynein play a role in the regulation of the activity of the outer dynein arm? (2) If so, is regulation mediated by the inner–outer dynein linker structure revealed by cryo-EM tomography [57,58]? (3) Are there functional interactions among the inner dynein arms?

One surprise is that conserved protein kinases (including PKA and CK1) and phosphatases (including PP1 and PP2A) are targeted and anchored in the axoneme and play a role in the regulation of motility [11]. Current questions include: (1) Are the axonemal kinases and phosphatases involved in I1-dynein regulation localized on each outer doublet of the axoneme? (2) How are the otherwise ubiquitous enzymes targeted and anchored on the axonemal microtubules? One model is the localization of PKA by axonemal AKAPs [106,107]; analogous anchoring proteins may exist for all axonemal kinases and phosphatases. (3) What is the location of the enzymes on the outer doublet microtubules? Predictably, since the axonemal kinases and phosphatases are not randomly positioned or freely diffusible, they must be anchored near the key substrates including I1 dynein. (4) What is the stoichiometry of each kinase and phosphatase in the axoneme? For example, if CK1 is associated with I1 dynein on every outer doublet microtubule [105], then there must be an equal stoichiometry of I1 dynein and CK1. Consistent with this prediction, CK1 appears to be an abundant axonemal protein [104]. However, we do not know the relative stoichiometry of PP1 or PP2A in the axoneme. (5) Given the pharmacological evidence for a role of PKA in phosphoregulation in *Chlamydomonas* axonemes [103], what are the subunits and genes encoding PKA in *Chlamydomonas*?

Changes in calcium concentration also alter flagellar waveform and I1-dynein assembly is important for control of waveform. (6) What is the link between calcium regulation of beating and the central pair/radial spoke/I1 pathway? (7) How do the radial spokes interact with the central pair projections to transmit signals to the outer doublet microtubules? And (8) what are the structural and chemical links between the radial spokes and the inner dynein arms?

References

[1] P. Satir, S.T. Christensen, Overview of structure and function of mammalian cilia, Annu. Rev. Physiol. 69 (2007) 377–400.

[2] D.M. Woolley, Flagellar oscillation: A commentary on proposed mechanisms, Biol. Rev. Camb. Philos. Soc. 85 (2010) 453–470.

[3] S.C. Goetz, K.V. Anderson, The primary cilium: A signalling centre during vertebrate development, Nat. Rev. Genet. 11 (2010) 331–344.

[4] G.J. Pazour, R.A. Bloodgood, Targeting proteins to the ciliary membrane, Curr. Top. Dev. Biol. 85 (2008) 115–149.

[5] R. Rohatgi, W.J. Snell, The ciliary membrane, Curr. Opin. Cell. Biol. 22 (2010) 541–546.

[6] B.T. Emmer, D. Maric, D.M. Engman, Molecular mechanisms of protein and lipid targeting to ciliary membranes, J. Cell Sci. 123 (2010) 529–536.

[7] Q. Hu, L. Milenkovic, H. Jin, M.P. Scott, M.V. Nachury, E.T. Spiliotis, W.J. Nelson, A septin diffusion barrier at the base of the primary cilium maintains ciliary membrane protein distribution, Science 329 (2010) 436–439.

[8] A.S. Shah, Y. Ben-Shahar, T.O. Moninger, J.N. Kline, M.J. Welsh, Motile cilia of human airway epithelia are chemosensory, Science 325 (2009) 1131–1134.

[9] B. Craige, C.C. Tsao, D.R. Diener, Y. Hou, K.F. Lechtreck, J.L. Rosenbaum, G.B. Witman, CEP290 tethers flagellar transition zone microtubules to the membrane and regulates flagellar protein content, J. Cell Biol. 190 (2010) 927–940.

[10] M.E. Porter, W.S. Sale, The 9 + 2 axoneme anchors multiple inner arm dyneins and a network of kinases and phosphatases that control motility, J. Cell Biol. 151 (2000) F37–F42.

[11] C.A. Elam, W.S. Sale, M. Wirschell, The regulation of dynein-driven microtubule sliding in *Chlamydomonas* flagella by axonemal kinases and phosphatases, Method. Cell. Biol. 92 (2009) 133–151.

[12] M. Wirschell, D. Nicastro, M.E. Porter, W.S. Sale, The regulation of axonemal bending, in: G.B. Witman (Ed.), Second ed., The Chlamydomonas Sourcebook: Cell Motility and Behavior, vol. 3 Academic Press, Oxford, 2009, pp. 253–282.

[13] C.J. Brokaw, Control of flagellar bending: A new agenda based on dynein diversity, Cell Motil. Cytoskeleton 28 (1994) 199–204.

[14] R. Kamiya, Functional diversity of axonemal dyneins as studied in *Chlamydomonas* mutants, Int. Rev. Cytol. 219 (2002) 115–155.

[15] S.M. King, R. Kamiya, Axonemal dyneins: Assembly, structure, and force generation, in: G.B. Witman (Ed.), Second ed., The *Chlamydomonas* Sourcebook: Cell Motility and Behavior, vol. 3 Academic Press, Oxford, 2009, pp. 131–208.

[16] M. Salathe, Regulation of mammalian ciliary beating, Annu. Rev. Physiol. 69 (2007) 401–422.

[17] S.M. King, Sensing the mechanical state of the axoneme and integration of Ca^{2+} signaling by outer arm dynein, Cytoskeleton (Hoboken) 67 (2010) 207–213.

[18] B.H. Gibbons, I.R. Gibbons, The effect of partial extraction of dynein arms on the movement of reactivated sea-urchin sperm, J. Cell Sci. 13 (1973) 337–357.

[19] D.R. Mitchell, J.L. Rosenbaum, A motile *Chlamydomonas* flagellar mutant that lacks outer dynein arms, J. Cell Biol. 100 (1985) 1228–1234.

[20] R. Kamiya, M. Okamoto, A mutant of *Chlamydomonas reinhardtii* that lacks the flagellar outer dynein arm but can swim, J. Cell Sci. 74 (1985) 181–191.

[21] C.J. Brokaw, R. Kamiya, Bending patterns of *Chlamydomonas* flagella: IV. Mutants with defects in inner and outer dynein arms indicate differences in dynein arm function, Cell Motil. Cytoskeleton 8 (1987) 68–75.

[22] P. Satir, Studies on cilia. 3. Further studies on the cilium tip and a "sliding filament" model of ciliary motility, J. Cell Biol. 39 (1968) 77–94.

[23] K.E. Summers, I.R. Gibbons, Adenosine triphosphate-induced sliding of tubules in trypsin-treated flagella of sea-urchin sperm, Proc. Natl. Acad. Sci. USA 68 (1971) 3092–3096.
[24] C. Shingyoji, A. Murakami, K. Takahashi, Local reactivation of Triton-extracted flagella by iontophoretic application of ATP, Nature 265 (1977) 269–270.
[25] C.J. Brokaw, Direct measurements of sliding between outer doublet microtubules in swimming sperm flagella, Science 243 (1989) 1593–1596.
[26] C.J. Brokaw, Thinking about flagellar oscillation, Cell Motil. Cytoskeleton 66 (2009) 425–436.
[27] C.B. Lindemann, K.A. Lesich, Flagellar and ciliary beating: The proven and the possible, J. Cell Sci. 123 (2010) 519–528.
[28] C.B. Lindemann, The geometric clutch as a working hypothesis for future research on cilia and flagella, Ann. N.Y. Acad. Sci. 1101 (2007) 477–493.
[29] C.B. Lindemann, K.S. Kanous, A model for flagellar motility, Int. Rev. Cytol. 173 (1997) 1–72.
[30] K. Oiwa, H. Sakakibara, Recent progress in dynein structure and mechanism, Curr. Opin. Cell. Biol. 17 (2005) 98–103.
[31] S.M. King, Axonemal dyneins winch the cilium, Nat. Struct. Mol. Biol. 17 (2010) 673–674.
[32] W.S. Sale, P. Satir, Direction of active sliding of microtubules in *Tetrahymena* cilia, Proc. Natl. Acad. Sci. USA 74 (1977) 2045–2049.
[33] L.A. Fox, W.S. Sale, Direction of force generated by the inner row of dynein arms on flagellar microtubules, J. Cell Biol. 105 (1987) 1781–1787.
[34] J. Wais-Steider, P. Satir, Effect of vanadate on gill cilia: Switching mechanism in ciliary beat, J. Supramol. Struct. 11 (1979) 339–347.
[35] P. Satir, T. Matsuoka, Splitting the ciliary axoneme: Implications for a "switch-point" model of dynein arm activity in ciliary motion, Cell Motil. Cytoskeleton 14 (1989) 345–358.
[36] K.F. Lechtreck, P. Delmotte, M.L. Robinson, M.J. Sanderson, G.B. Witman, Mutations in hydin impair ciliary motility in mice, J. Cell Biol. 180 (2008) 633–643.
[37] K.F. Lechtreck, G.B. Witman, *Chlamydomonas reinhardtii* hydin is a central pair protein required for flagellar motility, J. Cell Biol. 176 (2007) 473–482.
[38] E.F. Smith, Hydin seek: Finding a function in ciliary motility, J. Cell Biol. 176 (2007) 403–404.
[39] R. Kamiya, Exploring the function of inner and outer dynein arms with *Chlamydomonas* mutants, Cell Motil. Cytoskeleton 32 (1995) 98–102.
[40] S. Aoyama, R. Kamiya, Cyclical interactions between two outer doublet microtubules in split flagellar axonemes, Biophys. J. 89 (2005) 3261–3268.
[41] K. Hayashibe, C. Shingyoji, R. Kamiya, Induction of temporary beating in paralyzed flagella of *Chlamydomonas* mutants by application of external force, Cell Motil. Cytoskeleton 37 (1997) 232–239.
[42] Y. Morita, C. Shingyoji, Effects of imposed bending on microtubule sliding in sperm flagella, Curr. Biol. 14 (2004) 2113–2118.
[43] S. Hayashi, C. Shingyoji, Mechanism of flagellar oscillation-bending-induced switching of dynein activity in elastase-treated axonemes of sea urchin sperm, J. Cell Sci. 121 (2008) 2833–2843.
[44] C.J. Brokaw, Computer simulation of flagellar movement. I. Demonstration of stable bend propagation and bend initiation by the sliding filament model, Biophys. J. 12 (1972) 564–586.
[45] C.J. Brokaw, Computer simulation of flagellar movement. VI. Simple curvature-controlled models are incompletely specified, Biophys. J. 48 (1985) 633–642.
[46] C.B. Lindemann, K.S. Kanous, "Geometric clutch" hypothesis of axonemal function: Key issues and testable predictions, Cell Motil. Cytoskeleton 31 (1995) 1–8.

[47] R.L. Morris, M.P. Hoffman, R.A. Obar, S.S. McCafferty, I.R. Gibbons, A.D. Leone, J. Cool, E.L. Allgood, A.M. Musante, K.M. Judkins, B.J. Rossetti, A.P. Rawson, D.R. Burgess, Analysis of cytoskeletal and motility proteins in the sea urchin genome assembly, Dev. Biol. 300 (2006) 219–237.
[48] D.E. Wilkes, H.E. Watson, D.R. Mitchell, D.J. Asai, Twenty-five dyneins in *Tetrahymena*: A re-examination of the multidynein hypothesis, Cell Motil. Cytoskeleton 65 (2008) 342–351.
[49] T. Yagi, K. Uematsu, Z. Liu, R. Kamiya, Identification of dyneins that localize exclusively to the proximal portion of *Chlamydomonas* flagella, J. Cell Sci. 122 (2009) 1306–1314.
[50] M. Wirschell, T. Hendrickson, W.S. Sale, Keeping an eye on I1: I1 dynein as a model for flagellar dynein assembly and regulation, Cell Motil. Cytoskeleton 64 (2007) 569–579.
[51] R. Bower, K. VanderWaal, E. O'Toole, L. Fox, C. Perrone, J. Mueller, M. Wirschell, R. Kamiya, W.S. Sale, M.E. Porter, IC138 defines a subdomain at the base of the I1 dynein that regulates microtubule sliding and flagellar motility, Mol. Biol. Cell 20 (2009) 3055–3063.
[52] M. Wirschell, C. Yang, P. Yang, L. Fox, H.A. Yanagisawa, R. Kamiya, G.B. Witman, M.E. Porter, W.S. Sale, IC97 is a novel intermediate chain of I1 dynein that interacts with tubulin and regulates interdoublet sliding, Mol. Biol. Cell 20 (2009) 3044–3054.
[53] K. Ikeda, R. Yamamoto, M. Wirschell, T. Yagi, R. Bower, M.E. Porter, W.S. Sale, R. Kamiya, A novel ankyrin-repeat protein interacts with the regulatory proteins of inner arm dynein f (I1) of *Chlamydomonas reinhardtii*, Cell Motil. Cytoskeleton 66 (2009) 448–456.
[54] N. Kotani, H. Sakakibara, S.A. Burgess, H. Kojima, K. Oiwa, Mechanical properties of inner-arm dynein-f (dynein I1) studied with *in vitro* motility assays, Biophys. J. 93 (2007) 886–894.
[55] U.W. Goodenough, J.E. Heuser, Substructure of inner dynein arms, radial spokes, and the central pair/projection complex of cilia and flagella, J. Cell Biol. 100 (1985) 2008–2018.
[56] D. Nicastro, J.R. McIntosh, W. Baumeister, 3D structure of eukaryotic flagella in a quiescent state revealed by cryo-electron tomography, Proc. Natl. Acad. Sci. USA 102 (2005) 15889–15894.
[57] D. Nicastro, C. Schwartz, J. Pierson, R. Gaudette, M.E. Porter, J.R. McIntosh, The molecular architecture of axonemes revealed by cryoelectron tomography, Science 313 (2006) 944–948.
[58] K.H. Bui, H. Sakakibara, T. Movassagh, K. Oiwa, T. Ishikawa, Molecular architecture of inner dynein arms *in situ* in *Chlamydomonas reinhardtii* flagella, J. Cell Biol. 183 (2008) 923–932.
[59] K.H. Bui, H. Sakakibara, T. Movassagh, K. Oiwa, T. Ishikawa, Asymmetry of inner dynein arms and inter-doublet links in *Chlamydomonas* flagella, J. Cell Biol. 186 (2009) 437–446.
[60] S.A. Burgess, D.A. Carter, S.D. Dover, D.M. Woolley, The inner dynein arm complex: Compatible images from freeze-etch and thin section methods of microscopy, J. Cell Sci. 100 (Pt. 2) (1991) 319–328.
[61] U.W. Goodenough, B. Gebhart, V. Mermall, D.R. Mitchell, J.E. Heuser, High-pressure liquid chromatography fractionation of *Chlamydomonas* dynein extracts and characterization of inner-arm dynein subunits, J. Mol. Biol. 194 (1987) 481–494.
[62] G. Piperno, Z. Ramanis, E.F. Smith, W.S. Sale, Three distinct inner dynein arms in *Chlamydomonas* flagella: Molecular composition and location in the axoneme, J. Cell Biol. 110 (1990) 379–389.
[63] M.E. Porter, J. Power, S.K. Dutcher, Extragenic suppressors of paralyzed flagellar mutations in *Chlamydomonas reinhardtii* identify loci that alter the inner dynein arms, J. Cell Biol. 118 (1992) 1163–1176.
[64] L.M. DiBella, S.M. King, Dynein motors of the *Chlamydomonas* flagellum, Int. Rev. Cytol. 210 (2001) 227–268.

[65] D.N. Mastronarde, E.T. O'Toole, K.L. McDonald, J.R. McIntosh, M.E. Porter, Arrangement of inner dynein arms in wild-type and mutant flagella of *Chlamydomonas*, J. Cell Biol. 118 (1992) 1145–1162.
[66] R. Kamiya, E. Kurimoto, E. Muto, Two types of *Chlamydomonas* flagellar mutants missing different components of inner-arm dynein, J. Cell Biol. 112 (1991) 441–447.
[67] G. Piperno, Z. Ramanis, The proximal portion of *Chlamydomonas* flagella contains a distinct set of inner dynein arms, J. Cell Biol. 112 (1991) 701–709.
[68] O. Kagami, S. Takada, R. Kamiya, Microtubule translocation caused by three subspecies of inner-arm dynein from *Chlamydomonas* flagella, FEBS Lett. 264 (1990) 179–182.
[69] M. LeDizet, G. Piperno, The light chain p28 associates with a subset of inner dynein arm heavy chains in *Chlamydomonas* axonemes, Mol. Biol. Cell 6 (1995) 697–711.
[70] M. LeDizet, G. Piperno, *ida*4-1, *ida*4-2, and *ida*4-3 are intron splicing mutations affecting the locus encoding p28, a light chain of *Chlamydomonas* axonemal inner dynein arms, Mol. Biol. Cell 6 (1995) 713–723.
[71] R. Yamamoto, M. Hirono, R. Kamiya, Discrete PIH proteins function in the cytoplasmic preassembly of different subsets of axonemal dyneins, J. Cell Biol. 190 (2010) 65–71.
[72] T. Yagi, I. Minoura, A. Fujiwara, R. Saito, T. Yasunaga, M. Hirono, R. Kamiya, An axonemal dynein particularly important for flagellar movement at high viscosity. Implications from a new *Chlamydomonas* mutant deficient in the dynein heavy chain gene DHC9, J. Biol. Chem. 280 (2005) 41412–41420.
[73] L.C. Gardner, E. O'Toole, C.A. Perrone, T. Giddings, M.E. Porter, Components of a "dynein regulatory complex" are located at the junction between the radial spokes and the dynein arms in *Chlamydomonas* flagella, J. Cell Biol. 127 (1994) 1311–1325.
[74] T. Heuser, M. Raytchev, J. Krell, M.E. Porter, D. Nicastro, The dynein regulatory complex is the nexin link and a major regulatory node in cilia and flagella, J. Cell Biol. 187 (2009) 921–933.
[75] S.J. King, W.B. Inwood, E.T. O'Toole, J. Power, S.K. Dutcher, The bop2-1 mutation reveals radial asymmetry in the inner dynein arm region of *Chlamydomonas reinhardtii*, J. Cell Biol. 126 (1994) 1255–1266.
[76] H.J. Hoops, G.B. Witman, Outer doublet heterogeneity reveals structural polarity related to beat direction in *Chlamydomonas* flagella, J. Cell Biol. 97 (1983) 902–908.
[77] E.F. Smith, W.S. Sale, Structural and functional reconstitution of inner dynein arms in *Chlamydomonas* flagellar axonemes, J. Cell Biol. 117 (1992) 573–581.
[78] R. Yamamoto, T. Yagi, R. Kamiya, Functional binding of inner-arm dyneins with demembranated flagella of *Chlamydomonas* mutants, Cell Motil. Cytoskeleton 63 (2006) 258–265.
[79] A. Koutoulis, G.J. Pazour, C.G. Wilkerson, K. Inaba, H. Sheng, S. Takada, G.B. Witman, The *Chlamydomonas reinhardtii ODA*3 gene encodes a protein of the outer dynein arm docking complex, J. Cell Biol. 137 (1997) 1069–1080.
[80] S. Takada, C.G. Wilkerson, K. Wakabayashi, R. Kamiya, G.B. Witman, The outer dynein arm-docking complex: Composition and characterization of a subunit (*oda1*) necessary for outer arm assembly, Mol. Biol. Cell 13 (2002) 1015–1029.
[81] D.M. Casey, K. Inaba, G.J. Pazour, S. Takada, K. Wakabayashi, C.G. Wilkerson, R. Kamiya, G.B. Witman, DC3, the 21-kDa subunit of the outer dynein arm-docking complex (ODA-DC), is a novel EF-hand protein important for assembly of both the outer arm and the ODA-DC, Mol. Biol. Cell 14 (2003) 3650–3663.
[82] M. Wirschell, G. Pazour, A. Yoda, M. Hirono, R. Kamiya, G.B. Witman, Oda5p, a novel axonemal protein required for assembly of the outer dynein arm and an associated adenylate kinase, Mol. Biol. Cell 15 (2004) 2729–2741.
[83] E.F. Smith, W.S. Sale, Microtubule binding and translocation by inner dynein arm subtype I1, Cell Motil. Cytoskeleton 18 (1991) 258–268.

[84] P. Yang, W.S. Sale, The Mr 140,000 intermediate chain of chlamydomonas flagellar inner arm dynein is a WD-repeat protein implicated in dynein arm anchoring, Mol. Biol. Cell 9 (1998) 3335–3349.
[85] T.W. Hendrickson, C.A. Perrone, P. Griffin, K. Wuichet, J. Mueller, P. Yang, M.E. Porter, W.S. Sale, IC138 is a WD-repeat dynein intermediate chain required for light chain assembly and regulation of flagellar bending, Mol. Biol. Cell 12 (2004) 5431–5442.
[86] A. Harrison, P. Olds-Clarke, S.M. King, Identification of the t complex-encoded cytoplasmic dynein light chain tctex1 in inner arm I1 supports the involvement of flagellar dyneins in meiotic drive, J. Cell Biol. 140 (1998) 1137–1147.
[87] L.M. DiBella, S.E. Benashski, H.W. Tedford, A. Harrison, R.S. Patel-King, S.M. King, The Tctex1/Tctex2 class of dynein light chains. Dimerization, differential expression, and interaction with the LC8 protein family, J. Biol. Chem. 276 (2001) 14366–14373.
[88] L.M. DiBella, M. Sakato, R.S. Patel-King, G.J. Pazour, S.M. King, The LC7 light chains of *Chlamydomonas* flagellar dyneins interact with components required for both motor assembly and regulation, Mol. Biol. Cell 15 (10) (2004) 4633–4646.
[89] L.M. DiBella, E.F. Smith, R.S. Patel-King, K. Wakabayashi, S.M. King, A novel Tctex2-related light chain is required for stability of inner dynein arm I1 and motor function in the *Chlamydomonas* flagellum, J. Biol. Chem. 279 (2004) 21666–21676.
[90] C.A. Perrone, S.H. Myster, R. Bower, E.T. O'Toole, M.E. Porter, Insights into the structural organization of the I1 inner arm dynein from a domain analysis of the 1 beta dynein heavy chain, Mol. Biol. Cell 11 (2000) 2297–2313.
[91] C.A. Perrone, P. Yang, E. O'Toole, W.S. Sale, M.E. Porter, The *Chlamydomonas* IDA7 locus encodes a 140-kDa dynein intermediate chain required to assemble the I1 inner arm complex, Mol. Biol. Cell 9 (1998) 3351–3365.
[92] S.H. Myster, J.A. Knott, K.M. Wysocki, E. O'Toole, M.E. Porter, Domains in the 1alpha dynein heavy chain required for inner arm assembly and flagellar motility in, *Chlamydomonas*. J. Cell Biol. 146 (1999) 801–818.
[93] P. Yang, C. Yang, M. Wirschell, S. Davis, Novel LC8 mutations have disparate effects on the assembly and stability of flagellar complexes, J. Biol. Chem. (2009) M109.050666.
[94] L.M. Dibella, O. Gorbatyuk, M. Sakato, K. Wakabayashi, R.S. Patel-King, G.J. Pazour, G.B. Witman, S.M. King, Differential light chain assembly influences outer arm Dynein motor function, Mol. Biol. Cell 16 (2005) 5661–5674.
[95] A.B. Bowman, R.S. Patel-King, S.E. Benashski, J.M. McCaffery, L.S.B. Goldstein, S.M. King, *Drosophila roadblock* and *Chlamydomonas* LC7: A conserved family of dynein-associated proteins involved in axonal transport, flagellar motility, and mitosis, J. Cell Biol. 146 (1999) 165–180.
[96] C.A. Tanner, P. Rompolas, R.S. Patel-King, O. Gorbatyuk, K. Wakabayashi, G.J. Pazour, S.M. King, Three members of the LC8/DYNLL family are required for outer arm dynein motor function, Mol. Biol. Cell 19 (2008) 3724–3734.
[97] E. Barbar, Dynein light chain LC8 is a dimerization hub essential in diverse protein networks, Biochemistry 47 (2008) 503–508.
[98] S.J. Susalka, K.K. Pfister, Cytoplasmic dynein subunit heterogeneity: Implications for axonal transport, J. Neurocytol. 29 (2000) 819–829.
[99] H. Sakakibara, H. Kojima, Y. Sakai, E. Katayama, K. Oiwa, Inner-arm dynein c of *Chlamydomonas* flagella is a single-headed processive motor, Nature 400 (1999) 586–590.
[100] S.A. Burgess, M.L. Walker, H. Sakakibara, P.J. Knight, K. Oiwa, Dynein structure and power stroke, Nature 421 (2003) 715–718.
[101] S.A. Burgess, M.L. Walker, H. Sakakibara, K. Oiwa, P.J. Knight, The structure of dynein-c by negative stain electron microscopy, J. Struct. Biol. 146 (2004) 205–216.
[102] C. DiPetrillo, E. Smith, Calcium regulation of ciliary motility analysis of axonemal calcium-binding proteins, Method. Cell Biol. 92 (2009) 163–180.

[103] D.R. Howard, G. Habermacher, D.B. Glass, E.F. Smith, W.S. Sale, Regulation of *Chlamydomonas* flagellar dynein by an axonemal protein kinase, J. Cell Biol. 127 (1994) 1683–1692.
[104] P. Yang, W.S. Sale, Casein kinase I is anchored on axonemal doublet microtubules and regulates flagellar dynein phosphorylation and activity, J. Biol. Chem. 275 (2000) 18905–18912.
[105] A. Gokhale, M. Wirschell, W.S. Sale, Regulation of dynein-driven microtubule sliding by the axonemal protein kinase CK1 in *Chlamydomonas* flagella, J. Cell Biol. 186 (2009) 817–824.
[106] A.R. Gaillard, D.R. Diener, J.L. Rosenbaum, W.S. Sale, Flagellar radial spoke protein 3 is an A-kinase anchoring protein (AKAP), J. Cell Biol. 153 (2001) 443–448.
[107] A.R. Gaillard, L.A. Fox, J.M. Rhea, B. Craige, W.S. Sale, Disruption of the A-kinase anchoring domain in flagellar radial spoke protein 3 results in unregulated axonemal cAMP-dependent protein kinase activity and abnormal flagellar motility, Mol. Biol. Cell 17 (2006) 2626–2635.
[108] G. Habermacher, W.S. Sale, Regulation of flagellar dynein by an axonemal type-1 phosphatase in *Chlamydomonas*, J. Cell Sci. 109 (Pt. 7) (1996) 1899–1907.
[109] G. Habermacher, W.S. Sale, Regulation of flagellar dynein by phosphorylation of a 138-kD inner arm dynein intermediate chain, J. Cell Biol. 136 (1997) 167–176.
[110] P. Yang, L. Fox, R.J. Colbran, W.S. Sale, Protein phosphatases PP1 and PP2A are located in distinct positions in the *Chlamydomonas* flagellar axoneme, J. Cell Sci. 113 (Pt. 1) (2000) 91–102.
[111] B.H. Gibbons, I.R. Gibbons, Flagellar movement and adenosine triphosphatase activity in sea urchin sperm extracted with triton X-100, J. Cell Biol. 54 (1972) 75–97.
[112] R. Kamiya, G.B. Witman, Submicromolar levels of calcium control the balance of beating between the two flagella in demembranated models of *Chlamydomonas*, J. Cell Biol. 98 (1984) 97–107.
[113] C.J. Brokaw, I.R. Gibbons, Localized activation of bending in proximal, medial and distal regions of sea-urchin sperm flagella, J. Cell Sci. 13 (1973) 1–10.
[114] C.K. Omoto, C.J. Brokaw, Bending patterns of *Chlamydomonas* flagella: II. Calcium effects on reactivated *Chlamydomonas* flagella, Cell Motil. 5 (1985) 53–60.
[115] E. Hasegawa, H. Hayashi, S. Asakura, R. Kamiya, Stimulation of *in vitro* motility of *Chlamydomonas* axonemes by inhibition of cAMP-dependent phosphorylation, Cell Motil. Cytoskeleton 8 (1987) 302–311.
[116] C.G. DiPetrillo, E.F. Smith, Pcdp1 is a central apparatus protein that binds Ca(2+)-calmodulin and regulates ciliary motility, J. Cell Biol. 189 (2010) 601–612.
[117] E.F. Smith, Regulation of flagellar dynein by calcium and a role for an axonemal calmodulin and calmodulin-dependent kinase, Mol. Biol. Cell 13 (2002) 3303–3313.
[118] E.E. Dymek, E.F. Smith, A conserved CaM and radial spoke associated complex mediates regulation of flagellar dynein activity, J. Cell Biol. 179 (2007) 515–526.
[119] M.J. Wargo, E.E. Dymek, E.F. Smith, Calmodulin and PF6 are components of a complex that localizes to the C1 microtubule of the flagellar central apparatus, J. Cell Sci. 118 (2005) 4655–4665.
[120] P. Yang, D.R. Diener, J.L. Rosenbaum, W.S. Sale, Localization of calmodulin and dynein light chain LC8 in flagellar radial spokes, J. Cell Biol. 153 (2001) 1315–1326.
[121] P.V. Bayly, B.L. Lewis, P.S. Kemp, R.B. Pless, S.K. Dutcher, Efficient spatiotemporal analysis of the flagellar waveform of *Chlamydomonas reinhardtii*, Cytoskeleton (Hoboken) 67 (2010) 56–69.
[122] W.S. Sale, L.A. Fox, E.F. Smith, Assays of axonemal dynein-driven motility, Method. Cell Biol 39 (1993) 89–104.
[123] H. Bannai, M. Yoshimura, K. Takahashi, C. Shingyoji, Calcium regulation of microtubule sliding in reactivated sea urchin sperm flagella, J. Cell Sci. 113 (Pt. 5) (2000) 831–839.

[124] S. Kamimura, K. Takahashi, Direct measurement of the force of microtubule sliding in flagella, Nature 293 (1981) 566–568.
[125] C.B. Lindemann, I.R. Gibbons, Adenosine triphosphate-induced motility and sliding of filaments in mammalian sperm extracted with Triton X-100, J. Cell Biol. 65 (1975) 147–162.
[126] Y. Mogami, K. Takahashi, Calcium and microtubule sliding in ciliary axonemes isolated from *Paramecium caudatum*, J. Cell Sci. 61 (1983) 107–121.
[127] T. Okagaki, R. Kamiya, Microtubule sliding in mutant *Chlamydomonas* axonemes devoid of outer or inner dynein arms, J. Cell Biol. 103 (1986) 1895–1902.
[128] K. Summers, ATP-induced sliding of microtubules in bull sperm flagella, J. Cell Biol. 60 (1974) 321–324.
[129] S.L. Tamm, S. Tamm, Alternate patterns of doublet microtubule sliding in ATP-disintegrated macrocilia of the *ctenophore Beroe*, J. Cell Biol. 99 (1984) 1364–1371.
[130] G.B. Witman, J. Plummer, G. Sander, *Chlamydomonas* flagellar mutants lacking radial spokes and central tubules. Structure, composition, and function of specific axonemal components, J. Cell Biol. 76 (1978) 729–747.
[131] E. Kurimoto, R. Kamiya, Microtubule sliding in flagellar axonemes of *Chlamydomonas* mutants missing inner- or outer-arm dynein: Velocity measurements on new types of mutants by an improved method, Cell Motil. Cytoskeleton 19 (1991) 275–281.
[132] E.F. Smith, P. Yang, The radial spokes and central apparatus: Mechano-chemical transducers that regulate flagellar motility, Cell Motil. Cytoskeleton 57 (2004) 8–17.
[133] B. Huang, Z. Ramanis, D.J. Luck, Suppressor mutations in *Chlamydomonas* reveal a regulatory mechanism for flagellar function, Cell 28 (1982) 115–124.
[134] G. Piperno, K. Mead, W. Shestak, The inner dynein arms I2 interact with a "dynein regulatory complex" in *Chlamydomonas* flagella, J. Cell Biol. 118 (1992) 1455–1463.
[135] G. Rupp, E. O'Toole, L.C. Gardner, B.F. Mitchell, M.E. Porter, The sup-pf-2 mutations of *Chlamydomonas* alter the activity of the outer dynein arms by modification of the gamma-dynein heavy chain, J. Cell Biol. 135 (1996) 1853–1865.
[136] G. Rupp, M.E. Porter, A subunit of the dynein regulatory complex in *Chlamydomonas* is a homologue of a growth arrest-specific gene product, J. Cell Biol. 162 (2003) 47–57.
[137] E.F. Smith, W.S. Sale, Regulation of dynein-driven microtubule sliding by the radial spokes in flagella, Science 257 (1992) 1557–1559.
[138] S.J. King, S.K. Dutcher, Phosphoregulation of an inner dynein arm complex in *Chlamydomonas reinhardtii* is altered in phototactic mutant strains, J. Cell Biol. 136 (1997) 177–191.
[139] G. Habermacher, W.S. Sale, Regulation of dynein-driven microtubule sliding by an axonemal kinase and phosphatase in *Chlamydomonas* flagella, Cell Motil. Cytoskeleton 32 (1995) 106–109.
[140] O. Kagami, R. Kamiya, Translocation and rotation of microtubules caused by multiple species of *Chlamydomonas* inner-arm dynein, J. Cell Sci. 103 (1992) 653–664.
[141] G. Piperno, Regulation of dynein activity within *Chlamydomonas* flagella, Cell Motil. Cytoskel 32 (1995) 103–105.
[142] S.H. Myster, J.A. Knott, E. O'Toole, M.E. Porter, The *Chlamydomonas* Dhc1 gene encodes a dynein heavy chain subunit required for assembly of the I1 inner arm complex, Mol. Biol. Cell 8 (1997) 607–620.
[143] K. Kikushima, R. Kamiya, Clockwise translocation of microtubules by flagellar inner-arm dyneins *in vitro*, Biophys. J 94 (2008) 4014–4019.
[144] M. LeDizet, G. Piperno, *ida4-1, ida4-2*, and *ida4-3* are intron splicing mutations affecting the locus encoding p28, a light chain of *Chlamydomonas* axonemal inner dynein arms, Mol. Biol. Cell 6 (1995) 713–723.
[145] T. Kato-Minoura, M. Hirono, R. Kamiya, *Chlamydomonas* inner-arm dynein mutant, ida5, has a mutation in an actin-encoding gene, J. Cell Biol. 137 (1997) 649–656.

[146] T. Kato, O. Kagami, T. Yagi, R. Kamiya, Isolation of two species of *Chlamydomonas reinhardtii* flagellar mutants, *ida5* and *ida6*, that lack a newly identified heavy chain of the inner dynein arm, Cell Struct. Funct 18 (1993) 371–377.
[147] H.A. Yanagisawa, R. Kamiya, A tektin homologue is decreased in *Chlamydomonas* mutants lacking an axonemal inner-arm dynein, Mol. Biol. Cell 15 (2004) 2105–2115.
[148] G. Piperno, K. Mead, M. LeDizet, A. Moscatelli, Mutations in the 'dynein regulatory complex' alter the ATP-insensitive binding sites for inner arm dyneins in *Chlamydomonas* axonemes, J. Cell Biol. 125 (1994) 1109–1117.
[149] B. Huang, G. Piperno, D.J. Luck, Paralyzed flagella mutants of *Chlamydomonas reinhardtii* defective for axonemal doublet microtubule arms, J. Biol. Chem. 254 (1979) 3091–3099.

In this chapter

12

Flagellar Motility and the Dynein Regulatory Complex

Mary E. Porter
Department of Genetics, Cell Biology, and Development, University of Minnesota, Minneapolis, MN, USA

12.1 Introduction

Eucaryotic cilia and flagella are highly conserved, microtubule-based structures that play fundamental roles in sensory transduction and cell motility. Defects in the assembly or motility of these structures can have disastrous consequences for an organism. In humans, defects in ciliary motility result in defects in the development of the left–right body axis, hydrocephalus, chronic respiratory disease, and male sterility (see [1] and Chapter 24).

Most motile cilia and flagella are constructed using a 9+2 arrangement of nine outer-doublet microtubules arranged in a ring around a pair of single microtubules (the central pair) to form the axoneme. Each outer doublet contains a series of accessory structures that repeat every 96 nm along the length of the axoneme. Most prominent are the inner and outer dynein arms, the molecular motors that drive microtubule sliding in the axoneme [2,3]. Each outer doublet is also connected to its neighbor by a second set of linkers, the nexin links, which are thought to limit dynein-driven sliding during the flagellar beat. The outer doublets are connected to the central-pair microtubules by radial spokes that attach to the outer doublets in close proximity to the inner dynein arms. The radial spoke heads make contact with a sheath of asymmetrically arranged projections on the central-pair microtubules.

The outer- and inner-arm dyneins are attached to the A-tubules of the outer doublets by specific, ATP-insensitive binding sites. The motor domains of the dynein arms walk along the B-tubule of the neighboring doublet in an ATP-sensitive fashion and thereby generate sliding forces between the doublets. Because the outer doublets are firmly attached to basal bodies at their base and crosslinked by nexin along their length, microtubule sliding is limited and ultimately converted to axonemal bending [4]. Both the outer- and inner-arm dyneins are "minus"-end-directed motors and push the adjacent doublets towards the

Dyneins DOI: 10.1016/B978-0-12-382004-4.10012-3
Copyright © 2012 by Elsevier Inc. All rights reserved

flagellar tip during axonemal bending [5,6]. Dyneins on one side of the axoneme induce bending in one direction, whereas dyneins on the opposite of the axoneme induce bending in the opposite direction [4]. Therefore, to generate complex waveforms, dynein activity must be "switched" on and off from one side of the axoneme to the other [7]. Moreover, there must be additional mechanisms for modifying dynein activity to alter waveforms in response to intracellular and extracellular signals. Finally, all of these mechanisms must be built into the structure of the axoneme, given the ability to "reactivate" motility with the isolated organelle.

Currently there are three very different views of how dynein activity might be switched during the flagellar beat cycle. One view is that the fundamental mechanics of the dynein cross-cycle coupled with the linear arrangement of dynein motors along the length of the outer doublet results in their sequential activation and termination during microtubule sliding (the "sliding control" model). Several versions of this model have been computer-simulated with increasing sophistication over the years (reviewed in [8–11]). Another view is that the structure of the axoneme during flagellar bending alters the activity of dynein cross-bridges by changes in doublet curvature or doublet spacing (the "curvature control" and "geometric clutch" models). Changes in curvature or spacing increase or decrease the probability that a dynein arm can cross-bridge with the neighboring doublet (reviewed in [9,10,12,13]). If the doublets are close enough, cross-bridges will form and the doublets will begin to slide and bend; however, at a critical point, sufficient stress or tension (transverse tension or t-force) will develop to override the adhesiveness of the cross-bridges and inactivate the dyneins [12,13]. These models are influenced by factors that affect the affinity of the dynein cross-bridges (e.g. nucleotide concentrations) or the behavior of the nexin linkages. Both models have significant theoretical and experimental support, and both have been the subjects of recent reviews [9–11,14–16].

The third view is that dynein activity is modulated by a series of mechanical and enzymatic interactions that begin with the central-pair microtubules and their projections. The central pair projections make contact with the radial-spoke heads in an asymmetric fashion in response to axonemal bending. Differences in strain or tension are transduced through the radial-spoke stalks and a dynein regulatory complex (DRC) to different subsets of inner dynein arms to activate or inhibit their activity. This model cannot apply to many of the motile 9+0 cilia and flagella seen in nature, but it is based on a large body of work, primarily with *Chlamydomonas* flagellar mutants, demonstrating that the central-pair and radial-spoke complex regulates the velocity of dynein-driven sliding in the axoneme (reviewed in [17–19]; Chapter 11). However, very little is known about the nature of the DRC and how it might function as an intermediate in this pathway.

In this chapter, we begin with a brief review of the work on the central-pair microtubules and radial spokes, which are required for flagellar motility in

Chlamydomonas under physiological conditions [20]. We then focus on the identification and characterization of two groups of extragenic suppressor mutations that can restore motility to paralyzed central pair/radial spoke defective mutants [21–24]. The first group of suppressor mutations has demonstrated that specific changes in both the outer and inner dynein arms can override defects in the central-pair/radial-spoke complex to restore motility [25–28]. Characterization of the second group of suppressors, the *drc* mutants, has revealed that the DRC serves both as an adaptor for the binding of specific inner-arm dynein isoforms and as part of the nexin link that resists microtubule sliding [23,24, 28–31]. We will also review recent efforts to identify nexin–DRC subunits and localize them within the substructure of the DRC. Finally, we will revisit the proposed functions of the DRC and nexin links and discuss possible future directions for research.

12.2 The Central Pair, Radial Spokes, and Dynein Regulatory Complex

The central pair/radial spoke model for the regulation of flagellar motility is that mechanical interactions between the central pair and radial spokes are converted into a biochemical signaling pathway that ultimately alters the phosphorylation state of the dynein arms within the 96 nm repeat (reviewed in [17–18] and Chapter 11). Mutations that block assembly of the central-pair microtubules result in complete flagellar paralysis in *Chlamydomonas* [20,32] and lead to chronic respiratory disease, male infertility, and hydrocephaly in vertebrates [33,34–37]. The two microtubules, C1 and C2, differ with respect to the structure and composition of their associated projections [35,36,38–44]. The asymmetry of the projections is critical for the activation of dyneins on specific outer-doublet microtubules [45,46], and defects in the assembly of individual projection domains can alter waveform or beat frequency or lead to arrest at switch points [35,38,40]. Each projection domain is a multi-subunit complex composed of large scaffolding proteins and additional subunits associated with calcium signaling, energy metabolism, and/or novel kinesin isoforms [35,41,43,47,48].

The passive rotation of the central-pair complex and its projections during the flagellar beat cycle results in periodic interactions with the radial spoke heads [45,49–52]. These interactions are thought to induce mechanical strain in the radial spoke stalk, which results in local control of dynein activity within the 96 nm axoneme repeat. How changes in tension or strain in the radial spoke are translated into transient activation of dynein-arm activity is not well understood. However, several studies have identified multiple signaling molecules as structural components of the radial spokes, including a novel A-kinase anchoring protein (AKAP), calmodulin, a GAF-domain protein, a Ca^{2+}-stimulated nucleoside

diphosphate kinase (NDK), and several other subunits with diverse calcium-binding and protein-interaction domains [53–57]. Moreover, pharmacological studies have provided indirect evidence that the radial spokes modulate the activity of kinases (PKA, CKI) and phosphatases (PP2A) associated with the outer-doublet microtubules (reviewed in [17,18] and Chapter 11). Microtubule-sliding velocities are reduced in axonemes from paralyzed flagellar mutants, but sliding velocities can be increased by treatment with protein kinase inhibitors ([58–61] and Chapter 11). The precise location of these axonemal enzymes on the outer doublets is unknown, but it is presumed that they must be anchored in proximity to the dynein arms (Fig. 12.1). The critical target substrates within the dynein arms are largely unknown, with the exception of an I1-dynein intermediate chain (IC) known as IC138 [60,62–66].

Additional support for the model of the central-pair/radial-spoke complex as an activator of dynein arm activity has come from the characterization of extragenic suppressor mutations. The extragenic suppressors were isolated by mutagenesis of paralyzed central-pair and radial-spoke mutant strains and then screening for cells that had recovered sufficient motility to accumulate in the upper portion of liquid cultures [21]. Several of the suppressors were second-site mutations in

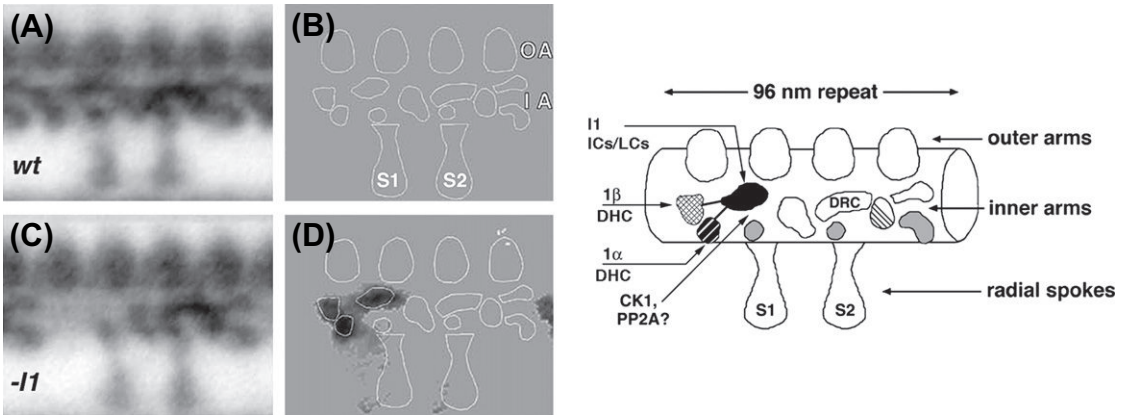

Figure 12.1 Views of the 96 nm repeat obtained by two-dimensional averaging of fixed axonemes. Isolated wild-type and I1 mutant (*pf9-2*) axonemes were fixed and processed for thin sectioning. Longitudinal sections containing clear views of the 96 nm repeat with outer arms, inner arms, and radial spokes were imaged, digitized, aligned, and averaged. (A) An average of the wild-type repeat with the outer arms on the top, two radial spokes on the bottom, and a series of densities in the inner-arm region. (B) A diagram showing an outline of the major densities seen in the wild-type repeat. (C) An average of the 96 nm repeat from a mutant (*pf9*) that lacks the I1 dynein. Note the missing density on the left, proximal to the first radial spoke. (D) A difference plot comparing the wild-type and I1 mutant axonemes. The only statistically significant difference is the tri-lobed structure corresponding to the I1 dynein. (E) A diagram of the 96 nm repeat summarizing the location of the three major domains of the I1 dynein (the 1-α dynein HC motor domain, the 1-β dynein HC domain, and the IC–LC domain); the three single-headed, inner-arm dyneins missing in *ida4* (the three grey shaded densities); and the crescent-shaped domain above radial spoke 2 corresponding to the DRC. *(A–D) modified from [28]. (E) modified from [17].*

Table 12.1 Dynein Heavy Chain Suppressor Mutations

Mutants	Locus Name	Gene Product	Motility Phenotype	Dynein Defect	References
sup-pf-1	*ODA4*	β dynein HC	WT waveform, reduced beat frequency	Outer arms present; altered β dynein HC	[21,25,27,67]
sup-pf-2	*ODA2*	γ dynein HC	WT waveform, reduced beat frequency	Outer arms present; altered γ dynein HC	[21,26,27,68]
pf9-2	*IDA1 (PF9)*	1-α dynein HC	altered waveform, slow swimming	I1 dynein (*f*) missing	[22,78,84]

other genes that rescued some form of motility without restoring the missing central-pair or radial-spoke structures. The bypass suppressor mutations revealed the presence of a control system that globally inhibits dynein activity when the central pair and/or radial spokes are missing. The model suggested that, when this control system is mutated, inhibition is removed and at least some of the dynein arms become more active [21,67,68]. When the double mutant strains were backcrossed to remove the original central-pair or radial-spoke mutation, many of the suppressor mutants also displayed motility defects of their own [21,67,68].

Initial studies indicated that the extragenic suppressors could be sorted into at least two classes: mutations that affect certain dynein heavy chains (HCs) (*sup-pf-1*, *sup-pf-2*, and *pf9-2*) and mutations that affect the assembly of a group of tightly bound axonemal polypeptides but whose location within the axoneme was unknown (*pf2*, *pf3*, *sup-pf-3*, *sup-pf-4*, and *sup-pf-5*) [21–23]. These mutants are listed in Tables 12.1 and 12.2 and will be discussed in turn.

12.3 The Dynein Heavy Chain Suppressors

The *sup-pf-1* and *sup-pf-2* mutations reside in the genes that encode the β and γ dynein HCs of the outer arm [21,25,26] (see Table 12.1). Although several suppressor alleles have been isolated in each locus [25–27], the sequence defects have only been identified in two *sup-pf-1* alleles. Both are in-frame deletions within the coiled-coil domains of the microtubule-binding stalk of the β dynein HC [25]. Measurements of flagellar beat frequency indicated that the *sup-pf-1* mutations reduce the activity of the outer dynein arms *in situ* without affecting outer dynein arm assembly [25,27,67,69]. In contrast, mutations in the β dynein HC gene that block assembly of the outer arm (*oda4*) or only the β motor domain (*oda4-s7*) fail to suppress flagellar paralysis in radial-spoke or central-pair mutants [25,69]. These observations suggested that specific changes in the β dynein HC cross-bridge cycle are required for suppression, and that reductions in outer-arm

Table 12.2 Polypeptide Deficiencies Observed in *drc* Mutants

Polypeptide Defects[2]		Strain				
Subunit	**Size**	**Wild-type**	***sup-pf-4***	***sup-pf-3***	***pf2***	***pf3***
DRC1	**83 kD**	+	+	+	+	–
DRC2	**70 kD**	+	+	+	+	–
DRC3	**62 kD**	+	+	+/–	–	+/–
DRC4	**55 kD**	+	+	+/–	–	+
DRC5	**40 kD**	+	–	–	–	–
DRC6	**29 kD**	+	–	–	–	–
DRC7[1]	**192 kD**	+	+	+/–	–	+/–
I2/I3 dynein HCs[3]		+++	+++	++	++	+
Dynein "e" [4]		+	+	+/–	+/–	–
Dynein "b" [4]		+	+	+	+/–	+
Actin[3]		+++	+++	+++	++	++
Centrin[3]		++	++	++	+	+
p28[3]		+++	+++	++	++	+
Other polypeptides						
RSP13[5]		+	+	+	+	–
Tektin[6]		+++	+++	+++	+++	+

[1] *Quantitative data on DRC7 is limited.*
[2] *[24].*
[3] *[23].*
[4] *[29].*
[5] *[139].*
[6] *[98].*
+, component present; +/–, component reduced; –, component lacking.

activity might facilitate coordination with the activities of the multiple inner-arm dyneins in the central pair/radial spoke mutants [25,70].

The *sup-pf-2* mutants display more diverse phenotypes with respect to outer-arm assembly, but in general ~50% or more of the outer-arm structures and associated polypeptides remain [26,27]. Interestingly, the *sup-pf-2-1* assembly defects were seen more frequently on outer doublets 3 and 6–9 [26]. This bias in assembly may be related to the asymmetric beat pattern of *Chlamydomonas* flagella and the distortion experienced by specific outer doublets [71]. However, even when all outer arms are present, flagellar beat frequencies are reduced in *sup-pf-2* mutants [26,27,68]. The mutant lesions have not been identified, but complementation tests demonstrated that the *sup-pf-2* mutations reside in the gene encoding the γ dynein HC (*ODA2*/*PF28*) [26,27]. However, mutations in the γ dynein HC gene that prevent assembly of the outer dynein arms (*oda2*) or the γ motor domain (*oda2-t*) fail to suppress paralysis [26,71], similarly to the phenotypes described above for the β dynein HC.

The requirement for the presence of modified β or γ dynein HCs suggests that the outer arms must be assembled, but their activity must be altered in some very specific way to restore motility. One hypothesis is that the mutated dynein HCs do not receive the inhibitory signals associated with the loss of the radial spokes [26,27]. Consistent with this hypothesis, measurements of microtubule sliding with axonemes from radial-spoke mutants and suppressed strains demonstrated that sliding velocities are increased in the double mutants ([26,58]; G. Habermacher, G. Rupp, W. Sale, and M. E. Porter, unpublished results). These observations suggested that inhibition of the inner dynein arms by defects in the central pair or radial spokes results in the failure to coordinate multiple motors moving at different intrinsic velocities [70]. However, compensatory changes in the activity of the outer arm might permit coordination between the two sets of motors that results in at least some motility in the absence of signals from the radial spokes. This hypothesis has gained additional support from a series of elegant experiments in which paralyzed central-pair or radial-spoke mutants can be induced to beat by manipulation of nucleotide concentrations, solvent conditions, or mechanical stimulation, but only if the outer arms are present [70,72–75]. Thus, there are two different systems within the axoneme – the inner arms, which are subject to regulation by the central pair and radial spokes, and the outer arms, which can be regulated by mechanical input – whose activities must be coordinated [70]. The proposed coordination between the different dynein motors suggested the presence of physical linkages between the outer- and inner-arm dyneins that might couple their activity. Recent descriptions of axoneme structure by cryo-electron tomography (cryo-ET) have provided new evidence that such linkages do exist [31,76,77]. More studies are needed to identify the specific polypeptides that form these linkages and to determine how they might coordinate dynein-arm activity.

The first evidence to suggest that the I1 dynein might be a specific target of the central pair/radial spoke pathway was the isolation of an extragenic suppressor (*pf9-2*) of the temperature-sensitive central-pair mutant *pf16R3* [22]. A defect in the assembly of the I1 inner-arm dynein could partially suppress the paralysis phenotype at the restrictive temperature (see Table 12.1 and Fig. 12.1). Mutations in the I1 dynein are also associated with defects in the flagellar waveform and phototaxis [63,78]. Pharmacological and reconstitution studies of microtubule sliding in isolated axonemes further implicated the I1 dynein, and more specifically IC138, as a target for regulation by the central pair/radial spoke pathway and phototaxis pathways ([62–65,79] and Chapter 11). The localization of an IC138 sub-complex (IC138, IC97, LC7b, and FAP120) at the base of the I1 dynein, between the first radial spoke and the outer dynein arms, provided additional evidence for the presence of regulatory components that could potentially coordinate activities between the inner and outer dynein arms [65,80]. Whether the IC138 sub-complex forms part of the first outer-inner

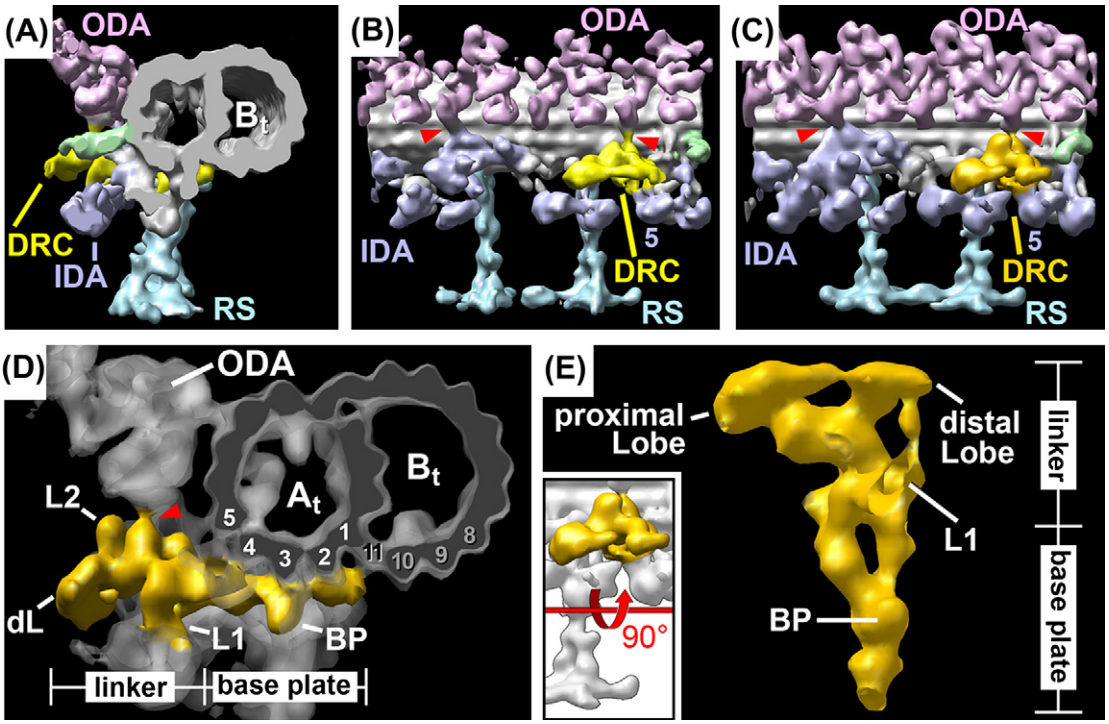

Figure 12.2 Three-dimensional views of the 96 nm repeat and the wild-type DRC by cryo-ET. Isolated axonemes from a wild-type strain (WT) or a rescued *pf2* mutant with a wild-type phenotype (pWT) were rapidly frozen and imaged directly by cryo-ET. Tilt series images of intact axonemes were collected, aligned, and averaged in three dimensions. The results are shown here as three-dimensional isosurface renderings of the outer doublet in cross-sectional view as seen from the distal end of the 96 nm repeat (A,D) or in longitudinal view from the perspective of the neighboring B-tubule (B,C). In longitudinal view, the DRC appears as a yellow (B) or gold (C) crescent-shaped structure at the distal end of the 96 nm repeat, above radial spoke 2. This view is similar to the DRC structure seen by two-dimensional averaging in Figure 12.1E. The two radial spokes are shown in light blue. The outer dynein arms (four per repeat) are shown in violet and the inner dynein arms are shown in darker blue. There are two connections between the outer and the inner dynein arms (OID1 and OID2) that are marked by two red arrowheads. The first (OID1) links the I1 dynein to the outer dynein arms and the second (OID2) links the DRC to the outer dynein arms. In (D) the DRC is viewed in gold and the rest of the outer doublet is shown in grey. Two major domains can be seen in cross-section: a base-plate that reaches from the B11 structure of the B-tubule and wraps around the underside of the A-tubule to protofilament A4, and a linker that reaches from the A-tubule into the interdoublet space to make contact with the neighboring B-tubule. In (E), the DRC is shown alone as viewed from its underside. The crescent-shaped linker can be resolved into several subdomains, including the proximal and distal lobes that contact the neighboring B-tubule. *Modified from [31].*

dynein (OID1) linker seen by cryo-ET [76] remains to be determined (Fig. 12.2). Cryo-ET of other mutants that affect the assembly of different I1 subunits would also be informative [65,80–83].

The *pf9*/*ida1*/*pf30* mutations fall within the *DHC1* gene that encodes the 1-α dynein HC of the I1 dynein [84,85]. Transformation with *DHC1* constructs

encoding N-terminal HC fragments that lack the 1-α motor domain results in the reassembly of the 1-α tail domain, the full-length 1-β dynein HC, and all of the I1 IC and LC subunits [85,86]. Mutations in the *DHC10* gene encoding the 1-β dynein HC also disrupt I1 assembly, and transformation with 1-β dynein HC fragments will likewise rescue assembly of the other I1-dynein subunits [86,87]. Interestingly, strains containing a single-headed I1 dynein with a 1-β motor domain are almost fully functional with respect to both the recovery of flagellar motility and the regulation of microtubule sliding by the radial spoke phosphorylation pathway [85,86]. However, strains containing a single-headed I1 dynein with only the 1-α motor domain are significantly slower with respect to both their microtubule-sliding velocities and forward-swimming velocities [86,87]. These and other observations suggest that, even within the I1 dynein, the activities of the two motor domains are distinct and that one function of the 1-α dynein HC may be to limit microtubule sliding by the 1-β dynein HC [86,87]. Moreover, *in vitro* microtubule-gliding assays further suggest that the addition of I1 dynein can decrease the activity of the faster, single-headed inner-arm dynein *c* [88]. Thus, under certain conditions, the I1 dyneins may actually resist microtubule sliding ([86,88] and Chapter 11). Further work is needed to understand the detailed physical interactions between the two I1 dynein HCs and the IC138 regulatory sub-complex, and how these interactions may be modulated by phosphorylation and/or interactions with the radial spokes or other dynein isoforms.

12.4 The Dynein Regulatory Complex and the Inner Dynein Arms

The second class of bypass suppressors that restore motility to radial-spoke and central-pair mutant strains are characterized by defects in the assembly of a group of tightly bound axonemal polypeptides commonly referred to as the dynein regulatory complex (DRC) [21,23,24]. The DRC is a complex of at least seven proteins ranging in size from ~29 to ~190 kD and missing to varying degrees in the different mutants (Table 12.2). Initial studies noted that the missing DRC polypeptides were distinct from those associated with structures such as the dynein arms, central-pair microtubules, and radial spokes [21]. However, subsequent analysis of motility phenotypes showed that some of the DRC mutants (*pf2, pf3*) displayed defects in their flagellar waveforms similar to those observed with inner-arm mutant strains [78]. These observations prompted several groups to analyze the assembly of inner-arm subunits in both inner-arm mutants and *drc* mutants using improved biochemical and structural approaches. The assembly and organization of the inner-arm dyneins are covered in depth in Chapters 7, 8, 9, and 11, and so we will only review major points relevant to the DRC here.

The isolation of motility mutants lacking specific subsets of inner-arm dyneins [22,89,90] combined with improvements in the resolution and purification of dynein subspecies by FPLC identified at least eight different dynein HCs organized with various ICs and LCs into seven distinct inner-arm subspecies [89,91,92]. The two-headed I1 dynein or dynein *f* contains the two dynein HCs mentioned above (1-α and 1-β), three ICs, and several LCs (reviewed in [92] and Chapters 7 and 11). Analysis of I1 mutants by thin-section electron microscopy and computer image averaging demonstrated that the I1 dynein is a tri-lobed structure located at the proximal end of the 96 nm repeat (Fig. 12.1) but present all along the length of the outer doublets [28,89]. The positions of the two motor domains and the IC138 regulatory sub-complex within the I1 dynein were revealed by analysis of mutants lacking these domains [65,85,87]. Cryo-ET has confirmed this overall organization and revealed additional substructure within the I1 dynein, including the proximal linker to the outer dynein arms (OID1) ([76,77] and see Fig. 12.2). Interestingly, the assembly of I1 dynein is largely unaffected in the *drc* mutants [28,29], although there is some evidence for an additional linker between the base of I1 and the DRC [31].

The six major single-headed dynein subspecies (*a*, *b*, *c*, *d*, *e*, and *g*) are each associated with an actin subunit but can be separated into two groups based on their association with one of two LC subunits, p28 or centrin. Quantitative densitometry of both dynein HC and LC subunits demonstrated significant deficiencies in the assembly of single-headed dyneins in the *drc* mutants [23,24] (see Table 12.2). The defects are most severe in *pf3* and *sup-pf-5*, but also seen to a lesser degree in *pf2* and *sup-pf-3*. These observations lead to the proposal that the DRC serves as an adaptor for the assembly of a subset of inner-arm dyneins [23,24,28].

Computer averaging of electron microscopy images identified the inner-arm subspecies most closely associated with the DRC (Fig. 12.1) but also demonstrated the presence of other structures within the 96 nm repeat [28,29]. Mutations in the *IDA4* gene encoding p28 disrupt the assembly of inner-arm subspecies *a*, *c*, and *d* [91,93,94]. These three dyneins do not co-assemble *in situ* but are instead correlated with the assembly of single-headed dyneins (I2, I4, and I6) at three distinct sites within the 96 nm repeat, one at the base of each radial spoke (radial spoke 1 and radial spoke 2) and a third at the distal end of the repeat [29,76,77]. Only subspecies *c*, located near radial spoke 2, is missing in the *DHC9* mutant *ida9* [95]. More recent work has identified two minor dynein HC subspecies (DHC3 and DHC4) that are also associated with p28 and missing in *ida4*, but these minor dyneins are restricted to the proximal region of the axoneme [96]. Image averaging of *pf2* and *pf3* axonemes has demonstrated that there are deficiencies in the assembly of p28-associated dyneins in the *drc* mutants, particularly in the region around radial spoke 2 [29,31,77].

The fourth single-headed inner-arm dynein (subspecies *e*) identified within the 96 nm repeat is a centrin-associated dynein (IA5) that is directly associated with

the DRC [29,31]. Assembly of subspecies *e* is disrupted in the inner-arm mutant *ida6* and the *drc* mutant *pf3* [29,97]. Interestingly, *ida6* and *pf3* are also associated with defects in the assembly of tektin [98], which is thought to be a major component of the *pf* ribbon in most species [99]. Collectively these observations suggested that *ida6* might be a previously unrecognized *drc* mutant. More recent work has confirmed that *ida6* is associated with both biochemical and structural defects in the DRC (D. Tritschler, R. Bower, E. O'Toole, and M. E. Porter, unpublished results).

12.5 The Dynein Regulatory Complex and Nexin Link

Although several *drc* mutants are associated with significant deficiencies in the assembly of inner-arm dyneins, the most striking defect observed by image averaging of thin sections is the loss of a crescent-shaped structure at the base of radial spoke 2, in between the inner and outer dynein arms (Fig. 12.1) [28–30]. This structure is missing in all of the *drc* mutants, with the exception of *sup-pf-4* (Table 12.3). The crescent was predicted to be the DRC as it is ideally positioned to mediate signals, either mechanical, chemical, or both, between the radial spoke and the inner and outer dynein arms [28,29]. However, these early studies also recognized that the DRC is located in close proximity to the site where the nexin link is thought to attach to the A-tubule [28,100–102]). Both Mastronarde et al. [28] and Woolley [100] speculated that the DRC might be part of the nexin link, but the complexity of structures in thin-sectioned material did not permit a definitive conclusion. However, recent three-dimensional images of the axoneme by cryo-ET have provided a clearer view of the structures in the 96 nm repeat [31,76,77].

The nexin links were identified in early electron microscopy studies as flexible filaments that interconnect the A-tubule of one doublet to the B-tubule of the neighboring outer doublet. They were first described in isolated *Tetrahymena* axonemes from which the dynein arms, radial spokes, and central pair structures had been removed by prolonged dialysis at low ionic strength [2,3,103,104]. They were then visualized in intact cilia following nine-fold rotation of axoneme cross-sections to enhance structural periodicities [103] and given the name "nexin" [105]. The nexin links are thought to be responsible for maintaining the cylindrical structure of the nine outer doublets within the axoneme, even after chemical extraction of most of the tubulin to produce a ciliary remnant [106,107]. The nexin link is also thought to be intimately associated with components of the stable protofilament ribbon, including tektin [99,107,108]. These observations have lead to the expectation that mutations in nexin components would likely disrupt the organization of the outer doublet microtubules.

Table 12.3 Summary of Structural Components Present or Absent in *drc* Mutants

Structural Component (kDa)	Strain				
	WT	***sup-pf-4***	***sup-pf-3***	***pf2***	***pf3***
DRC LINKER (1000–1200)					
Connection to neighboring B-tubule					
Proximal lobe (~350)	+	+	–	–	–
Distal lobe (~120)	+	–	–	–	–
Linker projections					
L1 (50–80)	+	+	+/–	–	+/–
L2	+	–	–	–	–
OID linker 2	+	+	+/–	–	+/–
Central linker region					
Central linker	+	+	+/–	–	+/–
Docking subunit (~60)	+	+	+	+	+
DRC BASE-PLATE (300–350)					
B11–A3 section	+	+	+	+	–
Connection to B11	+	+	+	+	–
B-tubule hole	+	+	+	+	–
INNER DYNEIN ARMS					
IA 4	+	+	–/+	–/+	–
IA 5	+	+	+	–/+	(–)

+, component present; +/–, component reduced; (–), component almost completely reduced; –, component lacking. Modified from [31].

When viewed in longitudinal section, the nexin links repeat every 96 nm and are often inclined at an angle between neighboring doublets [20,102,109,110]. Analysis of isolated axonemes by negative staining or other conditions that cause the outer doublets to splay apart has suggested that the nexin links are highly elastic and can stretch nearly ten times their original length without breaking [106,109,111]. However, other studies of actively bending axonemes have indicated that nexin links do not stretch under normal conditions but may instead undergo cycles of lateral displacement [100,101,110,112].

The suggestion that the nexin links are the primary component that provides resistance to dynein-driven sliding is based on observations of flagellar axonemes during protease treatment [20,113,114]. Protease digestion disrupts both the radial spokes and the nexin links with approximately the same time course as it sensitizes the axonemes to ATP-induced disintegration [113,114]. However, ATP-induced sliding disintegration can also be induced in *pf14* axonemes lacking radial spokes, but only if they are first treated with protease [20]. These observations suggested that the nexin links alone are sufficient to limit outer-doublet sliding [20].

Cryo-ET of wild-type axonemes indicated that one end of the nexin linkage is anchored to the A-tubule close to the base of radial spoke 2 and the proposed

location of the DRC [76]. The nexin link then zigzags to form a bifurcated attachment to the neighboring B-tubule. The crescent-shaped density of the DRC extends several nanometers away from the surface of the A-tubule but also makes contact with the outer dynein arms by a second OID linker [76]. These images suggested that there is considerable overlap between the DRC and the nexin link, which is consistent with previous speculation [28,30,100].

Cryo-ET of *drc* mutant axonemes has finally resolved the relationship between these two structures: the DRC is the nexin link [31]. By comparing averaged tomograms of the two most severely defective drc mutants, *pf2* and *pf3*, with those of wild-type and a rescued strain (Table 12.3), Heuser et al. [31] found that the DRC is significantly more complex and extended (~50 nm) than previously realized (Fig. 12.2). The DRC contains two major domains, the base-plate and the linker. The base-plate is attached to the underside of the A-tubule and extends from the junction between the A-tubule and B-tubule to protofilament A4 of the A-tubule (using the protofilament numbering scheme described in [115]). The base-plate is ~300–350 kD in size and it is completely missing in *pf3* (Fig. 12.3).

The DRC linker begins at protofilament A4 of the A-tubule and projects into the interdoublet space towards the neighboring B-tubule (Fig. 12.2). Its total mass is ~1–1.2 MD and it contains several subdomains or protrusions (Table 12.3). One of these protrusions is the OID2 linker that connects the DRC to the outer dynein arms [76]. The second protrusion is a linker that connects the DRC to inner-arm dynein IA5. As the DRC linker approaches the neighboring outer doublet, it branches into two distinct lobes, both of which make contact with protofilament B8 of the B-tubule. Nearly all of the DRC linker is missing in *pf2* axonemes, and a large portion is also missing in *pf3*. As the DRC is the only structure that connects the outer doublets besides the dynein arms, the most reasonable conclusion was that the DRC must be the same structure as the nexin link [31].

The most recent images of the wild-type and mutant axonemes show a significant increase in the resolution of axoneme sub-structures (~3.2 nm versus ~4.3 nm) [31,76,116]. These advances have made it possible to identify multiple connections between the DRC–nexin link and other structures within the axoneme. These include connections between the base-plate and the B11 density at the A-tubule–B-tubule junction, between the base-plate and radial spoke 2, and between the base-plate and the tail domain of IA4 [31]. The images also confirm the defects in the assembly of inner-arm subspecies seen in earlier studies [23,24,29,77].

12.6 Localization of Dynein Regulatory Complex Subunits Within the Nexin Link

Analysis of the biochemical and structural defects observed in the different *drc* mutants has provided a preliminary model for the localization of subunits within

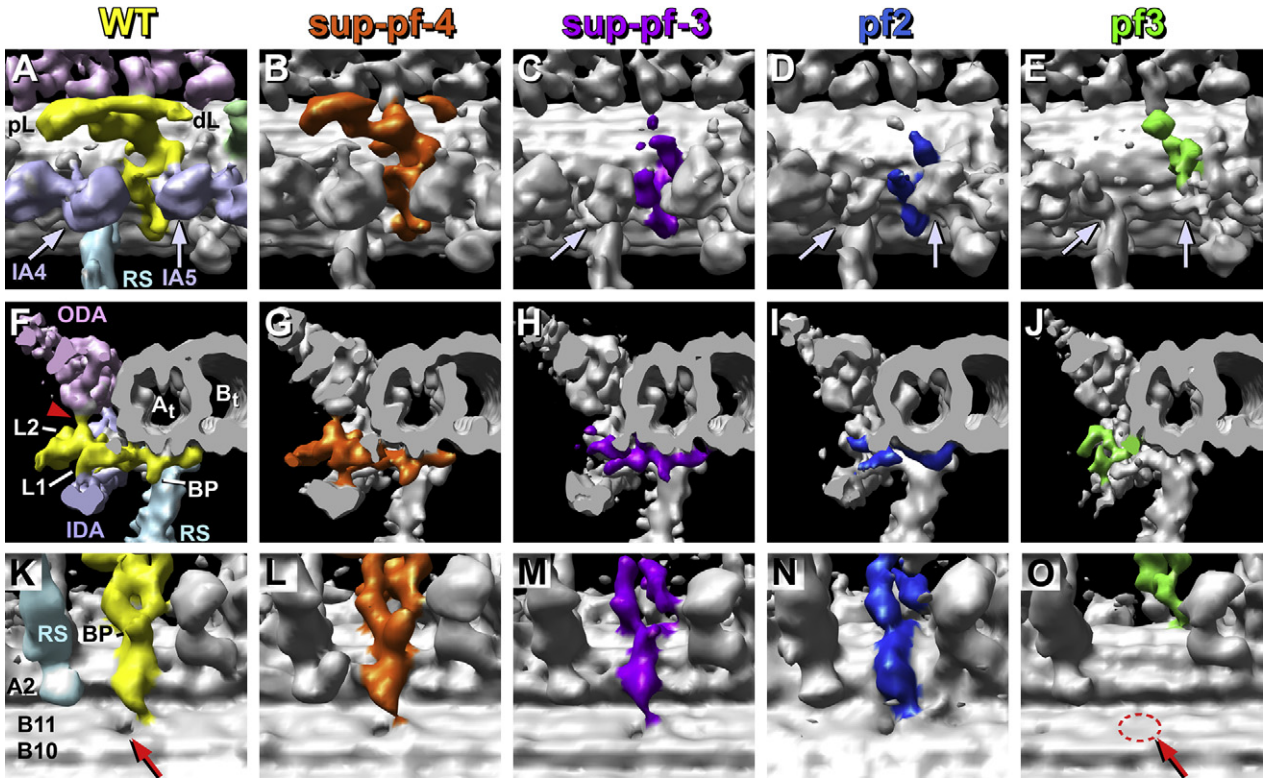

Figure 12.3 Close-up views of the DRC in wild-type and *drc* mutant axonemes. The wild-type DRC structure is shown in yellow in a longitudinal view of the linker (A), a cross-sectional view of the DRC (F), and a close-up view of the base-plate as it attaches to the B11 structure of the B-tubule (K). The DRC in *sup-pf-4* is shown in brown. Structural changes are relatively small. The overall structure of the linker and base-plate is normal (G,L) but the distal lobe of the linker and one of the linker projections are missing in *sup-pf-4* (B). This is the likely location of DRC5 and DRC6. *sup-pf-3* is shown in purple (C,H,M) and *pf2* in dark blue (D,I,N). Both mutants lack most of the linker region; only a small portion close to the A-tubule remains. The missing linker region is the likely location of DRC3, DRC4, and DRC7. Inner-arms IA4 and IA5 (grey arrows in C,D) are also reduced. *pf3* is shown in green; it is the most defective strain (E,J,N). More of the linker remains (E), but the base-plate is completely missing (J) and there is no attachment to the B11 structure (N). The base-plate is the likely location of DRC1 and DRC2. A hole in the B11 structure is visible in wild-type and other mutants, but the hole is missing in *pf3* (see red arrows in K,O). *Modified from [31].*

different domains of the nexin–DRC link [31]. The *sup-pf-4* strain is most similar to wild type with respect to motility and the structure of the nexin link. Only two DRC subunits, DRC5 (~40 kD) and DRC6 (~29 kD), have been identified as missing in *sup-pf-4* [21]. No structural defects were observed in two-dimensional averages of thin-sectioned material [29], but cryo-ET has shown that the most distal region of the linker, closest to the B-tubule, is missing in *sup-pf-4* [31]. This site is the likely location of DRC5 and DRC6. However, the missing density is ~250 kD, which is significantly larger than the sum of the two missing subunits (~69 kD). Thus, there may be multiple copies of DRC5 and DRC6 and/or additional polypeptides also located in this region.

The *pf2* and *sup-pf-3* strains are most similar with respect to their structural and biochemical defects (Table 12.2). Both mutants lack a major portion of the linker region, which corresponds to the crescent-shaped domain seen previously in two-dimensional averages of thin-sectioned material [29,31]. Missing structures in *pf2* include both the proximal and distal lobes of the linker that connect to the B-tubule, the various protrusions that connect to inner-arm IA5 and the outer dynein arms (OID2), and the central portion of the linker. Only the base-plate and a small density of ~60 kD close to the A-tubule remain [31]. *pf2* axonemes lack DRC3–DRC7, but DRC1 and DRC2 are present at wild-type levels [21,24]. These results suggest that DRC3–DRC7 are located in the linker, and DRC1 and DRC2 are located in the base-plate. Given the estimated size of the linker (~1–1.2 MD), there may be additional DRC subunits that are located in this region but were not detected as missing in previous studies.

DRC4 has been identified as the *PF2* gene product, and transformation with wild-type or epitope-tagged copies of PF2/DRC4 rescued both the motility defects and assembly of missing structures [30,31]. These observations indicate that DRC4 plays a critical role in the assembly of the linker region. *sup-pf-3* is an unusual DRC4 mutation that results in the assembly of truncated DRC4 subunits (R. Bower, D. Tritschler, and M. E. Porter, unpublished results). The presence of the truncated subunits results in the assembly of a larger part of the linker in *sup-pf-3* and further suggests that DRC4 is located near the base of the linker region. Chemical crosslinking of DRC4 indicates a close association with three axonemal polypeptides of 65–85 kD [30]. They may correspond to other DRC subunits that are missing in *pf2*, or they may represent subunits located in the base of the linker that are involved in mediating its attachment to the A-tubule. Interestingly, the initial chemical crosslinking experiments did not detect a direct interaction between DRC4 and tubulin *in situ* [30], even though tubulin binding by a DRC4 ortholog (Gas8) has been reported *in vitro* [117].

The *pf3* mutant has the most severe structural and biochemical defects (Tables 12.2 and 12.3). The base-plate structure is gone, and most of the linker region is also missing, except for ~130–200 kD located close to the A-tubule [31].

Similarly, DRC1 and DRC2 are completely missing, and many of the linker subunits are significantly reduced, with the possible exception of DRC4 (Table 12.2). These observations are consistent with the assignment of DRC1 and DRC2 to the base-plate, DRC5 and DRC6 to the distal lobe of the linker, DRC3–DRC7 to the central portion of the linker, and DRC4 to a site near the base of the linker region [31].

The base-plate appears to be directly connected to the B11 filament at the junction between the A- and B-tubules [31]. Immediately adjacent to this site, a small 3–4 nm "hole" is observed in the wall of the B-tubule. The hole is not observed in *pf3* when the base-plate is missing [31]. The composition of the B11 filament and the nature of the hole are not well understood, but earlier studies have suggested that the nexin link may be closely associated with the *pf* ribbon, including tektin [98,99,107]. Tektin is also reduced in the *pf3* and *ida6* mutants [98], and tektin mutants in mice are associated with defects in the assembly of inner dynein arms [118]. The exact location of the *pf* ribbon within the A-tubule is controversial, but it is tempting to speculate that it may be located in close proximity to the nexin–DRC link and play a role in determining its spacing on the outer doublets [99].

12.7 Identification and Characterization of Dynein Regulatory Complex and Nexin Subunits

12.7.1 DRC4/Trypanin/Gas8

DRC4 is the only DRC subunit that has been clearly characterized at the molecular level [30], although several other polypeptides have recently been proposed as candidate subunits for the nexin link [108,119,120]. *DRC4* was identified by rescue of a *pf2* mutation that had been tagged by plasmid insertion; it encodes a highly conserved coiled-coil protein that appears to be ubiquitous in organisms that assemble motile axonemes [30].

The DRC4 ortholog in trypanosomes is trypanin, a polypeptide required for optimal flagellar motility [121,122]. Knockdown of trypanin by RNA interference (RNAi) can partially suppress the flagellar paralysis associated with central-pair mutations, which is consistent with a role in mediating signals between the central pair/radial spoke complex and the dynein arms [123]. DRC4/trypanin is essential for the viability of the bloodstream form of trypanosomes [124], which suggests that inhibition of flagellar motility might be an attractive target for the treatment of sleeping sickness (reviewed in [125]).

Vertebrate orthologs of DRC4 are known as GAS11 in humans and GAS8 in mice and zebrafish [126–128]. *Gas8* was first described as a gene in mouse fibroblasts

whose expression could be stimulated by growth arrest induced by serum starvation [129,130]. Both Gas8 mRNA and protein are highly enriched in mouse testis and ciliated epithelia of the respiratory and reproductive tracts [127]. Recent work in zebrafish has shown that GAS8 is required for ciliary motility in vertebrates [128]. Knockdown of GAS8 by antisense morpholinos resulted in hydrocephaly, neural tube cell death, left–right axis defects, and defects in ciliary motility and otolith biogenesis. Thus, defects in genes encoding components of the nexin–DRC link might well be the underlying cause of disease in a subset of patients with primary ciliary dyskinesia (PCD) ([1,131]; see Chapter 24).

Whether DRC4 has additional functions beyond a role in flagellar motility is unclear. Several investigators have detected high levels of Gas8/Gas11 transcripts in tissues that assemble non-motile, primary cilia including heart, liver, and kidney ([126,127]; G. Rupp and M. E. Porter, unpublished results). These observations prompted a search for Gas8 in primary cilia, but thus far the evidence has been largely negative. Antibody staining of tissue culture cells indicated some staining at the base of primary cilia in a collecting duct cell line, as well as pericentrosomal co-localization with Golgi markers in COS7 cells [132]. These authors suggested that Gas8/Gas11 may function to regulate cytoplasmic dyneins involved in intraflagellar transport and ciliary assembly [132]. Others have reported associations between GAS8 and Rab3b [133] and between GAS8 and the influenza A virus protein NS1 [134] using yeast two-hybrid and co-immunoprecipitation assays. Whether these interactions are functionally significant *in vivo* is unknown.

12.7.2 Candidate Nexin Subunits

Rib72 is a major non-tubulin component of the *pf* ribbon that has also been proposed as a candidate subunit of the nexin link [108]. This proposal is based on the sensitivity of the Rib72 polypeptide to protease digestion during ATP-induced sliding disintegration and immuno-electron microscopy staining of intact axonemes with a Rib72 antibody at ~100 nm intervals. However, more stringent extraction conditions using Sarkosyl to break down the axoneme to *pf* ribbons resulted in antibody labeling at ~24 nm intervals. The epitope recognized by the Rib72 antibody appears to be partially masked in intact axonemes but more accessible after Sarkosyl extraction. These observations may be more consistent with a model in which Rib72 is involved in the specification of the 96 nm repeat and nexin binding [99] rather than an integral subunit of the nexin—DRC link.

The PACRG (Parkin co-regulated gene) encodes a conserved axonemal polypeptide that was first described as the cause of male sterility in a mouse mutant strain with a large deletion of chromosome 17 [135]. Comparative genomics has shown that PACRG is widely expressed in ciliated organisms [136]. Knockdown of the two PACRG isoforms in trypanosomes by RNAi results in defects in flagellar motility and integrity of the axoneme [120]. Electron microscopy analysis revealed that one or more outer-doublet microtubules is missing or displaced from the central ring of the axoneme in PACRG knockdown strains, but other

aspects of axoneme structure are normal. The authors proposed that PACRG might be a component of the nexin link that functions to maintain axonemal integrity [120]. Interestingly, PACRG has also been identified in Sarkosyl-extracted *Chlamydomonas* axonemes as a polypeptide that potentially interacts with Rib72 by blot overlay [137]. Like Rib72, localization of PACRG in the axoneme by antibody staining required pretreatment with low (0.1−0.3%) concentrations of Sarkosyl. However, PACRG is more readily extracted from the axoneme by higher concentrations of detergent than Rib72, suggesting that it is not an integral component of the ribbon. Immuno-electron microscopy localization of PARCG indicated that it is frequently found inbetween adjacent outer doublets in axoneme cross-sections. However, by negative staining, PACRG is more densely distributed along the length of frayed axonemes than might be expected for a nexin link component [137]. Additional work is needed to evaluate the relationship between PACRG, Rib72, and the nexin link.

Work in trypanosomes has identified another group of closely related proteins as potential subunits of the nexin link [119]. TbCMF-9/-76/-76b are three coiled-coil proteins that are highly conserved in species with motile flagella (CMF=components of motile flagella). Knockdown of TbCMF-9 and TbCMF-76b resulted in cells with reduced motility and defects in outer doublet connections in ~44% of axoneme cross-sections [119,138]. A TbCMF-9−GFP (green fluorescent protein) fusion protein is localized along the length of the flagellum, and no defects were observed in cross-sections of the basal bodies or transition zones. These findings are consistent with a model in which the TbCMF-9/-76/-76b proteins are required along the length of the axoneme to stabilize the connections between outer-doublet microtubules [119]. Closely related orthologs include the coiled-coil domain-containing protein CCDC147 in vertebrates and FAP189 and FAP58 in *Chlamydomonas*. It would be interesting to determine whether these proteins are bona fide subunits of the nexin−DRC link or axonemal polypeptides otherwise required for outer-doublet integrity.

The nexin−DRC link is intimately associated with several structures in the 96 nm repeat, including the radial spokes and the inner and outer dynein arms [23,24,29,31,76]. Several of the *drc* mutations have secondary effects on the assembly of inner-arm and radial-spoke subunits [29,31,139]. These interactions are poorly understood and merit more serious investigation. In addition, recent work has identified another complex that may be connected to the DRC. The calmodulin-and-radial-spoke-associated complex (CRC) was identified in axonemal extracts as a group of three polypeptides (FAP91, FAP61, and FAP251) that co-immunoprecipitate with calmodulin and the radial spokes in low calcium buffers [140]. Calmodulin is a subunit of both the central pair and radial spokes (reviewed in [18]), but it is present at wild-type levels in *drc* mutants [140]. However, co-immunoprecipitation of the CRC with calmodulin is disrupted in the *drc* mutants *pf2* and *pf3*. Thus, the interaction between calmodulin and the CRC is altered in the absence of the nexin−DRC link [140]. Further work is needed to

characterize the physical location of the CRC within the 96 nm repeat and its relationship to both the radial spokes and the DRC.

12.7.3 Strategies and Criteria for the Identification of Dynein Regulatory Complex–Nexin Subunits

In addition to the studies described above, work is ongoing in several laboratories to identify additional DRC subunits. Strategies include the characterization of polypeptides that co-purify and co-immunoprecipitate with DRC4, chromosome walking to *DRC* loci, the analysis of missing spots on two-dimensional gels, and quantitative comparison of wild-type and mutant axonemes by iTRAQ labeling and MS/MS. Several candidates have been identified, but there is not yet a uniform consensus on the composition of the DRC. Given that the *drc* mutations affect the assembly of multiple structures, it is not sufficient to simply catalog missing polypeptides. The challenge for the future will be to identify which polypeptides are bona fide subunits of the nexin link versus components of DRC-associated structures. Criteria should include co-purification with the isolated DRC and evidence of direct physical interactions with known DRC subunits. In addition, as more candidates are identified, we need to determine their relative stoichiometries, assess how they interact with one another, and localize each subunit more precisely within the substructure of the nexin link. Given the size and complexity of the nexin link (~1.5 MD), we are just at the beginning of this endeavor.

12.8 Function of the Dynein Regulatory Complex–Nexin Link in Motility and Future Directions

Nexin linkages appear to be a unique feature of motile cilia and flagella, whether or not radial spokes and central-pair microtubules are present. They are obviously present in the motile 9+0 flagella of eel sperm [141,142] and likely present in the motile cilia of the embryonic node [143]. However, high-resolution electron microscopy studies on non-motile, primary cilia are limited, and it is difficult to clearly identify interdoublet linkages, even when images are reinforced by nine-fold rotation [144], although links between outer-doublet microtubules and the ciliary membrane are often prominent [145]. Recent work has recognized that the 9+0 pattern of primary cilia is frequently modified by the movement of one or more doublets into the core of the axoneme [144,146]. These authors suggest that the term "9v" (variable) is a more accurate description of axoneme architecture for primary cilia in a wide variety of tissues and organisms. In addition, most of the polypeptides that have been proposed as potential subunits of the nexin link are only expressed in organisms with motile flagella [30,108,119,120,137].

Most investigators have assumed that the nexin links are essential for the integrity of the ring of outer doublets in the axoneme. It was therefore surprising that none of the *drc* mutants shows any defects in the arrangement of the outer-doublet microtubules [28,29,31]. In addition, some of the *drc* mutants (e.g. *sup-pf-3* and *sup-pf-4*) display nearly wild-type motility [68]. These observations suggest that other structures, such as the dynein arms and radial spoke, are sufficient to maintain axoneme integrity *in vivo*, and/or that protease digestion may not be as selective for the nexin—DRC links as was previously believed. The identification of other components that help to maintain outer-doublet integrity should be a high priority. An interesting possibility is that a specific subset of inner-arm dyneins may be involved [96].

The nexin links are also believed to provide mechanical resistance to dynein-driven sliding, a key feature of many models for flagellar motility (reviewed in [10,11]). If mutations in the central pair/radial spoke complex inhibit or reduce dynein-driven sliding, then mutations in the nexin link could suppress paralysis by reducing resistance to sliding. Reduced resistance to microtubule sliding may also be a key property displayed by other suppressor mutations that affect the outer-arm dynein HCs and the I1 dynein (Table 12.1). This hypothesis would be consistent with the original model suggesting that the wild-type function of the DRC is to globally inhibit dynein activity in the absence of signals from the radial spokes [68]. It could be tested by direct measurement of sliding resistance in *drc* and other suppressor mutants [147]. How signals from the central pair/radial spoke complex might alter the conformation or activities of the nexin—DRC link in wild-type flagella is an open question. Is this strictly a mechanical interaction, or does it also involve the axonemal kinases and phosphatases that appear to be regulated by the central pair/radial spoke pathway (reviewed in [148] and Chapter 11)? Clear answers will require more detailed knowledge about specific interactions between the radial spokes, the axonemal enzymes, and nexin—DRC components.

It is also uncertain what happens to the nexin—DRC links during interdoublet sliding; that is, do they stretch and relax or do they release and reattach? Biophysical experiments using vanadate treatment to inactivate dyneins followed by measurements of interdoublet elasticity have provided support for both models [147,149,150]. Direct observations of the nexin links in actively beating flagella may ultimately be required to settle this question, but this will be challenging given that high-resolution views of axoneme structure require three-dimensional correlation averaging of multiple 96 nm repeats. The continued development of classification methods that will allow the investigator to identify different conformational states within the 96 nm repeat will likely be crucial to resolving this and other questions about the behavior(s) of the various axonemal components during flagellar bending [116,151].

Although it has been nearly 50 years since the original description of the nexin link [2] and nearly 30 years since the isolation of the dynein regulatory mutations [21], it has taken several steps in the development of imaging technologies for us to finally "see" the relationship between the nexin link and the DRC [28,31,100]. However, many challenges still remain. At the moment we are in a phase of molecular "bird-watching," as we forge ahead with the identification and characterization of nexin–DRC subunits. However, we still need to identify more selective mutations that affect specific subdomains of the nexin–DRC link, without disrupting so many other axonemal substructures. Perhaps even more daunting is the need to develop new biophysical strategies with which to probe the functions of the nexin–DRC link and finally understand its role in the regulation of dynein-based flagellar motility. Clearly we still have much to learn about how the various parts of the axoneme work together to produce such a complex and elegant form of cellular motility.

Acknowledgments

Many thanks to the past and present members of my laboratory for their hard work and dedication to our studies on flagellar dynein and its regulation. I am also grateful to many wonderful collaborators over the years, including Susan Dutcher, David Mitchell, Dick Linck, Winfield Sale, and Maureen Wirschell. A special thanks to my collaborators at the Boulder Laboratory for 3D Fine Structure, David Mastronarde, Eileen O'Toole, and Dick McIntosh, for their tireless efforts to push the envelope and see new details of axoneme structure, and to Thomas Heuser and Daniela Nicastro at Brandeis University, who have now brought our studies into a third dimension. Our work is supported by a grant (GM55667) from the National Institutes of Health.

References

[1] M. Fliegauf, T. Benzing, H. Omran, When cilia go bad: Cilia defects and ciliopathies, Nat. Rev. Mol. Cell Biol. 8 (2007) 880–893.
[2] I.R. Gibbons, Studies on the protein components of cilia from *Tetrahymena pyriformis*, Proc. Natl. Acad. Sci. USA 50 (1963) 1002–1010.
[3] I.R. Gibbons, Chemical dissection of the cilia, Arch. Biol. (Liege). 76 (1965) 317–352.
[4] P. Satir, Studies on cilia III. Further studies on the cilium tip and a "sliding filament" model of ciliary motility, J. Cell Biol. 39 (1968) 77–94.
[5] W.S. Sale, P. Satir, The direction of active sliding of microtubules in *Tetrahymena cilia*. Proc. Natl. Acad. Sci. USA 74 (1977) 2045–2049.
[6] L.A. Fox, W.S. Sale, Direction of force generated by the inner row of dynein arms on flagellar microtubules, J. Cell Biol. 105 (1987) 1781–1787.
[7] P. Satir, Switching mechanisms in the control of ciliary motility, Mod. Cell Biol. 4 (1985) 1–46.
[8] I.H. Riedel-Kruse, A. Hilfinger, J. Howard, F. Julicher, How molecular motors shape the flagellar beat, HFSP J. 1 (2007) 192–208.
[9] C.J. Brokaw, Thinking about flagellar oscillation, Cell Motil. Cytoskeleton 66 (2009) 425–436.

[10] C.B. Lindemann, K.A. Lesich, Flagellar and ciliary beating: The proven and the possible, J. Cell Sci. 123 (2010) 519–528.
[11] D.M. Woolley, Flagellar oscillation: A commentary on proposed mechanisms, Biol. Rev. Camb. Philos. Soc. 85 (2010) 453–470.
[12] C.B. Lindemann, A "geometric clutch" hypothesis to explain oscillations of the axoneme of cilia and flagella, J. Theor. Biol. 168 (1994) 175–189.
[13] C.B. Lindemann, A model of flagellar and ciliary functioning which uses the forces transverse to the axoneme as the regulator of dynein activation, Cell Motil. Cytoskel. 29 (1994) 141–154.
[14] C.J. Brokaw, Simulation of cyclic dynein-driven sliding, splitting, and reassociation in an outer doublet pair, Biophys. J. 97 (2009) 2939–2947.
[15] S. Aoyama, R. Kamiya, Cyclical interactions between two outer doublet microtubules in split flagellar axonemes, Biophys. J. 89 (2005) 3261–3268.
[16] C.B. Lindemann, D.R. Mitchell, Evidence for axonemal distortion during the flagellar beat of *Chlamydomonas*. Cell Motil. Cytoskeleton 64 (2007) 580–589.
[17] M.E. Porter, W.S. Sale, The 9 + 2 axoneme anchors multiple inner arm dyneins and a network of kinases and phosphatases that control motility, J. Cell Biol. 151 (2000) F37–F42.
[18] E.F. Smith, P. Yang, The radial spokes and central apparatus: Mechano-chemical transducers that regulate flagellar motility, Cell Motil. Cytoskeleton 57 (2004) 8–17.
[19] I. Nakano, T. Kobayashi, M. Yoshimura, C. Shingyoji, Central-pair-linked regulation of microtubule sliding by calcium in flagellar axonemes, J. Cell Sci. 116 (2003) 1627–1636.
[20] G.B. Witman, J. Plummer, G. Sander, *Chlamydomonas* flagellar mutants lacking radial spokes and central tubules. Structure, composition, and function of specific axonemal components, J. Cell Biol. 76 (1978) 729–747.
[21] B. Huang, Z. Ramanis, D.J. Luck, Suppressor mutations in *Chlamydomonas* reveal a regulatory mechanism for flagellar function, Cell 28 (1982) 115–124.
[22] M.E. Porter, J. Power, S.K. Dutcher, Extragenic suppressors of paralyzed flagellar mutations in *Chlamydomonas reinhardtii* identify loci that alter the inner dynein arms, J. Cell Biol. 118 (1992) 1163–1176.
[23] G. Piperno, K. Mead, W. Shestak, The inner dynein arms I2 interact with a "dynein regulatory complex" in *Chlamydomonas* flagella, J. Cell Biol. 118 (1992) 1455–1463.
[24] G. Piperno, K. Mead, M. LeDizet, A. Moscatelli, Mutations in the "dynein regulatory complex" alter the ATP-insensitive binding sites for inner arm dyneins in *Chlamydomonas* axonemes, J. Cell Biol. 125 (1994) 1109–1117.
[25] M.E. Porter, J.A. Knott, L.C. Gardner, D.K. Mitchell, S.K. Dutcher, Mutations in the *SUP-PF-1* locus of *Chlamydomonas reinhardtii* identify a regulatory domain in the beta-dynein heavy chain, J. Cell Biol. 126 (1994) 1495–1507.
[26] G. Rupp, E. O'Toole, L.C. Gardner, B.F. Mitchell, M.E. Porter, The *sup-pf-2* mutations of *Chlamydomonas* alter the activity of the outer dynein arms by modification of the γ-dynein heavy chain, J. Cell Biol. 135 (1996) 1853–1865.
[27] B.F. Mitchell, L.E. Grulich, M.M. Mader, Flagellar quiescence in *Chlamydomonas*: Characterization and defective quiescence in cells carrying *sup-pf-1* and *sup-pf-2* outer dynein arm mutations, Cell Motil. Cytoskeleton 57 (2004) 186–196.
[28] D.N. Mastronarde, E.T. O'Toole, K.L. McDonald, J.R. McIntosh, M.E. Porter, Arrangement of inner dynein arms in wild-type and mutant flagella of *Chlamydomonas*. J. Cell Biol. 118 (1992) 1145–1162.
[29] L.C. Gardner, E. O'Toole, C.A. Perrone, T. Giddings, M.E. Porter, Components of a "dynein regulatory complex" are located at the junction between the radial spokes and the dynein arms in *Chlamydomonas* flagella, J. Cell Biol. 127 (1994) 1311–1325.

[30] G. Rupp, M.E. Porter, A subunit of the dynein regulatory complex in *Chlamydomonas* is a homologue of a growth arrest-specific gene product, J. Cell Biol. 162 (2003) 47–57.
[31] T. Heuser, M. Raytchev, J. Krell, M.E. Porter, D. Nicastro, The dynein regulatory complex is the nexin link and a major regulatory node in cilia and flagella, J. Cell Biol. 187 (2009) 921–933.
[32] G.M.W. Adams, B. Huang, G. Piperno, D.J.L. Luck, The central pair microtubular complex of *Chlamydomonas* flagella: Polypeptide composition as revealed by analysis of mutants, J. Cell Biol. 91 (1981) 69–76.
[33] R. Sapiro, I. Kostetskii, P. Olds-Clarke, G.L. Gerton, G.L. Radice, I.J. Strauss, Male infertility, impaired sperm motility, and hydrocephalus in mice deficient in sperm-associated antigen 6, Mol. Cell Biol. 22 (2002) 6298–6305.
[34] W. Stannard, A. Rutman, C. Wallis, C. O'Callaghan, Central microtubular agenesis causing primary ciliary dyskinesia, Am. J. Respir. Crit. Care. Med. 169 (2004) 634–637.
[35] K.F. Lechtreck, G.B. Witman, *Chlamydomonas reinhardtii* hydin is a central pair protein required for flagellar motility, J. Cell Biol. 176 (2007) 473–482.
[36] C.G. DiPetrillo, E.F. Smith, Pcdp1 is a central apparatus protein that binds Ca(2+)-calmodulin and regulates ciliary motility, J. Cell Biol. 189 (2010) 601–612.
[37] K.F. Lechtreck, P. Delmotte, M.L. Robinson, M.J. Sanderson, G.B. Witman, Mutations in Hydin impair ciliary motility in mice, J. Cell Biol. 180 (2008) 633–643.
[38] S.K. Dutcher, B. Huang, D.J.L. Luck, Genetic dissection of the central pair microtubules of the flagella of *Chlamydomonas reinhardtii*, J. Cell Biol. 98 (1984) 229–236.
[39] E.F. Smith, P.A. Lefebvre, The role of central apparatus components in flagellar motility and microtubule assembly, Cell Motil. Cytoskel. 38 (1997) 1–8.
[40] D.R. Mitchell, W.S. Sale, Characterization of a *Chlamydomonas* insertional mutant that disrupts flagellar central pair microtubule-associated structures, J. Cell Biol. 144 (1999) 293–304.
[41] G. Rupp, E. O'Toole, M.E. Porter, The *Chlamydomonas PF6* locus encodes a large alanine/proline-rich polypeptide that is required for assembly of a central pair projection and regulates flagellar motility, Mol. Biol. Cell 12 (2001) 739–751.
[42] D.R. Mitchell, Reconstruction of the projection periodicity and surface architecture of the flagellar central pair complex, Cell Motil. Cytoskeleton 55 (2003) 188–199.
[43] H. Zhang, D.R. Mitchell, Cpc1, a *Chlamydomonas* central pair protein with an adenylate kinase domain, J. Cell Sci. 117 (2004) 4179–4188.
[44] M.J. Wargo, E.E. Dymek, E.F. Smith, Calmodulin and PF6 are components of a complex that localizes to the C1 microtubule of the flagellar central apparatus, J. Cell Sci. 118 (2005) 4655–4665.
[45] D.R. Mitchell, Orientation of the central pair complex during flagellar bend formation in *Chlamydomonas*, Cell Motil. Cytoskeleton 56 (2003) 120–129.
[46] M.J. Wargo, E.F. Smith, Asymmetry of the central apparatus defines the location of active microtubule sliding in *Chlamydomonas* flagella, Proc. Natl. Acad. Sci. USA 100 (2003) 137–142.
[47] B.F. Mitchell, L.B. Pedersen, M. Feely, J.L. Rosenbaum, D.R. Mitchell, ATP production in *Chlamydomonas reinhardtii* flagella by glycolytic enzymes, Mol. Biol. Cell 16 (2005) 4509–4518.
[48] M. Bernstein, P.L. Beech, S.G. Katz, J.L. Rosenbaum, A new kinesin-like protein (Klp1) localized to a single microtubule of the *Chlamydomonas* flagellum, J. Cell Biol. 125 (1994) 1313–1326.
[49] C.K. Omoto, C. Kung, The pair of central tubules rotates during ciliary beat in *Paramecium*, Nature 279 (1979) 532–534.
[50] C. Omoto, C. Kung, Rotation and twist of the central-pair microtubules in the cilia of *Paramecium*. J. Cell Biol. 87 (1980) 33–46.

[51] C.K. Omoto, I.R. Gibbons, R. Kamiya, C. Shingyoji, K. Takahashi, G.B. Witman, Rotation of the central pair microtubules in eukaryotic flagella, Mol. Biol. Cell 10 (1999) 1–4.
[52] D.R. Mitchell, M. Nakatsugawa, Bend propagation drives central pair rotation in *Chlamydomonas reinhardtii* flagella, J. Cell Biol. 166 (2004) 709–715.
[53] A.R. Gaillard, D.R. Diener, J.L. Rosenbaum, W.S. Sale, Flagellar radial spoke protein 3 is an A-kinase anchoring protein (AKAP), J. Cell Biol. 153 (2001) 443–448.
[54] R.S. Patel-King, O. Gorbatyuk, S. Takebe, S.M. King, Flagellar radial spokes contain a Ca^{2+}-stimulated nucleoside diphosphate kinase, Mol. Biol. Cell 15 (2004) 3891–3902.
[55] P. Yang, D.R. Diener, J.L. Rosenbaum, W.S. Sale, Localization of calmodulin and dynein light chain LC8 in flagellar radial spokes, J. Cell Biol. 153 (2001) 1315–1326.
[56] P. Yang, C. Yang, W.S. Sale, Flagellar radial spoke protein 2 is a calmodulin binding protein required for motility in *Chlamydomonas reinhardtii*, Eukaryot. Cell 3 (2004) 72–81.
[57] P. Yang, D.R. Diener, C. Yang, T. Kohno, G.J. Pazour, J.M. Dienes, N.S. Agrin, S.M. King, W.S. Sale, R. Kamiya, J.L. Rosenbaum, G.B. Witman, Radial spoke proteins of *Chlamydomonas* flagella, J. Cell Sci. 119 (2006) 1165–1174.
[58] E.F. Smith, W.S. Sale, Regulation of dynein-driven microtubule sliding by the radial spokes in flagella, Science 257 (1992) 1557–1559.
[59] D.R. Howard, G. Habermacher, D.B. Glass, E.F. Smith, W.S. Sale, Regulation of *Chlamydomonas* flagellar dynein by an axonemal protein kinase, J. Cell Biol. 127 (1994) 1683–1692.
[60] A. Gokhale, M. Wirschell, W.S. Sale, Regulation of dynein-driven microtubule sliding by the axonemal protein kinase CK1 in *Chlamydomonas* flagella, J. Cell Biol. 186 (2009) 817–824.
[61] E.F. Smith, Regulation of flagellar dynein by calcium and a role for an axonemal calmodulin and calmodulin-dependent kinase, Mol. Biol. Cell 13 (2002) 3303–3313.
[62] G. Habermacher, W.S. Sale, Regulation of flagellar dynein by phosphorylation of a 138-kD inner arm dynein intermediate chain, J. Cell Biol. 136 (1997) 167–176.
[63] S.J. King, S.K. Dutcher, Phosphoregulation of an inner dynein arm complex in *Chlamydomonas reinhardtii* is altered in phototactic mutant strains, J. Cell Biol. 136 (1997) 177–191.
[64] T.W. Hendrickson, C.A. Perrone, P. Griffin, K. Wuichet, J. Mueller, P. Yang, M.E. Porter, W.S. Sale, IC138 is a WD-repeat dynein intermediate chain required for light chain assembly and regulation of flagellar bending, Mol. Biol. Cell 15 (2004) 5431–5442.
[65] R. Bower, K. VanderWaal, E. O'Toole, L. Fox, C. Perrone, J. Mueller, M. Wirschell, R. Kamiya, W.S. Sale, M.E. Porter, IC138 defines a subdomain at the base of the I1 dynein that regulates microtubule sliding and flagellar motility, Mol. Biol. Cell 20 (2009) 3055–3063.
[66] J. Boesger, V. Wagner, W. Weisheit, M. Mittag, Analysis of flagellar phosphoproteins from *Chlamydomonas reinhardtii*, Eukaryot. Cell 8 (2009) 922–932.
[67] C.J. Brokaw, D.J. Luck, B. Huang, Analysis of the movement of *Chlamydomonas* flagella: the function of the radial-spoke system is revealed by comparison of wild-type and mutant flagella, J. Cell Biol. 92 (1982) 722–732.
[68] C.J. Brokaw, D.J.L. Luck, Bending patterns of *Chlamydomonas* flagella III. A radial spoke deficient mutant and a central pair deficient mutant, Cell Motil. 5 (1985) 195–208.
[69] H. Sakakibara, S. Takada, S.M. King, G.B. Witman, R. Kamiya, A *Chlamydomonas* outer-arm dynein mutant with a truncated beta heavy chain, J. Cell Biol. 122 (1993) 653–661.
[70] R. Kamiya, Functional diversity of axonemal dyneins as studied in *Chlamydomonas* mutants, Int. Rev. Cytol. 219 (2002) 115–155.
[71] Z. Liu, H. Takazaki, Y. Nakazawa, M. Sakato, T. Yagi, T. Yasunaga, S.M. King, R. Kamiya, Partially functional outer-arm dynein in a novel *Chlamydomonas* mutant expressing a truncated gamma heavy chain, Eukaryot. Cell 7 (2008) 1136–1145.

[72] C.K. Omoto, T. Yagi, E. Kurimoto, R. Kamiya, The ability of paralyzed flagella mutants of *Chlamydomonas* to move, Cell Motil. Cytoskeleton 33 (1996) 88–94.
[73] E. Frey, C.J. Brokaw, C.K. Omoto, Reactivation at low ATP distinguishes among classes of paralyzed flagella mutants, Cell Motil. Cytoskeleton 38 (1997) 91–99.
[74] K. Hayashibe, C. Shingyoji, R. Kamiya, Induction of temporary beating in paralyzed flagella of *Chlamydomonas* mutants by application of external force, Cell Motil. Cytoskeleton 37 (1997) 232–239.
[75] T. Yagi, R. Kamiya, Vigorous beating of *Chlamydomonas* axonemes lacking central pair/radial spoke structures in the presence of salts and organic compounds, Cell Motil. Cytoskeleton 46 (2000) 190–199.
[76] D. Nicastro, C. Schwartz, J. Pierson, R. Gaudette, M.E. Porter, J.R. McIntosh, The molecular architecture of axonemes revealed by cryoelectron tomography, Science 313 (2006) 944–948.
[77] K.H. Bui, H. Sakakibara, T. Movassagh, K. Oiwa, T. Ishikawa, Molecular architecture of inner dynein arms *in situ* in *Chlamydomonas reinhardtii* flagella, J. Cell Biol. 183 (2008) 923–932.
[78] C.J. Brokaw, R. Kamiya, Bending patterns of *Chlamydomonas* flagella: IV. Mutants with defects in inner and outer dynein arms indicate differences in dynein arm function, Cell Motil. Cytoskeleton 8 (1987) 68–75.
[79] P. Yang, W.S. Sale, Casein kinase I is anchored on axonemal doublet microtubules and regulates flagellar dynein phosphorylation and activity, J. Biol. Chem. 275 (2000). 18905–18912.
[80] L.M. DiBella, M. Sakato, R.S. Patel-King, G.J. Pazour, S.M. King, The LC7 light chains of *Chlamydomonas* flagellar dyneins interact with components required for both motor assembly and regulation, Mol. Biol. Cell 15 (2004) 4633–4646.
[81] L.M. DiBella, E.F. Smith, R.S. Patel-King, K. Wakabayashi, S.M. King, A novel Tctex2-related light chain is required for stability of inner dynein arm I1 and motor function in the *Chlamydomonas* flagellum, J. Biol. Chem. 279 (2004). 21666–21676.
[82] K. Ikeda, R. Yamamoto, M. Wirschell, T. Yagi, R. Bower, M.E. Porter, W.S. Sale, R. Kamiya, A novel ankyrin-repeat protein interacts with the regulatory proteins of inner arm dynein f(I1) of *Chlamydomonas reinhardtii*, Cell Motil. Cytoskeleton 66 (2009) 448–456.
[83] M. Wirschell, C. Yang, P. Yang, L. Fox, H.A. Yanagisawa, R. Kamiya, G.B. Witman, M.E. Porter, W.S. Sale, IC97 is a novel intermediate chain of I1 dynein that interacts with tubulin and regulates interdoublet sliding, Mol. Biol. Cell 20 (2009) 3044–3054.
[84] S.H. Myster, J.A. Knott, E. O'Toole, M.E. Porter, The *Chlamydomonas Dhc1* gene encodes a dynein heavy chain subunit required for assembly of the I1 inner arm complex, Mol. Biol. Cell 8 (1997) 607–620.
[85] S.H. Myster, J.A. Knott, K.M. Wysocki, E. O'Toole, M.E. Porter, Domains in the 1α dynein heavy chain required for inner arm assembly and flagellar motility in *Chlamydomonas*, J. Cell Biol. 146 (1999) 801–818.
[86] S. Toba, L.A. Fox, H. Sakakibara, M.E. Porter, K. Oiwa, W.S. Sale, Distinct roles of the 1alpha and 1beta heavy dyneins of the inner arm dynein I1 of *Chlamydomonas* flagella, Mol. Biol. Cell. 22 (2011) 342–353.
[87] C.A. Perrone, S.H. Myster, R. Bower, E.T. O'Toole, M.E. Porter, Insights into the structural organization of the I1 inner arm dynein from a domain analysis of the 1beta dynein heavy chain, Mol. Biol. Cell 11 (2000) 2297–2313.
[88] N. Kotani, H. Sakakibara, S.A. Burgess, H. Kojima, K. Oiwa, Mechanical properties of inner-arm dynein-f (dynein I1) studied with *in vitro* motility assays, Biophys. J. 93 (2007) 886–894.
[89] G. Piperno, Z. Ramanis, E.F. Smith, W.S. Sale, Three distinct inner dynein arms in *Chlamydomonas* flagella: Molecular composition and location in the axoneme, J. Cell Biol. 110 (1990) 379–389.

[90] R. Kamiya, E. Kurimoto, E. Muto, Two types of *Chlamydomonas* flagellar mutants missing different components of inner-arm dynein, J. Cell Biol. 112 (1991) 441–447.
[91] O. Kagami, R. Kamiya, Translocation and rotation of microtubules caused by multiple species of *Chlamydomonas* inner-arm dynein, J. Cell Sci. 103 (1992) 653–664.
[92] M. Wirschell, T. Hendrickson, W.S. Sale, Keeping an eye on I1: I1 dynein as a model for flagellar dynein assembly and regulation, Cell Motil. Cytoskeleton 64 (2007) 569–579.
[93] M. LeDizet, G. Piperno, *ida4-1*, *ida4-2*, and *ida4-3* are intron splicing mutations affecting the locus encoding p28, a light chain of *Chlamydomonas* axonemal inner dynein arms, Mol. Biol. Cell 6 (1995) 713–723.
[94] M. LeDizet, G. Piperno, The light chain p28 associates with a subset of inner dynein arm heavy chains in *Chlamydomonas* axonemes, Mol. Biol. Cell 6 (1995) 697–711.
[95] T. Yagi, I. Minoura, A. Fujiwara, R. Saito, T. Yasunaga, M. Hirono, R. Kamiya, An axonemal dynein particularly important for flagellar movement at high viscosity. Implications from a new *Chlamydomonas* mutant deficient in the dynein heavy chain gene DHC9, J. Biol. Chem. 280 (2005). 41412–41420.
[96] T. Yagi, K. Uematsu, Z. Liu, R. Kamiya, Identification of dyneins that localize exclusively to the proximal portion of *Chlamydomonas* flagella, J. Cell Sci. 122 (2009) 1306–1314.
[97] T. Kato, O. Kagami, T. Yagi, R. Kamiya, Isolation of two species of *Chlamydomonas reinhardtii* flagellar mutants, *ida5* and *ida6*, that lack a newly identified heavy chain of the inner dynein arm, Cell Struct. Funct. 18 (1993) 371–377.
[98] H.A. Yanagisawa, R. Kamiya, A tektin homologue is decreased in *Chlamydomonas* mutants lacking an axonemal inner-arm dynein, Mol. Biol. Cell 15 (2004) 2105–2115.
[99] P.W. Setter, E. Malvey-Dorn, W. Steffen, R.E. Stephens, R.W. Linck, Tektin interactions and a model for molecular functions, Exp. Cell Res. 312 (2006) 2880–2896.
[100] D.M. Woolley, Studies on the eel sperm flagellum. I. The structure of the inner dynein arm complex, J. Cell Sci. 110 (1997) 85–94.
[101] U.W. Goodenough, J.E. Heuser, Structure of the soluble and in situ ciliary dyneins visualized by quick-freeze deep-etch microscopy, in: F.D. Warner, P. Satir, I.R. Gibbons (Eds.), Cell Movement. The Dynein ATPases, Alan R. Liss, Inc., New York, 1989, pp. 121–140.
[102] S.A. Burgess, D.A. Carter, S.D. Dover, D.M. Woolley, The inner dynein arm complex: Compatible images from freeze-etch and thin section methods of microscopy, J. Cell Sci. 100 (1991) 319–328.
[103] R.D. Allen, A reinvestigation of cross-sections of cilia, J. Cell Biol. 37 (1968) 825–831.
[104] R.E. Stephens, Thermal fractionation of outer fiber doublet microtubules into A- and B-subfiber components, J. Mol. Biol. 47 (1970) 353–363.
[105] R.E. Stephens, Isolation of nexin – the linkage protein responsible for the maintenance of the nine-fold configuration of flagellar axonemes, Biol. Bull. 139 (1970) 1.
[106] R. Linck, Chemical and structural differences between cilia and flagella from the Lamellibranch mollusc, *Aequipecten irradians*, J. Cell Sci. 12 (1973) 951–981.
[107] R.E. Stephens, S. Oleszko-Szuts, R.W. Linck, Retention of ciliary ninefold structure after removal of microtubules, J. Cell Sci. 92 (1989) 391–402.
[108] K. Ikeda, J.A. Brown, T. Yagi, J.M. Norrander, M. Hirono, E. Eccleston, R. Kamiya, R.W. Linck, Rib72, a conserved protein associated with the ribbon compartment of flagellar A-microtubules and potentially involved in the linkage between outer doublet microtubules, J. Biol. Chem. 278 (2003) 7725–7734.
[109] F.D. Warner, Ciliary inter-microtubule bridges, J. Cell Sci. 20 (1976) 101–114.
[110] F.D. Warner, Organization of interdoublet links in *Tetrahymena* cilia, Cell Motil. 3 (1983) 321–332.

[111] G.E. Olson, R.W. Linck, Observations of the structural components of flagellar axonemes and central pair microtubules from rat sperm, J. Ultrastruct. Res. 61 (1977) 21–43.
[112] H.H. Bozkurt, D.M. Woolley, Morphology of nexin links in relation to interdoublet sliding in the sperm flagellum, Cell Motil. Cytoskel. 24 (1993) 109–118.
[113] K.E. Summers, I.R. Gibbons, Effects of trypsin digestion on flagellar structures and their relationship to motility, J. Cell Biol. 58 (1973) 618–629.
[114] C.J. Brokaw, Elastase digestion of demembranated sperm flagella, Science (Wash. D.C.) 207 (1980) 1365–1367.
[115] R.W. Linck, R.E. Stephens, Functional protofilament numbering of ciliary, flagellar, and centriolar microtubules, Cell Motil. Cytoskeleton 64 (2007) 489–495.
[116] D. Nicastro, Cryo-electron microscope tomography to study axonemal organization, Meth. Cell Biol. 91 (2009) 1–39.
[117] J.M. Bekker, J.R. Colantonio, A.D. Stephens, W.T. Clarke, S.J. King, K.L. Hill, R.H. Crosbie, Direct interaction of Gas11 with microtubules: Implications for the dynein regulatory complex, Cell Motil. Cytoskeleton 64 (2007) 461–473.
[118] H. Tanaka, N. Iguchi, Y. Toyama, K. Kitamura, T. Takahashi, K. Kaseda, M. Maekawa, Y. Nishimune, Mice deficient in the axonemal protein Tektin-t exhibit male infertility and immotile-cilium syndrome due to impaired inner arm dynein function, Mol. Cell Biol. 24 (2004) 7958–7964.
[119] D.M. Baron, K.S. Ralston, Z.P. Kabututu, K.L. Hill, Functional genomics in *Trypanosoma brucei* identifies evolutionarily conserved components of motile flagella, J. Cell Sci. 120 (2007) 478–491.
[120] H.R. Dawe, H. Farr, N. Portman, M.K. Shaw, K. Gull, The Parkin co-regulated gene product, PACRG, is an evolutionarily conserved axonemal protein that functions in outer-doublet microtubule morphogenesis, J. Cell Sci. 118 (2005) 5421–5430.
[121] K.L. Hill, N.R. Hutchings, P.M. Grandgenett, J.E. Donelson, T lymphocyte-triggering factor of African trypanosomes is associated with the flagellar fraction of the cytoskeleton and represents a new family of proteins that are present in several divergent eukaryotes, J. Biol. Chem. 275 (2000). 39369–39378.
[122] N.R. Hutchings, J.E. Donelson, K.L. Hill, Trypanin is a cytoskeletal linker protein and is required for cell motility in African trypanosomes, J. Cell Biol. 156 (2002) 867–877.
[123] K.S. Ralston, A.G. Lerner, D.R. Diener, K.L. Hill, Flagellar motility contributes to cytokinesis in *Trypanosoma brucei* and is modulated by an evolutionarily conserved dynein regulatory system, Eukaryot. Cell 5 (2006) 696–711.
[124] K.S. Ralston, K. L. Hill, Trypanin, a component of the flagellar dynein regulatory complex, is essential in bloodstream form African trypanosomes. *PLoS Pathog.* 2 (2006) e101.
[125] K.S. Ralston, K.L. Hill, The flagellum of *Trypanosoma brucei*: New tricks from an old dog, Int. J. Parasitol. 38 (2008) 869–884.
[126] S.A. Whitmore, C. Settasatian, J. Crawford, K.M. Lower, B. McCallum, R. Seshadri, C.J. Cornelisse, E.W. Moerland, A. Cleton-Jansen, A.J. Tipping, C.G. Mathew, M. Savnio, A. Savoia, P. Verlander, A.D. Auerbach, C. Van Berkel, J.C. Pronk, N.A. Doggett, D.F. Callen, Characterization and screening for mutations of the growth arrest-specific 11 (*GAS11*) and *C16orf3* genes at 16q24.3 in breast cancer, Genomics 52 (1998) 325–331.
[127] S.D. Yeh, Y.J. Chen, A.C. Chang, R. Ray, B.R. She, W.S. Lee, H.S. Chiang, S.N. Cohen, S. Lin-Chao, Isolation and properties of *Gas8*, a growth arrest-specific gene regulated during male gametogenesis to produce a protein associated with the sperm motility apparatus, J. Biol. Chem. 277 (2002) 6311–6317.
[128] J.R. Colantonio, J. Vermot, D. Wu, A.D. Langenbacher, S. Fraser, J.N. Chen, K.L. Hill, The dynein regulatory complex is required for ciliary motility and otolith biogenesis in the inner ear, Nature 457 (2009) 205–209.

[129] D.G. Brenner, S. LIn-Chao, S.N. Cohen, Analysis of mammalian cell genetic regulation *in situ* by using retrovirus-derived "portable exons" carrying the *Escherichia coli* lacZ gene, Proc. Natl. Acad. Sci. USA 86 (1989) 5517–5521.
[130] C.J. Lih, S.N. Cohen, C. Wang, S. Lin-Chao, The platelet derived-growth factor α-receptor is encoded by a growth arrest-specific gene, Proc. Natl. Acad. Sci. USA 93 (1996). 4617–4462.
[131] B. Carlen, S. Lindberg, U. Stenram, Absence of nexin links as a possible cause of primary ciliary dyskinesia, Ultrastruct. Pathol. 27 (2003) 123–126.
[132] J.R. Colantonio, J.M. Bekker, S.J. Kim, K.M. Morrissey, R.H. Crosbie, K.L. Hill, Expanding the role of the dynein regulatory complex to non-axonemal functions: Association of GAS11 with the Golgi apparatus, Traffic 7 (2006) 538–548.
[133] N. Nishimura, K. Araki, W. Shinahara, Y. Nakano, K. Nishimura, H. Higashio, T. Sasaki, Interaction of Rab3B with microtubule-binding protein Gas8 in NIH 3T3 cells, Arch. Biochem. Biophys. 474 (2008) 136–142.
[134] L. Zhao, L. Xu, X. Zhou, Q. Zhu, Z. Yang, C. Zhang, X. Zhu, M. Yu, Y. Zhang, X. Zhao, P. Huang, Interaction of influenza virus NS1 protein with growth arrest-specific protein 8, Virol. J. 6 (2009) 218.
[135] D. Lorenzetti, C.E. Bishop, M.J. Justice, Deletion of the Parkin coregulated gene causes male sterility in the quaking (viable) mouse mutant, Proc. Natl. Acad. Sci. USA 101 (2004) 8402–8407.
[136] J.B. Li, J.M. Gerdes, C.J. Haycraft, Y. Fan, T.M. Teslovich, H. May-Simera, H. Li, O.E. Blacque, L. Li, C.C. Leitch, R.A. Lewis, J.S. Green, P.S. Parfrey, M.R. Leroux, W.S. Davidson, P.L. Beales, L.M. Guay-Woodford, B.K. Yoder, G.D. Stormo, N. Katsanis, S.K. Dutcher, Comparative genomics identifies a flagellar and basal body proteome that includes the BBS5 human disease gene, Cell 117 (2004) 541–552.
[137] K. Ikeda, T. Ikeda, K. Morikawa, R. Kamiya, Axonemal localization of *Chlamydomonas* PACRG, a homologue of the human Parkin-coregulated gene product, Cell Motil. Cytoskeleton 64 (2007) 814–821.
[138] R. Broadhead, H.R. Dawe, H. Farr, S. Griffiths, S.R. Hart, N. Portman, M.K. Shaw, M.L. Ginger, S.J. Gaskell, P.G. McKean, K. Gull, Flagellar motility is required for the viability of the bloodstream trypanosome, Nature 440 (2006) 224–227.
[139] G. Piperno, Regulation of dynein activity within *Chlamydomonas* flagella, Cell Motil. Cytoskeleton 32 (1995) 103–105.
[140] E.E. Dymek, E.F. Smith, A conserved CaM and radial spoke associated complex mediates regulation of flagellar dynein activity, J. Cell Biol. 179 (2007) 515–526.
[141] B.H. Gibbons, I.R. Gibbons, B. Baccetti, Structure and motility of the 9+0 flagellum of eel spermatozoa, J. Submicrosc. Cytol. 15 (1983) 15–20.
[142] B.H. Gibbons, B. Baccetti, I.R. Gibbons, Live and reactivated motility in the 9+0 flagellum of *Anguilla* sperm, Cell Motil. 5 (1985) 333–350.
[143] T. Caspary, C.E. Larkins, K.V. Anderson, The graded response to Sonic Hedgehog depends on cilia architecture, Dev. Cell 12 (2007) 767–778.
[144] H. Hagiwara, N. Ohwada, T. Aoki, T. Suzuki, K. Takata, The primary cilia of secretory cells in the human oviduct mucosa, Med. Mol. Morphol. 41 (2008) 193–198.
[145] L.A. Perkins, E.M. Hedgecock, J.N. Thomson, J.G. Culotti, Mutant sensory cilia in the nematode *Caenorhabditis elegans*, Dev. Biol. 117 (1986) 456–487.
[146] E. Gluenz, J.L. Hoog, A.E. Smith, H.R. Dawe, M.K. Shaw, K. Gull, Beyond 9+0: Non-canonical axoneme structures characterize sensory cilia from protists to humans, FASEB J. 24 (2010) 3117–3121.
[147] I. Minoura, T. Yagi, R. Kamiya, Direct measurement of inter-doublet elasticity in flagellar axonemes, Cell Struct. Funct. 24 (1999) 27–33.

[148] M. Wirschell, D. Nicastro, M.E. Porter, W.S. Sale, The regulation of axonemal bending, in: G.B. Witman (Ed.), *The* Chlamydomonas *Sourcebook, Cell Motility and Behavior*, Academic Press, San Diego, 2009, pp. 253–282.
[149] D.W. Pelle, C.J. Brokaw, K.A. Lesich, C.B. Lindemann, Mechanical properties of the passive sea urchin sperm flagellum, Cell Motil. Cytoskeleton 66 (2009) 721–735.
[150] C.B. Lindemann, L.J. Macauley, K.A. Lesich, The counterbend phenomenon in dynein-disabled rat sperm flagella and what it reveals about the interdoublet elasticity, Biophys. J. 89 (2005) 1165–1174.
[151] T. Movassagh, K.H. Bui, H. Sakakibara, K. Oiwa, T. Ishikawa, Nucleotide-induced global conformational changes of flagellar dynein arms revealed by *in situ* analysis, Nat. Struct. Mol. Biol. 17 (2010) 761–767.

In this chapter

13

Regulation of Dynein in Ciliary and Flagellar Movement

Chikako Shingyoji
Department of Biological Sciences, Graduate School of Science, University of Tokyo, Tokyo, Japan

13.1 Introduction

Eukaryotic flagella and cilia are cell organelles having a complex yet highly conserved internal machinery known as the "9+2" structure (Fig. 13.1A). The evolutionary origin of the 9+2 structure is unknown but may be close to that of primitive eukaryotes, which dates back about 15 billion years. Since then, the 9+2 structure may have remained basically unchanged because this highly successful design drives the cilia and flagella of all the eukaryotes that possess them, from algae to humans. The first recognition of the 9+2 structure of the axoneme (the internal core of a flagellum and cilium) was made in plant sperm flagella by electron microscopy [1]. The diversity of the axonemal structures, with deviations from the "typical" 9+2 type, has been demonstrated in spermatozoa of various animal species, particularly insects [2]. The different structures of sperm tails are probably related to the different patterns of their movement.

Flagella and cilia are identical in structure, but it is convenient to retain separate terms for them. Those that undulate like a whip with symmetric travelling waves are called flagella (Fig. 13.1B) while those that beat with an oar-like action with alternation of so-called "effective" (1–5 in Fig. 13.1C) and "recovery" (6–12 in Fig. 13.1C) strokes are called cilia. Flagella are commonly longer than cilia. The characteristic oscillatory bending movements of cilia and flagella produce the directional liquid flow (upward in Fig. 13.1B; rightward in Fig. 13.1C) surrounding them. The sperm flagella of marine invertebrates, for example the sea urchin (Fig. 13.2A), beat with a nearly planar waveform at about 40–50 Hz. The sperm swim at a speed of about a hundred to several hundred μm/s. The propulsive force of flagella and cilia results almost wholly from their viscous interaction with the medium, in which the Reynolds number, which is the ratio of inertial to viscous forces, is 10^{-4} to 10^{-6} for individual flagella and 10^{-2} to 10^{-1} for individual spermatozoa [3]. Thus, the flagella must beat against the high drag

Dyneins DOI: 10.1016/B978-0-12-382004-4.10013-5
Copyright © 2012 by Elsevier Inc. All rights reserved.

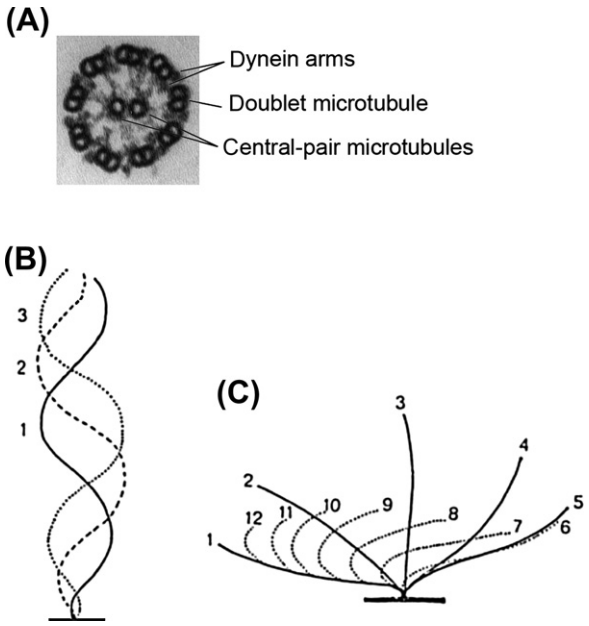

Figure 13.1 Basic structure and beating patterns of flagella and cilia. (A) An electron micrograph showing the internal structure (axoneme) of a flagellum, called the "9+2" structure, consisting of nine doublet microtubules surrounding the central-pair microtubules, in transverse section. Dynein arms are projecting from the A-tubule of each doublet towards the B-tubule of the adjacent doublet. Schematic drawings showing sequential waveforms of flagellar (B) and ciliary (C) movements. The waveforms with numbers indicate the order of movement. The direction of wave propagation in (B) is upward, which is the same as the direction of the propulsive force. In the ciliary movement in (C), the effective stroke (1–5) but not the recovery stroke (6–12) produces the propulsive force, which is rightward.

force of the medium. How do they solve this problem? An answer is found in the mechanism of microtubule sliding driven by the dyneins in the 9+2 structure.

In the 9+2 pattern, nine doublet microtubules surround the central pair microtubules. Dynein molecules (the so-called dynein arms in the axoneme) occur in two regular rows, the outer and inner arms, along each of the nine doublet microtubules (Figs. 13.1A and 13.2B). They are minus-end-directed motor proteins and cause sliding movement of the adjoining doublet microtubules towards their plus ends, which is towards the distal ends of cilia and flagella. For the linear sliding force generated by dynein to cause the rhythmic bending waves, the activity of dynein must be controlled. There are several apparently paradoxical questions concerning the regulatory mechanism of dynein motility in cilia and flagella: How do dyneins that exert unidirectional force on the microtubule (Fig. 13.2C) generate bidirectional oscillatory bending (Fig. 13.2A; Movie 13.1)? How does microtubule sliding at the nine interdoublet sites in the axoneme (Fig. 13.2B) produce planar bending waves (Fig. 13.2A)? How does microtubule sliding, which can occur in any region along the axoneme, produce bending

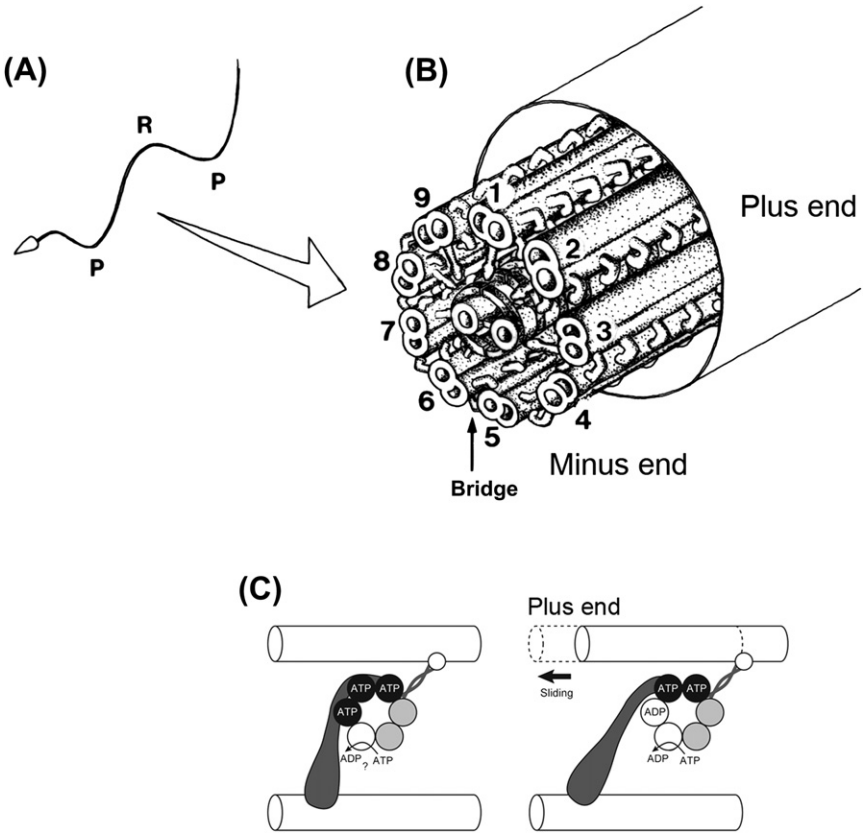

Figure 13.2 The architecture of a flagellum and microtubule sliding induced by dynein. (A) A sea urchin spermatozoon shows planar oscillatory beating with alternate formation of principal (P) and reverse (R) bends. The beat plane is the plane containing doublet 1 and the "5-6 bridges," and the distal and proximal ends of a flagellum correspond to the so-called plus and minus ends of microtubules, respectively (B). The dynein-driven microtubule sliding involves changes to the tail–head interactions without a change of orientation of the stalk relative to the head (C: left, before sliding; right, during sliding). For simplicity, although the outer-arm dynein of the sea urchin sperm flagella consists of two heads with slender stalks and tails, the dynein is depicted here as one ring of six AAA domains with the stalk and tail (C).

waves propagating from base to tip of the flagellum or cilium? Clues as to the answers to these questions seem to be found in the structural and functional uniqueness of the 9+2 axoneme.

This chapter provides an overview of the regulation of dynein motile activity underlying the oscillatory bending movement of cilia and flagella. The basic mechanism of dynein regulation is thought to be common to flagella and cilia of many species, but there are differences in some of its features. We will therefore mainly describe the knowledge obtained from studies on sea urchin sperm flagella, referring to other species when necessary.

13.2 Basic Features of the Components of Cilia and Flagella

13.2.1 Dynein Arms

In SDS-plyacrylamide gel electrophoresis of axonemal proteins, dynein occurs in four or more major electrophoretically separable bands at high molecular regions above 300 kDa, with several bands in the middle (around 60–120 kDa) and low (around 10–20 kDa) molecular regions, which respectively correspond to the heavy chains (HCs), intermediate chains (ICs), and light chains (LCs) [4]. In the sea urchin sperm flagella, the four bands that appear in the high molecular region in an acrylamide gradient gel are called – from the highest to the lowest molecular regions – the C, A, D, and B bands. One of the bands represents the outer dynein arms. The outer arms can be selectively extracted from demembranated flagella when the axonemes are treated with 0.6 M KCl solution. The HCs of the isolated crude outer-arm dynein as well as the purified dynein (21 S dynein) are the main polypeptides of the A band. Each of the outer arms of sea urchin sperm flagella consists of two HCs (α and β), three ICs, and six LCs.

Dynein arms are regularly arranged along the doublet microtubules. The outer arms are arrayed at intervals of 24 nm, which is common to many species [5,6]. Unlike the outer arms, which consist of uniform members, the inner arms consist of sets of several kinds of dyneins [7]. The inner arms of *Chlamydomonas* flagella consist of seven kinds of dynein arms and the sets of these multiple arms repeat with a 96 nm periodicity along the doublet microtubules [8,9]. It is interesting that this periodicity corresponds to that of the interdoublet (or nexin) links and to the repeating unit of the radial spokes. This may indicate a functional relationship between the radial spokes and the inner arms, and/or between the interdoublet links and the inner arms [10]. Recent ultrastructural findings regarding the arrangement of dynein molecules in the axoneme are described in Chapter 8.

Dynein is a motor protein that hydrolyzes ATP and converts its chemical energy to mechanical work to induce microtubule sliding. The mechanism of chemomechanical energy transduction in dynein has not been elucidated. However, it seems to be related to the structural features of the dynein molecule. Dynein belongs to the AAA^+ superfamily (ATPases associated with various cellular activities) and its motor domain (or "head") is composed of six AAA^+ modules [11,12]. The dynein HC comprises a ring-shaped "head" with a "stalk," a "linker," and a "tail" (tail formerly known as the "stem"). In the axonemal dynein, the tail binds to the A-tubule of the doublet while the stalk interacts with the B-tubule of the adjacent doublet. In the control of dynein motile activity, conformational changes of not only the stalk but also the linker-tail are involved [13–15].

Four of the six AAA^+ modules (hereafter called AAA1–AAA4) of the dynein motor domain possess a conserved phosphate-binding loop called the P-loop (P1–P4)

[16–18], and AAA1 is considered the primary hydrolytic site [11,16,19]. In cytoplasmic dynein the other three sites are nucleotide-binding and/or hydrolyzing sites and have distinct roles in the regulation of dynein function [20–22].

In axonemal dynein, AAA2, AAA3, and AAA4 are non-catalytic nucleotide-binding sites involved in the regulation of dynein motile activity. More precisely, the binding of both ADP [23–26] and ATP [23] to AAA2–AAA4, together with hydrolysis at AAA1, seems to be essential for the microtubule-sliding activity of dynein. According to whether these regulatory nucleotide-binding sites bind ATP or ATP and ADP, the activity of dyneins in the axoneme seems to change between the two states (or modes). In the case of ATP binding, the dyneins form cross-bridges between doublets (we call this state "ATP inhibition") (Fig. 13.2C, left), while in the case of ATP and ADP binding the dynein causes microtubule sliding (we call this state "ADP activation") (Fig. 13.2C, right). For flagellar bending, dynein arms in the states of ATP inhibition and ADP activation are both necessary [27]. ADP binding, which is probably related to protein phosphorylation, may be a key signal in terms of switching on dynein activity in flagellar motility [28].

13.2.2 Microtubules

All the microtubules of the axoneme are built up of α- and β-tubulin heterodimers in an 8 nm axial repeat [29]; this periodicity probably determines the unit step of dynein motility [30]. The structural polarity of these microtubules is related to the polarity of their growth; namely, to which end of a growing microtubule tubulin subunits can add. Bidirectional growth of microtubules can be induced when axonemes are incubated with purified tubulin, but the distally added tubules are considerably longer than those added at the proximal end of the axoneme [31]. Thus, the proximal (or basal) end of both the doublet microtubules and the central-pair microtubules is the so-called minus end, which is the more stable end, of the microtubule. In doublet microtubules, only the complete A-tubule is able to form extensions *in vitro*.

The αβ-tubulin heterodimer is subject to a large number of post-translational modifications [32]. Among them, tyrosination/detyrosination, polyglycylation, glutamylation, and polyglutamylation in the tubulin of axonemal doublet microtubules and of the central-pair microtubules have been reported to affect the motility of *Chlamydomonas* flagella, *Tetrahymena* cilia, and sea urchin sperm flagella [33–38].

Singlet microtubules polymerized from tubulin dimers are slender rods about 25 nm in diameter and a few microns in length. They are almost straight in solution when observed under dark-field illumination, while doublet microtubules without dynein arms, which are prepared by dialysis of demembranated flagella, show a coiled conformation forming left-handed helices. The shape of the helices changes with pH; the coiled form becomes larger at pH 7.4 in both pitch and diameter compared to at pH 8.3. Ca^{2+} also affects the helices; the

diameter of the helices at above 10^{-7} M Ca^{2+} is smaller than that at lower Ca^{2+} concentrations [39].

The mechanical properties of the singlet and doublet microtubules and their organization are the major determinants of the mechanical properties of flagella. Thus, the flexural rigidity (or stiffness) of the microtubules determines the bending moment of flagella. The flexural rigidity of a singlet microtubule from bovine brain is about 26×10^{-24} Nm^2 [40]. It increases with the presence of dynein, which forms a dynein–microtubule complex [39]. The flexural rigidity of microtubules in flagella has been inferred from the bending stiffness of sperm. The stiffness of a demembranated flagellum showing rigor waves under an ATP-free condition, where dynein is expected to form cross-bridges between the doublet microtubules, is about 11×10^{-21} Nm^2 [41]. In the presence of ATP and vanadate, the flexural rigidity of a sperm flagellum is about $1–2\times10^{-21}$ Nm^2 [41,42], from which the flexural rigidity of a single microtubule is estimated to be about $20–30\times10^{-24}$ Nm^2, assuming that there is no crosslinking between the doublet microtubules [40]. Thus, the flexural rigidity of microtubules in flagella changes with the state of dynein activity. The post-translational modification along microtubules may be another factor that modulates their flexural rigidity. Systematic analysis of changes in flexural rigidity of the microtubules along a flagellum seems important for further understanding of its contribution to the regulation of flagellar movement.

13.2.3 Beat Plane and the Central-Pair Microtubules

When the 9+2 structure is viewed from base to tip, the dynein arms are seen projecting clockwise from the A-tubules towards the B-tubules of the adjacent doublets. In a typical arrangement, an imaginary line vertically bisecting the line through the microtubules of the central pair passes through one of the doublets on one side and a unique bridge-like structure between two of the doublets on the other side. The doublet on the imaginary line is conventionally designated as doublet number 1 and the remaining doublets are numbered in a clockwise direction; that is, in the direction in which the dynein arms project. The bridge mentioned above occurs between the doublets number 5 and 6 and is called the "5–6 bridge" (Fig. 13.2B). In axonemes lacking the 5–6 bridge, other structural characteristics are used for clockwise numbering; for example, in *Chlamydomonas* flagella, number 1 is assigned to the doublet that does not have an outer arm. Ultrastructural observations have shown that, in protease-treated axonemes, sliding can occur between any adjacent two of the nine doublets. This indicates that any dynein arm in any region along the flagella can produce force to move the adjacent doublet.

EM studies have also shown that the beat plane of many flagella and cilia is perpendicular to the plane of the central-pair microtubules. This does not, however, presuppose a fixed orientation of the plane of the central pair in the 9+2

structure. Thus, electron microscopy observations of the central pair of *Paramecium*, instantaneously fixed and serially sectioned, have suggested that the central pair rotates 360° per beat cycle with respect to the nine doublets [43,44]. This interpretation has since been supported by various studies made on flagella of other species [45–49]. Although there are motile flagella that naturally lack the central pair, indicating that the central pair is not needed for bending *per se*, a large majority of axonemes possess the central pair, and mutants defective in them are paralyzed under physiological (i.e. high) ATP conditions. It is postulated that the central pair (more precisely, the central-pair/radial-spoke system) may act as a "distributor," regulating the activity of dynein to impose a higher-order regulation on the default movement of cilia and flagella, thus enabling a more complex waveform and/or high-speed beating [50].

13.3 Regulation of Microtubule Sliding in the Axoneme

13.3.1 Microtubule Sliding in Trypsin-Treated Axonemes

A milestone in the study of ciliary and flagellar movement after the discovery of dynein was the demonstration of microtubule sliding in the axoneme of sea urchin spermatozoa [51]. When the flagellar axonemes were fragmented, treated with trypsin, and then exposed to Mg-ATP under a dark-field microscope, they showed disintegration into individual doublet microtubules as the doublets slid past each other. The trypsin treatment caused disruption of the axonemal substructures, such as the interdoublet links, that connect the doublet microtubules. Ultrastructural observations of negatively stained doublets showed that sliding could occur between any two of the nine doublets of an axonemal fragment [52]. This experimental method for observing sliding has been very useful in elucidating the basic properties of dynein motile activity, such as the polarity of dynein force generation, which is now known to occur towards the proximal end of the flagellum [53,54].

The disintegration of axonemes induced by this method was used to determine the velocity of microtubule sliding, which is a basic parameter for understanding the regulation of dynein activity in flagella. The sliding velocity determined in this way increased with an increase in the concentration of ATP. However, the profiles of the velocity increase obtained by two different groups [55,56] were not consistent. The non-stoichiometric relationship between the rate of ATP hydrolysis and ATP-dependent microtubule sliding in trypsin-treated axonemes suggested possible damage to the regulatory mechanism by trypsin [57]. Later studies have revealed that trypsin treatment of the axonemes not only disrupts the interdoublet links and a part of the radial spokes [58–60] but also induces fragmentation of dynein HCs [59–62], which increases dynein ATPase activity.

Therefore, trypsin treatment of dyneins is not suitable for the analysis of their motile ability in flagella and cilia.

13.3.2 Microtubule Sliding in Elastase-Treated Axonemes

Elastase is another protease that induces disintegration of the axoneme by microtubule sliding in the presence of ATP. Elastase and trypsin differ in their effects on the flagellar waveform of reactivated sperm [63,64], suggesting that they disrupt different structural components. After elastase treatment, dynein HCs still appear as four bands in acrylamide gel electrophoretic patterns, similarly to intact dynein, while trypsin-treated dyneins are fragmented into smaller polypeptides [60]. Both the radial spokes and interdoublet links are digested heavily by trypsin, but only slightly by elastase [58].

The velocity of microtubule sliding in elastase-treated axonemes increases in proportion to the increase in ATP concentration (0.01−3.0 mM). The double reciprocal plots of these two parameters is linear at lower Mg-ATP (0.007−0.16 mM), with V_{max} and K_m of 11.0 μm/s and 7.1×10^{-2} mM, respectively (E. Nakajima and C. Shingyoji, 2006, unpublished data), indicating that the relationship between these two parameters obeys Michaelis−Menten kinetics at lower Mg-ATP concentrations.

In both the trypsin-treated and elastase-treated axonemes, the first microtubule sliding splits the axoneme longitudinally into two parts, each consisting mainly of a bundle of doublet microtubules. In most of the trypsin-treated axonemes the splitting is followed by separation of the doublet bundles into individual doublets, whereas in about a third of the elastase-treated axonemes no further sliding occurs in the presence of higher concentrations of ATP ($\geq$0.1 mM). Interestingly, in the presence of lower concentrations of ATP the elastase-treated axonemes show sliding disintegration into individual doublets like the trypsin-treated axonemes (Fig. 13.3A, B).

13.3.3 Patterns of Splitting in Elastase-Treated Axonemes

The microtubule sliding that induces splitting in elastase-treated axonemes shows unique characteristics [65,66]: (1) At lower ATP ($<$0.1 mM) they split into individual doublets by sliding, while at higher ATP, in particular at physiological concentrations of ATP (several mM), 20−30% of the elastase-treated axonemes split into two doublet bundles (Figs. 13.3B and 13.4A,B; Movie 13.2). (2) At high Ca^{2+}, the splitting into two bundles at high ATP becomes dominant (60%) (Fig. 13.4A,B). (3) When they split into two bundles, the activity of the dynein arms on the thinner bundles is dominant at both lower and higher Ca^{2+}, as a result moving the thicker bundle towards the plus end of the microtubules relative to the thinner bundle (Fig. 13.4C). (4) Ultrastructural studies of the split doublet bundles show that the splitting occurs on both sides of the central-pair

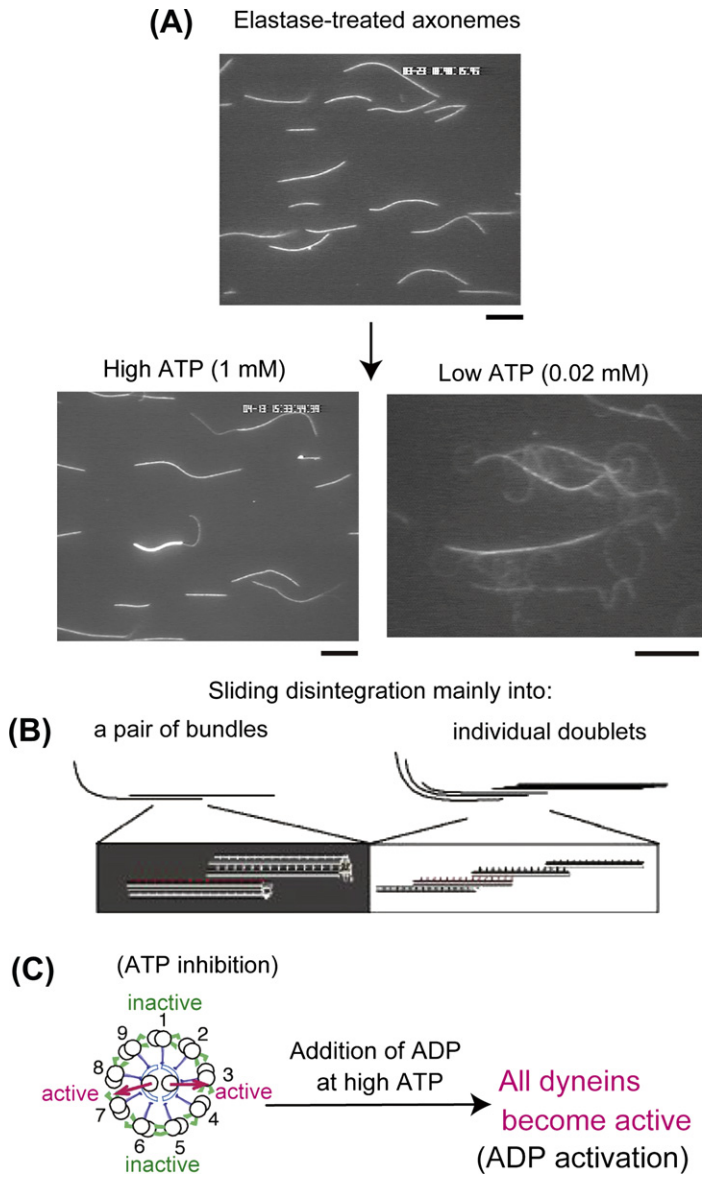

Figure 13.3 Characteristic splitting of the elastase-treated axonemes. Video images (A) and their diagrammatic illustrations (B) showing the characteristic microtubule sliding of elastase-treated axonemes into (mainly) a pair of bundles (left) and individual doublets (right) under high and low ATP conditions, respectively. Dynein arms on both sides of the central pair are active but those in other positions are inactive at high ATP, in which the regulation of dynein activity causes splitting of the axoneme into a pair of bundles (A, B, and C, left; refer also to Movie 13.2). The inhibition of some dynein activity at high ATP (ATP inhibition) can be released by the addition of ADP, resulting in the sliding disintegration of elastase-treated axonemes into individual doublets (C, right). Scale bar in (A) = 10 μm.

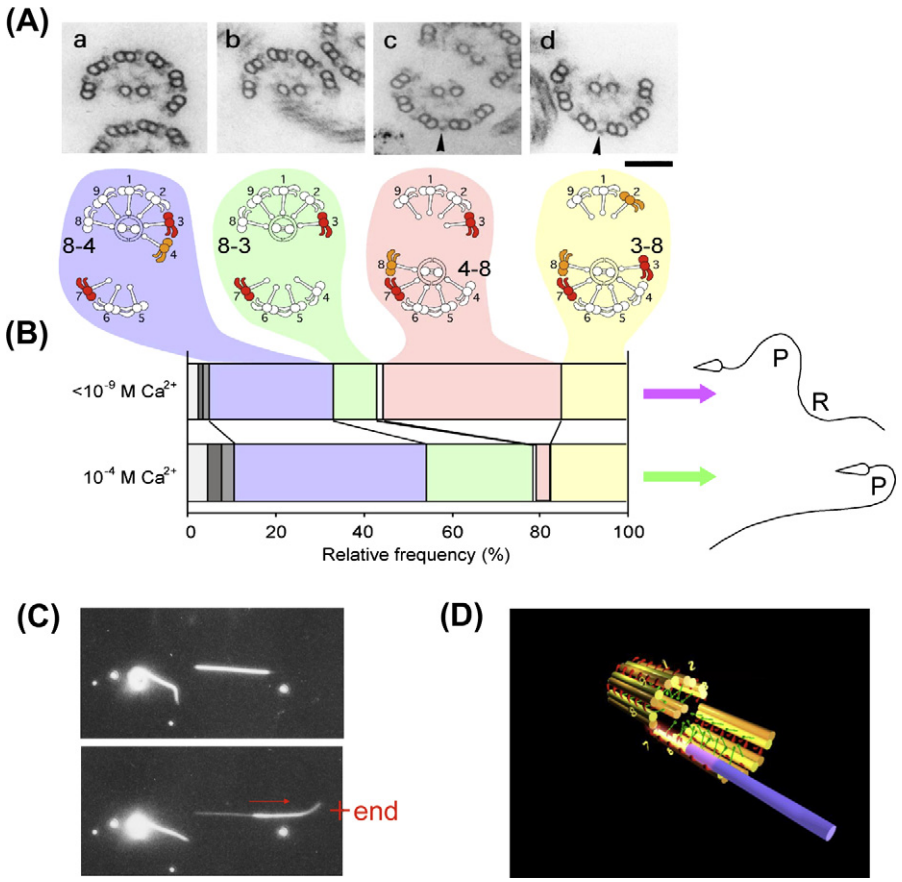

Figure 13.4 Splitting patterns of elastase-treated axonemes (A and B). Electron microscopic observation of axonemes split at 1 mM ATP (A) confirms that the thicker and thinner bundles consist of groups of specific members of the doublets (B), suggesting that the splitting takes place along the plane of the central pair. Ca^{2+}-dependent changes of splitting patterns (B) seem to be related to the Ca^{2+}-dependent changes of the waveform of reactivated flagella. At low Ca^{2+}, principal (P) and reverse (R) bends are alternately formed, while at high Ca^{2+} only principal bends are formed (B, right). To induce the separation of elastase-treated axonemes (C), the dynein arms on the thinner bundle but not those on the thicker bundle should be active. This was confirmed by the observation that the sliding of the thicker bundles (C, upper and lower panels, respectively, shown before and after the sliding induced by 1 mM ATP) occurred exclusively toward the plus-end of the microtubules (away from the head) at high rates of 84% (at low Ca^{2+}) and 92% (at high Ca^{2+}). (D) A schematic diagram showing the sliding of a microtubule (blue rod) on the dynein arms exposed along the thinner bundle obtained by splitting of elastase-treated axonemes. (A–C) modified from figures 3 and 4 in [66]. Scale bar in (A) = 100 nm.

microtubules and the number of doublets in each of the two bundles is more or less fixed: 90% of the thicker bundles containing five or six doublets with the central pair show mainly four patterns of 8–4, 8–3, 4–8, and 3–8, where the numbers denote the doublet numbers (Fig. 13.4A). The thinner bundles

corresponding to these patterns should consist of doublets 5–7, 4–7, 9–3, and 9–2, respectively. Higher concentrations of Ca^{2+} increase the occurrence of the 8–4 and 8–3 patterns and decrease that of the 4–8 and 3–8 patterns (Fig. 13.4B; see also figure 3 in [66]).

The characteristic splitting indicates the following three important points regarding the regulation of dynein activity. First, although dynein arms on any doublet microtubule can induce sliding between adjacent doublets, when the axonemes split into two bundles at physiological ATP concentrations, some of the dyein arms are kept inactive by a certain mechanism that suppresses the dynein activity and allows dynein cross-bridges to form between the doublets at high concentrations of ATP. Second, the central-pair microtubules override the ATP inhibition of dynein activity. The central pair may remove the inhibitory effect of ATP on the chemomechanical cycle of dyneins, probably through changing the mechanical and/or chemical signals. When the axonemes split, the more-active dyneins are on doublet 7 of the thinner bundles and the less-active dyneins are on doublet 3 of the thicker bundles. The difference in dynein activity (the dynein–microtubule affinity and the velocity of microtubule sliding) on doublet 7 and doublet 3 of the thinner and thicker bundles can be directly observed as the behavior of microtubules that interact with the dynein arms exposed on the thinner and thicker doublet bundles [66] (Fig. 13.4D).

Lastly, the splitting patterns of elastase-treated axonemes into two doublet bundles reflect the regulation of dynein activity during flagellar beating. As described above: (1) the dynein arms on the thinner bundles, but not those on the thicker bundles, are active, producing microtubule sliding and thereby splitting the axonemes into paired bundles; and (2) the occurrence of the 8–4 and 8–3 patterns and of the 4–8 and 3–8 patterns are similar at lower Ca^{2+}, whereas the 8–4 and 8–3 patterns become dominant with an increase in the Ca^{2+} concentration. It is known that the Ca^{2+} concentration relates to the waveform of the reactivated flagella: alternate formation of principal (P) and reverse (R) bends occurs at low Ca^{2+} concentrations, whereas the flagellar waveform becomes asymmetric, finally showing quiescence with a large P-bend at high Ca^{2+} concentrations [67–70]. Thus, the occurrence of the 4–8 pattern is related to the R-bend formation and that of the 8–4 and 8–3 patterns is related to the P-bend formation (Fig. 13.4B). Switching the activity of dynein arms between doublets 7 and 3 is the basis for the alternate formation of the P- and R-bends.

The splitting of axonemes into two doublet bundles was first demonstrated in lateral cilia of freshwater mussel gills [71] and observations by electron microscopy showed splitting at fixed doublet sites near the central pair of the 9+2 structure in sea urchin sperm flagella, mussel gill cilia, and rat sperm flagella [69,72,73]. Based on the observation of displacement of adjacent doublets at the end of the recovery and effective strokes [74], it was suggested that the dyneins on doublet numbers 1, 2, 3, and 4 are active while those on doublets 6, 7, 8, and

9 are passive during the effective stroke, and the converse must occur during the recovery stroke. Based on these observations, a "switch-point" hypothesis of ciliary activity was proposed in which the dynein activity alternates between the two halves of the axoneme [71,75]. More recently, our findings in sea urchin sperm flagella (Figs. 13.3 and 13.4) have indicated that dyneins on doublets 7 and 3, respectively, are responsible for inducing interdoublet sliding to form P- and R-bends and that switching the activity between these dyneins is essential for flagellar movement (Fig. 13.3C; see also Section 13.5). A basically similar switching mechanism between interdoublet sites has been suggested in *Chlamydomonas* flagella, regardless of the central pair rotation during their beat cycle [76].

13.4 Sliding Microtubule Theory and Bend Formation

The sliding microtubule theory, first put forward in the 1950s [77] following morphological observations of dynein arms, postulated that sliding between microtubules within the axonemes is the motive force of flagellar (or ciliary) beating. This theory, which contradicted the then-prevalent contraction theory, was supported by the ultrastructural observation that the tip of the cilium was fixed during beating [78] and by the demonstration of ATP-dependent sliding of microtubules in trypsin-treated axonemes [51].

To produce a bend in the sliding microtubule model, there should be local differences in the amount of sliding along the axoneme. This was clearly demonstrated by experiments involving local, brief reactivation of flagellar axonemes of sea urchin spermatozoa by iontophoretic application of ATP [79] (Fig. 13.5A). Unlike bath application of ATP to demembranated sperm flagella, which induces beating, a local brief application of a small amount of ATP (0.13 nC) induced the formation of a pair of similar bends in opposite directions and this bending was fixed until subsequent ATP applications (Fig. 13.5B; Movie 13.3). This experiment showed that the bends were formed (as a result of microtubule sliding caused by dynein arms that had been exposed to ATP) at the boundaries between the ATP-activated region (a few μm in length) and adjoining regions, where microtubule sliding does not occur in the absence of ATP. By ATP iontophoresis, local bends could be formed in any region along the flagellar axoneme, indicating that bending is not restricted to the basal region but can be induced in any region of the flagellum. Thus, it became clear that a difference in the amount of sliding produces bending (Fig. 13.5C). To support the sliding microtubule model even further, direct, real-time changes in the sliding displacement of doublet microtubules were demonstrated by using gold beads bound to the axoneme in beating sea urchin and tunicate sperm flagella [80,81].

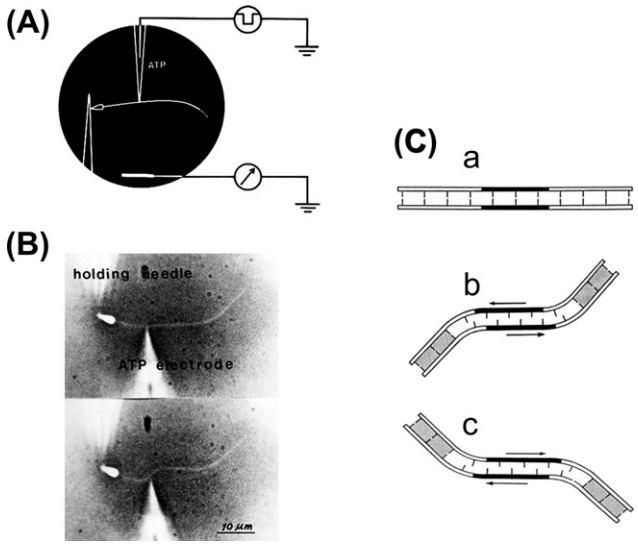

Figure 13.5 Responses of a demembranated flagellum to localized reactivation. The Triton-extracted sea urchin spermatozoon was attached by its head to a polylysine-coated glass microneedle and ATP was applied iontophoretically from a glass micropipette whose tip was brought close to the flagellum. (A) Diagram showing the procedure of ATP iontophoresis. (B) Responses of a flagellum to ATP iontophoresis, printed from a cine-film, showing the spermatozoon before (upper) and about 0.4 s after ATP application. *Reproduced from [79].* (C) Diagram showing how local active sliding (indicated by arrows) between two flexible filaments is converted into bending. (a) Without sliding. (b) If sliding is restrained on both sides of the active region, two bends are formed in opposite directions. (c) The same condition as (b), but the direction of active sliding is opposite to (b), which produces two bends each in the opposite directions to those of the bends in (b).

In the local reactivation experiments, local bending could be induced repeatedly in an additive manner by repetitive application of ATP [58] (Fig. 13.6A,B). Furthermore, when the local bending reached a certain point the direction of the bending reversed, so that the bending alternated between two opposite directions, just like that found in normally beating flagella. Thus, oscillatory bending can occur in any region of the axoneme, and in this case the bending is also planar. These studies indicate that the basic mechanism underlying the regulation of the microtubule-sliding activity of dynein to induce oscillatory bending is located in the "9+2" structure; planar bending tells us that the activity of the dynein arms must be coordinated so that at any moment some arms are active while others are not.

The elastase-treated axonemes showed localized bending in response to repetitive activation by ATP iontophoresis, as in the untreated axonemes [58] (Fig. 13.6C). This is interesting because bath application of ATP to elastase-treated axonemes induces microtubule sliding (Fig. 13.3A), which is quite different from the beating induced in untreated axonemes. As the elastase-treated axonemes retain the capability for oscillatory bending when they are activated locally by ATP

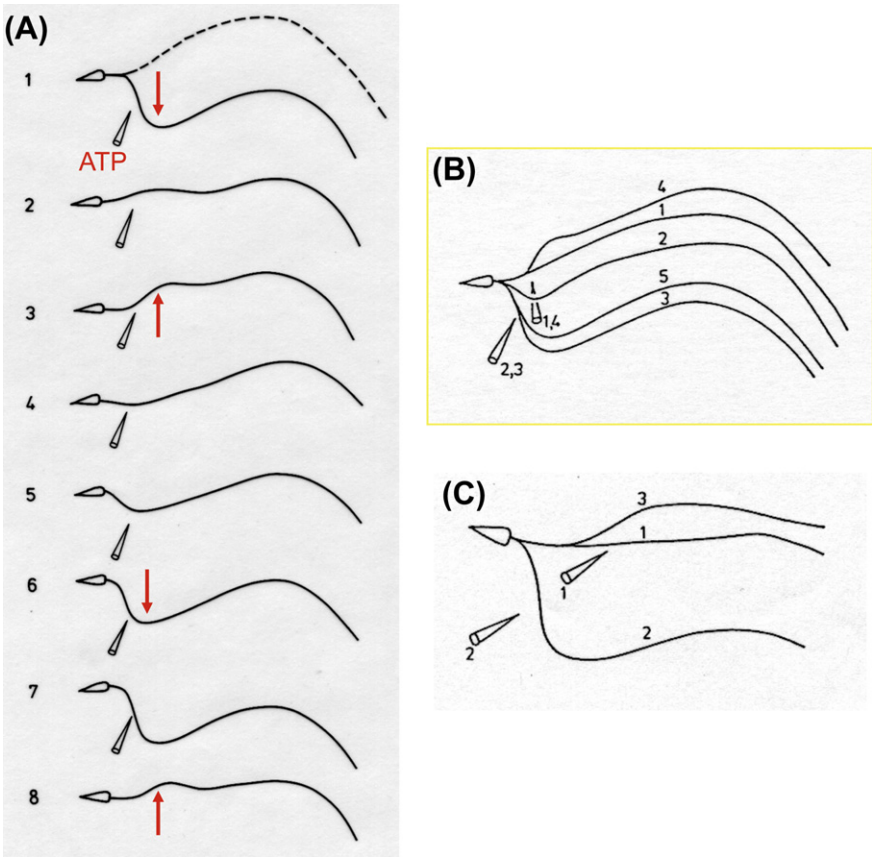

Figure 13.6 Responses of demembranated intact (A, B) and elastase-treated (C) axonemes to repetitive local reactivation by ATP iontophoresis. Sequential tracings in (A) and superimposed tracings in (B) were obtained from a cine-film recording of the same spermatozoon. Each number indicates the sequential order of response. The formation of paired bends alternated between two opposite directions (indicated with arrows in (A)). *Reproduced from [58].*

iontophoresis, while the trypsin-treated axonemes lack such an ability to oscillate [58], the regulatory system responsible for oscillation may still remain after elastase treatment. Thus, these results support the view that the splitting behavior of elastase-treated axonemes (Fig. 13.4) reflects the regulation of dynein activity in beating flagella.

It was previously thought that the interdoublet links are responsible for restricting free sliding of doublet microtubules in the axoneme. However, the observation that elastase-treated axonemes are still capable of continuous beating for more than a minute at 1 mM ATP [28] indicates that, in addition to the interdoublet links, dynein cross-bridges play an important role as linkers between the doublets during flagellar motility at high (physiological) concentrations of ATP [27]. It is probable that the ATP-dependent crosslinking state of dynein arms is involved in the regulation of dynein activity during flagellar beating.

13.5 The Mechanism of Oscillation

How can we examine the mechanism regulating the coordinated activity of dynein that produces the difference in the amount of microtubule sliding during flagellar oscillation? Experiments that will reveal this mechanism are awaited, but there are many technical difficulties to be overcome. One of the difficulties concerns how to analyze microtubule sliding in a flagellum that can oscillate. One way of understanding the mechanism is to use mathematical analysis. Another relies on an experiment using elastase-treated axonemes.

13.5.1 Theoretical Models of Oscillation and the Oscillator

Building on the classic mathematical analysis by Machin [82], the idea of a mechanochemical oscillator in flagella has been proposed and evolved into a model in which the active sliding process is controlled by the curvature of the flagellum [83]. Computer simulation using the curvature-controlled model showed that the control specification can generate oscillation and bending wave propagation in reactivated flagella, but is insufficient to completely determine the characteristics of their movement: particularly, it was not possible to explain why removal of the outer arms resulted in decreased beat frequency but little change in the bending pattern [84–86]. An alternative simulation model, which incorporates different cross-bridge models for the inner and outer arms, with different force–velocity curves, fits the real situation well and suggests that the inner-dynein arms may generate most (90% or more) of the power output [87].

A theoretical model that considers the "transverse" force, which develops between the outer doublets of the axoneme as the regulator for activating and inactivating the dynein and organizing the flagellar beat, was proposed by Lindemann, based on a "geometric clutch" hypothesis [88–90]. The geometric clutch mechanism predicts that imposed (passive) bending will initiate episodes of dynein engagement and can consequently synchronize the onset of sliding and the phase of the beat cycle. A simulation based on this hypothesis generates spontaneous stable oscillations. Use of a control function that depends not only on curvature but also on the cumulative shear force on the doublets permits global feedback to the activity state of the local segment. The model overcomes a problem in the curvature control approach [91,92] and provides a framework that may be useful in explaining the operation of the axoneme. A modification of this model that uses force–velocity relationships for the outer- and inner-arm dyneins similar to those described by Brokaw [87], where the inner arms contribute most of the driving force at low shear velocities, can simulate the oscillation after removal of the outer-arm dynein [90].

The oscillatory capability is associated with active sliding throughout the flagellum and is not a unique property of its basal end. This suggests that the mechanochemical oscillator is a mechanism for producing oscillatory sliding of microtubules independently of flagellar bending. Oscillatory models based on the

oscillatory microtubule sliding caused by the activity of dynein cross-bridge cycling [93,94] suggest the possibility that oscillatory sliding may occur in fragments of axonemes that do not bend. In fragmented axonemes, the so-called motility-uncoupled ATPase activity is very low compared to the motility-coupled ATPase activity determined during flagellar beating [95,64]. This suggests a low possibility of oscillatory sliding within axonemal fragments. However, highly sensitive measurement of the movement of beads [96] attached to the doublet microtubules of axonemal fragments obtained from sea urchin sperm flagella revealed oscillation [97]. The oscillation is of a low amplitude (from 4 to 36 nm, reflecting the size of tubulin repeats) and high frequency that changes with the ATP concentration (~300 Hz at 1 mM ATP) [98]. This indicates a possible oscillatory behavior of the dynein arms and/or the microtubule sliding within the axonemes, but the low amplitude is not enough to explain oscillatory sliding with an amplitude of more than 50 nm in beating flagella [99].

Our study has shown oscillation of dynein force with an amplitude of about 32 nm, a similar amplitude to that of the high-frequency oscillation of the axoneme [100]. This indicates that oscillation is an intrinsic property of dynein itself. Although we do not know whether the mechanism of regular oscillation of flagella involves the probabilistic behavior of single dynein molecules, the mechanochemical oscillator may be incorporated into microtubule sliding as a result of dynein force generation. These findings, however, do not exclude the possible dependence of the mechanochemical oscillator on bending.

13.5.2 Mechanical Activation and Flagellar Oscillation

Certain aspects of flagellar movement — for example, beat frequency and wave initiation — can be modified by mechanical manipulation of the flagellum [47,48,101,102]. It has also been shown that inactive dynein arms in the axoneme are activated by bending the doublet microtubules [103,104]. The activity of the dynein arms thus appears to be modulated, in some cases enhanced, by the mechanical environment or mechanical "signals." It seems probable that bending of the doublet microtubules constitutes an important factor in the self-regulatory feedback system underlying flagellar oscillation [104]. Our studies on demembranated and motionless flagella at low ATP have shown that mechanical signals are important factors governing flagellar oscillation [27,105].

Demembranated flagella that are immotile at low ATP (2.0–3.0 μM), which is around the threshold concentration for beating, become motile and oscillate when they are distorted with two microneedles, one attached to the head and the other to the distal end of the flagellum (Movie 13.4). However, simple bending of the axoneme so as to increase the angle of a single bend does not induce oscillation (Fig. 13.7A). A key step for inducing oscillation by imposed bending is to form a pair of bends (Fig. 13.7B) [105]. This effective bending, which produces

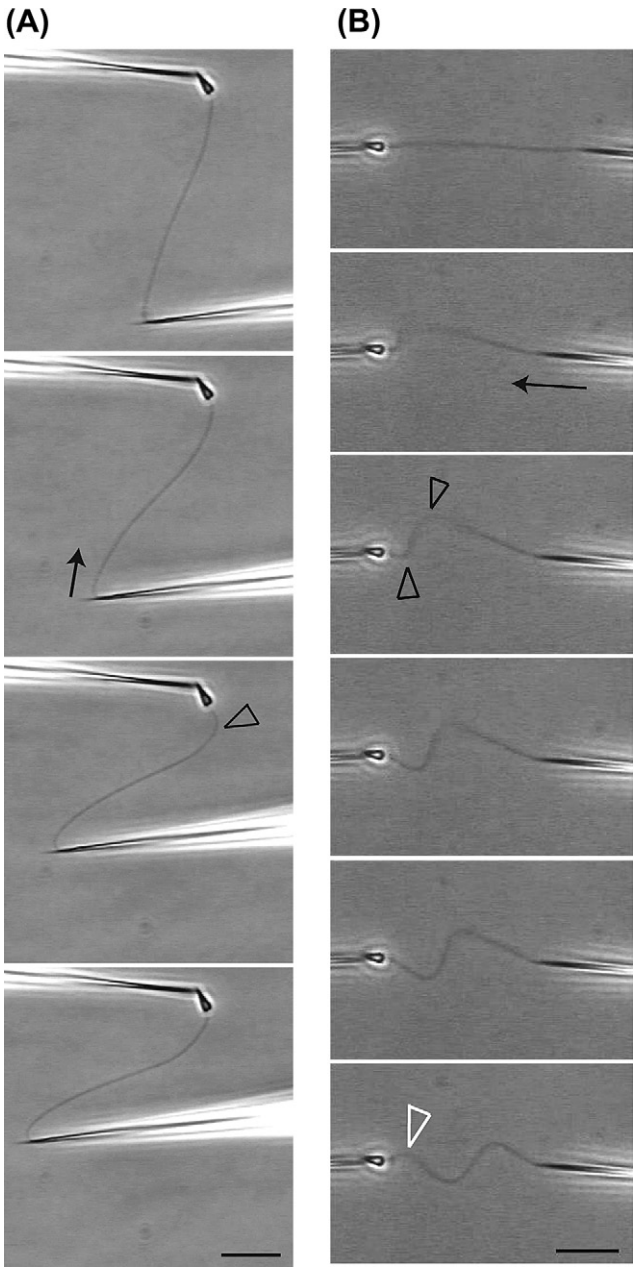

Figure 13.7 Bending-induced oscillation in immotile flagella at 2.0 μM ATP. Sequential video images showing imposed bending with two microneedles, one (left microneedle) attached to the head and the other (right microneedle) to the end of the flagellum. Bending of the flagellum by moving the right microneedle towards the head (arrows) induced a bend near the head (A) and a pair of bends (B) (black arrowheads). The bending-induced single bend (A) did not induce a new flagellar response, while the paired bends (B) induced a new bend (white arrowhead) in the proximal region of the flagellum that was followed by oscillation. The oscillation continued under the mechanical constraint. Scale bar = 10 μm.

differences in the amount of microtubule sliding along the flagellum (Fig. 13.5), may be related to the direction-dependent factor important for the bending-induced reversal described by Hayashi and Shingyoji [106]. There is a regional difference in the axoneme in terms of responsiveness to the distortion: a smaller amount of bending induces oscillation only in the proximal one third of the axoeneme, indicating a higher sensitivity of the proximal dyneins to the mechanical signal. This may be related to the wave propagation toward the tip of the flagella. The bending-induced oscillation continues under the mechanical constraint but is terminated by the removal of the constraint by detaching the microneedle from the distal end of the flagellum. In the presence of a low concentration of ADP (2.0–2.5 μM) in addition to ATP (2.0–2.5 μM), however, the removal of the microneedle does not terminate the oscillation [105]. This indicates that the presence of ADP is necessary for switching dynein activity and thus oscillatory bending (Fig. 13.2C).

13.5.3 Mechanical Induction of the Switching of Dynein Activity

Microtubule sliding in elastase-treated axonemes, which is restricted to specific interdoublet sites beside the central pair, is associated with the regulation of dynein motile activity at high ATP concentrations. Thus, the central pair plays a key role in the regulation of dynein activity at high ATP. If the distribution of active dyneins in the elastase-treated axonemes reflects the regulation of dynein activity in beating flagella, switching between the active and the inactive dyneins should be induced by a mechanical signal of bending. Furthermore, the direction of bending must be an important factor involved in switching.

In the elastase-treated axonemal fragments, a high ATP concentration (1 mM) at high Ca^{2+} (10^{-4} M) induces sliding disintegration, which splits the axoneme into two doublet bundles of unequal thickness, mainly because of the activity of the dynein arms on doublet 7 [66,106]. This is depicted in Figure 13.8C as forward sliding, in which the thinner bundle moves leftward. Successive applications of ATP, released from caged ATP by repetitive UV flashes, induce further sliding of the thinner bundle in the same (forward) direction. However, bending the region of overlap between the two bundles by more than 90° can induce in some fragments a reversal of the direction of sliding between the bundles (Fig. 13.8C, backward sliding; Movies 13.5 and 13.6) [104]. The reversal is probably induced by switching the dynein activity from doublet 7 to doublet 3 (or 2). The rate of reversal (about 48%) in the axonemal fragments is not high, meaning that bending itself is not the sole dynein-regulating factor related to the switching mechanism. In contrast, when the bending direction is controlled by using elastase-treated Ca^{2+}-induced quiescent flagella, as shown in Figure 13.8A,B, reversal of the sliding direction is induced at a high rate (71%), depending on the direction of the imposed bending [27,106].

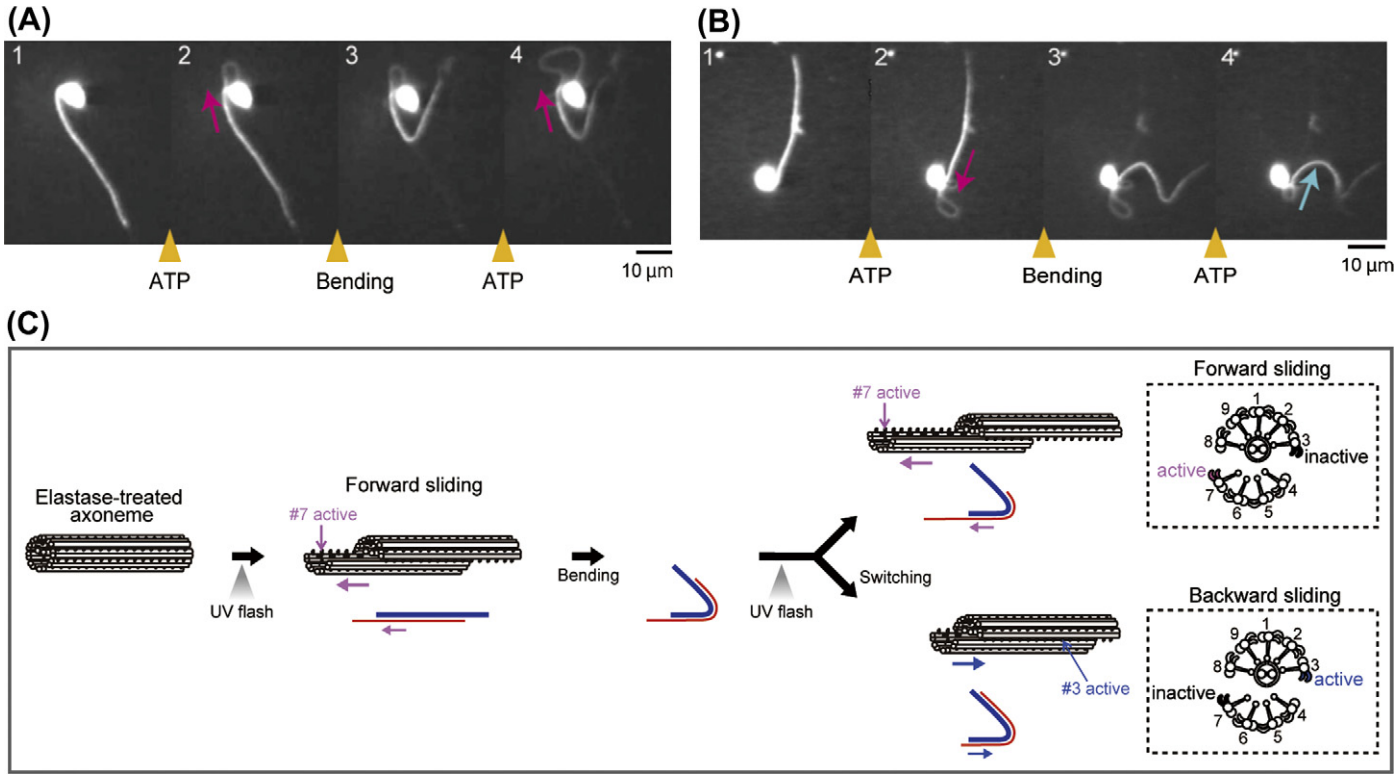

Figure 13.8 Bending-induced reversal of microtubule sliding. (A,B): Video images showing forward (red arrows in (A) and (B2)) and backward (blue arrow in (B4)) sliding before and after imposed bending (Bending). Sliding was induced by UV flashes in the elastase-treated quiescent flagella that had a P-bend at the base. Bending was applied in the same direction as the P-bend (A) and in the opposite direction (B). (C) Diagram showing an interpretation of the experiment. *Modified from figure 3 of [106,107].*

Furthermore, in the elastase-treated axonemal fragments the rate of bending-induced reversal is increased by the presence of ADP [107]. It is tempting to speculate that bending-induced activation of dynein arms on doublet 3 occurs upon ADP binding to dynein, but ADP binding to the regulatory sites of dyneins on doublet 3 has not been demonstrated when their activity is switched on by bending. It seems likely that stable ADP binding to dynein is necessary for the bending-induced activation of dynein in the ATP-inhibited state, but regulation of the activity of dynein that is already active may not involve association and dissociation of ADP with dynein during beating. In other words, once ADP binds to dynein, the dynein can probably respond more sensitively to mechanical signals than before the ADP binding [107].

In the protease-untreated axonemes, active sliding occurs between the doublet groups 8–4 and 5–7 (or 8–3 and 4–7) for a P-bend formation and between 4–8 and 9–3 (or 3–8 and 9–2) for an R-bend formation (Fig. 13.9). The central-pair microtubules are located in the doublet groups of 8-4 or 4-8, so during beating the position of the central pair may alternate between the doublet 1 side (in the 8–4 (or 8–3) group) and the doublet 5 side (in the 4–8 (or 3–8) group). In this respect, the diameter of the oscillation of axonemes of sea uchin sperm flagella is interesting [108]. In this study, transverse oscillatory motion of the axoneme diameter (through the doublet 1–doublet 5 axis) with maximum amplitude of $\sim$10 nm and frequency of $\sim$300 Hz was recorded using modified atomic force microscopy.

13.6 Outlook

The study of flagellar and ciliary movement over the last 50 or more years has revealed the basic features of its mechanism. It is now known that dynein is not a simple force-generating motor: by responding to the mechanical signal associated with flagellar bending, it can dynamically switch its functional mode from the inactive cross-bridging state to the active sliding state in the presence of constant, physiologically high, concentrations of ATP. The different modes of dynein functions are determined by the position in the 9+2 structure as well as by the phase of beating: the central-pair microtubules are responsible for determining dynein activity and the dyneins in the plane of the central pair behave differently from those in the beat plane that is perpendicular to the central pair plane.

In beating flagella, cyclical bending is produced by regulating the activity of all dynein arms in the bend plane as well as by switching the dynein activity in the plane of the central pair in the interbend regions (Fig. 13.9). To understand flagellar oscillation, we need to elucidate the mechanism regulating the combination of these dynein functions. The disintegration of axonemes into smaller bundles or individual doublets induced by bending, which was observed frequently in axonemal fragments [104], was infrequent in quiescent flagella [106]. This suggests that the activation of all dynein arms by imposed bending

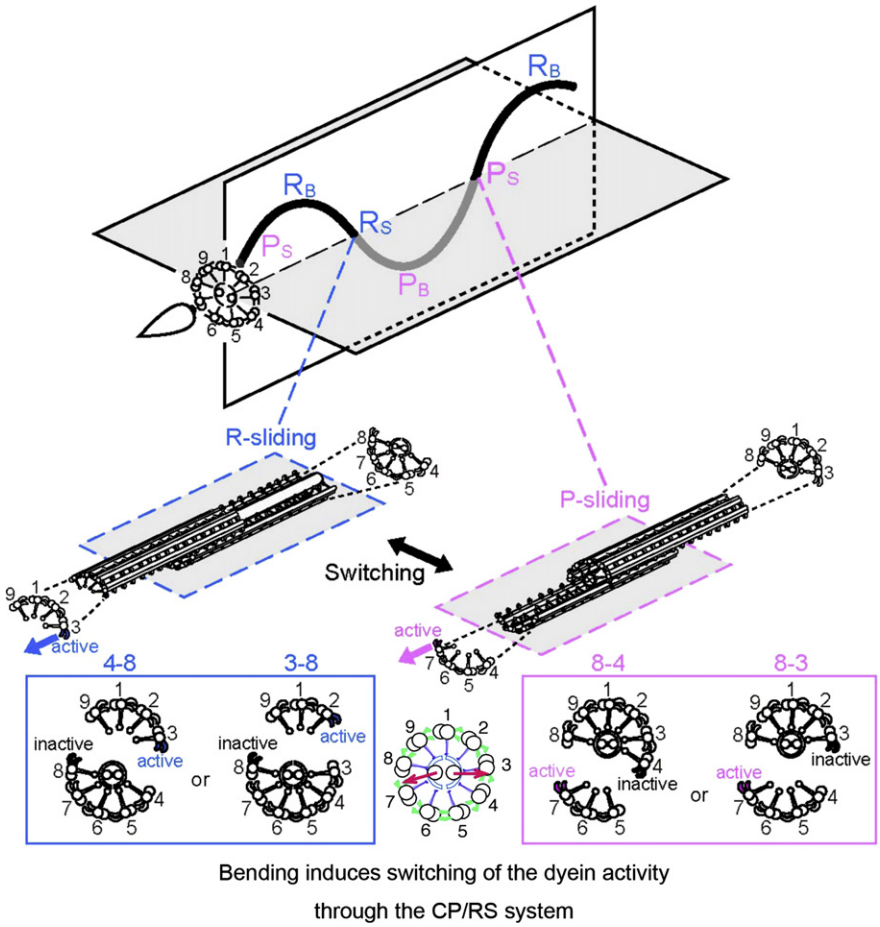

Figure 13.9 Diagrams showing the possible regulation of dynein activity in a switching model of beating flagella. In the sea urchin sperm flagellum, principal and reverse bends (P_B and R_B) are cyclically formed in the plane of beat (white), which is perpendicular to the plane of the central pair (grey). The formation of P_B and R_B is due to P-sliding (P_S) and R-sliding (R_S), respectively, induced by the dynein arms of doublets 7 and 3 (or 2). The model is based on our previous studies, shown in Figures 13.3–13.6 and 13.8. In the locally reactivated axonemes (Figs. 13.5 and 13.6), microtubule sliding occurs only in the region (interbend region) between the pair of opposite bends and a reversal of the sliding direction between the two bends leads to alternation of the direction of these bends. Coupling of the mechanism regulating microtubule sliding in the paired bend formation with the regulation that induces a reversal of the sliding direction in the bending region (Fig. 13.8) may constitute a basis for the coordination of cyclical bend formation and propagation.

requires that the force be applied to dynein arms in the direction not parallel to the beat plane. In addition to the change in the dynein attachment state resulting from the shear induced by the imposed bending, distortion of the axoneme could occur along the doublets in the bend plane, tilting the radial spokes and changing the geometric relationship between the doublets. These factors may activate

the dynein arms on the doublets in the bend plane, and are probably linked to the switching of the activity of dynein on both sides of the central pair. Thus, the combination of the regulation of the activity of all dynein arms in the beat plane and the mechanism for switching the dynein activity on both sides of the central pair is essential for flagellar beating.

How the motile activity of dynein is switched on and off by the mechanical signal of bending – probably through nucleotide binding to the dynein heads, conformational and functional changes to the dynein tail and stalk, and the flexural rigidity of microtubules – is one of the important questions that the future must answer.

Acknowledgments

I thank Prof. Keiichi Takahashi for valuable discussions and the members of my group, past and present, who have collaborated with me on dynein and sea urchin sperm flagella (M. Yoshimura, T. Kobayashi, H. Imai, I. Nakano, Y. Inoue, Y. Morita, R. Ishikawa, A. Yoshimura, S. Hayashi, Y. Kambara, M. Wada, H. Yoke, and Y. Watanabe).

References

[1] I. Manton, B. Clark, An electron microscope study of the spermatozoid of Sphagnum, J. Exp. Botany 3 (1952) 265–275.
[2] B.A. Afzelius, The flagellar apparatus of marine spermatozoa: Evolutionary and functionary aspects, Symp. Soc. Exp. Biol. 35 (1982) 495–519.
[3] I.R. Gibbons, Cilia and flagella of eukaryotes, J. Cell Biol. 91 (1981) 107s–124s.
[4] C.W. Bell, C.L. Fraser, W.S. Sale, W.J. Tang, I.R. Gibbons, Preparation and purification of dynein, Method. Cell Biol. 24A (1982) 373–397.
[5] F.D. Warner, D.R. Mitchell, C.R. Perkins, Structural conformation of the ciliary ATPase dynein, J. Mol. Biol. 114 (1977) 367–384.
[6] G.B. Witman, N. Minervini, Dynein arm conformation and mechanochemical transduction in the eukaryotic flagellum, Symp. Soc. Exp. Biol. 35 (1982) 203–224.
[7] W.S. Sale, L.A. Fox, S.A. Milgram, Composition and organization of the inner row dynein arms, in: F.D. Warner, P. Satir, I.R. Gibbons (Eds.), Cell Movement, Volume 1: The Dynein ATPases, Alan R. Liss Inc., New York, 1989, pp. 89–102.
[8] G.B. Witman, Introduction to cilia and flagella, in: R.A. Bloodgood (Ed.), Ciliary and Flagellar Membranes, Plenum Publishing Corporation, New York, 1990, pp. 1–30.
[9] R. Kamiya, Functional diversity of axonemal dyneins as studied in *Chlamydomonas* mutants, Int. Rev. Cytol. 219 (2002) 115–155.
[10] T. Heuser, M. Raytchev, J. Krell, M.E. Porter, D. Nicastro, The dynein regulatory complex is the nexin link and major regulatory node in cilia and flagella, J. Cell Biol. 187 (2009) 921–933.
[11] G. Mocz, I.R. Gibbons, Model for the motor component of dynein heavy chain based on homology to the AAA family of oligomeric ATPases, Structure 9 (2001) 93–103.
[12] M. Samsó, M. Rademacher, J. Frank, M.P. Koonce, Structural characterization of a dynein motor domain, J. Mol. Biol. 276 (1998) 927–937.
[13] I.R. Gibbons, J.E. Garbarino, C.E. Tan, S.L. Reck-Peterson, R.D. Vale, A.P. Carter, The affinity of the dynein microtubule-binding domain is modulated by the conformation of its coiled-coil stalk, J. Biol. Chem. 280 (2005) 23960–23965.
[14] H. Ueno, T. Yasunaga, C. Shingyoji, K. Hirose, Dynein pulls microtubules without rotating its stalk, Proc. Natl. Acad. Sci. USA 105 (2008) 19702–19707.

[15] A.J. Roberts, N. Numata, M.L. Walker, Y.S. Kato, B. Malkova, T. Kon, R. Ohkura, F. Arisaka, P.J. Knight, K. Sutoh, S.A. Burgess, AAA^+ ring and linker swing mechanism in the dynein motor, Cell 136 (2009) 485–495.
[16] I.R. Gibbons, B.H. Gibbons, G. Mocz, D.J. Asai, Multiple nucleotide-binding sites in the sequence of dynein β chain, Nature 352 (1991) 640–643.
[17] K. Ogawa, Four ATP-binding sites in the midregion of the β heavy chain of dynein, Nature 352 (1991) 643–645.
[18] M.P. Koonce, P.M. Grissom, J.R. McIntosh, Dynein from *Dictyostelium*: Primary structure comparisons between a cytoplasmic motor enzyme and flagellar dynein, J. Cell Biol. 119 (1992) 1597–1604.
[19] G. Mocz, I.R. Gibbons, Phase partition analysis of nucleotide binding to axonemal dynein, Biochemistry 35 (1996) 9204–9211.
[20] A. Silvanovich, M.G. Li, M. Serr, S. Mische, T.S. Hays, The third P-loop domain in cytoplasmic dynein heavy chain is essential for dynein motor function and ATP-sensitive microtubule binding, Mol. Biol. Cell 14 (2003) 1355–1365.
[21] T. Kon, M. Nishiura, R. Ohkura, Y.Y. Toyoshima, K. Sutoh, Distinct functions of nucleotide-binding/hydrolysis sites in the four AAA modules of cytoplasmic dynein, Biochemistry 43 (2004) 11266–11274.
[22] Y. Takahashi, M. Edamatsu, Y.Y. Toyoshima, Multiple ATP-hydorolyzing sites that potentially function in cytoplasmic dynein, Proc. Natl. Acad. Sci. USA 101 (2004) 12865–12869.
[23] Y. Inoue, C. Shingyoji, The roles of noncatalytic ATP binding and ADP binding in the regulation of dynein motile activity in flagella, Cell Motil. Cytoskel. 64 (2007) 690–704.
[24] K. Kikushima, T. Yagi, R. Kamiya, Slow ADP-dependent acceleration of microtubule translocation produced by an axonemal dynein, FEBS Lett. 563 (2004) 119–122.
[25] K. Shiroguchi, Y.Y. Toyoshima, Regulation of monomeric dynein activity by ATP and ADP concentrations, Cell Motil. Cytoskel. 49 (2001) 189–199.
[26] T. Yagi, ADP-dependent microtubule translocation by flagellar inner-arm dyneins, Cell Struct. Funct. 25 (2000) 263–267.
[27] C. Shingyoji, Analysis of the role of nucleotides in axonemal dynein function, Method. Cell Biol. 92 (2009) 113–131.
[28] A. Yoshimura, I. Nakano, C. Shingyoji, Inhibition by ATP and activation by ADP in the regulation of flagellar movement in sea urchin sperm, Cell Motil. Cytoskel. 64 (2007) 777–793.
[29] F.D. Warner, The fine structure of the ciliary and flagellar axoneme, in: M.A. Sleigh (Ed.), *Cilia and Flagella*, Academic Press, New York, 1974, pp. 11–37.
[30] H. Sakakibara, H. Kojima, Y. Sakai, E. Katayama, K. Oiwa, Inner-arm dynein c of *Chlamydomonas* flagella is a single-headed processive motor, Nature 400 (1999) 586–590.
[31] C. Allen, G.G. Borisy, Structural polarity and directional growth of microtubules of *Chlamydomonas* flagella, J. Mol. Biol. 90 (1974) 381–402.
[32] S. Westermann, K. Weber, Post-translational modifications regulate microtubule function, Nature Rev. Mol. Cell Biol. 4 (2003) 938–947.
[33] M.H. Bré, V. Redeker, M. Quibell, J. Damanaden-Delome, C. Bressac, J. Cosson, P. Huitorel, J.M. Schmitter, J. Rossler, T. Johnson, A. Adoutte, N. Levilliers, Axonemal tubulin polyglycylation probed with two monoclonal antibodies: Widespread evolutionary distribution, appearance during spermatozoan maturation and possible function in motility, J. Cell Sci. 109 (1996) 727–738.
[34] L. Multigner, I. Pignot-Paintrand, Y. Saoudi, D. Job, U. Plessmann, M. Rüdiger, K. Weber, The A and B tubules of the outer doublets of sea urchin sperm axonemes are composed of different tubulin variants, Biochemistry 35 (1996) 10862–10871.
[35] K.A. Johnson, The axonemal microtubules of the *Chlamydomonas* flagellum differ in tubulin isoform content, J. Cell Sci. 111 (1998) 313–320.

[36] L. Xia, B. Hai, Y. Gao, D. Bumette, R. Thazhath, J. Duan, M.H. Bré, N. Levillers, M.A. Gorovsky, J. Gaertig, Polyglycylation of tubulin is essential and affects cell motility and division of *Tetrahymena thermophila*, J. Cell Biol. 149 (2000) 1097–1106.
[37] S. Suryavanshi, B. Edde, L.A. Fox, S. Guerrero, R. Hard, T. Hennessey, A. Kabi, D. Malison, D. Pennock, W.S. Sale, D. Wloga, J. Gaertig, Tubulin glutamylation regulates ciliary motility by altering inner dynein activity, Curr. Biol. 20 (2010) 435–440.
[38] T. Kubo, H. Yanagisawa, T. Yagi, M. Hirono, R. Kamiya, Tubulin polyglutamylation regulates axonemal motility by modulating activities of inner-arm dyneins, Curr. Biol. 20 (2010) 441–445.
[39] T. Miki-Noumura, Dark-field microscopic study of microtubules in solution, Int. Rev. Cytol. 122 (1990) 65–104.
[40] J. Howard, Mechanics of the cytoskeleton, in: Mechanics of Motor Proteins and the Cytoskeleton, Sinauer Associates, Inc, Massachusetts, 2001, pp. 135–149.
[41] M. Okuno, Y. Hiramoto, Direct measurements of the stiffness of echinoderm sperm flagella, J. Exp. Biol. 79 (1979) 235–243.
[42] M. Okuno, Inhibition and relaxation of sea urchin sperm flagella by vanadate, J. Cell Biol. 85 (1980) 712–725.
[43] C.K. Omoto, C. Kung, The pair of central tubules rotates during ciliary beat in *Paramecium*, Nature 279 (1979) 532–534.
[44] C.K. Omoto, C. Kung, Rotation and twist of the central-pair microtubules in the cilia of *Paramecium*, J. Cell Biol. 87 (1980) 33–46.
[45] C.K. Omoto, G.B. Witman, Functionally significant central-pair rotation in a primitive eukaryotic flagellum, Nature 290 (1981) 708–710.
[46] R. Kamiya, Extrusion and rotation of the central-pair microtubules in detergent-treated *Chlamydomonas* flagella, Cell Motil. Cytoskel. (Suppl. 1) (1982) 169–173.
[47] I.R. Gibbons, C. Shingyoji, A. Murakami, K. Takahashi, Spontaneous recovery after experimental manipulation of the plane of beat in sperm flagella, Nature 325 (1987) 351–352.
[48] C. Shingyoji, I.R. Gibbons, A. Murakami, K. Takahashi, Effect of imposed head vibration on the stability and waveform of flagellar beating in sea urchin spermatozoa, J. Exp. Biol. 156 (1991) 63–80.
[49] K. Takahashi, C. Shingyoji, J. Katada, D. Eshel, I.R. Gibbons, Polarity in spontaneous unwinding after prior rotation of the flagellar beat plane in sea-urchin spermatozoa, J. Cell Sci. 98 (1991) 183–189.
[50] C.K. Omoto, I.R. Gibbons, R. Kamiya, C. Shingyoji, K. Takahashi, G.B. Witman, Rotation of the central pair microtubules in eukaryotic flagella, Mol. Biol. Cell 10 (1999) 1–4.
[51] K.E. Summers, I.R. Gibbons, Adenosine triphosphate-induced sliding of tubules in trypsin-treated flagella of sea-urchin sperm, Proc. Natl. Acad. Sci. USA 68 (1971) 3092–3096.
[52] K.E. Summers, I.R. Gibbons, Effects of trypsin digestion on flagellar structures and their relationship to motility, J. Cell Biol. 58 (1973) 618–629.
[53] W.S. Sale, P. Satir, Splayed *Tetrahymena* cilia: A system for analyzing sliding and axonemal spoke arrangements, J. Cell Biol. 71 (1976) 589–605.
[54] W.S. Sale, P. Satir, Direction of active sliding of microtubules in *Tetrahymena* cilia, Proc. Natl. Acad. Sci. USA 74 (1977) 2045–2049.
[55] Y. Yano, T. Miki-Noumura, Sliding velocity between outer doublet microtubules of sea-urchin sperm axonemes, J. Cell Sci. 44 (1980) 169–186.
[56] K. Takahashi, C. Shingyoji, S. Kamimura, Microtubule sliding in reactivated flagella, Symp. Soc. Exp. Biol. 35 (1982) 159–177.
[57] S. Kamimura, M. Yano, H. Shimizu, ATP hydrolysis coupled to microtubule sliding in sea-urchin sperm flagella, J. Biochem. 97 (1985) 1509–1515.
[58] C. Shingyoji, K. Takahashi, Cyclical bending movements induced locally by successive iontophoretic application of ATP to an elastase-treated flagellar axoneme, J. Cell Sci. 108 (1995) 1359–1369.

[59] K. Inaba, Conformational changes of dynein: Mapping and sequence analysis of ATP/vanadate-dependent trypsin-sensitive sites on the outer arm dynein β heavy chain from sea urchin sperm flagella, J. Biochem. 127 (2000) 1115–1120.
[60] H. Imai, C. Shingyoji, Effects of trypsin-digested outer-arm dynein fragments on the velocity of microtubule sliding in elastase-digested flagellar axonemes, Cell Struct. Funct. 28 (2003) 71–86.
[61] K. Ogawa, Studies on flagellar ATPase from sea urchin spermatozoa. II. Effects of trypsin digestion on the enzyme, Biochim. Biopys. Acta 293 (1973) 514–525.
[62] R.A. Ow, W.-J.Y. Tang, G. Mocz, I.R. Gibbons, Tryptic digestion of dynein 1 in low salt medium. Origin and properties of fragment A, J. Biol. Chem. 262 (1987) 3409–3414.
[63] C.J. Brokaw, Elastase digestion of demembranated sperm flagella, Science 207 (1980) 1365–1367.
[64] C.J. Brokaw, T.F. Simonick, Mechanochemical coupling in flagella: V. Effects of viscosity on movement and ATP-dephosphorylation of triton-demembranated sea-urchin spermatozoa, J. Cell Sci. 23 (1977) 227–241.
[65] M. Yoshimura, C. Shingyoji, Effects of the central pair apparatus on microtubule sliding velocity in sea urchin sperm flagella, Cell Struct. Funct. 24 (1999) 43–54.
[66] I. Nakano, T. Kobayashi, M. Yoshimura, C. Shingyoji, Central-pair-linked regulation of microtubule sliding by calcium in flagellar axonemes, J. Cell Sci. 116 (2003) 1627–1636.
[67] C.J. Brokaw, Calcium-induced asymmetrical beating of Triton-demembranated sea urchin sperm flagella, J. Cell Biol. 82 (1979) 401–411.
[68] B.H. Gibbons, I.R. Gibbons, Calcium-induced quiescence in reactivated sea urchin sperm, J. Cell Biol. 84 (1980) 13–27.
[69] W.S. Sale, The axonemal axis and Ca^{2+}-induced asymmetry of active microtubule sliding in sea urchin sperm tails, J. Cell Biol. 102 (1986) 2042–2052.
[70] H. Bannai, M. Yoshimura, C. Shingyoji, Calcium regulation of microtubule sliding in reactivated sea urchin sperm flagella, J. Cell Sci. 113 (2000) 831–839.
[71] J. Wais-Steider, P. Satir, Effect of vanadate on gill cilia: Switching mechanism in ciliary beat, J. Supramol. Struct. 11 (1979) 339–347.
[72] P. Satir, T. Matsuoka, Splitting the ciliary axoneme: Implications for a "switch-point" model of dynein arm activity in ciliary motion, Cell Motil. Cytoskel. 14 (1989) 345–358.
[73] C.B. Lindemann, A. Orlando, K.S. Kanous, The flagellar beat of rat sperm is organized by the interaction of two functionally distinct populations of dynein bridges with a stable central axonemal partition, J. Cell Sci. 102 (1992) 249–260.
[74] P. Satir, W.S. Sale, Tails of *Tetrahymena*, J. Protozool. 24 (1977) 498–501.
[75] P. Satir, Switching mechanisms in the control of ciliary motility, Modern Cell Biol. 4 (1985) 1–46.
[76] E.F. Smith, Regulation of flagellar dynein by the axonemal central apparatus, Cell Motil. Cytoskel. 52 (2002) 33–42.
[77] B. Afzelius, Electron microscopy of the sperm tail, J. Biophys. Biochem. Cytol. 5 (1959) 269–278.
[78] P. Satir, Studies on cilia: III. Further studies on the cilium tip and a "sliding filament" model of ciliary motility, J. Cell Biol. 39 (1968) 77–94.
[79] C. Shingyoji, A. Murakami, K. Takahashi, Local reactivation of Triton-extracted flagella by iontophoretic application of ATP, Nature 265 (1977) 269–270.
[80] C.J. Brokaw, Direct measurements of sliding between outer doublet microtubules in swimming sperm flagella, Science 243 (1989) 1593–1596.
[81] C.J. Brokaw, Microtubule sliding in swimming sperm flagella: Direct and indirect measurements on sea urchin and tunicate spermatozoa, J. Cell Biol. 114 (1991) 1201–1215.
[82] K.E. Machin, Wave propagation along flagella, J. Exp. Biol. 35 (1958) 796–806.

[83] C.J. Brokaw, Bend propagation by a sliding filament model for flagella, J. Exp. Biol. 55 (1971) 289–304.
[84] C.J. Brokaw, Computer simulation of flagellar movement. I. Demonstration of stable bend propagation and bend initiation by the sliding filament model, Biophys. J. 12 (1972) 564–586.
[85] C.J. Brokaw, Computer simulation of flagellar movement. VI. Simple curvature-controlled models are incompletely specified, Biophys. J. 48 (1985) 633–642.
[86] C.J. Brokaw, Control of flagellar bending: A new agenda based on dynein diversity, Cell Motil. Cytoskel. 28 (1994) 199–204.
[87] C.J. Brokaw, Computer simulation of flagellar movement: VII. Conventional but functionally different cross-bridge models for inner and outer arm dyneins can explain the effects of outer arm dynein removal, Cell Motil. Cytoskel. 42 (1999) 134–148.
[88] C.B. Lindemann, A "Geometric Clutch" hypothesis to explain oscillations of the axoneme of cilia and flagella, J. Theor. Biol. 168 (1994) 175–189.
[89] C.B. Lindemann, A model of flagellar and ciliary functioning which uses the forces transverse to the axoneme as the regulator of dynein activation, Cell Motil. Cytoskel. 29 (1994) 141–154.
[90] C.B. Lindemann, Geometric clutch model version 3: The role of the inner and outer arm dyneins in the ciliary beat, Cell Motil. Cytoskel. 52 (2002) 242–254.
[91] C.J. Brokaw, Bending-wave propagation by microtubules and flagella, Math. Biosci. 90 (1988) 247–263.
[92] C.J. Brokaw, Operation and regulation of the flagellar oscillator, in: F.D. Warner, P. Satir, I.R. Gibbons (Eds.), Cell Movement, volume 1, Alan R. Liss, N.Y, 1989, pp. 267–279.
[93] C.J. Brokaw, Cross-bridge behavior in a sliding filament model for flagella, in: S. Inoué, R.E. Stephens (Eds.), Molecules and Cell Movement, Raven Press, New York, 1975, pp. 165–179.
[94] M. Murase, H. Shimizu, A model of flagellar movement based on cooperative dynamics of dynein-tubulin cross-bridges, J. Theor. Biol. 119 (1986) 409–433.
[95] B.H. Gibbons, I.R. Gibbons, Flagellar movement and adenosine triphosphatase activity in sea urchin sperm extracted with Triton X-100, J. Cell Biol. 54 (1972) 75–97.
[96] S. Kamimura, Direct measurement of nanometric displacement under an optical microscope, Applied Optics 26 (1987) 3425–3427.
[97] S. Kamimura, R. Kamiya, High-frequency nanometre-scale vibration in "quiescent" flagellar axonemes, Nature 340 (1989) 476–478.
[98] S. Kamimura, R. Kamiya, High-frequency vibration in flagellar axonemes with amplitudes reflecting the size of tubulin, J. Cell Biol. 116 (1992) 1443–1454.
[99] C.J. Brokaw, Flagellar oscillation: New vibes from beads, J. Cell Sci. 95 (1990) 527–530.
[100] C. Shingyoji, H. Higuchi, M. Yoshimura, E. Katayama, T. Yanagida, Dynein arms are oscillating force generators, Nature 393 (1998) 711–714.
[101] M. Okuno, Y. Hiramoto, Mechanical stimulation of starfish sperm flagella, J. Exp. Biol. 65 (1976) 401–413.
[102] C. Shingyoji, K. Yoshimura, D. Eshel, K. Takahashi, I.R. Gibbons, Effect of beat frequency on the velocity of microtubule sliding in reactivated sea urchin sperm flagella under imposed head vibration, J. Exp. Biol. 198 (1995) 645–653.
[103] K. Hayashibe, C. Shingyoji, R. Kamiya, Induction of temporary beating in paralyzed flagella of *Chlamydomonas* mutants by application of external force, Cell Motil. Cytoskel. 37 (1997) 232–239.
[104] Y. Morita, C. Shingyoji, Effects of imposed bending on microtubule sliding in sperm flagella, Curr. Biol. 14 (2004) 2113–2118.
[105] R. Ishikawa, C. Shingyoji, Induction of beating by imposed bending or mechanical pulse in demembranated, motionless sea urchin sperm flagella at very low ATP concentrations, Cell Struct. Funct. 32 (2007) 17–27.

[106] S. Hayashi, C. Shingyoji, Mechanism of flagellar oscillation − Bending-induced switching of dynein activity in elastase-treated axonemes of sea urchin sperm, J. Cell Sci. 121 (2008) 2833−2843.
[107] S. Hayashi, C. Shingyoji, Bending-induced switching of dynein activity in elastase-treated axonemes of sea urchin sperm − Roles of Ca^{2+} and ADP, Cell Motil. Cytoskel. 66 (2009) 292−301.
[108] H.M. Sakakibara, Y. Kunioka, T. Yamada, S. Kamimura, Diameter oscillation of axonemes in sea-urchin sperm flagella, Biophys. J. 86 (2004) 346−352.

In this chapter

14

Dynein and Intraflagellar Transport

George B. Witman
Department of Cell Biology, University of Massachusetts Medical School, Worcester, MA, USA

14.1 Introduction

This chapter, first provides a brief background on intraflagellar transport (IFT) and then reviews the studies culminating in the identification of the dynein motor that powers retrograde IFT. Next the known subunits of this dynein are described, their specific functions, and how they fit together in the intact motor. Finally, the function of the dynein in recycling IFT proteins and other flagellar components, in transporting signals from the cilium to the cell body, in ciliary maintenance, and so on, is discussed[1]. The evolutionary history of this dynein is only touched upon here and is treated in a broader context in Chapter 2 (on dynein evolution). Although not discussed further, it should be noted that defects in this dynein cause human diseases such as Jeune asphyxiating thoracic dystrophy and short-rib polydactyly syndrome [1,2].

The nomenclature of the dynein motor (and dynein subunits) responsible for retrograde IFT is complex and problematic, with different names used in different organisms and even within the same organism at different times and by different investigators. Because the dynein is present only in organisms that have cilia and flagella, its primary function is certainly IFT, and some publications have referred to it simply as "IFT dynein." However, such a term implies that IFT is its only function, a risky assumption given that IFT proteins are present in cells with no cilia [3] and that the motor may have roles in the cell body (see Section 14.6.5). Therefore, this chapter will use "cytoplasmic dynein 2" or simply "dynein 2" to refer to the intact motor. The commonly accepted name DHC1b will be used to refer to the cytoplasmic dynein 2 heavy chain (HC) in *Chlamydomonas reinhardtii* and some other invertebrates, and the current mammalian name Dync2h1 will be used to refer to the cytoplasmic dynein 2 HC in mammals [4]. The names of the

[1] *Because cilia and flagella are essentially identical organelles, the terms "cilia" and "flagella" will be used interchangeably throughout this chapter.*

Dyneins DOI: 10.1016/B978-0-12-382004-4.10014-7
Copyright © 2012 by Elsevier Inc. All rights reserved.

Table 14.1 Cytoplasmic Dynein 2 Subunit Names and Aliases[1]

Subunit	*C. reinhardtii*	*T. thermophila*	*Ca. elegans*	*H. sapiens*
Heavy chain	DHC1b	DYH2	DHC1b (CHE-3)	DYNC2H1 (DHC2, DHC1b, DNCHC2)
Intermediate chain	FAP133	D2IC	N.A.	WD-34
Light-intermediate chain	D1bLIC	D2LIC	XBX-1	DYNC2LI1 (D2LIC, LIC3)
Light chain 8	LC8 (FLA14)	LC8	DLC-1	DYNLL1 (DLC8, PIN) DYNLL2 (DLC8B)

[1] *Aliases are given in parentheses.*

cytoplasmic dynein 2 light-intermediate chain (LIC) in *C. reinhardtii* and mammals are derivatives of the HC designations. To aid the reader in following the literature, Table 14.1 summarizes the nomenclature, including former names and aliases, for the various cytoplasmic dynein 2 subunits in *C. reinhardtii*, *Caenorhabditis elegans*, *Tetrahymena thermophila*, and *Homo sapiens*.

14.2 Intraflagellar Transport

IFT is the active movement of multi-subunit particles along axonemal doublet microtubules in the space between the outer-doublet microtubules and the membrane of cilia and flagella [5,6,7]. IFT particles are usually moved steadily and without pause from the base to the tip of the flagellum and then back to the base, where there is a large concentration of IFT particles in close association with the basal body (see Fig. 14.1C, wild type). Movement of particles in the base-to-tip direction is termed anterograde IFT; movement in the opposite direction is termed retrograde IFT. IFT was first described by Kozminski et al. [8] in flagella of the unicellular algae *C. reinhardtii* and *Chlamydomonas moewusii*; the IFT machinery has since been shown to be present in almost all ciliated organisms. IFT particles themselves are made up of two sub-complexes: complex A, containing at least six subunits, and complex B, containing at least 13 subunits. IFT particles moving in the anterograde direction carry, as cargo, precursors for axonemal assembly, which occurs at the tip of the flagellum. The retrograde IFT motor returns the IFT particles and the anterograde IFT motor as well as axonemal turnover products to the cell body. IFT also transports membrane proteins and signals from the flagellum to the cell body and vice versa. Evidence from several organisms suggests that anterograde IFT is mediated by complex B whereas retrograde IFT is mediated by complex A [7]. IFT is necessary for both the assembly and maintenance of most types of cilia and flagella.

Using differential interference contrast light microscopy, Kozminski et al. [8] observed that IFT particles in *C. moewusii* flagella moved anterogradely at ~2 μm/s and retrogradely at 3.5 μm/s. This suggested that the movement involved two different motor mechanisms; possible motors that were considered at that time

were myosin, cytoplasmic dynein, kinesin, kinesin-related proteins, and even a single motor with bidirectional capability. Shortly thereafter, it was found that anterograde IFT in *C. reinhardtii* required a kinesin HC termed FLA10 [9]. FLA10 is now known to be one subunit of heterotrimeric kinesin-2. In *C. reinhardtii*, FLA10 is associated with the kinesin HC FLA8 and the kinesin-2-associated protein KAP. The orthologous motor contains Kif3A, Kif3B, and KAP3 in mammals and KLP-11, KLP-20, and KAP-1 in *Ca. elegans*. In some cilia, including *Ca. elegans* sensory cilia and mammalian photoreceptor cilia, anterograde IFT also is powered by a homodimeric member of the kinesin-2 family known as OSM-3 in *Ca. elegans* and Kif17 in mammals. Additional kinesins may have special roles in IFT and ciliary assembly and signaling [10–13].

14.3 Discovery of the Cytoplasmic Dynein 2 Heavy Chain and Early Proposals for its Function

The cytoplasmic dynein 2 HC was identified first by Gibbons et al. [14] in an analysis of cDNAs encoding dynein HCs from sea urchin embryos. In total, 15 dynein HC isoforms were identified. In phylogenetic analyses, one of these, termed DHC1a, was closely related to the previously known conventional cytoplasmic dynein 1 HC sequences from the slime mold *Dictyostelium discoideum* and the rat, and its expression was not induced by deciliation of the embryos. Most of the rest grouped with a known axonemal dynein HC (the β dynein HC), and their expression was induced by deciliation, suggesting that they were likely to be axonemal dyneins. However, one, termed DHC1b, was enigmatic in that its sequence was most closely related to that of the cytoplasmic dynein HC, yet its expression was induced by deciliation. Gibbons and colleagues speculated that DHC1b might play a role in the transport of materials for ciliary regeneration or could be a true axonemal dynein HC that for unknown reasons resembles the cytoplasmic dynein HC. Tanaka et al. [15] identified a closely related isoform in rat brain, which they predicted was a cytoplasmic translocater like conventional cytoplasmic dynein 1. The expression of this isoform — now termed Dync2h1 — was much higher in testis than in brain, consistent with a function in flagellar formation; they noted that the protein might function in IFT.

On the other hand, Vaisberg et al. [16] reported, on the basis of both northern and western blot analyses, that Dync2h1 was expressed in several mammalian tissues and cell lines not known to make cilia or flagella. Using an antibody generated against a bacterially expressed fragment of Dync2h1, they found that Dync2h1 was localized to the Golgi apparatus in several cell lines and that injection of the antibody into normal rat kidney (NRK) epithelial cells led to dispersal of the Golgi. They concluded that Dync2h1 was a cytoplasmic dynein HC necessary to maintain normal arrangement of the Golgi membranes. However, this localization is controversial because later localization of Dync2h1 in

NRK cells by immunofluorescence microscopy failed to confirm its presence in the Golgi apparatus [17].

Criswell et al. [18] reported that rat Dync2h1 was expressed in all tissues examined, including non-ciliated tissues. In cultured rat tracheal epithelial (RTE) cells that were induced to differentiate into ciliated cells by creation of an air–liquid interface in the culture, Dync2h1 was expressed at a low level prior to differentiation, and expression increased during ciliation. In contrast, expression of the conventional cytoplasmic dynein 1 HC was high and remained unchanged during differentiation, whereas expression of axonemal dynein HCs was not detected prior to differentiation and increased during ciliation. Using immunofluorescence microscopy and an antibody to a synthetic Dync2h1 peptide, they detected Dync2h1 at the apical ends of ciliated RTE cells but not in the cilia. They concluded that Dync2h1 is a second cytoplasmic dynein HC isoform possibly involved in the transport of ciliary precursors from the interior to the apical end of polarized epithelial cells. Using the same antibody in western blots, Criswell and Asai [19] observed that Dync2h1 is much more abundant in testis than in brain.

14.4 Identification of Cytoplasmic Dynein 2 as The Intraflagellar Transport Retrograde Motor

The first evidence that retrograde IFT was powered by a dynein came from studies by Pazour et al. [20] of *C. reinhardtii* insertional mutants lacking the *FLA14* gene, which encodes the dynein light chain (LC) LC8. Cells of the mutant had short flagella in which anterograde IFT appeared to be normal but retrograde IFT was absent. Electron microscopy revealed that the short flagella contained large amounts of electron-dense material resembling IFT particles, and biochemical analysis of isolated flagella confirmed that they had abnormally high levels of IFT-particle proteins and kinesin-2. This buildup of IFT particles in the flagellum presumably was the result of loss of retrograde IFT: because anterograde IFT was present, the IFT particles were transported into the flagella, where they accumulated in the absence of retrograde IFT to return them to the cell body. Because LC8 was known to be a subunit of both mammalian cytoplasmic dynein 1 and *C. reinhardtii* inner- and outer-arm dynein, it seemed likely that the retrograde IFT motor was a dynein. The evidence pointed specifically to a cytoplasmic dynein, because mutants defective in inner- or outer-arm dyneins have normal IFT.

The possible involvement of cytoplasmic dynein in retrograde IFT was consistent with studies of Collet et al. [21] of the *Ca. elegans* OSM-6 protein, an IFT-particle protein homologous to *C. reinhardtii* IFT52. Although the function of OSM-6 was then unknown, analysis of OSM-6 expression and of the phenotype

of *osm-6* mutants suggested to Collet and colleagues that it was a component of sensory cilia and had a role in the growth of axonemes. Importantly, OSM-6-GFP (OSM-6 tagged with green fluorescent protein) accumulated in the dendritic endings of ciliated neurons of mutants defective in the *che-3* gene, which encodes a dynein HC (W. Grant, personal communication, cited in [21,22]). Previous ultrastructural studies had revealed that the neuronal cilia of *che-3* mutants are short with bulb-shaped endings filled with electron-dense material [23,24]. Collet and colleagues suggested that the OSM-6-GFP accumulation was associated with the bulb-shaped endings of the sensory cilia. In a phylogenetic analysis of dynein HCs, the predicted *che-3* gene product grouped with the cytoplasmic dynein 2 HC of human, rat, mouse, sea urchin, and *Tetrahymena* [20]. This together with the results from the *C. reinhardtii* LC8 mutant led Pazour and colleagues [20] to propose that cytoplasmic dynein 2 might be the motor for retrograde IFT.

In *C. reinhardtii*, the cytoplasmic dynein 2 HC is termed DHC1b[2], and its gene is strongly induced by deflagellation [25,26]. To investigate the function of DHC1b in this organism, Pazour et al. [25] and Porter et al. [26] screened collections of *C. reinhardtii* insertional mutants for deletion or disruption of the *DHC1b* gene and identified apparently null mutants. The cells grew at wild-type rates, indicating that DHC1b is not required for essential cell functions, and the Golgi apparatus appeared to be normal. However, the mutants had short, stumpy flagella (Fig. 14.1A), and ultrastructural analysis revealed that these flagella contained large amounts of electron-dense material resembling IFT particles (Fig. 14.1B). Immunofluorescence microscopy confirmed that this material was composed of IFT-particle proteins and revealed that there was a complete redistribution of the IFT particles from the basal body region into the short flagella (Fig. 14.1C) [25]. This phenotype, which is similar to that of the LC8 mutant [20] but more severe, indicated that loss of DHC1b caused a defect in retrograde IFT that resulted in accumulation of IFT particles within the flagellum (Fig. 14.2). Immunofluorescence microscopy using an antibody to *C. reinhardtii* DHC1b showed that in wild-type cells the protein was located primarily in the peri-basal body region and in spots along the flagella – a pattern virtually identical to that observed for the IFT-particle protein IFT172 (Fig. 14.1C, wild type) and the IFT anterograde motor subunit FLA10 [25]. Immunoblotting of purified wild-type flagella and flagellar fractions confirmed the presence of DHC1b in the flagellum, predominantly in the detergent- and ATP-soluble fractions, a result similar to that obtained for kinesin-2 and the IFT-particle protein IFT139 but distinct from that obtained for an axonemal dynein HC [25]. Thus, the cellular distribution and localization of DHC1b was consistent with it being the retrograde motor for IFT.

[2]C. reinhardtii *lacks conventional cytoplasmic dynein 1. The sequence once termed pcr4 [25] and DHC1a [26] is now known to encode an axonemal dynein HC (T. Yagi, M. Kikkawa, and R. Kamiya, personal communication).*

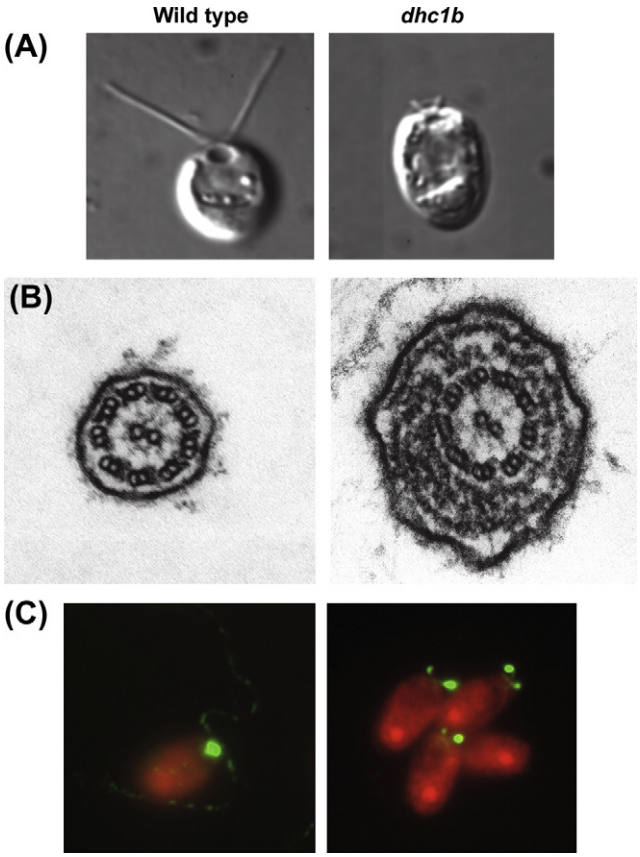

Figure 14.1 Comparison of *C. reinhardtii* wild-type (left) and *dhc1b* mutant (right) cells. (A) Differential interference contrast images. The flagella, normally 10–12 μm long in wild type, are less than 1 μm long in the mutant. (B) Electron micrographs of cross-sections of flagella. Wild-type flagella have a typical "9+2" axoneme surrounded closely by a flagellar membrane; IFT particles are only occasionally observed in the space between the doublet microtubules and the membrane. In the mutant, the axoneme is structurally normal but the space between the axoneme and the flagellar membrane is filled with layer upon layer of IFT particles, which distend the flagellar membrane. (C) Immunofluorescence micrographs of cells labeled with an antibody to the IFT-particle protein IFT172. In wild type, IFT172 is localized primarily to the peri-basal body region of the cell, with less intense localization to discrete puncta along the entire length of the flagella. In the *dhc1b* mutant, the IFT particles have completely redistributed and are detectable only in the short flagella. Autofluorescence of the cell body is shown in red. *Reproduced from [25].*

It was concluded that DHC1b was a cytoplasmic dynein HC that powered retrograde IFT and was essential for flagellar assembly.

The above findings in *C. reinhardtii* shed light on some of the observations previously made in sea urchin embryos and mammalian cells. The demonstration that DHC1b is necessary for flagellar assembly explained why expression of this

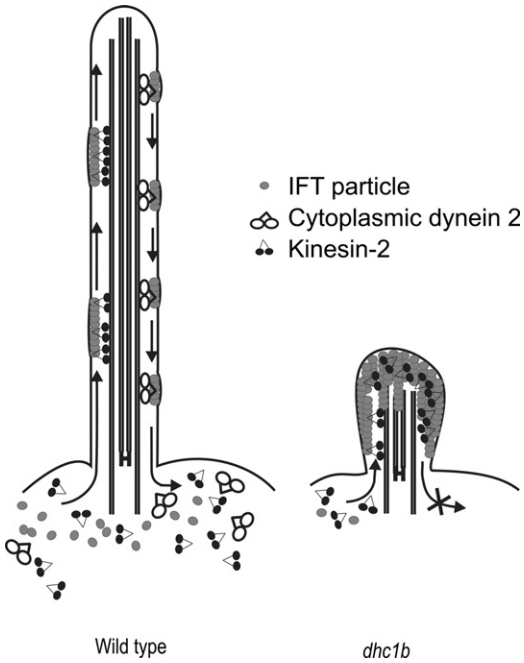

Figure 14.2 Model for IFT in wild-type *C. reinhardtii* (left) and the *dhc1b* mutant (right). In wild-type cells, IFT particles are moved continuously from the peri-basal body pool into the flagellum and then transported anterogradely along the axoneme by kinesin-2. At the tip of the flagellum, kinesin-2 is inactivated and cytoplasmic dynein 2 is activated with the result that the IFT particles are returned to the cell body by dynein 2. In the *dhc1b* mutant, kinesin-2 is still active and can move IFT particles from the peri-basal body pool into the flagella. However, in the absence of dynein 2 to return the particles to the cell body, the particles accumulate in the flagella and the peri-basal body pool becomes depleted of particles. *Modified from [25].*

isoform is induced during ciliogenesis [14,18] and why it is so abundant in testis [15,19]. The fact that cytoplasmic dynein 2 is likely to be necessary for assembly of non-motile cilia, including the primary cilia present on most cell types, likely accounts for why Dync2h1 is expressed in cells and tissues that do not produce motile cilia [16,18]. That cytoplasmic dynein 2 is normally concentrated in the peri-basal body region likely explains why Dync2h1 appeared to be localized specifically to the apical regions but not the cilia of ciliated RTE cells [18]; because the peri-basal body staining is much brighter than the ciliary staining, ciliary staining could easily have been overlooked.

Further evidence for an involvement of DHC1b specifically in retrograde IFT came from studies of *Ca. elegans*. Using time-lapse fluorescence microscopy, Signor et al. [22] observed that, in wild-type worms, GFP-tagged versions of the heterodimeric kinesin-2 subunit KAP and the IFT-particle protein OSM-6 moved anterogradely and retrogradely in both neuronal dendrites and the sensory cilia at the tips of the dendrites. The retrograde rate (1.1 μm/s) was the same for both

GFP-labeled proteins, suggesting that they were being moved by the same motor. However, in the DHC1b mutant (*che-3*), retrograde transport of both proteins was inhibited in the cilia but not in the dendrites. As mentioned above, *che-3* mutant cilia are truncated and have bulbous tips; however, the proximal 2.6 μm of the cilia are relatively normal, and in this region anterograde transport of OSM-6-GFP was observed to continue unabated. Moreover, in wild-type *Ca. elegans* cilia, both KAP-GFP and OSM-6-GFP are enriched at degenerate basal bodies termed "transition zones." However, in the *che-3* mutant these proteins are depleted at the transition zones and abnormally enriched at the tips of the cilia, presumably because they are not returned to the transition zones in the absence of retrograde IFT. The authors concluded that DHC1b is specifically required for the retrograde transport of IFT particles and kinesin-2 in *Ca. elegans* cilia.

14.5 Structure and Subunit Content of Cytoplasmic Dynein 2

Known subunits of cytoplasmic dynein 2 include the HC, an intermediate chain (IC), a LIC, and the LC8 (Table 14.1). It is possible that additional subunits, especially LCs, remain to be discovered.

14.5.1 DHC1b/Dync2h1

Cytoplasmic dynein 2 HCs are similar in overall domain organization to conventional cytoplasmic dynein 1 HCs but are slightly shorter (e.g. 4207 versus 4646 amino acids in humans). They contain six AAA+ modules in their central and C-terminal regions, the first four of which contain P-loop motifs (Fig. 14.3A) [17]. As in other dynein HCs, the first P-loop (P1) is very highly conserved [25,27] and is likely to be the primary site of ATP hydrolysis related to force production. Among DHC1b/Dync2h1 sequences, P2 is more conserved than either P3 or P4; this differs from the cytoplasmic dynein 1 HC, in which P3 is more conserved than P2 or P4, and from axonemal dynein HCs, in which P4 is more conserved than P2 or P3 [26]. Therefore, P2 may be especially important in cytoplasmic dynein 2 function. Between AAA4 and AAA5 are predicted coiled-coil domains [17,27] that form the microtubule-binding stalk [28]. The N-terminal one-third of DHC1b/Dync2h1 is quite divergent from cytoplasmic dynein 1 HCs except for regions corresponding to the LIC binding site and part of the IC binding site. As discussed below (Section 14.5.6), dynein 2 is likely to be "two headed" — that is, a homodimer with regard to its two HCs.

14.5.2 Light-Intermediate Chain

A cytoplasmic dynein 2 LIC has been characterized from mammals [17,29], where it is termed Dync2li1; from *Ca. elegans* [30], where it is termed XBX-1; and from

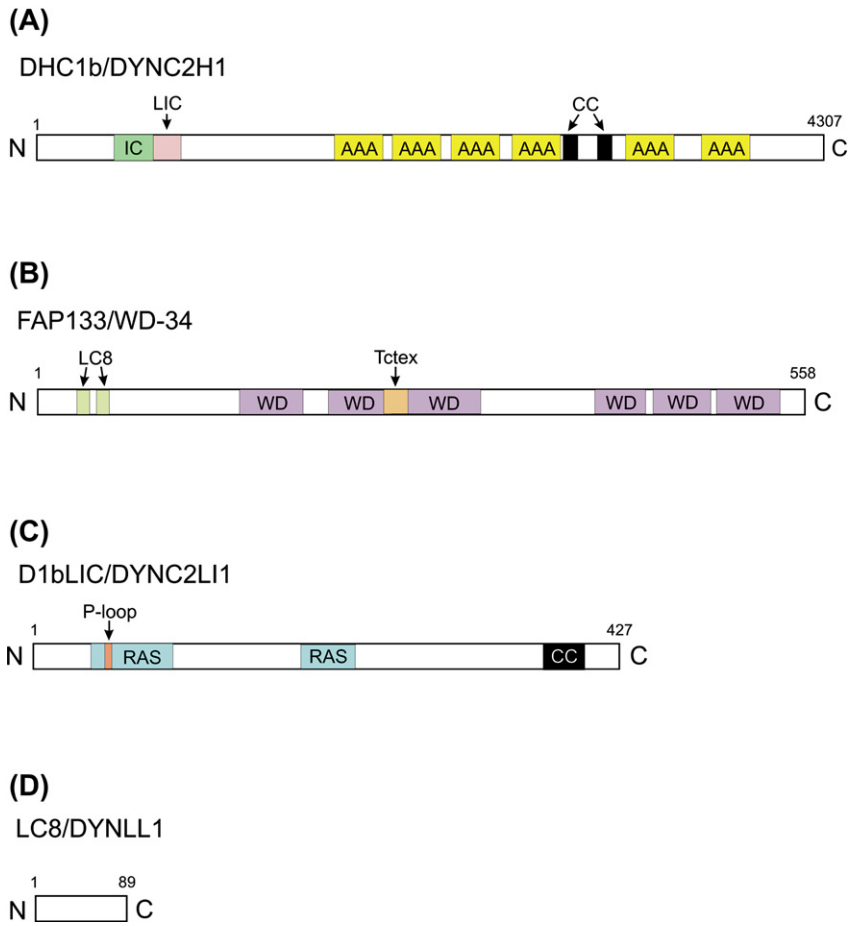

Figure 14.3 Cytoplasmic dynein 2 subunits. (A) Diagram of rat Dync2h1. AAA, AAA domains; CC, coiled-coil domain; IC, intermediate-chain binding site; LIC, light-intermediate chain binding site. Modified from [17]. (B) Diagram of *C. reinhardtii* FAP133. WD, WD-repeat domain; LC8, degenerate LC8 binding motifs; Tctex, sequence that matches Tctex1-binding site in other ICs. Modified from [37]. (C) Diagram of *C. reinhardtii* D1bLIC. CC, coiled-coil domain; RAS, putative RAS signature motif; P-loop, P-loop motif. Modified from [31]. (D) Diagram of human DYNLL1. (B–D) are drawn to scale.

C. reinhardtii [31,32], where it is termed D1bLIC. The cytoplasmic dynein 2 LIC has sequence homology to other dynein LICs and is most closely related to the cytoplasmic dynein 1 LIC Dync1li2. Cytoplasmic dynein 2 LICs that have been characterized range in predicted size from ~40 kD in mammals to 46.5 kD in *C. reinhardtii*; the larger size in *C. reinhardtii* results from an extra alanine-rich region of ~60 amino acids at the C-terminus [31]. Like many other members of the dynein LIC family, the mammalian and *C. reinhardtii* proteins have a predicted

P-loop near their N-termini, suggesting that the protein might bind ATP/GTP; however, the *Ca. elegans* LIC lacks this P-loop. A coiled-coil region is predicted near the C-terminus (Fig. 14.3C). Possible RAS signature motifs — that is, conserved sequences shared with the RAS family of small GTPases, which generally serve as molecular switches — have also been reported in this as well as cytoplasmic dynein 1 LICs [29,31], suggesting a regulatory role. Nothing more is currently known about the function of these sites, although it should be noted that the *C. reinhardtii* flagellar proteome contains numerous small GTPases [33] and that the IFT-particle protein IFT27 is predicted to be a small G protein [34].

Several lines of evidence indicate that this LIC is associated with the cytoplasmic dynein 2 HC. The two proteins co-sediment in sucrose density gradients and co-immunoprecipitate [17,29,31,32]; moreover, in mammals the LIC associates specifically with Dync2h1 and not with the cytoplasmic dynein 1 HC [17,29]. Most immunofluorescence microscopy analyses have found that both proteins are present in cilia and flagella and enriched at their bases [17,31,32]; however, Grissom et al. [29] reported that both proteins localized to the Golgi apparatus throughout the cell cycle. Biochemical analyses in *C. reinhardtii* showed that both proteins partition identically in flagellar fractions and are present predominantly in the detergent- and ATP-soluble flagellar fractions [31,32]. *C. reinhardtii* D1bLIC is reduced in amount in *dhc1b* mutants [31,32] and vice versa [32], providing genetic evidence that the two proteins are part of the same complex and indicating that each subunit is necessary for stabilization of the other.

Studies of the cytoplasmic dynein 2 LIC in *Ca. elegans* have provided insight into this subunit's function. In *Ca. elegans*, the dynein 2 LIC is termed XBX-1 because its gene contains an X-box promoter that mediates regulation of the gene by the DAF-19 transcription factor, which also regulates expression of *Ca. elegans* IFT complex B genes and many other genes associated with IFT [30,35]. Schafer et al. [30] observed that XBX-1-YFP (XBX-1 tagged with yellow fluorescent protein) is enriched at the transition zone and present in the ciliary shaft of phasmid neuronal cilia, where it undergoes both anterograde and retrograde transport. In an *xbx-1* mutant, the neuronal cilia are short with bulb-like distal swellings that accumulate IFT-particle proteins, a phenotype similar to that of *che-3* mutants defective in DHC1b and mutants defective in proteins of IFT complex A, which also is thought to be involved in retrograde IFT [7]. These observations indicated that XBX-1 has a role in retrograde IFT. Interestingly, XBX-1-YFP did not accumulate in the bulbous swellings of IFT complex A mutants, despite the apparent role of complex A in retrograde IFT, and both anterograde and retrograde transport of XBX-1-YFP were observed in these mutants. These results indicated that retrograde movement of XBX-1 does not depend on complex A and raised the possibility that XBX-1 connects the IFT particle to the cytoplasmic dynein 2 HC during retrograde transport. Schafer and colleagues also observed that XBX-1 accumulated in the swollen tips of cilia of the *che-3* mutant. This result is in

contrast to that of Perrone et al. [31], who observed no accumulation of D1bLIC in the swollen tips of a *C. reinhardtii dhc1b* mutant. However, the *che-3* mutant used in the *Ca. elegans* studies has a nonsense mutation in the middle of the gene that likely would result in expression of a truncated DHC1b that retains its N-terminal domain, including the LIC binding site [27], whereas the *C. reinhardtii dhc1b* mutant is likely to be null. Together, these results: (1) confirm that the LIC binding site is located in the N-terminal half of DHC1b, (2) indicate that the LIC is carried out to the tip of the *che-3* cilium by virtue of its association with the truncated DHC1b, and (3) show that the LIC cannot be transported to the tip of the flagellum in the complete absence of DHC1b.

Additional information on cytoplasmic dynein 2 LIC function has come from studies by Hou et al. [32] of a *C. reinhardtii d1blic* null mutant. As was the case for the *C. reinhardtii dhc1b* mutant [25], this mutant grows normally and has an apparently normal Golgi apparatus but has short flagella that accumulate IFT-particle proteins, which is indicative of a defect that specifically affects retrograde IFT. The flagella are not as short as in the *dhc1b* mutant, suggesting that cytoplasmic dynein 2 retains some function in the absence of D1bLIC. Importantly, although IFT particles accumulated in the swollen tips of the flagella, immunofluorescence microscopy revealed that DHC1b is normally distributed in the *d1blic* cells, suggesting that DHC1b retains motor activity and can move out of the flagellum even in the absence of D1bLIC. The results also strongly suggest that D1bLIC has a role in binding the IFT particle to DHC1b, a conclusion consistent with the observations of XBX-1-YFP in the complex A mutants of *Ca. elegans* [30].

The function, if any, of the D1bLIC P-loop remains unknown. Transformation of the mutant *C. reinhardtii d1blic* mutant with constructs designed to express D1bLIC proteins carrying mutations known to disrupt P-loop function in other proteins completely rescued the *d1blic* phenotype [32]. The rescued cells had normal-length flagella and normal IFT particle distribution. Mating, which is dependent on IFT [36], also appeared to be normal. Therefore, the P-loop does not appear to be essential for D1bLIC's function in IFT, a finding consistent with its absence in *Ca. elegans* XBX-1.

14.5.3 FAP133, a Cytoplasmic Dynein 2 Intermediate Chain

Although all other dyneins having two HCs also have two ICs of the WD-repeat family, no such IC had been identified for cytoplasmic dynein 2 in any of the biochemical studies cited above. In a screen for *C. reinhardtii* genes encoding proteins related to rat conventional cytoplasmic dynein 1's IC2, Rompolas et al. [37] identified a previously uncharacterized gene, annotated as *FAP133*, that was a candidate for a cytoplasmic dynein 2 IC. FAP133 previously had been shown to be in the flagellar proteome with a distribution in the flagellar subfractions similar

to that of D1bLIC but different from that of axonemal dynein subunits [33]. Rompolas and colleagues found that the gene is upregulated by deflagellation, as expected for a protein involved in flagellar assembly or function. FAP133 is predicted to be a 61-kD protein with six WD-repeat domains spanning the C-terminal two-thirds of the molecule; a seventh degenerate WD-repeat domain may be present between repeats three and four (Fig. 14.3B) [37]. These presumably form a β-propeller structure. The protein also contains two degenerate LC8 binding sites near its N-terminus and, closer to the center but still in the N-terminal half of the molecule, a motif that in other dynein ICs is associated with binding of the dynein LC Tctex1 (see Section 14.5.5).

Detailed characterization of FAP133 clearly demonstrated that it is associated with cytoplasmic dynein 2 [37]. FAP133 distributed in various flagellar fractions in a pattern apparently identical to that of D1bLIC, co-sedimented in sucrose gradients with both DHC1b and D1bLIC, and co-fractionated with both DHC1b and D1bLIC by gel-filtration column chromatography. Antibodies to FAP133 co-immunoprecipitated DHC1b and D1bLIC. Immunofluorescence microscopy showed that FAP133 was localized primarily to the peri-basal body region and to puncta along the flagella, a cellular distribution identical to that of DHC1b and D1bLIC. In *C. reinhardtii* mutants lacking DHC1b and D1bLIC, FAP133 redistributes from the peri-basal body region to the center of the cell, indicating that DHC1b and D1bLIC are required for tethering of FAP133 at the basal body. A FAP133 mutant has not yet been reported in any organism, but knockdown of the *Trypanosoma brucei* homolog (*T. brucei*; database ID 927.3.5540) by RNA interference (RNAi) caused cells to accumulate in multicellular clusters due to a failure to complete cell division, which in *T. brucei* requires flagellar motility [38].

Rompolas et al. [37] also observed that FAP133 readily dissociates from the DHC1b/D1bLIC complex, which raises the possibility that this interaction is regulated *in vivo* and also likely explains why FAP133 was not detected in earlier studies. By use of gentle procedures, they obtained a Superose-6 gel filtration fraction containing DHC1b, D1bLIC, FAP133, LC8, the kinesin-2 subunit FLA10, and the IFT complex A protein IFT139, but not IFT complex B protein IFT81. The same proteins plus IFT81 were co-immunoprecipitated from a flagellar matrix fraction by the antibody to FAP133. These results strongly suggested that cytoplasmic dynein 2 is associated with IFT complex A and kinesin-2, but that these associations are lost by traditional methods for purifying the complex.

Concurrently with the publication of the above studies of Rompolas et al. [37], Wickstead and Gull [39] published a comparative genomic analysis of dynein sequences that identified a new dynein IC family of unknown function; they named this family WDRD34 for the human WD-repeat (domain) containing protein 34, which is a family member. FAP133 is also a member of this family and

thus identifies the family as a clade likely to be specific to cytoplasmic dynein 2. Close homologs are present in most organisms with cilia, including vertebrates, sea urchin, insects, and numerous protists [37,39]. Surprisingly, no homolog of FAP133 has been identified in *Ca. elegans*. This raised the possibility that this dynein IC has a function specific to motile cilia [37]. However, this apparently is not the case, because knockdown of the zebrafish homolog resulted in defects in the photoreceptor connecting cilium and outer segment similar to those seen when the cytoplasmic dynein 2 HC or LIC was knocked down [40].

14.5.4 LC8

Despite the genetic evidence for a connection between LC8 and retrograde IFT [20], LC8 did not co-purify with DHC1b in an early biochemical study of cytoplasmic dynein 2's subunits [31]. Biochemical evidence that LC8 (Fig. 14.3D) is a subunit of cytoplasmic dynein 2 finally was provided by Rompolas et al. [37]. When freshly prepared *C. reinhardtii* freeze-thaw flagella extracts (i.e. the flagellar matrix) were fractionated by sucrose density gradient centrifugation, LC8 sedimented in three peaks: one at 18 S containing DHC1b, D1bLIC, and FAP133; a second at 10 S containing FAP133; and a third near the top of the gradient. Also, as noted in Section 14.5.3, LC8 was present in gel filtration fractions containing DHC1b, D1bLIC, and FAP133. Finally, when FAP133 was immunoprecipitated from the flagellar matrix fraction, LC8 in particular was highly enriched in the resulting pellet, which also contained DHC1b. These results strongly suggested that LC8 is indeed a subunit of dynein 2 and that FAP133 and LC8 interact. Further experiments confirmed this interaction. Fractionation of the flagellar matrix by anion exchange chromatography yielded two peaks of FAP133; when the fractions representing each of these peaks were pooled and subjected to sucrose gradient centrifugation, in both cases FAP133 and LC8 co-sedimented at 10 S. Therefore, LC8 interacts strongly with FAP133 to form a sub-complex that makes up part of cytoplasmic dynein 2 but is readily dissociated from it. Based on the sedimentation properties of the sub-complex, Rompolas and colleagues predicted that it is likely to contain two subunits of FAP133 and two of LC8. The finding that FAP133 and LC8 interact is consistent with the prediction that FAP133 contains degenerate LC8 binding sites.

In *C. reinhardtii fla14* cells (lacking LC8), DHC1b, D1bLIC, and FAP133 are concentrated in the peri-basal body region [31,37]. Therefore, cytoplasmic dynein 2 is targeted to the peri-basal body region even in the absence of LC8. Also in *fla14* cells, DHC1b, D1bLIC, and FAP133 do not appear to enter the flagellar stubs as assessed by immunofluorescence microscopy. This is in contrast to the IFT-particle proteins, which are greatly enriched in flagella in the absence of LC8 [20]. Interpretation of the failure to detect dynein 2 subunits in *fla14* flagella by immunofluorescence microscopy alone is complicated by conflicting data on the stability of DHC1b in the absence of LC8 (cf. figure 2D of [31] with

figure 7A of [37]); the apparent lack of these dynein 2 subunits in *fla14* flagella should be confirmed by quantitative western blot analyses of the ratios of dynein 2 subunits in isolated flagella and cell bodies of *fla14* compared to wild type. In any case, dynein 2 does not accumulate in *fla14* flagella in the same way that IFT particles do. One possible explanation is that LC8 is required for loading the dynein 2 complex onto the anterograde IFT machinery for transport into the flagellar compartment. Another possibility is that, in the absence of LC8, as in the absence of D1bLIC [32], dynein 2 enters and exits the flagellum more or less normally but does not return IFT particles to the base of the flagellum. These possibilities probably could be distinguished by the quantitative western blot analyses discussed above. It also should be noted that *fla14* flagella are longer than *dhc1b* mutant flagella, suggesting that some dynein 2 function remains in the absence of LC8.

14.5.5 A Tctex1/Tctex2 Light Chain?

Most if not all other two-headed dyneins also contain a subunit that is a member of the Tctex1/Tctex2 family of dynein LCs. In an analysis of *Ca. elegans* genes containing an X-box promoter motif, which regulates the expression of *xbx-1* and many other genes associated with IFT, Efimenko et al. [35] identified a gene (*dylt-2*) encoding a Tctex1/Tctex2 family member that they named XBX-2. In phylogenetic analyses, XBX-2 grouped most closely with *C. reinhardtii* Tctex2/LC2 and Tctex2b, which are LCs of axonemal outer-arm and inner-arm dyneins, respectively [39]. However, *Ca. elegans* lacks axonemal dyneins. Efimenko and colleagues found that XBX-2-GFP is highly expressed in ciliated sensory organs and moves along phasmid ciliary axonemes in both anterograde and retrograde directions. Therefore, XBX-2 is a strong candidate for being another dynein 2 LC. In mammalian cytoplasmic dynein 1, Tctex1 (Dynlt1) binds directly to the dynein IC via the motif R/KR/KXXR/K [41], which is also present in the *C. reinhardtii* outer-arm dynein ICs IC1 and IC2 [42]. *C. reinhardtii* FAP133 also contains a perfect copy of this motif, suggesting that it may bind a Tctex1/Tctex2 family member. However, as noted above, no homolog of FAP133 exists in *Ca. elegans*. Therefore, further studies will be necessary to determine whether XBX-2 is a subunit of dynein 2 in *Ca. elegans* and whether dynein 2 from other organisms contains a Tctex1/Tctex2 LC.

14.5.6 Overall Architecture of Cytoplasmic Dynein 2 and the Roles of its Subunits

Whether cytoplasmic dynein 2 is one-headed or two-headed has not yet been demonstrated directly by electron microscopy. In sucrose gradients, mammalian cytoplasmic dynein 2 has been reported to sediment between 12 S and 17 S [16,17,19], and *C. reinhardtii* dynein 2 at 18 S–19 S and 12 S depending on extraction conditions [31,37]. Because two-headed dyneins tend to sediment

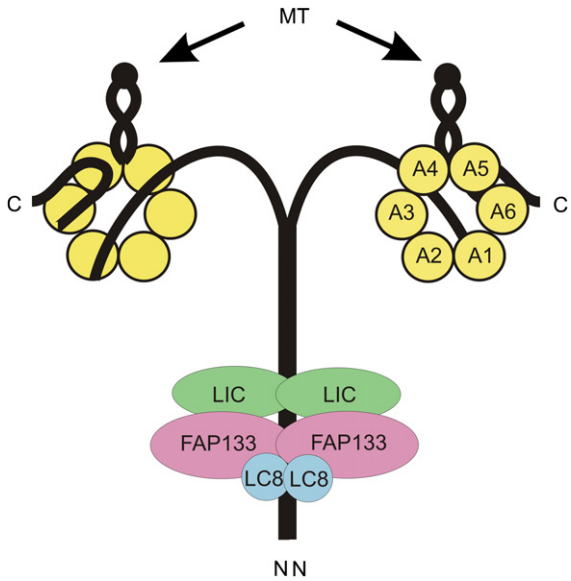

Figure 14.4 Diagram illustrating the predicted architecture of cytoplasmic dynein 2. Two HCs interact via their N-terminal regions to form a homodimer. N, N-terminal ends of the HCs; C, C-terminal ends of the HCs. The six AAA+ domains (A1–A6) of each HC form a ring-shaped globular head. "Top" and "bottom" views of the heads are shown for the left and right HCs, respectively, to illustrate how part of the N-terminal region crosses the AAA+ ring just before continuing into AAA1 and how the C-terminus extends from AAA6. Between AAA4 and AAA5 is the coiled-coil stalk terminating in the microtubule-binding domain (MT). A LIC is attached to the N-terminal domain of each HC. A FAP133 dimer binds to the HC dimer and an LC8 dimer is bound to the FAP133 dimer. The arrangements of the N-terminal region as it crosses the AAA+ ring structure and of the C-terminus are based on data from conventional cytoplasmic dynein 1 [63,64].

around 18 S and single-headed dyneins around 12 S, this strongly suggests that cytoplasmic dynein 2 is a two-headed dynein (Fig. 14.4) and that under certain conditions the two HCs dissociate from each other to sediment at 12 S.

Inasmuch as each dynein HC contains a LIC binding site in its N-terminal half ([17]; and see Section 14.5.1), the holoenzyme, like other two-headed dyneins, presumably contains two copies of the LIC subunit as well. Based on its sedimentation properties, the FAP133/LC8 sub-complex is also predicted to contain two copies of each of its subunits. Because DHC1b, D1bLIC, and FAP133 retain their localization in the peri-basal body region of the *C. reinhardtii fla14* mutant lacking LC8 [31,37], Rompolas et al. [37] proposed that the FAP133 dimer binds directly to the N-terminal region of DHC1b and that LC8 is not necessary for this interaction. Therefore, the association of LC8 with the holoenzyme is likely mediated by FAP133. Under harsher conditions of extraction and fractionation, the FAP133–LC8 sub-complex dissociates from DHC1b and sediments at 10 S, and the two dynein HCs dissociate from each other and sediment at 12 S.

To summarize what is known about the possible roles of the different dynein 2 subunits, the LIC is important for the stabilization of the HC, and vice versa [31,32]; LC8 also may be important for stabilizing DHC1b [37]. In the absence of the LIC, the small amount of dynein 2 that remains appears to be normally distributed in the cell [32], suggesting that dynein 2 *sans* the LIC is able to couple to the IFT machinery for anterograde transport by kinesin-2 and retains enough motor activity to power its return to the cell body. However, the LIC appears to be essential for coupling IFT particles to dynein 2 for retrograde transport [30,32]. LC8 may be necessary to couple dynein 2 to the anterograde machinery for transport to the flagellar tip [31,37], but further studies are required to confirm this.

14.6 Function of Cytoplasmic Dynein 2 and Retrograde Intraflagellar Transport

14.6.1 Recycling of Intraflagellar Transport Components

A primary function of cytoplasmic dynein 2 in most organisms examined is the return of IFT particles and probably the anterograde IFT motors to the base of the cilium for reuse in anterograde IFT. This is clearly evidenced by the phenotypes of *dhc1b*/*dync2h1*, *d1blic*/*xbx-1*, and LC8 mutants in *C. reinhardtii* [20,25,26,32], *Ca. elegans* [21,22,27,30], and mice (Fig. 14.5) [43,44], all of which accumulate IFT particles in short, swollen cilia. This phenotype indicates that the IFT particles, which are carried into the cilium by anterograde IFT, are not retrieved from the cilium in the absence of dynein 2 function.

14.6.2 Return of Turnover Products to the Cell Body

In addition to retrieving components of the IFT machinery from the flagellum, retrograde IFT returns axonemal and membrane proteins back to the cell body. The flagellar axoneme undergoes continual turnover [45,46], and cytoplasmic dynein 2 functions in returning the products of this turnover to the cell body. This has been demonstrated most clearly for the radial spokes, which are large multi-subunit components of the axonemes of motile cilia. In *C. reinhardtii*, extraction of radial spokes from the axoneme yields a 20 S complex containing the known radial spoke proteins and presumably representing the intact radial spoke. Qin et al. [47] found that wild-type cells contain both 12 S and 20 S radial spoke complexes in their cytoplasm and soluble flagellar membrane plus matrix fraction. The 12 S complex alone is present in the cytoplasm of mutants lacking flagella and thus appears to be a precursor of the 20 S complex; conversion of the 12 S complex to the 20 S complex is believed to occur concomitantly with incorporation of the radial spoke into the axoneme. In wild-type cells, the 12 S form is greatly enriched relative to the 20 S form in the membrane plus matrix of regenerating flagella, as would be expected for a component in transit to the flagellar tip during rapid

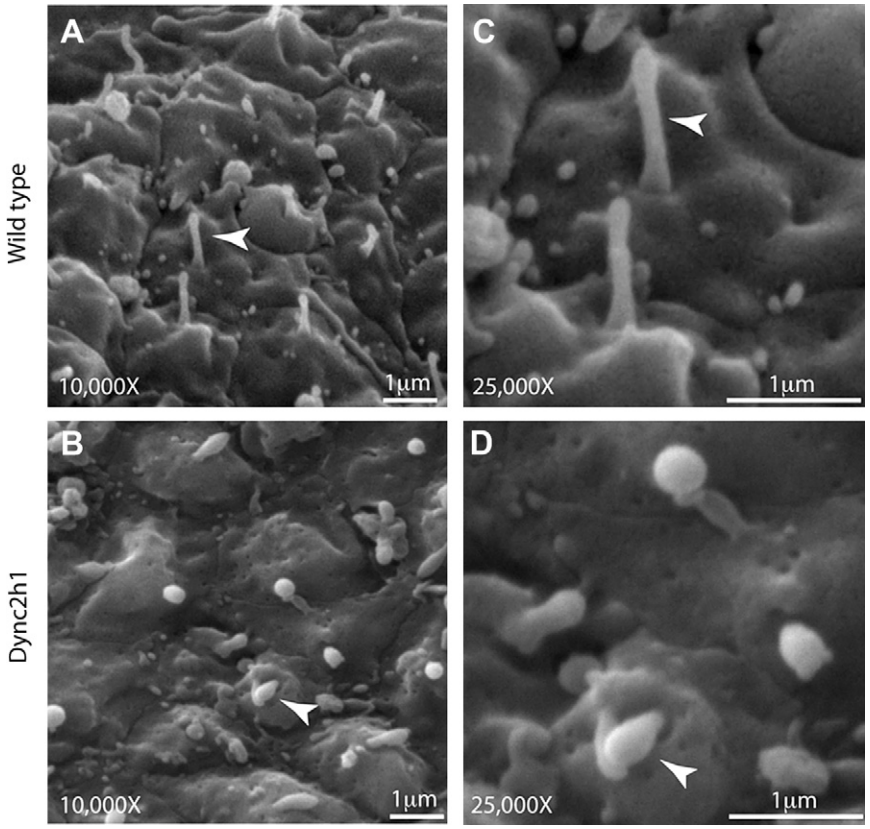

Figure 14.5 Scanning electron micrographs of primary cilia (*arrowheads*) in the forebrain neuroectoderm of E10.5-day embryos of wild-type (top) and *dync2h1* mutant (bottom) mice. (C and D) show higher magnifications of (A and B). Note the short swollen appearance of the mutant cilia. The *dynch21* mice have a nonsense mutation that generates a stop codon predicted to result in a protein truncated at amino acid 397 — that is, very early in the amino acid sequence. *Reproduced from [44].*

assembly of the flagellar axoneme. In contrast, blocking IFT at restrictive temperature in the temperature-sensitive *fla10* (kinesin-2) mutant reduces the relative amount of the 12 S complex in the membrane plus matrix fraction, again as would be expected if the 12 S complex is being transported to the flagellar tip for assembly into the axoneme. Under the same conditions, which cause the flagella to slowly disassemble, the 20 S complex accumulated in the flagella, as would be expected if it is a product of axonemal turnover or disassembly removed from the flagellum by IFT. In *fla14* mutants lacking LC8, both the 12 S and the 20 S complexes are present in the flagellar membrane plus matrix, but the 20 S complex is absent from the cell body. Similarly, the 20 S form is absent from the

cell body of *dhc1b* mutants. These observations indicate that the 20 S complex is no longer recycled to the cell body in the absence of a functional dynein 2. Qin et al. [47] concluded that retrograde IFT carries the 20 S radial spoke complex, a product of axonemal turnover, out of the flagellum and back to the cell body.

Polycystin-2, a transmembrane protein present in many types of cilia, also appears to be removed from the cilium by IFT. When IFT is impaired by defects in either the anterograde motor or complex B, polycystin-2 accumulates in the resulting short cilia of *Ca. elegans* [48], *C. reinhardtii* [49], and the mammalian kidney [50]. This strongly suggests that polycystin-2 is trafficked out of the cilium by retrograde IFT.

Retrograde IFT of some proteins may be mediated by the BBSome. The BBSome is a large complex containing at least eight proteins, seven of which cause the human disease Bardet-Biedl syndrome (BBS) when defective [51]. Lechtreck et al. [52] showed that in *C. reinhardtii* the BBSome undergoes both anterograde and retrograde IFT in association with a subset of IFT particles; it appears to be a cargo adapter for IFT. Defects in individual BBSome subunits led to the accumulation in the flagella of several proteins that are not normally detected there [52]. Many of these proteins are predicted to be myristoylated and palmitoylated (K.-F. Lechtreck and G.B. Witman, unpublished results) and are associated with the flagellar membrane, presumably through their fatty-acid modifications. How these proteins get into the flagellum is not clear; they could have a function in the flagellum and be continually trafficked through the organelle at very low levels, or they could be non-flagellar proteins that leak into the flagellar compartment due to an inefficiency of the flagellar sorting machinery. In any case, the time-dependent accumulation of these proteins in *bbs* mutant flagella but not wild-type flagella indicated that they are normally removed from the flagella by the BBSome, which in turn is trafficked by IFT. At least one of these proteins also accumulated in the flagella of a hypomorphic *dhc1b* mutant, which is consistent with removal of the protein from the flagellum by cytoplasmic dynein 2 via the BBSome [52].

14.6.3 Signal Transduction

Cytoplasmic dynein 2 also has an important role in the transduction of signals from the cilium to the cell body. This has been studied extensively for vertebrate hedgehog (Hh) signaling, which occurs in the primary cilium [13,43,44,53,54]. Important components of this pathway include: (1) sonic hedgehog (Shh), a secreted protein that is an important ligand for the Hh signaling pathway during development; (2) patched 1 (Ptch1), a transmembrane protein that is the receptor for Shh; (3) smoothened (Smo), a seven-pass transmembrane protein that acts downstream of Ptch1; (4) Gli2, a transcription factor that functions as the primary activator of Hh target gene expression; (5) Gli3, a transcription factor that can function as an activator of Hh target genes when full length but that is proteolytically processed to function as the primary repressor of Hh target

genes; and (6) Sufu, a negative regulator of Hh signaling. In unstimulated cells, Smo is associated primarily with vesicles in the cell body; Ptch1 is localized to the base of the cilium, where it may regulate entry of Smo into the ciliary compartment; and Gli2, Gli3, and Sufu are localized to the tip of the cilium. Following stimulation of cells by Shh, Ptch1 moves out of the cilium and Smo moves into the cilium. Gli2 is then activated, moves out of the cilium, and enters the nucleus to activate transcription of Hh target genes. It is hypothesized that, at the ciliary tip, Smo antagonizes the activity of Sufu, thereby promoting the activation of Gli2 in a manner not yet determined but that results in the exit of Gli2 from the cilium.

Ocbina and Anderson [53] examined this process in mouse embryonic fibroblasts derived from embryos homozygous for the *tian-tian* allele of *Dync2h1*. *Dync2h1*^{ttn} mice have a 38-amino-acid in-frame deletion within the fourth AAA+ domain of Dync2h1; this appears to disrupt Dync2h1's function because the cilia are shorter than those of wild-type cells and have bulges similar to those observed in the cilia of other organisms that have defects in dynein 2, as well as in the cilia of mice with an apparently null mutation in *Dync2h1* (Fig. 14.5). Treatments that activated the Hh pathway in wild-type cells failed to activate the pathway in these mutant mouse embryonic fibroblasts, indicating that retrograde IFT is essential for activation of the pathway. It was also observed that, in the *Dync2h1*^{ttn} cells, Smo was enriched in the primary cilia even in the absence of the Hh ligand, indicating that Smo is continuously trafficked through the cilium at a baseline level and accumulates in the cilium when dynein 2 is unable to carry it back to the cytoplasm. However, even though Smo was concentrated in their cilia, these mutant mouse embryonic fibroblasts failed to respond to activators of the Hh pathway; this result strongly suggested that activated Gli2 is moved out of the cilium by retrograde IFT and that this export is blocked in the Dync2h1 mutant cells.

Consistent with this, Kim et al. [54] used shRNA to knock down Dync2h1 in confluent NIH 3T3 cells and observed that Gli2 in addition to Smo accumulated in the primary cilium; nevertheless, treatment of the cells with Shh failed to activate expression of an Hh-target gene reporter, an effect likely resulting from blocked export of activated Gli2 from the cilium and, as a result, reduced nuclear accumulation of Gli2. Based on these results, Kim and colleagues proposed that Smo and Gli2 are continuously shuttled through the cilium, that Gli2 is continuously sampling the signaling environment of the ciliary compartment, and that Shh-stimulated accumulation of Smo in the cilium alters this trafficking in such a way that Gli2 accumulates at the ciliary tip, is subsequently moved from the cilium to the cell body by dynein 2, and from there enters the nucleus to activate Hh target genes. In addition, proteolytic processing of Gli3 to its repressor form requires Dync2h1 [43,44,55]. It has been proposed that Gli3, like Gli2 and Smo, is moved continuously in and out of the cilium, and that at the ciliary tip of unstimulated cells it undergoes a post-translational modification that primes it for further modification and proteolytic processing to the repressor form following its removal from

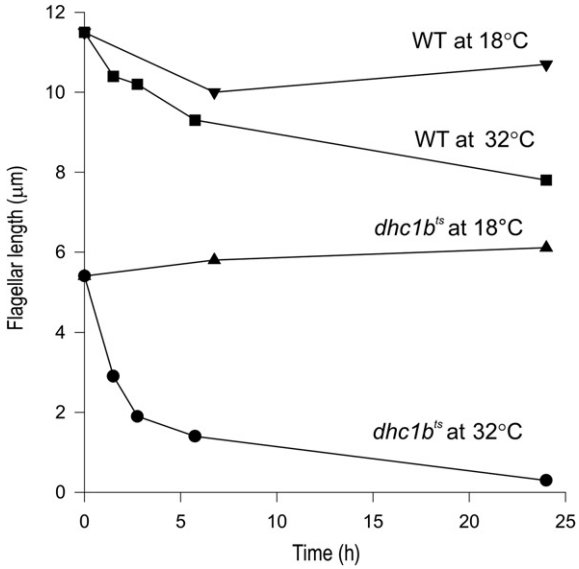

Figure 14.6 Dynein 2 is required for maintenance of flagellar length. At permissive temperature (18°C), flagella of a *C. reinhardtii* temperature-sensitive *dhc1b* mutant (*dhc1b*^{ts}) are variable in length but have an average length about one-half that of wild-type (WT) flagella. Upon shift to non-permissive temperature (32°C), the flagella of the mutant rapidly shorten, averaging less than half their original length after ~2.5 h. In wild type, the same temperature shift results in only a slight shortening of the flagella. *Reproduced from [56].*

the cilium by dynein 2; the resulting Gli3 repressor then enters the nucleus to prevent expression of Hh-target genes [55].

14.6.4 Flagellar Maintenance

Dynein 2 is required for the *maintenance* of fully formed flagella. This is illustrated by the phenotype of a *C. reinhardtii dhc1b* temperature-sensitive mutant [56]. At permissive temperature, this mutant has reduced levels of DHC1b and has variable-length flagella, some of which accumulate IFT particles. When shifted to non-permissive temperature, the amount of DHC1b protein in the cell body decreases further and the flagella shorten, losing over half their length in 150 min (Fig. 14.6). This rate of shortening is comparable to that observed when *fla10* cells are shifted to non-permissive temperature, blocking anterograde IFT [9]. In the case of the *dhc1b* temperature-sensitive mutant, shortening most likely occurs because IFT components are no longer being recycled at the restrictive temperature, which in turn impairs replacement of proteins lost due to turnover at the tip of the axoneme [46]. However, it also is possible that shortening occurs through disruption of a DHC1b-dependent signaling pathway that monitors and controls flagellar length.

14.6.5 Other Functions

Cytoplasmic dynein 2 may have a different, or additional, function in some other organisms. Rajagopalan et al. [57] examined the function of dynein 2 in *T. thermophila* cells in which either the catalytic P1 loop of the HC was deleted or the first 192 amino acids of the LIC (termed D2LIC) were deleted. In both cases, fewer cilia were produced and the cells had impaired motility, but the cilia appeared ultrastructurally normal and did not have swollen tips or accumulate IFT particles as in *C. reinhardtii*, *Ca. elegans*, and mouse mutants with defects in dynein 2. The main effect appeared to be on ciliary length. Compared to wild-type cells, mutant cells had a broader range of ciliary length, including abnormally short cilia and some abnormally long cilia. The kinetics of ciliary regeneration after deciliation were also examined in the D2LIC knockout cells; the cilia regrew more slowly than those of wild-type cells [58]. Rajagopalan et al. [57] concluded that the function of dynein 2 for retrograde IFT is not conserved in *T. thermophila*. They suggested that dynein 2 may be transporting ciliary precursors from the cytoplasm to the base of the cilium, a function that would be consistent with the localization of dynein 2 to the apical ends of ciliated epithelial cells ([18]; see Section 14.3). There are at least two possibilities that might explain why IFT particles do not accumulate in cilia of *T. thermophila* with defects in dynein 2 [57]: (1) retrograde IFT is powered by a different motor in *T. thermophila*, the genome of which is predicted to encode four minus-end-directed kinesin-like proteins, and (2) for unknown reasons, retrograde IFT is simply not required, as appears to be the case for the parasitic protozoan *Toxoplasma gondii* and the centric diatom *Thalassiosira pseudonana*, both of which lack dynein 2 and, in the case of the latter, IFT complex A [39,59].

Most organisms have only a single cytoplasmic dynein 2 HC gene, but trypanosomatids such as *Trypanosoma* and *Leishmania* have, in addition to one conventional dynein 1 HC gene, two dynein 2 HC genes [60]. Phylogenetic analysis indicates that the two dynein 2 HC genes are likely the result of a gene duplication that occurred after the trypanosomatids diverged from other groups of organisms. The two dynein 2 HC genes appear to have different functions. Adhiambo et al. [60] used homologous gene replacement to sequentially disrupt each of the two *Leishmania mexicana* genes, termed *LmxDHC2.1* and *LmxDHC2.2*. *L. mexicana* is diploid throughout its lifecycle, and, although both alleles of *LmxDHC2.1* were disrupted in multiple cell lines, the disrupted alleles invariably occurred together with a copy of the wild-type gene, suggesting aneuploidy of the chromosome containing *LmxDHC2.1*. This is a common occurrence when essential genes are disrupted in *L. mexicana*, and suggested that *LmxDHC2.1* is an essential gene. In contrast, disruption of *LmxDHC2.2* resulted in promastigote-stage cells with very short flagella and an abnormal cell shape. Unlike the cilia of mutants of *C. reinhardtii*, *Ca. elegans*, and mice with defects in dynein 2, these short flagella were not swollen and did not accumulate electron-dense material resembling IFT particles. Adhiambo and

colleagues suggested that this difference may result from the greater stability of the *L. mexicana* flagellum, from a difference in regulation of the steady-state concentrations of unassembled flagellar proteins, or from an inability to recruit flagellar proteins to the base of the flagellum in the absence of this dynein HC gene. Kohl et al. [61] used inducible RNAi to knock down one of the dynein 2 HC genes (*TbDHC1b*) in promastigote-stage *T. brucei* and observed no effect on the existing flagellum, but new flagellar assembly was blocked and cell shape and size were dramatically perturbed. The latter effects were attributed to inhibition of assembly of the new flagellum, which in *T. brucei* is attached along its entire length to the cell body by a specialized structure termed the flagellar attachment zone. Kohl and colleagues proposed that the flagellar attachment zone has a role in cytoskeleton elongation, basal body/kinetoplast segregation, and determination of the site of cytokinesis; the inability to form a new flagellum affected assembly of the new flagellar attachment zone, with consequent defects in cytokinesis and cell shape determination. However, in *L. mexicana*, the flagellum is not attached to the cell body along its length and there is no flagellar attachment zone. Therefore, Adhiambo et al. [60] concluded that *LmxDHC2.2* has a more direct role in determining cell shape. Certainly, it will be of great interest to learn more about the functions of each of the two dynein 2 HC genes in trypanosomatids.

14.6.6 Dynein 2 is not Required for Retrograde Transport of Arrestin in Photoreceptor Outer Segments

In vertebrate photoreceptors, opsins are transported by anterograde IFT through the connecting cilium to the outer segment, and subsequently shed from the tip of the outer segment. Thus, the bulk of protein transport through the connecting cilium is unidirectional in the anterograde direction. However, arrestin is moved from the outer segment to the inner segment during dark adaptation and transducin is moved from the outer segment to the inner segment during light adaptation, raising the possibility that these proteins might be transported by retrograde IFT. To examine this, Krock et al. [40] used morpholino oligonucleotides to knock down the *dync2-h1*, *dync2-i1*, and *dync2-li1* genes, encoding the cytoplasmic dynein 2 HC, IC, and LIC, respectively, in zebrafish embryos; they then compared the movement of arrestin during light and dark adaptation in the morphant and control embryos. Although the knockdowns caused changes in outer-segment morphology consistent with inhibition of IFT, no effect on arrestin movement was observed. They concluded that retrograde translocation of arrestin does not require dynein 2. Rather, this movement may be the result of diffusion (reviewed in [62]), providing a cautionary reminder that not all retrograde movement of proteins in cilia is necessarily driven by IFT.

14.7 Conclusion

The basic function of cytoplasmic dynein 2 as the motor for retrograde IFT is now well-established, and its general molecular architecture can be predicted with confidence. However, much remains to be learned about this unique and important dynein. It is likely that our knowledge of its subunit composition – and in particular of its LCs – is still incomplete. There is virtually no information available on how its motor and cargo-binding activities are controlled; our understanding of these activities would undoubtedly benefit from additional biochemical and genetic analyses, as well as from *in vitro* motility studies using purified microtubules and other defined components, which have not yet been carried out. Undoubtedly, the currently intense focus on investigating ciliary function and assembly (and disassembly) will provide more information on the role of dynein 2 in the transport of specific proteins and signals out of the cilium. Whether dynein 2 functions as a microtubule motor in other places where IFT particles are found besides the cilium is an important question that has yet to be addressed. Finally, questions remain about the function of dynein 2 in organisms such as *T. thermophila*, where it may not be required for ciliary assembly *per se*, and in trypanosomatids, which encode two dynein 2 HC genes, one of which may be essential. Clearly, there is sufficient work still to be done on dynein 2 to keep students of dynein occupied for many years to come.

Acknowledgments

I thank Drs. Yuqing Hou and Gregory Pazour for helpful comments on the manuscript, and gratefully acknowledge support from NIH grant GM030626, the Grousbeck Family Foundation, and the Robert W. Booth Endowment at the University of Massachusetts Medical School.

References

[1] N. Dagoneau, M. Goulet, D. Geneviève, Y. Sznajer, J. Martinovic, S. Smithson, C. Huber, G. Baujat, E. Flori, L. Tecco, D. Cavalcanti, A.L. Delezoide, V. Serre, M. Le Merrer, A. Munnich, V. Cormier-Daire, *DYNC2H1* mutations cause asphyxiating thoracic dystrophy and short rib-polydactyly syndrome, type III, Am. J. Hum. Genet. 84 (2009) 706–711.

[2] A.E. Merrill, B. Merriman, C. Farrington-Rock, N. Camacho, E.T. Sebald, V.A. Funari, M.J. Schibler, M.H. Firestein, Z.A. Cohn, M.A. Priore, A.K. Thompson, D.L. Rimoin, S.F. Nelson, D.H. Cohn, D. Krakow, Ciliary abnormalities due to defects in the retrograde transport protein DYNC2H1 in short-rib polydactyly syndrome, Am. J. Hum. Genet. 84 (2009) 542–549.

[3] F. Finetti, S.R. Paccani, M.G. Riparbelli, E. Giacomello, G. Perinetti, G.J. Pazour, J.L. Rosenbaum, C.T. Baldari, Intraflagellar transport is required for polarized recycling of the TCR/CD3 complex to the immune synapse, Nat. Cell Biol. 11 (2009) 1332–1339.

[4] K.K. Pfister, E.M.C. Fisher, I.R. Gibbons, T.S. Hays, E.L.F. Holzbaur, J.R. McIntosh, M.E. Porter, T.A. Schroer, K.T. Vaughan, G.B. Witman, S.M. King, R.B. Vallee, Cytoplasmic dynein nomenclature, J. Cell Biol. 171 (2005) 411–413.

[5] J.L. Rosenbaum, G.B. Witman, Intraflagellar transport, Nat. Rev. Mol. Cell Biol. 3 (2002) 813–825.

[6] J.M. Scholey, Intraflagellar transport, Annu. Rev. Cell Dev. Biol. 19 (2003) 423–443.
[7] L.B. Pedersen, J.L. Rosenbaum, Ciliary assembly and maintenance, Curr. Top. Dev. Biol. 85 (2008) 23–61.
[8] K.G. Kozminski, K.A. Johnson, P. Forscher, J.L. Rosenbaum, A motility in the eukaryotic flagellum unrelated to flagellar beating, Proc. Natl. Acad. Sci. USA 90 (1993) 5519–5523.
[9] K.G. Kozminski, P.L. Beech, J.L. Rosenbaum, The *Chlamydomonas* kinesin-like protein FLA10 is involved in motility associated with the flagellar membrane, J. Cell Biol. 131 (1995) 1517–1527.
[10] J.M. Scholey, Intraflagellar transport motors in cilia: Moving along the cell's antenna, J. Cell Biol. 180 (2008) 23–29.
[11] S. Endoh-Yamagami, M. Evangelista, D. Wilson, X. Wen, J.W. Theunissen, K. Phamluong, M. Davis, S.J. Scales, M.J. Solloway, F.J. de Sauvage, A.S. Peterson, The mammalian Cos2 homolog Kif7 plays an essential role in modulating Hh signal transduction during development, Curr. Biol. 19 (2009) 1320–1326.
[12] T. Piao, M. Luo, L. Wang, Y. Guo, D. Li, P. Li, W.J. Snell, J. Pan, A microtubule depolymerizing kinesin functions during both flagellar disassembly and flagellar assembly in *Chlamydomonas*, Proc. Natl. Acad. Sci. USA 106 (2009) 4713–4718.
[13] S.C. Goetz, K.V. Anderson, The primary cilium: A signaling centre during vertebrate development, Nat. Rev. Genet. 11 (2010) 331–344.
[14] B.H. Gibbons, D.J. Asai, W.-J. Tang, T.S. Hays, I.R. Gibbons, Phylogeny and expression of axonemal and cytoplasmic dynein genes in sea urchins, Mol. Biol. Cell 5 (1994) 57–70.
[15] Y. Tanaka, Z. Zhang, N. Hirokawa, Identification and molecular evolution of new dynein-like protein sequences in rat brain, J. Cell Sci. 108 (1995) 1883–1893.
[16] E.A. Vaisberg, P.M. Grissom, J.R. McIntosh, Mammalian cells express three distinct dynein heavy chains that are localized to different cytoplasmic organelles, J. Cell Biol. 133 (1996) 831–842.
[17] A. Mikami, S.H. Tynan, T. Hama, K. Luby-Phelps, T. Saito, J.E. Crandall, J.C. Besharse, R.B. Vallee, Molecular structure of cytoplasmic dynein 2 and its distribution in neuronal and ciliated cells, J. Cell Sci. 115 (2002) 4801–4808.
[18] P.S. Criswell, L.E. Ostrowski, D.J. Asai, A novel cytoplasmic dynein heavy chain: Expression of DHC1b in mammalian ciliated epithelial cells, J. Cell Sci. 109 (1996) 1891–1898.
[19] P.S. Criswell, D.J. Asai, Evidence for four cytoplasmic dynein heavy chain isoforms in rat testis, Mol. Biol. Cell 9 (1998) 237–347.
[20] G.J. Pazour, C.G. Wilkerson, G.B. Witman, A dynein light chain is essential for the retrograde particle movement of intraflagellar transport (IFT), J. Cell Biol. 141 (1998) 979–992.
[21] J. Collet, C.A. Spike, E.A. Lundquist, J.E. Shaw, R.K. Herman, Analysis of *osm-6*, a gene that affects sensory cilium structure and sensory neuron function in *Caenorhabditis elegans*, Genetics 148 (1998) 187–200.
[22] D. Signor, K.P. Wedaman, J.T. Orozco, N.D. Dwyer, C.I. Bargmann, L.S. Rose, J.M. Scholey, Role of a class DHC1b dynein in retrograde transport of IFT motors and IFT raft particles along cilia, but not dendrites, in chemosensory neurons of living *Caenorhabditis elegans*, J. Cell Biol. 147 (1999) 519–530.
[23] J.A. Lewis, J.A. Hodgkins, Specific neuroanatomical changes in chemosensory mutants of the nematode *Caenorhabditis elegans*, J. Comp. Neurol. 172 (1977) 489–510.
[24] P.S. Albert, S.J. Brown, D.L. Riddle, Sensory control of dauer larva formation in *Caenorhabditis elegans*, J. Comp. Neurol. 198 (1981) 435–451.
[25] G.J. Pazour, B.L. Dickert, G.B. Witman, The DHC1b (DHC2) isoform of cytoplasmic dynein is required for flagellar assembly, J. Cell Biol. 144 (1999) 473–481.
[26] M.E. Porter, R. Bower, J.A. Knott, P. Byrd, W. Dentler, Cytoplasmic dynein heavy chain 1b is required for flagellar assembly in *Chlamydomonas*, Mol. Biol. Cell 10 (1999) 693–712.

[27] S.R. Wicks, C.J. de Vries, H.G.A.M. van Luenen, R.H.A. Plasterk, CHE-3, a cytosolic dynein heavy chain, is required for sensory cilia structure and function in *Caenorhabditis elegans*, Dev. Biol. 221 (2000) 295–307.
[28] M.A. Gee, J.E. Heuser, R.B. Vallee, An extended microtubule-binding structure within the dynein motor domain, Nature 390 (1997) 636–639.
[29] P.M. Grissom, E.A. Vaisberg, J.R. McIntosh, Identification of a novel light intermediate chain (D2LIC) for mammalian cytoplasmic dynein 2, Mol. Biol. Cell 13 (2002) 817–829.
[30] J.C. Schafer, C.J. Haycraft, J.H. Thomas, B.K. Yoder, P. Swoboda, XBX-1 encodes a dynein light intermediate chain required for retrograde intraflagellar transport and cilia assembly in *Caenorhabditis elegans*, Mol. Biol. Cell 14 (2003) 2057–2070.
[31] C.A. Perrone, D. Tritschler, P. Taulman, R. Bower, B.K. Yoder, M.E. Porter, A novel dynein light intermediate chain colocalizes with the retrograde motor for intraflagellar transport at sites of axoneme assembly in *Chlamydomonas* and mammalian cells, Mol. Biol. Cell 14 (2003) 2041–2056.
[32] Y. Hou, G.J. Pazour, G.B. Witman, A dynein light intermediate chain, D1bLIC, is required for retrograde intraflagellar transport, Mol. Biol. Cell 15 (2004) 4382–4394.
[33] G.J. Pazour, N. Agrin, J. Leszyk, G.B. Witman, Proteomic analysis of a eukaryotic cilium, J. Cell Biol. 170 (2005) 103–113.
[34] H. Qin, Z. Wang, D. Diener, J. Rosenbaum, Intraflagellar transport protein 27 is a small G protein involved in cell-cycle control, Curr. Biol. 17 (2007) 193–202.
[35] E. Efimenko, K. Bubb, H.Y. Mak, T. Holzman, M.R. Leroux, G. Ruvkun, J.H. Thomas, P. Swoboda, Analysis of *xbx* genes in *C. elegans*, Development 132 (2005) 1923–1934.
[36] J. Pan, W.J. Snell, Kinesin-II is required for flagellar sensory transduction during fertilization in *Chlamydomonas*, Mol. Biol. Cell 13 (2002) 1417–1426.
[37] R. Rompolas, L.B. Pedersen, R.S. Patel-King, S.M. King, *Chlamydomonas* FAP133 is a dynein intermediate chain associated with the retrograde intraflagellar transport motor, J. Cell Sci. 120 (2007) 3653–3665.
[38] D.M. Baron, K.S. Ralston, Z.P. Kabututu, K.L. Hill, Functional genomics in *Trypanosoma brucei* identifies evolutionarily conserved components of motile flagella, J. Cell Sci. 120 (2007) 478–491.
[39] B. Wickstead, K. Gull, Dyneins across eukaryotes: A comparative genomic analysis, Traffic 8 (2007) 1708–1721.
[40] B.L. Krock, I. Mills-Henry, B.D. Perkins, Retrograde intraflagellar transport by cytoplasmic dynein-2 is required for outer segment extension in vertebrate photoreceptors but not arrestin translocation, Invest. Ophth. Vis. Sci. 50 (2009) 5463–5471.
[41] Y.-K. Mok, K.W.-H. Lo, M. Zhang, Structure of Tctex-1 and its interaction with cytoplasmic dynein intermediate chain, J. Biol. Chem. 276 (2001). 14067–14074.
[42] S.M. King, R. Kamiya, Axonemal dyneins: Assembly, structure, and force generation, in: G.B. Witman (Ed.), The *Chlamydomonas* Sourcebook. Vol. 3. Cell Motility and Behavior, Elsevier, New York, 2009, pp. 445–478.
[43] D. Huangfu, K.V. Anderson, Cilia and hedgehog responsiveness in the mouse, Proc. Natl. Acad. Sci. USA 102 (2005). 11325–11330.
[44] S.R. May, A.M. Ashique, M. Karlen, B. Wang, Y. Shen, K. Zarbalis, J. Reiter, J. Ericson, A.S. Peterson, Loss of the retrograde motor for IFT disrupts localization of Smo to cilia and prevents the expression of both activator and repressor functions of Gli, Dev. Biol. 287 (2005) 378–389.
[45] K.A. Johnson, J.L. Rosenbaum, Polarity of flagellar assembly in *Chlamydomonas*, J. Cell Biol. 119 (1992) 1605–1611.
[46] W.F. Marshall, J.L. Rosenbaum, Intraflagellar transport balances continuous turnover of outer doublet microtubules: Implications for flagellar length control, J. Cell Biol. 155 (2001) 405–414.

[47] H. Qin, D.R. Diener, S. Geimer, D.G. Cole, J.L. Rosenbaum, Intraflagellar transport (IFT) cargo: IFT transports flagellar precursors to the tip and turnover products to the cell body, J. Cell Biol. 164 (2004) 255–266.
[48] H. Qin, J.L. Rosenbaum, M.M. Barr, An autosomal recessive polycystic kidney disease gene homolog is involved in intraflagellar transport in *C. elegans* ciliated sensory neurons, Curr. Biol. 11 (2001) 457–461.
[49] K. Huang, D.R. Diener, A. Mitchell, G.J. Pazour, G.B. Witman, J.L. Rosenbaum, Function and dynamics of PKD2 in *Chlamydomonas reinhardtii* flagella, J. Cell Biol. 179 (2007) 501–514.
[50] G.J. Pazour, J.T. San Agustin, J.A. Follit, J.L. Rosenbaum, G.B. Witman, Polycystin-2 localizes to kidney cilia and the ciliary level is elevated in *orpk* mice with polycystic kidney disease, Curr. Bio. 12 (2002) R378–R380.
[51] M.V. Nachury, A.V. Loktev, Q. Zhang, C.J. Westlake, J. Peranen, A. Merdes, D.C. Slusarski, R.H. Scheller, J.F. Bazan, V.C. Sheffield, P.K. Jackson, A core complex of BBS proteins cooperates with the GTPase Rab8 to promote ciliary membrane biogenesis, Cell. 129 (2007) 1201–1213.
[52] K.-F. Lechtreck, E.C. Johnson, T. Sakai, D. Cochran, B.A. Ballif, J. Rush, G.J. Pazour, M. Ikebe, G.B. Witman, The *Chlamydomonas reinhardtii* BBSome is an IFT cargo required for export of specific signaling proteins from flagella, J. Cell Biol. 187 (2009) 1117–1132.
[53] P.J.R. Ocbina, K.V. Anderson, Intraflagellar transport, cilia, and mammalian Hedgehog signaling: Analysis in mouse embryonic fibroblasts, Dev. Dynam. 237 (2008) 2030–2038.
[54] J. Kim, M. Kato, P.A. Beachy, Gli2 trafficking links Hedgehog-dependent activation of Smoothened in the primary cilium to transcriptional activation in the nucleus, Proc. Natl. Acad. Sci. USA 106 (2009) 21666–21671.
[55] X. Wen, C.K. Lai, M. Evangelista, J.-A. Hongo, F.J. de Sauvage, S.J. Scales, Kinetics of Hedgehog-dependent full-length Gli3 accumulation in primary cilia and subsequent degradation, Mol. Cell Biol. 30 (2010) 1910–1922.
[56] G.J. Pazour, B.L. Dickert, G.B. Witman, The DHC1b (DHC2) isoform of cytoplasmic dynein is necessary for flagellar maintenance as well as flagellar assembly, Mol. Biol. Cell 10 (Supplement) (1999) 369a.
[57] V. Rajagopalan, A. Subramanian, D.E. Wilkes, D.G. Pennock, D.J. Asai, Dynein-2 affects the regulation of ciliary length but is not required for ciliogenesis in *Tetrahymena thermophila*, Mol. Biol. Cell 20 (2009) 708–720.
[58] D.J. Asai, V. Rajagopalan, D.E. Wilkes, Dynein-2 and ciliogenesis in *Tetrahymena*, Cell Motil. Cytoskel. 66 (2009) 673–677.
[59] S.S. Merchant, S.E. Prochnik, O. Vallon, E.H. Harris, S.J. Karpowicz, G.B. Witman, A. Terry, A. Salamov, L.K. Fritz-Laylin, L. Maréchal-Drouard, W.F. Marshall, L.H. Qu, D.R. Nelson, A.A. Sanderfoot, M.H. Spalding, V.V. Kapitonov, Q. Ren, P. Ferris, E. Lindquist, H. Shapiro, S.M. Lucas, J. Grimwood, J. Schmutz, P. Cardol, H. Cerutti, G. Chanfreau, C.L. Chen, V. Cognat, M.T. Croft, R. Dent, S. Dutcher, E. Fernández, H. Fukuzawa, D. González-Ballester, D. González-Halphen, A. Hallmann, M. Hanikenne, M. Hippler, W. Inwood, K. Jabbari, M. Kalanon, R. Kuras, P.A. Lefebvre, S.D. Lemaire, A.V. Lobanov, M. Lohr, A. Manuell, I. Meier, L. Mets, M. Mittag, T. Mittelmeier, J.V. Moroney, J. Moseley, C. Napoli, A.M. Nedelcu, K. Niyogi, S.V. Novoselov, I.T. Paulsen, G. Pazour, S. Purton, J.P. Ral, D.M. Riaño-Pachón, W. Riekhof, L. Rymarquis, M. Schroda, D. Stern, J. Umen, R. Willows, N. Wilson, S.L. Zimmer, J. Allmer, J. Balk, K. Bisova, C.J. Chen, M. Elias, K. Gendler, C. Hauser, M.R. Lamb, H. Ledford, J.C. Long, J. Minagawa, M.D. Page, J. Pan, W. Pootakham, S. Roje, A. Rose, E. Stahlberg, A.M. Terauchi, P. Yang, S. Ball, C. Bowler, C.L. Dieckmann, V.N. Gladyshev, P. Green, R. Jorgensen, S. Mayfield, B. Mueller-Roeber, S. Rajamani, R.T. Sayre, P. Brokstein, I. Dubchak, D. Goodstein, L. Hornick, Y.W. Huang, J. Jhaveri, Y. Luo, D. Martínez, W.C. Ngau, B. Otillar, A. Poliakov, A. Porter, L. Szajkowski,

G. Werner, K. Zhou, I.V. Grigoriev, D.S. Rokhsar, A.R. Grossman, The *Chlamydomonas* genome reveals the evolution of key animal and plant functions, Science 318 (2007) 245–251.

[60] C. Adhiambo, J.D. Forney, D.J. Asai, J.H. LeBowitz, The two cytoplasmic dynein-2 isoforms in *Leishmania* perform separate functions, Mol. Biochem. Parasit. 143 (2005) 216–225.

[61] L. Kohl, D. Robinson, P. Bastin, Novel roles for the flagellum in cell morphogenesis and cytokinesis of trypanosomes, EMBO J. 22 (2003) 5336–5346.

[62] P.D. Calvert, K.J. Strissel, W.E. Schiesser, E.N. Pugh Jr., V.Y. Arshavsky, Light-driven translocation of signaling proteins in vertebrate photoreceptors, Trends Cell Bio. 16 (2006) 560–568.

[63] A.J. Roberts, N. Numata, M.L. Walker, Y.S. Kato, B. Malkova, T. Kon, R. Ohkura, F. Arisaka, P.J. Knight, K. Sutoh, S.A. Burgess, AAA+ ring and linker swing mechanism in the dynein motor, Cell 136 (2009) 485–495.

[64] A.P. Carter, R.D. Vale, Communication between the AAA+ ring and microtubule-binding domain of dynein, Biochem. Cell Biol. 88 (2010) 15–21.

In this chapter

15

Cytoplasmic Dynein Function Defined by Subunit Composition

K. Kevin Pfister [1], Kevin W.-H. Lo [2]

[1] Cell Biology Department, University of Virginia School of Medicine, Charlottesville, VA, USA
[2] Department of Orthopaedic Surgery, University of Connecticut Health Center, Farmington, CT, USA

15.1 Introduction

Multicellular organisms need to move a variety of organelles and proteins to specific cellular locations in order to maintain proper cell function, including cell polarity. To accomplish this, cells use motor proteins (mechanochemical ATPases) that transport cargo along roads made of polarized filaments. The members of the kinesin family are primarily used to move cargo to microtubule plus ends, which are often located in the periphery of the cell, and cytoplasmic dynein moves cargo toward microtubule minus ends, found in the cell center [1–4]. Cells have considerable flexibility to regulate transport to microtubule plus ends as there are over 45 different genes encoding for kinesin motors [5]. However, there is only one gene for the cytoplasmic dynein motor [1]. Understanding how the single cytoplasmic dynein motor suffices for the proper organization of organelles in the cytoplasm is the subject of considerable investigation, especially as cells have approximately 13 genes encoding the dynein motors used in flagella [6–8]. Interestingly, flagella also contain a dynein complex whose subunits are most closely related to those found in cytoplasmic dynein; however, to date this second cytoplasmic dynein complex has been found to have a role only in intraflagellar transport [1,9].

Cytoplasmic dynein 1 is a large protein complex composed of six subunits, the motor containing heavy chain (HC) and five smaller subunits (referred to here as the base subunits), which make up the base of the complex. Most of the base subunits have been implicated in cargo binding, and vertebrates have at least two genes for each of these subunits [1,10]. The core of the cytoplasmic dynein complex is a dimer of the HC (DYNC1H). Attached to the HC N-terminal region are a dimer of the intermediate chain (IC) (DYNC1I1 and DYNC1I2) and a dimer of the light-intermediate chain (LIC) (DYNC1LI1 and DYNC1LI2). Bound to the IC

Dyneins DOI: 10.1016/B978-0-12-382004-4.10015-9
Copyright © 2012 by Elsevier Inc. All rights reserved.

dimer are three pairs of LCs, which are also present as dimers: the Tctex1 family (DYNC1LT1 and DYNC1LT3), the Roadblock family (DYNC1LRB1 and DYNC1LRB2), and the LC8 family (DYNC1LL1 and DYNC1LL2). All of these subunits copurify with dynein isolated from brain by microtubule affinity, standard biochemical purification methods, and immunoprecipitation using antibodies to the IC or LCs [11–15]. However, there has been no systematic effort to purify or characterize dynein complexes based on the isoform composition of the different base subunits.

This chapter discusses the functional roles of the different subunits and evaluates the evidence supporting the hypothesis that differential regulation of cytoplasmic dynein is accomplished by utilizing different isoforms of the five base subunits to create functionally distinct cytoplasmic dynein complexes (Table 15.1). Starting with two genes for each subunit and assuming: (1) uniform tissue expression of all the subunit isoforms; and (2) that each subunit only forms homodimers, cells have the potential to generate 32 distinct dynein complexes. When the alternative splicing of the IC mRNA that occurs in vertebrates and *Drosophila* is taken into account, the number of potential dynein complexes could be increased six- to

Table 15.1 Composition of Cytoplasmic Dynein 1[a]. Summary of the Cytoplasmic Dynein 1 Subunit Isoforms and their known Expression Patterns

Subunit	Name	Expression
Heavy chain	DYNC1H1 (HC)	ubiquitous
Intermediate chain	DYNC1I1[b] (IC-1)	IC-1A brain (neuron) IC-1B brain (neuron) IC-1C brain (neuron)/testis/ovary
	DYNC1I2[c] (IC-2) IC-2C	ubiquitous IC-2B brain (neuron)/testis/liver IC-2A brain
Light intermediate chain	DYNC1LIC1 (LIC 1) DYNC1LIC2 (LIC 2)	ubiquitous ubiquitous
Light chains		
Tctex1 family	DYNLT1	ubiquitous
	DYNLT3	ubiquitous
Road-block family[d]	DYNLRB1	ubiquitous
	DYNLRB2	kidney/liver
LC8 family	DYNLL1	ubiquitous
	DYNLL2	ubiquitous

[a]All subunits are present as homodimers. The formal subunit name is followed by the descriptive abbreviation used in the text in parentheses.

[b]Data is from analyses in the rat and mouse. Note that the two additional IC-1 isoforms identified in the mouse (not listed) were found exclusively in brain.

[c]Data is primarily from analyses in the rat. Note that a different expression pattern was identified in the mouse. All the IC-2 isoforms identified in the mouse, with the exception of IC-2C, were found exclusively in the brain.

[d]Data is from rodent tissues [62]. In human tissues DYNLRB2 was found in the brain [100].

twelve-fold [16,17]. Supporting a role for the base subunits in cytoplasmic dynein regulation and cargo binding are the observations that pieces of the HC will move in the absence of the other subunits [18,19] and that genetic mutations of the base subunits will suppress HC mutations [20]. The dynein complexes produced through the recruitment of different isoforms of the base subunits would be subject to other regulatory mechanisms, such as those provided by dynactin or Lis1/NudE (see Chapters 16 and 19).

15.2 Heavy Chain (DYNC1H)

The HC DYNC1H is the force-producing component of the dynein complex. It is the largest subunit, with a molecular mass of approximately 530 kDa. Only a single cytoplasmic HC species has been discovered. This is in contrast to the 13 different HC species reported in the inner and outer dynein arm structures of the flagellar axoneme [6,21]. It is also observed that higher plants function without this protein [9]. The C-terminal region of the HC is the force-generating domain of the dynein complex. This region has the appearance of beads arranged in a doughnut shape that also has a projecting stalk. The beads correspond to six AAA domains [22–24]. AAA domains are regions of potential ATP binding and hydrolysis, and thus they generate the energy required for translocation [25]. The first four AAA domains are capable of binding ATP [26]. A coiled-coil stalk (around 15 nm long) projects from the region between the fourth and fifth AAA domains and the tip of this stalk binds to and "walks" along the microtubule via a repeated cycle of attachment and detachment in conjunction with the hydrolysis of ATP by the first AAA domain [24,27]. The HC forms a dimer and the dimerization region is located at the N-terminus. Interestingly, the dimerization region overlaps with the light intermediate chain (LIC) and IC binding sites [15].

15.3 Light Intermediate Chain (DYNC1LI)

Two genes for the LIC, DYNC1LI1 and DYNC1LI2, are present in most vertebrates. The limited expression data available suggest that both are expressed ubiquitously as they are found in various cultured cells. Multiple protein isoforms, including phospho-isoforms of the LICs from various sources, have also been observed with two-dimensional electrophoresis [28–31]. The LICs also contain a predicted nucleotide-binding domain similar to that found in the ABC transporter family of ATPases [29,32]. In overexpression assays, the two DYNC1LI family members form only homodimers, and immunoprecipitation studies indicate that LIC isoform binding to the dynein HC is mutually exclusive [15].

There is considerable evidence that dynein populations distinguished by the LIC isoforms have different functions in cultured cells. Cytoplasmic dynein with LIC 1, not LIC 2, is necessary for dynein binding to pericentrin and direct binding to adenovirus hexons [33,34]. During cell division, LIC 1 localizes to the mitotic spindle and midbody, while LIC 2 localizes to spindle poles [35]. Depletion of LIC 1 in cultured cells leads to defects in mitotic checkpoint signaling, in particular a delay in metaphase and defective transport of Mad1/2 and ZW10, but not BubR1, from kinetochores [36]. RNA interference (RNAi) depletion studies also show a role for dynein with LIC 1 in the maintenance of endoplasmic reticulum–Golgi transport, while dynein with LIC 2 is important for endosomal function and cytokinesis [37]. LIC 2 associates with Par3 and is important for centrosome orientation [38]. In Xenopus, only one of three LICs identified with SDS-PAGE co-purified with melanosomes [39]. Phosphorylation of the LICs has been correlated with reduced dynein binding to membrane-bounded organelles during mitosis [40–42] and with dynein's role in the checkpoint [36]. To date no functional role for the LIC ATP-binding region has been identified; for example, mutations of the ATP-binding region had no effect on binding to the HC or pericentrin [34].

Fungal species also provide insight into the roles of the LICs in dynein function. In the filamentous fungi *Aspergillus nidulans*, the LICs are necessary for IC binding to the HC [43]. In the fission yeast *Schizosaccharomyces pombe*, the LIC is necessary for dynein HC localization to spindle pole bodies [44]. In the budding yeast *Saccharomyces cerevisiae*, dynein HC localization to cortical dots requires the LICs, but targeting of the dynein HC to microtubule plus ends does not depend on the LICs [45].

15.4 Intermediate Chain (DYNC1I)

The IC, also known as DYNC1I or IC, serves as a scaffold in the dynein complex, directly interacting with all the other subunits of the dynein complex and various other cargo proteins including the dynein motor activator, dynactin [1,46]. The IC's C-terminus contains seven WD repeats, which are presumed to form a β propeller structure responsible for interacting with HC [47–49]. The far N-terminus of the molecule contains a coiled-coil that binds to the p150 subunit of dynactin [50]. This is followed by a serine-rich region that is bracketed by the two regions of alternative splicing. Next comes the binding sites for two of the LC families, LC8 (DYNLL) and Tctex1 (DYNLT) [51,52], while the binding region for the Roadblock (DYNLRB) LC family is just upstream of the first WD-repeat domain [46,53,54]. The dimerization domain of the rat ICs was identified by independent groups using biochemical and structural analytical techniques: it is located immediately N-terminal to the roadblock LC-binding region [46,55]. IC dimerization did not require the binding of any LCs. Recent structural studies of the *Drosophila* IC found that IC dimerization required LC binding and that the

roadblock binding site partially overlapped with the proposed IC dimerization domain [56,57]. These results, and the distinctive alternative splicing pattern of *Drosophila* mRNA, suggest that that some subdomains of the IC may not be well-conserved among higher and lower eukaryotes [58].

There are two IC genes in vertebrates and both undergo alternative splicing at their N-termini. While IC alternative splicing was first studied in rat and fruit flies, recently a more systematic survey of alternative splicing in mouse has been completed [16]. This study suggests that 12 different protein isoforms are possible in the mouse. Interestingly, 11 different mRNAs from the IC-2 gene were identified. This was because the IC-2 gene has two different promoters and first exons. However, as the first exon does not contribute to the protein coding sequence, six different IC-2 protein isoforms can be produced. The presence of two different promoters suggests the possibility of fine regulation of the expression of the IC-2 isoforms. To date, only six IC isoforms have been identified in rat, three splice variants for each of the two genes [17,50,59,60].

The properties of the rat ICs have been extensively characterized. All six isoforms of the rat ICs are capable of forming homo- and hetero-dimers when they are overexpressed in cultured cells [46]. Interestingly, these studies utilized the same assay, which was used to show that the LICs form only homodimers [34]. The functional significance of IC heterodimer formation is unclear. While it is known that IC homodimers bind HCs and LCs, subunit binding has not been shown for IC heterodimers. Homodimers may be more likely to bind the other dynein subunits [61]. But it has also been hypothesized that heterodimer formation by dynein subunits will enlarge the number of potential dynein motor subtypes available for cargo-binding specificity [62]. There is also evidence that IC phosphorylation is important for regulating dynein function on membrane-bounded organelles and kinetochores [30,63,64].

One IC-2 isoform, known as IC-2C, is found in almost all cell types and tissues and it is often the only isoform present in most cultured cells [17]. Although the IC-2B isoform is commonly found in most rat organs, to date it has only been found in cultured neurons and neuroblastoma cell lines [11,17,31,59]. Interestingly, in rat pheochromocytoma (PC12) cells, the IC isoform expression pattern changes upon nerve-growth-factor-induced differentiation from primarily IC-2C to predominantly IC-2B [31]. All the IC-1 isoforms are found in adult mouse and rat brain tissues, although their relative expression levels are highly regulated during brain development. IC-2C is found earliest in the brain, while the other isoforms appear only after embryonic day 13 [17,59,60]. Four IC isoforms are found in cultured embryonic hippocampal and cortical neurons [59,60]. The IC-1 isoforms appear to be restricted to brain and neural tissues in rat and mouse, with the exception of the IC-1C isoform, which is found in testis and ovary. Since axons have their microtubule plus ends pointing to axon terminals, dynein complexes must be transported into the axon in order to be positioned at the terminals to

move material back to the cell bodies. In adult optic nerves, dynein complexes with IC-2C are transported more rapidly toward the terminus than dynein complexes containing the other IC isoforms [65,66].

These expression patterns indicate that dyneins with different IC isoforms cannot be important for dynein regulation in fibroblasts but may be important for regulation of dynein function in neurons. Consistent with this, we found that cultured neurons that express two IC-1 and two IC-2 isoforms use dynein containing the IC-1 isoforms to transport TrkB-containing signaling endosomes. Interestingly, PC12 neuroblastoma cells, which do not express IC-1 isoforms, utilize an IC-2 isoform to transport signaling endosomes [67]. It is possible that the ICs were recruited for neuronal dynein regulation due to the particular requirements that transport in long neuronal axons place on motor function. The observation that neurons often display the first phenotypes observed in dynein or kinesin mutations in mice and *Drosophila* suggest that transport in long axons pushes the motor protein's capacities to their limits [68–74].

15.5 DynII (LC8 Light Chain)

The DYNLL LC is the smallest subunit in the dynein motor complex and was the first LC subunit shown to be a stoichiometric component of the cytoplasmic dynein 1 complex [11]. The DYNLL family has two genes, DYNLL1 and DYNLL2. The DYNLL isoforms form homo- and heterodimers in overexpression assays [12]. Both members of the DYNLL family bind directly to all six dynein IC isoforms in a yeast two-hybrid binding assay [12].

There has been growing realization that DYNLL has roles independent of the dynein complex. The data supporting this include: (1) sucrose gradient fractionation of mammalian cytosol revealing that most of the DYNLL is not associated with the dynein complex while the other subunits are exclusively associated with the complex [11,12]; and (2) the finding that DYNLL interacts with targets that are not connected with dynein or microtubule-based transport [75,76]. Among the large number of protein complexes with which DYNLL has been shown to associate are flagellar outer-arm dynein, flagellar I1 inner-arm dynein, flagellar radial spokes, myosin Va, neuronal nitric oxide synthase, the swallow transcription factor, p21-activated kinase-1, and the p53 binding protein-1 [11,21,75–83]. The initial studies on the binding of DYNLL to the IC and other proteins led to the proposal that DYNLL functions as a cargo adaptor between the dynein motor complex and the proteins [52].

Two consensus sequences in DYNLL-interacting proteins have been identified using various *in vitro* binding assays, the amino acid sequence "K/R*X*TQT," and the GIQVD-like motif [52,77,84]. On the basis of various biophysical and biochemical analyses on the structure of DYNLL with its interacting targets, it has been proposed that the DYNLL dimer is essential for the dimerization of various

target-binding proteins [75,85,86]. Interestingly, reports have suggested that the dimerization of DYNLL is regulated by different stimuli such as phosphorylation and pH change, and the dimer formation of DYNLL is correlated to the bioactivity of its interacting proteins [87,88].

Both DYNLL isoforms co-purify with cytoplasmic dynein from brain [14], but few other studies on their relative expression patterns have been published. DYNLL2 alone binds myosin Va and the alternatively spliced exon B of Myosin Va is an important part of the binding site [83,89]. To date, no specific dynein functions have been linked to the different DYNLL isoforms. However, it has been shown that DYNLL2 selectively binds Bcl-2-modifying factor (Bmf) whereas DYNLL1 binds preferably to BH3-only proapoptotic protein (Bim) [90,91]. Such distinct protein–protein interaction may be important for regulating the Bmf and Bim proteins in response to apoptotic stimulations.

15.6 DYNLT (Tctex1 Light Chain)

The DYNLT (Tctex1) family has two members, DYNLT1 and DYNLT3 [1,92]. Both DYNLT1 and DYNLT3 interacted with all six IC isoforms in a yeast two-hybrid assay [12]. Yeast two-hybrid and co-immunoprecipitation overexpression assays demonstrated that both members of the DYNLT family were capable of forming homo- and hetero-dimers. However, only homodimers were assembled into functional dynein complexes [12]. This finding indicates that the heterodimers were not functional. This finding also points to a pitfall in using overexpression studies to elucidate the relative roles of DYNLT1 and DYNLT3, as overexpression of one isoform results in the formation of functional homodimers of that isoform but drives all of the other isoforms into non-functional heterodimers. Thus, phenotypes that are observed after expression of one family member are caused by failure to assemble dynein complexes containing the other family member [93]. It has also been suggested that, like the DYNLL family, the two DYNLT family members have roles independent of their association with cytoplasmic dynein [94,95].

From limited expression studies, it is thought that both DYNLT family members are found in most fetal and adult tissues and most cultured cells [92,93,96]. In interphase cells, DYNLT1 localizes predominantly to the Golgi apparatus whereas DYNLT3 was distributed throughout the cytoplasm [93,94,97]. In mitotic cells, both DYNLT1 and DYNLT3 were distributed along spindle fibers [93,97]. However, siRNA reduction in the level of DYNLT3 caused a delay in mitosis while reduction of intracellular DYNLT1 levels with an *in vivo* molecular trap had no effect on mitotic progression [97,98]. This is consistent with the finding that DYNLT3 binds to the checkpoint protein Bub3 [97]. Knockdown of DYNLT1 with the *in vivo* trap also rapidly disrupted the organization of lysosomes and early endosomes and, more slowly, the Golgi [98]. Consistent with this, dynein containing DYNLT1 has been implicated in the transport of rhodopsin to apical

membranes [93]. DYNLT1 has also been linked with the transport of many individual proteins, but, as in the case of DYNLL, the functional significance of this binding is uncertain. Interestingly, there is a single DYNLT family member in *Drosophila* and, while null mutations result in male sterility, they demonstrate that it is dispensable for other essential dynein functions [99].

15.7 DYNLRB (Roadblock Light Chain)

In mammalian cells two DYNLRB LC genes have been identified, DYNLRB1 and DYNLRB2. Expression studies revealed that DYNLRB1 mRNA is found in all human tissues while DYNLRB2 mRNA expression is restricted to certain tissues including kidney and testis, and it is not found in brain [62,100]. Both members of the DYNLRB family bind directly to all of the IC isoforms [53]. An *in vitro* pull-down assay and *in vivo* yeast two-hybrid expression system demonstrated that both DYNLRB1 and DYNLRB2 are capable of forming homo- and heterodimers [62]. DYNLRB was found to localize along microtubules in the form of punctuate structures in neuroblastoma cells [62].

Unlike DYNLL and DYNLT, the functional role of DYNLRB in the dynein complex is not clearly defined. In *Drosophila*, DYNLRB (also known as LC7) is essential for proper axonal transport and dendrite growth. Mutation of the DYNLRB gene results in mitotic defects, accumulation of axonal cargoes, and larval or pupal lethality, suggesting that DYNLRB plays a significant role in dynein assembly and regulation. Recent structural analysis of the DYNLRB and IC complex revealed that the IC undergoes a disorder-to-order transition upon DYNLRB binding, suggesting that DYNLRB was able to stabilize the IC fragment in solution [56].

Only a handful of DYNLRB interacting partners have been identified. Apart from the dynein IC, DYNLRB1 specifically binds to the small GTPase Rab6, to the human reduced folate carrier, and to the TGFβ receptor [101–104]. However, to date none of the DYNLRB binding proteins appear to be directly connected to dynein-mediated translocation. Thus, it remains to be determined if DYNLRB isoforms contribute to specific dynein functions. Similar to the members of other dynein LC families, the two isoforms of DYNLRB have been reported to interact specifically with other protein targets. In one study, DYNLRB2 was found to be responsible for Smad3-dependent TGFβ signaling by selectively interacting with TGFβ receptor type II, while DYNLRB1 was involved exclusively in Smad2-dependent TGFβ signaling [105,106].

15.8 Conclusion

The data described above conclusively show that distinct dynein functions are correlated with dynein complexes containing different isoforms of either the IC,

the LIC, or the DYNLT LC. The data suggest that the LIC and DYNLT isoforms are specific for different cellular "housekeeping" dynein functions, while dynein complexes with different IC isoforms are utilized for neuron-specific functions. Thus, at present, there is good evidence for four different functionally distinct dynein complexes in fibroblasts and most likely six in neurons. However, several important data remain to be established. There are no studies showing specific dynein functions for the isoforms of the DYNLL or DYNLRB LCs, possibly because of a lack of specific reagents. Most importantly, there are no studies on the potential functions of dynein complexes containing various combinations of the subunit isoforms. Thus, the number of potential combinations of dynein base subunits that exist and their functional significance remain to be determined.

Acknowledgments

This work was supported by a grant from the National Institute of General Medical Science.

References

[1] K.K. Pfister, P.R. Shah, H. Hummerich, A. Russ, J. Cotton, A.A. Annuar, S.M. King, E.M. Fisher, Genetic analysis of the cytoplasmic dynein subunit families, PLoS Genet. 2 (2006) e1.

[2] I.R. Gibbons, Dynein family of motor proteins: Present status and future questions, Cell Motil. Cytoskeleton 32 (1995) 136–144.

[3] R.B. Vallee, J.C. Williams, D. Varma, L.E. Barnhart, Dynein: An ancient motor protein involved in multiple modes of transport, J. Neurobiol. 58 (2004) 189–200.

[4] H. Miki, Y. Okada, N. Hirokawa, Analysis of the kinesin superfamily: Insights into structure and function, Trends Cell Biol. 15 (2005) 467–476.

[5] N. Hirokawa, Y. Noda, Y. Tanaka, S. Niwa, Kinesin superfamily motor proteins and intracellular transport, Nat. Rev. Mol. Cell Biol. 10 (2009) 682–696.

[6] B.H. Gibbons, D.J. Asai, W.J. Tang, T.S. Hays, I.R. Gibbons, Phylogeny and expression of axonemal and cytoplasmic dynein genes in sea urchins, Mol. Biol. Cell 5 (1994) 57–70.

[7] K.T. Vaughan, A. Mikami, B.M. Paschal, E.L. Holzbaur, S.M. Hughes, C.J. Echeverri, K.J. Moore, D.J. Gilbert, N.G. Copeland, N.A. Jenkins, R.B. Vallee, Multiple mouse chromosomal loci for dynein-based motility, Genomics 36 (1996) 29–38.

[8] R.L. Morris, M.P. Hoffman, R.A. Obar, S.S. McCafferty, I.R. Gibbons, A.D. Leone, J. Cool, E.L. Allgood, A.M. Musante, K.M. Judkins, B.J. Rossetti, A.P. Rawson, D.R. Burgess, Analysis of cytoskeletal and motility proteins in the sea urchin genome assembly, Dev. Biol. 300 (2006) 219–237.

[9] B. Wickstead, K. Gull, Dyneins across eukaryotes: A comparative genomic analysis, Traffic 8 (2007) 1708–1721.

[10] K.K. Pfister, E.M. Fisher, I.R. Gibbons, T.S. Hays, E.L. Holzbaur, J.R. McIntosh, M.E. Porter, T.A. Schroer, K.T. Vaughan, G.B. Witman, S.M. King, R.B. Vallee, Cytoplasmic dynein nomenclature, J. Cell Biol. 171 (2005) 411–413.

[11] S.M. King, E. Barbarese, J.F. Dillman III, R.S. Patel-King, J.H. Carson, K.K. Pfister, Brain cytoplasmic and flagellar outer arm dyneins share a highly conserved Mr 8,000 light chain, J. Biol. Chem. 271 (1996) 19358–19366.

[12] K.W. Lo, J.M. Kogoy, B.A. Rasoul, S.M. King, K.K. Pfister, Interaction of the DYNLT (TCTEX1/RP3) light chains and the intermediate chains reveals novel intersubunit regulation during assembly of the dynein complex, J. Biol. Chem. 282 (2007) 36871–36878.
[13] S.M. King, J.F. Dillman 3rd, S.E. Benashski, R.J. Lye, R.S. Patel-King, K.K. Pfister, The mouse t-complex-encoded protein Tctex-1 is a light chain of brain cytoplasmic dynein, J. Biol. Chem. 271 (1996) 32281–32287.
[14] M.J. Wilson, M.W. Salata, S.J. Susalka, K.K. Pfister, Light chains of mammalian cytoplasmic dynein: Identification and characterization of a family of LC8 light chains, Cell Motil. Cytoskeleton 49 (2001) 229–240.
[15] S.H. Tynan, M.A. Gee, R.B. Vallee, Distinct but overlapping sites within the cytoplasmic dynein heavy chain for dimerization and for intermediate chain and light intermediate chain binding, J. Biol. Chem. 275 (2000) 32769–32774.
[16] A. Kuta, W. Deng, A. Morsi El-Kadi, G.T. Banks, M. Hafezparast, K.K. Pfister, E.M. Fisher, Mouse cytoplasmic dynein intermediate chains: Identification of new isoforms, alternative splicing and tissue distribution of transcripts, PLoS One 5 (2010) e11682.
[17] K.R. Myers, K.W. Lo, R.J. Lye, J.M. Kogoy, V. Soura, M. Hafezparast, K.K. Pfister, Intermediate chain subunit as a probe for cytoplasmic dynein function: Biochemical analyses and live cell imaging in PC12 cells, J. Neurosci. Res. 85 (2007) 2640–2647.
[18] C. Cho, S.L. Reck-Peterson, R.D. Vale, Regulatory ATPase sites of cytoplasmic dynein affect processivity and force generation, J. Biol. Chem. 283 (2008) 25839–25845.
[19] L.C. Kapitein, M.A. Schlager, M. Kuijpers, P.S. Wulf, M. van Spronsen, F.C. MacKintosh, C.C. Hoogenraad, Mixed microtubules steer dynein-driven cargo transport into dendrites, Curr. Biol. 20 (2010) 290–299.
[20] S.M. O'Rourke, M.D. Dorfman, J.C. Carter, B. Bowerman, Dynein modifiers in *C. elegans*: Light chains suppress conditional heavy chain mutants, PLoS Genet. 3 (2007) e128.
[21] S.M. King, R. Kamiya, Axonemal dyneins: Assembly, structure, and force generation, in: G.W. Witman, E.H. Harris (Eds.), The *Chlamydomas* Sourcebook, Cell Motility and Behavior, Elsevier/Academic Press, Oxford, 2009, pp. 31–208.
[22] M. Samso, M.P. Koonce, 25 Angstrom resolution structure of a cytoplasmic dynein motor reveals a seven-member planar ring, J. Mol. Biol. 340 (2004) 1059–1072.
[23] G. Mocz, I.R. Gibbons, Model for the motor component of dynein heavy chain based on homology to the AAA family of oligomeric ATPases, Structure (Camb.) 9 (2001) 93–103.
[24] M.A. Gee, J.E. Heuser, R.B. Vallee, An extended microtubule-binding structure within the dynein motor domain, Nature 390 (1997) 636–639.
[25] A.F. Neuwald, L. Aravind, J.L. Spouge, E.V. Koonin, AAA^{+}: A class of chaperone-like ATPases associated with the assembly, operation, and disassembly of protein complexes, Genome Res. 9 (1999) 27–43.
[26] K. Ogawa, Four ATP-binding sites in the midregion of the beta heavy chain of dynein, Nature 352 (1991) 643–645.
[27] M.P. Koonce, Identification of a microtubule-binding domain in a cytoplasmic dynein heavy chain, J. Biol. Chem. 272 (1997) 19714–19718.
[28] S.R. Gill, D.W. Cleveland, T.A. Schroer, Characterization of DLC-A and DLC-B, two families of cytoplasmic dynein light chain subunits, Mol. Biol. Cell 5 (1994) 645–654.
[29] S.M. Hughes, K.T. Vaughan, J.S. Herskovits, R.B. Vallee, Molecular analysis of a cytoplasmic dynein light intermediate chain reveals homology to a family of ATPases, J. Cell Sci. 108 (Pt 1) (1995) 17–24.
[30] J.F. Dillman 3rd, K.K. Pfister, Differential phosphorylation *in vivo* of cytoplasmic dynein associated with anterogradely moving organelles, J. Cell Biol. 127 (1994) 1671–1681.

[31] M.W. Salata, J.F. Dillman 3rd, R.J. Lye, K.K. Pfister, Growth factor regulation of cytoplasmic dynein intermediate chain subunit expression preceding neurite extension, J. Neurosci. Res. 65 (2001) 408–416.
[32] J.H. Yoder, M. Han, Cytoplasmic dynein light intermediate chain is required for discrete aspects of mitosis in *Caenorhabditis elegans*, Mol. Biol. Cell 12 (2001) 2921–2933.
[33] K.H. Bremner, J. Scherer, J. Yi, M. Vershinin, S.P. Gross, R.B. Vallee, Adenovirus transport via direct interaction of cytoplasmic dynein with the viral capsid hexon subunit, Cell Host Microbe 6 (2009) 523–535.
[34] S.H. Tynan, A. Purohit, S.J. Doxsey, R.B. Vallee, Light intermediate chain 1 defines a functional subfraction of cytoplasmic dynein which binds to pericentrin, J. Biol. Chem. 275 (2000) 32763–32768.
[35] C.P. Horgan, S.R. Hanscom, M.W. McCaffrey, Dynein LIC1 localises to the mitotic spindle and midbody and LIC2 localises to spindle poles during cell division, Cell Biol. Int. 35 (2010) 171–178.
[36] M.V. Sivaram, T.L. Wadzinski, S.D. Redick, T. Manna, S.J. Doxsey, Dynein light intermediate chain 1 is required for progress through the spindle assembly checkpoint, EMBO J. 28 (2009) 902–914.
[37] K.J. Palmer, H. Hughes, D.J. Stephens, Specificity of cytoplasmic dynein subunits in discrete membrane-trafficking steps, Mol. Biol. Cell 20 (2009) 2885–2899.
[38] J. Schmoranzer, J.P. Fawcett, M. Segura, S. Tan, R.B. Vallee, T. Pawson, G.G. Gundersen, Par3 and dynein associate to regulate local microtubule dynamics and centrosome orientation during migration, Curr. Biol. 19 (2009) 1065–1074.
[39] A.R. Reilein, A.S. Serpinskaya, R.L. Karcher, D.L. Dujardin, R.B. Vallee, V.I. Gelfand, Differential regulation of dynein-driven melanosome movement, Biochem. Biophys. Res. Commun. 309 (2003) 652–658.
[40] V.J. Allan, R.D. Vale, Cell cycle control of microtubule-based membrane transport and tubule formation *in vitro*, J. Cell Biol. 113 (1991) 347–359.
[41] K.R. Dell, C.W. Turck, R.D. Vale, Mitotic phosphorylation of the dynein light intermediate chain is mediated by cdc2 kinase, Traffic 1 (2000) 38–44.
[42] V. Allan, Protein phosphatase 1 regulates the cytoplasmic dynein-driven formation of endoplasmic reticulum networks *in vitro*, J. Cell Biol. 128 (1995) 879–891.
[43] J. Zhang, S. Li, S. Musa, H. Zhou, X. Xiang, Dynein light intermediate chain in *Aspergillus nidulans* is essential for the interaction between heavy and intermediate chains, J. Biol. Chem. 284 (2009) 34760–34768.
[44] I. Fujita, A. Yamashita, M. Yamamoto, Contribution of dynein light intermediate and intermediate chains to subcellular localization of the dynein-dynactin motor complex in *Schizosaccharomyces pombe*, Genes Cells 15 (2010) 359–372.
[45] W.L. Lee, M.A. Kaiser, J.A. Cooper, The offloading model for dynein function: Differential function of motor subunits, J. Cell Biol. 168 (2005) 201–207.
[46] K.W. Lo, H.M. Kan, K.K. Pfister, Identification of a novel region of the cytoplasmic dynein intermediate chain important for dimerization in the absence of the light chains, J. Biol. Chem. 281 (2006) 9552–9559.
[47] R.D. Vale, The molecular motor toolbox for intracellular transport, Cell 112 (2003) 467–480.
[48] S. Ma, L. Trivinos-Lagos, R. Graf, R.L. Chisholm, Dynein intermediate chain mediated dynein–dynactin interaction is required for interphase microtubule organization and centrosome replication and separation in *Dictyostelium*, J. Cell Biol. 147 (1999) 1261–1274.
[49] T.W. Hendrickson, C.A. Perrone, P. Griffin, K. Wuichet, J. Mueller, P. Yang, M.E. Porter, W.S. Sale, IC138 is a WD-repeat dynein intermediate chain required for light chain assembly and regulation of flagellar bending, Mol. Biol. Cell 15 (2004) 5431–5442.

[50] K.T. Vaughan, R.B. Vallee, Cytoplasmic dynein binds dynactin through a direct interaction between the intermediate chains and p150Glued, J. Cell Biol. 131 (1995) 1507–1516.
[51] Y.K. Mok, K.W. Lo, M. Zhang, Structure of Tctex-1 and its interaction with cytoplasmic dynein intermediate chain, J. Biol. Chem. 276 (2001) 14067–14074.
[52] K.W. Lo, S. Naisbitt, J.S. Fan, M. Sheng, M. Zhang, The 8-kDa dynein light chain binds to its targets via a conserved (K/R)XTQT motif, J. Biol. Chem. 276 (2001) 14059–14066.
[53] S.J. Susalka, K. Nikulina, M.W. Salata, P.S. Vaughan, S.M. King, K.T. Vaughan, K.K. Pfister, The roadblock light chain binds a novel region of the cytoplasmic dynein intermediate chain, J. Biol. Chem. 277 (2002) 32939–32946.
[54] J. Song, J.L. Markley, Cautionary tail: The presence of an N-terminal tag on dynein light-chain Roadblock/LC7 affects its interaction with a functional partner, Protein Pept. Lett. 14 (2007) 265–268.
[55] J.C. Williams, P.L. Roulhac, A.G. Roy, R.B. Vallee, M.C. Fitzgerald, W.A. Hendrickson, Structural and thermodynamic characterization of a cytoplasmic dynein light chain-intermediate chain complex, Proc. Natl. Acad. Sci. USA 104 (2007) 10028–10033.
[56] J. Hall, Y. Song, P.A. Karplus, E. Barbar, The crystal structure of dynein intermediate chain-light chain roadblock complex gives new insights into dynein assembly, J. Biol. Chem. 285 (2010) 22566–22575.
[57] A. Nyarko, E. Barbar, Light chain-dependent self-association of dynein intermediate chain, J. Biol. Chem. 286 (2011) 1556–1566.
[58] D.I. Nurminsky, M.V. Nurminskaya, E.V. Benevolenskaya, Y.Y. Shevelyov, D.L. Hartl, V.A. Gvozdev, Cytoplasmic dynein intermediate-chain isoforms with different targeting properties created by tissue-specific alternative splicing, Mol. Cell Biol. 18 (1998) 6816–6825.
[59] K.K. Pfister, M.W. Salata, J.F. Dillman 3rd, E. Torre, R.J. Lye, Identification and developmental regulation of a neuron-specific subunit of cytoplasmic dynein, Mol. Biol. Cell 7 (1996) 331–343.
[60] K.K. Pfister, M.W. Salata, J.F. Dillman 3rd, K.T. Vaughan, R.B. Vallee, E. Torre, R.J. Lye, Differential expression and phosphorylation of the 74-kDa intermediate chains of cytoplasmic dynein in cultured neurons and glia, J. Biol. Chem. 271 (1996) 1687–1694.
[61] S. Tauhata, J. Burke, E. Joseph, W.S. Lane, S.M. King, K.K. Pfister, P.S. Vaughan, K.T. Vaughan, A new model for cytoplasmic dynein subunit complexity, Mol. Biol. Cell 16 (2005). Abstract #974.
[62] K. Nikulina, R.S. Patel-King, S. Takebe, K.K. Pfister, S.M. King, The Roadblock light chains are ubiquitous components of cytoplasmic dynein that form homo- and heterodimers, Cell Motil. Cytoskeleton 57 (2004) 233–245.
[63] P.S. Vaughan, J.D. Leszyk, K.T. Vaughan, Cytoplasmic dynein intermediate chain phosphorylation regulates binding to dynactin, J. Biol. Chem. 276 (2001) 26171–26179.
[64] J. Whyte, J.R. Bader, S.B. Tauhata, M. Raycroft, J. Hornick, K.K. Pfister, W.S. Lane, G.K. Chan, E.H. Hinchcliffe, P.S. Vaughan, K.T. Vaughan, Phosphorylation regulates targeting of cytoplasmic dynein to kinetochores during mitosis, J. Cell Biol. 183 (2008) 819–834.
[65] J.F. Dillman 3rd, L.P. Dabney, S. Karki, B.M. Paschal, E.L. Holzbaur, K.K. Pfister, Functional analysis of dynactin and cytoplasmic dynein in slow axonal transport, J. Neurosci. 16 (1996) 6742–6752.
[66] J.F. Dillman 3rd, K.K. Pfister, Differential phosphorylation *in vivo* of cytoplasmic dynein in anterograde and whole cell compartments, Biophys. J. 68 (1995) 226S.
[67] J. Ha, K.W. Lo, K.R. Myers, T.M. Carr, M.K. Humsi, B.A. Rasoul, R.A. Segal, K.K. Pfister, A neuron-specific cytoplasmic dynein isoform preferentially transports TrkB signaling endosomes, J. Cell Biol. 181 (2008) 1027–1039.

[68] M. Hafezparast, R. Klocke, C. Ruhrberg, A. Marquardt, A. Ahmad-Annuar, S. Bowen, G. Lalli, A.S. Witherden, H. Hummerich, S. Nicholson, P.J. Morgan, R. Oozageer, J.V. Priestley, S. Averill, V.R. King, S. Ball, J. Peters, T. Toda, A. Yamamoto, Y. Hiraoka, M. Augustin, D. Korthaus, S. Wattler, P. Wabnitz, C. Dickneite, S. Lampel, F. Boehme, G. Peraus, A. Popp, M. Rudelius, J. Schlegel, H. Fuchs, M. Hrabe de Angelis, G. Schiavo, D.T. Shima, A.P. Russ, G. Stumm, J.E. Martin, E.M. Fisher, Mutations in dynein link motor neuron degeneration to defects in retrograde transport, Science 300 (2003) 808–812.

[69] H.S. Ilieva, K. Yamanaka, S. Malkmus, O. Kakinohana, T. Yaksh, M. Marsala, D.W. Cleveland, Mutant dynein (Loa) triggers proprioceptive axon loss that extends survival only in the SOD1 ALS model with highest motor neuron death, Proc. Natl. Acad. Sci. USA 105 (2008) 12599–12604.

[70] I. Puls, S.J. Oh, C.J. Sumner, K.E. Wallace, M.K. Floeter, E.A. Mann, W.R. Kennedy, G. Wendelschafer-Crabb, A. Vortmeyer, R. Powers, K. Finnegan, E.L. Holzbaur, K.H. Fischbeck, C.L. Ludlow, Distal spinal and bulbar muscular atrophy caused by dynactin mutation, Ann. Neurol. 57 (2005) 687–694.

[71] L. Dupuis, A. Fergani, K.E. Braunstein, J. Eschbach, N. Holl, F. Rene, J.L. Gonzalez De Aguilar, B. Zoerner, B. Schwalenstocker, A.C. Ludolph, J.P. Loeffler, Mice with a mutation in the dynein heavy chain 1 gene display sensory neuropathy but lack motor neuron disease, Exp. Neurol. 215 (2009) 146–152.

[72] M. Martin, S.J. Iyadurai, A. Gassman, J.G. Gindhart Jr., T.S. Hays, W.M. Saxton, Cytoplasmic dynein, the dynactin complex, and kinesin are interdependent and essential for fast axonal transport, Mol. Biol. Cell 10 (1999) 3717–3728.

[73] J.G. Gindhart Jr., C.J. Desai, S. Beushausen, K. Zinn, L.S. Goldstein, Kinesin light chains are essential for axonal transport in *Drosophila*, J. Cell Biol. 141 (1998) 443–454.

[74] M. McGrail, T.S. Hays, The microtubule motor cytoplasmic dynein is required for spindle orientation during germline cell divisions and oocyte differentiation in *Drosophila*, Development 124 (1997) 2409–2419.

[75] E. Barbar, Dynein light chain LC8 is a dimerization hub essential in diverse protein networks, Biochemistry 47 (2008) 503–508.

[76] C.M. Lightcap, G. Kari, L.E. Arias-Romero, J. Chernoff, U. Rodeck, J.C. Williams, Interaction with LC8 is required for Pak1 nuclear import and is indispensable for zebrafish development, PLoS One 4 (2009) e6025.

[77] K.W. Lo, H.M. Kan, L.N. Chan, W.G. Xu, K.P. Wang, Z. Wu, M. Sheng, M. Zhang, The 8-kDa dynein light chain binds to p53-binding protein 1 and mediates DNA damage-induced p53 nuclear accumulation, J. Biol. Chem. 280 (2005) 8172–8179.

[78] K.K. Pfister, R.B. Fay, G.B. Witman, Purification and polypeptide composition of dynein ATPases from *Chlamydomonas* flagella, Cell Motil. 2 (1982) 525–547.

[79] P. Yang, D.R. Diener, J.L. Rosenbaum, W.S. Sale, Localization of calmodulin and dynein light chain LC8 in flagellar radial spokes, J. Cell Biol. 153 (2001) 1315–1326.

[80] S.R. Jaffrey, S.H. Snyder, PIN: An associated protein inhibitor of neuronal nitric oxide synthase, Science 274 (1996) 774–777.

[81] F. Schnorrer, K. Bohmann, C. Nusslein-Volhard, The molecular motor dynein is involved in targeting swallow and bicoid RNA to the anterior pole of *Drosophila* oocytes, Nat. Cell Biol. 2 (2000) 185–190.

[82] S.E. Benashski, A. Harrison, R.S. Patel-King, S.M. King, Dimerization of the highly conserved light chain shared by dynein and myosin V, J. Biol. Chem. 272 (1997) 20929–20935.

[83] W. Wagner, E. Fodor, A. Ginsburg, J.A. Hammer 3rd, The binding of DYNLL2 to myosin Va requires alternatively spliced exon B and stabilizes a portion of the myosin's coiled-coil domain, Biochemistry 45 (2006) 11564–11577.

[84] J. Fan, Q. Zhang, H. Tochio, M. Li, M. Zhang, Structural basis of diverse sequence-dependent target recognition by the 8 kDa dynein light chain, J. Mol. Biol. 306 (2001) 97–108.
[85] L. Wang, M. Hare, T.S. Hays, E. Barbar, Dynein light chain LC8 promotes assembly of the coiled-coil domain of swallow protein, Biochemistry 43 (2004) 4611–4620.
[86] G. Benison, E. Barbar, NMR analysis of dynein light chain dimerization and interactions with diverse ligands, Method. Enzymol. 455 (2009) 237–258.
[87] Y. Jung, H. Kim, S.H. Min, S.G. Rhee, W. Jeong, Dynein light chain LC8 negatively regulates NF-kappaB through the redox-dependent interaction with IkappaBalpha, J. Biol. Chem. 283 (2008) 23863–23871.
[88] J. Hall, A. Hall, N. Pursifull, E. Barbar, Differences in dynamic structure of LC8 monomer, dimer, and dimer-peptide complexes, Biochemistry 47 (2008) 11940–11952.
[89] S. Naisbitt, J. Valtschanoff, D.W. Allison, C. Sala, E. Kim, A.M. Craig, R.J. Weinberg, M. Sheng, Interaction of the postsynaptic density-95/guanylate kinase domain-associated protein complex with a light chain of myosin-V and dynein, J. Neurosci. 20 (2000) 4524–4534.
[90] C.L. Day, H. Puthalakath, G. Skea, A. Strasser, I. Barsukov, L.Y. Lian, D.C. Huang, M.G. Hinds, Localization of dynein light chains 1 and 2 and their pro-apoptotic ligands, Biochem. J. 377 (2004) 597–605.
[91] H. Puthalakath, A. Villunger, L.A. O'Reilly, J.G. Beaumont, L. Coultas, R.E. Cheney, D.C. Huang, A. Strasser, Bmf: A proapoptotic BH3-only protein regulated by interaction with the myosin V actin motor complex, activated by anoikis, Science 293 (2001) 1829–1832.
[92] S.M. King, E. Barbarese, J.F. Dillman 3rd, S.E. Benashski, K.T. Do, R.S. Patel-King, K.K. Pfister, Cytoplasmic dynein contains a family of differentially expressed light chains, Biochemistry 37 (1998) 15033–15041.
[93] A.W. Tai, J.Z. Chuang, C.H. Sung, Cytoplasmic dynein regulation by subunit heterogeneity and its role in apical transport, J. Cell Biol. 153 (2001) 1499–1509.
[94] T.Y. Yeh, J.Z. Chuang, C.H. Sung, Dynein light chain rp3 acts as a nuclear matrix-associated transcriptional modulator in a dynein-independent pathway, J. Cell Sci. 118 (2005) 3431–3443.
[95] J.Z. Chuang, T.Y. Yeh, F. Bollati, C. Conde, F. Canavosio, A. Caceres, C.H. Sung, The dynein light chain Tctex-1 has a dynein-independent role in actin remodeling during neurite outgrowth, Dev. Cell 9 (2005) 75–86.
[96] L.M. DiBella, S.E. Benashski, H.W. Tedford, A. Harrison, R.S. Patel-King, S.M. King, The Tctex1/Tctex2 class of dynein light chains. Dimerization, differential expression, and interaction with the LC8 protein family, J. Biol. Chem. 276 (2001) 14366–14373.
[97] K.W. Lo, J.M. Kogoy, K.K. Pfister, The DYNLT3 light chain directly links cytoplasmic dynein to a spindle checkpoint protein, Bub3, J. Biol. Chem. 282 (2007) 11205–11212.
[98] D. Varma, A. Dawn, A. Ghosh-Roy, S.J. Weil, K.M. Ori-McKenney, Y. Zhao, J. Keen, R.B. Vallee, J.C. Williams, Development and application of *in vivo* molecular traps reveals that dynein light chain occupancy differentially affects dynein-mediated processes, Proc. Natl. Acad. Sci. USA. 107 (2010) 3493–3498.
[99] M.G. Li, M. Serr, E.A. Newman, T.S. Hays, The Drosophila tctex-1 light chain is dispensable for essential cytoplasmic dynein functions but is required during spermatid differentiation, Mol. Biol. Cell 15 (2004) 3005–3014.
[100] J. Jiang, L. Yu, X. Huang, X. Chen, D. Li, Y. Zhang, L. Tang, S. Zhao, Identification of two novel human dynein light chain genes, DNLC2A and DNLC2B, and their expression changes in hepatocellular carcinoma tissues from 68 Chinese patients, Gene 281 (2001) 103–113.
[101] B.F. Wanschers, R. van de Vorstenbosch, M.A. Schlager, D. Splinter, A. Akhmanova, C.C. Hoogenraad, B. Wieringa, J.A. Fransen, A role for the Rab6B Bicaudal-D1 interaction in retrograde transport in neuronal cells, Exp. Cell Res. 313 (2007) 3408–3420.

[102] B. Ashokkumar, S.M. Nabokina, T.Y. Ma, H.M. Said, Identification of dynein light chain road block-1 as a novel interaction partner with the human reduced folate carrier, Am. J. Physiol. Gastrointest. Liver Physiol. 297 (2009) G480–G487.
[103] Q. Tang, C.M. Staub, G. Gao, Q. Jin, Z. Wang, W. Ding, R.E. Aurigemma, K.M. Mulder, A novel transforming growth factor-beta receptor-interacting protein that is also a light chain of the motor protein dynein, Mol. Biol. Cell 13 (2002) 4484–4496.
[104] W. Ding, Q. Tang, V. Espina, L.A. Liotta, D.T. Mauger, K.M. Mulder, A transforming growth factor-beta receptor-interacting protein frequently mutated in human ovarian cancer, Cancer Res. 65 (2005) 6526–6533.
[105] Q. Jin, W. Ding, K.M. Mulder, Requirement for the dynein light chain km23–1 in a Smad2-dependent transforming growth factor-beta signaling pathway, J. Biol. Chem. 282 (2007) 19122–19132.
[106] Q. Jin, G. Gao, K.M. Mulder, Requirement of a dynein light chain in TGFbeta/Smad3 signaling, J. Cell Physiol. 221 (2009) 707–715.

In this chapter

16

Studies of Lissencephaly and Neurodegenerative Disease Reveal Novel Aspects of Cytoplasmic Dynein Regulation

Kassandra M. Ori-McKenney[1,2], Richard J. McKenney[2], Richard B. Vallee[1,2]

[1] Department of Biological Sciences, Columbia University, New York, NY, USA
[2] Department of Pathology and Cell Biology, Columbia University, New York, NY, USA

16.1 Introduction

The major form of cytoplasmic dynein (dynein 1) is involved in a very wide range of functions. Mammalian brain cytoplasmic dynein was found to produce force toward the microtubule minus end, the first such motor with this property [1]. It supported microtubule gliding at rates of >1 μm/s at room temperature, corresponding to 2−3 μm/s at physiological temperatures and consistent with the very fast rates of retrograde vesicular transport in axons and other cell types.

A substantial variety of cargoes that are subject to rapid minus-end-directed dynein transport have been identified, including vesicular organelles, viruses, RNP particles, immunophilin-associated steroid receptors [2], and injury signals [3]. However, cytoplasmic dynein is now also known to be important for the movement of large structures, such as nuclei at rates at least 100−500-fold slower ($\leq$0.5 μm/min) than retrograde vesicular transport [4]. Cytoplasmic dynein has also been implicated in static generation of tension along microtubules, in which movement may not occur at all. One such example is seen in neuronal growth cones, where cortical dynein anchors polymerizing microtubules, allowing them to resist retrograde actin flow and promoting growth cone advance [5]. Cortical dynein-mediated tension on microtubule arrays has also been implicated in neuronal and non-neuronal cell migration, mitotic spindle orientation and centration, and other functions involving high forces and slow movement [6]. Thus, one motor protein is involved in a broad continuum of physiologically important functions, which range from very fast transport of small macromolecules and

Dyneins DOI: 10.1016/B978-0-12-382004-4.10016-0
Copyright © 2012 by Elsevier Inc. All rights reserved.

membranes to very slow transport of large structures and static force generation. Major questions in the cytoplasmic dynein field concern the ability of this single protein complex to recognize and interact with a wide range of cargo types, but also to participate in such a broad range of mechanochemical roles.

The answers to these questions have seemed likely to reside in the diversity of cytoplasmic dynein subunit isoforms and a still-growing list of regulatory proteins. Most of the latter have been implicated in the important function of subcellular targeting. One such factor, dynactin, has also been found to enhance dynein processivity – that is, its run length along microtubules *in vitro* [7,8]. How this behavior is related to *in vivo* function remains to be tested directly, but it seems likely to increase over all transport efficiency. In contrast to dynactin, further evidence has revealed that the dynein accessory factors LIS1, NudE, and NudEL contribute to the regulation of dynein force production [9,10].

Understanding how these factors alter dynein function requires knowledge of how they interact with the motor but also of the inherent range of behaviors of which dynein is capable. The dynein motor domain alone has proven to be a wonder of evolutionary engineering, with at least two to four functional ATPase sites and a diversity of functional and regulatory domains [11–14].

Much of what is known regarding intra- and extramolecular dynein regulation has come from basic research, but recent clues have emerged from the investigation of mechanisms underlying cytoplasmic dynein-related diseases, as reviewed here. These studies have broad implications for understanding dynein regulation, which we also discuss.

16.2 Extramolecular Regulation of Cytoplasmic Dynein Force Generation by LIS1 and NudE/NudEL

LIS1 was initially identified as the causative gene for type 1 lissencephaly (smooth brain) [15]. A LIS1 ortholog, *NUDF*, was shortly thereafter identified in the dynein-driven nuclear distribution (nud) pathway in the filamentous fungus *Aspergillus nidulans* [16]. Another gene in the pathway, *NUDE*, was found to suppress the *nudF* phenotype [17]. *Aspergillus* NUDE has been found to have two vertebrate homologs, NudE (gene name *Nde1*) and NudEL (NudE-like (*Ndel1*)) [18–20]. LIS1, NudE, NudEL, and cytoplasmic dynein have all been implicated in neuronal migration and proliferation during mammalian brain development [4,21–23]. These proteins are required for the mitotic divisions of neural progenitor cells, axon elongation, growth cone advance, and in centrosome and nuclear translocation in live radially migrating cells (reviewed in [6]).

Lissencephaly is caused by sporadic missense or deletion mutations in the LIS1 gene, resulting in haploinsufficiency of the LIS1 protein [24,25]. In addition to its

role in the dynein pathway, LIS1 was initially identified as a noncatalytic subunit of platelet-activating factor acetylhydrolase (PAFAH). However, mice lacking the catalytic subunits exhibit no defects in brain development [26,27], supporting a primary role for altered cytoplasmic dynein function in lissencephaly. Recent work has indicated that overexpression of the catalytic subunits in COS7 cells causes Golgi disruption, characteristic of dynein perturbation. LIS1 overexpression rescued this defect, suggesting that the PAFAH catalytic subunits might act as a sink for free LIS1, preventing it from interacting with dynein [28].

LIS1 localizes to several sites of dynein action, including the kinetochore and the metaphase-prometaphase cell cortex [29], the plus ends of microtubules [30–32], the leading edge of migrating cells [33], and the late G2 nuclear envelope [30,34]. Interestingly, there are no reports for an association of LIS1 with vesicular dynein cargoes such as endosomes, lysosomes, and the Golgi apparatus, but some [35–37], though not all [29,38], studies have reported that LIS1 perturbation affects the distribution of these structures.

Tests for a role for LIS1 in dynein recruitment to subcellular cargo sites have been limited. An early study indicated that LIS1 mutations in *Drosophila* reduced levels of cytoplasmic dynein at the cortex of *Drosophila* oocytes [39]. However, analysis of the binding hierarchy for dynein-related kinetochore proteins found no effect of LIS1 dominant negatives on dynein recruitment to these sites. In contrast, LIS1 levels were reduced by dynein and dynactin dominant negatives, suggesting that LIS1 associates with kinetochores via cytoplasmic dynein [30,38,40]. These results suggest that, at least at kinetochores, LIS1 serves not in dynein recruitment but in some other regulatory capacity.

NudE and NudEL, however, have clear roles in dynein and LIS1 recruitment at diverse subcellular sites, including kinetochores [41,42], centrosomes, the late G2 nuclear envelope [34], and the leading edge of migrating fibroblasts [41]. NudE and NudEL have also been implicated in dynein-based vesicular trafficking [43,44], and their ablation by RNA interference (RNAi) reduced the amount of dynein bound to a crude membrane fraction [35].

Pairwise interactions among LIS1, NudE or NudEL, and cytoplasmic dynein have been identified and characterized in some detail. NudE and NudEL each interact with LIS1 through an extended N-terminal coiled-coil domain [18] and with dynein through an intrinsically disordered C-terminal domain [18,43] (Fig. 16.1A). NudEL was found to interact with the dynein heavy chain (HC) in a yeast two-hybrid screen [18]. However, little support for this specific interaction was obtained in biochemical assays [10,41]. Instead, strong interactions were observed between NudE and the dynein ICs (DYNC1I1/2) and LC 1 (LC8/DYNLL1) [10,41], each of which are located at the base of the dynein molecule (Fig. 16.2).

LIS1 has been found to interact in mammalian cell coexpression assays with multiple sites within both dynein and dynactin [38]. Among these, most intriguingly, is the

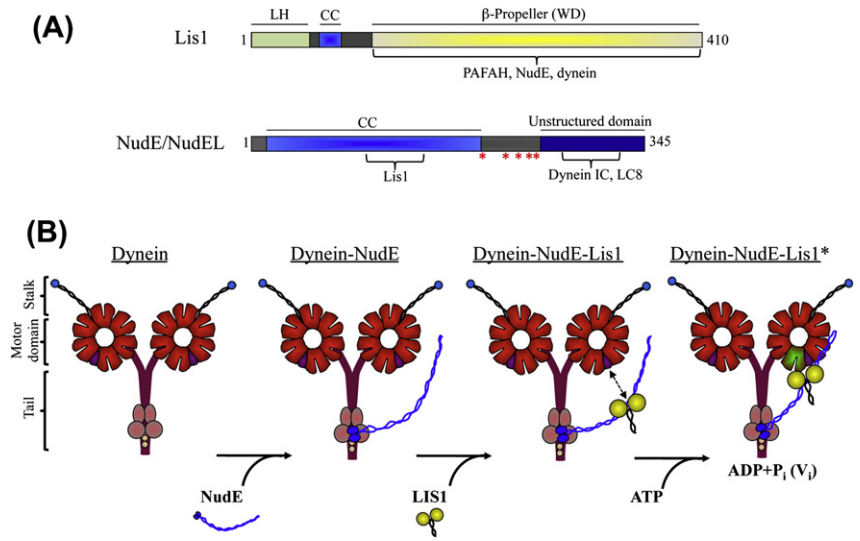

Figure 16.1 LIS1 and NudE regulate dynein force production. (A) Diagrams of LIS1 and NudE or NudEL polypeptides showing domain organization and known protein–protein interaction sites. LIS1 contains an N-terminal LIS homology domain (LH) that facilitates dimerization, a small central coiled coil, and C-terminal WD40 repeats that mediate protein–protein interactions. NudE/NudEL contain a highly elongated N-terminal coiled-coil domain that interacts with LIS1 and a C-terminal unstructured domain that binds dynein, likely through the IC and LC8 subunits. Known phosphorylation sites are marked with red asterisks. LH, LIS homology; CC, coiled coil; PAFAH, platelet-activating factor acetylhydrolase. (B) Step-wise assembly of a dynein–NudE–LIS1 complex. NudE binds to the base of the dynein molecule through direct interactions with the IC and LC8. The elongated coiled-coil region of NudE binds LIS1 and is thought to position it near the dynein motor domains where LIS1 binds to the AAA1 subdomain specifically during the pre-powerstroke (ADP-P_i – green subdomain) state of the ATP hydrolysis cycle. LIS1, in turn, enhances dynein–microtubule binding, thus allowing the motor to remain bound to microtubules for prolonged periods of time under load. (B) Reproduced with permission from [10].

AAA1 site within the motor domain [18,38], the primary site of ATP hydrolysis [45,46] (Fig. 16.2B). Despite this observation, the effects of LIS1 on dynein ATPase activity have been relatively weak and inconsistent between laboratories [9,10,47].

We have explored the roles of LIS1 and NudE in dynein regulation *in vitro* using purified components. In contrast with earlier yeast two-hybrid and immunoprecipitation results [18,38], baculovirus-expressed LIS1 showed little detectable interaction with purified brain dynein *in vitro* [10]. However, the addition of purified NudE, which binds to LIS1 and the dynein complex individually (Fig. 16.1A), linked the three components together in a stable, stoichiometric triple complex. LIS1 displayed no detectable interaction with the purified dynein motor domain [48]. Strikingly, however, LIS1 and the motor domain formed a stable complex in the presence of ATP and vanadate (VO_4) (Fig. 16.1B). This condition mimics the transition state of the dynein cross-bridge cycle, and is thought to correspond to the pre-powerstroke state [11,12,49,50]. The interaction between dynein and microtubules is weak in the presence of ATP-VO_4.

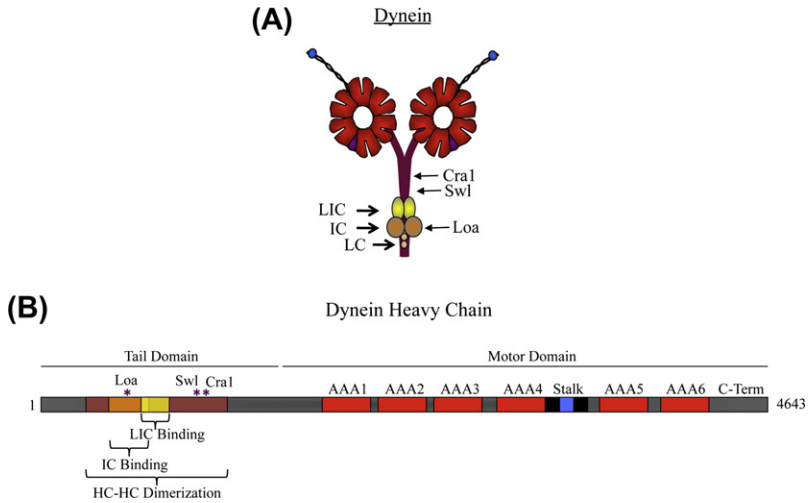

Figure 16.2 Mutations that cause motor neuron disease and sensory neuropathy reside in the N-terminal region of the dynein HC. (A) Cartoon of the cytoplasmic dynein complex, and (B) bar diagram of the dynein HC. Locations of known neurodegenerative mutations are indicated.

Remarkably, however, LIS1 enhanced dynein–microtubule cosedimentation five-fold under these conditions, supporting a role for LIS1 in regulating motor activity at this key step in the powerstroke cycle. In contrast to LIS1, NudE potently inhibited the ability of dynein to bind to microtubules, consistent with effects reported for NudEL [9]. Together, these results implied potential and perhaps very different roles for NudE and LIS1 in the dynein cross-bridge cycle.

To test this possibility directly, we carried out single-molecule assays with the laboratory of Steve Gross. Purified LIS1 had no effect on the velocity or processivity of dynein, though it did induce pauses in dynein travel at elevated concentrations. However, the most striking LIS1 effect was enhancement of the ability of dynein to remain bound to microtubules under load. Direct analysis of dynein detachment kinetics from microtubules revealed an approximately five-fold increase in the average time to detachment, which is very similar to the increase in microtubule-binding affinity seen in our biochemical analysis [10].

In contrast to LIS1, but consistent with our biochemical analysis, NudE alone strongly inhibited the binding of single dynein molecules to microtubules in the laser trap assay. Nonetheless, LIS1 reversed this effect and the proteins together produce an increase in the ability of dynein to remain associated with microtubules under loads similar to that for LIS1 alone. To test whether NudE served in linking LIS1 to dynein, as suggested in our biochemical analysis, we incubated dynein-coated beads with either LIS1 alone or NudE and LIS1 together, and then removed unbound protein via centrifugation. The effect of LIS1 alone on dynein was largely reversed, whereas it persisted when NudE was present. These results supported a role for NudE in

recruiting LIS1 to dynein. The basis for the inhibitory effect of NudE alone in dynein function is still unknown, though it could represent a regulatory mechanism for blocking dynein function at subcellular sites until LIS1 were available.

In vivo cargo transport is likely to involve multiple motors [51,52], especially with increased cargo size and resistance to movement. To relate our single-molecule findings to intracellular transport, we carried out multi-motor assays as well as *in silico* modeling of multiple motor transport, using the single-molecule kinetic parameters measured in the presence of NudE and LIS1. Optical trapping was used to restrain beads coated with two to three dynein motors and the effects of the addition of NudE-LIS1 were assayed. The addition of NudE and LIS1 strongly increased the number of beads that were able to escape the optical trap, demonstrating enhanced dynein force production under multi-motor conditions [10]. Computer simulations similarly predicted a strong increase in the ability of multiple dyneins to work under load resulting from the decreased microtubule detachment kinetics observed for dynein in the presence of LIS1.

A puzzling feature of lissencephaly has been the manifestation of phenotypic effects solely in the brain, when LIS1 also functions along with dynein in mitosis [29] and cell migration in both neuronal and non-neuronal cells [33]. The answer likely lies in the effects of LIS1 on dynein motor output. Aspects of cytoplasmic dynein-based transport that are particularly sensitive to reduced LIS1 expression generally involve large cellular structures, such as nuclei and the entire microtubule cytoskeleton through narrow cellular processes [4]. Indeed, nuclei undergo extreme distortions during neuronal migration, suggesting large resistance to movement [4]. Such forms of "high load" transport are much slower (e.g. 0.3 μm/min for radially migrating neocortical neurons [4]) than the fast, retrograde transport of small vesicular cargoes (1−5 μm/s). Why the effects of LIS1 inhibition have been observed in the transport of vesicular cargo, and why in some studies but not others, is uncertain. We speculate that smaller cargoes could periodically encounter relatively high resistance to their forward advance, either from cellular impediments or from plus-end-directed motor proteins acting in opposition to cytoplasmic dynein, requiring LIS1-mediated enhanced dynein force production.

16.3 Intramolecular Regulation of Dynein Processivity and Implications for Neurodegeneration

Mutations in cytoplasmic dynein and dynactin can cause motor neuron disease and sensory neurodegeneration in humans and mice [53−58]. Three different dynein mutant mouse strains have been generated by chemical mutagenesis and identified in screens for neurodegeneration. Surprisingly, all three mutations mapped to sites within the N-terminal region of the cytoplasmic dynein HC [53,59], corresponding to the tail portion of the molecule. The Loa (Legs at odd

angles) mutation consists of a single amino acid change, amino acid F580Y, within the region of the HC implicated by earlier studies in IC binding and HC dimerization [60,61]. The Cra1 (Cramping 1) mutation further downstream at residue Y1055C, as well as the Swl (Sprawling) mutation, which results in an alanine substitution for amino acids 1040−1043, resides within the HC dimerization region (Fig. 16.2). All mutations cause early-onset sensory neuropathy in the heterozygous animals [54,55,59]. The Loa and Cra1 homozygotes die within 24 h of birth due to an inability to feed, whereas Swl homozygotes exhibit early embryonic lethality [53,59]. Defects in the average rate of retrograde transport were observed in both the Loa homozygous and Loa heterozygous animals, potentially contributing to the neurodegeneration phenotype [53,56].

The Loa mutant mouse has received the most attention of the three mutant strains. Despite the clear effect of the mutation on axonal transport and neuronal viability, no apparent change was detected in cytoplasmic dynein levels, though the stability of the complex, its mechanochemical and cargo-binding properties, and its interactions with regulatory factors were not tested.

We reasoned that identification of the molecular basis for the mutant phenotype should be of value in understanding neurodegenerative disease and might, in addition, provide novel insights into cytoplasmic dynein regulation and function. To address this question, we purified wild-type and the heterozygous Loa mutant dyneins. In the brain cytosolic extracts we observed a small but reproducible tendency for a fraction of the ICs to dissociate from the mutant dynein complex. This effect was lost with purification, though the mutant dynein remained more susceptible to dissociation by treatment with the chaotropic agent, potassium iodide. The purified wild-type and heterozygous dyneins were completely indistinguishable in subunit composition. Tissue was limited for the Loa/Loa mice, in part because they die perinatally. Therefore, we carried out a partial microtubule affinity-based purification, followed by immunoisolation. This approach was adequate for single-molecule, but not biochemical, analysis [62].

Basal ATPase activity was unchanged for the Loa/+ dynein, but, surprisingly, the K_m for microtubules was increased. This result suggested a decrease in microtubule-binding affinity for mutant dynein during its ATP hydrolysis cycle. Microtubule-pelleting assays revealed that microtubule binding for the Loa/+ dynein was unaffected in the absence of ATP but was dramatically reduced in the presence of ATP. To test the effects of the Loa mutation at the single-molecule level, we used both polystyrene-bead- and quantum-dot-based single-molecule assays. Velocity, stall force, and step size were unchanged for the purified Loa/+ dynein. However, the Loa/+ dynein exhibited a 23% reduction in run length compared with wild-type dynein. Loa/Loa dynein exhibited a 50% reduction in run length. We also found impaired processivity in bead assays involving multiple dynein molecules, suggesting that this defect is likely relevant under physiological transport conditions. Computational modeling supported this conclusion. We also computationally

tested the behavior of physiological dynein regulators, which increase processivity in *in vitro* assays. This analysis revealed that the Loa processivity defect should persist in the presence of *in vivo* factors such as dynactin. To test directly for processivity effects *in vivo*, we conducted high-resolution tracking of lysosome/late endosome transport in axons of cultured wild-type and Loa hippocampal neurons. This analysis revealed a clear two-to-five-fold reduction in vesicular run lengths that was closely matched in our computational modeling of the Loa processivity defect [62].

Together, the *in vitro* and *in vivo* experiments strongly supported an effect of the Loa mutation on the dynein–microtubule interaction. To gain further insight into the molecular basis for the mechanism responsible for altered Loa dynein processivity, we examined the reported tendency of cytoplasmic dynein to step laterally on the microtubule surface [63,64]. Purified wild-type mouse cytoplasmic dynein exhibited clear evidence of lateral stepping, as previously reported for dynein from other species. Strikingly, we observed a significant increase in the frequency of lateral stepping for the Loa/+ mutant protein [62].

These results suggest that the Loa mutation affects the dynein–microtubule interaction by altering the coordinate behavior of the two motor domains. The mutation is separated from the motor domains of dynein by some 1 500 amino acids, and in the folded dynein molecule by an estimated minimum of 20 nm [11]. Yet, the Loa mutation occurs in the only known site of interaction between the dynein HCs. We reason, therefore, that the dynein tail contributes to the relative positioning of the motor domains on the microtubule surface and, potentially, the coordination of their mechanochemical cycles. Such coordination is thought to contribute to processive transport by motor proteins in general [65]. As one motor domain undergoes ATP hydrolysis and advances along its track, the other must remain bound in the apo state to prevent premature dissociation of the motor complex. This behavior is most likely controlled by a gating mechanism, in which one motor domain restrains the other from advancing prematurely through its cross-bridge cycle [66–68]. This could be achieved by direct interaction of motors at specific states in their ATPase cycles. Alternatively, the motor domains could influence each other through an indirect, intramolecular mechanism [65]. Gating has been demonstrated in kinesins and myosins and is predicted for cytoplasmic dynein to explain its processive behavior, but the underlying mechanism is not yet understood. An artificially crosslinked dimeric dynein is processive, supporting direct communication between motor domains. However, the Loa defect suggests that the dynein tail further contributes to proper motor gating. We tested for altered gating by measuring the K_m for ATP. Loa dynein had a decreased K_{mATP} compared with wild-type dynein. This is consistent with premature ATP binding by the apo motor domain, which would be expected to increase the frequency with which the dynein complex would detach from the microtubule. We also found a subtly decreased stability of the Loa mutant dynein complex, suggesting that an abnormal linkage within the base of the Loa dynein molecule may disrupt the coordination between the two motor domains by altering their relative positioning and ability to properly gate each other (Fig. 16.3).

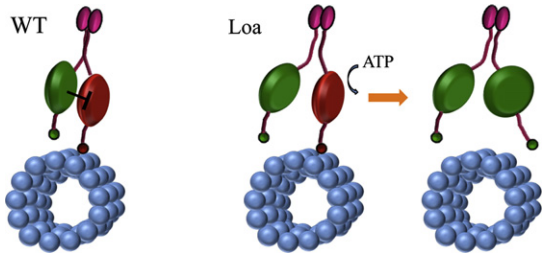

Figure 16.3 Proposed effect of Loa mutation on coordination between dynein motor domains. Dynein has been speculated to use a gating mechanism to coordinate the stepping and hydrolysis cycles of the two motor domains. This is shown diagrammatically, with a stepping motor domain (green) inhibiting a tightly bound motor domain (red) from binding ATP. In Loa dynein, this gating behavior is proposed to be defective, allowing premature ATP binding and premature release of the dynein complex from the microtubule. This model provides an explanation for altered microtubule binding affinity in the Loa mutant dynein [62]. Furthermore, because the Loa mutation is at the opposite end of the dynein HC from the motor domains, miscoordination between motors must reflect a failure in long-range communication within the dynein complex. This possibility is supported by an increase in wandering behavior by the dynein complex on the surface of the microtubule [62].

These results provide the first direct evidence that processivity defects can cause disease. This possibility has also been raised due to the effects of dynactin mutations, which also cause neurodegeneration [57,58]. However, it is not yet known which aspect of the dynactin phenotype is responsible for this effect. A G59S mutation in the CAP-Gly (cytoskeleton-associated protein, glycine-rich) microtubule-binding region of the major dynactin subunit $p150^{Glued}$ has been implicated in lower motor neuron degeneration in a human family [58]. However, removal of the entire CAP-Gly region had no effect on the ability of dynactin to stimulate dynein processivity [8]. How the $p150^{Glued}$ G59S mutation affects neuronal behavior and viability remains to be understood more completely, but the degeneration phenotype could involve some other aspect of dynactin function or result from mutant $p150^{Glued}$ misfolding and aggregation [69]. Disruption of the dynactin complex by overexpression of its 50 kDa dynamitin subunit also results in late-onset progressive motor neuron degeneration [57]. Retrograde axonal transport was inhibited, though whether through a defect in processivity or, perhaps, its recruitment of dynein to membrane vesicles is unknown.

16.4 Conclusion

The dyneins, and especially the major cytoplasmic form, appear to be subject to a very complex array of regulatory mechanisms. Analysis of lissencephaly and a form of neurodegeneration has provided insight into two distinct mechanisms by which dynein motor behavior may be modulated. Our own evidence indicates that LIS1 affects the dynein powerstroke, identifying a new requirement for external regulatory factors in high-load cytoplasmic dynein functions. Thus, a protein capable of rapid transport of diverse vesicular and macromolecular structures can also transport large, slow-moving structures.

The Loa phenotype involves a defect in long-range communication within the cytoplasmic dynein complex. Whether this effect is a reflection of a normal intramolecular regulatory mechanism is unclear. Analysis of the Loa mutation has implicated the tail region of the dynein HC in coordination between motor domains. Is the dynein tail a target of physiological regulation? A number of observations suggest that this might be the case. NudE and dynactin each interact with the dynein ICs. How these interactions translate into inhibition of the dynein–microtubule interaction in the case of NudE or enhanced processivity in the case of dynactin is unknown. Truncated forms of dynactin retain their effect on dynein processivity [8]; whether the anti-processive effects of NudE require the full-length molecule or can be mimicked by its IC-binding region alone remains to be tested. Thus, dynactin, and conceivably NudE, may act in part through the dynein tail, perhaps by upregulating or downregulating an inherent form of tail-mediated motor coordination.

References

[1] B.M. Paschal, R.B. Vallee, Retrograde transport by the microtubule associated protein MAP 1C, Nature 330 (1987) 181–183.

[2] J.M. Harrell, P.J. Murphy, Y. Morishima, H. Chen, J.F. Mansfield, M.D. Galigniana, W.B. Pratt, Evidence for glucocorticoid receptor transport on microtubules by dynein, J. Biol. Chem. 279 (2004) 54647–54654.

[3] S. Hanz, E. Perlson, D. Willis, J.Q. Zheng, R. Massarwa, J.J. Huerta, M. Koltzenburg, M. Kohler, J. van-Minnen, J.L. Twiss, M. Fainzilber, Axoplasmic importins enable retrograde injury signaling in lesioned nerve, Neuron 40 (2003) 1095–1104.

[4] J.W. Tsai, K.H. Bremner, R.B. Vallee, Dual subcellular roles for LIS1 and dynein in radial neuronal migration in live brain tissue, Nat. Neurosci. 10 (2007) 970–979.

[5] P.W. Grabham, M. Bennecib, G.E. Seale, D.J. Goldberg, R.B. Vallee, Cytoplasmic dynein and LIS1 are required for growth cone remodeling and fast neurite outgrowth, J. Neurosci. 27 (2007) 5823–5832.

[6] R.B. Vallee, G.E. Seale, J.W. Tsai, Emerging roles for myosin II and cytoplasmic dynein in migrating neurons and growth cones, Trends Cell Biol. 19 (2009) 347–355.

[7] S.J. King, T.A. Schroer, Dynactin increases the processivity of the cytoplasmic dynein motor, Nat. Cell Biol. 2 (2000) 20–24.

[8] J.R. Kardon, S.L. Reck-Peterson, R.D. Vale, Regulation of the processivity and intracellular localization of *Saccharomyces cerevisiae* dynein by dynactin, Proc. Natl. Acad. Sci. USA 106 (2009) 5669–5674.

[9] M. Yamada, S. Toba, Y. Yoshida, K. Haratani, D. Mori, Y. Yano, Y. Mimori-Kiyosue, T. Nakamura, K. Itoh, S. Fushiki, M. Setou, A. Wynshaw-Boris, T. Torisawa, Y.Y. Toyoshima, S. Hirotsune, LIS1 and NDEL1 coordinate the plus-end-directed transport of cytoplasmic dynein, EMBO J. 27 (2008) 2471–2483.

[10] R.J. McKenney, M. Vershinin, A. Kunwar, R.B. Vallee, S.P. Gross, LIS1 and NudE induce a persistent dynein force-producing state, Cell 141 (2010) 304–314.

[11] S.A. Burgess, M.L. Walker, H. Sakakibara, P.J. Knight, K. Oiwa, Dynein structure and power stroke, Nature 421 (2003) 715–718.

[12] A.J. Roberts, N. Numata, M.L. Walker, Y.S. Kato, B. Malkova, T. Kon, R. Ohkura, F. Arisaka, P.J. Knight, K. Sutoh, S.A. Burgess, AAA^+ ring and linker swing mechanism in the dynein motor, Cell 136 (2009) 485–495.

[13] N. Numata, T. Kon, T. Shima, K. Imamula, T. Mogami, R. Ohkura, K. Sutoh, Molecular mechanism of force generation by dynein, a molecular motor belonging to the AAA^+ family, Biochem. Soc. Trans. 36 (2008) 131–135.

[14] A.P. Carter, R.D. Vale, Communication between the AAA^+ ring and microtubule-binding domain of dynein, Biochem. Cell Biol. 88 (2010) 15–21.
[15] O. Reiner, R. Carrozzo, Y. Shen, M. Wehnert, F. Faustinella, W.B. Dobyns, C.T. Caskey, D.H. Ledbetter, Isolation of a Miller-Dieker lissencephaly gene containing G protein b-subunit-like repeats, Nature 364 (1993) 717–721.
[16] X. Xiang, A.H. Osmani, S.A. Osmani, M. Xin, N.R. Morris, NudF, a nuclear migration gene in *Aspergillus nidulans*, is similar to the human LIS-1 gene required for neuronal migration, Mol. Biol. Cell 6 (1995) 297–310.
[17] V.P. Efimov, N.R. Morris, The LIS1-related NUDF protein of *Aspergillus nidulans* interacts with the coiled-coil domain of the NUDE/RO11 protein, J. Cell Biol. 150 (2000) 681–688.
[18] S. Sasaki, A. Shionoya, M. Ishida, M.J. Gambello, J. Yingling, A. Wynshaw-Boris, S. Hirotsune, A LIS1/NUDEL/cytoplasmic dynein heavy chain complex in the developing and adult nervous system, Neuron 28 (2000) 681–696.
[19] Y. Feng, E.C. Olson, P.T. Stukenberg, L.A. Flanagan, M.W. Kirschner, C.A. Walsh, LIS1 regulates CNS lamination by interacting with mNudE, a central component of the centrosome, Neuron 28 (2000) 665–679.
[20] M. Niethammer, D.S. Smith, R. Ayala, J. Peng, J. Ko, M.S. Lee, M. Morabito, L.H. Tsai, NUDEL is a novel Cdk5 substrate that associates with LIS1 and cytoplasmic dynein, Neuron 28 (2000) 697–711.
[21] J.W. Tsai, Y. Chen, A.R. Kriegstein, R.B. Vallee, LIS1 RNA interference blocks neural stem cell division, morphogenesis, and motility at multiple stages, J. Cell Biol. 170 (2005) 935–945.
[22] Y. Feng, C.A. Walsh, Mitotic spindle regulation by nde1 controls cerebral cortical size, Neuron 44 (2004) 279–293.
[23] S. Sasaki, D. Mori, K. Toyo-oka, A. Chen, L. Garrett-Beal, M. Muramatsu, S. Miyagawa, N. Hiraiwa, A. Yoshiki, A. Wynshaw-Boris, S. Hirotsune, Complete loss of Ndel1 results in neuronal migration defects and early embryonic lethality, Mol. Cell Biol. 25 (2005) 7812–7827.
[24] O. Reiner, U. Albrecht, M. Gordon, K.A. Chianese, C. Wong, O. Gal-Gerber, T. Sapir, L.D. Siracusa, A.M. Buchberg, C.T. Caskey, G. Eichele, Lissencephaly gene (*LIS1*). expression in the CNS suggests a role in neuronal migration, J. Neurosci. 15 (1995) 3730–3738.
[25] C. Lo Nigro, C.S. Chong, A.C. Smith, W.B. Dobyns, R. Carrozzo, D.H. Ledbetter, Point mutations and an intragenic deletion in LIS1, the lissencephaly causative gene in isolated lissencephaly sequence and Miller-Dieker syndrome, Hum. Mol. Genet. 6 (1997) 157–164.
[26] H. Koizumi, N. Yamaguchi, M. Hattori, T.O. Ishikawa, J. Aoki, M.M. Taketo, K. Inoue, H. Arai, Targeted disruption of intracellular type I platelet activating factor-acetylhydrolase catalytic subunits causes severe impairment in spermatogenesis, J. Biol. Chem. 278 (2003) 12489–12494.
[27] W. Yan, A.H. Assadi, A. Wynshaw-Boris, G. Eichele, M.M. Matzuk, G.D. Clark, Previously uncharacterized roles of platelet-activating factor acetylhydrolase 1b complex in mouse spermatogenesis, Proc. Natl. Acad. Sci. USA 100 (2003) 7189–7194.
[28] C. Ding, X. Liang, L. Ma, X. Yuan, X. Zhu, Opposing effects of Ndel1 and alpha1 or alpha2 on cytoplasmic dynein through competitive binding to Lis1, J. Cell Sci. 122 (2009) 2820–2827.
[29] N.E. Faulkner, D.L. Dujardin, C.Y. Tai, K.T. Vaughan, C.B. O'Connell, Y. Wang, R.B. Vallee, A role for the lissencephaly gene LIS1 in mitosis and cytoplasmic dynein function, Nat. Cell. Biol. 2 (2000) 784–791.
[30] F.M. Coquelle, M. Caspi, F.P. Cordelieres, J.P. Dompierre, D.L. Dujardin, C. Koifman, P. Martin, C.C. Hoogenraad, A. Akhmanova, N. Galjart, J.R. De Mey, O. Reiner, LIS1, CLIP-170's key to the dynein/dynactin pathway, Mol. Cell Biol. 22 (2002) 3089–3102.
[31] W.L. Lee, J.R. Oberle, J.A. Cooper, The role of the lissencephaly protein Pac1 during nuclear migration in budding yeast, J. Cell Biol. 160 (2003) 355–364.
[32] X. Xiang, LIS1 at the microtubule plus end and its role in dynein-mediated nuclear migration, J. Cell Biol. 160 (2003) 289–290.

[33] D.L. Dujardin, L.E. Barnhart, S.A. Stehman, E.R. Gomes, G.G. Gundersen, R.B. Vallee, A role for cytoplasmic dynein and LIS1 in directed cell movement, J. Cell Biol. 163 (2003) 1205–1211.
[34] S. Hebbar, M.T. Mesngon, A.M. Guillotte, B. Desai, R. Ayala, D.S. Smith, Lis1 and Ndel1 influence the timing of nuclear envelope breakdown in neural stem cells, J. Cell Biol. 182 (2008) 1063–1071.
[35] C. Lam, M.A. Vergnolle, L. Thorpe, P.G. Woodman, V.J. Allan, Functional interplay between LIS1, NDE1 and NDEL1 in dynein-dependent organelle positioning, J. Cell Sci. 123 (2010) 202–212.
[36] D.S. Smith, M. Niethammer, R. Ayala, Y. Zhou, M.J. Gambello, A. Wynshaw-Boris, L.H. Tsai, Regulation of cytoplasmic dynein behaviour and microtubule organization by mammalian Lis1, Nat. Cell. Biol. 2 (2000) 767–775.
[37] M.E. Bechler, A.M. Doody, E. Racoosin, L. Lin, K.H. Lee, W.J. Brown, The phospholipase complex PAFAH Ib regulates the functional organization of the Golgi complex, J. Cell Biol. 190 (2010) 45–53.
[38] C.Y. Tai, D.L. Dujardin, N.E. Faulkner, R.B. Vallee, Role of dynein, dynactin, and CLIP-170 interactions in LIS1 kinetochore function, J. Cell Biol. 156 (2002) 959–968.
[39] A. Swan, T. Nguyen, B. Suter, *Drosophila* lissencephaly-1 functions with Bic-D and dynein in oocyte determination and nuclear positioning, Nat. Cell Biol. 1 (1999) 444–449.
[40] D. Varma, P. Monzo, S.A. Stehman, R.B. Vallee, Direct role of dynein motor in stable kinetochore–microtubule attachment, orientation, and alignment, J. Cell Biol. 182 (2008) 1045–1054.
[41] S.A. Stehman, Y. Chen, R.J. McKenney, R.B. Vallee, NudE and NudEL are required for mitotic progression and are involved in dynein recruitment to kinetochores, J. Cell Biol. 178 (2007) 583–594.
[42] M.A. Vergnolle, S.S. Taylor, Cenp-F links kinetochores to Ndel1/Nde1/Lis1/dynein microtubule motor complexes, Curr. Biol. 17 (2007) 1173–1179.
[43] Y. Liang, W. Yu, Y. Li, Z. Yang, X. Yan, Q. Huang, X. Zhu, Nudel functions in membrane traffic mainly through association with Lis1 and cytoplasmic dynein, J. Cell Biol. 164 (2004) 557–566.
[44] Q. Zhang, F. Wang, J. Cao, Y. Shen, Q. Huang, L. Bao, X. Zhu, Nudel promotes axonal lysosome clearance and endo-lysosome formation via dynein-mediated transport, Traffic 10 (2009) 1337–1349.
[45] T. Kon, M. Nishiura, R. Ohkura, Y.Y. Toyoshima, K. Sutoh, Distinct functions of nucleotide-binding/hydrolysis sites in the four AAA modules of cytoplasmic dynein, Biochemistry 43 (2004) 11266–11274.
[46] T. Kon, T. Mogami, R. Ohkura, M. Nishiura, K. Sutoh, ATP hydrolysis cycle-dependent tail motions in cytoplasmic dynein, Nat. Struct. Mol. Biol. 12 (2005) 513–519.
[47] M.T. Mesngon, C. Tarricone, S. Hebbar, A.M. Guillotte, E.W. Schmitt, L. Lanier, A. Musacchio, S.J. King, D.S. Smith, Regulation of cytoplasmic dynein ATPase by Lis1, J. Neurosci. 26 (2006) 2132–2139.
[48] P. Hook, A. Mikami, B. Shafer, B.T. Chait, S.S. Rosenfeld, R.B. Vallee, Long range allosteric control of cytoplasmic dynein ATPase activity by the stalk and C-terminal domains, J. Biol. Chem. 280 (2005) 33045–33054.
[49] K. Imamula, T. Kon, R. Ohkura, K. Sutoh, The coordination of cyclic microtubule association/dissociation and tail swing of cytoplasmic dynein, Proc. Natl. Acad. Sci. USA 104 (2007) 16134–16139.
[50] T. Shimizu, K.A. Johnson, Presteady state kinetic analysis of vanadate-induced inhibition of the dynein ATPase, J. Biol. Chem. 258 (1983) 13833–13840.
[51] V. Soppina, A.K. Rai, A.J. Ramaiya, P. Barak, R. Mallik, Tug-of-war between dissimilar teams of microtubule motors regulates transport and fission of endosomes, Proc. Natl. Acad. Sci. USA 106 (2009) 19381–19386.
[52] A.G. Hendricks, E. Perlson, J.L. Ross, H.W. Schroeder 3rd, M. Tokito, E.L. Holzbaur, Motor coordination via a tug-of-war mechanism drives bidirectional vesicle transport, Curr. Biol. 20 (2010) 697–702.

[53] M. Hafezparast, R. Klocke, C. Ruhrberg, A. Marquardt, A. Ahmad-Annuar, S. Bowen, G. Lalli, A.S. Witherden, H. Hummerich, S. Nicholson, P.J. Morgan, R. Oozageer, J.V. Priestley, S. Averill, V.R. King, S. Ball, J. Peters, T. Toda, A. Yamamoto, Y. Hiraoka, M. Augustin, D. Korthaus, S. Wattler, P. Wabnitz, C. Dickneite, S. Lampel, F. Boehme, G. Peraus, A. Popp, M. Rudelius, J. Schlegel, H. Fuchs, M.H. de Angelis, G. Schiavo, D.T. Shima, A.P. Russ, G. Stumm, J.E. Martin, E.M. Fisher, Mutations in dynein link motor neuron degeneration to defects in retrograde transport, Science 300 (2003) 808–812.
[54] H.S. Ilieva, K. Yamanaka, S. Malkmus, O. Kakinohana, T. Yaksh, M. Marsala, D.W. Cleveland, Mutant dynein (Loa) triggers proprioceptive axon loss that extends survival only in the SOD1 ALS model with highest motor neuron death, Proc. Natl. Acad. Sci. USA 105 (2008) 12 599–12 604.
[55] L. Dupuis, A. Fergani, K.E. Braunstein, J. Eschbach, N. Holl, F. Rene, J.L. Gonzalez De Aguilar, B. Zoerner, B. Schwalenstocker, A.C. Ludolph, J.P. Loeffler, Mice with a mutation in the dynein heavy chain 1 gene display sensory neuropathy but lack motor neuron disease, Exp. Neurol. 215 (2009) 146–152.
[56] E. Perlson, G.B. Jeong, J.L. Ross, R. Dixit, K.E. Wallace, R.G. Kalb, E.L. Holzbaur, A switch in retrograde signaling from survival to stress in rapid-onset neurodegeneration, J. Neurosci. 29 (2009) 9903–9917.
[57] B.H. LaMonte, K.E. Wallace, B.A. Holloway, S.S. Shelly, J. Ascano, M. Tokito, T. Van Winkle, D.S. Howland, E.L. Holzbaur, Disruption of dynein/dynactin inhibits axonal transport in motor neurons causing late-onset progressive degeneration, Neuron 34 (2002) 715–727.
[58] I. Puls, C. Jonnakuty, B.H. LaMonte, E.L. Holzbaur, M. Tokito, E. Mann, M.K. Floeter, K. Bidus, D. Drayna, S.J. Oh, R.H. Brown, C.L. Ludlow, K.H. Fischbeck, Mutant dynactin in motor neuron disease, Nat. Genet. 33 (2003) 455–456.
[59] X.J. Chen, E.N. Levedakou, K.J. Millen, R.L. Wollmann, B. Soliven, B. Popko, Proprioceptive sensory neuropathy in mice with a mutation in the cytoplasmic dynein heavy chain 1 gene, J. Neurosci. 27 (2007) 14515–14524.
[60] A. Habura, I. Tikhonenko, R.L. Chisholm, M.P. Koonce, Interaction mapping of a dynein heavy chain. Identification of dimerization and intermediate-chain binding domains, J. Biol. Chem. 274 (1999) 15447–15453.
[61] S.H. Tynan, M.A. Gee, R.B. Vallee, Distinct but overlapping sites within the cytoplasmic dynein heavy chain for dimerization and for intermediate chain and light intermediate chain binding, J. Biol. Chem. 275 (2000) 32769–32774.
[62] K.M. Ori-McKenney, J. Xu, S.P. Gross, R.B. Vallee, A cytoplasmic dynein tail mutation impairs motor processivity, Nat. Cell Biol. 12 (2010) 1228–1234.
[63] Z. Wang, S. Khan, M.P. Sheetz, Single cytoplasmic dynein molecule movements: Characterization and comparison with kinesin, Biophys. J. 69 (1995) 2011–2023.
[64] S.L. Reck-Peterson, A. Yildiz, A.P. Carter, A. Gennerich, N. Zhang, R.D. Vale, Single-molecule analysis of dynein processivity and stepping behavior, Cell 126 (2006) 335–348.
[65] A. Gennerich, R.D. Vale, Walking the walk: How kinesin and dynein coordinate their steps, Curr. Opin. Cell Biol. 21 (2009) 59–67.
[66] N.R. Guydosh, S.M. Block, Backsteps induced by nucleotide analogs suggest the front head of kinesin is gated by strain, Proc. Natl. Acad. Sci. USA 103 (2006) 8054–8059.
[67] H.L. Sweeney, H. Park, A.B. Zong, Z. Yang, P.R. Selvin, S.S. Rosenfeld, How myosin VI coordinates its heads during processive movement, EMBO J. 26 (2007) 2682–2692.
[68] A. Yildiz, M. Tomishige, A. Gennerich, R.D. Vale, Intramolecular strain coordinates kinesin stepping behavior along microtubules, Cell 134 (2008) 1030–1041.
[69] J.R. Levy, C.J. Sumner, J.P. Caviston, M.K. Tokito, S. Ranganathan, L.A. Ligon, K.E. Wallace, B.H. LaMonte, G.G. Harmison, I. Puls, K.H. Fischbeck, E.L. Holzbaur, A motor neuron disease-associated mutation in $p150^{Glued}$ perturbs dynactin function and induces protein aggregation, J. Cell Biol. 172 (2006) 733–745.

In this chapter

17

Insights into Cytoplasmic Dynein Function and Regulation from Fungal Genetics

Xin Xiang
Department of Biochemistry and Molecular Biology, Uniformed Services University of the Health Sciences – F. Edward Hébert School of Medicine, Bethesda, MD, USA

17.1 Introduction

Cytoplasmic dynein is a minus-end-directed microtubule motor important for mitosis, retrograde vesicle transport, and organelle distribution [1–3]. It is a multi-protein complex, and the dynein heavy chain (HC) within the complex is an ATPase responsible for ATP-dependent motility along microtubules [4,5]. The function of cytoplasmic dynein *in vivo* is regulated by several factors including another multi-protein complex, dynactin [6]; LIS1, a human disease lissencephaly gene product; and NudE/NudEL, which interact with LIS1 [7–9]. Over the years, studies in several fungal organisms have made great contributions to our current understanding of cytoplasmic dynein function and regulation *in vivo*. This chapter covers the discovery of dynein's function in the positioning of nuclei and mitotic spindles, and genetic studies that link the function of LIS1 and NudE/NudEL to the dynein pathway. It also reviews studies on the functions and regulatory mechanisms of the microtubule plus-end accumulation of cytoplasmic dynein, as well as studies on the biochemical functions of different proteins in the dynein and dynactin complexes. Some aspects of dynein function and regulation that are not covered here have been discussed in other recent reviews [10,11].

17.2 Discoveries of Dynein Function in Spindle Orientation/Nuclear Migration

The function of cytoplasmic dynein in positioning the mitotic spindles was first discovered in the budding yeast *Saccharomyces cerevisiae* by using

Dyneins DOI: 10.1016/B978-0-12-382004-4.10017-2
Copyright © 2012 by Elsevier Inc. All rights reserved.

a reverse-genetic approach [12,13]. The dynein HC gene in *S. cerevisiae* was identified based on its sequence homology with HCs in other eukaryotic organisms, which was followed by the construction and analysis of the dynein HC deletion/disruption mutants [12,13]. In the absence of dynein HC, budding mother cells containing two or occasionally more nuclei and budding daughter cells with no nuclei are found in a fraction of cells (about 14%) at 30°C, and the percentage of cells with this abnormal phenotype increases when cells are incubated at lower temperatures (Fig. 17.1). In the cells with abnormal nuclear distribution, mitotic spindles are not properly oriented and fail to move through the bud neck, suggesting that dynein is required for positioning the spindle. Since dynein is a minus-end-directed motor and the spindle pole body represents the minus ends of astral microtubules emanating from the spindle pole bodies, it was proposed that dynein is most likely anchored to a cortical site, either at the neck or the bud, to pull the astral microtubules and the attached spindle towards the daughter cell [12,13]. This notion has been strongly supported by the

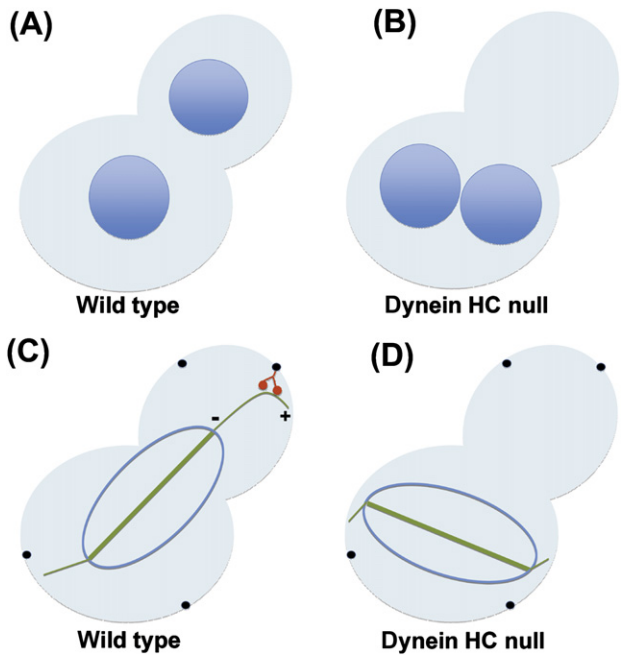

Figure 17.1 Diagrams showing the phenotypes of wild-type and null mutants of dynein heavy chain (HC) in *S. cerevisiae*, and how dynein functions to move the mitotic spindle. Unlike wild type, in which daughter nuclei are segregated properly into the mother and the bud (A), a fraction of the dynein mutant mother cells abnormally contain two daughter nuclei after anaphase DNA segregation (B). This results from the fact that spindles in the dynein mutant often fail to orientate properly, which is in contrast to wild type, in which spindles are orientated along the mother–bud axis (C,D). Also shown in (C) is a model in which dynein (red) anchored at the Num1 sites (black dots) at the bud cortex walks along an astral microtubule towards its minus end, located at the bud-proximal spindle pole body, thereby pulling the spindle toward the bud [12–16].

identification of the cortical Num1 protein, which interacts with dynein, and the finding that cortical association of Num1 is required for dynein-mediated microtubule sliding and spindle positioning [14–17].

Despite a defect in spindle movement towards the bud, dynein null mutants in *S. cerevisiae* are able to form normal colonies under normal growth conditions, and this could be due to several factors. First, anucleated daughter cells do not bud off because of the presence of a spindle-positioning checkpoint that prevents mitotic exit and cytokinesis when a spindle pole does not enter the bud, which allows time for compensatory forces to orientate the spindle [12,18]. Second, the Kar9-Bim1-Kip3 pathway allows nuclear movement toward the bud neck before anaphase by using the pulling force of a myosin-V motor on microtubule plus ends and the plus-end depolymerase activity of the Kip3 kinesin-8, which prevents the spindles from being pushed back to mother cells [19–23]. This pathway is partially redundant to the dynein pathway and these two pathways may also communicate with each other at the molecular level to ensure proper positioning of the spindle [24,25].

Functional studies of cytoplasmic dynein in the multinucleated filamentous fungi *Aspergillus nidulans* and *Neurospora crassa* were initiated by a classic forward-genetic approach (Table 17.1) [26–28]. In 1975, Ron Morris isolated the first several nuclear distribution (*nud*) mutants in *A. nidulans* [26], and the *nudA* gene was later cloned by cosmid complementation and identified as the coding gene for cytoplasmic dynein HC [27]. The *nud* mutants defective in the dynein pathway form colonies that are significantly smaller than a wild-type colony [27], which facilitates not only cloning of *nud* genes by complementation but also the isolation

Table 17.1 *A. nidulans nud* Genes and *N. crassa ropy* (or *ro*) Genes

nud genes	*ropy* (or *ro*) genes
nudA (HC) [27] *nudG* (LC8) [130] *nudI* (IC) [133] *nudN* (LIC) [131]	*ro*-1 (HC) [28]
nudK (Arp1) [143] *nudM* (p150) [97] *nudR* (p62) [144]	*ro*-2 (p62) [39] *ro*-3 (p150) [38] *ro*-4 (Arp1) [28] *ro*-7 (Arp11) [39] *ro*-10 (p24) [72] *ro*-12 (p25) [39]
nudC (mNudC/NudCL) [29] *nudF* (LIS1) [30] *nudE* (NudE/NudEL) [71]	*ro*-11 (NudE/NudEL) [72]

This table lists only published *nud* and *ropy* genes identified by forward-genetic approaches. The genes encode proteins of the dynein complex (the first block) and the dynactin complex (the second block) and also proteins not in the dynein–dynactin complexes (the third block). Mammalian proteins encoded by the homologous genes are indicated in parentheses.

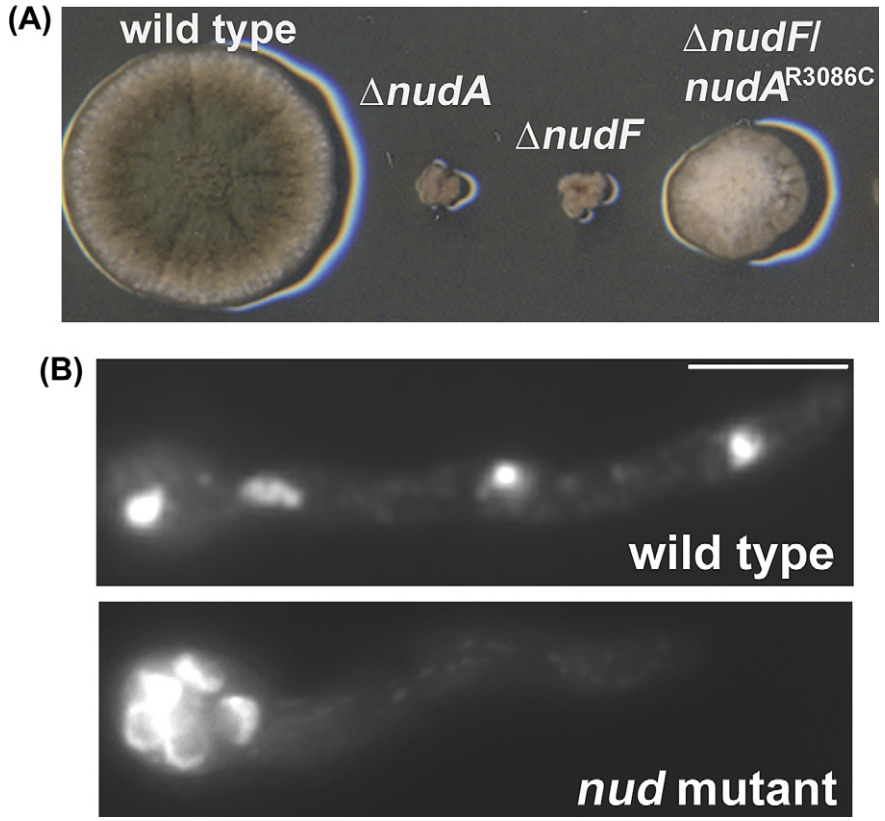

Figure 17.2 Colony-growth and nuclear-distribution phenotypes of *nud* mutants in *A. nidulans* [27,140]. (A) Colony phenotypes of the △*nudA* (dynein HC) and △*nudF* (LIS1) mutants and a △*nudF* mutant containing a suppressor mutation in the *nudA* gene. Modified with permission from [140]. (B) Nuclear-distribution phenotype of a typical *nud* mutant as revealed by DAPI staining of nuclei. While multiple nuclei are evenly distributed in wild type, multiple nuclei are clustered at the spore end of a germ tube in a *nud* mutant. Bar = 5 μm.

of additional *nud* mutants and/or their suppressors (Fig. 17.2). In contrast to the elongated hyphae of wild type, where multiple nuclei are distributed more or less evenly, the hyphae of a *nud* mutant contain nuclei that are clustered together [26]. The nud phenotype is also obvious in germ tubes formed upon spore germination. While wild-type nuclei are evenly distributed along a germ tube, nuclei of a *nud* mutant fail to move out of the spore end, resulting in the appearance of a nuclear cluster at the spore end and a nuclei-free germ tube (Fig. 17.2). Although this phenotype suggested a defect in nuclear movement, an alternative interpretation for it was that a failure in the separation of nuclei after divisions resulted in the formation of a cluster too large to enter the relatively narrow germ tube. To address this possibility, double mutants were made containing both a *nud* mutation and

a mitotic mutation that causes the cells to be blocked at G2 with a single nucleus [27,29]. It was shown that the single nucleus is still unable to move into the germ tube, strongly suggesting that dynein is required for nuclear migration [27,29].

A. nidulans dynein is also critical for conidiation (asexual spore production), a process consisting of steps that resemble yeast budding during which the movement of a single nucleus into the bud is important [30–33]. In fact, the ApsA (anucleate primary sterigmata) protein of *A. nidulans*, which is similar to the budding yeast Num1, is essential for this process [32,33]. It is also interesting to note that *A. nidulans* dynein mutants show an abnormality in the position of septation (a process analogous to cytokinesis although it does not strictly follow each nuclear division in filamentous fungi) [31,34–36]. While the first septum is usually formed near the spore end in a wild-type germ tube, it is often formed far away from the spore end in a dynein loss-of-function mutant [31,35]. The abnormally positioned septum seems to block nuclei from leaking out to other hyphal compartments, thereby acerbating the nud phenotype [35]. In support of this view, mutations that delay septation can partially suppress the nud phenotype of dynein mutants and allow a *nud* mutant colony to grow better [35,36].

In *N. crassa*, dynein is also important for nuclear distribution in elongated hyphae [28]. *N. crassa* dynein mutants exhibit a curled hyphae (ropy) phenotype and therefore are also called the *ropy* (or *ro*) mutants [28]. Interestingly, genetic dissection of the dynein pathway was started by a screen for suppressors of a serine/threonine kinase *cot*1 mutant defective in hyphal growth [37], and the screen identified many *ropy* (or *ro*) mutants [28,38]. The *ro*-1 gene was cloned by cosmid complementation and it encodes the cytoplasmic dynein HC [28]. Most *ropy* mutants in the dynein pathway exhibit a nuclear-distribution defect in elongated hyphae, characterized by the presence of nuclear clumps in one region and nuclei-free hyphal segments in nearby regions [28]. The curled hyphal growth in the *ropy* mutants is unlikely to be caused by the nuclear-distribution defect, which is evidenced by the existence of the *ro*-12 mutant, which does not exhibit a nuclear-distribution defect [39].

The role of dynein in positioning nuclei/spindles has also been found in several other fungal organisms such as *Nectria haematococca*, *Ustilago maydis*, *Ashbya gossypii*, *Aspergillus oryzae*, and *Candida albicans* [40–46]. Moreover, this role appears to be well-conserved in higher eukaryotic organisms including worms, flies, and mammals [8,47,48]. It is interesting to note that in the dimorphic basidiomycetes *U. maydis*, where two separate genes encode two polypeptides that combine to function as a dynein HC [42], dynein-mediated nuclear migration into the daughter cell helps to strip off the nuclear envelope, thereby ensuring open mitosis [43]. In the fission yeast *Schizosaccharomyces pombe*, dynein is not required for nuclear positioning during the mitotic cycle but plays a role in moving the prophase nucleus back and forth during meiosis, which may help to align the homologous chromosomes for recombination before nuclear division [49–51].

17.3 Identification of Dynein Regulators Using Fungal Genetics

Cytoplasmic dynein is a complex containing the HC motor and other subunits including intermediate chains (ICs), light-intermediate chains (LICs), and light chains (LCs) that bind to the HC's tail domain [4]. The dynein IC interacts directly with the dynactin complex that is thought to link dynein to membranous vesicles and also to enhance dynein processivity [6,52–54]. Fungal genetics not only made the functional link between individual subunits of the dynein–dynactin complexes and the *in vivo* function of dynein, but also allowed the identification of several dynein regulators such as LIS1, NudE/NudEL, and mNudC/NudCL that had not been isolated as components of the dynein and dynactin complexes.

In *A. nidulans*, the *nudC* gene was the first cloned *nud* gene and it encodes a small protein with 212 amino acids [29]. Although the deletion mutant of *nudC* is lethal and exhibits a defect in cell wall formation, the *nudC*3 mutation, *nudC*^{L146P}, produces a nud phenotype [29,55,56]. NUDC homologs in higher eukaryotic systems are found and these proteins appear to have both dynein-dependant and dynein-independent functions, and may have a chaperone activity and affect protein stability [57–64].

The *nudF* gene was initially cloned as an extra-copy suppressor of the *nudC*3 mutant [30]. It completely rescued the nud phenotype of the *nudF* mutants, and further genetic analyses confirmed its identity as the *nudF* gene [30]. The suppression of the *nudC*3 phenotype by extra copies of *nudF* was explained by the finding that the level of the NUDF protein is decreased in the *nudC*3 mutant [30]. NUDF is a protein containing multiple WD-40 repeats and also a coiled-coil domain at the N-terminus, and it shares high sequence identity (42%) with the human LIS1 protein encoded by a causal gene of human type 1 lissencephaly [30,65]. Lissencephaly (smooth brain) is a disease manifested by severe mental retardation, epilepsy, and early death, and it is caused by a neuronal migration defect [66]. The high homology between NUDF and LIS1 has linked nuclear migration and cell migration at the molecular level, and provided a strong support for the concept of nucleokinesis, during which the movement of the nucleus within the cell is an essential step of cell migration [48,67]. The *nudF* gene functions in the cytoplasmic dynein pathway [30,68], indicating that the function of LIS1 is connected to that of cytoplasmic dynein in mammalian cells, and this idea has been strongly supported by data on the physical interactions and functions of these proteins [7,9,48,69]. It should also be pointed out that a LIS1 homolog in *Chlamydomonas* is present in flagella, where it interacts with components of the outer dynein arm [70]. In addition, both LIS1 and NUDC are present in cilia of mammalian cells [70]. Thus, unlike the dynactin complex, which seems to be specifically required for the functions of cytoplasmic dynein [54], LIS1 and its

homologs may have evolved to regulate the functions of both cytoplasmic dynein and axonemal dynein.

The *nudE* gene was cloned as a multi-copy suppressor of a *nudF* ts mutant and, like *nudF*, it is also important for nuclear distribution [71]. NUDE contains a N-terminal coiled-coil domain and is homologous to RO11 in *N. crassa* [71,72]. NUDE and NUDF/LIS1 interact physically, and the N-terminal half of NUDE that interacts with NUDF/LIS1 is sufficient for NUDE function [71]. The *nudE* deletion mutant, however, shows a less severe defect in nuclear distribution and forms a healthier colony compared to that of the *nudF* (LIS1) deletion mutant [71,73]. Multiple copies of *nudE* suppresses the phenotype of a *nudF* mutant in an allele-specific manner, suggesting that overexpression of NUDE cannot bypass NUDF function. However, overexpression of NUDF/LIS1 completely suppresses the phenotype of the *nudE* deletion mutant [74]. These results suggest that NUDF/LIS1 works downstream of NUDE, and the function of NUDE is dispensable if an excess amount of NUDF is present in the cell [74].

In *S. cerevisiae*, many proteins in the dynein pathway including Pac1, the LIS1 homolog, were discovered in a screen for mutations synthetically lethal with loss of a kinesin-5 motor, Cin8 [75]. In addition, a screen for cold-sensitive haploid null mutants with a higher than normal percentage of binucleate cells has led to the identification of the NudE homolog Ndl1 [76]. The ndl1 null mutant shows a defect in spindle positioning as judged by an increased number of binucleate cells at a low temperature and also by the presence late-anaphase spindles in the mother cells, but the defect is less severe than that exhibited by a dynein null mutant [76]. This is consistent with results from *A. nidulans* and suggests that, in these fungi, NUDE plays a less critical role in the dynein pathway than other core components such as dynein HC and LIS1 [71,76]. Results on the genetic interaction between Pac1/LIS1 and Ndl1/NUDE obtained from *S. cerevisiae* are similar to that in *A. nidulans* [76]. While overexpression of Ndl1 cannot suppress the *pac1* null mutant phenotype, overexpression of Pac1 is able to suppress the *ndl1* null mutant phenotype [76]. This further strengthens the notion that NUDF/Pac1 is more directly involved in dynein function than NUDE/Ndl1, and NUDE/Ndl1 functions to facilitate the function of NUDF/Pac1 in the dynein pathway.

Like LIS1, NUDE homologs in high eukaryotes (NudE and NudEL, also called Nde1 and Ndel1 in some publications) participate in cellular functions that involve cytoplasmic dynein, although LIS1, NudE, and NudEL also have dynein-independent functions [7,69,77–89]. Importantly, purified LIS1 combined with NudE causes an enhancement of dynein force production *in vitro*, indicating that these dynein regulators would help the motor to move processively along microtubules when loaded with heavy cargoes [9]. NudE enhances LIS1–dynein interaction, which may help LIS1 to exert its regulation on the dynein motor [9].

17.4 Dissecting the Mechanism and Function of the Microtubule-Plus-End Accumulation of Cytoplasmic Dynein

Despite being a minus-end-directed motor, cytoplasmic dynein and its regulators are found to accumulate at the microtubule plus ends. In mammalian cells, dynactin localizes at the microtubule plus ends but dynein's plus-end accumulation was not easily detected [90–92]. However, in filamentous fungi and budding yeast, cytoplasmic dynein, dynactin, and LIS1 homologs such as NUDF and Pac1 are all found to accumulate at the plus ends of microtubules [93–99]. It was first described in *A. nidulans* that green fluorescent protein (GFP)-labeled dynein HC molecules form comet-like structures at the dynamic plus ends of cytoplasmic microtubules near the hyphal tip (Fig. 17.3) [93,94]. This behavior is similar to that of a class of proteins termed the "microtubule plus-end-tracking proteins" (+TIPs), which includes CLIP-170 and EB1 in mammalian cells [100]. However, while the GFP-labeled mammalian +TIPs highlight the growing plus ends, dynein and its regulators in fungi are not only observed at the growing plus ends but also at the shrinking plus ends [100]. In *S. cerevisiae*, a homolog of CLIP-170 (the first described +TIP), Bik1, is also found to associate with both the shrinking and growing ends [101]. When these proteins are associated with the shrinking ends, the comet-like structures appear to move backwards and, thus, this phenomenon is termed "backtracking" [101]. Backtracking is likely to be related to the kinesin-driven mechanism of plus-end accumulation, in which plus-end-directed kinesins continuously replenish the plus ends with +TIPs [97,98,101]. In filamentous hyphae of *A. nidulans* and *U. maydis*, kinesin-1 is required for the plus-end accumulation of dynein [97,98]. In *S. cerevisiae*, the Kip2 kinesin-7 is important for the plus-end accumulation of dynein and Bik1 [101]. The direct role of Kip2 in driving Bik1 to the plus ends is demonstrated by the physical association between these two proteins and by their co-migration towards the plus ends [101]. Dynein may take a ride with Bik1 and Pac1, which interacts with Bik1 [96], to the plus ends, as fluorescent dynein spots are also observed to move along microtubules towards the plus ends [102]. Alternatively, the plus-end accumulated Bik1 and Pac1 may recruit and/or retain dynein at the plus ends [11].

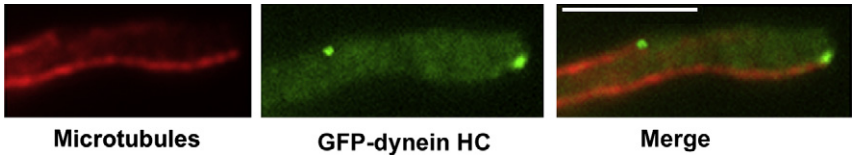

Figure 17.3 Microtubule plus-end localization of dynein HC in *A. nidulans* [94]. Rhodamine-labeled microtubules (red), GFP-labeled dynein HC (green), and a merged image are shown. Bar = 5 μm. *Modified with permission from [94].*

Besides the plus-end-directed kinesins, other proteins are also found to be important for the plus-end accumulation of dynein. In *A. nidulans*, dynein and dynactin are dependent upon each other, and also on kinsin-1, for their plus-end accumulation, but NUDF/LIS1 is not required [97]. In *S. pombe*, dynein and dynactin are also dependent upon each other for their localization to the sites where microtubule plus ends interact with the cortex [103]. However, in *S. cerevisiae*, Pac1 (LIS1), Bik1 (CLIP-170), and Kip2, but not dynactin, are important for the plus-end accumulation of dynein [95,96,101]. Thus, the mechanisms of dynein's plus-end accumulation are not the same among these fungi, although in both *A. nidulans* and *S. cerevisiae* the plus-end accumulation of dynactin depends on dynein [97,99,104]. In the filamentous hyphae of *U. maydis*, dynactin and kinesin-1, but not LIS1, are important for dynein's plus-end accumulation, which is similar to the results from *A. nidulans* [98]. Thus, filamentous fungi may use a similar mechanism for targeting dynein to the plus ends, which is different from that used in budding yeast.

In *S. cerevisiae*, where dynein is important for the orientation/positioning of the mitotic spindle but not for vesicle transport, the accumulation of dynein at the plus ends of astral microtubules is important for dynein-mediated spindle movement toward the bud [11,95,96]. Dyneins at the dynamic plus ends are thought to be delivered/offloaded to the cortical Num1 sites in a dynactin-dependant manner, and, when dynein molecules anchored at these sites move towards the minus ends of astral microtubules emanated from the bud-proximal spindle pole, the spindle is pulled toward the bud (Fig. 17.4) [95,96]. Although the offloading process has yet to be directly observed, this model is very well accepted and is largely consistent with the available data. For example, in the absence of Pac1/LIS1, a lack of dynein accumulation at the plus ends is well-

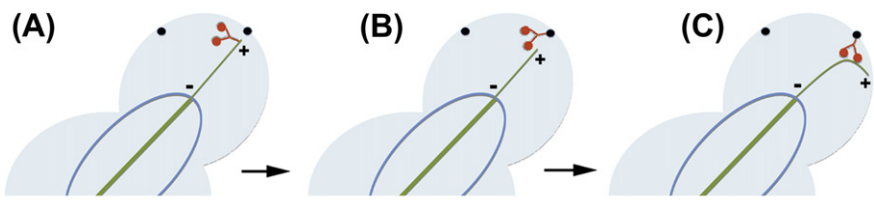

Figure 17.4 A model illustrating that *S. cerevisiae* dynein at the microtubule plus end is delivered/offloaded to a cortical Num1 site (black dot), where it is anchored and exerts its pulling force on an astral microtubule by walking towards its minus end [95,96]. For simplicity, non-HC dynein subunits are not shown and only one dynein HC dimer (red) is depicted at the plus end, although a recent study suggests that there are about seven HC dimers per plus end (105). (A) Dynein is located at the dynamic plus end of an astral microtubule. In this diagram, the dynein tail is attached to the microtubule, which reflects a possible configuration in which dynein is not able to leave the plus end as a minus-end-directed motor. (B) Dynein is delivered/offloaded from the plus end to the cortical Num1 site. (C) Dynein anchored at the Num1 site walks towards the minus end of the astral microtubule, thereby pulling the spindle.

correlated with a lack of dynein at the cortical sites [105]. In the *num*1 null mutant or in a dynactin null mutant, however, the signal intensity of plus-end dynein comets is increased, consistent with a failure in offloading plus-end dynein to the cortical sites [95,96]. In addition, plus-end tracking of dynein is most prominent during anaphase [96], a stage when dynein and Num1 are both needed for pulling astral microtubules [15,16]. Kip2 becomes abundant at a similar stage; it transports Bik1 to the plus ends to ensure that microtubules are long enough to allow delivery of plus-end dynein to the cortex [101]. Dynactin, whose function is implicated in the offloading of plus-end dynein to the cortex [95,96,99], accumulates at the plus ends of astral microtubules only at anaphase, which is regulated by the She1 protein [104]. In the *she1* null mutant, dynactin accumulates prematurely to the plus end, leading to spindle movement before anaphase [104]. Regulatory mechanisms are also present to ensure that dynein is asymmetrically distributed so that anaphase spindle movement occurs in a direction toward the bud, and that the pulling force from the bud is balanced by that from the mother so that one daughter cell will not contain the whole spindle and end up with two daughter nuclei [106,107]. It should be pointed out that *S. cerevisiae* dynein also plays a role in nuclear migration before anaphase [18]. In the presence of a DNA replication inhibitor or a mutation that prevents formation of a bipolar spindle, nuclear migration/penetration to the bud still depends on dynein [18]. The mechanistic details of dynein-mediated nuclear migration are not completely understood and need to be further studied.

In *S. pombe*, the Num1 homolog is important for dynein-mediated nuclear oscillation during prophase of meiosis [108,109], and a laser-ablation experiment shows that pulling force rather than pushing force is responsible for the movements at this stage [110]. Fluorescent dynein molecules accumulate at the plus ends and are also seen as spots along astral microtubules, presumably representing cortically anchored dynein walking along microtubules [110]. Dynein molecules are more concentrated on the leading microtubule than on the trailing microtubule, which may result from microtubule-length-dependent dynein attachment and load-dependent dynein detachment mechanisms [110]. When the leading microtubule is being pulled, dynein detaches from the trailing microtubule, due to a change in motor behavior upon an increase in load [110,111]. This self-organized change in motor distribution could lead to the back-and-forth movements of the nucleus [110].

A cortical dynein-pulling mechanism may also work to some extent in filamentous fungi, especially for spindle elongation and movement during mitosis. In *U. maydis*, dynein is responsible for the pulling force that drives anaphase B spindle elongation, as shown by laser cutting and live-cell imaging experiments [112]. Moreover, the results of the imaging experiments suggest that dynein molecules at the ends of astral microtubules can be off-loaded to the cortex, and the cortical dynein is used to pull the astral microtubules [112]. In *A. nidulans*, the cortical protein ApsA (Num1 homolog) required for nuclear migration

into the primary sterigmata (the bud-like structures of the asexual-spore-bearing condidiophore) is also important for the movements of mitotic spindles in hyphae [32,33,113]. However, since ApsA is not required for dynein-mediated interphase nuclear distribution, movement of multiple interphase nuclei towards the hyphal tip may use other mechanisms. While microtubule dynamics at the plus ends is important for enabling the plus ends to search for the cortical anchoring sites during spindle positioning, it may also play a critical role during the migration of interphase nuclei. The function of dynein in regulating microtubule dynamics at the plus ends, either directly or indirectly, has been found in several fungi including *S. cerevisiae*, *A. nidulans*, and *U. maydis*. In these fungi, loss of dynein function results in longer and more stable microtubules [94,114,115]. In *A. nidulans*, a β-tubulin mutation that causes hyperstabilization of microtubules blocks nuclear migration [116]. In addition, the nud phenotype of dynein mutants is partially suppressed by an α-tubulin mutation; by a low concentration of benomyl, a microtubule-destabilizing drug; and also by an ApsB mutation that suppresses the generation of microtubules from its organizing center [113,117]. More astonishingly, in *A. gossypii*, nuclei are clustered at the hyphal tip in the absence of dynein (in contrast to the appearance of the nuclear cluster at the spore end of the hyphae in other fungi), and this nuclear-clustering phenotype is completely suppressed by benomyl [44]. It has also been shown in *A. gossypii* that, in the absence of microtubules, other forces such as cytoplasmic streaming may carry the nuclei toward the hyphal tip [118]. Together, these results suggest that dynein function in interphase nuclear migration may be related to its effect on microtubule dynamics.

In filamentous hyphae, dynein is important for the retrograde movement of membranous cargoes during interphase (Fig. 17.5) [119–122], and dynein accumulation at the plus ends of cytoplasmic microtubules may facilitate motor–cargo interaction near the hyphal tip (Fig. 17.6) [98,122,123]. As first demonstrated in *U. maydis*, while kinesin-3 drives the movement of early endosomes towards microtubule plus ends, dynein, dynactin, and LIS1 (but not CLIP-170) are crucial for the retrograde transport of early endosomes [98]. At the

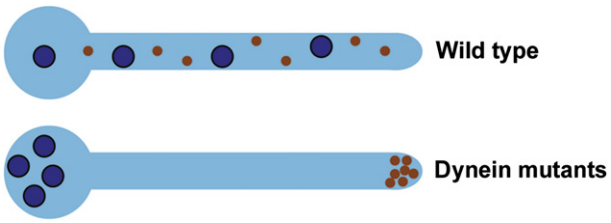

Figure 17.5 A diagram showing that, in filamentous fungi, dynein is not only important for nuclear distribution but also essential for the retrograde movement of early endosomes [98,121,122]. In the absence of dynein function, nuclei (blue circle) abnormally accumulate at the spore end and early endosomes (brown circles) abnormally accumulate at the hyphal tip.

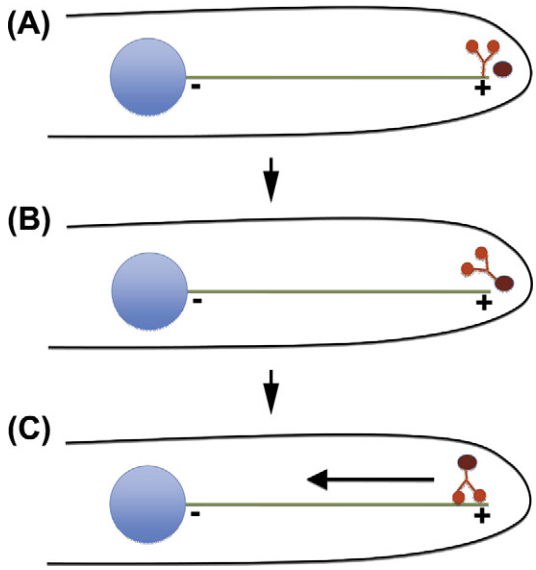

Figure 17.6 A model illustrating the role of microtubule-plus-end dynein in the retrograde transport of vesicles inside a filamentous hypha. For simplicity, only one dynein molecule is depicted at the plus end. (A) Dynein is located at the dynamic plus end of a cytoplasmic microtubule that may search and capture the vesicle; for example, an early endosome (brown circle). In this diagram, the dynein tail is attached to the microtubule, which reflects a possible configuration in which dynein is not able to leave the plus end as a minus-end-directed motor. (B) Dynein binds to the early endosome when the motor and the cargo encounter each other. (C) Dynein moves towards the microtubule minus end, carrying the early endosome as a load.

hyphal tip region of *U. maydis*, most (about 75%) of the dynein-driven early endosome movements start at the microtubule plus ends and, thus, the microtubule plus end has been considered as a "dynein-loading zone" [98]. In *A. nidulans*, the main site of endocytosis is located at a collar behind the hyphal apex [124–126], which is close to the microtubule plus ends facing the hyphal tip. Endocytic vesicles formed at other regions of the hyphae may need to be transported to the plus ends before they can undergo dynein-mediated minus-end-directed transport [122]. In *U. maydis* and *A. nidulans*, a deficiency in dynein function causes early endosomes to accumulate abnormally at the hyphal tip [98,122,127]. In hyphae lacking kinesin-1, dynein fails to accumulate at the plus ends [97,98] and a buildup of early endosomes at the hyphal tip becomes obvious, similarly to what has been observed in dynein loss-of-function mutants [98,122,123,127]. Thus, the plus-end accumulation of dynein is important for the retrograde movement of early endosomes [98,122]. Dynein isolated from the kinesin-1 null cells has normal ATPase activity, suggesting that the plus-end accumulation of dynein is not a prerequisite for dynein ATPase activation [123].

Thus, loss of retrograde transport of early endosomes in the absence of kinesin-1 is most likely caused by a failure in motor–cargo interaction rather than in motor activation. While the chance of interaction between a dynein molecule along a microtubule and an early endosome is relatively low, the plus-end accumulation of dynein may significantly enhance the opportunity for dynein–cargo interaction.

17.5 Understanding The Functions of Various Components of the Dynein and Dynactin Complexes

17.5.1 Proteins in the Cytoplasmic Dynein Complex

Cytoplasmic dynein HC contains an N-terminal stem region (or tail) and a C-terminal motor unit containing six AAA (ATPase associated with a variety of cellular activities) domains that are organized into a ring-like structure [4,5,128]. The tail of HC is involved in dimerization, and also contains binding sites for the ICs and LICs [4]. The IC directly binds the p150 subunit of the dynactin complex [6] and also contains binding sites for all three LCs: LC8, Tctex1, and LC7/Roadblock (Rob1) [4,129].

Functions of various non-HC dynein subunits have been studied by fungal genetics. In *A. nidulans*, the gene encoding LC8 was cloned as the *nudG* gene that complemented the ts *nudG*8 mutant, and this result demonstrates the function of LC8 in dynein-mediated nuclear distribution [130]. Interestingly, deletion of *nudG* does not apparently affect dynein function at lower temperatures but diminishes the microtubule plus-end localization of dynein and causes nuclear clustering at higher temperatures [31]. The more recently characterized Rob1 homolog RobA in *A. nidulans* is also important for nuclear distribution at a higher temperature [131]. However, the double null mutant of LC8 and RobA (Rob1 homolog) exhibits a severe nud phenotype at both lower and higher temperatures [131]. The Tctex1 LC in *A. nidulans* is not required for dynein-mediated nuclear migration [131]. In *S. pombe*, however, the Tctex1 homolog plays a role in dynein-mediated prophase movement of nuclei during meiosis and also in achiasmate segregation [50,132], and its effect on dynein localization has been observed [50]. Both the IC and the LIC are essential for dynein function in *A. nidulans* and *S. cerevisiae* [131,133,134]. In *A. nidulans*, both the IC and the LIC are important for the accumulation of the HC to microtubule plus ends [131,133], and the LIC is important for the interaction between the HC and the IC [131].

The motor property of the HC has been studied in *S. cerevisiae*, and these studies have had a great impact on our understanding of the dynein motor mechanism [111,135]. Dynein HC purified from *S. cerevisiae* walks along microtubules processively, and after each step the center mass of the motor moves forward about 8 nm (although occasionally a 16 nm or 24 nm step size is detected) [135].

Table 17.2 *In vivo* Functions of Dynein HC AAA domains in *S. cerevisiae and A. nidulans*

AAA domains	Dynein-Mediated Nuclear Positioning	Dynein-Mediated Early-Endosome Transport	Microtubule-Plus-End Accumulation of Dynein
AAA1			
ATP binding	Essential [136]	Essential [123]	Essential [123]
ATP hydrolysis	Essential [136]	Essential [123]	Not essential [123]
AAA2			
ATP binding	Not essential [136]		Not essential [96]
ATP hydrolysis	Not essential [136]		
AAA3			
ATP binding	Essential [136]		Not essential [105]
ATP hydrolysis	Essential [136]		
AAA4			
ATP binding	Not essential [136]		
ATP hydrolysis	Not essential [136]		

The conclusions are based on the effects of Walker A (p-loop) and Walker B mutations implicated in abolishing ATP binding and hydrolysis, respectively, based on analyses of other AAA ATPases [136]. HC-encoding DNA fragments containing point mutations [105,123,136] and a small deletion [96] were introduced into the genomes of *S. cerevisiae* [96,105,136] and *A. nidulans* [123] to replace the wild-type HC genes, followed by phenotypic analyses.

The ability to walk depends on the C-terminal motor domain plus the linker region immediately upstream of the motor domain, and also the formation of the HC dimer [135]. Purified dynein motors missing the HC N-terminal tail (or stem) region, if artificially linked to form dimers, are able to walk, and this ability to walk is independent of dynein regulators such as Pac1 (LIS1) and other dynein subunits such as the IC and the LIC [135]. In *S. cerevisiae*, functions of the Walker A (implicated in ATP binding) and Walker B (implicated in ATP hydrolysis) regions of the first four AAA domains have been analyzed (Table 17.2) [136]. Specifically, each mutant HC gene containing a Walker A mutation implicated in abolishing ATP binding, or a Walker B mutation implicated in abolishing ATP hydrolysis, is introduced into the genome to replace the endogenous HC gene via homologous recombination [136]. The results suggest that ATP binding and hydrolysis at the first and the third AAA domains are critical for dynein function in spindle positioning, while those of AAA2 and AAA4, despite being implicated in modulating dynein–microtubule interaction, are not critical for dynein-mediated spindle positioning [136]. Dynein HC containing a mutation that affects ATP hydrolysis at AAA3 is still able to walk processively along microtubules but with a significantly reduced velocity [137]. Interestingly, a mutation that affects ATP hydrolysis at AAA4 significantly increases motor processivity, which may be related to an increased affinity of the mutant dynein to microtubules [137].

Different domains of the HC are also studied to determine their functions in dynein localization *in vivo*. In *S. cerevisiae*, while the N-terminal tail domain binds to cortical sites more effectively than the full-length dynein HC, the C-terminal motor domain is sufficient for microtubule plus-end accumulation of dynein,

most likely due to its interaction with Pac1/LIS1 [105]. An small deletion of the AAA2 P-loop involved in ATP binding results in a non-functional HC that still localizes to the plus ends, suggesting that the plus-end accumulation does not need the full function of the dynein motor [96]. Similarly, HC with the AAA3 Walker A mutation (implicated in ATP binding) also localizes to the plus ends [105]. It is intriguing that, although the AAA3 Walker A mutation prevents dynein from being released from microtubules with ATP [136], it does not cause dynein to localize along microtubules like a rigor mutant [105]. In *A. nidulans*, while HC with the AAA1 Walker B mutation affecting ATP hydrolysis still accumulates at the plus ends, the Walker A mutation implicated in abolishing ATP binding causes dynein to localize along microtubules [123]. Since AAA1 is the major ATP hydrolyzing site [138,139], this result indicates that the ATPase activity of dynein is not required for its plus-end localization. Interestingly, *nudA*^{R3086C}, a missense mutation of an arginine residue of AAA4, which represents an arginine finger (P. Höök and R.B. Vallee, personal communication), decreases HC's plus-end accumulation and enhances its localization along microtubules [140]. This mutation partially suppresses the nuclear-distribution defect of the *nudF* (LIS1) null mutant [140], and the mechanism of suppression remains an interesting topic to be investigated.

17.5.2 Proteins of the Dynactin Complex

The dynactin complex was initially discovered as a complex required for *in vitro* vesicle transport by dynein [6]. Within the dynactin complex, the Arp1 (actin-related protein 1) subunit forms an actin-like mini-filament of 37 nm that is implicated in binding to membranous cargoes [6]. One end of the Arp1 filament is associated with a barbed-end capping protein and the other end binds to the pointed-end complex that contains Arp11, p62, p25, and p27 [6]. The p150^{Glued} subunit (called p150 for simplicity), together with p50 (dynamitin) and p24, constitute a shoulder-sidearm complex. As first demonstrated in *N. crassa* and *S. cerevisiae*, the Arp1 subunit, which forms the backbone of the dynactin complex, is important for dynein-mediated nuclear migration/spindle orientation in fungi [28,141–143], thus implicating the dynactin complex in this biological process *in vivo*. In both *N. crassa* and *A. nidulans*, deletion or downregulation of the Arp1-encoding gene results in a significant decrease in the protein level of p150 [72,144], although this does not seem to be the case in *S. cerevisiae* [99,145]. It seems likely that the presence of Arp1 may positively influence the folding/stability of p150 in some cell types.

Fungal genetic studies have provided insights into the functions of different domains of p150. In *N. crassa*, an analysis of a *ro*-3 (p150) mutant suggests that the C-terminus of p150 negatively regulates the binding of dynein–dynactin to membranous organelles [146]. The mutant p150, which lacks the second coiled-coil domain and the C-terminal basic domain, enhances dynactin–membrane interaction. On the other hand, the recombinant protein of the C-terminal region

blocks dynactin–membrane binding in the cell extract [146]. While the exact mechanism of this regulation remains an interesting issue to be addressed, it is possible that the C-terminus of p150 may physically block the interaction between the Arp1 filament and membranous cargoes [146]. Recently, functions of the N-terminus of p150 containing a microtubule-binding region have been studied. The microtubule-binding region contains the CAP-Gly (cytoskeleton-associated protein, glycine-rich) domain, which interacts with microtubules, and also a basic domain downstream of it, and *in vitro* data suggest that the basic domain allows dynactin to skate along microtubules whereas the CAP-Gly domain causes p150 to bind tightly to microtubules [147]. Purified dynactin from *S. cerevisiae* promotes the processivity of purified dynein, which is consistent with previous results [6,145]. However, the region of p150 required for this function involves the first coiled-coil domain rather than the N-terminal microtubule-binding region [145]. In addition, p150 isolated from an Arp1 deletion mutant is not able to promote processivity of dynein *in vitro* [145]. Thus, the effect of p150 on dynein processivity may be related to mechanisms other than a microtubule-tethering function provided by the microtubule-binding region [145]. Whether this N-terminal microtubule-binding region influences the *in vivo* functions of dynein becomes an interesting topic in the field. In *Drosophila* S2 cells, a construct containing a deletion of the N-terminal microtubule-binding domain (MTBD) rescues the vesicle transport defect caused by p150 RNA interference (RNAi), suggesting that the microtubule-binding region is not required for the processive movement of membranous organelles [148]. A similar result obtained by analyzing a p150 isoform that misses the N-terminal CAP-Gly and basic microtubule-binding region in Hela cells is consistent with this notion [149]. Recently, the function of the p150 microtubule-binding region in *S. cerevisiae* has been addressed by using a deletion mutant missing this region. Although a p150 null mutant is defective in anaphase spindle poisoning [150], p150 mutants specifically missing the CAP-Gly domain do not exhibit an obvious defect in anaphase spindle positioning [145,151]. However, by observing preanaphase spindle movement in the *kar9* null mutant, a role of this domain in the initial movement of the nucleus into the bud neck has been revealed [151]. As mentioned earlier, the Kar9 pathway helps to position the nucleus near the bud neck before anaphase [19–23]. It has been found that preanaphase spindles undergo dynein-dependant back-and-forth movements across the bud neck, and the amplitudes of these oscillations increase dramatically upon loss of Kar9, indicating that Kar9 may restrain these dynein-dependent movements in order to keep the nucleus close to the neck [152]. Without the CAP-Gly domain, the percentage of preanaphase spindles that crossed the neck in the *kar9* null mutant was significantly decreased [151]. Further observations on the change of nuclear shape during these movements suggest that the defect caused by the CAP-Gly deletion is in the initial movement across the neck rather than the subsequent oscillations [151]. Since deletion of the CAP-Gly domain affects neither the speed nor the duration of dynein-dependant sliding of free microtubules along the

cortex, this domain is most likely only important for dynein function when the load is high [151].

Two proteins located on top of the Arp1 filament — p50 and p24 (the shoulder) — are also important for spindle orientation/nuclear migration [72,99,144, 153,154]. In *S. cerevisiae*, both p50 (Jnm1) and p24 are important for the association between Arp1 and p150 [99,150]. The presence of p50 is essential for the interaction between p150 and p24 [99]. The presence of p24 also enhances the interaction between p150 and p50 [99,154], but has little effect on the interaction between p50 and Arp1 [154]. In *N. crassa*, RO10 is the p24 homolog and, similar to Arp1, RO10/p24 is important for the stability of p150 [72].

In *N. crassa* and *A. nidulans*, functions of the pointed-end proteins such as Arp11 and p62 are important for nuclear distribution [39,144]. However, the function of the *S. cerevisiae* Arp11 homolog Arp10 is not critical for dynein-mediated spindle positioning in a wild-type background, and it only becomes critical in an Arp1 mutant background [155,156]. In *A. nidulans*, downregulation of Arp11 expression severely lowers the amount of Arp1 associated with p150 [144], suggesting that the Arp1 filament is shortened and/or the interaction between p150 and Arp1 is weakened in the absence of Arp11. This is similarly observed in *S. cerevisiae* [99], suggesting that the function of Arp11 in the integrity of the Arp1 filament is evolutionarily conserved, but the integrity of the intact Arp1 filament may be more crucial in filamentous fungi than in budding yeast. Arp11 and p62 in *A. nidulans* also appear to negatively regulate dynein—dynactin interaction [144]. Upon downregulation of the genes encoding Arp11 and p62, the association between p150 and the dynein complex is enhanced, which may possibly interfere with dynein motor function [144]. It is also important to note that the p25 protein at the pointed end is not required for nuclear migration but is important for vesicle transport in *N. crassa* [39]. Thus, p25 may be specifically required for targeting dynein—dynactin to membranous cargoes. However, biochemical studies from *N. crassa* suggest that the interaction between dynactin and the membrane is enhanced without p25 or other pointed-end proteins such as Arp11 and p62 [39]. Thus, the functions of these pointed-end proteins may be multi-fold and deserve to be studied in more detail.

17.6 Conclusions

Over the last twenty years, fungal genetic studies have made unique and important contributions to the understanding of dynein function and regulation. These studies have not only revealed the function of dynein in nuclear migration/spindle positioning but also linked several evolutionarily conserved regulators such as LIS1 and NudE/NudEL to dynein function. Fungal genetics combined with live-cell imaging have also led to a basic understanding of the function and mechanism of the microtubule plus-end accumulation of cytoplasmic dynein. In

addition, biochemical studies done in fungal organisms have provided insights not only into the dynein motor mechanism but also into the regulatory roles of proteins in the dynein pathway.

It is worth pointing out that fungal model organisms are in general very well suited for detailed biochemical characterization of the proteins involved in dynein function. Although fungal dynein participates in mitotic functions including spindle assembly and elongation [112,157–162], it is not essential for nuclear division in most fungal model organisms. While loss of dynein causes embryonic lethality in mice [163], dynein null mutations in major fungal model organisms are not lethal (with the exception of *U. maydis*, in which dynein and LIS1 are both required for cell survival [42,164]). Thus, null mutants or conditional null mutants in the dynein pathway can grow to allow biochemical characterization of the specific defects. With the available methods for purifying dynein and its regulators in fungi [135,140,144,165] and the relative easiness of creating gene deletion and specific mutations in the haploid fungal organisms, fungi will continue to serve as excellent model systems for detailed mechanistic studies of the proteins involved in the *in vivo* function of the dynein motor.

Finally, it should be pointed out that a lot more mechanistic details still need to be learned about how dynein is regulated to participate in the movement of nuclei/spindles and/or membranous organelles. The accumulation of dynein at the microtubule plus ends is important for these biological functions of dynein in fungi. At the microtubule plus ends, there are many other proteins – such as CLIP-170, EB1, and other motor proteins – that are important for regulating microtubule dynamics and may affect the interactions of microtubule plus ends with the cell cortex and/or membranous cargoes [100,166,167]. Thus, the biological role of dynein and its regulation at the plus end will need to be studied in such a context. While studies in budding yeast have provided insights into the mechanism of dynein-mediated spindle positioning, dynein-powered movements of membranous cargoes occur in filamentous fungi but not in budding yeast. Thus, filamentous fungi will need to be used for uncovering mechanisms that control membranous cargo transport, in particular how dynein molecules at the dynamic microtubule plus ends are targeted to membranous cargoes and how this process is regulated. Fungal genetic methods should be of great use to these studies. For example, well-designed genetic screens should lead to the discovery not only of molecules that physically link dynein to various membranous cargoes but also of those that regulate this process, and the available genomic information should facilitate both forward-genetic and reverse-genetic approaches.

Acknowledgments

I thank Peter Höök and Richard Vallee for communicating to me the results of their sequence analysis on arginine fingers of dynein HCs prior to publication, and Stephen M. King for

helpful suggestions. Research projects on *A. nidulans* dynein in the author's lab were supported by NIH (GM069527), CNP (Comprehensive Neuroscience Program)-DoD and a USUHS intramural grant.

References

[1] S. Karki, E.L. Holzbaur, Cytoplasmic dynein and dynactin in cell division and intracellular transport, Curr. Opin. Cell Biol. 11 (1999) 45–53.
[2] T. Soldati, M. Schliwa, Powering membrane traffic in endocytosis and recycling, Nat. Rev. Mol. Cell Biol. 7 (2006) 897–908.
[3] Y. Mao, D. Varma, R. Vallee, Emerging functions of force-producing kinetochore motors, Cell Cycle 9 (2010) 715–719.
[4] K.K. Pfister, P.R. Shah, H. Hummerich, A. Russ, J. Cotton, A.A. Annuar, S.M. King, E.M. Fisher, Genetic analysis of the cytoplasmic dynein subunit families, PLoS Genet. 2 (2006) e1.
[5] S.M. King, AAA domains and organization of the dynein motor unit, J. Cell Sci. 113 (Pt 14) (2000) 2521–2526.
[6] T.A. Schroer, Dynactin, Annu. Rev. Cell Dev. Biol. 20 (2004) 759–779.
[7] A. Wynshaw-Boris, Lissencephaly and LIS1: Insights into the molecular mechanisms of neuronal migration and development, Clin. Genet. 72 (2007) 296–304.
[8] N.R. Morris, Nuclear migration. From fungi to the mammalian brain, J. Cell Biol. 148 (2000) 1097–1101.
[9] R.J. McKenney, M. Vershinin, A. Kunwar, R.B. Vallee, S.P. Gross, LIS1 and NudE induce a persistent dynein force-producing state, Cell 141 304–314.
[10] G. Steinberg, Preparing the way: Fungal motors in microtubule organization, Trends Microbiol. 15 (2007) 14–21.
[11] J.K. Moore, M.D. Stuchell-Brereton, J.A. Cooper, Function of dynein in budding yeast: Mitotic spindle positioning in a polarized cell, Cell Motil. Cytoskeleton 66 (2009) 546–555.
[12] Y.Y. Li, E. Yeh, T. Hays, K. Bloom, Disruption of mitotic spindle orientation in a yeast dynein mutant, Proc. Natl. Acad. Sci. USA 90 (1993) 10096–10100.
[13] D. Eshel, L.A. Urrestarazu, S. Vissers, J.C. Jauniaux, J.C. van Vliet-Reedijk, R.J. Planta, I.R. Gibbons, Cytoplasmic dynein is required for normal nuclear segregation in yeast, Proc. Natl. Acad. Sci. USA 90 (1993) 11172–11176.
[14] M. Farkasovsky, H. Kuntzel, Cortical Num1p interacts with the dynein intermediate chain Pac11p and cytoplasmic microtubules in budding yeast, J. Cell Biol. 152 (2001) 251–262.
[15] N.R. Adames, J.A. Cooper, Microtubule interactions with the cell cortex causing nuclear movements in *Saccharomyces cerevisiae*, J. Cell Biol. 149 (2000) 863–874.
[16] R.A. Heil-Chapdelaine, J.R. Oberle, J.A. Cooper, The cortical protein Num1p is essential for dynein-dependent interactions of microtubules with the cortex, J. Cell Biol. 151 (2000) 1337–1344.
[17] X. Tang, J.J. Punch, W.L. Lee, A CAAX motif can compensate for the PH domain of Num1 for cortical dynein attachment, Cell Cycle 8 (2009) 3182–3190.
[18] E. Yeh, R.V. Skibbens, J.W. Cheng, E.D. Salmon, K. Bloom, Spindle dynamics and cell cycle regulation of dynein in the budding yeast, *Saccharomyces cerevisiae*, J. Cell Biol. 130 (1995) 687–700.
[19] R.K. Miller, M.D. Rose, Kar9p is a novel cortical protein required for cytoplasmic microtubule orientation in yeast, J. Cell Biol. 140 (1998) 377–390.
[20] H. Yin, D. Pruyne, T.C. Huffaker, A. Bretscher, Myosin V orientates the mitotic spindle in yeast, Nature 406 (2000) 1013–1015.
[21] D.L. Beach, J. Thibodeaux, P. Maddox, E. Yeh, K. Bloom, The role of the proteins Kar9 and Myo2 in orienting the mitotic spindle of budding yeast, Curr. Biol. 10 (2000) 1497–1506.

[22] E. Hwang, J. Kusch, Y. Barral, T.C. Huffaker, Spindle orientation in *Saccharomyces cerevisiae* depends on the transport of microtubule ends along polarized actin cables, J. Cell Biol. 161 (2003) 483–488.
[23] M.L. Gupta Jr., P. Carvalho, D.M. Roof, D. Pellman, Plus end-specific depolymerase activity of Kip3, a kinesin-8 protein, explains its role in positioning the yeast mitotic spindle, Nat. Cell Biol. 8 (2006) 913–923.
[24] J.K. Moore, S. D'Silva, R.K. Miller, The CLIP-170 homologue Bik1p promotes the phosphorylation and asymmetric localization of Kar9p, Mol. Biol. Cell 17 (2006) 178–191.
[25] R.K. Miller, S. D'Silva, J.K. Moore, H.V. Goodson, The CLIP-170 orthologue Bik1p and positioning the mitotic spindle in yeast, Curr. Top. Dev. Biol. 76 (2006) 49–87.
[26] N.R. Morris, Mitotic mutants of *Aspergillus nidulans*, Genet. Res. 26 (1975) 237–254.
[27] X. Xiang, S.M. Beckwith, N.R. Morris, Cytoplasmic dynein is involved in nuclear migration in *Aspergillus nidulans*, Proc. Natl. Acad. Sci. USA 91 (1994) 2100–2104.
[28] M. Plamann, P.F. Minke, J.H. Tinsley, K.S. Bruno, Cytoplasmic dynein and actin-related protein Arp1 are required for normal nuclear distribution in filamentous fungi, J. Cell Biol. 127 (1994) 139–149.
[29] A.H. Osmani, S.A. Osmani, N.R. Morris, The molecular cloning and identification of a gene product specifically required for nuclear movement in *Aspergillus nidulans*, J. Cell Biol. 111 (1990) 543–551.
[30] X. Xiang, A.H. Osmani, S.A. Osmani, M. Xin, N.R. Morris, NudF, a nuclear migration gene in *Aspergillus nidulans*, is similar to the human LIS-1 gene required for neuronal migration, Mol. Biol. Cell 6 (1995) 297–310.
[31] B. Liu, X. Xiang, Y.R. Lee, The requirement of the LC8 dynein light chain for nuclear migration and septum positioning is temperature dependent in *Aspergillus nidulans*, Mol. Microbiol. 47 (2003) 291–301.
[32] R. Fischer, W.E. Timberlake, *Aspergillus nidulans* apsA (anucleate primary sterigmata) encodes a coiled-coil protein required for nuclear positioning and completion of asexual development, J. Cell Biol. 128 (1995) 485–498.
[33] R. Suelmann, N. Sievers, R. Fischer, Nuclear traffic in fungal hyphae: *In vivo* study of nuclear migration and positioning in *Aspergillus nidulans*, Mol. Microbiol. 25 (1997) 757–769.
[34] T.D. Wolkow, S.D. Harris, J.E. Hamer, Cytokinesis in *Aspergillus nidulans* is controlled by cell size, nuclear positioning and mitosis, J. Cell Sci. 109 (Pt 8) (1996) 2179–2188.
[35] B. Liu, N.R. Morris, A spindle pole body-associated protein, SNAD, affects septation and conidiation in *Aspergillus nidulans*, Mol. Gen. Genet. 263 (2000) 375–387.
[36] J.M. Kim, C.J. Zeng, T. Nayak, R. Shao, A.C. Huang, B.R. Oakley, B. Liu, Timely septation requires SNAD-dependent spindle pole body localization of the septation initiation network components in the filamentous fungus *Aspergillus nidulans*, Mol. Biol. Cell 20 (2009) 2874–2884.
[37] O. Yarden, M. Plamann, D.J. Ebbole, C. Yanofsky, cot-1, a gene required for hyphal elongation in *Neurospora crassa*, encodes a protein kinase, EMBO J. 11 (1992) 2159–2166.
[38] J.H. Tinsley, P.F. Minke, K.S. Bruno, M. Plamann, p150Glued, the largest subunit of the dynactin complex, is nonessential in *Neurospora* but required for nuclear distribution, Mol. Biol. Cell 7 (1996) 731–742.
[39] I.H. Lee, S. Kumar, M. Plamann, Null mutants of the neurospora actin-related protein 1 pointed-end complex show distinct phenotypes, Mol. Biol. Cell 12 (2001) 2195–2206.
[40] S. Inoue, B.G. Turgeon, O.C. Yoder, J.R. Aist, Role of fungal dynein in hyphal growth, microtubule organization, spindle pole body motility and nuclear migration, J. Cell Sci. 111 (Pt 11) (1998) 1555–1566.
[41] J. Maruyama, H. Nakajima, K. Kitamoto, Novel role of cytoplasmic dynein motor in maintenance of the nuclear number in conidia through organized conidiation in *Aspergillus oryzae*, Biochem. Biophys. Res. Commun. 307 (2003) 900–906.

[42] A. Straube, W. Enard, A. Berner, R. Wedlich-Soldner, R. Kahmann, G. Steinberg, A split motor domain in a cytoplasmic dynein, EMBO J. 20 (2001) 5091–5100.
[43] A. Straube, I. Weber, G. Steinberg, A novel mechanism of nuclear envelope break-down in a fungus: Nuclear migration strips off the envelope, EMBO J. 24 (2005) 1674–1685.
[44] C. Alberti-Segui, F. Dietrich, R. Altmann-Johl, D. Hoepfner, P. Philippsen, Cytoplasmic dynein is required to oppose the force that moves nuclei towards the hyphal tip in the filamentous ascomycete *Ashbya gossypii*, J. Cell Sci. 114 (2001) 975–986.
[45] R. Martin, A. Walther, J. Wendland, Deletion of the dynein heavy-chain gene DYN1 leads to aberrant nuclear positioning and defective hyphal development in *Candida albicans*, Eukaryot. Cell 3 (2004) 1574–1588.
[46] K.R. Finley, K.J. Bouchonville, A. Quick, J. Berman, Dynein-dependent nuclear dynamics affect morphogenesis in *Candida albicans* by means of the Bub2p spindle checkpoint, J. Cell Sci. 121 (2008) 466–476.
[47] P. Gönczy, Mechanisms of spindle positioning: Focus on flies and worms, Trends Cell Biol. 12 (2002) 332–339.
[48] L.H. Tsai, J.G. Gleeson, Nucleokinesis in neuronal migration, Neuron 46 (2005) 383–388.
[49] A. Yamamoto, R.R. West, J.R. McIntosh, Y. Hiraoka, A cytoplasmic dynein heavy chain is required for oscillatory nuclear movement of meiotic prophase and efficient meiotic recombination in fission yeast, J. Cell Biol. 145 (1999) 1233–1249.
[50] F. Miki, K. Okazaki, M. Shimanuki, A. Yamamoto, Y. Hiraoka, O. Niwa, The 14-kDa dynein light chain-family protein Dlc1 is required for regular oscillatory nuclear movement and efficient recombination during meiotic prophase in fission yeast, Mol. Biol. Cell 13 (2002) 930–946.
[51] D.Q. Ding, A. Yamamoto, T. Haraguchi, Y. Hiraoka, Dynamics of homologous chromosome pairing during meiotic prophase in fission yeast, Dev. Cell 6 (2004) 329–341.
[52] S. Karki, E.L. Holzbaur, Affinity chromatography demonstrates a direct binding between cytoplasmic dynein and the dynactin complex, J. Biol. Chem. 270 (1995) 28806–28811.
[53] K.T. Vaughan, R.B. Vallee, Cytoplasmic dynein binds dynactin through a direct interaction between the intermediate chains and p150Glued, J. Cell Biol. 131 (1995) 1507–1516.
[54] S.J. King, T.A. Schroer, Dynactin increases the processivity of the cytoplasmic dynein motor, Nat. Cell Biol. 2 (2000) 20–24.
[55] Y.H. Chiu, N.R. Morris, Genetic and molecular analysis of a tRNA(Leu) missense suppressor of nudC3, a mutation that blocks nuclear migration in *Aspergillus nidulans*, Genetics 145 (1997) 707–714.
[56] Y.H. Chiu, X. Xiang, A.L. Dawe, N.R. Morris, Deletion of nudC, a nuclear migration gene of *Aspergillus nidulans*, causes morphological and cell wall abnormalities and is lethal, Mol. Biol. Cell 8 (1997) 1735–1749.
[57] A.L. Dawe, K.A. Caldwell, P.M. Harris, N.R. Morris, G.A. Caldwell, Evolutionarily conserved nuclear migration genes required for early embryonic development in *Caenorhabditis elegans*, Dev. Genes Evol. 211 (2001) 434–441.
[58] J.P. Aumais, S.N. Williams, W. Luo, M. Nishino, K.A. Caldwell, G.A. Caldwell, S.H. Lin, L.Y. Yu-Lee, Role for NudC, a dynein-associated nuclear movement protein, in mitosis and cytokinesis, J. Cell Sci. 116 (2003) 1991–2003.
[59] T. Zhou, W. Zimmerman, X. Liu, R.L. Erikson, A mammalian NudC-like protein essential for dynein stability and cell viability, Proc. Natl. Acad. Sci. USA 103 (2006) 9039–9044.
[60] L.M. Faircloth, P.F. Churchill, G.A. Caldwell, K.A. Caldwell, The microtubule-associated protein, NUD-1, exhibits chaperone activity *in vitro*, Cell Stress Chaperon. 14 (2009) 95–103.
[61] J. Riera, P.S. Lazo, The mammalian NudC-like genes: A family with functions other than regulating nuclear distribution, Cell Mol. Life Sci. 66 (2009) 2383–2390.

[62] M. Nishino, Y. Kurasawa, R. Evans, S.H. Lin, B.R. Brinkley, L.Y. Yu-Lee, NudC is required for Plk1 targeting to the kinetochore and chromosome congression, Curr. Biol. 16 (2006) 1414–1421.
[63] M. Yamada, S. Toba, T. Takitoh, Y. Yoshida, D. Mori, T. Nakamura, A.H. Iwane, T. Yanagida, H. Imai, L.Y. Yu-Lee, T. Schroer, A. Wynshaw-Boris, S. Hirotsune, mNUDC is required for plus-end-directed transport of cytoplasmic dynein and dynactins by kinesin-1, EMBO J. 29 (2010) 517–531.
[64] Y. Yang, X. Yan, Y. Cai, Y. Lu, J. Si, T. Zhou, NudC-like protein 2 regulates the LIS1/dynein pathway by stabilizing LIS1 with Hsp90, Proc. Natl. Acad. Sci. USA 107 (2010) 3499–3504.
[65] O. Reiner, R. Carrozzo, Y. Shen, M. Wehnert, F. Faustinella, W.B. Dobyns, C.T. Caskey, D.H. Ledbetter, Isolation of a Miller-Dieker lissencephaly gene containing G protein beta-subunit-like repeats, Nature 364 (1993) 717–721.
[66] W.B. Dobyns, O. Reiner, R. Carrozzo, D.H. Ledbetter, Lissencephaly. A human brain malformation associated with deletion of the LIS1 gene located at chromosome 17p13, Jama 270 (1993) 2838–2842.
[67] N.R. Morris, V.P. Efimov, X. Xiang, Nuclear migration, nucleokinesis and lissencephaly, Trends Cell Biol. 8 (1998) 467–470.
[68] D.A. Willins, B. Liu, X. Xiang, N.R. Morris, Mutations in the heavy chain of cytoplasmic dynein suppress the nudF nuclear migration mutation of *Aspergillus nidulans*, Mol. Gen. Genet. 255 (1997) 194–200.
[69] R.B. Vallee, J.W. Tsai, The cellular roles of the lissencephaly gene LIS1, and what they tell us about brain development, Genes Dev. 20 (2006) 1384–1393.
[70] L.B. Pedersen, P. Rompolas, S.T. Christensen, J.L. Rosenbaum, S.M. King, The lissencephaly protein Lis1 is present in motile mammalian cilia and requires outer arm dynein for targeting to *Chlamydomonas* flagella, J. Cell Sci. 120 (2007) 858–867.
[71] V.P. Efimov, N.R. Morris, The LIS1-related NUDF protein of *Aspergillus nidulans* interacts with the coiled-coil domain of the NUDE/RO11 protein, J. Cell Biol. 150 (2000) 681–688.
[72] P.F. Minke, I.H. Lee, J.H. Tinsley, K.S. Bruno, M. Plamann, *Neurospora crassa* ro-10 and ro-11 genes encode novel proteins required for nuclear distribution, Mol. Microbiol. 32 (1999) 1065–1076.
[73] V.P. Efimov, J. Zhang, X. Xiang, CLIP-170 homologue and NUDE play overlapping roles in NUDF localization in *Aspergillus nidulans*, Mol. Biol. Cell 17 (2006) 2021–2034.
[74] V.P. Efimov, Roles of NUDE and NUDF proteins of *Aspergillus nidulans*: Insights from intracellular localization and overexpression effects, Mol. Biol. Cell 14 (2003) 871–888.
[75] J.R. Geiser, E.J. Schott, T.J. Kingsbury, N.B. Cole, L.J. Totis, G. Bhattacharyya, L. He, M.A. Hoyt, *Saccharomyces cerevisiae* genes required in the absence of the CIN8-encoded spindle motor act in functionally diverse mitotic pathways, Mol. Biol. Cell 8 (1997) 1035–1050.
[76] J. Li, W.L. Lee, J.A. Cooper, NudEL targets dynein to microtubule ends through LIS1, Nat. Cell Biol. 7 (2005) 686–690.
[77] H. Arai, H. Koizumi, J. Aoki, K. Inoue, Platelet-activating factor acetylhydrolase (PAF-AH), J. Biochem. 131 (2002) 635–640.
[78] Y. Feng, C.A. Walsh, Mitotic spindle regulation by Nde1 controls cerebral cortical size, Neuron 44 (2004) 279–293.
[79] J. Guo, Z. Yang, W. Song, Q. Chen, F. Wang, Q. Zhang, X. Zhu, Nudel contributes to microtubule anchoring at the mother centriole and is involved in both dynein-dependent and -independent centrosomal protein assembly, Mol. Biol. Cell 17 (2006) 680–689.
[80] S.S. Kholmanskikh, H.B. Koeller, A. Wynshaw-Boris, T. Gomez, P.C. Letourneau, M.E. Ross, Calcium-dependent interaction of Lis1 with IQGAP1 and Cdc42 promotes neuronal motility, Nat. Neurosci. 9 (2006) 50–57.

[81] Y. Liang, W. Yu, Y. Li, Z. Yang, X. Yan, Q. Huang, X. Zhu, Nudel functions in membrane traffic mainly through association with Lis1 and cytoplasmic dynein, J. Cell Biol. 164 (2004) 557–566.
[82] Y. Liang, W. Yu, Y. Li, L. Yu, Q. Zhang, F. Wang, Z. Yang, J. Du, Q. Huang, X. Yao, X. Zhu, Nudel modulates kinetochore association and function of cytoplasmic dynein in M phase, Mol. Biol. Cell 18 (2007) 2656–2666.
[83] L. Ma, M.Y. Tsai, S. Wang, B. Lu, R. Chen, J.R. Iii, X. Zhu, Y. Zheng, Requirement for Nudel and dynein for assembly of the lamin B spindle matrix, Nat. Cell Biol. 11 (2009) 247–256.
[84] M.D. Nguyen, T. Shu, K. Sanada, R.C. Lariviere, H.C. Tseng, S.K. Park, J.P. Julien, L.H. Tsai, A NUDEL-dependent mechanism of neurofilament assembly regulates the integrity of CNS neurons, Nat. Cell. Biol. 6 (2004) 595–608.
[85] M. Rehberg, J. Kleylein-Sohn, J. Faix, T.H. Ho, I. Schulz, R. Graf, Dictyostelium LIS1 is a centrosomal protein required for microtubule/cell cortex interactions, nucleus/centrosome linkage, and actin dynamics, Mol. Biol. Cell 16 (2005). 2759-2571.
[86] Y. Shan, L. Yu, Y. Li, Y. Pan, Q. Zhang, F. Wang, J. Chen, X. Zhu, Nudel and FAK as antagonizing strength modulators of nascent adhesions through paxillin, PLoS Biol. 7 (2009) e1000116.
[87] Y. Shen, N. Li, S. Wu, Y. Zhou, Y. Shan, Q. Zhang, C. Ding, Q. Yuan, F. Zhao, R. Zeng, X. Zhu, Nudel binds Cdc42GAP to modulate Cdc42 activity at the leading edge of migrating cells, Dev. Cell 14 (2008) 342–353.
[88] T. Shu, R. Ayala, M.D. Nguyen, Z. Xie, J.G. Gleeson, L.H. Tsai, Ndel1 operates in a common pathway with LIS1 and cytoplasmic dynein to regulate cortical neuronal positioning, Neuron 44 (2004) 263–277.
[89] S.A. Stehman, Y. Chen, R.J. McKenney, R.B. Vallee, NudE and NudEL are required for mitotic progression and are involved in dynein recruitment to kinetochores, J. Cell Biol. 178 (2007) 583–594.
[90] C. Valetti, D.M. Wetzel, M. Schrader, M.J. Hasbani, S.R. Gill, T.E. Kreis, T.A. Schroer, Role of dynactin in endocytic traffic: effects of dynamitin overexpression and colocalization with CLIP-170, Mol. Biol. Cell 10 (1999) 4107–4120.
[91] K.T. Vaughan, S.H. Tynan, N.E. Faulkner, C.J. Echeverri, R.B. Vallee, Colocalization of cytoplasmic dynein with dynactin and CLIP-170 at microtubule distal ends, J. Cell Sci. 112 (Pt 10) (1999) 1437–1447.
[92] P.S. Vaughan, P. Miura, M. Henderson, B. Byrne, K.T. Vaughan, A role for regulated binding of p150(Glued) to microtubule plus ends in organelle transport, J. Cell Biol. 158 (2002) 305–319.
[93] X. Xiang, G. Han, D.A. Winkelmann, W. Zuo, N.R. Morris, Dynamics of cytoplasmic dynein in living cells and the effect of a mutation in the dynactin complex actin-related protein Arp1, Curr. Biol. 10 (2000) 603–606.
[94] G. Han, B. Liu, J. Zhang, W. Zuo, N.R. Morris, X. Xiang, The *Aspergillus* cytoplasmic dynein heavy chain and NUDF localize to microtubule ends and affect microtubule dynamics, Curr. Biol. 11 (2001) 719–724.
[95] W.L. Lee, J.R. Oberle, J.A. Cooper, The role of the lissencephaly protein Pac1 during nuclear migration in budding yeast, J. Cell Biol. 160 (2003) 355–364.
[96] B. Sheeman, P. Carvalho, I. Sagot, J. Geiser, D. Kho, M.A. Hoyt, D. Pellman, Determinants of *S. cerevisiae* dynein localization and activation: Implications for the mechanism of spindle positioning, Curr. Biol. 13 (2003) 364–372.
[97] J. Zhang, S. Li, R. Fischer, X. Xiang, Accumulation of cytoplasmic dynein and dynactin at microtubule plus ends in *Aspergillus nidulans* is kinesin dependent, Mol. Biol. Cell 14 (2003) 1479–1488.
[98] J.H. Lenz, I. Schuchardt, A. Straube, G. Steinberg, A dynein loading zone for retrograde endosome motility at microtubule plus-ends, EMBO J. 25 (2006) 2275–2286.

[99] J.K. Moore, J. Li, J.A. Cooper, Dynactin function in mitotic spindle positioning, Traffic 9 (2008) 510–527.
[100] P. Carvalho, J.S. Tirnauer, D. Pellman, Surfing on microtubule ends, Trends Cell Biol. 13 (2003) 229–237.
[101] P. Carvalho, M.L. Gupta Jr., M.A. Hoyt, D. Pellman, Cell cycle control of kinesin-mediated transport of Bik1 (CLIP-170) regulates microtubule stability and dynein activation, Dev. Cell 6 (2004) 815–829.
[102] F. Caudron, A. Andrieux, D. Job, C. Boscheron, A new role for kinesin-directed transport of Bik1p (CLIP-170) in *Saccharomyces cerevisiae*, J. Cell Sci. 121 (2008) 1506–1513.
[103] T. Niccoli, A. Yamashita, P. Nurse, M. Yamamoto, The p150-Glued Ssm4p regulates microtubular dynamics and nuclear movement in fission yeast, J. Cell Sci. 117 (2004) 5543–5556.
[104] J.B. Woodruff, D.G. Drubin, G. Barnes, Dynein-driven mitotic spindle positioning restricted to anaphase by She1p inhibition of dynactin recruitment, Mol. Biol. Cell 20 (2009) 3003–3011.
[105] S.M. Markus, J.J. Punch, W.L. Lee, Motor- and tail-dependent targeting of dynein to microtubule plus ends and the cell cortex, Curr. Biol. 19 (2009) 196–205.
[106] S. Grava, F. Schaerer, M. Faty, P. Philippsen, Y. Barral, Asymmetric recruitment of dynein to spindle poles and microtubules promotes proper spindle orientation in yeast, Dev. Cell 10 (2006) 425–439.
[107] K.E. Ross, O. Cohen-Fix, A role for the FEAR pathway in nuclear positioning during anaphase, Dev. Cell 6 (2004) 729–735.
[108] A. Yamashita, M. Yamamoto, Fission yeast Num1p is a cortical factor anchoring dynein and is essential for the horse-tail nuclear movement during meiotic prophase, Genetics 173 (2006) 1187–1196.
[109] T.T. Saito, D. Okuzaki, H. Nojima, Mcp5, a meiotic cell cortex protein, is required for nuclear movement mediated by dynein and microtubules in fission yeast, J. Cell Biol. 173 (2006) 27–33.
[110] S.K. Vogel, N. Pavin, N. Maghelli, F. Julicher, I.M. Tolic-Norrelykke, Self-organization of dynein motors generates meiotic nuclear oscillations, PLoS Biol. 7 (2009) e1000087.
[111] A. Gennerich, A.P. Carter, S.L. Reck-Peterson, R.D. Vale, Force-induced bidirectional stepping of cytoplasmic dynein, Cell 131 (2007) 952–965.
[112] G. Fink, I. Schuchardt, J. Colombelli, E. Stelzer, G. Steinberg, Dynein-mediated pulling forces drive rapid mitotic spindle elongation in *Ustilago maydis*, EMBO J. 25 (2006) 4897–4908.
[113] D. Veith, N. Scherr, V.P. Efimov, R. Fischer, Role of the spindle-pole-body protein ApsB and the cortex protein ApsA in microtubule organization and nuclear migration in *Aspergillus nidulans*, J. Cell Sci. 118 (2005) 3705–3716.
[114] J.L. Carminati, T. Stearns, Microtubules orient the mitotic spindle in yeast through dynein-dependent interactions with the cell cortex, J. Cell Biol. 138 (1997) 629–641.
[115] L. Adamikova, A. Straube, I. Schulz, G. Steinberg, Calcium signaling is involved in dynein-dependent microtubule organization, Mol. Biol. Cell 15 (2004) 1969–1980.
[116] B.R. Oakley, N.R. Morris, A beta-tubulin mutation in *Aspergillus nidulans* that blocks microtubule function without blocking assembly, Cell 24 (1981) 837–845.
[117] D.A. Willins, X. Xiang, N.R. Morris, An alpha tubulin mutation suppresses nuclear migration mutations in *Aspergillus nidulans*, Genetics 141 (1995) 1287–1298.
[118] C. Lang, S. Grava, T. van den Hoorn, R. Trimble, P. Philippsen, S.L. Jaspersen, Mobility, microtubule nucleation and structure of microtubule-organizing centers in multinucleated hyphae of *Ashbya gossypii*, Mol. Biol. Cell 21 (2010) 18–28.
[119] S. Seiler, M. Plamann, M. Schliwa, Kinesin and dynein mutants provide novel insights into the roles of vesicle traffic during cell morphogenesis in *Neurospora*, Curr. Biol. 9 (1999) 779–785.

[120] R. Wedlich-Soldner, I. Schulz, A. Straube, G. Steinberg, Dynein supports motility of endoplasmic reticulum in the fungus *Ustilago maydis*, Mol. Biol. Cell 13 (2002) 965–977.
[121] R. Wedlich-Soldner, A. Straube, M.W. Friedrich, G. Steinberg, A balance of KIF1A-like kinesin and dynein organizes early endosomes in the fungus *Ustilago maydis*, EMBO J. 21 (2002) 2946–2957.
[122] J.F. Abenza, A. Pantazopoulou, J.M. Rodriguez, A. Galindo, M.A. Peñalva, Long-distance movement of *Aspergillus nidulans* early endosomes on microtubule tracks, Traffic 10 (2009) 57–75.
[123] J. Zhang, L. Zhuang, Y. Lee, J.F. Abenza, M.A. Peñalva., X. Xiang, The microtubule-plus-end localization of *Aspergillus dynein* is important for dynein-early-endosome interaction but not for dynein ATPase activation, J. Cell Sci. 123 (2010) 3596–3604.
[124] N. Taheri-Talesh, T. Horio, L. Araujo-Bazan, X. Dou, E.A. Espeso, M.A. Peñalva, S.A. Osmani, B.R. Oakley, The tip growth apparatus of *Aspergillus nidulans*, Mol. Biol. Cell 19 (2008) 1439–1449.
[125] L. Araujo-Bazan, M.A. Peñalva, E.A. Espeso, Preferential localization of the endocytic internalization machinery to hyphal tips underlies polarization of the actin cytoskeleton in *Aspergillus nidulans*, Mol. Microbiol. 67 (2008) 891–905.
[126] S. Upadhyay, B.D. Shaw, The role of actin, fimbrin and endocytosis in growth of hyphae in *Aspergillus nidulans*, Mol. Microbiol. 68 (2008) 690–705.
[127] N. Zekert, R. Fischer, The *Aspergillus nidulans* kinesin-3 UncA motor moves vesicles along a subpopulation of microtubules, Mol. Biol. Cell 20 (2009) 673–684.
[128] A.J. Roberts, N. Numata, M.L. Walker, Y.S. Kato, B. Malkova, T. Kon, R. Ohkura, F. Arisaka, P.J. Knight, K. Sutoh, S.A. Burgess, AAA^{+} ring and linker swing mechanism in the dynein motor, Cell 136 (2009) 485–495.
[129] S.M. King, The dynein microtubule motor, Biochim. Biophys. Acta 1496 (2000) 60–75.
[130] S.M. Beckwith, C.H. Roghi, B. Liu, N. Ronald Morris, The "8-kD" cytoplasmic dynein light chain is required for nuclear migration and for dynein heavy chain localization in *Aspergillus nidulans*, J. Cell Biol. 143 (1998) 1239–1247.
[131] J. Zhang, S. Li, S. Musa, H. Zhou, X. Xiang, Dynein light intermediate chain in *Aspergillus nidulans* is essential for the interaction between heavy and intermediate chains, J. Biol. Chem. 284 (2009) 34760–34768.
[132] L. Davis, G.R. Smith, Dynein promotes achiasmate segregation in *Schizosaccharomyces pombe*, Genetics 170 (2005) 581–590.
[133] J. Zhang, G. Han, X. Xiang, Cytoplasmic dynein intermediate chain and heavy chain are dependent upon each other for microtubule end localization in *Aspergillus nidulans*, Mol. Microbiol. 44 (2002) 381–392.
[134] W.L. Lee, M.A. Kaiser, J.A. Cooper, The offloading model for dynein function: Differential function of motor subunits, J. Cell Biol. 168 (2005) 201–207.
[135] S.L. Reck-Peterson, A. Yildiz, A.P. Carter, A. Gennerich, N. Zhang, R.D. Vale, Single-molecule analysis of dynein processivity and stepping behavior, Cell 126 (2006) 335–348.
[136] S.L. Reck-Peterson, R.D. Vale, Molecular dissection of the roles of nucleotide binding and hydrolysis in dynein's AAA domains in *Saccharomyces cerevisiae*, Proc. Natl. Acad. Sci. USA 101 (2004) 1491–1495.
[137] C. Cho, S.L. Reck-Peterson, R.D. Vale, Regulatory ATPase sites of cytoplasmic dynein affect processivity and force generation, J. Biol. Chem. 283 (2008) 25839–25845.
[138] I.R. Gibbons, A. Lee-Eiford, G. Mocz, C.A. Phillipson, W.J. Tang, B.H. Gibbons, Photosensitized cleavage of dynein heavy chains. Cleavage at the "V1 site" by irradiation at 365 nm in the presence of ATP and vanadate, J. Biol. Chem. 262 (1987) 2780–2786.
[139] M.A. Gee, J.E. Heuser, R.B. Vallee, An extended microtubule-binding structure within the dynein motor domain, Nature 390 (1997) 636–639.

[140] L. Zhuang, J. Zhang, X. Xiang, Point mutations in the stem region and the fourth AAA domain of cytoplasmic dynein heavy chain partially suppress the phenotype of NUDF/LIS1 loss in *Aspergillus nidulans*, Genetics 175 (2007) 1185–1196.
[141] L. Muhua, T.S. Karpova, J.A. Cooper, A yeast actin-related protein homologous to that in vertebrate dynactin complex is important for spindle orientation and nuclear migration, Cell 78 (1994) 669–679.
[142] M.J. Robb, M.A. Wilson, P.J. Vierula, A fungal actin-related protein involved in nuclear migration, Mol. Gen. Genet. 247 (1995) 583–590.
[143] X. Xiang, W. Zuo, V.P. Efimov, N.R. Morris, Isolation of a new set of *Aspergillus nidulans* mutants defective in nuclear migration, Curr. Genet. 35 (1999) 626–630.
[144] J. Zhang, L. Wang, L. Zhuang, L. Huo, S. Musa, S. Li, X. Xiang, Arp11 affects dynein-dynactin interaction and is essential for dynein function in *Aspergillus nidulans*, Traffic 9 (2008) 1073–1087.
[145] J.R. Kardon, S.L. Reck-Peterson, R.D. Vale, Regulation of the processivity and intracellular localization of *Saccharomyces cerevisiae* dynein by dynactin, Proc. Natl. Acad. Sci. USA 106 (2009) 5669–5674.
[146] S. Kumar, Y. Zhou, M. Plamann, Dynactin–membrane interaction is regulated by the C-terminal domains of p150(Glued), EMBO Rep. 2 (2001) 939–944.
[147] T.L. Culver-Hanlon, S.A. Lex, A.D. Stephens, N.J. Quintyne, S.J. King, A microtubule-binding domain in dynactin increases dynein processivity by skating along microtubules, Nat. Cell. Biol. 8 (2006) 264–270.
[148] H. Kim, S.C. Ling, G.C. Rogers, C. Kural, P.R. Selvin, S.L. Rogers, V.I. Gelfand, Microtubule binding by dynactin is required for microtubule organization but not cargo transport, J. Cell Biol. 176 (2007) 641–651.
[149] R. Dixit, J.R. Levy, M. Tokito, L.A. Ligon, E.L. Holzbaur, Regulation of dynactin through the differential expression of p150Glued isoforms, J. Biol. Chem. 283 (2008) 33611–33619.
[150] J.A. Kahana, G. Schlenstedt, D.M. Evanchuk, J.R. Geiser, M.A. Hoyt, P.A. Silver, The yeast dynactin complex is involved in partitioning the mitotic spindle between mother and daughter cells during anaphase B, Mol. Biol. Cell 9 (1998) 1741–1756.
[151] J.K. Moore, D. Sept, J.A. Cooper, Neurodegeneration mutations in dynactin impair dynein-dependent nuclear migration, Proc. Natl. Acad. Sci. USA 106 (2009) 5147–5152.
[152] E. Yeh, C. Yang, E. Chin, P. Maddox, E.D. Salmon, D.J. Lew, K. Bloom, Dynamic positioning of mitotic spindles in yeast: Role of microtubule motors and cortical determinants, Mol. Biol. Cell 11 (2000) 3949–3961.
[153] J.N. McMillan, K. Tatchell, The JNM1 gene in the yeast *Saccharomyces cerevisiae* is required for nuclear migration and spindle orientation during the mitotic cell cycle, J. Cell Biol. 125 (1994) 143–158.
[154] I.A. Amaro, M. Costanzo, C. Boone, T.C. Huffaker, The *Saccharomyces cerevisiae* homolog of p24 is essential for maintaining the association of p150Glued with the dynactin complex, Genetics 178 (2008) 703–709.
[155] S.W. Clark, M.D. Rose, Alanine scanning of Arp1 delineates a putative binding site for Jnm1/dynamitin and Nip100/p150Glued, Mol. Biol. Cell 16 (2005) 3999–4012.
[156] S.W. Clark, M.D. Rose, Arp10p is a pointed-end-associated component of yeast dynactin, Mol. Biol. Cell 17 (2006) 738–748.
[157] W.S. Saunders, D. Koshland, D. Eshel, I.R. Gibbons, M.A. Hoyt, *Saccharomyces cerevisiae* kinesin- and dynein-related proteins required for anaphase chromosome segregation, J. Cell Biol. 128 (1995) 617–624.
[158] V.P. Efimov, N.R. Morris, A screen for dynein synthetic lethals in *Aspergillus nidulans* identifies spindle assembly checkpoint genes and other genes involved in mitosis, Genetics 149 (1998) 101–116.

[159] S. Li, C.E. Oakley, G. Chen, X. Han, B.R. Oakley, X. Xiang, Cytoplasmic dynein's mitotic spindle pole localization requires a functional anaphase-promoting complex, gamma-tubulin, and NUDF/LIS1 in *Aspergillus nidulans*, Mol. Biol. Cell 16 (2005) 3591–3605.
[160] E.L. Grishchuk, I.S. Spiridonov, J.R. McIntosh, Mitotic chromosome biorientation in fission yeast is enhanced by dynein and a minus-end-directed, kinesin-like protein, Mol. Biol. Cell 18 (2007) 2216–2225.
[161] T. Courtheoux, G. Gay, C. Reyes, S. Goldstone, Y. Gachet, S. Tournier, Dynein participates in chromosome segregation in fission yeast, Biol. Cell 99 (2007) 627–637.
[162] A. Gerson-Gurwitz, N. Movshovich, R. Avunie, V. Fridman, K. Moyal, B. Katz, M.A. Hoyt, L. Gheber, Mid-anaphase arrest in *S. cerevisiae* cells eliminated for the function of Cin8 and dynein, Cell Mol. Life Sci. 66 (2009) 301–313.
[163] A. Harada, Y. Takei, Y. Kanai, Y. Tanaka, S. Nonaka, N. Hirokawa, Golgi vesiculation and lysosome dispersion in cells lacking cytoplasmic dynein, J. Cell Biol. 141 (1998) 51–59.
[164] M. Valinluck, S. Ahlgren, M. Sawada, K. Locken, F. Banuett, Role of the nuclear migration protein Lis1 in cell morphogenesis in *Ustilago maydis*, Mycologia, 102 493–512.
[165] C. Ahn, N.R. Morris, Nudf, a fungal homolog of the human LIS1 protein, functions as a dimer *in vivo*, J. Biol. Chem. 276 (2001) 9903–9909.
[166] X. Wu, X. Xiang, J.A. Hammer 3rd, Motor proteins at the microtubule plus-end, Trends Cell Biol. 16 (2006) 135–143.
[167] A. Akhmanova, M.O. Steinmetz, Tracking the ends: A dynamic protein network controls the fate of microtubule tips, Nat. Rev. Mol. Cell Biol. 9 (2008) 309–322.

In this chapter

18

Genetic Insights into Mammalian Cytoplasmic Dynein Function Provided by Novel Mutations in the Mouse

Anna Kuta [1], *Majid Hafezparast* [2], *Giampietro Schiavo* [3], *Elizabeth M.C. Fisher* [1]

[1] *Department of Neurodegenerative Disease, Institute of Neurology, University College London, London, UK*
[2] *School of Life Sciences, University of Sussex, Brighton, UK*
[3] *Molecular Neuropathology Laboratory, Cancer Research, UK London Research Institute, London, UK*

18.1 Why, and How, We Work with Mice to Learn About Mammalian Genes such as the Dynein Subunits

The data streaming out of genome sequencing projects support what we already know to be true from evolutionary studies: all living things are related because we all have distant, or not so distant, common ancestors. Humans and mice are both placental mammals and we diverged from our last common ancestor about 74 million years ago. Our relatedness means we share similar genomes – approximately 99% of mouse genes have a homolog in the human genome [32] – as well as similar biochemistry and physiology. Therefore, we can study other organisms to learn about the evolutionary relationships of the dynein gene family [13,20,33] and about dynein function because generally, though with exceptions, what is biologically true for a mouse is true for a human and a rat, and vice versa.

In all work with living animals, there are huge ethical issues. Our ability to work with mice entails a general acceptance from society that some animal research is allowed if it can be justified medically and also a personal consideration of our individual stance on what is acceptable.

In genetic studies we often work with mutants in order to perturb the system and so learn about gene and protein function. For investigating cytoplasmic dynein in

Dyneins DOI: 10.1016/B978-0-12-382004-4.10018-4
Copyright © 2012 by Elsevier Inc. All rights reserved.

mammals, our organism of choice for study is the mouse. This is because we can genetically modify the mouse genome with a precision that is not yet possible for other mammals. Conversely, we can also investigate animals with novel, random mutations in their genomes, and this can give us unexpected insight into gene and protein function. We can put together an "allelic series" of mice that have different mutations within a single gene of interest, and use careful phenotypic analysis of these animals to give us information about protein function in the whole organism that would be impossible to glean from cell or tissue culture studies. This includes behavioral analysis of mutant mice. Furthermore, we have built up over 100 years of mouse genetic resources, such as inbred lines, transgenic strains, and knockout strains, and these resources do not exist for other laboratory mammals (yet) [24]. Finally, we can breed mutants together as a way of looking for interactions between different genes and proteins; sometimes this has given us unexpected insight into novel pathways in specific cell types.

The cytoplasmic dynein complex is made up of individual dynein proteins. We know comparatively little about these subunits and what they do in the complex. We know which genes encode the individual subunits [13,20,33], we know they have diverse patterns of expression (for example see [4,17,21,31]), and the array of different subunits and their different expression may indicate we have multiple motor complexes with specialized functions [19]. In addition, individual subunits can have roles outside the complex itself, as clearly demonstrated for the dynein light chain (LC) subunit DYNLT (Tctex1) [5,6]. Through working with mouse mutants with different dynein subunit mutations, we can slowly build up a detailed picture of dynein subunit function in the whole mammalian organism.

18.2 Approaches to Working with Mouse Mutants to Learn About Dynein Function

18.2.1 The Genotype-Driven Approach (Reverse Genetics)

The genotype-driven or "reverse-genetics" approach to working with mouse mutants and studying dynein function involves creating mice with specific mutations in individual genes of interest – in our case, the genes encoding cytoplasmic dynein subunits (Fig. 18.1). We can then assess the biology of the mouse in different systems – for example, the behaviour, physiology, cell biology, and biochemistry of individual tissues – to examine how a single mutation alters dynein function compared to the equivalent wild-type dynein subunit. This allows us to make a genotype–phenotype correlation and, for example, to assess the function of different domains within the protein.

There are many different ways of making a mouse with a mutation in an individual gene, and the technology that allows us to do this is being refined continuously. Genotype-driven mouse mutants fall into two broad groups.

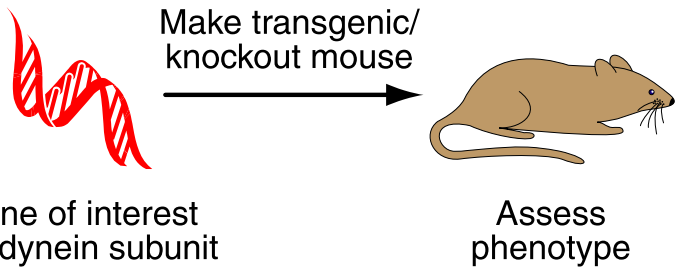

Figure 18.1 The genotype-driven or reverse genetics approach to understanding gene function, which starts with a known gene of interest.

(1) Transgenic animals. These mice carry an extra copy of the gene of interest (often a human gene) somewhere in the genome in addition to the endogenous genes. These mice overexpress the gene of interest because they carry more than the endogenous two copies of the gene. The pattern of expression of the transgene depends on the promoter in the transgene construct, which may or may not be the endogenous promoter of the gene. Transgenes may have the normal gene sequence or they may carry a mutant version of the gene of interest.

Transgene constructs insert randomly into the genome and they may disrupt endogenous genes. This feature of transgenes has been used in some projects to create "gene trap" mouse mutants, in which random endogenous genes are disrupted and then the site of insertion is ascertained. Most gene-trap mice have gene function knocked out.

(2) Gene-targeted animals. In these animals, the gene of interest may be knocked out or otherwise altered within the endogenous locus. A refinement on gene targeting is to create mice carrying conditional or inducible mutations. These allow expression of the gene of interest to be switched off or on by the use of carefully tailored genetic systems. This means that gene expression can be changed in individual cell types at specific times.

There are many other ways of targeting a gene of interest and creating a specific change to help answer a biological question. One other type of mouse is a knockin animal, in which a sequence of interest such as a novel protein domain is placed within the gene under investigation.

Transgenic and gene-targeted mice are powerful resources used by biologists to understand normal and mutant gene function. They can be precisely designed to change just a single nucleotide within the entire genome of a mouse or to switch off gene expression in one cell type, for example. As these types of mice have proven to be so important for biological and medical research, several large-scale programs have been set up to create gene-targeted mice with mutations in every known gene. Many of these mice are being made with conditional mutations so that the gene of interest may be deleted in a temporally or spatially controlled

manner. Current programs to generate gene-targeted animals include the European Conditional Mouse Mutagenesis Program (EUCOMM) (http://www.eucomm.org), the (Canadian) North American Conditional Mouse Mutagenesis Project (NorCOMM) (http://www.norcomm.org), the American Knockout Mouse Project (KOMP) (http://www.komp.org), and sites such as http://www.knockoutmouse.org, which are helpful for finding out whether a gene of interest has a knockout mouse available.

All these mouse resources, including transgenic animals, gene-trap mice, knockout mice, and conditional mutants, may be used to study the individual cytoplasmic dynein subunits and to tease out the interactions of these proteins. For example, Hirokawa and colleagues created a cytoplasmic dynein heavy chain (HC) knockout mouse and showed that a null mutation (i.e. no expression of the dynein HC) resulted in early embryonic death [12], demonstrating that this subunit is essential for embryonic development.

18.2.2 The Phenotype-Driven Approach (Forward Genetics)

The phenotype-driven or "forward-genetics" approach to studying mouse mutants entails starting with a mouse that has a phenotype of interest, such as problems with locomotion — the way it walks, for example — and then using standard molecular genetics techniques to identify the unknown mutant gene (Fig. 18.2). This approach makes no assumptions about the genes or pathways involved in the phenotype and can highlight previously unknown roles for well-known genes. For example, a mouse with a strange gait (the "Legs at odd angles" mouse) was found to have a mutation in the dynein HC gene [11] and (see Section 18.7.2) highlighted the role of this individual dynein subunit in the functioning of neurons in the motor and sensory systems of the body [3,11,14]. Forward-genetics approaches have been extensively exploited in yeast and other model systems but are perhaps less well known in mammals, although genes of clinical and other interest have been identified in mice, rats, pigs, and many other mammals.

There are only a few hundred spontaneously occurring mouse mutants known, and so one problem with the phenotype-driven approach was to find animals

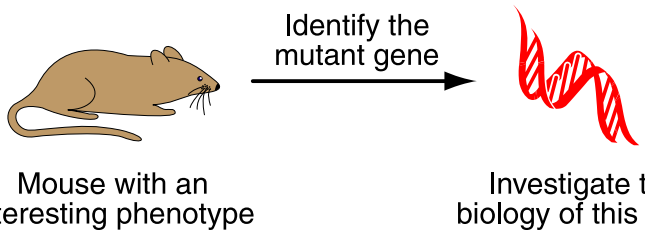

Figure 18.2 The phenotype-driven or forward genetics approach to understanding gene function, which starts with a mouse that has a phenotype of interest.

with phenotypes of interest. This meant making more mutant mice. There are several ways to do this, but one of the best ways is to use the powerful chemical mutagen ENU (*N*-ethyl-*N*-nitrosourea), which randomly mutates single nucleotides in the genome. Thus, mutant mice have minimal mutations at the DNA level, and, as ENU mutations are random, all transcribed and non-transcribed sequences may be affected – leading to coding, splice site, and many other changes in both conventional protein coding genes and other sequences such as microRNAs [1].

As the phenotype-driven approach is so powerful for informing us about the biology of phenotypes of interest, including medical phenotypes, and often shows us both novel genes and novel functions for known genes, ENU mutagenesis programs have been set up around the world to generate tens of thousands of new mice with random point mutations and phenotypes of interest to all areas of biological and medical research. The Legs at odd angles and Cramping 1 dynein HC mutant mouse strains came out of two such programs, one in the United Kingdom and one in Germany.

The ENU mutagenesis programs generate far too many mice to keep them alive in animal houses and so individual mouse mutant strains are frozen down by either embryo or sperm freezing. These frozen archives are also DNA archives so that they are also used for the genotype-driven approach: DNAs in the archive are screened for mutations in specific genes of interest, usually by some form of high-throughput mutation detection protocol. If a mutant DNA sample is found with a mutation in the gene of interest that can be confirmed by DNA sequencing, the strain is rederived from the frozen sample and then the potential phenotype of the mouse can be studied to gain new insight into protein function.

There are several other ways of generating mice with phenotypes of interest arising from random changes in the genome. One such approach is through mutagenesis with radiation. Although radiation may cause widespread damage to the DNA, such mice have a long history in biological and medical research, particularly after World War II and during the Cold War, when there was intense interest in the effects of radiation. The Sprawling mouse has locomotor deficits and came out of a radiation experiment in the early 1970s; the causative gene was identified in 2007 by Chen, Popko, and colleagues [3] and turned out to be the cytoplasmic dynein HC 1 (see Section 18.7.3).

18.3 Accessing Information About Mouse Mutants

There are many different databases and publications containing information about individual mouse mutants. In addition http://www.knockoutmouse.org, which is the place to look for mouse mutants available or being made by

international gene targeting projects, another excellent website is the Mouse Genome Informatics (MGI) website (http://www.informatics.jax.org). This well-curated site contains information about all mutants published in the literature or on the internet, regardless of the type of mutation. Searching MGI with a gene name results in a large amount of useful information about the gene, such as where it maps, what protein domains it encodes, what clones are available, and also what alleles of the gene are known in mice including knockout alleles, gene-trapped alleles, and chemically and radiation-induced mutant alleles. Some information is also given about mouse phenotypes resulting from these different alleles.

18.4 Genetic Background is Important

In studying mouse mutants it is important to be aware that the effects of all genes are modified by other genes – the genetic background – of the animal. These "modifiers" can encode proteins that lie within the same pathway or complex as the gene/protein of interest. This phenotype-modifying effect of genetic background is also found in the human population but is often more pronounced in mice, where we tend to work with inbred lines that have genetic backgrounds that are identical *within* the inbred line but can be quite disparate *between* inbred lines. In other words, a phenotype that occurs on one genetic background of mice, may look quite different or even disappear on a different inbred line.

18.5 Mouse Strains with Mutations in Cytoplasmic Dynein Subunits

The cytoplasmic dynein complex 1 consists of up to 11 different subunits (Table 18.1). Each subunit is encoded by a single gene, and these genes and the subunits they encode have an official abbreviation that is approved by the international committees that decide on mouse and human nomenclature. Prior to the standardization of the cytoplasmic dynein subunit names, the HC alone was referred to by 15 different names in the literature [21,22]. The new standardized abbreviation starts with "Dync1" for proteins thought to lie exclusively in the cytoplasmic dynein complex 1. The abbreviations for LCs, which are thought to be shared with other types of dynein complex, start with just "Dyn." Each subunit is then given a letter relating to its molecular weight: h for the HC, i for the intermediate chains (ICs), li for the light-intermediate chains (LICs), and l for the LCs. The three families of LCs are distinguished by the letters T, RB, and L, which refer to their original names in literature: the Tctex1 light chains, the Roadblock light chains, and the LC8 LCs [21,22].

Table 18.1 Mouse Cytoplasmic Dynein Subunits and Where they Map in the Mouse Genome

Gene Name	Official Gene Abbreviation	Chromosome	Maximum mRNA Length (Gene Accession Number)	Maximum Number of Exons	Protein Size (Protein Accession Number)
Cytoplasmic dynein 1 heavy chain 1	*Dync1h1*	12	14 398 nt (NM_030238)	77	4644 aa (NP_084514)
Cytoplasmic dynein 1 intermediate chain 1	*Dync1i1*	6	2 579 nt (NM_010063)	17	628 aa (NP_034193)
Cytoplasmic dynein 1 intermediate chain 2	*Dync1i2*	2	2 457 nt (NM_010064)	17	612 aa (NP_034194)
Cytoplasmic dynein 1 light-intermediate chain 1	*Dyncli1*	9	2 046 nt (NM_146229)	13	523 aa (NP_666341)
Cytoplasmic dynein 1 light-intermediate chain 2	*Dync1li2*	8	3 145 nt (NM_001013380)	13	492 aa (NP_001013398)
Cytoplasmic dynein Tctex light chain 1	*Dynlt1*	17[1]	791 nt (NM_009342)	5	113 aa (NP_033368)
Cytoplasmic dynein Tctex light chain 3	*Dynlt3*	X	2 154 nt (NM_025975)	5	116 aa (NP_080251)
Cytoplasmic dynein Roadblock light chain 1	*Dynlrb1*	2	643 nt (NM_025947)	4	96 aa (NP_080223)
Cytoplasmic dynein Roadblock light chain 2	*Dynlrb2*	8	515 nt (NM_029297)	4	96 aa (NP_083573)
Cytoplasmic dynein LC8 light chain 1	*Dynll1*	5	652 nt (NM_019682)	3	89 aa (NP_062656)
Cytoplasmic dynein LC8 light chain 2	*Dynll2*	11	2 441 nt (NM_026556)	3	89 aa (NP_080832)

[1] *This locus is now known to consist of six related genes.*

Information taken from the Mouse Genome Informatics website: http://www.informatics.jax.org, 2010. aa, amino acids; nt, nucleotide. accession numbers for mRNA and protein are shown in brackets.

A search of the Mouse Genome Informatics website reveals that most cytoplasmic dynein subunit-encoding genes have mutant alleles, and the vast majority of these are gene-trap alleles. However, very few mutant alleles have been analyzed for their phenotype in mice. Furthermore, to our knowledge there are no naturally occurring mutations in humans or mice that have been identified.

The only mammalian cytoplasmic dynein subunits for which mutations have been published are in mice, and are in (1) the gene encoding the dynein HC *Dync1h1*, (2) a transgenic mouse carrying a mutant *Dynll1* LC gene, and (3) the various "T-complex" mouse mutants carrying alleles of the cytoplasmic dynein Tctex1 LC

genes, *Dynlt1*, which are so complex they deserve an individual chapter to themselves (see Chapter 21).

Here we discuss *Dync1h1* mutant mice as a paradigm of what we can learn from an allelic series of mutations within the same gene. We look at how each mutation was made, the phenotypes, and what they tell us collectively about the function of the dynein HC DYNC1H1.

18.6 A Further Note on Nomenclature

The naming of both human and mouse genes and mutations is controlled by nomenclature committees for both organisms and is standardized so that each gene or mutation has a unique name that is the same in both organisms, and there is no room for confusion between different genes. The standard nomenclature for the dynein genes is as we use in this chapter [21,22]. The standard notation for mouse mutants was revised in 2006 and is available at http://www.informatics.jax.org/mgihome/nomen/gene.shtml.

If the gene is unidentified, the mutant mouse strain is given a name that tells us something about the mouse phenotype, such as "Legs at odd angles," "Cramping 1," and "Sprawling," and we use an italicised two-to-four-letter abbreviation (here "*Loa*," "*Cra1*," and "*Swl*," respectively).

Once the gene has been identified, the mutant mouse strain is named by giving the gene name (e.g. *Dync1h1*) followed immediately by the name of the mutation in superscript; for example, $Dync1h1^{Loa}$, $Dync1h1^{Cra1}$, and $Dync1h1^{Swl}$.

When we need to write about homozygous, heterozygous, or wild-type animals, we use the notation $Dync1h1^{Loa/Loa}$, $Dync1h1^{Loa/+}$, and $Dync1h1^{+/+}$, where $+$ represents the wild-type allele.

For gene-targeted mutations, such as the *Dync1h1* knockout mouse, the superscript starts with "tm" to denote that this is a targeted mutation, then there is a serial number from the laboratory that made the mouse, followed by a code for that laboratory – in this case the code is "Noh," denoting the laboratory of Professor Nobutaka Hirokawa, which made the HC knockout.

18.7 An Allelic Series of Mutations in the Mouse Cytoplasmic Dynein Heavy Chain Gene, *Dync1h1*

Here we will discuss a gene-targeted *Dync1h1* knockout mutation, two chemically induced mouse mutations, and a radiation-induced mouse mutation (Table 18.2).

Table 18.2 The Four Published Cytoplasmic Dynein Heavy Chain Mouse Mutants

Mouse Strain Name	Abbreviation	Mutation	References
Cytoplasmic dynein 1 heavy chain 1 knockout	*Dync1h1*^{tm1Noh}	Gene-targeted knockout	[12]
Legs at odd angles	*Dync1h1*^{Loa}	Point mutation causing a single amino acid change	[11]
Cramping 1	*Dync1h1*^{Cra1}	Point mutation causing a single amino acid change	[11]
Sprawling	*Dync1h1*^{Swl}	Deletion resulting in a coding change	[3]

18.7.1 A *Dync1h1* Gene-Targeted Knockout Mouse, *Dync1h1*^{tm1Noh}

The first mutation in *Dync1h1* in a mouse was produced by Hirokawa, Harada, and colleagues in Japan in 1998 [12]. These authors reported that heterozygous animals displayed no discernable abnormalities. They went on to interbreed heterozygous knockout animals to try to produce homozygous null mice; however, they found no homozygotes in the litters. A developmental analysis revealed that homozygous null embryos developed sufficiently to be implanted but died at embryonic day 8.5, at about a third of the way through gestation (which is approximately 21 days in a mouse). Interestingly, Hirokawa and colleagues detected low levels of *Dync1h1* mRNA in the null embryos (blastocysts), which they believe was due to maternal contribution.

Further analysis of cells in the null embryos at the blastocyst stage showed that their Golgi complex had an aberrant morphology and cellular distribution. The Golgi complex was highly fragmented and was distributed throughout the cytoplasm, whereas control wild-type cells had intact cisternae located around the nucleus. The Golgi complex was also smaller in mutant compared to wild-type cells. Endosomes and lysosomes also displayed abnormal peripheral localization at the edges of cells, rather than the perinuclear distribution seen in control cells. The dynactin complex was also abnormally distributed — in wild-type control cells it was found in punctuate structures near the centrosome, whereas in the null cells it was still localized to punctuate structures but these were distributed throughout the cytoplasm. In contrast, the localizations of the endoplasmic reticulum and mitochondria were similar in control and *Dync1h1* null cells. Thus, this interesting mouse mutant highlights that the maintenance of Golgi apparatus and the homeostasis of the endosomal pathway are both dependent on the presence of dynein HC 1 and, furthermore, having no functional copies of this gene results in early embryonic lethality [12].

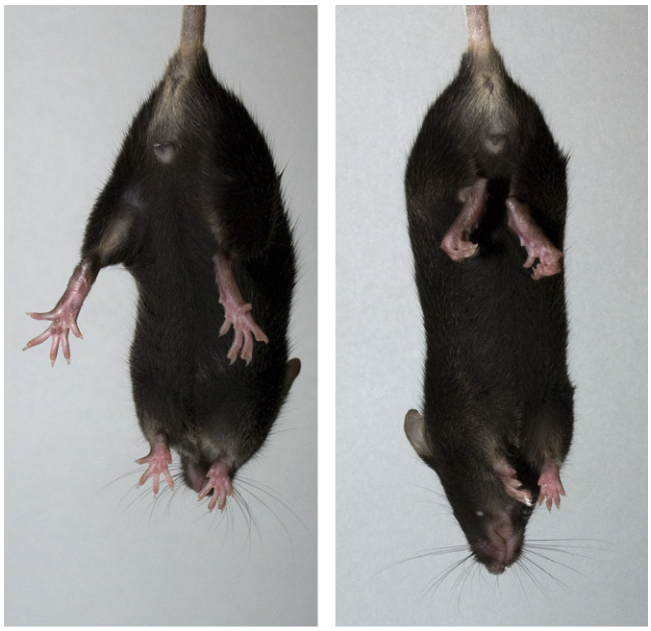

Figure 18.3 Photograph of two littermates suspended by the tail. The mouse on the left is a wild-type mouse and the mouse on the right is a *Dync1h1*^{Loa} heterozygous mouse. Note the different positions of the limbs in each mouse. The *Dync1h1*^{Loa} heterozygote is exhibiting the typical signs of a mouse with a neuromuscular deficit.

18.7.2 Analyzing Two Chemically Induced Mutations in *Dync1h1*

The identification of two chemically induced mutant alleles of *Dync1h1* came about from two separate phenotype-driven mouse genetics projects. Both projects were driven by groups with an interest in mice with movement deficits. One group working in London and at the UK Medical Research Council Mammalian Genetics Unit (MRC Harwell, near Oxford, UK) was analyzing a novel mouse strain called the "Legs at odd angles" (*Loa*) mouse. This mouse had been so named because when the animals were suspended by the tail for up to 30 s they clenched in their limbs, which is a generic sign of neuromuscular damage in mice (Fig. 18.3). The second group, working at Ingenium Pharmaceuticals near Munich in Germany, had independently identified a novel strain called the "Cramping 1" mouse (*Cra1*), which had a very similar phenotype. These groups started working together because a member of the German group spotted a poster from a member of the British group at a mouse genetics meeting in Scotland and realized that both teams were probably looking at alleles of

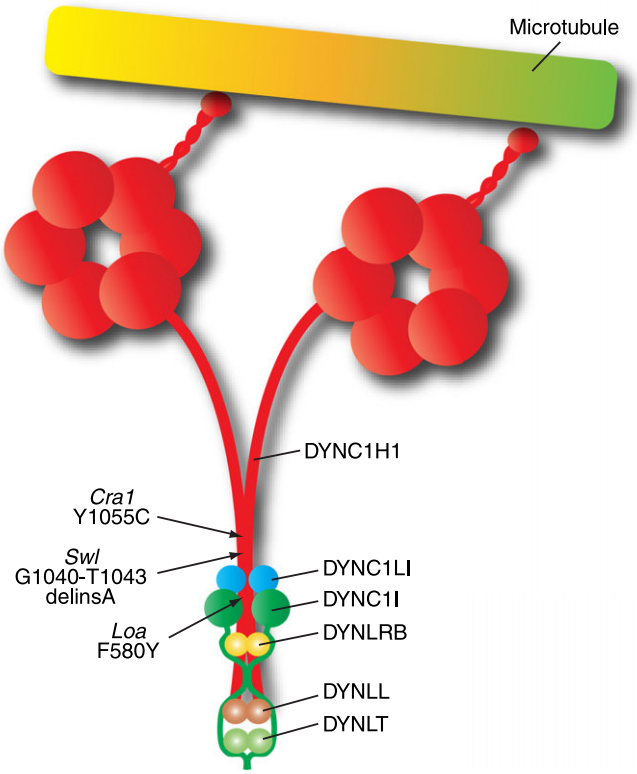

Figure 18.4 Schematic of where all the published heavy chain mutations lie within the dynein complex.

the same gene. This led to a cooperative effort to characterize both mouse models.

Both the *Loa* and *Cra1* strains had come out of chemical mutagenesis experiments with ENU at MRC Harwell and at the German ENU project, respectively. Thus, both groups knew that it was likely their mice each carried a single point mutation that was causing the abnormal phenotype, but they did not know which gene(s) was affected. The groups independently carried out standard genetic techniques to identify the mutant gene and, as expected, found single base pair mutations in what then turned out to be the dynein HC gene, *Dync1h1* [11].

The mutation in the *Dync1h1*^{Loa} mouse leads to a phenylalanine being changed to a tyrosine at amino acid 580 of the dynein HC, which lies within the overlapping HC homodimerisation and binding domains to dynein ICs [27] (Fig. 18.4). In the *Dync1h1*^{Cra1} mouse, the mutation results in a change at position 1055 from tyrosine to cysteine, which lies within the homodimerisation domain [27]. Both mouse strains have similar phenotypes but generally the *Dync1h1*^{Cra1} mutation is

more severe, although heterozygous *Dync1h1*^{Loa} and *Dync1h1*^{Cra1} animals live up to at least two years (an average lifespan in a laboratory mouse).

Characterising the phenotypes of these animals extended the work of Hirokawa and colleagues by showing that many systems were affected in these mice, which had relatively subtle mutations: just a single amino acid change in 0.5 MDa of dynein HC protein. However, both the *Dync1h1*^{Loa} and *Dync1h1*^{Cra1} animals also had abnormalities in Golgi complex distribution, highlighting the impact of Hirokawa's findings with the *Dync1h1* knockout animal. It is worth noting that, despite the number of phenotypes so far found in the *Dync1h1*^{Loa} and *Dync1h1*^{Cra1} mice, they have a normal lifespan and fertility.

As well as the limb grasping/clenching phenotype, heterozygous mutants have progressive movement deficits in that they often walk with a strange low-based reptilian-like gait, and the severity of this abnormal way of walking increases as the animals age. These gait abnormalities were originally reported to arise from a mild loss of motor neurons (the neurons that extend from the brain, through the spinal cord, and out to the muscles) in the spinal cord of both mice [11], but, as the *Dync1h1*^{Loa} mouse was subsequently found to have a severe loss of proprioceptors (sensory neurons that detect muscle length and tension within the body to provide information to the brain about where the limbs are), it is likely that the movement disorder in heterozygous animals is primarily a sensory deficit [3,14].

The situation in *Dync1h1*$^{Loa/Loa}$ and *Dync1h1*$^{Cra1/Cra1}$ homozygotes is markedly more severe. *Dync1h1*$^{Loa/Loa}$ homozygotes die in late gestation or at birth from unknown causes; newborns have an inability to feed or move. Both mutants have a pronounced loss of lower motor neurons (anterior horn cells) in the spinal cord, ranging from 50% loss in *Dync1h1*$^{Loa/Loa}$ homozygotes to 80% loss in *Dync1h1*$^{Cra1/Cra1}$ homozygotes when compared to wild-type littermates. Apoptosis was shown to be greatly enhanced in homozygous motor neurons in the anterior horn of the spinal cord from both mutants. Interestingly, these cells also contained inclusions that stained positive for ubiquitin, superoxide dismutase 1, CDK5, and neurofilaments, which are a combination of proteins known to be deposited in forms of the human neurodegenerative disease amyotrophic lateral sclerosis (ALS) – although neither the *Dync1h1*^{Loa} nor *Dync1h1*^{Cra1} mice constitute a model for human ALS, which is an aggressive lethal disorder in which motor neurons die and which generally occurs in mid-life [11].

The "housekeeping" functions of the dynein HC, highlighted by the knockout animal, were investigated. Abnormalities in the formation of the Golgi complex were revealed in stressed cells, but it seemed unlikely that these would account for the locomotor and neuronal phenotypes found in the mutant mice. An analysis of neuronal development in *Dync1h1*^{Loa} and *Dync1h1*^{Cra1} heterozygotes and homozygotes revealed abnormalities in facial motor neuron development. Branching and elongation of peripheral sensory nerves was also found to be

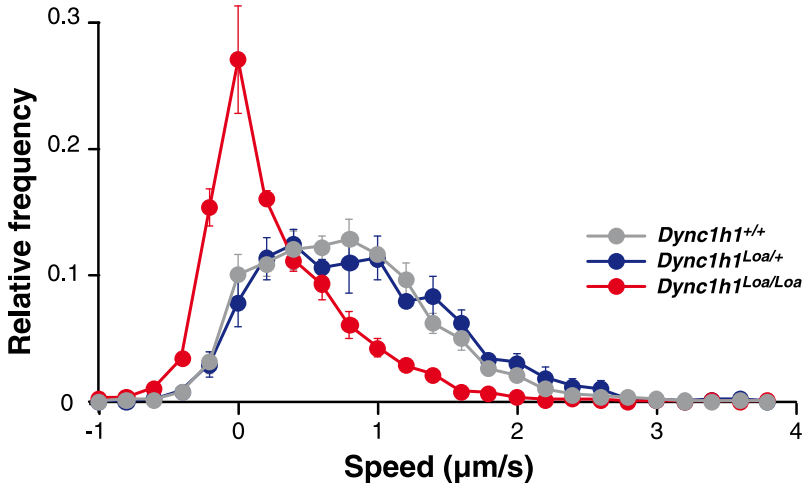

Figure 18.5 Axonal transport in embryonic motor neurons from wildtype, *Dync1h1*$^{Loa/+}$, and *Dync1h1*$^{Loa/Loa}$ mice.

impaired in the developing embryo, and, again, homozygotes were more badly affected than heterozygotes.

At the cellular level, an important question that needed to be addressed was "do the *Dync1h1*^{Loa} and *Dync1h1*^{Cra1} mutations affect axonal transport?," which is thought to be a primary role of cytoplasmic dynein in neurons. A kinetic analysis was undertaken of embryonic motor neurons from *Dync1h1*^{Loa} mice; it showed that heterozygous animals have rates of retrograde axonal transport similar to wild-type littermates (Fig. 18.5). However, the picture in homozygous *Dync1h1*$^{Loa/Loa}$ motor neurons is completely different: here, homozygous mutants have strikingly reduced rates of transport. This analysis has yet to be carried out in *Dync1h1*$^{Cra1/Cra1}$ homozygous mice, although the results are expected to be similar to *Dync1h1*$^{Loa/Loa}$ homozygotes.

To try to understand why the *Dync1h1*^{Loa} mutation gives rise to aberrant axonal transport, Deng, Hafezparast, and colleagues studied the assembly of the dynein complex and its interaction with dynactin [7]. They showed that the mutant dynein compromises the interaction of dynein LICs and ICs with the HC, which consequently impairs the interaction of dynactin with the dynein complex. This could explain the retrograde transport defect and neurodegeneration in the *Dync1h1*$^{Loa/Loa}$ homozygotes, as dynactin is essential for dynein processivity and for tethering cargo to dynein. Ore-McKenney, Vallee, and colleagues carried out a subsequent study using single-molecule and live-cell imaging to look at the processivity of this dynein [18]. They found the mutant dynein has an inhibition of motor run length and significantly altered motor domain coordination. Thus, these data have given new insight into the molecular functioning of dynein.

Thus, two relatively subtle point mutations in the *Dync1h1* gene, which do not involve the ATPase domains, revealed its critical functions within the nervous system and a variety of other tissues. It is still not clear whether aspects of this phenotype arise from a gain or loss of function of the dynein HC 1, whether parts of the phenotype arise from the entire cytoplasmic dynein working abnormally as a motor complex, or whether there are individual deficits that arise from specific functions of the HC alone. There is considerably more that the biology of these fascinating mutant mice can tell us about the cytoplasmic dynein complex and its individual components.

18.7.3 A Radiation-Induced Mutant of *Dync1h1*

A radiation-induced mutant mouse, the Sprawling mouse (*Swl*), was produced in the early 1970s at MRC Harwell and showed an early-onset sensory neuropathy with a loss of muscle spindles although a normal lifespan [8]. Thirty-three years later, Chen, Popko, and colleagues, working in Chicago, USA, identified the mutant gene in this mouse strain and found that the phenotype arose from a nine-base-pair deletion at residues 1040–1043 resulting in four amino acids (glycine, isoleucine, valine, and threonine) changing into a single alanine in the cargo-binding domain of the dynein HC protein [3].

Dync1h1$^{Swl/+}$ heterozygous animals are similar to *Dync1h1*$^{Loa/+}$ and *Dync1h1*-$^{Cra1/+}$ mutants in that they clench their limbs when suspended by the tail and have an abnormal gait and posture. In investigating this mutant, Chen, Popko, and co-authors compared it to the *Dync1h1*$^{Loa/+}$ mouse and showed, for the first time, a striking loss of proprioceptors in both mutants [3]. The H reflex, which is an electrophysiological measure of proprioceptor function, supported the histopathological findings, and the authors also showed that *Dync1h1*$^{Swl/+}$ heterozygotes have 88% fewer muscle spindles in the hindlimbs than their wild-type littermates. The proprioceptive defects almost certainly resulted from degeneration that occurred in the proprioceptive system, starting *in utero* in both *Dync1h1*$^{Swl/+}$ and *Dync1h1*$^{Loa/+}$. Subsequently, these findings for the *Dync1h1*^{Loa} mouse were confirmed by Ilieva, Cleveland, and colleagues [14]. Dupuis and colleagues then reported that *Dync1h1*$^{Cra1/+}$ mice also have similar proprioceptive losses but their neuromuscular junctions are normal and – in contrast to previous findings – there is no loss of motor neurons in these heterozygous animals [9]. Ilieva, Cleveland, and colleagues also reported a significant loss of γ motor neurons, which synapse onto the muscle spindles in skeletal muscle, in *Dync1h1*^{Loa} mice, but no loss of the large α motor neurons [14].

In contrast to the *Dync1h1*^{Loa} and *Dync1h1*^{Cra1} mutations, the *Dync1h1*^{Swl} phenotype is reported as not progressive and no significant loss of α motor neurons (large motor neurons) was found.

18.8 Overall Conclusions from the *Dync1h1* Mutant Mice

The four published *Dync1h1* mutant mice combine to tell us that the dynein HC is important for normal function of the Golgi apparatus, the endoplasmic reticulum, and the endocytic pathway. These mice have also shown us that this subunit has a specific role in the nervous system both during development and in ageing, and that sensory, proprioceptive, neurons are particularly dependent on the function of the HC. Why this should be remains a mystery. We assume that the main role of the HC in sensory neurons is axonal transport and that aberrations in retrograde trafficking of endosomes containing survival and differentiation signals lead to loss of proprioceptors. However, it remains formally possible that the dynein HC has independent functions in this type of neuron.

In addition, we are left with some interesting contradictions with respect to the motor phenotype of the heterozygous *Dync1h1*$^{Swl/+}$, *Dync1h1*$^{Loa/+}$, and *Dync1h1*$^{Cra1/+}$ mice – although it is possible, but unlikely, that genetic background may modify this mild phenotype and account for some of the differences found in different laboratories.

18.9 The MMTV-DLC^{S88A} Transgenic Mouse

Phosphorylation of serine 88 in dynein LC DYNLL1 (also known as LC8) has been shown to regulate DYNLL1 dimerisation [28] and its interaction with the proapoptotic protein BIM [22,28]. In 2008, Song, Kumar, and colleagues published a transgenic mouse strain, MMTV-DLC^{S88A}, that carries a transgene expressing a mutated form of the DYNLL1 under an MMTV (murine mammary tumor virus) promoter for expression of the transgene in the mammary glands [25]. The serine-to-alanine mutation at position 88 abolished the phosphorylation of this residue of the LC and caused a phenotype in the MMTV-DLC^{S88A} mouse line of increased apoptosis and involution in mammary glands, suggesting that serine 88 phosphorylation acts as a molecular switch for dimer–monomer transition and subsequently interaction with other proteins [25].

18.10 Using Mouse Genetics to Further Unravel the Role of the Cytoplasmic Dynein Heavy Chain

Mouse mutants have given and will continue to give novel insight into the role of cytoplasmic dynein, insights that would have been impossible to gain from *in vitro*

studies. In addition, one aspect of working with genetic mouse models that can give information about the interactions of proteins of interest is to cross different mouse strains and analyze the phenotype of the resulting progeny. In 2005, heterozygous *Dync1h1*$^{Loa/+}$ mice were crossed with the SOD1^{G93A} transgenic mice [16]. The latter strain (TgSOD1^{G93A}) carries a human transgene array of a mutant superoxide dismutase 1 gene, which is causative for ALS in both humans and mice. TgSOD1^{G93A} mice typically die at about 125 days of age (depending on genetic background) from motor neuron loss and with pathophysiological symptoms resembling ALS in humans.

Somewhat surprisingly, the double mutant progeny that carried the human transgene array and the *Loa* mutation in *Dync1h1* lived for 28% longer than their TgSOD1^{G93A} littermates or parents. The double mutants had a delay in disease onset and death, although a similar time course of disease. Axonal transport was analysed in embryonic motor neurons derived from progeny of the cross, using a fluorescently labeled fragment of the tetanus toxin. This showed two surprising results: axonal retrograde transport in TgSOD1^{G93A} was delayed compared to wild-type and *Dync1h1*$^{Loa/+}$ littermates, whereas it was faster in the TgSOD1^{G93A}–*Dync1h1*$^{Loa/+}$ double mutants [16]. This result may indicate an unexpected interaction, either direct or indirect, between Dync1h1 and mutant (and possibly wild-type) SOD1 [10,34].

The extension of lifespan in TgSOD1^{G93A}–*Dync1h1*$^{Loa/+}$ double mutants was also shown by two other groups: Chen, Popko, and colleagues, who found a 21% increase in the lifespan of these mice compared to TgSOD1^{G93A} littermates [3]; and Ilieva, Cleveland, and colleagues, who reported a 9% increase [14]. The latter group crossed their *Dync1h1*$^{Loa/+}$ mice with two other transgenic animals with different mutations in SOD1 that also give models of ALS; they found no ameliorating effect of the dynein subunit mutation, which they suggest may reflect a difference in SOD1 protein levels in the transgenics.

Interestingly, Teuchert and colleagues reported that TgSOD1^{G93A}–*Dync1h1*$^{Cra1/+}$ double mutants also have a delayed disease onset compared to TgSOD1^{G93A} littermates [26], but this effect is not seen in TgSOD1^{G93A}–*Dync1h1*$^{Swl/+}$ double mutants [3], indicating that different members of this dynein subunit allelic series may well have different interactions. This also highlights the use of having an allelic series of mutants for helping to tease out protein–protein interactions that take place in different domains.

New research indicates that the role of the dynein HC mutation in ameliorating the effect of the TgSOD1^{G93A} transgene may lie in a surprising alteration in mitochondrial function that is found in the *Dync1h1*$^{Loa/+}$ and TgSOD1^{G93A}–*Dync1h1*$^{Loa/+}$ double mutant mice [10]. Morsi El-Kadi, Hafezparast, and colleagues have shown that in the double mutants the *Dync1h1*^{Loa} mutation leads to a significant reduction in the amount of toxic SOD1^{G93A} protein in the mitochondrial matrix, resulting in amelioration of the defects in mitochondrial

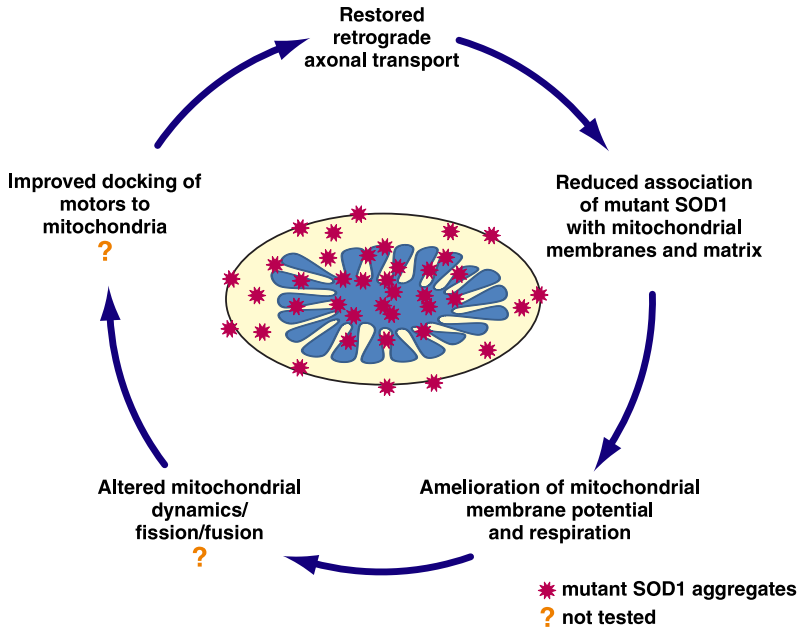

Figure 18.6 Effects of the *Dync1h1*^{Loa} mutation on the TgSOD1^{G93A} mouse phenotype. mSOD1, mutant SOD1; ●, mSOD1 aggregates; ?, not tested yet.

membrane potential and respiration. The precise mechanism by which mutant dynein affects the differential deposition of SOD1^{G93A} in the double mutants and its role in ameliorating mitochondrial function is not understood yet. But, taking into account the role of dynein in mitochondrial transport and possibly mitochondrial fission [30], it is likely that the *Dync1h1*^{Loa} mutation improves the transport of mitochondria and that the improved transport could make them less prone to mutant SOD1 association, leading to ameliorated membrane potential and respiration and/or reducing the association of mutant SOD1 protein with the mitochondrial membranes via an as-yet-unknown mechanism; thus, the *Dync1h1*^{Loa} mutation could restore the docking of dynein (and kinesin) to the mitochondria to improve its transport (Fig. 18.6) [10,29].

The unexpected outcome of crossing the *Dync1h1*$^{Loa/+}$ and TgSOD1^{G93A} mice has prompted other crosses with the dynein HC subunit mutants. Ravikumar, Acevedo-Arozena, Rubinsztein, and colleagues crossed the *Dync1h1*$^{Loa/+}$ mouse with a mouse model of the neurodegenerative disorder Huntington's disease (*Hdh*$^{HD/+}$) [23]. They found that the Huntington's phenotype, including tremor onset, motor coordination, and muscle function, was enhanced in compound heterozygote animals. This effect likely resulted from effects of the dynein mutation on the autosome–lysosome fusion process – showing a potential novel role for the dynein HC subunit in this pathway.

In other mouse models of neurological disorders, the *Dync11h*$^{Loa/+}$ has had no effect on phenotype [2].

18.11 Conclusion

Mouse models with genetic mutations have outstanding potential in telling us about normal gene function. Although mutant mice of different sorts, mainly gene-trap mutants, are available for all the cytoplasmic dynein subunits, only mice with mutations in the dynein HC have so far been analysed. Of these, four mutations have been published and this allelic series shows different phenotypes even between the two strains of animals with point mutations. However, they all indicate that the cytoplasmic dynein HC is essential for life and is intimately involved with the correct functioning of the sensory nervous system. Thus, this protein has both a housekeeping and a more specialized role(s), although it is not clear whether it acts outside the dynein complex.

Other vertebrate systems such as zebrafish are being developed for the study of genetic mutation, and a zebrafish *Dync1h1* has recently been published that results in complete disruption of photoreceptor morphogenesis [15].

Acknowledgments

We thank Dr Zhe-Xi Luo of the Carnegie Museum of Natural History for helpful comments and Mr Ray Young for graphics. Our work is supported by grants from Cancer Research UK, the ENDOCYTE Research and Training Network funded by the European Union, the UK Medical Research Council, and the Wellcome Trust.

References

[1] A. Acevedo-Arozena, S. Wells, P. Potter, M. Kelly, R.D. Cox, S.D. Brown, ENU mutagenesis, a way forward to understand gene function, Annu. Rev. Genomics Hum. Genet. 9 (2008) 49–69.

[2] G.T. Banks, V. Bros-Facer, H.P. Williams, R. Chia, F. Achilli, J.B. Bryson, L. Greensmith, E.M. Fisher, Mutant glycyl-tRNA synthetase (Gars) ameliorates SOD1(G93A) motor neuron degeneration phenotype but has little affect on Loa dynein heavy chain mutant mice, PLoS One 4 (2009) e6218.

[3] X.J. Chen, E.N. Levedakou, K.J. Millen, R.L. Wollmann, B. Soliven, B. Popko, Proprioceptive sensory neuropathy in mice with a mutation in the cytoplasmic dynein heavy chain 1 gene, J. Neurosci. 27 (2007) 14515–14524.

[4] J.Z. Chuang, T.A. Milner, C.H. Sung, Subunit heterogeneity of cytoplasmic dynein: Differential expression of 14 kDa dynein light chains in rat hippocampus, J. Neurosci. 21 (2001) 5501–5512.

[5] J.Z. Chuang, T.Y. Yeh, F. Bollati, C. Conde, F. Canavosio, A. Caceres, C.H. Sung, The dynein light chain Tctex-1 has a dynein-independent role in actin remodeling during neurite outgrowth, Dev. Cell 9 (2005) 75–86.

[6] C. Conde, C. Arias, M. Robin, A. Li, M. Saito, J.Z. Chuang, A.C. Nairn, C.H. Sung, A. Caceres, Evidence for the involvement of Lfc and Tctex-1 in axon formation, J. Neurosci. 30 (2010) 6793–6800.
[7] W. Deng, C. Garrett, B. Dombert, V. Soura, G. Banks, E.M.C. Fisher, M.P. van der Brug, M. Hafezparast, Neurodegeneration mutation in cytoplasmic dynein alters its organisation and dynein-dynactin and dynein-kinesin interactions, J. Biol. Chem. 285 (2010) 39922–39934.
[8] L.W. Duchen, A dominant hereditary sensory disorder in the mouse with deficiency of muscle spindles: The mutant Sprawling, J. Physiol. 237 (1974) 10P–11P.
[9] L. Dupuis, A. Fergani, K.E. Braunstein, J. Eschbach, N. Holl, F. Rene, J.L. Gonzalez De Aguilar, B. Zoerner, B. Schwalenstocker, A.C. Ludolph, J.P. Loeffler, Mice with a mutation in the dynein heavy chain 1 gene display sensory neuropathy but lack motor neuron disease, Exp. Neurol. 215 (2009) 146–152.
[10] A.M. El Kadi, V. Bros-Facer, W. Deng, A. Philpott, E. Stoddart, G. Banks, G.S. Jackson, E.M. Fisher, M.R. Duchen, L. Greensmith, A.L. Moore, M. Hafezparast, The legs at odd angles (Loa) mutation in cytoplasmic dynein ameliorates mitochondrial function in SOD1G93A mouse model for motor neuron disease, J. Biol. Chem. 285 (2010) 18627–18639.
[11] M. Hafezparast, R. Klocke, C. Ruhrberg, A. Marquardt, A. Ahmad-Annuar, S. Bowen, G. Lalli, A.S. Witherden, H. Hummerich, S. Nicholson, P.J. Morgan, R. Oozageer, J.V. Priestley, S. Averill, V.R. King, S. Ball, J. Peters, T. Toda, A. Yamamoto, Y. Hiraoka, M. Augustin, D. Korthaus, S. Wattler, P. Wabnitz, C. Dickneite, S. Lampel, F. Boehme, G. Peraus, A. Popp, M. Rudelius, J. Schlegel, H. Fuchs, M.H. de Angelis, G. Schiavo, D.T. Shima, A.P. Russ, G. Stumm, J.E. Martin, E.M. Fisher, Mutations in dynein link motor neuron degeneration to defects in retrograde transport, Science 300 (2003) 808–812.
[12] A. Harada, Y. Takei, Y. Kanai, Y. Tanaka, S. Nonaka, N. Hirokawa, Golgi vesiculation and lysosome dispersion in cells lacking cytoplasmic dynein, J. Cell Biol. 141 (1998) 51–59.
[13] P. Hook, R.B. Vallee, The dynein family at a glance, J. Cell Sci. 119 (2006) 4369–4371.
[14] H.S. Ilieva, K. Yamanaka, S. Malkmus, O. Kakinohana, T. Yaksh, M. Marsala, D.W. Cleveland, Mutant dynein (Loa) triggers proprioceptive axon loss that extends survival only in the SOD1 ALS model with highest motor neuron death, Proc. Natl. Acad. Sci. USA 105 (2008) 12599–12604.
[15] C. Insinna, L.M. Baye, A. Amsterdam, J.C. Besharse, B.A. Link, Analysis of a zebrafish dync1h1 mutant reveals multiple functions for cytoplasmic dynein 1 during retinal photoreceptor development, Neural Dev. 5 (2010) 12.
[16] D. Kieran, M. Hafezparast, S. Bohnert, J.R.T. Dick, J. Martin, G. Schiavo, E.M.C. Fisher, L. Greensmith, A mutation in dynein rescues axonal transport defects and extends the lifespan of ALS mice, J. Cell Biol. 169 (2005) 561–567.
[17] A. Kuta, W. Deng, A. Morsi El-Kadi, G.T. Banks, M. Hafezparast, K.K. Pfister, E.M.C. Fisher, Mouse cytoplasmic dynein intermediate chains: Identification of new isoforms, alternative splicing and tissue distribution of transcripts, PLoS One 5 (2010) e11682.
[18] K.M. Ori-McKenney, J. Xu, S.P. Gross, R.B. Vallee, A cytoplasmic dynein tail mutation impairs motor processivity, Nat. Cell Biol. 12 (2010) 1228–1234.
[19] K.J. Palmer, H. Hughes, D.J. Stephens, Specificity of cytoplasmic dynein subunits in discrete membrane-trafficking steps, Mol. Biol. Cell 20 (2009) 2885–2899.
[20] K.K. Pfister, E.M. Fisher, I.R. Gibbons, T.S. Hays, E.L. Holzbaur, J.R. McIntosh, M.E. Porter, T.A. Schroer, K.T. Vaughan, G.B. Witman, S.M. King, R.B. Vallee, Cytoplasmic dynein nomenclature, J. Cell Biol. 171 (2005) 411–413.
[21] K.K. Pfister, P.R. Shah, H. Hummerich, A. Russ, J. Cotton, A.A. Annuar, S.M. King, E.M. Fisher, Genetic analysis of the cytoplasmic dynein subunit families, PLoS Genet. 2 (2006) e1.

[22] H. Puthalakath, D.C. Huang, L.A. O'Reilly, S.M. King, A. Strasser, The proapoptotic activity of the Bcl-2 family member Bim is regulated by interaction with the dynein motor complex, Mol. Cell 3 (1999) 287–296.
[23] B. Ravikumar, A. Acevedo-Arozena, S. Imarisio, Z. Berger, C. Vacher, C.J. O'Kane, S.D. Brown, D.C. Rubinsztein, Dynein mutations impair autophagic clearance of aggregate-prone proteins, Nat. Genet. 37 (2005) 771–776.
[24] L.M. Silver, Mouse genetics, Oxford University Press, Oxford, 1995.
[25] C. Song, W. Wen, S.K. Rayala, M. Chen, J. Ma, M. Zhang, R. Kumar, Serine 88 phosphorylation of the 8-kDa dynein light chain 1 is a molecular switch for its dimerization status and functions, J. Biol. Chem. 283 (2008) 4004–4013.
[26] M. Teuchert, D. Fischer, B. Schwalenstoecker, H.J. Habisch, T.M. Bockers, A.C. Ludolph, A dynein mutation attenuates motor neuron degeneration in SOD1(G93A) mice, Exp. Neurol. 198 (2006) 271–274.
[27] S.H. Tynan, M.A. Gee, R.B. Vallee, Distinct but overlapping sites within the cytoplasmic dynein heavy chain for dimerization and for intermediate chain and light intermediate chain binding, J. Biol. Chem. 275 (2000) 32769–32774.
[28] R.K. Vadlamudi, R. Bagheri-Yarmand, Z. Yang, S. Balasenthil, D. Nguyen, A.A. Sahin, P. den Hollander, R. Kumar, Dynein light chain 1, a p21-activated kinase 1-interacting substrate, promotes cancerous phenotypes, Cancer Cell 5 (2004) 575–585.
[29] V.C. Vande, T.M. Miller, N.R. Cashman, D.W. Cleveland, Selective association of misfolded ALS-linked mutant SOD1 with the cytoplasmic face of mitochondria, Proc. Natl. Acad. Sci. USA 105 (2008) 4022–4027.
[30] A. Varadi, L.I. Johnson-Cadwell, V. Cirulli, Y. Yoon, V.J. Allan, G.A. Rutter, Cytoplasmic dynein regulates the subcellular distribution of mitochondria by controlling the recruitment of the fission factor dynamin-related protein-1, J. Cell Sci. 117 (2004) 4389–4400.
[31] R.A. Wang, M. Zhao, M.L. Meistrich, R. Kumar, Stage-specific expression of dynein light chain-1 and its interacting kinase, p21-activated kinase-1, in rodent testes: Implications in spermiogenesis, J. Histochem. Cytochem. 53 (2005) 1235–1243.
[32] R.H. Waterston, K. Lindblad-Toh, E. Birney, J. Rogers, J.F. Abril, P. Agarwal, R. Agarwala, R. Ainscough, M. Alexandersson, P. An, S.E. Antonarakis, J. Attwood, R. Baertsch, J. Bailey, K. Barlow, S. Beck, E. Berry, B. Birren, T. Bloom, P. Bork, M. Botcherby, N. Bray, M.R. Brent, D.G. Brown, S.D. Brown, C. Bult, J. Burton, J. Butler, R.D. Campbell, P. Carninci, S. Cawley, F. Chiaromonte, A.T. Chinwalla, D.M. Church, M. Clamp, C. Clee, F.S. Collins, L.L. Cook, R.R. Copley, A. Coulson, O. Couronne, J. Cuff, V. Curwen, T. Cutts, M. Daly, R. David, J. Davies, K.D. Delehaunty, J. Deri, E.T. Dermitzakis, C. Dewey, N.J. Dickens, M. Diekhans, S. Dodge, I. Dubchak, D.M. Dunn, S.R. Eddy, L. Elnitski, R.D. Emes, P. Eswara, E. Eyras, A. Felsenfeld, G.A. Fewell, P. Flicek, K. Foley, W.N. Frankel, L.A. Fulton, R.S. Fulton, T.S. Furey, D. Gage, R.A. Gibbs, G. Glusman, S. Gnerre, N. Goldman, L. Goodstadt, D. Grafham, T.A. Graves, E.D. Green, S. Gregory, R. Guigo, M. Guyer, R.C. Hardison, D. Haussler, Y. Hayashizaki, L.W. Hillier, A. Hinrichs, W. Hlavina, T. Holzer, F. Hsu, A. Hua, T. Hubbard, A. Hunt, I. Jackson, D.B. Jaffe, L.S. Johnson, M. Jones, T.A. Jones, A. Joy, M. Kamal, E.K. Karlsson, D. Karolchik, A. Kasprzyk, J. Kawai, E. Keibler, C. Kells, W.J. Kent, A. Kirby, D.L. Kolbe, I. Korf, R.S. Kucherlapati, E.J. Kulbokas, D. Kulp, T. Landers, J.P. Leger, S. Leonard, I. Letunic, R. Levine, J. Li, M. Li, C. Lloyd, S. Lucas, B. Ma, D.R. Maglott, E.R. Mardis, L. Matthews, E. Mauceli, J.H. Mayer, M. McCarthy, W.R. McCombie, S. McLaren, K. McLay, J.D. McPherson, J. Meldrim, B. Meredith, J.P. Mesirov, W. Miller, T.L. Miner, E. Mongin, K.T. Montgomery, M. Morgan, R. Mott, J.C. Mullikin, D.M. Muzny, W.E. Nash, J.O. Nelson, M.N. Nhan, R. Nicol, Z. Ning, C. Nusbaum, M.J. O'Connor, Y. Okazaki, K. Oliver, E. Overton-Larty, L. Pachter, G. Parra, K.H. Pepin, J. Peterson, P. Pevzner, R. Plumb, C.S. Pohl, A. Poliakov, T.C. Ponce, C.P. Ponting, S. Potter, M. Quail, A. Reymond, B.A. Roe, K.M. Roskin, E.M. Rubin, A.G. Rust, R. Santos, V. Sapojnikov, B. Schultz, J. Schultz, M.S. Schwartz, S. Schwartz, C. Scott, S. Seaman, S. Searle, T. Sharpe,

A. Sheridan, R. Shownkeen, S. Sims, J.B. Singer, G. Slater, A. Smit, D.R. Smith, B. Spencer, A. Stabenau, N. Stange-Thomann, C. Sugnet, M. Suyama, G. Tesler, J. Thompson, D. Torrents, E. Trevaskis, J. Tromp, C. Ucla, A. Ureta-Vidal, J.P. Vinson, A.C. Von Niederhausern, C.M. Wade, M. Wall, R.J. Weber, R.B. Weiss, M.C. Wendl, A.P. West, K. Wetterstrand, R. Wheeler, S. Whelan, J. Wierzbowski, D. Willey, S. Williams, R.K. Wilson, E. Winter, K.C. Worley, D. Wyman, S. Yang, S.P. Yang, E.M. Zdobnov, M.C. Zody, E.S. Lander, Initial sequencing and comparative analysis of the mouse genome, Nature 420 (2002) 520–562.

[33] B. Wickstead, K. Gull, Dyneins across eukaryotes: A comparative genomic analysis, Traffic 8 (2007) 1708–1721.

[34] F. Zhang, A.L. Strom, K. Fukada, S. Lee, L.J. Hayward, H. Zhu, Interaction between familial amyotrophic lateral sclerosis (ALS)-linked SOD1 mutants and the dynein complex, J. Biol. Chem. 282 (2007) 16691–16699.

In this chapter

19

The Role of Dynactin in Dynein-Mediated Motility

Trina A. Schroer, Frances K.Y. Cheong
Department of Biology, Johns Hopkins University, Baltimore, MD, USA

19.1 Introduction

Dynactin is a multi-subunit complex that was first identified as a biochemical activity required for dynein-driven vesicle movement along microtubules *in vitro* [1,2]. It has since been found to be required for most types of dynein-based motility *in vivo*. Its best-understood functions involve transport of membrane-bound organelles toward microtubule minus ends [3–8]. Dynein and dynactin also play essential roles in mitotic processes, including transport of checkpoint proteins from kinetochores to spindle poles, spindle pole organization, and chromosome movement [9–19].

A thorough understanding of dynactin's composition and subunit organization has been gained through a combination of biochemical, ultrastructural, and molecular cloning work (reviewed in [20]). Genetic studies in budding yeast, filamentous fungi, *Drosophila melanogaster*, and *Caenorhabditis elegans* have firmly established that dynactin is an essential part of the cytoplasmic dynein motor [21–30]. In *Drosophila*, the "rough eye" phenotype caused by a mutation in the dynactin subunit *Glued* ($p150^{Glued}$) gene can be suppressed or enhanced by mutations in dynein heavy chain (HC) [22]. In the filamentous fungus *Neurospora crassa*, the same nuclear clumping defects and inhibition of nuclear migration that yield a so-called "ropy" phenotype are seen in null mutations of dynein HC (*ro-1*), dynactin $p150^{Glued}$ (*ro-3*), and other dynein and dynactin subunits [25,28,30]. Nuclear migration defects are also seen in *Aspergillus nidulans* (another filamentous fungus) cells bearing cytoplasmic dynein and dynactin mutations (the nuclear distribution, or *nud* mutants) [29]. In the budding yeast *Saccharomyces cerevisiae*, dynein and dynactin act together at the cortex to pull the nucleus from the mother cell into the bud during mitosis [24,31].

19.2 Structure and Composition of Dynactin

Unlike cytoplasmic dynein, which is an identically symmetric complex consisting of pairs of HCs, intermediate chains (ICs), light-intermediate chains (LICs), and

Dyneins DOI: 10.1016/B978-0-12-382004-4.10019-6
Copyright © 2012 by Elsevier Inc. All rights reserved.

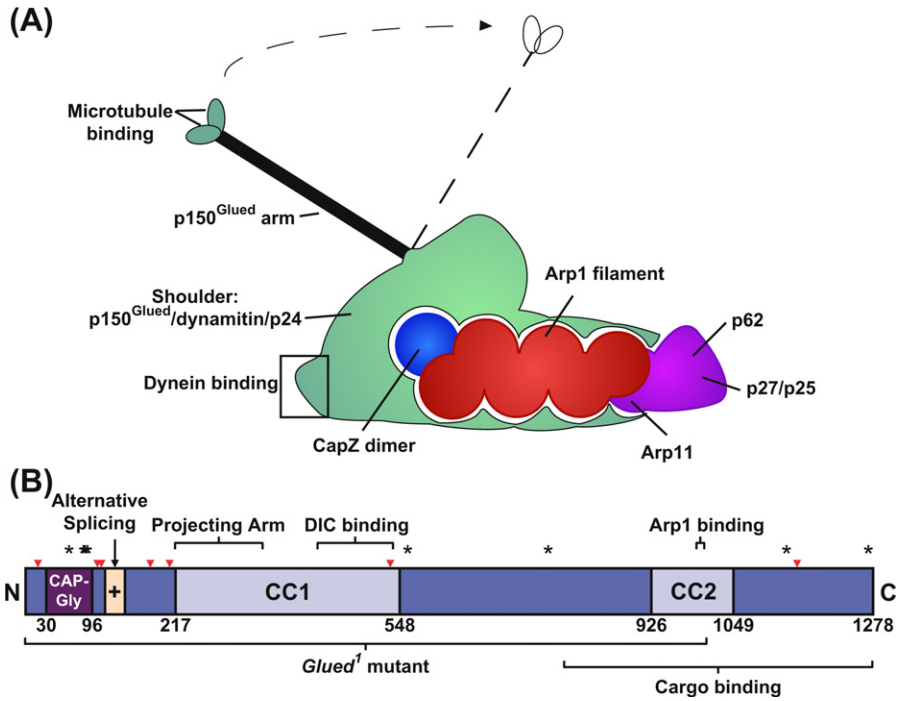

Figure 19.1 (Top) Cartoon representation of dynactin (as of late 2010) showing the position and relative size of the three structural domains. The projecting arm (a dimer of $p150^{Glued}$ AA ≈220–350) is in black; the green ovals represent the globular heads that contain the CAP-Gly and basic domains. The dotted line is provided to remind the reader of the extreme conformational flexibility of the junction between the arm and the rest of the dynactin molecule that has been observed in electron microscopy images of individual molecules [33,98]. The shoulder domain ($p150^{Glued}$ AA 350–end, dynamitin, and p24 in a 2:4:2 ratio [32]) is in green. The rest of the molecule is the Arp1 minifilament domain. The Arp1 polymer (which contains a single G-actin monomer; not indicated) is red. CapZ is blue. The pointed-end complex (Arp11, p62, p27, and p25) is purple. This representation is based on a 3.4 nm resolution three-dimensional-averaged electron microscopy image of negatively stained chick embryo brain dynactin (H. Imai, A. Narita, T. A. Schroer, and Y. Maeda, manuscript in preparation). (Bottom) Representation of the human $p150^{Glued}$ sequence indicating known features. The microtubule-binding CAP-Gly motif (AA 30–96) is purple and the basic domain (+; AA 115–145) is yellow. Alternative splicing of exons 5, 6, and 7 yields basic domains of varying sizes; one splice form contains an internal ATG site that can be translated to form a shorter isoform [50]. CC1 and CC2 are the two predicted α-helical coiled-coil domains. Dynein intermediate chain (DIC) binds in the vicinity of AA ≈ 415–530 [54]. A putative Arp1 binding site (AA 1005–1019) was identified in [81]. The archetypal *Drosophila* $Glued^{1}$ mutation yields a $p150^{Glued}$ form that terminates prematurely in CC2 and is no longer associated with the Arp1 filament domain. Several potential binding partners (see **Section 19.4.3** for details) appear to interact with the C-terminal portion ("cargo-binding"). Red arrowheads indicate sites that have been found to be phosphorylated *in vivo* [99–103]. Asterisks mark the positions of naturally occurring mutations that correlate with neurological defects [43,44,104,105].

light chains (LCs), dynactin contains 11 distinct subunits and is highly asymmetric (Fig. 19.1). Dynactin has three structural domains: a 24 nm-long *projecting arm* formed by the N-terminal (AA (amino acids) 1−≈350) of the subunit p150^{Glued}; a 37×8 nm structure (the *Arp1 filament domain*) comprising a short polymer of the actin-related protein, Arp1, plus CapZ, actin, Arp11, p62, p27, and p25 [20,32,33]; and a chevron-shaped *shoulder* that links the two. The shoulder is thought to comprise the rest of p150^{Glued}, plus dynamitin (p50) and p24 [32].

p150^{Glued} has two distinct microtubule-binding sites in each of the small globular domains seen at the distal tip of the projecting arm. These are discussed in detail in Section 19.3. The Arp1 polymer is of uniform length and bears a close resemblance to a short polymer of F-actin. It is capped on the barbed end by the heterodimeric conventional actin capping protein, CapZ [33]. Arp11 caps the opposite end of the Arp1 filament where it associates with the p62, p25, and p27 subunits. Together, this entire heterotetrameric structure is referred to as the pointed-end complex [32,33]. The Arp1 filament domain is believed to be largely responsible for binding cargo.

19.3 Known Activities of Dynactin

19.3.1 Microtubule Binding

Dynactin binds microtubules via the p150^{Glued} subunit, two copies of which are present in the dynactin molecule. Each p150^{Glued} monomer contains two distinct microtubule interaction motifs that are adjacent to each other in the N-terminal region of the protein (Fig. 19.1). The first (AA 30−96) is a canonical CAP-Gly (cytoskeleton-associated protein, glycine-rich) motif [34]. Its structure has been determined at high resolution [35−38] and is very similar to other CAP-Gly structures [39,40]. CAP-Gly motifs can bind microtubules either directly or indirectly. This can involve high-affinity interactions with the amino acid triad EEF/Y but they can also bind zinc fingers, and at least one CAP-Gly variant binds proline-rich domains [40] (summarized in [41]). The structural basis for the difference in binding preference has been determined and maps to a single surface loop [37]. The p150^{Glued} CAP-Gly motif is believed to interact with microtubules indirectly, via microtubule-binding proteins such as EB1 (see below). Naturally occurring mutations in the CAP-Gly motif that cause embryonic lethality in homozygotes [42] and dominant motor neuron defects in heterozygotes [43,44] destabilize the structure [45] and reduce its affinity for the microtubule-binding protein EB1 [46]. That these mutations have such profound effects emphasizes the importance of the CAP-Gly motif for proper dynactin function in metazoan organisms.

Immediately adjacent to the CAP-Gly motif is a short tract of basic amino acids that supports low-affinity interactions with microtubules. This so-called "basic domain" (AA 115−145) supports one-dimensional diffusion, or "skating," on the microtubule lattice. Skating behavior is only seen for artificially engineered

p150^{Glued} mutants that lack the CAP-Gly motif [47]. Naturally occurring p150^{Glued} splice isoforms exist that differ in the length of the basic domain. This has been proposed to result in different microtubule-binding properties [48,49]; the ubiquitous form with a shorter basic domain interacts with microtubules less strongly than a neuron-specific form with a slightly longer basic domain. When exogenously expressed in cells, the form with the shorter basic domain interacts with microtubule plus ends selectively, whereas the form with the longer basic domain form decorates the entire microtubule lattice. Alternative splicing in neurons also yields a form that lacks the CAP-Gly motif [50]. Thus, neurons may have p150^{Glued} isoforms that range in microtubule-binding potential from high (long basic domain) to low (no CAP-Gly, short basic domain). This may reflect the diversity and importance of intracellular transport phenomena in neurons. Conversely, budding yeast p150^{Glued} (Nip100p) has the CAP-Gly motif but not the basic domain, which may reflect the unique way in which yeasts use the dynein/dynactin motor.

Although CAP-Gly motifs are capable of binding microtubules directly and with high affinity, their interactions with microtubules can be very complex. They can bind directly to the C-terminus of α-tubulin (via the last three amino acids, EEY) but also to the same motif in microtubule-binding proteins such as CLIP-170 and the EB (end-binding) family [51]. Indirect binding is believed to be the predominant mode by which p150^{Glued} interacts with microtubules. It is possible that the p150^{Glued} basic domain provides a means for "fine-tuning" dynactin's interactions with microtubules by supporting or stabilizing intermolecular contacts, perhaps leading to the formation of even more complex networks of microtubule-binding proteins. We will return to the question of how microtubule binding impacts dynactin function later.

19.3.2 Dynein Binding

The dynactin subunit p150^{Glued} also plays a key role in dynactin–dynein interaction by binding to the cytoplasmic dynein IC. This dynein subunit is highly similar to the ICs that tether axonemal dyneins to the A-tubule of the microtubule doublet. Biochemical studies aimed at identifying binding partners for the cytoplasmic dynein IC revealed strong associations with p150^{Glued} [52,53]. This interaction involves the extreme N-terminus (AA 1–≈35) of the IC [54], which is predicted to be intrinsically disordered [55]. The binding site on p150^{Glued} has been shown to lie within the region AA ≈220–550 [4]. This portion of p150^{Glued} comprises two distinct structures: the coiled-coil stalk portion of the projecting arm (AA ≈220–350) and the adjacent region (AA ≈350–550), which is also predicted to fold into a coiled coil. p150^{Glued} AA ≈350–550 is thought to be contained within the body of the dynactin molecule, where it most likely sits at the barbed end of the Arp1 polymer. This portion of p150^{Glued} is required for dynactin activity *in vivo* [56], which is consistent with the notion that it contains the dynein binding site. In agreement with this, the IC binding site has been

mapped to AA 415–530 [54]. The idea that cytoplasmic dynein binds dynactin at a site near the base of the projecting arm, and not on the arm itself, means that dynein and dynactin are tethered to each other some distance, possibly as far as 30 nm, from the microtubule surface (Fig. 19.2). This binding geometry has the potential to confer great flexibility on the dynein–dynactin complex and may be important for observed behaviors such as avoidance of obstacles, lateral "wandering" on the microtubule lattice, and short apparent reversals in direction. Extreme flexibility of the joint between dynactin's projecting arm and the rest of the dynactin molecule is probably essential for its ability to stay associated with dynein and undergo dynamic interactions with microtubules, as dynein walks along the microtubule lattice.

19.4 Dynactin Function in Dynein-Based Motility

19.4.1 Dynactin as a Cargo Adaptor

Dynactin and dynein are components of the same genetic pathway, and mutations in subunits of either molecule appear to have a similar set of cellular consequences. Dynein's function is very clear: to coordinate the energy of ATP hydrolysis with a conformational change that results in directional movement along the microtubule lattice. What, then, is the function of dynactin? A clue comes from the simplicity of the dynein gene family compared to the kinesins. Eukaryotic genomes contain a multitude of kinesin motors that perform overlapping and distinct functions but rely on only one (or two) cytoplasmic dyneins to drive a huge range of motile phenomena. Thus, it makes sense that a "one-size-fits-all" motor such as cytoplasmic dynein would require an accessory component such as dynactin to tailor its activity to allow it to perform its many functions.

Cytoplasmic dynein drives a truly dizzying range of behaviors. In animal cells, it plays important roles in both mitosis and interphase. In mitosis, it contributes to nuclear envelope breakdown, organization of microtubules at spindle poles, and the dynamic behaviors of kinetochores and kinetochore proteins. In both mitosis and interphase, dynein can power rotation and repositioning of microtubule arrays relative to the cell cortex. In interphase, dynein drives the inward movement and contributes to steady-state positioning of most, if not all, of the cell's internal membranes. In fact, just about any subcellular particle, whether ribonucleoprotein, a preassembled complex of pericentriolar material, a protein aggregate destined for degradation, or an invading viral capsid, will use dynein to propel it toward microtubule minus ends. Some of these cargoes may be able to bind dynein independently of dynactin. Dynein–membrane binding is still seen in *Drosophila* mutants that lack Arp1 [57] although membrane transport is profoundly impaired. However, even if dynein–membrane

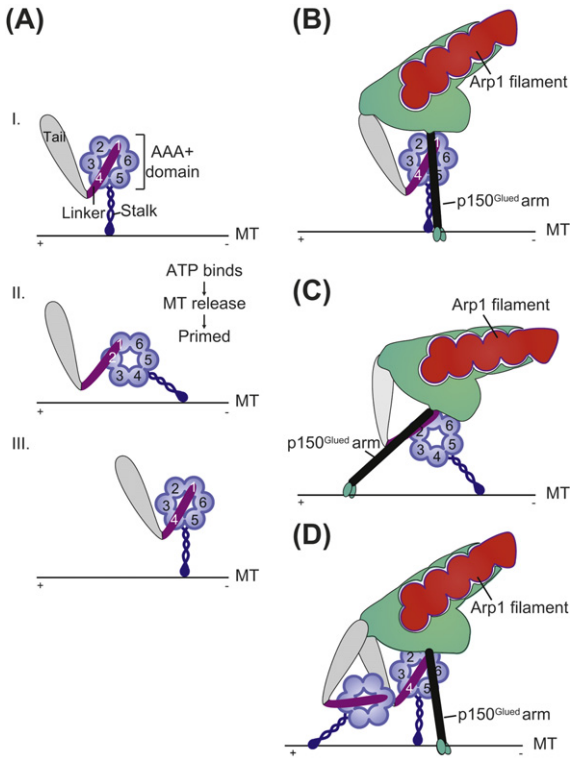

Figure 19.2 Proposed dynactin–cytoplasmic dynein interaction modes. (A) The mechanical cycle of a half dynein molecule (one HC and associated subunits). The AAA^+ domain (purple), linker (magenta), and microtubule binding stalk (blue) are indicated. The tail domain (grey) contains the N-terminal portion of the HC complexed with ICs, LICs, and LCs. Panel I: At the end of a mechanochemical cycle ("step"), the dynein head is bound to the microtubule. ATP binding at AAA1 allows the stalk to be released from the microtubule. Panel II: Coupled to the ATP hydrolytic cycle at AAA1, the head moves relative to the linker. The stalk and its terminal microtubule-binding site are now in a different position relative to the microtubule. This state is referred to as "primed" in [89]. Panel III: The microtubule-binding site reattaches to the microtubule, in conjunction with a second large-scale movement of the head relative to the linker. This is referred to as the "power stroke" in [106]. The relative positions of the head and linker are the same as they were at the beginning of the cycle. Modified from [89]. (B and C) Hypothetical models depicting possible interactions between the $p150^{Glued}$ arm and the mechanical components of the head. The reader should note that the $p150^{Glued}$ arm may be able to swivel freely relative to the rest of the dynactin molecule, permitting a wide range of binding modes to dynein and the microtubule. The structural basis of the interaction between dynactin and the unstructured N-terminus of the dynein IC has not yet been determined and it is possible that this junction is also flexible. In (B), the arm is proximal to the stalk and/or AAA^+ domains. This might contribute to the communication between the site of ATP hydrolysis (AAA1) and the stalk that is necessary to drive the conformational changes in the stalk that correlate with different affinities of its microtubule-binding site for the microtubule [95–97]. In (C), the arm is in proximity to the linker and/or AAA^+ domains. This might facilitate or govern the relative movements of these structures relative to each other during either the priming step or the powerstroke illustrated in (A). (D) Hypothetical model showing one possible mode of interaction between a dynactin molecule with a two-headed cytoplasmic dynein molecule. The reader should note that the $p150^{Glued}$ arm could be positioned between the two heads or it could be outside either head.

binding can persist in the absence of dynactin under artificial circumstances such as these, it is still the case that the vast majority of dynein–cargo interactions involve dynactin.

The necessity of dynactin for proper dynein function is made abundantly clear by genetic studies. The $p150^{Glued}$ subunit plays two key roles, as detailed above, but neither $p150^{Glued}$ by itself nor the free Arp1 filament domain is a functional substitute for the complete dynactin molecule. *Glued*[1], the archetypal *Drosophila* dynactin mutant, encodes a truncated form of $p150^{Glued}$ (AA ≈1–1020; Fig. 19.1) that is stable in cells but is no longer associated with the Arp1 polymer. Overexpression of the dynactin subunit dynamitin has a similar effect as it causes $p150^{Glued}$ to be released from the rest of the dynactin molecule. In both cases, free $p150^{Glued}$ (or $p150^{Glued}$ fragments) and an intact Arp1 filament domain are present, yet cells show a similar spectrum of organelle localization and mitotic defects to cells lacking dynein. These findings demonstrate clearly that functions provided by the Arp1 filament are as important for dynactin activity as the ability of $p150^{Glued}$ to bind dynein and microtubules. The most obvious function is cargo binding.

19.4.2 Cargo Interactions of the Arp1 Filament

Two components of the Arp1 filament domain have been implicated in cargo binding: the Arp1 filament itself and the pointed-end complex that sits at the end distal to the $p150^{Glued}$ arm. In electron microscopy images, the Arp1 filament closely resembles a short polymer of conventional F-actin. Such a structure provides two fairly flat potential binding surfaces whose areas are approximately 6–8 nm × 40 nm. The surface of each Arp1 monomer contains a high proportion of basic residues, suggesting that this part of the structure may support electrostatic interactions with acidic lipid head groups [58]. Arp1 has been reported to bind to spectrin, specifically the β III isoform that is associated with the Golgi complex [58–61], which may provide an additional mode of membrane binding.

Arp1 may be ubiquitous among eukaryotes, but this is not true of all components of the Arp1 filament. The pointed-end complex subunits p62, p27, and p25 are absent from yeasts, indicating that, unlike all other subunits, they are not uniformly essential for dynactin function. Unlike most eukaryotes, yeasts do not use dynein to power the movement of internal membranes other than the nucleus. For this reason, it has been speculated that the pointed-end complex represents a dynactin subdomain that is specialized for membrane targeting and/or other behaviors not seen in yeast. However, whether or not p62, p27, and p25 interact with membranes remains largely unknown. The pointed-end complex subunit p62 has been implicated in dynactin targeting to the nuclear envelope [62,63]. Work from our lab has revealed that p27 and p25 are required for proper targeting of

dynactin to recycling endosomes (T. Y. Yeh, B. R. Scipioni, and T. A. Schroer, manuscript in preparation). However, no specific binding partner(s) have been identified, leaving the molecular details of how the pointed-end complex contributes to membrane binding an enigma.

19.4.3 Cargo Interactions with the Shoulder–Sidearm Complex

The dynactin subunits dynamitin and the C-terminal region of $p150^{Glued}$ (AA ≈880–end) have been reported to bind to an eclectic array of potential dynein cargoes. Both are part of the shoulder-sidearm complex. When the isolated shoulder-sidearm complex is viewed via electron microscopy, it bears a very close resemblance to the bulky dynactin shoulder and projecting arm [32]. This suggests that dynamitin and the C-terminal portion of $p150^{Glued}$ associate with each other to form a compact, roughly globular structure. However, their precise locations in the intact dynactin molecule are unknown so the possibility that portions of each are exposed on the dynactin surface and able to support cargo binding interactions cannot be excluded.

Evidence that dynamitin and the $p150^{Glued}$ C-terminus bind cargo molecules has come from yeast two-hybrid screens and protein affinity methods. Molecules suggested to bind the $p150^{Glued}$ C-terminus include the microtubule-associated protein tau [64], the huntingtin-associated protein HAP1 [65], and sorting nexin 6 (SNX6) [66]. Membrane-associated proteins such as RILP (Rab7-interacting lysosomal protein) [67] and the Jnk kinase scaffold proteins JIP 3 and 4 [68] have also emerged as possible binding partners. Similar strategies have led to reports that dynamitin binds ZW10 (a protein associated with both membranes and kinetochores) [15], Bicaudal D [69], the dynein/dynactin pathway protein LIS1 [70], calmodulin and Mac-MARCKS (a protein involved in the coordination of membrane–cytoskeleton signaling events) [71], and α-E-catenin [72]. Studies involving overexpression of various proteins in cells followed by affinity isolation have revealed possible interactions of these same dynactin subunits with molecules such as cyclophilin A [73] and 14-3-3 [74].

Despite all this work, a comprehensive picture of how dynactin binds membranous cargoes has not yet emerged. A likely scenario is that dynactin associates with membranes via multiple interactions that vary in both affinity and specificity. Electrostatic interactions between the Arp1 polymer and acidic lipid head groups may confer general stickiness, whereas a preference for binding to certain membranes may be determined by specific interactions with molecules such as those listed above. To add to the complexity, extrinsic proteins such as BicD [75] may serve to stabilize and/or modulate dynactin–membrane binding. Definitive answers to this important and elusive question will surely come in the future.

19.4.4 Dynactin as a Processivity Enhancer

Dynactin's first known activity was its ability to allow purified cytoplasmic dynein to power long-range (>1 um) movement of membrane vesicles *in vitro* [2]. In the absence of dynactin, dynein allowed vesicles to bind microtubules and undergo short-range, bidirectional excursions, but obviously directed motility was not observed. Although not appreciated at the time, this seminal study provided the first evidence that dynactin is able to enhance dynein processivity. For many motors, processive activity involves the presence of multiple motors, and a large body of recent biophysical work has established that dynein-driven membrane motility *in vivo* involves as many as eight active dynein molecules per cargo particle [76–79]. Thus, the earliest observation that dynactin could enhance dynein processivity might simply have been a reflection of its ability to increase the number of dyneins bound to the vesicle surface. However, other work has shown that dynactin can enhance the processivity of single dynein molecules [56,80]. Whether or not dynactin has any effect on processive dynein-based movement *in vivo* is a source of great controversy.

Processive activity of any enzyme requires a minimum of two substrate binding sites, one that undergoes cycles of attachment and detachment and a second to tether the enzyme to the substrate during the detached phase. Many cytoskeletal motors solve this problem by having two heads that work alternately so one is always attached. Other motors use a secondary, non-motor, site to stay bound to the filament. Dyneins are relatively non-processive, so the discovery that $p150^{Glued}$ contains its own microtubule-binding sites carried obvious implications [81]. In the case of bovine cytoplasmic dynein, the processivity enhancement seen in the presence of dynactin can be reversed by an antibody that blocks the N-terminal, microtubule-binding domain (MTBD) [80]. Processivity of budding yeast dynein is also enhanced by dynactin, but in this case the MTBD is not required [56].

Studies in whole cells in culture have also led to the conclusion that microtubule binding by $p150^{Glued}$ is not required for processive dynein movement. When $p150^{Glued}$ in cultured *Drosophila* S2 cells was replaced with a form lacking the MTBD, peroxisomes and other organelles moved indistinguishably from controls [82]. However, these cells exhibited profound spindle defects, suggesting that the MTBD is important for dynactin function in other contexts. HeLa cells expressing engineered mutant forms of $p150^{Glued}$ and fibroblasts isolated from humans bearing the destabilizing CAP-Gly mutation also show minimal alteration of endomembrane architecture [48,83]. Replacement of $p150^{Glued}$ (Nip100p) in budding yeast with a similarly truncated form yields no obvious phenotype, suggesting that microtubule binding is not essential in this system [45,56]. However, close inspection reveals impaired initiation of movement of the nucleus into and through the bud neck, suggesting that microtubule binding by $p150^{Glued}$ is important for dynein-based movement of

particularly challenging loads [45]. Furthermore, destabilizing mutations in the CAP-Gly domain are lethal when homozygous in mammals and have clear consequences for the long-term health of motor neurons in heterozygotes, as described in Section 19.3.1. Taken together, this work suggests that dynactin's ability to bind microtubules is not required for processive dynein-based movement in many contexts. However, cells that require especially-long-range movement or movement of very large cargoes may place a heavy burden on the dynein/dynactin motor machinery. In neurons, this might lead to deterioration of cell integrity that accumulates over time.

19.4.5 Other Modes of Dynein Activation

Thanks to the concerted efforts of a number of laboratories, we are slowly starting to understand how the chemical and mechanical cycles of cytoplasmic dynein are coupled to allow this unusual motor to walk along the microtubule lattice [84–89]. This work has provided a clear, but superficial, picture of how ATP hydrolysis at one site might be translated into a change in microtubule affinity at another (Fig. 19.2A). By necessity, this work has focused on severely truncated forms of just one dynein subunit, the HC. However, the intact dynein molecule contains several other subunits, including the dynactin-binding IC, and it is not at all clear how these subunits, let alone dynactin, might impact the behavior of the motor as a whole. Dynactin has no apparent effect on dynein's enzymatic activity in simple ATPase assays [80], but this does not mean it does not have other, important, effects on the dynein motile cycle. In other words, the possibility remains open that dynactin is a true activator of the dynein motor, in ways upon which we can only speculate.

The most likely dynactin domain to interact with the dynein motor domain is the 24 nm long projecting arm. The arm is an α-helical coiled coil that appears rigid by itself but is docked to the Arp1 filament domain via a highly flexible hinge (Fig. 19.1). This organization allows the arm to act as a stiff rod that can swivel freely relative to the rest of the dynactin and any bound cargo. It is safe to assume that the MTBD at the tip of the arm contacts the microtubule within stepping distance (8–32 nm) of dynein's microtubule-binding site. Interaction between the distal tip of the dynein tail and the end of the Arp1 filament domain could position the arm so that it reaches all the way across the dynein head (Fig. 19.2B–D). Here, it might interact with any of the mechanical elements of the motor domain: AAA^{+} domain, linker, or microtubule-binding stalk. A $p150^{Glued}$ fragment that contains the projecting arm (CC1; AA $\approx$220–550) is a highly effective inhibitor of dynein-based motility [4,90–93]. This fragment contains the dynein-binding site and is generally assumed to suppress motility by competitively inhibiting the dynein/dynactin interaction. However, a complementary fragment of the dynein IC is a poor inhibitor by comparison [4], raising the possibility that CC1 might affect dynein activity directly. It would be highly

worthwhile for this $p150^{Glued}$ fragment to be tested for its ability to alter the behavior of dynein in single-molecule assays.

Given our rudimentary understanding of the cytoplasmic dynein mechanochemical cycle, at this point there is only a limited number of possibilities for how the $p150^{Glued}$ arm might participate (Fig. 19.2B,C). It might interact with the linker or AAA^+ domain to facilitate the linker sweep that occurs during the ATP hydrolytic cycle [89], a process that is still not fully understood (reviewed in [94]). For example, if the linker acts as a rigid lever, lateral association with the $p150^{Glued}$ arm might help to increase its rigidity to make the sweep more efficient. If movement of the linker relative to the AAA^+ domain involves a conformational change in the linker, association with the $p150^{Glued}$ arm might facilitate this. If the linker moves by skipping between binding sites on the head, $p150^{Glued}$ binding to either the linker or the AAA^+ domain might enhance the process. It is also possible that the $p150^{Glued}$ arm interacts with dynein's microtubule-binding stalk to assist the conformational changes that occur either at the head/stalk junction [89] or along the length of the stalk [95–97] and that correlate with changes in microtubule affinity. Finally, dynactin might facilitate the head-to-head coordination that is thought to be important for optimal motor activity [79]. At present, existing assays that allow head-to-head coordination to be evaluated are few and highly challenging, so exploration of this possibility may have to wait. However, whether dynactin might have an impact on the behavior of a single dynein head is testable, at least in principle.

A final question that is left unaddressed above and in all models of cytoplasmic dynein motor activity is how many dynactins are coupled to a single dynein motor. If dynactin contributes to head-to-head coordination, only one dynactin might be needed for every dynein (Fig. 19.2D). However, if dynactin contributes to the mechanochemical cycle of a single dynein head, it would make sense for each head to be associated with its own dynactin (i.e. in a 2:1 dynactin:dynein ratio). Current estimates of the stoichiometry of dynein and dynactin on membranes lie tantalizingly between 1 and 2 [78], in support of either possibility. Hopefully, more insight into this question and the many other mysteries that still surround dynactin and the roles it plays in cytoplasmic dynein function will soon be forthcoming.

References

[1] S.R. Gill, T.A. Schroer, I. Szilak, E.R. Steuer, M.P. Sheetz, D.W. Cleveland, Dynactin, a conserved, ubiquitously expressed component of an activator of vesicle motility mediated by cytoplasmic dynein, J. Cell Biol. 115 (1991) 1639–1650.

[2] T.A. Schroer, M.P. Sheetz, Two activators of microtubule-based vesicle transport, J. Cell Biol. 115 (1991) 1309–1318.

[3] J.K. Burkhardt, C.J. Echeverri, T. Nilsson, R.B. Vallee, Overexpression of the dynamitin (p50) subunit of the dynactin complex disrupts dynein-dependent maintenance of membrane organelle distribution, J. Cell Biol. 139 (1997) 469–484.

[4] S.J. King, C.L. Brown, K.C. Maier, N.J. Quintyne, T.A. Schroer, Analysis of the dynein–dynactin interaction *in vitro* and *in vivo*, Mol. Biol. Cell 14 (2003) 5089–5097.
[5] C. Roghi, V.J. Allan, Dynamic association of cytoplasmic dynein heavy chain 1a with the Golgi apparatus and intermediate compartment, J. Cell Sci. 112 (1999) 4673–4685.
[6] J.F. Presley, K.J.M. Zaal, T.A. Schroer, N.B. Cole, J. Lippincott-Schwartz, ER to Golgi transport visualized in living cells, Nature 389 (1997) 81–85.
[7] C. Valetti, D.M. Wetzel, M. Schrader, M.J. Hasbani, S.R. Gill, T.E. Kreis, T.A. Schroer, Role of dynactin in endocytic traffic: Effects of dynamitin overexpression and colocalization with CLIP-170, Mol. Biol. Cell 10 (1999) 4107–4120.
[8] S.W. Deacon, A.S. Serpinskaya, P.S. Vaughan, M. Lopez Fanarraga, I. Vernos, K.T. Vaughan, V.I. Gelfand, Dynactin is required for bidirectional organelle transport, J. Cell Biol. 160 (2003) 297–301.
[9] C.J. Echeverri, B.M. Paschal, K.T. Vaughan, R.B. Vallee, Molecular characterization of 50 kD subunit of dynactin reveals function for the complex in chromosome alignment and spindle organization during mitosis, J. Cell Biol. 132 (1996) 617–633.
[10] P. Gonczy, S. Pichler, M. Kirkham, A.A. Hyman, Cytoplasmic dynein is required for distinct aspects of MTOC positioning, including centrosome separation, in the one cell stage *Caenorhabditis elegans* embryo, J. Cell Biol. 147 (1999) 135–150.
[11] R. Heald, R. Tournebize, T. Blank, R. Sandaltzopoulos, P. Becker, A. Hyman, E. Karsenti, Self-organization of microtubules into bipolar spindles around artificial chromosomes in *Xenopus* egg extracts, Nature 382 (1996) 420–425.
[12] B.J. Howell, B.F. McEwen, J.C. Canman, D.B. Hoffman, E.M. Farrar, C.L. Rieder, E.D. Salmon, Cytoplasmic dynein/dynactin drives kinetochore protein transport to the spindle poles and has a role in mitotic spindle checkpoint inactivation, J. Cell Biol. 155 (2001) 1159–1172.
[13] Y.-Y. Li, E. Yeh, T. Hays, K. Bloom, Disruption of mitotic spindle orientation in a yeast dynein mutant, Proc. Natl. Acad. Sci. USA 90 (1993) 10096–10100.
[14] C.M. Pfarr, M. Coue, P.M. Grissom, T.S. Hays, M.E. Porter, J.R. McIntosh, Cytoplasmic dynein localizes to kinetochores during mitosis, Nature 345 (1990) 263–265.
[15] D.A. Starr, B.C. Williams, T.S. Hays, M.L. Goldberg, ZW10 helps recruit dynactin and dynein to the kinetochore, J. Cell Biol. 142 (1998) 763–774.
[16] E.R. Steuer, T.A. Schroer, L. Wordeman, M.P. Sheetz, Localization of cytoplasmic dynein to mitotic spindles and kinetochores, Nature 345 (1990) 266–268.
[17] E.A. Vaisberg, M.P. Koonce, J.R. McIntosh, Cytoplasmic dynein plays a role in mammalian mitotic spindle formation, J. Cell Biol. 123 (1993) 849–858.
[18] E. Yeh, R.V. Skibbens, J.W. Cheng, E.D. Salmon, K. Bloom, Spindle dynamics and cell cycle regulation of dynein in the budding yeast, *Saccharomyces cerevisiae*, J. Cell Biol. 130 (1995) 687–700.
[19] I.B. Clark, D.I. Meyer, Overexpression of normal and mutant Arp1alpha (centractin) differentially affects microtubule organization during mitosis and interphase, J. Cell Sci. 112 (Pt 20) (1999) 3507–3518.
[20] T.A. Schroer, Dynactin, Annu. Rev. Cell Dev. Biol. 20 (2004) 759–779.
[21] S.W. Clark, D.I. Meyer, ACT3: A putative centractin homolog in *S. cerevisiae* is required for proper orientation of the mitotic spindle, J. Cell Biol. 127 (1994) 129–138.
[22] M. McGrail, J. Gepner, A. Silvanovich, S. Ludmann, M. Serr, T.S. Hays, Regulation of cytoplasmic dynein function *in vivo* by the *Drosophila* glued complex, J. Cell Biol. 131 (1995) 411–425.
[23] J.N. McMillan, K. Tatchell, The JNM1 gene in the yeast *Saccharomyces cerevisiae* is required for nuclear migration and spindle orientation during the mitotic cell cycle, J. Cell Biol. 125 (1994) 143–158.
[24] L. Muhua, T.S. Karpova, J.A. Cooper, A yeast actin-related protein homologous to that found in vertebrate dynactin complex is important for spindle orientation and nuclear migration, Cell 78 (1994) 669–679.

[25] M. Plamann, P.F. Minke, J.H. Tinsley, K.S. Bruno, Cytoplasmic dynein and actin-related protein Arp1 are required for normal nuclear distribution in filamentous fungi, J. Cell Biol. 127 (1994) 139–149.
[26] T.A. Schroer, New insights into the interaction of cytoplasmic dynein with the actin-related protein, Arp1, J. Cell Biol. 127 (1994) 1–4.
[27] B. Sonnichsen, L.B. Koski, A. Walsh, P. Marschall, B. Neumann, M. Brehm, A.M. Alleaume, J. Artelt, P. Bettencourt, E. Cassin, M. Hewitson, C. Holz, M. Khan, S. Lazik, C. Martin, B. Nitzsche, M. Ruer, J. Stamford, M. Winzi, R. Heinkel, M. Roder, J. Finell, H. Hantsch, S.J. Jones, M. Jones, F. Piano, K.C. Gunsalus, K. Oegema, P. Gonczy, A. Coulson, A.A. Hyman, C.J. Echeverri, Full-genome RNAi profiling of early embryogenesis in *Caenorhabditis elegans*, Nature 434 (2005) 462–469.
[28] J.H. Tinsley, P.F. Minke, K.S. Bruno, M. Plamann, p150^{Glued}, the largest subunit of the dynactin complex, is nonessential in *Neurospora* but required for nuclear distribution, Mol. Biol. Cell 7 (1996) 731–742.
[29] X. Xiang, W. Zuo, V.P. Efimov, N.R. Morris, Isolation of a new set of *Aspergillus nidulans* mutants defective in nuclear migration, Curr. Genet. 35 (1999) 626–630.
[30] P.F. Minke, I.H. Lee, J.H. Tinsley, K.S. Bruno, M. Plamann, *Neurospora crassa* ro-10 and ro-11 genes encode novel proteins required for nuclear distribution, Mol. Microbiol. 32 (1999) 1065–1076.
[31] J.A. Kahana, G. Schlenstedt, D.M. Evanchuk, J.A. Geiser, M.A. Hoyt, P.A. Silver, The yeast dynactin complex is involved in partitioning the mitotic spindle between mother and daughter cells during anaphase B, Mol. Biol. Cell 9 (1998) 1741–1756.
[32] D.M. Eckley, S.R. Gill, K.A. Melkonian, J.B. Bingham, H.V. Goodson, J.E. Heuser, T.A. Schroer, Analysis of dynactin subcomplexes reveals a novel actin-related protein associated with the Arp1 filament pointed end, J. Cell Biol. 147 (1999) 307–319.
[33] D.A. Schafer, S.R. Gill, J.A. Cooper, J.E. Heuser, T.A. Schroer, Ultrastructural analysis of the dynactin complex, An actin-related protein is a component of a filament that resembles f-actin, J. Cell Biol. 126 (1994) 403–412.
[34] K. Riehemann, C. Sorg, Sequence homologies between four cytoskeleton-associated proteins, Trends Biochem. Sci. 18 (1993) 82–83.
[35] I. Hayashi, A. Wilde, T.K. Mal, M. Ikura, Structural basis for the activation of microtubule assembly by the EB1 and p150^{Glued} complex, Mol. Cell 19 (2005) 449–460.
[36] S. Honnappa, O. Okhrimenko, R. Jaussi, H. Jawhari, I. Jelesarov, F.K. Winkler, M.O. Steinmetz, Key interaction modes of dynamic +TIP networks, Mol. Cell 23 (2006) 663–671.
[37] M.J. Plevin, I. Hayashi, M. Ikura, Characterization of a conserved "threonine clasp" in CAP-Gly domains: Role of a functionally critical OH/pi interaction in protein recognition, J. Am. Chem. Soc. 130 (2008) 14918–14919.
[38] S. Sun, A. Siglin, J.C. Williams, T. Polenova, Solid-state and solution NMR studies of the CAP-Gly domain of mammalian dynactin and its interaction with microtubules, J. Am. Chem. Soc. 131 (2009) 10113–10126.
[39] S. Li, J. Finley, Z.J. Liu, S.H. Qiu, H. Chen, C.H. Luan, M. Carson, J. Tsao, D. Johnson, G. Lin, J. Zhao, W. Thomas, L.A. Nagy, B. Sha, L.J. DeLucas, B.C. Wang, M. Luo, Crystal structure of the cytoskeleton-associated protein (CAP-Gly) domain, J. Biol. Chem. 277 (2002) 48596–48601.
[40] K. Saito, T. Kigawa, S. Koshiba, K. Sato, Y. Matsuo, A. Sakamoto, T. Takagi, M. Shirouzu, T. Yabuki, E. Nunokawa, E. Seki, T. Matsuda, M. Aoki, Y. Miyata, N. Hirakawa, M. Inoue, T. Terada, T. Nagase, R. Kikuno, M. Nakayama, O. Ohara, A. Tanaka, S. Yokoyama, The CAP-Gly domain of CYLD associates with the proline-rich sequence in NEMO/IKKgamma, Structure 12 (2004) 1719–1728.
[41] M.O. Steinmetz, A. Akhmanova, Capturing protein tails by CAP-Gly domains, Trends Biochem. Sci. 33 (2008) 535–545.
[42] C. Lai, X. Lin, J. Chandran, H. Shim, W.J. Yang, H. Cai, The G59S mutation in p150(glued) causes dysfunction of dynactin in mice, J. Neurosci. 27 (2007) 13982–13990.

[43] I. Puls, C. Jonnakuty, B.H. LaMonte, E.L. Holzbaur, M. Tokito, E. Mann, M.K. Floeter, K. Bidus, D. Drayna, S.J. Oh, R.H. Brown Jr., C.L. Ludlow, K.H. Fischbeck, Mutant dynactin in motor neuron disease, Nat. Genet. 33 (2003) 455–456.
[44] M.J. Farrer, M.M. Hulihan, J.M. Kachergus, J.C. Dachsel, A.J. Stoessl, L.L. Grantier, S. Calne, D.B. Calne, B. Lechevalier, F. Chapon, Y. Tsuboi, T. Yamada, L. Gutmann, B. Elibol, K.P. Bhatia, C. Wider, C. Vilarino-Guell, O.A. Ross, L.A. Brown, M. Castanedes-Casey, D.W. Dickson, Z.K. Wszolek, DCTN1 mutations in Perry syndrome, Nat. Genet. 41 (2009) 163–165.
[45] J.K. Moore, D. Sept, J.A. Cooper, Neurodegeneration mutations in dynactin impair dynein-dependent nuclear migration, Proc. Natl. Acad. Sci. USA 106 (2009) 5147–5152.
[46] S. Ahmed, S. Sun, A.E. Siglin, T. Polenova, J.C. Williams, Disease-associated mutations in the p150(Glued) subunit destabilize the CAP-gly domain, Biochemistry 49 (2010) 5083–5085.
[47] T.L. Culver-Hanlon, S.A. Lex, A.D. Stephens, N.J. Quintyne, S.J. King, A microtubule-binding domain in dynactin increases dynein processivity by skating along microtubules, Nat. Cell Biol. 8 (2006) 264–270.
[48] R. Dixit, J.R. Levy, M. Tokito, L.A. Ligon, E.L. Holzbaur, Regulation of dynactin through the differential expression of $p150^{Glued}$ isoforms, J. Biol. Chem. 283 (2008) 33611–33619.
[49] O.N. Zhapparova, S.A. Bryantseva, L.V. Dergunova, N.M. Raevskaya, A.V. Burakov, O.B. Bantysh, N.A. Shanina, E.S. Nadezhdina, Dynactin subunit p150Glued isoforms notable for differential interaction with microtubules, Traffic 10 (2009) 1635–1646.
[50] M.K. Tokito, D.S. Howland, V.M.-Y. Lee, E.L.F. Holzbaur, Functionally distinct isoforms of dynactin are expressed in human neurons, Mol. Biol. Cell 7 (1996) 1167–1180.
[51] A. Weisbrich, S. Honnappa, R. Jaussi, O. Okhrimenko, D. Frey, I. Jelesarov, A. Akhmanova, M.O. Steinmetz, Structure–function relationship of CAP-Gly domains, Nat. Struct. Mol. Biol. 14 (2007) 959–967.
[52] K.T. Vaughan, R.B. Vallee, Cytoplasmic dynein binds dynactin through a direct interaction between the intermediate chains and $p150^{Glued}$, J. Cell Biol. 131 (1995) 1507–1516.
[53] S. Karki, E.L.F. Holzbaur, Affinity chromatography demonstrates a direct binding between cytoplasmic dynein and the dynactin complex, J. Biol. Chem. 270 (1995) 28806–28811.
[54] A. Roberts-Siglin, S. Tan, M. Poenie, J.C. Williams, Fine mapping of the dynein–dynactin interface, Mol. Biol. Cell (ASCB abstract) (2008).
[55] J.C. Williams, P.L. Roulhac, A.G. Roy, R.B. Vallee, M.C. Fitzgerald, W.A. Hendrickson, Structural and thermodynamic characterization of a cytoplasmic dynein light chain-intermediate chain complex, Proc. Natl. Acad. Sci. USA 104 (2007) 10028–10033.
[56] J.R. Kardon, S.L. Reck-Peterson, R.D. Vale, Regulation of the processivity and intracellular localization of *Saccharomyces cerevisiae* dynein by dynactin, Proc. Natl. Acad. Sci. USA 106 (2009) 5669–5674.
[57] M. Haghnia, V. Cavalli, S.B. Shah, K. Schimmelpfeng, R. Brusch, G. Yang, C. Herrera, A. Pilling, L.S. Goldstein, Dynactin is required for coordinated bidirectional motility, but not for dynein membrane attachment, Mol. Biol. Cell 18 (2007) 2081–2089.
[58] V. Muresan, M.C. Stankewich, W. Steffen, J.S. Morrow, E.L. Holzbaur, B.J. Schnapp, Dynactin-dependent, dynein-driven vesicle transport in the absence of membrane proteins, A role for spectrin and acidic phospholipids, Mol. Cell 7 (2001) 173–183.
[59] E.A. Holleran, M.K. Tokito, S. Karki, E.L.F. Holzbaur, Centractin (Arp1) associates with spectrin revealing a potential mechanism to link dynactin to intracellular organelles, J. Cell Biol. 135 (1996) 1815–1829.
[60] K.A. Beck, J.A. Buchanan, V. Malhotra, W.J. Nelson, Golgi spectrin: Identification of an erythroid beta-spectrin homolog associated with the Golgi complex, J. Cell Biol. 127 (1994) 707–723.
[61] E.A. Holleran, L.A. Ligon, M. Tokito, M.C. Stankewich, J.S. Morrow, E.L. Holzbaur, Beta III spectrin binds to the Arp1 subunit of dynactin, J. Biol. Chem. 276 (2001) 36598–36605.

[62] D. Salina, K. Bodoor, D.M. Eckley, T.A. Schroer, J.B. Rattner, B. Burke, Cytoplasmic dynein as a facilitator of nuclear envelope breakdown, Cell 108 (2002) 97–107.
[63] C. Payne, V. Rawe, J. Ramalho-Santos, C. Simerly, G. Schatten, Preferentially localized dynein and perinuclear dynactin associate with nuclear pore complex proteins to mediate genomic union during mammalian fertilization, J. Cell Sci. 116 (2003) 4727–4738.
[64] E. Magnani, J. Fan, L. Gasparini, M. Golding, M. Williams, G. Schiavo, M. Goedert, L.A. Amos, M.G. Spillantini, Interaction of tau protein with the dynactin complex, EMBO J. 26 (2007) 4546–4554.
[65] S. Engelender, A.H. Sharp, V. Colomer, M.K. Tokito, A. Lanahan, P. Worley, E.L. Holzbaur, C.A. Ross, Huntingtin-associated protein 1 (HAP1) interacts with the p150Glued subunit of dynactin, Hum. Mol. Genet. 6 (1997) 2205–2212.
[66] T. Wassmer, N. Attar, M. Harterink, J.R. van Weering, C.J. Traer, J. Oakley, B. Goud, D.J. Stephens, P. Verkade, H.C. Korswagen, P.J. Cullen, The retromer coat complex coordinates endosomal sorting and dynein-mediated transport, with carrier recognition by the trans-Golgi network, Dev. Cell 17 (2009) 110–122.
[67] M. Johansson, N. Rocha, W. Zwart, I. Jordens, L. Janssen, C. Kuijl, V.M. Olkkonen, J. Neefjes, Activation of endosomal dynein motors by stepwise assembly of Rab7-RILP-$p150^{Glued}$, ORP1L, and the receptor betalll spectrin, J. Cell Biol. 176 (2007) 459–471.
[68] G. Montagnac, J.B. Sibarita, S. Loubery, L. Daviet, M. Romao, G. Raposo, P. Chavrier, ARF6 Interacts with JIP4 to control a motor switch mechanism regulating endosome traffic in cytokinesis, Curr. Biol. 19 (2009) 184–195.
[69] C.C. Hoogenraad, A. Akhmanova, S.A. Howell, B.R. Dortland, C.I. De Zeeuw, R. Willemsen, P. Visser, F. Grosveld, N. Galjart, Mammalian Golgi-associated Bicaudal-D2 functions in the dynein–dynactin pathway by interacting with these complexes, EMBO J. 20 (2001) 4041–4054.
[70] C.Y. Tai, D.L. Dujardin, N.E. Faulkner, R.B. Vallee, Role of dynein, dynactin, and CLIP-170 interactions in LIS1 kinetochore function, J. Cell Biol. 156 (2002) 959–968.
[71] L. Yue, S. Lu, J. Garces, T. Jin, J. Li, Protein kinase C-regulated dynamitin-macrophage-enriched myristoylated alanine-rice C kinase substrate interaction is involved in macrophage cell spreading, J. Biol. Chem. 275 (2000) 23948–23956.
[72] W.H. Lien, V.I. Gelfand, V. Vasioukhin, Alpha-E-catenin binds to dynamitin and regulates dynactin-mediated intracellular traffic, J. Cell Biol. 183 (2008) 989–997.
[73] M.D. Galigniana, Y. Morishima, P.A. Gallay, W.B. Pratt, Cyclophilin-A is bound through its peptidylprolyl isomerase domain to the cytoplasmic dynein motor protein complex, J. Biol. Chem. 279 (2004) 55754–55759.
[74] T. Nakamura, T. Hayashi, Y. Mimori-Kiyosue, F. Sakaue, K. Matsuura, S. Iemura, T. Natsume, T. Akiyama, The PX-RICS-14-3-3zeta/theta complex couples N-cadherin-beta-catenin with dynein–dynactin to mediate its export from the endoplasmic reticulum, J. Biol. Chem. 285 (2010) 16145–16154.
[75] M. Dienstbier, X. Li, Bicaudal-D and its role in cargo sorting by microtubule-based motors, Biochem. Soc. Trans. 37 (2009) 1066–1071.
[76] V. Soppina, A.K. Rai, A.J. Ramaiya, P. Barak, R. Mallik, Tug-of-war between dissimilar teams of microtubule motors regulates transport and fission of endosomes, Proc. Natl. Acad. Sci. USA 106 (2009) 19381–19386.
[77] V. Levi, A.S. Serpinskaya, E. Gratton, V. Gelfand, Organelle transport along microtubules in *Xenopus* melanophores: Evidence for cooperation between multiple motors, Biophys. J. 90 (2006) 318–327.
[78] A.G. Hendricks, E. Perlson, J.L. Ross, H.W. Schroeder 3rd, M. Tokito, E.L. Holzbaur, Motor coordination via a tug-of-war mechanism drives bidirectional vesicle transport, Curr. Biol. 20 (2010) 697–702.
[79] K.M. Ori-McKenney, J. Xu, S.P. Gross, R.B. Vallee, A cytoplasmic dynein tail mutation impairs motor processivity, Nat. Cell. Biol. 12 (2010) 1228–1234.

[80] S.J. King, T.A. Schroer, Dynactin increases the processivity of the cytoplasmic dynein motor, Nat. Cell Biol. 2 (2000) 20–24.
[81] C.M. Waterman-Storer, S. Karki, E.L. Holzbaur, The $p150^{Glued}$ component of the dynactin complex binds to both microtubules and the actin-related protein centractin (Arp-1), Proc. Natl. Acad. Sci. USA 92 (1995) 1634–1638.
[82] H. Kim, S.C. Ling, G.C. Rogers, C. Kural, P.R. Selvin, S.L. Rogers, V.I. Gelfand, Microtubule binding by dynactin is required for microtubule organization but not cargo transport, J. Cell Biol. 176 (2007) 641–651.
[83] J.R. Levy, C.J. Sumner, J.P. Caviston, M.K. Tokito, S. Ranganathan, L.A. Ligon, K.E. Wallace, B.H. LaMonte, G.G. Harmison, I. Puls, K.H. Fischbeck, E.L. Holzbaur, A motor neuron disease-associated mutation in $p150^{Glued}$ perturbs dynactin function and induces protein aggregation, J. Cell Biol. 172 (2006) 733–745.
[84] T. Kon, T. Mogami, R. Ohkura, M. Nishiura, K. Sutoh, ATP hydrolysis cycle-dependent tail motions in cytoplasmic dynein, Nat. Struct. Mol. Biol. 12 (2005) 513–519.
[85] X. Meng, M. Samso, M.P. Koonce, A flexible linkage between the dynein motor and its cargo, J. Mol. Biol. 357 (2006) 701–706.
[86] T. Shima, T. Kon, K. Imamula, R. Ohkura, K. Sutoh, Two modes of microtubule sliding driven by cytoplasmic dynein, Proc. Natl. Acad. Sci. USA 103 (2006) 17736–17740.
[87] S.L. Reck-Peterson, A. Yildiz, A.P. Carter, A. Gennerich, N. Zhang, R.D. Vale, Single-molecule analysis of dynein processivity and stepping behavior, Cell 126 (2006) 335–348.
[88] T. Mogami, T. Kon, K. Ito, K. Sutoh, Kinetic characterization of tail swing steps in the ATPase cycle of *Dictyostelium* cytoplasmic dynein, J. Biol. Chem. 282 (2007) 21639–21644.
[89] A.J. Roberts, N. Numata, M.L. Walker, Y.S. Kato, B. Malkova, T. Kon, R. Ohkura, F. Arisaka, P.J. Knight, K. Sutoh, S.A. Burgess, K. Imamula, I.R. Gibbons, AAA^{+} ring and linker swing mechanism in the dynein motor helix sliding in the stalk coiled coil of dynein couples ATPase and microtubule binding, Cell 136 (2009) 485–495.
[90] N.J. Quintyne, S.R. Gill, D.M. Eckley, C.L. Crego, D.A. Compton, T.A. Schroer, Dynactin is required for microtubule anchoring at fibroblast centrosomes, J. Cell Biol. 147 (1999) 321–334.
[91] J. Gaetz, T.M. Kapoor, Dynein/dynactin regulate metaphase spindle length by targeting depolymerizing activities to spindle poles, J. Cell Biol. 166 (2004) 465–471.
[92] D.M. Kwinter, K. Lo, P. Mafi, M.A. Silverman, Dynactin regulates bidirectional transport of dense-core vesicles in the axon and dendrites of cultured hippocampal neurons, Neuroscience 162 (2009) 1001–1010.
[93] H. Si, S.C. Verma, M.A. Lampson, Q. Cai, E.S. Robertson, Kaposi's sarcoma-associated herpesvirus-encoded LANA can interact with the nuclear mitotic apparatus protein to regulate genome maintenance and segregation, J. Virol. 82 (2008) 6734–6746.
[94] A. Houdusse, A.P. Carter, Dynein swings into action, Cell 136 (2009) 395–396.
[95] T. Kon, K. Imamula, A.J. Roberts, R. Ohkura, P.J. Knight, I.R. Gibbons, S.A. Burgess, K. Sutoh, Helix sliding in the stalk coiled coil of dynein couples ATPase and microtubule binding, Nat. Struct. Mol. Biol. 16 (2009) 325–333.
[96] A.P. Carter, J.E. Garbarino, E.M. Wilson-Kubalek, W.E. Shipley, C. Cho, R.A. Milligan, R.D. Vale, I.R. Gibbons, Structure and functional role of dynein's microtubule-binding domain, Science 322 (2008) 1691–1695.
[97] L. McNaughton, I. Tikhonenko, N.K. Banavali, D.M. LeMaster, M.P. Koonce, A low affinity ground state conformation for the dynein microtubule binding domain, J. Biol. Chem. 285 (2010) 15994–16002.
[98] H. Imai, A. Narita, T.A. Schroer, Y. Maeda, Two-dimensional averaged images of the dynactin complex revealed by single particle analysis, J. Mol. Biol. 359 (2006) 833–839.
[99] P.S. Vaughan, P. Miura, M. Henderson, B. Byrne, K.T. Vaughan, A role for regulated binding of p150(Glued) to microtubule plus ends in organelle transport, J. Cell Biol. 158 (2002) 305–319.

[100] B.A. Ballif, J. Villen, S.A. Beausoleil, D. Schwartz, S.P. Gygi, Phosphoproteomic analysis of the developing mouse brain, Mol. Cell. Proteomics 3 (2004) 1093–1101.
[101] N. Dephoure, C. Zhou, J. Villen, S.A. Beausoleil, C.E. Bakalarski, S.J. Elledge, S.P. Gygi, A quantitative atlas of mitotic phosphorylation, Proc. Natl. Acad. Sci. USA 105 (2008) 10762–10767.
[102] H. Li, X.S. Liu, X. Yang, B. Song, Y. Wang, X. Liu, Polo-like kinase 1 phosphorylation of p150Glued facilitates nuclear envelope breakdown during prophase, Proc. Natl. Acad. Sci. USA 107 (2010) 14633–14638.
[103] J.V. Olsen, M. Vermeulen, A. Santamaria, C. Kumar, M.L. Miller, L.J. Jensen, F. Gnad, J. Cox, T.S. Jensen, E.A. Nigg, S. Brunak, M. Mann, Quantitative phosphoproteomics reveals widespread full phosphorylation site occupancy during mitosis, Sci. Signal. 3 (2010).
[104] C. Munch, R. Sedlmeier, T. Meyer, V. Homberg, A.D. Sperfeld, A. Kurt, J. Prudlo, G. Peraus, C.O. Hanemann, G. Stumm, A.C. Ludolph, Point mutations of the p150 subunit of dynactin (DCTN1) gene in ALS, Neurology 63 (2004) 724–726.
[105] C. Munch, A. Rosenbohm, A.D. Sperfeld, I. Uttner, S. Reske, B.J. Krause, R. Sedlmeier, T. Meyer, C.O. Hanemann, G. Stumm, A.C. Ludolph, Heterozygous R1101K mutation of the DCTN1 gene in a family with ALS and FTD, Ann. Neurol. 58 (2005) 777–780.
[106] A.P. Carter, R.D. Vale, Communication between the AAA^{+} ring and microtubule-binding domain of dynein, Biochem. Cell Biol. 88 (2010) 15–21.

In this chapter

20

Roles of Cytoplasmic Dynein During Mitosis

Kevin T. Vaughan
Department of Biological Sciences, University of Notre Dame, Notre Dame, IN, USA

20.1 Introduction

Cytoplasmic dynein is an abundant microtubule motor protein implicated widely in intracellular transport. A role for dynein as a mitotic motor for chromosome movement has been considered for decades. However, investigations into mitotic dynein activity have intensified recently with the development of new model systems, the identification of dynein binding partners, and the use of genetic and siRNA screens.

In contrast to other mitotic motor proteins that display some degree of cell-cycle-stage-specific expression, dynein does not appear to change in abundance or subunit composition across the cell cycle. Also in contrast to some other proteins, dynein does not appear to contain mitosis-specific isoforms of key subunits. The core dynein holoenzyme is thought to contain a pair of catalytic heavy chains (HCs), intermediate chains (ICs), and light-intermediate chains (LICs) in addition to a series of three distinct light chain (LC) dimers. The HCs encode the motor activity of the complex, whereas the remaining subunits are arranged at the base of the motor to mediate cargo binding [1]. In addition to these core proteins, a panel of accessory proteins including LIS-1 [2], nudE/EL [3], nudC [4], and dynactin [5,6,7] have been shown to modulate dynein activity.

Despite its apparent lack of complexity at the genetic or protein levels, dynein is more functionally diverse than any other mitotic microtubule motor protein examined to date (Fig. 20.1). At the cell cortex, dynein is thought to interact with astral microtubules for spindle rotation [8,9], spindle centering [10], and the generation of tension through the spindle poles [11]. At spindle poles, dynein plays a crucial role in delivering newly synthesized components to the microtubule-organizing centers (MTOCs) [12]. Dynein also links interdigitating microtubules within the spindle and tethers kinetochore fibers to microtubules projected from each centrosome [13,14]. Finally, dynein is prominent at kinetochores, where roles in microtubule capture [15], regulation of the angle of

Dyneins DOI: 10.1016/B978-0-12-382004-4.10020-2
Copyright © 2012 by Elsevier Inc. All rights reserved.

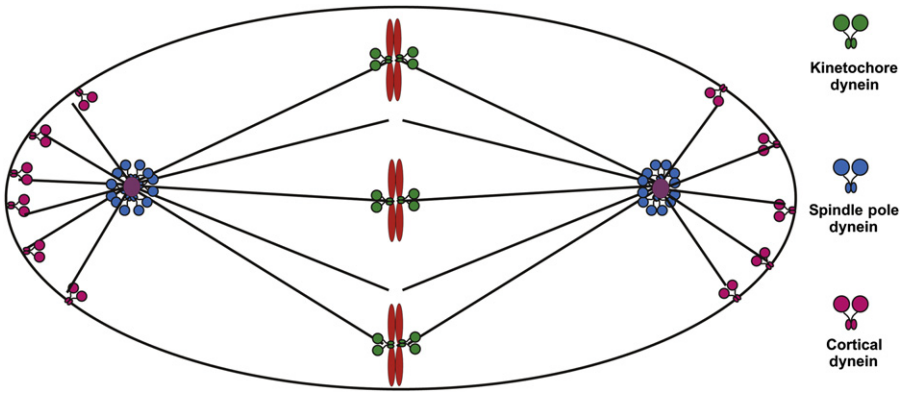

Figure 20.1 Complexity of cytoplasmic dynein localizations during mitosis. Dynein has been implicated in essential functions at kinetochores, spindle poles, and the cell cortex. Although the timing of these localizations can be somewhat shifted, inhibition of each population impairs mitotic progress.

microtubule attachment [16], chromosome movement [17], and checkpoint protein transport [18,19,20] have each been proposed. The mechanisms that allow dynein to participate in such a wide range of activities are currently unclear. This chapter summarizes what is known about this question and proposes novel models for functional complexity.

20.2 Model Systems of Mitotic Dynein

Budding yeasts have provided a broad foundation of work on mitotic dynein, taking advantage of mutants in dynein subunits, dynactin subunits, and homologs of other dynein accessory proteins. Although roles for dynein at kinetochores and spindle poles in budding yeast have not been eliminated completely, the specificity of mutant phenotypes for spindle positioning supports a primary role in linking the astral microtubule to the cell cortex [8,21,22]. The ability of cortically anchored dynein to capture astral microtubules and draw the spindle through the bud neck is thought to be shared with cortical dynein function in higher eukaryotes. Particularly interesting is the fact that cortical dynein is thought to be targeted to the cell cortex through a novel "off-loading" model [23]. Because this behavior has not been observed in other systems, further work will be needed to test the off-loading model in other cell types. Less work on dynein has been completed in fission yeast, although recent studies suggest that *Schizosaccharomyces pombe* dynein might function at kinetochores and spindle pole bodies [24].

Genetic screens in filamentous fungi (*Aspergillus nidulans* and *Neurospora crassa*) were largely responsible for the identification of many dynein accessory proteins

[25,26]. Because dynein is required for nuclear dispersal in growing hyphae, dynein mutants induce the *nud* [25] or *ropy* [26] phenotypes, where accumulations of nuclei are apparent. Subsequently, this analysis of nuclear translocation and microtubule anchoring has been extended to models of nuclear translocation in neurons [27]. More specific roles for dynein in mitotic spindle elongation have been studied in the corn pathogen *Ustilago maydis* [28,29].

An initial advantage of the use of *Caenorhabditis elegans* was a systematic siRNA screen that identified roles for dynein in pronuclear migration and spindle positioning [10,30]. Subsequently, analysis of kinetochore function has also proven possible [31]. Similarly, *Drosophila* mutants have contributed broadly to our understanding of mitotic dynein [17,20,32]. In some cases, fly mutants in eye development reflect defective function in dynein or dynein accessory proteins [33,34]. In others, fly embryos provide an elegant model system for imaging [32].

Several vertebrate model systems have paved the way for progress in dissecting mitotic dynein. *Xenopus* egg extracts have been used extensively to study spindle assembly and the roles of dynein in organizing and focusing microtubules in mitotic spindles [35,36]. One tool in these studies has been the depletion of specific dynein subunits or accessory proteins. For imaging of mitotic dynein, cultured cell lines have been a workhorse system. Cultured cells provide the advantages of simplified imaging, synchronization, transfection of plasmid constructs, and siRNA/shRNA.

Our understanding of mitotic dynein function reflects the integration of work from each of these model systems. What emerges is a daunting list of activities that either require dynein or are augmented by dynein.

20.3 Spindle Pole Dynein

As cells move from G2 into M phase, the first prominent population of mitotic dynein resides at the spindle poles. This is consistent with a role for dynein in transporting newly synthesized protein to the MTOCs for proper function [12]. Although this aspect of dynein function is not unique to mitosis, the localization of dynein to the duplicated spindle poles is striking prior to nuclear envelope breakdown and precedes any substantial accumulation of mitotic dynein to the cell cortex or kinetochores. Among the proteins undergoing transport to the spindle poles are pericentrin [37] and NUMA [14,38].

As the spindle poles migrate to opposite sides of the nuclear envelope during prophase, independent radial microtubule arrays begin to form together with the incorporation of existing microtubules into these arrays [39]. The pattern of dynein localization extends outside the centrosomes somewhat during this period [9,40], perhaps reflecting additional populations of dynein that are associated with the overlapping microtubules (Fig. 20.2). The dynein co-factor dynactin

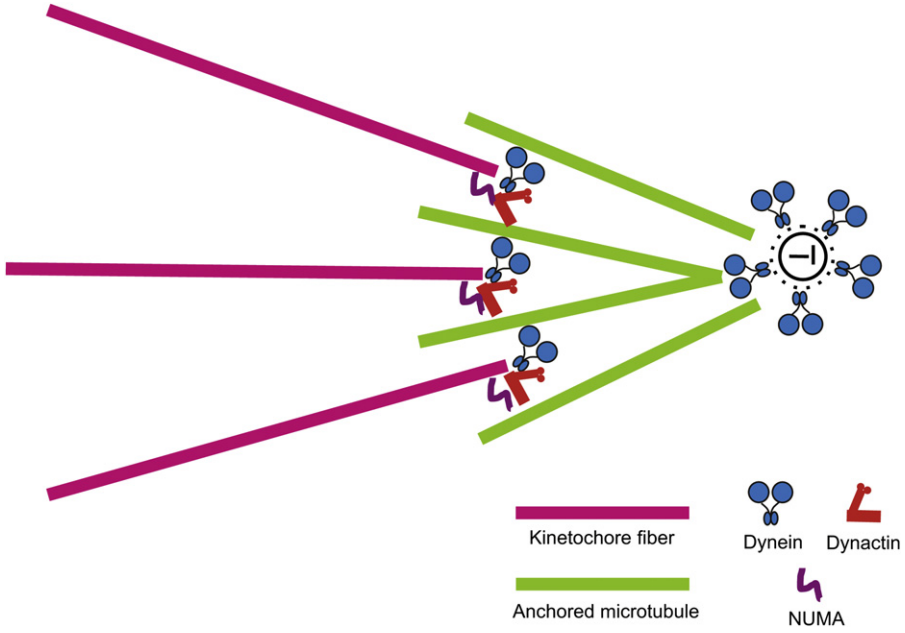

Figure 20.2 Overlapping populations of dynein at mitotic spindle poles. Dynein consistently localizes to the centrosome proper and mimics γ-tubulin. However dynein also localizes to the developing spindle pole, where it is proposed to function with dynactin and NUMA to link kinetochore fibers to microtubules nucleating from the MTOCs.

mimics this pattern of dynein accumulation [41,42]. Consistently with this model, a trimerix complex of dynein, dynactin, and NUMA is thought to tether and crosslink microtubules to each spindle pole [14,43]. Additional proteins such as CEP215 [44], RHAMM [45], and CDK5RAP2 [46] are likely to affect dynein localization as well.

The significance of the spindle pole localization for dynein is complicated by the overlapping roles dynein plays as a motile complex transporting MTOC components and a more static complex crosslinking microtubules (Fig. 20.2). Elegant studies in *Xenopus* egg extracts allow some separation of these functions. Spindles formed in the absence of dynein failed to focus tightly [35], reflecting the ability of dynein–dynactin–NUMA to interact with multiple microtubules simultaneously. This model is also supported by dynein inhibition in mammalian cells [13].

Once bipolar spindles have formed and the centrosomes of the spindle poles have separated somewhat from tightly focused kinetochore fibers, the distinction between these two populations of dynein becomes blurred. This is complicated further after kinetochore dynein becomes activated for pole-ward motility near metaphase. This leads to prominent spindle labeling that overlaps with spindle poles and centrosomes [19]. The specific signatures of each population at this stage are not known. Future work will need to focus on markers that allow the analysis of individual dynein subsets within these mixtures.

20.4 Cortical Dynein

During progression through mitosis, the next population of dynein that is considered functions at the cell cortex. This population has been very challenging to image and was originally predicted based on the abnormal behavior of microtubules in budding-yeast dynein null mutants [8]. This dynein subset has been detected subsequently in higher eukaryotes [9,47,48]; however, molecular signatures for this population remain unknown.

The primary functions for cortical dynein are to interact with astral microtubules and to position the spindle (Fig. 20.3). In budding yeast, cortical dynein is most important in the bud, where pulling forces are used to draw the spindle into the bud neck. In mammalian systems, cortical dynein interacts with astral microtubules from both spindle poles to rotate the spindle along the long axis of the cell [9]. Depending on the model system, cortical dynein is also thought to mediate the positioning of the spindle in the cell center for symmetric division, or towards one pole for asymmetric division. Because the ultimate location of the cytokinetic cleavage plane is closely related to spindle position, this aspect of dynein activity is crucial for accurate cell cleavage.

Cortical dynein is also widely thought to function in concert with Eg5 to mediate spindle elongation during anaphase B [11,49]. Our current knowledge of cortical

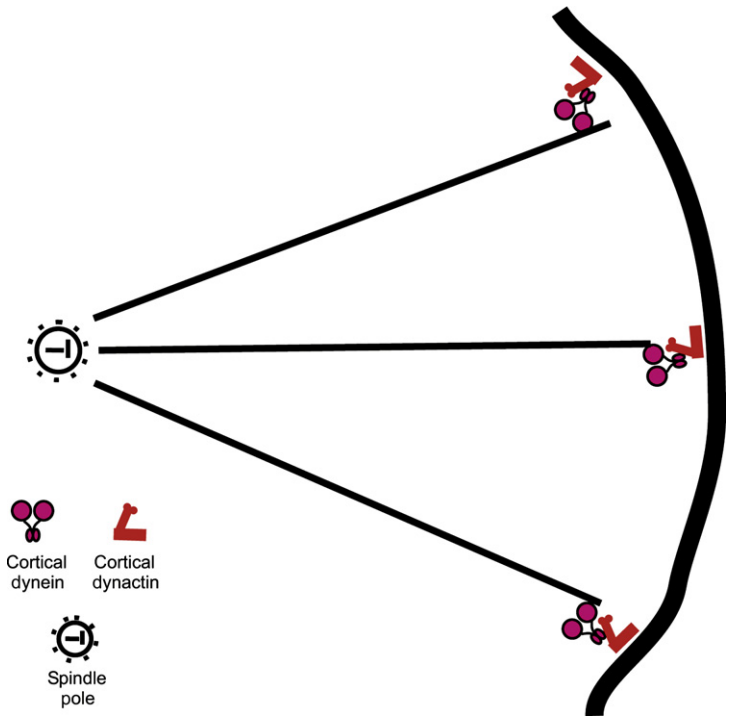

Figure 20.3 Localization of mitotic dynein to the cell cortex. Although more difficult to image than other populations, cortical dynein is proposed to tether astral microtubules and mediate microtubule pulling forces. These activities allow dynein to drive spindle rotation and positioning.

dynein benefits from genetic work in budding yeast where cortical-binding partners have been identified. Cortical dynein is delivered to the bud cortex through the coordinated actions of microtubule tip-tracking proteins and plus-end-directed motors. An elegant off-loading process has been described to explain how dynein is attached to the cortical surface [50]. Fewer details are known about cortical dynein in higher eukaryotes, and the plus-end-directed delivery model remains under investigation. Clues into cortical dynein targeting have emerged in non-mitotic systems [51], raising the possibility that mitotic dynein targeting shares a similar mechanism. Clearly more work will be needed to understand how cortical dynein differs from other dynein populations. Insights into the specific functions of cortical dynein will also require methods to separate this subset from other forms of dynein at spindle poles and kinetochores.

20.5 Kinetochore Dynein

Most of our knowledge about kinetochore dynein emerges from work in higher eukaryotes, including *Drosophila*, *C. elegans*, and mammalian cell lines. Although there is some evidence for kinetochore dynein activity in fission yeast, work in budding yeast suggests that dynein is not involved in microtubule capture, chromosome movement, or checkpoint signaling. Consistent with this model, dynein is not detected at kinetochores during intranuclear yeast mitosis.

In metazoans, dynein is detected at kinetochores only after nuclear envelope breakdown [52,53] and it is proposed to play a direct role in nuclear envelope breakdown itself [54]. Initial antibody staining studies revealed prominent accumulation from nuclear envelope breakdown to metaphase [42,52,53]. There is consensus from subsequent studies that dynein is no longer prominent at kinetochores after the metaphase–anaphase transition. However, live-imaging studies in *Drosophila* suggest some accumulation during anaphase [32]. This aspect of kinetochore dynein function has been confusing until recently because dynein was initially proposed to be the dominant-minus-end-directed motor for anaphase chromosome movement [55,56]. More recent studies have suggested alternative functions for kinetochore dynein that are more important during prometaphase.

These include initial microtubule capture [17,57], correcting inappropriate microtubule attachments [16], achieving biorientation, and early aspects of congression [17,57]. Late in prometaphase, dynein is thought to function primarily in the silencing of the spindle assembly checkpoint [18–20]. This is achieved by disassembling the outer kinetochore scaffold through pole-ward transport. By physically translocating these proteins from the kinetochores towards spindle poles, dynein is proposed to disrupt the local environment at kinetochores required for activation of anaphase inhibitors (i.e. mad2). It is also possible that dynein provides the mechanical force for this disassembly. Consistently with this model, inhibition of dynein-driven transport allows continued production of anaphase inhibitors at metaphase and a delay in anaphase onset or

metaphase arrest [19,42]. Although existing probes do not reveal significant amounts of dynein at kinetochores after anaphase onset in mammalian systems, it remains unclear whether this reflects a loss of detection or a loss of accumulation. Given the dynamics of recruitment and release for proteins in the fibrous corona, it is also unclear whether the platform for dynein recruitment continues to assemble after anaphase onset.

A number of proteins have been identified as dynein-binding proteins at kinetochores, including dynactin [41,42], LIS-1 [47], nudE/EL [58], nudC [59], zw10 [19,57,60], and spindly [31,61–63]. Some of these proteins are proposed to recruit dynein initially to kinetochores. Consistently with this model, depletion of these proteins using dominant-negative mutants or siRNA/shRNA reveals reduction in the total levels of dynein at kinetochores. One complication is that some of these components are responsible for recruiting others. *Zw10*, for example, is thought to be required for the recruitment of dynactin [64], spindly [61], and dynein [19]. Thus, depletion of *zw10* affects dynein interactions at multiple levels.

Another complication is that the specific function of these candidates is not understood completely. Dynactin was proposed initially to recruit dynein to kinetochores [42]; however, dynactin is also associated with dynein undergoing motility [6,19]. NudE/EL and LIS-1 have been studied recently in regulating the persistence of microtubule binding under conditions approaching stall force [65]. The specific contributions of nudC [59] and spindly [31,61,62,66] remain under investigation. Given this complexity of dynein-binding proteins at kinetochores, it remains unclear whether all of these proteins play a role in recruiting dynein to kinetochores or whether they each play a different role. It is also possible that multiple populations of dynein exist at kinetochores and each is recruited independently. This could explain how a single version of dynein could be coordinated to execute so many functions.

Potentially explaining some of this complexity, a mitotic phosphorylation site was identified recently in the dynein ICs that is required for recruitment to kinetochores [19]. The phosphorylated form of dynein binds directly to the checkpoint protein *zw10* and is prominent throughout prometaphase. This interaction is independent of dynactin. However, after chromosomes become bioriented and begin to align at the metaphase plate, this dynein undergoes dephosphorylation, which is mediated by PP1γ. Dephosphorylation of dynein allows binding to shift to dynactin, a transition that is linked to the pole-ward transport implicated in checkpoint silencing. Consistently with this model, depletion of kinetochore dynactin through p50 (dynamitin) expression or inhibition of PP1γ both result in a loss of dynein-driven checkpoint silencing and metaphase arrest [19].

In this context, it is interesting that depletion of most of the candidate binding partners for dynein elicit the same metaphase arrest or delay. Spindly depletion induces metaphase arrest across multiple model systems. Dominant-negative

LIS-1 and NudE/EL constructs also delay anaphase onset. This suggests that these proteins play an important role in activating the motile form of dynein at metaphase, which is the form required for checkpoint silencing. Only one of these candidates, *zw10*, produces a different effect after depletion. Loss of *zw10* induces premature anaphase onset [67,68], an outcome thought to reflect the inability to produce sufficient quantities of anaphase inhibitors during prometaphase. Consistently with this idea, the RZZ complex is thought to recruit mad2 to kinetochores [69]. Interestingly, *zw10* depletion also blocks the recruitment of dynein to kinetochores [19,60]. This raises the possibility that dynein contributes to the structural requirements for checkpoint activation. However, additional work will be needed to test this possibility.

As a result of these studies, a new explanation for the complexity of dynein binding proteins at kinetochores could be that dynein interacts sequentially with proteins that regulate dynein for specific steps in a pathway. Current data suggest that dynein is recruited to kinetochores through the interaction with *zw10* and

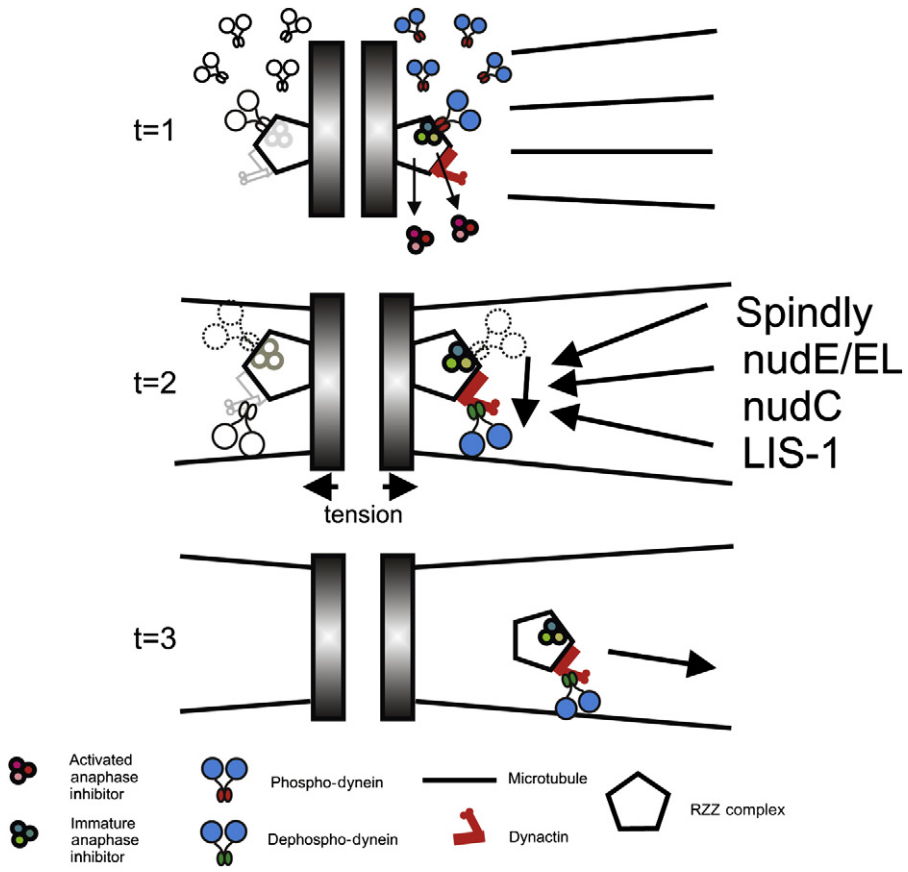

Figure 20.4 Sequential contributions of dynein binding proteins at kinetochores. A new model for the complexity of dynein binding partners at kinetochores is supported by recent studies that suggest dynein is recruited by an interaction with *zw10* but subsequently leaves through an interaction with dynactin. This new model predicts that the remaining dynein binding partners contribute to molecular transitions and the activation of dynein for motility.

leaves the kinetochore in a complex with dynactin [19]. The events between these "bookend" events remain unclear (Fig. 20.4). A number of predicted functions are not yet accounted for. The transition in binding from *zw10* to dynactin, for example, is likely to involve an intermediate state in which dynein is temporarily bound to neither. How is dynein retained at kinetochores during this transition? Does dynein produce force continuously at kinetochores across all the events in prometaphase or is dynein activated as a motor under the appropriate conditions? Which proteins are responsible for sensing these conditions and activating dynein? Finally, it remains possible that independent populations of dynein exist at kinetochores with distinct functions. New experiments to inhibit specific forms of dynein will be required to test this model.

20.6 Phosphorylation

Although extensive isoform or subunit heterogeneity does not appear to provide an explanation for the diversity of dynein functions during mitosis, some promising clues emerge from analysis of post-translation modifications. Mitotic phosphorylation of dynein, for example, has been detected across multiple model systems. The dynein ICs are consistent targets for phosphorylation in X*enopus* egg extracts [70] and mammalian cells [19]. The dynein LICs are also phosphorylated in models of mitosis [71–73]; however, phosphorylation-dependent binding partners or localizations have not been reported. Some of the dynein LCs are known to be phosphorylated [74], but the functions of this phosphorylation are not known. Comprehensive MS/MS analysis of mitotic dynein reveals phosphorylation of dynein HCs as well [75], but these MS/MS studies require some additional work for function to be ascertained. Given the advances that have resulted from analysis of kinetochore dynein and phosphorylation, it is likely that subunit-specific phosphorylation will explain some of the functional diversity of mitotic dynein. The signaling pathways and targeting mechanisms that explain this phosphorylation will be very important.

20.7 Future Questions

One of the challenges in studying dynein at each mitotic site is that there is some functional overlap between each population. Disruption of spindle pole dynein, for example, is likely to affect other populations of dynein, thereby complicating interpretation. The molecular signatures that define each subset need to be better understood before we can make progress. Specific tools to disrupt one population without affecting others will also be very powerful.

20.8 Conclusions

Mitotic dynein performs a wide range of functions, distinguishing this motor from other mitotic motor proteins. The specific contributions of each dynein

population are being deciphered, but more work will be required before the critical experiments can be performed. Among the unresolved questions are: (1) What are the functions of site-specific accessory proteins? And (2) what aspect of dynein complexity explains site-specific targeting? New technologies and strategies are beginning to solve these problems.

References

[1] R.D. Vale, The molecular motor toolbox for intracellular transport, Cell 112 (2003) 467–480.

[2] X. Xiang, A.H. Osmani, S.A. Osmani, M. Xin, N.R. Morris, *NudF*, a nuclear migration gene in *Apsergillus nidulans*, is similar to the Human LIS-1 gene required for neuronal migration, Mol. Biol. Cell 6 (1995) 297–310.

[3] V.P. Efimov, N.R. Morris, The LIS1-related NUDF protein of *Aspergillus nidulans* interacts with the coiled-coil domain of the NUDE/RO11 protein, J. Cell Biol. 150 (2000) 681–688.

[4] S.M. Morris, U. Albrecht, O. Reiner, G. Eichele, L. Yu-Lee, The lissencephaly gene product Lis1, a protein involved in neuronal migration, interacts with a nuclear movement protein, NudC, Current Biology 8 (1998) 603–606.

[5] T.A. Schroer, M.P. Sheetz, Two activators of microtubule-based vesicle transport, J. Cell Biol. 115 (1991) 1309–1318.

[6] S.R. Gill, T.A. Schroer, I. Szilak, E.R. Steuer, M.P. Sheetz, D.W. Cleveland, Dynactin, a conserved, ubiquitously expressed component of an activator of vesicle motility mediated by cytoplasmic dynein, J. Cell Biol. 115 (1991) 1639–1650.

[7] E.L. Holzbaur, J.A. Hammarback, B.M. Paschal, N.G. Kravit, K.K. Pfister, R.B. Vallee, Homology of a 150K cytoplasmic dynein-associated polypeptide with the Drosophila gene Glued, Nature 351 (1991) 579–583. Erratum appears in Nature 360(6405), 695(1992).

[8] J.L. Carminati, T. Stearns, Microtubules orient the mitotic spindle in yeast through dynein-dependent interactions with the cell cortex, J. Cell Biol. 138 (1997) 629–641.

[9] C.B. O'Connell, Y.L. Wang, Mammalian spindle orientation and position respond to changes in cell shape in a dynein-dependent fashion, Mol. Biol. Cell 11 (2000) 1765–1774.

[10] P. Gonczy, S. Pichler, M. Kirkham, A.A. Hyman, Cytoplasmic dynein is required for distinct aspects of MTOC positioning, including centrosome separation, in the one cell stage *Caenorhabditis elegans* embryo, J. Cell Biol. 147 (1999) 135–150.

[11] E.A. Vaisberg, M.P. Koonce, J.R. McIntosh, Cytoplasmic dynein plays a role in mammalian mitotic spindle formation, J. Cell Biol. 123 (1993) 849–858.

[12] A. Young, J.B. Dictenberg, A. Purohit, R. Tuft, S.J. Doxsey, Cytoplasmic dynein-mediated assembly of pericentrin and gamma tubulin onto centrosomes, Mol. Biol. Cell 11 (2000) 2047–2056.

[13] T. Gaglio, M.A. Dionne, D.A. Compton, Mitotic spindle poles are organized by structural and motor proteins in addition to centrosomes, J. Cell Biol. 138 (1997) 1055–1066.

[14] T. Gaglio, A. Saredi, D.A. Compton, NuMA is required for the organization of microtubules into aster-like mitotic arrays, J. Cell Biol. 131 (1995) 693–708.

[15] T.J. Mitchison, M.W. Kirschner, Properties of the kinetochore *in vitro*. II. Microtubule capture and ATP-dependent translocation, J. Cell Biol. 101 (1985) 766–777.

[16] D. Varma, P. Monzo, S.A. Stehman, R.B. Vallee, Direct role of dynein motor in stable kinetochore-microtubule attachment, orientation, and alignment, J. Cell Biol. 182 (2008) 1045–1054.

[17] M.S. Savoian, M.L. Goldberg, C.L. Rieder, The rate of poleward chromosome motion is attenuated in *Drosophila* zw10 and rod mutants, Nat. Cell Biol. 2 (2000) 948–952.

[18] B.J. Howell, B.F. McEwen, J.C. Canman, D.B. Hoffman, E.M. Farrar, C.L. Rieder, E.D. Salmon, Cytoplasmic dynein/dynactin drives kinetochore protein transport to the spindle poles and has a role in mitotic spindle checkpoint inactivation, J. Cell Biol. 155 (2001) 1159–1172.

[19] J. Whyte, J.R. Bader, S.B. Tauhata, M. Raycroft, J. Hornick, K.K. Pfister, W.S. Lane, G.K. Chan, E.H. Hinchcliffe, P.S. Vaughan, K.T. Vaughan, Phosphorylation regulates targeting of cytoplasmic dynein to kinetochores during mitosis, J. Cell Biol. 183 (2008) 819–834.

[20] E. Wojcik, R. Basto, M. Serr, F. Scaerou, R. Karess, T. Hays, Kinetochore dynein: Its dynamics and role in the transport of the Rough deal checkpoint protein, Nat. Cell Biol. 3 (2001) 1001–1007.

[21] N.R. Adames, J.A. Cooper, Microtubule interactions with the cell cortex causing nuclear movements in *Saccharomyces cerevisiae*, J. Cell Biol. 149 (2000) 863–874.

[22] D. Eshel, L.A. Urrestarazu, S. Vissers, J.C. Jauniaux, J.C. van Vliet-Reedijk, R.J. Planta, I.R. Gibbons, Cytoplasmic dynein is required for normal nuclear segregation in yeast, Proc. Natl. Acad. Sci. USA 90 (1993) 11172–11176.

[23] L. Lee, J.S. Tirnauer, J. Li, S.C. Schuyler, J.Y. Liu, D. Pellman, Positioning of the mitotic spindle by a cortical-microtubule capture mechanism, Science 287 (2000) 2260–2262.

[24] E.L. Grishchuk, I.S. Spiridonov, J.R. McIntosh, Mitotic chromosome biorientation in fission yeast is enhanced by dynein and a minus-end-directed, kinesin-like protein, Mol. Biol. Cell 18 (2007) 2216–2225.

[25] X. Xiang, S.M. Beckwith, N.R. Morris, Cytoplasmic dynein is involved in nuclear migration in *Aspergillus nidulans*, Proc. Natl. Acad. Sci. USA 91 (1994) 2100–2104.

[26] M. Plamann, P.F. Minke, J.H. Tinsley, K.S. Bruno, Cytoplasmic dynein and actin-related protein Arp1 are required for normal nuclear distribution in filamentous fungi, J. Cell Biol. 127 (1994) 139–149.

[27] J.W. Tsai, K.H. Bremner, R.B. Vallee, Dual subcellular roles for LIS1 and dynein in radial neuronal migration in live brain tissue, Nat. Neurosci. 10 (2007) 970–979.

[28] G. Fink, I. Schuchardt, J. Colombelli, E. Stelzer, G. Steinberg, Dynein-mediated pulling forces drive rapid mitotic spindle elongation in *Ustilago maydis*, EMBO J. 25 (2006) 4897–4908.

[29] G. Fink, G. Steinberg, Dynein-dependent motility of microtubules and nucleation sites supports polarization of the tubulin array in the fungus *Ustilago maydis*, Mol. Biol. Cell 17 (2006) 3242–3253.

[30] B. Sonnichsen, L.B. Koski, A. Walsh, P. Marschall, B. Neumann, M. Brehm, A.M. Alleaume, J. Artelt, P. Bettencourt, E. Cassin, M. Hewitson, C. Holz, M. Khan, S. Lazik, C. Martin, B. Nitzsche, M. Ruer, J. Stamford, M. Winzi, R. Heinkel, M. Roder, J. Finell, H. Hantsch, S.J. Jones, M. Jones, F. Piano, K.C. Gunsalus, K. Oegema, P. Gonczy, A. Coulson, A.A. Hyman, C.J. Echeverri, Full-genome RNAi profiling of early embryogenesis in *Caenorhabditis elegans*, Nature 434 (2005) 462–469.

[31] R. Gassmann, A. Essex, J.S. Hu, P.S. Maddox, F. Motegi, A. Sugimoto, S.M. O'Rourke, B. Bowerman, I. McLeod, J.R. Yates 3rd, K. Oegema, I.M. Cheeseman, A. Desai, A new mechanism controlling kinetochore-microtubule interactions revealed by comparison of two dynein-targeting components: SPDL-1 and the Rod/Zwilch/Zw10 complex, Genes Dev. 22 (2008) 2385–2399.

[32] D.J. Sharp, G.C. Rogers, J.M. Scholey, Cytoplasmic dynein is required for poleward chromosome movement during mitosis in drosophila embryos, Nat. Cell Biol. 2 (2000) 922–930.

[33] A. Swaroop, M.L. Paco-Larson, A. GarenDustin, P., Molecular genetics of a transposon-induced dominant mutation in the *Drosophila* locus glued, Proc. Natl. Acad. Sci. USA 82 (1985) 1751–1755.

[34] M. McGrail, J. Gepner, A. Silvanovich, S. Ludmann, M. Serr, T.S. Hays, Regulation of cytoplasmic dynein function *in vivo* by the *Drosophila* Glued complex, J. Cell Biol. 131 (1995) 411–425.

[35] R. Heald, R. Tournebize, T. Blank, R. Sandaltzopoulos, P. Becker, A. Hyman, E. Karsenti, Self-organization of microtubules into bipolar spindles around artificial chromosomes in *Xenopus* egg extracts, Nature 382 (1996) 420–425.
[36] R. Heald, R. Tournebize, A. Habermann, E. Karsenti, A. Hyman, Spindle assembly in *Xenopus* egg extracts: Respective roles of centrosomes and microtubule self-organization, J. Cell Biol. 138 (1997) 615–628.
[37] A. Purohit, S.H. Tynan, R. Vallee, S.J. Doxsey, Direct interaction of pericentrin with cytoplasmic dynein light intermediate chain contributes to mitotic spindle organization, J. Cell Biol. 147 (1999) 481–492.
[38] A. Merdes, K. Ramyar, J.D. Vechio, D.W. Cleveland, A complex of NuMA and cytoplasmic dynein is essential for mitotic spindle assembly, Cell 87 (1996) 447–458.
[39] N.M. Rusan, U.S. Tulu, C. Fagerstrom, P. Wadsworth, Reorganization of the microtubule array in prophase/prometaphase requires cytoplasmic dynein-dependent microtubule transport, J. Cell Biol. 158 (2002) 997–1003.
[40] N.J. Quintyne, S.R. Gill, D.M. Eckley, C.L. Crego, D.A. Compton, T.A. Schroer, Dynactin is required for microtubule anchoring at centrosomes, J. Cell Biol. 147 (1999) 321–334.
[41] B.M. Paschal, E.L. Holzbaur, K.K. Pfister, S. Clark, D.I. Meyer, R.B. Vallee, Characterization of a 50-kDa polypeptide in cytoplasmic dynein preparations reveals a complex with p150GLUED and a novel actin, J. Biol. Chem. 268 (1993) 15 318–15 323.
[42] C.J. Echeverri, B.M. Paschal, K.T. Vaughan, R.B. Vallee, Molecular characterization of the 50-kD subunit of dynactin reveals function for the complex in chromosome alignment and spindle organization during mitosis, J. Cell Biol. 132 (1996) 617–633.
[43] A. Merdes, R. Heald, K. Samejima, W.C. Earnshaw, D.W. Cleveland, Formation of spindle poles by dynein/dynactin-dependent transport of NuMA, J. Cell Biol. 149 (2000) 851–862.
[44] S. Lee, K. Rhee, CEP215 is involved in the dynein-dependent accumulation of pericentriolar matrix proteins for spindle pole formation, Cell Cycle 9 (2010) 774–783.
[45] C.A. Maxwell, J.J. Keats, M. Crainie, X. Sun, T. Yen, E. Shibuya, M. Hendzel, G. Chan, L.M. Pilarski, RHAMM is a centrosomal protein that interacts with dynein and maintains spindle pole stability, Mol. Biol. Cell 14 (2003) 2262–2276.
[46] A.R. Barr, J.V. Kilmartin, F. Gergely, CDK5RAP2 functions in centrosome to spindle pole attachment and DNA damage response, J. Cell Biol. 189 (2010) 23–39.
[47] N.E. Faulkner, D.L. Dujardin, C.Y. Tai, K.T. Vaughan, C.B. O'Connell, Y. Wang, R.B. Vallee, A role for the lissencephaly gene LIS1 in mitosis and cytoplasmic dynein function, Nat. Cell Biol. 2 (2000) 784–791.
[48] D.L. Dujardin, R.B. Vallee, Dynein at the cortex, Curr. Opin. Cell Biol. 14 (2002) 44–49.
[49] W.S. Saunders, D. Koshland, D. Eshel, I.R. Gibbons, M.A. Hoyt, *Saccharomyces cerevisiae* kinesin- and dynein-related proteins required for anaphase chromosome segregation, J. Cell Biol. 128 (1995) 617–624.
[50] W.L. Lee, M.A. Kaiser, J.A. Cooper, The offloading model for dynein function: Differential function of motor subunits, J. Cell Biol. 168 (2005) 201–207.
[51] A.F. Palazzo, H.L. Joseph, Y.J. Chen, D.L. Dujardin, A.S. Alberts, K.K. Pfister, R.B. Vallee, G.G. Gundersen, Cdc42, dynein, and dynactin regulate MTOC reorientation independent of Rho-regulated microtubule stabilization, Curr. Biol. 11 (2001) 1536–1541.
[52] C.M. Pfarr, M. Coue, P.M. Grissom, T.S. Hays, M.E. Porter, J.R. McIntosh, Cytoplasmic dynein is localized to kinetochores during mitosis, Nature 345 (1990) 263–265.
[53] E.R. Steuer, L. Wordeman, T.A. Schroer, M.P. Sheetz, Localization of cytoplasmic dynein to mitotic spindles and kinetochores, Nature 345 (1990) 266–268.
[54] D. Salina, K. Bodoor, D.M. Eckley, T.A. Schroer, J.B. Rattner, B. Burke, Cytoplasmic dynein as a facilitator of nuclear envelope breakdown, Cell 108 (2002) 97–107.
[55] C.L. Rieder, S.P. Alexander, Kinetochores are transported poleward along a single astral microtubule during chromosome attachment to the spindle in newt lung cells, J. Cell Biol. 110 (1990) 81–95.

[56] C.L. Rieder, The formation, structure, and composition of the mammalian kinetochore and kinetochore fiber, Int. Rev. Cytol. 79 (1982) 1–58.
[57] Z. Yang, U.S. Tulu, P. Wadsworth, C.L. Rieder, Kinetochore dynein is required for chromosome motion and congression independent of the spindle checkpoint, Curr. Biol. 17 (2007) 973–980.
[58] S.A. Stehman, Y. Chen, R.J. McKenney, R.B. Vallee, NudE and NudEL are required for mitotic progression and are involved in dynein recruitment to kinetochores, J. Cell Biol. 178 (2007) 583–594.
[59] T. Zhou, W. Zimmerman, X. Liu, R.L. Erikson, A mammalian NudC-like protein essential for dynein stability and cell viability, Proc. Natl. Acad. Sci. USA 103 (2006) 9039–9044.
[60] G.J. Kops, Y. Kim, B.A. Weaver, Y. Mao, I. McLeod, J.R. Yates 3rd, M. Tagaya, D.W. Cleveland, ZW10 links mitotic checkpoint signaling to the structural kinetochore, J. Cell Biol. 169 (2005) 49–60.
[61] E.R. Griffis, N. Stuurman, R.D. Vale, Spindly, a novel protein essential for silencing the spindle assembly checkpoint, recruits dynein to the kinetochore, J. Cell Biol. 177 (2007) 1005–1015.
[62] Y.W. Chan, L.L. Fava, A. Uldschmid, M.H. Schmitz, D.W. Gerlich, E.A. Nigg, A. Santamaria, Mitotic control of kinetochore-associated dynein and spindle orientation by human Spindly, J. Cell Biol. 185 (2009) 859–874.
[63] M. Barisic, B. Sohm, P. Mikolcevic, C. Wandke, V. Rauch, T. Ringer, M. Hess, G. Bonn, S. Geley, Spindly/CCDC99 is required for efficient chromosome congression and mitotic checkpoint regulation, Mol. Biol. Cell 21 (2010) 1968–1981.
[64] D.A. Starr, B.C. Williams, T.S. Hays, M.L. Goldberg, ZW10 helps recruit dynactin and dynein to the kinetochore, J. Cell Biol. 142 (1998) 763–774.
[65] R.J. McKenney, M. Vershinin, A. Kunwar, R.B. Vallee, S.P. Gross, LIS1 and NudE induce a persistent dynein force-producing state, Cell 141 (2010) 304–314.
[66] R. Gassmann, A.J. Holland, D. Varma, X. Wan, F. Civril, D.W. Cleveland, K. Oegema, E.D. Salmon, A. Desai, Removal of Spindly from microtubule-attached kinetochores controls spindle checkpoint silencing in human cells, Genes Dev. 24 (2010) 957–971.
[67] R. Basto, R. Gomes, R.E. Karess, Rough deal and Zw10 are required for the metaphase checkpoint in *Drosophila*, Nat. Cell Biol. 2 (2000) 939–943.
[68] R.E. Karess, D.M. Glover, Rough deal: A gene required for proper mitotic segregation in *Drosophila*, J. Cell Biol. 109 (1989) 2951–2961.
[69] E. Buffin, C. Lefebvre, J. Huang, M.E. Gagou, R.E. Karess, Recruitment of Mad2 to the kinetochore requires the Rod/Zw10 complex, Curr. Biol. 15 (2005) 856–861.
[70] C.Y. Huang, C.P. Chang, C.L. Huang, J.E. Ferrell Jr., M phase phosphorylation of cytoplasmic dynein intermediate chain and p150(Glued), J. Biol. Chem. 274 (1999) 14262–14269.
[71] K.R. Dell, C.W. Turck, R.D. Vale, Mitotic phosphorylation of the dynein light intermediate chain is mediated by cdc2 kinase, Traffic 1 (2000) 38–44.
[72] S.G. Addinall, P.S. Mayr, S. Doyle, J.K. Sheehan, P.G. Woodman, V.J. Allan, Phosphorylation by cdc2-CyclinB1 kinase releases cytoplasmic dynein from membranes, J. Biol. Chem. 276 (2001) 15939–15944.
[73] M.V. Sivaram, T.L. Wadzinski, S.D. Redick, T. Manna, S.J. Doxsey, Dynein light intermediate chain 1 is required for progress through the spindle assembly checkpoint, EMBO J. 28 (2009) 902–914.
[74] C. Song, W. Wen, S.K. Rayala, M. Chen, J. Ma, M. Zhang, R. Kumar, Serine 88 phosphorylation of the 8-kDa dynein light chain 1 is a molecular switch for its dimerization status and functions, J. Biol. Chem. 283 (2008) 4004–4013.
[75] H. Daub, J.V. Olsen, M. Bairlein, F. Gnad, F.S. Oppermann, R. Korner, Z. Greff, G. Keri, O. Stemmann, M. Mann, Kinase-selective enrichment enables quantitative phosphoproteomics of the kinome across the cell cycle, Mol. Cell 31 (2008) 438–448.

In this chapter

21

Does Dynein Influence the Non-Mendelian Inheritance of Chromosome 17 Homologs in Male Mice?

Stephen H. Pilder
Department of Anatomy and Cell Biology, Temple University School of Medicine, Philadelphia, PA, USA

21.1 Introduction

Modern mouse *t*-haplotypes are closely related members of a family of inversion polymorphisms of the proximal one-third of chromosome 17 (the *t*-complex). These variants descended from a common ancestor ~10 000–100 000 years ago and presently exist at a relatively low equilibrium frequency in feral populations of all subspecies of the *Mus musculus* species complex [1]. All family members are characterized by four nearly-region-spanning, non-overlapping, megabase-pair inversions relative to the wild-type (+) form of the region (Fig. 21.1) [2]. Because these inversions suppress recombination between + and *t*, the progeny of a +/*t*-heterozygous parent usually receives either *t* or + en bloc.

Intriguingly, males, but not females, heterozygous for a *t*-haplotype transmit the variant *t*-homolog to >95% of their progeny, a phenotype known as transmission ratio distortion (TRD) or meiotic drive. The huge selective advantage in favor of the driving *t*-chromosome is offset by a number of forces, the two most often cited being: (1) most *t*-haplotypes carry recessive embryonic lethal mutations and (2) males homozygous for a non-lethal *t*-haplotype (t^X/t^X) or doubly heterozygous for two complementing lethal *t*-haplotypes (t^X/t^Y) are consistently sterile [3,4].

The *t*-haplotypes were discovered over eighty years ago, yet for most of that time this large chromosomal expanse has hidden its most fascinating secrets – the identities of the genes that cause the non-Mendelian inheritance of *t* from +/*t*-heterozygous males and the sterility of *t*/*t*-males – in its nearly impenetrable inversions. Nonetheless, just prior to the era of genomics and proteomics, Lyon [4,5] elucidated the genetic basis of *t*-related male TRD and sterility by following the effects on chromosomal transmission and fertility of males carrying a series of

Dyneins DOI: 10.1016/B978-0-12-382004-4.10021-4
Copyright © 2012 by Elsevier Inc. All rights reserved.

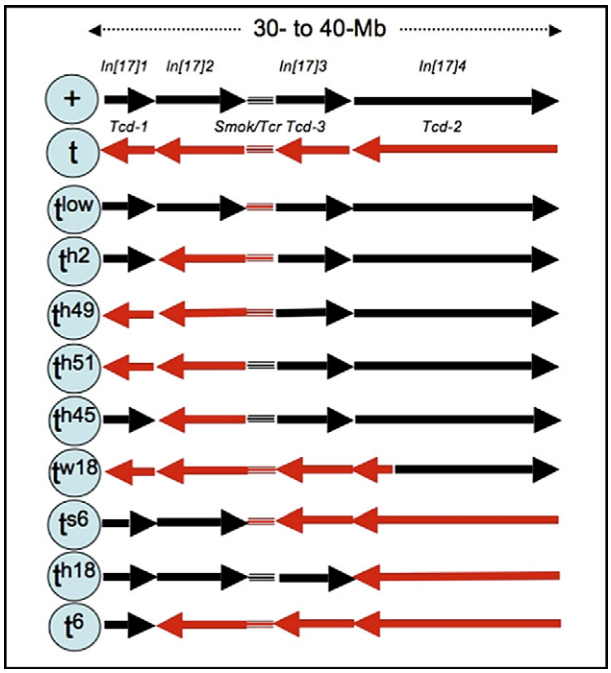

Figure 21.1 Organization of complete and partial *t*-haplotypes. Centromeric regions are denoted by circles on the left side of the diagram with the name of each chromosome indicated within the circle (+ denotes wild-type chromosome 17, *t* indicates a complete *t*-haplotype, and *t* followed by a superscript indicates a partial *t*-haplotype). Black bars indicate +-DNA, red bars, *t*-DNA, and arrowheads represent the relative orientation of inverted segments of chromatin in + versus *t*. The positions of inversions 1–4 (*In[17]1-In[17]4*) are shown above the wild-type chromosome and the locations of distorters (*Tcd1–3*) and *Smok/Tcr* are indicated between the wild-type and complete *t*-haplotype regional representations. The uninverted *Smok* and *Tcr* loci are represented by either a black or red triplicate of lines without arrows, respectively. Inversions and the *Smok/Tcr* region are drawn approximately to scale.

rare recombinants between +- and *t*-homologs known as partial *t*-haplotypes (Fig. 21.1). The result of Lyon's labor was a cogent hypothesis that proposed a model containing the following tenets: (1) TRD occurs only when the *t*-allele of a cis-acting factor called the *t*-complex responder (Tcr) is present heterozygously; (2) the *t*-alleles of three both cis- and trans-acting factors of varying strengths called *t*-complex distorters (Tcds) operate additively on the Tcr to drive the transmission of whatever chromosome is carrying the *t*-allele of Tcr to higher levels; (3) if Tcd^ts are absent, the chromosome containing Tcr^t is transmitted to only 10–20% of the progeny; (4a) homozygosity for Tcd-2^t or (4b) heterozygosity for Tcd-2^t plus homozygosity for Tcd-1^t (and thus lack of appropriate complementing wild-type function) causes male sterility (in the case of (4b), the specific combination of *t*-alleles causes profound subfertility, rather than absolute sterility as in (4a)); and (5) *Tcr* maps centrally in the *t*-complex, *Tcd-1* is near its

proximal end, *Tcd-2* is located distally, and *Tcd-3* maps between *Tcr* and *Tcd-2* (Fig. 21.1). Together, these findings suggested that the *Tcr* alleles are expressed during the haploid phase of spermatogenesis (spermiogenesis) and are somehow retained in the cell of origin, despite the fact that male germ cells derived from the same stem cell (spermatogonium) develop in a syncitium that allows the transfer of mRNAs and proteins between daughter cells. This implies that the allelic nature of *Tcr* determines the fate of each daughter cell, since it is assumed that they are otherwise identical.

High resolution marker mapping studies at the dawn of the genomics era [2] placed *Tcd-1* in the centromeric inversion (*In[17]1*), *Tcd-3* in the middle inversion (*In[17]3*), *Tcd-2* in the large distal inversion (*In[17]4*), and *Tcr* in a small uninverted region of the *t*-complex between *In[17]2* and *In[17]3* (Fig. 21.1). Additionally, Silver and Olds-Clarke [6] demonstrated that, unlike other known cases of male meiotic drive, where the wild-type chromosome-carrying spermatid is destroyed during development, equal quantities of +-homolog-carrying and *t*-homolog-carrying sperm from +/*t*-males are present in the female uterus 90 min after coitus. The consensus conclusion derived from these data is that the function of the +-carrying sperm produced by a +/*t*-heterozygous male must be relatively more defective in its capacity to fertilize than the *t*-carrying sperm produced by the same male.

Following this logic, Olds-Clarke and Johnson [7] published a comprehensive study of the effects of complete *t*-haplotypes on sperm function in fertilization. Cauda epididymal (mature) sperm from +/+, t^X/+, t^Y/+, and t^X/t^Y males were incubated in either *in vitro* fertilization medium minus the addition of exogenous calcium (IVF−, a minimal medium that does not support fertilization *in vitro*) or a medium that does support fertilization *in vitro* (IVF, a minimal medium containing 1.7 mM added Ca^{2+}). Three key events that measure the fertilizing capacity of sperm − hyperactivated motility (a type of vigorous but non-linear flagellar movement required for fertility), *in vitro* capacitation (the ability to undergo the acrosome reaction quickly when challenged by zona pellucida proteins), and the spontaneous acrosome reaction − were determined over a 4 h time course and compared between genotypes. As expected, no significant difference between genotypes for these three important calcium-dependent events was observed in IVF− medium. However, in IVF medium, sperm from t^X/+, t^Y/+, and t^X/t^Y males exhibited only minor differences from sperm produced by +/+ males in their ability to capacitate and spontaneously undergo acrosomal exocytosis, yet highly significant differences in the initiation and maintenance of the hyperactivated state of motility: after 1 h in IVF medium, nearly 60% of spermatozoa from t^X/+ and t^Y/+ males exhibited hyperactivated motility, compared to a high of about 35% of sperm from +/+ males at 2 h of incubation. Quantitatively, the +/*t*-precocious hyperactivation phenotype was attributable to a rapid decline in linearity to ultra-low t^X/t^Y levels, accompanied by a more gradual drop in curvilinear velocity (or vigorous movement) to a mean

approximately half way between the means of wild-type and t^X/t^Y levels by 4 h of incubation. However, the flagella of nearly all sperm from t^X/t^Y males demonstrated premature hyperactivation by 5 min of incubation, although this flagellar phenotype abruptly ended as a precipitous decline in vigor accompanying the constant, abnormally low level of linearity ensued. Additionally, the flagella of 90–95% of the motile sperm from t^X/t^Y males became "frozen" in an aberrant curvature phenotype called "curlicue," a chronic negative bend throughout the entire flagellum (Fig. 21.2A, B). The movement of these sperm resembled little more than non-rhythmic twitching in place, producing slow circular swimming.

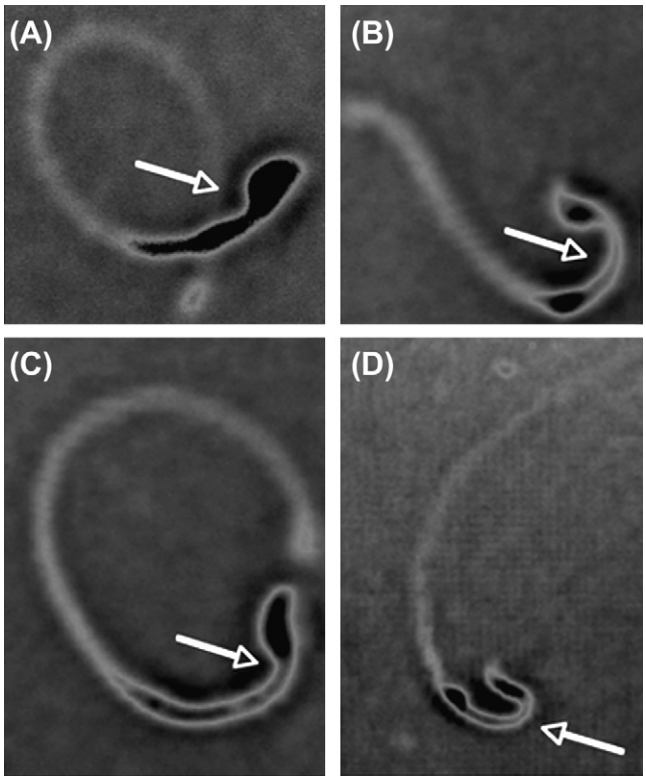

Figure 21.2 The "curlicue" and "fishhook" flagellar curvature phenotypes. High-speed (Adobe Photoshop "solarized") photographs captured from videotapes recorded at 30 frames per second of motile t^X/t^Y-sperm (A,B) and $+/t$-sperm (C,D) swimming in an 80 μm-deep slide chamber in complete IVF medium. The lightly minced caudae epididymides of test males were incubated at 37°C in 5% CO_2 in air for 15 min to allow sperm to swim out of the caudae. After removal of epididymal tissue, sperm were incubated for an additional 15 min in fresh media before videotaping for 5 min on slides maintained at 37°C. Arrows indicate that the bend of the middle piece of $+/t$-sperm is generally more acute than that of t^X/t^Y-sperm. However, it is noteworthy that both forms of curvature are always negative (direction of curvature of the flagellum is always opposite to the direction of curvature of the sperm head). The chronic nature of this one-sided curvature suggests that both phenotypes may result from defects in the ability of dyneins to promote a recovery stroke.

Interestingly, from the earliest time point and beyond, an increasingly high percentage of the flagella of sperm from $t^X/+$ and $t^Y/+$ mice exhibited a flagellar curvature phenotype called "fishhook" (Fig. 21.2C, D), in which the middle piece of the flagellum displayed an almost chronic negative bend while the principal piece displayed nearly normal curvature, with abnormal bending occurring only infrequently in that portion of the flagellum. The abnormality of this phenotype, however, had more to do with its premature occurrence rather than the occurrence itself, since wild-type sperm flagella display a fishhook-like phenotype when the axonemal free Ca^{2+} concentration rises to high levels [8].

Surprisingly, membrane-minus flagella of sperm from $+/t$ males reactivated in calcium-containing medium had been shown to display a negative curvature phenotype significantly more rapidly than the membrane-minus, reactivated flagella of sperm from $+/+$ males [9]. Taken together, these results suggested that the altered motility of sperm produced by *t*-bearing males was a calcium-dependent phenomena and that the calcium hypersensitive element(s) were intrinsic to the axonemal and/or periaxonemal structures of the mouse sperm tail.

Independent studies 14 years apart also revealed that, at early time points (up to 2 h of incubation in IVF medium), the swimming speed, path shape, and flagellar beat frequency of sperm populations from $+/t$ males were bimodally distributed [7,10]: one peak was closer to the unimodal peak of sperm from $+/+$ males, which exhibited vigorous, progressive motility and a consistent beat pattern, while the other was closer to the unimodal peak of sperm from t^X/t^Y males, which displayed slow, non-progressive motility, with no regular beat configuration. These data tied TRD to altered sperm motility, with half of the sperm population (presumed to be the *t*-sperm population) exhibiting relatively better flagellar function than the other half (presumed to be the $+$-sperm population).

Armed with convincing models of the genetic and functional bases of *t*-related male TRD and sterility, plus technological advances in physical gene mapping and analysis, investigators began a series of systematic searches for the elusive Tcr and Tcd factors. Several of these studies were published somewhat before the final determination that altered flagellar function was most likely at the heart of *t*-TRD and male sterility, primarily relying on novel differential cDNA subtraction, transcription, and sequence analyses to compare $+$- and *t*-alleles of genes physically linked to either the large *Tcr* or *Tcd* loci via restriction fragment length polymorphisms. Interestingly, among the first Tcd candidates isolated by these techniques were two flagellar dynein light chains (LCs) (although their identities as such did not become apparent until later), aptly named *t*-complex testis expressed-1 and -2 (*Tctex1* and *Tctex2*), mapping to the *Tcd-1* and *Tcd-3* loci (Fig. 21.3), respectively [11–13]. These early investigations were followed by a string of studies that employed mice heterozygous for a *t*-haplotype and a series of interspecific recombinant chromosome 17 homologs (*S*-$+$ homologs), which were either able or unable to rescue the flagellar phenotypes associated

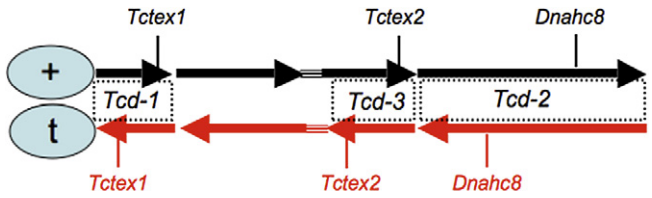

Figure 21.3 The location of three axonemal dynein subunits in the *t*-complex. +- and *t*-chromosomes are shown as in Figure 21.1, and the relative positions of *Tctex1*, *Tctex2* (inner- and outer-arm LCs, respectively), and *Dnahc8*, a unique, principal piece-specific outer-arm γ HC subunit, are indicated.

with *t*/*t*-male sterility. Therefore, mice carrying various *S*-+/*t* chromosome 17 genotypes were employed to map the key factors responsible for the curlicue phenotype within two sub-megabase regions of the large *Tcd-2* locus [14–18]. The first of three genes localized in this way was identified as *Dnahc8* (Fig. 21.3), a gene encoding a sperm-specific γ-type axonemal outer-dynein-arm heavy chain (HC), restricted to the flagellar principal piece in mice and (putatively) in other mammals [19–22].

The following sections summarize some of the properties of these three dynein subunits (in addition to their physical map locations) that for nearly 15 years have supported the idea that dyneins influence TRD.

21.2 Properties of *Tctex1*

Tctex1 (*Dynlt1*), the first member of a family of structurally homologous dynein LCs, maps to the *Tcd-1* locus in the most proximal *t*-inversion (*In[17]1*). Though it was unknown at the time of its identification, *Tctex1* is represented in wild-type *In [17]1* as five genes encoding identical proteins (Ensembl Genome Database, NCBI m37 Mouse Assembly). Though the number of *t*-haplotype copies has not yet been elucidated, the *t*-protein is homologous in sequence and identical in length to its wild-type counterpart (Fig. 21.4A). Regardless of gene number, the steady-state level of $Tctex1^{t}$ mRNA is four-fold that of $Tctex1^{+}$ mRNA in the testis. In addition, *Tctex1* is expressed at a higher level in the testis than in other tissues [13].

Although first characterized as a LC subunit of brain cytoplasmic dynein 1 [23], Tctex1 was subsequently localized to the dimeric axonemal inner dynein arm I1 in the flagella of *Chlamydomonas reinhardtii* and also to the mouse sperm tail [24]. Significantly, recent findings have demonstrated that inner-arm I1 appears to play a central regulatory role in coordinating flagellar beating and determining waveform in response to signals transduced from the central pair of axonemal microtubules through the radial spokes of the axoneme [25,26]. More recently, an additional *Chlamydomonas* sequence homolog of *Tctex1* was shown to be a dynein LC (LC9) bound to the intermediate chains (ICs) of the outer dynein arm [27]. The data from deletion mutants strongly suggest that its absence has a negative effect on flagellar beat frequency.

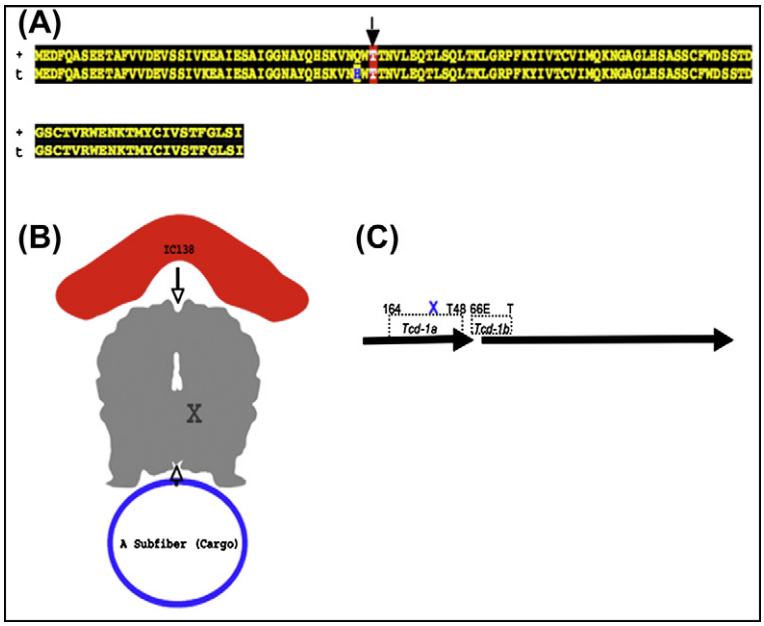

Figure 21.4 ***Tctex1* sequence, structure, and location in *Tcd-1a*.** (A) Upper sequence representing five wild-type copies of *Tctex1* is shown aligned to the *t*-amino acid sequence below. The *t*-sequence closely aligns with the wild-type sequence Tctex1−1 except for three amino acid changes, only one of which is considered likely to have an effect on function (shown as a blue letter on a yellow background). The threonine whose phosphorylation status might be affected by this change is shown in all three proteins as a white letter on a red background and indicated by the vertical arrow. (B) A freehand sketch of one view of the solution structure of dimeric Tctex1 (gray); from [29] with arrows above and below pointing at the location of the intermonomer groove between them. The picture indicates that the dimer binds an IC (above) and interacts directly with cargo (below) at opposite poles. The "X" marks the location of the Q→H mutation in the *t*-haplotype protein. (C) Division of *Tcd-1* into *Tcd-1a* and *Tcd-1b*, with *Tctex1* (blue "X") located in the former sublocus. The approximate boundaries of these loci are: *D17Mit164* (*164*) proximally and *D17Leh48* (*T48*) distally for *Tcd-1a*, and *D17Leh66E* proximally and the locus of *Brachyury* (*T*) for *Tcd-1b*.

In late 1999, Herrmann and colleagues identified *Tcr* and demonstrated that it encoded a fusion product of sperm motility kinase 1 (*Smok1*) and another unrelated kinase [28] whose expression was spermiogenesis-specific. Almost six years later, but before any *Tcd* had been positively identified, the solution structure of Tctex1 was solved [29], revealing that dimeric Tctex1 is most likely bound to both the "cargo" subunit of axonemal microtubule doublets (the A subfiber) and to the dynein intermediate chain IC138 at opposite ends of the Tctex1 dimer (Fig. 21.4B). Interestingly, a single mutation (out of three) in Tctex1^{t} ($Q_{41}H$) alters a highly conserved residue that is exposed close to the intermonomer groove (Fig. 21.4A). This mutation directly abuts an exposed serine in the *Chlamydomonas* Tctex1 structure (a threonine in mouse Tctex1), producing a potential new target for phosphorylation. Additionally, during the time interval between the

identification of *Tcr* and solving the structure of Tctex1, analysis of chromosomal deletions of, within, and surrounding the *Tcd-1* locus suggested that: (1) Tcd-1 was a hypomorph or amorph [30] and (2) the locus could be divided into at least two subloci (Fig. 21.4C): *Tcd-1a* (possibly containing *Tctex1* near its distal end) and a more distal *Tcd-1b* sublocus [31,32].

21.3 Properties of *Tctex2*

Tctex2 (*Tcte3*) was first identified in the same cDNA subtractive screening experiment in which *Tctex1* was isolated [13]. Subsequent mapping studies placed it in the proximal end of *In[17]4* [11], but higher-resolution mapping and sequencing has since positioned it distally in *In[17]3* (Ensembl Genome Database, NCBI m37 Mouse Assembly).

Initially, *Tctex2* was described as a gene(s) encoding a membrane-associated protein found exclusively on the surface of the sperm tail [12], but its identity as a structural homolog of Tctex1 and an outer-arm axonemal dynein LC (LC2) in *Chlamydomonas* flagella was later demonstrated [33]. Unlike *Tctex1*, the *t*-haplotype form of *Tctex2* shows an abnormally low level of mRNA expression, and its sequence contains numerous in-frame but potentially deleterious mutations [12]. In addition, targeted deletion of *Tctex2* in *Chlamydomonas* results in the loss of outer-dynein-arm assembly and subsequent ultra-slow, jerky flagellar movement. Moreover, these deletion mutants fail to appropriately respond to photoshock, a calcium-dependent property of the outer dynein arm consisting of backward swimming in response to intense light [34]. Thus, although untested, it is possible that the multiple amino acid changes in the Tctex2^{t} may have a calcium-sensitive gain-of-function (hypermorphic) effect.

Interestingly, in wild-type mouse chromosome 17, *Tctex2* is present in three nearly identical copies (Fig. 21.5), each separated from the next more-distal copy by a distance of approximately 17 kb. Homozygous deletion of the most proximal copy results in several incompletely penetrant phenotypes, including sterility due to asthenozoospermia in some cases and poor sperm motility in others [35]. These poorly motile sperm exhibit an inability to move from the uterus into the oviduct, previously demonstrated to be a deficiency of sperm from males carrying two *t*-haplotypes [36].

21.4 Properties of *Dnahc8*

Interspecific recombinant chromosome 17 homolog mapping was initially employed to determine the origin, number, and extent of the *t*-inversions [2]. Two useful byproducts of these experiments were: (1) *Mus musculus* males heterozygous for an introgressed chromosome 17 homolog (*S*; from the aboriginal mouse species, *Mus spretus*) and the endogenous wild-type chromosome 17 homolog (+) were fertile (*S*/+ males), while *Mus musculus* males

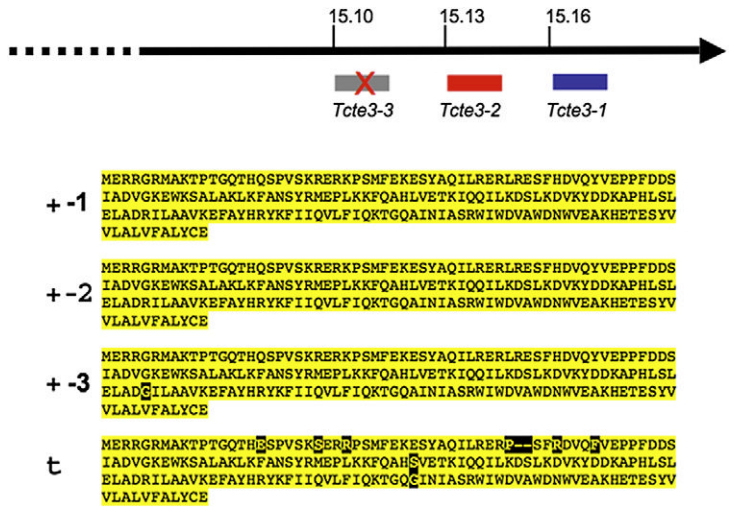

Figure 21.5 Physical map location of wild-type paralogs of *Tctex2* (*Tcte3*) and comparison of the +- and *t*-sequences. (Top) Physical map positions of three wild-type paralogs of *Tctex2* in *In[17]3*. Numbers are in megabase pairs from the centromere and all three genes are transcribed toward the centromere. The red "X" in *Tcte3-3* indicates that it has undergone homozygous deletion from the genome by targeted disruption [35] resulting in incompletely penetrant sperm motility and azoospermia (due to increased testicular apoptosis) phenotypes but no other notable problems. (Bottom) comparison of the amino-acid sequences of the wild-type (+) and *t*-haplotype (*t*) homologs of *Tctex2* demonstrating numerous potentially deleterious mutations in the *t*-homolog (yellow letters on a black background).

heterozygous for the *S*-chromosome 17 homolog and the endogenous chromosome 17 *t*-variant were, without exception, sterile (*S*/*t* males); and (2) the *S*-homolog and the +-homolog were capable of recombination at wild-type rates in the three inversions that housed the *Tcd* loci. Thus, males heterozygous for a large assortment of *S*-+ recombinant chromosome 17 homologs and a complete *t*-haplotype were employed in breeding studies to map *t*-sterility loci within large inversions to a high resolution [15–18,37–39].

Motility of sperm from sterile recombinants was assessed quantitatively by computer-assisted sperm motility analysis (CASA) and high-resolution video microscopy. Physical mapping of recombinant breakpoints from informative chromosome 17 homologs eventually led to the identification of three factors that together appeared to cause male sterility, precocious hyperactivation and curlicue in ~95% of motile sperm flagella. Each factor was mapped to a sub-megabase region of the distal one-third of $In[17]4^{+}$ (Fig. 21.6A), with the most proximal of these containing the axonemal dynein HC, *Dnahc8* [20,40–42]. Interestingly, the *S*-allele of *Dnahc8* turned out to be a null allele in the *Mus musculus* background, suggesting that the hemizygous (or homozygous) $Dnahc8^{t}$ allele was a major cause of flagellar dysfunction in male $Tcd\text{-}2^{t}$ *homozygotes*.

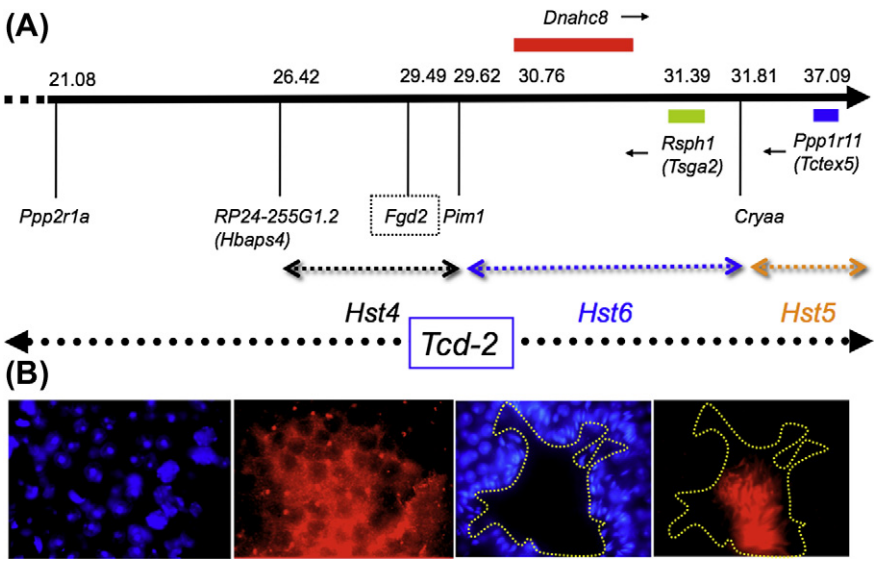

Figure 21.6 Physical map location of *Dnahc8* in *In[17]4* and expression of DNAHC8 in the testis. (A) *Dnahc8* is located in the proximal half of the *Hst6* locus between *Fgd2*, located in the *Hst4* locus, and *Rsph1*, located more distally in the *Hst6* locus. The *Hst6* locus plus the *Hst5* locus have been subdivided into three subloci (*curlicueA*, *curlicueB1*, and *curlicueB2* [40]), based on the location of a trio of genes whose *t*-alleles are thought to be responsible for expression of the "curlicue" phenotype (*Dnahc8*, *Rsph1*, and *Ppp1r11* [41]). (B) Immunohistochemistry of wild-type testis sections probed with an affinity-purified antibody raised against a portion of the unique N-terminal extension of DNAHC8. In panels 1 and 3 from the left, DAPI staining has been utilized to show nuclear morphology. Immunofluorescent localizations of DNAHC8 in panels 2 and 4 (sections showing earlier and later stages of spermatid development, respectively) demonstrate intense, punctate fluorescence over the region of round spermatids approximately where flagellar growth would originate in panel 2, and equally intense fluorescence in the center of the lumen of a seminiferous tubule section in panel 4, an area where the principal piece of sperm tails resides. The dashed yellow borders in panels 3 and 4 define the outer boundaries of the lumen.

Sequence analysis of *Dnahc8*$^{+}$ demonstrated that the mRNA was composed of 93 exons totaling more than 14 kb, within a genomic region of over 250 kb. Phylogenetic analysis of the computer-generated translation product of this message demonstrated that DNAHC8 was most closely related to the *Chlamydomonas* axonemal outer-dynein-arm γ-HC. Both $+/+$ and t/t mice produced two alternatively spliced transcripts, the more abundant one coding for a protein of 4732 amino acids and the less abundant and less stable transcript encoding a C-terminally truncated protein of 4203 residues [21,22].

Expression of the gene was testis specific, and transcription of both $+$- and *t*-alleles occurred exclusively in late pachytene primary and secondary spermatocytes. Translation was also specific to these cells, as mRNAs were not observed in round or elongating spermatids by *in situ* hybridization [21]. Both $+$- and *t*-polypeptides were visualized by immunohistochemistry and immunocytochemistry of the testis and cauda epididymal sperm, respectively, and were

shown to localize to the cytoplasm of pachytene spermatocytes, the tail bud in round spermatids, and the principal piece of the flagellum in testicular and cauda epididymal sperm (Fig. 21.6B). These findings demonstrated that, at least in mammals, the subunits of the outer dynein arm are not identical from the base to the tip of the tail [22].

Significantly, comparative sequence analysis of isolated *t*- and +-cDNAs indicated that the *t*-message contains 17 non-synonymous mutations scattered throughout the protein, several coding for non-conservative changes at otherwise highly conserved residues in all mammalian genomes thus far annotated [22]. Of particular interest were two mutations, one ($P_{3408}T$) occurring at the end of the outward α-helical branch of the anti-parallel coiled-coil stalk upon which sits the ATP-dependent microtubule-binding site. This mutation aligns with a residue formerly reported to play a significant role in ATP-dependent microtubule binding in cytoplasmic dyneins and thus could affect microtubule translocation [22,43].

The second mutation of interest ($G_{127}R$) occurs at the N-terminus of the most highly conserved region of the unique mammalian DNAHC8 N-terminal extension [21,22]. The exchange of arginine for what is always a hydrophobic residue in all annotated wild-type mammalian DNAHC8 orthologous protein sequences creates a PKC phosphorylation target of a completely conserved flanking serine/threonine residue (S_{129} in mouse). This serine resides just upstream of a highly conserved serine-/arginine-/lysine-rich region and an IQ calmodulin-binding motif (Fig. 21.7A). While yet untested, it is possible that phosphorylation of S_{129} might alter the conformation of the region and thus modify the behavior of the downstream IQ motif, potentially affecting the way in which a (putative) calmodulin LC (LC4 in *Chlamydomonas*) binds to DNAHC8 and/or interacts with the A subfiber of the outer microtubule doublet [44,45].

The DNAHC8 N-terminal 167-amino-acid sequence is completely unrelated to any region found in any other dynein, and the N-terminal 75% of the mouse sequence appears to be similar only to the orthologous sequences in mammals. Interestingly, in mouse DNAHC8, the first $\sim$60 residues of the N-terminus are 25% glu/asp (mostly glu) and $\sim$36% pro with no basic residues. This sequence has similarity in its proline content and position to a region of GAPDS known to anchor it to the fibrous sheath of mammalian sperm [46]. While the significance of this feature is unknown at this time, it is tempting to speculate that the unique N-terminus of DNAHC8 has a role in targeting this HC and the dynein particle to which it belongs to the developing principal piece of the sperm tail where the fibrous sheath, a mammalian-specific periaxonemal structure [47], resides [15,16]. More importantly, Smok/Tcr has been recently localized exclusively to the principal piece of the sperm tail by immunocytochemical approaches using both light and transmission electron microscopy, where it appears to be linked to both the longitudinal columns and circumferential ribs of the fibrous sheath and

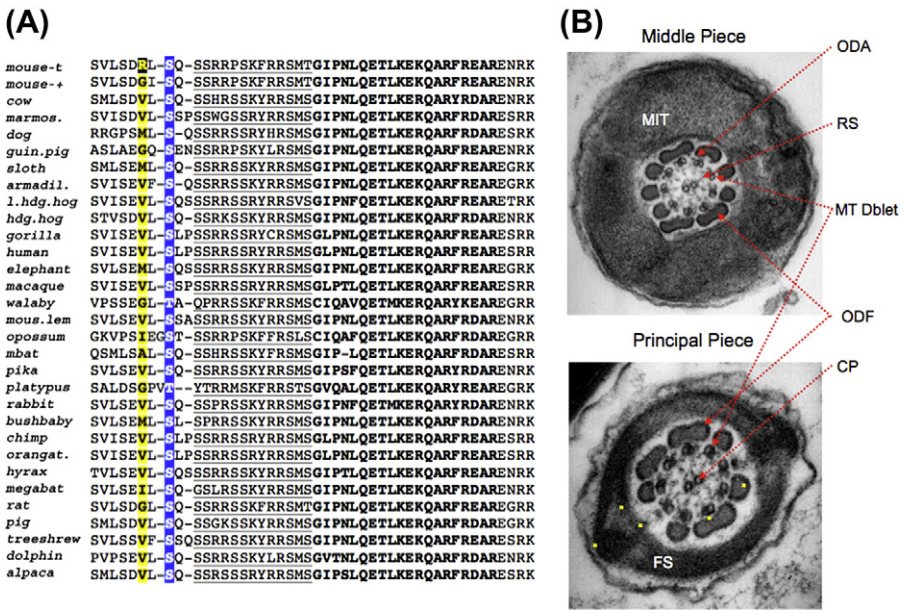

Figure 21.7 The unique N-terminal region of mammalian DNAHC8. (A) The first mutation in DNAHC8^{t} is a non-conservative change at the N-terminus of the most highly conserved region of the unique DNAHC8 N-terminal extension. This region contains a serine-/arginine-/lysine-rich sequence (underlined) upstream of a putative IQ calmodulin-binding motif (bold lettering). At the very N-terminus of this sequence, there is less conservation, but certain amino acids retain specific character traits in all annotated mammalian proteomes. An alignment of the *t*-haplotype sequence with the wild-type mouse sequence and 29 additional annotated mammalian sequences demonstrates that the first mutation in DNAHC8^{t} occurs at a residue that is always hydrophobic in wild-type orthologs (black letters on yellow background), and changes this residue (a glycine in the case of the +-mouse sequence) to an arginine (yellow letters on black background). Bioinformatic analyses of this change with numerous programs indicate that the change would promote phosphorylation by a protein kinase C-like enzyme of a completely conserved serine/threonine (white letters on blue background) two amino acids (in the mouse) downstream of the $G_{127}R$ mutation. The effect of this mutation, if any, has not been ascertained, but it is tempting to speculate that a conformational change related to such a phosphorylation event could have a deleterious effect on any interaction of the downstream IQ motif with a calmodulin LC. (B) Transmission electron micrographs of cross-sections through the middle piece (top) and principal piece (bottom) of the mammalian sperm tail. MIT corresponds to the mitochondrial sheath, a middle-piece-specific periaxonemal structure, and FS indicates the fibrous sheath, a principal-piece-specific periaxonemal structure. Other structures found throughout the flagellum: CP, central pair of singlet microtubules; MT Dblet, microtubule doublet; ODA, outer dynein arms; ODF, outer dense fibers; RS, radial spokes. Both DNAHC8 and Smok/Tcr localize specifically to structures in the principal piece, with the yellow dots indicating sites of Smok/Tcr localization in the FS, ODF, and between the ODF and outer doublet microtubules, putatively in the vicinity of the N-terminus of DNAHC8 at the base of the outer dynein arm.

the inner surface of the outer dense fibers (Fig. 21.7B), adjacent to the outer doublet microtubules of the axoneme, close to the outer dynein arms [48].

21.5 Chromosomal Deletion Analysis Modifies Lyon's Model

Lyon predicted that homozygosity for distorters was the basis for male sterility [4]. In support of this hypothesis, Lyon later demonstrated that a large deletion (T22H) on a wild-type chromosome that eliminated the entire *Tcd-1* locus could completely recapitulate the *Tcd-1* effects on male sterility and TRD when respectively heterozygous with a complete or distal partial *t*-haplotype containing *Tcr* [30]. These data reinforced the idea that the *Tcd-1* distorter was identical to the *Tcd-1* sterility gene, since both appeared to display severe loss-of-function (hypomorphic or amorphic) phenotypes.

As previously stated, data had already suggested that the *Tcd-1* locus could be divided into at least two subloci — *Tcd-1a* and *Tcd-1b* — and sterility was shown to map exclusively to *Tcd-1a* [31]. Since *Tctex1* mapped within the *Tcd-1a* sublocus, it remained a candidate for both the distorter, *Tcd-1a*, and the associated sterility factor.

A more recent analysis of the *Tcd-1a* sublocus employed BAC transgenesis in an effort to rescue male sterility and/or TRD caused by deletion of the *Tcd-1a* region [49]. A BAC containing two proximal genes from the locus, the testis-expressed genes *Synj2* and *Serac1* (whose *t*-alleles carry deleterious mutations) but not *Tctex1*, was capable of rescuing the sterility phenotype caused by deletion of the locus but had no effect on TRD (Fig. 21.8). These results suggested that, while $Tctex1^t$ might still be the *Tcd-1a* distorter component, it was not the cause of male sterility mapping to the *Tcd-1a* locus, thus modifying

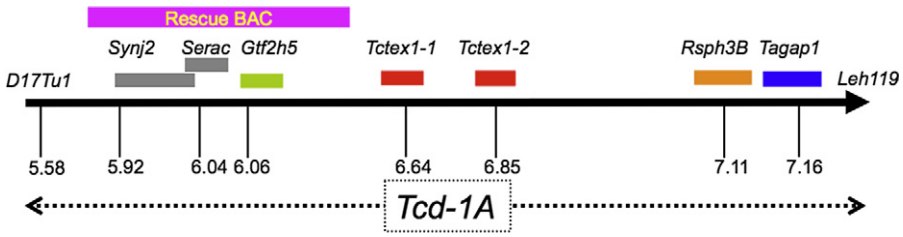

Figure 21.8 The position of the sterility genes in *Tcd-1a* relative to distorter candidates. The physical map positions of testis-expressed *Synj2* and *Serac* are shown in relationship to the physical locations of *Tctex1—1*, *Tctex1—2*, *Rsph3b*, and *Tagap1* in the *Tcd-1a* locus. Numbers indicate megabase pairs from the centromere. A chromosome carrying a deletion of the entire region causes: (1) male sterility when in trans to a complete *t*-haplotype, and (2) elevation of the transmission level of the t^6 partial *t*-haplotype (see Fig. 21.1) when in trans to it. A BAC transgene carrying only *Synj2* and *Serac* (and *Gtf2h5*, a gene not expressed in the testis) is able to rescue fertility in the first case but has no effect on TRD in the second case, indicating that not all sterility genes are distorters and vice versa.

Lyon's original concept of identity between at least one of the *t*-distorters and *t*-sterility genes.

21.6 Identification of Tcds

Prior to the discovery of any of the *Tcd* genes by Herrmann and colleagues, but after his laboratory had identified *Tcr* and described it as a member of a family of "sperm motility kinases" ($Smok^{Tcr}$, encoding a dominant negative kinase), Herrmann and colleagues reasoned that, since *Tcr* appeared to be a loss-of-function kinase, *Tcd*

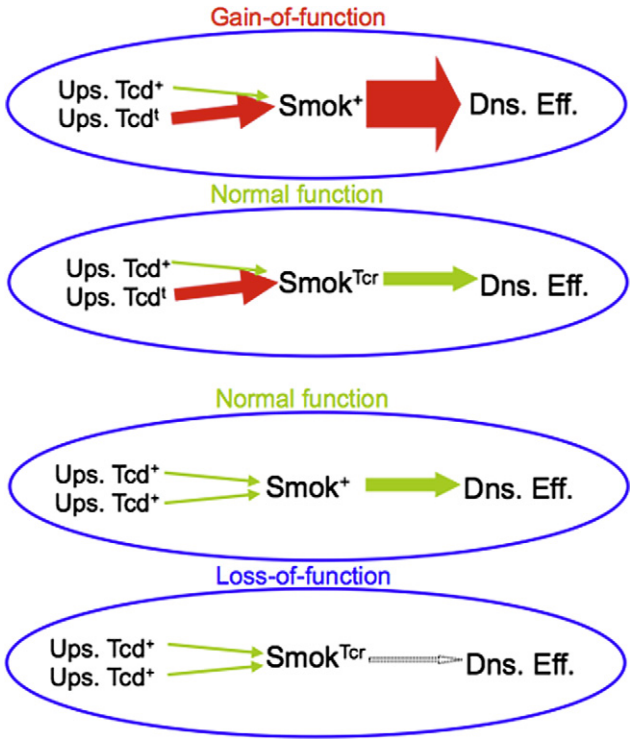

Figure 21.9 Model of TRD with distorters acting only upstream of Smok/Tcr. *Tcr* ($Smok^{Tcr}$) encodes a dominant loss-of-function kinase, a variant of wild-type Smok ($Smok^{+}$), and each is present only in the cell of its origin. Thus, in sperm from a +/*t*-male, the activity of wild-type Smok in +-sperm is boosted to aberrantly high levels when activated by upstream gain-of—function *t*-distorters (Ups.-Tcd^{t}), leading to dysregulation of downstream effector (Dns. Eff.) molecules and relatively poor sperm motility (top oval: gain-of-function effect). However, the same upstream gain-of-function *t*-distorters are present in *t*-sperm and they restore Tcr activity to nearly wild-type levels, thus promoting nearly wild-type motility (second oval: normal function effect). When only +-distorters (Ups.-Tcd^{+}) are present, a $Smok^{+}$-containing sperm behaves just like a wild-type sperm from a +/+-male (third oval: normal function effect), but a Tcr-containing sperm fails to sufficiently activate downstream effector molecules (bottom oval: loss-of-function effect).

genes would most likely code for products that act in signaling pathways upstream of Tcr to enhance Tcr activity in *t*-sperm to near wild-type Smok1 levels, while, at the same time, driving wild-type Smok1 activity in +-sperm to aberrantly high levels [28]. Thus, according to this simple and elegant model of TRD, distorters should act upstream of Smok/Tcr as either amorphic/hypomorphic negative regulators of Smok/Tcr activity or hypermorphic positive regulators of Smok/Tcr activity, but not as downstream targets (such as dyneins) (Fig. 21.9A). In fact, in the ensuing search for distorters by Herrmann and colleagues, this description of what distorters must or must not look like became one of four key limiting criteria for identifying *Tcd* candidate genes whose function in TRD could then be tested in transgenic mice. The other three criteria were identical to those used by most investigators since Lyon first proposed her model of TRD [5], and included: (1) genomic location of the candidate, (2) testis expression of the candidate, and (3) substantial differences in sequence and/or expression of the *t*-allele of the candidate relative to those properties of the wild-type allele.

Interestingly, in the decade since the identification of *Tcr*, the new strategy of limiting *Tcd* genes to those that encode upstream hypermorphic activators or hypomorphic inhibitors of Smok/Tcr action has resulted in the identification of two genes that appear to have distorter activity. Both genes encode Rho-GTPase (putatively RhoA) regulators. The first, *Tagap1*, is a *Tcd-1a* candidate (presently named $Tagap1^{Tcd1A}$), coding for a GTPase-activating protein (GAP), a negative regulator of RhoA activity [50].

A single copy on wild-type chromosome 17 is ubiquitously expressed but shows a relatively low level of mRNA expression in testis. Four copies are present in *t*-haplotypes, each containing multiple non-synonymous mutations. Although the *t*-isoforms constitute three distinct polymorphic classes, each has an intact Rho-GAP domain. Additionally, *t*-allele mRNA expression levels are considerably higher than +-allele levels in testis.

Because chromosomal deletion analysis had already demonstrated that *Tcd-1* is amorphic or hypomorphic, it follows that deletion of $Tagap1^{+}$ should demonstrate positive TRD when the deletion is in trans to t^6, a partial *t*-haplotype lacking only the $Tcd\text{-}1^t$ alleles (see Fig. 21.1). Furthermore, an overexpressing wild-type allele of *Tagap1* should demonstrate negative TRD when in trans from t^6. However, tests of both hypermorphic and amorphic alleles of $Tagap1^{+}$ demonstrated that hypermorphic $Tagap1^{+}$ caused a small but significant elevation of t^6 transmission (88% versus 80% for control $+/t^6$ males), while targeted deletion of $Tagap1^{+}$ caused a significantly greater depression of t^6 transmission. Thus, for $Tagap1^t$ to demonstrate positive TRD, it would have to be a hypermorph. The explanation given for this apparent contradiction was that *Tagap1* must be hypostatic to *Tcd-1b* (or synergize with it) and the resultant must encode a hypomorph/amorph of a Smok/Tcr inhibitor. However, because the steady-state level and functionality of the $Tagap1^t$ protein was not assessed, it is conceivable that $Tagap1^t$, whose multiple

isoforms carry numerous potentially deleterious mutations, could demonstrate dominant negative activity and, thus, be a hypomorph. A "suppressor of meiotic drive" function for *Tagap1*^{t} would be consistent with such a finding. Evidence of suppressors of drive has been obtained in TRD experiments using laboratory strains where TRD is not continually monitored and selective pressure for drive has been removed [1].

Using the same criteria as those used to identify *Tagap1* as a strong candidate for *Tcd-1a*, Herrmann's lab identified a *Tcd-2* candidate gene, *Fgd2*, coding for a guanine nucleotide exchange factor, a promoter of the Rho active state [51]. *Fgd2*$^{+}$ is located just proximal to the *Hybrid Sterility 6* (*Hst6*) locus containing *Dnahc8* [16,20], and lies within the *Hybrid Sterility 4* (*Hst4*) locus (see Fig. 21.6A) [37]. Although the *t*-allele codes for a protein that differs from the wild-type isoform by only a single amino acid ($S_{234}G$), the +- and *t*-isoforms demonstrate different mRNA expression profiles in the testis.

Wild-type *Fgd2* mRNA is ubiquitous, and testis expression commences in early spermatocytes. Two isoforms are expressed, a non-abundant full-length mRNA and an abundant shorter isoform, transcribed from a promoter within the gene. Because translation of the shorter transcript would produce a polypeptide that deletes much of the N-terminus of the guanine nucleotide exchange factor domain, it was suggested that a product of this abundant isoform might act as a dominant inhibitor of the larger, less-abundant isoform. Alternatively, the shorter transcript might undergo nonsense mediated decay, as appears possible in Bauer et al. [51].

As for transcription of *t*-mRNA, the wild-type transcript abundance pattern appeared to be reversed, with *t*/*t* producing at least three-fold more of the longer testis mRNA than most wild-type inbred strains of mice, but also considerably less of the shorter transcript. The enhanced expression level of the longer mRNA in *t*/*t* mice suggested that *Fgd2*^{t} would encode a hypermorph of a positive regulator of Smok/Tcr activity. Indeed, targeted deletion of the locus on a wild-type chromosome reduced the transmission of a partial *t*-haplotype containing only *Tcd-1* and *Tcr* (*t*^{h49}; see Fig. 21.1) from 47 to 35% when in trans to *t*^{h49}, suggesting that a hypermorphic *t*-allele should raise the transmission level of *t*^{h49} by up to 24%. However, a test of a gain-of-function allele was not performed, thus precluding our ability to know with any sense of accuracy exactly how high it might elevate the transmission level of *t*^{h49}. Nonetheless, the *t*-allele of *Fgd2* is an excellent candidate for a distorter, and has been designated *Fgd2*^{Tcd2}.

21.7 What About Dyneins?

After many years of searching for the molecular basis of *t*-TRD, have we finally come close to the end of the journey? Maybe. Maybe not. Olds-Clarke's

cautionary thoughts about being overly restrictive when defining the molecular basis of sperm capacitation [52] apply, and are herein paraphrased with regard to meiotic drive: TRD may be, in many ways, like World War II, with several different theatres of operation, related only by the need for coordinating their activities around Tcr and one common end: to transmit the *t*-haplotype to all progeny (and, thus, win the Great Chromosomal War). In other words, it matters little whether a protein acts upstream or downstream of Tcr: if it increases the transmission level of the *t*-haplotype at the expense of the transmission of the +-chromosome, it must be a distorter. Thus, it may be too early to restrict all potential mutant downtream effectors (Fig. 21.10) of Smok/Tcr function from consideration as conditionally defective mediators (downstream distorters) of the Smok/Tcr signal that act to raise moderately distorted transmission levels of *t* to even higher levels.

This idea is in some ways reinforced by the evolutionary history of *t*-haplotypes. Numerous studies suggest an ancient origin for *t*-haplotypes dating back more than 2 million years [2,53,54]. However, modern *t*-haplotypes are very closely related at the phylogentic level, indicating that they must be very recent descendants of a common ancestor [55]. To reconcile an ancient origin with the phylogenetic relatedness of contemporary *t*-haplotypes, Ardlie and Silver [1] suggested that, if suppressors of meiotic drive were, at one time, widespread in feral populations of mice, the perseverance of *t*-haplotypes in the population would require recurrent mutation to higher distorting alleles of already existing distorters and the addition of new distorter loci, subsequently locked in by selection for inversions. Given the intricate, non-linear evolutionary history of contemporary *t*-haplotypes, plus Olds-Clarke's caution, one could propose a model of TRD that takes into account mutant downstream effectors of Smok/Tcr activity whose punishing effects are meted out conditionally as responses to increasing levels of Smok/Tcr activity.

That being said, although it has been common knowledge for some time that mutant dynein subunits present in the mouse sperm tail axoneme (at least one of them exclusively) map to three of the *Tcd* loci, the fact is that none of them have ever been directly tested for their potential effects on TRD. Instead, naturally occurring or targeted deletions of wild-type isoforms have been employed, more often than not in *Chlamydomonas* (but occassionally in mice), to investigate both qualitative and quantitative downstream effects on dynein arm assembly, dynein function, or fertility, while the potential effects of the *t*-alleles of these subunits (and other flagellar components mapping to the *t*-complex; see Fig. 21.10) on TRD have not been assessed *in vivo*. Some of these assessments may be technically difficult. However, experiments similar to those devised by Herrmann's group [50,51] to identify *Tagap1* and *Fgd2* as likely upstream distorters are feasible and should be performed on the plethora of already-identified potential downstream effector molecules mapping to *Tcd* loci, some already known to carry potentially deleterious mutations [40,41]. So stay tuned.

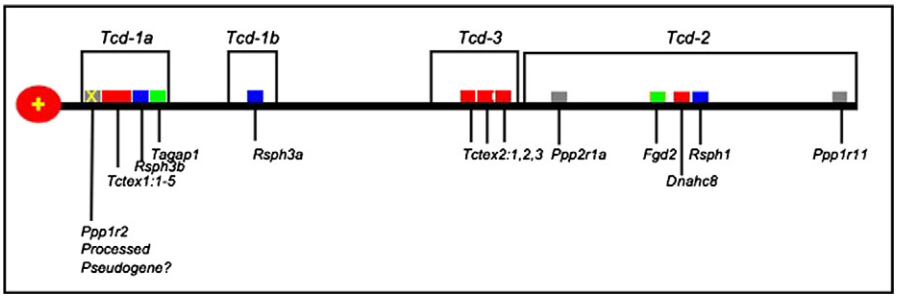

Figure 21.10 Mapped *Tcd* candidates. The relative map positions within known distorter loci on the wild-type chromosome of 14 potential or (all but) proven distorters are shown as squares. Red, dynein subunits; blue, radial spoke proteins; green, regulators of Rho activity; gray, ser/thr protein phosphatase 1 and 2 regulatory or scaffolding subunits. All are expressed in testis and most have been shown to be sperm proteins. The candidacies of *Tctex1*, *Tctex2*, *Dnahc8*, *Fgd2*, and *Tagap1* have already been described in Sections 21.2, 21.3, 21.4, 21.5, and 21.6. Other candidates are as follows; (1) *Rsph1* (*Tsga2*, *Meichroacidin*, *Morn 40*, *Rsp44*) encodes a radial spoke protein that in mouse is also found in abundance in both the FS and ODF of the sperm tail [40,56]. Our (unpublished) preliminary evidence from co-immunoprecipitation studies suggests that it binds to both activity-promoting regulatory subunits and inhibitory subunits of ser/thr protein phosphatase 1 (PP1) in testis and sperm, and to IQUB, a sperm-specific calmodulin binding protein. Thus, it is potentially active as a calcium-sensitive switching mechanism in signaling pathways in the sperm tail. The *t*-allele carries numerous potentially deleterious mutations at highly conserved sites in all mammalian sequences. It could act either upstream or downstream of Smok/Tcr and it is a *Tcd-2* candidate; (2) *Rsph3a* and *Rsph3b* are paralogous radial spoke protein sequences. The former maps to the *Tcd-1b* locus and the latter to the *Tcd-1a* locus, just proximal to *Tagap1.* In mammals, radial spoke protein 3 is an A-kinase anchoring protein (AKAP), binding to ERK1/2 [57]. It also binds IQUB in sperm. Whether the *t*-sequence of either or both is mutated or expressed differently from the allelic +-sequence is unknown; (3) *Ppp1r11* (formerly *Tctex5*; [11] encodes an evolutionary ancient and powerful inhibitory subunit of PP1. It is present in catalytically inactive complexes with PP1γ2 in the testis and sperm [58], and genetic evidence suggests that it has a synergistic relationship with *Rsph1* in the expression of "curlicue" [40,41]. The *t*-variant carries numerous non-conservative mutations at otherwise completely conserved residues in mammalian orthologs [41]. Our (unpublished) preliminary co-immunoprecipitation data suggest that it interacts with RSPH1 in the testis and sperm tail. Because the inhibition of ser/thr phosphatase activity promotes vigorous, progressive sperm motility, *Ppp1r11* can be considered a downstream *Tcd-2* candidate; (4) *Ppp2r1a* codes for the major scaffolding subunit of ser/thr protein phosphatase 2A (PP2A). It is expressed in the testis and is found in sperm, and maps to the proximal end of the *Tcd-2* locus. The sequence and expression of its *t*-allele have not been studied; (5) An allele of what is believed to be a processed pseudogene copy of *Ppp1r2*, another ubiquitous inhibitor of PP1, is located between *Serac* and *Tctex1* (*Gm5490*; Ensembl Mouse Genome Database NCBI-M37). It appears to be a single exon paralog of *Ppp1r2*, with an intact coding region and relatively few mutations, none of which encode frame shifts or premature stop codons. Our preliminary (unpublished) data suggest it produces a testis-specific transcript that can code for a PPP1R2 variant with an additional 109-amino-acid N-terminal extension containing interesting features (not shown as part of the Ensembl transcript). Whether this transcript is, indeed, translated is not yet known. Interestingly, the entire sequence is absent from *t*-haplotypes.

References

[1] K.G. Ardlie, L.M. Silver, Low frequency of mouse *t* haplotypes in wild populations is not explained by modifiers of meiotic drive, Genetics 144 (1996) 1787–1797.

[2] M.F. Hammer, J. Schimenti, L.M. Silver, Evolution of mouse chromosome 17 and the origin of inversions associated with t haplotypes, Proc. Natl. Acad. Sci. USA 86 (1989) 3261–3265.

[3] D. Bennett, The T-locus of the mouse, Cell 6 (1975) 441–454.

[4] M.F. Lyon, Male sterility of the mouse t-complex is due to homozygosity of the distorter genes, Cell 44 (1986) 357–363.

[5] M.F. Lyon, Transmission ratio distortion in mouse *t*-haplotypes is due to multiple distorter genes acting on a responder locus, Cell 37 (1984) 621–628.

[6] L.M. Silver, P. Olds-Clarke, Transmission ratio distortion of mouse *t*-haplotypes is not a consequence of wild-type sperm degeneration, Dev. Biol. 105 (1984) 250–252.

[7] P. Olds-Clarke, L.R. Johnson, *t*-Haplotypes in the mouse compromise sperm flagellar function, Dev. Biol. 155 (1993) 14–25.

[8] D.F. Katz, E.Z. Drobnis, J.W. Overstreet, Factors regulating mammalian sperm migration through the female reproductive tract and oocyte vestments, Gamete Res. 22 (1989) 443–469.

[9] C.B. Lindemann, J.S. Goltz, K.S. Kanous, T.K. Gardner, P. Olds-Clarke, Evidence for an increased sensitivity to Ca^{2+} in the flagella of sperm from t^{w32}/+mice, Mol. Reprod. Dev. 26 (1990) 69–77.

[10] D.F. Katz, R.P. Erickson, M. Nathanson, Beat frequency is bimodally distributed in spermatozoa from T/t12 mice, J. Exp. Zool. 210 (1979) 529–535.

[11] H. Ha, C.A. Howard, Y.I. Yeom, K. Abe, H. Uehara, K. Artzt, D. Bennett, Several testis-expressed genes in the mouse t-complex have expression differences between wild-type and t-mutant mice, Dev. Genet. 12 (1991) 318–332.

[12] L.Y. Huw, A.S. Goldsborough, K. Willison, K. Artzt, Tctex2: A sperm tail surface protein mapping to the *t*-complex, Dev. Biol. 170 (1995) 183–194.

[13] E. Lader, H.S. Ha, M. O'Neill, K. Artzt, D. Bennett, Tctex-1: A candidate gene family for a mouse *t* complex sterility locus, Cell 58 (1989) 969–979.

[14] L.R. Johnson, S.H. Pilder, P. Olds-Clarke, The cellular basis for interaction of sterility factors in the mouse *t* haplotype, Genet. Res. (Camb.) 66 (1995) 189–193.

[15] D.M. Phillips, S.H. Pilder, P.J. Olds-Clarke, L.M. Silver, Factors that may regulate assembly of the mammalian sperm tail deduced from a mouse *t* complex mutation, Biol. Reprod. 49 (1993) 1347–1352.

[16] S.H. Pilder, P. Olds-Clarke, D.M. Phillips, L.M. Silver, Hybrid sterility-6: A mouse *t* complex locus controlling sperm flagellar assembly and movement, Dev. Biol. 159 (1993) 631–642.

[17] A.A. Redkar, P. Olds-Clarke, L.M. Dugan, S.H. Pilder, High resolution mapping of sperm function defects in the t complex fourth inversion, Mamm. Genome 9 (1998) 825–830.

[18] S.A. Samant, J. Fossella, L.M. Silver, S.H. Pilder, Mapping and cloning recombinant breakpoints demarcating the hybrid sterility 6-specific sperm tail assembly defect, Mamm. Genome 10 (1999) 88–94.

[19] M. Fliegauf, H. Olbrich, J. Horvath, J.H. Wildhaber, M.A. Zariwala, M. Kennedy, M.R. Knowles, H. Omran, Mis-localization of DNAH5 and DNAH9 in respiratory cells from primary ciliary dyskinesia patients, Am. J. Respir. Crit. Care Med. 171 (12) (2005) 1343–1349.

[20] J. Fossella, S.A. Samant, L.M. Silver, S.M. King, K.T. Vaughan, P. Olds-Clarke, K.A. Johnson, A. Mikami, R.B. Vallee, S.H. Pilder, An axonemal dynein at the Hybrid Sterility 6 locus: Implications for *t* haplotype-specific male sterility and the evolution of species barriers, Mamm. Genome 11 (2000) 8–15.

[21] S.A. Samant, O. Ogunkua, L. Hui, J. Fossella, S.H. Pilder, The *t* complex distorter 2 candidate gene, *Dnahc8*, encodes at least two testis-specific axonemal dynein heavy chains that differ extensively at their amino and carboxyl termini, Dev. Biol. 250 (2002) 24–43.

[22] S.A. Samant, O.O. Ogunkua, L. Hui, J. Lu, Y. Han, J.M. Orth, S.H. Pilder, The mouse t complex distorter/sterility candidate, Dnahc8, expresses a γ-type axonemal dynein heavy chain isoform confined to the principal piece of the sperm tail, Dev. Biol. 285 (2005) 57–69.
[23] S.M. King, J.F. Dillman 3rd, S.E. Benashski, R.J. Lye, S. Patel-King, K.K. Pfister, The mouse *t*-complex-encoded protein Tctex-1 is a light chain of brain cytoplasmic dynein, J. Biol. Chem. 271 (1996) 32281–32287.
[24] A. Harrison, P. Olds-Clarke, S.M. King, Identification of the *t* complex-encoded cytoplasmic dynein light chain TcTex-1 in inner arm I1 supports the involvement of flagellar dyneins in meiotic drive, J. Cell Biol. 140 (1998) 1137–1147.
[25] N. Kotani, H. Sakakibara, S.A. Burgess, H. Kojima, K. Oiwa, Mechanical properties of inner-arm dynein-f (dynein I1) studied with in vitro motility assays, Biophys. J. 93 (2007) 886–894.
[26] C.B. Lindemann, K.A. Lesich, Flagellar and ciliary beating: The proven and the possible, J. Cell Sci. 123 (2010) 519–528.
[27] L.M. DiBella, O. Gorbatyuk, M. Sakato, K. Wakabayashi, R.S. Patel-King, G.J. Pazour, G.B. Witman, S.M. King, Differential light chain assembly influences outer arm dynein motor function, Mol. Biol. Cell 16 (2005) 5661–5674.
[28] B.G. Herrmann, B. Koschorz, K. Wertz, K.J. McLaughlin, A. Kispert, A protein kinase encoded by the t complex responder gene causes non-mendelian inheritance, Nature 402 (1999) 141–146.
[29] H. Wu, M.W. Maciejewski, S. Takebe, S.M. King, Solution structure of the Tctex1 dimer reveals a mechanism for dynein–cargo interactions, Structure 13 (2005) 213–223.
[30] M.F. Lyon, Deletion of mouse t-complex distorter-1 produces an effect like that of the t-form of the distorter, Genet. Res. 59 (1992) 27–33.
[31] M.F. Lyon, J.C. Schimenti, E.P. Evans, Narrowing the critical regions for mouse t complex transmission ratio distortion factors by use of deletions, Genetics 155 (2000) 793–801.
[32] A. Planchart, Y. You, J.C. Schimenti, Physical mapping of male fertility and meiotic drive QTLs in the mouse *t* complex using chromosome deficiencies, Genetics 155 (2000) 803–812.
[33] R.S. Patel-King, S.E. Benashski, A. Harrison, S.M. King, A *Chlamydomonas* homologue of the putative murine *t* complex distorter Tctex-2 is an outer arm dynein light chain, J. Cell Biol. 137 (1997) 1081–1090.
[34] G.J. Pazour, A. Koutoulis, S.E. Benashski, B.L. Dickert, H. Sheng, R.S. Patel-King, S.M. King, G.B. Witman, LC2, the *Chlamydomonas* homologue of the *t* complex-encoded protein Tctex2, is essential for outer dynein arm assembly, Mol. Biol. Cell 10 (1999) 3507–3520.
[35] S. Rashid, P. Grzmil, J.-D. Drenckhahn, A. Meinhardt, I. Adham, W. Engel, J. Neesen, Disruption of the murine dynein light chain gene Tcte3-3 results in asthenozoospermia, Reproduction 139 (2010) 99–111.
[36] P. Olds-Clarke, Motility characteristics of sperm from the uterus and oviducts of female mice after mating to congenic males differing in sperm transport and fertility, Biol. Reprod. 34 (1986) 453–467.
[37] S.H. Pilder, M.F. Hammer, L.M. Silver, A novel mouse chromosome 17 hybrid sterility locus: Implications for the origin of *t* haplotypes, Genetics 129 (1991) 237–246.
[38] S.H. Pilder, Identification and linkage mapping of Hst7, a new *M. spretus*/ *M. m. domesticus* chromosome 17 hybrid sterility locus, Mamm. Genome. 8 (1997) 290–291.
[39] S.H. Pilder, P. Olds-Clarke, J.M. Orth, W.F. Jester, L. Dugan, Hst7: A male sterility mutation perturbing sperm motility, flagellar assembly, and mitochondrial sheath differentiation, J. Androl. 18 (1997) 663–671.
[40] L. Hui, J. Lu, Y. Han, S.H. Pilder, The mouse T complex gene Tsga2, encoding polypeptides located in the sperm tail and anterior acrosome, maps to a locus associated with sperm motility and sperm-egg interaction abnormalities, Biol. Reprod. 74 (2006) 633–643.

[41] S.H. Pilder, J. Lu, Y. Han, L. Hui, S.A. Samant, O.O. Olugbemiga, K.W. Meyers, L. Cheng, S. Vijayaraghavan, The molecular basis of "curlicue": A sperm motility abnormality linked to the sterility of *t* haplotype homozygous male mice, Soc. Reprod. Fertil. Suppl. 63 (2007) 123–133.
[42] K.T. Vaughn, A. Mikami, B.M. Paschal, E.L.F. Holzbaur, S.M. Hughes, C.J. Echeverri, K.J. Moore, D.J. Gilbert, N.G. Copeland, N.A. Jenkins, R.B. Vallee, Multiple mouse chromosomal loci for dynein-based motility, Genomics 36 (1996) 29–38.
[43] M.P. Koonce, I. Tikhonenko, Functional elements within the dynein microtubule-binding domain, Mol. Biol. Cell 11 (2000) 523–529.
[44] S.M. King, Sensing the mechanical state of the axoneme and integration of Ca^{2+} signaling by outer arm dynein, Cytoskeleton 67 (2010) 207–213.
[45] M. Sakato, H. Sakakibara, S.M. King, *Chlamydomonas* outer arm dynein alters conformation in response to Ca^{2+}, Mol. Biol. Cell 18 (2007) 3620–3634.
[46] D.O. Bunch, J.E. Welch, P.L. Magyar, E.M. Eddy, D.A. O'Brien, Glyceraldehyde 3-phosphate dehydrogenase-S protein distribution during mouse spermatogenesis, Biol. Reprod. 58 (1998) 834–841.
[47] D.W. Fawcett, The mammalian spermatozoon, Dev. Biol. 44 (1975) 394–436.
[48] N. Veron, H. Bauer, A.Y. Weiße, G. Luder, M. Werber, B.G. Herrmann, Retention of gene products in syncytial spermatids promotes non-Mendelian inheritance as revealed by the *t* complex responder, Genes Dev. 23 (2009) 2705–2710.
[49] J.C. Schimenti, J.L. Reynolds, A. Planchart, Mutations in *Serac1* or *Synj2* cause proximal *t* haplotype-mediated male mouse sterility but not transmission ratio distortion, Proc. Natl. Acad. Sci. USA 102 (2005) 3342–3347.
[50] H. Bauer, J. Willert, B. Koschorz, B.G. Herrmann, The *t* complex-encoded GTPase-activating protein Tagap1 acts as a transmission ratio distorter in mice, Nat. Genet. 37 (2005) 969–973.
[51] H. Bauer, N. Veron, J. Willert, B.G. Herrmann, The t-complex-encoded guanine nucleotide exchange factor *Fgd2* reveals that two opposing signaling pathways promote transmission ratio distortion in the mouse, Gene. Dev. 21 (2007) 143–147.
[52] P. Olds-Clarke, Unresolved issues in mammalian fertilization, Int. Rev. Cytol. 232 (2003) 129–184.
[53] C. Delarbre, Y. Kashi, P. Boursot, J.S. Beckmann, P. Kourilsky, F. Bonhomme, G. Gachelin, Phylogenetic distribution in the genus Mus of *t* complex-specific DNA and protein markers: Inferences on the origin of *t*-haplotypes, Mol. Biol. Evol. 5 (1988) 120–133.
[54] J. Klein, M. Nizetic, Z. Golubic, M. Dembic, F. Figueroa, Evolution of the H-2 genes on *t* chromosomes, in: B. Pernis, H.J. Vogel (Eds.), Cell Biology of the Major Histocompatability Complex, Academic Press, New York, 1985, pp. 97–106.
[55] M.F. Hammer, L.M. Silver, Phylogenetic analysis of the alpha-globin pseudogene-4 (*Hba-ps4*) locus in the house mouse species complex reveals a stepwise evolution of *t* haplotypes, Mio. Biol. Evol. 10 (1993) 971–1001.
[56] K. Tokuhiro, M. Hirose, Y. Miyagawa, A. Tsujimura, S. Irie, A. Isotani, M. Okabe, Y. Toyama, C. Ito, K. Toshimori, K. Takeda, S. Oshio, H. Tainaka, J. Tsuchida, A. Okuyama, Y. Nishimune, H. Tanaka, Meichroacidin containing the membrane occupation and recognition nexus motif is essential for spermatozoa morphogenesis, J. Biol. Chem. 283 (2008) 19039–19048.
[57] A. Jivan, S. Earnest, Y.-C. Juang, M.H. Cobb, Radial spoke protein 3 is a mammalian protein kinase A-anchoring protein that binds ERK1/2, J. Biol. Chem. 284 (2009) 29437–29445.
[58] L. Cheng, S. Pilder, A.C. Nairn, S. Ramdas, S. Vijayaraghavan, PP1gamma2 and PPP1R11 are parts of a multimeric complex in developing testicular germ cells in which their steady state levels are reciprocally related, PLoS One 4 (2009) e4861.

In this chapter

22

Role of Dynein in Viral Pathogenesis

Andrew J. Mouland, Miroslav P. Milev

HIV-1 RNA Trafficking Laboratory, Lady Davis Institute for Medical Research – Sir Mortimer B. Davis Jewish General Hospital, Montréal, QC, Canada; Department of Medicine, Division of Experimental Medicine, McGill University, Montréal, QC, Canada; Department of Microbiology and Immunology, McGill University, Montréal, QC, Canada

22.1 General Tenets of Virus–Host Interactions

A general principal of the interaction between viruses and the host is how viruses facilitate their existence and propagation by co-opting host cell components, membranes, proteins, and machineries to their advantage. This is true for virtually every aspect of the replication cycle of viruses from virus entry to the generation of progeny virus particles following assembly. Thus, this chapter will describe the state of the art machineries that viruses use from viral infection (entry) to the end stage, when new, progeny virus particles disseminate from cells. This may be a harsh process, in that several viruses promote dramatic rearrangement of cellular organelles and eventual catastrophy of the cell leading to cell death via apoptosis and cell lysis. Indeed, there are few instances of a peaceful coexistence between host cell and virus, with dramatic virus-mediated modulations of host cell signaling, morphology, and organellar rearrangements being more common. The grand challenge of this field of research is the identification of suitable targets and the development of novel candidate anti-viral drugs.

22.2 Blocking Dynein Function in Virus-Infected Cells: Potential Drug Development to Poison Viral Replication Steps

Realistically, the development of drugs that target dynein activities during viral replication would rely on the disruption of characterized and specific interactions between viral proteins and dynein. Whether this would be appropriate for all viruses is questionable. For example, viruses that swiftly infect and destroy cells by

Dyneins DOI: 10.1016/B978-0-12-382004-4.10022-6
Copyright © 2012 by Elsevier Inc. All rights reserved.

rapidly programming apoptosis might not be good candidates. On the other hand, viruses that are latent in cellular tissue reservoirs, for example retroviruses, might be more suitable since the re-activation of the expression of this type of virus would require viability during the viral expression stage. For example, currently there are no cures for several viral diseases and no effective vaccines despite some promising results [1–3]. The two characterized replication steps of human immunodeficiency virus type 1 (HIV-1) that require and/or utilize dynein function (i.e. viral ingress and egress) may very well both be targeted with future anti-viral compounds [4]. Nevertheless, a plethora of drugs that target processes of the viral replication cycle including virus entry, reverse transcription of the viral RNA genome, viral import into the nucleus, integration into the host genome, and viral maturation [5–10] are mainstays (e.g. Fig. 22.1). These have been instrumental in maintaining the quality of life and life expectancy of infected individuals. However, in addition to unwanted metabolic side effects induced by drugs, HIV-1's ability to adapt leads to sequence variation in the viral genetic material and the inevitable development of resistance to all current drug therapies [11], leading to treatment failure. Thus, there is an urgent need to identify additional therapeutic targets for drug design to block viral replication that succumbs to adaptation. Recent discoveries demonstrate the potential of stopping HIV-1 by targeting the machineries and host proteins used for viral assembly [12,13] or by blocking host cell protein function [14–18], and indeed these methods can be used for other viruses. These new strategies have provided optimism for the development of a new generation of anti-viral compounds in the fight against HIV-1 infection and progression to acquired immunodeficiency syndrome (AIDS). Likewise, for viruses such as Herpes simplex virus type 1 (HSV-1) and the hepatitis C virus (HCV), both major human pathogens with high medical importance, the use of motor proteins during ingress and egress make these machineries highly suitable for drug targeting. Because viruses are parasitic in nature, an even greater reason exists to fully understand the molecular mechanisms underlying host cell protein function and viruses' dependence on these for additional rounds of infection. This is the general thrust of all research on the molecular biology of viruses that can potentially have an impact on human health and disease outcomes.

22.2.1 Virus Infection and Ingress

The mechanisms by which viruses gain entry into cells rely on two fundamental cellular processes: membrane fusion and endocytosis (Figs. 22.1 and 22.2). Whereas freely diffusing virus can find target cells expressing the appropriate receptors, albeit inefficiently, other phenomena that enable more directed targeting and greater efficiency exist. This includes virus cell surfing, which occurs on thin, actin-rich membrane extensions such as filopodia and nanotubes. For many viruses, this extracellular trafficking is critical to virus transmission from one cell to another (e.g. coronavirus severe acute respiratory syndrome (SARS-CoV), respiratory syncitial virus, HIV-1, murine leukemia virus, and human T-cell leukemia virus type 1 (HTLV-1); see also Section 22.8). Motility of viruses towards the cell

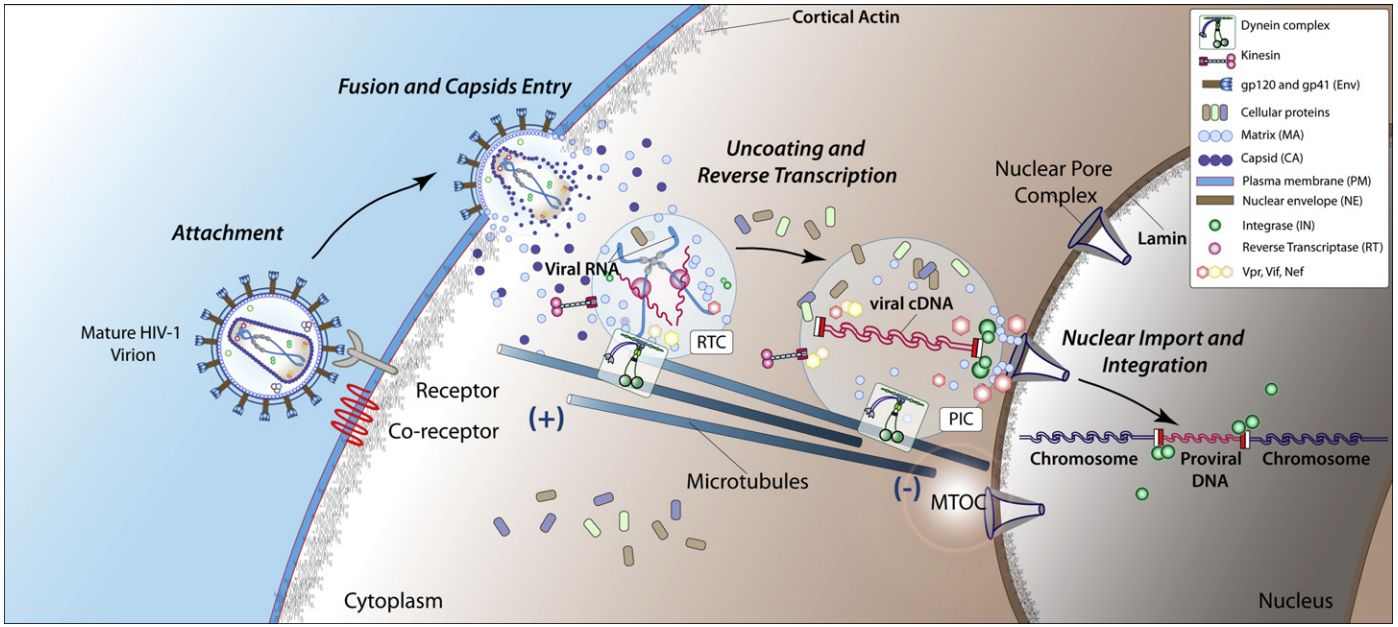

Figure 22.1 Early replication steps of retroviruses. Viral entry of HIV-1 (shown here) and other retroviruses is characterized by receptor–ligand interactions followed by viral entry. The outer envelope of retroviruses fuses with the plasma membrane to release the viral core that contains the genomic RNA. In retroviruses such as human foamy virus, a specific interaction with dynein is achieved and immunoneutralization experiments show that this translocation toward the nucleus occurs in a dynein-dependent manner. During this translocation step, the viral genomic RNA is reverse-transcribed to complementary DNA to generate the pre-integration complex. At the nuclear pore, the pre-integration complex is transported into the nucleus for eventual integration into the host DNA. Additional details on the specific virus–dynein interactions are discussed in the text.

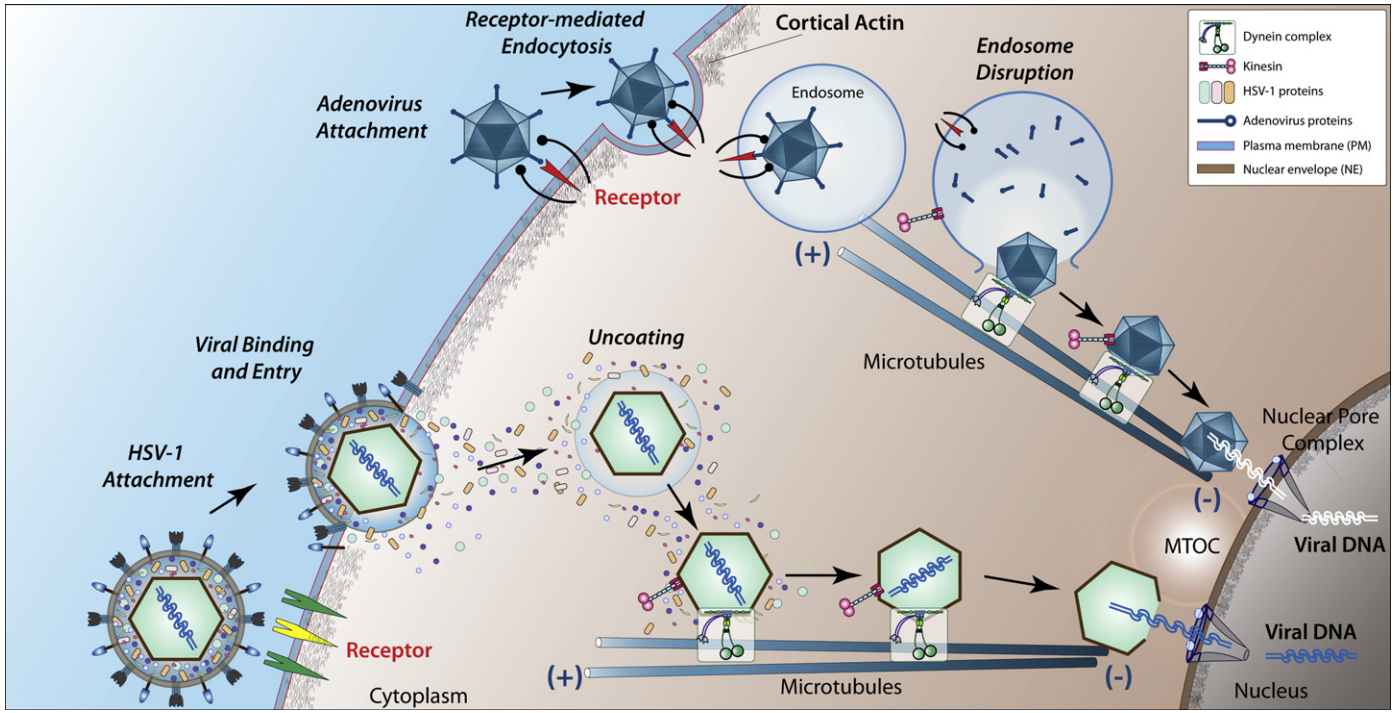

Figure 22.2 Early replication steps of HSV-1 and adenovirus. Viral entry is characterized by receptor–ligand interaction followed by viral entry. The attachment of adenoviruses to the membrane of the target cell is mediated by the viral fiber protein and cellular Coxsackie/adenovirus receptor. Following this step, a second interaction between viral capsid proteins and integrins on the cell surface occurs that leads to internalisation of the virus through endocytosis. The toxic activity of the viral proteins is later responsible for disruption of the endosomal membrane and delivery of the viral particle into the cytoplasm. In contrast, the entry of HSV-1 into cells requires interaction between virion envelope glycoproteins and cell surface glycosaminoglycans. Following this event is the direct fusion of the virion envelope and cell plasma membrane to allow the entry of the viral capsid into the cytoplasm. Intracellular trafficking is mediated by virus–dynein interactions followed by translocation toward the nucleus on microtubules powered by the minus-end motor, dynein. Both HSV-1 and adenovirus have nuclear intermediates and the viral genetic material is transferred into the nucleus for transcription. Details of the specific virus–dynein interactions are discussed in the text.

body relies principally on the myosin II motor, which propels receptor-tethered virus particles towards the cell body [19–21]. Active actin remodeling at the cell body makes the membrane vulnerable and more penetrable to virus infection and viral entry, by the two mechanisms above. Neurotropic viruses are met with the particular challenge of transporting the virus to the cell body and then onward toward the nucleus, which can be several thousand micrometers away. For other viruses such as HIV-1 and HTLV-1, which infect smaller, monocytic T cells, the distances to travel are seemingly smaller but the viruses encounter identical physical, cytoplasmic impediments to infection [22].

22.3 Direct Interactions with Dynein for Viral Entry: Trafficking Towards the Nucleus by Various Viruses

As the virus penetrates into the cytoplasm, viruses initiate their voyage towards the nucleus. One of several possibilities then occurs, depending on whether the virus requires a nuclear intermediate or whether a juxtanuclear domain represents its destination. Nevertheless, viruses are devoid of translocation capability and must now rely on the host to take them where they need to go. For example, upon virus entry the adenovirus capsid hexon subunit interacts with dynein intermediate chain (IC) but not dynactin, a multi-subunit protein complex that is required for cytoplasmic dynein activity and processivity [23,24] (Figs. 22.2 and 22.3; Table 22.1). This event has been shown to be pH dependent and therefore, following the post-entry acidification of the endosomes, efficient transport via this interaction can occur. Adenovirus targeting to the nucleus is also enhanced by direct activation of p38/MAP kinase pathway. The activation of this pathway may represent a countermeasure of sorts to the innate response to infection elicited by the host cell ([25] and see Section 22.4). Adenovirus interactions with dynein TCTEL1 (also known as DYNLT1 or Tctex1) may also influence later steps in the virus' replication cycle when the decision is made to either induce or repress the signals that lead to apoptosis [26]. Likewise, via an interaction between the later-expressed viral envelope protein p54 and dynein LC-8 [27], the African swine fever virus can be propelled towards the nucleus on microtubules but cannot elicit the activation of caspases and induce apoptosis [27,28]. Ebolavirus' interaction with DLC-8 has also been mapped to a short, consensus five-amino acid motif (SQTQT) in the viral protein VP-35 [29]. This viral protein has multiple functions during viral replication, but most important is its ability to suppress interferon synthesis following infection and its capacity to bind RNA, both of which are critical for pathogenesis. While research into this virus is impractical because it requires enhanced biosafety conditions, the little that we have learned about ebolavirus molecular biology will have a positive impact on human health in the long-term. Another virus that is studied with difficulty is the hantavirus, which is transmitted from the excrement of small rodents to humans. However, some

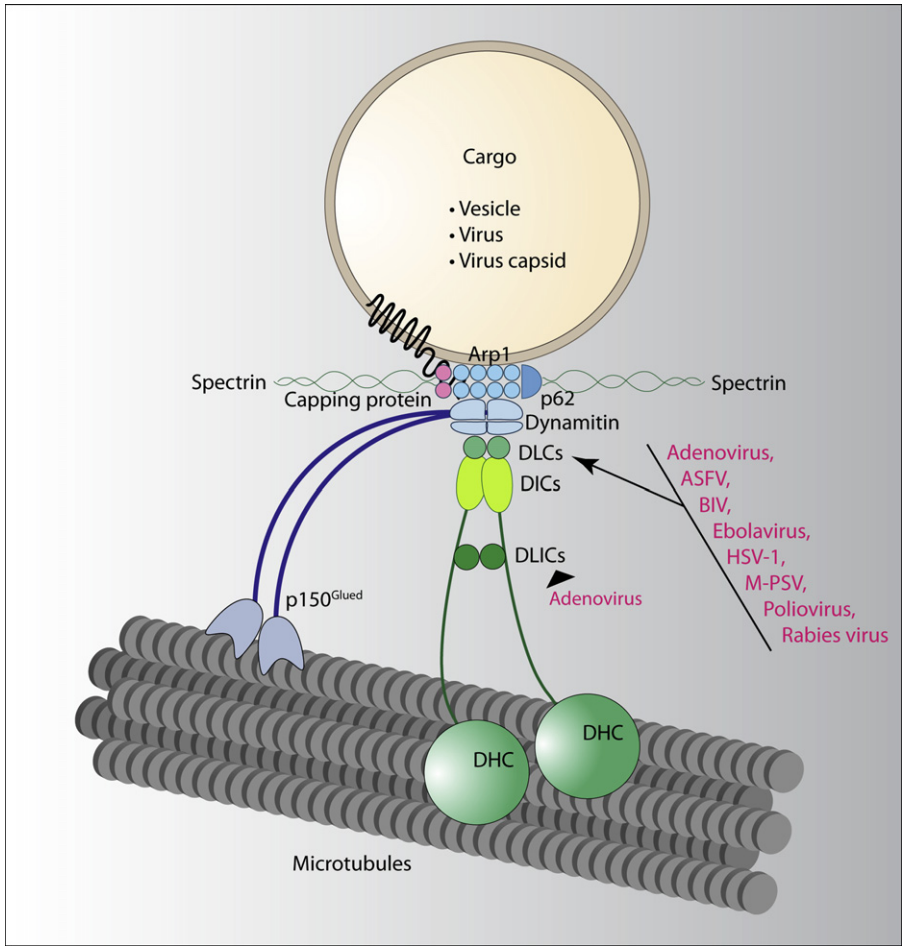

Figure 22.3 Structure of the dynein/dynactin complex and interacting viruses. The dynein motor complex is shown bearing cargo (e.g. vesicles, virus, viral capsids) with its major subdomains – dynein light chains (DLCs), dynein intermediate chains (DICs), dynein light-intermediate chains (DLICs), and dynein HCs (DHCs) – described in Chapter 15. Examples of virus interactions with dynein LCs as well as the dynein ICs are indicated on the right. Discussions of specific interactions are found in the text. The dynactin complex consists of 11 different polypeptide subunits. Some of them are present in more than one copy per complex. The octameric polymer of the actin-related protein-1 (Arp1) resembles a short actin filament. As with conventional actin, Arp1 can hydrolyze ATP and form filaments. Arp1 binds directly to spectrin. The dynactin subunit p62 functions in linking dynein and dynactin to the cortical cytoskeleton. Spectrin is an important constituent of the cytoskeletal network, underlies the plasma membrane, and controls the distribution of the integral membrane proteins.

progress towards elucidating the role of the hantaviral nucleocapsid protein during virus replication has been made. Nucleocapsid, an RNA-binding protein is found to traffic to the endoplasmic reticulum and Golgi intermediate compartment. This was found to depend on dynein motor activity, since the

Table 22.1 Viruses that Interact with Dynein Components During Replication

Virus[1]	Virus Interaction Domain	Dynein Component[2]	References
Adeno-associated virus	Capsid	Dynein	[24]
Adenovirus	Capsid FIP-1	Dynein light and light-intermediate chain; TCTEL1	[23–26,72,123,124]
African swine fever virus	P54 (13 amino acid motif)	DLC-8	[27,28]
Bovine immunodeficiency virus	Capsid	DLC-8	[51]
Ebolavirus	VP35	DLC-8	[29]
Hantaan virus	Unknown	Unknown	[30]
Hepatitis B virus	Unknown	Unknown	[82]
Hepatitis C virus	Unknown	Unknown	[83]
Hepatitis E virus	Vp13	Dynein	[125]
Herpes simplex virus 1	VP26 capsid	RP3, Tctex-1	[31,32,34,126–130]
Equine herpesvirus	Unknown	Unknown (acetylated tubulin)	[33]
Kaposi's sarcoma herpesvirus	Unknown	Unknown (acetylated tubulin)	[48]
Mason–Pfizer simian virus	Matrix	DYNLT1 (Tctex-1)	[102,103]
Bovine immunodeficiency virus	Capsid	LC8	[51]
Human foamy virus	Capsid	LC8	[50]
Human immunodeficiency virus type 1	Pre-integration complex	Dynein	[49,92,94]
Human papillomavirus	Minor capsid L2	DYNLT1 and DYNLT3	[40,41]
Poliovirus	Receptor CD155	Tctex-1	[35,36,38,131]
Rabies virus	P phosphoprotein	DYNLL (LC8)	[42–47]
Sirevirus	Hopie Gag extension	DLC-8	[132]
Vaccinia virus	Unknown	Unknown	[107,117,133]

[1] *Alphabetically organized; most viruses are discussed in the text.*
[2] *The name of the dynein subunit as stated in the cited references is indicated. However, it is important to note that for several components multiple names have been used in the literature to refer to the same protein.*

expression of dynamitin/p50 dispersed nucleocapsid within the cytoplasm [30]. Nevertheless, while nucleocapsid can bind microtubules, no direct interaction between the nucleocapsid and dynein has been characterized to date [30].

HSV-1 entry also requires nuclear targeting and HSV-1 is one of the most thoroughly studied viruses in this field. Typically, it infects cells via epithelial

cells on oral mucous membranes and then transmits to sensory neurons to establish a latent infection that can be reactivated. The initial stages of infection following entry rely on an interaction between HSV-1 VP26 capsid protein and a dynein light chain (LC) of the Tctex-1 family, DYNLT1 and DYNLT3, as verified using a variety of *in vitro* experimental analyses ([31]; Figs. 22.2 and 22.3). The viral capsid protein was also found to be associated with microtubules. However, contrary evidence that did not support a direct role for VP26 has been made available and suggests roles for additional components that recruit the dynein motor to HSV-1 capsids [32]. The role of dynein appears to transcend species since the major horse pathogen, equine herpesvirus type 1 (EHV-1), also utilizes dynein following viral entry to infect cells efficiently [33]. However, in this case the virus causes the acetylation of tubulin, eliciting microtubule stabilization. This appears to be a guarantee to provide a stable trafficking scaffold for EHV-1 to reach the nucleus.

However, recent evidence regarding HSV-1 indicates that the scenario is not so simple. Beate Sodeik's group tested the role of 23 viral proteins that are potentially exposed to the cytoplasm during viral ingress and egress of HSV-1. These analyses revealed that multiple inner viral tegument proteins including pUS3, pUL36, pUL37, ICP0, pUL14, pUL16, and pUL21 recruited dynein and dynactin but also were able to recruit the opposing motor proteins, kinesin-1 and kinesin-2, simultaneously [34] (Fig. 22.2). These results explained to a certain extent how HSV-1 capsids exhibited both plus- and minus-end movements, a likely scenario for most viruses that hijack the motor proteins and the microtubule network for intracellular translocation. The involvement of dynein in poliovirus entry and shuttling towards the cell body is also still being worked out. The interaction between the poliovirus single-membrane-spanning receptor CD155 and dynein LC Tctex-1 was believed to be responsible for intracellular trafficking following entry [35], but recent models suggest a slightly more complex scenario. Studies using motor neurons from transgenic mice revealed that retrograde transport of poliovirus was both receptor-dependent and receptor-independent [36]. Importantly, poliovirus protein 3A, a characterized anti-apoptotic protein, was shown to interact with the type 1 lissencephaly protein (LIS-1), a key regulator of cytoplasmic dynein. While the authors promoted the idea that this was relevant for cell viability, the virus–host interaction could represent another regulatory point at which poliovirus controls intracellular trafficking that may also include other motor proteins [37,38]. Moreover, a growing number of studies show that many viruses are able to recruit and interact with both dynein and kinesin motors, a finding that would be consistent with intracellular trafficking of vesicles and endosomal membranes that harbor both motor proteins [39].

Some of the viral factors with characterized interactions with dynein fulfill additional roles during virus replication. Human papillomavirus infection is again characterized by a well-documented interaction between its capsid L2 protein

and the dynein LCs DYNLT1 and DYNLT 3 [40,41]. However, L2 is found to accompany the viral DNA in the nucleus, suggesting that it plays a dual role in the early events of viral replication for this virus. Rabies virus is another case in point, where initial characterization of an interaction between the phosphoprotein P with dynein light chain LC8 (DYNLL) in *in vitro* and *in vivo* studies was shown to be important during viral replication [42–45]. Certainly these data indicate a reliance on the dynein motor and stable microtubules for ingress, but an additional role for the P protein has been uncovered, this time in a much later viral replication step, in transcriptional regulation [46,47]. By mutating the LC8 binding domain of rabies virus P, the authors revealed that this major effect was independent of its role in intracellular (cytoplasmic) trafficking [46,47]. Because mutating the binding sites only attenuated infection, it is likely that this virus guarantees its replication and propagation by multiple means that could include additional interactions with motor proteins mediated by other viral proteins.

Similarly to EHV-1, human herpesvirus 8 (HHV-8), also known as Kaposi's sarcoma-associated herpesvirus, also induces the stabilization of microtubules by actetylating tubulin as a result of the viral-induced activation of Rho GTPases in primo infection [48]. The HHV-8 herpesvirus contributes to the development of Kaposi's sarcoma, an otherwise rare form of cancer that is sometimes associated with HIV-1-infected patients who have developed AIDS, and to some B-cell lymphomas. In the virus that causes AIDS, after fusion with the plasma membrane, the core, containing the genomic RNA and the viral and host-cell proteins, is transported along microtubules in a dynein-dependent manner toward the nucleus [49] (Fig. 22.1). The ability of HIV-1 to interact with the dynein motor is shared with many of the viruses above. However, HIV-1 RNA must be reverse-transcribed into double-stranded cDNA and then transported into the nucleus for integration into the host-cell genome. This defines retroviral infection as a genetic disease since the genomic material, in the form of a proviral DNA, can propagate from one cell to another during cell division. Detailed correlative electron and confocal imaging have provided a snapshot of the physical space and revealed apparent tethering of the HIV-1 capsid to what seemed to be a motor (like dynein) protein bound to microtubules. This was supported further by experiments that employed the microtubule-disrupting drug nocodazole and by dynein immuno-neutralization injection experiments. Both of the retroviruses human foamy virus and bovine immunodeficiency virus also utilize this mode of transport during viral entry to traffic toward the nucleus with characterized interactions between retroviral capsid proteins and DLC-1 (aks DYNLL or LC8), in which tethering to microtubules was shown to be the result of DLC-1 binding to microtubules [50,51]. This machinery could be targeted by small peptides, as was done to inhibit productive HIV-1 infection [4]. Section 22.4 contains a discussion of how viruses utilise dynein during egress and assembly.

22.4 Innate Immune Response to Viral Infection

Viral infection exposes cells to viral RNA and DNA, inevitably leading to innate anti-viral host responses. Generally, these innate anti-viral responses represent fundamental defense mechanisms of the cell to incoming pathogens and are initiated through the recognition of viral products, such as the viral dsRNA and DNA by the pathogen-recognition toll-like receptors [52,53]. The Toll-like receptor family consists of more than 10 members that are expressed on the cell surface membrane or endosomes. Interferon is generally synthesized following the initial recognition events and has a number of effects on cell function including the induction of interferon-stimulated genes (ISG). These ISG's include those encoding cytokines and the double-stranded RNA-activated protein kinase (PKR) and their expression creates a highly inhospitable environment for viruses [54,55]. Other interferon-stimulated genes encode HIV-1 restriction factors such as tetherin [56] and TRIM5a [57], which can severely limit HIV-1 replication [58].

However, viruses are notoriously efficient at counteracting these innate anti-viral responses following virus infection by creating a host cell environment that is more favourable to viral replication [59,60]. Viruses can block interferon synthesis, intracellular trafficking, and release of anti-viral cytokines from cells, thereby promoting viral replication [61,62]. Furthermore, complex retroviruses, such as HIV-1, encode auxiliary factors that counteract interferon-induced virus restriction factors such as tetherin [63,64] and viruses such as reovirus, the vaccinia virus [65,66]. Others express genes that can have a severe impact on PKR function. Other viruses such as HCV elicit parallel pathways to downregulate the synthesis of ISG mRNAs. This is achieved by the super-induction of PKR and eIF2α phosphorylation, processes known to severely limit both cellular and viral mRNA translation. The result of this virus-induced situation is the suppression of cap-dependent mRNA translation and the preferential synthesis of HCV proteins via the canonical cap-independent translation using an internal ribosome entry site [55,67,68]. Of note are reovirus mRNAs, which are translated over cellular mRNAs, even in the presence of a phosphorylated eIF2α and the assembly of translationally silent stress granules [69]. These aspects of virus–host biology are currently the focus of intense research: if we can block the viruses' ability to commandeer innate responses, the natural course of events against infection and viral disease will prevail, thereby limiting the toll on human lives.

The transit of viral capsids towards the nucleus may in fact be considered to be an early step of the cell's innate immune response to infection. Cellular surveillance machineries may consider incoming virus particles as "foreign" or aggregates of proteins and thus traffic them to the microtubule-organizing center (MTOC) for aggresome formation. Aggresomes are proteinaceous bodies in which accumulate proteins destined for degradation; they usually assemble at juxtanuclear

domains situated around the MTOC. Thus, dynein motors are largely responsible for the transport of cargo to this site [70]. However, a strong link between virus replication and aggresome formation exists, supporting the view that viruses capitalize on the cell's response to traffic material to these sites of aggregation [70,71]. Hantavirus has also been shown to accumulate in vimentin cage-like structures that are characteristic of aggresomes at the MTOC [30]. The association of virus assembly sites with aggresomes may also allow viruses to immobilize and inactivate proteins that would otherwise inhibit infection, such as the demonstrated degradation of the MRE11–RAD50–NBS1 complex, which, if active, may damage viral DNA during adenovirus infection [72].

22.5 Dyneins and Stress Granule Assembly: A Novel Concept in Innate Responses to Viral Infection

Stress granules have been the focus of numerous recent investigations. They are aggregations of translationally silent ribonucleoproteins forming discrete yet prominent cytoplasmic foci 1–5 μm in diameter. Stress granules assemble as a result of various cellular stresses mediated by both eIF2α-dependent and -independent mechanisms [73,74]. Stress granule assembly is induced via a stress-induced phosphorylation of eIF2α (by PKR, for instance) that reduces the availability of the eIF2α/tRNAi Met/GTP ternary complex responsible for translation initiation codon recognition of an mRNA. Under these conditions, the assembly of the translation initiation complex disassembles and promotes the formation of stress granules that harbor translationally silent mRNAs.

Some viral infections induce the assembly of stress granules, including reovirus and respiratory syncitial virus [69,75], but others block their assembly during infection; for example, HIV-1, West Nile virus, rotavirus, and poliovirus [76–78]. Interestingly, the assembly of stress granules depends on dynein and microtubules [79,80]. Considering this dependence on dynein activity for assembly, it is possible that viruses co-opt factors of the dynein motor complex during infection, but as a consequence either induce or silence stress granule assembly. This is an emerging field of endeavor [81] but, all told, stress granules and other silencing ribonucleoprotein bodies may represent "dangerous" areas and structures of the cell that viral replication complexes, proteins, and RNAs/DNAs would need to avoid to guarantee expression and survival.

22.6 Dynein Involvement in Viral Egress and Assembly

While the use of minus-end-directed dynein motor activity to direct viral capsids towards the nucleus is common to many diverse viruses (Table 22.1), the

implication of dynein during viral egress, during the transit of viral components towards the cell periphery and the assembly of most viruses, is not immediately apparent. Indeed, studies on hantavirus and the hepatitis viruses reveal that dynein motors contribute to localization and perhaps juxtapositioning of the viral components required for assembly at virus factories [30,82,83]. Specific proteins from the hepatitis B virus (HBV) and HCV, for example, elicit changes in the localization of viral and cellular components and appear to be dependent on dynein activity. Disrupting dynein function via dynamitin/p50 overexpression, for instance, disrupts both nuclear targeting as well as lipid droplet organization around the MTOC; both are critical to viral assembly [82,83]. The trafficking of HSV-1 to the Golgi complex may depend on dynein activities during the acquisition of membrane immediately prior to cell exit. Recent investigations have revealed that dynein exhibits plus-end movement that is controlled by LIS-1 and tubulins and the tethering of mammalian NUDC to kinesin-1 (a plus-end-directed motor) [84,85]. There is clearly support for the presence of both dynein and kinesin motors driving viral components toward assembly sites [86]. Paradoxically, regulatory genes of HTLV-1 and HIV-1 both enhance and disrupt microtubule integrity and polarization [87–89], but this may directly relate to the timing of the replication cycle.

22.7 Using Dynein To Traffic to Virus Assembly Domains

Integrated targeting of viral components must be coordinated by retroviruses to complete assembly at the plasma membrane. Concerted aggregation of viral proteins and the genomic material, a large 9–12 kb RNA, should be achieved in a small space at the plasma membrane. Retroviruses such as HIV-1 engineer additional targeting strategies that have been worked out by extensive analyses. For instance, membrane targeting domains called lipid rafts and tetraspanin-rich domains serve as scaffolds for viral assembly [90,91]. These exist at internal limiting membranes and at the plasma membrane. Dynein's implication in viral RNA targeting was first revealed by the observation of an aggregation of HIV-1 genomic RNA at the MTOC when heterogeneous nuclear ribonucleoprotein RNA binding proteins were depleted in HIV-1-expressing cells [92]. While this suggested that minus-end transport was not disrupted (since the RNA could readily traffic to the MTOC following export from the nucleus), a blockade to outbound RNA traffic from the MTOC was observed. A critical event in the replication of this virus includes the selection of viral RNA for encapsidation into progeny viruses. This must be done in a regulated manner since only two copies of the viral RNA genome are selected for encapsidation into each virus. The MTOC region has been identified as the site of genomic RNA selection using both biophysical fluorescence resonance energy transfer experiments [93] and by indirect measurements by microscopy and virological assays [92]. The genomic RNA was

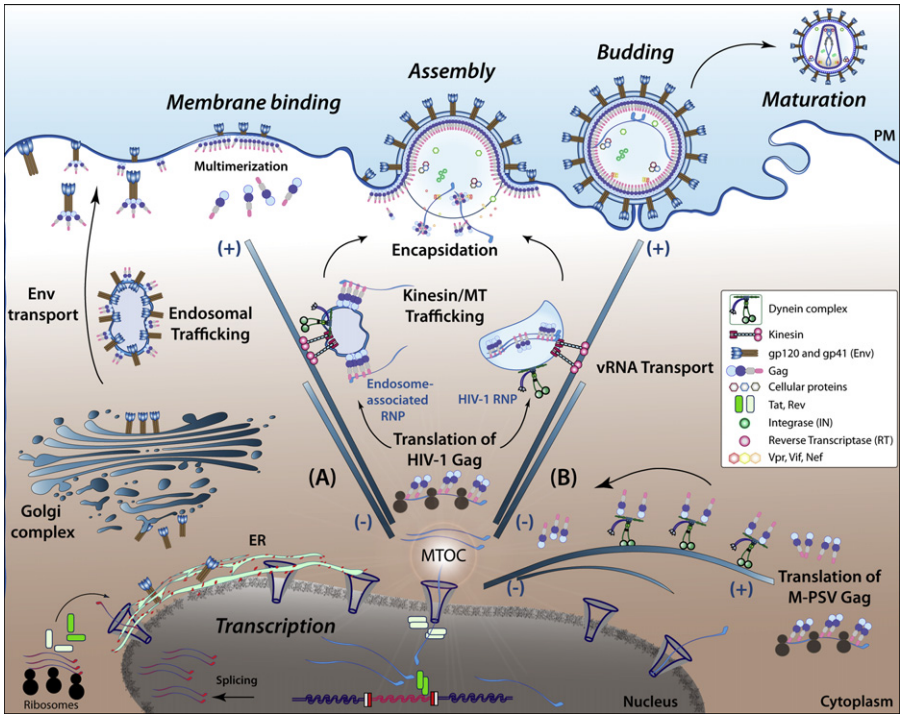

Figure 22.4 Late replication steps of the retroviruses HIV-1 and M-PSV, which require dynein activity. The late stages of retroviral replication are characterized by transcription of the proviral DNA and the generation of a genomic RNA (blue squiggle) in the nucleus. Upon nuclear export, the RNA must be translated to make the major structural protein Gag (as well Gag/Pol, which encodes viral enzymes) in a juxtanuclear domain. The genomic RNA of M-PSV follows the same fate to the cytoplasm but the synthesis of M-PSV Gag is followed by Gag trafficking to the MTOC that is mediated by a specific interaction with dynein, as described in Section 22.7, with the cognate genomic RNA where this virus assembles. The genomic RNA and Gag of HIV-1 have potentially two fates: the genomic RNA is used for translation of Gag polyprotein and, also, the RNA must be selected for and encapsidated into new virus particles. Gag binds and selects for the genomic RNA at the MTOC region, and these viral components must be trafficked to the plasma membrane (PM) for virus assembly. This can be achieved by the association of Gag with intracellular endosomal membranes via a myristoylation domain of matrix (A) or the assembly of a ribonucleoprotein complex containing Gag and the RNA (B). Both complexes contain multiple host factors (not shown). The trafficking toward the plasma membrane is achieved in a multi-subunit complex that likely contains both minus- and plus-end motor proteins, dynein and kinesin. Other components of these retroviruses (e.g. envelope (Env) protein) take the secretory pathway via the endoplasmic reticulum (ER) and Golgi (on left), leading the assembly and budding of new viruses.

then shown to assemble into ribonucleoproteins for trafficking on endosomal membranes. The localization of these endosomal membrane-associated ribonucleoproteins, which harbor viral structural and host proteins along with the viral genomic RNA, was tightly controlled by dynein activity [92,94] (Fig. 22.4). Using siRNA against the dynein heavy chain (HC) or by overexpressing dynamitin/p50, the viral ribonucleoproteins were released along with late endosomal membranes to the cell periphery [94], indicating that there was an active positioning in the

cytoplasm by the minus-end activity of dynein. Because virtually all models for RNA trafficking propose a coordinated tug of war between the activities of opposing motor forces (e.g. the motor proteins dynein and kinesin are in the same complex but one beats out the other to dictate the direction in which a complex, viral capsid, vesicle, or ribonucleoprotein moves on microtubules [86,95–97]; Fig. 22.4), both motor activities should be present on the retroviral ribonucleoproteins during viral egress.

The expression of Rab7-interacting lysosomal protein (RILP) has a dramatic effect on HIV-1 genomic RNA localization in HIV-1-expressing cells by rerouting the RNA to the MTOC. This effect, in fact, could be due to RILP's ability to directly interact with the subunits of endosomal sorting complex required for transport (ESCRT)-II (EAP20 and EAP36) [98,99], or to small Rab GTPases to which RILP binds on endosomal membranes. Alternatively, this localization phenotype could be the result of RILP's ability to recruit components of the dynein/dynactin complex ($p150^{glued}$) or the dynein motor itself [100,101].

The Mason-Pfizer simian virus (M-PSV) utilizes dynein LC (DYNLT1) Tctex-1 to target intracellular viral assembly sites adjacent to the nucleus, at the MTOC [102,103] (Fig. 22.4). Thus, in contrast to the assembly pathway taken by HIV-1, for M-PSV, a D-type retrovirus, assembly occurs at the MTOC. A morphogenetic switch mediated by a hydrophobic pocket in the amino-terminal matrix domain of Gag directs an interaction with the dynein LC DYNLT1 and is responsible for targeting to this unique assembly domain, at least when compared to the assembly pathway taken by HIV-1 and other retroviruses [103]. Interestingly, a single point mutation in the dynein-binding domain not only prevents DYNLT1 binding but changes the site of assembly to that exhibited by HIV-1: the plasma membrane (Fig. 22.4). Thus, although the assembly sites may be different for HIV-1 and M-PSV, for example, this type of switch might not be at play for genomic RNA trafficking of these retroviruses since, by inference, the M-PSV genomic RNA might also be packaged at the MTOC like that of HIV-1 [93]. Nevertheless, retroviral genomic RNA localization might also be dictated by nuclear trafficking events, perhaps associated with the viral regulatory protein Rev or chromosome region maintenance 1 (CRM1) nuclear export factors that have been localized to the MTOC region [104]. Morphological switches mediated by specific interactions with organelles and motor proteins will likely determine trafficking polarity in cells and the winner in the dynein–kinesin tug of war. Gag, host proteins, and the viral RNA, present on endosomal membranes, may be cargo that is available for directed transport on microtubules toward plasma membrane assembly sites (Fig. 22.4). Interactions of viral proteins with dynein mediators such as LIS-1 and other host proteins [37,84,85] could very well provide the switch from minus-end to plus-end motor-directed traffic. Curiously, the HIV-1 regulatory protein, Tat, enhances microtubule polymerization [87] and interacts with LIS-1 protein [105], whereas HIV-1 Rev, vaccinia virus, and African swine fever virus break down microtubules [88,106,107].

22.8 Cell-to-Cell Transmission

Recent investigations into virus cell-to-cell transmission have revealed that several viruses from different classes are capable of being transmitted directly from one cell to another. These include the Rous sarcoma virus, murine leukemia virus, HIV-1, HTLV-1, and the coronavirus SARS-CoV, amongst others. Cell-to-cell transmission of viruses requires the intimate association of infected and non-infected target cells. This type of transmission is also more likely to occur in densely populated tissues, in which viruses can propagate efficiently.

The most details are known for retroviruses and onco-retroviruses, which bud from the cell surface and transmit via a "virological synapse." This synapse is formed by receptor–ligand interactions between cell adhesion molecules and is similar to the immunological cytotoxic T-cell synapse during an immune response [108,109]. The intercellular space is referred to as the virological synapse into which virus particles bud. Viruses are then able to efficiently infect the immediately juxtaposed cell, and this can enhance the infectious potential over 100-fold and may provide for a privileged site where viruses will not be recognized by immune surveillance machinery [110]. Targeting to this domain is aided by the reorganization of the microtubule network, including the dramatic repositioning of the MTOC towards the cell-to-cell junction, which is dependent on the viral regulatory protein Tax in HTLV-1 and the Ras-MEK-ERK signaling pathway [111]. The repositioning of the MTOC was found to be dependent both on diacylglycerol concentrations and on dynein activity [112]. Reversed polarity of microtubules is induced by the close juxtapositioning of the MTOC at the plasma membrane, resulting in the possibility that the minus-end motor dynein may traffic viral components towards the microtubule minus ends at the cell-to-cell junction. This could represent and consolidate some of the observations for dynein's involvement in intracellular trafficking events of structural proteins and viral genomic RNA during egress before virus budding [92]. Nevertheless, multiple cell-to-cell contact sites (polysynapses) were identified for HIV-1 in T-cells [113]. While this does not reconcile the polarization of a single MTOC during cell-to-cell transmission, in the oncoretrovirus HTLV-1, the viral protein Tax yields cells with multiple centrosomes in infected cells [114] that could contribute to virus propagation.

Viral cell-to-cell transmission also occurs on cell membrane extensions termed filopodia or cytonemes and nanotubes, but transmission does not necessarily require direct cell-to-cell juxtapositioning [19–21]. Propulsion of viruses from an infected cell to another is achieved via myosin II–actin retrograde movement, resulting in shuttling of virus-coupled cell surface receptors on membrane extensions towards the cell body. The transmission of several viruses is enhanced by these processes but nevertheless does not appear to depend on dynein activity before the viral capsid penetrates into the cell at the cell body.

22.9 Virus Export from Virus Factories

Several viruses, including poxviruses and the vaccinia virus, replicate in cytoplasmic virus factories. The recruitment of transcription and translation factors and the engineering of virus-specific membranes and smaller "organelles" all contribute to the biogenesis of these virus factories [83,115,116]. Both the vaccinia virus and HSV-1 must acquire membrane at the Golgi complex or at juxtanuclear sites, according to current concepts, before exiting the cell [117,118], and this may require active transport that could include the activity of the dynein motor and an intact microtubule cytoskeleton for this directed targeting during viral egress.

22.10 Concluding Remarks

The intracellular translocation of viral components continues to be an extremely enriching area of study (see also [119–121] and for other pathogens [122]). Viruses are inherently immotile and studies on how they are able to commandeer, recruit, and utilise the host cell translocation machinery are continually shedding light on the workings of the cell's major trafficking machineries. Viruses must also mount countermeasures against anti-viral innate responses while making their way through the host's cytoplasm. This is usually achieved by utilizing constitutive cellular processes and by directly interacting with host motor proteins and other factors.

Viruses likely harbor and make use of both plus- and minus-end-directed microtubule motor activities during their replication cycles. On this subject, the following are some of the major questions for the future to answer:

- What are the primary mechanisms for the recruitment of molecular motor proteins?
- What determines directionality?
- What viral and host factors are involved?
- Are there molecular switches that occur to dictate the directionality of motor-protein-containing capsids?
- Are these dictated by viral gene products that are expressed in a time-dependent manner?

Acknowledgments

The authors acknowledge the generous support of the Canadian Institutes of Health Research, the *Fonds pour la recherche en santè du Québec*, and the McGill University Fraser, Monat, and McPherson Scholarships program.

References

[1] M.P. Girard, G.P. Bansal, HIV/AIDS vaccines: A need for new concepts? Int. Rev. Immunol. 27 (2008) 447–471.

[2] S. Rerks-Ngarm, P. Pitisuttithum, S. Nitayaphan, J. Kaewkungwal, J. Chiu, R. Paris, N. Premsri, C. Namwat, M. de Souza, E. Adams, M. Benenson, S. Gurunathan, J. Tartaglia, J.G. McNeil, D.P. Francis, D. Stablein, D.L. Birx, S. Chunsuttiwat, C. Khamboonruang, P. Thongcharoen, M.L. Robb, N.L. Michael, P. Kunasol, J.H. Kim, Vaccination with ALVAC and AIDSVAX to prevent HIV-1 infection in Thailand, New Eng. J. Med. 361 (2009) 2209–2220.
[3] T. Zhou, I. Georgiev, X. Wu, Z.Y. Yang, K. Dai, A. Finzi, Y. Do Kwon, J. Scheid, W. Shi, L. Xu, Y. Yang, J. Zhu, M.C. Nussenzweig, J. Sodroski, L. Shapiro, G.J. Nabel, J.R. Mascola, P.D. Kwong, Structural basis for broad and potent neutralization of HIV-1 by antibody VRC01, Science 329 (2010) 1060–1064.
[4] D.R. Fontenot, P. den Hollander, E.M. Vela, R. Newman, J.K. Sastry, R. Kumar, Dynein light chain 1 peptide inhibits human immunodeficiency virus infection in eukaryotic cells, Biochem. Biophys. Res. Commun. 363 (2007) 901–907.
[5] B.R. Cullen, Nuclear mRNA export: Insights from virology, Trends Biochem. Sci. 28 (2003) 419–424.
[6] I. Hauber, D. Bevec, J. Heukeshoven, F. Kratzer, F. Horn, A. Choidas, T. Harrer, J. Hauber, Identification of cellular deoxyhypusine synthase as a novel target for antiretroviral therapy, J. Clin. Invest. 115 (2005) 76–85.
[7] E. Dejesus, D. Berger, M. Markowitz, C. Cohen, T. Hawkins, P. Ruane, R. Elion, C. Farthing, L. Zhong, A.K. Cheng, D. McColl, B.P. Kearney, Antiviral activity, pharmacokinetics, and dose response of the HIV-1 integrase inhibitor GS-9137 (JTK-303) in treatment-naive and treatment-experienced patients, J. Acquir. Immune Defic. Syndr. 43 (2006) 1–5.
[8] S.C. Piller, L. Caly, D.A. Jans, Nuclear import of the pre-integration complex (PIC): The Achilles heel of HIV? Curr. Drug Targets 4 (2003) 409–429.
[9] J. Zhou, X. Yuan, D. Dismuke, B.M. Forshey, C. Lundquist, K.H. Lee, C. Aiken, C.H. Chen, Small-molecule inhibition of human immunodeficiency virus type 1 replication by specific targeting of the final step of virion maturation, J. Virol. 78 (2004) 922–929.
[10] F. Li, R. Goila-Gaur, K. Salzwedel, N.R. Kilgore, M. Reddick, C. Matallana, A. Castillo, D. Zoumplis, D.E. Martin, J.M. Orenstein, G.P. Allaway, E.O. Freed, C.T. Wild, PA-457: A potent HIV inhibitor that disrupts core condensation by targeting a late step in Gag processing, Proc. Natl. Acad. Sci. USA 100 (2003). 13 555–13 560.
[11] T. Bar-Magen, R.D. Sloan, D.A. Donahue, B.D. Kuhl, A. Zabeida, H. Xu, M. Oliveira, D.J. Hazuda, M.A. Wainberg, Identification of novel mutations responsible for resistance to MK-2048, a second-generation HIV-1 integrase inhibitor, J. Virol. 84 (2010) 9210–9216.
[12] C.S. Adamson, K. Salzwedel, E.O. Freed, Virus maturation as a new HIV-1 therapeutic target, Expert Opin. Ther. Tar. 13 (2009) 895–908.
[13] A.A. Waheed, E.O. Freed, Peptide inhibitors of HIV-1 egress, ACS Chem. Biol. 3 (2008) 745–747.
[14] F.D. Bushman, N. Malani, J. Fernandes, I. D'Orso, G. Cagney, T.L. Diamond, H. Zhou, D.J. Hazuda, A.S. Espeseth, R. Konig, S. Bandyopadhyay, T. Ideker, S.P. Goff, N.J. Krogan, A.D. Frankel, J.A. Young, S.K. Chanda, Host cell factors in HIV replication: Meta-analysis of genome-wide studies, PLoS Pathog 5 (2009) e1000437.
[15] C.S. Adamson, E.O. Freed, Novel approaches to inhibiting HIV-1 replication, Antivir. Res. 85 (2010) 119–141.
[16] P. An, C.A. Winkler, Host genes associated with HIV/AIDS: Advances in gene discovery, Trends Genet. 26 (2010) 119–131.
[17] N. Arhel, F. Kirchhoff, Host proteins involved in HIV infection: New therapeutic targets, Biochim. Biophys. Acta 1802 (2010) 313–321.
[18] R. Cantin, S. Methot, M.J. Tremblay, Plunder and stowaways: Incorporation of cellular proteins by enveloped viruses, J. Virol. 79 (2005) 6577–6587.
[19] S. Sowinski, C. Jolly, O. Berninghausen, M.A. Purbhoo, A. Chauveau, K. Kohler, S. Oddos, P. Eissmann, F.M. Brodsky, C. Hopkins, B. Onfelt, Q. Sattentau, D.M. Davis, Membrane

nanotubes physically connect T cells over long distances presenting a novel route for HIV-1 transmission, Nat. Cell. Biol. 10 (2008) 211–219.
[20] M.J. Lehmann, N.M. Sherer, C.B. Marks, M. Pypaert, W. Mothes, Actin- and myosin-driven movement of viruses along filopodia precedes their entry into cells, J. Cell Biol. 170 (2005) 317–325.
[21] N.M. Sherer, M.J. Lehmann, L.F. Jimenez-Soto, C. Horensavitz, M. Pypaert, W. Mothes, Retroviruses can establish filopodial bridges for efficient cell-to-cell transmission, Nat. Cell. Biol. 9 (2007) 310–315.
[22] K. Luby-Phelps, Cytoarchitecture and physical properties of cytoplasm: Volume, viscosity, diffusion, intracellular surface area, Int. Rev. Cytol 192 (2000) 189–221.
[23] K.H. Bremner, J. Scherer, J. Yi, M. Vershinin, S.P. Gross, R.B. Vallee, Adenovirus transport via direct interaction of cytoplasmic dynein with the viral capsid hexon subunit, Cell Host Microbe. 6 (2009) 523–535.
[24] S.A. Kelkar, K.K. Pfister, R.G. Crystal, P.L. Leopold, Cytoplasmic dynein mediates adenovirus binding to microtubules, J. Virol. 78 (2004). 10 122–10 132.
[25] M. Suomalainen, M.Y. Nakano, K. Boucke, S. Keller, U.F. Greber, Adenovirus-activated PKA and p38/MAPK pathways boost microtubule-mediated nuclear targeting of virus, EMBO J. 20 (2001) 1310–1319.
[26] S.A. Lukashok, L. Tarassishin, Y. Li, M.S. Horwitz, An adenovirus inhibitor of tumor necrosis factor alpha-induced apoptosis complexes with dynein and a small GTPase, J. Virol. 74 (2000) 4705–4709.
[27] C. Alonso, J. Miskin, B. Hernaez, P. Fernandez-Zapatero, L. Soto, C. Canto, I. Rodriguez-Crespo, L. Dixon, J.M. Escribano, African swine fever virus protein p54 interacts with the microtubular motor complex through direct binding to light-chain dynein, J. Virol. 75 (2001) 9819–9827.
[28] B. Hernaez, G. Diaz-Gil, M. Garcia-Gallo, J. Ignacio Quetglas, I. Rodriguez-Crespo, L. Dixon, J.M. Escribano, C. Alonso, The African swine fever virus dynein-binding protein p54 induces infected cell apoptosis, FEBS Lett. 569 (2004) 224–228.
[29] T. Kubota, M. Matsuoka, T.H. Chang, M. Bray, S. Jones, M. Tashiro, A. Kato, K. Ozato, Ebolavirus VP35 interacts with the cytoplasmic dynein light chain 8, J. Virol. 83 (2009) 6952–6956.
[30] H.N. Ramanathan, D.H. Chung, S.J. Plane, E. Sztul, Y.K. Chu, M.C. Guttieri, M. McDowell, G. Ali, C.B. Jonsson, Dynein-dependent transport of the hantaan virus nucleocapsid protein to the endoplasmic reticulum-Golgi intermediate compartment, J. Virol. 81 (2007) 8634–8647.
[31] M.W. Douglas, R.J. Diefenbach, F.L. Homa, M. Miranda-Saksena, F.J. Rixon, V. Vittone, K. Byth, A.L. Cunningham, Herpes simplex virus type 1 capsid protein VP26 interacts with dynein light chains RP3 and Tctex1 and plays a role in retrograde cellular transport, J. Biol. Chem. 279 (2004). 28 522–28 530.
[32] K. Dohner, K. Radtke, S. Schmidt, B. Sodeik, Eclipse phase of herpes simplex virus type 1 infection: Efficient dynein-mediated capsid transport without the small capsid protein VP26, J. Virol. 80 (2006) 8211–8224.
[33] A.R. Frampton Jr., H. Uchida, J. von Einem, W.F. Goins, P. Grandi, J.B. Cohen, N. Osterrieder, J.C. Glorioso, Equine herpesvirus type 1 (EHV-1) utilizes microtubules, dynein, and ROCK1 to productively infect cells, Vet. Microbiol. 141 (2010) 12–21.
[34] K. Radtke, D. Kieneke, A. Wolfstein, K. Michael, W. Steffen, T. Scholz, A. Karger, B. Sodeik, Plus- and minus-end directed microtubule motors bind simultaneously to herpes simplex virus capsids using different inner tegument structures, PLoS Pathog. 6 (2010) e1000991.
[35] S. Mueller, X. Cao, R. Welker, E. Wimmer, Interaction of the poliovirus receptor CD155 with the dynein light chain Tctex-1 and its implication for poliovirus pathogenesis, J. Biol. Chem. 277 (2002) 7897–7904.

[36] S. Ohka, M. Sakai, S. Bohnert, H. Igarashi, K. Deinhardt, G. Schiavo, A. Nomoto, Receptor-dependent and -independent axonal retrograde transport of poliovirus in motor neurons, J. Virol. 83 (2009) 4995–5004.
[37] M. Yamada, S. Toba, Y. Yoshida, K. Haratani, D. Mori, Y. Yano, Y. Mimori-Kiyosue, T. Nakamura, K. Itoh, S. Fushiki, M. Setou, A. Wynshaw-Boris, T. Torisawa, Y.Y. Toyoshima, S. Hirotsune, LIS1 and NDEL1 coordinate the plus-end-directed transport of cytoplasmic dynein, EMBO J. 27 (2008) 2471–2483.
[38] A.A. Kondratova, N. Neznanov, R.V. Kondratov, A.V. Gudkov, Poliovirus protein 3A binds and inactivates LIS1, causing block of membrane protein trafficking and deregulation of cell division, Cell Cycle (Georgetown, Tex.) 4 (2005) 1403–1410.
[39] S. Ma, R.L. Chisholm, Cytoplasmic dynein-associated structures move bidirectionally *in vivo*, J. Cell Sci. 115 (2002) 1453–1460.
[40] L. Florin, K.A. Becker, C. Lambert, T. Nowak, C. Sapp, D. Strand, R.E. Streeck, M. Sapp, Identification of a dynein interacting domain in the papillomavirus minor capsid protein l2, J. Virol. 80 (2006) 6691–6696.
[41] M.A. Schneider, G.A. Spoden, L. Florin, C. Lambert, Identification of the dynein light chains required for human papillomavirus infection, Cellular Microbiology 13 (2010) 32–46.
[42] Y. Jacob, H. Badrane, P.E. Ceccaldi, N. Tordo, Cytoplasmic dynein LC8 interacts with lyssavirus phosphoprotein, J. Virol. 74 (2000) 10217–10222.
[43] T. Mebatsion, Extensive attenuation of rabies virus by simultaneously modifying the dynein light chain binding site in the P protein and replacing Arg333 in the G protein, J. Virol. 75 (2001). 11 496–11 502.
[44] P. Rasalingam, J.P. Rossiter, T. Mebatsion, A.C. Jackson, Comparative pathogenesis of the SAD-L16 strain of rabies virus and a mutant modifying the dynein light chain binding site of the rabies virus phosphoprotein in young mice, Virus Res. 111 (2005) 55–60.
[45] H. Raux, A. Flamand, D. Blondel, Interaction of the rabies virus P protein with the LC8 dynein light chain, J. Virol. 74 (2000) 10212–10216.
[46] N. Poisson, E. Real, Y. Gaudin, M.C. Vaney, S. King, Y. Jacob, N. Tordo, D. Blondel, Molecular basis for the interaction between rabies virus phosphoprotein P and the dynein light chain LC8: Dissociation of dynein-binding properties and transcriptional functionality of P, J. Gen. Virol. 82 (2001) 2691–2696.
[47] G.S. Tan, M.A. Preuss, J.C. Williams, M.J. Schnell, The dynein light chain 8 binding motif of rabies virus phosphoprotein promotes efficient viral transcription, Proc. Natl. Acad. Sci. USA 104 (2007) 7229–7234.
[48] P.P. Naranatt, H.H. Krishnan, M.S. Smith, B. Chandran, Kaposi's sarcoma-associated herpesvirus modulates microtubule dynamics via RhoA-GTP-diaphanous 2 signaling and utilizes the dynein motors to deliver its DNA to the nucleus, J. Virol. 79 (2005) 1191–1206.
[49] D. McDonald, M. Vodicka, G. Lucero, Y. Svitkina, G. Borisy, M. Emerman, T.J. Hope, Visualization of the intracellular behavior of HIV in living cells, J. Cell Biol. 159 (2002) 441–452.
[50] C. Petit, M.L. Giron, J. Tobaly-Tapiero, P. Bittoun, E. Real, Y. Jacob, N. Tordo, H. De The, A. Saib, Targeting of incoming retroviral Gag to the centrosome involves a direct interaction with the dynein light chain 8, J. Cell Sci. 116 (2003) 3433–3442.
[51] Y. Su, W. Qiao, T. Guo, J. Tan, Z. Li, Y. Chen, X. Li, Y. Li, J. Zhou, Q. Chen, Microtubule-dependent retrograde transport of bovine immunodeficiency virus, Cell. Microbiol. 12 (2010) 1098–1107.
[52] M. Carty, A.G. Bowie, Recent insights into the role of toll-like receptors in viral infection, Clin. Exp. Immunol. 161 (2010) 397–406.
[53] A.J. Thompson, S.A. Locarnini, Toll-like receptors, RIG-I-like RNA helicases and the antiviral innate immune response, Immunol. Cell Biol. 85 (2007) 435–445.
[54] D.R. Taylor, S.B. Lee, P.R. Romano, D.R. Marshak, A.G. Hinnebusch, M. Esteban, M.B. Mathews, Autophosphorylation sites participate in the activation of the double-stranded-RNA-activated protein kinase PKR, Mol. Cell. Biol. 16 (1996) 6295–6302.

[55] C.A. Bonjardim, P.C. Ferreira, E.G. Kroon, Interferons: Signaling, antiviral and viral evasion, Immunol. Lett. 122 (2009) 1–11.
[56] J.L. Douglas, J.K. Gustin, K. Viswanathan, M. Mansouri, A.V. Moses, K. Fruh, The great escape: Viral strategies to counter BST-2/tetherin, PLoS Pathog. 6 (2010) e1000913.
[57] L. Carthagena, A. Bergamaschi, J.M. Luna, A. David, P.D. Uchil, F. Margottin-Goguet, W. Mothes, U. Hazan, C. Transy, G. Pancino, S. Nisole, Human TRIM gene expression in response to interferons, PLoS One 4 (2009) e4894.
[58] R.N. Douville, J. Hiscott, The interface between the innate interferon response and expression of host retroviral restriction factors, Cytokine 52 (2010) 108–115.
[59] S. Schutz, P. Sarnow, How viruses avoid stress, Cell Host Microbe. 2 (2007) 284–285.
[60] T.H. Mogensen, J. Melchjorsen, C.S. Larsen, S.R. Paludan, Innate immune recognition and activation during HIV infection, Retrovirology 7 (2010) 54.
[61] E. Martinelli, C. Cicala, D. Van Ryk, D.J. Goode, K. Macleod, J. Arthos, A.S. Fauci, HIV-1 gp120 inhibits TLR9-mediated activation and IFN-α secretion in plasmacytoid dendritic cells, Proc. Natl. Acad. Sci. USA 104 (2007) 3396–3401.
[62] B.P. Doehle, F. Hladik, J.P. McNevin, M.J. McElrath, M. Gale Jr., Human immunodeficiency virus type 1 mediates global disruption of innate antiviral signaling and immune defenses within infected cells, J. Virol. 83 (2009) 10395–10405.
[63] S.J. Neil, T. Zang, P.D. Bieniasz, Tetherin inhibits retrovirus release and is antagonized by HIV-1 Vpu, Nature 451 (2008) 425–430.
[64] K.N. Bishop, R.K. Holmes, A.M. Sheehy, M.H. Malim, APOBEC-mediated editing of viral RNA, Science 305 (2004) 645.
[65] Z. Yue, A.J. Shatkin, Double-stranded RNA-dependent protein kinase (PKR) is regulated by reovirus structural proteins, Virology 234 (1997) 364–371.
[66] P.R. Romano, F. Zhang, S.L. Tan, M.T. Garcia-Barrio, M.G. Katze, T.E. Dever, A.G. Hinnebusch, Inhibition of double-stranded RNA-dependent protein kinase PKR by vaccinia virus E3: Role of complex formation and the E3 N-terminal domain, Mol. Cell. Biol. 18 (1998) 7304–7316.
[67] U. Garaigorta, F.V. Chisari, Hepatitis C virus blocks interferon effector function by inducing protein kinase R phosphorylation, Cell Host Microbe. 6 (2009) 513–522.
[68] N. Arnaud, S. Dabo, P. Maillard, A. Budkowska, K.I. Kalliampakou, P. Mavromara, D. Garcin, J. Hugon, A. Gatignol, D. Akazawa, T. Wakita, E.F. Meurs, Hepatitis C virus controls interferon production through PKR activation, PLoS One 5 (2010) e10575.
[69] J.A. Smith, S.C. Schmechel, A. Raghavan, M. Abelson, C. Reilly, M.G. Katze, R.J. Kaufman, P.R. Bohjanen, L.A. Schiff, Reovirus induces and benefits from an integrated cellular stress response, J. Virol. 80 (2006) 2019–2033.
[70] T. Wileman, Aggresomes and pericentriolar sites of virus assembly: Cellular defense or viral design? Annu. Rev. Microbiol. 61 (2007) 149–167.
[71] T. Wileman, Aggresomes and autophagy generate sites for virus replication, Science 312 (2006) 875–878.
[72] Y. Liu, A. Shevchenko, A. Shevchenko, A.J. Berk, Adenovirus exploits the cellular aggresome response to accelerate inactivation of the MRN complex, J. Virol 79 (2005). 14 004–14 016.
[73] M.E. Bordeleau, R. Cencic, L. Lindqvist, M. Oberer, P. Northcote, G. Wagner, J. Pelletier, RNA-mediated sequestration of the RNA helicase eIF4A by Pateamine A inhibits translation initiation, Chem. Biol. 13 (2006) 1287–1295.
[74] R. Mazroui, R. Sukarieh, M.E. Bordeleau, R.J. Kaufman, P. Northcote, J. Tanaka, I. Gallouzi, J. Pelletier, Inhibition of ribosome recruitment induces stress granule formation independently of eukaryotic initiation factor 2alpha phosphorylation, Mol. Biol. Cell 17 (2006) 4212–4219.
[75] H. Montero, M. Rojas, C.F. Arias, S. Lopez, Rotavirus infection induces the phosphorylation of eIF2alpha but prevents the formation of stress granules, J. Virol. 82 (2008) 1496–1504.

[76] L.G. Abrahamyan, L. Chatel-Chaix, L. Ajamian, M.P. Milev, A. Monette, J.F. Clement, R. Song, M. Lehmann, L. Desgroseillers, M. Laughrea, G. Boccaccio, A.J. Mouland, Novel Staufen1 ribonucleoproteins prevent formation of stress granules but favour encapsidation of HIV-1 genomic RNA, J. Cell Sci. 123 (2010) 369–383.
[77] M.M. Emara, M.A. Brinton, Interaction of TIA-1/TIAR with West Nile and dengue virus products in infected cells interferes with stress granule formation and processing body assembly, Proc. Natl. Acad. Sci. USA 104 (2007) 9041–9046.
[78] J.P. White, A.M. Cardenas, W.E. Marissen, R.E. Lloyd, Inhibition of cytoplasmic mRNA stress granule formation by a viral proteinase, Cell Host Microbe. 2 (2007) 295–305.
[79] M. Loschi, C.C. Leishman, N. Berardone, G.L. Boccaccio, Dynein and kinesin regulate stress-granule and P-body dynamics, J. Cell Sci. 122 (2009) 3973–3982.
[80] N.P. Tsai, Y.C. Tsui, L.N. Wei, Dynein motor contributes to stress granule dynamics in primary neurons, Neuroscience 159 (2009) 647–656.
[81] C.J. Beckham, R. Parker, P bodies, stress granules, and viral life cycles, Cell Host Microbe. 3 (2008) 206–212.
[82] S. Kim, H.Y. Kim, S. Lee, S.W. Kim, S. Sohn, K. Kim, H. Cho, Hepatitis B virus x protein induces perinuclear mitochondrial clustering in microtubule- and dynein-dependent manners, J. Virol. 81 (2007) 1714–1726.
[83] S. Boulant, M.W. Douglas, L. Moody, A. Budkowska, P. Targett-Adams, J. McLauchlan, Hepatitis C virus core protein induces lipid droplet redistribution in a microtubule- and dynein-dependent manner, Traffic 9 (2008) 1268–1282.
[84] M. Yamada, S. Toba, T. Takitoh, Y. Yoshida, D. Mori, T. Nakamura, A.H. Iwane, T. Yanagida, H. Imai, L.Y. Yu-Lee, T. Schroer, A. Wynshaw-Boris, S. Hirotsune, mNUDC is required for plus-end-directed transport of cytoplasmic dynein and dynactins by kinesin-1, EMBO J. 29 (2010) 517–531.
[85] T. Torisawa, A. Nakayama, K. Furuta, M. Yamada, S. Hirotsune, Y.Y. Toyoshima, Functional dissection of LIS1 and NDEL1 towards understanding the molecular mechanism of cytoplasmic dynein regulation, J. Biol. Chem. 286 (2010) 1959–1965.
[86] N. Mizuno, S. Toba, M. Edamatsu, J. Watai-Nishii, N. Hirokawa, Y.Y. Toyoshima, M. Kikkawa, Dynein and kinesin share an overlapping microtubule-binding site, EMBO J. 23 (2004) 2459–2467.
[87] J. de Mareuil, M. Carre, P. Barbier, G.R. Campbell, S. Lancelot, S. Opi, D. Esquieu, J.D. Watkins, C. Prevot, D. Braguer, V. Peyrot, E.P. Loret, HIV-1 Tat protein enhances microtubule polymerization, Retrovirology 2 (2005) 5.
[88] N.R. Watts, D.L. Sackett, R.D. Ward, M.W. Miller, P.T. Wingfield, S.S. Stahl, A.C. Steven, HIV-1 rev depolymerizes microtubules to form stable bilayered rings, J. Cell Biol. 150 (2000) 349–360.
[89] M. Nejmeddine, A.L. Barnard, Y. Tanaka, G.P. Taylor, C.R. Bangham, Human T-lymphotropic virus, type 1, tax protein triggers microtubule reorientation in the virological synapse, J. Biol. Chem. 280 (2005) 29653–29660.
[90] Z. Liao, L.M. Cimakasky, R. Hampton, D.H. Nguyen, J.E. Hildreth, Lipid rafts and hiv pathogenesis: Host membrane cholesterol is required for infection by hiv type 1, AIDS Res. Hum. Retroviruses 17 (2001) 1009–1019.
[91] M. Thali, The roles of tetraspanins in HIV-1 replication, Curr. Top. Microbiol. 339 (2009) 85–102.
[92] K. Levesque, M. Halvorsen, L. Abrahamyan, L. Chatel-Chaix, V. Poupon, H. Gordon, L. DesGroseillers, A. Gatignol, A.J. Mouland, Trafficking of HIV-1 RNA is mediated by heterogeneous nuclear ribonucleoprotein A2 expression and impacts on viral assembly, Traffic 7 (2006) 1177–1193.
[93] E. Poole, P. Strappe, H.P. Mok, R. Hicks, A.M. Lever, HIV-1 Gag-RNA interaction occurs at a perinuclear/centrosomal site; analysis by confocal microscopy and FRET, Traffic 6 (2005) 741–755.

[94] M. Lehmann, M.P. Milev, L. Abrahamyan, X.J. Yao, N. Pante, A.J. Mouland, Intracellular transport of human immunodeficiency virus type 1 genomic RNA and viral production are dependent on dynein motor function and late endosome positioning, J. Biol. Chem. 284 (2009). 14 572–14 585.
[95] W.S. Sossin, L. DesGroseillers, Intracellular trafficking of RNA in neurons, Traffic 7 (2006) 1581–1589.
[96] C. Kural, H. Kim, S. Syed, G. Goshima, V.I. Gelfand, P.R. Selvin, Kinesin and dynein move a peroxisome *in vivo*: A tug-of-war or coordinated movement? Science 308 (2005) 1469–1472.
[97] J.H. Carson, H. Cui, E. Barbarese, The balance of power in RNA trafficking, Curr. Opin. Neurobiol. 11 (2001) 558–563.
[98] C. Progida, M.R. Spinosa, A. De Luca, C. Bucci, RILP interacts with the VPS22 component of the ESCRT-II complex, Biochem. Biophys. Res. Commun. 347 (2006) 1074–1079.
[99] T. Wang, W. Hong, RILP interacts with VPS22 and VPS36 of ESCRT-II and regulates their membrane recruitment, Biochem. Biophys. Res. Commun. 350 (2006) 413–423.
[100] M. Johansson, N. Rocha, W. Zwart, I. Jordens, L. Janssen, C. Kuijl, V.M. Olkkonen, J. Neefjes, Activation of endosomal dynein motors by stepwise assembly of Rab7-RILP-p150^{Glued}, ORP1L, and the receptor βIII spectrin, J. Cell Biol. 176 (2007) 459–471.
[101] B. Short, C. Preisinger, J. Schaletzky, R. Kopajtich, F.A. Barr, The Rab6 GTPase regulates recruitment of the dynactin complex to Golgi membranes, Curr. Biol. 12 (2002) 1792–1795.
[102] J.N. Sfakianos, R.A. LaCasse, E. Hunter, The M-PMV cytoplasmic targeting-retention signal directs nascent Gag polypeptides to a pericentriolar region of the cell, Traffic 4 (2003) 660–670.
[103] J. Vlach, J. Lipov, M. Rumlova, V. Veverka, J. Lang, P. Srb, Z. Knejzlik, I. Pichova, E. Hunter, R. Hrabal, T. Ruml, D-retrovirus morphogenetic switch driven by the targeting signal accessibility to Tctex-1 of dynein, Proc. Natl. Acad. Sci. USA 105 (2008) 10565–10570.
[104] M. Forgues, M.J. Difilippantonio, S.P. Linke, T. Ried, K. Nagashima, J. Feden, K. Valerie, K. Fukasawa, X.W. Wang, Involvement of Crm1 in hepatitis B virus X protein-induced aberrant centriole replication and abnormal mitotic spindles, Mol. Cell Biol. 23 (2003) 5282–5292.
[105] N. Epie, T. Ammosova, T. Sapir, Y. Voloshin, W.S. Lane, W. Turner, O. Reiner, S. Nekhai, HIV-1 Tat interacts with LIS1 protein, Retrovirology 2 (2005) 6.
[106] N. Jouvenet, T. Wileman, African swine fever virus infection disrupts centrosome assembly and function, J. Gen. Virol. 86 (2005) 589–594.
[107] A. Ploubidou, V. Moreau, K. Ashman, I. Reckmann, C. Gonzalez, M. Way, Vaccinia virus infection disrupts microtubule organization and centrosome function, EMBO J. 19 (2000) 3932–3944.
[108] V. Piguet, Q. Sattentau, Dangerous liaisons at the virological synapse, J. Clin. Invest. 114 (2004) 605–610.
[109] G. Vasiliver-Shamis, M.L. Dustin, C.E. Hioe, HIV-1 virological synapse is not simply a copycat of the immunological synapse, Viruses 2 (2010) 1239–1260.
[110] C. Jolly, Q.J. Sattentau, Retroviral spread by induction of virological synapses, Traffic 5 (2004) 643–650.
[111] M. Nejmeddine, V.S. Negi, S. Mukherjee, Y. Tanaka, K. Orth, G.P. Taylor, C.R. Bangham, HTLV-1-Tax and ICAM-1 act on T-cell signal pathways to polarize the microtubule-organizing center at the virological synapse, Blood 114 (2009) 1016–1025.
[112] E.J. Quann, E. Merino, T. Furuta, M. Huse, Localized diacylglycerol drives the polarization of the microtubule-organizing center in T cells, Nat. Immunol. 10 (2009) 627–635.
[113] D. Rudnicka, J. Feldmann, F. Porrot, S. Wietgrefe, S. Guadagnini, M.C. Prevost, J. Estaquier, A.T. Haase, N. Sol-Foulon, O. Schwartz, Simultaneous cell-to-cell transmission of human immunodeficiency virus to multiple targets through polysynapses, J. Virol. 83 (2009) 6234–6246.

[114] A. Pumfery, C. de la Fuente, F. Kashanchi, HTLV-1 Tax: Centrosome amplification and cancer, Retrovirology 3 (2006) 50.
[115] C. Netherton, K. Moffat, E. Brooks, T. Wileman, A guide to viral inclusions, membrane rearrangements, factories, and viroplasm produced during virus replication, Adv. Virus Res. 70 (2007) 101–182.
[116] G.C. Katsafanas, B. Moss, Colocalization of transcription and translation within cytoplasmic poxvirus factories coordinates viral expression and subjugates host functions, Cell Host Microbe. 2 (2007) 221–228.
[117] B.M. Ward, Visualization and characterization of the intracellular movement of vaccinia virus intracellular mature virions, J. Virol. 79 (2005) 4755–4763.
[118] G. Remillard-Labrosse, C. Mihai, J. Duron, G. Guay, R. Lippe, Protein kinase D-dependent trafficking of the large herpes simplex virus type 1 capsids from the TGN to plasma membrane, Traffic 10 (2009) 1074–1083.
[119] P.L. Leopold, K.K. Pfister, Viral strategies for intracellular trafficking: Motors and microtubules, Traffic 7 (2006) 516–523.
[120] U.F. Greber, M. Way, A superhighway to virus infection, Cell 124 (2006) 741–754.
[121] K. Dohner, C.H. Nagel, B. Sodeik, Viral stop-and-go along microtubules: Taking a ride with dynein and kinesins, Trends Microbiol. 13 (2005) 320–327.
[122] T. Henry, J.P. Gorvel, S. Meresse, Molecular motors hijacking by intracellular pathogens, Cell. Microbiol. 8 (2006) 23–32.
[123] M. Gazzola, C.J. Burckhardt, B. Bayati, M. Engelke, U.F. Greber, P. Koumoutsakos, A stochastic model for microtubule motors describes the *in vivo* cytoplasmic transport of human adenovirus, PLoS Comput. Biol. 5 (2009) e1000623.
[124] H. Mabit, M.Y. Nakano, U. Prank, B. Saam, K. Dohner, B. Sodeik, U.F. Greber, Intact microtubules support adenovirus and herpes simplex virus infections, J. Virol. 76 (2002) 9962–9971.
[125] H. Kannan, S. Fan, D. Patel, I. Bossis, Y.J. Zhang, The hepatitis E virus open reading frame 3 product interacts with microtubules and interferes with their dynamics, J. Virol. 83 (2009) 6375–6382.
[126] K. Dohner, A. Wolfstein, U. Prank, C. Echeverri, D. Dujardin, R. Vallee, B. Sodeik, Function of dynein and dynactin in herpes simplex virus capsid transport, Mol. Biol. Cell 13 (2002) 2795–2809.
[127] B. Sodeik, M.W. Ebersold, A. Helenius, Microtubule-mediated transport of incoming herpes simplex virus 1 capsids to the nucleus, J. Cell Biol. 136 (1997) 1007–1021.
[128] K.S. Topp, L.B. Meade, J.H. LaVail, Microtubule polarity in the peripheral processes of trigeminal ganglion cells: Relevance for the retrograde transport of herpes simplex virus, J. Neurosci. 14 (1994) 318–325.
[129] A. Wolfstein, C.H. Nagel, K. Radtke, K. Dohner, V.J. Allan, B. Sodeik, The inner tegument promotes herpes simplex virus capsid motility along microtubules *in vitro*, Traffic 7 (2006) 227–237.
[130] G.J. Ye, K.T. Vaughan, R.B. Vallee, B. Roizman, The herpes simplex virus 1 U(L)34 protein interacts with a cytoplasmic dynein intermediate chain and targets nuclear membrane, J. Virol. 74 (2000) 1355–1363.
[131] E. Gonzalez Duran, R.M. del Angel, J.S. Salas Benito, *In vitro* interaction of poliovirus with cytoplasmic dynein, Intervirology 50 (2007) 214–218.
[132] E.R. Havecker, X. Gao, D.F. Voytas, The Sireviruses, a plant-specific lineage of the Ty1/copia retrotransposons, interact with a family of proteins related to dynein light chain 8, Plant Physiology 139 (2005) 857–868.
[133] E. Herrero-Martinez, K.L. Roberts, M. Hollinshead, G.L. Smith, Vaccinia virus intracellular enveloped virions move to the cell periphery on microtubules in the absence of the A36R protein, J. Gen. Virol. 86 (2005) 2961–2968.

In this chapter

23

Cytoplasmic Dynein Dysfunction and Neurodegenerative Disease

Armen J. Moughamian, Erika L.F. Holzbaur
Department of Physiology, University of Pennsylvania School of Medicine, Philadelphia, PA, USA

23.1 Introduction

Active, directed transport along cytoplasmic microtubules is a characteristic feature of mammalian cells. The transport of organelles, vesicles, and proteins along the microtubule cytoskeleton is driven by both kinesins and cytoplasmic dynein. This transport is essential for normal intracellular trafficking, including both biosynthetic and degradative pathways. However, microtubule-based transport is especially important in large cells, which cannot rely on diffusion to efficiently distribute proteins or organelles. Directed transport is also critical in polarized cells, where the localized trafficking of components to specific cellular destinations is required for normal cellular function.

Neurons are both large and polarized, so these cells would be expected to be particularly reliant on microtubule-based transport (Fig. 23.1). In fact, neurons are uniquely vulnerable to defects in dynein function. Mutations in cytoplasmic dynein and/or its activator dynactin result in neurological defects in humans as well as in model organisms including *Drosophila* and mice. Here, we review the critical roles dynein plays in neurons and then discuss the effects that dynein and dynactin mutations have on neuronal function. Finally, we discuss neurodegenerative diseases in which dynein dysfunction is not the proximal cause but may be a key contributor to the pathological state. The important role of the dynein motor in intracellular trafficking and transport makes it likely that defects in this pathway contribute to a number of neurodegenerative diseases, including amyotrophic lateral sclerosis (ALS) and Huntington's disease (HD).

Dyneins DOI: 10.1016/B978-0-12-382004-4.10023-8
Copyright © 2012 by Elsevier Inc. All rights reserved.

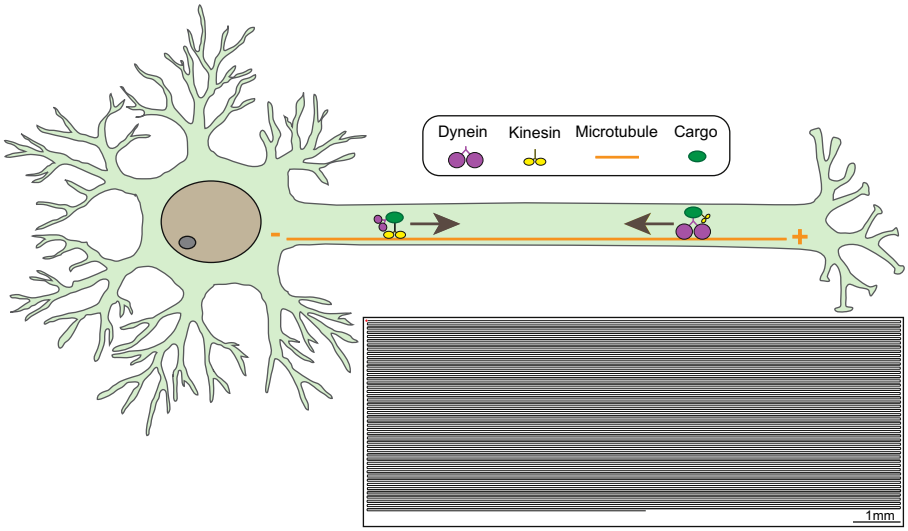

Figure 23.1 Axonal transport. Neurons are polarized cells with dendritic and axonal projections projecting from the cell body. Microtubules in the axon are uniformly oriented with the plus ends outward. The plus-end-directed microtubule motor, kinesin, transports cargos from the cell body to the distal axon and synapse, while the minus-end-directed microtubule motor, dynein, transports cargos from the axon back to the cell body. In dendrites, microtubules are organized with mixed polarity, making the analysis of dendritic trafficking more complex. Cargos move along microtubules with multiple motors attached; bidirectional transport may be regulated via scaffolding proteins, but may also involve a stochastic tug-of-war mechanism [5,79]. (Inset) To-scale representation of an α motor neuron illustrating the vast distances that microtubule motors must traverse in order to maintain the distal axon and synapse. An α motor neuron projecting from the lumbar spinal cord to a muscle in the foot has a typical cell body diameter of 50 mm (shown in red, top left of inset) and an axon length of approximately 1 m. Inset adapted with permission from a drawing by Peter Hollenbeck.

23.2 Cytoplasmic Dynein Drives Intracellular Transport in Neurons

23.2.1 Intracellular Trafficking

In neurons, the microtubule array is polarized within the soma (cell body) and the axon, with minus ends directed toward the cell center and plus ends directed outward. Cytoplasmic dynein is the major, perhaps only, long-distance minus-end-directed motor for vesicles and organelles. Thus, dynein drives the inward motility of diverse cellular compartments involved in both biosynthetic and degradative pathways in the cell. For example, dynein drives vesicles moving from the endoplasmic reticulum to the Golgi complex during the synthesis of membrane-associated and secreted proteins [1], and also drives the motility of the lysosomal compartment essential for normal degradation [2–5]. Loss of dynein

function is predicted to have significant effects on the normal housekeeping functions of the cell [3]. However, it remains unclear whether the observed lethality upon dynein knockout is due to a trafficking deficiency or instead to a defect in cell division [6].

Dynein has a role in early endosomal formation, motility, maturation, and sorting [7–9], processes that are critical for normal neuronal function. In small, nonpolarized cells such as HeLa, loss of dynein affects organelle positioning but does not appear to significantly affect the kinetics of endocytosis or recycling [10]. However, in larger, polarized cells such as neurons, defects induced by dynein dysfunction are likely to become more critical. For example, studies in *Drosophila* have shown that dynein is essential to maintain normal synaptic vesicle recycling during high-frequency stimulation [9].

23.2.2 Degradative Pathways

Neurons are post-mitotic, making them particularly reliant on efficient degradative processes to remove misfolded or aggregated proteins or dysfunctional organelles. Many of the major neurodegenerative diseases, including ALS, HD, Alzheimer's disease, and Parkinson's disease are characterized pathologically by the accumulation of protein aggregates. This suggests that neurons may be uniquely vulnerable to even minor dysfunction of degradative pathways, including lysosomal and proteosomal pathways, aggresome formation, and autophagic clearance of organelles. In conjunction with kinesin-1 and kinesin-2, dynein is known to drive the bidirectional transport of lysosomes [5]. While it has not been directly demonstrated that defects in lysosomal motility lead to defects in protein degradation [10], it remains a compelling hypothesis that the bidirectional movement of lysosomes throughout both axonal and dendritic processes enhances the efficient clearance of misfolded or aging proteins, or small protein aggregates. The continuous bidirectional motility of lysosomes may thus serve as a surveillance mechanism allowing for efficient clearance of protein aggregates from extended neuronal processes. Consistent with this hypothesis, it has been shown that very subtle defects in Rab7 function are sufficient to cause one form of Charcot–Marie–Tooth disease (type 2B) [11,12]. Rab7 has been shown to regulate the association of dynein with the lysosomal compartment [4], so a defect in Rab7-dependent regulation may potentially affect either the localization or motility of lysosomes in affected patients.

Significant links between motor activity and proteosomal function have not been established, but dynein has been shown to drive aggresome formation. Aggresomes are accumulations of filamentous proteins and entrapped organelles in inclusions near the nucleus [13]. Dynein drives the inward movement of the components of this structure [14], potentially through a link mediated by the microtubule-associated deacetylase HDAC6 [15]. However, it remains unclear whether aggresomes have a role in normal cellular processes or are

instead induced in cell culture by the overexpression of misfolded or mutant proteins.

lDynein function also appears to be critical for autophagy. This essential cellular process removes aggregated proteins and old or damaged organelles such as mitochondria and is upregulated under conditions of cellular stress such as starvation. Neurons are clearly dependent on autophagy, as neuron-specific knockout of either of two essential autophagy genes, Atg5 and Atg7, leads to degeneration in the cerebellar and cerebral cortices [16,17]. Dynein likely drives autophagosome motility along neuronal processes [18] and has also been proposed to mediate efficient fusion of autophagosomes with lysosomes [19].

23.2.3 Axonal and Dendritic Transport

Perhaps the best-studied role of dynein in neurons is driving the robust retrograde motility of vesicles and organelles along the axon. This activity was first demonstrated in classic nerve ligation assays by Hirokawa et al. [20,21], in which dynein-associated organelles were observed to accumulate both proximally and distally to the site of ligature, while kinesin-associated organelles accumulated on the proximal side only. This result was interpreted as evidence that dynein motors, synthesized in the cytoplasm, are passively transported outward along the axon by kinesins, where they become activated and drive vesicle transport back to the cell body. In contrast, kinesins may take a one-way trip, driving anterograde transport outward along the axon followed by degradation at the distal terminal. Subsequent studies have shown that multiple members of the kinesin superfamily drive anterograde movement along the axon, including kinesin-1, kinesin-2, and kinesin-3, while cytoplasmic dynein remains the only known motor for fast retrograde motility.

Classic studies on axonal transport identified two major forms of motility: a fast phase and a slower phase. Fast axonal transport rates are reported as ~100–400 mm/day (1–4 μm/s) and slow axonal transport rates are ~0.1–4 mm/day (1–40 nm/s) [25]. Fast axonal transport has been studied with an array of approaches including live cell imaging of cargos including lysosomal and mitochondrial markers, synaptic protein cargos, amyloid precursor protein (APP), fluorescently labeled Rabs, NGF-bound quantum dots, and tetanus toxin. These studies have provided many new insights into the mechanisms involved. Much of the observed transport is bidirectional, with cargos such as lysosomes and mitochondria alternating in movement in either the anterograde or retrograde direction [5,22]. In contrast, other dynein cargos, such as NGF-associated signaling endosomes, show pronounced unidirectional motility [23–25]. Additionally, the speed of motility is cargo specific; some cargos such as APP move significantly faster than other cargos such as mitochondria. While the motors driving fast axonal transport were identified relatively rapidly [20,21], the mechanisms driving the much slower transport of proteins such as neurofilaments

remained less clear for many years. Insight into the process came from a breakthrough study demonstrating that the net slow movement of neurofilaments was the result of short bursts of rapid movement separated by prolonged pauses with no movement [26]. Consistent with this analysis, kinesin-1A and dynein have been identified as the motors for the bidirectional slow transport of neurofilaments along the axon [27,28].

The uniform polarity of microtubule organization in axons makes it relatively easy to assess the mechanisms driving transport. In contrast, the more complex, mixed polarity of microtubules in dendrites has slowed the analysis of transport in this compartment. However, recent studies suggest that, while kinesin-1 transports cargo into the axon, dynein is required for the polarized targeting of cargos such as AMPA receptors to dendrites [29]. Further complicating the issue are recent studies that demonstrate a critical role for dynein in the initial establishment of the mixed microtubule polarity of dendrites [30]. While the mechanisms involved remain to be determined, this represents an additional role for dynein required for normal neuronal function.

In summary, cytoplasmic dynein is essential for the normal function of multiple intracellular trafficking pathways in higher eukaryotes. However, the large, polarized morphology and post-mitotic nature of neurons make these cells uniquely vulnerable to even subtle defects in dynein function. Unlike the functional redundancy of the kinesin motor system, a single cytoplasmic dynein motor is responsible for most minus-end-directed vesicular and organelle motility. Thus, defects in dynein would be expected to have a critical effect on neuronal function. This point has been illustrated in both humans and animal models, in which mutations in dynein or an associated protein such as dynactin cause neuron-specific phenotypes including developmental defects and/or motor, sensory, and central-nervous-system degeneration.

23.3 Dynein Function in Developing Neurons

In addition to the roles for dynein in mature neurons discussed above, dynein also has a critical role in the developing nervous system, reviewed in Chapter 16. Dynein helps to drive nucleokinesis, the movement of nuclei during the robust migration of neurons that occurs in the developing brain and nervous system. Consistent with this critical role, mutations in the dynein regulatory protein Lis1 lead to a severe developmental disease called lissencephaly (reviewed in [31]). Patients with this defect have a “smooth brain,” with accompanying mental retardation, among other defects, the disrupted migration of neurons during development leads to misformation of the cortex. Mouse models with knockout of Lis1 or the co-regulatory proteins NDE1 (formerly NudE) and NDEL1 (formerly NudEL) support a key role for dynein in this process [32,33].

23.4 Dynein Dysfunction in Neurodegeneration

23.4.1 Dynactin Mutations

To date, no disease-associated mutations have been reported in human genes encoding subunits of cytoplasmic dynein. However, mutations in multiple dynein-associated proteins have been shown to cause neurodegenerative disease (Fig. 23.2). The first of these mutations to be identified was the G59S mutation in the $p150^{Glued}$ subunit of dynactin, encoded by the DCTN1 gene [34]. Dynactin is a highly conserved accessory or activator complex for dynein. Dynactin is required for most or all dynein-mediated functions discovered to date, including those discussed above, such as vesicle trafficking and axonal transport (Fig. 23.2). In a range of model systems, mutations in dynactin have a similar phenotype to mutations in dynein.

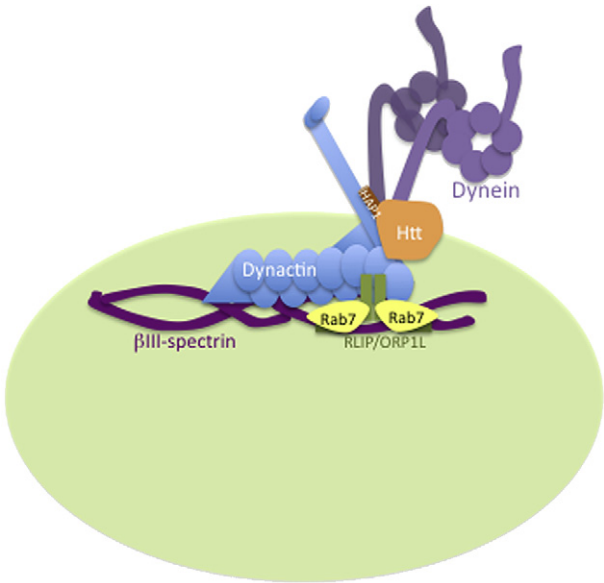

Figure 23.2 Model for the vesicle-associated dynein motor complex: Mutations in either dynein or dynein-interacting proteins lead to neurodegeneration. Cytoplasmic dynein binds to dynactin; this association is required for the intracellular transport of vesicles and organelles. Dynein also binds to huntingtin (Htt) [43]. The Htt-binding protein HAP1 in turn binds to the $p150^{Glued}$ subunit of dynactin, forming a complex that facilitates dynein-mediated transport [44]. An adaptor complex consisting of Rab7, RILP, ORP1L, and βIII-spectrin recruits dynein to some endosomal cargos [47,48,80]. Mutations in dynein cause neurodegeneration in mice [64], and mutations in dynactin, Htt, Rab7, and βIII-spectrin induce neurodegeneration in humans [34,41,44,46,49,81].

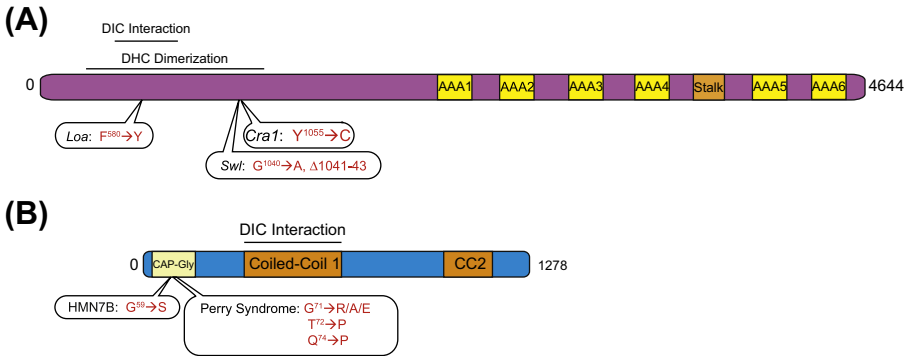

Figure 23.3 Neurodegenerative mutations in cytoplasmic dynein HC and the p150^{Glued} subunit of dynactin. (A) The dynein HC is a large protein containing six AAA-ATPase domains and a microtubule binding stalk near the C-terminus responsible for binding to the microtubule and producing force. At the N-terminus of the dynein HC there is a dimerization domain as well as binding determinants for dynein IC. The *Loa*, *Cra1*, and *Swl* mutations are all located in this N-terminal region [64,65]. (B) The p150^{Glued} subunit of dynactin contains two coiled-coil domains, the first of which is responsible for both the dimerization of p150^{Glued} and attachment to the dynein motor via a direct interaction with dynein IC. The N-terminus of p150^{Glued} contains a highly conserved CAP-Gly domain that interacts directly with microtubules and the microtubule plus-end complex. Mutations in the CAP-Gly domain of p150^{Glued} cause two distinct autosomal dominant neurodegenerative diseases, hereditary motor neuropathy VIIB (HMN7B) and Perry syndrome [34,41].

The p150^{Glued} subunit of dynactin binds to dynein via a direct association with dynein intermediate chain (IC) [35,36]. p150^{Glued} also mediates the direct association of dynactin with microtubules, via a highly conserved N-terminal CAP-Gly (cytoskeletal-associated protein, glycine-rich) domain (Fig. 23.3) [37]. There is a single gene, DCTN1, encoding p150^{Glued} in humans [38], so the mutant protein is expressed in all tissues. However, affected individuals have a motor-neuron-specific disease, hereditary motor neuropathy VIIB (HMN7B), also known as distal spinal and bulbar muscular atrophy (dSBMA) [34,39]. The G59S mutation in DCTN1 is autosomal dominant. Biochemical and cellular approaches indicate that the mutant protein is likely misfolded and meta-stable. Non-neuronal cells may efficiently clear the defective polypeptide, leaving sufficient wild-type protein for normal function. However, the misfolded p150^{Glued} polypeptide accumulates in aggregates in motor neurons in affected patients; dynein is also recruited to these aggregates [39,40]. While these observations suggest that the G59S mutation adversely affects protein folding or stability, functional studies indicate that the mutation also inhibits dynactin function [40]. Both loss of dynein/dynactin activity and the toxic accumulation of aggregated proteins are likely to contribute to disease in patients with HMN7B, which has been extensively studied in mouse models (Sections 23.5.3 and 23.5.4).

Intriguingly, a more recent genetic study has shown that mutations in the same CAP-Gly domain of p150^{Glued} cause a distinct and lethal form of

neurodegeneration known as Perry syndrome [41]. Perry syndrome is an autosomal dominant disorder consisting of Parkinsonism accompanied by depression, weight loss, and hypoventilation. All known genetically inherited forms of the disease have been shown to result from mutations in DCTN1, clustered within the CAP-Gly domain (Fig. 23.3). These mutations (G71R, G71E, G71A, T72P, and Q74P) are predicted to affect dynactin function [41], but it remains unclear why these changes induce a significantly different disease affecting a different population of neurons from the previously characterized G59S mutation in the same domain. Further research will be required to answer this question.

23.4.2 Dynein and Huntingtin

Mutations in other dynein-associated proteins are also directly linked to human disease (Fig. 23.2). The best-studied of these proteins is huntingtin. Expansion of a polyglutamine repeat in the N-terminus of huntingtin, from $\leq$35 repeats in normal individuals to $>$35 in affected individuals, is the sole cause of HD. HD is a fatal neurodegenerative disorder that primarily affects medium spiny neurons in the basal ganglia and is characterized by chorea, loss of motor coordination, and cognitive decline. Pathogenic expansion of the normal polyglutamine sequence leads to increased aggregation of the huntingtin protein in both cell body and nucleus, and induces an array of cellular changes including alterations in gene expression (reviewed in [42]).

It remains unclear whether the autosomal dominant disease is caused entirely by a toxic gain of function, or whether loss of normal huntingtin function contributes. Part of this uncertainty stems from the fact that the normal function of huntingtin is not well understood. However, recent work has shown that huntingtin binds directly to cytoplasmic dynein [43] and indirectly to both dynactin and kinesin-1 (reviewed in [44]). This has led to a model in which huntingtin may play a role in regulating bidirectional vesicle transport along microtubules. Huntingtin has also been proposed to integrate the microtubule and actin cytoskeletons, either by regulating the association of endosomes with microtubules and actin filaments [45] or by regulating organelle-associated actin polymerization [10].

23.4.3 Rab7 and βIII-Spectrin

Two other mutations in dynein-associated proteins may specifically affect motor–cargo associations. Rab7 is a small GTPase involved in the regulation of late endosomes and lysosomes. A mutation in Rab7 was identified as the cause of Charcot–Marie–Tooth disease type 2B, a disorder characterized primarily by the length-dependent degeneration of sensory neurons [46]. Detailed structural and biochemical studies have shown that the mutation causes a relatively mild misregulation of Rab7 function [12]. Rab7 has been shown to be key to the recruitment of dynein to late endosomes and lysosomes, via a mechanism that

includes RLIP, ORPIL, and βIII spectrin, so it is possible that this misregulation of Rab7 activity affects the motility of lysosomes along extended axonal processes [4].

βIII spectrin is a dynactin-binding protein proposed to be directly involved in the association of the dynein–dynactin motor with vesicular cargos [47,48]. Recent work has shown that mutations in βIII spectrin are the cause of spinocerebellar ataxia type 5 (SCA5) [49]. Modeling of these mutations in *Drosophila* has shown that expression of the mutant protein affects axonal transport, which is consistent with a role for βIII in dynein-mediated trafficking within the neuron [50].

23.5 Dynein Mutations in Model Organisms

23.5.1 *Drosophila*

The vertebrate protein $p150^{Glued}$, the largest subunit of dynactin, was initially identified in part as a result of its homology with the product of the *Drosophila* gene *Glued* (*Gl*) [51]. The Gl^1 mutation is an autosomal dominant defect caused by a transposon insertion leading to the expression of a truncated form of the polypeptide [52]. This truncated polypeptide cannot bind to the Arp1 filament that forms the base of the dynactin complex, and thus is proposed to lead to the detachment of dynein from vesicular cargo [53].

Flies expressing the Gl^1 mutation have a rough eye phenotype, a readout for defects in neurodevelopment and/or neurodegeneration. Electon microscopy analysis shows pronounced defects in the morphology of some neurons in the optic lobe, and genetic studies show that the defect is cell autonomous [54]. Live imaging studies have demonstrated axonal transport defects in neurons in the Gl^1 fly [22], while genetic analysis has shown that the product of the *Glued* gene interacts genetically with both dynein and kinesin [55]. More recently, a study modeling a human SCA5-associated mutation in βIII-spectrin using *Drosophila* has shown defects in axonal transport as well as synaptic disruption [50].

23.5.2 *Caenorhabditis elegans*

Studies examining dynein function in *Caenorhabditis elegans* strongly support a key role for the motor in retrograde axonal transport [56,57]. An interesting recent study [58] examined the role of cyclin-dependent kinases in the regulation of neuronal transport, leading to the hypothesis that cyclin-dependent kinases such as CDK-5 regulate polarized trafficking by controlling dynein motor function. This is an intriguing model but more research is required to fully understand the regulation of microtubule-based transport in the neuron.

23.5.3 Mouse Models of Hereditary Motor Neuropathy VIIB

Mouse models may be the most informative in relating defects in dynein function to neurodegenerative disease. The first model in which this question was examined was a transgenic mouse engineered to overexpress the dynamitin subunit of dynactin in motor neurons, leading to a cell-type-specific inhibition of dynein–dynactin function [59]. The resulting mouse line develops a late-onset, slowly progressive degeneration of motor neurons that resembles the disease course observed in patients expressing the G59S mutation in DCTN1.

More recently, this G59S mutation has been modeled, in both knockin and transgenic models [60–62]. There is some variability in the phenotypes observed in the resulting lines. Both the knockin G59S mouse and one of the transgenic models develop progressive motor neuron degeneration very slowly, consistent with the disease course in humans, while a second transgenic line displays more marked degeneration that is fatal within ~10 months [61]. Pronounced defects in axonal transport were not observed [62], but all three models display destabilization of the neuromuscular junction. Marked changes in membranous organelles within the cell body were also noted, most significantly the proliferation of tertiary lysosomes and lipofuscin granules [62].

These studies have suggested that the pathogenesis resulting from mutations in the dynein pathway may not be solely the result of disruptions in axonal transport. Synaptic defects are observed in numerous models of dynein/dynactin dysfunction. Destabilization of the presynaptic terminal was first observed in mutant Gl^{1} flies; presynaptic defects have subsequently been observed in both fly and mouse models [60,62,63]. Together these data suggest that the dynein complex may have an additional neuron-specific cellular function at the synapse beyond the well-characterized role of the motor in minus-end-directed transport.

23.5.4 The *Loa*, *Cra1*, and *Swl* Mouse Models

Three lines of mice with mutations in dynein heavy chain (HC) have now been characterized in some detail (see Chapter 18). Two lines, *Loa* (Legs-at-odd-angles) and *Cra1* (Cramping-1), have point mutations in the N-terminal tail domain of cytoplasmic dynein HC, and *Swl* (Sprawling) mice have a three-amino-acid residue deletion, also in the tail domain of dynein HC [64,65] (Fig. 23.3). As the tail domain of dynein mediates both HC dimerization and the association between dynein HC and dynein IC, these mutations are predicted to affect the integrity of the holo-dynein complex. Biochemical and biophysical characterization of dynein purified from both heterozygous and homozygous *Loa* mice further supports this interpretation [66].

Both the *Loa* and *Cra1* phenotypes were initially interpreted as motor neuron defects [64]. The characterization of the *Swl* mouse as primarily a sensory defect due to the abnormal developmental of proprioceptive neurons [65] led to the re-examination of this interpretation [67,68]. Further studies have also found significant deficits in striatal neuron morphology in *Cra1* mice [69]. As dynein HC is encoded by a single gene whose expression is required for the normal function of all neurons, it is likely that all three lines exhibit pleiotropic defects, both developmental and degenerative. While it is possible that analysis of the specific mutations involved might provide insight into cell-type-specific functions, it is perhaps more likely that multiple pathways are affected and that neurons are differentially sensitive to these defects based on other variables such as specific requirements for continued trophic factor support, neuronal specific morphologies, or sensitivity to defects in degradative pathway function.

23.6 Dynein's Role in the Pathogenesis of Common Neurodegenerative Disease

The neurodegenerative diseases discussed above are caused directly by mutations in dynein-associated proteins. However, it is likely that the overall number of patients affected directly by mutations in this pathway is relatively low. There is no genetic or functional redundancy for most aspects of the cytoplasmic dynein pathway, so mutations must be relatively mild in order for affected individuals to survive development. In patients with mutations in DCTN1, for example, dynein–dynactin function is only mildly compromised and the symptoms do not become apparent until two or more decades have passed.

However, dysfunction of the dynein pathway is implicated in the pathogenesis of a much broader range of neurodegenerative disease. Trafficking and transport defects may be at the heart of pathogenesis in a number of major diseases. For example, specific deficits in axonal transport have been measured in animal models of ALS, HD, Parkinson's disease, and Alzheimer's disease (reviewed in [70]).

23.6.1 Amyotrophic Lateral Sclerosis

In ALS, defects in fast axonal transport have been noted early in the disease process, with retrograde defects more significant than anterograde defects both *in vitro* and *in vivo* [24,71,72]. Furthermore, it is not just the velocity of transport that is affected. There are pronounced changes in the cargo being transported in the retrograde direction along the axon, including marked changes in key signaling molecules [24]. Thus, the regulation of both motors and their cargos are of vital importance for maintaining neuronal health.

One example of how the nature of cargo transported by dynein is changed due to alterations in the cellular environment occurs during axonal injury. Following injury to the axon, the retrograde transport of neurotrophins may cease [73]. Instead, dynein drives the transport of stress signals to the nucleus [74]. A similar process may occur in neurodegeneration, with axonal transport mediating the signaling between the cell periphery and the nucleus [24,70].

23.6.2 Huntington's Disease

Axonal transport deficits have also been noted in models of HD [75]. The disease-associated protein huntingtin binds directly to dynein and also associates with both dynactin and kinesin-1 [43]. The phosphorylation state of huntingtin affects its association with kinesin, leading to a model in which huntingtin acts as switch for bidirectional transport [76] and thus affects the efficiency of delivery and/or uptake of the essential neurotrophic factor BDNF [77]. Expression of mutant huntingtin in patients with HD may disrupt this regulation, leading to defects in axonal transport [44].

23.6.3 Parkinson's Disease and Alzheimer's Disease

In the variant form of Parkinson's disease known as Perry syndrome, disease is caused by mutations in dynactin [41]. Other familial forms of Parkinson's disease have been linked to genes affecting mitophagy, the process of clearance of defective mitochondria by autophagy [70]. Dynein has been implicated in the autophagy of aggregated proteins [18] and may also promote mitophagy, although more research into the mechanisms involved is required. In contrast, in Alzheimer's disease, there have been no direct links as of yet to dynein dysfunction, but interesting progress on the role of tau in axonal transport may provide some further insights [78].

23.7 Conclusions

The identification of cytoplasmic dynein as an essential minus-end-directed motor in higher eukaryotes has led to a much deeper understanding of the role of active transport in the neuron. Many of the key pathways involved have been illuminated, but many important questions remain. The significance of these questions to neurodegenerative disease is becoming increasingly clear with the identification of human mutations in the dynein-associated protein dynactin, Lis1, Rab7, and βIII spectrin. This is now a very rapidly progressing field, where basic research is informing clinical discoveries and in turn clinical observations are accelerating our understanding of basic cellular processes.

References

[1] J.F. Presley, N.B. Cole, T.A. Schroer, K. Hirschberg, K.J. Zaal, J. Lippincott-Schwartz, ER-to-Golgi transport visualized in living cells, Nature 389 (1997) 81–85.

[2] J.K. Burkhardt, C.J. Echeverri, T. Nilsson, R.B. Vallee, Overexpression of the dynamitin (p50) subunit of the dynactin complex disrupts dynein-dependent maintenance of membrane organelle distribution, J. Cell Biol. 139 (1997) 469–484.

[3] A. Harada, Y. Takei, Y. Kanai, Y. Tanaka, S. Nonaka, N. Hirokawa, Golgi vesiculation and lysosome dispersion in cells lacking cytoplasmic dynein, J. Cell Biol. 141 (1998) 51–59.

[4] I. Jordens, M. Fernandez-Borja, M. Marsman, S. Dusseljee, L. Janssen, J. Calafat, H. Janssen, R. Wubbolts, J. Neefjes, The Rab7 effector protein RILP controls lysosomal transport by inducing the recruitment of dynein–dynactin motors, Curr. Biol. 11 (2001) 1680–1685.

[5] A.G. Hendricks, E. Perlson, J.L. Ross, H.W. Schroeder 3rd, M. Tokito, E.L. Holzbaur, Motor coordination via a tug-of-war mechanism drives bidirectional vesicle transport, Curr. Biol. 20 (2010) 697–702.

[6] K.H. Siller, M. Serr, R. Steward, T.S. Hays, C.Q. Doe, Live imaging of *Drosophila* brain neuroblasts reveals a role for Lis1/dynactin in spindle assembly and mitotic checkpoint control, Mol. Biol. Cell 16 (2005) 5127–5140.

[7] O.J. Driskell, A. Mironov, V.J. Allan, P.G. Woodman, Dynein is required for receptor sorting and the morphogenesis of early endosomes, Nat. Cell. Biol. 9 (2007) 113–120.

[8] K.J. Palmer, H. Hughes, D.J. Stephens, Specificity of cytoplasmic dynein subunits in discrete membrane-trafficking steps, Mol. Biol. Cell 20 (2009) 2885–2899.

[9] X. Li, H. Kuromi, L. Briggs, D.B. Green, J.J. Rocha, S.T. Sweeney, S.L. Bullock, Bicaudal-D binds clathrin heavy chain to promote its transport and augments synaptic vesicle recycling, EMBO J. 29 (2010) 992–1006.

[10] J.P. Caviston, A.L. Zajac, M. Tokito, E.L. Holzbaur, Huntingtin coordinates the dynein-mediated dynamic positioning of endosomes and lysosomes, Mol. Biol. Cell 22 (2010) 478–492.

[11] L. Cogli, F. Piro, C. Bucci, Rab7 and the CMT2B disease, Biochem. Soc. Trans. 37 (2009) 1027–1031.

[12] B.A. McCray, E. Skordalakes, J.P. Taylor, Disease mutations in Rab7 result in unregulated nucleotide exchange and inappropriate activation, Hum. Mol. Genet. 19 (2010) 1033–1047.

[13] J.A. Olzmann, L. Li, L.S. Chin, Aggresome formation and neurodegenerative diseases: Therapeutic implications, Curr. Med. Chem. 15 (2008) 47–60.

[14] J.A. Johnston, M.E. Illing, R.R. Kopito, Cytoplasmic dynein/dynactin mediates the assembly of aggresomes, Cell Motil. Cytoskeleton 53 (2002) 26–38.

[15] Y. Kawaguchi, J.J. Kovacs, A. McLaurin, J.M. Vance, A. Ito, T.P. Yao, The deacetylase HDAC6 regulates aggresome formation and cell viability in response to misfolded protein stress, Cell 115 (2003) 727–738.

[16] T. Hara, K. Nakamura, M. Matsui, A. Yamamoto, Y. Nakahara, R. Suzuki-Migishima, M. Yokoyama, K. Mishima, I. Saito, H. Okano, N. Mizushima, Suppression of basal autophagy in neural cells causes neurodegenerative disease in mice, Nature 441 (2006) 885–889.

[17] M. Komatsu, S. Waguri, T. Chiba, S. Murata, J. Iwata, I. Tanida, T. Ueno, M. Koike, Y. Uchiyama, E. Kominami, K. Tanaka, Loss of autophagy in the central nervous system causes neurodegeneration in mice, Nature 441 (2006) 880–884.

[18] B. Ravikumar, A. Acevedo-Arozena, S. Imarisio, Z. Berger, C. Vacher, C.J. O'Kane, S.D. Brown, D.C. Rubinsztein, Dynein mutations impair autophagic clearance of aggregate-prone proteins, Nat. Genet. 37 (2005) 771–776.

[19] S. Kimura, T. Noda, T. Yoshimori, Dynein-dependent movement of autophagosomes mediates efficient encounters with lysosomes, Cell Struct. Funct. 33 (2008) 109–122.

[20] N. Hirokawa, R. Sato-Yoshitake, T. Yoshida, T. Kawashima, Brain dynein (MAP1C) localizes on both anterogradely and retrogradely transported membranous organelles *in vivo*, J. Cell Biol. 111 (1990) 1027–1037.
[21] N. Hirokawa, R. Sato-Yoshitake, N. Kobayashi, K.K. Pfister, G.S. Bloom, S.T. Brady, Kinesin associates with anterogradely transported membranous organelles *in vivo*, J. Cell Biol. 114 (1991) 295–302.
[22] A.D. Pilling, D. Horiuchi, C.M. Lively, W.M. Saxton, Kinesin-1 and dynein are the primary motors for fast transport of mitochondria in *Drosophila* motor axons, Mol. Biol. Cell 17 (2006) 2057–2068.
[23] B. Cui, C. Wu, L. Chen, A. Ramirez, E.L. Bearer, W.P. Li, W.C. Mobley, S. Chu, One at a time, live tracking of NGF axonal transport using quantum dots, Proc. Natl. Acad. Sci. USA 104 (2007) 13666–13671.
[24] E. Perlson, G.-B. Jeong, J.L. Ross, R. Dixit, K.E. Wallace, R.G. Kalb, E.L.F. Holzbaur, A switch in retrograde signaling from survival to stress in rapid-onset neurodegeneration, J. Neurosci. 29 (2009) 9903–9917.
[25] R.B. Vallee, G.S. Bloom, Mechanisms of fast and slow axonal transport, Annu. Rev. Neurosci. 14 (1991) 59–92.
[26] L. Wang, C.L. Ho, D. Sun, R.K. Liem, A. Brown, Rapid movement of axonal neurofilaments interrupted by prolonged pauses, Nat. Cell. Biol. 2 (2000) 137–141.
[27] A. Uchida, N.H. Alami, A. Brown, Tight functional coupling of kinesin-1A and dynein motors in the bidirectional transport of neurofilaments, Mol. Biol. Cell 20 (2009) 4997–5006.
[28] O.I. Wagner, J. Ascano, M. Tokito, J.F. Leterrier, P.A. Janmey, E.L. Holzbaur, The interaction of neurofilaments with the microtubule motor cytoplasmic dynein, Mol. Biol. Cell 15 (2004) 5092–5100.
[29] L.C. Kapitein, M.A. Schlager, M. Kuijpers, P.S. Wulf, M. van Spronsen, F.C. MacKintosh, C.C. Hoogenraad, Mixed microtubules steer dynein-driven cargo transport into dendrites, Curr. Biol. 20 (2010) 290–299.
[30] Y. Zheng, J. Wildonger, B. Ye, Y. Zhang, A. Kita, S.H. Younger, S. Zimmerman, L.Y. Jan, Y.N. Jan, Dynein is required for polarized dendritic transport and uniform microtubule orientation in axons, Nat. Cell. Biol. 10 (2008) 1172–1180.
[31] A. Wynshaw-Boris, T. Pramparo, Y.H. Youn, S. Hirotsune, Lissencephaly: Mechanistic insights from animal models and potential therapeutic strategies, Semin. Cell Dev. Biol. 21 823-830.
[32] Y. Feng, C.A. Walsh, Mitotic spindle regulation by Nde1 controls cerebral cortical size, Neuron 44 (2004) 279–293.
[33] S. Sasaki, D. Mori, K. Toyo-oka, A. Chen, L. Garrett-Beal, M. Muramatsu, S. Miyagawa, N. Hiraiwa, A. Yoshiki, A. Wynshaw-Boris, S. Hirotsune, Complete loss of Ndel1 results in neuronal migration defects and early embryonic lethality, Mol. Cell Biol. 25 (2005) 7812–7827.
[34] I. Puls, C. Jonnakuty, B.H. LaMonte, E.L. Holzbaur, M. Tokito, E. Mann, M.K. Floeter, K. Bidus, D. Drayna, S.J. Oh, R.H. Brown Jr., C.L. Ludlow, K.H. Fischbeck, Mutant dynactin in motor neuron disease, Nat. Genet. 33 (2003) 455–456.
[35] S. Karki, E.L. Holzbaur, Affinity chromatography demonstrates a direct binding between cytoplasmic dynein and the dynactin complex, J. Biol. Chem. 270 (1995) 28806–28811.
[36] K.T. Vaughan, R.B. Vallee, Cytoplasmic dynein binds dynactin through a direct interaction between the intermediate chains and $p150^{Glued}$, J. Cell Biol. 131 (1995) 1507–1516.
[37] C.M. Waterman-Storer, S. Karki, E.L. Holzbaur, The $p150^{Glued}$ component of the dynactin complex binds to both microtubules and the actin-related protein centractin (Arp-1), Proc. Natl. Acad. Sci. USA 92 (1995) 1634–1638.
[38] M.K. Tokito, E.L. Holzbaur, The genomic structure of DCTN1, a candidate gene for limb-girdle muscular dystrophy (LGMD2B), Biochim. Biophys. Acta 1442 (1998) 432–436.

[39] I. Puls, S.J. Oh, C.J. Sumner, K.E. Wallace, M.K. Floeter, E.A. Mann, W.R. Kennedy, G. Wendelschafer-Crabb, A. Vortmeyer, R. Powers, K. Finnegan, E.L. Holzbaur, K.H. Fischbeck, C.L. Ludlow, Distal spinal and bulbar muscular atrophy caused by dynactin mutation, Ann. Neurol. 57 (2005) 687–694.
[40] J.R. Levy, C.J. Sumner, J.P. Caviston, M.K. Tokito, S. Ranganathan, L.A. Ligon, K.E. Wallace, B.H. LaMonte, G.G. Harmison, I. Puls, K.H. Fischbeck, E.L. Holzbaur, A motor neuron disease-associated mutation in $p150^{Glued}$ perturbs dynactin function and induces protein aggregation, J. Cell Biol. 172 (2006) 733–745.
[41] M.J. Farrer, M.M. Hulihan, J.M. Kachergus, J.C. Dachsel, A.J. Stoessl, L.L. Grantier, S. Calne, D.B. Calne, B. Lechevalier, F. Chapon, Y. Tsuboi, T. Yamada, L. Gutmann, B. Elibol, K.P. Bhatia, C. Wider, C. Vilarino-Guell, O.A. Ross, L.A. Brown, M. Castanedes-Casey, D.W. Dickson, Z.K. Wszolek, DCTN1 mutations in Perry syndrome, Nat. Genet. 41 (2009) 163–165.
[42] C. Zuccato, M. Valenza, E. Cattaneo, Molecular mechanisms and potential therapeutical targets in Huntington's disease, Physiol. Rev. 90 (2010) 905–981.
[43] J.P. Caviston, J.L. Ross, S.M. Antony, M. Tokito, E.L. Holzbaur, Huntingtin facilitates dynein/dynactin-mediated vesicle transport, Proc. Natl. Acad. Sci. USA 104 (2007) 10045–10050.
[44] J.P. Caviston, E.L. Holzbaur, Huntingtin as an essential integrator of intracellular vesicular trafficking, Trends Cell Biol. 19 (2009) 147–155.
[45] A. Pal, F. Severin, B. Lommer, A. Shevchenko, M. Zerial, Huntingtin-HAP40 complex is a novel Rab5 effector that regulates early endosome motility and is upregulated in Huntington's disease, J. Cell Biol. 172 (2006) 605–618.
[46] K. Verhoeven, P. De Jonghe, K. Coen, N. Verpoorten, M. Auer-Grumbach, J.M. Kwon, D. FitzPatrick, E. Schmedding, E. De Vriendt, A. Jacobs, V. Van Gerwen, K. Wagner, H.P. Hartung, V. Timmerman, Mutations in the small GTP-ase late endosomal protein RAB7 cause Charcot-Marie-Tooth type 2B neuropathy, Am. J. Hum. Genet. 72 (2003) 722–727.
[47] E.A. Holleran, M.K. Tokito, S. Karki, E.L. Holzbaur, Centractin (ARP1) associates with spectrin revealing a potential mechanism to link dynactin to intracellular organelles, J. Cell Biol. 135 (1996) 1815–1829.
[48] V. Muresan, M.C. Stankewich, W. Steffen, J.S. Morrow, E.L. Holzbaur, B.J. Schnapp, Dynactin-dependent, dynein-driven vesicle transport in the absence of membrane proteins: A role for spectrin and acidic phospholipids, Mol. Cell. 7 (2001) 173–183.
[49] Y. Ikeda, K.A. Dick, M.R. Weatherspoon, D. Gincel, K.R. Armbrust, J.C. Dalton, G. Stevanin, A. Durr, C. Zuhlke, K. Burk, H.B. Clark, A. Brice, J.D. Rothstein, L.J. Schut, J.W. Day, L.P. Ranum, Spectrin mutations cause spinocerebellar ataxia type 5, Nat. Genet. 38 (2006) 184–190.
[50] D.N. Lorenzo, M.G. Li, S.E. Mische, K.R. Armbrust, L.P. Ranum, T.S. Hays, Spectrin mutations that cause spinocerebellar ataxia type 5 impair axonal transport and induce neurodegeneration in *Drosophila*, J. Cell Biol. 189 (2010) 143–158.
[51] E.L. Holzbaur, J.A. Hammarback, B.M. Paschal, N.G. Kravit, K.K. Pfister, R.B. Vallee, Homology of a 150K cytoplasmic dynein-associated polypeptide with the *Drosophila* gene Glued, Nature 351 (1991) 579–583.
[52] A. Swaroop, M.L. Paco-Larson, A. Garen, Molecular genetics of a transposon-induced dominant mutation in the *Drosophila* locus Glued, Proc. Natl. Acad. Sci. USA 82 (1985) 1751–1755.
[53] M. McGrail, J. Gepner, A. Silvanovich, S. Ludmann, M. Serr, T.S. Hays, Regulation of cytoplasmic dynein function *in vivo* by the *Drosophila* Glued complex, J. Cell Biol. 131 (1995) 411–425.
[54] S.H. Garen, D.R. Kankel, Golgi and genetic mosaic analyses of visual system mutants in *Drosophila* melanogaster, Dev. Biol. 96 (1983) 445–466.

[55] M. Martin, S.J. Iyadurai, A. Gassman, J.G. Gindhart Jr., T.S. Hays, W.M. Saxton, Cytoplasmic dynein, the dynactin complex, and kinesin are interdependent and essential for fast axonal transport, Mol. Biol. Cell 10 (1999) 3717–3728.
[56] S.P. Koushika, A.M. Schaefer, R. Vincent, J.H. Willis, B. Bowerman, M.L. Nonet, Mutations in *Caenorhabditis elegans* cytoplasmic dynein components reveal specificity of neuronal retrograde cargo, J. Neurosci. 24 (2004) 3907–3916.
[57] K. Murthy, J.M. Bhat, S.P. Koushika, *In vivo* imaging of retrogradely transported synaptic vesicle proteins in *Caenorhabditis elegans* neurons, Traffic 12 (2010) 89–101.
[58] C.Y. Ou, V.Y. Poon, C.I. Maeder, S. Watanabe, E.K. Lehrman, A.K. Fu, M. Park, W.Y. Fu, E.M. Jorgensen, N.Y. Ip, K. Shen, Two cyclin-dependent kinase pathways are essential for polarized trafficking of presynaptic components, Cell 141 (2010) 846–858.
[59] B.H. LaMonte, K.E. Wallace, B.A. Holloway, S.S. Shelly, J. Ascano, M. Tokito, T. Van Winkle, D.S. Howland, E.L. Holzbaur, Disruption of dynein/dynactin inhibits axonal transport in motor neurons causing late-onset progressive degeneration, Neuron 34 (2002) 715–727.
[60] C. Lai, X. Lin, J. Chandran, H. Shim, W.J. Yang, H. Cai, The G59S mutation in p150(glued) causes dysfunction of dynactin in mice, J. Neurosci. 27 (2007) 13982–13990.
[61] F.M. Laird, M.H. Farah, S. Ackerley, A. Hoke, N. Maragakis, J.D. Rothstein, J. Griffin, D.L. Price, L.J. Martin, P.C. Wong, Motor neuron disease occurring in a mutant dynactin mouse model is characterized by defects in vesicular trafficking, J. Neurosci. 28 (2008) 1997–2005.
[62] E.S. Chevalier-Larsen, K.E. Wallace, C.R. Pennise, E.L. Holzbaur, Lysosomal proliferation and distal degeneration in motor neurons expressing the G59S mutation in the $p150^{Glued}$ subunit of dynactin, Hum. Mol. Genet. 17 (2008) 1946–1955.
[63] B.A. Eaton, R.D. Fetter, G.W. Davis, Dynactin is necessary for synapse stabilization, Neuron 34 (2002) 729–741.
[64] M. Hafezparast, R. Klocke, C. Ruhrberg, A. Marquardt, A. Ahmad-Annuar, S. Bowen, G. Lalli, A.S. Witherden, H. Hummerich, S. Nicholson, P.J. Morgan, R. Oozageer, J.V. Priestley, S. Averill, V.R. King, S. Ball, J. Peters, T. Toda, A. Yamamoto, Y. Hiraoka, M. Augustin, D. Korthaus, S. Wattler, P. Wabnitz, C. Dickneite, S. Lampel, F. Boehme, G. Peraus, A. Popp, M. Rudelius, J. Schlegel, H. Fuchs, M. Hrabe de Angelis, G. Schiavo, D.T. Shima, A.P. Russ, G. Stumm, J.E. Martin, E.M. Fisher, Mutations in dynein link motor neuron degeneration to defects in retrograde transport, Science 300 (2003) 808–812.
[65] X.J. Chen, E.N. Levedakou, K.J. Millen, R.L. Wollmann, B. Soliven, B. Popko, Proprioceptive sensory neuropathy in mice with a mutation in the cytoplasmic dynein heavy chain 1 gene, J. Neurosci. 27 (2007) 14515–14524.
[66] K.M. Ori-McKenney, J. Xu, S.P. Gross, R.B. Vallee, A cytoplasmic dynein tail mutation impairs motor processivity, Nat. Cell. Biol. 12 1228-1234.
[67] H.S. Ilieva, K. Yamanaka, S. Malkmus, O. Kakinohana, T. Yaksh, M. Marsala, D.W. Cleveland, Mutant dynein (*Loa*). triggers proprioceptive axon loss that extends survival only in the SOD1 ALS model with highest motor neuron death, Proc. Natl. Acad. Sci. USA 105 (2008) 12599–12604.
[68] L. Dupuis, A. Fergani, K.E. Braunstein, J. Eschbach, N. Holl, F. Rene, J.L. Gonzalez De Aguilar, B. Zoerner, B. Schwalenstocker, A.C. Ludolph, J.P. Loeffler, Mice with a mutation in the dynein heavy chain 1 gene display sensory neuropathy but lack motor neuron disease, Exp. Neurol. 215 (2009) 146–152.
[69] K.E. Braunstein, J. Eschbach, K. Rona-Voros, R. Soylu, E. Mikrouli, Y. Larmet, F. Rene, J.L. De Aguilar, J.P. Loeffler, H.P. Muller, S. Bucher, T. Kaulisch, H.G. Niessen, J. Tillmanns, K. Fischer, B. Schwalenstocker, J. Kassubek, B. Pichler, D. Stiller, A. Petersen, A.C. Ludolph, L. Dupuis, A point mutation in the dynein heavy chain gene leads to striatal atrophy and compromises neurite outgrowth of striatal neurons, Hum. Mol. Genet. 19 (2010) 4385–4398.

[70] E. Perlson, S. Maday, M.M. Fu, A.J. Moughamian, E.L. Holzbaur, Retrograde axonal transport: Pathways to cell death? Trends Neurosci. 33 (2010) 335–344.
[71] L.A. Ligon, B.H. LaMonte, K.E. Wallace, N. Weber, R.G. Kalb, E.L. Holzbaur, Mutant superoxide dismutase disrupts cytoplasmic dynein in motor neurons, NeuroReport 16 (2005) 533–536.
[72] L.G. Bilsland, E. Sahai, G. Kelly, M. Golding, L. Greensmith, G. Schiavo, Deficits in axonal transport precede ALS symptoms *in vivo*, Proc. Natl. Acad. Sci. USA 107 (2010) 20523–20528.
[73] H.M. Heerssen, M.F. Pazyra, R.A. Segal, Dynein motors transport activated Trks to promote survival of target-dependent neurons, Nat. Neurosci. 7 (2004) 596–604.
[74] E. Perlson, S. Hanz, K. Ben-Yaakov, Y. Segal-Ruder, R. Seger, M. Fainzilber, Vimentin-dependent spatial translocation of an activated MAP kinase in injured nerve, Neuron 45 (2005) 715–726.
[75] S. Gunawardena, L.S. Her, R.G. Brusch, R.A. Laymon, I.R. Niesman, B. Gordesky-Gold, L. Sintasath, N.M. Bonini, L.S. Goldstein, Disruption of axonal transport by loss of huntingtin or expression of pathogenic polyQ proteins in *Drosophila*, Neuron 40 (2003) 25–40.
[76] E. Colin, D. Zala, G. Liot, H. Rangone, M. Borrell-Pages, X.J. Li, F. Saudou, S. Humbert, Huntingtin phosphorylation acts as a molecular switch for anterograde/retrograde transport in neurons, EMBO J. 27 (2008) 2124–2134.
[77] L.R. Gauthier, B.C. Charrin, M. Borrell-Pages, J.P. Dompierre, H. Rangone, F.P. Cordelieres, J. De Mey, M.E. MacDonald, V. Lessmann, S. Humbert, F. Saudou, Huntingtin controls neurotrophic support and survival of neurons by enhancing BDNF vesicular transport along microtubules, Cell 118 (2004) 127–138.
[78] K.A. Vossel, K. Zhang, J. Brodbeck, A.C. Daub, P. Sharma, S. Finkbeiner, B. Cui, L. Mucke, Tau reduction prevents Abeta-induced defects in axonal transport, Science 330 (2010) 198.
[79] S.P. Gross, Hither and yon: A review of bi-directional microtubule-based transport, Phys. Biol. 1 (2004) R1–R11.
[80] M. Johansson, N. Rocha, W. Zwart, I. Jordens, L. Janssen, C. Kuijl, V.M. Olkkonen, J. Neefjes, Activation of endosomal dynein motors by stepwise assembly of Rab7-RILP-p150^{Glued}, ORP1L, and the receptor betalll spectrin, J. Cell Biol. 176 (2007) 459–471.
[81] The Huntington's Disease Collaborative Research Group, A novel gene containing a trinucleotide repeat that is expanded and unstable on Huntington's disease chromosomes, Cell 72 (1993) 971–983.

In this chapter

24

Dynein Dysfunction as a Cause of Primary Ciliary Dyskinesia and Other Ciliopathies

Anita Becker-Heck, Niki T. Loges, Heymut Omran
Klinik und Poliklinik für Kinder und Jugendmedizin, Allgemeine Pädiatrie, Universitätsklinik Münster, Münster, Germany

24.1 Introduction

Cilia are highly conserved organelles extending from almost every cell type of the human body. Their core structure – the axoneme – consists of nine doublet microtubules composed of α- and β-tubulin. The average length and diameter are 6 μm and 0.2 to 0.3 μm, respectively [80]. These complex organelles consist of hundreds of different proteins that have been characterized in various proteomics studies. In the human system, axonemes display either a 9+2 or 9+0 pattern. In 9+2 cilia, the nine outer doublets surround two single microtubules, whereas the single central microtubules are missing in 9+0 cilia. Other organisms also display other axonemal structures; for example, in rabbits 9+4 axonemes have been described. Most non-motile cilia have 9+0 axonemes.

Cilia can be divided into two classes – motile and immotile. Motile cilia have large motor protein complexes (dynein arm complexes) attached to their outer doublets that generate the force required to produce cilia bending. Primary ciliary dyskinesia (PCD) is a rare hereditary disorder affecting approximately 1 in 20 000 individuals and is characterized by abnormal motility of cilia or flagella. The clinical phenotype is very complex, because defective cilia/flagella motility in various cell types such as respiratory epithelial cells, ependymal cells lining the brain ventricles, embryonic nodal cells, fallopian tube cells, and sperm cells can contribute to distinct disease manifestations. In addition in some PCD variants, molecular defects do not only affect motile but also non-motile cilia types, resulting in even more complex phenotypes. However, all PCD patients suffer from recurrent respiratory infections of the upper and lower airways due to defective mucociliary airway clearance. Dysfunction of motile cilia at the

Dyneins DOI: 10.1016/B978-0-12-382004-4.10024-X
Copyright © 2012 by Elsevier Inc. All rights reserved.

embryonic node causes *situs inversus* in approximately half of the PCD individuals and has been referred to as Kartagener's syndrome.

24.2 Ultrastructure of Motile Cilia

In *Chlamydomonas* the core structure of motile cilia is the "9+2" axoneme, which consists of multiple protein complexes (Fig. 24.1). It contains a central pair of two single microtubules surrounded by nine outer microtubule doublets. The microtubular doublets are composed of heterodimers of α- and

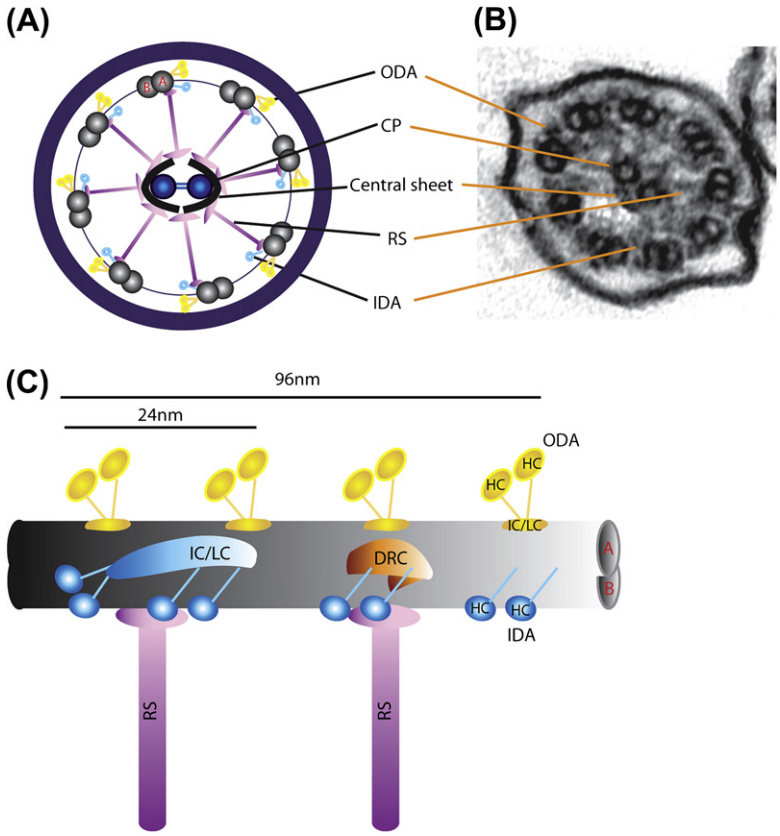

Figure 24.1 Ultrastructure of a motile 9+2 cilium. (A) Schematic diagram of a cross-section of a respiratory cilium indicating the different axonemal components. Nine outer microtubule doublets (microtubule A + B) surround two single central microtubules (CP: central pair). Attached to the outer microtubule A are the outer dynein arms (ODAs) and inner dynein arms (IDAs). The radial spokes (RSs) link the central pair and the outer microtubule doublets. (B) Transmission electron microscopy photograph of a respiratory cilium depicting the axonemal structure in a healthy control. (C) Schematic diagram of the axoneme in length based on findings obtained in *Chlamydomonas*.

β-tubulin assembled into 13 and 11 protofilaments (in microtubules A and B, respectively). The outer microtubule doublets are connected to each other by the DRC linker [29] and to the central pair by radial spokes. Major structures attached to each outer microtubule A are the outer and inner dynein arms, which are composed of dynein heavy chains (HCs) (400–500 kDa), intermediate chains (ICs) (45–140 kDa), and light chains (LCs) (8–28 kDa). The conserved central and C-terminal segments of the HCs form the globular head (motor domain) whereas the N-terminal region interacts with ICs and LCs [56,79]. Axonemal dyneins are arranged in two rows along the axoneme in a 96 nm characteristic repeat. In *Chlamydomonas reinhardtii* these repeats consist of four outer dynein arms, one dimeric inner dynein arm, and six monomeric inner dynein arms [43]. The dynein arms are AAA (ATPases associated with various cellular activities)-type motor protein-complexes that convert the chemical energy of ATP binding and hydrolysis into mechanical force [9]. Due to ATP-dependent conformational changes and transient binding to neighbouring doublets, the dynein motors generate the force required for ciliary bending based on the sliding between outer microtubule doublets – the outer dynein arms regulate the beat frequency whereas the inner dynein arms regulate the waveform of flagellar beating [8]. The central pair–radial spoke system, together with the dynein regulatory complex (DRC) attached to the outer microtubule A next to the radial spokes and the inner dynein arms, are thought to govern the motile machinery of the nine outer doublets by acting as a mechanochemical transducer [24,74,90]. Intracellular second messengers such as cAMP and cGMP, as well as intracellular calcium concentration, have been shown to be involved in ciliary beat regulation [80]. cAMP regulates the ciliary beat through activation of protein kinase A [81]; Schmid et al. [86] could demonstrate that a CO_2/HCO_3-sensitive soluble adenylyl cyclase expressed in human epithelial axonemes can regulate ciliary beat frequency by controlling the levels of cAMP produced [87].

24.3 Outer Dynein Arms

Most of the knowledge about outer dynein arm composition originates from studies in the green alga *Chlamydomonas reinhardtii* [14]. A wild-type strain was mutagenized by UV light and 35 strains of *Chlamydomonas* mutants missing the entire outer dynein arm were isolated by screening slow-swimming phenotypes. They comprised 10 independent genetic loci (*oda1-10*) including those of previously isolated mutants *oda38* [41] and *pf28* [54]. The 10 loci were distinct from *pf13* and *pf22*, loci for nonmotile mutants missing the outer arm [33]. These results indicated that at least 12 genes are responsible for the assembly of the outer dynein arms [38]. In the alga *Chlamydomonas*, only one distinct type of outer dynein arm complex is known. The complex contains three HCs (α-, β-, and

γ-HCs), two ICs, nine LCs, three docking complex proteins, and at least two other associated proteins [66].

Based on homology searches using the BLAST algorithms [4], Pazour et al. have identified five human outer dynein arm HC orthologs of *Chlamydomonas* β- and γ-HCs [66]. Orthologs of the β-HC are DNAH11 (chromosome 7p21), DNAH17 (chromosome 17q25), and DNAH9 (chromosome 17p12). *DNAH17*, however, very likely represents a non-functional pseudogene. Orthologs of the γ-HC are DNAH5 (chromosome 5p15) and DNAH8 (chromosome 6p21). No human ortholog of the *Chlamydomonas* α-HC has been identified. These findings are consistent with the concept that, like other vertebrates, human outer dynein arm complexes contain only two outer dynein arm HCs. However, because more than one human outer dynein arm HC ortholog has been identified, humans may have more than one distinct type of outer dynein arm complex. The expression pattern of some of the four genes encoding outer dynein arm HCs has been analyzed. Northern blot analyses revealed specific expression of *DNAH5* in the lung, brain, and testis [63]. Using the *in situ* hybridization technique, Kispert et al. found that the cellular expression of the murine ortholog *Mdnah5* (alias *Dnahc5*) is confined in the lung to ciliated respiratory cells of the upper and lower airways [45]. In addition, the ependymal cells lining the brain ventricles, which are also covered by multiple motile cilia, express *Mdnah5* [36]. Cells of the embryonic node, which carry one specialized motile monocilium, also express *Mdnah5* [63]. Reed et al. studied in detail the expression of *DNAH9* [78], also referred to as *DNEL1*. They demonstrated specific expression in the lung, using Northern blot analysis. Reverse transcriptase-polymerase chain reaction (RT-PCR) analyses revealed RNA messages in cultured respiratory cells of tracheal and nasal origin. In addition, Reed et al. analyzed protein expression, using specific monoclonal anti-DNAH9 antibodies [78]. Immunohistochemistry and Western blot analyses showed that the outer dynein arm-HC DNAH9 is present in respiratory cilia and sperm flagella [78]. Immunoelectron microscopy demonstrated that DNAH9 localizes to one subfiber of the doublet microtubules surrounding the two singlet (central-complex) tubules in respiratory ciliary axonemes. RT-PCR identified *DNAH11* (*Dnahc11*) expression in trachea, testis, and lung [11]. The mouse ortholog *lrd* (left–right dynein) is specifically expressed at the embryonic node [93]. Samant et al. [82] showed that the expression of both Dnahc8 isoforms, the mouse ortholog of human DNAH8, is testis-specific in the adult mouse, unlike most other previously characterized mammalian axonemal HCs. However, detailed expression analyses of human DNAH8 have not yet been performed.

To investigate the molecular mechanisms involved in human outer dynein arm generation and function, specific antibodies were used to analyze the subcellular localization of the axonemal outer dynein arm HCs DNAH5 and DNAH9 in respiratory epithelial and sperm cells [21]. Confocal immunofluorecence imaging revealed characteristic patterns of subcellular localization of the analyzed outer dynein arm components. In wild-type respiratory cells,

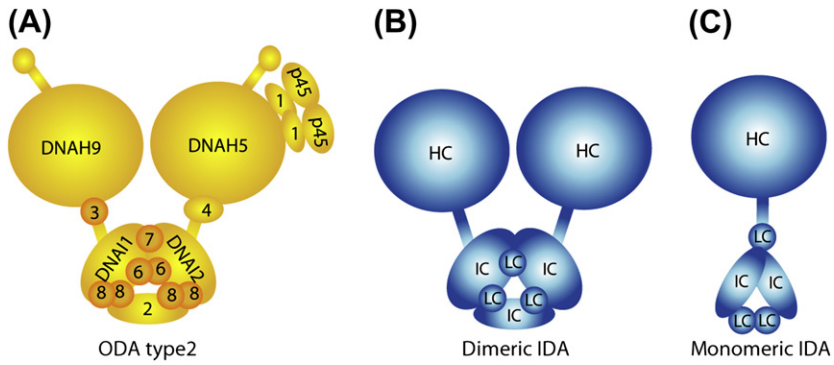

Figure 24.2 Schematic figure depicting probable protein composition of human outer and inner dynein arms. (A) The outer dynein arms are composed of two dynein HCs (DNAH5 and DNAH9 for type 2), two or three ICs, and several LCs. (B) The dimeric inner dynein arm of *Chlamydomonas*, composed of two HCs, three ICs, and three LCs. (C) The monomeric inner dynein arm of *Chlamydomonas* with one HC, two ICs, and three LCs.

the outer dynein arm HC DNAH5 is present throughout the entire length of the ciliary axoneme, whereas the outer dynein arm HC DNAH9 localizes only to the distal ciliary compartment. Thus, human outer dynein arm complexes vary in their composition along the respiratory ciliary axoneme and the axoneme of the sperm tail, and this composition also differs between these two cell types. These data indicate that in respiratory cilia and sperm tails at least two outer dynein arm types are present: type 1 (DNAH9 negative and DNAH5 positive, proximal) and type 2 (DNAH9 and DNAH5 positive, distal) (Fig. 24.2A). The spatial diversity of outer dynein arm HCs along the axonemes probably contributes to the typical beating characteristics of cilia and sperm flagella and likewise to the various beat modes of other motile cilia types (e.g. ependymal and nodal cilia).

24.4 Inner Dynein Arms

Using a *Chlamydomonas reinhardtii* mutant with missing outer dynein arms, dynein was extracted from axonemes of the mutant *oda1* and fractionated into seven distinct subspecies containing different HCs – named a–g. Seven inner dynein arm isoforms – one heterodimeric (two-headed) isoform (f or I1; Fig. 24.2B) located proximal of the radial spoke 1 [72] and six monomeric isoforms (a–e and g or I2 and I3; Fig. 24.2C) repeating every 96 nm along the entire axoneme – have been reported. The inner dynein arm subgroup I2 – composed of different one-headed inner dynein arms – is located between radial spokes 1 and 2, and the subgroup I3 – also composed of different monomeric inner dynein arms – is located distal of radial spoke 2 (Fig. 24.1C). Each inner dynein arm plays a distinct role in the generation and control of motility. Mutant flagella

of *Chlamydomonas reinhardtii* missing distinct inner dynein arm components beat almost at normal frequency but with a reduced amplitude [39]. Furthermore, Kamiya et al. identified that all inner dynein arm subspecies (except subspecies f) are able to translocate microtubules *in vitro* and all subspecies (except b) generate microtubule rotation at the same time. Therefore, the inner dynein arm system appears to be involved in the initiation of a flagellar bend and the amplitude of the flagellar wave [8,40]. The inner dynein arms consist of several subunits of HCs, ICs, and LCs. The two-headed isoform (I1) is composed of two dynein HCs (1α and 1β), three ICs (97, 138, and 140 kDa), and three LCs (8, 11, and 14 kDa) (Fig. 24.2B; [27,70,75,77]. The β-HC of the inner dynein arm I1 is Dhc10, which is essential for the assembly and activity of the inner dynein arm I1 [71]. Dhc10 – whose human homolog is DNAH2 – contains the typical axonemal HC sequences: coiled-coil domains and multiple P-loops (phosphate-binding loops). Another component of the inner dynein arm I1 is IC138, which is thought to transmit signals between the radial spokes and the dynein HC of I1 [44], whereas the attachment to the outer microtubule doublet is mediated by IC140. The single-headed isoforms (I2) are composed of single dynein HCs and interact with actin and p28 (for the dyneins a, c, and d) or actin and centrin (for the dyneins b, e, and g) [46,98]. In *ida4 Chlamydomonas* mutants, p28 – an axonemal LC – is completely missing, resulting in the absence of a subset of dynein HCs in the subgroup I2; this indicates that p28 – whose human homolog is DNALI1 – is necessary for the assembly of a subset of inner dynein arms or for their binding to the outer microtubule A. The function of actin and centrin in the inner dynein arms is unknown – but it is known that in other cytoskeletal structures actin and centrin are involved in Ca^{2+}-dependent regulatory cellular processes [76, 83]).

To date, little is known about the composition of the inner dynein arm complexes in mammalian cells, although in mammalian cells they seem to be as heterogeneous as in *Chlamydomonas*. Neesen et al. analysed the first-described mammalian dynein HC – Mdhc7 (the human homolog is DNAH1) – in mice by deleting the P1-loop (the motif responsible for ATP hydrolysis). Loss of *Mdhc7* function resulted in reduced beat amplitude of sperm flagella, leading to male infertility [58]. By comparing healthy respiratory cells with cells from PCD patients showing absence of inner dynein arms in electron-microscopy analyses, DNAH7 – a dynein HC of the inner dynein arms localizing along the whole axoneme – was identified [101]. It shares all known features of axonemal HCs including four P-loops and two coiled-coil domains. By BLAST searches, Pazour et al. identified further human orthologous inner dynein arm HC genes – *DNAH14*, *DNAH1*, *DNAH12*, *DNAH10*, *DNAH2*, and *DNAH6* [66]. So far no molecular defect responsible for isolated inner dynein arm defects has been reported in PCD patients. However, several genetic defects characterized by combined defects of either outer dynein arms and inner dynein arms or DRC and inner dynein arms have been identified. All of these defects result in abnormalities of I2-inner

dynein arm types because they are characterized by the absence of DNALI1 (ortholog of p28) from the ciliary axonemes. These defects will be discussed in more detail below.

24.5 Ciliopathies

Cilia assemble on most cell types of the human body to perform diverse biological functions. Defects in motile or immotile cilia are associated with various human diseases – collectively referred to as ciliopathies [20].

The function of non-motile 9+0 cilia includes mechano- and chemosensation, as well as photoreception and olfaction. These 9+0 cilia are often also called primary cilia. Furthermore, it is known that primary cilia play an essential role in several signal transduction pathways such as the Hedgehog pathway. Diseases linked with primary cilia dysfunction are very diverse. Cystic kidney disease disorders such as nephronophthisis (NPHP) (OMIM 256100) are supposed to originate from aberrant mechanosensory function and/or cellular signaling processes caused by defective renal monocilia. Other disease manifestations include *situs inversus*, pancreatic and hepatic fibrosis, and retinal degeneration, all linked to cilia dysfunction. To date, mutations in various genes linked to NPHP [32,62,89] have been identified and all are associated with cilia dysfunction. Bardet-Biedl syndrome (BBS) (OMIM 209900) is a genetically heterogeneous disorder including symptoms such as retinal degeneration, cognitive impairment, obesity, diabetes, polydactyly, *situs inversus*, and renal abnormalities. To date, 14 BBS genes have been identified, of which at least seven assemble into a core complex – the BBSome – that is proposed to regulate the RAB8 (a small GTPase)-dependent vesicular trafficking of membrane proteins from the Golgi into the ciliary membrane [57]. By preventing Rab8 (GTP) production in zebrafish, ciliation is blocked and the classical BBS phenotype results, indicating that the BBSome may regulate the entry of proteins to the cilium or on IFT (intraflagellar transport) particles. Oral-facial-digital type 1 (OFD1) (OMIM 311200) syndrome is a heterogeneous developmental disorder characterized by polydactyly, central nervous system disorders, and in 15% of cases cystic kidney disease [13]. The OFD1 protein localizes to the basal body of the cilium and is involved in the complex mechanism of ciliary generation, because *ofd1*-deficient mice lack node cilia and display left–right body asymmetry defects [19]. Patients with Almström syndrome (ALMS) (OMIM 203800) display similar phenotypes to BBS patients; in addition, these patients show cardiomyopathy and liver and kidney dysfunction but do not have polydactyly. The ALMS1 protein also localizes to the basal body and the centrosome. ALMS1 appears to be important for ciliogenesis and the inactivation of the *ALMS1* gene results in the prevention of Ca^{2+} influx into the cytosol [37]. Interestingly, there is increasing evidence that, in patients with ciliopathies such NPHP, BBS, and

OFD1, dysfunction of respiratory cilia can also be observed, suggesting that the genetic defects not only affect non-motile but also motile cila.

24.5.1 Nodal Cilia

Patterning of the left–right (L/R) axis is a complex process that involves establishment of a midline and orientation of the left–right asymmetry with respect to the anteriorposterior (A/P) and dorsoventral (D/V) axes. Defects in one or more of these processes result in randomization or loss of asymmetry and in changes in numbers and placement of organs (i.e. bilateral spleens). In organisms such as fishes and frogs, the D/V and A/P axes are determined at fertilization by the entry position of the sperm and distribution of the yolk [25]. In mammals, such as humans and mice, the cylindrically symmetrical embryo implants itself into the wall of the uterus. The D/V axis is specified as the proximal-distal axis from the implantation site. Subsequently, the A/P axis is randomly determined in the plane at right angles to the D/V axis [7]. Once the D/V and A/P axes are determined, the L/R axis is established. A link between motile cilia dysfunction and defects in establishing left–right body asymmetry originated from observations that half of individuals with PCD have their organs in reversed orientation, a condition called *situs inversus totalis* (also referred to as Kartagener' syndrome), which is consistent with randomization of left–right asymmetry [17].

The first morphological asymmetry apparent is the heart loop [42], but L/R asymmetric gene expression precedes morphological changes. Many studies have suggested the node as a morphological structure important for L/R determination (Fig. 24.3A; [30,51,60]). The node of mouse embryos appears as a roughly triangular depression with the apex point toward the anterior. This nodal pit is covered by Reichert's membrane and the cavity is filled with extraembryonic fluid. The ventral embryonic surface of the nodal pit consists of a few hundred monociliated cells (Fig. 24.3A). Monocilia from nodal pit cells – so-called nodal cilia – appear as rod-like protrusions approximately 5 μm in length and 0.3 μm in diameter [30]. Nonaka et al. demonstrated that 9+0 nodal cilia contain motor protein complexes such as dynein arms and are motile. In addition they found that dysfunction of motile monocilia at the embryonic node is associated with randomization of left–right body asymmetry [60]. A similar phenotype was observed in the *inversus viscerum* (*iv*) mouse carrying recessive mutations in the axonemal dynein HC gene *Lrd* (*left–right dynein*), the ortholog of the human axonemal dynein HC gene *DNAH11* [93]. Lrd is exclusively expressed by nodal cells at 7.5 days postcoitum [93]. In embryos heterozygous for *iv*, nodal cilia rotated as rapidly as those in wild-type embryos [61]. This rapid movement produces a leftward flow of extraembryonic fluid in the ventral node, referred to as nodal flow [60]. In contrast, the nodal cilia in *iv* homozygous embryos appeared rigid and rarely moved, resulting in *situs inversus* [61]. Interestingly,

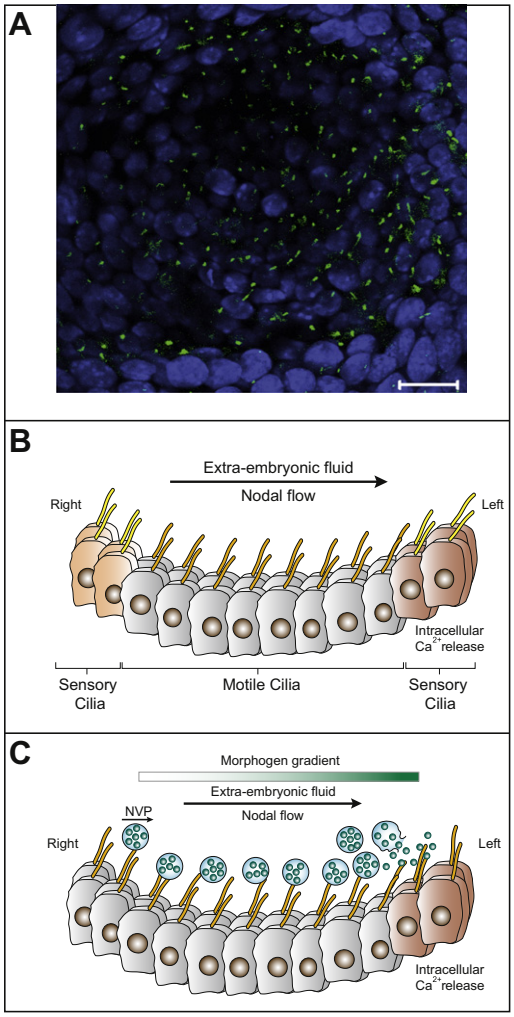

Figure 24.3 Mouse node and current models for establishing left–right asymmetry. (A) High-resolution immunofluorescence picture of the mouse node at E8.0. Cilia are stained with an antibody directed against acetylated α-tubulin (green); nuclei are stained with Hoechst 33342 (blue). Scale bar represents 20 μm. (B and C) The two current models explaining the mechanisms involved in establishing left–right body asymmetry. In the "two-cilia model" (B), motile cilia in the center of the node create a leftward nodal flow that is mechanically sensed through passive bending of non-motile sensory cilia at the border of the node. Bending of the cilia on the left side leads to a left-sided intracellular release of Ca^{2+} that initiates asymmetric expression of signaling molecules (morphogen gradient). The nodal vesicular parcel (NVP) model (C) predicts that vesicles filled with morphogens (such as sonic hedgehog and retinoic acid) are secreted from the right side and transported to the left side of the embryonic node by nodal flow, where they fragment. The resulting initiation of left-sided intracellular Ca^{2+} release induces downstream signalling events (such as expression of Lefty and Nodal) that break bilaterality. In this model, the flow of extra-embryonic fluid is not detected by cilia-based mechanosensation.

laterality defects were always accompanied by an abnormality in nodal flow, suggesting that lack of nodal flow results in randomization of laterality. Indeed, artificially generated rightward flow that was sufficiently rapid to reverse the intrinsic leftward nodal flow resulted in reversal of laterality in wild-type embryos. The artificial flow was also able to direct the situs of mutant mouse embryos with immotile cilia [59]. These results provided evidence for the role of mechanical fluid flow in L–R patterning. Similar laterality-breaking mechanisms have also been proposed for zebrafish (involving Kupffer's vesicle), birds (Hensen's node), and amphibians (Spemann's organizer) [18]. In humans, mutations in several genes coding for axonemal dyneins (*DNAI1*, *DNAI2*, *DNAH5*, *DNAH11*) resulting in randomization of L/R body asymmetry have been described [5,26,31,49,63,88,100].

Two models have been proposed for how nodal flow might contribute to left–right asymmetry. The "two cilia" model [51] predicts that there are two distinct types of cilia and that nodal flow is generated by motile cilia (characterized by Lrd expression) and sensed by non-motile, mechanosensory cilia (characterized by polycystin-2 expression) at the periphery of the node. The "morphogen gradient" model predicts that the nodal flow results in a leftward gradient of a hypothetical morphogen (Fig. 24.3B). Tanaka et al. identified nodal vesicular parcels (NVPs) filled with sonic hedgehog and retinoic acid molecules. The secretion and release of NVPs is triggered by fibroblast growth factor signaling. NVPs are transported by the nodal flow, where they eventually fragment close to the left lateral wall of the ventral node, releasing their contents (Fig. 24.3C; [94]. Both models described an asymmetric Ca^{2+} release, which is probably involved in the subsequent proceedings of left–right determination, which in turn is based on asymmetric expression of signaling molecules, such as nodal and lefty, and transcription factors, such as Pitx2 (paired-like homeodomain transcription factor-2).

24.5.2 Ependymal Cilia and Hydrocephalus

In the brain ventricles, the synchronized beating of the ependymal 9+2 cilia creates a laminar flow of cerebrospinal fluid above the ependymal cell surface and through the cerebral aqueduct, which is termed ependymal flow [36]. A link between ependymal cilia dysfunction and enlargement of the brain ventricles (hydrocephalus) was shown by analysis of several mouse models with altered function of motile cilia. Mice lacking the axonemal dynein HC Dnahc5 (Mdnah5); the axonemal protein SPAG6; the central pair protein Hydin; or proteins involved in ciliogenesis, such as IFT88 (Tg737) or FOXJ1 (forkhead box J1; also known as HFH-4), which regulates generation of motile cilia, develop hydrocephalus [12,35,47,84,95]. Unlike in mice, in humans ependymal ciliary dysmotility is not sufficient to cause hydrocephalus but increases the risk for aqueduct closure and hydrocephalus formation. Furthermore, analysis of neuron migration in the brain of *Tg737*^{orpk} mutant mice found that the lack of

ependymal flow resulted in disturbed directional migration of neuroblasts in the subventricular zone, suggesting that ependymal flow is required for the formation of a concentration gradient of guidance molecules [85]. Alternatively, other functional roles of IFT proteins might be responsible for this complex phenotype.

24.5.3 Sperm Flagella and Male Infertility

The ultrastructure of the sperm flagellum and the motile 9+2 cilium are very similar but not identical, which might explain why sperm flagella dysfunction is often, but not necessarily, associated with PCD and vice versa [55]. Interestingly, male infertility of PCD patients might not necessarily be caused by a defect of sperm motility, but may also result from defective transportation of sperm cells through the ductuli efferentes. Parts of the ductuli efferentes epithelium are lined by motile cilia, which beat in the direction of the epididymis.They probably assist in the transportation of spermatozoa out of the testes, since sperm at this stage are still not activated and therefore are non-motile [1].

24.5.4 Fallopian Tubes and Female Infertility

The fallopian tube plays an essential role in gamete transport, fertilization, and the early development of the embryo. It consists of two major cell types — ciliated and secretory cells. It is supposed that ciliary action plays an important role in the transfer of gametes and embryos. Indeed, women with PCD (or Kartagener's syndrome) have been reported to suffer from sub-fertility (Afzelius 1978; [50,67]. However, the exact role of the cilia in the fallopian tube is not clear and it is possible that motile cilia lining the fallopian tube — similar to respiratory cilia in the airways — exert a role in the clearance of the female reproductive system. Female infertility can occur in PCD but is not as frequent as that observed in male patients (H. Omran, personal communication).

24.6 Primary Cilia Dyskinesia

PCD is a rare hereditary disorder affecting approximately 1 in 20 000 (live births) and results from abnormalities in the structure and/or function of motile cilia and their motility. The disease phenotype is characterized by chronic upper and lower airway infections, which can cause substantial damage to the lungs. In most PCD variants, the genetic defects not only affect function of motile 9+2 cilia but also result in defective 9+0 motile cilia at the embryonic node. In these PCD variants the genetic defect regularly causes randomization of left–right asymmetry. Thus, about half of PCD patients display a *situs inversus* (referred to as Kartagener's syndrome). Interestingly, *situs ambiguous* (heterotaxy) is present in ~6% of PCD patients, demonstrating the important role of nodal flow

in preventing the complex cardiac defects often observed in *situs ambiguous* patients.

Björn Afzelius and others were the first to show that respiratory cilia from patients with Kartagener's syndrome often lack dynein arms on the outer doublet microtubules, resulting in an immotile cilia syndrome [3,68]. Since then, many defects in the ultrastructure and/or function of motile cilia have been identified. Because in many patients defects of cilia beating were recognized, the original name of the disease (immotile cilia syndrome) was changed to PCD.

24.6.1 Genetic Defects in Primary Cilia Dyskinesia

PCD is characterized by an extensive genetic heterogeneity. Genetic defects can alter composition and/or function of many distinct protein complexes either important for cilia beat generation or regulation. In Section 24.8 we group and summarize all genes – known so far – responsible for PCD.

24.7 Molecular Defects Affecting Outer Dynein Arm Components

The most commonly encountered ultrastructural defects in PCD are characterized by defects of the outer dynein arms. Mutations in genes encoding different components of outer dynein arm complexes cause distinct structural and/or functional defects of the outer dynein arms. So far, mutations in five genes (*DNAI1*, *DNAH5*, *DNAH11*, *DNAI2*, and *TXNDC3*) have been identified and will be discussed in detail.

24.7.1 DNAI1

DNAI1 was screened in PCD patients based on a candidate approach, because *Chlamydomonas oda9* mutants deficient in the axonemal intermediate outer dynein arm chain IC78 (now known as IC1) display an axonemal defect resembling those frequently observed in PCD patients with outer dynein arm defects. It was the first gene identified to be responsible for PCD [69]. It is located on chromosome 9p21-p13 and encodes the human intermediate chain IC1. Analysis of human mutant *DNAI1* respiratory cells with anti-DNAH5 and anti-DNAI2 antibodies revealed that DNAI1 is probably essential for the assembly of outer dynein arm type 2 as the outer dynein arm HC DNAH5 does not localize along the whole axoneme but can still be assembled within the proximal axoneme [20].

24.7.2 DNAH5

To identify additional genes responsible for PCD, Omran et al. [64] used a homozygosity mapping strategy and detected on chromosome 5p15

a novel PCD locus. Within the critical genetic interval they localized the potential candidate gene *DNAH5* (with 80 exons). In the *Chlamydomonas reinhardtii* mutant *oda2*, mutations in the γ-HC (the ortholog of *DNAH5*) result in slow-swimming algae with ultrastructural outer dynein arm defects [97]. Patients who carry *DNAH5* mutations consistently display axonemal outer dynein arm defects. Other clinical manifestations include randomization of left–right body asymmetry [21,31,63]. Mutations in *DNAH5* are detected in 28% of PCD cases – the rate is even higher (~50%) when PCD cases are pre-selected for outer dynein arm defects, highlighting the important role of DNAH5 for the aetiology of PCD. DNAH5 is a HC of the outer dynein arms and localizes along the entire axoneme. Consistently in patients with *DNAH5* mutations, the DNAH5 protein is regularly absent from the whole ciliary axoneme. Thus, DNAH5 is present in both human outer dynein arm types – in type 1 outer dynein arms (positive for DNAH5 and negative for DNAH9) and in type 2 outer dynein arms (positive for both dynein HCs – DNAH5 and DNAH9).

24.7.3 DNAH11

DNAH11 is one of the two human orthologs of the *Chlamydomonas* β-HC. The gene comprises 82 exons and has been associated with Kartagener's syndrome with normal axonemal ultrastructure [5]. As a patient with homozygous nonsense mutations in *DNAH11* also suffered from cystic fibrosis, it was first uncertain whether mutations in *DNAH11* solely cause defects of laterality or also result in PCD. Recently, several patients with PCD/Kartagener's syndrome (cystic fibrosis was excluded) have been identified with *DNAH11* mutations, thus confirming the role of *DNAH11* in the pathogenesis of PCD [88]. Interestingly, the phenotype of respiratory cilia is characterized by an abnormal beating pattern with reduced amplitudes and recovery strokes and increased beating frequency but normal ultrastructure. Consistently, respiratory cilia of patients with *DNAH11* mutations display normal localization for the outer dynein arm components DNAH5, DNAH9, and DNAI2.

24.7.4 DNAI2

DNAI2, the human ortholog of the *Chlamydomonas* intermediate outer dynein arm chain IC69 (now known as IC2), was identified recently to be essential for outer dynein arm assembly along the whole axoneme [49]. All patients identified with loss-of-function mutations had no *DNAI2* expression in respiratory cells and suffered from chronic lung disease, and four out of six patients displayed *situs inversus*. Further analysis revealed that DNAI2 is a component of both outer dynein arm types. In patients with *DNAI2* mutations, DNAH5 as well as DNAH9 were absent from the axoneme.

24.7.5 TXNDC3

TXNDC3 is a thioredoxin nucleoside diphosphate kinase (NDK) and is orthologous to the outer dynein arm component IC1 in sea urchin. TXNDC3 in humans has been shown by Duriez et al. [15] to be expressed in nasal cells, trachea, and testis. *Chlamydomonas* has two TXNDC3 orthologs (LC3 and LC5), which have been shown to interact with the HCs [28]. So far a single patient with mutations in *TXNDC3* has been reported. Electron microscopy found abnormal outer dynein arms in some cross-sections whereas other appeared normal.

24.8 Molecular Defects Affecting Outer and Inner Dynein Arms

Mechanisms responsible for cytoplasmic preassembly of dynein components, loading of those complexes onto the IFT machinery, and delivery as well as anchoring of dynein motor complexes to their destined axonemal sites are only poorly understood. Very recently genetic defects responsible for combined defects of outer- and inner-dynein-arm components are being reported. So far two genes (*KTU*; *LRRC50*) involved in the cytoplasmic preassembly process of dynein arms have been identified. Because many proteins are involved in this complex process, it is very likely that several other genetic defects will soon be reported.

24.8.1 Kintoun

The first gene reported to encode a protein involved in cytoplasmic preassembly of dynein arms was *kintoun* (*ktu*). This gene was first identified in a medaka mutant and was found to be mutated in the *pf13* mutant of *Chlamydomonas*. In humans, mutations in the *KTU* gene result in PCD and Kartagener's syndrome. Dysfunction of KTU leads to reduction of outer dynein arms and absence of inner dynein arms containing DNALI1 from the ciliary axoneme and results in loss of ciliary motility [65]. Biochemical studies in *Chlamydomonas* and mice showed that Ktu/PF13 interacts with dynein intermediate and HCs [65], suggesting that KTU is involved in preassembly of dynein arm complexes in the cytoplasm before they are loaded onto the IFT machinery for delivery to the ciliary compartment [22].

24.8.2 LRRC50

The second gene identified encodes a protein involved in preassembly of dynein arms *LRRC50* (leucine repeat rich containing protein 50). *LRRC50* was considered as a strong candidate for PCD because the reported ultrastructural phenotype of cilia and flagella in zebrafish and *Chlamydomonas* algae carrying mutations in orthologous genes showed defects of outer dynein arm and inner dynein arm structures [22,23,92,96]. Large genomic deletions as well as point mutations in

the human *LRRC50* gene result in a PCD variant with combined outer dynein arm and inner dynein arm defects. Functional analyses showed that LRRC50 deficiency disrupts assembly of outer dynein arm complexes containing DNAH9 (distally) and DNAH5 and DNAI2 (distally and proximally), as well as DNALI1-containing inner dynein arm complexes, resulting in absence of these dynein arms from the ciliary axoneme, in turn leading to immotile cilia [48]. These findings suggest that LRRC50 plays a role in preassembly of distinct dynein-arm complexes. Indeed, in parallel, P. Duquesnoy et al. [16] demonstrated that in *Chlamydomonas* and *Trypanosoma brucei* ODA7 is located primarily in the cell body and RNA interference (RNAi)-induced silencing of *ODA7* in *Trypanosoma brucei* indicated that some dynein-arm components are assembled but remain in the cytoplasm. The absence of ODA7 in both organisms results in flagellar hypomotility with selective defects of outer dynein arms and inner dynein arms.

24.9 Molecular Defects Affecting the Central Pair and Radial Spokes

24.9.1 RSPH9 (C6orf206) and RSPH4A

In *Chlamydomonas*, the radial spoke is a conserved macromolecular complex containing at least 23 proteins. The complex repeats in pairs every 96 nm along the axoneme. It is anchored to the outer microtubule doublet close to the inner dynein arms and the DRC and extends to the central pair [99]. Thus, its position along the axoneme is perfect for relaying signals from the central pair to the dynein arms. Despite the fact that in 1979 Sturgess et al. had already described patients with missing radial spokes resulting in immotile respiratory cilia and sperm flagella [91], little is known about the composition and the exact function of radial spokes in humans. BLAST searches with *Chlamydomonas* radial spoke proteins identified several radial spoke homologs in humans, providing new candidate genes in patients with radial spoke defects. Indeed, Castleman et al. recently identified by linkage analysis two genes mutated in PCD patients with central microtubule pair defects [10]. The identification of *RSPH9* (*C6orf206*) and *RSPH4A* revealed a new group of proteins related to PCD. Both proteins are components of the axonemal radial spoke head in motile cilia.

From *Chlamydomonas* mutants it is known that the central pair/radial spoke system is essential for regulating beating as mutants lacking this system do not swim. The defects in these genes cause an abnormal rotary beating pattern with normal beat velocity, like in 9+0 cilia. Consistently, electron-microscopy analysis in these patients revealed in some cross-sections ciliary transposition defects with 9+0 or 8+1 microtubule configurations. It is important to note that these defects in the tubule composition are only present in small areas along the ciliary axonemes. This explains why electron microscopy analyses can be apparently normal in patients with *RSPH9* (*C6orf206*) and *RSPH4A* mutations [10].

24.10 Molecular Defects Affecting Dynein Regulatory Complexes and Inner Dynein Arms

24.10.1 CCDC39 and CCDC40

Very recently a novel group of PCD variants was characterized by the absence of GAS11 (a component of the DRC; Fig. 24.4A–C) and the inner dynein arm component DNALI1 (Fig. 24.4G–I) from the ciliary axonemes. Transmission electron microscopy found characteristic changes involving reduced number of inner dynein arms, eccentric central pairs, abnormal alignment of outer doublets, and occasional displacement of outer doublets (Fig. 24.5G–N), and a beating pattern characterized by a severely reduced amplitude with rigid axonemes. The clinical phenotype of this novel PCD variant is characterized by chronic airway disease, randomization of left–right asymmetry, and immotile sperm tails. Based on candidate approaches in dog, fish, and mice, the genes *CCDC39* and *CCDC40* were identified as possible candidate genes [6,53]. Mutational analyses of PCD patients with the above-described characteristics found changes in *CCDC39* and *CCDC40* in 13% and 60% of affected loss-of function mutations, respectively [6,53]. Both genes encode for uncharacterized coiled-coil domain-containing proteins. *FAP59*, the orthlog of *CCDC39* in *Chlamydomonas*, was predicted to be essential for ciliary motility as orthologs do not exist in non-ciliated organisms [52]. CCDC39 and CCDC40 are axonemal proteins whose absence results in the failure to correctly assemble DNALI1-containing inner dynein arm complexes and the DRC (Fig. 24.4D–F,K–M), thereby causing axonemal disorganization and dyskinetic ciliary beating. Since CCDC39, which normally localizes along the whole axoneme (Fig. 24.5B), is also missing in patients carrying *CCDC40* loss-of-function mutations (Fig. 24.5E), both proteins may interact with each other. Our findings indicate that both proteins possibly physically interact with other axonemal components and serve as a structural part of the axoneme, possibly as a new DRC component. This is consistent with findings that mutations in genes encoding DRC components in *Chlamydomonas* – like PF2 – cause a similar ultrastructural phenotype in flagella including the failure to assemble the DRC and the DNALI1-containing inner dynein arms [34,73,74]. As proposed for *PF2*, *CCDC39* and *CCDC40* could therefore encode for proteins involved in the stability of the DRC complex by interacting with one or several DRC subunits. Alternatively, it is possible that CCDC39 and CCDC40 are important for the cytoplasmic preassembly of axonemal proteins, and/or axonemal targeting/transport of the axonemal components GAS11 and DNALI1, because they were also found in the apical cytoplasm. However, so far nothing is known about the process of cytoplasmic preassembly and axonemal targeting/delivery of DRC complexes.

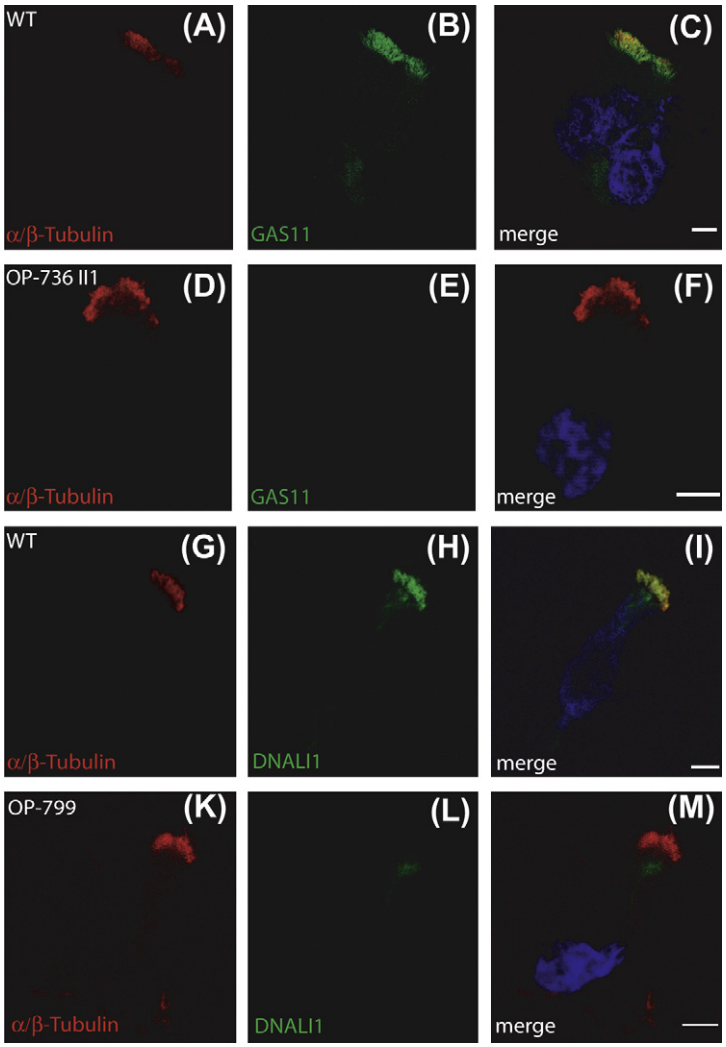

Figure 24.4 High-resolution immunofluorescence analyses. Epithelial cells were stained with α-/β-tubulin as ciliary marker (red in (A,D,G,K)). In respiratory epithelial cells of healthy controls GAS11 (green) localizes along the entire length of the axoneme (B), whereas, in patient OP-736II1 carrying loss-of-function mutations in *CCDC39*, GAS11 is completely missing (E). DNALI1 (green) also localizes along the entire length of the axoneme in respiratory epithelial cells of healthy control (H) and is completely absent in patient OP-*799* (L) carrying loss-of-function mutations in *CCDC40*. (C,F,I,M) Merge figures: yellow staining means co-localization of both proteins. Nuclei were stained with Hoechst 33342 (blue). Scale bars display 5 μm.

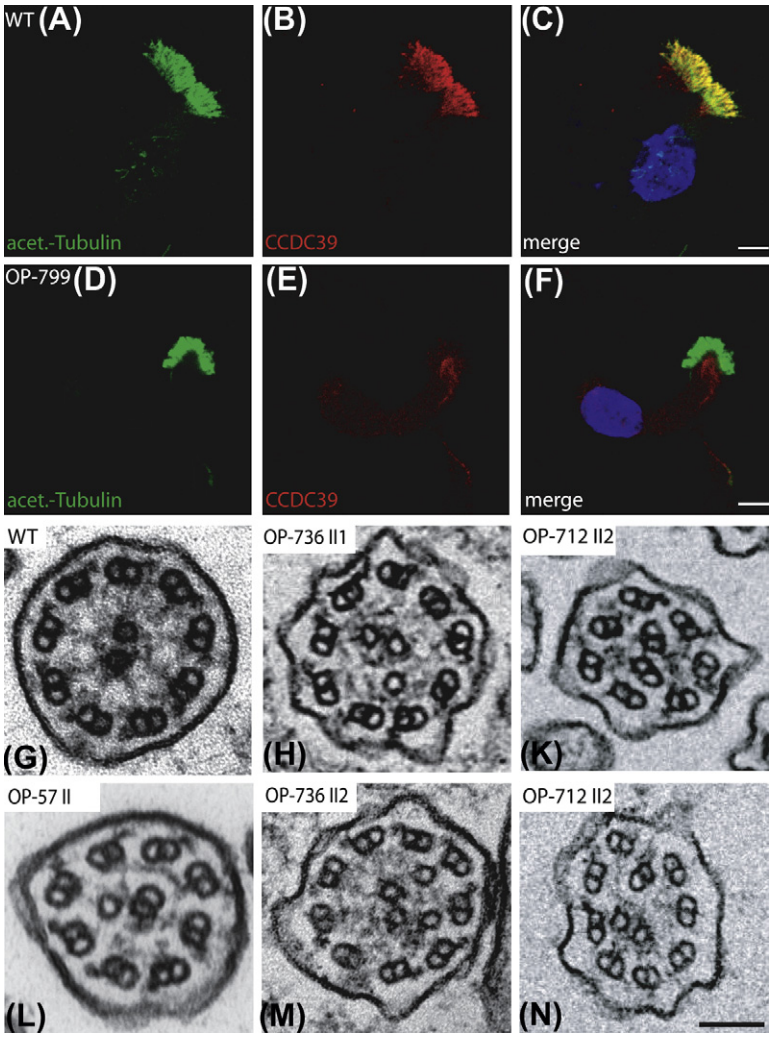

Figure 24.5 Localization of CCDC39 and axonemal ultrastructure. (A,D) Respiratory epithelial cells stained with acetylated α-tubulin (green) as marker for the ciliary axoneme. In respiratory ciliary cells of healthy controls, CCDC39 (red) localizes along the whole length of the axoneme (B). In patient OP-799 carrying loss-of-function mutations in *CCDC40*, CCDC39 is completely absent from the axoneme (E). (C,F) Merge figures: yellow staining means co-localization of both proteins. White scale bars represent 5 μm. (G) Axonemal ultrastructure of a healthy control. (H–N) Axonemal ultrastructure of patients carrying either *CCDC39* or *CCDC40* mutations show defects of the lining of the outer doublets as well as delocalization of the central pairs. Black scale bar displays 0.1 μm.

References

[1] B.A. Afzelius, Cilia-related diseases, J. Pathol. 204 (4) (2004) 470–477.

[2] B.A. Afzelius, P. Camner, B. Mossberg, On the function of cilia in the female reproductive tract, Fertil. Steril. 29 (1) (1978) 72–74.

[3] B.A. Afzelius, R. Eliasson, O. Johnsen, C. Lindholmer, Lack of dynein arms in immotile human spermatozoa, J. Cell Biol. 66 (2) (1975) 225–232.

[4] S.F. Altschul, W. Gish, W. Miller, E.W. Myers, D.J. Lipman, Basic local alignment search tool, J. Mol. Biol. 215 (1990) 403–410.

[5] L. Bartoloni, J.L. Blouin, Y. Pan, C. Gehrig, A.K. Maiti, N. Scamuffa, C. Rossier, M. Jorissen, M. Armengot, M. Meeks, H.M. Mitchison, E.M. Chung, C.D. Delozier-Blanchet, W.J. Craigen, S.E. Antonarakis, Mutations in the *DNAH11* (axonemal heavy chain dynein type 11) gene cause one form of *situs inversus totalis* and most likely primary ciliary dyskinesia, Proc. Natl. Acad. Sci. 99 (2002) 10282–10286.

[6] A. Becker-Heck, I.E. Zohn, N. Okabe, A. Pollock, K.B. Lenhart, J. Sullivan-Brown, J. McSheene, N.T. Loges, H. Olbrich, K. Haeffner, M. Fliegauf, J. Horvath, R. Reinhardt, K.G. Nielsen, J.K. Marthin, G. Baktai, K.V. Anderson, R. Geisler, L. Niswander, H. Omran, R.D. Burdine, The coiled-coil domain containing protein CCDC40 is essential for motile cilia function and left–right axis formation, Nat. Genet. 43 (2010) 79–84.

[7] R.S. Beddington, E.J. Robertson, Axis development and early asymmetry in mammals, Cell 96 (1999) 195–209.

[8] C.J. Brokaw, R. Kamiya, Bending patterns of *Chlamydomonas* flagella: IV. Mutants with defects in inner and outer dynein arms indicate differences in dynein arm function, Cell Motil. Cytoskeleton 8 (1) (1987) 68–75.

[9] S.A. Burgess, M.L. Walker, H. Sakakibara, P.J. Knight, K. Oiwa, Dynein structure and power stroke, Nature 13 (2003) 715–718.

[10] V.H. Castleman, L. Romio, R. Chodhari, R.A. Hirst, S.C. de Castro, K.A. Parker, P. Ybot-Gonzalez, R.D. Emes, S.W. Wilson, C. Wallis, C.A. Johnson, R.J. Herrera, A. Rutman, M. Dixon, A. Shoemark, A. Bush, C. Hogg, R.M. Gardiner, O. Reish, N.D. Greene, C. O'Callaghan, S. Purton, E.M. Chung, H.M. Mitchison, Mutations in radial spoke head protein genes RSPH9 and RSPH4A cause primary ciliary dyskinesia with central-microtubular-pair abnormalities, Am. J. Hum. Genet. 84 (2) (2009) 197–209.

[11] C. Chapelin, B. Duriez, F. Magnino, M. Goossens, E. Escudier, S. Amselem, Isolation of several human axonemal dynein heavy chain genes: Genomic structure of the catalytic site, phylogenetic analysis and chromosomal assignment, FEBS Lett. 412 (1997) 325–330.

[12] J. Chen, H.J. Knowles, J.L. Hebert, B.P. Hackett, Mutation of the mouse hepatocyte nuclear factor/forkhead homologue 4 gene results in an absence of cilia and random left-right asymmetry, J. Clin. Invest. 102 (1998) 1077–1082.

[13] E. Coll, R. Torra, J. Pascual, A. Botey, J. Ara, L. Pérez, F. Ballesta, A. Darnell, Sporadic orofaciodigital syndrome type I presenting as end-stage renal disease, Nephrol. Dial. Transplant. 12 (5) (1997) 1040–1042.

[14] L.M. DiBella, S.M. King, Dynein motor of the *Chlamydomonas* flagellum, Int. Rev. Cytol. 210 (2001) 227–268.

[15] B. Duriez, P. Duquesnoy, E. Escudier, A.M. Bridoux, D. Escalier, I. Rayet, E. Marcos, A.M. Vojtek, J.F. Bercher, S. Amselem, A common variant in combination with a nonsense mutation in a member of the thioredoxin family causes primary ciliary dyskinesia, Proc. Natl. Acad. Sci. USA 104 (9) (2007) 3336–3341.

[16] P. Duquesnoy, E. Escudier, L. Vincensini, J. Freshour, A.M. Bridoux, A. Coste, A. Deschildre, J. de Blic, M. Legendre, G. Montantin, H. Tenreiro, A.M. Vojtek, C. Loussert, A. Clément, D. Escalier, P. Bastin, D.R. Mitchell, S. Amselem, Loss-of-function mutations in the human ortholog of *Chlamydomonas reinhardtii* ODA7 disrupt dynein arm assembly and cause primary ciliary dyskinesia, Am. J. Hum. Genet. 85 (6) (2009) 890–896.

[17] L. El Zein, H. Omran, P. Bouvagnet, Lateralization defects and ciliary dyskinesia: Lessons from algae, Trends Genet. 19 (2003) 162–167.
[18] J.J. Essner, K.J. Vogan, M.K. Wagner, C.J. Tabin, H.J. Yost, M. Brueckner, Conserved function for embryonic nodal cilia, Nature 418 (2002) 37–38.
[19] M.I. Ferrante, A. Zullo, A. Barra, S. Bimonte, N. Messaddeq, M. Studer, P. Dollé, B. Franco, Oral-facial-digital type I protein is required for primary cilia formation and left–right axis specification, Nat. Genet. 38 (1) (2006) 112–117.
[20] M. Fliegauf, T. Benzing, H. Omran, When cilia go bad: Cilia defects and ciliopathies, Nat. Rev. Mol. Cell Biol. 8 (11) (2007) 880–893.
[21] M. Fliegauf, H. Olbrich, J. Horvath, J.H. Wildhaber, M.A. Zariwala, M. Kennedy, M.R. Knowles, H. Omran, Mislocalization of DNAH5 and DNAH9 in respiratory cells from patients with primary ciliary dyskinesia, Am. J. Respir. Crit. Care Med. 171 (2005) 1343–1349.
[22] M.E. Fowkes, D.R. Mitchell, The role of preassembled cytoplasmic complexes in assembly of flagellar dynein subunits, Mol. Biol. Cell 9 (1998) 2337–2347.
[23] J. Freshour, R. Yokoyama, D.R. Mitchell, *Chlamydomonas* flagellar outer row dynein assembly protein ODA7 interacts with both outer row and I1 inner row dyneins, J. Biol. Chem. 282 (8) (2006) 5404–5412.
[24] L.C. Gardner, E. O'Toole, C.A. Perrone, T. Giddings, M.E. Porter, Components of a "dynein regulatory complex" are located at the junction between the radial spokes and the dynein arms in *Chlamydomonas* flagella, J. Cell Biol. 127 (5) (1994) 1311–1325.
[25] S.F. Gilbert, Developmental Biology, 7th edition, Sinauer Associates Inc, Sunderland, MA, 2003.
[26] C. Guichard, M.C. Harricane, J.J. Lafitte, P. Godard, M. Zaegel, V. Tack, G. Lalau, P. Bouvagnet, Axonemal dynein intermediate-chain gene (DNAI1) mutations result in *situs inversus* and primary ciliary dyskinesia (Kartagener syndrome), Am. J. Hum. Genet. 68 (2001) 1030–1035.
[27] A. Harrison, P. Olds-Clarke, S.M. King, Identification of the t complex-encoded cytoplasmic dynein light chain tctex1 in inner arm I1 supports the involvement of flagellar dyneins in meiotic drive, J. Cell Biol. 140 (5) (1998) 1137–1147.
[28] A. Harrison, M. Sakato, H.W. Tedford, S.E. Benashski, R.S. Patel-King, S.M. King, Redox-based control of the gamma heavy chain ATPase from *Chlamydomonas* outer arm dynein, Cell Motil. Cytoskeleton 52 (3) (2002) 131–143.
[29] T. Heuser, M. Raytchev, J. Krell, M.E. Porter, D. Nicastro, The dynein regulatory complex is the nexin link and a major regulatory node in cilia and flagella, J. Cell Biol. 187 (6) (2009) 921–933.
[30] N. Hirokawa, Y. Tanaka, Y. Okada, Left–right determination: Involvement of molecular motor KIF3, cilia, and nodal flow, Cold Spring Harb. Perspect. Biol. 1 (1) (2009) a000802.
[31] N. Hornef, H. Olbrich, J. Horvath, M.A. Zariwala, M. Fliegauf, N.T. Loges, J. Wildhaber, P.G. Noone, M. Kennedy, S.E. Antonarakis, J.L. Blouin, L. Bartoloni, T. Nüsslein, P. Ahrens, M. Griese, H. Kuhl, R. Sudbrak, M.R. Knowles, R. Reinhardt, H. Omran, *DNAH5* mutations are a common cause of primary ciliary dyskinesia with outer dynein arm defects, Am. J. Respir. Crit. Care Med. 174 (2006) 120–126.
[32] F. Hildebrandt, E. Otto, C. Rensing, H.G. Nothwang, M. Vollmer, J. Adolphs, H. Hanusch, M. Brandis, A novel gene encoding an SH3 domain protein is mutated in nephronophthisis type 1, Nat. Genet. 17 (2) (1997) 149–153.
[33] B. Huang, G. Piperno, D.J.L. Luck, Paralyzed flagella mutants of *Chlamydomonas reinhardtii* defective for axonemal doublet microtubule arms, J. Biol. Chem. 254 (1979) 3091–3099.
[34] B. Huang, Z. Ramanis, D.J. Luck, Suppressor mutations in *Chlamydomonas* reveal a regulatory mechanism for flagellar function, Cell 28 (1) (1982) 115–124.

[35] I. Ibanez-Tallon, N. Heintz, H. Omran, To beat or not to beat: Roles of cilia in development and disease, Hum. Mol. Genet. 12 (2003) 27–35.
[36] I. Ibanez-Tallon, A. Pagenstecher, M. Fliegauf, H. Olbrich, A. Kispert, U.P. Ketelsen, A. North, N. Heintz, H. Omran, Dysfunction of axonemal dynein heavy chain Mdnah5 inhibits ependymal flow and reveals a novel mechanism for hydrocephalus formation, Hum. Mol. Genet. 13 (2004) 2133–2141.
[37] G. Li, R. Vega, K. Nelms, N. Gekakis, C. Goodnow, P. McNamara, H. Wu, N.A. Hong, R. Glynne, A role for Alström syndrome protein, alms1, in kidney ciliogenesis and cellular quiescence, PLoS Genet. 3 (1) (2007) e8.
[38] R. Kamiya, Mutations at twelve independent loci result in absence of outer dynein arms in *Chylamydomonas reinhardtii*, J. Cell Biol. 107 (1988) 2253–2258.
[39] R. Kamiya, Exploring the function of inner and outer dynein arms with *Chlamydomonas* mutants, Cell Motil. Cytoskeleton 32 (1995) 98–102.
[40] R. Kamiya, E. Kurimoto, H. Sakakibara, T. Okagaki, A genetic approach to the function of inner and outer arm dynein, in: F.D. Warner, P. Satir, I.R. Gibbons (Eds.), Cell Movement, vol. 1, Alan R. Liss, Inc, New York, 1989, pp. 49–60.
[41] R. Kamiya, M. Okamoto, A mutant of *Chlamydomonas reinhardtii* that lacks the flagellar outer dynein arm but can swim, J. Cell Sci. 74 (1985) 181–191.
[42] M.H. Kaufmann, The Atlas of Mouse Development, first ed, Elsevier Academic Press, San Diego, CA, 1995.
[43] S.M. King, Axonemal dyneins winch the cilium, Nat. Struct. Mol. Biol. 17 (2010) 673–674.
[44] S.J. King, S.K. Dutcher, Phosphoregulation of an inner dynein arm complex in *Chlamydomonas reinhardtii* is altered in phototactic mutant strains, J. Cell Biol. 136 (1) (1997) 177–191.
[45] A. Kispert, M. Petry, H. Olbrich, A. Volz, U.P. Ketelsen, J. Horvath, R. Melkaoui, H. Omran, M. Zariwala, P.G. Noone, M. Knowles, Genotype–phenotype correlations in PCD patients carrying *DNAH5* mutations, Thorax 58 (2003) 552–554.
[46] M. LeDizet, G. Piperno, The light chain p28 associates with a subset of inner dynein arm heavy chains in *Chlamydomonas* axonemes, Mol. Biol. Cell 6 (1995) 697–711.
[47] K.F. Lechtreck, P. Delmotte, M.L. Robinson, M.J. Sanderson, G.B. Witman, Mutations in *Hydin* impair ciliary motility in mice, J. Cell Biol. 180 (2008) 633–643.
[48] N.T. Loges, H. Olbrich, A. Becker-Heck, K. Häffner, A. Heer, C. Reinhard, M. Schmidts, A. Kispert, M.A. Zariwala, M.W. Leigh, M.R. Knowles, H. Zentgraf, H. Seithe, G. Nürnberg, P. Nürnberg, R. Reinhardt, H. Omran, Deletions and point mutations of *LRRC50* cause primary ciliary dyskinesia due to dynein arm defects, Am. J. Hum. Genet. 85 (6) (2009) 883–889.
[49] N.T. Loges, H. Olbrich, L. Fenske, H. Mussaffi, J. Horvath, M. Fliegauf, H. Kuhl, G. Baktai, E. Peterffy, R. Chodhari, E.M. Chung, A. Rutman, C. O'Callaghan, H. Blau, L. Tiszlavicz, K. Voelkel, M. Witt, E. Zietkiewicz, J. Neesen, R. Reinhardt, H.M. Mitchison, H. Omran, *DNAI2* mutations cause primary ciliary dyskinesia with defects in the outer dynein arm, Am. J. Hum. Genet. 83 (2008) 547–558.
[50] R.A. Lyons, E. Saridogan, O. Djahanbakhch, The reproductive significance of human fallopian tube cilia, Hum. Reprod. Update 12 (4) (2006) 363–372.
[51] J. McGrath, M. Brueckner, Cilia are at the heart of vertebrate left–right asymmetry, Curr. Opin. Genet. Dev. 13 (2003) 385–392.
[52] S.S. Merchant, S.E. Prochnik, O. Vallon, E.H. Harris, S.J. Karpowicz, G.B. Witman, A. Terry, A. Salamov, L.K. Fritz-Laylin, L. Maréchal-Drouard, W.F. Marshall, L.H. Qu, D.R. Nelson, A.A. Sanderfoot, M.H. Spalding, V.V. Kapitonov, Q. Ren, P. Ferris, E. Lindquist, H. Shapiro, S.M. Lucas, J. Grimwood, J. Schmutz, P. Cardol, H. Cerutti, G. Chanfreau, C.L. Chen, V. Cognat, M.T. Croft, R. Dent, S. Dutcher, E. Fernández, H. Fukuzawa, D. González-Ballester, D. González-Halphen, A. Hallmann, M. Hanikenne, M. Hippler, W. Inwood,

K. Jabbari, M. Kalanon, R. Kuras, P.A. Lefebvre, S.D. Lemaire, A.V. Lobanov, M. Lohr, A. Manuell, I. Meier, L. Mets, M. Mittag, T. Mittelmeier, J.V. Moroney, J. Moseley, C. Napoli, A.M. Nedelcu, K. Niyogi, S.V. Novoselov, I.T. Paulsen, G. Pazour, S. Purton, J.P. Ral, D.M. Riaño-Pachón, W. Riekhof, L. Rymarquis, M. Schroda, D. Stern, J. Umen, R. Willows, N. Wilson, S.L. Zimmer, J. Allmer, J. Balk, K. Bisova, C.J. Chen, M. Elias, K. Gendler, C. Hauser, M.R. Lamb, H. Ledford, J.C. Long, J. Minagawa, M.D. Page, J. Pan, W. Pootakham, S. Roje, A. Rose, E. Stahlberg, A.M. Terauchi, P. Yang, S. Ball, C. Bowler, C.L. Dieckmann, V.N. Gladyshev, P. Green, R. Jorgensen, S. Mayfield, B. Mueller-Roeber, S. Rajamani, R.T. Sayre, P. Brokstein, I. Dubchak, D. Goodstein, L. Hornick, Y.W. Huang, J. Jhaveri, Y. Luo, D. Martínez, W.C. Ngau, B. Otillar, A. Poliakov, A. Porter, L. Szajkowski, G. Werner, K. Zhou, I.V. Grigoriev, D.S. Rokhsar, A.R. Grossman, The *Chlamydomonas* genome reveals the evolution of key animal and plant functions, Science 318 (5848) (2007) 245–250.

[53] A.C. Merveille, E.E. Davis, A. Becker-Heck, M. Legendre, I. Amirav, G. Bataille, J. Belmont, N. Beydon, F. Billen, A. Clément, C. Clercx, A. Coste, R. Crosbie, J. de Blic, S. Deleuze, P. Duquesnoy, D. Escalier, E. Escudier, M. Fliegauf, J. Horvath, K. Hill, M. Jorissen, J. Just, A. Kispert, M. Lathrop, N.T. Loges, J.K. Marthin, Y. Momozawa, G. Montantin, K.G. Nielsen, H. Olbrich, J.F. Papon, I. Rayet, G. Roger, M. Schmidts, H. Tenreiro, J.A. Towbin, D. Zelenika, H. Zentgraf, M. Georges, A.S. Lequarré, N. Katsanis, H. Omran, S. Amselem, CCDC39 is required for assembly of inner dynein arms and the dynein regulatory complex and for normal ciliary motility in humans and dogs, Nat. Genet. 43 (2010) 72–78.

[54] D.R. Mitchell, J.L. Rosenbaum, A motile *Chlamydomonas* flagellar mutant that lacks outer dynein arms, J. Cell Biol. 100 (1985) 1228–1234.

[55] N.C. Munro, D.C. Currie, K.S. Lindsay, T.A. Ryder, A. Rutman, A. Dewar, M.A. Greenstone, W.F. Hendry, P.J. Cole, Fertility in men with primary ciliary dyskinesia presenting with respiratory infection, Thorax 49 (1994) 684–687.

[56] S.H. Myster, J.A. Knott, K.M. Wysocki, E. O'Toole, M.E. Porter, Domains in the 1alpha dynein heavy chain required for inner arm assembly and flagellar motility in *Chlamydomonas*, J. Cell Biol. 146 (4) (1999) 801–818.

[57] M.V. Nachury, A.V. Loktev, Q. Zhang, C.J. Westlake, J. Peränen, A. Merdes, D.C. Slusarski, R.H. Scheller, J.F. Bazan, V.C. Sheffield, P.K. Jackson, A core complex of BBS proteins cooperates with the GTPase Rab8 to promote ciliary membrane biogenesis, Cell 129 (6) (2007) 1201–1213.

[58] J. Neesen, R. Kirschner, M. Ochs, A. Schmiedl, B. Habermann, C. Mueller, A.F. Holstein, T. Nuesslein, I. Adham, W. Engel, Disruption of an inner arm dynein heavy chain gene results in asthenozoospermia and reduced ciliary beat frequency, Hum. Mol. Genet. 10 (11) (2001) 1117–1128.

[59] S. Nonaka, H. Shiratori, Y. Saijoh, H. Hamada, Determination of left–right patterning of the mouse embryo by artificial nodal flow, Nature 418 (2002) 96–99.

[60] S. Nonaka, Y. Tanaka, Y. Okada, S. Takeda, A. Harada, Y. Kanai, M. Kido, N. Hirokawa, Randomization of left–right asymmetry due to loss of nodal cilia generating leftward flow of extraembryonic fluid in mice lacking KIF3B motor protein, Cell 95 (1998) 829–837.

[61] Y. Okada, S. Nonaka, Y. Tanaka, Y. Saijoh, H. Hamada, N. Hirokawa, Abnormal nodal flow precedes *situs inversus* in iv and inv mice, Mol. Cell 4 (1999) 459–468.

[62] H. Olbrich, M. Fliegauf, J. Hoefele, A. Kispert, E. Otto, A. Volz, M.T. Wolf, G. Sasmaz, U. Trauer, R. Reinhardt, R. Sudbrak, C. Antignac, N. Gretz, G. Walz, B. Schermer, T. Benzing, F. Hildebrandt, H. Omran, Mutations in a novel gene, *NPHP3*, cause adolescent nephronophthisis, tapeto-retinal degeneration and hepatic fibrosis, Nat. Genet. 34 (4) (2003) 455–459.

[63] H. Olbrich, K. Haffner, A. Kispert, A. Volkel, A. Volz, G. Sasmaz, R. Reinhardt, S. Hennig, H. Lehrach, N. Konietzko, M. Zariwala, P.G. Noone, M. Knowles, H.M. Mitchison, M. Meeks, E.M. Chung, F. Hildebrandt, R. Sudbrak, H. Omran, Mutations in *DNAH5* cause

primary ciliary dyskinesia and randomization of left–right asymmetry, Nat. Genet. 30 (2002) 143–144.
[64] H. Omran, K. Haffner, A. Volkel, J. Kuehr, U.-P. Ketelsen, U.H. Ross, N. Konietzko, T. Wienker, M. Brandis, F. Hildebrandt, Homozygosity mapping of a gene locus for primary ciliary dyskinesia on chromosome 5p and identification of the heavy dynein chain DNAH5 as a candidate gene, Am. J. Respir. Cell Mol. Biol. 23 (2000) 696–702.
[65] H. Omran, D. Kobayashi, H. Olbrich, T. Tsukahara, N.T. Loges, H. Hagiwara, Q. Zhang, G. Leblond, E. O'Toole, C. Hara, H. Mizuno, H. Kawano, M. Fliegauf, T. Yagi, S. Koshida, A. Miyawaki, H. Zentgraf, H. Seithe, R. Reinhardt, Y. Watanabe, R. Kamiya, D.R. Mitchell, H. Takeda, Ktu/PF13 is required for cytoplasmic pre-assembly of axonemal dyneins, Nature 456 (7222) (2008) 611–616.
[66] G.J. Pazour, N. Agrin, B.L. Walker, G.B. Witman, Identification of predicted human outer dynein arm genes: Candidates for primary ciliary dyskinesia genes, J. Med. Genet. 43 (2006) 62–73.
[67] H. Pedersen, Absence of dynein arms in endometrial cilia: Cause of infertility? Acta Obstet. Gynecol. Scand. 62 (6) (1983) 625–627.
[68] H. Pedersen, H. Rebbe, Absence of arms in the axoneme of immobile human spermatozoa, Biol. Reprod. 12 (5) (1975) 541–544.
[69] G. Pennarun, E. Escudier, C. Chapelin, A.M. Bridoux, V. Cacheux, G. Roger, A. Clément, M. Goossens, S. Amselem, B. Duriez, Loss-of-function mutations in a human gene related to *Chlamydomonas reinhardtii* dynein *IC78* result in primary ciliary dyskinesia, Am. J. Hum. Genet. 65 (6) (1999) 1508–1519.
[70] C.A. Perrone, P. Yang, E. O'Toole, W.S. Sale, M.E. Porter, The *Chlamydomonas* IDA7 locus encodes a 140-kDa dynein intermediate chain required to assemble the I1 inner arm complex, Mol. Biol. Cell 9 (1998) 3351–3365.
[71] C.A. Perrone, S.H. Myster, R. Bower, E.T. O'Toole, M.E. Porter, Insights into the structural organization of the I1 inner arm dynein from a domain analysis of the 1beta dynein heavy chain, Mol. Biol. Cell 11 (7) (2000) 2297–2313.
[72] G. Piperno, Isolation of radial spoke heads from *Chlamydomonas* axonemes, Method. Cell. Biol. 47 (1995) 381–383.
[73] G. Piperno, K. Mead, M. LeDizet, A. Moscatelli, Mutations in the "dynein regulatory complex" alter the ATP-insensitive binding sites for inner arm dyneins in *Chlamydomonas* axonemes, J. Cell Biol. 125 (5) (1994) 1109–1117.
[74] G. Piperno, K. Mead, W. Shestak, The inner dynein arms I2 interact with a "dynein regulatory complex" in *Chlamydomonas* flagella, J. Cell Biol. 118 (6) (1992) 1455–1463.
[75] G. Piperno, Z. Ramanis, The proximal portion of *Chlamydomonas* flagella contains a distinct set of inner dynein arms, J. Cell Biol. 112 (4) (1991) 701–709.
[76] T.D. Pollard, J.A. Cooper, Actin and actin-binding proteins. A critical evaluation of mechanisms and functions, Annu. Rev. Biochem. 55 (1986) 987–1035.
[77] M.E. Porter, J. Power, S.K. Dutcher, Extragenic suppressors of paralyzed flagellar mutations in *Chlamydomonas reinhardtii* identify loci that alter the inner dynein arms, J. Cell Biol. 118 (5) (1992) 1163–1176.
[78] W. Reed, J.L. Carson, B.M. Moats-Staats, T. Lucier, P. Hu, L. Brighton, T.M. Gambling, C.H. Huang, M.W. Leigh, A.M. Collier, Characterization of an axonemal dynein heavy chain expressed early in airway epithelial ciliogenesis, Am. J. Respir. Cell Mol. Biol. 23 (2000) 734–741.
[79] H. Sakakibara, S. Takada, S.M. King, G.B. Witman, R. Kamiya, A *Chlamydomonas* outer arm dynein mutant with a truncated beta heavy chain, J. Cell Biol. 122 (3) (1993) 653–661.
[80] M. Salathe, Regulation of mammalian ciliary beating, Annu. Rev. Physiol. 69 (2007) 401–422.

[81] M. Salathe, M.M. Pratt, A. Wanner, Cyclic AMP-dependent phosphorylation of a 26 kD axonemal protein in ovine cilia isolated from small tissue pieces, Am. J. Respir. Cell Mol. Biol. 9 (1993) 306–314.
[82] S.A. Samant, O. Ogunkua, L. Hui, J. Fossella, S.H. Pilder, The T complex distorter 2 candidate gene, *Dnahc8*, encodes at least two testis-specific axonemal dynein heavy chains that differ extensively at their amino and carboxyl termini, Dev. Biol. 250 (2002) 24–43.
[83] M.A. Sanders, J.L. Salisbury, Centrin-mediated microtubule severing during flagellar excision in *Chlamydomonas reinhardtii*, J. Cell Biol. 108 (5) (1989) 1751–1760.
[84] R. Sapiro, I. Kostetskii, P. Olds-Clarke, G.L. Gerton, G.L. Radice, J.F. Strauss III, Male infertility, impaired sperm motility, and hydrocephalus in mice deficient in sperm-associated antigen 6, Mol. Cell Biol. 22 (2002) 6298–6305.
[85] K. Sawamoto, H. Wichterle, O. Gonzalez-Perez, J.A. Cholfin, M. Yamada, N. Spassky, N.S. Murcia, J.M. Garcia-Verdugo, O. Marin, J.L. Rubenstein, M. Tessier-Lavigne, H. Okano, A. Alvarez-Buylla, New neurons follow the flow of cerebrospinal fluid in the adult brain, Science 311 (2006) 629–632.
[86] A. Schmid, G. Bai, N. Schmid, M. Zaccolo, L.E. Ostrowski, G.E. Conner, N. Fregien, M. Salathe, Real-time analysis of cAMP-mediated regulation of ciliary motility in single primary human airway epithelial cells, J. Cell Sci. 15 (2006) 4176–4186.
[87] A. Schmid, Z. Sutto, M.C. Nlend, G. Horvath, N. Schmid, J. Buck, L.R. Levin, G.E. Conner, N. Fregien, M. Salathe, Soluble adenylyl cyclase is localized to cilia and contributes to ciliary beat frequency regulation via production of cAMP, J. Gen. Physiol. 130 (2007) 99–109.
[88] G.C. Schwabe, K. Hoffmann, N.T. Loges, D. Birker, C. Rossier, M.M. de Santi, H. Olbrich, M. Fliegauf, M. Failly, U. Liebers, M. Collura, G. Gaedicke, S. Mundlos, U. Wahn, J.L. Blouin, B. Niggemann, H. Omran, S.E. Antonarakis, L. Bartoloni, Primary ciliary dyskinesia associated with normal axoneme ultrastructure is caused by *DNAH11* mutations, Hum. Mutat. 29 (2008) 289–298.
[89] R.J. Simms, L. Eley, J.A. Sayer, Nephronophthisis, Eur. J. Hum. Genet. 17 (4) (2008) 406–416.
[90] E.F. Smith, P. Yang, The radial spokes and central apparatus: Mechano-chemical transducers that regulate flagellar motility, Cell Motil. Cytoskeleton 57 (1) (2004) 8–17.
[91] J.M. Sturgess, J. Chao, J. Wong, N. Aspin, J.A. Turner, Cilia with defective radial spokes: A cause of human respiratory disease, N. Engl. J. Med. 11 (1979) 53–56.
[92] J. Sullivan-Brown, J. Schottenfeld, N. Okabe, C.L. Hostetter, F.C. Serluca, S.Y. Thiberge, R.D. Burdine, Zebrafish mutations affecting cilia motility share similar cystic phenotypes and suggest a mechanism of cyst formation that differs from pkd2 morphants, Dev. Biol. 314 (2) (2007) 261–275.
[93] D.M. Supp, D.P. Witte, S.S. Potter, M. Brueckner, Mutation of an axonemal dynein affects left–right asymmetry in inversus viscerum mice, Nature 389 (1997) 963–996.
[94] Y. Tanaka, Y. Okada, N. Hirokawa, FGF-induced vesicular release of sonic hedgehog and retinoic acid in leftward nodal flow is critical for left–right determination, Nature 435 (2005) 172–177.
[95] P.D. Taulman, C.J. Haycraft, D.F. Balkovetz, B.K. Yoder, Polaris, a protein involved in left–right axis patterning, localizes to basal bodies and cilia, Mol. Biol. Cell 12 (2001) 589–599.
[96] E. van Rooijen, R.H. Giles, E.E. Voest, C. van Rooijen, S. Schulte-Merker, F.J. van Eeden, LRRC50, a conserved ciliary protein implicated in polycystic kidney disease, J. Am. Soc. Nephrol. 19 (6) (2008) 1128–1138.
[97] C.G. Wilkerson, S.M. King, G.B. Witman, Molecular analysis of the gamma heavy chain of *Chlamydomonas* flagellar outer-arm dynein, J. Cell Sci. 107 (1994) 497–506.

[98] H.A. Yanagisawa, R. Kamiya, Association between actin and light chains in *Chlamydomonas* flagellar inner-arm dyneins, Biochem. Biophys. Res. Commun. 26 (2001) 443–447.
[99] P. Yang, D.R. Diener, C. Yang, T. Kohno, G.J. Pazour, J.M. Dienes, N.S. Agrin, S.M. King, W.S. Sale, R. Kamiya, J.L. Rosenbaum, G.B. Witman, Radial spoke proteins of *Chlamydomonas flagella*, J. Cell Sci. 15 (2006) 1165–1174.
[100] M.A. Zariwala, M.W. Leigh, F. Ceppa, M.P. Kennedy, P.G. Noone, J.L. Carson, M.J. Hazucha, A. Lori, J. Horvath, H. Olbrich, N.T. Loges, A.M. Bridoux, G. Pennarun, B. Duriez, E. Escudier, H.M. Mitchison, R. Chodhari, E.M. Chung, L.C. Morgan, R.U. de Iongh, J. Rutland, U. Pradal, H. Omran, S. Amselem, M.R. Knowles, Mutations of *DNAI1* in primary ciliary dyskinesia: evidence of founder effect in a common mutation, Am. J. Respir. Crit. Care Med. 174 (2006) 858–866.
[101] Y.J. Zhang, W.K. O'Neal, S.H. Randell, K. Blackburn, M.B. Moyer, R.C. Boucher, L.E. Ostrowski, Identification of dynein heavy chain 7 as an inner arm component of human cilia that is synthesized but not assembled in a case of primary ciliary dyskinesia, J. Biol. Chem. 17 (2002) 17906–17915.

Index

B

C

H